

P-ADIC LENGTH SCALE HYPOTHESIS
AND DARK MATTER HIERARCHY

Matti Pitkänen

Köydenpunojankatu D 11, 10900, Hanko, Finland

Preface

This book belongs to a series of online books summarizing the recent state Topological Geometrodynamics (TGD) and its applications. TGD can be regarded as a unified theory of fundamental interactions but is not the kind of unified theory as so called GUTs constructed by graduate students at seventies and eighties using detailed recipes for how to reduce everything to group theory. Nowadays this activity has been completely computerized and it probably takes only a few hours to print out the predictions of this kind of unified theory as an article in the desired format. TGD is something different and I am not ashamed to confess that I have devoted the last 32 years of my life to this enterprise and am still unable to write The Rules.

I got the basic idea of Topological Geometrodynamics (TGD) during autumn 1978, perhaps it was October. What I realized was that the representability of physical space-times as 4-dimensional surfaces of some higher-dimensional space-time obtained by replacing the points of Minkowski space with some very small compact internal space could resolve the conceptual difficulties of general relativity related to the definition of the notion of energy. This belief was too optimistic and only with the advent of what I call zero energy ontology the understanding of the notion of Poincare invariance has become satisfactory.

It soon became clear that the approach leads to a generalization of the notion of space-time with particles being represented by space-time surfaces with finite size so that TGD could be also seen as a generalization of the string model. Much later it became clear that this generalization is consistent with conformal invariance only if space-time is 4-dimensional and the Minkowski space factor of imbedding space is 4-dimensional.

It took some time to discover that also the geometrization of also gauge interactions and elementary particle quantum numbers could be possible in this framework: it took two years to find the unique internal space providing this geometrization involving also the realization that family replication phenomenon for fermions has a natural topological explanation in TGD framework and that the symmetries of the standard model symmetries are much more profound than pragmatic TOE builders have believed them to be. If TGD is correct, main stream particle physics chose the wrong track leading to the recent deep crisis when people decided that quarks and leptons belong to same multiplet of the gauge group implying instability of proton.

There have been also longstanding problems.

- Gravitational energy is well-defined in cosmological models but is not conserved. Hence the conservation of the inertial energy does not seem to be consistent with the Equivalence Principle. Furthermore, the imbeddings of Robertson-Walker cosmologies turned out to be vacuum extremals with respect to the inertial energy. About 25 years was needed to realize that the sign of the inertial energy can be also negative and in cosmological scales the density of inertial energy vanishes: physically acceptable universes are creatable from vacuum. Eventually this led to the notion of zero energy ontology which deviates dramatically from the standard ontology being however consistent with the crossing symmetry of quantum field theories. In this framework the quantum numbers are assigned with zero energy states located at the boundaries of so called causal diamonds defined as intersections of future and past directed light-cones. The notion of energy-momentum becomes length scale dependent since one has a scale hierarchy for causal diamonds. This allows to understand the non-conservation of energy as apparent. Equivalence Principle generalizes and has a formulation in terms of coset representations of Super-Virasoro algebras providing also a justification for p-adic thermodynamics.
- From the beginning it was clear that the theory predicts the presence of long ranged classical electro-weak and color gauge fields and that these fields necessarily accompany classical electromagnetic fields. It took about 26 years to gain the maturity to admit the obvious: these fields are classical correlates for long range color and weak interactions assignable to dark matter. The only possible conclusion is that TGD physics is a fractal consisting of an entire hierarchy of fractal copies of standard model physics. Also the understanding of electro-weak massivation and screening of weak charges has been a long standing problem, and 32 years was needed to discover that what I call weak form of electric-magnetic duality gives a satisfactory solution of the problem and provides also surprisingly powerful insights to the mathematical structure of quantum TGD.

I started the serious attempts to construct quantum TGD after my thesis around 1982. The original optimistic hope was that path integral formalism or canonical quantization might be enough to construct the quantum theory but the first discovery made already during first year of TGD was that these formalisms might be useless due to the extreme non-linearity and enormous vacuum degeneracy of the theory. This turned out to be the case.

- It took some years to discover that the only working approach is based on the generalization of Einstein's program. Quantum physics involves the geometrization of the infinite-dimensional "world of classical worlds" (WCW) identified as 3-dimensional surfaces. Still few years had to pass before I understood that general coordinate invariance leads to a more or less unique solution of the problem and implies that space-time surfaces are analogous to Bohr orbits. Still a couple of years and I discovered that quantum states of the Universe can be identified as classical spinor fields in WCW. Only quantum jump remains the genuinely quantal aspect of quantum physics.
- During these years TGD led to a rather profound generalization of the space-time concept. Quite general properties of the theory led to the notion of many-sheeted space-time with sheets representing physical subsystems of various sizes. At the beginning of 90s I became dimly aware of the importance of p-adic number fields and soon ended up with the idea that p-adic thermodynamics for a conformally invariant system allows to understand elementary particle massivation with amazingly few input assumptions. The attempts to understand p-adicity from basic principles led gradually to the vision about physics as a generalized number theory as an approach complementary to the physics as an infinite-dimensional spinor geometry of WCW approach. One of its elements was a generalization of the number concept obtained by fusing real numbers and various p-adic numbers along common rationals. The number theoretical trinity involves besides p-adic number fields also quaternions and octonions and the notion of infinite prime.
- TGD inspired theory of consciousness entered the scheme after 1995 as I started to write a book about consciousness. Gradually it became difficult to say where physics ends and consciousness theory begins since consciousness theory could be seen as a generalization of quantum measurement theory by identifying quantum jump as a moment of consciousness and by replacing the observer with the notion of self identified as a system which is conscious as long as it can avoid entanglement with environment. "Everything is conscious and consciousness can be only lost" summarizes the basic philosophy neatly. The idea about p-adic physics as physics of cognition and intentionality emerged also rather naturally and implies perhaps the most dramatic generalization of the space-time concept in which most points of p-adic space-time sheets are infinite in real sense and the projection to the real imbedding space consists of discrete set of points. One of the most fascinating outcomes was the observation that the entropy based on p-adic norm can be negative. This observation led to the vision that life can be regarded as something in the intersection of real and p-adic worlds. Negentropic entanglement has interpretation as a correlate for various positively colored aspects of conscious experience and means also the possibility of strongly correlated states stable under state function reduction and different from the conventional bound states and perhaps playing key role in the energy metabolism of living matter.
- One of the latest threads in the evolution of ideas is only slightly more than six years old. Learning about the paper of Laurent Nottale about the possibility to identify planetary orbits as Bohr orbits with a gigantic value of gravitational Planck constant made once again possible to see the obvious. Dynamical quantized Planck constant is strongly suggested by quantum classical correspondence and the fact that space-time sheets identifiable as quantum coherence regions can have arbitrarily large sizes. During summer 2010 several new insights about the mathematical structure and interpretation of TGD emerged. One of these insights was the realization that the postulated hierarchy of Planck constants might follow from the basic structure of quantum TGD. The point is that due to the extreme non-linearity of the classical action principle the correspondence between canonical momentum densities and time derivatives of the imbedding space coordinates is one-to-many and the natural description of the situation is in terms of local singular covering spaces of the imbedding space. One could speak about effective value of Planck

constant coming as a multiple of its minimal value. The implications of the hierarchy of Planck constants are extremely far reaching so that the significance of the reduction of this hierarchy to the basic mathematical structure distinguishing between TGD and competing theories cannot be under-estimated.

From the point of view of particle physics the ultimate goal is of course a practical construction recipe for the S-matrix of the theory. I have myself regarded this dream as quite too ambitious taking into account how far reaching re-structuring and generalization of the basic mathematical structure of quantum physics is required. It has indeed turned out that the dream about explicit formula is unrealistic before one has understood what happens in quantum jump. Symmetries and general physical principles have turned out to be the proper guide line here. To give some impressions about what is required some highlights are in order.

- With the emergence of zero energy ontology the notion of S-matrix was replaced with M-matrix which can be interpreted as a complex square root of density matrix representable as a diagonal and positive square root of density matrix and unitary S-matrix so that quantum theory in zero energy ontology can be said to define a square root of thermodynamics at least formally.
- A decisive step was the strengthening of the General Coordinate Invariance to the requirement that the formulations of the theory in terms of light-like 3-surfaces identified as 3-surfaces at which the induced metric of space-time surfaces changes its signature and in terms of space-like 3-surfaces are equivalent. This means effective 2-dimensionality in the sense that partonic 2-surfaces defined as intersections of these two kinds of surfaces plus 4-D tangent space data at partonic 2-surfaces code for the physics. Quantum classical correspondence requires the coding of the quantum numbers characterizing quantum states assigned to the partonic 2-surfaces to the geometry of space-time surface. This is achieved by adding to the modified Dirac action a measurement interaction term assigned with light-like 3-surfaces.
- The replacement of strings with light-like 3-surfaces equivalent to space-like 3-surfaces means enormous generalization of the super conformal symmetries of string models. A further generalization of these symmetries to non-local Yangian symmetries generalizing the recently discovered Yangian symmetry of $\mathcal{N} = 4$ supersymmetric Yang-Mills theories is highly suggestive. Here the replacement of point like particles with partonic 2-surfaces means the replacement of conformal symmetry of Minkowski space with infinite-dimensional super-conformal algebras. Yangian symmetry provides also a further refinement to the notion of conserved quantum numbers allowing to define them for bound states using non-local energy conserved currents.
- A further attractive idea is that quantum TGD reduces to almost topological quantum field theory. This is possible if the Kähler action for the preferred extremals defining WCW Kähler function reduces to a 3-D boundary term. This takes place if the conserved currents are so called Beltrami fields with the defining property that the coordinates associated with flow lines extend to single global coordinate variable. This ansatz together with the weak form of electric-magnetic duality reduces the Kähler action to Chern-Simons term with the condition that the 3-surfaces are extremals of Chern-Simons action subject to the constraint force defined by the weak form of electric magnetic duality. It is the latter constraint which prevents the trivialization of the theory to a topological quantum field theory. Also the identification of the Kähler function of WCW as Dirac determinant finds support as well as the description of the scattering amplitudes in terms of braids with interpretation in terms of finite measurement resolution coded to the basic structure of the solutions of field equations.
- In standard QFT Feynman diagrams provide the description of scattering amplitudes. The beauty of Feynman diagrams is that they realize unitarity automatically via the so called Cutkosky rules. In contrast to Feynman's original beliefs, Feynman diagrams and virtual particles are taken only as a convenient mathematical tool in quantum field theories. QFT approach is however plagued by UV and IR divergences and one must keep mind open for the possibility that a genuine progress might mean opening of the black box of the virtual particle.

In TGD framework this generalization of Feynman diagrams indeed emerges unavoidably. Light-like 3-surfaces replace the lines of Feynman diagrams and vertices are replaced by 2-D partonic

2-surfaces. Zero energy ontology and the interpretation of parton orbits as light-like "wormhole throats" suggests that virtual particles do not differ from on mass shell particles only in that the four- and three- momenta of wormhole throats fail to be parallel. The two throats of the wormhole defining virtual particle would contact carry on mass shell quantum numbers but for virtual particles the four-momenta need not be parallel and can also have opposite signs of energy. Modified Dirac equation suggests a number theoretical quantization of the masses of the virtual particles. The kinematic constraints on the virtual momenta are extremely restrictive and reduce the dimension of the sub-space of virtual momenta and if massless particles are not allowed (IR cutoff provided by zero energy ontology naturally), the number of Feynman diagrams contributing to a particular kind of scattering amplitude is finite and manifestly UV and IR finite and satisfies unitarity constraint in terms of Cutkosky rules. What is remarkable that fermionic propagators are massless propagators but for on mass shell four-momenta. This gives a connection with the twistor approach and inspires the generalization of the Yangian symmetry to infinite-dimensional super-conformal algebras.

What I have said above is strongly biased view about the recent situation in quantum TGD and I have left all about applications to the introductions of the books whose purpose is to provide a bird's eye of view about TGD as it is now. This vision is single man's view and doomed to contain unrealistic elements as I know from experience. My dream is that young critical readers could take this vision seriously enough to try to demonstrate that some of its basic premises are wrong or to develop an alternative based on these or better premises. I must be however honest and tell that 32 years of TGD is a really vast bundle of thoughts and quite a challenge for anyone who is not able to cheat himself by taking the attitude of a blind believer or a light-hearted debunker trusting on the power of easy rhetoric tricks.

Matti Pitkänen

Hanko,

September 15, 2010

Acknowledgements

Neither TGD nor these books would exist without the help and encouragement of many people. The friendship with Heikki and Raija Haila and their family have kept me in contact with the everyday world and without this friendship I would not have survived through these lonely 32 years most of which I have remained unemployed as a scientific dissident. I am happy that my children have understood my difficult position and like my friends have believed that what I am doing is something valuable although I have not received any official recognition for it.

During last decade Tapio Tammi has helped me quite concretely by providing the necessary computer facilities and being one of the few persons in Finland with whom to discuss about my work. I have had also stimulating discussions with Samuli Penttinen who has also helped to get through the economical situations in which there seemed to be no hope. The continual updating of fifteen online books means quite a heavy bureaucracy at the level of bits and without a systemization one ends up with endless copying and pasting and internal consistency is soon lost. Pekka Rapinoja has offered his help in this respect and I am especially grateful for him for my Python skills. Also Matti Vallinkoski has helped me in computer related problems.

The collaboration with Lian Sidoroff was extremely fruitful and she also helped me to survive economically through the hardest years. The participation to CASYS conferences in Liege has been an important window to the academic world and I am grateful for Daniel Dubois and Peter Marcer for making this participation possible. The discussions and collaboration with Eduardo de Luna and Istvan Dienes stimulated the hope that the communication of new vision might not be a mission impossible after all. Also blog discussions have been very useful. During these years I have received innumerable email contacts from people around the world. In particular, I am grateful for Mark McWilliams and Ulla Matfolk for providing links to possibly interesting web sites and articles. These contacts have helped me to avoid the depressive feeling of being some kind of Don Quixote of Science and helped me to widen my views: I am grateful for all these people.

In the situation in which the conventional scientific communication channels are strictly closed it is important to have some loop hole through which the information about the work done can at

least in principle leak to the publicity through the iron wall of the academic censorship. Without any exaggeration I can say that without the world wide web I would not have survived as a scientist nor as individual. Homepage and blog are however not enough since only the formally published result is a result in recent day science. Publishing is however impossible without a direct support from power holders- even in archives like arXiv.org.

Situation changed for five years ago as Andrew Adamatsky proposed the writing of a book about TGD when I had already got used to the thought that my work would not be published during my life time. The Prespacetime Journal and two other journals related to quantum biology and consciousness - all of them founded by Huping Hu - have provided this kind of loop holes. In particular, Dainis Zeps, Phil Gibbs, and Arkadiusz Jadczyk deserve my gratitude for their kind help in the preparation of an article series about TGD catalyzing a considerable progress in the understanding of quantum TGD. Also the viXra archive founded by Phil Gibbs and its predecessor Archive Freedom have been of great help: Victor Christianto deserves special thanks for doing the hard work needed to run Archive Freedom. Also the Neuroquantology Journal founded by Sultan Tarlaci deserves a special mention for its publication policy. And last but not least: there are people who experience as a fascinating intellectual challenge to spoil the practical working conditions of a person working with something which might be called unified theory: I am grateful for the people who have helped me to survive through the virus attacks, an activity which has taken roughly one month per year during the last half decade and given a strong hue of grey to my hair.

For a person approaching his sixty year birthday it is somewhat easier to overcome the hard feelings due to the loss of academic human rights than for an inpatient youngster. Unfortunately the economic situation has become increasingly difficult during the twenty years after the economic depression in Finland which in practice meant that Finland ceased to be a constitutional state in the strong sense of the word. It became possible to depose people like me from the society without fear about public reactions and the classification as dropout became a convenient tool of ridicule to circumvent the ethical issues. During last few years when the right wing has held the political power this trend has been steadily strengthening. In this kind of situation the concrete help from individuals has been and will be of utmost importance. Against this background it becomes obvious that this kind of work is not possible without the support from outside and I apologize for not being able to mention all the people who have helped me during these years.

Matti Pitkänen

Hanko,

September 15, 2010

Contents

1	Introduction	1
1.1	Background	1
1.2	Basic Ideas of TGD	1
1.2.1	TGD as a Poincare invariant theory of gravitation	2
1.2.2	TGD as a generalization of the hadronic string model	2
1.2.3	Fusion of the two approaches via a generalization of the space-time concept	2
1.3	The five threads in the development of quantum TGD	2
1.3.1	Quantum TGD as configuration space spinor geometry	2
1.3.2	p-Adic TGD	3
1.3.3	TGD as a generalization of physics to a theory consciousness	4
1.3.4	TGD as a generalized number theory	7
1.3.5	Dynamical quantized Planck constant and dark matter hierarchy	8
1.4	Bird's eye of view about the topics of the book	11
1.5	The contents of the book	11
1.5.1	Part I: p-Adic description of particle massivation	11
1.5.2	Part II: Applications of p-adic length scale hypothesis and dark matter hierarchy	18
I	P-ADIC DESCRIPTION OF PARTICLE MASSIVATION	31
2	Overall View About TGD from Particle Physics Perspective	33
2.1	Introduction	33
2.2	Some aspects of quantum TGD	34
2.2.1	New space-time concept	34
2.2.2	Zero energy ontology	35
2.2.3	The hierarchy of Planck constants	36
2.2.4	p-Adic physics and number theoretic universality	37
2.3	Symmetries of quantum TGD	39
2.3.1	General Coordinate Invariance	39
2.3.2	Generalized conformal symmetries	40
2.3.3	Equivalence Principle and super-conformal symmetries	40
2.3.4	Extension to super-conformal symmetries	40
2.3.5	Space-time supersymmetry in TGD Universe	41
2.3.6	Twistorial approach, Yangian symmetry, and generalized Feynman diagrams	45
2.4	Weak form electric-magnetic duality and color and weak forces	51
2.4.1	Could a weak form of electric-magnetic duality hold true?	52
2.4.2	Magnetic confinement, the short range of weak forces, and color confinement	55
2.5	Quantum TGD very briefly	58
2.5.1	Physics as infinite-dimensional geometry	58
2.5.2	Physics as generalized number theory	59
2.5.3	Questions	60
2.5.4	Modified Dirac action	65
2.5.5	Three Dirac operators and their interpretation	67
2.6	The role of twistors in quantum TGD	69
2.6.1	Could the Grassmannian program be realized in TGD framework?	69

2.6.2	Could TGD allow formulation in terms of twistors	76
2.7	Finiteness of generalized Feynman diagrams zero energy ontology	87
2.7.1	Virtual particles as pairs of on mass shell particles in ZEO	87
2.7.2	Loop integrals are manifestly finite	88
2.7.3	Taking into account magnetic confinement	89
3	Elementary Particle Vacuum Functionals	99
3.1	Introduction	99
3.2	Identification of elementary particles	100
3.2.1	The evolution of the topological ideas about elementary particles	101
3.2.2	Graviton and other stringy states	103
3.2.3	Spectrum of non-stringy states	104
3.3	Basic facts about Riemann surfaces	105
3.3.1	Mapping class group	105
3.3.2	Teichmueller parameters	107
3.3.3	Hyper-ellipticity	108
3.3.4	Theta functions	109
3.4	Elementary particle vacuum functionals	110
3.4.1	Extended Diff invariance and Lorentz invariance	110
3.4.2	Conformal invariance	111
3.4.3	Diff invariance	111
3.4.4	Cluster decomposition property	112
3.4.5	Finiteness requirement	113
3.4.6	Stability against the decay $g \rightarrow g_1 + g_2$	113
3.4.7	Stability against the decay $g \rightarrow g - 1$	113
3.4.8	Continuation of the vacuum functionals to higher genus topologies	115
3.5	Explanations for the absence of the $g > 2$ elementary particles from spectrum	116
3.5.1	Hyper-ellipticity implies the separation of $g \leq 2$ and $g > 2$ sectors to separate worlds	116
3.5.2	What about $g > 2$ vacuum functionals which do not vanish for hyper-elliptic surfaces?	116
3.5.3	Should higher elementary particle families be heavy?	117
3.6	Elementary particle vacuum functionals for dark matter	117
3.6.1	Connection between Hurwitz zetas, quantum groups, and hierarchy of Planck constants?	117
3.6.2	Could Hurwitz zetas relate to dark matter?	118
4	Massless States and Particle Massivation	127
4.1	Introduction	127
4.1.1	Physical states as representations of super-symplectic and Super Kac-Moody algebras	128
4.1.2	Particle massivation	128
4.1.3	What next?	131
4.2	Identification of elementary particles	131
4.2.1	Partons as wormhole throats and particles as bound states of wormhole contacts	131
4.2.2	Family replication phenomenon topologically	132
4.3	Non-topological contributions to particle masses from p-adic thermodynamics	135
4.3.1	Partition functions are not changed	136
4.3.2	Fundamental length and mass scales	139
4.3.3	Color degrees of freedom	141
4.3.4	Spectrum of elementary particles	145
4.3.5	Some probabilistic considerations	147
4.4	Modular contribution to the mass squared	148
4.4.1	Conformal symmetries and modular invariance	149
4.4.2	The physical origin of the genus dependent contribution to the mass squared	150
4.4.3	Generalization of Θ functions and quantization of p-adic moduli	152
4.4.4	The calculation of the modular contribution $\langle \Delta h \rangle$ to the conformal weight	155

4.5	General mass formulas for non-Higgsy contributions	155
4.5.1	General mass squared formula	156
4.5.2	Color contribution to the mass squared	156
4.5.3	Modular contribution to the mass of elementary particle	156
4.5.4	Thermal contribution to the mass squared	157
4.5.5	The contribution from the deviation of ground state conformal weight from negative integer	157
4.5.6	General mass formula for Ramond representations	159
4.5.7	General mass formulas for NS representations	159
4.5.8	Primary condensation levels from p-adic length scale hypothesis	160
4.6	Fermion masses	160
4.6.1	Charged lepton mass ratios	161
4.6.2	Neutrino masses	162
4.6.3	Quark masses	168
4.7	Higgsy aspects of particle massivation	172
4.7.1	Can p-adic thermodynamics explain the masses of intermediate gauge bosons?	172
4.7.2	Comparison of TGD Higgs and with MSSM Higgs	173
4.7.3	How TGD based description of particle massivation relates to Higgs mechanism	176
5	p-Adic Particle Massivation: Hadron Masses	185
5.1	Introduction	185
5.1.1	Construction of U and D matrices	185
5.1.2	Observations crucial for the model of hadron masses	186
5.1.3	A possible model for hadron	189
5.2	Quark masses	189
5.2.1	Basic mass formulas	189
5.2.2	The p-adic length scales associated with quarks and quark masses	190
5.2.3	Are scaled up variants of quarks also there?	193
5.3	Topological mixing of quarks	196
5.3.1	Mixing of the boundary topologies	196
5.3.2	The constraints on U and D matrices from quark masses	197
5.3.3	Constraints from CKM matrix	199
5.4	Construction of U , D , and CKM matrices	202
5.4.1	The constraints from CKM matrix and number theoretical conditions	202
5.4.2	How strong number theoretic conditions one can pose on U and D matrices?	203
5.4.3	Could rational unitarity make sense?	203
5.4.4	The parametrization suggested by the mass squared conditions	206
5.4.5	Thermodynamical model for the topological mixing	207
5.4.6	U and D matrices from the knowledge of top quark mass alone?	212
5.5	Hadron masses	217
5.5.1	The definition of the model for hadron masses	218
5.5.2	The anatomy of hadronic space-time sheet	220
5.5.3	Pseudoscalar meson masses	224
5.5.4	Baryonic mass differences as a source of information	226
5.5.5	Color magnetic spin-spin splitting	227
5.5.6	Color magnetic spin-spin interaction and super-symplectic contribution to the mass of hadron	228
5.5.7	Summary about the predictions for hadron masses	234
5.5.8	Some critical comments	237
6	p-Adic Particle Massivation: New Physics	243
6.1	Introduction	243
6.1.1	Basic new physics predictions	243
6.1.2	Outline of the topics of the chapter	243
6.2	Exotic particles predicted by TGD	244
6.2.1	Higher gauge boson families	245
6.2.2	Does TGD allow the counterpart of space-time super-symmetry	248

6.2.3	The physics of $M - \bar{M}$ systems forces the identification of vertices as branchings of partonic 2-surfaces	252
6.2.4	Super-symplectic bosons	253
6.2.5	A new twist in the spin puzzle of proton	254
6.2.6	Fractally scaled up versions of quarks	257
6.2.7	What M_{89} Hadron Physics would look like?	258
6.2.8	Could neutrinos appear in several p-adic mass scales?	260
6.2.9	Topological evaporation and the concept of Pomeron	263
6.2.10	Wild speculations about non-perturbative aspects of hadron physics and exotic Super Virasoro representations	264
6.3	The incredibly shrinking proton	266
6.3.1	Basic facts and notions	267
6.3.2	A model for the coupling between standard states and flux tube states	270
6.3.3	Are exotic flux tube bound states possible?	276
6.4	Comments about new physics predicted by TGD at LHC	278
6.4.1	Particles as wormhole contacts	278
6.4.2	New physics at LHC is approximately unavoidable	279
6.4.3	How TGD based description of particle massivation relates to Higgs mechanism?	281
6.4.4	First rumors about supersymmetric partners from LHC	284
6.5	Simulating Big Bang in laboratory	286
6.5.1	Experimental arrangement and findings	287
6.5.2	TGD based model for the quark-gluon plasma	289
6.5.3	Further experimental findings and theoretical ideas	291
6.5.4	Are ordinary black-holes replaced with super-symplectic black-holes in TGD Universe?	294
6.5.5	Very cautious conclusions	296
6.5.6	Five years later	297
6.5.7	Mersenne primes and mass scales	298
6.5.8	Cosmic strings and cosmic rays	299
6.5.9	Centauro type events, Cygnus X-3 and M_{89} hadrons	302
6.5.10	TGD based explanation of the exotic events	303
6.5.11	Cosmic ray spectrum and exotic hadrons	306
6.5.12	Ultrahigh energy cosmic rays as super-symplectic quanta?	308
6.6	TGD based explanation for the anomalously large direct CP violation in $K \rightarrow 2\pi$ decay	310
6.6.1	How to solve the problems in TGD framework	310
6.6.2	Basic notations and concepts	312
6.6.3	Separation of short and long distance physics using operator product expansion	314
6.7	Appendix	317
6.7.1	Effective Feynman rules and the effect of top quark mass on the effective action	317
6.7.2	U and D matrices from the knowledge of top quark mass alone?	319
6.8	Figures and Illustrations	331

II P-ADIC LENGTH SCALE HYPOTHESIS AND DARK MATTER HIERARCHY 335

7	Recent Status of Lepto-Hadron Hypothesis	337
7.1	Introduction	337
7.2	Lepto-hadron hypothesis	340
7.2.1	Anomalous e^+e^- pairs in heavy ion collisions	340
7.2.2	Lepto-pions and generalized PCAC hypothesis	342
7.2.3	Lepto-pion decays and PCAC hypothesis	345
7.2.4	Lepto-pions and weak decays	348
7.2.5	Orthopositronium puzzle and lepto-pion in photon photon scattering	350
7.2.6	Spontaneous vacuum expectation of lepto-pion field as source of lepto-pions	351
7.2.7	Sigma model and creation of lepto-hadrons in electromagnetic fields	352
7.2.8	Classical model for lepto-pion production	355

7.2.9	Quantum model for lepton production	357
7.3	Further developments	369
7.3.1	How to observe leptonic color?	369
7.3.2	New experimental evidence	370
7.3.3	Evidence for τ -hadrons	372
7.3.4	Could lepto-hadrons be replaced with bound states of exotic quarks?	382
7.3.5	About the masses of lepto-hadrons	382
7.4	APPENDIX	383
7.4.1	Evaluation of lepton production amplitude	383
7.4.2	Production amplitude in quantum model	392
7.4.3	Evaluation of the singular parts of the amplitudes	395
8	TGD and Nuclear Physics	403
8.1	Introduction	403
8.1.1	p-Adic length scale hierarchy	403
8.1.2	TGD based view about dark matter	405
8.1.3	The identification of long range classical weak gauge fields as correlates for dark massless weak bosons	406
8.1.4	Dark color force as a space-time correlate for the strong nuclear force?	407
8.1.5	Tritium beta decay anomaly	410
8.1.6	Cold fusion and Trojan horse mechanism	410
8.2	Model for the nucleus based on exotic quarks	410
8.2.1	The notion of color bond	411
8.2.2	Are the quarks associated with color bonds dark or p-adically scaled down quarks?	411
8.2.3	Electro-weak properties of exotic and dark quarks	412
8.2.4	How the statistics of exotic and ordinary quarks relate to each other?	412
8.3	Model of strong nuclear force based on color bonds between exotic quarks	413
8.3.1	A model for color bonds in terms of color flux tubes	413
8.3.2	About the energetics of color bonds	415
8.4	How the color bond model relates to the ordinary description of nuclear strong interactions?	417
8.4.1	How strong isospin emerges?	417
8.4.2	How to understand the emergence of harmonic oscillator potential and spin-orbit interaction?	419
8.4.3	Binding energies and stability of light nuclei	421
8.4.4	Strong correlation between proton and neutron numbers and magic numbers	423
8.4.5	A remark about stringy description of strong reactions	426
8.4.6	Nuclear strings and DNA strands	426
8.5	Neutron halos, tetra-neutron, and "sticky toffee" model of nucleus	427
8.5.1	Tetraneutron	427
8.5.2	The formation of neutron halo and TGD	427
8.5.3	The "sticky toffee" model of Chris Illert for alpha decays	428
8.6	Tritium beta decay anomaly	429
8.6.1	Tritium beta decay anomaly	429
8.6.2	Could TGD based exotic nuclear physics explain the anomaly?	431
8.6.3	The model based on dark neutrinos	433
8.6.4	Some other apparent anomalies made possible by dark neutrinos	435
8.7	Cold fusion and Trojan horse mechanism	436
8.7.1	Exotic quarks and charged color bonds as a common denominator of anomalous phenomena	436
8.7.2	The experiments of Ditmire <i>et al</i>	438
8.7.3	Brief summary of cold fusion	438
8.7.4	TGD inspired model of cold fusion	440
8.7.5	Do nuclear reaction rates depend on environment?	443

9	Nuclear String Hypothesis	451
9.1	Introduction	451
9.1.1	$A > 4$ nuclei as nuclear strings consisting of $A \leq 4$ nuclei	451
9.1.2	Bose-Einstein condensation of color bonds as a mechanism of nuclear binding	452
9.1.3	Giant dipole resonance as de-coherence of Bose-Einstein condensate of color bonds	452
9.1.4	Dark nuclear strings as analogs of DNA-, RNA- and amino-acid sequences and baryonic realization of genetic code	452
9.2	Some variants of the nuclear string hypothesis	452
9.2.1	Could linking of nuclear strings give rise to heavier stable nuclei?	452
9.2.2	Nuclear strings as connected sums of shorter nuclear strings?	453
9.2.3	Is knotting of nuclear strings possible?	453
9.3	Could nuclear strings be connected sums of alpha strings and lighter nuclear strings?	453
9.3.1	Does the notion of elementary nucleus make sense?	453
9.3.2	Stable nuclei need not fuse to form stable nuclei	454
9.3.3	Formula for binding energy per nucleon as a test for the model	454
9.3.4	Decay characteristics and binding energies as signatures of the decomposition of nuclear string	455
9.3.5	Are magic numbers additive?	455
9.3.6	Stable nuclei as composites of lighter nuclei and necessity of tetra-neutron?	456
9.3.7	What are the building blocks of nuclear strings?	456
9.4	Light nuclei as color bound Bose-Einstein condensates of ${}^4\text{He}$ nuclei	458
9.4.1	How to explain the maximum of E_B for iron?	458
9.4.2	Scaled up QCD with Bose-Einstein condensate of ${}^4\text{He}$ nuclei explains the growth of E_B	458
9.4.3	Why E_B decreases for heavier nuclei?	460
9.5	What QCD binds nucleons to $A \leq 4$ nuclei?	462
9.5.1	The QCD associated with nuclei lighter than ${}^4\text{He}$	462
9.5.2	The QCD associated with ${}^4\text{He}$	464
9.5.3	What about tetra-neutron?	464
9.5.4	What could be the general mass formula?	465
9.5.5	Nuclear strings and cold fusion	466
9.5.6	Strong force as a scaled and dark electro-weak force?	469
9.6	Giant dipole resonance as a dynamical signature for the existence of Bose-Einstein condensates?	470
9.6.1	De-coherence at the level of ${}^4\text{He}$ nuclear string	470
9.6.2	De-coherence inside ${}^4\text{He}$ nuclei	470
9.6.3	De-coherence inside $A = 3$ nuclei and pygmy resonances	473
9.6.4	De-coherence and the differential topology of nuclear reactions	473
9.7	Cold fusion, plasma electrolysis, biological transmutations, and burning salt water	475
9.7.1	The data	475
9.7.2	$H_{1.5}O$ anomaly and nuclear string model	476
9.7.3	A model for the observations of Mizuno	479
9.7.4	Comparison with the model of deuterium cold fusion	482
9.7.5	What happens to OH bonds in plasma electrolysis?	483
9.7.6	A model for plasma electrolysis	485
9.7.7	Comparison with the reports about biological transmutations	489
9.7.8	Are the abundances of heavier elements determined by cold fusion in interstellar medium?	490
9.7.9	Tests and improvements	491
9.7.10	Burning salt water by radio-waves and cold fusion by plasma electrolysis	493
9.7.11	GSI anomaly	494
9.8	Dark nuclear strings as analogs of DNA-, RNA- and amino-acid sequences and baryonic realization of genetic code?	496
9.8.1	States in the quark degrees of freedom	498
9.8.2	States in the flux tube degrees of freedom	499
9.8.3	Analog of DNA, RNA, aminoacids, and of translation and transcription mechanisms	499

9.8.4	Understanding the symmetries of the code	500
9.8.5	Some comments about the physics behind the code	501
10	Dark Nuclear Physics and Condensed Matter	509
10.1	Introduction	509
10.1.1	Dark rules	509
10.1.2	Some implications	513
10.2	A generalization of the notion of imbedding space as a realization of the hierarchy of Planck constants	514
10.2.1	Hierarchy of Planck constants and the generalization of the notion of imbedding space	514
10.2.2	Could the dynamics of Kähler action predict the hierarchy of Planck constants?	520
10.3	General ideas about dark matter	523
10.3.1	How the scaling of \hbar affects physics and how to detect dark matter?	523
10.3.2	General view about dark matter hierarchy and interactions between relatively dark matters	523
10.3.3	How dark matter and visible matter interact?	525
10.3.4	Could one demonstrate the existence of large Planck constant photons using ordinary camera or even bare eyes?	526
10.3.5	Dark matter and exotic color and electro-weak interactions	529
10.3.6	Anti-matter and dark matter	531
10.4	Dark variants of nuclear physics	532
10.4.1	Constraints from the nuclear string model	532
10.4.2	Constraints from the anomalous behavior of water	533
10.4.3	Exotic chemistries and electromagnetic nuclear darkness	534
10.5	Has dark matter been observed?	536
10.5.1	Optical rotation of a laser beam in a magnetic field	536
10.5.2	Do nuclear reaction rates depend on environment?	537
10.6	Water and new physics	540
10.6.1	The 41 anomalies of water	540
10.6.2	The model	544
10.6.3	Further comments on 41 anomalies	550
10.6.4	Genes and water memory	551
10.6.5	Burning water and photosynthesis	555
10.7	Connection with mono-atomic elements, cold fusion, and sono-luminescence?	558
10.7.1	Mono-atomic elements as dark matter and high T_c super-conductors?	559
10.7.2	Connection with cold fusion?	564
10.7.3	Sono-luminescence, classical Z^0 force, and hydrodynamic hierarchy of p-adic length scales	567
10.8	Dark atomic physics	569
10.8.1	Dark atoms and dark cyclotron states	570
10.8.2	Could q-Laguerre equation relate to the claimed fractionation of the principal quantum number for hydrogen atom?	571
11	Dark Forces and Living Matter	585
11.1	Introduction	585
11.1.1	Evidence for long range weak forces and new nuclear physics	585
11.1.2	Dark rules	587
11.1.3	Weak form of electric magnetic duality, screening of weak charges, and color confinement?	589
11.1.4	Dark weak forces and almost vacuum extremals	590
11.2	Weak form electric-magnetic duality and color and weak forces	591
11.2.1	Could a weak form of electric-magnetic duality hold true?	592
11.2.2	Magnetic confinement, the short range of weak forces, and color confinement	595
11.3	Dark matter hierarchy, genetic machinery, and the un-reasonable selectivity of biocatalysis	597
11.3.1	Dark atoms and dark cyclotron states	598

11.3.2	Spontaneous decay and completion of dark fractional atoms as a basic mechanisms of bio-chemistry?	599
11.3.3	The new view about hydrogen bond and water	601
11.4	TGD based model for cell membrane as sensory receptor	604
11.4.1	Could cell correspond to almost vacuum extremal?	605
11.4.2	General model for qualia and sensory receptor	611
11.4.3	Some implications of the model of cell membrane as sensory receptor	612
11.4.4	A general model of qualia and sensory receptor	612
11.4.5	Detailed model for the qualia	614
11.4.6	Overall view about qualia	617
11.4.7	About detailed identification of the qualia	617
12	Super-Conductivity in Many-Sheeted Space-Time	625
12.1	Introduction	625
12.1.1	General ideas about super-conductivity in many-sheeted space-time	625
12.1.2	TGD inspired model for high T_c superconductivity	627
12.2	General TGD based view about super-conductivity	629
12.2.1	Basic phenomenology of super-conductivity	629
12.2.2	Universality of the parameters in TGD framework	631
12.2.3	Quantum criticality and super-conductivity	633
12.2.4	Space-time description of the mechanisms of super-conductivity	635
12.2.5	Super-conductivity at magnetic flux tubes	638
12.3	TGD based model for high T_c super conductors	640
12.3.1	Some properties of high T_c super conductors	640
12.3.2	TGD inspired vision about high T_c superconductivity	642
13	Quantum Hall effect and Hierarchy of Planck Constants	653
13.1	Introduction	653
13.2	About theories of quantum Hall effect	655
13.2.1	Quantum Hall effect as a spontaneous symmetry breaking down to a discrete subgroup of the gauge group	655
13.2.2	Witten-Chern-Simons action and topological quantum field theories	655
13.2.3	Chern-Simons action for anyons	657
13.2.4	Topological quantum computation using braids and anyons	657
13.3	Hierarchy of Planck constants and the generalization of the notion of imbedding space	658
13.3.1	The evolution of physical ideas about hierarchy of Planck constants	658
13.3.2	The most general option for the generalized imbedding space	659
13.3.3	About the phase transitions changing Planck constant	660
13.3.4	How one could fix the spectrum of Planck constants?	661
13.3.5	Preferred values of Planck constants	661
13.3.6	How Planck constants are visible in Kähler action?	662
13.3.7	Could the dynamics of Kähler action predict the hierarchy of Planck constants?	662
13.4	Weak form electric-magnetic duality and its implications	665
13.4.1	Could a weak form of electric-magnetic duality hold true?	666
13.4.2	Magnetic confinement, the short range of weak forces, and color confinement	669
13.4.3	Could Quantum TGD reduce to almost topological QFT?	673
13.4.4	A general solution ansatz based on almost topological QFT property	675
13.4.5	Hydrodynamic picture in fermionic sector	678
13.5	How to define Dirac determinant?	684
13.5.1	Dirac determinant when the number of eigenvalues is infinite	684
13.5.2	Hyper-octonionic primes	686
13.5.3	Three basic options for the pseudo-momentum spectrum	687
13.5.4	Expression for the Dirac determinant for various options	689
13.6	Quantum Hall effect, charge fractionization, and hierarchy of Planck constants	697
13.6.1	Quantum Hall effect	698
13.6.2	A simple model for fractional quantum Hall effect	698
13.6.3	Description of QHE in terms of hierarchy of Planck constants	700

13.6.4	In what kind of situations do anyons emerge?	705
13.6.5	What happens in FQHE?	706
1	Appendix	715
A-1	Basic properties of CP_2 and elementary facts about p-adic numbers	715
A-1.1	CP_2 as a manifold	715
A-1.2	Metric and Kähler structure of CP_2	715
A-1.3	Spinors in CP_2	718
A-1.4	Geodesic sub-manifolds of CP_2	718
A-2	CP_2 geometry and standard model symmetries	719
A-2.1	Identification of the electro-weak couplings	719
A-2.2	Discrete symmetries	722
A-3	Basic facts about induced gauge fields	723
A-3.1	Induced gauge fields for space-times for which CP_2 projection is a geodesic sphere	723
A-3.2	Space-time surfaces with vanishing em, Z^0 , or Kähler fields	723
A-4	p-Adic numbers and TGD	726
A-4.1	p-Adic number fields	726
A-4.2	Canonical correspondence between p-adic and real numbers	727

List of Figures

3.1	Definition of the canonical homology basis	105
3.2	Definition of the Dehn twist	106
5.1	Fermilab semileptonic histogram for the distribution of the mass of top quark candidate (FERMILAB-PUB-94/097-E).	194
5.2	Fermilab D0 semileptonic histogram for the distribution of the mass of top quark candidate (hep-ex/9703008, April 26, 1994	195
6.1	There are some indications that cosmic gamma ray flux contains a peak in the energy interval $10^{10} - 10^{11}$ eV. Figure is taken from [80].	331
6.2	332
6.3	Standard model contributions to the matching of the quark operators in the effective flavor-changing Lagrangian	333
7.1	Differential cross section $\sin^2(\theta) \times \frac{d^2\sigma}{2E d^3p}$ for τ -pion production for $\gamma_1 = 1.0319 \times 10^3$ in the rest system of antiproton for $\delta = 1.5$. $m(\pi_\tau)$ defines the unit of energy and nb is the unit for cross section. The ranges of θ and ϕ are $(0, \pi)$ and $(0, \pi/2)$	366
7.2	Differential cross section $\sin^2(\theta) \times \frac{d^2\sigma}{2E d^3p}$ for τ -pion production for $\gamma_1 = 1.090 \times 10^3$ in the rest system of antiproton for $\delta = 1.5$. $m(\pi_\tau)$ defines the unit of energy and nb is the unit for cross section. The ranges of θ and ϕ are $(0, \pi)$ and $(0, \pi/2)$	379
7.3	Evaluation of k_y -integral using residue calculus.	391
7.4	Evaluation of k_x -integral using residue calculus.	391
9.1	The comparison of photoneutron cross sections $^{16}O(\gamma, xn)$ obtained in one BR-experiment (Moscow State University) and two QMA experiments carried out at Saclay (France) Livermore (USA). Figure is taken from [28] where also references to experiments can be found.	472
9.2	Pygmy resonances in ^{44}Ca and ^{48}Ca up to 11 MeV. Figure is taken from [41].	474
9.3	Illustration of a possible vision about dark nucleus as a nuclear string consisting of rotating baryonic strings.	497
1	The real norm induced by canonical identification from 2-adic norm.	728

Chapter 1

Introduction

1.1 Background

T(opological) G(eometro)D(ynamics) is one of the many attempts to find a unified description of basic interactions. The development of the basic ideas of TGD to a relatively stable form took time of about half decade [27]. The great challenge is to construct a mathematical theory around these physically very attractive ideas and I have devoted the last twenty-three years for the realization of this dream and this has resulted in seven online books about TGD and eight online books about TGD inspired theory of consciousness and of quantum biology.

Quantum T(opological)D(ynamics) as a classical spinor geometry for infinite-dimensional configuration space, p-adic numbers and quantum TGD, and TGD inspired theory of consciousness have been for last decade of the second millenium the basic three strongly interacting threads in the tapestry of quantum TGD.

For few yeas ago the discussions with Tony Smith generated a fourth thread which deserves the name 'TGD as a generalized number theory'. The work with Riemann hypothesis made time ripe for realization that the notion of infinite primes could provide, not only a reformulation, but a deep generalization of quantum TGD. This led to a thorough and extremely fruitful revision of the basic views about what the final form and physical content of quantum TGD might be.

The fifth thread came with the realization that by quantum classical correspondence TGD predicts an infinite hierarchy of macroscopic quantum systems with increasing sizes, that it is not at all clear whether standard quantum mechanics can accommodate this hierarchy, and that a dynamical quantized Planck constant might be necessary and certainly possible in TGD framework. The identification of hierarchy of Planck constants whose values TGD "predicts" in terms of dark matter hierarchy would be natural. This also led to a solution of a long standing puzzle: what is the proper interpretation of the predicted fractal hierarchy of long ranged classical electro-weak and color gauge fields. Quantum classical correspondences allows only single answer: there is infinite hierarchy of p-adically scaled up variants of standard model physics and for each of them also dark hierarchy. Thus TGD Universe would be fractal in very abstract and deep sense.

TGD forces the generalization of physics to a quantum theory of consciousness, and represent TGD as a generalized number theory vision leads naturally to the emergence of p-adic physics as physics of cognitive representations. The seven online books [1, 2, 5, 6, 3, 4, 7] about TGD and eight online books about TGD inspired theory of consciousness and of quantum biology [8, 9, 10, 11, 12, 15, 13, 14] are warmly recommended to the interested reader.

1.2 Basic Ideas of TGD

The basic physical picture behind TGD was formed as a fusion of two rather disparate approaches: namely TGD is as a Poincare invariant theory of gravitation and TGD as a generalization of the old-fashioned string model.

1.2.1 TGD as a Poincare invariant theory of gravitation

The first approach was born as an attempt to construct a Poincare invariant theory of gravitation. Space-time, rather than being an abstract manifold endowed with a pseudo-Riemannian structure, is regarded as a surface in the 8-dimensional space $H = M_+^4 \times CP_2$, where M_+^4 denotes the interior of the future light cone of the Minkowski space (to be referred as light cone in the sequel) and $CP_2 = SU(3)/U(2)$ is the complex projective space of two complex dimensions [45, 44, 47, 17]. The identification of the space-time as a submanifold [33, 30] of $M^4 \times CP_2$ leads to an exact Poincare invariance and solves the conceptual difficulties related to the definition of the energy-momentum in General Relativity. The actual choice $H = M_+^4 \times CP_2$ implies the breaking of the Poincare invariance in the cosmological scales but only at the quantum level. It soon however turned out that submanifold geometry, being considerably richer in structure than the abstract manifold geometry, leads to a geometrization of all basic interactions. First, the geometrization of the elementary particle quantum numbers is achieved. The geometry of CP_2 explains electro-weak and color quantum numbers. The different H-chiralities of H -spinors correspond to the conserved baryon and lepton numbers. Secondly, the geometrization of the field concept results. The projections of the CP_2 spinor connection, Killing vector fields of CP_2 and of H -metric to four-surface define classical electro-weak, color gauge fields and metric in X^4 .

1.2.2 TGD as a generalization of the hadronic string model

The second approach was based on the generalization of the mesonic string model describing mesons as strings with quarks attached to the ends of the string. In the 3-dimensional generalization 3-surfaces correspond to free particles and the boundaries of the 3- surface correspond to partons in the sense that the quantum numbers of the elementary particles reside on the boundaries. Various boundary topologies (number of handles) correspond to various fermion families so that one obtains an explanation for the known elementary particle quantum numbers. This approach leads also to a natural topological description of the particle reactions as topology changes: for instance, two-particle decay corresponds to a decay of a 3-surface to two disjoint 3-surfaces.

1.2.3 Fusion of the two approaches via a generalization of the space-time concept

The problem is that the two approaches seem to be mutually exclusive since the orbit of a particle like 3-surface defines 4-dimensional surface, which differs drastically from the topologically trivial macroscopic space-time of General Relativity. The unification of these approaches forces a considerable generalization of the conventional space-time concept. First, the topologically trivial 3-space of General Relativity is replaced with a "topological condensate" containing matter as particle like 3-surfaces "glued" to the topologically trivial background 3-space by connected sum operation. Secondly, the assumption about connectedness of the 3-space is given up. Besides the "topological condensate" there is "vapor phase" that is a "gas" of particle like 3-surfaces (counterpart of the "baby universes" of GRT) and the nonconservation of energy in GRT corresponds to the transfer of energy between the topological condensate and vapor phase.

1.3 The five threads in the development of quantum TGD

The development of TGD has involved four strongly interacting threads: physics as infinite-dimensional geometry; p-adic physics; TGD inspired theory of consciousness and TGD as a generalized number theory. In the following these five threads are briefly described.

1.3.1 Quantum TGD as configuration space spinor geometry

A turning point in the attempts to formulate a mathematical theory was reached after seven years from the birth of TGD. The great insight was "Do not quantize". The basic ingredients to the new approach have served as the basic philosophy for the attempt to construct Quantum TGD since then and are the following ones:

1. Quantum theory for extended particles is free(!), classical(!) field theory for a generalized Schrödinger amplitude in the configuration space CH consisting of all possible 3-surfaces in H . "All possible" means that surfaces with arbitrary many disjoint components and with arbitrary internal topology and also singular surfaces topologically intermediate between two different manifold topologies are included. Particle reactions are identified as topology changes [35, 32, 29]. For instance, the decay of a 3-surface to two 3-surfaces corresponds to the decay $A \rightarrow B + C$. Classically this corresponds to a path of configuration space leading from 1-particle sector to 2-particle sector. At quantum level this corresponds to the dispersion of the generalized Schrödinger amplitude localized to 1-particle sector to two-particle sector. All coupling constants should result as predictions of the theory since no nonlinearities are introduced.
2. Configuration space is endowed with the metric and spinor structure so that one can define various metric related differential operators, say Dirac operator, appearing in the field equations of the theory.

1.3.2 p-Adic TGD

The p-adic thread emerged for roughly ten years ago as a dim hunch that p-adic numbers might be important for TGD. Experimentation with p-adic numbers led to the notion of canonical identification mapping reals to p-adics and vice versa. The breakthrough came with the successful p-adic mass calculations using p-adic thermodynamics for Super-Virasoro representations with the super-Kac-Moody algebra associated with a Lie-group containing standard model gauge group. Although the details of the calculations have varied from year to year, it was clear that p-adic physics reduces not only the ratio of proton and Planck mass, the great mystery number of physics, but all elementary particle mass scales, to number theory if one assumes that primes near prime powers of two are in a physically favored position. Why this is the case, became one of the key puzzlers and led to a number of arguments with a common gist: evolution is present already at the elementary particle level and the primes allowed by the p-adic length scale hypothesis are the fittest ones.

It became very soon clear that p-adic topology is not something emerging in Planck length scale as often believed, but that there is an infinite hierarchy of p-adic physics characterized by p-adic length scales varying to even cosmological length scales. The idea about the connection of p-adics with cognition motivated already the first attempts to understand the role of the p-adics and inspired 'Universe as Computer' vision but time was not ripe to develop this idea to anything concrete (p-adic numbers are however in a central role in TGD inspired theory of consciousness). It became however obvious that the p-adic length scale hierarchy somehow corresponds to a hierarchy of intelligences and that p-adic prime serves as a kind of intelligence quotient. Ironically, the almost obvious idea about p-adic regions as cognitive regions of space-time providing cognitive representations for real regions had to wait for almost a decade for the access into my consciousness.

There were many interpretational and technical questions crying for a definite answer. What is the relationship of p-adic non-determinism to the classical non-determinism of the basic field equations of TGD? Are the p-adic space-time region genuinely p-adic or does p-adic topology only serve as an effective topology? If p-adic physics is direct image of real physics, how the mapping relating them is constructed so that it respects various symmetries? Is the basic physics p-adic or real (also real TGD seems to be free of divergences) or both? If it is both, how should one glue the physics in different number field together to get *The Physics*? Should one perform p-adicization also at the level of the configuration space of 3-surfaces? Certainly the p-adicization at the level of super-conformal representation is necessary for the p-adic mass calculations. Perhaps the most basic and most irritating technical problem was how to precisely define p-adic definite integral which is a crucial element of any variational principle based formulation of the field equations. Here the frustration was not due to the lack of solution but due to the too large number of solutions to the problem, a clear symptom for the sad fact that clever inventions rather than real discoveries might be in question.

Despite these frustrating uncertainties, the number of the applications of the poorly defined p-adic physics grew steadily and the applications turned out to be relatively stable so that it was clear that the solution to these problems must exist. It became only gradually clear that the solution of the problems might require going down to a deeper level than that represented by reals and p-adics.

1.3.3 TGD as a generalization of physics to a theory consciousness

General coordinate invariance forces the identification of quantum jump as quantum jump between entire deterministic quantum histories rather than time=constant snapshots of single history. The new view about quantum jump forces a generalization of quantum measurement theory such that observer becomes part of the physical system. Thus a general theory of consciousness is unavoidable outcome. This theory is developed in detail in the books [8, 9, 10, 11, 12, 15, 13, 14].

Quantum jump as a moment of consciousness

The identification of quantum jump between deterministic quantum histories (configuration space spinor fields) as a moment of consciousness defines microscopic theory of consciousness. Quantum jump involves the steps

$$\Psi_i \rightarrow U\Psi_i \rightarrow \Psi_f ,$$

where U is informational "time development" operator, which is unitary like the S-matrix characterizing the unitary time evolution of quantum mechanics. U is however only formally analogous to Schrödinger time evolution of infinite duration although there is *no* real time evolution involved. It is not however clear whether one should regard U-matrix and S-matrix as two different things or not: U -matrix is a completely universal object characterizing the dynamics of evolution by self-organization whereas S-matrix is a highly context dependent concept in wave mechanics and in quantum field theories where it at least formally represents unitary time translation operator at the limit of an infinitely long interaction time. The S-matrix understood in the spirit of superstring models is however something very different and could correspond to U-matrix.

The requirement that quantum jump corresponds to a measurement in the sense of quantum field theories implies that each quantum jump involves localization in zero modes which parameterize also the possible choices of the quantization axes. Thus the selection of the quantization axes performed by the Cartesian outsider becomes now a part of quantum theory. Together these requirements imply that the final states of quantum jump correspond to quantum superpositions of space-time surfaces which are macroscopically equivalent. Hence the world of conscious experience looks classical. At least formally quantum jump can be interpreted also as a quantum computation in which matrix U represents unitary quantum computation which is however not identifiable as unitary translation in time direction and cannot be 'engineered'.

The notion of self

The concept of self is absolutely essential for the understanding of the macroscopic and macro-temporal aspects of consciousness. Self corresponds to a subsystem able to remain un-entangled under the sequential informational 'time evolutions' U . Exactly vanishing entanglement is practically impossible in ordinary quantum mechanics and it might be that 'vanishing entanglement' in the condition for self-property should be replaced with 'subcritical entanglement'. On the other hand, if space-time decomposes into p-adic and real regions, and if entanglement between regions representing physics in different number fields vanishes, space-time indeed decomposes into selves in a natural manner.

It is assumed that the experiences of the self after the last 'wake-up' sum up to single average experience. This means that subjective memory is identifiable as conscious, immediate short term memory. Selves form an infinite hierarchy with the entire Universe at the top. Self can be also interpreted as mental images: our mental images are selves having mental images and also we represent mental images of a higher level self. A natural hypothesis is that self S experiences the experiences of its subselves as kind of abstracted experience: the experiences of subselves S_i are not experienced as such but represent kind of averages $\langle S_{ij} \rangle$ of sub-subselves S_{ij} . Entanglement between selves, most naturally realized by the formation of join along boundaries bonds between cognitive or material space-time sheets, provides a possible a mechanism for the fusion of selves to larger selves (for instance, the fusion of the mental images representing separate right and left visual fields to single visual field) and forms wholes from parts at the level of mental images.

Relationship to quantum measurement theory

The third basic element relates TGD inspired theory of consciousness to quantum measurement theory. The assumption that localization occurs in zero modes in each quantum jump implies that the world of conscious experience looks classical. It also implies the state function reduction of the standard quantum measurement theory as the following arguments demonstrate (it took incredibly long time to realize this almost obvious fact!).

1. The standard quantum measurement theory a la von Neumann involves the interaction of brain with the measurement apparatus. If this interaction corresponds to entanglement between microscopic degrees of freedom m with the macroscopic effectively classical degrees of freedom M characterizing the reading of the measurement apparatus coded to brain state, then the reduction of this entanglement in quantum jump reproduces standard quantum measurement theory provide the unitary time evolution operator U acts as flow in zero mode degrees of freedom and correlates completely some orthonormal basis of configuration space spinor fields in non-zero modes with the values of the zero modes. The flow property guarantees that the localization is consistent with unitarity: it also means 1-1 mapping of quantum state basis to classical variables (say, spin direction of the electron to its orbit in the external magnetic field).
2. Since zero modes represent classical information about the geometry of space-time surface (shape, size, classical Kähler field,...), they have interpretation as effectively classical degrees of freedom and are the TGD counterpart of the degrees of freedom M representing the reading of the measurement apparatus. The entanglement between quantum fluctuating non-zero modes and zero modes is the TGD counterpart for the $m - M$ entanglement. Therefore the localization in zero modes is equivalent with a quantum jump leading to a final state where the measurement apparatus gives a definite reading.

This simple prediction is of utmost theoretical importance since the black box of the quantum measurement theory is reduced to a fundamental quantum theory. This reduction is implied by the replacement of the notion of a point like particle with particle as a 3-surface. Also the infinite-dimensionality of the zero mode sector of the configuration space of 3-surfaces is absolutely essential. Therefore the reduction is a triumph for quantum TGD and favors TGD against string models.

Standard quantum measurement theory involves also the notion of state preparation which reduces to the notion of self measurement. Each localization in zero modes is followed by a cascade of self measurements leading to a product state. This process is obviously equivalent with the state preparation process. Self measurement is governed by the so called Negentropy Maximization Principle (NMP) stating that the information content of conscious experience is maximized. In the self measurement the density matrix of some subsystem of a given self localized in zero modes (after ordinary quantum measurement) is measured. The self measurement takes place for that subsystem of self for which the reduction of the entanglement entropy is maximal in the measurement. In p-adic context NMP can be regarded as the variational principle defining the dynamics of cognition. In real context self measurement could be seen as a repair mechanism allowing the system to fight against quantum thermalization by reducing the entanglement for the subsystem for which it is largest (fill the largest hole first in a leaking boat).

Selves self-organize

The fourth basic element is quantum theory of self-organization based on the identification of quantum jump as the basic step of self-organization [25]. Quantum entanglement gives rise to the generation of long range order and the emergence of longer p-adic length scales corresponds to the emergence of larger and larger coherent dynamical units and generation of a slaving hierarchy. Energy (and quantum entanglement) feed implying entropy feed is a necessary prerequisite for quantum self-organization. Zero modes represent fundamental order parameters and localization in zero modes implies that the sequence of quantum jumps can be regarded as hopping in the zero modes so that Haken's classical theory of self organization applies almost as such. Spin glass analogy is a further important element: self-organization of self leads to some characteristic pattern selected by dissipation as some valley of the "energy" landscape.

Dissipation can be regarded as the ultimate Darwinian selector of both memes and genes. The mathematically ugly irreversible dissipative dynamics obtained by adding phenomenological dissipation terms to the reversible fundamental dynamical equations derivable from an action principle can be understood as a phenomenological description replacing in a well defined sense the series of reversible quantum histories with its envelope.

Classical non-determinism of Kähler action

The fifth basic element are the concepts of association sequence and cognitive space-time sheet. The huge vacuum degeneracy of the Kähler action suggests strongly that the absolute minimum space-time is not always unique. For instance, a sequence of bifurcations can occur so that a given space-time branch can be fixed only by selecting a finite number of 3-surfaces with time like(!) separations on the orbit of 3-surface. Quantum classical correspondence suggest an alternative formulation. Space-time surface decomposes into maximal deterministic regions and their temporal sequences have interpretation a space-time correlate for a sequence of quantum states defined by the initial (or final) states of quantum jumps. This is consistent with the fact that the variational principle selects preferred extremals of Kähler action as generalized Bohr orbits.

In the case that non-determinism is located to a finite time interval and is microscopic, this sequence of 3-surfaces has interpretation as a simulation of a classical history, a geometric correlate for contents of consciousness. When non-determinism has long lasting and macroscopic effect one can identify it as volitional non-determinism associated with our choices. Association sequences relate closely with the cognitive space-time sheets defined as space-time sheets having finite time duration and psychological time can be identified as a temporal center of mass coordinate of the cognitive space-time sheet. The gradual drift of the cognitive space-time sheets to the direction of future force by the geometry of the future light cone explains the arrow of psychological time.

p-Adic physics as physics of cognition and intentionality

The sixth basic element adds a physical theory of cognition to this vision. TGD space-time decomposes into regions obeying real and p-adic topologies labelled by primes $p = 2, 3, 5, \dots$. p-Adic regions obey the same field equations as the real regions but are characterized by p-adic non-determinism since the functions having vanishing p-adic derivative are pseudo constants which are piecewise constant functions. Pseudo constants depend on a finite number of positive binary digits of arguments just like numerical predictions of any theory always involve decimal cutoff. This means that p-adic space-time regions are obtained by gluing together regions for which integration constants are genuine constants. The natural interpretation of the p-adic regions is as cognitive representations of real physics. The freedom of imagination is due to the p-adic non-determinism. p-Adic regions perform mimicry and make possible for the Universe to form cognitive representations about itself. p-Adic physics space-time sheets serve also as correlates for intentional action.

A more more precise formulation of this vision requires a generalization of the number concept obtained by fusing reals and p-adic number fields along common rationals (in the case of algebraic extensions among common algebraic numbers). This picture is discussed in [21]. The application this notion at the level of the imbedding space implies that imbedding space has a book like structure with various variants of the imbedding space glued together along common rationals (algebraics). The implication is that genuinely p-adic numbers (non-rationals) are strictly infinite as real numbers so that most points of p-adic space-time sheets are at real infinity, outside the cosmos, and that the projection to the real imbedding space is discrete set of rationals (algebraics). Hence cognition and intentionality are almost completely outside the real cosmos and touch it at a discrete set of points only.

This view implies also that purely local p-adic physics codes for the p-adic fractality characterizing long range real physics and provides an explanation for p-adic length scale hypothesis stating that the primes $p \simeq 2^k$, k integer are especially interesting. It also explains the long range correlations and short term chaos characterizing intentional behavior and explains why the physical realizations of cognition are always discrete (say in the case of numerical computations). Furthermore, a concrete quantum model for how intentions are transformed to actions emerges.

The discrete real projections of p-adic space-time sheets serve also space-time correlate for a logical thought. It is very natural to assign to p-adic binary digits a p -valued logic but as such this kind

of logic does not have any reasonable identification. p-Adic length scale hypothesis suggest that the $p = 2^k - n$ binary digits represent a Boolean logic B^k with k elementary statements (the points of the k -element set in the set theoretic realization) with n taboos which are constrained to be identically true.

1.3.4 TGD as a generalized number theory

Quantum T(opological)D(ynamics) as a classical spinor geometry for infinite-dimensional configuration space, p-adic numbers and quantum TGD, and TGD inspired theory of consciousness, have been for last ten years the basic three strongly interacting threads in the tapestry of quantum TGD. For few years ago the discussions with Tony Smith generated a fourth thread which deserves the name 'TGD as a generalized number theory'. It involves three separate threads: the fusion of real and various p-adic physics to a single coherent whole by requiring number theoretic universality discussed already, the formulation of quantum TGD in terms of hyper-counterparts of classical number fields identified as sub-spaces of complexified classical number fields with Minkowskian signature of the metric defined by the complexified inner product, and the notion of infinite prime.

The role of classical number fields

The vision about the physical role of the classical number fields relies on the notion of number theoretic compactification stating that space-time surfaces can be regarded as surfaces of either M^8 or $M^4 \times CP_2$. As surfaces of M^8 identifiable as space of hyper-octonions they are hyper-quaternionic or co-hyper-quaternionic- and thus maximally associative or co-associative. This means that their tangent space is either hyper-quaternionic plane of M^8 or an orthogonal complement of such a plane. These surface can be mapped in natural manner to surfaces in $M^4 \times CP_2$ [19] provided one can assign to each point of tangent space a hyper-complex plane $M^2(x) \subset M^4$. One can also speak about $M^8 - H$ duality.

This vision has very strong predictive power. It predicts that the extremals of Kähler action correspond to either hyper-quaternionic or co-hyper-quaternionic surfaces such that one can assign to tangent space at each point of space-time surface a hyper-complex plane $M^2(x) \subset M^4$. As a consequence, the M^4 projection of space-time surface at each point contains $M^2(x)$ and its orthogonal complement. These distributions are integrable implying that space-time surface allows dual slicings defined by string world sheets Y^2 and partonic 2-surfaces X^2 . The existence of this kind of slicing was earlier deduced from the study of extremals of Kähler action and christened as Hamilton-Jacobi structure. The physical interpretation of $M^2(x)$ is as the space of non-physical polarizations and the plane of local 4-momentum.

One can fairly say, that number theoretical compactification is responsible for most of the understanding of quantum TGD that has emerged during last years. This includes the realization of Equivalence Principle at space-time level, dual formulations of TGD as Minkowskian and Euclidian string model type theories, the precise identification of preferred extremals of Kähler action as extremals for which second variation vanishes (at least for deformations representing dynamical symmetries) and thus providing space-time correlate for quantum criticality, the notion of number theoretic braid implied by the basic dynamics of Kähler action and crucial for precise construction of quantum TGD as almost-topological QFT, the construction of configuration space metric and spinor structure in terms of second quantized induced spinor fields with modified Dirac action defined by Kähler action realizing automatically the notion of finite measurement resolution and a connection with inclusions of hyper-finite factors of type II_1 about which Clifford algebra of configuration space represents an example.

Infinite primes

The discovery of the hierarchy of infinite primes and their correspondence with a hierarchy defined by a repeatedly second quantized arithmetic quantum field theory gave a further boost for the speculations about TGD as a generalized number theory. The work with Riemann hypothesis led to further ideas.

After the realization that infinite primes can be mapped to polynomials representable as surfaces geometrically, it was clear how TGD might be formulated as a generalized number theory with infinite primes forming the bridge between classical and quantum such that real numbers, p-adic numbers, and various generalizations of p-adics emerge dynamically from algebraic physics as various completions of

the algebraic extensions of rational (hyper-)quaternions and (hyper-)octonions. Complete algebraic, topological and dimensional democracy would characterize the theory.

What is especially satisfying is that p-adic and real regions of the space-time surface could emerge automatically as solutions of the field equations. In the space-time regions where the solutions of field equations give rise to in-admissible complex values of the imbedding space coordinates, p-adic solution can exist for some values of the p-adic prime. The characteristic non-determinism of the p-adic differential equations suggests strongly that p-adic regions correspond to 'mind stuff', the regions of space-time where cognitive representations reside. This interpretation implies that p-adic physics is physics of cognition. Since Nature is probably extremely brilliant simulator of Nature, the natural idea is to study the p-adic physics of the cognitive representations to derive information about the real physics. This view encouraged by TGD inspired theory of consciousness clarifies difficult interpretational issues and provides a clear interpretation for the predictions of p-adic physics.

1.3.5 Dynamical quantized Planck constant and dark matter hierarchy

By quantum classical correspondence space-time sheets can be identified as quantum coherence regions. Hence the fact that they have all possible size scales more or less unavoidably implies that Planck constant must be quantized and have arbitrarily large values. If one accepts this then also the idea about dark matter as a macroscopic quantum phase characterized by an arbitrarily large value of Planck constant emerges naturally as does also the interpretation for the long ranged classical electro-weak and color fields predicted by TGD. Rather seldom the evolution of ideas follows simple linear logic, and this was the case also now. In any case, this vision represents the fifth, relatively new thread in the evolution of TGD and the ideas involved are still evolving.

Dark matter as large \hbar phase

D. Da Rocha and Laurent Nottale [78] have proposed that Schrödinger equation with Planck constant \hbar replaced with what might be called gravitational Planck constant $\hbar_{gr} = \frac{GmM}{v_0}$ ($\hbar = c = 1$). v_0 is a velocity parameter having the value $v_0 = 144.7 \pm .7$ km/s giving $v_0/c = 4.6 \times 10^{-4}$. This is rather near to the peak orbital velocity of stars in galactic halos. Also subharmonics and harmonics of v_0 seem to appear. The support for the hypothesis coming from empirical data is impressive.

Nottale and Da Rocha believe that their Schrödinger equation results from a fractal hydrodynamics. Many-sheeted space-time however suggests astrophysical systems are not only quantum systems at larger space-time sheets but correspond to a gigantic value of gravitational Planck constant. The gravitational (ordinary) Schrödinger equation would provide a solution of the black hole collapse (IR catastrophe) problem encountered at the classical level. The resolution of the problem inspired by TGD inspired theory of living matter is that it is the dark matter at larger space-time sheets which is quantum coherent in the required time scale [38].

Already before learning about Nottale's paper I had proposed the possibility that Planck constant is quantized [42] and the spectrum is given in terms of logarithms of Beraha numbers: the lowest Beraha number B_3 is completely exceptional in that it predicts infinite value of Planck constant. The inverse of the gravitational Planck constant could correspond a gravitational perturbation of this as $1/\hbar_{gr} = v_0/GMm$. The general philosophy would be that when the quantum system would become non-perturbative, a phase transition increasing the value of \hbar occurs to preserve the perturbative character and at the transition $n = 4 \rightarrow 3$ only the small perturbative correction to $1/\hbar(3) = 0$ remains. This would apply to QCD and to atoms with $Z > 137$ as well.

TGD predicts correctly the value of the parameter v_0 assuming that cosmic strings and their decay remnants are responsible for the dark matter. The harmonics of v_0 can be understood as corresponding to perturbations replacing cosmic strings with their n-branched coverings so that tension becomes n^2 -fold: much like the replacement of a closed orbit with an orbit closing only after n turns. $1/n$ -sub-harmonic would result when a magnetic flux tube split into n disjoint magnetic flux tubes. Also a model for the formation of planetary system as a condensation of ordinary matter around quantum coherent dark matter emerges [38].

Dark matter as a source of long ranged weak and color fields

Long ranged classical electro-weak and color gauge fields are unavoidable in TGD framework. The smallness of the parity breaking effects in hadronic, nuclear, and atomic length scales does not however seem to allow long ranged electro-weak gauge fields. The problem disappears if long range classical electro-weak gauge fields are identified as space-time correlates for massless gauge fields created by dark matter. Also scaled up variants of ordinary electro-weak particle spectra are possible. The identification explains chiral selection in living matter and unbroken $U(2)_{ew}$ invariance and free color in bio length scales become characteristics of living matter and of bio-chemistry and bio-nuclear physics. An attractive solution of the matter antimatter asymmetry is based on the identification of also antimatter as dark matter.

p-Adic and dark matter hierarchies and hierarchy of moments of consciousness

Dark matter hierarchy assigned to a spectrum of Planck constant having arbitrarily large values brings additional elements to the TGD inspired theory of consciousness.

1. Macroscopic quantum coherence can be understood since a particle with a given mass can in principle appear as arbitrarily large scaled up copies (Compton length scales as \hbar). The phase transition to this kind of phase implies that space-time sheets of particles overlap and this makes possible macroscopic quantum coherence.
2. The space-time sheets with large Planck constant can be in thermal equilibrium with ordinary ones without the loss of quantum coherence. For instance, the cyclotron energy scale associated with EEG turns out to be above thermal energy at room temperature for the level of dark matter hierarchy corresponding to magnetic flux quanta of the Earth's magnetic field with the size scale of Earth and a successful quantitative model for EEG results [43].

Dark matter hierarchy leads to detailed quantitative view about quantum biology with several testable predictions [43]. The applications to living matter suggests that the basic hierarchy corresponds to a hierarchy of Planck constants coming as $\hbar(k) = \lambda^k(p)\hbar_0$, $\lambda \simeq 2^{11}$ for $p = 2^{127-1}$, $k = 0, 1, 2, \dots$ [43]. Also integer valued sub-harmonics and integer valued sub-harmonics of λ might be possible. Each p-adic length scale corresponds to this kind of hierarchy and number theoretical arguments suggest a general formula for the allowed values of Planck constant λ depending logarithmically on p-adic prime [34]. Also the value of \hbar_0 has spectrum characterized by Beraha numbers $B_n = 4\cos^2(\pi/n)$, $n \geq 3$, varying by a factor in the range $n > 3$ [34]. It must be however emphasized that the relation of this picture to the model of quantized gravitational Planck constant \hbar_{gr} appearing in Nottale's model is not yet completely understood.

The general prediction is that Universe is a kind of inverted Mandelbrot fractal for which each bird's eye of view reveals new structures in long length and time scales representing scaled down copies of standard physics and their dark variants. These structures would correspond to higher levels in self hierarchy. This prediction is consistent with the belief that 75 per cent of matter in the universe is dark.

1. *Living matter and dark matter*

Living matter as ordinary matter quantum controlled by the dark matter hierarchy has turned out to be a particularly successful idea. The hypothesis has led to models for EEG predicting correctly the band structure and even individual resonance bands and also generalizing the notion of EEG [43]. Also a generalization of the notion of genetic code emerges resolving the paradoxes related to the standard dogma [22, 43]. A particularly fascinating implication is the possibility to identify great leaps in evolution as phase transitions in which new higher level of dark matter emerges [43].

It seems safe to conclude that the dark matter hierarchy with levels labelled by the values of Planck constants explains the macroscopic and macro-temporal quantum coherence naturally. That this explanation is consistent with the explanation based on spin glass degeneracy is suggested by following observations. First, the argument supporting spin glass degeneracy as an explanation of the macro-temporal quantum coherence does not involve the value of \hbar at all. Secondly, the failure of the perturbation theory assumed to lead to the increase of Planck constant and formation of macroscopic quantum phases could be precisely due to the emergence of a large number of new degrees

of freedom due to spin glass degeneracy. Thirdly, the phase transition increasing Planck constant has concrete topological interpretation in terms of many-sheeted space-time consistent with the spin glass degeneracy.

2. Dark matter hierarchy and the notion of self

The vision about dark matter hierarchy leads to a more refined view about self hierarchy and hierarchy of moments of consciousness [16, 43]. The larger the value of Planck constant, the longer the subjectively experienced duration and the average geometric duration $T(k) \propto \lambda^k$ of the quantum jump.

Quantum jumps form also a hierarchy with respect to p-adic and dark hierarchies and the geometric durations of quantum jumps scale like \hbar . Dark matter hierarchy suggests also a slight modification of the notion of self. Each self involves a hierarchy of dark matter levels, and one is led to ask whether the highest level in this hierarchy corresponds to single quantum jump rather than a sequence of quantum jumps. The averaging of conscious experience over quantum jumps would occur only for sub-selves at lower levels of dark matter hierarchy and these mental images would be ordered, and single moment of consciousness would be experienced as a history of events. The quantum parallel dissipation at the lower levels would give rise to the experience of flow of time. For instance, hadron as a macro-temporal quantum system in the characteristic time scale of hadron is a dissipating system at quark and gluon level corresponding to shorter p-adic time scales. One can ask whether even entire life cycle could be regarded as a single quantum jump at the highest level so that consciousness would not be completely lost even during deep sleep. This would allow to understand why we seem to know directly that this biological body of mine existed yesterday.

The fact that we can remember phone numbers with 5 to 9 digits supports the view that self corresponds at the highest dark matter level to single moment of consciousness. Self would experience the average over the sequence of moments of consciousness associated with each sub-self but there would be no averaging over the separate mental images of this kind, be their parallel or serial. These mental images correspond to sub-selves having shorter wake-up periods than self and would be experienced as being time ordered. Hence the digits in the phone number are experienced as separate mental images and ordered with respect to experienced time.

3. The time span of long term memories as signature for the level of dark matter hierarchy

The simplest dimensional estimate gives for the average increment τ of geometric time in quantum jump $\tau \sim 10^4 CP_2$ times so that $2^{127} - 1 \sim 10^{38}$ quantum jumps are experienced during secondary p-adic time scale $T_2(k = 127) \simeq 0.1$ seconds which is the duration of physiological moment and predicted to be fundamental time scale of human consciousness [34]. A more refined guess is that $\tau_p = \sqrt{p}\tau$ gives the dependence of the duration of quantum jump on p-adic prime p . By multi-p-fractality predicted by TGD and explaining p-adic length scale hypothesis, one expects that at least $p = 2$ -adic level is also always present. For the higher levels of dark matter hierarchy τ_p is scaled up by \hbar/\hbar_0 . One can understand evolutionary leaps as the emergence of higher levels at the level of individual organism making possible intentionality and memory in the time scale defined τ [22].

Higher levels of dark matter hierarchy provide a neat quantitative view about self hierarchy and its evolution. For instance, EEG time scales corresponds to $k = 4$ level of hierarchy and a time scale of .1 seconds [16, 43], and EEG frequencies correspond at this level dark photon energies above the thermal threshold so that thermal noise is not a problem anymore. Various levels of dark matter hierarchy would naturally correspond to higher levels in the hierarchy of consciousness and the typical duration of life cycle would give an idea about the level in question.

The level would determine also the time span of long term memories as discussed in [43]. $k = 7$ would correspond to a duration of moment of conscious of order human lifetime which suggests that $k = 7$ corresponds to the highest dark matter level relevant to our consciousness whereas higher levels would in general correspond to transpersonal consciousness. $k = 5$ would correspond to time scale of short term memories measured in minutes and $k = 6$ to a time scale of memories measured in days.

The emergence of these levels must have meant evolutionary leap since long term memory is also accompanied by ability to anticipate future in the same time scale. This picture would suggest that the basic difference between us and our cousins is not at the level of genome as it is usually understood but at the level of the hierarchy of magnetic bodies [22, 43]. In fact, higher levels of dark matter hierarchy motivate the introduction of the notions of super-genome and hyper-genome. The genomes of entire organ can join to form super-genome expressing genes coherently. Hyper-genomes would

result from the fusion of genomes of different organisms and collective levels of consciousness would express themselves via hyper-genome and make possible social rules and moral.

1.4 Bird's eye of view about the topics of the book

The book is devoted to the applications of p-adic length scale hypothesis and dark matter hierarchy.

1. p-Adic length scale hypothesis states that primes $p \simeq 2^k$, k integer, in particular prime, define preferred p-adic length scales. Physical arguments supporting this hypothesis are based on the generalization of Hawking's area law for blackhole entropy so that it applies in case of elementary particles.
2. A much deeper number theory based justification for this hypothesis is based on the generalization of the number concept fusing real number fields and p-adic number fields among common rationals or numbers in their non-trivial algebraic extensions. This approach also justifies the notion of multi-p-fractality and allows to understand scaling law in terms of simultaneous $p \simeq 2^k$ - and 2-fractality.
3. Certain anomalous empirical findings inspire in TGD framework the hypothesis about the existence of entire hierarchy of phases of matter identifiable as dark matter. The levels of dark matter hierarchy are labeled by the values of dynamical quantized Planck constant. The justification for the hypothesis provided by quantum classical correspondence and the fact the sizes of space-time sheets identifiable as quantum coherence regions can be arbitrarily large.

The organization of the book is following.

1. The first part of the book is devoted to the description of elementary particle massivation in terms of p-adic thermodynamics. In the first two chapters general theory is represented and the remaining three chapters are devoted to the detailed calculation of masses of elementary particles and hadrons, and to various new physics suggested or predicted by the resulting scenario.
2. The second part of the book is devoted to the application of p-adic length scale hypothesis above elementary particle length scales. The notions of topological condensation and evaporation are formulated. The so called leptohadron physics, originally developed on basis of experimental anomalies, is discussed as a particular instance of an infinite fractal hierarchy of copies of standard model physics, predicted by TGD and consistent with what is known about ordinary elementary particle physics.

TGD based view about nuclear physics involves light exotic quarks as a essential element, and dark nuclear physics could have implications also at the level of condensed matter physics and biology. Quite surprisingly, the model for dark 3-quarks states consisting of u and d quarks leads to the identification of quantum states of three-quark system as counterparts of 64 DNA and RNA codons and 20 amino-acids and of the analog of genetic code identical with the vertebrate genetic code. This suggests that dark nuclear physics with scaled up sizes of nucleon of order atomic size could play key role in living matter and provide the realization of genetic code at deeper level. Water memory would be one application of this vision.

TGD based view about high T_c superconductors involves also in an essential manner dark matter and is summarized in the closing chapter.

The seven online books about TGD [1, 2, 5, 6, 3, 4, 7] and eight online books about TGD inspired theory of consciousness and quantum biology [8, 9, 10, 11, 12, 15, 13, 14] are warmly recommended for the reader willing to get overall view about what is involved.

1.5 The contents of the book

1.5.1 Part I: p-Adic description of particle massivation

In this part of the book a p-adic description of particle massivation using p-adic thermodynamics and TGD variant of Higgs mechanism is developed.

Overall View About TGD from Particle Physics Perspective

Topological Geometro-dynamics is able to make rather precise and often testable predictions. In this and two other articles I want to describe the recent over all view about the aspects of quantum TGD relevant for particle physics.

In the first chapter I concentrate the heuristic picture about TGD with emphasis on particle physics.

- First I represent briefly the basic ontology: the motivations for TGD and the notion of many-sheeted space-time, the concept of zero energy ontology, the identification of dark matter in terms of hierarchy of Planck constant which now seems to follow as a prediction of quantum TGD, the motivations for p-adic physics and its basic implications, and the identification of space-time surfaces as generalized Feynman diagrams and the basic implications of this identification.
- Symmetries of quantum TGD are discussed. Besides the basic symmetries of the imbedding space geometry allowing to geometrize standard model quantum numbers and classical fields there are many other symmetries. General Coordinate Invariance is especially powerful in TGD framework allowing to realize quantum classical correspondence and implies effective 2-dimensionality realizing strong form of holography. Super-conformal symmetries of super string models generalize to conformal symmetries of 3-D light-like 3-surfaces and one can understand the generalization of Equivalence Principle in terms of coset representations for the two super Virasoro algebras associated with lightlike boundaries of so called causal diamonds defined as intersections of future and past directed lightcones (*CDs*) and with light-like 3-surfaces. Super-conformal symmetries imply generalization of the space-time supersymmetry in TGD framework consistent with the supersymmetries of minimal supersymmetric variant of the standard model. Twistorial approach to gauge theories has gradually become part of quantum TGD and the natural generalization of the Yangian symmetry identified originally as symmetry of $\mathcal{N} = 4$ SYMs is postulated as basic symmetry of quantum TGD.
- The so called weak form of electric-magnetic duality has turned out to have extremely far reaching consequences and is responsible for the recent progress in the understanding of the physics predicted by TGD. The duality leads to a detailed identification of elementary particles as composite objects of massless particles and predicts new electro-weak physics at LHC. Together with a simple postulate about the properties of preferred extremals of Kähler action the duality allows also to realized quantum TGD as almost topological quantum field theory giving excellent hopes about integrability of quantum TGD.
- There are two basic visions about the construction of quantum TGD. Physics as infinite-dimensional Kähler geometry of world of classical worlds (WCW) endowed with spinor structure and physics as generalized number theory. These visions are briefly summarized as also the practical constructing involving the concept of Dirac operator. As a matter fact, the construction of TGD involves three Dirac operators. The Kähler Dirac equation holds true in the interior of space-time surface and its solutions have a natural interpretation in terms of description of matter, in particular condensed matter. Chern-Simons Dirac action is associated with the light-like 3-surfaces and space-like 3-surfaces at ends of space-time surface at light-like boundaries of *CD*. One can assign to it a generalized eigenvalue equation and the matrix valued eigenvalues correspond to the the action of Dirac operator on momentum eigenstates. Momenta are however not usual momenta but pseudo-momenta very much analogous to region momenta of twistor approach. The third Dirac operator is associated with super Virasoro generators and super Virasoro conditions define Dirac equation in WCW. These conditions characterize zero energy states as modes of WCW spinor fields and code for the generalization of *S*-matrix to a collection of what I call *M*-matrices defining the rows of unitary *U*-matrix defining unitary process.
- Twistor approach has inspired several ideas in quantum TGD during the last years and it seems that the Yangian symmetry and the construction of scattering amplitudes in terms of Grassmannian integrals generalizes to TGD framework. This is due to ZEO allowing to assume that all particles have massless fermions as basic building blocks. ZEO inspires the hypothesis that incoming and outgoing particles are bound states of fundamental fermions associated with

wormhole throats. Virtual particles would also consist of on mass shell massless particles but without bound state constraint. This implies very powerful constraints on loop diagrams and there are excellent hopes about their finiteness. Twistor approach also inspires the conjecture that quantum TGD allows also formulation in terms of 6-dimensional holomorphic surfaces in the product $CP_3 \times CP_3$ of two twistor spaces and general arguments allow to identify the partial differential equations satisfied by these surfaces.

Elementary particle vacuum functionals

Genus-generation correspondence is one of the basic ideas of TGD approach. In order to answer various questions concerning the plausibility of the idea, one should know something about the dependence of the elementary particle vacuum functionals on the vibrational degrees of freedom for the partonic 2-surface.

The construction of the elementary particle vacuum functionals based on Diff invariance, 2-dimensional conformal symmetry, modular invariance plus natural stability requirements indeed leads to an essentially unique form of the vacuum functionals and one can understand why $g > 0$ bosonic families are experimentally absent and why lepton numbers are conserved separately.

An argument suggesting that the number of the light fermion families is three, is developed. The crux of the argument is that the partonic 2-surfaces coding for quantum states are for the maxima of Kähler action hyper-elliptic, that is possess Z_2 conformal symmetry, which for $g > 2$ implies that elementary particle vacuum functional vanishes.

Massless states and particle massivation

This chapter represents the most recent view about elementary particle massivation in TGD framework. This topic is necessarily quite extended since many several notions and new mathematics is involved. Therefore the calculation of particle masses involves five chapters. In the following my goal is to provide an up-to-date summary whereas the chapters are unavoidably a story about evolution of ideas.

The identification of the spectrum of light particles reduces to two tasks: the construction of massless states and the identification of the states which remain light in p-adic thermodynamics. The latter task is relatively straightforward. The thorough understanding of the massless spectrum requires however a real understanding of quantum TGD. It would be also highly desirable to understand why p-adic thermodynamics combined with p-adic length scale hypothesis works. A lot of progress has taken place in these respects during last years.

Zero energy ontology providing a detailed geometric view about bosons and fermions, the generalization of S -matrix to what I call M -matrix, the notion of finite measurement resolution characterized in terms of inclusions of von Neumann algebras, the derivation of p-adic coupling constant evolution and p-adic length scale hypothesis from the first principles, the realization that the counterpart of Higgs mechanism involves generalized eigenvalues of the modified Dirac operator: these are represent important steps of progress during last years with a direct relevance for the understanding of particle spectrum and massivation although the predictions of p-adic thermodynamics are not affected.

During 2010 a further progress took place. These steps of progress relate closely to zero energy ontology, bosonic emergence, the realization of the importance of twistors in TGD, and to the discovery of the weak form of electric-magnetic duality. Twistor approach and the understanding of the Chern-Simons Dirac operator served as a midwife in the process giving rise to the birth of the idea that all particles at fundamental level are massless and that both ordinary elementary particles and string like objects emerge from them. Even more, one can interpret virtual particles as being composed of these massless on mass shell particles assignable to wormhole throats so that four-momentum conservation poses extremely powerful constraints on loop integrals and makes them manifestly finite.

The weak form of electric-magnetic duality led to the realization that elementary particles correspond to bound states of two wormhole throats with opposite Kähler magnetic charges with second throat carrying weak isospin compensating that of the fermion state at second wormhole throat. Both fermions and bosons correspond to wormhole contacts: in the case of fermions topological condensation generates the second wormhole throat. This means that altogether four wormhole throats are involved with both fermions, gauge bosons, and gravitons (for gravitons this is unavoidable in any case). For p-adic thermodynamics the mathematical counterpart of string corresponds to a wormhole

contact with size of order CP_2 size with the role of its ends played by wormhole throats at which the signature of the induced 4-metric changes. The key observation is that for massless states the throats of spin 1 particle must have opposite three-momenta so that gauge bosons are necessarily massive, even photon and other particles usually regarded as massless must have small mass which in turn cancels infrared divergences and give hopes about exact Yangian symmetry generalizing that of $\mathcal{N} = 4$ SYM. Besides this there is weak "stringy" contribution to the mass assignable to the magnetic flux tubes connecting the two wormhole throats at the two space-time sheets.

1. Physical states as representations of super-symplectic and Super Kac-Moody algebras

Physical states are assumed to belong to the representation of super-symplectic algebra and Super Kac-Moody algebra assignable $SO(2) \times SU(3) \times SU(2)_{rot} \times U(2)_{ew}$ associated with the 2-D surfaces X^2 defined by the intersections of light-like 3-surfaces with $\delta M_{\pm}^4 \times CP_2$. These 2-surfaces have interpretation as partons.

Yangian algebras associated with the super-conformal algebras and motivated by twistorial approach generalize the super-conformal symmetry and make it multi-local in the sense that generators can act on several partonic 2-surfaces simultaneously. These partonic 2-surfaces generalize the vertices for the external massless particles in twistor Grassmann diagrams. The implications of this symmetry are yet to be deduced but one thing is clear: Yangians are tailor made for the description of massive bound states formed from several partons identified as partonic 2-surfaces.

2. Particle massivation

Particle massivation can be regarded as a generation of thermal conformal weight identified as mass squared and due to a thermal mixing of a state with vanishing conformal weight with those having higher conformal weights. The observed mass squared is not p-adic thermal expectation of mass squared but that of conformal weight so that there are no problems with Lorentz invariance.

One can imagine several microscopic mechanisms of massivation. The following proposal is the winner in the fight for survival between several competing scenarios.

1. Instead of energy, the Super Kac-Moody Virasoro (or equivalently super-symplectic) generator L_0 (essentially mass squared) is thermalized in p-adic thermodynamics (and also in its real version assuming it exists). The fact that mass squared is thermal expectation of conformal weight guarantees Lorentz invariance. That mass squared, rather than energy, is a fundamental quantity at CP_2 length scale is also suggested by a simple dimensional argument (Planck mass squared is proportional to \hbar so that it should correspond to a generator of some Lie-algebra (Virasoro generator $L_0!$)).
2. By Equivalence Principle the thermal average of mass squared can be calculated either in terms of thermodynamics for either super-symplectic of Super Kac-Moody Virasoro algebra and p-adic thermodynamics is consistent with conformal invariance.
3. There is also a modular contribution to the mass squared, which can be estimated using elementary particle vacuum functionals in the conformal modular degrees of freedom of the partonic 2-surface. It dominates for higher genus partonic 2-surfaces. For bosons both Virasoro and modular contributions seem to be negligible and could be due to the smallness of the p-adic temperature.
4. A long standing problem has been whether coupling to Higgs boson is needed to explain gauge boson masses via a generation of Higgs vacuum expectation having possibly interpretation in terms of a coherent state. The deviation Δh of the total ground state conformal weight from negative integer gives rise to Higgs type contribution to the thermal mass squared and dominates in case of gauge bosons for which p-adic temperature is small. In the case of fermions this contribution to the mass squared is small. It is natural to relate Δh to the generalized eigenvalues of Chern-Simons Dirac operator.
5. A natural identification of the non-integer contribution to the conformal weight is as Higgsy and stringy contributions to the vacuum conformal weight (strings are now "weak strings"). In twistor approach the generalized eigenvalues of Chern-Simons Dirac operator for external particles indeed correspond to light-like momenta and when the three-momenta are opposite this gives rise to non-vanishing mass. Higgs is necessary to give longitudinal polarizations

for gauge bosons and also gauge bosons usually regarded as exactly massless particles would naturally receive small mass in this manner so that Higgs would disappear completely from the spectrum. The theoretical motivation for a small mass would be exact Yangian symmetry. Higgs vacuum expectation assignable to coherent state of Higgs bosons is not needed to explain the boson masses. Twistorial consideration suggest that Higgs disappears completely from the spectrum and this might happen also for its super counterpart.

p-Adic thermodynamics is what gives to this approach its predictive power.

1. p-Adic temperature is quantized by purely number theoretical constraints (Boltzmann weight $\exp(-E/kT)$ is replaced with p^{L_0/T_p} , $1/T_p$ integer) and fermions correspond to $T_p = 1$ whereas $T_p = 1/n$, $n > 1$, seems to be the only reasonable choice for gauge bosons.
2. p-Adic thermodynamics forces to conclude that CP_2 radius is essentially the p-adic length scale $R \sim L$ and thus of order $R \simeq 10^{3.5} \sqrt{\hbar G}$ and therefore roughly $10^{3.5}$ times larger than the naive guess. Hence p-adic thermodynamics describes the mixing of states with vanishing conformal weights with their Super Kac-Moody Virasoro excitations having masses of order $10^{-3.5}$ Planck mass.

p-Adic particle massivation: hadron masses

In this chapter the results of the calculation of elementary particle masses will be used to construct a model predicting hadron masses.

1. Topological mixing of quarks

In TGD framework CKM mixing is induced by topological mixing of quarks (that is 2-dimensional topologies characterized by genus). Number theoretical constraints on topological mixing can be realized by assuming that topological mixing leads to a thermodynamical equilibrium. This gives an upper bound of 1200 for the number of different U and D matrices and the input from top quark mass and $\pi^+ - \pi^0$ mass difference implies that physical U and D matrices can be constructed as small perturbations of matrices expressible as direct sum of essentially unique 2×2 and 1×1 matrices. The maximally entropic solutions can be found numerically by using the fact that only the probabilities p_{11} and p_{21} can be varied freely. The solutions are unique in the accuracy used, which suggests that the system allows only single thermodynamical phase.

The matrices U and D associated with the probability matrices can be deduced straightforwardly in the standard gauge. The U and D matrices derived from the probabilities determined by the entropy maximization turn out to be unitary for most values of n_1 and n_2 . This is a highly non-trivial result and means that mass and probability constraints together with entropy maximization define a sub-manifold of $SU(3)$ regarded as a sub-manifold in 9-D complex space. The choice $(n(u), n(c)) = (4, n)$, $n < 9$, does not allow unitary U whereas $(n(u), n(c)) = (5, 6)$ does. This choice is still consistent with top quark mass and together with $n(d) = n(s) = 5$ it leads to a rather reasonable CKM matrix with a value of CP breaking invariant within experimental limits. The elements V_{i3} and V_{3i} , $i = 1, 2$ are however roughly twice larger than their experimental values deduced assuming standard model. V_{31} is too large by a factor 1.6. The possibility of scaled up variants of light quarks could lead to too small experimental estimates for these matrix elements. The whole parameter space has not been scanned so that better candidates for CKM matrices might well exist.

2. Higgs contribution to fermion masses is negligible

There are good reasons to believe that Higgs expectation for the fermionic space-time sheets is vanishing although fermions couple to Higgs. Thus p-adic thermodynamics would explain fermion masses completely. This together with the fact that the prediction of the model for the top quark mass is consistent with the most recent limits on it, fixes the CP_2 mass scale with a high accuracy to the maximal one obtained if second order contribution to electron's p-adic mass squared vanishes. This is very strong constraint on the model.

3. The p-adic length scale of quark is dynamical

The assumption about the presence of scaled up variants of light quarks in light hadrons leads to a surprisingly successful model for pseudo scalar meson masses using only quark masses and the

assumption mass squared is additive for quarks with same p-adic length scale and mass for quarks labelled by different primes p . This conforms with the idea that pseudo scalar mesons are Goldstone bosons in the sense that color Coulombic and magnetic contributions to the mass cancel each other. Also the mass differences between hadrons containing different numbers of strange and heavy quarks can be understood if s , b and c quarks appear as several scaled up versions.

This hypothesis yields surprisingly good fit for meson masses but for some mesons the predicted mass is slightly too high. The reduction of CP_2 mass scale to cure the situation is not possible since top quark mass would become too low. In case of diagonal mesons for which quarks correspond to same p-adic prime, quark contribution to mass squared can be reduced by ordinary color interactions and in the case of non-diagonal mesons one can require that quark contribution is not larger than meson mass.

4. Super-canonical bosons at hadronic space-time sheet can explain the constant contribution to baryonic masses

Quarks explain only a small fraction of the baryon mass and that there is an additional contribution which in a good approximation does not depend on baryon. This contribution should correspond to the non-perturbative aspects of QCD.

A possible identification of this contribution is in terms of super-canonical gluons predicted by TGD. Baryonic space-time sheet with $k = 107$ would contain a many-particle state of super-canonical gluons with net conformal weight of 16 units. This leads to a model of baryons masses in which masses are predicted with an accuracy better than 1 per cent. Super-canonical gluons also provide a possible solution to the spin puzzle of proton.

Hadronic string model provides a phenomenological description of non-perturbative aspects of QCD and a connection with the hadronic string model indeed emerges. Hadronic string tension is predicted correctly from the additivity of mass squared for $J = 2$ bound states of super-canonical quanta. If the topological mixing for super-canonical bosons is equal to that for U type quarks then a 3-particle state formed by 2 super-canonical quanta from the first generation and 1 quantum from the second generation would define baryonic ground state with 16 units of conformal weight.

In the case of mesons pion could contain super-canonical boson of first generation preventing the large negative contribution of the color magnetic spin-spin interaction to make pion a tachyon. For heavier bosons super-canonical boson need not to be assumed. The preferred role of pion would relate to the fact that its mass scale is below QCD Λ .

5. Description of color magnetic spin-spin splitting in terms of conformal weight

What remains to be understood are the contributions of color Coulombic and magnetic interactions to the mass squared. There are contributions coming from both ordinary gluons and super-canonical gluons and the latter is expected to dominate by the large value of color coupling strength.

Conformal weight replaces energy as the basic variable but group theoretical structure of color magnetic contribution to the conformal weight associated with hadronic space-time sheet ($k = 107$) is same as in case of energy. The predictions for the masses of mesons are not so good than for baryons, and one might criticize the application of the format of perturbative QCD in an essentially non-perturbative situation.

The comparison of the super-canonical conformal weights associated with spin 0 and spin 1 states and spin 1/2 and spin 3/2 states shows that the different masses of these states could be understood in terms of the super-canonical particle contents of the state correlating with the total quark spin. The resulting model allows excellent predictions also for the meson masses and implies that only pion and kaon can be regarded as Goldstone boson like states. The model based on spin-spin splittings is consistent with the model.

To sum up, the model provides an excellent understanding of baryon and meson masses. This success is highly non-trivial since the fit involves only the integers characterizing the p-adic length scales of quarks and the integers characterizing color magnetic spin-spin splitting plus p-adic thermodynamics and topological mixing for super-canonical gluons. The next challenge would be to predict the correlation of hadron spin with super-canonical particle content in case of long-lived hadrons.

p-Adic Particle Massivation: New Physics

TGD certainly predicts a lot of new physics, actually infinite hierarchies of fractal copies of standard model physics, but the precise characterization of predictions has varied as the interpretation of the theory has evolved during years. No attempt to discuss systematically the spectrum of various exotic bosons and fermions, basically due to the ground states created by color super-canonical and Kac-Moody generators, will be made. Rather, the attempt is to summarize the new physics expected on basis of recent interpretation of quantum TGD.

1. Basic new physics predictions

For a long time the belief was that TGD allows no sparticles: super-generators with vanishing conformal weight simply vanish. It however turned that TGD leads to a generalization of space-time supersymmetry for which the fermionic oscillator operators associated with the modes of the induced spinor field define via their anti-commutators SUSY algebra serving as the basic building brick for various super-conformal algebras. This means quite a dramatic extension of the ordinary space-time supersymmetry since the number of spinor modes can be infinite and also a generalization of the SUSY formalism. This super-symmetry is broken from the beginning. The minimal breaking would mean different p-adic length scale for particles and their super-partners but otherwise identical mass formulae. This makes theory quite predictive.

TGD predicts a rich spectrum of massless states for which ground states of negative super-canonical conformal weight are created by colored super-generators. By color confinement these states do not however give rise to macroscopic long range forces. A hierarchy color and weak physics is predicted. Also dark matter hierarchy corresponding to a hierarchy of Planck constants brings in a hierarchy of variants of standard model physics labeled by the values of Planck constant. Thus in TGD the question is not about predicting some exotic particle but entire fractal hierarchies of copies of standard model physics.

The family replication for fermions correspond in case of gauge bosons prediction of bosons labelled by genera of the two lightlike wormhole throats associated with the wormhole contact representing boson. There are very general arguments predicting that the number of fermionic genera is three and this means that gauge bosons can be arranged into genus-SU(3) singlet and octet. Octet corresponds to exotic gauge bosons and its members should develop Higgs expectation value. Completely symmetric coupling between Higgs octet and boson octet allows also the bosons with vanishing genus-SU(3) quantum numbers to develop mass.

Higgs field is predicted and its vacuum expectation value explains boson masses. By a general argument p-adic temperature for bosons is low and this means that Higgs contribution to the gauge boson mass dominates. Only p-adic thermodynamics is needed to explain fermion masses and the masses of super-canonical bosons and their super counterparts. There is an argument suggesting that vacuum expectation value of Higgs at fermion space-time sheets is not possible. Almost universality of the topological mixing inducing also CKM mixing allows to predict mass spectrum of these states.

2. Summary of new physics effects

Various new physics effects are discussed.

1. There is a brief discussion of family replication phenomenon in the case of gauge bosons based on the identification of gauge bosons as wormhole contacts. Also an argument forcing the identification of partonic vertices as branchings of partonic 2-surfaces is developed.
2. ALEPH anomaly is interpreted in terms of a fractal copy of b-quark corresponding to $k=197$.
3. The possible signatures of M_{89} hadron physics in e^+e^- annihilation experiments are discussed using a naive scaling of ordinary hadron physics.
4. It is found that the newly born concept of Pomeron of Regge theory could be identified as the sea of perturbative QCD.
5. In p-adic context exotic representations of Super Virasoro with $M^2 \propto p^k$, $k = 1, 2, \dots$ are possible. For $k = 1$ the states of these representations have same mass scale as elementary particles although in real context the masses would be gigantic. This inspires the question whether non-perturbative aspects of hadron physics could be assigned to the presence of these

representations. The prospects for this are promising. Pion mass is almost exactly equal to the mass of lowest state of the exotic representation for $k = 107$ and Regge slope for rotational excitations of hadrons is predicted with three per cent accuracy assuming that they correspond to the states of $k = 101$ exotic Super Virasoro representations. This leads to the idea that hadronization and fragmentation correspond to phase transitions between ordinary and exotic Super Virasoro representations and that there is entire fractal hierarchy of hadrons inside hadrons and QCD:s inside QCD:s corresponding to p-adic length scales $L(k)$, $k = 107, 103, 101, 97, \dots$

3. Anomalously large direct CP breaking in $K - \bar{K}$ system and exotic gluons

The recently observed anomalously large direct CP breaking in $K_L \rightarrow \pi\pi$ decays is explained in terms of loop corrections due to the predicted 2 exotic gluons having masses around 33.6 GeV. It will be also found that the TGD version of the chiral field theory believed to provide a phenomenological low energy description of QCD differs from its standard model version in that quark masses are replaced in TGD framework with shifts of quark masses induced by the vacuum expectation values of the scalar meson fields. This conforms with the TGD view about Higgs mechanism as causing only small mass shifts. It must be however emphasized that there is an argument suggesting that the vacuum expectation value of Higgs in fermionic case does not even make sense.

1.5.2 Part II: Applications of p-adic length scale hypothesis and dark matter hierarchy

Recent status of lepto-hadron hypothesis

TGD suggests strongly the existence of lepto-hadron physics. Lepto-hadrons are bound states of color excited leptons and the anomalous production of e^+e^- pairs in heavy ion collisions finds a nice explanation as resulting from the decays of lepto-hadrons with basic condensate level $k = 127$ and having typical mass scale of one MeV . The recent indications on the existence of a new fermion with quantum numbers of muon neutrino and the anomaly observed in the decay of orthopositronium give further support for the lepto-hadron hypothesis. There is also evidence for anomalous production of low energy photons and e^+e^- pairs in hadronic collisions.

The identification of lepto-hadrons as a particular instance in the predicted hierarchy of dark matters interacting directly only via graviton exchange allows to circumvent the lethal counter arguments against the lepto-hadron hypothesis (Z^0 decay width and production of colored lepton jets in e^+e^- annihilation) even without assumption about the loss of asymptotic freedom.

PCAC hypothesis and its sigma model realization lead to a model containing only the coupling of the lepto-pion to the axial vector current as a free parameter. The prediction for e^+e^- production cross section is of correct order of magnitude only provided one assumes that lepto-pions decay to lepto-nucleon pair $e_{ex}^+e_{ex}^-$ first and that lepto-nucleons, having quantum numbers of electron and having mass only slightly larger than electron mass, decay to lepton and photon. The peculiar production characteristics are correctly predicted. There is some evidence that the resonances decay to a final state containing $n > 2$ particle and the experimental demonstration that lepto-nucleon pairs are indeed in question, would be a breakthrough for TGD.

During 18 years after the first published version of the model also evidence for colored μ has emerged. Towards the end of 2008 CDF anomaly gave a strong support for the colored excitation of τ . The lifetime of the light long lived state identified as a charged τ -pion comes out correctly and the identification of the reported 3 new particles as p-adically scaled up variants of neutral τ -pion predicts their masses correctly. The observed muon jets can be understood in terms of the special reaction kinematics for the decays of neutral τ -pion to 3 τ -pions with mass scale smaller by a factor 1/2 and therefore almost at rest. A spectrum of new particles is predicted. The discussion of CDF anomaly led to a modification and generalization of the original model for lepto-pion production and the predicted production cross section is consistent with the experimental estimate.

TGD and Nuclear Physics

This chapter is devoted to the possible implications of TGD for nuclear physics. In the original version of the chapter the focus was in the attempt to resolve the problems caused by the incorrect interpretation of the predicted long ranged weak gauge fields. What seems to be a breakthrough in

this respect came only quite recently (2005), more than a decade after the first version of this chapter, and is based on TGD based view about dark matter inspired by the developments in the mathematical understanding of quantum TGD. In this approach condensed matter nuclei can be either ordinary, that is behave essentially like standard model nuclei, or be in dark matter phase in which case they generate long ranged dark weak gauge fields responsible for the large parity breaking effects in living matter. This approach resolves trivially the objections against long range classical weak fields.

The basic criterion for the transition to dark matter phase having by definition large value of \hbar is that the condition $\alpha Q_1 Q_2 \simeq 1$ for appropriate gauge interactions expressing the fact that the perturbation series does not converge. The increase of \hbar makes perturbation series converging since the value of α is reduced but leaves lowest order classical predictions invariant.

This criterion can be applied to color force and inspires the hypothesis that valence quarks inside nucleons correspond to large \hbar phase whereas sea quark space-time sheets correspond to the ordinary value of \hbar . This hypothesis is combined with the earlier model of strong nuclear force based on the assumption that long color bonds with p-adically scaled down quarks with mass of order MeV at their ends are responsible for the nuclear strong force.

1. *Is strong force due to color bonds between exotic quark pairs?*

The basic assumptions are following.

1. Valence quarks correspond to large \hbar phase with p-adic length scale $L(k_{eff} = 129) = L(107)/v_0 \simeq 2^{11}L(107) \simeq 5 \times 10^{-12}$ m whereas sea quarks correspond to ordinary \hbar and define the standard size of nucleons.
2. Color bonds with length of order $L(127) \simeq 2.5 \times 10^{-12}$ m and having quarks with ordinary \hbar and p-adically scaled down masses $m_q(dark) \simeq v_0 m_q$ at their ends define kind of rubber bands connecting nucleons. The p-adic length scale of exotic quarks differs by a factor 2 from that of dark valence quarks so that the length scales in question can couple naturally. This large length scale as also other p-adic length scales correspond to the size of the topologically quantized field body associated with system, be it quark, nucleon, or nucleus.
3. Valence quarks and even exotic quarks can be dark with respect to both color and weak interactions but not with respect to electromagnetic interactions. The model for binding energies suggests darkness with respect to weak interactions with weak boson masses scaled down by a factor v_0 . Weak interactions remain still weak. Quarks and nucleons as defined by their $k = 107$ sea quark portions condense at scaled up weak space-time sheet with $k_{eff} = 111$ having p-adic size 10^{-14} meters. The estimate for the atomic number of the heaviest possible nucleus comes out correctly.

The wave functions of the nucleons fix the boundary values of the wave functionals of the color magnetic flux tubes idealizable as strings. In the terminology of M-theory nucleons correspond to small branes and color magnetic flux tubes to strings connecting them.

2. *General features of strong interactions*

This picture allows to understand the general features of strong interactions.

1. Quantum classical correspondence and the assumption that the relevant space-time surfaces have 2-dimensional CP_2 projection implies Abelianization. Strong isospin group can be identified as the $SU(2)$ subgroup of color group acting as isotropies of space-time surfaces. and the $U(1)$ holonomy of color gauge potential defines a preferred direction of strong isospin. Dark color isospin corresponds to strong isospin. The correlation of dark color with weak isospin of the nucleon is strongly suggested by quantum classical correspondence.
2. Both color singlet spin 0 pion type bonds and colored spin 1 bonds are allowed and the color magnetic spin-spin interaction between the exotic quark and anti-quark is negative in this case. p-p and n-n bonds correspond to oppositely colored spin 1 bonds and p-n bonds to colorless spin 0 bonds for which the binding energy is free times higher. The presence of colored bonds forces the presence of neutralizing dark gluon condensate favoring states with $N - P > 0$.

3. Shell model based on harmonic oscillator potential follows naturally from this picture in which the magnetic flux tubes connecting nucleons take the role of springs. Spin-orbit interaction can be understood in terms of the color force in the same way as it is understood in atomic physics.

3. Nuclear binding energies

1. The binding energies per nucleon for $A \leq 4$ nuclei can be understood if they form closed string like structures, nuclear strings, so that only two color bonds per nucleon are possible. This could be understood if ordinary quarks and exotic quarks possessing much smaller mass behave as if they were identical fermions. p-Adic mass calculations support this assumption. Also the average behavior of binding energy for heavier nuclei is predicted correctly.
2. For nuclei with $P = N$ all color bonds can be pion type bonds and have thus largest color magnetic spin-spin interaction energy. The increase of color Coulombic binding energy between colored exotic quark pairs and dark gluons however favors $N > P$ and explains also the formation of neutron halo outside $k = 111$ space-time sheet.
3. Spin-orbit interaction provides the standard explanation for magic numbers. If the maximum of the binding energy per nucleon is taken as a criterion for magic, also $Z=N=4,6,12$ are magic. The alternative TGD based explanation for magic numbers $Z = N = 4, 6, 8, 12, 20$ would be in terms of regular Platonic solids. Experimentally also other magic numbers are known for neutrons. The linking of nuclear strings provides a possible mechanism producing new magic nuclei from lighter magic nuclei.

4. Stringy description of nuclear reactions

The view about nucleus as a collection of linked nuclear strings suggests stringy description of nuclear reactions. Microscopically the nuclear reactions would correspond to re-distribution of exotic quarks between the nucleons in reacting nuclei.

5. Anomalies and new nuclear physics

The TGD based explanation of neutron halo has been already mentioned. The recently observed tetra-neutron states are difficult to understand in the standard nuclear physics framework since Fermi statistics does not allow this kind of state. The identification of tetra-neutron as an alpha particle containing two negatively charged color bonds allows to circumvent the problem. A large variety of exotic nuclei containing charged color bonds is predicted.

The proposed model explains the anomaly associated with the tritium beta decay. What has been observed is that the spectrum intensity of electrons has a narrow bump near the endpoint energy. Also the maximum energy E_0 of electrons is shifted downwards. I have considered two explanations for the anomaly. The original models are based on TGD variants of original models involving belt of dark neutrinos or antineutrinos along the orbit of Earth. Only recently (towards the end of year 2008) I realized that nuclear string model provides much more elegant explanation of the anomaly and has also the potential to explain much more general anomalies.

Cold fusion has not been taken seriously by the physics community but the situation has begun to change gradually. There is an increasing evidence for the occurrence of nuclear transmutations of heavier elements besides the production of ${}^4\text{He}$ and ${}^3\text{H}$ whereas the production rate of ${}^3\text{He}$ and neutrons is very low. These characteristics are not consistent with the standard nuclear physics predictions. Also Coulomb wall and the absence of gamma rays and the lack of a mechanism transferring nuclear energy to the electrolyte have been used as an argument against cold fusion. TGD based model relying on the notion of charged color bonds explains the anomalous characteristics of cold fusion.

Nuclear String Hypothesis

Nuclear string hypothesis is one of the most dramatic almost-predictions of TGD. The hypothesis in its original form assumes that nucleons inside nucleus form closed nuclear strings with neighboring nuclei of the string connected by exotic meson bonds consisting of color magnetic flux tube with quark and anti-quark at its ends. The lengths of flux tubes correspond to the p-adic length scale of electron

and therefore the mass scale of the exotic mesons is around 1 MeV in accordance with the general scale of nuclear binding energies. The long lengths of em flux tubes increase the distance between nucleons and reduce Coulomb repulsion. A fractally scaled up variant of ordinary QCD with respect to p-adic length scale would be in question and the usual wisdom about ordinary pions and other mesons as the origin of nuclear force would be simply wrong in TGD framework as the large mass scale of ordinary pion indeed suggests.

1. *A > 4 nuclei as nuclear strings consisting of A ≤ 4 nuclei*

In this article a more refined version of nuclear string hypothesis is developed.

1. It is assumed ${}^4\text{He}$ nuclei and $A < 4$ nuclei and possibly also nucleons appear as basic building blocks of nuclear strings. $A \leq 4$ nuclei in turn can be regarded as strings of nucleons. Large number of stable lightest isotopes of form $A = 4n$ supports the hypothesis that the number of ${}^4\text{He}$ nuclei is maximal. Even the weak decay characteristics might be reduced to those for $A < 4$ nuclei using this hypothesis.
2. One can understand the behavior of nuclear binding energies surprisingly well from the assumptions that total *strong* binding energy associated with $A \leq 4$ building blocks is *additive* for nuclear strings.
3. In TGD framework tetra-neutron is interpreted as a variant of alpha particle obtained by replacing two meson-like stringy bonds connecting neighboring nucleons of the nuclear string with their negatively charged variants. For heavier nuclei tetra-neutron is needed as an additional building brick.

2. *Bose-Einstein condensation of color bonds as a mechanism of nuclear binding*

The attempt to understand the variation of the nuclear binding energy and its maximum for Fe leads to a quantitative model of nuclei lighter than Fe as color bound Bose-Einstein condensates of pion like colored states associated with color flux tubes connecting ${}^4\text{He}$ nuclei. The color contribution to the total binding energy is proportional to n^2 , where n is the number of color bonds. Fermi statistics explains the reduction of E_B for the nuclei heavier than Fe . Detailed estimate favors harmonic oscillator model over free nucleon model with oscillator strength having interpretation in terms of string tension.

Fractal scaling argument allows to understand ${}^4\text{He}$ and lighter nuclei as strings of nucleons with nucleons bound together by color bonds. Three fractally scaled variants of QCD corresponding $A > 4$, $A = 4$, and $A < 4$ nuclei are involved. The binding energies of also $A \leq 4$ are predicted surprisingly accurately by applying simple p-adic scaling to the model of binding energies of heavier nuclei.

3. *Giant dipole resonance as de-coherence of Bose-Einstein condensate of color bonds*

Giant resonances and so called pygmy resonances are interpreted in terms of de-coherence of the Bose-Einstein condensates associated with $A \leq 4$ nuclei and with the nuclear string formed from $A \leq 4$ nuclei. The splitting of the Bose-Einstein condensate to pieces costs a precisely defined energy. For ${}^4\text{He}$ de-coherence the model predicts singlet line at 12.74 MeV and triplet at ~ 27 MeV spanning 4 MeV wide range.

The de-coherence at the level of nuclear string predicts 1 MeV wide bands 1.4 MeV above the basic lines. Bands decompose to lines with precisely predicted energies. Also these contribute to the width. The predictions are in rather good agreement with experimental values. The so called pygmy resonance appearing in neutron rich nuclei can be understood as a de-coherence for $A = 3$ nuclei. A doublet at ~ 8 MeV and MeV spacing is predicted. The prediction for the position is correct.

4. *Dark nuclear strings as analogs of as analogs of DNA-, RNA- and amino-acid sequences and baryonic realization of genetic code*

A speculative picture proposing a connection between homeopathy, water memory, and phantom DNA effect is discussed and on basis of this connection a vision about how the tqc hardware represented by the genome is actively developed by subjecting it to evolutionary pressures represented by a virtual world representation of the physical environment. The speculation inspired by this vision is that genetic code as well as DNA-, RNA- and amino-acid sequences should have representation in terms

of nuclear strings. The model for dark baryons indeed leads to an identification of these analogs and the basic numbers of genetic code including also the numbers of aminoacids coded by a given number of codons are predicted correctly. Hence it seems that genetic code is universal rather than being an accidental outcome of the biological evolution.

Dark Nuclear Physics and Condensed Matter

In this chapter the possible effects of dark matter in nuclear physics and condensed matter physics are considered. The spirit of the discussion is necessarily rather speculative since the vision about the hierarchy of Planck constants is only 5 years old. The most general form of the hierarchy would involve both singular coverings and factors spaces of CD (causal diamond of M^4) defined as intersection of future and past directed light-cones) and CP_2 . There are grave objections against the allowance of factor spaces. In this case Planck constant could be smaller than its standard value and there are very few experimental indications for this. Quite recently came the realization that the hierarchy of Planck constants might emerge from the basic quantum TGD as a consequence of the extreme non-linearity of field equations implying that the correspondence between the derivatives of imbedding space coordinates and canonical momentum is many-to-one. This makes natural to the introduction of covering spaces of CD and CP_2 . Planck constant would be effectively replaced with a multiple of ordinary Planck constant defined by the number of the sheets of the covering. The space-like 3-surfaces at the ends of the causal diamond and light-like 3-surfaces defined by wormhole throats carrying elementary particle quantum numbers would be quantum critical in the sense of being unstable against decay to many-sheeted structures. Charge fractionization could be understood in this scenario. Biological evolution would have the increase of the Planck constant as as one aspect. The crucial scaling of the size of CD by Planck constant can be justified by a simple argument. Note that primary p-adic length scales would scale as $\sqrt{\hbar}$ rather than \hbar as assumed in the original model.

1. *What darkness means?*

Dark matter is identified as matter with non-standard value of Planck constant. The weak form of darkness states that only some field bodies of the particle consisting of flux quanta mediating bound state interactions between particles become dark. One can assign to each interaction a field body (em, Z^0 , W , gluonic, gravitational) and p-adic prime and the value of Planck constant characterize the size of the particular field body. One might even think that particle mass can be assigned with its em field body and that Compton length of particle corresponds to the size scale of em field body.

Nuclear string model suggests that the sizes of color flux tubes and weak flux quanta associated with nuclei can become dark in this sense and have size of order atomic radius so that dark nuclear physics would have a direct relevance for condensed matter physics. If this happens, it becomes impossible to make a reductionistic separation between nuclear physics and condensed matter physics and chemistry anymore.

2. *What dark nucleons are?*

The basic hypothesis is that nuclei can make a phase transition to dark phase in which the size of both quarks and nuclei is measured in Angstroms. For the less radical option this transition could happen only for the color, weak, and em field bodies. Proton connected by dark color bonds super-nuclei with inter-nucleon distance of order atomic radius might be crucial for understanding the properties of water and perhaps even the properties of ordinary condensed matter. Large \hbar phase for weak field body of D and Pd nuclei with size scale of atom would explain selection rules of cold fusion.

3. *Anomalous properties of water and dark nuclear physics*

A direct support for partial darkness of water comes from the $H_{1.5}O$ chemical formula supported by neutron and electron diffraction in attosecond time scale. The explanation could be that one fourth of protons combine to form super-nuclei with protons connected by color bonds and having distance sufficiently larger than atomic radius.

The crucial property of water is the presence of molecular clusters. Tetrahedral clusters allow an interpretation in terms of magic $Z=8$ protonic dark nuclei. The icosahedral clusters consisting of 20 tetrahedral clusters in turn have interpretation as magic dark dark nuclei: the presence of the dark dark matter explains large portion of the anomalies associated with water and explains the unique role of water in biology. In living matter also higher levels of dark matter hierarchy are predicted to

be present. The observed nuclear transmutation suggest that also light weak bosons are present.

4. *Implications of the partial darkness of condensed matter*

The model for partially dark condensed matter inspired by nuclear string model and the model of cold fusion inspired by it allows to understand the low compressibility of the condensed matter as being due to the repulsive weak force between exotic quarks, explains large parity breaking effects in living matter, and suggests a profound modification of the notion of chemical bond having most important implications for bio-chemistry and understanding of bio-chemical evolution.

Dark Forces and Living Matter

The unavoidable presence of classical long ranged weak (and also color) gauge fields in TGD Universe has been a continual source of worries for more than two decades. The basic question has been whether Z^0 charges of elementary particles are screened in electro-weak length scale or not. Same question must be raised in the case of color charges. For a long time the hypothesis was that the charges are feeded to larger space-time sheets in this length scale rather than screened by vacuum charges so that an effective screening results in electro-weak length scale. This hypothesis turned out to be a failure and was replaced with the idea that the non-linearity of field equations (only topological half of Maxwell's equations holds true) implies the generation of vacuum charge densities responsible for the screening.

The weak form of electric-magnetic duality led to the identification of the long sought for mechanism causing the weak screening in electroweak scales. The basic implication of the duality is that Kähler electric charges of wormhole throats representing particles are proportional to Kähler magnetic charges so that the CP_2 projections of the wormhole throats are homologically non-trivial. The Kähler magnetic charges do not create long range monopole fields if they are neutralized by wormhole throats carrying opposite monopole charges and weak isospin neutralizing the axial isospin of the particle's wormhole throat. One could speak of confinement of weak isospin. The weak field bodies of elementary fermions would be replaced with string like objects with a length of order W boson Compton length. Electro-magnetic flux would be feeded to electromagnetic field body where it would be feeded to larger space-time sheets. Similar mechanism could apply in the case of color quantum numbers. Weak charges would be therefore screened for ordinary matter in electro-weak length scale but dark electro-weak bosons correspond to much longer symmetry breaking length scale for weak field body. Large values of Planck constant would make it possible to zoop up elementary particles and study their internal structure without any need for gigantic accelerators.

In this chapter possible implications of the dark weak force for the understanding of living matter are discussed. The basic question is how classical Z^0 fields could make itself visible. Large parity breaking effects in living matter suggests which direction one should look for the answer to the question. One possible answer is based on the observation that for vacuum extremals classical electromagnetic and Z^0 fields are proportional to each other and this means that the electromagnetic charges of dark fermions standard are replaced with effective couplings in which the contribution of classical Z^0 force dominates. This modifies dramatically the model for the cell membrane as a Josephson junction and raises the scale of Josephson energies from IR range just above thermal threshold to visible and ultraviolet. The amazing finding is that the Josephson energies for biologically important ions correspond to the energies assigned to the peak frequencies in the biological activity spectrum of photoreceptors in retina suggesting. This suggests that almost vacuum extremals and thus also classical Z^0 fields are in a central role in the understanding of the functioning of the cell membrane and of sensory qualia. This would also explain the large parity breaking effects in living matter.

A further conjecture is that EEG and its predicted fractally scaled variants which same energies in visible and UV range but different scales of Josephson frequencies correspond to Josephson photons with various values of Planck constant. The decay of dark ELF photons with energies of visible photons would give rise to bunches of ordinary ELF photons. Biophotons in turn could correspond to ordinary visible photons resulting in the phase transition of these photons to photons with ordinary value of Planck constant. This leads to a very detailed view about the role of dark electromagnetic radiation in biomatter and also to a model for how sensory qualia are realized. The general conclusion might be that most effects due to the dark weak force are associated with almost vacuum extremals.

Super-Conductivity in Many-Sheeted Space-Time

In this chapter a model for high T_c super-conductivity as quantum critical phenomenon is developed. The relies on the notions of quantum criticality, dynamical quantized Planck constant requiring a generalization of the 8-D imbedding space to a book like structure, and many-sheeted space-time. In particular, the notion of magnetic flux tube as a carrier of supra current of central concept.

With a sufficient amount of twisting and weaving these basic ideas one ends up to concrete model for high T_c superconductors as quantum critical superconductors consistent with the qualitative facts that I am personally aware. The following minimal model looks the most realistic option found hitherto.

1. The general idea is that magnetic flux tubes are carriers of supra currents. In anti-ferromagnetic phases these flux tube structures form small closed loops so that the system behaves as an insulator. Some mechanism leading to a formation of long flux tubes must exist. Doping creates holes located around stripes, which become positively charged and attract electrons to the flux tubes.
2. The higher critical temperature T_{c1} corresponds to a formation local configurations of parallel spins assigned to the holes of stripes giving rise to a local dipole fields with size scale of the order of the length of the stripe. Conducting electrons form Cooper pairs at the magnetic flux tube structures associated with these dipole fields. The elongated structure of the dipoles favors angular momentum $L = 2$ for the pairs. The presence of magnetic field favors Cooper pairs with spin $S = 1$.
3. Stripes can be seen as 1-D metals with delocalized electrons. The interaction responsible for the energy gap corresponds to the transversal oscillations of the magnetic flux tubes inducing oscillations of the nuclei of the stripe. These transverse phonons have spin and their exchange is a good candidate for the interaction giving rise to a mass gap. This could explain the BCS type aspects of high T_c super-conductivity.
4. Above T_c supra currents are possible only in the length scale of the flux tubes of the dipoles which is of the order of stripe length. The reconnections between neighboring flux tube structures induced by the transverse fluctuations give rise to longer flux tubes structures making possible finite conductivity. These occur with certain temperature dependent probability $p(T, L)$ depending on temperature and distance L between the stripes. By criticality $p(T, L)$ depends on the dimensionless variable $x = TL/\hbar$ only: $p = p(x)$. At critical temperature T_c transverse fluctuations have large amplitude and makes $p(x_c)$ so large that very long flux tubes are created and supra currents can run. The phenomenon is completely analogous to percolation.
5. The critical temperature $T_c = x_c \hbar/L$ is predicted to be proportional to \hbar and inversely proportional to L (, which is indeed to be the case). If flux tubes correspond to a large value of \hbar , one can understand the high value of T_c . Both Cooper pairs and magnetic flux tube structures represent dark matter in TGD sense.
6. The model allows to interpret the characteristic spectral lines in terms of the excitation energy of the transversal fluctuations and gap energy of the Cooper pair. The observed 50 meV threshold for the onset of photon absorption suggests that below T_c also $S = 0$ Cooper pairs are possible and have gap energy about 9 meV whereas $S = 1$ Cooper pairs would have gap energy about 27 meV. The flux tube model indeed predicts that $S = 0$ Cooper pairs become stable below T_c since they cannot anymore transform to $S = 1$ pairs. Their presence could explain the BCS type aspects of high T_c super-conductivity. The estimate for $\hbar/\hbar_0 = r$ from critical temperature T_{c1} is about $r = 3$ contrary to the original expectations inspired by the model of of living system as a super-conductor suggesting much higher value. An unexpected prediction is that coherence length is actually r times longer than the coherence length predicted by conventional theory so that type I super-conductor could be in question with stripes serving as duals for the defects of type I super-conductor in nearly critical magnetic field replaced now by ferromagnetic phase.
7. TGD suggests preferred values for $r = \hbar/\hbar_0$. For the most general option the values of \hbar are products and ratios of two integers n_a and n_b . Ruler and compass integers defined by the products of distinct Fermat primes and power of two are number theoretically favored values for

these integers because the phases $\exp(i2\pi/n_i)$, $i \in \{a, b\}$, in this case are number theoretically very simple and should have emerged first in the number theoretical evolution via algebraic extensions of p-adics and of rationals. p-Adic length scale hypothesis favors powers of two as values of r . The hypothesis that Mersenne primes $M_k = 2^k - 1$, $k \in \{89, 107, 127\}$, and Gaussian Mersennes $M_{G,k} = (1+i)k - 1$, $k \in \{113, 151, 157, 163, 167, 239, 241.. \}$ (the number theoretical miracle is that all the four p-adic length scales with $k \in \{151, 157, 163, 167\}$ are in the biologically highly interesting range 10 nm-2.5 μm) define scaled up copies of electro-weak and QCD type physics with ordinary value of \hbar and that these physics are induced by dark variants of each other leads to a prediction for the preferred values of $r = 2^{k_d}$, $k_d = k_i - k_j$, and the resulting picture finds support from the ensuing models for biological evolution and for EEG.

At qualitative level the model explains various strange features of high T_c superconductors. One can understand the high value of T_c and ambivalent character of high T_c superconductors, the existence of pseudogap and scalings laws for observables above T_c , the role of stripes and doping and the existence of a critical doping, etc...

Quantum Hall effect and Hierarchy of Planck Constants

I have already earlier proposed the explanation of FQHE, anyons, and fractionization of quantum numbers in terms of hierarchy of Planck constants realized as a generalization of the imbedding space $H = M^4 \times CP_2$ to a book like structure. The book like structure applies separately to CP_2 and to causal diamonds ($CD \subset M^4$) defined as intersections of future and past directed light-cones. The pages of the Big Book correspond to singular coverings and factor spaces of CD (CP_2) glued along 2-D subspace of CD (CP_2) and are labeled by the values of Planck constants assignable to CD and CP_2 and appearing in Lie algebra commutation relations. The observed Planck constant \hbar , whose square defines the scale of M^4 metric corresponds to the ratio of these Planck constants. The key observation is that fractional filling factor results if \hbar is scaled up by a rational number.

In this chapter I try to formulate more precisely this idea. The outcome is a rather detailed view about anyons on one hand, and about the Kähler structure of the generalized imbedding space on the other hand.

1. The key idea in the formulation of quantum TGD in terms of modified Dirac equation associated with Kähler action is that the Dirac determinant defined by the generalized eigenvalues assignable to the Dirac operator D_K equals to the vacuum functional defined as the exponent of Kähler function in turn identifiable as Kähler action for a preferred extremal for which second variation of Kähler action vanishes at least for the variations responsible for dynamical symmetries. The interpretation is in terms of quantum criticality. This representation generalizes. One can add imaginary instanton term to the Kähler function and corresponding modified Dirac operator: the hypothesis is that the resulting Dirac determinant equals the exponent of Kähler action and imaginary instanton term.
2. Fundamental role is played by the assumption that the Kähler gauge potential of CP_2 contains a gauge part with no physical implications in the context of gauge theories but contributing to physics in TGD framework since $U(1)$ gauge transformations are representations of symplectic transformations of CP_2 . Also in the case of CD it makes also sense to speak about Kähler gauge potential. The gauge part codes for Planck constants of CD and CP_2 and leads to the identification of anyons as states associated with partonic 2-surfaces surrounding the tip of CD and fractionization of quantum numbers. Explicit formulas relating fractionized charges to the coefficients characterizing the gauge parts of Kähler gauge potentials of CD and CP_2 are proposed based on some empirical input.
3. One important implication is that Poincare and Lorentz invariance are broken inside given CD although they remain exact symmetries at the level of the geometry of world of classical worlds (WCW). The interpretation is as a breaking of symmetries forced by the selection of quantization axis.
4. Anyons would basically correspond to matter at 2-dimensional "partonic" surfaces of macroscopic size surrounding the tip of the light-cone boundary of CD and could be regarded as

gigantic elementary particle states with very large quantum numbers and by charge fractionization confined around the tip of CD . Charge fractionization and anyons would be basic characteristic of dark matter (dark only in relative sense). Hence it is not surprising that anyons would have applications going far beyond condensed matter physics. Anyonic dark matter concentrated at 2-dimensional surfaces would play key key role in the the physics of stars and black holes, and also in the formation of planetary system via the condensation of the ordinary matter around dark matter. This assumption was the basic starting point leading to the discovery of the hierarchy of Planck constants. In living matter membrane like structures would represent a key example of anyonic systems as the model of DNA as topological quantum computer indeed assumes.

5. One of the basic questions has been whether TGD forces the hierarchy of Planck constants realized in terms of generalized imbedding space or not. The condition that the choice of quantization axes has a geometric correlate at the imbedding space level motivated by quantum classical correspondence of course forces the hierarchy: this has been clear from the beginning. It is now clear that first principle description of anyons requires the hierarchy in TGD Universe. The hierarchy reveals also new light to the huge vacuum degeneracy of TGD and reduces it dramatically at pages for which CD corresponds to a non-trivial covering or factor space, which suggests that mathematical existence of the theory necessitates the hierarchy of Planck constants.

Bibliography

Books about TGD

- [1] M. Pitkänen (2006), *Topological Geometroynamics: Overview*.
http://tgd.wippiespace.com/public_html/tgdview/tgdview.html.
- [2] M. Pitkänen (2006), *Quantum Physics as Infinite-Dimensional Geometry*.
http://tgd.wippiespace.com/public_html/tgdgeom/tgdgeom.html.
- [3] M. Pitkänen (2006), *Physics in Many-Sheeted Space-Time*.
http://tgd.wippiespace.com/public_html/tgdclass/tgdclass.html.
- [4] M. Pitkänen (2006), *p-Adic length Scale Hypothesis and Dark Matter Hierarchy*.
http://tgd.wippiespace.com/public_html/paddark/paddark.html.
- [5] M. Pitkänen (2006), *Quantum TGD*.
http://tgd.wippiespace.com/public_html/tgdquant/tgdquant.html.
- [6] M. Pitkänen (2006), *TGD as a Generalized Number Theory*.
http://tgd.wippiespace.com/public_html/tgdnumber/tgdnumber.html.
- [7] M. Pitkänen (2006), *TGD and Fringe Physics*.
http://tgd.wippiespace.com/public_html/freenergy/freenergy.html.

Books about TGD Inspired Theory of Consciousness and Quantum Biology

- [8] M. Pitkänen (2006), *TGD Inspired Theory of Consciousness*.
http://tgd.wippiespace.com/public_html/tgdconsc/tgdconsc.html.
- [9] M. Pitkänen (2006), *Bio-Systems as Self-Organizing Quantum Systems*.
http://tgd.wippiespace.com/public_html/bioselforg/bioselforg.html.
- [10] M. Pitkänen (2006), *Quantum Hardware of Living Matter*.
http://tgd.wippiespace.com/public_html/bioware/bioware.html.
- [11] M. Pitkänen (2006), *Bio-Systems as Conscious Holograms*.
http://tgd.wippiespace.com/public_html/hologram/hologram.html.
- [12] M. Pitkänen (2006), *Genes and Memes*.
http://tgd.wippiespace.com/public_html/genememe/genememe.html.
- [13] M. Pitkänen (2006), *Magnetospheric Consciousness*.
http://tgd.wippiespace.com/public_html/magnconsc/magnconsc.html.
- [14] M. Pitkänen (2006), *Mathematical Aspects of Consciousness Theory*.
http://tgd.wippiespace.com/public_html/mathconsc/mathconsc.html.
- [15] M. Pitkänen (2006), *TGD and EEG*.
http://tgd.wippiespace.com/public_html/tgdeeg/tgdeeg.html.

References to the chapters of the books about TGD

- [16] The chapter *TGD as a Generalized Number Theory: Quaternions, Octonions, and their Hyper Counterparts* of [6].
http://tgd.wippiespace.com/public_html/tgdnumber/tgdnumber.html#visionb.
- [17] The chapter *TGD as a Generalized Number Theory: p-Adicization Program* of [6].
http://tgd.wippiespace.com/public_html/tgdnumber/tgdnumber.html#visiona.
- [18] The chapter *Dark Forces and Living Matter* of [4].
http://tgd.wippiespace.com/public_html/paddark/paddark.html#darkforces.
- [19] M. Pitkänen (2006), *Physics in Many-Sheeted Space-Time*.
http://tgd.wippiespace.com/public_html/tgdclass/tgdclass.html.
- [20] The chapter *Was von Neumann Right After All* of [5].
http://tgd.wippiespace.com/public_html/tgdquant/tgdquant.html#vNeumann.
- [21] The chapter *TGD and Astrophysics* of [3].
http://tgd.wippiespace.com/public_html/tgdclass/tgdclass.html#astro.

References to the chapters of the books about TGD Inspired Theory of Consciousness and Quantum Biology

- [22] The chapter *Many-Sheeted DNA* of [12].
http://tgd.wippiespace.com/public_html/genememe/genememe.html#genecodec.
- [23] The chapter *Topological Quantum Computation in TGD Universe* of [12].
http://tgd.wippiespace.com/public_html/genememe/genememe.html#tqc.
- [24] The chapter *Dark Matter Hierarchy and Hierarchy of EEGs* of [15].
http://tgd.wippiespace.com/public_html/tgdeeg/tgdeeg.html#eegdark.
- [25] The chapter *Quantum Theory of Self-Organization* of [9].
http://tgd.wippiespace.com/public_html/bioselforg/bioselforg.html#selforgac.
- [26] The chapter *Genes and Memes* of [12].
http://tgd.wippiespace.com/public_html/genememe/genememe.html#genememec.

Articles related to TGD

- [27] Pitkänen, M. (1983) International Journal of Theor. Phys. ,22, 575.

Mathematics

- [28] T. Eguchi, B. Gilkey, J. Hanson (1980). Phys. Rep. 66, 6, 1980.
- [29] Wallace (1968): *Differential Topology*. W. A. Benjamin, New York.
- [30] Spivak, M. (1970): *Differential Geometry I,II,III,IV*. Publish or Perish. Boston.
- [31] Hawking, S.,W. and Pope, C., N. (1978): *Generalized Spin Structures in Quantum Gravity*. Physics Letters Vol 73 B, no 1.
- [32] Thom, R. (1954): Commentarii Math. Helvet., 28, 17.
- [33] Eisenhart (1964), *Riemannian Geometry*. Princeton University Press.

-
- [34] G. W. Gibbons, C. N. Pope (1977): *CP₂ as gravitational instanton*. Commun. Math. Phys. 55, 53.
- [35] Milnor, J. (1965): *Topology from Differential Point of View*. The University Press of Virginia.
- [36] Pope, C., N. (1980): *Eigenfunctions and Spin^c Structures on CP₂* D.A.M.T.P. preprint.

Cosmology and astrophysics

- [37] D. Da Roacha and L. Nottale (2003), *Gravitational Structure Formation in Scale Relativity*. astro-ph/0310036.

Part I

**P-ADIC DESCRIPTION OF
PARTICLE MASSIVATION**

Chapter 2

Overall View About TGD from Particle Physics Perspective

2.1 Introduction

Topological Geometroynamics is able to make rather precise and often testable predictions. In this and two other articles I want to describe the recent over all view about the aspects of quantum TGD relevant for particle physics.

During these 32 years TGD has become quite an extensive theory involving also applications to quantum biology and quantum consciousness theory. Therefore it is difficult to decide in which order to proceed. Should one represent first the purely mathematical theory as done in the articles in Prespacetime Journal [34]? Or should one start from the TGD inspired heuristic view about space-time and particle physics and represent the vision about construction of quantum TGD briefly after that? In this and other two chapters I have chosen the latter approach since the emphasis is on the applications on particle physics.

Second problem is to decide about how much material one should cover. If the representation is too brief no-one understands and if it is too detailed no-one bothers to read. I do not know whether the outcome was a success or whether there is any way to success but in any case I have been sweating a lot in trying to decide what would be the optimum dose of details.

In the first chapter I concentrate the heuristic picture about TGD with emphasis on particle physics.

- First I represent briefly the basic ontology: the motivations for TGD and the notion of many-sheeted space-time, the concept of zero energy ontology, the identification of dark matter in terms of hierarchy of Planck constant which now seems to follow as a prediction of quantum TGD, the motivations for p-adic physics and its basic implications, and the identification of space-time surfaces as generalized Feynman diagrams and the basic implications of this identification.
- Symmetries of quantum TGD are discussed. Besides the basic symmetries of the imbedding space geometry allowing to geometrize standard model quantum numbers and classical fields there are many other symmetries. General Coordinate Invariance is especially powerful in TGD framework allowing to realize quantum classical correspondence and implies effective 2-dimensionality realizing strong form of holography. Super-conformal symmetries of super string models generalize to conformal symmetries of 3-D light-like 3-surfaces and one can understand the generalization of Equivalence Principle in terms of coset representations for the two super Virasoro algebras associated with lightlike boundaries of so called causal diamonds defined as intersections of future and past directed lightcones (*CDs*) and with light-like 3-surfaces. Super-conformal symmetries imply generalization of the space-time supersymmetry in TGD framework consistent with the supersymmetries of minimal supersymmetric variant of the standard model. Twistorial approach to gauge theories has gradually become part of quantum TGD and the natural generalization of the Yangian symmetry identified originally as symmetry of $\mathcal{N} = 4$ SYMs is postulated as basic symmetry of quantum TGD.

- The so called weak form of electric-magnetic duality has turned out to have extremely far reaching consequences and is responsible for the recent progress in the understanding of the physics predicted by TGD. The duality leads to a detailed identification of elementary particles as composite objects of massless particles and predicts new electro-weak physics at LHC. Together with a simple postulate about the properties of preferred extremals of Kähler action the duality allows also to realized quantum TGD as almost topological quantum field theory giving excellent hopes about integrability of quantum TGD.
- There are two basic visions about the construction of quantum TGD. Physics as infinite-dimensional Kähler geometry of world of classical worlds (WCW) endowed with spinor structure and physics as generalized number theory. These visions are briefly summarized as also the practical constructing involving the concept of Dirac operator. As a matter fact, the construction of TGD involves three Dirac operators. The Kähler Dirac equation holds true in the interior of space-time surface and its solutions have a natural interpretation in terms of description of matter, in particular condensed matter. Chern-Simons Dirac action is associated with the light-like 3-surfaces and space-like 3-surfaces at ends of space-time surface at light-like boundaries of CD . One can assign to it a generalized eigenvalue equation and the matrix valued eigenvalues correspond to the action of Dirac operator on momentum eigenstates. Momenta are however not usual momenta but pseudo-momenta very much analogous to region momenta of twistor approach. The third Dirac operator is associated with super Virasoro generators and super Virasoro conditions define Dirac equation in WCW. These conditions characterize zero energy states as modes of WCW spinor fields and code for the generalization of S -matrix to a collection of what I call M -matrices defining the rows of unitary U -matrix defining unitary process.
- Twistor approach has inspired several ideas in quantum TGD during the last years and it seems that the Yangian symmetry and the construction of scattering amplitudes in terms of Grassmannian integrals generalizes to TGD framework. This is due to ZEO allowing to assume that all particles have massless fermions as basic building blocks. ZEO inspires the hypothesis that incoming and outgoing particles are bound states of fundamental fermions associated with wormhole throats. Virtual particles would also consist of on mass shell massless particles but without bound state constraint. This implies very powerful constraints on loop diagrams and there are excellent hopes about their finiteness. Twistor approach also inspires the conjecture that quantum TGD allows also formulation in terms of 6-dimensional holomorphic surfaces in the product $CP_3 \times CP_3$ of two twistor spaces and general arguments allow to identify the partial differential equations satisfied by these surfaces.

The discussion of this chapter is rather sketchy and the reader interesting in details can consult the books about TGD [1, 2, 3, 5, 6, 4, 39].

2.2 Some aspects of quantum TGD

In the following I summarize very briefly those basic notions of TGD which are especially relevant for the applications to particle physics. The representation will be practically formula free. The article series published in Prespacetime Journal [34] describes the mathematical theory behind TGD. The seven books about TGD [1, 2, 3, 4, 6, 5, 7] provide a detailed summary about the recent state of TGD.

2.2.1 New space-time concept

The physical motivation for TGD was what I have christened the energy problem of General Relativity. The notion of energy is ill-defined because the basic symmetries of empty space-time are lost in the presence of gravity. The way out is based on assumption that space-times are imbeddable as 4-surfaces to certain 8-dimensional space by replacing the points of 4-D empty Minkowski space with 4-D very small internal space. This space -call it S - is unique from the requirement that the theory has the symmetries of standard model: $S = CP_2$, where CP_2 is complex projective space with 4 real dimensions [49], is the unique choice.

The replacement of the abstract manifold geometry of general relativity with the geometry of surfaces brings the shape of surface as seen from the perspective of 8-D space-time and this means additional degrees of freedom giving excellent hopes of realizing the dream of Einstein about geometrization of fundamental interactions.

The work with the generic solutions of the field equations assignable to almost any general coordinate invariant variational principle led soon to the realization that the space-time in this framework is much more richer than in general relativity.

1. Space-time decomposes into space-time sheets with finite size: this lead to the identification of physical objects that we perceive around us as space-time sheets. For instance, the outer boundary of the table is where that particular space-time sheet ends. Besides sheets also string like objects and elementary particle like objects appear so that TGD can be regarded also as a generalization of string models obtained by replacing strings with 3-D surfaces.
2. Elementary particles are identified as topological inhomogenities glued to these space-time sheets. In this conceptual framework material structures and shapes are not due to some mysterious substance in slightly curved space-time but reduce to space-time topology just as energy-momentum currents reduce to space-time curvature in general relativity.
3. Also the view about classical fields changes. One can assign to each material system a field identity since electromagnetic and other fields decompose to topological field quanta. Examples are magnetic and electric flux tubes and flux sheets and topological light rays representing light propagating along tube like structure without dispersion and dissipation making em ideal tool for communications [40]. One can speak about field body or magnetic body of the system.

Field body indeed becomes the key notion distinguishing TGD inspired model of quantum biology from competitors but having applications also in particle physics since also leptons and quarks possess field bodies. The is evidence for the Lamb shift anomaly of muonic hydrogen [54] and the color magnetic body of u quark whose size is somewhat larger than the Bohr radius could explain the anomaly [20].

2.2.2 Zero energy ontology

In standard ontology of quantum physics physical states are assumed to have positive energy. In zero energy ontology physical states decompose to pairs of positive and negative energy states such that all net values of the conserved quantum numbers vanish. The interpretation of these states in ordinary ontology would be as transitions between initial and final states, physical events. By quantum classical correspondences zero energy states must have space-time and imbedding space correlates.

1. Positive and negative energy parts reside at future and past light-like boundaries of causal diamond (CD) defined as intersection of future and past directed light-cones and visualizable as double cone. The analog of CD in cosmology is big bang followed by big crunch. CD s for a fractal hierarchy containing CD s within CD s. Disjoint CD s are possible and CD s can also intersect.
2. p-Adic length scale hypothesis [20] motivates the hypothesis that the temporal distances between the tips of the intersecting light-cones come as octaves $T = 2^n T_0$ of a fundamental time scale T_0 defined by CP_2 size R as $T_0 = R/c$. One prediction is that in the case of electron this time scale is .1 seconds defining the fundamental biorhythm. Also in the case u and d quarks the time scales correspond to biologically important time scales given by 10 ms for u quark and by and 2.5 ms for d quark [45]. This means a direct coupling between microscopic and macroscopic scales.

Zero energy ontology conforms with the crossing symmetry of quantum field theories meaning that the final states of the quantum scattering event are effectively negative energy states. As long as one can restrict the consideration to either positive or negative energy part of the state ZEO is consistent with positive energy ontology. This is the case when the observer characterized by a particular CD studies the physics in the time scale of much larger CD containing observer's CD as a sub- CD . When the time scale sub- CD of the studied system is much shorter than the time scale of

sub- CD characterizing the observer, the interpretation of states associated with sub- CD is in terms of quantum fluctuations.

ZEO solves the problem which results in any theory assuming symmetries giving rise to conservation laws. The problem is that the theory itself is not able to characterize the values of conserved quantum numbers of the initial state. In ZEO this problem disappears since in principle any zero energy state is obtained from any other state by a sequence of quantum jumps without breaking of conservation laws. The fact that energy is not conserved in general relativity based cosmologies can be also understood since each CD is characterized by its own conserved quantities. As a matter fact, one must be speak about average values of conserved quantities since one can have a quantum superposition of zero energy states with the quantum numbers of the positive energy part varying over some range.

For thermodynamical states this is indeed the case and this leads to the idea that quantum theory in ZEO can be regarded as a "complex square root" of thermodynamics obtained as a product of positive diagonal square root of density matrix and unitary S -matrix. M -matrix defines time-like entanglement coefficients between positive and negative energy parts of the zero energy state and replaces S -matrix as the fundamental observable. In standard quantum measurement theory this time-like entanglement would be reduced in quantum measurement and regenerated in the next quantum jump if one accepts Negentropy Maximization Principle (NMP) [45] as the fundamental variational principle. Various M -matrices define the rows of the unitary U matrix characterizing the unitary process part of quantum jump. From the point of view of consciousness theory the importance of ZEO is that conservation laws in principle pose no restrictions for the new realities created in quantum jumps: free will is maximal.

2.2.3 The hierarchy of Planck constants

The motivations for the hierarchy of Planck constants come from both astrophysics and biology [27, 43]. In astrophysics the observation of Nottale [78] that planetary orbits in solar system seem to correspond to Bohr orbits with a gigantic gravitational Planck constant motivated the proposal that Planck constant might not be constant after all [38, 27].

This led to the introduction of the quantization of Planck constant as an independent postulate. It has however turned that quantized Planck constant in effective sense could emerge from the basic structure of TGD alone. Canonical momentum densities and time derivatives of the imbedding space coordinates are the field theory analogs of momenta and velocities in classical mechanics. The extreme non-linearity and vacuum degeneracy of Kähler action imply that the correspondence between canonical momentum densities and time derivatives of the imbedding space coordinates is 1-to-many: for vacuum extremals themselves 1-to-infinite.

A convenient technical manner to treat the situation is to replace imbedding space with its n -fold singular covering. Canonical momentum densities to which conserved quantities are proportional would be same at the sheets corresponding to different values of the time derivatives. At each sheet of the covering Planck constant is effectively $\hbar = n\hbar_0$. This splitting to multisheeted structure can be seen as a phase transition reducing the densities of various charges by factor $1/n$ and making it possible to have perturbative phase at each sheet (gauge coupling strengths are proportional to $1/\hbar$ and scaled down by $1/n$). The connection with fractional quantum Hall effect [67] is almost obvious. At the more detailed level one finds that the spectrum of Planck constants would be given by $\hbar = n_a n_b \hbar_0$ [39].

This has many profound implications, which are wellcome from the point of view of quantum biology but the implications would be profound also from particle physics perspective and one could say that living matter represents zoomed up version of quantum world at elementary particle length scales.

1. Quantum coherence and quantum superposition become possible in arbitrary long length scales. One can speak about zoomed up variants of elementary particles and zoomed up sizes make it possible to satisfy the overlap condition for quantum length parameters used as a criterion for the presence of macroscopic quantum phases. In the case of quantum gravitation the length scale involved are astrophysical. This would conform with Penrose's intuition that quantum gravity is fundamental for the understanding of consciousness and also with the idea that consciousness cannot be localized to brain.

2. Photons with given frequency can in principle have arbitrarily high energies by $E = hf$ formula, and this would explain the strange anomalies associated with the interaction of ELF em fields with living matter [113]. Quite generally the cyclotron frequencies which correspond to energies much below the thermal energy for ordinary value of Planck constant could correspond to energies above thermal threshold.
3. The value of Planck constant is a natural characterizer of the evolutionary level and biological evolution would mean a gradual increase of the largest Planck constant in the hierarchy characterizing given quantum system. Evolutionary leaps would have interpretation as phase transitions increasing the maximal value of Planck constant for evolving species. The space-time correlate would be the increase of both the number and the size of the sheets of the covering associated with the system so that its complexity would increase.
4. The phase transitions changing Planck constant change also the length of the magnetic flux tubes. The natural conjecture is that biomolecules form a kind of Indra's net connected by the flux tubes and \hbar changing phase transitions are at the core of the quantum bio-dynamics. The contraction of the magnetic flux tube connecting distant biomolecules would force them near to each other making possible for the bio-catalysis to proceed. This mechanism could be central for DNA replication and other basic biological processes. Magnetic Indra's net could be also responsible for the coherence of gel phase and the phase transitions affecting flux tube lengths could induce the contractions and expansions of the intracellular gel phase. The reconnection of flux tubes would allow the restructuring of the signal pathways between biomolecules and other subsystems and would be also involved with ADP-ATP transformation inducing a transfer of negentropic entanglement [43]. The braiding of the magnetic flux tubes could make possible topological quantum computation like processes and analog of computer memory realized in terms of braiding patterns[44].
5. p-Adic length scale hypothesis and hierarchy of Planck constants suggest entire hierarchy of zoomed up copies of standard model physics with range of weak interactions and color forces scaling like \hbar . This is not conflict with the known physics for the simple reason that we know very little about dark matter (partly because we might be making misleading assumptions about its nature). One implication is that it might be someday to study zoomed up variants particle physics at low energies using dark matter.

Dark matter would make possible the large parity breaking effects manifested as chiral selection of bio-molecules [45]. What is required is that classical Z^0 and W fields responsible for parity breaking effects are present in cellular length scale. If the value of Planck constant is so large that weak scale is some biological length scale, weak fields are effectively massless below this scale and large parity breaking effects become possible.

For the solutions of field equations which are almost vacuum extremals Z^0 field is non-vanishing and proportional to electromagnetic field. The hypothesis that cell membrane corresponds to a space-time sheet near a vacuum extremal (this corresponds to criticality very natural if the cell membrane is to serve as an ideal sensory receptor) leads to a rather successful model for cell membrane as sensory receptor with lipids representing the pixels of sensory qualia chart. The surprising prediction is that bio-photons [64] and bundles of EEG photons can be identified as different decay products of dark photons with energies of visible photons. Also the peak frequencies of sensitivity for photoreceptors are predicted correctly [27].

2.2.4 p-Adic physics and number theoretic universality

p-Adic physics [19, 4] has become gradually a key piece of TGD inspired biophysics. Basic quantitative predictions relate to p-adic length scale hypothesis and to the notion of number theoretic entropy. Basic ontological ideas are that life resides in the intersection of real and p-adic worlds and that p-adic space-time sheets serve as correlates for cognition and intentionality. Number theoretical universality requires the fusion of real physics and various p-adic physics to single coherent whole. On implication is the generalization of the notion of number obtained by fusing real and p-adic numbers to a larger structure.

p-Adic number fields

p-Adic number fields Q_p [82] -one for each prime p - are analogous to reals in the sense that one can speak about p-adic continuum and that also p-adic numbers are obtained as completions of the field of rational numbers. One can say that rational numbers belong to the intersection of real and p-adic numbers. p-Adic number field Q_p allows also an infinite number of its algebraic extensions. Also transcendental extensions are possible. For reals the only extension is complex numbers.

p-Adic topology defining the notions of nearness and continuity differs dramatically from the real topology. An integer which is infinite as a real number can be completely well defined and finite as a p-adic number. In particular, powers p^n of prime p have p-adic norm (magnitude) equal to p^{-n} in Q_p so that at the limit of very large n real magnitude becomes infinite and p-adic magnitude vanishes.

p-Adic topology is rough since p-adic distance $d(x, y) = d(x - y)$ depends on the lowest binary digit of $x - y$ only and is analogous to the distance between real points when approximated by taking into account only the lowest digit in the decimal expansion of $x - y$. A possible interpretation is in terms of a finite measurement resolution and resolution of sensory perception. p-Adic topology looks somewhat strange. For instance, p-adic spherical surface is not infinitely thin but has a finite thickness and p-adic surfaces possess no boundary in the topological sense. Ultrametricity is the technical term characterizing the basic properties of p-adic topology and is coded by the inequality $d(x - y) \leq \text{Min}\{d(x), d(y)\}$. p-Adic topology brings in mind the decomposition of perceptive field to objects.

Motivations for p-adic number fields

The physical motivations for p-adic physics came from the observation that p-adic thermodynamics -not for energy but infinitesimal scaling generator of so called super-conformal algebra [70] acting as symmetries of quantum TGD [2]- predicts elementary particle mass scales and also masses correctly under very general assumptions [4]. The calculations are discussed in more detail in the second article of the series. In particular, the ratio of proton mass to Planck mass, the basic mystery number of physics, is predicted correctly. The basic assumption is that the preferred primes characterizing the p-adic number fields involved are near powers of two: $p \simeq 2^k$, k positive integer. Those nearest to power of two correspond to Mersenne primes $M_n = 2^n - 1$. One can also consider complex primes known as Gaussian primes, in particular Gaussian Mersennes $M_{G,n} = (1 + i)^n - 1$.

It turns out that Mersennes and Gaussian Mersennes are in a preferred position physically in TGD based world order. What is especially interesting that the length scale range 10 nm-2.5 μ assignable to DNA contains as many as 4 Gaussian Mersennes corresponding to $n = 151, 157, 163, 167$ [27]. This number theoretical miracle supports the view that p-adic physics is especially important for the understanding of living matter.

The philosophical for p-adic numbers fields come from the question about the possible physical correlates of cognition and intention [53]. Cognition forms representations of the external world which have finite cognitive resolution and the decomposition of the perceptive field to objects is an essential element of these representations. Therefore p-adic space-time sheets could be seen as candidates of thought bubbles, the mind stuff of Descartes. One can also consider p-adic space-time sheets as correlates of intentions. The quantum jump in which p-adic space-time sheet is replaced with a real one could serve as a quantum correlate of intentional action. This process is forbidden by conservation laws in standard ontology: one cannot even compare real and p-adic variants of the conserved quantities like energy in the general case. In zero energy ontology the net values of conserved quantities for zero energy states vanish so that conservation laws allow these transitions.

Rational numbers belong to the intersection of real and p-adic continua. An obvious generalization of this statement applies to real manifolds and their p-adic variants. When extensions of p-adic numbers are allowed, also some algebraic numbers can belong to the intersection of p-adic and real worlds. The notion of intersection of real and p-adic worlds has actually two meanings.

1. The intersection could consist of the rational and possibly some algebraic points in the intersection of real and p-adic partonic 2-surfaces at the ends of CD . This set is in general discrete. The interpretation could be as discrete cognitive representations.
2. The intersection could also have a more abstract meaning. For instance, the surfaces defined by rational functions with rational coefficients have a well-defined meaning in both real and p-adic

context and could be interpreted as belonging to this intersection. There is strong temptation to assume that intentions are transformed to actions only in this intersection. One could say that life resides in the intersection of real and p-adic worlds in this abstract sense.

Additional support for the idea comes from the observation that Shannon entropy $S = -\sum p_n \log(p_n)$ allows a p-adic generalization if the probabilities are rational numbers by replacing $\log(p_n)$ with $-\log(|p_n|_p)$, where $|x|_p$ is p-adic norm. Also algebraic numbers in some extension of p-adic numbers can be allowed. The unexpected property of the number theoretic Shannon entropy is that it can be negative and its unique minimum value as a function of the p-adic prime p it is always negative. Entropy transforms to information!

In the case of number theoretic entanglement entropy there is a natural interpretation for this. Number theoretic entanglement entropy would measure the information carried by the entanglement whereas ordinary entanglement entropy would characterize the uncertainty about the state of either entangled system. For instance, for p maximally entangled states both ordinary entanglement entropy and number theoretic entanglement negentropy are maximal with respect to R_p norm. Entanglement carries maximal information. The information would be about the relationship between the systems, a rule. Schrödinger cat would be dead enough to know that it is better to not open the bottle completely.

Negentropy Maximization Principle [45] coding the basic rules of quantum measurement theory implies that negentropic entanglement can be stable against the effects of quantum jumps unlike entropic entanglement. Therefore living matter could be distinguished from inanimate matter also by negentropic entanglement possible in the intersection of real and p-adic worlds. In consciousness theory negentropic entanglement could be seen as a correlate for the experience of understanding or any other positively colored experience, say love.

Negentropically entangled states are stable but binding energy and effective loss of relative translational degrees of freedom is not responsible for the stability. Therefore bound states are not in question. The distinction between negentropic and bound state entanglement could be compared to the difference between unhappy and happy marriage. The first one is a social jail but in the latter case both parties are free to leave but do not want to. The special characteristics of negentropic entanglement raise the question whether the problematic notion of high energy phosphate bond [111] central for metabolism could be understood in terms of negentropic entanglement. This would also allow an information theoretic interpretation of metabolism since the transfer of metabolic energy would mean a transfer of negentropy [43].

2.3 Symmetries of quantum TGD

Symmetry principles play key role in the construction of WCW geometry have become and deserve a separate explicit treatment even at the risk of repetitions.

2.3.1 General Coordinate Invariance

General coordinate invariance is certainly of the most important guidelines and is much more powerful in TGD framework than in GRT context.

1. General coordinate transformations as a gauge symmetry so that the diffeomorphic slices of space-time surface equivalent physically. 3-D light-like 3-surfaces defined by wormhole throats define preferred slices and allows to fix the gauge partially apart from the remaining 3-D variant of general coordinate invariance and possible gauge degeneracy related to the choice of the light-like 3-surface due to the Kac-Moody invariance. This would mean that the random light-likeness represents gauge degree of freedom except at the ends of the light-like 3-surfaces.
2. GCI can be strengthened so that the pairs of space-like ends of space-like 3-surfaces at CD s are equivalent with light-like 3-surfaces connecting them. The outcome is effective 2-dimensionality because their intersections at the boundaries of CD s must carry the physically relevant information.

2.3.2 Generalized conformal symmetries

One can assign Kac-Moody type conformal symmetries to light-like 3-surfaces as isometries of H localized with respect to light-like 3-surfaces. Kac Moody algebra essentially the Lie algebra of gauge group with central extension meaning that projective representation in which representation matrices are defined only modulo a phase factor. Kac-Moody symmetry is not quite a pure gauge symmetry.

One can assign a generalization of Kac-Moody symmetries to the boundaries of CD by replacing Lie-group of Kac Moody algebra with the group of symplectic (contact-) transformations [72] of H_+ provided with a degenerate Kähler structure made possible by the effective 2-dimensionality of δM_+^4 . The light-like radial coordinate of δM_+^4 plays the role of the complex coordinate of conformal transformations or their hyper-complex analogs. These symmetries are also localized with respect to the internal coordinates of the partonic 2-surface so that rather huge symmetry group is in question. The basic hypothesis is that these transformations with possible some restrictions on the dependence on the coordinates of X^2 define the isometries of WCW .

A further physically well-motivated hypothesis inspired by holography and extended GCI is that these symmetries extend so that they apply at the entire space-time sheet. This requires the slicing of space-time surface by partonic 2- surfaces and by stringy world sheets such that each point of stringy world sheet defines a partonic 2-surface and vice versa. This slicing has deep physical motivations since it realizes geometrically standard facts about gauge invariance (partonic 2-surface defines the space of physical polarizations and stringy space-time sheet corresponds to non-physical polarizations) and its existence is a hypothesis about the properties of the preferred extremals of Kähler action. There is a similar decomposition also at the level of CD and so called Hamilton-Jacobi coordinates for M_+^4 [36] define this kind of slicings. This slicing can induced the slicing of the space-time sheet. The number theoretic vision gives a further justification for this hypothesis and also strengthens it by postulating the presence of the preferred time direction having interpretation in terms of real unit of octonions. In ZEO this time direction corresponds to the time-like vector connecting the tips of CD .

Conformal symmetries would provide the realization of WCW as a union of symmetric spaces. Symmetric spaces are coset spaces of form G/H . The natural identification of G and H is as groups of X^2 -local symplectic transformations and local Kac-Moody group of X^2 -local H isometries. Quantum fluctuating (metrically non-trivial) degrees of freedom would correspond to symplectic transformations of H_+ and induced Kähler form at X^2 would define a local representation for zero modes: not necessarily all of them.

2.3.3 Equivalence Principle and super-conformal symmetries

Equivalence Principle (EP) is a second corner stone of General Relativity and together with GCI leads to Einstein's equations. What EP states is that inertial and gravitational masses are identical. In this form it is not well-defined even in GRT since the definition of gravitational and inertial four-momenta is highly problematic because Noether theorem is not available. The realization is in terms of local equations identifying energy momentum tensor with Einstein tensor.

Whether EP is realized in TGD has been a longstanding open question[35]. The problem has been that at the classical level EP in its GRT form can hold true only in long enough length scales and it took long time to realize that only the stringy form of this principle is required. The first question is how to identify the gravitational and inertial four-momenta. This is indeed possible. One can assign to the two types super-conformal symmetries assigned with light-like 3-surfaces and space-like 3-surfaces four-momenta to both. EP states that these four momenta are identical and is equivalent with the generalization of GCI and effective 2-dimensionality. The condition generalizes so that it applies to the generators of super-conformal algebras associated with the two super-conformal symmetries. This leads to a generalization of a standard mathematical construction of super-conformal theories known as coset representation [61]. What the construction states is that the differences of super-conformal generators defined by super-symmetric algebra and Kac-Moody algebra annihilate physical states.

2.3.4 Extension to super-conformal symmetries

The original idea behind the extension of conformal symmetries to super-conformal symmetries was the observation that isometry currents defining infinitesimal isometries of WCW have natural super-counterparts obtained by contracting the Killing vector fields with the complexified gamma matrices

of the imbedding space.

This vision has generalized considerably as the construction of WCW spinor structure in terms of modified Dirac action has developed. The basic philosophy behind this idea is that configuration space spinor structure must relate directly to the fermionic sector of quantum physics. In particular, modified gamma matrices should be expressible in terms of the fermionic oscillator operators associated with the second quantized induced spinor fields. The explicit realization of this program leads to an identification of rich spectrum of super-conformal symmetries and generalization of the ordinary notion of space-time supersymmetry. What happens that all fermionic oscillator operator generate broken super-symmetries whereas in SUSYs there is only finite number of them. One can however identify sub-algebra of super-conformal symmetries associated with right handed neutrino and this gives $\mathcal{N} = 1$ super-symmetry [90] of SUSYs [23].

2.3.5 Space-time supersymmetry in TGD Universe

It has been clear from the beginning that the notion of super-conformal symmetry crucial for the successes of super-string models generalizes in TGD framework. The answer to the question whether space-time SUSY makes sense in TGD framework has not been obvious at all but it seems now that the answer is affirmative. The evolution of the ideas relevant for the formulation of SUSY in TGD framework is summarized in the chapters of [5]. The chapters devoted to the notion of bosonic emergence [25], to the SUSY QFT limit of TGD [23], to twistor approach to TGD [30], and to the generalization of Yangian symmetry of $\mathcal{N} = 4$ SYM manifest in the Grassmannian twistor approach [97] to a multi-local variant of super-conformal symmetries [19] represent a gradual development of the ideas about how super-symmetric M -matrix could be constructed in TGD framework. A warning to the reader is in order. In their recent form these chapters do not represent the final outcome but just an evolution of ideas proceeding by trial and error. There are however good reasons to believe that the chapter about Yangian symmetry is nearest to the correct physical interpretation and mathematical formulation.

Contrary to the original expectations, TGD seems to allow a generalization of the space-time super-symmetry. This became clear with the increased understanding of the modified Dirac action [33, 55, 37]. The appearance of the momentum and color quantum numbers in the measurement interaction part of the modified Dirac action associated with the light-like wormhole throats [55] couples space-time degrees of freedom to quantum numbers and allows also to define SUSY algebra at fundamental level as anti-commutation relations of fermionic oscillator operators. Depending on the situation $\mathcal{N} = 2N$ SUSY algebra (an inherent cutoff on the number of fermionic modes at light-like wormhole throat) or fermionic part of super-conformal algebra with infinite number of oscillator operators results. The addition of fermion in particular mode would define particular super-symmetry. This super-symmetry is badly broken due to the dynamics of the modified Dirac operator which also mixes M^4 chiralities inducing massivation. Since right-handed neutrino has no electro-weak couplings the breaking of the corresponding super-symmetry should be weakest.

Zero energy ontology combined with the analog of the twistor approach to $\mathcal{N} = 4$ SYMs and weak form of electric-magnetic duality has actually led to this kind of formulation [19]. What is new that also virtual particles have massless fermions as their building blocks. This implies manifest finiteness of loop integrals so that the situation simplifies dramatically. What is also new element that physical particles and also string like objects correspond to bound states of massless fermions.

The question is whether this SUSY has a realization as a SUSY algebra at space-time level and whether the QFT limit of TGD could be formulated as a generalization of SUSY QFT. There are several problems involved.

1. In TGD framework super-symmetry means addition of fermion to the state and since the number of spinor modes is larger states with large spin and fermion numbers are obtained. This picture does not fit to the standard view about super-symmetry. In particular, the identification of theta parameters as Majorana spinors and super-charges as Hermitian operators is not possible.
2. The belief that Majorana spinors are somehow an intrinsic aspect of super-symmetry is however only a belief. Weyl spinors meaning complex theta parameters are also possible. Theta parameters can also carry fermion number meaning only the supercharges carry fermion number and are non-hermitian. The general classification of super-symmetric theories indeed demonstrates

that for $D = 8$ Weyl spinors and complex and non-hermitian super-charges are possible. The original motivation for Majorana spinors might come from MSSM assuming that right handed neutrino does not exist. This belief might have also led to string theories in $D = 10$ and $D = 11$ as the only possible candidates for TOE after it turned out that chiral anomalies cancel. It indeed turns out that TGD view about space-time SUSY is internally consistent. Even more, the separate conservation of quark and lepton number is essential for the internal consistency of this view [23].

3. The massivation of particles is the basic problem of both SUSYs and twistor approach. I have discussed several solutions to this problem [30, 19]. The simplest and most convincing solution of the problem is following and inspired by twistor Grassmannian approach to $\mathcal{N} = 4$ SYM and the generalization of the Yangian symmetry of this theory. In zero energy ontology one can construct physical particles as bound states of massless particles associated with the opposite wormhole throats. If the particles have opposite 3-momenta the resulting state is automatically massive. In fact, this forces massivation of also spin one bosons since the fermion and antifermion must move in opposite directions for their spins to be parallel so that the net mass is non-vanishing: note that this means that even photon, gluons, and graviton have small mass. This mechanism makes topologically condensed fermions massive and p-adic thermodynamics allows to describe the massivation in terms of zero energy states and M -matrix. Bosons receive to their mass besides the small mass coming from thermodynamics also a contribution which is counterpart of the contribution coming from Higgs vacuum expectation value and Higgs gives rise to longitudinal polarizations. No Higgs potential is however needed. The cancellation of infrared divergences necessary for exact Yangian symmetry and the observation that even photon receives small mass suggest that scalar Higgs would disappear completely from the spectrum.

Basic data bits

Let us first summarize the data bits about possible relevance of super-symmetry for TGD before the addition of the 3-D measurement interaction term to the modified Dirac action [33, 55].

1. Right-handed covariantly constant neutrino spinor ν_R defines a super-symmetry in CP_2 degrees of freedom in the sense that Dirac equation is satisfied by covariant constancy and there is no need for the usual ansatz $\Psi = D\Psi_0$ giving $D^2\Psi = 0$. This super-symmetry allows to construct solutions of Dirac equation in CP_2 [44, 17, 47, 45].
2. In $M^4 \times CP_2$ this means the existence of massless modes $\Psi = \not{p}\Psi_0$, where Ψ_0 is the tensor product of M^4 and CP_2 spinors. For these solutions M^4 chiralities are not mixed unlike for all other modes which are massive and carry color quantum numbers depending on the CP_2 chirality and charge. As matter fact, covariantly constant right-handed neutrino spinor mode is the only color singlet. The mechanism leading to non-colored states for fermions is based on super-conformal representations for which the color is neutralized [26, 18]. The negative conformal weight of the vacuum also cancels the enormous contribution to mass squared coming from mass in CP_2 degrees of freedom.
3. Right-handed covariantly constant neutrino allows to construct the gamma matrices of the world of classical worlds (WCW) as fermionic counterparts of Hamiltonians of WCW. This gives rise super-symplectic symmetry algebra having interpretation also as a conformal algebra. Also more general super-conformal symmetries exist.
4. Space-time (in the sense of Minkowski space M^4) super-symmetry in the conventional sense of the word is impossible in TGD framework since it would require require Majorana spinors. In 8-D space-time with Minkowski signature of metric Majorana spinors are definitely ruled out by the standard argument leading to super string model. Majorana spinors would also break separate conservation of lepton and baryon numbers in TGD framework.

Could one generalize super-symmetry?

Could one then consider a more general space-time super-symmetry with "space-time" identified as space-time surface rather than Minkowski space?

1. The TGD variant of the super-symmetry could correspond quite concretely to the addition to fermion and boson states right-handed neutrinos. Since right-handed neutrinos do not have electro-weak interactions, the addition might not appreciably affect the mass formula although it could affect the p-adic prime defining the mass scale.
2. The problem is to understand what this addition of the right-handed neutrino means. To begin with, notice that in TGD Universe fermions reside at light-like 3-surfaces at which the signature of induced metric changes. Bosons correspond to pairs of light-like wormhole throats with wormhole contact having Euclidian signature of the induced metric. The long standing problem has been that for bosons with parallel light-like four-momenta with same sign of energy the spins of fermion and antifermion are opposite so that one would obtain only scalar bosons!

I have considered several solutions to the problem but the final solution came from the basic problem of twistor approach to $\mathcal{N} = 4$ SUSY. This theory is believed to be UV finite but has IR divergences spoiling the Yangian SUSY. These infinities cancel if the physical particles are bound states of pairs of wormhole throats with light-like momenta. Just the requirement that spin is equal to one forces massivation. This is true for all spin 1 particles, also those regarded as massless. Massivation of the photon is not a problem if the mass corresponds to the IR cutoff determined by the largest causal diamond (CD) defining the measurement resolution. For electron the size of CD corresponds to the size scale of Earth. The basic prediction is that Higgs disappears completely from the spectrum so that this mechanism is testable at LHC.

The first proposal to the solution of problem was that either fermion or antifermion in the boson state carries what might be called un-physical polarization in the standard conceptual framework. This means that it has negative energy but three-momentum parallel to that of the second wormhole throat. The assumption that the bosonic wormhole throats correspond to positive and negative energy space-time sheets realizes this constraint in the framework of zero energy ontology. It however turned out that for light-like momenta these states have more natural interpretation in terms of virtual bosons able to have space-like momenta. This means that one can realize virtual particles as pairs of on mass shell wormhole throats with either sign of energy and 3-momentum so that the basic condition of twistorial approach is satisfied. The conservation of 4-momentum at vertices gives extremely powerful kinematical constraints so that there are excellent hopes about cancellation of UV divergences of loop integrals.

3. The super-symmetry as an addition to the fermion state a second wormhole throats carrying right handed neutrino quantum numbers does not make sense since the resulting state cannot be distinguished from gauge boson or Higgs type particle. The light-like 3-surfaces can however carry fermion numbers up to the number of modes of the induced spinor field, which is expected to be infinite inside string like objects having wormhole throats at ends and finite when one has space time sheets containing the throats [55]. In very general sense one could say that each mode defines a very large broken N -super-symmetry with the value of N depending on state and light-like 3-surface. The breaking of this super-symmetry would come from electro-weak -, color -, and gravitational interactions. Right-handed neutrino would by its electro-weak and color inertness define a minimally broken super-symmetry.
4. What this addition of the right handed neutrinos or more general fermion modes could precisely mean? One cannot assign fermionic oscillator operators to right handed neutrinos which are covariantly constant in both M^4 and CP_2 degrees of freedom since the modes with vanishing energy (frequency) cannot correspond to fermionic oscillator operator creating a physical state since one would have $a = a^\dagger$. The intuitive view is that all the spinor modes move in an exactly collinear manner -somewhat like quarks inside hadron do approximately.

Modified Dirac equation briefly

The answer to the question what "collinear motion" means mathematically emerged from the recent progress in the understanding of the modified Dirac equation.

1. The modified Dirac action involves two terms. Besides the original 4-D modified Dirac action there is measurement interaction which can be localized to wormhole throat or to any light-like 3-surfaces "parallel" to it in the slicing of space-time sheet by light-like 3-surfaces. This term

correlates space-time geometry with quantum numbers assignable to super-conformal representations and is also necessary to obtain almost-stringy propagator.

2. The modified Dirac equation with measurement action added reads as

$$\begin{aligned} D_K \Psi &= 0 , \\ D_3 \Psi &= (D_{C-S} + Q \times O) \Psi = 0 , \\ [D_3, D_K] \Psi &= 0 . \end{aligned} \tag{2.3.1}$$

- (a) D_K corresponds formally to 4-D massless Dirac equation in X^4 . D_3 realizes measurement interaction. D_{C-S} is the 3-D modified Dirac action defined by Chern-Simons action.
- (b) Q is linear in Cartan algebra generators of the isometry algebra of imbedding space (color isospin and hypercharge plus four-momentum or two components of four momentum and spin and boost in direction of 3-momentum). Q is expressible as

$$Q = Q_A \partial_\alpha h^k g^{AB} j_{Bk} \hat{\Gamma}_{CS}^\alpha . \tag{2.3.2}$$

Here Q_A is Cartan algebra generator acting on physical states. Physical states must be eigen states of Q_A since otherwise the equations do not make sense. g^{AB} is the inverse of the matrix defined by the imbedding space inner product of Killing vector fields j_A^k and j_B^l : its existence allows only Cartan algebra charges. $\hat{\Gamma}_{CS}^\alpha$ is the modified gamma matrix associated with the Chern-Simons action.

- (c) In general case the modified gamma matrices are defined in terms of action density L as

$$\hat{\Gamma}^\alpha = \frac{\partial L}{\partial_\alpha h^k} \gamma^k . \tag{2.3.3}$$

γ^k denotes imbedding space gamma matrices.

- (d) The operator O characterizes the conserved fermionic current to which Cartan algebra generators of isometries couple. The simplest conserved currents correspond to quark or lepton currents and corresponding vectorial isospin- and spin currents [55]. Besides this there is an infinite hierarchy of conserved currents relating to quantum criticality and in one-one correspondence with vanishing second variations of Kähler action for preferred extremal. These couplings allow to represent measurement interaction for any observable.
3. The equation $D_3 \nu_R = 0$ would reduce for vanishing color charges and covariantly constant spinor to the analog of algebraic fermionic on mass shell condition $p_A \gamma^A \nu_R = 0$ since Q is obtained by projecting the total four-momentum of the parton state interpreted as a vector-field of H to the space-time surface and by replacing ordinary gamma matrices with the modified ones. This equation cannot be exact since Q depends on the point of the light-like 3-surface so that covariant constancy fails and D_{C-S} cannot annihilate the state. This is the space-time correlate for the breaking of super-symmetry. The action of the Cartan algebra generators is purely algebraic and on the state of super-conformal representations rather than that of a differential operator on spinor field. The modified equation implies that all spinor modes represent fermions moving collinearly in the sense an equation with the same total four-momentum and total color quantum numbers is satisfied by all of them. Note that p_A represents the total four-momentum of the state rather than individual four-momenta of fermions.

TGD counterpart of space-time super-symmetry

This picture allows to define more precisely what one means with the approximate super-symmetries in TGD framework.

1. One can in principle construct many-fermion states containing both fermions and anti-fermions at given light-like 3-surface. The four-momenta of states related by super-symmetry need not be same. Super-symmetry breaking is present and has as the space-time correlate the deviation of the modified gamma matrices from the ordinary M^4 gamma matrices. In particular, the fact that $\hat{\Gamma}^\alpha$ possesses CP_2 part in general means that different M^4 chiralities are mixed: a space-time correlate for the massivation of the elementary particles.
2. For right-handed neutrino super-symmetry breaking is expected to be smallest but also in the case of the right-handed neutrino mode mixing of M^4 chiralities takes place and breaks the TGD counterpart of super-symmetry.
3. The fact that all helicities in the state are physical for a given light-like 3-surface has important implications. For instance, the addition of a right-handed antineutrino to right-handed (left-handed) electron state gives scalar (spin 1) state. Also states with fermion number two are obtained from fermions. For instance, for e_R one obtains the states $\{e_R, e_R\nu_R\bar{\nu}_R, e_R\bar{\nu}_R, e_R\nu_R\}$ with lepton numbers $(1, 1, 0, 2)$ and spins $(1/2, 1/2, 0, 1)$. For e_L one obtains the states $\{e_L, e_L\nu_R\bar{\nu}_R, e_L\bar{\nu}_R, e_L\nu_R\}$ with lepton numbers $(1, 1, 0, 2)$ and spins $(1/2, 1/2, 1, 0)$. In the case of gauge boson and Higgs type particles -allowed by TGD but not required by p-adic mass calculations- gauge boson has 15 super partners with fermion numbers $[2, 1, 0, -1, -2]$.

The cautious conclusion is that the recent view about quantum TGD allows the analog of super-symmetry which is necessary broken and for which the multiplets are much more general than for the ordinary super-symmetry. Right-handed neutrinos might however define something resembling ordinary super-symmetry to a high extent. The question is how strong prediction one can deduce using quantum TGD and proposed super-symmetry.

1. For a minimal breaking of super-symmetry only the p-adic length scale characterizing the super-partner differs from that for partner but the mass of the state is same. This would allow only a discrete set of masses for various super-partners coming as half octaves of the mass of the particle in question. A highly predictive model results.
2. The quantum field theoretic description should be based on QFT limit of TGD formulated in terms of bosonic emergence [25]. This formulation should allow to calculate the propagators of the super-partners in terms of fermionic loops.
3. This TGD variant of space-time super-symmetry resembles ordinary super-symmetry in the sense that selection rules due to the right-handed neutrino number conservation and analogous to the conservation of R-parity hold true. The states inside super-multiplets have identical electro-weak and color quantum numbers but their p-adic mass scales can be different. It should be possible to estimate reaction rates using rules very similar to those of super-symmetric gauge theories.
4. It might be even possible to find some simple generalization of standard super-symmetric gauge theory to get rough estimates for the reaction rates. There are however problems. The fact that spins $J = 0, 1, 2, 3/2, 2$ are possible for super-partners of gauge bosons forces to ask whether these additional states define an analog of non-stringy strong gravitation. Note that graviton in TGD framework corresponds to a pair of wormhole throats connected by flux tube (counterpart of string) and for gravitons one obtains 2^8 -fold degeneracy.

2.3.6 Twistorial approach, Yangian symmetry, and generalized Feynman diagrams

There has been impressive steps in the understanding of $\mathcal{N} = 4$ maximally supersymmetric YM theory possessing 4-D super-conformal symmetry. This theory is related by AdS/CFT duality to certain string theory in $AdS_5 \times S^5$ background. Second stringy representation was discovered by Witten and is based on 6-D Calabi-Yau manifold defined by twistors. The unifying proposal is that so called Yangian symmetry is behind the mathematical miracles involved.

The notion of Yangian symmetry would have a generalization in TGD framework obtained by replacing conformal algebra with appropriate super-conformal algebras. Also a possible realization

of twistor approach and the construction of scattering amplitudes in terms of Yangian invariants defined by Grassmannian integrals is considered in TGD framework and based on the idea that in zero energy ontology one can represent massive states as bound states of massless particles. There is also a proposal for a physical interpretation of the Cartan algebra of Yangian algebra allowing to understand at the fundamental level how the mass spectrum of n-particle bound states could be understood in terms of the n-local charges of the Yangian algebra.

Twistors were originally introduced by Penrose to characterize the solutions of Maxwell's equations. Kähler action is Maxwell action for the induced Kähler form of CP_2 . The preferred extremals allow a very concrete interpretation in terms of modes of massless non-linear field. Both conformally compactified Minkowski space identifiable as so called causal diamond and CP_2 allow a description in terms of twistors. These observations inspire the proposal that a generalization of Witten's twistor string theory relying on the identification of twistor string world sheets with certain holomorphic surfaces assigned with Feynman diagrams could allow a formulation of quantum TGD in terms of 3-dimensional holomorphic surfaces of $CP_3 \times CP_3$ mapped to 6-surfaces dual $CP_3 \times CP_3$, which are sphere bundles so that they are projected in a natural manner to 4-D space-time surfaces. Very general physical and mathematical arguments lead to a highly unique proposal for the holomorphic differential equations defining the complex 3-surfaces conjectured to correspond to the preferred extremals of Kähler action.

Background

I am outsider as far as concrete calculations in $\mathcal{N} = 4$ SUSY are considered and the following discussion of the background probably makes this obvious. My hope is that the reader had patience to not care about this and try to see the big pattern.

The developments began from the observation of Parke and Taylor [85] that n-gluon tree amplitudes with less than two negative helicities vanish and those with two negative helicities have unexpectedly simple form when expressed in terms of spinor variables used to represent light-like momentum. In fact, in the formalism based on Grassmannian integrals the reduced tree amplitude for two negative helicities is just "1" and defines Yangian invariant. The article *Perturbative Gauge Theory As a String Theory In Twistor Space* [86] by Witten led to so called Britto-Cachazo-Feng-Witten (BCFW) recursion relations for tree level amplitudes [92, 89] allowing to construct tree amplitudes using the analogs of Feynman rules in which vertices correspond to maximally helicity violating tree amplitudes (2 negative helicity gluons) and propagator is massless Feynman propagator for boson. The progress inspired the idea that the theory might be completely integrable meaning the existence of infinite-dimensional un-usual symmetry. This symmetry would be so called Yangian symmetry [19] assigned to the super counterpart of the conformal group of 4-D Minkowski space.

Drumond, Henn, and Plefka represent in the article *Yangian symmetry of scattering amplitudes in $\mathcal{N} = 4$ super Yang-Mills theory* [94] an argument suggesting that the Yangian invariance of the scattering amplitudes is an intrinsic property of planar $\mathcal{N} = 4$ super Yang Mills at least at tree level.

The latest step in the progress was taken by Arkani-Hamed, Bourjaily, Cachazo, Carot-Huot, and Trnka and represented in the article *Yangian symmetry of scattering amplitudes in $\mathcal{N} = 4$ super Yang-Mills theory* [97]. At the same day there was also the article of Rutger Boels entitled *On BCFW shifts of integrands and integrals* [96] in the archive. Arkani-Hamed *et al* argue that a full Yangian symmetry of the theory allows to generalize the BCFW recursion relation for tree amplitudes to all loop orders at planar limit (planar means that Feynman diagram allows imbedding to plane without intersecting lines). On mass shell scattering amplitudes are in question.

Yangian symmetry

The notion equivalent to that of Yangian was originally introduced by Faddeev and his group in the study of integrable systems. Yangians are Hopf algebras which can be assigned with Lie algebras as the deformations of their universal enveloping algebras. The elegant but rather cryptic looking definition is in terms of the modification of the relations for generating elements [19]. Besides ordinary product in the enveloping algebra there is co-product Δ which maps the elements of the enveloping algebra to its tensor product with itself. One can visualize product and co-product in terms of particle reactions. Particle annihilation is analogous to annihilation of two particle so single one and co-product is analogous to the decay of particle to two. Δ allows to construct higher generators of the

algebra.

Lie-algebra can mean here ordinary finite-dimensional simple Lie algebra, Kac-Moody algebra or Virasoro algebra. In the case of SUSY it means conformal algebra of M^4 - or rather its super counterpart. Witten, Nappi and Dolan have described the notion of Yangian for super-conformal algebra in very elegant and concrete manner in the article *Yangian Symmetry in D=4 superconformal Yang-Mills theory* [95]. Also Yangians for gauge groups are discussed.

In the general case Yangian resembles Kac-Moody algebra with discrete index n replaced with a continuous one. Discrete index poses conditions on the Lie group and its representation (adjoint representation in the case of $\mathcal{N} = 4$ SUSY). One of the conditions is that the tensor product $R \otimes R^*$ for representations involved contains adjoint representation only once. This condition is non-trivial. For $SU(n)$ these conditions are satisfied for any representation. In the case of $SU(2)$ the basic branching rule for the tensor product of representations implies that the condition is satisfied for the product of any representations.

Yangian algebra with a discrete basis is in many respects analogous to Kac-Moody algebra. Now however the generators are labelled by non-negative integers labeling the light-like incoming and outgoing momenta of scattering amplitude whereas in the case of Kac-Moody algebra also negative values are allowed. Note that only the generators with non-negative conformal weight appear in the construction of states of Kac-Moody and Virasoro representations so that the extension to Yangian makes sense.

The generating elements are labelled by the generators of ordinary conformal transformations acting in M^4 and their duals acting in momentum space. These two sets of elements can be labelled by conformal weights $n = 0$ and $n = 1$ and their mutual commutation relations are same as for Kac-Moody algebra. The commutators of $n = 1$ generators with themselves are however something different for a non-vanishing deformation parameter h . Serre's relations characterize the difference and involve the deformation parameter h . Under repeated commutations the generating elements generate infinite-dimensional symmetric algebra, the Yangian. For $h = 0$ one obtains just one half of the Virasoro algebra or Kac-Moody algebra. The generators with $n > 0$ are $n + 1$ -local in the sense that they involve $n + 1$ -forms of local generators assignable to the ordered set of incoming particles of the scattering amplitude. This non-locality generalizes the notion of local symmetry and is claimed to be powerful enough to fix the scattering amplitudes completely.

How to generalize Yangian symmetry in TGD framework?

As far as concrete calculations are considered, I have nothing to say. I am just perplexed. It is however possible to keep discussion at general level and still say something interesting (as I hope!). The key question is whether it could be possible to generalize the proposed Yangian symmetry and geometric picture behind it to TGD framework.

1. The first thing to notice is that the Yangian symmetry of $\mathcal{N} = 4$ SUSY in question is quite too limited since it allows only single representation of the gauge group and requires massless particles. One must allow all representations and massive particles so that the representation of symmetry algebra must involve states with different masses, in principle arbitrary spin and arbitrary internal quantum numbers. The candidates are obvious: Kac-Moody algebras [62] and Virasoro algebras[70] and their super counterparts. Yangians indeed exist for arbitrary super Lie algebras. In TGD framework conformal algebra of Minkowski space reduces to Poincare algebra and its extension to Kac-Moody allows to have also massive states.
2. The formal generalization looks surprisingly straightforward at the formal level. In zero energy ontology one replaces point like particles with partonic two-surfaces appearing at the ends of light-like orbits of wormhole throats located to the future and past light-like boundaries of causal diamond ($CD \times CP_2$ or briefly CD). Here CD is defined as the intersection of future and past directed light-cones. The polygon with light-like momenta is naturally replaced with a polygon with more general momenta in zero energy ontology and having partonic surfaces as its vertices. Non-point-likeness forces to replace the finite-dimensional super Lie-algebra with infinite-dimensional Kac-Moody algebras and corresponding super-Virasoro algebras assignable to partonic 2-surfaces.

3. This description replaces disjoint holomorphic surfaces in twistor space with partonic 2-surfaces at the boundaries of $CD \times CP_2$ so that there seems to be a close analogy with Cachazo-Svrcek-Witten picture. These surfaces are connected by either light-like orbits of partonic 2-surface or space-like 3-surfaces at the ends of CD so that one indeed obtains the analog of polygon.

What does this then mean concretely (if this word can be used in this kind of context;-)?

1. At least it means that ordinary Super Kac-Moody and Super Virasoro algebras associated with isometries of $M^4 \times CP_2$ annihilating the scattering amplitudes must be extended to a co-algebras with a non-trivial deformation parameter. Kac-Moody group is thus the product of Poincare and color groups. This algebra acts as deformations of the light-like 3-surfaces representing the light-like orbits of particles which are extremals of Chern-Simon action with the constraint that weak form of electric-magnetic duality holds true. I know so little about the mathematical side that I cannot tell whether the condition that the product of the representations of Super-Kac-Moody and Super-Virasoro algebras contains adjoint representation only once, holds true in this case. In any case, it would allow all representations of finite-dimensional Lie group in vertices whereas $\mathcal{N} = 4$ SUSY would allow only the adjoint.
2. Besides this ordinary kind of Kac-Moody algebra there is the analog of Super-Kac-Moody algebra associated with the light-cone boundary which is metrically 3-dimensional. The finite-dimensional Lie group is in this case replaced with infinite-dimensional group of symplectomorphisms of $\delta M_{+/-}^4$ made local with respect to the internal coordinates of partonic 2-surface. A coset construction is applied to these two Virasoro algebras so that the differences of the corresponding Super-Virasoro generators and Kac-Moody generators annihilate physical states. This implies that the corresponding four-momenta are same: this expresses the equivalence of gravitational and inertial masses. A generalization of the Equivalence Principle is in question. This picture also justifies p-adic thermodynamics applied to either symplectic or isometry Super-Virasoro and giving thermal contribution to the vacuum conformal and thus to mass squared.
3. The construction of TGD leads also to other super-conformal algebras and the natural guess is that the Yangians of all these algebras annihilate the scattering amplitudes.
4. Obviously, already the starting point symmetries look formidable but they still act on single partonic surface only. The discrete Yangian associated with this algebra associated with the closed polygon defined by the incoming momenta and the negatives of the outgoing momenta acts in multi-local manner on scattering amplitudes. It might make sense to speak about polygons defined also by other conserved quantum numbers so that one would have generalized light-like curves in the sense that state are massless in 8-D sense.

Is there any hope about description in terms of Grassmannians?

At technical level the successes of the twistor approach rely on the observation that the amplitudes can be expressed in terms of very simple integrals over sub-manifolds of the space consisting of k -dimensional planes of n -dimensional space defined by delta function appearing in the integrand. These integrals define super-conformal Yangian invariants appearing in twistorial amplitudes and the belief is that by a proper choice of the surfaces of the twistor space one can construct all invariants. One can construct also the counterparts of loop corrections by starting from tree diagrams and annihilating pair of particles by connecting the lines and quantum entangling the states at the ends in the manner dictated by the integration over loop momentum. These operations can be defined as operations for Grassmannian integrals in general changing the values of n and k . This description looks extremely powerful and elegant and most importantly involves only the external momenta.

The obvious question is whether one could use similar invariants in TGD framework to construct the momentum dependence of amplitudes.

1. The first thing to notice is that the super algebras in question act on infinite-dimensional representations and basically in the world of classical worlds assigned to the partonic 2-surfaces correlated by the fact that they are associated with the same space-time surface. This does not promise anything very practical. On the other hand, one can hope that everything related to other than M^4 degrees of freedom could be treated like color degrees of freedom in $\mathcal{N} = 4$ SYM

and would boil down to indices labeling the quantum states. The Yangian conditions coming from isometry quantum numbers, color quantum numbers, and electroweak quantum numbers are of course expected to be highly non-trivial and could fix the coefficients of various singlets resulting in the tensor product of incoming and outgoing states.

2. The fact that incoming particles can be also massive seems to exclude the use of the twistor space. The following observation however raises hopes. The Dirac propagator for wormhole throat is massless propagator but for what I call pseudo momentum. It is still unclear how this momentum relates to the actual four-momentum. Could it be actually equal to it? The recent view about pseudo-momentum does not support this view but it is better to keep mind open. In any case this finding suggests that twistorial approach could work in in more or less standard form. What would be needed is a representation for massive incoming particles as bound states of massless partons. In particular, the massive states of super-conformal representations should allow this kind of description.

Could zero energy ontology allow to achieve this dream?

1. As far as divergence cancellation is considered, zero energy ontology suggests a totally new approach producing the basic nice aspects of QFT approach, in particular unitarity and coupling constant evolution. The big idea related to zero energy ontology is that all virtual particle particles correspond to wormhole throats, which are pairs of on mass shell particles. If their momentum directions are different, one obtains time-like continuum of virtual momenta and if the signs of energy are opposite one obtains also space-like virtual momenta. The on mass shell property for virtual partons (massive in general) implies extremely strong constraints on loops and one expect that only very few loops remain and that they are finite since loop integration reduces to integration over much lower-dimensional space than in the QFT approach. There are also excellent hopes about Cutkoski rules.
2. Could zero energy ontology make also possible to construct massive incoming particles from massless ones? Could one construct the representations of the super conformal algebras using only massless states so that at the fundamental level incoming particles would be massless and one could apply twistor formalism and build the momentum dependence of amplitudes using Grassmannian integrals.

One could indeed construct on mass shell massive states from massless states with momenta along the same line but with three-momenta at opposite directions. Mass squared is given by $M^2 = 4E^2$ in the coordinate frame, where the momenta are opposite and of same magnitude. One could also argue that partonic 2-surfaces carrying quantum numbers of fermions and their superpartners serve as the analogs of point like massless particles and that topologically condensed fermions and gauge bosons plus their superpartners correspond to pairs of wormhole throats. Stringy objects would correspond to pairs of wormhole throats at the same space-time sheet in accordance with the fact that space-time sheet allows a slicing by string worlds sheets with ends at different wormhole throats and defining time like braiding.

The weak form of electric magnetic duality indeed supports this picture. To understand how, one must explain a little bit what the weak form of electric magnetic duality means.

1. Elementary particles correspond to light-like orbits of partonic 2-surfaces identified as 3-D surfaces at which the signature of the induced metric of space-time surface changes from Euclidian to Minkowskian and 4-D metric is therefore degenerate. The analogy with black hole horizon is obvious but only partial. Weak form of electric-magnetic duality states that the Kähler electric field at the wormhole throat and also at space-like 3-surfaces defining the ends of the space-time surface at the upper and lower light-like boundaries of the causal diamond is proportional to Kähler magnetic field so that Kähler electric flux is proportional Kähler magnetic flux. This implies classical quantization of Kähler electric charge and fixes the value of the proportionality constant.
2. There are also much more profound implications. The vision about TGD as almost topological QFT suggests that Kähler function defining the Kähler geometry of the "world of classical

worlds" (WCW) and identified as Kähler action for its preferred extremal reduces to the 3-D Chern-Simons action evaluated at wormhole throats and possible boundary components. Chern-Simons action would be subject to constraints. Wormhole throats and space-like 3-surfaces would represent extremals of Chern-Simons action restricted by the constraint force stating electric-magnetic duality (and realized in terms of Lagrange multipliers as usual).

If one assumes that Kähler current and other conserved currents are proportional to current defining Beltrami flow whose flow lines by definition define coordinate curves of a globally defined coordinate, the Coulombic term of Kähler action vanishes and it reduces to Chern-Simons action if the weak form of electric-magnetic duality holds true. One obtains almost topological QFT. The absolutely essential attribute "almost" comes from the fact that Chern-Simons action is subject to constraints. As a consequence, one obtains non-vanishing four-momenta and WCW geometry is non-trivial in M^4 degrees of freedom. Otherwise one would have only topological QFT not terribly interesting physically.

Consider now the question how one could understand stringy objects as bound states of massless particles.

1. The observed elementary particles are not Kähler monopoles and there much exist a mechanism neutralizing the monopole charge. The only possibility seems to be that there is opposite Kähler magnetic charge at second wormhole throat. The assumption is that in the case of color neutral particles this throat is at a distance of order intermediate gauge boson Compton length. This throat would carry weak isospin neutralizing that of the fermion and only electromagnetic charge would be visible at longer length scales. One could speak of electro-weak confinement. Also color confinement could be realized in analogous manner by requiring the cancellation of monopole charge for many-parton states only. What comes out are string like objects defined by Kähler magnetic fluxes and having magnetic monopoles at ends. Also more general objects with three strings branching from the vertex appear in the case of baryons. The natural guess is that the partons at the ends of strings and more general objects are massless for incoming particles but that the 3-momenta are in opposite directions so that stringy mass spectrum and representations of relevant super-conformal algebras are obtained. This description brings in mind the description of hadrons in terms of partons moving in parallel apart from transversal momentum about which only momentum squared is taken as observable.
2. Quite generally, one expects for the preferred extremals of Kähler action the slicing of space-time surface with string world sheets with stringy curves connecting wormhole throats. The ends of the stringy curves can be identified as light-like braid strands. Note that the strings themselves define a space-like braiding and the two braidings are in some sense dual. This has a concrete application in TGD inspired quantum biology, where time-like braiding defines topological quantum computer programs and the space-like braidings induced by it its storage into memory. Stringlike objects defining representations of super-conformal algebras must correspond to states involving at least two wormhole throats. Magnetic flux tubes connecting the ends of magnetically charged throats provide a particular realization of stringy on mass shell states. This would give rise to massless propagation at the parton level. The stringy quantization condition for mass squared would read as $4E^2 = n$ in suitable units for the representations of super-conformal algebra associated with the isometries. For pairs of throats of the same wormhole contact stringy spectrum does not seem plausible since the wormhole contact is in the direction of CP_2 . One can however expect generation of small mass as deviation of vacuum conformal weight from half integer in the case of gauge bosons.

If this picture is correct, one might be able to determine the momentum dependence of the scattering amplitudes by replacing free fermions with pairs of monopoles at the ends of string and topologically condensed fermions gauge bosons with pairs of this kind of objects with wormhole throat replaced by a pair of wormhole throats. This would mean suitable number of doublings of the Grassmannian integrations with additional constraints on the incoming momenta posed by the mass shell conditions for massive states.

Could zero energy ontology make possible full Yangian symmetry?

The partons in the loops are on mass shell particles have a discrete mass spectrum but both signs of energy are possible for opposite wormhole throats. This implies that in the rules for constructing loop amplitudes from tree amplitudes, propagator entanglement is restricted to that corresponding to pairs of partonic on mass shell states with both signs of energy. As emphasized in [97], it is the Grassmannian integrands and leading order singularities of $\mathcal{N} = 4$ SYM, which possess the full Yangian symmetry. The full integral over the loop momenta breaks the Yangian symmetry and brings in IR singularities. Zero energy ontologist finds it natural to ask whether QFT approach shows its inadequacy both via the UV divergences and via the loss of full Yangian symmetry. The restriction of virtual partons to discrete mass shells with positive or negative sign of energy imposes extremely powerful restrictions on loop integrals and resembles the restriction to leading order singularities. Could this restriction guarantee full Yangian symmetry and remove also IR singularities?

Could Yangian symmetry provide a new view about conserved quantum numbers?

The Yangian algebra has some properties which suggest a new kind of description for bound states. The Cartan algebra generators of $n = 0$ and $n = 1$ levels of Yangian algebra commute. Since the co-product Δ maps $n = 0$ generators to $n = 1$ generators and these in turn to generators with high value of n , it seems that they commute also with $n \geq 1$ generators. This applies to four-momentum, color isospin and color hyper charge, and also to the Virasoro generator L_0 acting on Kac-Moody algebra of isometries and defining mass squared operator.

Could one identify total four momentum and Cartan algebra quantum numbers as sum of contributions from various levels? If so, the four momentum and mass squared would involve besides the local term assignable to wormhole throats also n-local contributions. The interpretation in terms of n-parton bound states would be extremely attractive. n-local contribution would involve interaction energy. For instance, string like object would correspond to $n = 1$ level and give $n = 2$ -local contribution to the momentum. For baryonic valence quarks one would have 3-local contribution corresponding to $n = 2$ level. The Yangian view about quantum numbers could give a rigorous formulation for the idea that massive particles are bound states of massless particles.

2.4 Weak form electric-magnetic duality and color and weak forces

The notion of electric-magnetic duality [65] was proposed first by Olive and Montonen and is central in $\mathcal{N} = 4$ supersymmetric gauge theories. It states that magnetic monopoles and ordinary particles are two different phases of theory and that the description in terms of monopoles can be applied at the limit when the running gauge coupling constant becomes very large and perturbation theory fails to converge. The notion of electric-magnetic self-duality is more natural since for CP_2 geometry Kähler form is self-dual and Kähler magnetic monopoles are also Kähler electric monopoles and Kähler coupling strength is by quantum criticality renormalization group invariant rather than running coupling constant. The notion of electric-magnetic (self-)duality emerged already two decades ago in the attempts to formulate the Kähler geometric of world of classical worlds. Quite recently a considerable step of progress took place in the understanding of this notion [22]. What seems to be essential is that one adopts a weaker form of the self-duality applying at partonic 2-surfaces. What this means will be discussed in the sequel.

Every new idea must be of course taken with a grain of salt but the good sign is that this concept leads to precise predictions. The point is that elementary particles do not generate monopole fields in macroscopic length scales: at least when one considers visible matter. The first question is whether elementary particles could have vanishing magnetic charges: this turns out to be impossible. The next question is how the screening of the magnetic charges could take place and leads to an identification of the physical particles as string like objects identified as pairs magnetic charged wormhole throats connected by magnetic flux tubes.

1. The first implication is a new view about electro-weak massivation reducing it to weak confinement in TGD framework. The second end of the string contains particle having electroweak isospin neutralizing that of elementary fermion and the size scale of the string is electro-weak

scale would be in question. Hence the screening of electro-weak force takes place via weak confinement realized in terms of magnetic confinement.

2. This picture generalizes to the case of color confinement. Also quarks correspond to pairs of magnetic monopoles but the charges need not vanish now. Rather, valence quarks would be connected by flux tubes of length of order hadron size such that magnetic charges sum up to zero. For instance, for baryonic valence quarks these charges could be $(2, -1, -1)$ and could be proportional to color hyper charge.
3. The highly non-trivial prediction making more precise the earlier stringy vision is that elementary particles are string like objects in electro-weak scale: this should become manifest at LHC energies.
4. The weak form electric-magnetic duality together with Beltrami flow property of Kähler leads to the reduction of Kähler action to Chern-Simons action so that TGD reduces to almost topological QFT and that Kähler function is explicitly calculable. This has enormous impact concerning practical calculability of the theory.
5. One ends up also to a general solution ansatz for field equations from the condition that the theory reduces to almost topological QFT. The solution ansatz is inspired by the idea that all isometry currents are proportional to Kähler current which is integrable in the sense that the flow parameter associated with its flow lines defines a global coordinate. The proposed solution ansatz would describe a hydrodynamical flow with the property that isometry charges are conserved along the flow lines (Beltrami flow). A general ansatz satisfying the integrability conditions is found. The solution ansatz applies also to the extremals of Chern-Simons action and to the conserved currents associated with the modified Dirac equation defined as contractions of the modified gamma matrices between the solutions of the modified Dirac equation. The strongest form of the solution ansatz states that various classical and quantum currents flow along flow lines of the Beltrami flow defined by Kähler current (Kähler magnetic field associated with Chern-Simons action). Intuitively this picture is attractive. A more general ansatz would allow several Beltrami flows meaning multi-hydrodynamics. The integrability conditions boil down to two scalar functions: the first one satisfies massless d'Alembert equation in the induced metric and the the gradients of the scalar functions are orthogonal. The interpretation in terms of momentum and polarization directions is natural.
6. The general solution ansatz works for induced Kähler Dirac equation and Chern-Simons Dirac equation and reduces them to ordinary differential equations along flow lines. The induced spinor fields are simply constant along flow lines of induced spinor field for Dirac equation in suitable gauge. Also the generalized eigen modes of the modified Chern-Simons Dirac operator can be deduced explicitly if the throats and the ends of space-time surface at the boundaries of CD are extremals of Chern-Simons action. Chern-Simons Dirac equation reduces to ordinary differential equations along flow lines and one can deduce the general form of the spectrum and the explicit representation of the Dirac determinant in terms of geometric quantities characterizing the 3-surface (eigenvalues are inversely proportional to the lengths of strands of the flow lines in the effective metric defined by the modified gamma matrices).

2.4.1 Could a weak form of electric-magnetic duality hold true?

Holography means that the initial data at the partonic 2-surfaces should fix the configuration space metric. A weak form of this condition allows only the partonic 2-surfaces defined by the wormhole throats at which the signature of the induced metric changes. A stronger condition allows all partonic 2-surfaces in the slicing of space-time sheet to partonic 2-surfaces and string world sheets. Number theoretical vision suggests that hyper-quaternionicity *resp.* co-hyperquaternionicity constraint could be enough to fix the initial values of time derivatives of the imbedding space coordinates in the space-time regions with Minkowskian *resp.* Euclidian signature of the induced metric. This is a condition on modified gamma matrices and hyper-quaternionicity states that they span a hyper-quaternionic sub-space.

Definition of the weak form of electric-magnetic duality

One can also consider alternative conditions possibly equivalent with this condition. The argument goes as follows.

1. The expression of the matrix elements of the metric and Kähler form of WCW in terms of the Kähler fluxes weighted by Hamiltonians of δM_{\pm}^4 at the partonic 2-surface X^2 looks very attractive. These expressions however carry no information about the 4-D tangent space of the partonic 2-surfaces so that the theory would reduce to a genuinely 2-dimensional theory, which cannot hold true. One would like to code to the WCW metric also information about the electric part of the induced Kähler form assignable to the complement of the tangent space of $X^2 \subset X^4$.
2. Electric-magnetic duality of the theory looks a highly attractive symmetry. The trivial manner to get electric magnetic duality at the level of the full theory would be via the identification of the flux Hamiltonians as sums of the magnetic and electric fluxes. The presence of the induced metric is however troublesome since the presence of the induced metric means that the simple transformation properties of flux Hamiltonians under symplectic transformations -in particular color rotations- are lost.
3. A less trivial formulation of electric-magnetic duality would be as an initial condition which eliminates the induced metric from the electric flux. In the Euclidian version of 4-D YM theory this duality allows to solve field equations exactly in terms of instantons. This approach involves also quaternions. These arguments suggest that the duality in some form might work. The full electric magnetic duality is certainly too strong and implies that space-time surface at the partonic 2-surface corresponds to piece of CP_2 type vacuum extremal and can hold only in the deep interior of the region with Euclidian signature. In the region surrounding wormhole throat at both sides the condition must be replaced with a weaker condition.
4. To formulate a weaker form of the condition let us introduce coordinates (x^0, x^3, x^1, x^2) such (x^1, x^2) define coordinates for the partonic 2-surface and (x^0, x^3) define coordinates labeling partonic 2-surfaces in the slicing of the space-time surface by partonic 2-surfaces and string world sheets making sense in the regions of space-time sheet with Minkowskian signature. The assumption about the slicing allows to preserve general coordinate invariance. The weakest condition is that the generalized Kähler electric fluxes are apart from constant proportional to Kähler magnetic fluxes. This requires the condition

$$J^{03}\sqrt{g_4} = K J_{12} . \quad (2.4.1)$$

A more general form of this duality is suggested by the considerations of [37] reducing the hierarchy of Planck constants to basic quantum TGD and also reducing Kähler function for preferred extremals to Chern-Simons terms [63] at the boundaries of CD and at light-like wormhole throats. This form is following

$$J^{n\beta}\sqrt{g_4} = K\epsilon \times \epsilon^{n\beta\gamma\delta} J_{\gamma\delta}\sqrt{g_4} . \quad (2.4.2)$$

Here the index n refers to a normal coordinate for the space-like 3-surface at either boundary of CD or for light-like wormhole throat. ϵ is a sign factor which is opposite for the two ends of CD . It could be also opposite of opposite at the opposite sides of the wormhole throat. Note that the dependence on induced metric disappears at the right hand side and this condition eliminates the potentials singularity due to the reduction of the rank of the induced metric at wormhole throat.

5. Information about the tangent space of the space-time surface can be coded to the configuration space metric with loosing the nice transformation properties of the magnetic flux Hamiltonians

if Kähler electric fluxes or sum of magnetic flux and electric flux satisfying this condition are used and K is symplectic invariant. Using the sum

$$J_e + J_m = (1 + K)J , \quad (2.4.3)$$

where J can denote the Kähler magnetic flux, makes it possible to have a non-trivial configuration space metric even for $K = 0$, which could correspond to the ends of a cosmic string like solution carrying only Kähler magnetic fields. This condition suggests that it can depend only on Kähler magnetic flux and other symplectic invariants. Whether local symplectic coordinate invariants are possible at all is far from obvious, If the slicing itself is symplectic invariant then K could be a non-constant function of X^2 depending on string world sheet coordinates. The light-like radial coordinate of the light-cone boundary indeed defines a symplectically invariant slicing and this slicing could be shifted along the time axis defined by the tips of CD .

Electric-magnetic duality physically

What could the weak duality condition mean physically? For instance, what constraints are obtained if one assumes that the quantization of electro-weak charges reduces to this condition at classical level?

1. The first thing to notice is that the flux of J over the partonic 2-surface is analogous to magnetic flux

$$Q_m = \frac{e}{\hbar} \oint B dS = n .$$

n is non-vanishing only if the surface is homologically non-trivial and gives the homology charge of the partonic 2-surface.

2. The expressions of classical electromagnetic and Z^0 fields in terms of Kähler form [46] read as

$$\begin{aligned} \gamma &= \frac{eF_{em}}{\hbar} = 3J - \sin^2(\theta_W)R_{03} , \\ Z^0 &= \frac{g_Z F_Z}{\hbar} = 2R_{03} . \end{aligned} \quad (2.4.4)$$

Here R_{03} is one of the components of the curvature tensor in vielbein representation and F_{em} and F_Z correspond to the standard field tensors. From this expression one can deduce

$$J = \frac{e}{3\hbar} F_{em} + \sin^2(\theta_W) \frac{g_Z}{6\hbar} F_Z . \quad (2.4.5)$$

3. The weak duality condition when integrated over X^2 implies

$$\begin{aligned} \frac{e^2}{3\hbar} Q_{em} + \frac{g_Z^2 p}{6} Q_{Z,V} &= K \oint J = Kn , \\ Q_{Z,V} &= \frac{I_V^3}{2} - Q_{em} , \quad p = \sin^2(\theta_W) . \end{aligned} \quad (2.4.6)$$

Here the vectorial part of the Z^0 charge rather than as full Z^0 charge $Q_Z = I_L^3 + \sin^2(\theta_W)Q_{em}$ appears. The reason is that only the vectorial isospin is same for left and right handed components of fermion which are in general mixed for the massive states.

The coefficients are dimensionless and expressible in terms of the gauge coupling strengths and using $\hbar = r\hbar_0$ one can write

$$\begin{aligned} \alpha_{em} Q_{em} + p \frac{\alpha_Z}{2} Q_{Z,V} &= \frac{3}{4\pi} \times rnK , \\ \alpha_{em} &= \frac{e^2}{4\pi\hbar_0} , \quad \alpha_Z = \frac{g_Z^2}{4\pi\hbar_0} = \frac{\alpha_{em}}{p(1-p)} . \end{aligned} \quad (2.4.7)$$

4. There is a great temptation to assume that the values of Q_{em} and Q_Z correspond to their quantized values and therefore depend on the quantum state assigned to the partonic 2-surface. The linear coupling of the modified Dirac operator to conserved charges implies correlation between the geometry of space-time sheet and quantum numbers assigned to the partonic 2-surface. The assumption of standard quantized values for Q_{em} and Q_Z would be also seen as the identification of the fine structure constants α_{em} and α_Z . This however requires weak isospin invariance.

The value of K from classical quantization of Kähler electric charge

The value of K can be deduced by requiring classical quantization of Kähler electric charge.

1. The condition that the flux of $F^{03} = (\hbar/g_K)J^{03}$ defining the counterpart of Kähler electric field equals to the Kähler charge g_K would give the condition $K = g_K^2/\hbar$, where g_K is Kähler coupling constant which should be invariant under coupling constant evolution by quantum criticality. Within experimental uncertainties one has $\alpha_K = g_K^2/4\pi\hbar_0 = \alpha_{em} \simeq 1/137$, where α_{em} is finite structure constant in electron length scale and \hbar_0 is the standard value of Planck constant.
2. The quantization of Planck constants makes the condition highly non-trivial. The most general quantization of r is as rationals but there are good arguments favoring the quantization as integers corresponding to the allowance of only singular coverings of CD and CP_2 . The point is that in this case a given value of Planck constant corresponds to a finite number of pages of the "Big Book". The quantization of the Planck constant implies a further quantization of K and would suggest that K scales as $1/r$ unless the spectrum of values of Q_{em} and Q_Z allowed by the quantization condition scales as r . This is quite possible and the interpretation would be that each of the r sheets of the covering carries (possibly same) elementary charge. Kind of discrete variant of a full Fermi sphere would be in question. The interpretation in terms of anyonic phases [24] supports this interpretation.
3. The identification of J as a counterpart of eB/\hbar means that Kähler action and thus also Kähler function is proportional to $1/\alpha_K$ and therefore to \hbar . This implies that for large values of \hbar Kähler coupling strength $g_K^2/4\pi$ becomes very small and large fluctuations are suppressed in the functional integral. The basic motivation for introducing the hierarchy of Planck constants was indeed that the scaling $\alpha \rightarrow \alpha/r$ allows to achieve the convergence of perturbation theory: Nature itself would solve the problems of the theoretician. This of course does not mean that the physical states would remain as such and the replacement of single particles with anyonic states in order to satisfy the condition for K would realize this concretely.

The weak form of electric-magnetic duality has surprisingly strong implications for basic view about quantum TGD as following considerations show.

2.4.2 Magnetic confinement, the short range of weak forces, and color confinement

The weak form of electric-magnetic duality has surprisingly strong implications if one combines it with some very general empirical facts such as the non-existence of magnetic monopole fields in macroscopic length scales.

How can one avoid macroscopic magnetic monopole fields?

Monopole fields are experimentally absent in length scales above order weak boson length scale and one should have a mechanism neutralizing the monopole charge. How electroweak interactions become short ranged in TGD framework is still a poorly understood problem. What suggests itself is the neutralization of the weak isospin above the intermediate gauge boson Compton length by neutral Higgs bosons. Could the two neutralization mechanisms be combined to single one?

1. In the case of fermions and their super partners the opposite magnetic monopole would be a wormhole throat. If the magnetically charged wormhole contact is electromagnetically neutral but has vectorial weak isospin neutralizing the weak vectorial isospin of the fermion only the electromagnetic charge of the fermion is visible on longer length scales. The distance of this wormhole throat from the fermionic one should be of the order weak boson Compton length. An interpretation as a bound state of fermion and a wormhole throat state with the quantum numbers of a neutral Higgs boson would therefore make sense. The neutralizing throat would have quantum numbers of $X_{-1/2} = \nu_L \bar{\nu}_R$ or $X_{1/2} = \bar{\nu}_L \nu_R$. $\nu_L \bar{\nu}_R$ would not be neutral Higgs boson (which should correspond to a wormhole contact) but a super-partner of left-handed neutrino obtained by adding a right handed neutrino. This mechanism would apply separately to the fermionic and anti-fermionic throats of the gauge bosons and corresponding space-time sheets and leave only electromagnetic interaction as a long ranged interaction.
2. One can of course wonder what is the situation for the bosonic wormhole throats feeding gauge fluxes between space-time sheets. It would seem that these wormhole throats must always appear as pairs such that for the second member of the pair monopole charges and I_V^3 cancel each other at both space-time sheets involved so that one obtains at both space-time sheets magnetic dipoles of size of weak boson Compton length. The proposed magnetic character of fundamental particles should become visible at TeV energies so that LHC might have surprises in store!

Magnetic confinement and color confinement

Magnetic confinement generalizes also to the case of color interactions. One can consider also the situation in which the magnetic charges of quarks (more generally, of color excited leptons and quarks) do not vanish and they form color and magnetic singlets in the hadronic length scale. This would mean that magnetic charges of the state $q_{\pm 1/2} - X_{\mp 1/2}$ representing the physical quark would not vanish and magnetic confinement would accompany also color confinement. This would explain why free quarks are not observed. To how degree then quark confinement corresponds to magnetic confinement is an interesting question.

For quark and antiquark of meson the magnetic charges of quark and antiquark would be opposite and meson would correspond to a Kähler magnetic flux so that a stringy view about meson emerges. For valence quarks of baryon the vanishing of the net magnetic charge takes place provided that the magnetic net charges are $(\pm 2, \mp 1, \mp 1)$. This brings in mind the spectrum of color hyper charges coming as $(\pm 2, \mp 1, \mp 1)/3$ and one can indeed ask whether color hyper-charge correlates with the Kähler magnetic charge. The geometric picture would be three strings connected to single vertex. Amusingly, the idea that color hypercharge could be proportional to color hyper charge popped up during the first year of TGD when I had not yet discovered CP_2 and believed on $M^4 \times S^2$.

p-Adic length scale hypothesis and hierarchy of Planck constants defining a hierarchy of dark variants of particles suggest the existence of scaled up copies of QCD type physics and weak physics. For p-adically scaled up variants the mass scales would be scaled by a power of $\sqrt{2}$ in the most general case. The dark variants of the particle would have the same mass as the original one. In particular, Mersenne primes $M_k = 2^k - 1$ and Gaussian Mersennes $M_{G,k} = (1 + i)^k - 1$ has been proposed to define zoomed copies of these physics. At the level of magnetic confinement this would mean hierarchy of length scales for the magnetic confinement.

One particular proposal is that the Mersenne prime M_{89} should define a scaled up variant of the ordinary hadron physics with mass scaled up roughly by a factor $2^{(107-89)/2} = 512$. The size scale of color confinement for this physics would be same as the weak length scale. It would look more natural that the weak confinement for the quarks of M_{89} physics takes place in some shorter scale and M_{61} is the first Mersenne prime to be considered. The mass scale of M_{61} weak bosons would

be by a factor $2^{(89-61)/2} = 2^{14}$ higher and about 1.6×10^4 TeV. M_{89} quarks would have virtually no weak interactions but would possess color interactions with weak confinement length scale reflecting themselves as new kind of jets at collisions above TeV energies.

In the biologically especially important length scale range 10 nm -2500 nm there are as many as four Gaussian Mersennes corresponding to $M_{G,k}$, $k = 151, 157, 163, 167$. This would suggest that the existence of scaled up scales of magnetic-, weak- and color confinement. An especially interesting possibly testable prediction is the existence of magnetic monopole pairs with the size scale in this range. There are recent claims about experimental evidence for magnetic monopole pairs [77].

Magnetic confinement and stringy picture in TGD sense

The connection between magnetic confinement and weak confinement is rather natural if one recalls that electric-magnetic duality in super-symmetric quantum field theories means that the descriptions in terms of particles and monopoles are in some sense dual descriptions. Fermions would be replaced by string like objects defined by the magnetic flux tubes and bosons as pairs of wormhole contacts would correspond to pairs of the flux tubes. Therefore the sharp distinction between gravitons and physical particles would disappear.

The reason why gravitons are necessarily stringy objects formed by a pair of wormhole contacts is that one cannot construct spin two objects using only single fermion states at wormhole throats. Of course, also super partners of these states with higher spin obtained by adding fermions and anti-fermions at the wormhole throat but these do not give rise to graviton like states [23]. The upper and lower wormhole throat pairs would be quantum superpositions of fermion anti-fermion pairs with sum over all fermions. The reason is that otherwise one cannot realize graviton emission in terms of joining of the ends of light-like 3-surfaces together. Also now magnetic monopole charges are necessary but now there is no need to assign the entities X_{\pm} with gravitons.

Graviton string is characterized by some p-adic length scale and one can argue that below this length scale the charges of the fermions become visible. Mersenne hypothesis suggests that some Mersenne prime is in question. One proposal is that gravitonic size scale is given by electronic Mersenne prime M_{127} . It is however difficult to test whether graviton has a structure visible below this length scale.

What happens to the generalized Feynman diagrams is an interesting question. It is not at all clear how closely they relate to ordinary Feynman diagrams. All depends on what one is ready to assume about what happens in the vertices. One could of course hope that zero energy ontology could allow some very simple description allowing perhaps to get rid of the problematic aspects of Feynman diagrams.

1. Consider first the recent view about generalized Feynman diagrams which relies zero energy ontology. A highly attractive assumption is that the particles appearing at wormhole throats are on mass shell particles. For incoming and outgoing elementary bosons and their super partners they would be positive it resp. negative energy states with parallel on mass shell momenta. For virtual bosons they the wormhole throats would have opposite sign of energy and the sum of on mass shell states would give virtual net momenta. This would make possible twistor description of virtual particles allowing only massless particles (in 4-D sense usually and in 8-D sense in TGD framework). The notion of virtual fermion makes sense only if one assumes in the interaction region a topological condensation creating another wormhole throat having no fermionic quantum numbers.
2. The addition of the particles X^{\pm} replaces generalized Feynman diagrams with the analogs of stringy diagrams with lines replaced by pairs of lines corresponding to fermion and $X_{\pm 1/2}$. The members of these pairs would correspond to 3-D light-like surfaces glued together at the vertices of generalized Feynman diagrams. The analog of 3-vertex would not be splitting of the string to form shorter strings but the replication of the entire string to form two strings with same length or fusion of two strings to single string along all their points rather than along ends to form a longer string. It is not clear whether the duality symmetry of stringy diagrams can hold true for the TGD variants of stringy diagrams.
3. How should one describe the bound state formed by the fermion and X^{\pm} ? Should one describe the state as superposition of non-parallel on mass shell states so that the composite state would

be automatically massive? The description as superposition of on mass shell states does not conform with the idea that bound state formation requires binding energy. In TGD framework the notion of negentropic entanglement has been suggested to make possible the analogs of bound states consisting of on mass shell states so that the binding energy is zero [45]. If this kind of states are in question the description of virtual states in terms of on mass shell states is not lost. Of course, one cannot exclude the possibility that there is infinite number of this kind of states serving as analogs for the excitations of string like object.

4. What happens to the states formed by fermions and $X_{\pm 1/2}$ in the internal lines of the Feynman diagram? Twistor philosophy suggests that only the higher on mass shell excitations are possible. If this picture is correct, the situation would not change in an essential manner from the earlier one.

The highly non-trivial prediction of the magnetic confinement is that elementary particles should have stringy character in electro-weak length scales and could behaving to become manifest at LHC energies. This adds one further item to the list of non-trivial predictions of TGD about physics at LHC energies [20].

2.5 Quantum TGD very briefly

There are two basic approaches to the construction of quantum TGD. The first approach relies on the vision of quantum physics as infinite-dimensional Kähler geometry [78] for the "world of classical worlds" (WCW) identified as the space of 3-surfaces in in certain 8-dimensional space. Essentially a generalization of the Einstein's geometrization of physics program is in question. The second vision is the identification of physics as a generalized number theory involving p-adic number fields and the fusion of real numbers and p-adic numbers to a larger structure, classical number fields, and the notion of infinite prime.

With a better resolution one can distinguish also other visions crucial for quantum TGD. Indeed, the notion of finite measurement resolution realized in terms of hyper-finite factors, TGD as almost topological quantum field theory, twistor approach, zero energy ontology, and weak form of electric-magnetic duality play a decisive role in the actual construction and interpretation of the theory. One can however argue that these visions are not so fundamental for the formulation of the theory than the first two.

2.5.1 Physics as infinite-dimensional geometry

It is good to start with an attempt to give overall view about what the dream about physics as infinite-dimensional geometry is. The basic vision is generalization of the Einstein's program for the geometrization of classical physics so that entire quantum physics would be geometrized. Finite-dimensional geometry is certainly not enough for this purposed but physics as infinite-dimensional geometry of what might be called world of classical worlds (WCW) -or more neutrally configuration space of 3-surfaces of some higher-dimensional imbeddign space- might make sense. The requirement that the Hermitian conjugation of quantum theories has a geometric realization forces Kähler geometry for WCW. WCW defines the fixed arena of quantum physics and physical states are identified as spinor fields in WCW. These spinor fields are classical and no second quantization is needed at this level. The justification comes from the observation that infinite-dimensional Clifford algebra [63] generated by gamma matrices allows a natural identification as fermionic oscillator algebra.

The basic challenges are following.

1. Identify WCW.
2. Provide WCW with Kähler metric and spinor structure
3. Define what spinors and spinor fields in WCW are.

There is huge variety of finite-dimensional geometries and one might think that in infinite-dimensional case one might be drowned with the multitude of possibilities. The situation is however exactly opposite. The loop spaces associated with groups have a unique Kähler geometry due to the simple

condition that Riemann connection exists mathematically [68]. This condition requires that the metric possesses maximal symmetries. Thus raises the vision that infinite-dimensional Kähler geometric existence is unique once one poses the additional condition that the resulting geometry satisfies some basic constraints forced by physical considerations.

The observation about the uniqueness of loop geometries leads also to a concrete vision about what this geometry could be. Perhaps WCW could be regarded as a union of symmetric spaces [75] for which every point is equivalent with any other. This would simplify the construction of the geometry immensely and would mean a generalization of cosmological principle to infinite-D context [37, 51].

This still requires an answer to the question why $M^4 \times CP_2$ is so unique. Something in the structure of this space must distinguish it in a unique manner from any other candidate. The uniqueness of M^4 factor can be understood from the miraculous conformal symmetries of the light-cone boundary but in the case of CP_2 there is no obvious mathematical argument of this kind although physically CP_2 is unique [49]. The observation that $M^4 \times CP_2$ has dimension 8, the space-time surfaces have dimension 4, and partonic 2-surfaces, which are the fundamental objects by holography have dimension 2, suggests that classical number fields [79, 71, 67] are involved and one can indeed end up to the choice $M^4 \times CP_2$ from physics as generalized number theory vision by simple arguments [19, 52]. In particular, the choices M^8 -a subspace of complexified octonions (for octonions see [67]), which I have used to call hyper-octonions- and $M^4 \times CP_2$ can be regarded as physically equivalent: this "number theoretical compactification" is analogous to spontaneous compactification in M-theory. No dynamical compactification takes place so that $M^8 - H$ duality is a more appropriate term.

2.5.2 Physics as generalized number theory

Physics as a generalized number theory (for an overview about number theory see [69]) program consists of three separate threads: various p-adic physics and their fusion together with real number based physics to a larger structure [21, 53], the attempt to understand basic physics in terms of classical number fields [19, 52] (in particular, identifying associativity condition as the basic dynamical principle), and infinite primes [17, 55], whose construction is formally analogous to a repeated second quantization of an arithmetic quantum field theory. In this article a summary of the philosophical ideas behind this dream and a summary of the technical challenges and proposed means to meet them are discussed.

The construction of p-adic physics and real physics poses formidable looking technical challenges: p-adic physics should make sense both at the level of the imbedding space, the "world of classical worlds" (WCW), and space-time and these physics should allow a fusion to a larger coherent whole. This forces to generalize the notion of number by fusing reals and p-adics along rationals and common algebraic numbers. The basic problem that one encounters is definition of the definite integrals and harmonic analysis [77] in the p-adic context [20]. It turns out that the representability of WCW as a union of symmetric spaces [75] provides a universal group theoretic solution not only to the construction of the Kähler geometry of WCW but also to this problem. The p-adic counterpart of a symmetric space is obtained from its discrete invariant by replacing discrete points with p-adic variants of the continuous symmetric space. Fourier analysis [77] reduces integration to summation. If one wants to define also integrals at space-time level, one must pose additional strong constraints which effectively reduce the partonic 2-surfaces and perhaps even space-time surfaces to finite geometries and allow assign to a given partonic 2-surface a unique power of a unique p-adic prime characterizing the measurement resolution in angle variables. These integrals might make sense in the intersection of real and p-adic worlds defined by algebraic surfaces.

The dimensions of partonic 2-surface, space-time surface, and imbedding space suggest that classical number fields might be highly relevant for quantum TGD. The recent view about the connection is based on hyper-octonionic representation of the imbedding space gamma matrices, and the notions of associative and co-associative space-time regions defined as regions for which the modified gamma matrices span quaternionic or co-quaternionic plane at each point of the region. A further condition is that the tangent space at each point of space-time surface contains a preferred hyper-complex (and thus commutative) plane identifiable as the plane of non-physical polarizations so that gauge invariance has a purely number theoretic interpretation. WCW can be regarded as the space of sub-algebras of the local octonionic Clifford algebra [63] of the imbedding space defined by space-time surfaces with the property that the local sub-Clifford algebra spanned by Clifford algebra valued functions restricted

at them is associative or co-associative in a given region.

The recipe for constructing infinite primes is structurally equivalent with a repeated second quantization of an arithmetic super-symmetric quantum field theory. At the lowest level one has fermionic and bosonic states labeled by finite primes and infinite primes correspond to many particle states of this theory. Also infinite primes analogous to bound states are predicted. This hierarchy of quantizations can be continued indefinitely by taking the many particle states of the previous level as elementary particles at the next level. Construction could make sense also for hyper-quaternionic and hyper-octonionic primes although non-commutativity and non-associativity pose technical challenges. One can also construct infinite number of real units as ratios of infinite integers with a precise number theoretic anatomy. The fascinating finding is that the quantum states labeled by standard model quantum numbers allow a representation as wave functions in the discrete space of these units. Space-time point becomes infinitely richly structured in the sense that one can associate to it a wave function in the space of real (or octonionic) units allowing to represent the WCW spinor fields. One can speak about algebraic holography or number theoretic Brahman=Atman identity and one can also say that the points of imbedding space and space-time surface are subject to a number theoretic evolution.

2.5.3 Questions

The experience has shown repeatedly that a correct question and identification of some weakness of existing vision is what can only lead to a genuine progress. In the following I discuss the basic questions, which have stimulated progress in the challenge of constructing WCW geometry.

What is WCW?

Concerning the identification of WCW I have made several guesses and the progress has been basically due to the gradual realization of various physical constraints and the fact that standard physics ontology is not enough in TGD framework.

1. The first guess was that WCW corresponds to all possible space-like 3-surfaces in $H = M^4 \times CP_2$, where M^4 denotes Minkowski space and CP_2 denotes complex projective space of two complex dimensions having also representation as coset space $SU(3)/U(2)$ (see the separate article summarizing the basic facts about CP_2 and how it codes for standard model symmetries [46, 48]). What led to the this particular choice H was the observation that the geometry of H codes for standard model quantum numbers and that the generalization of particle from point like particle to 3-surface allows to understand also remaining quantum numbers having no obvious explanation in standard model (family replication phenomenon). What is important to notice is that Poincare symmetries act as exact symmetries of M^4 rather than space-time surface itself: this realizes the basic vision about Poincare invariant theory of gravitation. This lifting of symmetries to the level of imbedding space and the new dynamical degrees of freedom brought by the sub-manifold geometry of space-time surface are absolutely essential for entire quantum TGD and distinguish it from general relativity and string models. There is however a problem: it is not obvious how to get cosmology.
2. The second guess was that WCW consists of space-like 3-surfaces in $H_+ = M_+^4 \times CP_2$, where M_+^4 future light-cone having interpretation as Big Bang cosmology at the limit of vanishing mass density with light-cone property time identified as the cosmic time. One obtains cosmology but loses exact Poincare invariance in cosmological scales since translations lead out of future light-cone. This as such has no practical significance but due to the metric 2-dimensionality of light-cone boundary δM_+^4 the conformal symmetries of string model assignable to finite-dimensional Lie group generalize to conformal symmetries assignable to an infinite-dimensional symplectic group of $S^2 \times CP_2$ and also localized with respect to the coordinates of 3-surface. These symmetries are simply too beautiful to be important only at the moment of Big Bang and must be present also in elementary particle length scales. Note that these symmetries are present only for 4-D Minkowski space so that a partial resolution of the old conundrum about why space-time dimension is just four emerges.
3. The third guess was that the light-like 3-surfaces in H or H_+ are more attractive than space-like 3-surfaces. The reason is that the infinite-D conformal symmetries characterize also light-like

3-surfaces because they are metrically 2-dimensional. This leads to a generalization of Kac-Moody symmetries [62] of super string models with finite-dimensional Lie group replaced with the group of isometries of H . The natural identification of light-like 3-surfaces is as 3-D surfaces defining the regions at which the signature of the induced metric changes from Minkowskian $(1, -1, -1, -1)$ to Euclidian $(-1 - 1 - 1 - 1)$ - I will refer these surfaces as throats or wormhole throats in the sequel. Light-like 3-surfaces are analogous to blackhole horizons and are static because strong gravity makes them light-like. Therefore also the dimension 4 for the space-time surface is unique.

This identification leads also to a rather unexpected physical interpretation. Single lightlike wormhole throat carriers elementary particle quantum numbers. Fermions and their superpartners are obtained by glueing Euclidian regions (deformations of so called CP_2 type vacuum extremals of Kähler action) to the background with Minkowskian signature. Bosons are identified as wormhole contacts with two throats carrying fermion *resp.* antifermionic quantum numbers. These can be identified as deformations of CP_2 vacuum extremals between between two parallel Minkowskian space-time sheets. One can say that bosons and their superpartners emerge. This has dramatic implications for quantum TGD [19] and QFT limit of TGD [25].

The question is whether one obtains also a generalization of Feynman diagrams. The answer is affirmative. Light-like 3-surfaces or corresponding Euclidian regions of space-time are analogous to the lines of Feynman diagram and vertices are replaced by 2-D surface at which these surfaces glued together. One can speak about Feynman diagrams with lines thickened to light-like 3-surfaces and vertices to 2-surfaces. The generalized Feynman diagrams are singular as 3-manifolds but the vertices are non-singular as 2-manifolds. Same applies to the corresponding space-time surfaces and space-like 3-surfaces. Therefore one can say that WCW consists of generalized Feynman diagrams- something rather different from the original identification as space-like 3-surfaces and one can wonder whether these identification could be equivalent.

4. The fourth guess was a generalization of the WCW combining the nice aspects of the identifications $H = M^4 \times CP_2$ (exact Poincare invariance) and $H = M^4_+ \times CP_2$ (Big Bang cosmology). The idea was to generalize WCW to a union of basic building bricks -causal diamonds (CDs) - which themselves are analogous to Big Bang-Big Crunch cosmologies breaking Poincare invariance, which is however regained by the allowance of union of Poincare transforms of the causal diamonds.

The starting point is General Coordinate Invariance (GCI). It does not matter, which 3-D slice of the space-time surface one choose to represent physical data as long as slices are related by a diffeomorphism of the space-time surface. This condition implies holography in the sense that 3-D slices define holograms about 4-D reality.

The question is whether one could generalize GCI in the sense that the descriptions using space-like and light-like 3-surfaces would be equivalent physically. This requires that finite-sized space-like 3-surfaces are somehow equivalent with light-like 3-surfaces. This suggests that the light-like 3-surfaces must have ends. Same must be true for the space-time surfaces and must define preferred space-like 3-surfaces just like wormhole throats do. This makes sense only if the 2-D intersections of these two kinds of 3-surfaces -call them partonic 2-surfaces- and their 4-D tangent spaces carry the information about quantum physics. A strengthening of holography principle would be the outcome. The challenge is to understand, where the intersections defining the partonic 2-surfaces are located.

Zero energy ontology (ZEO) allows to meet this challenge.

- (a) Assume that WCW is union of sub-WCWs identified as the space of light-like 3-surfaces assignable to $CD \times CP_2$ with given CD defined as an intersection of future and past directed lightcones of M^4 . The tips of CD s have localization in M^4 and one can perform for CD both translations and Lorentz boost for CD s. Space-time surfaces inside CD define the basic building brick of WCW. Also unions of CD s allowed and the CD s belonging to the union can intersect. One can of course consider the possibility of intersections and analogy with the set theoretic realization of topology.
- (b) ZEO property means that the light-like boundaries of these objects carry positive and negative energy states, whose quantum numbers are opposite. Everything can be created

from vacuum and can be regarded as quantum fluctuations in the standard vocabulary of quantum field theories.

- (c) Space-time surfaces inside CDs begin from the lower boundary and end to the upper boundary and in ZEO it is natural to identify space-like 3-surfaces as pairs of space-like 3-surfaces at these boundaries. Light-like 3-surfaces connect these boundaries.
- (d) The generalization of GCI states that the descriptions based on space-like 3-surfaces must be equivalent with that based on light-like 3-surfaces. Therefore only the 2-D intersections of light-like and space-like 3-surfaces - partonic 2-surfaces- and their 4-D tangent spaces (4-surface is there!) matter. Effective 2-dimensionality means a strengthened form of holography but does not imply exact 2-dimensionality, which would reduce the theory to a mere string model like theory. Once these data are given, the 4-D space-time surface is fixed and is analogous to a generalization of Bohr orbit to infinite-D context. This is the first guess. The situation is actually more delicate due to the non-determinism of Kähler action motivating the interaction of the hierarchy of CDs within CDs .

In this framework one obtains cosmology: CDs represent a fractal hierarchy of big bang-big crunch cosmologies. One obtains also Poincare invariance. One can also interpret the non-conservation of gravitational energy in cosmology which is an empirical fact but in conflict with exact Poincare invariance as it is realized in positive energy ontology [35, 16]. The reason is that energy and four-momentum in zero energy ontology correspond to those assignable to the positive energy part of the zero energy state of a particular CD . The density of energy as cosmologist defines it is the statistical average for given CD : this includes the contributions of sub- CDs . This average density is expected to depend on the size scale of CD density is should therefore change as quantum dispersion in the moduli space of CDs takes place and leads to large time scale for any fixed sub- CD .

Even more, one obtains actually quantum cosmology! There is large variety of CDs since they have position in M^4 and Lorentz transformations change their shape. The first question is whether the M^4 positions of both tips of CD can be free so that one could assign to both tips of CD momentum eigenstates with opposite signs of four-momentum. The proposal, which might look somewhat strange, is that this not the case and that the proper time distance between the tips is quantized in octaves of a fundamental time scale $T = R/c$ defined by CP_2 size R . This would explain p-adic length scale hypothesis which is behind most quantitative predictions of TGD. That the time scales assignable to the CD of elementary particles correspond to biologically important time scales [43] forces to take this hypothesis very seriously.

The interpretation for T could be as a cosmic time quantized in powers of two. Even more general quantization is proposed to take place. The relative position of the second tip with respect to the first defines a point of the proper time constant hyperboloid of the future light cone. The hypothesis is that one must replace this hyperboloid with a lattice like structure. This implies very powerful cosmological predictions finding experimental support from the quantization of redshifts for instance [16]. For quite recent further empirical support see [110].

One should not take this argument without a grain of salt. Can one really realize zero energy ontology in this framework? The geometric picture is that translations correspond to translations of CDs . Translations should be done independently for the upper and lower tip of CD if one wants to speak about zero energy states but this is not possible if the proper time distance is quantized. If the relative M^4_+ coordinate is discrete, this pessimistic conclusion is strengthened further.

The manner to get rid of problem is to assume that translations are represented by quantum operators acting on states at the light-like boundaries. This is just what standard quantum theory assumes. An alternative- purely geometric- way out of difficulty is the Kac-Moody symmetry associated with light-like 3-surfaces meaning that local M^4 translations depending on the point of partonic 2-surface are gauge symmetries. For a given translation leading out of CD this gauge symmetry allows to make a compensating transformation which allows to satisfy the constraint.

This picture is roughly the recent view about WCW . What deserves to be emphasized is that a very concrete connection with basic structures of quantum field theory emerges already at the level of

basic objects of the theory and GCI implies a strong form of holography and almost stringy picture.

Some Why's

In the following I try to summarize the basic motivations behind quantum TGD in form of various Why's.

1. Why WCW?

Einstein's program has been extremely successful at the level of classical physics. Fusion of general relativity and quantum theory has however failed. The generalization of Einstein's geometrization program of physics from classical physics to quantum physics gives excellent hopes about the success in this project. Infinite-dimensional geometries are highly unique and this gives hopes about fixing the physics completely from the uniqueness of the infinite-dimensional Kähler geometric existence.

2. Why spinor structure in WCW?

Gamma matrices defining the Clifford algebra [63] of WCW are expressible in terms of fermionic oscillator operators. This is obviously something new as compared to the view about gamma matrices as bosonic objects. There is however no deep reason denying this kind of identification. As a consequence, a geometrization of fermionic oscillator operator algebra and fermionic statistics follows as also geometrization of super-conformal symmetries [70, 62] since gamma matrices define super-generators of the algebra of WCW isometries extended to a super-algebra.

3. Why Kähler geometry?

Geometrization of the bosonic oscillator operators in terms of WCW vector fields and fermionic oscillator operators in terms of gamma matrices spanning Clifford algebra. Gamma matrices span hyper-finite factor of type II_1 and the extremely beautiful properties of these von Neuman algebras [60] (one of the three von Neuman algebras that von Neumann suggests as possible mathematical frameworks behind quantum theory) lead to a direct connection with the basic structures of modern physics (quantum groups, non-commutative geometries,.. [56]).

A further reason why is the finiteness of the theory.

- (a) In standard QFTs there are two kinds of divergences. Action is a local functional of fields in 4-D sense and one performs path integral over **all** 4-surfaces to construct S-matrix. Mathematically path integration is a poorly defined procedure and one obtains diverging Gaussian determinants and divergences due to the local interaction vertices. Regularization provides the manner to get rid of the infinities but makes the theory very ugly.
- (b) Kähler function defining the Kähler geometry is expected to be non-local functional of the partonic 2-surface (Kähler action for a preferred extremal having as its ends the positive and negative energy 3-surfaces). Path integral is replaced with a functional integral which is mathematically well-defined procedure and one performs functional integral only over the partonic 2-surfaces rather than all 4-surfaces (holography). The exponent of Kähler function defines a unique vacuum functional. The local divergences of local quantum field theories since there are no local interaction vertices. Also the divergences associated with the Gaussian determinant and metric determinant cancel since these two determinants cancel each other in the integration over WCW. As a matter fact, symmetric space property suggest a much more elegant manner to perform the functional integral by reducing it to harmonic analysis in infinite-dimensional symmetric space [55].
- (c) One can imagine also the possibility of divergences in fermionic degrees of freedom but it has turned out that the generalized Feynman diagrams in ZEO are manifestly finite. Even more: it is quite possible that only finite number of these diagrams give non-vanishing contributions to the scattering amplitude. This is essentially due to the new view about virtual particles, which are identified as bound states of on mass shell states assigned with the throats of wormhole contacts so that the integration over loop momenta of virtual particles is extremely restricted [55].

4. Why infinite-dimensional symmetries?

WCW must be a union of symmetric spaces in order that the Riemann connection exists (this generalizes the finding of Freed for loop groups [68]). Since the points of symmetric spaces are metrically equivalent, the geometrization becomes tractable although the dimension is infinite. A union of symmetric spaces is required because 3-surfaces with a size of galaxy and electron cannot be metrically equivalent. Zero modes distinguish these surfaces and can be regarded as purely classical degrees of freedom whereas the degrees of freedom contributing to the WCW line element are quantum fluctuating degrees of freedom.

One immediate implication of the symmetric space property is constant curvature space property meaning that the Ricci tensor proportional to metric tensor. Infinite-dimensionality means that Ricci scalar either vanishes or is infinite. This implies vanishing of Ricci tensor and vacuum Einstein equations for WCW.

5. Why $M^4 \times CP_2$?

This choice provides an explanation for standard model quantum numbers. The conjecture is that infinite-D geometry of 3-surfaces exists only for this choice. As noticed, the dimension of space-time surfaces and M^4 fixed by the requirement of generalized conformal invariance [83] making possible to achieve symmetric space property. If $M^4 \times CP_2$ is so special, there must be a good reason for this. Number theoretical vision [19, 52] indeed leads to the identification of this reason. One can assign the hierarchy of dimensions associated with partonic 2-surfaces, space-time surfaces and imbedding space to classical number fields and can assign to imbedding space what might be called hyper-octonionic structure. "Hyper" comes from the fact that the tangent space of H corresponds to the subspaces of complexified octonions with octonionic imaginary units multiplied by a commuting imaginary unit. The space-time regions would be either hyper-quaternionic or co-hyper-quaternionic so that associativity/co-associativity would become the basic dynamical principle at the level of space-time dynamics. Whether this dynamical principle is equivalent with the preferred extremal property of Kähler action remains an open conjecture.

6. Why zero energy ontology and why causal diamonds?

The consistency between Poincare invariance and GRT requires ZEO. In positive energy ontology only one of the infinite number of classical solutions is realized and partially fixed by the values of conserved quantum numbers so that the theory becomes obsolete. Even in quantum theory conservation laws mean that only those solutions of field equations with the quantum numbers of the initial state of the Universe are interesting and one faces the problem of understanding what the the initial state of the universe was. In ZEO these problems disappear. Everything is creatable from vacuum: if the physical state is mathematically realizable it is in principle reachable by a sequence of quantum jumps. There are no physically non-reachable entities in the theory. Zero energy ontology leads also to a fusion of thermodynamics with quantum theory. Zero energy states are defined as entangled states of positive and negative energy states and entanglement coefficients define what I call M -matrix identified as "complex square root" of density matrix expressible as a product of diagonal real and positive density matrix and unitary S -matrix [19].

There are several good reasons why for causal diamonds. ZEO requires CD s, the generalized form of GCI and strong form of holography (light-like and space-like 3-surfaces are physically equivalent representations) require CD s, and also the view about light-like 3-surfaces as generalized Feynman diagrams requires CD s. Also the classical non-determinism of Kähler action can be understood using the hierarchy CD s and the addition of CD s inside CD s to obtain a fractal hierarchy of them provides an elegant manner to understand radiative corrections and coupling constant evolution in TGD framework.

A strong physical argument in favor of CD s is the finding that the quantized proper time distance between the tips of CD fixed to be an octave of a fundamental time scale defined by CP_2 happens to define fundamental biological time scale for electron, u quark and d quark [43]: there would be a deep connection between elementary particle physics and living matter leading to testable predictions.

2.5.4 Modified Dirac action

The construction of the spinor structure for the world of classical worlds (WCW) leads to the vision that second quantized modified Dirac equation codes for the entire quantum TGD. Among other things this would mean that Dirac determinant would define the vacuum functional of the theory having interpretation as the exponent of Kähler function of WCW and Kähler function would reduce to Kähler action for a preferred extremal of Kähler action. In this chapter the recent view about the modified Dirac action are explained in more detail.

Identification of the modified Dirac action

The modified Dirac action involves several terms. The first one is 4-dimensional assignable to Kähler action. Second term is instanton term reducible to an expression restricted to wormhole throats or any light-like 3-surfaces parallel to them in the slicing of space-time surface by light-like 3-surfaces. The third term is assignable to Chern-Simons term and has interpretation as a measurement interaction term linear in Cartan algebra of the isometry group of the imbedding space in order to obtain stringy propagators and also to realize coupling between the quantum numbers associated with super-conformal representations and space-time geometry required by quantum classical correspondence.

This means that 3-D light-like wormhole throats carry induced spinor field which can be regarded as independent degrees of freedom having the spinor fields at partonic 2-surfaces as sources and acting as 3-D sources for the 4-D induced spinor field. The most general measurement interaction would involve the corresponding coupling also for Kähler action but is not physically motivated. There are good arguments in favor of Chern-Simons Dirac action and corresponding measurement interaction.

1. A correlation between 4-D geometry of space-time sheet and quantum numbers is achieved by the identification of exponent of Kähler function as Dirac determinant making possible the entanglement of classical degrees of freedom in the interior of space-time sheet with quantum numbers.
2. Cartan algebra plays a key role not only at quantum level but also at the level of space-time geometry since quantum critical conserved currents vanish for Cartan algebra of isometries and the measurement interaction terms giving rise to conserved currents are possible only for Cartan algebras. Furthermore, modified Dirac equation makes sense only for eigen states of Cartan algebra generators. The hierarchy of Planck constants realized in terms of the book like structure of the generalized imbedding space assigns to each CD (causal diamond) preferred Cartan algebra: in case of Poincare algebra there are two of them corresponding to linear and cylindrical M^4 coordinates.
3. Quantum holography and dimensional reduction hierarchy in which partonic 2-surface defined fermionic sources for 3-D fermionic fields at light-like 3-surfaces Y_l^3 in turn defining fermionic sources for 4-D spinors find an elegant realization. Effective 2-dimensionality is achieved if the replacement of light-like wormhole throat X_l^3 with light-like 3-surface Y_l^3 "parallel" with it in the definition of Dirac determinant corresponds to the $U(1)$ gauge transformation $K \rightarrow K + f + \bar{f}$ for Kähler function of WCW so that WCW Kähler metric is not affected. Here f is holomorphic function of WCW ("world of classical worlds") complex coordinates and arbitrary function of zero mode coordinates.
4. An elegant description of the interaction between super-conformal representations realized at partonic 2-surfaces and dynamics of space-time surfaces is achieved since the values of Cartan charges are feeded to the 3-D Dirac equation which also receives mass term at the same time. Almost topological QFT at wormhole throats results at the limit when four-momenta vanish: this is in accordance with the original vision about TGD as almost topological QFT.
5. A detailed view about the physical role of quantum criticality results. Quantum criticality fixes the values of Kähler coupling strength as the analog of critical temperature. Quantum criticality implies that second variation of Kähler action vanishes for critical deformations and the existence of conserved current except in the case of Cartan algebra of isometries. Quantum criticality allows to fix the values of couplings appearing in the measurement interaction by using

the condition $K \rightarrow K + f + \bar{f}$. p-Adic coupling constant evolution can be understood also and corresponds to scale hierarchy for the sizes of causal diamonds (CDs).

6. The inclusion of imaginary instanton term to the definition of the modified gamma matrices is not consistent with the conjugation of the induced spinor fields. Measurement interaction can be however assigned to both Kähler action and its instanton term. CP breaking, irreversibility and the space-time description of dissipation are closely related and the CP and T oddness of the instanton part of the measurement interaction term could provide first level description for dissipative effects. It must be however emphasized that the mere addition of instanton term to Kähler function could be enough.
7. A radically new view about matter antimatter asymmetry based on zero energy ontology emerges and one could understand the experimental absence of antimatter as being due to the fact antimatter corresponds to negative energy states. The identification of bosons as wormhole contacts is the only possible option in this framework.
8. Almost stringy propagators and a consistency with the identification of wormhole throats as lines of generalized Feynman diagrams is achieved. The notion of bosonic emergence leads to a long sought general master formula for the M -matrix elements. The counterpart for fermionic loop defining bosonic inverse propagator at QFT limit is wormhole contact with fermion and cutoffs in mass squared and hyperbolic angle for loop momenta of fermion and antifermion in the rest system of emitting boson have precise geometric counterpart.

Hyper-quaternionicity and quantum criticality

The conjecture that quantum critical space-time surfaces are hyper-quaternionic in the sense that the modified gamma matrices span a quaternionic subspace of complexified octonions at each point of the space-time surface is consistent with what is known about preferred extremals. The condition that both the modified gamma matrices and spinors are quaternionic at each point of the space-time surface leads to a precise ansatz for the general solution of the modified Dirac equation making sense also in the real context. The octonionic version of the modified Dirac equation is very simple since $SO(7,1)$ as vielbein group is replaced with G_2 acting as automorphisms of octonions so that only the neutral Abelian part of the classical electro-weak gauge fields survives the map.

Octonionic gamma matrices provide also a non-associative representation for the 8-D version of Pauli sigma matrices and encourage the identification of 8-D twistors as pairs of octonionic spinors conjectured to be highly relevant also for quantum TGD. Quaternionicity condition implies that octo-twistors reduce to something closely related to ordinary twistors.

The exponent of Kähler function as Dirac determinant for the modified Dirac action

Although quantum criticality in principle predicts the possible values of Kähler coupling strength, one might hope that there exists even more fundamental approach involving no coupling constants and predicting even quantum criticality and realizing quantum gravitational holography.

1. The Dirac determinant defined by the product of Dirac determinants associated with the light-like partonic 3-surfaces X_l^3 associated with a given space-time sheet X^4 is the simplest candidate for vacuum functional identifiable as the exponent of the Kähler function. Individual Dirac determinant is defined as the product of eigenvalues of the dimensionally reduced modified Dirac operator $D_{K,3}$ and there are good arguments suggesting that the number of eigenvalues is finite. p-Adicization requires that the eigenvalues belong to a given algebraic extension of rationals. This restriction would imply a hierarchy of physics corresponding to different extensions and could automatically imply the finiteness and algebraic number property of the Dirac determinants if only finite number of eigenvalues would contribute. The regularization would be performed by physics itself if this were the case.
2. It remains to be proven that the product of eigenvalues gives rise to the exponent of Kähler action for the preferred extremal of Kähler action. At this moment the only justification for the conjecture is that this the only thing that one can imagine.

3. A long-standing conjecture has been that the zeros of Riemann Zeta are somehow relevant for quantum TGD. Riemann zeta is however naturally replaced Dirac zeta defined by the eigenvalues of $D_{K,3}$ and closely related to Riemann Zeta since the spectrum consists essentially for the cyclotron energy spectra for localized solutions region of non-vanishing induced Kähler magnetic field and hence is in good approximation integer valued up to some cutoff integer. In zero energy ontology the Dirac zeta function associated with these eigenvalues defines "square root" of thermodynamics assuming that the energy levels of the system in question are expressible as logarithms of the eigenvalues of the modified Dirac operator defining kind of fundamental constants. Critical points correspond to approximate zeros of Dirac zeta and if Kähler function vanishes at criticality as it indeed should, the thermal energies at critical points are in first order approximation proportional to zeros themselves so that a connection between quantum criticality and approximate zeros of Dirac zeta emerges.
4. The discretization induced by the number theoretic braids reduces the world of classical worlds to effectively finite-dimensional space and configuration space Clifford algebra reduces to a finite-dimensional algebra. The interpretation is in terms of finite measurement resolution represented in terms of Jones inclusion $\mathcal{M} \subset \mathcal{N}$ of HFFs with \mathcal{M} taking the role of complex numbers. The finite-D quantum Clifford algebra spanned by fermionic oscillator operators is identified as a representation for the coset space \mathcal{N}/\mathcal{M} describing physical states modulo measurement resolution. In the sectors of generalized imbedding space corresponding to non-standard values of Planck constant quantum version of Clifford algebra is in question.

2.5.5 Three Dirac operators and their interpretation

The physical interpretation of Kähler Dirac equation is not at all straightforward. The following arguments inspired by effective 2-dimensionality suggest that the modified gamma matrices and corresponding effective metric could allow dual gravitational description of the physics associated with wormhole throats. This applies in particular to condensed matter physics.

Three Dirac equations

To begin with, Dirac equation appears in three forms in TGD.

1. The Dirac equation in world of classical worlds codes for the super Virasoro conditions for the super Kac-Moody and similar representations formed by the states of wormhole contacts forming the counterpart of string like objects (throats correspond to the ends of the string. This Dirac generalizes the Dirac of 8-D imbedding space by bringing in vibrational degrees of freedom. This Dirac equation should give as its solutions zero energy states and corresponding M-matrices generalizing S-matrix and their collection defining the unitary U-matrix whose natural application appears in consciousness theory as a coder of what Penrose calls U-process.
2. There is generalized eigenvalue equation for Chern-Simons Dirac operator at light-like wormhole throats. The generalized eigenvalue is $p^k \gamma_k$. The interpretation of pseudo-momentum p^k has been a problem but twistor Grassmannian approach suggests strongly that it can be interpreted as the counterpart of equally mysterious region momentum appearing in momentum twistor Grassmannian approach to $\mathcal{N} = 4$ SYM. The pseudo-/region momentum p is quantized (this does not spoil the basics of Grassmannian residues integral approach) and $1/p^k \gamma_k$ defines propagator in lines of generalized Feynman diagrams. The Yangian symmetry discovered generalizes in a very straightforward manner and leads also to the realization that TGD could allow also a twistorial formulation in terms of product $CP_3 \times CP_3$ of two twistor spaces [19]. General arguments lead to a proposal for explicit form for the solutions of field equation represented identified as holomorphic 6-surfaces in this space subject to additional partial differential equations for homogenous functions of projective twistor coordinates suggesting strongly the quantal interpretation as analogs of partial waves. Therefore quantum-classical correspondence would be realized in beautiful manner.
3. There is Kähler Dirac equation in the interior of space-time. In this equation the gamma matrices are replaced with modified gamma matrices defined by the contractions of canonical momentum

currents $T_k^\alpha = \partial L / \partial_\alpha h^k$ with imbedding space gamma matrices Γ_k . This replacement is required by internal consistency and by super-conformal symmetries.

Could Kähler Dirac equation provide a first principle justification for the light-hearted use of effective mass and the analog of Dirac equation in condensed matter physics? This would conform with the holographic philosophy. Partonic 2-surfaces with tangent space data and their light-like orbits would give hologram like representation of physics and the interior of space-time the 4-D representation of physics. Holography would have in the recent situation interpretation also as quantum classical correspondence between representations of physics in terms of quantized spinor fields at the light-like 3-surfaces on one hand and in terms of classical fields on the other hand.

The resulting dispersion relation for the square of the Kähler-Dirac operator assuming that induced like metric, Kähler field, etc. are very slowly varying contains quadratic and linear terms in momentum components plus a term corresponding to magnetic moment coupling. In general massive dispersion relation is obtained as is also clear from the fact that Kähler Dirac gamma matrices are combinations of M^4 and CP_2 gammas so that modified Dirac mixes different M^4 chiralities (basic signal for massivation). If one takes into account the dependence of the induced geometric quantities on space-time point dispersion relations become non-local.

Does energy metric provided the gravitational dual for condensed matter systems?

The modified gamma matrices define an effective metric via their anticommutators which are quadratic in components of energy momentum tensor (canonical momentum densities). This effective metric vanishes for vacuum extremals. Note that the use of modified gamma matrices guarantees among other things internal consistency and super-conformal symmetries of the theory. The physical interpretation has remained obscure hitherto although corresponding effective metric for Chern-Simons Dirac action has now a clear physical interpretation.

If the above argument is on the right track, this effective metric should have applications in condensed matter theory. In fact, energy metric has a natural interpretation in terms of effective light velocities which depend on direction of propagation. One can diagonalize the energy metric $g_e^{\alpha\beta}$ (contravariant form results from the anticommutators) and one can denote its eigenvalues by (v_0, v_i) in the case that the signature of the effective metric is $(1, -1, -1, -1)$. The 3-vector v_i/v_0 has interpretation as components of effective light velocity in various directions as becomes clear by thinking the d'Alembert equation for the energy metric. This velocity field could be interpreted as that of hydrodynamic flow. The study of the extremals of Kähler action shows that if this flow is actually Beltrami flow so that the flow parameter associated with the flow lines extends to global coordinate, Kähler action reduces to a 3-D Chern-Simons action and one obtains effective topological QFT. The conserved fermion current $\bar{\Psi}\Gamma_e^\alpha\Psi$ has interpretation as incompressible hydrodynamical flow.

This would give also a nice analogy with AdS/CFT correspondence allowing to describe various kinds of physical systems in terms of higher-dimensional gravitation and black holes are introduced quite routinely to describe condensed matter systems. In TGD framework one would have an analogous situation but with 10-D space-time replaced with the interior of 4-D space-time and the boundary of AdS representing Minkowski space with the light-like 3-surfaces carrying matter. The effective gravitation would correspond to the "energy metric". One can associate with it curvature tensor, Ricci tensor and Einstein tensor using standard formulas and identify effective energy momentum tensor associated as Einstein tensor with effective Newton's constant appearing as constant of proportionality. Note however that the besides ordinary metric and "energy" metric one would have also the induced classical gauge fields having purely geometric interpretation and action would be Kähler action. This 4-D holography would provide a precise, dramatically simpler, and also a very concrete dual description. This cannot be said about model of graphene based on the introduction of 10-dimensional black holes, branes, and strings chosen in more or less ad hoc manner.

This raises questions. Does this give a general dual gravitational description of dissipative effects in terms of the "energy" metric and induced gauge fields? Does one obtain the counterparts of black holes? Do the general theorems of general relativity about the irreversible evolution leading to black holes generalize to describe analogous fate of condensed matter systems caused by dissipation? Can one describe non-equilibrium thermodynamics and self-organization in this manner?

One might argue that the incompressible Beltrami flow defined by the dynamics of the preferred extremals is dissipationless and viscosity must therefore vanish locally. The failure of complete non-determinism of Kähler action however means generation of entropy since the knowledge about the

state decreases gradually. This in turn should have a phenomenological local description in terms of viscosity which characterizes the transfer of energy to shorter scales and eventually to radiation. The deeper description should be non-local and basically topological and might lead to quantization rules. For instance, one can imagine the quantization of the ratio η/s of the viscosity to entropy density as multiples of a basic unit defined by its lower bound (note that this would be analogous to Quantum Hall effect). For the first M-theory inspired derivation of the lower bound of η/s [98]. The lower bound for η/s is satisfied in good approximation by what should have been QCD plasma but found to be something different (RHIC and the first evidence for new physics from LHC [20]).

An encouraging sign comes from the observation that for so called massless extremals representing classically arbitrarily shaped pulses of radiation propagating without dissipation and dispersion along single direction the canonical momentum currents are light-like. The effective contravariant metric vanishes identically so that fermions cannot propagate in the interior of massless extremals! This is of course the case also for vacuum extremals. Massless extremals are purely bosonic and represent bosonic radiation. Many-sheeted space-time decomposes into matter containing regions and radiation containing regions. Note that when wormhole contact (particle) is glued to a massless extremal, it is deformed so that CP_2 projection becomes 4-D guaranteeing that the weak form of electric magnetic duality can be satisfied. Therefore massless extremals can be seen as asymptotic regions. Perhaps one could say that dissipation corresponds to a decoherence process creating space-time sheets consisting of matter and radiation. Those containing matter might be even seen as analogs blackholes as far as energy metric is considered.

2.6 The role of twistors in quantum TGD

2.6.1 Could the Grassmannian program be realized in TGD framework?

In the following the TGD based modification of the approach based on zero energy ontology is discussed in some detail. It is found that pseudo-momenta are very much analogous to region momenta and the approach leading to discretization of pseudo-mass squared for virtual particles - and even the discretization of pseudo-momenta - is consistent with the Grassmannian approach in the simple case considered and allow to get rid of IR divergences. Also the possibility that the number of generalized Feynman diagrams contributing to a given scattering amplitude is finite so that the recursion formula for the scattering amplitudes would involve only a finite number of steps (maximum number of loops) is considered. One especially promising feature of the residue integral approach with discretized pseudo-momenta is that it makes sense also in the p-adic context in the simple special case discussed since residue integral reduces to momentum integral (summation) and lower-dimensional residue integral.

What Yangian symmetry could mean in TGD framework?

The loss of the Yangian symmetry in the integrations over the region momenta x^a ($p^a = x^{a+1} - x^a$) assigned to virtual momenta seems to be responsible for many ugly features. It is basically the source of IR divergences regulated by "moving out on the Coulomb branch theory" so that IR singularities remain the problem of the theory. This raises the question whether the loss of Yangian symmetry is the signature for the failure of QFT approach and whether the restriction of loop momentum integrations to avoid both kind of divergences might be a royal road beyond QFT. In TGD framework zero energy ontology indeed leads to a concrete proposal based on the vision that virtual particles are something genuinely real.

The detailed picture is of course far from clear but to get an idea about what is involved one can look what kind of assumptions are needed if one wants to realize the dream that only a finite number of generalized Feynman diagrams contribute to a scattering amplitude which is Yangian invariant allowing a description using a generalization of the Grassmannian integrals.

1. Assume the bosonic emergence and its super-symmetric generalization holds true. This means that incoming and outgoing states are bound states of massless fermions assignable to wormhole throats but the fermions can opposite directions of three-momenta making them massive. Incoming and outgoing particles would consist of fermions associated with wormhole throats and would be characterized by a pair of twistors in the general situation and in general massive. This allows also string like mass squared spectrum for bound states having fermion and antifermion

at the ends of the string as well as more general n -particle bound states. Hence one can speak also about the emergence of string like objects. For virtual particles the fermions would be massive and have discrete mass spectrum. Also super partners containing several collinear fermions and antifermions at a given throat are possible. Collinearity is required by the generalization of SUSY. The construction of these states bring strongly in mind the merge procedure involving the replacement $Z^{n+1} \rightarrow Z^n$.

2. The basic question is how the momentum twistor diagrams and the ordinary Feynman diagrams behind them are related to the generalized Feynman diagrams.
 - (a) It is good to start from a common problem. In momentum twistor approach the relationship of region momenta to physical momenta remains somewhat mysterious. In TGD framework in turn the relationship of pseudo-momenta identified as generalized eigenvalues of the Chern-Simons Dirac operator at the lines of Feynman diagram (light-like wormhole throats) to the physical momenta has remained unclear. The identification of the pseudo-momentum as the TGD counterpart of the region momentum x looks therefore like a natural first guess.
 - (b) The identification $x_{a+1} - x_a = p_a$ with p_a representing light-like physical four-momentum generalizes in obvious manner. Also the identification of the light-like momentum of the external parton as pseudo-momentum looks natural. What is important is that this does not require the identification of the pseudo-momenta propagating along internal lines of generalized Feynman diagram as actual physical momenta since pseudo-momentum just like x is fixed only apart from an overall shift. The identification allows the physical four-momenta associated with the wormhole throats to be always on mass shell and massless: if the sign of the physical energy can be also negative space-like momentum exchanges become possible.
 - (c) The pseudo-momenta and light-like physical massless momenta at the lines of generalized Feynman diagrams on one hand, and region momenta and the light-like momenta associated with the collinear singularities on the other hand would be in very similar mutual relationship. Partonic 2-surfaces can carry large number of collinear light-like fermions and bosons since super-symmetry is extended. Generalized Feynman diagrams would be analogous to momentum twistor diagrams if this picture is correct and one could hope that the recursion relations of the momentum twistor approach generalize.
3. The discrete mass spectrum for pseudo-momentum would in the momentum twistor approach mean the restriction of x to discrete mass shells, and the obvious reason for worry is that this might spoil the Grassmannian approach relying heavily on residue integrals and making sense also p -adically. It seems however that there is no need to worry. In [97] the $M_{6,4,l=0}(1234AB)$ the integration over twistor variables z_A and z_B using "entangled" integration contour leads to 1-loop MHV amplitude $N^p MHV$, $p = 1$. The parametrization of the integration contour is $z_A = (\lambda_A, x\lambda_A)$, $z_B = (\lambda_B, x\lambda_B)$, where x is the M^4 coordinate representing the loop momentum. This boils down to an integral over $CP_1 \times CP_1 \times M^4$ [97]. The integrals over spheres CP_1 s are contour integrals so that only an ordinary integral over M^4 remains. The reduction to this kind of sums occurs completely generally thanks to the recursion formula.
4. The obvious implication of the restriction of the pseudo-momenta x on massive mass shells is the absence of IR divergences and one might hope that under suitable assumptions one achieves Yangian invariance. The first question is of course whether the required restriction of x to mass shells in z_A and z_B or possibly even algebraic discretization of momenta is consistent with the Yangian invariance. This seems to be the case: the integration contour reduces to entangled integration contour in $CP_1 \times CP_1$ not affected by the discretization and the resulting loop integral differs from the standard one by the discretization of masses and possibly also momenta with massless states excluded. Whether Yangian invariance poses also conditions on mass and momentum spectrum is an interesting question.
5. One can consider also the possibility that the incoming and outgoing particles - in general massive and to be distinguished from massless fermions appearing as their building blocks- have actually small masses presumably related to the IR cutoff defined by the size scale of the largest causal diamond involved. p -Adic thermodynamics could be responsible for this mass. Also

the binding of the wormhole throats can give rise to a small contribution to vacuum conformal weight possibly responsible for gauge boson masses. This would imply that a given n -particle state can decay to N -particle states for which N is below some limit. The fermions inside loops would be also massive. This allows to circumvent the IR singularities due to integration over the phase space of the final states (say in Coulomb scattering).

6. The representation of the off mass shell particles as pairs of wormhole throats with non-parallel four-momenta (in the simplest case only the three-momenta need be in opposite directions) makes sense and that the particles in question are on mass shell with mass squared being proportional to inverse of a prime number as the number theoretic vision applied to the modified Dirac equation suggests. On mass shell property poses extremely powerful constraints on loops and when the number of the incoming momenta in the loop increases, the number of constraints becomes larger than the number of components of loop momentum for the generic values of the external momenta. Therefore there are excellent hopes of getting rid of UV divergences.

A stronger assumption encouraged by the classical space-time picture about virtual particles is that the 3-momenta associated with throats of the same wormhole contact are always in same or opposite directions. Even this allows to have virtual momentum spectrum and non-trivial mass spectrum for them assuming that the three momenta are opposite.

7. The best that one can hope is that only a finite number of generalized Feynman diagrams contributes to a given reaction. This would guarantee that amplitudes belong to a finite-dimensional algebraic extension of rational functions with rational coefficients since finite sums do not lead out from a finite algebraic extension of rationals. The first problem are self energy corrections. The assumption that the mass non-renormalization theorems of SUSYs generalize to TGD framework would guarantee that the loops contributing to fermionic propagators (and their super-counterparts) do not affect them. Also the iteration of more complex amplitudes as analogs of ladder diagrams representing sequences of reactions $M \rightarrow M_1 \rightarrow M_2 \cdots \rightarrow N$ such that at each M_n in the sequence can appear as on mass shell state could give a non-vanishing contribution to the scattering amplitude and would mean infinite number of Feynman diagrams unless these amplitudes vanish. If N appears as a virtual state the fermions must be however massive on mass shell fermions by the assumption about on-mass shell states and one can indeed imagine a situation in which the decay $M \rightarrow N$ is possible when N consists of states made of massless fermions is possible but not when the fermions have non-vanishing masses. This situation seems to be consistent with unitarity. The implication would be that the recursion formula for the all loop amplitudes for a given reaction would give vanishing result for some critical value of loops.

Already these assumptions give good hopes about a generalization of the momentum Grassmann approach to TGD framework. Twistors are doubled as are also the Grassmann variables and there are wave functions correlating the momenta of the the fermions associated with the opposite wormhole throats of the virtual particles as well as incoming gauge bosons which have suffered massivation. Also wave functions correlating the massless momenta at the ends of string like objects and more general many parton states are involved but do not affect the basic twistor formalism. The basic question is whether the hypothesis of unbroken Yangian symmetry could in fact imply something resembling this picture. The possibility to discretize integration contours without losing the representation as residue integral quite generally is basic prerequisite for this and should be shown to be true.

How to achieve Yangian invariance without trivial scattering amplitudes?

In $\mathcal{N} = 4$ SYM the Yangian invariance implies that the MHV amplitudes are constant as demonstrated in [97]. This would mean that the loop contributions to the scattering amplitudes are trivial. Therefore the breaking of the dual super-conformal invariance by IR singularities of the integrand is absolutely essential for the non-triviality of the theory. Could the situation be different in TGD framework? Could it be possible to have non-trivial scattering amplitudes which are Yangian invariants. Maybe! The following heuristic argument is formulated in the language of super-twistors.

1. The dual conformal super generators of the super-Lie algebra $U(2, 2)$ acting as super vector fields reducing effectively to the general form $J = \eta_a^K \partial / \partial Z_a^J$ and the condition that they annihilate scattering amplitudes implies that they are constant as functions of twistor variables. When

particles are replaced with pairs of wormhole throats the super generators are replaced by sums $J_1 + J_2$ of these generators for the two wormhole throats and it might be possible to achieve the condition

$$(J_1 + J_2)M = 0 \quad (2.6.1)$$

with a non-trivial dependence on the momenta if the super-components of the twistors associated with the wormhole throats are in a linear relationship. This should be the case for bound states.

2. This kind of condition indeed exists. The condition that the sum of the super-momenta expressed in terms of super-spinors λ reduces to the sum of real momenta alone is not usually posed but in the recent case it makes sense as an additional condition to the super-components of the the spinors λ associated with the bound state. This quadratic condition is exactly of the same general form as the one following from the requirement that the sum of all external momenta vanishes for scattering amplitude and reads as

$$X = \lambda_1 \eta_1 + \lambda_2 \eta_2 = 0 \quad (2.6.2)$$

The action of the generators $\eta_1 \partial_{\lambda_1} + \eta_2 \partial_{\lambda_2}$ forming basic building blocks of the super generators on $p_1 + p_2 = \lambda_1 \lambda_1 + \lambda_2 \lambda_2$ appearing as argument in the scattering amplitude in the case of bound states gives just the quantity X , which vanishes so that one has super-symmetry. The generalization of this condition to n-parton bound state is obvious.

3. The argument does not apply to free fermions which have not suffered topological condensation and are therefore represented by CP_2 type vacuum extremal with single wormhole throat. If one accepts the weak form of electric-magnetic duality, one can circumvent this difficulty. The free fermions carry Kähler magnetic charge whereas physical fermions are accompanied by a bosonic wormhole throat carrying opposite Kähler magnetic charge and opposite electroweak isospin so that a ground state of string like object with size of order electroweak length scale is in question. In the case of quarks the Kähler magnetic charges need not be opposite since color confinement could involve Kähler magnetic confinement: electro-weak confinement holds however true also now. The above argument generalizes as such to the pairs formed by wormhole throats at the ends of string like object. One can of course imagine also more complex hybrids of these basic options but the general idea remains the same.

Note that the argument involves in an essential manner non-locality, which is indeed the defining property of the Yangian algebra and also the fact that physical particles are bound states. The massivation of the physical particles brings in the IR cutoff.

Number theoretical constraints on the pseudo-momenta

One can consider also further assumptions motivated by the recent view about the generalized eigenvalues of Chern-Simons Dirac operator having interpretation as pseudo-momentum. The details of this view need not of course be final.

1. Assume that the pseudo-momentum assigned to fermion lines by the modified Dirac equation [55] is the counterpart of region momentum as already explained and therefore does not directly correspond to the actual light-like four-momentum associated with partonic line of the generalized Feynman diagram. This assumption conforms with the assumption that incoming particles are built out of massless partonic fermions. It also implies that the propagators are massless propagators as required by twistorialization and Yangian generalization of super-conformal invariance.

2. Since (pseudo)-mass squared is number theoretically quantized as the length of a hyper-complex prime in preferred plane M^2 of pseudo-momentum space fermionic propagators are massless propagators with pseudo-masses restricted on discrete mass shells. Lorentz invariance suggests that M^2 cannot be common to all particles but corresponds to preferred reference frame for the virtual particle having interpretation as plane spanned by the quantization axes of energy and spin.
3. Hyper-complex primeness means also the quantization of pseudo-momentum components so that one has hyper-complex primes of form $\pm((p+1)/2, \pm(p-1)/1)$ corresponding to pseudo-mass squared $M^2 = p$ and hypercomplex primes $\pm(p, 0)$ with pseudo-mass squared $M^2 = p^2$. Space-like fermionic momenta are not needed since for opposite signs of energy wormhole throats can have space-like net momenta. If space-like pseudo-momenta are allowed/needed for some reason, they could correspond to space-like hyper-complex primes $\pm((p-1)/2, \pm(p+1)/1)$ and $\pm(0, p)$ so that one would obtain also discretization of space-like mass shells also. The number theoretical mass squared is proportional to p , whereas p-adic mass squared is proportional to $1/p$. For p-adic mass calculations canonical identification $\sum x_n p^n$ maps p-adic mass squared to its real counterpart. The simplest mapping consistent with this would be $(p_0, p_1) \rightarrow (p_0, p_1)/p$. This could be assumed from the beginning in real context and would mean that the mass squared scale is proportional to $1/p$.
4. Lorentz invariance requires that the preferred coordinate system in which this holds must be analogous to the rest system of the virtual fermion and thus depends on the virtual particle. In accordance with the general vision discussed in [55] Lorentz invariance could correspond to a discrete algebraic subgroup of Lorentz group spanned by transformation matrices expressible in terms of roots of unity. This would give a discrete version of mass shell and the preferred coordinate system would have a precise meaning also in the real context. Unless one allows algebraic extension of p-adic numbers p-adic mass shell reduces to the set of above number-theoretic momenta. For algebraic extensions of p-adic numbers the same algebraic mass shell is obtained as in real correspondence and is essential for the number theoretic universality. The interpretation for the algebraic discretization would be in terms of a finite measurement resolution. In real context this would mean discretization inducing a decomposition of the mass shell to cells. In the p-adic context each discrete point would be replaced with a p-adic continuum. As far as loop integrals are considered, this vision means that they make sense in both real and p-adic context and reduce to summations in p-adic context. This picture is discussed in detail in [55].
5. Concerning p-adicization the beautiful aspect of residue integral is that it makes sense also in p-adic context provided one can circumvent the problems related to the identification of p-adic counterpart of π requiring infinite-dimensional transcendental extension coming in powers of π . Together with the discretization of both real and virtual four-momenta this would allow to define also p-adic variants of the scattering amplitudes.

Could recursion formula allow interpretation in terms of zero energy ontology?

The identification of pseudo-momentum as a counterpart of region momentum suggests that generalized Feynman diagrams could be seen as a generalization of momentum twistor diagrams. Of course, the generalization from $\mathcal{N} = 4$ SYM to TGD is an enormous step in complexity and one must take all proposals in the following with a big grain of salt. For instance, the replacement of point-like particles with wormhole throats and the decomposition of gauge bosons to pairs of wormhole throats means that naive generalizations are dangerous.

With this in firmly in mind one can ask whether the recursion formula could allow interpretation in terms of zero energy states assigned to causal diamonds (CDs) containing CDs containing \dots . In this framework loops could be assigned with sub- CDs .

The interpretation of the leading order singularities forming the basic building blocks of the twistor approach in zero ontology is the basic source of questions. Before posing these questions recall the basic proposal that partonic fermions are massless but opposite signs of energy are possible for the opposite throats of wormhole contacts. Partons would be on mass shell but besides physical states identified as bound states formed from partons also more general intermediate states would be possible

but restricted by momentum conservation and mass shell conditions for partons at vertices. Consider now the questions.

1. Suppose that the massivation of virtual fermions and their super partners allows only ladder diagrams in which the intermediate states contain on mass shell massless states. Should one allow this kind of ladder diagrams? Can one identify them in terms of leading order singularities? Could one construct the generalized Feynman diagrams from Yangian invariant tree diagrams associated with the hierarchy of sub- CD s and using BCFW bridges and entangled pairs of massless states having interpretation as box diagrams with on mass shell momenta at microscopic level? Could it make sense to say that scattering amplitudes are represented by tree diagrams inside CD s in various scales and that the fermionic momenta associated with throats and emerging from sub- CD s are always massless?
2. Could BCFW bridge generalizes as such and could the interpretation of BCFW bridge be in terms of a scattering in which the four on mass shell massless partonic states (partonic throats have arbitrary fermion number) are exchanged between four sub- CD s. This admittedly looks somewhat artificial.
3. Could the addition of 2-particle zero energy state responsible for addition of loop in the recursion relations and having interpretation in terms of the cutting of line carrying loop momentum correspond to an addition of sub- CD such that the 2-particle zero energy state has its positive and negative energy part on its past and future boundaries? Could this mean that one cuts a propagator line by adding CD and leaves only the portion of the line within CD . Could the reverse operation mean to the addition of zero energy "thermally entangled" states in shorter time and length scales and assignable as a zero energy state to a sub- CD . Could one interpret the Cutkosky rule for propagator line in terms of this cutting or its reversal. Why only pairs would be needed in the recursion formula? Why not more general states? Does the recursion formula imply that they are included? Does this relate to the fact that these zero energy states have interpretation as single particle states in the positive energy ontology and that the basic building block of Feynman diagrams is single particle state? Could one regard the unitarity as an identity which states that the discontinuity of T-matrix characterizing zero energy state over cut is expressible in terms of TT^\dagger and T matrix is the relevant quantity?

Maybe it is again dangerous to try to draw too detailed correspondences: after all, point like particles are replaced by partonic two-surfaces in TGD framework.

4. If I have understood correctly the genuine l-loop term results from $l - 1$ -loop term by the addition of the zero energy pair and integration over $GL(2)$ as a representative of loop integral reducing $n + 2$ to n and calculating the added loop at the same time [97]. The integrations over the two momentum twistor variables associated with a line in twistor space defining off mass shell four-momentum and integration over the lines represent the integration over loop momentum. The reduction to $GL(2)$ integration should result from the delta functions relating the additional momenta to $GL(2)$ variables (note that $GL(2)$ performs linear transformations in the space spanned by the twistors Z_A and Z_B and means integral over the positions of Z_A and Z_B). The resulting object is formally Yangian invariant but IR divergences along some contours of integration breaks Yangian symmetry.

The question is what happens in TGD framework. The previous arguments suggests that the reduction of the the loop momentum integral to integrals over discrete mass shells and possibly to a sum over their discrete subsets does not spoil the reduction to contour integrals for loop integrals in the example considered in [97]. Furthermore, the replacement of mass continuum with a discrete set of mass shells should eliminate IR divergences and might allow to preserve Yangian symmetry. One can however wonder whether the loop corrections with on mass shell massless fermions are needed. If so, one would have at most finite number of loop diagrams with on mass shell fermionic momenta and one of the TGD inspired dreams already forgotten would be realized.

What about unitarity?

The approach of Arkani-Hamed and collaborators means that loop integral over four-momenta are replaced with residue integrals around a small sphere $p^2 = \epsilon$. This is very much reminiscent of my

own proposal for a few years ago based on the idea that the condition of twistorialization forces to accept only massless virtual states [25, 30]. I of course soon gave up this proposal as too childish.

This idea seems to however make a comeback in a modified form. At this time one would have only massive and quantized pseudo-momenta located at discrete mass shells. Can this picture be consistent with unitarity?

Before trying to answer this question one must make clear what one could assume in TGD framework.

1. Physical particles are in the general case massive and consist of collinear fermions at wormhole throats. External partons at wormhole throats must be massless to allow twistorial interpretation. Therefore massive states emerge. This applies also to stringy states.
2. The simplest assumption generalizing the childish idea is that on mass shell massless states for partons appear as both virtual particles and external particles. Space-like virtual momentum exchanges are possible if the virtual particles can consist of pairs of positive and negative energy fermions at opposite wormhole throats. Hence also partons at internal lines should be massless and this raises the question about the identification of propagators.
3. Generalized eigenvalue equation for Chern-Simons Dirac operator implies that virtual elementary fermions have massive and quantized pseudo-momenta whereas external elementary fermions are massless. The massive pseudo-momentum assigned with the Dirac propagator of a parton line cannot be identified with the massless real momentum assigned with the fermionic propagator line. The region momenta introduced in Grassmannian approach are something analogous.

As already explained, this brings in mind is the identification of this pseudo momentum as the counterpart of the region momentum of momentum twistor diagrams so that the external massless fermionic momenta would be differences of the pseudo-momenta. Indeed, since region momenta are determined apart from a common shift, they need not correspond to real momenta. Same applies to pseudo-momenta and one could assume that both internal and external fermion lines carry light-like pseudo-momenta and that external pseudo-momenta are equal to real momenta.

4. This picture has natural correspondence with twistor diagrams. For instance, the region momentum appearing in BCFW bridge defining effective propagator is in general massive although the underlying Feynman diagram would contain online massless momenta. In TGD framework massless lines of Feynman graphs associated with singularities would correspond to real momenta of massless fermions at wormhole throats. Also other canonical operations for Yangian invariants involve light-like momenta at the level of Feynman diagrams and would in TGD framework have a natural identification in terms of partonic momenta. Hence partonic picture would provide a microscopic description for the lines of twistor diagrams.

Let us assume being virtual particle means only that the discretized pseudo-momentum is on shell but massive whereas all real momenta of partons are light-like, and that negative partonic energies are possible. Can one formulate Cutkosky rules for unitarity in this framework? What could the unitarity condition

$$iDisc(T - T^\dagger) = -TT^\dagger$$

mean now? In particular, are the cuts associated with mass shells of physical particles or with mass shells of pseudo-momenta? Could these two assignments be equivalent?

1. The restriction of the partons to be massless but having both signs of energy means that the spectrum of intermediate states contains more states than the external states identified as bound states of partons with the same sign of energy. Therefore the summation over intermediate states does not reduce to a mere summation over physical states but involves a summation over states formed from massless partons with both signs of energy so that also space-like momentum exchanges become possible.
2. The understanding of the unitarity conditions in terms of Cutkosky rules would require that the cuts of the loop integrands correspond to mass shells for the virtual states which are also

physical states. Therefore real momenta have a definite sign and should be massless. Besides this bound state conditions guaranteeing that the mass spectrum for physical states is discrete must be assumed. With these assumptions the unitary cuts would not be assigned with the partonic light-cones but with the mass shells associated of physical particles.

3. There is however a problem. The pseudo-momenta of partons associated with the external partons are assumed to be light-like and equal to the physical momenta.
 - (a) If this holds true also for the intermediate physical states appearing in the unitarity conditions, the pseudo-momenta at the cuts are light-like and cuts must be assigned with pseudo-momentum light-cones. This could bring in IR singularities and spoil Yangian symmetry. The formation of bound states could eliminate them and the size scale of the largest CD involved would bring in a natural IR cutoff as the mass scale of the lightest particle. This assumption would however force to give up the assumption that only massive pseudo-momenta appear at the lines of the generalized Feynman diagrams.
 - (b) On the other hand, if pseudo-momenta are not regarded as a property of physical state and are thus allowed to be massive for the real intermediate states in Cutkosky rules, the cuts at parton level correspond to on mass shell hyperboloids and IR divergences are absent.

2.6.2 Could TGD allow formulation in terms of twistors

There are many questions to be asked. There would be in-numerable questions upwelling from my very incomplete understanding of the technical issues. In the following I restrict only to the questions which relate to the relationship of TGD approach to Witten's twistor string approach [86] and M-theory like frameworks. The arguments lead to an explicit proposal how the preferred extremals of Kähler action could correspond to holomorphic 4-surfaces in $CP_3 \times CP_3$. The basic motivation for this proposal comes from the observation that Kähler action is Maxwell action for the induced Kähler form and metric. Hence Penrose's original twistorial representation for the solutions of linear Maxwell's equations could have a generalization to TGD framework.

$M^4 \times CP_2$ from twistor approach

The first question which comes to mind relates to the origin of the Grassmannians. Do they have some deeper interpretation in TGD context. In twistor string theory Grassmannians relate to the moduli spaces of holomorphic surfaces defined by string world sheets in twistor space. Could partonic 2-surfaces have analogous interpretation and could one assign Grassmannians to their moduli spaces? If so, one could have rather direct connection with topological QFT defining twistor strings [86] and the almost topological QFT defining TGD. There are some hints to this direction which could be of course seen as figments of a too wild imagination.

1. The geometry of CD brings strongly in mind Penrose diagram for the conformally compactified Minkowski space [65], which indeed becomes CD when its points are replaced with spheres. This would suggest the information theoretic idea about interaction between observer and externals as a map in which M^4 is mapped to its conformal compactification represented by CD . Compactification means that the light-like points at the light-like boundaries of CD are identified and the physical counterpart for this in TGD framework is conformal invariance along light-rays along the boundaries of CD . The world of conscious observer for which CD is identified as a geometric correlate would be conformally compactified M^4 (plus CP_2 or course).
2. Since the points of the conformally compactified M^4 correspond to twistor pairs [93], which are unique only apart from opposite complex scalings, it would be natural to assign twistor space to CD and represent its points as pairs of twistors. This suggest an interpretation for the basic formulas of Grassmannian approach involving integration over twistors. The incoming and outgoing massless particles could be assigned at point-like limit light-like points at the lower and upper boundaries of CD and the lifting of the points of the light-cone boundary at partonic surfaces would give rise to the description in terms of ordinary twistors. The assumption that massless collinear fermions at partonic 2-surfaces are the basic building blocks of physical

particles at partonic 2-surfaces defined as many particles states involving several partonic 2-surfaces would lead naturally to momentum twistor description in which massless momenta and described by twistors and virtual momenta in terms of twistor pairs. It is important to notice that in TGD framework string like objects would emerge from these massless fermions.

3. Partonic 2-surfaces are located at the upper and lower light-like boundaries of the causal diamond (CD) and carry energies of opposite sign in zero energy ontology. Quite generally, one can assign to the point of the conformally compactified Minkowski space a twistor pair using the standard description. The pair of twistors is determined apart from $Gl(2)$ rotation. At the light-cone boundary M^4 points are light-like so that the two spinors of the two twistors differ from each other only by a complex scaling and single twistor is enough to characterize the space-time point this degenerate situation. The components of the twistor are related by the well known twistor equation $\mu^{a'} = -ix^{aa'}\lambda_a$. One can therefore lift each point of the partonic 2-surface to single twistor determined apart from opposite complex scalings of μ and λ so that the lift of the point would be 2-sphere. In the general case one must lift the point of CD to a twistor pair. The degeneracy of the points is given by $Gl(2)$ and each point corresponds to a 2-sphere in projective twistor space.
4. The new observation is that one can understand also CP_2 factor in twistor framework. The basic observation about which I learned in [93] (giving also a nice description of basics of twistor geometry) is that a pair (X, Y) of twistors defines a point of CD on one hand and complex 2-planes of the dual twistor space -which is nothing but CP_2 - by the equations

$$X_\alpha W^\alpha = 0 \quad , \quad Y_\alpha W^\alpha = 0 \quad .$$

The intersection of these planes is the complex line $CP_1 = S^2$. The action of $G(2)$ on the twistor pair affects the pair of surfaces CP_2 determined by these equations since it transforms the equations to their linear combination but not the the point of conformal CD resulting as projection of the sphere. Therefore twistor pair defines both a point of M^4 and assigns with it pair of CP_2 :s represented as holomorphic surfaces of the projective dual twistor space. Hence the union over twistor pairs defines $M^4 \times CP_2$ via this assignment if it is possible to choose "the other" CP_2 in a unique manner for all points of M^4 . The situation is similar to the assignment of a twistor to a point in the Grassmannian diagrams forming closed polygons with light-like edges. In this case one assigns to the the "region momenta" associated with the edge the twistor at the either end of the edge. One possible interpretation is that the two CP_2 :s correspond to the opposite ends of the CD . My humble hunch is that this observation might be something very deep.

Recall that the assignment of CP_2 to M^4 point works also in another direction. $M^8 - H$ duality associates with so called hyper-quaternionic 4-surface of M^8 allowing preferred hyper-complex plane at each point 4-surfaces of $M^4 \times CP_2$. The basic observation behind this duality is that the hyper-quaternionic planes (copies of M^4) with preferred choices of hyper-complex plane M^2 are parameterized by points of CP_2 . One can therefore assign to a point of CP_2 a copy of M^4 . Maybe these both assignments indeed belong to the core of quantum TGD. There is also an interesting analogy with Uncertainty Principle: complete localization in M^4 implies maximal uncertainty of the point in CP_2 and vice versa.

Does twistor string theory generalize to TGD?

With this background the key speculative questions seem to be the following ones.

1. Could one relate twistor string theory to TGD framework? Partonic 2-surfaces at the boundaries of CD are lifted to 4-D sphere bundles in twistor space. Could they serve as a 4-D counterpart for Witten's holomorphic twistor strings assigned to point like particles? Could these surfaces be actually lifts of the holomorphic curves of twistor space replaced with the product $CP_3 \times CP_2$ to 4-D sphere bundles? If I have understood correctly, the Grassmannians $G(n, k)$ can be assigned to the moduli spaces of these holomorphic curves characterized by the degree of the polynomial expressible in terms of genus, number of negative helicity gluons, and the number of loops for twistor diagram.

Could one interpret $G(n, k)$ as a moduli space for the δCD projections of n partonic 2-surfaces to which k negative helicity gluons and $n - k$ positive helicity gluons are assigned (or something more complex when one considers more general particle states)? Could quantum numbers be mapped to integer valued algebraic invariants? IF so, there would be a correlation between the geometry of the partonic 2-surface and quantum numbers in accordance with quantum classical correspondence.

2. Could one understand light-like orbits of partonic 2-surfaces and space-time surfaces in terms of twistors? To each point of the 2-surface one can assign a 2-sphere in twistor space CP_3 and CP_2 in its dual. These CP_2 s can be identified. One should be able to assign to each sphere S^2 at least one point of corresponding CP_2 s associated with its points in the dual twistor space and identified as single CP_2 union of CP_2 s in the dual twistor space a point of CP_2 or even several of them. One should be also able to continue this correspondence so that it applies to the light-like orbit of the partonic 2-surface and to the space-time surface defining a preferred extremal of Kähler action. For space-time sheets representable as graph of a map $M^4 \rightarrow CP_2$ locally one should select from a CP_2 assigned with a particular point of the space-time sheet a unique point of corresponding CP_2 in a manner consistent with field equations. For surfaces with lower dimensional M^4 projection one must assign a continuum of points of CP_2 to a given point of M^4 . What kind equations-could allow to realize this assignment? Holomorphy is strongly favored also by the number theoretic considerations since in this case one has hopes of performing integrals using residue calculus.
 - (a) Could two holomorphic equations in $CP_3 \times CP_2$ defining 6-D surfaces as sphere bundles over $M^4 \times CP_2$ characterize the preferred extremals of Kähler action? Could partonic 2-surfaces be obtained by posing an additional holomorphic equation reducing twistors to null twistors and thus projecting to the boundaries of CD ? A philosophical justification for this conjecture comes from effective 2-dimensionality stating that partonic 2-surfaces plus their 4-D tangent space data code for physics. That the dynamics would reduce to holomorphy would be an extremely beautiful result. Of course this is only an additional item in the list of general conjectures about the classical dynamics for the preferred extremals of Kähler action.
 - (b) One could also work in $CP_3 \times CP_3$. The first CP_3 would represent twistors endowed with a metric conformally equivalent to that of $M^{2,4}$ and having the covering of $SU(2, 2)$ of $SO(2, 4)$ as isometries. The second CP_3 defining its dual would have a metric consistent with the Calabi-Yau structure (having holonomy group $SU(3)$). Also the induced metric for canonically imbedded CP_2 s should be the standard metric of CP_2 having $SU(3)$ as its isometries. In this situation the linear equations assigning to M^4 points twistor pairs and $CP_2 \subset CP_3$ as a complex plane would hold always true. Besides this two holomorphic equations coding for the dynamics would be needed.
 - (c) The issues related to the induced metric are important. The conformal equivalence class of M^4 metric emerges from the 5-D light-cone of $M^{2,4}$ under projective identification. The choice of a proper projective gauge would select M^4 metric locally. Twistors inherit the conformal metric with signature $(2, 4)$ from the metric of 4+4 component spinors with metric having $(4, 4)$ signature. One should be able to assign a conformal equivalence class of Minkowski metric with the orbits of pairs of twistors modulo $GL(2)$. The metric of conformally compactified M^4 would be obtained from this metric by dropping from the line element the contribution to the S^2 fiber associated with M^4 point.
 - (d) Witten related [86] the degree d of the algebraic curve describing twistor string, its genus g , the number k of negative helicity gluons, and the number l of loops by the following formula

$$d = k - 1 + l \quad , \quad g \leq l \quad . \quad (2.6.3)$$

One should generalize the definition of the genus so that it applies to 6-D surfaces. For projective complex varieties of complex dimension n this definition indeed makes sense.

Algebraic genus [64] is expressible in terms of the dimensions of the spaces of closed holomorphic forms known as Hodge numbers $h^{p,q}$ as

$$g = \sum (-1)^{n-k} h^{k,0} . \quad (2.6.4)$$

The first guess is that the formula of Witten generalizes by replacing genus with its algebraic counterpart . This requires that the allowed holomorphic surfaces are projective curves of twistor space, that is described in terms of homogenous polynomials of the 4+4 projective coordinates of $CP_3 \times CP_3$.

What is the relationship of TGD to M-theory and F-theory?

There are also questions relating to the possible relationship to M-theory and F-theory.

1. Calabi-Yau-manifolds [74, 84] are central for the compactification in super string theory and emerge from the condition that the super-symmetry breaks down to $\mathcal{N} = 1$ SUSY. The dual twistor space CP_3 with Euclidian signature of metric is a Calabi-Yau manifold [86]. Could one have in some sense two Calabi-Yaus! Twistorial CP_3 can be interpreted as a four-fold covering and conformal compactification of $M^{2,4}$. I do not know whether Calabi-Yau property has a generalization to the situation when Euclidian metric is replaced with a conformal equivalence class of flat metrics with Minkowskian signature and thus having a vanishing Ricci tensor. As far as differential forms (no dependence on metric) are considered there should be no problems. Whether the replacement of the maximal holonomy group $SU(3)$ with its non-compact version $SU(1, 2)$ makes sense is not clear to me.
2. The lift of the CD to projective twistor space would replace $CD \times CP_2$ with 10-dimensional space which inspires the familiar questions about connection between TGD and M-theory. If Calabi-Yau with a Minkowskian signature of metric makes sense then the Calabi-Yau of the standard M-theory would be replaced with its Minkowskian counterpart! Could it really be that M-theory like theory based on $CP_3 \times CP_2$ reduces to TGD in $CD \times CP_2$ if an additional symmetry mapping 2-spheres of CP_3 to points of CD is assumed? Could the formulation based on 12-D $CP_3 \times CP_3$ correspond to F-theory which also has two time-like dimensions. Of course, the additional conditions defined by the maps to M^4 and CP_2 would remove the second time-like dimension which is very difficult to justify on purely physical grounds.
3. One can actually challenge the assumption that the first CP_3 should have a conformal metric with signature $(2, 4)$. Metric appears nowhere in the definition holomorphic functions and once the projections to M^4 and CP_2 are known, the metric of the space-time surface is obtained from the metric of $M^4 \times CP_2$. The previous argument for the necessity of the presence of the information about metric in the second order differential equation however suggests that the metric is needed.
4. The beginner might ask whether the 6-D 2-sphere bundles representing space-time sheets could have interpretation as Calabi-Yau manifolds. In fact, the Calabi-Yau manifolds defined as complete intersections in $CP_3 \times CP_3$ discovered by Tian and Yau are defined by three polynomials [84]. Two of them have degree 3 and depend on the coordinates of single CP_3 only whereas the third is bilinear in the coordinates of the CP_3 :s. Obviously the number of these manifolds is quite too small (taking into account scaling the space defined by the coefficients is 6-dimensional). All these manifolds are deformation equivalent. These manifolds have Euler characteristic $\chi = \pm 18$ and a non-trivial fundamental group. By dividing this manifold by Z_3 one obtains $\chi = \pm 6$, which guarantees that the number of fermion generations is three in heterotic string theory. This manifold was the first one proposed to give rise to three generations and $\mathcal{N} = 1$ SUSY.

What could the field equations be in twistorial formulation?

The fascinating question is whether one can identify the equations determining the 3-D complex surfaces of $CP_3 \times CP_3$ in turn determining the space-time surfaces.

The first thing is to clarify in detail how space-time $M^4 \times CP_2$ results from $CP_3 \times CP_3$. Each point $CP_3 \times CP_3$ define a line in third CP_3 having interpretation as a point of conformally compactified M^4 obtained by sphere bundle projection. Each point of either CP_3 in turn defines CP_2 in in fourth CP_3 as a 2-plane. Therefore one has $(CP_3 \times CP_3) \times (CP_3 \times CP_3)$ but one can reduce the consideration to $CP_3 \times CP_3$ fixing $M^4 \times CP_2$. In the generic situation 6-D surface in 12-D $CP_3 \times CP_3$ defines 4-D surface in the dual $CP_3 \times CP_3$ and its sphere bundle projection defines a 4-D surface in $M^4 \times CP_2$.

1. The vanishing of three holomorphic functions f^i would characterize 3-D holomorphic surfaces of 6-D $CP_3 \times CP_3$. These are determined by three real functions of three real arguments just like a holomorphic function of single variable is dictated by its values on a one-dimensional curve of complex plane. This conforms with the idea that initial data are given at 3-D surface. Note that either the first or second CP_3 can determine the CP_2 image of the holomorphic 3-surface unless one assumes that the holomorphic functions are symmetric under the exchange of the coordinates of the two CP_3 s. If symmetry is not assumed one has some kind of duality.
2. Effective 2-dimensionality means that 2-D partonic surfaces plus 4-D tangent space data are enough. This suggests that the 2 holomorphic functions determining the dynamics satisfy some second order differential equation with respect to their three complex arguments: the value of the function and its derivative would correspond to the initial values of the imbedding space coordinates and their normal derivatives at partonic 2-surface. Since the effective 2-dimensionality brings in dependence on the induced metric of the space-time surface, this equation should contain information about the induced metric.
3. The no-where vanishing holomorphic 3-form Ω , which can be regarded as a "complex square root" of volume form characterizes 6-D Calabi-Yau manifold [74, 84], indeed contains this information albeit in a rather implicit manner but in spirit with TGD as almost topological QFT philosophy. Both CP_3 s are characterized by this kind of 3-form if Calabi-Yau with (2, 4) signature makes sense.
4. The simplest second order- and one might hope holomorphic- differential equation that one can imagine with these ingredients is of the form

$$\Omega_1^{i_1 j_1 k_1} \Omega_2^{i_2 j_2 k_2} \partial_{i_1 i_2} f^1 \partial_{j_1 j_2} f^2 \partial_{k_1 k_2} f^3 = 0, \quad \partial_{ij} \equiv \partial_i \partial_j. \quad (2.6.5)$$

Since Ω_i is by its antisymmetry equal to $\Omega_i^{123} \epsilon^{ijk}$, one can divide Ω^{123} s away from the equation so that one indeed obtains holomorphic solutions. Note also that one can replace ordinary derivatives in the equation with covariant derivatives without any effect so that the equations are general coordinate invariant.

One can consider more complex equations obtained by taking instead of (f^1, f^2, f^3) arbitrary combinations (f^i, f^j, f^k) which results uniquely if one assumes anti-symmetrization in the labels (1, 2, 3). In the sequel only this equation is considered.

5. The metric disappears completely from the equations and skeptic could argue that this is inconsistent with the fact that it appears in the equations defining the weak form of electric-magnetic duality as a Lagrange multiplier term in Chern-Simons action. Optimist would respond that the representation of the 6-surfaces as intersections of three hyper-surfaces is different from the representation as imbedding maps $X^4 \rightarrow H$ used in the usual formulation so that the argument does not bite, and continue by saying that the metric emerges in any case when one endows space-time with the induced metric given by projection to M^4 .
6. These equations allow infinite families of obvious solutions. For instance, when some f^i depends on the coordinates of either CP_3 only, the equations are identically satisfied. As a special case one obtains solutions for which $f^1 = Z \cdot W$ and $(f^2, f^3) = (f^2(Z), f^3(W))$ This family contains also the Calabi-Yau manifold found by Yau and Tian, whose factor space was proposed as the first candidate for a compactification consistent with three fermion families.

7. One might hope that an infinite non-obvious solution family could be obtained from the ansatz expressible as products of exponential functions of Z and W . Exponentials are not consistent with the assumption that the functions f_i are homogenous polynomials of finite degree in projective coordinates so that the following argument is only for the purpose for learning something about the basic character of the equations.

$$\begin{aligned}
f^1 &= E_{a_1, a_2, a_3}(Z) E_{\hat{a}_1, \hat{a}_2, \hat{a}_3}(W) , & f^2 &= E_{b_1, b_2, b_3}(Z) E_{\hat{b}_1, \hat{b}_2, \hat{b}_3}(W) , \\
f^3 &= E_{c_1, c_2, c_3}(Z) E_{\hat{c}_1, \hat{c}_2, \hat{c}_3}(W) , & & \\
E_{a, b, c}(Z) &= \exp(az_1) \exp(bz_2) \exp(cz_3) .
\end{aligned} \tag{2.6.6}$$

The parameters a, b, c , and $\hat{a}, \hat{b}, \hat{c}$ can be arbitrary real numbers in real context. By the basic properties of exponential functions the field equations are algebraic. The conditions reduce to the vanishing of the products of determinants $\det(a, b, c)$ and $\det(\hat{a}, \hat{b}, \hat{c})$ so that the vanishing of either determinant is enough. Therefore the dependence can be arbitrary either in Z coordinates or in W coordinates. Linear superposition holds for the modes for which determinant vanishes which means that the vectors (a, b, c) or $(\hat{a}, \hat{b}, \hat{c})$ are in the same plane.

Unfortunately, the vanishing conditions reduce to the conditions $f^i(W) = 0$ for case a) and to $f^i(Z) = 0$ for case b) so that the conditions are equivalent with those obtained by putting the "wave vector" to zero and the solutions reduce to obvious ones. The lesson is that the equations do not commute with the multiplication of the functions f^i with nowhere vanishing functions of W and Z . The equation selects a particular representation of the surfaces and one might argue that this should not be the case unless the hyper-surfaces defined by f^i contain some physically relevant information. One could consider the possibility that the vanishing conditions are replaced with conditions $f^i = c_i$ with $f^i(0) = 0$ in which case the information would be coded by a family of space-time surfaces obtained by varying c_i .

One might criticize the above equations since they are formulated directly in the product $CP_3 \times CP_3$ of projective twistor by choosing a specific projective gauge by putting $z^4 = 1, w^4 = 1$. The manifestly projectively invariant formulation for the equations is in full twistor space so that 12-D space would be replaced with 16-D space. In this case one would have 4-D complex permutation symbol giving for these spaces Calabi-Yau structure with flat metric. The product of functions $f = z^4 = \text{constant}$ and $g = w^4 = \text{constant}$ would define the fourth function $f_4 = fg$ fixing the projective gauge

$$\epsilon^{i_1 j_1 k_1 l_1} \epsilon^{i_2 j_2 k_2 l_2} \partial_{i_1 i_2} f^1 \partial_{j_1 j_2} f^2 \partial_{k_1 k_2} f^3 \partial_{l_1 l_2} f^4 = 0 , \quad \partial_{ij} \equiv \partial_i \partial_j . \tag{2.6.7}$$

The functions f^i are homogenous polynomials of their twistor arguments to guarantee projective invariance. These equations are projectively invariant and reduce to the above form which means also loss of homogenous polynomial property. The undesirable feature is the loss of manifest projective invariance by the fixing of the projective gauge.

A more attractive ansatz is based on the idea that one must have one equation for each f^i to minimize the non-determinism of the equations obvious from the fact that there is single equation in 3-D lattice for three dynamical variables. The quartets (f^1, f^2, f^3, f^i) , $i = 1, 2, 3$ would define a possible minimally non-linear generalization of the equation

$$\epsilon^{i_1 j_1 k_1 l_1} \epsilon^{i_2 j_2 k_2 l_2} \partial_{i_1 i_2} f^1 \partial_{j_1 j_2} f^2 \partial_{k_1 k_2} f^m \partial_{l_1 l_2} f^4 = 0 , \quad \partial_{ij} \equiv \partial_i \partial_j , \quad m = 1, 2, 3 . \tag{2.6.8}$$

Note that the functions are homogenous polynomials of their arguments and analogous to spherical harmonics suggesting that they can allow a nice interpretation in terms of quantum classical correspondence.

The minimal non-linearity of the equations also conforms with the non-linearity of the field equations associated with Kähler action. Note that also in this case one can solve the equations by diagonalizing the dynamical coefficient matrix associated with the quadratic term and by identifying

the eigen-vectors of zero eigen values. One could consider also more complicated strongly non-linear ansätze such as (f^i, f^i, f^i, f^i) , $i = 1, 2, 3$, but these do not seem plausible.

1. *The explicit form of the equations using Taylor series expansion for multi-linear case*

In this section the equations associated with (f_1, f_2, f_3) ansatz are discussed in order to obtain a perspective about the general structure of the equations by using simpler (multilinearity) albeit probably non-realistic case as starting point. This experience can be applied directly to the (f^1, f^2, f^3, f^i) ansatz, which is quadratic in f^i .

The explicit form of the equations is obtained as infinite number of conditions relating the coefficients of the Taylor series of f^1 and f^2 . The treatment of the two variants for the equations is essentially identical and in the following only the manifestly projectively invariant form will be considered.

1. One can express the Taylor series as

$$\begin{aligned} f^1(Z, W) &= \sum_{m,n} C_{m,n} M_m(Z) M_n(W) , \\ f^2(Z, W) &= \sum_{m,n} D_{m,n} M_m(Z) M_n(W) , \\ f^3(Z, W) &= \sum_{m,n} E_{m,n} M_m(Z) M_n(W) , \\ M_{m \equiv (m_1, m_2, m_3)}(Z) &= z_1^{m_1} z_2^{m_2} z_3^{m_3} . \end{aligned} \quad (2.6.9)$$

2. The application of derivatives to the functions reduces to a simple algebraic operation

$$\partial_{ij}(M_m(Z) M_n(W)) = m_i n_j M_{m_1 - e_i}(Z) M_{n - e_j}(W) . \quad (2.6.10)$$

Here e_i denotes i :th unit vector.

3. Using the product rule $M_m M_n = M_{m+n}$ one obtains

$$\begin{aligned} &\partial_{ij}(M_m(Z) M_n(W)) \partial_{rs}(M_k(Z) M_l(W)) \\ &= m_i n_j k_r l_s \times M_{m - e_i}(Z) M_{n - e_j}(W) \times M_{k - e_r}(Z) M_{l - e_s}(W) \\ &= m_i n_j k_r l_s \times M_{m+k - e_i - e_r}(Z) \times M_{n+l - e_j - e_l}(W) . \end{aligned} \quad (2.6.11)$$

4. The equations reduce to the trilinear form

$$\begin{aligned} &\sum_{m,n,k,l,r,s} C_{m,n} D_{k,l} E_{r,s}(m, k, r)(n, l, s) M_{m+k+r-E}(Z) M_{n+l+s-E}(W) = 0 , \\ E &= e_1 + e_2 + e_3 , \quad (a, b, c) = \epsilon^{ijk} a_i b_j c_c . \end{aligned} \quad (2.6.12)$$

Here (a, b, c) denotes the determinant defined by the three index vectors involved. By introducing the summation indices

$$(M = m + k + r - E, k, r) , \quad (N = n + l + s - E, l, s)$$

one obtains an infinite number of conditions, one for each pair (M, N) . The condition for a given pair (M, N) reads as

$$\sum_{k,l,r,s} C_{M-k-r+E, N-l-s+E} D_{k,l} E_{r,s} \times (M-k-r+E, k, r)(N-l-s+E, l, s) = 0 . \quad (2.6.13)$$

These equations can be regarded as linear equations by regarding any matrix selected from $\{C, D, E\}$ as a vector of linear space. The existence solutions requires that the determinant associated with the tensor product of other two matrices vanishes. This matrix is dynamical. Same applies to the tensor product of any of the matrices.

5. Hyper-determinant [91] is the generalization of the notion of determinant whose vanishing tells that multilinear equations have solutions. Now the vanishing of the hyper-determinant defined for the tensor product of the three-fold tensor power of the vector space defined by the coefficients of the Taylor expansion should provide the appropriate manner to characterize the conditions for the existence of the solutions. As already seen, solutions indeed exist so that the hyper-determinant must vanish. The elements of the hyper matrix are now products of determinants for the exponents of the monomials involved. The non-locality of the Kähler function as a functional of the partonic surface leads to the argument that the field equations of TGD for vanishing n :th variations of Kähler action are multilinear and that a vanishing of a generalized hyper-determinant characterizes this [55].
6. Since the differential operators are homogenous polynomials of partial derivatives, the total degrees of $M_m(Z)$ and $M_m(W)$ defined as a sum $D = \sum m_i$ is reduced by one unit by the action of both operators ∂_{ij} . For given value of M and N only the products

$$M_m(Z)M_n(W)M_k(Z)M_r(W)M_s(Z)M_l(W)$$

for which the vector valued degrees $D_1 = m + k + r$ and $D_2 = n + l + s$ have the same value are coupled. Since the degree is reduced by the operators appearing in the equation, polynomial solutions for which f^i contain monomials labelled by vectors m_i, n_i, r_i for which the components vary in a finite range $(0, n_{max})$ look like a natural solution ansatz. All the degrees $D_i \leq D_{i,max}$ appear in the solution ansatz so that quite a large number of conditions is obtained.

What is nice is that the equation can be interpreted as a difference equation in 3-D lattice with "time direction" defined by the direction of the diagonal.

1. The counterparts of time=constant slices are the planes $n_1 + n_2 + n_3 = n$ defining outer surfaces of simplices having E as a normal vector. The difference equation does not seem to say nothing about the behavior in the transversal directions. M and N vary in the simplex planes satisfying $\sum M_i = T_1$, $\sum N_i = T_2$. It seems natural to choose $T_1 = T_2 = T$ so that Z and W dynamics corresponds to the same "time". The number of points in the $T = constant$ simplex plane increases with T which is analogous to cosmic expansion.
2. The "time evolution" with respect to T can be solved iteratively by increasing the value of $\sum M_i = N_i = T$ by one unit at each step. Suppose that the values of coefficients are known and satisfy the conditions for (m, k, r) and (n, l, s) up to the maximum value T for the sum of the components of each of these six vectors. The region of known coefficients -"past"- obviously corresponds to the interior of the simplex bounded by the plane $\sum M_i = \sum N_i = T$ having E as a normal. Let (m_{min}, n_{min}) , (k_{min}, l_{min}) and (r_{min}, s_{min}) correspond to the smallest values of 3-indices for which the coefficients are non-vanishing- this could be called the moment of "Big Bang". The simplest but not necessary assumption is that these indices correspond zero vectors $(0, 0, 0)$ analogous to the tip of light-cone.
3. For given values of M and N corresponding to same value of "cosmic time" T one can separate from the formula the terms which correspond to the un-known coefficients as the sum $C_{M+E, N+E} D_{0,0} E_{0,0} + D_{M+E, N+E} D_{0,0} C_{0,0} + E_{M+E, N+E} C_{0,0} D_{0,0}$. The remaining terms are by assumption already known. One can fix the normalization by choosing $C_{0,0} = D_{0,0} = E_{0,0} = 1$.

With these assumptions the equation reduces at each point of the outer boundary of the simplex to the form

$$C_{M+E,N+E} + D_{M+E,N+E} + E_{M+E,N+E} = X$$

where X is something already known and contain only data about points in the plane $m+k+r = M$ and $n+r+s = N$. Note that these planes have one "time like direction" unlike the simplex plane so that one could speak about a discrete analog of string world sheet in 3+3+3-D lattice space defined by a 2-plane with one time-like direction.

4. For each point of the simplex plane one has equation of the above form. The equation is non-deterministic since only constrain only the sum $C_{M+E,N+E} + D_{M+E,N+E} + E_{M+E,N+E}$ at each point of the simplex plane to a plane in the complex 3-D space defined by them. Hence the number of solutions is very large. The condition that the solutions reduce to polynomials poses conditions on the coefficients since the quantities X associated with the plane $T = T_{max}$ must vanish for each point of the simplex plane in this case. In fact, projective invariance means that the functions involved are homogenous functions in projective coordinates and thus polynomials and therefore reduce to polynomials of finite degree in 3-D treatment. This obviously gives additional condition to the equations.

2. The minimally non-linear option

The simple equation just discussed should be taken with a caution since the non-determinism seems to be too large if one takes seriously the analogy with classical dynamics. By the vacuum degeneracy also the time evolution associated with Kähler action breaks determinism in the standard sense of the word. The non-determinism is however not so strong and removed completely in local sense for non-vacuum extremals. One could also try to see the non-determinism as the analog for non-deterministic time evolution by quantum jumps.

One can however consider the already mentioned possibility of increasing the number of equations so that one would have three equations corresponding to the three unknown functions f^i so that the determinism associated with each step would be reduced. The equations in question would be of the same general form but with (f^1, f^2, f^3) replaced with some other combination.

1. In the genuinely projective situation where one can consider the (f^1, f^2, f^3, f^i) , $i = 1, 2, 3$ as a unique generalization of the equation. This would make the equations quadratic in f_i and reduce the non-determinism at given step of the time evolution. The new element is that now only monomials $M_m(z)$ associated with the f^i with same degree of homogeneity defined by $d = \sum m_i$ are consistent with projective invariance. Therefore the solutions are characterized by six integers $(d_{i,1}, d_{i,2})$ having interpretation as analogs of conformal weights since they correspond to eigenvalues of scaling operators. That homogenous polynomials are in question gives hopes that a generalization of Witten's approach might make sense. The indices m vary at the outer surfaces of the six 3-simplices defined by $(d_{i,1}, d_{i,2})$ and looking like tetrahedrons in 3-D space. The functions f^i are highly analogous to the homogenous functions appearing in group representations and quantum classical correspondence could be realized through the representation of the space-time surfaces in this manner.
2. The 3-determinants (a, b, c) appearing in the equations would be replaced by 4-determinants and the equations would have the same general form. One has

$$\begin{aligned} & \sum_{k,l,r,s,t,u} C_{M-k-r-t+E, N-l-s-u+E} D_{k,l} E_{r,s} C_{t,u} \times \\ & \times (M-k-r-t+E, k, r, t)(N-l-s-u+E, l, s, u) = 0 \ , \\ & E = e_1 + e_2 + e_3 + e_4 \ , \ (a, b, c, d) = \epsilon^{ijkl} a_i b_j c_k d_l \ . \end{aligned} \quad (2.6.14)$$

and its variants in which D and E appear quadratically. The values of M and N are restricted to the tetrahedrons $\sum M_i = \sum d_{k,1} + d_{1,i}$ and $\sum N_i = \sum d_{i,2} + d_{i,2}$, $i = 1, 2, 3$. Therefore

the dynamics in the index space is 3-dimensional. Since the index space is in a well-defined sense dual to CP_3 as is also the CP_3 in which the solutions are represented as counterparts of 3-surfaces, one could say that the 3-dimensionality of the dynamics corresponds to the dynamics of Chern-Simons action at space-like at the ends of CD and at light-like 3-surfaces.

3. The view based on 4-D time evolution is not useful since the solutions are restricted to time=constant plane in 4-D sense. The elimination of one of the projective coordinates would lead however to the analog of the above describe time evolution. In four-D context a more appropriate form of the equations is

$$\sum_{m,n,k,l,r,s} C_{m,n} D_{k,l} E_{r,s} C_{t,u}(m,k,r,t)(n,l,s,u) M_{m+k+r-E}(Z) M_{n+l+s-E}(W) = 0 \quad (2.6.15)$$

with similar equations for f^2 and f^3 . If one assumes that the CP_2 image of the holomorphic 3-surface is unique (it can correspond to either CP_3) the homogenous polynomials f^t must be symmetric under the exchange of Z and W so that the matrices C, D , and E are symmetric. This is equivalent to a replacement of the product of determinants with a sum of 16 products of determinants obtained by permuting the indices of each index pair (m, n) , (k, l) , (r, s) and (t, u) .

4. The number N_{cond} of conditions is given by the product $N_{cond} = N(d_M)N(d_N)$ of numbers of points in the two tetrahedrons defined by the total conformal weights

$$\sum M_r = d_M = \sum_k d_{k,1} + d_{i,1} \quad \text{and} \quad \sum N_r = d_N = \sum_k d_{k,2} + d_{i,2} \quad , \quad i = 1, 2, 3.$$

The number N_{coeff} of coefficients is

$$N_{coeff} = \sum_k n(d_{k,1}) + \sum_k n(d_{k,2}) \quad ,$$

where $n(d_{k,i})$ is the number points associated with the tetrahedron with conformal weight $d_{k,i}$. Since one has $n(d) \propto d^3$, N_{cond} scales as

$$N_{cond} \propto d_M^3 d_N^3 = \left(\sum_k d_{k,1} + d_{i,1} \right)^3 \times \left(\sum_k d_{k,2} + d_{i,2} \right)^3$$

whereas the number N_{coeff} of coefficients scales as

$$N_{coeff} \propto \sum_k (d_{k,1}^3 + d_{k,2}^3) \quad .$$

N_{cond} is clearly much larger than N_{coeff} so the solutions are analogous to partial waves and that the reduction of the rank for the matrices involved is an essential aspect of being a solution. The reduction of the rank for the coefficient matrices should reduce the effective number of coefficients so that solutions can be found. An interesting question is whether the coefficients are rationals with a suitable normalization allowed by independent conformal scalings. An analogy for the dynamics is quantum entanglement for 3+3 systems respecting the conservation of conformal weights and quantum classical correspondence taken to extreme suggests something like this.

5. One can interpret these equations as linear equations for the coefficients of the either linear term or as quadratic equations for the non-linear term. Also in the case of quadratic term one can apply general linear methods to identify the vanishing eigen values of the matrix of the quadratic form involved and to find the zero modes as solutions. The rank of the dynamically determined multiplier matrix must be non-maximal for the solutions to exist. One can imagine that the rank changes at critical surfaces in the space of Taylor coefficients meaning a multi-furcation in

the space determined by the coefficients of the polynomials. Also the degree of the polynomial can change at the critical point.

Solutions for which either determinant vanishes for all terms present in the solution exist. This is achieved if either the index vectors (m, l, r, t) or (n, l, s, u) in their respective parallel 3-planes are also in a 3-plane going through the origin. These solutions might be seen as the analogs of vacuum extremals of Chern-Simons action for which the CP_2 projection is at most 2-D Lagrangian manifold.

Quantum classical correspondence requires that the space-time surface carries also information about the momenta of partons. This information is quasi-continuous. Also information about zero modes should have representation in terms of the coefficients of the polynomials. Is this really possible if only products of polynomials of fixed conformal weights with strong restrictions on coefficients can be used? The counterpart for the vacuum degeneracy of Kähler action might resolve the problem. The analog for the construction of space-time surfaces as deformations of vacuum extremals would be starting from a trivial solution and adding to the building blocks of f^i some terms of same degree for which the wave vectors are not in the intersection of a 3-plane and simplex planes. The still existing "vacuum part" of the solution could carry the needed information.

6. One can take "obvious solutions" characterized by different common 3-planes for the "wave vectors" characterizing the 8 monomials $M_a(Z)$ and $M_b(W)$, $a \in \{m, k, r, t\}$ and $b \in \{n, l, s, u\}$. The coefficient matrices C, D, E, F are completely free. For the sum of these solutions the equations contain interaction terms for which at least two "wave vectors" belong to different 3-planes so that the corresponding 4-determinants are non-vanishing. The coefficients are not anymore free. Could the "obvious solutions" have interpretation in terms of different space-time sheets interacting via wormhole contacts? Or can one equate "obvious" with "vacuum" so that interaction between different vacuum space-time sheets via wormhole contact with 3-D CP_2 projection would deform vacuum extremals to non-vacuum extremals? Quantum classical correspondence inspires the question whether the products for functions f_i associated with an obvious solution associated with a particular plane correspond to a tensor products for quantum states associated with a particular partonic 2-surface or space-time sheet.
7. Effective 2-dimensionality realized in terms of the extremals of Chern-Simons actions with Lagrange multiplier term coming from the weak form of electric magnetic duality should also have a concrete counterpart if one takes the analogy with the extremals of Kähler action seriously. The equations can be transformed to 3-D ones by the elimination of the fourth coordinate but the interpretation in terms of discrete time evolution seems to be impossible since all points are coupled. The total conformal weights of the monomials vary in the range $[0, d_{1,i}]$ and $[0, d_{2,i}]$ so that the non-vanishing coefficients are in the interior of 3-simplex. The information about the fourth coordinate is preserved being visible via the four-determinants.
8. It should be possible to relate the hierarchy with respect to conformal weights would to the geometrization of loop integrals if a generalization of twistor strings is in question. One could hope that there exists a hierarchy of solutions with levels characterized by the rank of the matrices appearing in the linear representation. There is a temptation to associate this hierarchy with the hierarchy of deformations of vacuum extremals of Kähler action forming also a hierarchy. If this is the case the obvious solutions would correspond to vacuum extremals. At each step when the rank of the matrices involved decreases the solution becomes nearer to vacuum extremal and there should exist vanishing second variation of Kähler action. This structural similarity gives hopes that the proposed ansatz might work. Also the fact that a generalization of the Penrose's twistorial description for the solutions of Maxwell's equations to the situation when Maxwell field is induced from the Kähler form of CP_2 raises hopes. One must however remember that the consistency with other proposed solution ansätze and with what is believed to be known about the preferred extremals is an enormously powerful constraint and a mathematical miracle would be required.

2.7 Finiteness of generalized Feynman diagrams zero energy ontology

By effective 2-dimensionality partonic 2-surfaces plus the 4-D tangent space data at them code for quantum physics. The light-like orbits of partonic 2-surfaces in turn have interpretation as analogs of Feynman diagrams which correspond to 3-surfaces defining the regions at which the signature of the induced metric changes and 4-metric becomes degenerate. One could also identify the space-like regions of the space-time surfaces (deformed CP_2 type vacuum extremals, in particular wormhole throats) as the counterparts of generalized Feynman diagrams. The regions with Minkowskian signature of the induced metric would in turn correspond to the many-sheeted version of external space-time in which the particles move. A very concrete connection between particle and space-time geometry and topology is clearly in question.

Zero energy ontology has already led to the idea of interpreting the virtual particles as pairs of positive and negative energy wormhole throats. Hitherto I have taken it as granted that ordinary Feynman diagrammatics generalizes more or less as such. It is however far from clear what really happens in the vertices of the generalized Feynmann diagrams. The safest approach relies on the requirement that unitarity realized in terms of Cutkosky rules in ordinary Feynman diagrammatics allows a generalization. This requires loop diagrams. In particular, photon-photon scattering can take place only via a fermionic square loop so that it seems that loops must be present at least in the topological sense.

One must be however ready for the possibility that something unexpectedly simple might emerge. For instance, the vision about algebraic physics allows naturally only finite sums for diagrams and does not favor infinite perturbative expansions. Hence the true believer on algebraic physics might dream about finite number of diagrams for a given reaction type. For simplicity generalized Feynman diagrams without the complications brought by the magnetic confinement since by the previous arguments the generalization need not bring in anything essentially new.

The basic idea of duality in early hadronic models was that the lines of the dual diagram representing particles are only re-arranged in the vertices. This however does not allow to get rid of off mass shell momenta. Zero energy ontology encourages to consider a stronger form of this principle in the sense that the virtual momenta of particles could correspond to pairs of on mass shell momenta of particles. If also interacting fermions are pairs of positive and negative energy throats in the interaction region the idea about reducing the construction of Feynman diagrams to some kind of lego rules might work.

2.7.1 Virtual particles as pairs of on mass shell particles in ZEO

The first thing is to try to define more precisely what generalized Feynman diagrams are. The direct generalization of Feynman diagrams implies that both wormhole throats and wormhole contacts join at vertices.

1. A simple intuitive picture about what happens is provided by diagrams obtained by replacing the points of Feynman diagrams (wormhole contacts) with short lines and imagining that the throats correspond to the ends of the line. At vertices where the lines meet the incoming on mass shell quantum numbers would sum up to zero. This approach leads to a straightforward generalization of Feynman diagrams with virtual particles replaced with pairs of on mass shell throat states of type $++$, $--$, and $+-$. Incoming lines correspond to $++$ type lines and outgoing ones to $--$ type lines. The first two line pairs allow only time like net momenta whereas $+-$ line pairs allow also space-like virtual momenta. The sign assigned to a given throat is dictated by the the sign of the on mass shell momentum on the line. The condition that Cutkosky rules generalize as such requires $++$ and $--$ type virtual lines since the cut of the diagram in Cutkosky rules corresponds to on mass shell outgoing or incoming states and must therefore correspond to $++$ or $--$ type lines.
2. The basic difference as compared to the ordinary Feynman diagrammatics is that loop integrals are integrals over mass shell momenta and that all throats carry on mass shell momenta. In each vertex of the loop mass incoming on mass shell momenta must sum up to on mass shell momentum. These constraints improve the behavior of loop integrals dramatically and give

excellent hopes about finiteness. It does not however seem that only a finite number of diagrams contribute to the scattering amplitude besides tree diagrams. The point is that if a the reactions $N_1 \rightarrow N_2$ and $N_2 \rightarrow N_3$, where N_i denote particle numbers, are possible in a common kinematical region for N_2 -particle states then also the diagrams $N_1 \rightarrow N_2 \rightarrow N_3$ are possible. The virtual states N_2 include all all states in the intersection of kinematically allow regions for $N_1 \rightarrow N_2$ and $N_2 \rightarrow N_3$. Hence the dream about finite number possible diagrams is not fulfilled if one allows massless particles. If all particles are massive then the particle number N_2 for given N_1 is limited from above and the dream is realized.

3. For instance, loops are not possible in the massless case or are highly singular (bringing in mind twistor diagrams) since the conservation laws at vertices imply that the momenta are parallel. In the massive case and allowing mass spectrum the situation is not so simple. As a first example one can consider a loop with three vertices and thus three internal lines. Three on mass shell conditions are present so that the four-momentum can vary in 1-D subspace only. For a loop involving four vertices there are four internal lines and four mass shell conditions so that loop integrals would reduce to discrete sums. Loops involving more than four vertices are expected to be impossible.
4. The proposed replacement of the elementary fermions with bound states of elementary fermions and monopoles X_{\pm} brings in the analog of stringy diagrammatics. The 2-particle wave functions in the momentum degrees of freedom of fermions and X_{\pm} might allow more flexibility and allow more loops. Note however that there are excellent hopes about the finiteness of the theory also in this case.

2.7.2 Loop integrals are manifestly finite

One can make also more detailed observations about loops.

1. The simplest situation is obtained if only 3-vertices are allowed. In this case conservation of momentum however allows only collinear momenta although the signs of energy need not be the same. Particle creation and annihilation is possible and momentum exchange is possible but is always light-like in the massless case. The scattering matrices of supersymmetric YM theories would suggest something less trivial and this raises the question whether something is missing. Magnetic monopoles are an essential element of also these theories as also massivation and symmetry breaking and this encourages to think that the formation of massive states as fermion X_{\pm} pairs is needed. Of course, in TGD framework one has also high mass excitations of the massless states making the scattering matrix non-trivial.
2. In YM theories on mass shell lines would be singular. In TGD framework this is not the case since the propagator is defined as the inverse of the 3-D dimensional reduction of the modified Dirac operator D containing also coupling to four-momentum (this is required by quantum classical correspondence and guarantees stringy propagators),

$$\begin{aligned} D &= i\hat{\Gamma}^{\alpha} p_{\alpha} + \hat{\Gamma}^{\alpha} D_{\alpha} \ , \\ p_{\alpha} &= p_k \partial_{\alpha} h^k \ . \end{aligned} \tag{2.7.1}$$

The propagator does not diverge for on mass shell massless momenta and the propagator lines are well-defined. This is of course of essential importance also in general case. Only for the incoming lines one can consider the possibility that 3-D Dirac operator annihilates the induced spinor fields. All lines correspond to generalized eigenstates of the propagator in the sense that one has $D_3 \Psi = \lambda \gamma \Psi$, where γ is modified gamma matrix in the direction of the stringy coordinate emanating from light-like surface and D_3 is the 3-dimensional dimensional reduction of the 4-D modified Dirac operator. The eigenvalue λ is analogous to energy. Note that the eigenvalue spectrum depends on 4-momentum as a parameter.

3. Massless incoming momenta can decay to massless momenta with both signs of energy. The integration measure $d^2k/2E$ reduces to dx/x where $x \geq 0$ is the scaling factor of massless momentum. Only light-like momentum exchanges are however possible and scattering matrix is essentially trivial. The loop integrals are finite apart from the possible delicacies related to poles since the loop integrands for given massless wormhole contact are proportional to dx/x^3 for large values of x .
4. Irrespective of whether the particles are massless or not, the divergences are obtained only if one allows too high vertices as self energy loops for which the number of momentum degrees of freedom is $3N - 4$ for N -vertex. The construction of SUSY limit of TGD in [23] led to the conclusion that the parallelly propagating N fermions for given wormhole throat correspond to a product of N fermion propagators with same four-momentum so that for fermions and ordinary bosons one has the standard behavior but for $N > 2$ non-standard so that these excitations are not seen as ordinary particles. Higher vertices are finite only if the total number N_F of fermions propagating in the loop satisfies $N_F > 3N - 4$. For instance, a 4-vertex from which $N = 2$ states emanate is finite.

2.7.3 Taking into account magnetic confinement

What has been said above is not quite enough. As shown in the accompanying article and in [55] the weak form of electric-magnetic duality [65] leads to the picture about elementary particles as pairs of magnetic monopoles inspiring the notions of weak confinement based on magnetic monopole force. Also color confinement would have magnetic counterpart. This means that elementary particles would behave like string like objects in weak boson length scale. Therefore one must also consider the stringy case with wormhole throats replaced with fermion- X_{\pm} pairs (X_{\pm} is electromagnetically neutral and \pm refers to the sign of the weak isospin opposite to that of fermion) and their super partners.

1. The simplest assumption in the stringy case is that fermion- X_{\pm} pairs behave as coherent objects, that is scatter elastically. In more general case only their higher excitations identifiable in terms of stringy degrees of freedom would be created in vertices. The massivation of these states makes possible non-collinear vertices. An open question is how the massivation fermion- X_{\pm} pairs relates to the existing TGD based description of massivation in terms of Higgs mechanism and modified Dirac operator.
2. Mass renormalization could come from self energy loops with negative energy lines as also vertex normalization. By very general arguments supersymmetry implies the cancellation of the self energy loops but would allow non-trivial vertex renormalization [23].
3. If only 3-vertices are allowed, the loops containing only positive energy lines are possible if on mass shell fermion- X_{\pm} pair (or its superpartner) can decay to a pair of positive energy pair particles of same kind. Whether this is possible depends on the masses involved. For ordinary particles these decays are not kinematically possible below intermediate boson mass scale (the decays $F_1 \rightarrow F_2 + \gamma$ are forbidden kinematically or by the absence of flavor changing neutral currents whereas intermediate gauge bosons can decay to on mass shell fermion-antifermion pair).
4. The introduction of IR cutoff for 3-momentum in the rest system associated with the largest CD (causal diamond) looks natural as scale parameter of coupling constant evolution and p-adic length scale hypothesis favors the inverse of the size scale of CD coming in powers of two. This parameter would define the momentum resolution as a discrete parameter of the p-adic coupling constant evolution. This scale does not have any counterpart in standard physics. For electron, d quark, and u quark the proper time distance between the tips of CD corresponds to frequency of 10 Hz, 1280 Hz, and 160 Hz: all these frequencies define fundamental bio-rhythms [43].

These considerations have left completely untouched one important aspect of generalized Feynman diagrams: the necessity to perform a functional integral over the deformations of the partonic 2-surfaces at the ends of the lines- that is integration over WCW. Number theoretical universality requires that WCW and these integrals make sense also p-adically and in the following these aspects of generalized Feynman diagrams are discussed.

Bibliography

Books about TGD

- [1] M. Pitkänen (2006), *Topological Geometroynamics: Overview*.
http://tgd.wippiespace.com/public_html/tgdview/tgdview.html.
- [2] M. Pitkänen (2006), *Quantum Physics as Infinite-Dimensional Geometry*.
http://tgd.wippiespace.com/public_html/tgdgeom/tgdgeom.html.
- [3] M. Pitkänen (2006), *Physics in Many-Sheeted Space-Time*.
http://tgd.wippiespace.com/public_html/tgdclass/tgdclass.html.
- [4] M. Pitkänen (2006), *p-Adic length Scale Hypothesis and Dark Matter Hierarchy*.
http://tgd.wippiespace.com/public_html/paddark/paddark.html.
- [5] M. Pitkänen (2006), *Quantum TGD*.
http://tgd.wippiespace.com/public_html/tgdquant/tgdquant.html.
- [6] M. Pitkänen (2006), *TGD as a Generalized Number Theory*.
http://tgd.wippiespace.com/public_html/tgdnumber/tgdnumber.html.
- [7] M. Pitkänen (2006), *TGD and Fringe Physics*.
http://tgd.wippiespace.com/public_html/freenergy/freenergy.html.

Books about TGD Inspired Theory of Consciousness and Quantum Biology

- [8] M. Pitkänen (2006), *TGD Inspired Theory of Consciousness*.
http://tgd.wippiespace.com/public_html/tgdconsc/tgdconsc.html.
- [9] M. Pitkänen (2006), *Bio-Systems as Self-Organizing Quantum Systems*.
http://tgd.wippiespace.com/public_html/bioselforg/bioselforg.html.
- [10] M. Pitkänen (2006), *Quantum Hardware of Living Matter*.
http://tgd.wippiespace.com/public_html/bioware/bioware.html.
- [11] M. Pitkänen (2006), *Bio-Systems as Conscious Holograms*.
http://tgd.wippiespace.com/public_html/hologram/hologram.html.
- [12] M. Pitkänen (2006), *Genes and Memes*.
http://tgd.wippiespace.com/public_html/genememe/genememe.html.
- [13] M. Pitkänen (2006), *Magnetospheric Consciousness*.
http://tgd.wippiespace.com/public_html/magnconsc/magnconsc.html.
- [14] M. Pitkänen (2006), *Mathematical Aspects of Consciousness Theory*.
http://tgd.wippiespace.com/public_html/mathconsc/mathconsc.html.
- [15] M. Pitkänen (2006), *TGD and EEG*.
http://tgd.wippiespace.com/public_html/tgdeeg/tgdeeg.html.

References to the chapters of the books about TGD

- [16] The chapter *Construction of Configuration Space Kähler Geometry from Symmetry Principles* of [2].
http://tgd.wippiespace.com/public_html/tgdgeom/tgdgeom.html#compl1.
- [17] The chapter *Quantum Hall effect and Hierarchy of Planck Constants* [5].
http://tgd.wippiespace.com/public_html/tgdquant/tgdquant.html#anyontgd.
- [18] The chapter *Does the Modified Dirac Equation Define the Fundamental Action Principle?* of [2].
http://tgd.wippiespace.com/public_html/tgdgeom/tgdgeom.html#Dirac.
- [19] The chapter *TGD as a Generalized Number Theory: Quaternions, Octonions, and their Hyper Counterparts* of [6].
http://tgd.wippiespace.com/public_html/tgdnumber/tgdnumber.html#visionb.
- [20] The chapter *p-Adic Numbers and Generalization of Number Concept* of [6].
http://tgd.wippiespace.com/public_html/tgdnumber/tgdnumber.html#padmat.
- [21] The chapter *Quantum Field Theory Limit of TGD from Bosonic Emergence* of [5].
http://tgd.wippiespace.com/public_html/tgdquant/tgdquant.html#emergence.
- [22] M. Pitkänen (2006), *Physics in Many-Sheeted Space-Time*.
http://tgd.wippiespace.com/public_html/tgdclass/tgdclass.html.
- [23] The chapter *Construction of Quantum Theory: Symmetries* of [5].
http://tgd.wippiespace.com/public_html/tgdquant/tgdquant.html#quthe.
- [24] The chapter *p-Adic Particle Massivation: Hadron Masses* of [4].
http://tgd.wippiespace.com/public_html/paddark/paddark.html#mass3.
- [25] The chapter *p-Adic Particle Massivation: Elementary particle Masses* of [4].
http://tgd.wippiespace.com/public_html/paddark/paddark.html#mass2.
- [26] The chapter *TGD as a Generalized Number Theory: Infinite Primes* of [6].
http://tgd.wippiespace.com/public_html/tgdnumber/tgdnumber.html#visionc.
- [27] The chapter *p-Adic Particle Massivation: New Physics* of [4].
http://tgd.wippiespace.com/public_html/paddark/paddark.html#mass4.
- [28] The chapter *TGD as a Generalized Number Theory: p-Adicization Program* of [6].
http://tgd.wippiespace.com/public_html/tgdnumber/tgdnumber.html#visiona.
- [29] The chapter *Basic Extremals of Kähler Action* of [3].
http://tgd.wippiespace.com/public_html/tgdclass/tgdclass.html#class.
- [30] The chapter *TGD and Astrophysics* of [3].
http://tgd.wippiespace.com/public_html/tgdclass/tgdclass.html#astro.
- [31] The chapter *Configuration Space Spinor Structure* of [2].
http://tgd.wippiespace.com/public_html/tgdgeom/tgdgeom.html#cspin.
- [32] The chapter *The Relationship Between TGD and GRT* of [3].
http://tgd.wippiespace.com/public_html/tgdclass/tgdclass.html#tgdgrt.
- [33] The chapter *TGD and Cosmology* of [3].
http://tgd.wippiespace.com/public_html/tgdclass/tgdclass.html#cosmo.
- [34] The chapter *Identification of the Configuration Space Kähler Function* of [2].
http://tgd.wippiespace.com/public_html/tgdgeom/tgdgeom.html#kahler.
- [35] The chapter *Does TGD Predict the Spectrum of Planck Constants?* of [5].
http://tgd.wippiespace.com/public_html/tgdquant/tgdquant.html#Planck.

- [36] The chapter *Does the QFT Limit of TGD Have Space-Time Super-Symmetry?* of [5].
http://tgd.wippiespace.com/public_html/tgdquant/tgdquant.html#susy.
- [37] The chapter *Massless States and Particle Massivation* of [4].
http://tgd.wippiespace.com/public_html/paddark/paddark.html#mless.
- [38] The chapter *Quantum Astrophysics* of [3].
http://tgd.wippiespace.com/public_html/tgdclass/tgdclass.html#qastro.
- [39] The chapter *Construction of Quantum Theory: S-matrix* of [5].
http://tgd.wippiespace.com/public_html/tgdquant/tgdquant.html#towards.
- [40] The chapter *Twistors, N=4 Super-Conformal Symmetry, and Quantum TGD* of [5].
http://tgd.wippiespace.com/public_html/tgdquant/tgdquant.html#twistor.
- [41] The chapter *Yangian Symmetry, Twistors, and TGD* of [5].
http://tgd.wippiespace.com/public_html/tgdquant/tgdquant.html#Yangian.

References to the chapters of the books about TGD Inspired Theory of Consciousness and Quantum Biology

- [42] The chapter *p-Adic Physics as Physics of Cognition and Intention* of [8].
http://tgd.wippiespace.com/public_html/tgdconsc/tgdconsc.html#cognic.
- [43] The chapter *Evolution in Many-Sheeted Space-Time* of [12].
http://tgd.wippiespace.com/public_html/genememe/genememe.html#prebio.
- [44] The chapter *Quantum Model for Nerve Pulse* of [15].
http://tgd.wippiespace.com/public_html/tgdeeg/tgdeeg/tgdeeg.html#pulse.
- [45] The chapter *About the New Physics Behind Qualia* of [10].
http://tgd.wippiespace.com/public_html/bioware/bioware.html#newphys.
- [46] The chapter *Dark Matter Hierarchy and Hierarchy of EEGs* of [15].
http://tgd.wippiespace.com/public_html/tgdeeg/tgdeeg.html#eegdark.
- [47] The chapter *DNA as Topological Quantum Computer* of [12].
http://tgd.wippiespace.com/public_html/genememe/genememe.html#dnatqc.
- [48] The chapter *Quantum Antenna Hypothesis* of [10].
http://tgd.wippiespace.com/public_html/bioware/bioware.html#tubuc.
- [49] The chapter *Negentropy Maximization Principle* of [8].
http://tgd.wippiespace.com/public_html/tgdconsc/tgdconsc.html#nmpc.

Articles related to TGD

- [50] M. Pitkänen (2010), Article series in *Prespacetime Journal* Vol 1, No 3.
- [51] M. Pitkänen (2010), *Physics as Infinite-dimensional Geometry II: Configuration Space Kähler Geometry from Symmetry Principles*. *Prespacetime Journal* July Vol. 1 Issue 4 Page 562-580.
- [52] M. Pitkänen (2010), *Physics as Generalized Number Theory I: p-Adic Physics and Number Theoretic Universality*. *Prespacetime Journal* July Vol. 1 Issue 4 Page 68-94.
- [53] M. Pitkänen (2010), *Physics as Infinite-dimensional Geometry IV: Weak Form of Electric-Magnetic Duality and Its Implications*. *Prespacetime Journal* July Vol. 1 Issue 4 Page 562-580.
- [54] M. Pitkänen (2010), *Physics as Generalized Number Theory III: Infinite Primes*. *Prespacetime Journal* July Vol. 1 Issue 4 Page 153-181.

- [55] M. Pitkänen (2010), *Physics as Generalized Number Theory II: Classical Number Fields*. Prespacetime Journal July Vol. 1 Issue 4 Page 95-131.
- [56] M. Pitkänen (2010), *The Geometry of CP_2 and its Relationship to Standard Model*. Prespacetime Journal July Vol. 1 Issue 4 Page 182-192.
- [57] M. Pitkänen (2010), Article series in Prespacetime Journal Vol 1, No 3.
- [58] M. Pitkänen (2006) *Basic Properties of CP_2 and Elementary Facts about p -Adic Numbers*
http://tgd.wippiespace.com/public_html/pdfpool/append.pdf.

Mathematics

- [59] T. Eguchi, B. Gilkey, J. Hanson (1980). Phys. Rep. 66, 6, 1980.
- [60] J. Dixmier (1981), *Von Neumann Algebras*. Amsterdam: North-Holland Publishing Company. [First published in French in 1957: Les Algèbres d'Opérateurs dans l'Espace Hilbertien, Paris:Gauthier-Villars].
- [61] P. Goddard, A. Kent and D. Olive (1986), *Unitary representations of the Virasoro and super-Virasoro algebras*. Comm. Math. Phys. 103, no. 1, 105-119.
- [62] *Kac-Moody algebra*. http://en.wikipedia.org/wiki/KacMoody_algebra.
 P. Windey (1986), *Super-Kac-Moody algebras and supersymmetric 2d-free fermions*. Comm. in Math. Phys. Vol. 105, No 4.
 S. Kumar (2002), *Kac-Moody Groups, their Flag Varieties and Representation Theory*. Progress in Math. Vol 204. A Birkhauser Boston book. <http://www.springer.com/birkhauser/mathematics/book/978-0-8176-4227-3>.
- [63] *Clifford algebra*. http://en.wikipedia.org/wiki/Clifford_algebra.
- [64] *Algebraic genus*. http://en.wikipedia.org/wiki/Arithmetic_genus.
- [65] *Penrose diagram*. http://en.wikipedia.org/wiki/Penrose_diagram.
- [66] *Yangian symmetry*. <http://en.wikipedia.org/wiki/Yangian>.
- [67] *Octonions*. <http://en.wikipedia.org/wiki/Octonions>.
- [68] D. S. Freed (1985): *The Geometry of Loop Groups* (Thesis). Berkeley: University of California.
- [69] *Number theory*. http://en.wikipedia.org/wiki/Number_theory.
 T. M. Apostol (1976), *Introduction to Analytic Number Theory*. New York: Springer, ISBN 0-387-90163-9.
- [70] *Super Virasoro algebra*. http://en.wikipedia.org/wiki/Super_Virasoro_algebra.
 V. G. Knizhnik (1986), *Superconformal algebras in two dimensions*. Teoret. Mat. Fiz., Vol. 66, Number 1, pp. 102-108.
- [71] *Quaternions*. <http://en.wikipedia.org/wiki/Quaternion>.
- [72] *Symplectic manifold*. http://en.wikipedia.org/wiki/Symplectic_manifold.
Symplectic geometry. http://en.wikipedia.org/wiki/Symplectic_geometry.
 A. C. da Silva (2004), *Symplectic geometry*. <http://www.math.princeton.edu/~acannas/symplectic.pdf>.
- [73] Hawking, S.W. and Pope, C., N. (1978): *Generalized Spin Structures in Quantum Gravity*. Physics Letters Vol 73 B, no 1.
- [74] *Calabi-Yau manifold*. http://en.wikipedia.org/wiki/CalabiYau_manifold.
- [75] *Symmetric space*. http://en.wikipedia.org/wiki/Symmetric_space.

- [76] Pope, C., N. (1980): *Eigenfunctions and Spin^c Structures on CP₂* D.A.M.T.P. preprint.
- [77] *Harmonic analysis*. http://en.wikipedia.org/wiki/Harmonic_analysis.
- [78] *Kähler manifold*. http://en.wikipedia.org/wiki/Kähler_manifold.
- [79] *Fields*. [http://en.wikipedia.org/wiki/Field_\(mathematics\)](http://en.wikipedia.org/wiki/Field_(mathematics)).
D. A. Marcus (1977), *Number Fields*. Springer Verlag. <http://www.springer.com/mathematics/numbers/book/978-0-387-90279-1>.
- [80] G. W. Gibbons, C. N. Pope (1977): *CP₂ as gravitational instanton*. Commun. Math. Phys. 55, 53.
- [81] V. Jones (2003), *In and around the origin of quantum groups*. arXiv:math.OA/0309199.
C. Kassel (1995), *Quantum Groups*. SpringerVerlag.
C. Gomez, M. Ruiz-Altaba, G. Sierra (1996), *Quantum Groups and Two-Dimensional Physics*. Cambridge University Press.
- [82] L. Brekke and P. G. O. Freund (1993), *p-Adic Numbers in Physics*. Phys. Rep. vol. 233, No 1.
- [83] *Scale invariance vs. conformal invariance*. http://en.wikipedia.org/wiki/Conformal_field_theory#Scale_invariance_vs._conformal_invariance.
- [84] V. Bouchard (2005), *Lectures on complex geometry, Calabi-Yau manifolds and toric geometry*. <http://www.ulb.ac.be/sciences/ptm/pmif/Rencontres/ModaveI/CGL.ps>.

Theoretical physics

- [85] S. Parke and T. Taylor (1986), *An Amplitude for N gluon Scattering*, Phys. Rev. Lett. 56, 2459.
- [86] E. Witten (2003), *Perturbative Gauge Theory As a String Theory In Twistor Space*. <http://arxiv.org/abs/hep-th/0312171>.
- [87] *Montonen Olive Duality*. http://en.wikipedia.org/wiki/Montonen-Olive_duality.
- [88] R. Britto, F. Cachazo, B. Feng, and E. Witten (2005), *Direct Proof of Tree-level Recursion Relation in Yang-Mills Theory*. http://arxiv.org/PS_cache/hep-th/pdf/0501/0501052v2.pdf.
- [89] R. Britto, F. Cachazo, B. Feng, and E. Witten (2005), *Direct Proof of Tree-Level Recursion Relation in Yang-Mills Theory*, Phys. Rev. Lett. 94 (2005) 181602, <http://arxiv.org/abs/hep-th/0501052>.
- [90] *Super symmetry*. <http://en.wikipedia.org/wiki/SUSY>.
- [91] *Hyperdeterminant*. <http://en.wikipedia.org/wiki/Hyperdeterminant>.
- [92] F. Cachazo, P. Svrcek, and E. Witten (2004), *MHV Vertices and Tree Amplitudes In Gauge Theory*. <http://arXiv.org/pdf/hep-th/0403047v2>.
- [93] L. Mason and D. Skinner (2009), *Dual Superconformal Invariance, Momentum Twistors and Grassmannians*. <http://arxiv.org/pdf/0909.0250v2>.
- [94] J. Drummond, J. Henn, J. Plefka (2009), *Yangian symmetry of scattering amplitudes in N = 4 super Yang-Mills theory*. <http://cdsweb.cern.ch/record/1162372/files/jhep052009046.pdf>.
- [95] L. Dolan, C. R. Nappi, E. Witten (2004), *Yangian Symmetry in D = 4 superconformal Yang-Mills theory*. <http://arxiv.org/pdf/hep-th/0401243v2>.
- [96] R. Boels (2010), *On BCFW shifts of integrands and integrals*. <http://arxiv.org/abs/1008.3101>.

- [97] Nima Arkani-Hamed, Jacob L. Bourjaily, Freddy Cachazo, Simon Caron-Huot, Jaroslav Trnka(2010), *The All-Loop Integrand For Scattering Amplitudes in Planar $N = 4$ SYM*. http://arxiv.org/find/hep-th/1/au:+Bourjaily_J/0/1/0/all/0/1.
- [98] P. K. Kotvun *et al* (2010), *Viscosity in Strongly Interacting Quantum Field Theories from Black Hole Physics*. http://arxiv.org/PS_cache/hep-th/pdf/0405/0405231v2.pdf.
- [99] *Chern-Simons theory*. http://en.wikipedia.org/wiki/ChernSimons_theory.

Physics

- [100] Seongwan Park (1995), *Search for New Phenomena in CDF-I: Z' , W' , and leptoquarks*. Proceedings for the 10th Topical Workshop on Proton-Antiproton Collider Physics. Fermilab, Batavia, Illinois, 1995.Fermilab-Conf-95/155-E.<http://lss.fnal.gov/archive/1995/conf/Conf-95-155-E.pdf>.
- [101] S. Ambrosanio *et al* (1996), *Supersymmetric analysis and predictions based on the CDF $ee\gamma\gamma + E_T$ event*. arXiv:hep-ph/9602239v2.<http://arxiv.org/abs/hep-ph/9602239>.
- [102] J. D. Bjorken (1997), *Acta Phys. Polonica B. V. 28.p. 2773*.
- [103] *Lamb shift*. http://en.wikipedia.org/wiki/Lamb_shift.
- [104] J. Flowers (2010), *Quantum electrodynamics: A chink in the armour?*. Nature 466. 195-196. <http://www.nature.com/nature/journal/v466/n7303/pdf/466195a.pdf>.
- [105] Tommaso Dorigo (2009), *CDF Kisses Another New Physics Effect Bye-Bye*.http://www.scientificblogging.com/quantum_diaries_survivor/cdf_kisses_another_new_physics_effect_byebye.
- [106] *Fractional quantum Hall Effect*.http://en.wikipedia.org/wiki/Fractional_quantum_Hall_effect.
Fractional Quantum Hall Effect.<http://www.warwick.ac.uk/~phsbn/fqhe.htm>.
- [107] *Slow light*. http://en.wikipedia.org/wiki/Slow_light.
- [108] D. J. P. Morris *et al* (2009). *Dirac Strings and Magnetic Monopoles in Spin Ice $Dy_2Ti_2O_7$* . Science, Vol. 326, No. 5951, pp. 411-414.
H. Johnston (1010) *Magnetic monopoles spotted in spin ices*. <http://physicsworld.com/cws/article/news/40302>.
- [109] D. Da Roacha and L. Nottale (2003), *Gravitational Structure Formation in Scale Relativity*. astro-ph/0310036.
- [110] M. R. S. Hawkins (2010), *On time dilation in quasar light curves*. Montly Notices of the Royal Astronomical Society. <http://www3.interscience.wiley.com/journal/123345710/abstract?CRETRY=1&SRETRY=0>.
See also <http://matpitka.blogspot.com/2010/04/strange-quasars-do-not-show-time.html>.

Biology related references

- [111] *High energy phosphate*. http://en.wikipedia.org/wiki/High-energy_phosphate.
- [112] F. A. Popp, B.Ruth, W.Bahr, J. Boehm, P.Grass (1981),G.Grolig, M.Rattemeyer, H.G.Schmidt and P.Wulle:*Emission of Visible and Ultraviolet Radiationby Active Biological Systems*. Collective Phenomena (Gordon and Breach), 3, 187-214.
F. A.Popp, K. H. Li, and Q. Gu (eds.) (1992): *Recent Advances in Bio-photon Research and itsApplications*. World Scientific, Singapore-NewJersey.

- F.- A. Popp: *Photon-storage in biological systems*, in: *Electromagnetic Bio-Information*.pp.123-149. Eds. F.A.Popp, G.Becker, W.L.König, and W.Peschka. Urban& Schwarzenberg, Muenchen-Baltimore.
- F.-A. Popp (2001),*About the Coherence of Bio-photons*.
<http://www.datadiwan.de/iib/ib0201e1.htm>.
- F.-A. Popp and J.-J. Chang (2001), *Photon Sucking and the Basis of Biological Organization*.<http://www.datadiwan.de/iib/ib0201e3.htm>.
- F.-A.Popp and Y. Yan (2001), *Delayed Luminescence of Biological Systems in Terms of States*.<http://www.datadiwan.de/iib/pub2001-07.htm>.
- [113] C. F. Blackman (1994), "Effect of Electrical and Magnetic Fields on the Nervous System" in *The Vulnerable Brain and Environmental Risks, Vol. 3, Toxins in Air and Water* (eds. R. L. Isaacson and K. F. Jensen). Plenum Press, New York, pp.331-355.

Chapter 3

Elementary Particle Vacuum Functionals

3.1 Introduction

One of the basic ideas of TGD approach has been genus-generation correspondence: boundary components of the 3-surface should be carriers of elementary particle numbers and the observed fermion families should correspond to various boundary topologies. The details of the assumed correspondence have evolved during years.

1. The first proposal indeed indeed that both fermions and bosons correspond to boundary components so that the genus of the boundary component would classify the particles topologically. At this time I still believed that stringy diagrams would have a direct generalization in TGD framework implying that g would define additive quantum number effectively. Later it became clear that it is Feynman diagrams which must be generalized and the partons at primary vertices must have same genus. Stringy diagrams are still there but have totally different interpretation.
2. Boundary component was later replaced with the light-like surface at which the signature of the induced metric changes and it was natural to identify bosons as wormhole contacts carrying fermion and antifermion quantum numbers at opposite light-like worm-hole throats. Hence bosons would be labeled by pairs (g_1, g_2) of genera. For gravitons one had to assume pairs of wormhole contacts in order to obtain spin 2. Already at this stage it became clear that $SU(3)$ should act as a dynamical symmetry with fermions in triplet representation and bosons in octet and singlet representations. The light bosons would correspond to singlets which would guarantee universality of the couplings to fermion families.
3. For long time fermions were identified as single throats but twistorial program and the properties of Chern-Simons Dirac operator suggesting strongly that the fundamental entities must be massless, forced to replace physical fermion with a wormhole contact characterized by (g, g) and transforming like triplet with respect to $SU(3)$ as far as vertices are considered. The hypothesis that $SU(3)$ acts as dynamical symmetry for the reaction vertices has very powerful implications and allows only BFF type vertices required also by bosonic emergence and SUSY symmetry.
4. A further step in the evolution of ideas was the realization that electric-magnetic duality forces to identify all elementary particles as "weak" string like objects consisting of Kähler magnetic flux tubes with opposite magnetic charges at ends. This meant that all elementary particles - not only gravitons- are described by "weak" strings. Note that this stringy character should not be confused with that for wormhole contacts for which throats effectively play the role of string ends. One can say that fundamental objects are massless states at wormhole throats and that all elementary particles as well as string like objects emerge from them.

One might hope that this picture is not too far from the final one as far elementary particles are considered. If one accepts this picture the remaining question is why the number of genera is just three. Could this relate to the fact that $g \leq 2$ Riemann surfaces are always hyper-elliptic (have global

Z_2 conformal symmetry) unlike $g > 2$ surfaces? Why the complete bosonic de-localization of the light families should be restricted inside the hyper-elliptic sector? Does the Z_2 conformal symmetry make these states light and make possible delocalization and dynamical $SU(3)$ symmetry? Could it be that for $g > 2$ elementary particle vacuum functionals vanish for hyper-elliptic surfaces? If this the case and if the time evolution for partonic 2-surfaces changing g commutes with Z_2 symmetry then the vacuum functionals localized to $g \leq 2$ surfaces do not disperse to $g > 2$ sectors.

In order to provide answers to either series of questions one must know something about the dependence of the elementary particle state functionals on the geometric properties of the boundary component and in the sequel an attempt to construct what might be called elementary particle vacuum functionals, is made. Irrespective of what identification of interaction vertices is adopted, the arguments involved with the construction involve only the string model type vertices so that the previous discussion seems to apply more or less as such.

The basic assumptions underlying the construction are the following ones:

1. Elementary particle vacuum functionals depend on the geometric properties of the two-surface X^2 representing elementary particle.
2. Vacuum functionals possess extended Diff invariance: all 2-surfaces on the orbit of the 2-surface X^2 correspond to the same value of the vacuum functional. This condition is satisfied if vacuum functionals have as their argument, not X^2 as such, but some 2- surface Y^2 belonging to the unique orbit of X^2 (determined by the principle selecting preferred extremal of the Kähler action as a generalized Bohr orbit [37]) and determined in $Diff^3$ invariant manner.
3. Zero energy ontology allows to select uniquely the partonic two surface as the intersection of the wormhole throat at which the signature of the induced 4-metric changes with either the upper or lower boundary of $CD \times CP_2$. This is essential since otherwise one could not specify the vacuum functional uniquely.
4. Vacuum functionals possess conformal invariance and therefore for a given genus depend on a finite number of variables specifying the conformal equivalence class of Y^2 .
5. Vacuum functionals satisfy the cluster decomposition property: when the surface Y^2 degenerates to a union of two disjoint surfaces (particle decay in string model inspired picture), vacuum functional decomposes into a product of the vacuum functionals associated with disjoint surfaces.
6. Elementary particle vacuum functionals are stable against the two-particle decay $g \rightarrow g_1 + g_2$ and one particle decay $g \rightarrow g - 1$.

In the following the construction will be described in more detail.

1. Some basic concepts related to the description of the space of the conformal equivalence classes of Riemann surfaces are introduced and the concept of hyper-ellipticity is introduced. Since theta functions will play a central role in the construction of the vacuum functionals, also their basic properties are discussed.
2. After these preliminaries the construction of elementary particle vacuum functionals is carried out.
3. Possible explanations for the experimental absence of the higher fermion families are considered.

3.2 Identification of elementary particles

The developments in the formulation of quantum TGD which have taken place during the period 2005-2007 [37, 19] suggest dramatic simplifications of the general picture discussed in the earlier version of this chapter. p-Adic mass calculations [18, 17, 20] leave a lot of freedom concerning the detailed identification of elementary particles.

3.2.1 The evolution of the topological ideas about elementary particles

One of the basic ideas of TGD approach has been genus-generation correspondence: boundary components of the 3-surface should be carriers of elementary particle numbers and the observed fermion families should correspond to various boundary topologies.

With the advent of zero energy ontology this picture changed somewhat. It is the wormhole throats identified as light-like 3-surfaces at which with the induced metric of the space-time surface changes its signature from Minkowskian to Euclidian, which correspond to the light-like orbits of partonic 2-surfaces. One cannot of course exclude the possibility that also boundary components could allow to satisfy boundary conditions without assuming vacuum extremal property of nearby space-time surface. The intersections of the wormhole throats with the light-like boundaries of causal diamonds (CD s) identified as intersections of future and past directed light cones ($CD \times CP_2$ is actually in question but I will speak about CD s) define special partonic 2-surfaces and it is the moduli of these partonic 2-surfaces which appear in the elementary particle vacuum functionals naturally.

The first modification of the original simple picture comes from the identification of physical particles as bound states of pairs of wormhole contacts and from the assumption that for generalized Feynman diagrams stringy trouser vertices are replaced with vertices at which the ends of light-like wormhole throats meet. In this picture the interpretation of the analog of trouser vertex is in terms of propagation of same particle along two different paths. This interpretation is mathematically natural since vertices correspond to 2-manifolds rather than singular 2-manifolds which are just splitting to two disjoint components. Second complication comes from the weak form of electric-magnetic duality forcing to identify physical particles as weak strings with magnetic monopoles at their ends and one should understand also the possible complications caused by this generalization.

These modifications force to consider several options concerning the identification of light fermions and bosons and one can end up with a unique identification only by making some assumptions. Masslessness of all wormhole throats- also those appearing in internal lines- and dynamical $SU(3)$ symmetry for particle generations are attractive general enough assumptions of this kind. This means that bosons and their super-partners correspond to wormhole contacts with fermion and antifermion at the throats of the contact. Free fermions and their superpartners could correspond to CP_2 type vacuum extremals with single wormhole throat. It turns however that dynamical $SU(3)$ symmetry forces to identify massive (and possibly topologically condensed) fermions as (g, g) type wormhole contacts.

Do free fermions correspond to single wormhole throat or (g, g) wormhole?

The original interpretation of genus-generation correspondence was that free fermions correspond to wormhole throats characterized by genus. The idea of $SU(3)$ as a dynamical symmetry suggested that gauge bosons correspond to octet and singlet representations of $SU(3)$. The further idea that all lines of generalized Feynman diagrams are massless poses a strong additional constraint and it is not clear whether this proposal as such survives.

1. Twistorial program assumes that fundamental objects are massless wormhole throats carrying collinearly moving many-fermion states and also bosonic excitations generated by supersymplectic algebra. In the following consideration only purely bosonic and single fermion throats are considered since they are the basic building blocks of physical particles. The reason is that propagators for high excitations behave like p^{-n} , n the number of fermions associated with the wormhole throat. Therefore single throat allows only spins 0,1/2,1 as elementary particles in the usual sense of the word.
2. The identification of massive fermions (as opposed to free massless fermions) as wormhole contacts follows if one requires that fundamental building blocks are massless since at least two massless throats are required to have a massive state. Therefore the conformal excitations with CP_2 mass scale should be assignable to wormhole contacts also in the case of fermions. As already noticed this is not the end of the story: weak strings are required by the weak form of electric-magnetic duality.
3. If free fermions corresponding to single wormhole throat, topological condensation is an essential element of the formation of stringy states. The topological condensation of fermions by topological sum (fermionic CP_2 type vacuum extremal touches another space-time sheet) suggest $(g, 0)$

wormhole contact. Note however that the identification of wormhole throat is as 3-surface at which the signature of the induced metric changes so that this conclusion might be wrong. One can indeed consider also the possibility of (g, g) pairs as an outcome of topological condensation. This is suggested also by the idea that wormhole throats are analogous to string like objects and only this option turns out to be consistent with the BFF vertex based on the requirement of dynamical $SU(3)$ symmetry to be discussed later. The structure of reaction vertices makes it possible to interpret (g, g) pairs as $SU(3)$ triplet. If bosons are obtained as fusion of fermionic and antifermionic throats (touching of corresponding CP_2 type vacuum extremals) they correspond naturally to (g_1, g_2) pairs.

4. p-Adic mass calculations distinguish between fermions and bosons and the identification of fermions and bosons should be consistent with this difference. The maximal p-adic temperature $T = 1$ for fermions could relate to the weakness of the interaction of the fermionic wormhole throat with the wormhole throat resulting in topological condensation. This wormhole throat would however carry momentum and 3-momentum would in general be non-parallel to that of the fermion, most naturally in the opposite direction.

p-Adic mass calculations suggest strongly that for bosons p-adic temperature $T = 1/n, n > 1$, so that thermodynamical contribution to the mass squared is negligible. The low p-adic temperature could be due to the strong interaction between fermionic and antifermionic wormhole throat leading to the "freezing" of the conformal degrees of freedom related to the relative motion of wormhole throats.

5. The weak form of electric-magnetic duality forces second wormhole throat with opposite magnetic charge and the light-like momenta could sum up to massive momentum. In this case string tension corresponds to electroweak length scale. Therefore p-adic thermodynamics must be assigned to wormhole contacts and these appear as basic units connected by Kähler magnetic flux tube pairs at the two space-time sheets involved. Weak stringy degrees of freedom are however expected to give additional contribution to the mass, perhaps by modifying the ground state conformal weight.

Dynamical $SU(3)$ fixes the identification of fermions and bosons and fundamental interaction vertices

For 3 light fermion families $SU(3)$ suggests itself as a dynamical symmetry with fermions in fundamental $N = 3$ -dimensional representation and $N \times N = 9$ bosons in the adjoint representation and singlet representation. The known gauge bosons have same couplings to fermionic families so that they must correspond to the singlet representation. The first challenge is to understand whether it is possible to have dynamical $SU(3)$ at the level of fundamental reaction vertices.

This is a highly non-trivial constraint. For instance, the vertices in which n wormhole throats with same (g_1, g_2) glued along the ends of lines are not consistent with this symmetry. The splitting of the fermionic worm-hole contacts before the proper vertices for throats might however allow the realization of dynamical $SU(3)$. The condition of $SU(3)$ symmetry combined with the requirement that virtual lines resulting also in the splitting of wormhole contacts are always massless, leads to the conclusion that massive fermions correspond to (g, g) type wormhole contacts transforming naturally like $SU(3)$ triplet. This picture conforms with the identification of free fermions as throats but not with the naive expectation that their topological condensation gives rise to $(g, 0)$ wormhole contact.

The argument leading to these conclusions runs as follows.

1. The question is what basic reaction vertices are allowed by dynamical $SU(3)$ symmetry. FFB vertices are in principle all that is needed and they should obey the dynamical symmetry. The meeting of entire wormhole contacts along their ends is certainly not possible. The splitting of fermionic wormhole contacts before the vertices might be however consistent with $SU(3)$ symmetry. This would give two a pair of 3-vertices at which three wormhole lines meet along partonic 2-surfaces (rather than along 3-D wormhole contacts).
2. Note first that crossing gives all possible reaction vertices of this kind from $F(g_1)\bar{F}(g_2) \rightarrow B(g_1, g_2)$ annihilation vertex, which is relatively easy to visualize. In this reaction $F(g_1)$ and $\bar{F}(g_2)$ wormhole contacts split first. If one requires that all wormhole throats involved are

massless, the two wormhole throats resulting in splitting and carrying no fermion number must carry light-like momentum so that they cannot just disappear. The ends of the wormhole throats of the boson must be glued together with the end of the fermionic wormhole throat and its companion generated in the splitting of the wormhole. This means that fermionic wormhole first splits and the resulting throats meet at the partonic 2-surface.

This requires that topologically condensed fermions correspond to (g, g) pairs rather than $(g, 0)$ pairs. The reaction mechanism allows the interpretation of (g, g) pairs as a triplet of dynamical $SU(3)$. The fundamental vertices would be just the splitting of wormhole contact and 3-vertices for throats since $SU(3)$ symmetry would exclude more complex reaction vertices such as n -boson vertices corresponding to the gluing of n wormhole contact lines along their 3-dimensional ends. The couplings of singlet representation for bosons would have the same coupling to all fermion families so that the basic experimental constraint would be satisfied.

3. Both fermions and bosons cannot correspond to octet and singlet of $SU(3)$. In this case reaction vertices should correspond algebraically to the multiplication of matrix elements e_{ij} : $e_{ij}e_{kl} = \delta_{jk}e_{il}$ allowing for instance $F(g_1, g_2) + \bar{F}(g_2, g_3) \rightarrow B(g_1, g_3)$. Neither the fusion of entire wormhole contacts along their ends nor the splitting of wormhole throats before the fusion of partonic 2-surfaces allows this kind of vertices so that BFF vertex is the only possible one. Also the construction of QFT limit starting from bosonic emergence led to the formulation of perturbation theory in terms of Dirac action allowing only BFF vertex as fundamental vertex [23].
4. Weak electric-magnetic duality brings in an additional complication. $SU(3)$ symmetry poses also now strong constraints and it would seem that the reactions must involve copies of basic BFF vertices for the pairs of ends of weak strings. The string ends with the same Kähler magnetic charge should meet at the vertex and give rise to BFF vertices. For instance, $F\bar{F}B$ annihilation vertex would in this manner give rise to the analog of stringy diagram in which strings join along ends since two string ends disappear in the process.
5. This picture means that all elementary particles - not only gravitons- are described by "weak" strings involving four wormhole throats. Fundamental objects would be partonic 2-surfaces, which in principle can carry arbitrary high fermion numbers N but only $N = 1, 2$ correspond to particles with fermionic and bosonic propagators and the remaining ones correspond to propagators behaving like p^{-n} , $n > 2$, and having interpretation in terms of broken SUSY with a large value of \mathcal{N} identified as the number of fermionic modes. This compositeness of elementary particles should become manifest below weak length scale. Note that this stringy character should not be confused with that for the wormhole contacts for which conformal invariance implies that throats effectively play the role of string ends. One can say that fundamental objects are massless wormhole throats and that all elementary particles as well as string like objects emerge from them.

3.2.2 Graviton and other stringy states

Fermion and anti-fermion can give rise to only single unit of spin since it is impossible to assign angular momentum with the relative motion of wormhole throats. Hence the identification of graviton as single wormhole contact is not possible. The only conclusion is that graviton must be a superposition of fermion-anti-fermion pairs and boson-anti-boson pairs with coefficients determined by the coupling of the parton to graviton. Graviton-graviton pairs might emerge in higher orders. Fermion and anti-fermion would reside at the same space-time sheet and would have a non-vanishing relative angular momentum. Also bosons could have non-vanishing relative angular momentum and Higgs bosons must indeed possess it.

Gravitons are stable if the throats of wormhole contacts carry non-vanishing gauge fluxes so that the throats of wormhole contacts are connected by flux tubes carrying the gauge flux. The mechanism producing gravitons would be the splitting of partonic 2-surfaces via the basic vertex. A connection with string picture emerges with the counterpart of string identified as the flux tube connecting the wormhole throats. Gravitational constant would relate directly to the value of the string tension.

The development of the understanding of gravitational coupling has had many twists and it is perhaps to summarize the basic misunderstandings.

1. CP_2 length scale R , which is roughly $10^{3.5}$ times larger than Planck length $l_P = \sqrt{\hbar G}$, defines a fundamental length scale in TGD. The challenge is to predict the value of Planck length $\sqrt{\hbar G}$. The outcome was an identification of a formula for $R^2/\hbar G$ predicting that the magnitude of Kähler coupling strength α_K is near to fine structure constant in electron length scale (for ordinary value of Planck constant should be added here).
2. The emergence of the parton level formulation of TGD finally demonstrated that G actually appears in the fundamental parton level formulation of TGD as a fundamental constant characterizing the M^4 part of CP_2 Kähler gauge potential [33, 24]. This part is pure gauge in the sense of standard gauge theory but necessary to guarantee that the theory does not reduce to topological QFT. Quantum criticality requires that G remains invariant under p-adic coupling constant evolution and is therefore predictable in principle at least.
3. The TGD view about coupling constant evolution [26] predicts the proportionality $G \propto L_p^2$, where L_p is p-adic length scale. Together with input from p-adic mass calculations one ends up to two conclusions. The correct conclusion was that Kähler coupling strength is equal to the fine structure constant in the p-adic length scale associated with Mersenne prime $p = M_{127} = 2^{127} - 1$ assignable to electron [26]. I have considered also the possibility that α_K would be equal to electro-weak $U(1)$ coupling in this scale.
4. The additional - wrong- conclusion was that gravitons must always correspond to the p-adic prime M_{127} since G would otherwise vary as function of p-adic length scale. As a matter fact, the question was for years whether it is G or g_K^2 which remains invariant under p-adic coupling constant evolution. I found both options unsatisfactory until I realized that RG invariance is possible for both g_K^2 and G ! The point is that the exponent of the Kähler action associated with the piece of CP_2 type vacuum extremal assignable with the elementary particle is exponentially sensitive to the volume of this piece and logarithmic dependence on the volume fraction is enough to compensate the $L_p^2 \propto p$ proportionality of G and thus guarantee the constancy of G .

The explanation for the small value of the gravitational coupling strength serves as a test for the proposed picture. The exchange of ordinary gauge boson involves the exchange of single CP_2 type extremal giving the exponent of Kähler action compensated by state normalization. In the case of graviton exchange two wormhole contacts are exchanged and this gives second power for the exponent of Kähler action which is not compensated. It would be this additional exponent that would give rise to the huge reduction of gravitational coupling strength from the naive estimate $G \sim L_p^2$.

3.2.3 Spectrum of non-stringy states

The 1-throat character of fermions is consistent with the generation-genus correspondence. The 2-throat character of bosons predicts that bosons are characterized by the genera (g_1, g_2) of the wormhole throats. Note that the interpretation of fundamental fermions as wormhole contacts with second throat identified as a Fock vacuum is excluded.

The general bosonic wave-function would be expressible as a matrix M_{g_1, g_2} and ordinary gauge bosons would correspond to a diagonal matrix $M_{g_1, g_2} = \delta_{g_1, g_2}$ as required by the absence of neutral flavor changing currents (say gluons transforming quark genera to each other). 8 new gauge bosons are predicted if one allows all 3×3 matrices with complex entries orthonormalized with respect to trace meaning additional dynamical $SU(3)$ symmetry. Ordinary gauge bosons would be $SU(3)$ singlets in this sense. The existing bounds on flavor changing neutral currents give bounds on the masses of the boson octet. The 2-throat character of bosons should relate to the low value $T = 1/n \ll 1$ for the p-adic temperature of gauge bosons as contrasted to $T = 1$ for fermions.

If one forgets the complications due to the stringy states (including graviton), the spectrum of elementary fermions and bosons is amazingly simple and almost reduces to the spectrum of standard model. In the fermionic sector one would have fermions of standard model. By simple counting leptonic wormhole throat could carry $2^3 = 8$ states corresponding to 2 polarization states, 2 charge states, and sign of lepton number giving $8+8=16$ states altogether. Taking into account phase conjugates gives $16+16=32$ states.

In the non-stringy boson sector one would have bound states of fermions and phase conjugate fermions. Since only two polarization states are allowed for massless states, one obtains $(2 + 1) \times$

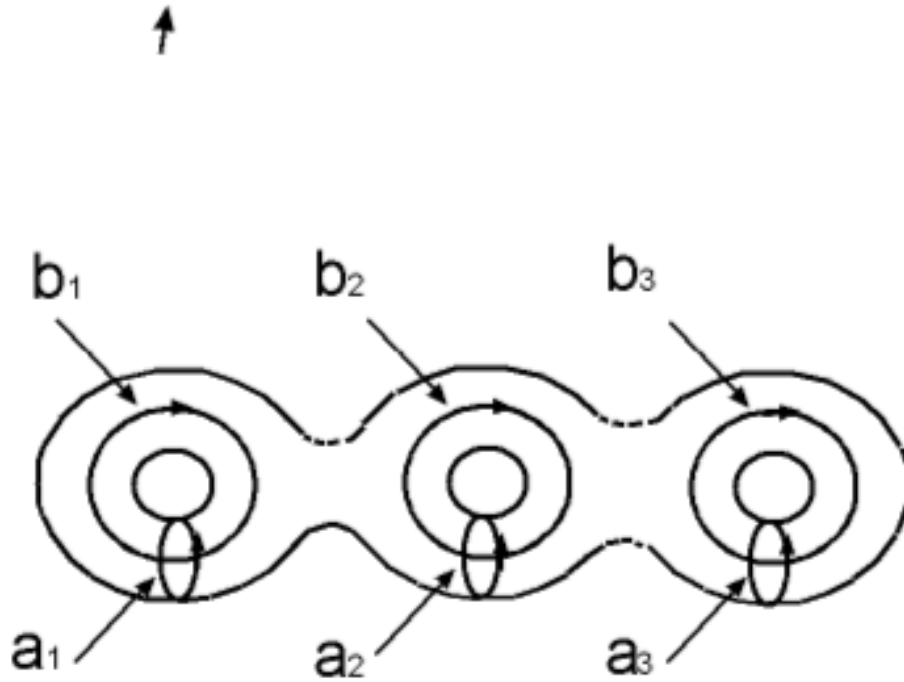


Figure 3.1: Definition of the canonical homology basis

$(3 + 1) = 12$ states plus phase conjugates giving $12+12=24$ states. The addition of color singlet states for quarks gives 48 gauge bosons with vanishing fermion number and color quantum numbers. Besides 12 electro-weak bosons and their 12 phase conjugates there are 12 exotic bosons and their 12 phase conjugates. For the exotic bosons the couplings to quarks and leptons are determined by the orthogonality of the coupling matrices of ordinary and boson states. For exotic counterparts of W bosons and Higgs the sign of the coupling to quarks is opposite. For photon and Z^0 also the relative magnitudes of the couplings to quarks must change. Altogether this makes $48+16+16=80$ states. Gluons would result as color octet states. Family replication would extend each elementary boson state into $SU(3)$ octet and singlet and elementary fermion states into $SU(3)$ triplets.

3.3 Basic facts about Riemann surfaces

In the following some basic aspects about Riemann surfaces will be summarized. The basic topological concepts, in particular the concept of the mapping class group, are introduced, and the Teichmüller parameters are defined as conformal invariants of the Riemann surface, which in fact specify the conformal equivalence class of the Riemann surface completely.

3.3.1 Mapping class group

The first homology group $H_1(X^2)$ of a Riemann surface of genus g contains $2g$ generators [31, 36, 37]: this is easy to understand geometrically since each handle contributes two homology generators. The so called canonical homology basis can be identified as in Fig. 3.3.1.

One can define the so called intersection number $J(a, b)$ for two elements a and b of the homology group as the number of intersection points for the curves a and b counting the orientation. Since $J(a, b)$ depends on the homology classes of a and b only, it defines an antisymmetric quadratic form in $H_1(X^2)$. In the canonical homology basis the non-vanishing elements of the intersection matrix are:

$$J(a_i, b_j) = -J(b_j, a_i) = \delta_{i,j} . \quad (3.3.1)$$

J clearly defines symplectic structure in the homology group.

The dual to the canonical homology basis consists of the harmonic one-forms $\alpha_i, \beta_i, i = 1, \dots, g$ on X^2 . These 1-forms satisfy the defining conditions

$$\begin{aligned} \int_{a_i} \alpha_j &= \delta_{i,j} & \int_{b_i} \alpha_j &= 0 \\ \int_{a_i} \beta_j &= 0 & \int_{b_i} \beta_j &= \delta_{i,j} \end{aligned} \quad (3.3.2)$$

The following identity helps to understand the basic properties of the Teichmueller parameters

$$\int_{X^2} \theta \wedge \eta = \sum_{i=1, \dots, g} \left[\int_{a_i} \theta \int_{b_i} \eta - \int_{b_i} \theta \int_{a_i} \eta \right] . \quad (3.3.3)$$

The existence of topologically nontrivial diffeomorphisms, when X^2 has genus $g > 0$, plays an important role in the sequel. Denoting by $Diff$ the group of the diffeomorphisms of X^2 and by $Diff_0$ the normal subgroup of the diffeomorphisms homotopic to identity, one can define the mapping class group M as the coset group

$$M = Diff/Diff_0 . \quad (3.3.4)$$

The generators of M are so called Dehn twists along closed curves a of X^2 . Dehn twist is defined by excising a small tubular neighborhood of a , twisting one boundary of the resulting tube by 2π and gluing the tube back into the surface: see Fig. 9.6.2.

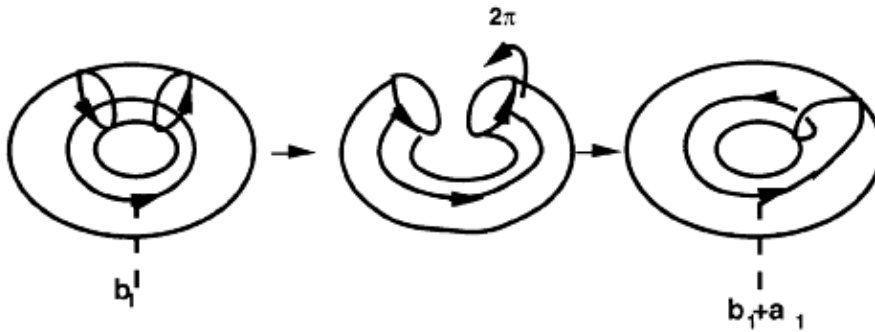


Figure 3.2: Definition of the Dehn twist

It can be shown that a minimal set of generators is defined by the following curves

$$a_1, b_1, a_1^{-1}a_2^{-1}, a_2, b_2, a_2^{-1}a_3^{-1}, \dots, a_g, b_g . \quad (3.3.5)$$

The action of these transformations in the homology group can be regarded as a symplectic linear transformation preserving the symplectic form defined by the intersection matrix. Therefore the matrix representing the action of $Diff$ on $H_1(X^2)$ is $2g \times 2g$ matrix M with integer entries leaving J invariant: $MJM^T = J$. Mapping class group is often referred also as a symplectic modular group and denoted by $Sp(2g, Z)$. The matrix representing the action of M in the canonical homology basis decomposes into four $g \times g$ blocks A, B, C and D

$$M = \begin{pmatrix} A & B \\ C & D \end{pmatrix} , \quad (3.3.6)$$

where A and D operate in the subspaces spanned by the homology generators a_i and b_i respectively and C and D map these spaces to each other. The notation $D = [A, B; C, D]$ will be used in the sequel: in this notation the representation of the symplectic form J is $J = [0, 1; -1, 0]$.

3.3.2 Teichmueller parameters

The induced metric on the two-surface X^2 defines a unique complex structure. Locally the metric can always be written in the form

$$ds^2 = e^{2\phi} dz d\bar{z} . \quad (3.3.7)$$

where z is local complex coordinate. When one covers X^2 by coordinate patches, where the line element has the above described form, the transition functions between coordinate patches are holomorphic and therefore define a complex structure.

The conformal transformations ξ of X^2 are defined as the transformations leaving invariant the angles between the vectors of X^2 tangent space invariant: the angle between the vectors X and Y at point x is same as the angle between the images of the vectors under Jacobian map at the image point $\xi(x)$. These transformations need not be globally defined and in each coordinate patch they correspond to holomorphic (anti-holomorphic) mappings as is clear from the diagonal form of the metric in the local complex coordinates. A distinction should be made between local conformal transformations and globally defined conformal transformations, which will be referred to as conformal symmetries: for instance, for hyper-elliptic surfaces the group of the conformal symmetries contains two-element group Z_2 .

Using the complex structure one can decompose one-forms to linear combinations of one-forms of type $(1,0)$ ($f(z, \bar{z})dz$) and $(0,1)$ ($f(z, \bar{z})d\bar{z}$). $(1,0)$ form ω is holomorphic if the function f is holomorphic: $\omega = f(z)dz$ on each coordinate patch.

There are g independent holomorphic one forms ω_i known also as Abelian differentials of the first kind [31, 36, 37] and one can fix their normalization by the condition

$$\int_{a_i} \omega_j = \delta_{ij} . \quad (3.3.8)$$

This condition completely specifies ω_i .

Teichmueller parameters Ω_{ij} are defined as the values of the forms ω_i for the homology generators b_j

$$\Omega_{ij} = \int_{b_j} \omega_i . \quad (3.3.9)$$

The basic properties of Teichmueller parameters are the following:

- i) The $g \times g$ matrix Ω is symmetric: this is seen by applying the formula (3.3.3) for $\theta = \omega_i$ and $\eta = \omega_j$.
- ii) The imaginary part of Ω is positive: $Im(\Omega) > 0$. This is seen by the application of the same formula for $\theta = \eta$. The space of the matrices satisfying these conditions is known as Siegel upper half plane.
- iii) The space of Teichmueller parameters can be regarded as a coset space $Sp(2g, R)/U(g)$ [36]: the action of $Sp(2g, R)$ is of the same form as the action of $Sp(2g, Z)$ and $U(g) \subset Sp(2g, R)$ is the isotropy group of a given point of Teichmueller space.
- iv) Teichmueller parameters are conformal invariants as is clear from the holomorphy of the defining one-forms.
- v) Teichmueller parameters specify completely the conformal structure of Riemann surface [37].

Although Teichmueller parameters fix the conformal structure of the 2-surface completely, they are not in one-to-one correspondence with the conformal equivalence classes of the two-surfaces:

- i) The dimension for the space of the conformal equivalence classes is $D = 3g - 3$, when $g > 1$ and smaller than the dimension of Teichmueller space given by $d = (g \times g + g)/2$ for $g > 3$: all Teichmueller matrices do not correspond to a Riemann surface. In TGD approach this does not produce any problems as will be found later.
- ii) The action of the topologically nontrivial diffeomorphisms on Teichmueller parameters is nontrivial and can be deduced from the action of the diffeomorphisms on the homology ($Sp(2g, Z)$ transformation) and from the defining condition $\int_{a_i} \omega_j = \delta_{i,j}$: diffeomorphisms correspond to elements $[A, B; C, D]$ of $Sp(2g, Z)$ and act as generalized Möbius transformations

$$\Omega \rightarrow (A\Omega + B)(C\Omega + D)^{-1} . \quad (3.3.10)$$

All Teichmueller parameters related by $Sp(2g, Z)$ transformations correspond to the same Riemann surface.

iii) The definition of the Teichmueller parameters is not unique since the definition of the canonical homology basis involves an arbitrary numbering of the homology basis. The permutation S of the handles is represented by same $g \times g$ orthogonal matrix both in the basis $\{a_i\}$ and $\{b_i\}$ and induces a similarity transformation in the space of the Teichmueller parameters

$$\Omega \rightarrow S\Omega S^{-1} . \quad (3.3.11)$$

Clearly, the Teichmueller matrices related by a similarity transformations correspond to the same conformal equivalence class. It is easy to show that handle permutations in fact correspond to $Sp(2g, Z)$ transformations.

3.3.3 Hyper-ellipticity

The motivation for considering hyper-elliptic surfaces comes from the fact, that $g > 2$ elementary particle vacuum functionals turn out to be vanishing for hyper-elliptic surfaces and this in turn will be later used to provide a possible explanation the non-observability of $g > 2$ particles.

Hyper-elliptic surface X can be defined abstractly as two-fold branched cover of the sphere having the group Z_2 as the group of conformal symmetries (see [36, 39, 37]). Thus there exists a map $\pi : X \rightarrow S^2$ so that the inverse image $\pi^{-1}(z)$ for a given point z of S^2 contains two points except at a finite number (say p) of points z_i (branch points) for which the inverse image contains only one point. Z_2 acts as conformal symmetries permuting the two points in $\pi^{-1}(z)$ and branch points are fixed points of the involution.

The concept can be generalized [39]: g -hyper-elliptic surface can be defined as a 2-fold covering of genus g surface with a finite number of branch points. One can consider also p -fold coverings instead of 2-fold coverings: a common feature of these Riemann surfaces is the existence of a discrete group of conformal symmetries.

A concrete representation for the hyper-elliptic surfaces [36] is obtained by studying the surface of C^2 determined by the algebraic equation

$$w^2 - P_n(z) = 0 , \quad (3.3.12)$$

where w and z are complex variables and $P_n(z)$ is a complex polynomial. One can solve w from the above equation

$$w_{\pm} = \pm \sqrt{P_n(z)} , \quad (3.3.13)$$

where the square root is determined so that it has a cut along the positive real axis. What happens that w has in general two roots (two-fold covering property), which coincide at the roots z_i of $P_n(z)$ and if n is odd, also at $z = \infty$: these points correspond to branch points of the hyper-elliptic surface and their number r is always even: $r = 2k$. w is discontinuous at the cuts associated with the square root in general joining two roots of $P_n(z)$ or if n is odd, also some root of P_n and the point $z = \infty$. The representation of the hyper-elliptic surface is obtained by identifying the two branches of w along the cuts. From the construction it is clear that the surface obtained in this manner has genus $k - 1$. Also it is clear that Z_2 permutes the different roots w_{\pm} with each other and that $r = 2k$ branch points correspond to fixed points of the involution.

The following facts about the hyper-elliptic surfaces [36, 37] turn out to be important in the sequel:

- i) All $g < 3$ surfaces are hyper-elliptic.
- ii) $g \geq 3$ hyper-elliptic surfaces are not in general hyper-elliptic and form a set of codimension 2 in the space of the conformal equivalence classes [36].

3.3.4 Theta functions

An extensive and detailed account of the theta functions and their applications can be found in the book of Mumford [36]. Theta functions appear also in the loop calculations of string model [31]. In the following the so called Riemann theta function and theta functions with half integer characteristics will be defined as sections (not strictly speaking functions) of the so called Jacobian variety.

For a given Teichmueller matrix Ω , Jacobian variety is defined as the $2g$ -dimensional torus obtained by identifying the points z of C^g (vectors with g complex components) under the equivalence

$$z \sim z + \Omega m + n \ , \tag{3.3.14}$$

where m and n are points of Z^g (vectors with g integer valued components) and Ω acts in Z^g by matrix multiplication.

The definition of Riemann theta function reads as

$$\Theta(z|\Omega) = \sum_n \exp(i\pi n \cdot \Omega \cdot n + i2\pi n \cdot z) \ . \tag{3.3.15}$$

Here \cdot denotes standard inner product in C^g . Theta functions with half integer characteristics are defined in the following manner. Let a and b denote vectors of C^g with half integer components (component either vanishes or equals to $1/2$). Theta function with characteristics $[a, b]$ is defined through the following formula

$$\Theta[a, b](z|\Omega) = \sum_n \exp [i\pi(n + a) \cdot \Omega \cdot (n + a) + i2\pi(n + a) \cdot (z + b)] \ . \tag{3.3.16}$$

A brief calculation shows that the following identity is satisfied

$$\Theta[a, b](z|\Omega) = \exp(i\pi a \cdot \Omega \cdot a + i2\pi a \cdot b) \times \Theta(z + \Omega a + b|\Omega) \tag{3.3.17}$$

Theta functions are not strictly speaking functions in the Jacobian variety but rather sections in an appropriate bundle as can be seen from the identities

$$\begin{aligned} \Theta[a, b](z + m|\Omega) &= \exp(i2\pi a \cdot m)\Theta[a, b](z|\Omega) \ , \\ \Theta[a, b](z + \Omega m|\Omega) &= \exp(\alpha)\Theta[a, b](z|\Omega) \ , \\ \exp(\alpha) &= \exp(-i2\pi b \cdot m)\exp(-i\pi m \cdot \Omega \cdot m - 2\pi m \cdot z) \ . \end{aligned} \tag{3.3.18}$$

The number of theta functions is 2^{2g} and same as the number of nonequivalent spinor structures defined on two-surfaces. This is not an accident [31]: theta functions with given characteristics turn out to be in a close relation to the functional determinants associated with the Dirac operators defined on the two-surface. It is useful to divide the theta functions to even and odd theta functions according to whether the inner product $4a \cdot b$ is even or odd integer. The numbers of even and odd theta functions are $2^{g-1}(2^g + 1)$ and $2^{g-1}(2^g - 1)$ respectively.

The values of the theta functions at the origin of the Jacobian variety understood as functions of Teichmueller parameters turn out to be of special interest in the following and the following notation will be used:

$$\Theta[a, b](\Omega) \equiv \Theta[a, b](0|\Omega) \ , \tag{3.3.19}$$

$\Theta[a, b](\Omega)$ will be referred to as theta functions in the sequel. From the defining properties of odd theta functions it can be found that they are odd functions of z and therefore vanish at the origin of the Jacobian variety so that only even theta functions will be of interest in the sequel.

An important result is that also some *even* theta functions vanish for $g > 2$ hyper-elliptic surfaces : in fact one can characterize $g > 2$ hyper-elliptic surfaces by the vanishing properties of the theta functions [36, 37]. The vanishing property derives from conformal symmetry (Z_2 in the case of hyper-elliptic surfaces) and the vanishing phenomenon is rather general [39]: theta functions tend to vanish for Riemann surfaces possessing discrete conformal symmetries. It is not clear (to the author) whether the presence of a conformal symmetry is in fact equivalent with the vanishing of some theta functions. As already noticed, spinor structures and the theta functions with half integer characteristics are in one-to-one correspondence and the vanishing of theta function with given half integer characteristics is equivalent with the vanishing of the Dirac determinant associated with the corresponding spinor structure or equivalently: with the existence of a zero mode for the Dirac operator [31]. For odd characteristics zero mode exists always: for even characteristics zero modes exist, when the surface is hyper-elliptic or possesses more general conformal symmetries.

3.4 Elementary particle vacuum functionals

The basic assumption is that elementary particle families correspond to various elementary particle vacuum functionals associated with the 2-dimensional boundary components of the 3-surface. These functionals need not be localized to a single boundary topology. Neither need their dependence on the boundary component be local. An important role in the following considerations is played by the fact that the minimization requirement of the Kähler action associates a unique 3-surface to each boundary component, the "Bohr orbit" of the boundary and this surface provides a considerable (and necessarily needed) flexibility in the definition of the elementary particle vacuum functionals. There are several natural constraints to be satisfied by elementary particle vacuum functionals.

3.4.1 Extended Diff invariance and Lorentz invariance

Extended Diff invariance is completely analogous to the extension of 3-dimensional Diff invariance to four-dimensional Diff invariance in the interior of the 3-surface. Vacuum functional must be invariant not only under diffeomorphisms of the boundary component but also under the diffeomorphisms of the 3- dimensional "orbit" Y^3 of the boundary component. In other words: the value of the vacuum functional must be same for any time slice on the orbit the boundary component. This is guaranteed if vacuum functional is functional of some two-surface Y^2 belonging to the orbit and defined in $Diff^3$ invariant manner.

An additional natural requirement is Poincare invariance. In the original formulation of the theory only Lorentz transformations of the light cone were exact symmetries of the theory. In this framework the definition of Y^2 as the intersection of the orbit with the hyperboloid $\sqrt{m_k m^k m^l} = a$ is $Diff^3$ and Lorentz invariant.

1. Interaction vertices as generalization of stringy vertices

For stringy diagrams Poincare invariance of conformal equivalence class and general coordinate invariance are far from being a trivial issues. Vertices are now not completely unique since there is an infinite number of singular 3-manifolds which can be identified as vertices even if one assumes space-likeness. One should be able to select a unique singular 3-manifold to fix the conformal equivalence class.

One might hope that Lorentz invariant invariant and general coordinate invariant definition of Y^2 results by introducing light cone proper time a as a height function specifying uniquely the point at which 3-surface is singular (stringy diagrams help to visualize what is involved), and by restricting the singular 3-surface to be the intersection of $a = \text{constant}$ hyperboloid of M^4 containing the singular point with the space-time surface. There would be non-uniqueness of the conformal equivalence class due to the choice of the origin of the light cone but the decomposition of the configuration space of 3-surfaces to a union of configuration spaces characterized by unions of future and past light cones could resolve this difficulty.

2. Interaction vertices as generalization of ordinary ones

If the interaction vertices are identified as intersections for the ends of space-time sheets representing particles, the conformal equivalence class is naturally identified as the one associated with the intersection of the boundary component or light like causal determinant with the vertex. Poincare invariance of the conformal equivalence class and generalized general coordinate invariance follow trivially in this case.

3.4.2 Conformal invariance

Conformal invariance implies that vacuum functionals depend on the conformal equivalence class of the surface Y^2 only. What makes this idea so attractive is that for a given genus g configuration space becomes effectively finite-dimensional. A second nice feature is that instead of trying to find coordinates for the space of the conformal equivalence classes one can construct vacuum functionals as functions of the Teichmueller parameters.

That one can construct this kind of functions as suitable functions of the Teichmueller parameters is not trivial. The essential point is that the boundary components can be regarded as submanifolds of $M_+^4 \times CP_2$: as a consequence vacuum functional can be regarded as a composite function:

$$2\text{-surface} \rightarrow \text{Teichmueller matrix } \Omega \text{ determined by the induced metric} \rightarrow \Omega_{vac}(\Omega)$$

Therefore the fact that there are Teichmueller parameters which do not correspond to any Riemann surface, doesn't produce any trouble. It should be noticed that the situation differs from that in the Polyakov formulation of string models, where one doesn't assume that the metric of the two-surface is induced metric (although classical equations of motion imply this).

3.4.3 Diff invariance

Since several values of the Teichmueller parameters correspond to the same conformal equivalence class, one must pose additional conditions on the functions of the Teichmueller parameters in order to obtain single valued functions of the conformal equivalence class.

The first requirement of this kind is the invariance under topologically nontrivial Diff transformations inducing $Sp(2g, Z)$ transformation $(A, B; C, D)$ in the homology basis. The action of these transformations on Teichmueller parameters is deduced by requiring that holomorphic one-forms satisfy the defining conditions in the transformed homology basis. It turns out that the action of the topologically nontrivial diffeomorphism on Teichmueller parameters can be regarded as a generalized Möbius transformation:

$$\Omega \rightarrow (A\Omega + B)(C\Omega + D)^{-1} . \quad (3.4.1)$$

Vacuum functional must be invariant under these transformations. It should be noticed that the situation differs from that encountered in the string models. In TGD the integration measure over the configuration space is Diff invariant: in string models the integration measure is the integration measure of the Teichmueller space and this is not invariant under $Sp(2g, Z)$ but transforms like a density: as a consequence the counterpart of the vacuum functional must be also modular covariant since it is the product of vacuum functional and integration measure, which must be modular invariant.

It is possible to show that the quantities

$$(\Theta[a, b]/\Theta[c, d])^4 . \quad (3.4.2)$$

and their complex conjugates are $Sp(2g, Z)$ invariants [36] and therefore can be regarded as basic building blocks of the vacuum functionals.

Teichmueller parameters are not uniquely determined since one can always perform a permutation of the g handles of the Riemann surface inducing a redefinition of the canonical homology basis (permutation of g generators). These transformations act as similarities of the Teichmueller matrix:

$$\Omega \rightarrow S\Omega S^{-1} , \quad (3.4.3)$$

where S is the $g \times g$ matrix representing the permutation of the homology generators understood as orthonormal vectors in the g -dimensional vector space. Therefore the Teichmueller parameters related by these similarity transformations correspond to the same conformal equivalence class of the Riemann surfaces and vacuum functionals must be invariant under these similarities.

It is easy to find out that these similarities permute the components of the theta characteristics: $[a, b] \rightarrow [S(a), S(b)]$. Therefore the invariance requirement states that the handles of the Riemann surface behave like bosons: the vacuum functional constructed from the theta functions is invariant under the permutations of the theta characteristics. In fact, this requirement brings in nothing new. Handle permutations can be regarded as $Sp(2g, Z)$ transformations so that the modular invariance alone guarantees invariance under handle permutations.

3.4.4 Cluster decomposition property

Consider next the behavior of the vacuum functional in the limit, when boundary component with genus g splits to two separate boundary components of genera g_1 and g_2 respectively. The splitting into two separate boundary components corresponds to the reduction of the Teichmueller matrix Ω^g to a direct sum of $g_1 \times g_1$ and $g_2 \times g_2$ matrices ($g_1 + g_2 = g$):

$$\Omega^g = \Omega^{g_1} \oplus \Omega^{g_2} \quad , \quad (3.4.4)$$

when a suitable definition of the Teichmueller parameters is adopted. The splitting can also take place without a reduction to a direct sum: the Teichmueller parameters obtained via $Sp(2g, Z)$ transformation from $\Omega^g = \Omega^{g_1} \oplus \Omega^{g_2}$ do not possess direct sum property in general.

The physical interpretation is obvious: the non-diagonal elements of the Teichmueller matrix describe the geometric interaction between handles and at this limit the interaction between the handles belonging to the separate surfaces vanishes. On the physical grounds it is natural to require that vacuum functionals satisfy cluster decomposition property at this limit: that is they reduce to the product of appropriate vacuum functionals associated with the composite surfaces.

Theta functions satisfy cluster decomposition property [36, 31]. Theta characteristics reduce to the direct sums of the theta characteristics associated with g_1 and g_2 ($a = a_1 \oplus a_2$, $b = b_1 \oplus b_2$) and the dependence on the Teichmueller parameters is essentially exponential so that the cluster decomposition property indeed results:

$$\Theta[a, b](\Omega^g) = \Theta[a_1, b_1](\Omega^{g_1})\Theta[a_2, b_2](\Omega^{g_2}) \quad . \quad (3.4.5)$$

Cluster decomposition property holds also true for the products of theta functions. This property is also satisfied by suitable homogenous polynomials of thetas. In particular, the following quantity playing central role in the construction of the vacuum functional obeys this property

$$Q_0 = \sum_{[a, b]} \Theta[a, b]^4 \bar{\Theta}[a, b]^4 \quad , \quad (3.4.6)$$

where the summation is over all even theta characteristics (recall that odd theta functions vanish at the origin of C^g).

Together with the $Sp(2g, Z)$ invariance the requirement of cluster decomposition property implies that the vacuum functional must be representable in the form

$$\Omega_{vac} = P_{M, N}(\Theta^4, \bar{\Theta}^4) / Q_{MN}(\Theta^4, \bar{\Theta}^4) \quad (3.4.7)$$

where the homogenous polynomials $P_{M, N}$ and $Q_{M, N}$ have same degrees (M and N as polynomials of $\Theta[a, b]^4$ and $\bar{\Theta}[a, b]^4$).

3.4.5 Finiteness requirement

Vacuum functional should be finite. Finiteness requirement is satisfied provided the numerator $Q_{M,N}$ of the vacuum functional is real and positive definite. The simplest quantity of this type is the quantity Q_0 defined previously and its various powers. $Sp(2g, Z)$ invariance and finiteness requirement are satisfied provided vacuum functionals are of the following general form

$$\Omega_{vac} = \frac{P_{N,N}(\Theta^4, \bar{\Theta}^4)}{Q_0^N}, \quad (3.4.8)$$

where $P_{N,N}$ is homogenous polynomial of degree N with respect to $\Theta[a, b]^4$ and $\bar{\Theta}[a, b]^4$. In addition $P_{N,N}$ is invariant under the permutations of the theta characteristics and satisfies cluster decomposition property.

3.4.6 Stability against the decay $g \rightarrow g_1 + g_2$

Elementary particle vacuum functionals must be stable against the genus conserving decays $g \rightarrow g_1 + g_2$. This decay corresponds to the limit at which Teichmueller matrix reduces to a direct sum of the matrices associated with g_1 and g_2 (note however the presence of $Sp(2g, Z)$ degeneracy). In accordance with the topological description of the particle reactions one expects that this decay doesn't occur if the vacuum functional in question vanishes at this limit.

In general the theta functions are non-vanishing at this limit and vanish provided the theta characteristics reduce to a direct sum of the odd theta characteristics. For $g < 2$ surfaces this condition is trivial and gives no constraints on the form of the vacuum functional. For $g = 2$ surfaces the theta function $\Theta(a, b)$, with $a = b = (1/2, 1/2)$ satisfies the stability criterion identically (odd theta functions vanish identically), when Teichmueller parameters separate into a direct sum. One can however perform $Sp(2g, Z)$ transformations giving new points of Teichmueller space describing the decay. Since these transformations transform theta characteristics in a nontrivial manner to each other and since all even theta characteristics belong to same $Sp(2g, Z)$ orbit [36, 31], the conclusion is that stability condition is satisfied provided $g = 2$ vacuum functional is proportional to the product of fourth powers of all even theta functions multiplied by its complex conjugate.

If $g > 2$ there always exists some theta functions, which vanish at this limit and the minimal vacuum functional satisfying this stability condition is of the same form as in $g = 2$ case, that is proportional to the product of the fourth powers of all even Theta functions multiplied by its complex conjugate:

$$\Omega_{vac} = \prod_{[a,b]} \Theta[a, b]^4 \bar{\Theta}[a, b]^4 / Q_0^N, \quad (3.4.9)$$

where N is the number of even theta functions. The results obtained imply that genus-generation correspondence is one to one for $g > 1$ for the minimal vacuum functionals. Of course, the multiplication of the minimal vacuum functionals with functionals satisfying all criteria except stability criterion gives new elementary particle vacuum functionals: a possible physical identification of these vacuum functionals is most naturally as some kind of excited states.

One of the questions posed in the beginning was related to the experimental absence of $g > 0$, possibly massless, elementary bosons. The proposed stability criterion suggests a nice explanation. The point is that elementary particles are stable against decays $g \rightarrow g_1 + g_2$ but not with respect to the decay $g \rightarrow g + sphere$. As a consequence the direct emission of $g > 0$ gauge bosons is impossible unlike the emission of $g = 0$ bosons: for instance the decay muon \rightarrow electron $+(g = 1)$ photon is forbidden.

3.4.7 Stability against the decay $g \rightarrow g - 1$

This stability criterion states that the vacuum functional is stable against single particle decay $g \rightarrow g - 1$ and, if satisfied, implies that vacuum functional vanishes, when the genus of the surface is smaller than g . In stringy framework this criterion is equivalent to a separate conservation of various lepton numbers: for instance, the spontaneous transformation of muon to electron is forbidden. Notice that

this condition doesn't imply that the vacuum functional is localized to a single genus: rather the vacuum functional of genus g vanishes for all surfaces with genus smaller than g . This hierarchical structure should have a close relationship to Cabibbo-Kobayashi-Maskawa mixing of the quarks.

The stability criterion implies that the vacuum functional must vanish at the limit, when one of the handles of the Riemann surface suffers a pinch. To deduce the behavior of the theta functions at this limit, one must find the behavior of Teichmueller parameters, when i :th handle suffers a pinch. Pinch implies that a suitable representative of the homology generator a_i or b_i contracts to a point.

Consider first the case, when a_i contracts to a point. The normalization of the holomorphic one-form ω_i must be preserved so that ω_i must behave as $1/z$, where z is the complex coordinate vanishing at pinch. Since the homology generator b_i goes through the pinch it seems obvious that the imaginary part of the Teichmueller parameter $\Omega_{ii} = \int_{b_i} \omega_i$ diverges at this limit (this conclusion is made also in [36]): $Im(\Omega_{ii}) \rightarrow \infty$.

Of course, this criterion doesn't cover all possible manners the pinch can occur: pinch might take place also, when the components of the Teichmueller matrix remain finite. In the case of torus topology one finds that $Sp(2g, Z)$ element $(A, B; C, D)$ takes $Im(\Omega) = \infty$ to the point C/D of real axis. This suggests that pinch occurs always at the boundary of the Teichmueller space: the imaginary part of Ω_{ij} either vanishes or some matrix element of $Im(\Omega)$ diverges.

Consider next the situation, when b_i contracts to a point. From the definition of the Teichmueller parameters it is clear that the matrix elements Ω_{kl} , with $k, l \neq i$ suffer no change. The matrix element Ω_{ki} obviously vanishes at this limit. The conclusion is that i :th row of Teichmueller matrix vanishes at this limit. This result is obtained also by deriving the $Sp(2g, Z)$ transformation permuting a_i and b_i with each other: in case of torus this transformation reads $\Omega \rightarrow -1/\Omega$.

Consider now the behavior of the theta functions, when pinch occurs. Consider first the limit, when $Im(\Omega_{ii})$ diverges. Using the general definition of $\Theta[a, b]$ it is easy to find out that all theta functions for which the i :th component a_i of the theta characteristic is non-vanishing (that is $a_i = 1/2$) are proportional to the exponent $exp(-\pi\Omega_{ii}/4)$ and therefore vanish at the limit. The theta functions with $a_i = 0$ reduce to $g-1$ dimensional theta functions with theta characteristic obtained by dropping i :th components of a_i and b_i and replacing Teichmueller matrix with Teichmueller matrix obtained by dropping i :th row and column. The conclusion is that all theta functions of type $\Theta(a, b)$ with $a = (1/2, 1/2, \dots, 1/2)$ satisfy the stability criterion in this case.

What happens for the $Sp(2g, Z)$ transformed points on the real axis? The transformation formula for theta function is given by [36, 31]

$$\Theta[a, b]((A\Omega + B)(C\Omega + D)^{-1}) = exp(i\phi)det(C\Omega + D)^{1/2}\Theta[c, d](\Omega) , \quad (3.4.10)$$

where

$$\begin{pmatrix} c \\ d \end{pmatrix} = \begin{pmatrix} A & B \\ C & D \end{pmatrix} \left(\begin{pmatrix} a \\ b \end{pmatrix} - \begin{pmatrix} (CD^T)_d/2 \\ (AB^T)_d/2 \end{pmatrix} \right) . \quad (3.4.11)$$

Here ϕ is a phase factor irrelevant for the recent purposes and the index d refers to the diagonal part of the matrix in question.

The first thing to notice is the appearance of the diverging square root factor, which however disappears from the vacuum functionals (P and Q have same degree with respect to thetas). The essential point is that theta characteristics transform to each other: as already noticed all even theta characteristics belong to the same $Sp(2g, Z)$ orbit. Therefore the theta functions vanishing at $Im(\Omega_{ii}) = \infty$ do not vanish at the transformed points. It is however clear that for a given Teichmueller parametrization of pinch some theta functions vanish always.

Similar considerations in the case $\Omega_{ik} = 0$, i fixed, show that all theta functions with $b = (1/2, \dots, 1/2)$ vanish identically at the pinch. Also it is clear that for $Sp(2g, Z)$ transformed points one can always find some vanishing theta functions. The overall conclusion is that the elementary particle vacuum functionals obtained by using $g \rightarrow g_1 + g_2$ stability criterion satisfy also $g \rightarrow g - 1$ stability criterion since they are proportional to the product of all even theta functions. Therefore

the only nontrivial consequence of $g \rightarrow g - 1$ criterion is that also $g = 1$ vacuum functionals are of the same general form as $g > 1$ vacuum functionals.

A second manner to deduce the same result is by restricting the consideration to the hyper-elliptic surfaces and using the representation of the theta functions in terms of the roots of the polynomial appearing in the definition of the hyper-elliptic surface [36]. When the genus of the surface is smaller than three (the interesting case), this representation is all what is needed since all surfaces of genus $g < 3$ are hyper-elliptic.

Since hyper-elliptic surfaces can be regarded as surfaces obtained by gluing two compactified complex planes along the cuts connecting various roots of the defining polynomial it is obvious that the process $g \rightarrow g - 1$ corresponds to the limit, when two roots of the defining polynomial coincide. This limit corresponds either to disappearance of a cut or the fusion of two cuts to a single cut. Theta functions are expressible as the products of differences of various roots (Thomae's formula [36])

$$\Theta[a, b]^4 \propto \prod_{i < j \in T} (z_i - z_j) \prod_{k < l \in CT} (z_k - z_l) , \quad (3.4.12)$$

where T denotes some subset of $\{1, 2, \dots, 2g\}$ containing $g + 1$ elements and CT its complement. Hence the product of all even theta functions vanishes, when two roots coincide. Furthermore, stability criterion is satisfied only by the product of the theta functions.

Lowest dimensional vacuum functionals are worth of more detailed consideration.

- i) $g = 0$ particle family corresponds to a constant vacuum functional: by continuity this vacuum functional is constant for all topologies.
- ii) For $g = 1$ the degree of P and Q as polynomials of the theta functions is 24: the critical number of transversal degrees of freedom in bosonic string model! Probably this result is not an accident.
- ii) For $g = 2$ the corresponding degree is 80 since there are 10 even genus 2 theta functions.

There are large numbers of vacuum functionals satisfying the relevant criteria, which do not satisfy the proposed stability criteria. These vacuum functionals correspond either to many particle states or to unstable single particle states.

3.4.8 Continuation of the vacuum functionals to higher genus topologies

From continuity it follows that vacuum functionals cannot be localized to single boundary topology. Besides continuity and the requirements listed above, a natural requirement is that the continuation of the vacuum functional from the sector g to the sector $g + k$ reduces to the product of the original vacuum functional associated with genus g and $g = 0$ vacuum functional at the limit when the surface with genus $g + k$ decays to surfaces with genus g and k : this requirement should guarantee the conservation of separate lepton numbers although different boundary topologies suffer mixing in the vacuum functional. These requirements are satisfied provided the continuation is constructed using the following rule:

Perform the replacement

$$\Theta[a, b]^4 \rightarrow \sum_{c, d} \Theta[a \oplus c, b \oplus d]^4 \quad (3.4.13)$$

for each fourth power of the theta function. Here c and d are Theta characteristics associated with a surface with genus k . The same replacement is performed for the complex conjugates of the theta function. It is straightforward to check that the continuations of elementary particle vacuum functionals indeed satisfy the cluster decomposition property and are continuous.

To summarize, the construction has provided hoped for answers to some questions stated in the beginning: stability requirements explain the separate conservation of lepton numbers and the experimental absence of $g > 0$ elementary bosons. What has not been explained is the experimental absence of $g > 2$ fermion families. The vanishing of the $g > 2$ elementary particle vacuum functionals for the hyper-elliptic surfaces however suggest a possible explanation: under some conditions on the surface X^2 the surfaces Y^2 are hyper-elliptic or possess some conformal symmetry so that elementary particle vacuum functionals vanish for them. This conjecture indeed might make sense since the surfaces Y^2 are determined by the asymptotic dynamics and one might hope that the surfaces Y^2 are analogous to the final states of a dissipative system.

3.5 Explanations for the absence of the $g > 2$ elementary particles from spectrum

The decay properties of the intermediate gauge bosons [54] are consistent with the assumption that the number of the light neutrinos is $N = 3$. Also cosmological considerations pose upper bounds on the number of the light neutrino families and $N = 3$ seems to be favored [38]. It must be however emphasized that p-adic considerations [20] encourage the consideration the existence of higher genera with neutrino masses such that they are not produced in the laboratory at present energies. In any case, for TGD approach the finite number of light fermion families is a potential difficulty since genus-generation correspondence suggests that the number of the fermion (and possibly also boson) families is infinite. Therefore one had better to find a good argument showing that the number of the observed neutrino families, or more generally, of the observed elementary particle families, is small also in the world described by TGD.

It will be later found that also TGD inspired cosmology requires that the number of the effectively massless fermion families must be small after Planck time. This suggests that boundary topologies with handle number $g > 2$ are unstable and/or very massive so that they, if present in the spectrum, disappear from it after Planck time, which correspond to the value of the light cone proper time $a \simeq 10^{-11}$ seconds.

In accordance with the spirit of TGD approach it is natural to wonder whether some geometric property differentiating between $g > 2$ and $g < 3$ boundary topologies might explain why only $g < 3$ boundary components are observable. One can indeed find a good candidate for this kind of property: namely hyper-ellipticity, which states that Riemann surface is a two-fold branched covering of sphere possessing two-element group Z_2 as conformal automorphisms. All $g < 3$ Riemann surfaces are hyper-elliptic unlike $g > 2$ Riemann surfaces, which in general do not possess this property. Thus it is natural to consider the possibility that hyper-ellipticity or more general conformal symmetries might explain why only $g < 2$ topologies correspond to the observed elementary particles.

As regards to the present problem the crucial observation is that some even theta functions vanish for the hyper-elliptic surfaces with genus $g > 2$ [36]. What is essential is that these surfaces have the group Z_2 as conformal symmetries. Indeed, the vanishing phenomenon is more general. Theta functions tend to vanish for $g > 2$ two-surfaces possessing discrete group of conformal symmetries [39]: for instance, instead of sphere one can consider branched coverings of higher genus surfaces.

From the general expression of the elementary particle vacuum functional it is clear that elementary particle vacuum functionals vanish, when Y^2 is hyper-elliptic surface with genus $g > 2$ and one might hope that this is enough to explain why the number of elementary particle families is three.

3.5.1 Hyper-ellipticity implies the separation of $g \leq 2$ and $g > 2$ sectors to separate worlds

If the vertices are defined as intersections of space-time sheets of elementary particles and if elementary particle vacuum functionals are required to have Z_2 symmetry, the localization of elementary particle vacuum functionals to $g \leq 2$ topologies occurs automatically. Even if one allows as limiting case vertices for which 2-manifolds are pinched to topologies intermediate between $g > 2$ and $g \leq 2$ topologies, Z_2 symmetry present for both topological interpretations implies the vanishing of this kind of vertices. This applies also in the case of stringy vertices so that also particle propagation would respect the effective number of particle families. $g > 2$ and $g \leq 2$ topologies would behave much like their own worlds in this approach. This is enough to explain the experimental findings if one can understand why the $g > 2$ particle families are absent as incoming and outgoing states or are very heavy.

3.5.2 What about $g > 2$ vacuum functionals which do not vanish for hyper-elliptic surfaces?

The vanishing of all $g \geq 2$ vacuum functionals for hyper-elliptic surfaces cannot hold true generally. There must exist vacuum functionals which do satisfy this condition. This suggest that elementary particle vacuum functionals for $g > 2$ states have interpretation as bound states of g handles and that the more general states which do not vanish for hyper-elliptic surfaces correspond to many-particle

states composed of bound states $g \leq 2$ handles and cannot thus appear as incoming and outgoing states. Thus $g > 2$ elementary particles would decouple from $g \leq 2$ states.

3.5.3 Should higher elementary particle families be heavy?

TGD predicts an entire hierarchy of scaled up variants of standard model physics for which particles do not appear in the vertices containing the known elementary particles and thus behave like dark matter [34]. Also $g > 2$ elementary particles would behave like dark matter and in principle there is no absolute need for them to be heavy.

The safest option would be that $g > 2$ elementary particles are heavy and the breaking of Z_2 symmetry for $g \geq 2$ states could guarantee this. p-Adic considerations lead to a general mass formula for elementary particles such that the mass of the particle is proportional to $\frac{1}{\sqrt{p}}$ [4]. Also the dependence of the mass on particle genus is completely fixed by this formula. What remains however open is what determines the p-adic prime associated with a particle with given quantum numbers. Of course, it could quite well occur that p is much smaller for $g > 2$ genera than for $g \leq 2$ genera.

3.6 Elementary particle vacuum functionals for dark matter

One of the open questions is how dark matter hierarchy reflects itself in the properties of the elementary particles. The basic questions are how the quantum phase $q = ep(2i\pi/n)$ makes itself visible in the solution spectrum of the modified Dirac operator D and how elementary particle vacuum functionals depend on q . Considerable understanding of these questions emerged recently. One can generalize modular invariance to fractional modular invariance for Riemann surfaces possessing Z_n symmetry and perform a similar generalization for theta functions and elementary particle vacuum functionals. In particular, without any further assumptions $n = 2$ dark fermions have only three families. The existence of space-time correlate for fermionic 2-valuedness suggests that fermions indeed correspond to $n = 2$, or more generally to even values of n , so that this result would hold quite generally. Elementary bosons (actually exotic particles) would correspond to $n = 1$, and more generally odd values of n , and could have also higher families.

3.6.1 Connection between Hurwitz zetas, quantum groups, and hierarchy of Planck constants?

The action of modular group $SL(2, \mathbb{Z})$ on Riemann zeta [35] is induced by its action on theta function [33]. The action of the generator $\tau \rightarrow -1/\tau$ on theta function is essential in providing the functional equation for Riemann Zeta. Usually the action of the generator $\tau \rightarrow \tau + 1$ on Zeta is not considered explicitly. The surprise was that the action of the generator $\tau \rightarrow \tau + 1$ on Riemann Zeta does not give back Riemann zeta but a more general function known as Hurwitz zeta $\zeta(s, z)$ for $z = 1/2$. One finds that Hurwitz zetas for certain rational values of argument define in a well defined sense representations of fractional modular group to which quantum group can be assigned naturally. This could allow to code the value of the quantum phase $q = exp(i2\pi/n)$ to the solution spectrum of the modified Dirac operator D .

Hurwitz zetas

Hurwitz zeta is obtained by replacing integers m with $m + z$ in the defining sum formula for Riemann Zeta:

$$\zeta(s, z) = \sum_m (m + z)^{-s} . \quad (3.6.1)$$

Riemann zeta results for $z = n$.

Hurwitz zeta obeys the following functional equation for rational $z = m/n$ of the second argument [32]:

$$\zeta\left(1-s, \frac{m}{n}\right) = \frac{2\Gamma(s)^s}{2\pi n} \sum_{k=1}^n \cos\left(\frac{\pi s}{2} - \frac{2\pi km}{n}\right) \zeta\left(s, \frac{k}{n}\right) . \quad (3.6.2)$$

The representation of Hurwitz zeta in terms of θ [32] is given by the equation

$$\int_0^\infty [\theta(z, it) - 1] t^{s/2} \frac{dt}{t} = \pi^{(1-s)/2} \Gamma\left(\frac{1-s}{2}\right) [\zeta(1-s, z) + \zeta(1-s, 1-z)] . \quad (3.6.3)$$

By the periodicity of theta function this gives for $z = n$ Riemann zeta.

The action of $\tau \rightarrow \tau + 1$ transforms $\zeta(s, 0)$ to $\zeta(s, 1/2)$

The action of the transformations $\tau \rightarrow \tau + 1$ on the integral representation of Riemann Zeta [35] in terms of θ function [33]

$$\theta(z; \tau) - 1 = 2 \sum_{n=1}^{\infty} [\exp(i\pi\tau)]^{n^2} \cos(2\pi n z) \quad (3.6.4)$$

is given by

$$\pi^{-s/2} \Gamma\left(\frac{s}{2}\right) \zeta(s) = \int_0^\infty [\theta(0; it) - 1] t^{s/2} \frac{dt}{t} . \quad (3.6.5)$$

Using the first formula one finds that the shift $\tau = it \rightarrow \tau + 1$ in the argument θ induces the shift $\theta(0; \tau) \rightarrow \theta(1/2; \tau)$. Hence the result is Hurwitz zeta $\zeta(s, 1/2)$. For $\tau \rightarrow \tau + 2$ one obtains Riemann Zeta.

Thus $\zeta(s, 0)$ and $\zeta(s, 1/2)$ behave like a doublet under modular transformations. Under the subgroup of modular group obtained by replacing $\tau \rightarrow \tau + 1$ with $\tau \rightarrow \tau + 2$ Riemann Zeta forms a singlet. The functional equation for Hurwitz zeta relates $\zeta(1-s, 1/2)$ to $\zeta(s, 1/2)$ and $\zeta(s, 1) = \zeta(s, 0)$ so that also now one obtains a doublet, which is not surprising since the functional equations directly reflects the modular transformation properties of theta functions. This doublet might be the proper object to study instead of singlet if one considers full modular invariance.

Hurwitz zetas form n -plets closed under the action of fractional modular group

The inspection of the functional equation for Hurwitz zeta given above demonstrates that $\zeta(s, m/n)$, $m = 0, 1, \dots, n$, form in a well-defined sense an n -plet under fractional modular transformations obtained by using generators $\tau \rightarrow -1/\tau$ and $\tau \rightarrow \tau + 2/n$. The latter corresponds to the unimodular matrix $(a, b; c, d) = (1, 2/n; 0, 1)$. These matrices obviously form a group. Note that Riemann zeta is always one member of the multiplet containing n Hurwitz zetas.

These observations bring in mind fractionization of quantum numbers, quantum groups corresponding to the quantum phase $q = \exp(i2\pi/n)$, and the inclusions for hyper-finite factors of type II_1 partially characterized by these quantum phases. Fractional modular group obtained using generator $\tau \rightarrow \tau + 2/n$ and Hurwitz zetas $\zeta(s, k/n)$ could very naturally relate to these and related structures.

3.6.2 Could Hurwitz zetas relate to dark matter?

These observations suggest a speculative application to quantum TGD.

Basic vision about dark matter

1. In TGD framework inclusions of HFFs of type II_1 are directly related to the hierarchy of Planck constants involving a generalization of the notion of imbedding space obtained by gluing together copies of 8-D $H = M^4 \times CP_2$ with a discrete bundle structure $H \rightarrow H/Z_{n_a} \times Z_{n_b}$ together along the 4-D intersections of the associated base spaces [39]. A book like structure results and various levels of dark matter correspond to the pages of this book. One can say that elementary particles proper are maximally quantum critical and live in the 4-D intersection of these imbedding spaces whereas their "field bodies" reside at the pages of the Big Book. Note that analogous book like structures results when real and various p-adic variants of the imbedding space are glued together along common algebraic points.
2. The integers n_a and n_b give Planck constant as $\hbar/\hbar_0 = n_a/n_b$, whose most general value is a rational number. In Platonic spirit one can argue that number theoretically simple integers involving only powers of 2 and Fermat primes are favored physically. Phase transitions between different matters occur at the intersection.
3. The inclusions $\mathcal{N} \subset \mathcal{M}$ of HFFs relate also to quantum measurement theory with finite measurement resolution with \mathcal{N} defining the measurement resolution so that N-rays replace complex rays in the projection postulate and quantum space \mathcal{M}/\mathcal{N} having fractional dimension effectively replaces \mathcal{M} .
4. Geometrically the fractional modular invariance would naturally relate to the fact that Riemann surface (partonic 2-surface) can be seen as an $n_a \times n_b$ -fold covering of its projection to the base space of H : fractional modular transformations corresponding to n_a and n_b would relate points at different sheets of the covering of M^4 and CP_2 . This means $Z_{n_a n_b} = Z_{n_a} \times Z_{n_b}$ conformal symmetry. This suggests that the fractionization could be a completely general phenomenon happening also for more general zeta functions.

What about exceptional cases $n = 1$ and $n = 2$?

Also $n = 1$ and $n = 2$ are present in the hierarchy of Hurwitz zetas (singlet and doublet). They do not correspond to allowed Jones inclusion since one has $n > 2$ for them. What could this mean?

1. It would seem that the fractionization of modular group relates to Jones inclusions ($n > 2$) giving rise to fractional statistics. $n = 2$ corresponding to the full modular group $Sl(2, \mathbb{Z})$ could relate to the very special role of 2-valued logic, to the degeneracy of $n = 2$ polygon in plane, to the very special role played by 2-component spinors playing exceptional role in Riemann geometry with spinor structure, and to the canonical representation of HFFs of type II_1 as fermionic Fock space (spinors in the world of classical worlds). Note also that $SU(2)$ defines the building block of compact non-commutative Lie groups and one can obtain Lie-algebra generators of Lie groups from n copies of $SU(2)$ triplets and posing relations which distinguish the resulting algebra from a direct sum of $SU(2)$ algebras.
2. Also $n = 2$ -fold coverings $M^4 \rightarrow M^4/Z_2$ and $CP_2 \rightarrow CP_2/Z_2$ seem to make sense. One can argue that by quantum classical correspondence the spin half property of imbedding space spinors should have space-time correlate. Could $n = 2$ coverings allow to define the space-time correlates for particles having half odd integer spin or weak isospin? If so, bosons would correspond to $n = 1$ and fermions to $n = 2$. One could of course counter argue that induced spinor fields already represent fermions at space-time level and there is no need for the doubling of the representation.

The trivial group Z_1 and Z_2 are exceptional since Z_1 does not define any quantization axis and Z_2 allows any quantization axis orthogonal to the line connecting two points. For $n \geq 3$ Z_n fixes the direction of quantization axis uniquely. This obviously correlates with $n \geq 3$ for Jones inclusions.

Dark elementary particle functionals

One might wonder what might be the dark counterparts of elementary particle vacuum functionals. Theta functions $\theta_{[a,b]}(z, \Omega)$ with characteristic $[a, b]$ for Riemann surface of genus g as functions of z

and Teichmueller parameters Ω are the basic building blocks of modular invariant vacuum functionals defined in the finite-dimensional moduli space whose points characterize the conformal equivalence class of the induced metric of the partonic 2-surface. Obviously, kind of spinorial variants of theta functions are in question with $g + g$ spinor indices for genus g .

The recent case corresponds to $g = 1$ Riemann surface (torus) so that a and b are $g = 1$ -component vectors having values 0 or $1/2$ and Hurwitz zeta corresponds to $\theta_{[0,1/2]}$. The four Jacobi theta functions listed in Wikipedia [33] correspond to these thetas for torus. The values for a and b are 0 and 1 for them but this is a mere convention.

The extensions of modular group to fractional modular groups obtained by replacing integers with integers shifted by multiples of $1/n$ suggest the existence of new kind of q-theta functions with characteristics $[a, b]$ with a and b being g -component vectors having fractional values k/n , $k = 0, 1, \dots, n-1$. There exists also a definition of q-theta functions working for $0 \leq |q| < 1$ but not for roots of unity [40]. The q-theta functions assigned to roots of unity would be associated with Riemann surfaces with additional Z_n conformal symmetry but not with generic Riemann surfaces and obtained by simply replacing the value range of characteristics $[a, b]$ with the new value range in the defining formula

$$\Theta[a, b](z|\Omega) = \sum_n \exp[i\pi(n+a) \cdot \Omega \cdot (n+a) + i2\pi(n+a) \cdot (z+b)] \quad . \quad (3.6.6)$$

for theta functions. If Z_n conformal symmetry is relevant for the definition of fractional thetas it is probably so because it would make the generalized theta functions sections in a bundle with a finite fiber having Z_n action.

This hierarchy would correspond to the hierarchy of quantum groups for roots of unity and Jones inclusions and one could probably define also corresponding zeta function multiplets. These theta functions would be building blocks of the elementary particle vacuum functionals for dark variants of elementary particles invariant under fractional modular group. They would also define a hierarchy of fractal variants of number theoretic functions: it would be interesting to see what this means from the point of view of Langlands program [38] discussed also in TGD framework [21] involving ordinary modular invariance in an essential manner.

This hierarchy would correspond to the hierarchy of quantum groups for roots of unity and Jones inclusions and one could probably define also corresponding zeta function multiplets. These theta functions would be building blocks of the elementary particle vacuum functionals for dark variants of elementary particles invariant under fractional modular group.

Hierarchy of Planck constants defines a hierarchy of quantum critical systems

Dark matter hierarchy corresponds to a hierarchy of conformal symmetries Z_n of partonic 2-surfaces with genus $g \geq 1$ such that factors of n define subgroups of conformal symmetries of Z_n . By the decomposition $Z_n = \prod_{p|n} Z_p$, where $p|n$ tells that p divides n , this hierarchy corresponds to an hierarchy of increasingly quantum critical systems in modular degrees of freedom. For a given prime p one has a sub-hierarchy $Z_p, Z_{p^2} = Z_p \times Z_p$, etc... such that the moduli at $n+1$:th level are contained by n :th level. In the similar manner the moduli of Z_n are sub-moduli for each prime factor of n . This mapping of integers to quantum critical systems conforms nicely with the general vision that biological evolution corresponds to the increase of quantum criticality as Planck constant increases.

The group of conformal symmetries could be also non-commutative discrete group having Z_n as a subgroup. This inspires a very short-lived conjecture that only the discrete subgroups of $SU(2)$ allowed by Jones inclusions are possible as conformal symmetries of Riemann surfaces having $g \geq 1$. Besides Z_n one could have tetrahedral and icosahedral groups plus cyclic group Z_{2n} with reflection added but not Z_{2n+1} nor the symmetry group of cube. The conjecture is wrong. Consider the orbit of the subgroup of rotational group on standard sphere of E^3 , put a handle at one of the orbits such that it is invariant under rotations around the axis going through the point, and apply the elements of subgroup. You obtain a Riemann surface having the subgroup as its isometries. Hence all discrete subgroups of $SU(2)$ can act even as isometries for some value of g .

The number theoretically simple ruler-and-compass integers having as factors only first powers of Fermat primes and power of 2 would define a physically preferred sub-hierarchy of quantum criticality

for which subsequent levels would correspond to powers of 2: a connection with p-adic length scale hypothesis suggests itself.

Spherical topology is exceptional since in this case the space of conformal moduli is trivial and conformal symmetries correspond to the entire $SL(2, C)$. This would suggest that only the fermions of lowest generation corresponding to the spherical topology are maximally quantum critical. This brings in mind Jones inclusions for which the defining subgroup equals to $SU(2)$ and Jones index equals to $M/N = 4$. In this case all discrete subgroups of $SU(2)$ label the inclusions. These inclusions would correspond to fiber space $CP_2 \rightarrow CP_2/U(2)$ consisting of geodesic spheres of CP_2 . In this case the discrete subgroup might correspond to a selection of a subgroup of $SU(2) \subset SU(3)$ acting non-trivially on the geodesic sphere. Cosmic strings $X^2 \times Y^2 \subset M^4 \times CP_2$ having geodesic spheres of CP_2 as their ends could correspond to this phase dominating the very early cosmology.

Fermions in TGD Universe allow only three families

What is nice that if fermions correspond to $n = 2$ dark matter with Z_2 conformal symmetry as strong quantum classical correspondence suggests, the number of ordinary fermion families is three without any further assumptions. To see this suppose that also the sectors corresponding to $M^4 \rightarrow M^4/Z_2$ and $CP_2 \rightarrow CP_2/Z_2$ coverings are possible. Z_2 conformal symmetry implies that partonic Riemann surfaces are hyper-elliptic. For genera $g > 2$ this means that some theta functions of $\theta_{[a,b]}$ appearing in the product of theta functions defining the vacuum functional vanish. Hence fermionic elementary particle vacuum functionals would vanish for $g > 2$ and only 3 fermion families would be possible for $n = 2$ dark matter.

This results can be strengthened. The existence of space-time correlate for the fermionic 2-valuedness suggests that fermions quite generally to even values of n , so that this result would hold for all fermions. Elementary bosons (actually exotic particles belonging to Kac-Moody type representations) would correspond to odd values of n , and could possess also higher families. There is a nice argument supporting this hypothesis. n -fold discretization provided by covering associated with H corresponds to discretization for angular momentum eigenstates. Minimal discretization for $2j + 1$ states corresponds to $n = 2j + 1$. $j = 1/2$ requires $n = 2$ at least, $j = 1$ requires $n = 3$ at least, and so on. $n = 2j + 1$ allows spins $j \leq n - 1/2$. This spin-quantum phase connection at the level of space-time correlates has counterpart for the representations of quantum $SU(2)$.

These rules would hold only for genuinely elementary particles corresponding to single partonic component and all bosonic particles of this kind are exotics (excitations in only "vibrational" degrees of freedom of partonic 2-surface with modular invariance eliminating quite a number of them.

Bibliography

Books about TGD

- [1] M. Pitkänen (2006), *Topological Geometroynamics: Overview*.
http://tgd.wippiespace.com/public_html/tgdview/tgdview.html.
- [2] M. Pitkänen (2006), *Quantum Physics as Infinite-Dimensional Geometry*.
http://tgd.wippiespace.com/public_html/tgdgeom/tgdgeom.html.
- [3] M. Pitkänen (2006), *Physics in Many-Sheeted Space-Time*.
http://tgd.wippiespace.com/public_html/tgdclass/tgdclass.html.
- [4] M. Pitkänen (2006), *p-Adic length Scale Hypothesis and Dark Matter Hierarchy*.
http://tgd.wippiespace.com/public_html/paddark/paddark.html.
- [5] M. Pitkänen (2006), *Quantum TGD*.
http://tgd.wippiespace.com/public_html/tgdquant/tgdquant.html.
- [6] M. Pitkänen (2006), *TGD as a Generalized Number Theory*.
http://tgd.wippiespace.com/public_html/tgdnumber/tgdnumber.html.
- [7] M. Pitkänen (2006), *TGD and Fringe Physics*.
http://tgd.wippiespace.com/public_html/freenergy/freenergy.html.

Books about TGD Inspired Theory of Consciousness and Quantum Biology

- [8] M. Pitkänen (2006), *TGD Inspired Theory of Consciousness*.
http://tgd.wippiespace.com/public_html/tgdconsc/tgdconsc.html.
- [9] M. Pitkänen (2006), *Bio-Systems as Self-Organizing Quantum Systems*.
http://tgd.wippiespace.com/public_html/bioselforg/bioselforg.html.
- [10] M. Pitkänen (2006), *Quantum Hardware of Living Matter*.
http://tgd.wippiespace.com/public_html/bioware/bioware.html.
- [11] M. Pitkänen (2006), *Bio-Systems as Conscious Holograms*.
http://tgd.wippiespace.com/public_html/hologram/hologram.html.
- [12] M. Pitkänen (2006), *Genes and Memes*.
http://tgd.wippiespace.com/public_html/genememe/genememe.html.
- [13] M. Pitkänen (2006), *Magnetospheric Consciousness*.
http://tgd.wippiespace.com/public_html/magnconsc/magnconsc.html.
- [14] M. Pitkänen (2006), *Mathematical Aspects of Consciousness Theory*.
http://tgd.wippiespace.com/public_html/mathconsc/mathconsc.html.
- [15] M. Pitkänen (2006), *TGD and EEG*.
http://tgd.wippiespace.com/public_html/tgdeeg/tgdeeg.html.

References to the chapters of the books about TGD

- [16] The chapter *p-Adic Particle Massivation: Hadron Masses* of [4].
http://tgd.wippiespace.com/public_html/paddark/paddark.html#mass3.
- [17] The chapter *p-Adic Particle Massivation: Elementary particle Masses* of [4].
http://tgd.wippiespace.com/public_html/paddark/paddark.html#mass2.
- [18] The chapter *p-Adic Particle Massivation: New Physics* of [4].
http://tgd.wippiespace.com/public_html/paddark/paddark.html#mass4.
- [19] M. Pitkänen (2006), *Physics in Many-Sheeted Space-Time*.
http://tgd.wippiespace.com/public_html/tgdclass/tgdclass.html.
- [20] The chapter *Quantum Hall effect and Hierarchy of Planck Constants* [5].
http://tgd.wippiespace.com/public_html/tgdquant/tgdquant.html#anyontgd.
- [21] The chapter *Langlands Program and TGD* of [6].
http://tgd.wippiespace.com/public_html/tgdnumber/tgdeeg/tgdnumber.html#Langlandia.
- [22] The chapter *Construction of Quantum Theory: S-matrix* of [5].
http://tgd.wippiespace.com/public_html/tgdquant/tgdquant.html#towards.
- [23] The chapter *Construction of Quantum Theory: Symmetries* of [5].
http://tgd.wippiespace.com/public_html/tgdquant/tgdquant.html#quthe.
- [24] The chapter *Configuration Space Spinor Structure* of [2].
http://tgd.wippiespace.com/public_html/tgdgeom/tgdgeom.html#cspin.
- [25] The chapter *Is it Possible to Understand Coupling Constant Evolution at Space-Time Level?* of [5].
http://tgd.wippiespace.com/public_html/tgdquant/tgdquant.html#rgflow.
- [26] The chapter *Was von Neumann Right After All* of [5].
http://tgd.wippiespace.com/public_html/tgdquant/tgdquant.html#vNeumann.
- [27] The chapter *An Overview about the Evolution of Quantum TGD* of [1].
http://tgd.wippiespace.com/public_html/tgdview/tgdview.html#evoI.
- [28] The chapter *Identification of the Configuration Space Kähler Function* of [2].
http://tgd.wippiespace.com/public_html/tgdgeom/tgdgeom.html#kahler.
- [29] The chapter *Elementary Particle Vacuum Functionals* of [4].
http://tgd.wippiespace.com/public_html/paddark/paddark.html#elvafu.
- [30] The chapter *Does TGD Predict the Spectrum of Planck Constants?* of [5].
http://tgd.wippiespace.com/public_html/tgdquant/tgdquant.html#Planck.

Mathematics

- [31] Alvarez-Gaume L., Moore G. and Vafa C. (1986): *Theta functions, Modular invariance and Strings*. Commun. Math. Phys. 106. 40-87.
- [32] *Hurwitz zeta function*. http://en.wikipedia.org/wiki/Hurwitz_zeta_function.
- [33] *Theta function*. http://en.wikipedia.org/wiki/Theta_function.
- [34] M. Redei and M. Stöltzner (eds) (2001), *John von Neumann and the Foundations of Quantum Physics*. Vol. 8, Dordrecht: Kluwer Academic Publishers. V. S. Sunder (1987), *An Invitation to von Neumann Algebras*. New York: Springer-Verlag.

- [35] *Riemann Zeta function*. http://en.wikipedia.org/wiki/Riemann_zeta.
- [36] Mumford, D.(1983,1984): *Tata Lectures on Theta I,II,III*. Birkhäuser.
- [37] Farkas, H., M. and Kra, I. (1980): *Riemann Surfaces*. Springer Verlag.
- [38] *Langlands program*.http://en.wikipedia.org/wiki/Langlands_program.
- [39] Accola, R. (1975): *Riemann Surfaces, Theta functions and Abelian Automorphism Groups*. Lecture Notes in Mathematics 483. Springer Verlag.
- [40] *Q-theta function*. http://en.wikipedia.org/wiki/Q-theta_function.

Particle and nuclear physics

- [41] Decamp *et al* (Aleph Collaboration)(1989): CERN-EP/89-141, preprint.
- [42] Denegri, D. *et al*(1989): *The number of neutrino species*. CERN EP/89-72, preprint.

Chapter 4

Massless States and Particle Massivation

4.1 Introduction

This article represents the most recent view about particle massivation in TGD framework. This topic is necessarily quite extended since many several notions and new mathematics is involved. Therefore the calculation of particle masses involves five chapters ([26, 22, 17, 20] of [4]). In the following my goal is to provide an up-to-date summary whereas the chapters are unavoidably a story about evolution of ideas.

The identification of the spectrum of light particles reduces to two tasks: the construction of massless states and the identification of the states which remain light in p-adic thermodynamics. The latter task is relatively straightforward. The thorough understanding of the massless spectrum requires however a real understanding of quantum TGD. It would be also highly desirable to understand why p-adic thermodynamics combined with p-adic length scale hypothesis works. A lot of progress has taken place in these respects during last years.

Zero energy ontology providing a detailed geometric view about bosons and fermions, the generalization of S -matrix to what I call M -matrix, the notion of finite measurement resolution characterized in terms of inclusions of von Neumann algebras, the derivation of p-adic coupling constant evolution and p-adic length scale hypothesis from the first principles, the realization that the counterpart of Higgs mechanism involves generalized eigenvalues of the modified Dirac operator: these are represent important steps of progress during last years with a direct relevance for the understanding of particle spectrum and massivation although the predictions of p-adic thermodynamics are not affected.

During 2010 a further progress took place as I wrote articles about TGD to Prespacetime journal [34]. These steps of progress relate closely to zero energy ontology, bosonic emergence, the realization of the importance of twistors in TGD, and to the discovery of the weak form of electric-magnetic duality. Twistor approach and the understanding of the Chern-Simons Dirac operator served as a midwife in the process giving rise to the birth of the idea that all particles at fundamental level are massless and that both ordinary elementary particles and string like objects emerge from them. Even more, one can interpret virtual particles as being composed of these massless on mass shell particles assignable to wormhole throats so that four-momentum conservation poses extremely powerful constraints on loop integrals and makes them manifestly finite.

The weak form of electric-magnetic duality led to the realization that elementary particles correspond to bound states of two wormhole throats with opposite Kähler magnetic charges with second throat carrying weak isospin compensating that of the fermion state at second wormhole throat. Both fermions and bosons correspond to wormhole contacts: in the case of fermions topological condensation generates the second wormhole throat. This means that altogether four wormhole throats are involved with both fermions, gauge bosons, and gravitons (for gravitons this is unavoidable in any case). For p-adic thermodynamics the mathematical counterpart of string corresponds to a wormhole contact with size of order CP_2 size with the role of its ends played by wormhole throats at which the signature of the induced 4-metric changes. The key observation is that for massless states the throats of spin 1 particle must have opposite three-momenta so that gauge bosons are necessarily

massive, even photon and other particles usually regarded as massless must have small mass which in turn cancels infrared divergences and give hopes about exact Yangian symmetry generalizing that of $\mathcal{N} = 4$ SYM. Besides this there is weak "stringy" contribution to the mass assignable to the magnetic flux tubes connecting the two wormhole throats at the two space-time sheets.

4.1.1 Physical states as representations of super-symplectic and Super Kac-Moody algebras

Physical states belong to the representation of super-symplectic algebra and Super Kac-Moody algebra assignable $SO(2) \times SU(3) \times SU(2)_{rot} \times U(2)_{ew}$ associated with the 2-D surfaces X^2 defined by the intersections of 3-D light like causal determinants with $\delta M_{\pm}^4 \times CP_2$. These 2-surfaces have interpretation as partons.

It has taken considerable effort to understand the relationship between super-symplectic and super Kac-Moody algebras and there are still many uncertainties involved. What looks like the most plausible option relies on the generalization of a coset construction proposed already for years ago but given up because of the lacking understanding of how SKM and SC algebras could be lifted to the level of imbedding space. The progress in the *Physics as generalized number theory* program provided finally a justification for the coset construction.

1. Assume a generalization of the coset construction in the sense that the differences of super Kac-Moody Virasoro generators (SKMV) and super-symplectic Virasoro generators (SSV) annihilate the physical states. The interpretation is in terms of TGD counterpart for Einstein's equations realizing Equivalence Principle. Mass squared is identified as the p-adic thermal expectation value of either *SKMV* or *SSV* conformal weight (gravitational or inertial mass) in a superposition of states with *SKMV* (*SSV*) conformal weight $n \geq 0$ annihilated by $SKMV - SSV$.
2. Construct first ground states with negative conformal weight annihilated by *SKMV* and *SSV* generators $G_n, L_n, n < 0$. Apply to these states generators of tensor factors of Super Viraroso algebras to obtain states with vanishing *SSV* and *SKMV* conformal weights. After this construct thermal states as superpositions of states obtained by applying *SKMV* generators and corresponding *SSV* generators $G_n, L_n, n > 0$. Assume that these states are annihilated by *SSV* and *SKMV* generators $G_n, L_n, n > 0$ and by the differences of all *SSV* and *SKMV* generators.
3. Super-symplectic algebra represents a completely new element and in the case of hadrons the non-perturbative contribution to the mass spectrum is easiest to understand in terms of super-symplectic thermal excitations contributing roughly 70 per cent to the p-adic thermal mass of the hadron. It must be however emphasized that by SKMV-SSV duality one can regard these contributions equivalently as SKM or SC contributions.

Yangian algebras associated with the super-conformal algebras and motivated by twistorial approach generalize the super-conformal symmetry and make it multi-local in the sense that generators can act on several partonic 2-surfaces simultaneously. These partonic 2-surfaces generalize the vertices for the external massless particles in twistor Grassmann diagrams [19]. The implications of this symmetry are yet to be deduced but one thing is clear: Yangians are tailor made for the description of massive bound states formed from several partons identified as partonic 2-surfaces. The preliminary discussion of what is involved can be found in [19].

4.1.2 Particle massivation

Particle massivation can be regarded as a generation of thermal conformal weight identified as mass squared and due to a thermal mixing of a state with vanishing conformal weight with those having higher conformal weights. The observed mass squared is not p-adic thermal expectation of mass squared but that of conformal weight so that there are no problems with Lorentz invariance.

One can imagine several microscopic mechanisms of massivation. The following proposal is the winner in the fight for survival between several competing scenarios.

1. The original observation was that the pieces of CP_2 type vacuum extremals representing elementary particles have random light-like curve as an M^4 projection so that the average motion

correspond to that of massive particle. Light-like randomness gives rise to classical Virasoro conditions. This picture generalizes since the basic dynamical objects are light-like but otherwise random 3-surfaces. The identification of elementary particles developed in three steps.

- (a) Fermions are identified as light-like 3-surfaces at which the signature of induced metric of deformed CP_2 type extremals changes from Euclidian to the Minkowskian signature of the background space-time sheet. Gauge bosons and Higgs correspond to wormhole contacts with light-like throats carrying fermion and antifermion quantum numbers. Gravitons correspond to pairs of wormhole contacts bound to string like object by the fluxes connecting the wormhole contacts. The randomness of the light-like 3-surfaces and associated super-conformal symmetries justify the use of thermodynamics and the question remains why this thermodynamics can be taken to be p-adic. The proposed identification of bosons means enormous simplification in thermodynamical description since all calculations reduced to the calculations to fermion level. This picture generalizes to include super-symmetry. The fermionic oscillator operators associated with the partonic 2-surfaces act as generators of badly broken SUSY and right-handed neutrino gives to the not so badly broken $\mathcal{N} = 1$ SUSY consistent with empirical facts.
 - (b) The next step was to realize that the topological condensation of fermion generates second wormhole throat which carries momentum but no fermionic quantum numbers. This is also needed to the massivation by p-adic thermodynamics applied to the analogs of string like objects defined by wormhole throats with throats taking the role of string ends. p-Adic thermodynamics did not however allow a satisfactory understanding of the gauge bosons masses and it was clear that Higgsy contribution should be present and dominate for gauge bosons. Gauge bosons should also somehow obtain their longitudinal polarizations and here Higgs like particles indeed predicted by the basic picture suggests itself strongly.
 - (c) A further step was the discovery of the weak form of electric-magnetic duality, which led to the realization that wormhole throats possess Kähler magnetic charge so that a wormhole throat with opposite magnetic charge is needed to compensate this charge. This wormhole throat can also compensate the weak isospin of the second wormhole throat so that weak confinement and massivation results. In the case of quarks magnetic confinement might take place in hadronic rather than weak length scale. Second crucial observation was that gauge bosons are necessarily massive since the light-like momenta at two throats must correspond to opposite three-momenta so that no Higgs potential is needed. This leads to a picture in which gauge bosons eat the Higgs scalars and also photon, gluons, and gravitons develop small mass.
2. The fundamental parton level description of TGD is based on almost topological QFT for light-like 3-surfaces. Dynamics is constrained by the requirement that CP_2 projection is for extremals of Chern-Simons action 2-dimensional and for off-shell states light-likeness is the only constraint. As a matter fact, the basic theory relies on the modified Dirac action associated with Chern-Simons action and Kähler action in the sense that the generalizes eigenmodes of Chern-Simons Dirac operator correspond to the zero modes of Kähler action localized to the light-like 3-surfaces representing partons. In this manner the data about the dynamics of Kähler action is feeded to the eigenvalue spectrum. Eigenvalues are interpreted as square roots of ground state conformal weights.
 3. The symmetries respecting light-likeness property give rise to Kac-Moody type algebra and super-symplectic symmetries emerge also naturally as well as $\mathcal{N} = 4$ character of super-conformal invariance. The coset construction for super-symplectic Virasoro algebra and Super Kac-Moody algebra identified in physical sense as sub-algebra of former implies that the four-momenta assignable to the two algebras are identical. The interpretation is in terms of the identity of gravitational inertial masses and generalization of Equivalence Principle.
 4. Instead of energy, the Super Kac-Moody Virasoro (or equivalently super-symplectic) generator L_0 (essentially mass squared) is thermalized in p-adic thermodynamics (and also in its real version assuming it exists). The fact that mass squared is thermal expectation of conformal weight guarantees Lorentz invariance. That mass squared, rather than energy, is a fundamental quantity at CP_2 length scale is also suggested by a simple dimensional argument (Planck mass

squared is proportional to \hbar so that it should correspond to a generator of some Lie-algebra (Virasoro generator $L_0!$)).

5. By Equivalence Principle the thermal average of mass squared can be calculated either in terms of thermodynamics for either super-symplectic of Super Kac-Moody Virasoro algebra and p-adic thermodynamics is consistent with conformal invariance.
6. There is also a modular contribution to the mass squared, which can be estimated using elementary particle vacuum functionals in the conformal modular degrees of freedom of the partonic 2-surface. It dominates for higher genus partonic 2-surfaces. For bosons both Virasoro and modular contributions seem to be negligible and could be due to the smallness of the p-adic temperature.
7. A long standing problem has been whether coupling to Higgs boson is needed to explain gauge boson masses via a generation of Higgs vacuum expectation having possibly interpretation in terms of a coherent state. Before the detailed model for elementary particles in terms of pairs of wormhole contacts at the ends of flux tubes the picture about the situation was as follows. From the beginning it was clear that is that ground state conformal weight must be negative. Then it became clear that the ground state conformal weight need not be a negative integer. The deviation Δh of the total ground state conformal weight from negative integer gives rise to Higgs type contribution to the thermal mass squared and dominates in case of gauge bosons for which p-adic temperature is small. In the case of fermions this contribution to the mass squared is small. The possible Higgs vacuum expectation makes sense only at QFT limit and would be naturally proportional to Δh so that the coupling to Higgs would only apparently cause gauge boson massivation. It is natural to relate Δh to the generalized eigenvalues of Chern-Simons Dirac operator.
8. A natural identification of the non-integer contribution to the conformal weight is as Higgsy and stringy contributions to the vacuum conformal weight. In twistor approach the generalized eigenvalues of Chern-Simons Dirac operator for external particles indeed correspond to light-like momenta and when the three-momenta are opposite this gives rise to non-vanishing mass. Higgs is necessary to give longitudinal polarizations for gauge bosons and also gauge bosons usually regarded as exactly massless particles would naturally receive small mass in this manner so that Higgs would disappear completely from the spectrum. The theoretical motivation for small mass would be exact Yangian symmetry. Higgs vacuum expectation assignable to coherent state of Higgs bosons is not needed to explain the boson masses.

An important question concerns the justification of p-adic thermodynamics.

1. The underlying philosophy is that real number based TGD can be algebraically continued to various p-adic number fields. This gives justification for the use of p-adic thermodynamics although the mapping of p-adic thermal expectations to real counterparts is not completely unique. The physical justification for p-adic thermodynamics is effective p-adic topology characterizing the 3-surface: this is the case if real variant of light-like 3-surface has large number of common algebraic points with its p-adic counterpart obeying same algebraic equations but in different number field. In fact, there is a theorem stating that for rational surfaces the number of rational points is finite and rational (more generally algebraic points) would naturally define the notion of number theoretic braid essential for the realization of number theoretic universality.
2. The most natural option is that the descriptions in terms of both real and p-adic thermodynamics make sense and are consistent. This option indeed makes if the number of generalized eigen modes of modified Dirac operator is finite. This is indeed the case if one accepts periodic boundary conditions for the Chern-Simons Dirac operator. In fact, the solutions are localized at the strands of braids [55]. This makes sense because the theory has hydrodynamic interpretation [55]. This reduces $\mathcal{N} = \infty$ to finite SUSY and realizes finite measurement resolution as an inherent property of dynamics.

The finite number of fermionic oscillator operators implies an effective cutoff in the number conformal weights so that conformal algebras reduce to finite-dimensional algebras. The first guess would be that integer label for oscillator operators becomes a number in finite field for

some prime. This means that one can calculate mass squared also by using real thermodynamics but the consistency with p-adic thermodynamics gives extremely strong number theoretical constraints on mass scale. This consistency condition allows also to solve the problem how to map a negative ground state conformal weight to its p-adic counterpart. Negative conformal weight is divided into a negative half odd integer part plus positive part Δh , and negative part corresponds as such to p-adic integer whereas positive part is mapped to p-adic number by canonical identification.

p-Adic thermodynamics is what gives to this approach its predictive power.

1. p-Adic temperature is quantized by purely number theoretical constraints (Boltzmann weight $\exp(-E/kT)$ is replaced with p^{L_0/T_p} , $1/T_p$ integer) and fermions correspond to $T_p = 1$ whereas $T_p = 1/n$, $n > 1$, seems to be the only reasonable choice for gauge bosons.
2. p-Adic thermodynamics forces to conclude that CP_2 radius is essentially the p-adic length scale $R \sim L$ and thus of order $R \simeq 10^{3.5} \sqrt{\hbar G}$ and therefore roughly $10^{3.5}$ times larger than the naive guess. Hence p-adic thermodynamics describes the mixing of states with vanishing conformal weights with their Super Kac-Moody Virasoro excitations having masses of order $10^{-3.5}$ Planck mass.

4.1.3 What next?

The successes of p-adic mass calculations are basically due to the power of super-conformal symmetries and of number theory. One cannot deny that the description of the Higgsy aspects of massivation and of hadrons involves phenomenological elements. There are however excellent hopes that it might be possible some day to calculate everything from first principles. The non-local Yangian symmetry generalizing the super-conformal algebras suggests itself strongly as a fundamental symmetry of quantum TGD. The generalized of the Yangian symmetry replaces points with partonic 2-surfaces being multi-local with respect to them, and leads to general formulas for multi-local operators representing four-momenta and other conserved charges of composite states. In TGD framework even elementary particles involve two wormhole contacts having each two wormhole throats identified as the fundamental partonic entities. Therefore Yangian approach would naturally define the first principle approach to the understanding of masses of elementary particles and their bound states (say hadrons). The power of this extended symmetry might be enough to deduce universal mass formulas. One of the future challenges would therefore be the mathematical and physical understanding of Yangian symmetry. This would however require the contributions of professional mathematicians.

4.2 Identification of elementary particles

4.2.1 Partons as wormhole throats and particles as bound states of wormhole contacts

The assumption that partonic 2-surfaces correspond to representations of Super Virasoro algebra has been an unchallenged assumption of the p-adic mass calculations for a long time although one might argue that these objects do not possess stringy characteristics, in particular they do not possess two ends. The progress in the understanding of the modified Dirac equation and the introduction of the weak form of electric magnetic duality [55] however forces to modify the picture about the origin of the string mass spectrum.

1. The weak form of electric-magnetic duality, the basic facts about modified Dirac equation and the proposed twistorialization of quantum TGD [19] force to conclude that both strings and bosons and their super-counterparts emerge from massless fermions moving collinearly at partonic two-surfaces. Stringy mass spectrum is consistent with this only if p-adic thermodynamics describes wormhole contacts as analogs of stringy objects having quantum numbers at the throats playing the role of string ends. For instance, the three-momenta of massless wormhole throats could be in opposite direction so that wormhole contact would become massive. The fundamental string like objects would therefore correspond to the wormhole contacts with size scale of order CP_2 length.

Already these objects must have a correct correlation between color and electroweak quantum numbers. The colored super-generators taking care that anomalous color is compensated can be assigned with purely bosonic quanta associated with the wormhole throats which carry no fermion number.

2. Second modification comes from the necessity to assume weak confinement in the sense that each wormhole throat carrying fermionic numbers is accompanied by a second wormhole throat carrying neutrino pair cancelling the net weak isospin so that only electromagnetic charge remains unscreened. This screening must take place in weak length scale so that ordinary elementary particles are predicted to be string like objects. This string tension has however nothing to do with the fundamental string tension responsible for the mass spectrum. This picture is forced also by the fact that fermionic wormhole throats necessarily carry Kähler magnetic charge [55] so that in the case of leptons the second wormhole throat must carry a compensating Kähler magnetic charge. In the case of quarks one can consider the possibility that magnetic charges are not neutralized completely in weak scale and that the compensation occurs in QCD length scale so that Kähler magnetic confinement would accompany color confinement. This means color magnetic confinement since classical color gauge fields are proportional to induced Kähler field.

These modifications do not seem to appreciably affect the results of calculations, which depend only on the number of tensor factors in super Virasoro representation, they are not taken explicitly into account in the calculations. The predictions of the general theory are consistent with the earliest mass calculations, and the earlier ad hoc parameters disappear. In particular, optimal lowest order predictions for the charged lepton masses are obtained and photon, gluon and graviton appear as essentially massless particles. What is new is the possibility to describe the massivation of gauge bosons by including the contribution from the string tension of weak string like objects: weak boson masses have indeed been the trouble makers and have forced to conclude that Higgs expectation might be needed unless some other mechanism contributes to the conformal vacuum weight of the ground state.

4.2.2 Family replication phenomenon topologically

One of the basic ideas of TGD approach has been genus-generation correspondence: boundary components of the 3-surface should be carriers of elementary particle numbers and the observed particle families should correspond to various boundary topologies.

With the advent of zero energy ontology this picture changed somewhat. It is the wormhole throats identified as light-like 3-surfaces at which the induced metric of the space-time surface changes its signature from Minkowskian to Euclidian, which correspond to the light-like orbits of partonic 2-surfaces. One cannot of course exclude the possibility that also boundary components could allow to satisfy boundary conditions without assuming vacuum extremal property of nearby space-time surface. The intersections of the wormhole throats with the light-like boundaries of causal diamonds (CD s) identified as intersections of future and past directed light cones ($CD \times CP_2$ is actually in question but I will speak about CD s) define special partonic 2-surfaces and it is the moduli of these partonic 2-surfaces which appear in the elementary particle vacuum functionals naturally.

The first modification of the original simple picture comes from the identification of physical particles as bound states of pairs of wormhole contacts and from the assumption that for generalized Feynman diagrams stringy trouser vertices are replaced with vertices at which the ends of light-like wormhole throats meet. In this picture the interpretation of the analog of trouser vertex is in terms of propagation of same particle along two different paths. This interpretation is mathematically natural since vertices correspond to 2-manifolds rather than singular 2-manifolds which are just splitting to two disjoint components. Second complication comes from the weak form of electric-magnetic duality forcing to identify physical particles as weak strings with magnetic monopoles at their ends and one should understand also the possible complications caused by this generalization.

These modifications force to consider several options concerning the identification of light fermions and bosons and one can end up with a unique identification only by making some assumptions. Masslessness of all wormhole throats- also those appearing in internal lines- and dynamical $SU(3)$ symmetry for particle generations are attractive general enough assumptions of this kind. This means that bosons and their super-partners correspond to wormhole contacts with fermion and antifermion

at the throats of the contact. Free fermions and their superpartners could correspond to CP_2 type vacuum extremals with single wormhole throat. It turns however that dynamical $SU(3)$ symmetry forces to identify massive (and possibly topologically condensed) fermions as (g, g) type wormhole contacts.

Do free fermions correspond to single wormhole throat or (g, g) wormhole?

The original interpretation of genus-generation correspondence was that free fermions correspond to wormhole throats characterized by genus. The idea of $SU(3)$ as a dynamical symmetry suggested that gauge bosons correspond to octet and singlet representations of $SU(3)$. The further idea that all lines of generalized Feynman diagrams are massless poses a strong additional constraint and it is not clear whether this proposal as such survives.

1. Twistorial program assumes that fundamental objects are massless wormhole throats carrying collinearly moving many-fermion states and also bosonic excitations generated by supersymplectic algebra. In the following consideration only purely bosonic and single fermion throats are considered since they are the basic building blocks of physical particles. The reason is that propagators for high excitations behave like p^{-n} , n the number of fermions associated with the wormhole throat. Therefore single throat allows only spins 0, 1/2, 1 as elementary particles in the usual sense of the word.
2. The identification of massive fermions (as opposed to free massless fermions) as wormhole contacts follows if one requires that fundamental building blocks are massless since at least two massless throats are required to have a massive state. Therefore the conformal excitations with CP_2 mass scale should be assignable to wormhole contacts also in the case of fermions. As already noticed this is not the end of the story: weak strings are required by the weak form of electric-magnetic duality.
3. If free fermions corresponding to single wormhole throat, topological condensation is an essential element of the formation of stringy states. The topological condensation of fermions by topological sum (fermionic CP_2 type vacuum extremal touches another space-time sheet) suggest $(g, 0)$ wormhole contact. Note however that the identification of wormhole throat is as 3-surface at which the signature of the induced metric changes so that this conclusion might be wrong. One can indeed consider also the possibility of (g, g) pairs as an outcome of topological condensation. This is suggested also by the idea that wormhole throats are analogous to string like objects and only this option turns out to be consistent with the BFF vertex based on the requirement of dynamical $SU(3)$ symmetry to be discussed later. The structure of reaction vertices makes it possible to interpret (g, g) pairs as $SU(3)$ triplet. If bosons are obtained as fusion of fermionic and antifermionic throats (touching of corresponding CP_2 type vacuum extremals) they correspond naturally to (g_1, g_2) pairs.
4. p-Adic mass calculations distinguish between fermions and bosons and the identification of fermions and bosons should be consistent with this difference. The maximal p-adic temperature $T = 1$ for fermions could relate to the weakness of the interaction of the fermionic wormhole throat with the wormhole throat resulting in topological condensation. This wormhole throat would however carry momentum and 3-momentum would in general be non-parallel to that of the fermion, most naturally in the opposite direction.

p-Adic mass calculations suggest strongly that for bosons p-adic temperature $T = 1/n$, $n > 1$, so that thermodynamical contribution to the mass squared is negligible. The low p-adic temperature could be due to the strong interaction between fermionic and antifermionic wormhole throat leading to the "freezing" of the conformal degrees of freedom related to the relative motion of wormhole throats.

5. The weak form of electric-magnetic duality forces second wormhole throat with opposite magnetic charge and the light-like momenta could sum up to massive momentum. In this case string tension corresponds to electroweak length scale. Therefore p-adic thermodynamics must be assigned to wormhole contacts and these appear as basic units connected by Kähler magnetic flux tube pairs at the two space-time sheets involved. Weak stringy degrees of freedom are however

expected to give additional contribution to the mass, perhaps by modifying the ground state conformal weight.

Dynamical $SU(3)$ fixes the identification of fermions and bosons and fundamental interaction vertices

For 3 light fermion families $SU(3)$ suggests itself as a dynamical symmetry with fermions in fundamental $N = 3$ -dimensional representation and $N \times N = 9$ bosons in the adjoint representation and singlet representation. The known gauge bosons have same couplings to fermionic families so that they must correspond to the singlet representation. The first challenge is to understand whether it is possible to have dynamical $SU(3)$ at the level of fundamental reaction vertices.

This is a highly non-trivial constraint. For instance, the vertices in which n wormhole throats with same (g_1, g_2) glued along the ends of lines are not consistent with this symmetry. The splitting of the fermionic worm-hole contacts before the proper vertices for throats might however allow the realization of dynamical $SU(3)$. The condition of $SU(3)$ symmetry combined with the requirement that virtual lines resulting also in the splitting of wormhole contacts are always massless, leads to the conclusion that massive fermions correspond to (g, g) type wormhole contacts transforming naturally like $SU(3)$ triplet. This picture conforms with the identification of free fermions as throats but not with the naive expectation that their topological condensation gives rise to $(g, 0)$ wormhole contact.

The argument leading to these conclusions runs as follows.

1. The question is what basic reaction vertices are allowed by dynamical $SU(3)$ symmetry. FFB vertices are in principle all that is needed and they should obey the dynamical symmetry. The meeting of entire wormhole contacts along their ends is certainly not possible. The splitting of fermionic wormhole contacts before the vertices might be however consistent with $SU(3)$ symmetry. This would give two a pair of 3-vertices at which three wormhole lines meet along partonic 2-surfaces (rather than along 3-D wormhole contacts).
2. Note first that crossing gives all possible reaction vertices of this kind from $F(g_1)\bar{F}(g_2) \rightarrow B(g_1, g_2)$ annihilation vertex, which is relatively easy to visualize. In this reaction $F(g_1)$ and $\bar{F}(g_2)$ wormhole contacts split first. If one requires that all wormhole throats involved are massless, the two wormhole throats resulting in splitting and carrying no fermion number must carry light-like momentum so that they cannot just disappear. The ends of the wormhole throats of the boson must be glued together with the end of the fermionic wormhole throat and its companion generated in the splitting of the wormhole. This means that fermionic wormhole first splits and the resulting throats meet at the partonic 2-surface.

his requires that topologically condensed fermions correspond to (g, g) pairs rather than $(g, 0)$ pairs. The reaction mechanism allows the interpretation of (g, g) pairs as a triplet of dynamical $SU(3)$. The fundamental vertices would be just the splitting of wormhole contact and 3-vertices for throats since $SU(3)$ symmetry would exclude more complex reaction vertices such as n -boson vertices corresponding the gluing of n wormhole contact lines along their 3-dimensional ends. The couplings of singlet representation for bosons would have same coupling to all fermion families so that the basic experimental constraint would be satisfied.

3. Both fermions and bosons cannot correspond to octet and singlet of $SU(3)$. In this case reaction vertices should correspond algebraically to the multiplication of matrix elements e_{ij} : $e_{ij}e_{kl} = \delta_{jk}e_{il}$ allowing for instance $F(g_1, g_2) + \bar{F}(g_2, g_3) \rightarrow B(g_1, g_3)$. Neither the fusion of entire wormhole contacts along their ends nor the splitting of wormhole throats before the fusion of partonic 2-surfaces allows this kind of vertices so that BFF vertex is the only possible one. Also the construction of QFT limit starting from bosonic emergence led to the formulation of perturbation theory in terms of Dirac action allowing only BFF vertex as fundamental vertex [23].
4. Weak electric-magnetic duality brings in an additional complication. $SU(3)$ symmetry poses also now strong constraints and it would seem that the reactions must involve copies of basic BFF vertices for the pairs of ends of weak strings. The string ends with the same Kähler magnetic charge should meet at the vertex and give rise to BFF vertices. For instance, $F\bar{F}B$ annihilation vertex would in this manner give rise to the analog of stringy diagram in which strings join along ends since two string ends disappear in the process.

If one accepts this picture the remaining question is why the number of genera is just three. Could this relate to the fact that $g \leq 2$ Riemann surfaces are always hyper-elliptic (have global Z_2 conformal symmetry) unlike $g > 2$ surfaces? Why the complete bosonic de-localization of the light families should be restricted inside the hyper-elliptic sector? Does the Z_2 conformal symmetry make these states light and make possible delocalization and dynamical $SU(3)$ symmetry? Could it be that for $g > 2$ elementary particle vacuum functionals vanish for hyper-elliptic surfaces? If this the case and if the time evolution for partonic 2-surfaces changing g commutes with Z_2 symmetry then the vacuum functionals localized to $g \leq 2$ surfaces do not disperse to $g > 2$ sectors.

The notion of elementary particle vacuum functional

Obviously one must know something about the dependence of the elementary particle state functionals on the geometric properties of the boundary component and in the sequel an attempt to construct what might be called elementary particle vacuum functionals, is made.

The basic assumptions underlying the construction are the following ones:

1. Elementary particle vacuum functionals depend on the geometric properties of the two-surface X^2 representing elementary particle.
2. Vacuum functionals possess extended Diff invariance: all 2-surfaces on the orbit of the 2-surface X^2 correspond to the same value of the vacuum functional. This condition is satisfied if vacuum functionals have as their argument, not X^2 as such, but some 2-surface Y^2 belonging to the unique orbit of X^2 (determined by the principle selecting preferred extremal of the Kähler action as a generalized Bohr orbit [37]) and determined in $Diff^3$ invariant manner.
3. Zero energy ontology allows to select uniquely the partonic two surface as the intersection of the wormhole throat at which the signature of the induced 4-metric changes with either the upper or lower boundary of $CD \times CP_2$. This is essential since otherwise one could not specify the vacuum functional uniquely.
4. Vacuum functionals possess conformal invariance and therefore for a given genus depend on a finite number of variables specifying the conformal equivalence class of Y^2 .
5. Vacuum functionals satisfy the cluster decomposition property: when the surface Y^2 degenerates to a union of two disjoint surfaces (particle decay in string model inspired picture), vacuum functional decomposes into a product of the vacuum functionals associated with disjoint surfaces.
6. Elementary particle vacuum functionals are stable against the decay $g \rightarrow g_1 + g_2$ and one particle decay $g \rightarrow g - 1$. This process corresponds to genuine particle decay only for stringy diagrams. For generalized Feynman diagrams the interpretation is in terms of propagation along two different paths simultaneously.

In [22] the construction of elementary particle vacuum functionals is described in more detail. This requires some basic concepts related to the description of the space of the conformal equivalence classes of Riemann surfaces and the concept of hyper-ellipticity. Since theta functions will play a central role in the construction of the vacuum functionals, also their basic properties are needed. Also possible explanations for the experimental absence of the higher fermion families are considered.

4.3 Non-topological contributions to particle masses from p-adic thermodynamics

In TGD framework p-adic thermodynamics provides a microscopic theory of particle massivation in the case of fermions. The idea is very simple. The mass of the particle results from a thermal mixing of the massless states with CP_2 mass excitations of super-conformal algebra. In p-adic thermodynamics the Boltzmann weight $\exp(-E/T)$ does not exist in general and must be replaced with p^{L_0/T_p} which exists for Virasoro generator L_0 if the inverse of the p-adic temperature is integer valued $T_p = 1/n$. The expansion in powers of p converges extremely rapidly for physical values of p , which are rather large. Therefore the three lowest terms in expansion give practically exact results. Thermal massivation

does not not necessarily lead to light states and this drops a large number of exotic states from the spectrum of light particles. The partition functions of N-S and Ramond type representations are not changed in TGD framework despite the fact that fermionic super generators carry fermion numbers and are not Hermitian. Thus the practical calculations are relatively straightforward.

In free fermion picture the p-adic thermodynamics in the boson sector is for fermion-antifermion states associated with the two throats of the bosonic wormhole. The question is whether the thermodynamical mass squared is just the sum of the two independent fermionic contributions for Ramond representations or should one use N-S type representation resulting as a tensor product of Ramond representations.

The overall conclusion about p-adic mass calculations is that fermionic mass spectrum is predicted in an excellent accuracy but that the thermal masses of the intermediate gauge bosons come 20-30 per cent to large for $T_p = 1$ and are completely negligible for $T_p = 1/2$. This forces to consider very seriously the possibility that thermal contribution to the bosonic mass is negligible and that TGD can, contrary to the original expectations, provide dynamical Higgs field as a fundamental field. The identification of Higgs as wormhole contact would provide this field. The bound state character of the boson states could be responsible for $T_p < 1$. For this option the Higgs contribution to fermion masses would be negligible.

A more plausible option is based on the identification of the Higgs like contribution in terms of the deviation of the ground state conformal weight from negative half integer. The negative ground state conformal weights in turn correspond to the squares of the generalized eigenvalues of the modified Dirac operator determined by the dynamics of Kähler action for preferred extremals.

A microscopic theory explaining the non-half integer contribution to the conformal weight follows from the identification of the physical elementary particles in terms of pairs of wormhole contacts with upper and lower throat pairs connected by Kähler magnetic flux tubes. This requires zero energy ontology, weak form of electric-magnetic duality, and twistor approach as theoretical ingredients. This gives also a nice connection with Higgs mechanism. TGD predicts scalar and pseudo scalar Higgs which correspond to SU(2) triplet and singlet and therefore same representations of SU(2) as electroweak gauge bosons. Higgs vacuum expectation is not needed and there are strong reasons to believe that also gauge bosons regarded usually as massless receive a small mass and scalar Higgs boson disappears completely from the spectrum. This could happen also for Higgsinos if they combine with gauginos to form massive fermions. Only pseudo scalar Higgs and its super partner would remain in the spectrum for this option unless they combine with possibly existing massless axial gauge bosons and their super partners to form massive states.

4.3.1 Partition functions are not changed

One must write Super Virasoro conditions for L_n and *both* G_n and G_n^\dagger rather than for L_n and G_n as in the case of the ordinary Super Virasoro algebra, and it is a priori not at all clear whether the partition functions for the Super Virasoro representations remain unchanged. This requirement is however crucial for the construction to work at all in the fermionic sector, since even the slightest changes for the degeneracies of the excited states can change light state to a state with mass of order m_0 in the p-adic thermodynamics.

Super conformal algebra

Super Virasoro algebra is generated by the bosonic the generators L_n (n is an integer valued index) and by the fermionic generators G_r , where r can be either integer (Ramond) or half odd integer (NS). G_r creates quark/lepton for $r > 0$ and antiquark/antilepton for $r < 0$. For $r = 0$, G_0 creates lepton and its Hermitian conjugate anti-lepton. The defining commutation and anti-commutation relations are the following:

$$\begin{aligned}
 [L_m, L_n] &= (m-n)L_{m+n} + \frac{c}{2}m(m^2-1)\delta_{m,-n} \ , \\
 [L_m, G_r] &= \left(\frac{m}{2} - r\right)G_{m+r} \ , \\
 [L_m, G_r^\dagger] &= \left(\frac{m}{2} - r\right)G_{m+r}^\dagger \ , \\
 \{G_r, G_s^\dagger\} &= 2L_{r+s} + \frac{c}{3}\left(r^2 - \frac{1}{4}\right)\delta_{m,-n} \ , \\
 \{G_r, G_s\} &= 0 \ , \\
 \{G_r^\dagger, G_s^\dagger\} &= 0 \ .
 \end{aligned} \tag{4.3.1}$$

By the inspection of these relations one finds some results of a great practical importance.

1. For the Ramond algebra G_0, G_1 and their Hermitian conjugates generate the $r \geq 0, n \geq 0$ part of the algebra via anti-commutations and commutations. Therefore all what is needed is to assume that Super Virasoro conditions are satisfied for these generators in case that G_0 and G_0^\dagger annihilate the ground state. Situation changes if the states are *not* annihilated by G_0 and G_0^\dagger since then one must assume the gauge conditions for both L_1, G_1 and G_1^\dagger besides the mass shell conditions associated with G_0 and G_0^\dagger , which however do not affect the number of the Super Virasoro excitations but give mass shell condition and constraints on the state in the cm spin degrees of freedom. This will be assumed in the following. Note that for the ordinary Super Virasoro only the gauge conditions for L_1 and G_1 are needed.
2. NS algebra is generated by $G_{1/2}$ and $G_{3/2}$ and their Hermitian conjugates (note that $G_{3/2}$ cannot be expressed as the commutator of L_1 and $G_{1/2}$) so that only the gauge conditions associated with these generators are needed. For the ordinary Super Virasoro only the conditions for $G_{1/2}$ and $G_{3/2}$ are needed.

Conditions guaranteing that partition functions are not changed

The conditions guaranteing the invariance of the partition functions in the transition to the modified algebra must be such that they reduce the number of the excitations and gauge conditions for a given conformal weight to the same number as in the case of the ordinary Super Virasoro.

1. The requirement that physical states are invariant under $G \leftrightarrow G^\dagger$ corresponds to the charge conjugation symmetry and is very natural. As a consequence, the gauge conditions for G and G^\dagger are not independent and their number reduces by a factor of one half and is the same as in the case of the ordinary Super Virasoro.
2. As far as the number of the thermal excitations for a given conformal weight is considered, the only remaining problem are the operators $G_n G_n^\dagger$, which for the ordinary Super Virasoro reduce to $G_n G_n = L_{2n}$ and do not therefore correspond to independent degrees of freedom. In present case this situation is achieved only if one requires

$$(G_n G_n^\dagger - G_n^\dagger G_n)|phys\rangle = 0 \ . \tag{4.3.2}$$

It is not clear whether this condition must be posed separately or whether it actually follows from the representation of the Super Virasoro algebra automatically.

Partition function for Ramond algebra

Under the assumptions just stated, the partition function for the Ramond states not satisfying any gauge conditions

$$Z(t) = 1 + 2t + 4t^2 + 8t^3 + 14t^4 + \dots \ , \tag{4.3.3}$$

which is identical to that associated with the ordinary Ramond type Super Virasoro.

For a Super Virasoro representation with $N = 5$ sectors, of main interest in TGD, one has

$$\begin{aligned} Z_N(t) &= Z^{N=5}(t) = \sum D(n)t^n \\ &= 1 + 10t + 60t^2 + 280t^3 + \dots \end{aligned} \quad (4.3.4)$$

The degeneracies for the states satisfying gauge conditions are given by

$$d(n) = D(n) - 2D(n-1) . \quad (4.3.5)$$

corresponding to the gauge conditions for L_1 and G_1 . Applying this formula one obtains for $N = 5$ sectors

$$d(0) = 1 , \quad d(1) = 8 , \quad d(2) = 40 , \quad d(3) = 160 . \quad (4.3.6)$$

The lowest order contribution to the p-adic mass squared is determined by the ratio

$$r(n) = \frac{D(n+1)}{D(n)} ,$$

where the value of n depends on the effective vacuum weight of the ground state fermion. Light state is obtained only provided the ratio is integer. The remarkable result is that for lowest lying states the ratio is integer and given by

$$r(1) = 8 , \quad r(2) = 5 , \quad r(3) = 4 . \quad (4.3.7)$$

It turns out that $r(2) = 5$ gives the best possible lowest order prediction for the charged lepton masses and in this manner one ends up with the condition $h_{vac} = -3$ for the tachyonic vacuum weight of Super Virasoro.

Partition function for NS algebra

For NS representations the calculation of the degeneracies of the physical states reduces to the calculation of the partition function for a single particle Super Virasoro

$$Z_{NS}(t) = \sum_n z(n/2)t^{n/2} . \quad (4.3.8)$$

Here $z(n/2)$ gives the number of Super Virasoro generators having conformal weight $n/2$. For a state with N active sectors (the sectors with a non-vanishing weight for a given ground state) the degeneracies can be read from the N-particle partition function expressible as

$$Z_N(t) = Z^N(t) . \quad (4.3.9)$$

Single particle partition function is given by the expression

$$Z(t) = 1 + t^{1/2} + t + 2t^{3/2} + 3t^2 + 4t^{5/2} + 5t^3 + \dots \quad (4.3.10)$$

Using this representation it is an easy task to calculate the degeneracies for the operators of conformal weight Δ acting on a state having N active sectors.

One can also derive explicit formulas for the degeneracies and calculation gives

$$\begin{aligned}
 D(0, N) &= 1 , & D(1/2, N) &= N , \\
 D(1, N) &= \frac{N(N+1)}{2} , & D(3/2, N) &= \frac{N}{6}(N^2 + 3N + 8) , \\
 D(2, N) &= \frac{N}{2}(N^2 + 2N + 3) , & D(5/2, N) &= 9N(N - 1) , \\
 D(3, N) &= 12N(N - 1) + 2N(N - 1) .
 \end{aligned} \tag{4.3.11}$$

as a function of the conformal weight $\Delta = 0, 1/2, \dots, 3$.

The number of states satisfying Super Virasoro gauge conditions created by the operators of a conformal weight Δ , when the number of the active sectors is N , is given by

$$d(\Delta, N) = D(\Delta, N) - D(\Delta - 1/2, N) - D(\Delta - 3/2, N) . \tag{4.3.12}$$

The expression derives from the observation that the physical states satisfying gauge conditions for $G^{1/2}$, $G^{3/2}$ satisfy the conditions for all Super Virasoro generators. For $T_p = 1$ light bosons correspond to the integer values of $d(\Delta + 1, N)/d(\Delta, N)$ in case that massless states correspond to thermal excitations of conformal weight Δ : they are obtained for $\Delta = 0$ only (massless ground state). This is what is required since the thermal degeneracy of the light boson ground state would imply a corresponding factor in the energy density of the black body radiation at very high temperatures. For the physically most interesting nontrivial case with $N = 2$ two active sectors the degeneracies are

$$d(0, 2) = 1 , \quad d(1, 2) = 1 , \quad d(2, 2) = 3 , \quad d(3, 2) = 4 . \tag{4.3.13}$$

N, Δ	0	1/2	1	3/2	2	5/2	3
2	1	1	1	3	3	4	4
3	1	2	3	9	11		
4	1	3	5	19	26		
5	1	4	10	24	150		

Table 3. Degeneracies $d(\Delta, N)$ of the operators satisfying NS type gauge conditions as a function of the number N of the active sectors and of the conformal weight Δ of the operator. Only those degeneracies, which are needed in the mass calculation for bosons assuming that they correspond to N-S representations are listed.

4.3.2 Fundamental length and mass scales

The basic difference between quantum TGD and super-string models is that the size of CP_2 is not of order Planck length but much larger: of order $10^{3.5}$ Planck lengths. This conclusion is forced by several consistency arguments, the mass scale of electron, and by the cosmological data allowing to fix the string tension of the cosmic strings which are basic structures in TGD inspired cosmology.

The relationship between CP_2 radius and fundamental p-adic length scale

One can relate CP_2 'cosmological constant' to the p-adic mass scale: for $k_L = 1$ one has

$$m_0^2 = \frac{m_1^2}{k_L} = m_1^2 = 2\Lambda . \tag{4.3.14}$$

$k_L = 1$ results also by requiring that p-adic thermodynamics leaves charged leptons light and leads to optimal lowest order prediction for the charged lepton masses. Λ denotes the 'cosmological constant' of CP_2 (CP_2 satisfies Einstein equations $G^{\alpha\beta} = \Lambda g^{\alpha\beta}$ with cosmological term).

The real counterpart of the p-adic thermal expectation for the mass squared is sensitive to the choice of the unit of p-adic mass squared which is by definition mapped as such to the real unit in canonical identification. Thus an important factor in the p-adic mass calculations is the correct identification of the p-adic mass squared scale, which corresponds to the mass squared unit and hence to the unit of the p-adic numbers. This choice does not affect the spectrum of massless states but can affect the spectrum of light states in case of intermediate gauge bosons.

1. For the choice

$$M^2 = m_0^2 \leftrightarrow 1 \tag{4.3.15}$$

the spectrum of L_0 is integer valued.

2. The requirement that all sufficiently small mass squared values for the color partial waves are mapped to real integers, would fix the value of p-adic mass squared unit to

$$M^2 = \frac{m_0^2}{3} \leftrightarrow 1 . \tag{4.3.16}$$

For this choice the spectrum of L_0 comes in multiples of 3 and it is possible to have a first order contribution to the mass which cannot be of thermal origin (say $m^2 = p$). This indeed seems to happen for electro-weak gauge bosons.

p-Adic mass calculations allow to relate m_0 to electron mass and to Planck mass by the formula

$$\begin{aligned} \frac{m_0}{m_{Pl}} &= \frac{1}{\sqrt{5 + Y_e}} \times 2^{127/2} \times \frac{m_e}{m_{Pl}} , \\ m_{Pl} &= \frac{1}{\sqrt{\hbar G}} . \end{aligned} \tag{4.3.17}$$

For $Y_e = 0$ this gives $m_0 = .2437 \times 10^{-3} m_{Pl}$.

This means that CP_2 radius R defined by the length $L = 2\pi R$ of CP_2 geodesic is roughly $10^{3.5}$ times the Planck length. More precisely, using the relationship

$$\Lambda = \frac{3}{2R^2} = M^2 = m_0^2 ,$$

one obtains for

$$L = 2\pi R = 2\pi \sqrt{\frac{3}{2}} \frac{1}{m_0} \simeq 3.1167 \times 10^4 \sqrt{\hbar G} \text{ for } Y_e = 0 . \tag{4.3.18}$$

The result came as a surprise: the first belief was that CP_2 radius is of order Planck length. It has however turned out that the new identification solved elegantly some long standing problems of TGD.

Y_e	0	.5	.7798
$(m_0/m_{Pl})10^3$.2437	.2323	.2266
$K_R \times 10^{-7}$	2.5262	2.7788	2.9202
$(L_R/\sqrt{\hbar G}) \times 10^{-4}$	3.1580	3.3122	3.3954
$K \times 10^{-7}$	2.4606	2.4606	2.4606
$(L/\sqrt{\hbar G}) \times 10^{-4}$	3.1167	3.1167	3.1167
K_R/K	1.0267	1.1293	1.1868

Table 1. Table gives the values of the ratio $K_R = R^2/G$ and CP_2 geodesic length $L = 2\pi R$ for $Y_e \in \{0, 0.5, 0.7798\}$. Also the ratio of K_R/K , where $K = 2 \times 3 \times 5 \times 7 \times 11 \times 13 \times 17 \times 19 \times 23 \times 2^{-3} * (15/17)$ is rational number producing R^2/G approximately is given.

The value of top quark mass favors $Y_e = 0$ and $Y_e = .5$ is largest value of Y_e marginally consistent with the limits on the value of top quark mass.

CP_2 radius as the fundamental p-adic length scale

The identification of CP_2 radius as the fundamental p-adic length scale is forced by the Super Virasoro invariance. The pleasant surprise was that the identification of the CP_2 size as the fundamental p-adic length scale rather than Planck length solved many long standing problems of older TGD.

1. The earliest formulation predicted cosmic strings with a string tension larger than the critical value giving the angle deficit 2π in Einstein's equations and thus excluded by General Relativity. The corrected value of CP_2 radius predicts the value k/G for the cosmic string tension with k in the range $10^{-7} - 10^{-6}$ as required by the TGD inspired model for the galaxy formation solving the galactic dark matter problem.
2. In the earlier formulation there was no idea as how to derive the p-adic length scale $L \sim 10^{3.5} \sqrt{\hbar G}$ from the basic theory. Now this problem becomes trivial and one has to predict gravitational constant in terms of the p-adic length scale. This follows in principle as a prediction of quantum TGD. In fact, one can deduce G in terms of the p-adic length scale and the action exponential associated with the CP_2 extremal and gets a correct value if α_K approaches fine structure constant at electron length scale (due to the fact that electromagnetic field equals to the Kähler field if Z^0 field vanishes).

Besides this, one obtains a precise prediction for the dependence of the Kähler coupling strength on the p-adic length scale by requiring that the gravitational coupling does not depend on the p-adic length scale. p-Adic prime p in turn has a nice physical interpretation: the critical value of α_K is same for the zero modes with given p . As already found, the construction of graviton state allows to understand the small value of the gravitational constant in terms of a de-coherence caused by multi-p fractality reducing the value of the gravitational constant from L_p^2 to G .

3. p-Adic length scale is also the length scale at which super-symmetry should be restored in standard super-symmetric theories. In TGD this scale corresponds to the transition to Euclidian field theory for CP_2 type extremals. There are strong reasons to believe that sparticles are however absent and that super-symmetry is present only in the sense that super-generators have complex conformal weights with $Re(h) = \pm 1/2$ rather than $h = 0$. The action of this super-symmetry changes the mass of the state by an amount of order CP_2 mass.

4.3.3 Color degrees of freedom

The ground states for the Super Virasoro representations correspond to spinor harmonics in $M^4 \times CP_2$ characterized by momentum and color quantum numbers. The correlation between color and electro-weak quantum numbers is wrong for the spinor harmonics and these states would be also hyper-massive. The super-symplectic generators allow to build color triplet states having negative vacuum conformal weights, and their values are such that p-adic massivation is consistent with the predictions of the earlier model differing from the recent one in the quark sector. In the following the construction and the properties of the color partial waves for fermions and bosons are considered. The discussion follows closely to the discussion of [17].

SKM algebra and counterpart of Super Virasoro conditions

The geometric part of SKM algebra is defined as an algebra respecting the light-likeness of the partonic 3-surface. It consists of X^3 -local conformal transformations of M_{\pm}^4 and $SU(3)$ -local $SU(3)$ rotations. The requirement that generators have well defined radial conformal weight with respect to the lightlike coordinate r of X^3 restricts M^4 conformal transformations to the group $SO(3) \times E^3$. This involves choice of preferred time coordinate. If the preferred M^4 coordinate is chosen to correspond to a preferred light-like direction in δM_{\pm}^4 characterizing the theory, a reduction to $SO(2) \times E^2$ more familiar from string models occurs. The algebra decomposes into a direct sum of sub-algebras mapped to themselves by the Kac-Moody algebra generated by functions depending on r only. SKM algebra contains also $U(2)_{ew}$ Kac-Moody algebra acting as holonomies of CP_2 and having no bosonic counterpart.

p-Adic mass calculations require $N = 5$ sectors of super-conformal algebra. These sectors correspond to the 5 tensor factors for the $SO(3) \times E^3 \times SU(3) \times U(2)_{ew}$ (or $SO(2) \times E^2 \times SU(3) \times U(2)_{ew}$) decomposition of the SKM algebra to gauge symmetries of gravitation, color and electro-weak interactions. These symmetries act on the intersections $X^2 = X_l^3 \cap X^7$ of 3-D light like causal determinants

(CDs) X_l^3 and 7-D light like CDs $X^7 = \delta M_+^4 \times CP_2$. This constraint leaves only the 2 transversal M^4 degrees of freedom since the translations in light like directions associated with X_l^3 and δM_+^4 are eliminated.

The algebra differs from the standard one in that super generators $G(z)$ carry lepton and quark numbers are not Hermitian as in super-string models (Majorana conditions are not satisfied). The counterparts of Ramond representations correspond to zero modes of a second quantized spinor field with vanishing radial conformal weight. Non-zero modes with generalized eigenvalues $\lambda = 1/2 + iy$, $y = \sum_k n_k y_k$, $n_k \geq 0$, of the modified Dirac operator with $s_k = 1/2 + iy_k$ a zero or Riemann Zeta, define ground states of N-S type super Virasoro representations.

What is new is the imaginary part of conformal weight which means that the arrow of geometric time manifests itself via the sign of the imaginary part y already at elementary particle level. More concretely, positive energy particle propagating to the geometric future is not equivalent with negative energy particle propagating to the geometric past. The strange properties of the phase conjugate provide concrete physical demonstration of this difference. p-Adic mass calculations suggest the interpretation of y in terms of a decay width of the particle.

The Ramond or N-S type Virasoro conditions satisfied by the physical states in string model approach are replaced by the formulas expressing mass squared as a conformal weight. The condition is not equivalent with super Virasoro conditions since four-momentum does not appear in super Virasoro generators. It seems possible to assume that the commutator algebra $[SKM, SC]$ and the commutator of $[SKMV, SSV]$ of corresponding Super Virasoro algebras annihilate physical states. This would give rise to the analog of Super Virasoro conditions which could be seen as a Dirac equation in the world of classical worlds.

1. CP_2 CM degrees of freedom

Important element in the discussion are center of mass degrees of freedom parameterized by imbedding space coordinates. By the effective 2-dimensionality it is indeed possible to assign to partons momenta and color partial waves and they behave effectively as free particles. In fact, the technical problem of the earlier scenario was that it was not possible to assign symmetry transformations acting only on the boundary components of 3-surface.

One can assign to each eigen state of color quantum numbers a color partial wave in CP_2 degrees of freedom. Thus color quantum numbers are not spin like quantum numbers in TGD framework except effectively in the length scales much longer than CP_2 length scale. The correlation between color partial waves and electro-weak quantum numbers is not physical in general: only the covariantly constant right handed neutrino has vanishing color.

2. Mass formula, and condition determining the effective string tension

Mass squared eigenvalues are given by

$$M^2 = m_{CP_2}^2 + kL_0 . \quad (4.3.19)$$

The contribution of CP_2 spinor Laplacian to the mass squared operator is in general not integer valued.

The requirement that mass squared spectrum is integer valued for color partial waves possibly representing light states fixes the possible values of k determining the effective string tension modulo integer. The value $k = 1$ is the only possible choice. The earlier choice $k_L = 1$ and $k_q = 2/3$, $k_B = 1$ gave integer conformal weights for the lowest possible color partial waves. The assumption that the total vacuum weight h_{vac} is conserved in particle vertices implied $k_B = 1$.

General construction of solutions of Dirac operator of H

The construction of the solutions of massless spinor and other d'Alembertians in $M_+^4 \times CP_2$ is based on the following observations.

1. d'Alembertian corresponds to a massless wave equation $M^4 \times CP_2$ and thus Kaluza-Klein picture applies, that is M_+^4 mass is generated from the momentum in CP_2 degrees of freedom. This implies mass quantization:

$$M^2 = M_n^2 ,$$

where M_n^2 are eigenvalues of CP_2 Laplacian. Here of course, ordinary field theory is considered. In TGD the vacuum weight changes mass squared spectrum.

2. In order to get a respectable spinor structure in CP_2 one must couple CP_2 spinors to an odd integer multiple of the Kähler potential. Leptons and quarks correspond to $n = 3$ and $n = 1$ couplings respectively. The spectrum of the electromagnetic charge comes out correctly for leptons and quarks.
3. Right handed neutrino is covariantly constant solution of CP_2 Laplacian for $n = 3$ coupling to Kähler potential whereas right handed 'electron' corresponds to the covariantly constant solution for $n = -3$. From the covariant constancy it follows that all solutions of the spinor Laplacian are obtained from these two basic solutions by multiplying with an appropriate solution of the scalar Laplacian coupled to Kähler potential with such a coupling that a correct total Kähler charge results. Left handed solutions of spinor Laplacian are obtained simply by multiplying right handed solutions with CP_2 Dirac operator: in this operation the eigenvalues of the mass squared operator are obviously preserved.
4. The remaining task is to solve scalar Laplacian coupled to an arbitrary integer multiple of Kähler potential. This can be achieved by noticing that the solutions of the massive CP_2 Laplacian can be regarded as solutions of S^5 scalar Laplacian. S^5 can indeed be regarded as a circle bundle over CP_2 and massive solutions of CP_2 Laplacian correspond to the solutions of S^5 Laplacian with $\exp(is\tau)$ dependence on S^1 coordinate such that s corresponds to the coupling to the Kähler potential:

$$s = n/2 .$$

Thus one obtains

$$D_5^2 = (D_\mu - iA_\mu \partial_\tau)(D^\mu - iA^\mu \partial_\tau) + \partial_\tau^2 \quad (4.3.20)$$

so that the eigen values of CP_2 scalar Laplacian are

$$m^2(s) = m_5^2 + s^2 \quad (4.3.21)$$

for the assumed dependence on τ .

5. What remains to do, is to find the spectrum of S^5 Laplacian and this is an easy task. All solutions of S^5 Laplacian can be written as homogenous polynomial functions of C^3 complex coordinates Z^k and their complex conjugates and have a decomposition into the representations of $SU(3)$ acting in natural manner in C^3 .
6. The solutions of the scalar Laplacian belong to the representations $(p, p + s)$ for $s \geq 0$ and to the representations $(p + |s|, p)$ of $SU(3)$ for $s \leq 0$. The eigenvalues $m^2(s)$ and degeneracies d are

$$\begin{aligned} m^2(s) &= \frac{2\Lambda}{3} [p^2 + (|s| + 2)p + |s|] , \quad p > 0 , \\ d &= \frac{1}{2} (p + 1)(p + |s| + 1)(2p + |s| + 2) . \end{aligned} \quad (4.3.22)$$

Λ denotes the 'cosmological constant' of CP_2 ($R_{ij} = \Lambda s_{ij}$).

Solutions of the leptonic spinor Laplacian

Right handed solutions of the leptonic spinor Laplacian are obtained from the ansatz of form

$$\nu_R = \Phi_{s=0} \nu_R^0 ,$$

where u_R is covariantly constant right handed neutrino and Φ scalar with vanishing Kähler charge. Right handed 'electron' is obtained from the ansatz

$$e_R = \Phi_{s=3} e_R^0 ,$$

where e_R^0 is covariantly constant for $n = -3$ coupling to Kähler potential so that scalar function must have Kähler coupling $s = n/2 = 3$ in order to get a correct Kähler charge. The d'Alembert equation reduces to

$$\begin{aligned} (D_\mu D^\mu - (1 - \epsilon)\Lambda)\Phi &= -m^2\Phi , \\ \epsilon(\nu) &= 1 , \quad \epsilon(e) = -1 . \end{aligned} \tag{4.3.23}$$

The two additional terms correspond to the curvature scalar term and $J_{kl}\Sigma^{kl}$ terms in spinor Laplacian. The latter term is proportional to Kähler coupling and of different sign for ν and e , which explains the presence of the sign factor ϵ in the formula.

Right handed neutrinos correspond to (p, p) states with $p \geq 0$ with mass spectrum

$$\begin{aligned} m^2(\nu) &= \frac{m_1^2}{3} [p^2 + 2p] , \quad p \geq 0 , \\ m_1^2 &\equiv 2\Lambda . \end{aligned} \tag{4.3.24}$$

Right handed 'electrons' correspond to $(p, p+3)$ states with mass spectrum

$$m^2(e) = \frac{m_1^2}{3} [p^2 + 5p + 6] , \quad p \geq 0 . \tag{4.3.25}$$

Left handed solutions are obtained by operating with CP_2 Dirac operator on right handed solutions and have the same mass spectrum and representational content as right handed leptons with one exception: the action of the Dirac operator on the covariantly constant right handed neutrino ($(p=0, p=0)$ state) annihilates it.

Quark spectrum

Quarks correspond to the second conserved H -chirality of H -spinors. The construction of the color partial waves for quarks proceeds along similar lines as for leptons. The Kähler coupling corresponds to $n = 1$ (and $s = 1/2$) and right handed U type quark corresponds to a right handed neutrino. U quark type solutions are constructed as solutions of form

$$U_R = u_R \Phi_{s=1} ,$$

where u_R possesses the quantum numbers of covariantly constant right handed neutrino with Kähler charge $n = 3$ ($s = 3/2$). Hence Φ_s has $s = -1$. For D_R one has

$$D_R = d_r \Phi_{s=2} .$$

d_R has $s = -3/2$ so that one must have $s = 2$. For U_R the representations $(p+1, p)$ with triality one are obtained and $p = 0$ corresponds to color triplet. For D_R the representations $(p, p+2)$ are obtained and color triplet is missing from the spectrum ($p = 0$ corresponds to $\bar{6}$).

The CP_2 contributions to masses are given by the formula

$$\begin{aligned}
 m^2(U, p) &= \frac{m_1^2}{3} [p^2 + 3p + 2] \quad , \quad p \geq 0 \quad , \\
 m^2(D, p) &= \frac{m_1^2}{3} [p^2 + 4p + 4] \quad , \quad p \geq 0 \quad .
 \end{aligned}
 \tag{4.3.26}$$

Left handed quarks are obtained by applying Dirac operator to right handed quark states and mass formulas and color partial wave spectrum are the same as for right handed quarks.

The color contributions to p-adic mass squared are integer valued if $m_0^2/3$ is taken as a fundamental p-adic unit of mass squared. This choice has an obvious relevance for p-adic mass calculations since canonical identification does not commute with a division by integer. More precisely, the images of number xp in canonical identification has a value of order 1 when x is a non-trivial rational whereas for $x = np$ the value is n/p and extremely is small for physically interesting primes. This choice does not however affect the spectrum of massless states but can affect the spectrum of light states in case of electro-weak gauge bosons.

4.3.4 Spectrum of elementary particles

The assumption that $k = 1$ holds true for all particles forces to modify the earlier construction of quark states. This turns out to be possible without affecting the p-adic mass calculations whose outcome depend in an essential manner on the ground state conformal weights h_{gr} of the fermions (which can be negative).

Leptonic spectrum

For $k = 1$ the leptonic mass squared is integer valued in units of m_0^2 only for the states satisfying

$$p \bmod 3 \neq 2 \quad .$$

Only these representations can give rise to massless states. Neutrinos correspond to (p, p) representations with $p \geq 1$ whereas charged leptons correspond to $(p, p + 3)$ representations. The earlier mass calculations demonstrate that leptonic masses can be understood if the ground state conformal weight is $h_{gr} = -1$ for charged leptons and $h_{gr} = -2$ for neutrinos.

The contribution of color partial wave to conformal weight is $h_c = (p^2 + 2p)/3$, $p \geq 1$, for neutrinos and $p = 1$ gives $h_c = 1$ (octet). For charged leptons $h_c = (p^2 + 5p + 6)/3$ gives $h_c = 2$ for $p = 0$ (decuplet). In both cases super-symplectic operator O must have a net conformal weight $h_{sc} = -3$ to produce a correct conformal weight for the ground state. p-adic considerations suggests the use of operators O with super-symplectic conformal weight $z = -1/2 - i \sum n_k y_k$, where $s_k = 1/2 + i y_k$ corresponds to zero of Riemann ζ . If the operators in question are color Hamiltonians in octet representation net super-symplectic conformal weight $h_{sc} = -3$ results. The tensor product of two octets with conjugate super-symplectic conformal weights contains both octet and decuplet so that singlets are obtained. What strengthens the hopes that the construction is not adhoc is that the same operator appears in the construction of quark states too.

Right handed neutrino remains essentially massless. $p = 0$ right handed neutrino does not however generate $N = 1$ space-time (or rather, imbedding space) super symmetry so that no sparticles are predicted. The breaking of the electro-weak symmetry at the level of the masses comes out basically from the anomalous color electro-weak correlation for the Kaluza-Klein partial waves implying that the weights for the ground states of the fermions depend on the electromagnetic charge of the fermion. Interestingly, TGD predicts leptohadron physics based on color excitations of leptons and color bound states of these excitations could correspond topologically condensed on string like objects but not fundamental string like objects.

Spectrum of quarks

Earlier arguments [17] related to a model of CKM matrix as a rational unitary matrix suggested that the string tension parameter k is different for quarks, leptons, and bosons. The basic mass formula read as

$$M^2 = m_{CP_2}^2 + kL_0 .$$

The values of k were $k_q = 2/3$ and $k_L = k_B = 1$. The general theory however predicts that $k = 1$ for all particles.

1. By earlier mass calculations and construction of CKM matrix the ground state conformal weights of U and D type quarks must be $h_{gr}(U) = -1$ and $h_{gr}(D) = 0$. The formulas for the eigenvalues of CP_2 spinor Laplacian imply that if m_0^2 is used as unit, color conformal weight $h_c \equiv m_{CP_2}^2$ is integer for $p \bmod = \pm 1$ for U type quark belonging to $(p+1, p)$ type representation and obeying $h_c(U) = (p^2 + 3p + 2)/3$ and for $p \bmod 3 = 1$ for D type quark belonging $(p, p+2)$ type representation and obeying $h_c(D) = (p^2 + 4p + 4)/3$. Only these states can be massless since color Hamiltonians have integer valued conformal weights.
2. In the recent case $p = 1$ states correspond to $h_c(U) = 2$ and $h_c(D) = 3$. $h_{gr}(U) = -1$ and $h_{gr}(D) = 0$ reproduce the previous results for quark masses required by the construction of CKM matrix. This forces the super-symplectic operator O to compensate the anomalous color to have a net conformal weight $h_{sc} = -3$ just as in the leptonic case. The facts that the values of p are minimal for spinor harmonics and the super-symplectic operator is same for both quarks and leptons suggest that the construction is not had hoc. The real justification would come from the demonstration that $h_{sc} = -3$ defines null state for SSV: this would also explain why h_{sc} would be same for all fermions.
3. It would seem that the tensor product of the spinor harmonic of quarks (as also leptons) with Hamiltonians gives rise to a large number of exotic colored states which have same thermodynamical mass as ordinary quarks (and leptons). Why these states have smaller values of p-adic prime than ordinary quarks and leptons, remains a challenge for the theory. Note that the decay widths of intermediate gauge bosons pose strong restrictions on the possible color excitations of quarks. On the other hand, the large number of fermionic color exotics can spoil the asymptotic freedom, and it is possible to have an entire p-adic length scale hierarchy of QCDs existing only in a finite length scale range without affecting the decay widths of gauge bosons.

The following table summarizes the color conformal weights and super-symplectic vacuum conformal weights for the elementary particles.

	L	ν_L	U	D	W	γ, G, g
h_{vac}	-3	-3	-3	-3	-2	0
h_c	2	1	2	3	2	0

Table 2. The values of the parameters h_{vac} and h_c assuming that $k = 1$. The value of $h_{vac} \leq -h_c$ is determined from the requirement that p-adic mass calculations give best possible fit to the mass spectrum.

Photon, graviton and gluon

For photon, gluon and graviton the conformal weight of the $p = 0$ ground state is $h_{gr} = h_{vac} = 0$. The crucial condition is that $h = 0$ ground state is non-degenerate: otherwise one would obtain several physically more or less identical photons and this would be seen in the spectrum of black-body radiation. This occurs if one can construct several ground states not expressible in terms of the action of the Super Virasoro generators.

Masslessness or approximate masslessness requires low enough temperature $T_p = 1/n$, $n > 1$ at least and small enough value of the possible contribution coming from the ground state conformal weight.

In NS thermodynamics the only possibility to get exactly massless states in thermal sense is to have $\Delta = 0$ state with one active sector so that NS thermodynamics becomes trivial due to the absence of the thermodynamical excitations satisfying the gauge conditions. For neutral gauge bosons this is indeed achieved. For $T_p = 1/2$, which is required by the mass spectrum of intermediate gauge bosons, the thermal contribution to the mass squared is however extremely small even for W boson.

4.3.5 Some probabilistic considerations

There are uniqueness problems related to the mapping of p-adic probabilities to real ones. These problems find a nice resolution from the requirement that the map respects probability conservation. The implied modification of the original mapping does not change measurably the predictions for the masses of light particles.

How unique the map of p-adic probabilities and mass squared values are mapped to real numbers is?

The mapping of p-adic thermodynamical probabilities and mass squared values to real numbers is not completely unique.

1. Canonical identification $I : \sum x_n p^n \rightarrow \sum x_n p^{-n}$ takes care of this mapping but does not respect the sum of probabilities so that the real images $I(p_n)$ of the probabilities must be normalized. This is a somewhat alarming feature.
2. The modification of the canonical identification mapping rationals by the formula $I(r/s) = I(r)/I(s)$ has appeared naturally in various applications, in particular because it respects unitarity of unitary matrices with rational elements with $r < p, s < p$. In the case of p-adic thermodynamic the formula $I(g(n)p^n/Z) \rightarrow I(g(n)p^n)/I(Z)$ would be very natural although Z need not be rational anymore. For $g(n) < p$ the real counterparts of the p-adic probabilities would sum up to one automatically for this option. One cannot deny that this option is more convincing than the original one. The generalization of this formula to map p-adic mass squared to a real one is obvious.
3. Options 1) and 2) differ dramatically when the $n = 0$ massless ground state has ground state degeneracy $D > 1$. For option 1) the real mass is predicted to be of order CP_2 mass whereas for option 2) it would be by a factor $1/D$ smaller than the minimum mass predicted by the option a). Thus option 2) would predict a large number of additional exotic states. For those states which are light for option 1), the two options make identical predictions as far as the significant two lowest order terms are considered. Hence this interpretation would not change the predictions of the p-adic mass calculations in this respect. Option 2) is definitely more in accord with the real physics based intuitions and the main role of p-adic thermodynamics would be to guarantee the quantization of the temperature and fix practically uniquely the spectrum of the "Hamiltonian".

Under what conditions the mapping of p-adic ensemble probabilities to real probabilities respects probability conservation?

One can consider also a more general situation. Assume that one has an ensemble consisting of independent elementary events such that the number of events of type i is N_i . The probabilities are given by $p_i = N_i/N$ and $N = \sum N_i$ is the total number of elementary events. Even in the case that N is infinite as a real number it is natural to map the p-adic probabilities to their real counterparts using the rational canonical identification $I(p_i) = I(N_i)/I(N)$. Of course, N_i and N exist as well defined p-adic numbers under very stringent conditions only.

The question is under what conditions this map respects probability conservation. The answer becomes obvious by looking at the pinary expansions of N_i and N . If the integers N_i (possibly infinite as real integers) have pinary expansions having no common pinary digits, the sum of probabilities is conserved in the map. Note that this condition can assign also to a finite ensemble with finite number of a unique value of p .

This means that the selection of a basis for independent events corresponds to a decomposition of the set of integers labelling pinary digits to disjoint sets and brings in mind the selection of orthonormalized basis of quantum states in quantum theory. What is physically highly non-trivial that this "orthogonalization" alone puts strong constraints on probabilities of the allowed elementary events. One can say that the probabilities define distributions of pinary digits analogous to non-negative probability amplitudes in the space of integers labelling pinary digits, and the probabilities of independent events must be orthogonal with respect to the inner product defined by point-wise multiplication in the space of pinary digits.

p-Adic thermodynamics for which Boltzman weights $g(E)exp(-E/T)$ are replaced by $g(E)p^{E/T}$ such that one has $g(E) < p$ and E/T is integer valued, satisfies this constraint. The quantization of E/T to integer values implies quantization of both T and "energy" spectrum and forces so called super conformal invariance in TGD applications, which is indeed a basic symmetry of the theory.

There are infinitely many ways to choose the elementary events and each choice corresponds to a decomposition of the infinite set of integers n labelling the powers of p to disjoint subsets. These subsets can be also infinite. One can assign to this kind of decomposition a resolution which is the poorer the larger the subsets involved are. p-Adic thermodynamics would represent the situation in which the resolution is maximal since each set contains only single binary digit. Note the analogy with the basis of completely localized wave functions in a lattice.

4.4 Modular contribution to the mass squared

The success of the p-adic mass calculations gives convincing support for the generation-genus correspondence. The basic physical picture is following.

1. Fermionic mass squared is dominated by partonic contribution, which is sum of cm and modular contributions: $M^2 = M^2(cm) + M^2(mod)$. Here 'cm' refers to the thermal contribution. Modular contribution can be assumed to depend on the genus of the boundary component only.
2. If Higgs contribution for diagonal (g, g) bosons (singlets with respect to "topological" $SU(3)$) dominates, the genus dependent contribution can be assumed to be negligible. This should be due to the bound state character of the wormhole contacts reducing thermal motion and thus the p-adic temperature.
3. Modular contribution to the mass squared can be estimated apart from an overall proportionality constant. The mass scale of the contribution is fixed by the p-adic length scale hypothesis. Elementary particle vacuum functionals are proportional to a product of all even theta functions and their conjugates, the number of even theta functions and their conjugates being $2N(g) = 2^g(2^g + 1)$. Also the thermal partition function must also be proportional to $2N(g)$:th power of some elementary partition function. This implies that thermal/ quantum expectation $M^2(mod)$ must be proportional to $2N(g)$. Since single handle behaves effectively as particle, the contribution must be proportional to genus g also. The success of the resulting mass formula encourages the belief that the argument is essentially correct.

The challenge is to construct theoretical framework reproducing the modular contribution to mass squared. There are two alternative manners to understand the origin modular contribution.

1. The realization that super-symplectic algebra is relevant for elementary particle physics leads to the idea that two thermodynamics are involved with the calculation of the vacuum conformal weight as a thermal expectation. The first thermodynamics corresponds to Super Kac-Moody algebra and second thermodynamics to super-symplectic algebra. This approach allows a first principle understanding of the origin and general form of the modular contribution without any need to introduce additional structures in modular degrees of freedom. The very fact that super-symplectic algebra does not commute with the modular degrees of freedom explains the dependence of the super-symplectic contribution on moduli.
2. The earlier approach was based on the idea that the modular contribution could be regarded as a quantum mechanical expectation value of the Virasoro generator L_0 for the elementary particle vacuum functional. Quantum treatment would require generalization the concepts of the moduli space and theta function to the p-adic context and finding an acceptable definition of the Virasoro generator L_0 in modular degrees of freedom. The problem with this interpretation is that it forces to introduce, not only Virasoro generator L_0 , but the entire super Virasoro algebra in modular degrees of freedom. One could also consider of interpreting the contribution of modular degrees of freedom to vacuum conformal weight as being analogous to that of CP_2 Laplacian but also this would raise the challenge of constructing corresponding Dirac operator. Obviously this approach has become obsolete.

The thermodynamical treatment taking into account the constraints from that p-adicization is possible might go along following lines.

1. In the real case the basic quantity is the thermal expectation value $h(M)$ of the conformal weight as a function of moduli. The average value of the deviation $\Delta h(M) = h(M) - h(M_0)$ over moduli space \mathcal{M} must be calculated using elementary particle vacuum functional as a modular invariant partition function. Modular invariance is achieved if this function is proportional to the logarithm of elementary particle vacuum functional: this reproduces the qualitative features basic formula for the modular contribution to the conformal weight. p-Adicization leads to a slight modification of this formula.
2. The challenge of algebraically continuing this calculation to the p-adic context involves several sub-tasks. The notions of moduli space \mathcal{M}_p and theta function must be defined in the p-adic context. An appropriately defined logarithm of the p-adic elementary particle vacuum functional should determine $\Delta h(M)$. The average of $\Delta h(M)$ requires an integration over \mathcal{M}_p . The problems related to the definition of this integral could be circumvented if the integral in the real case could be reduced to an algebraic expression, or if the moduli space is discrete in which case integral could be replaced by a sum.
3. The number theoretic existence of the p-adic Θ function leads to the quantization of the moduli so that the p-adic moduli space is discretized. Accepting the sharpened form of Riemann hypothesis [32], the quantization means that the imaginary *resp.* real parts of the moduli are proportional to integers *resp.* combinations of imaginary parts of zeros of Riemann Zeta. This quantization could occur also for the real moduli for the maxima of Kähler function. This reduces the problematic p-adic integration to a sum and the resulting sum defining $\langle \Delta h \rangle$ converges extremely rapidly for physically interesting primes so that only the few lowest terms are needed.

4.4.1 Conformal symmetries and modular invariance

The full SKM invariance means that the super-conformal fields depend only on the conformal moduli of 2-surface characterizing the conformal equivalence class of the 2-surface. This means that all induced metrics differing by a mere Weyl scaling have same moduli. This symmetry is extremely powerful since the space of moduli is finite-dimensional and means that the entire infinite-dimensional space of deformations of parton 2-surface X^2 degenerates to a finite-dimensional moduli spaces under conformal equivalence. Obviously, the configurations of given parton correspond to a fiber space having moduli space as a base space. Super-symplectic degrees of freedom could break conformal invariance in some appropriate sense.

Conformal and SKM symmetries leave moduli invariant

Conformal transformations and super Kac Moody symmetries must leave the moduli invariant. This means that they induce a mere Weyl scaling of the induced metric of X^2 and thus preserve its non-diagonal character $ds^2 = g_{z\bar{z}} dz d\bar{z}$. This is indeed true if

1. the Super Kac Moody symmetries are holomorphic isometries of $X^7 = \delta M_{\pm}^4 \times CP_2$ made local with respect to the complex coordinate z of X^2 , and
2. the complex coordinates of X^7 are holomorphic functions of z .

Using complex coordinates for X^7 the infinitesimal generators can be written in the form

$$J^{An} = z^n j^{Ak} D_k + \bar{z}^n j^{A\bar{k}} D_{\bar{k}} . \quad (4.4.1)$$

The intuitive picture is that it should be possible to choose X^2 freely. It is however not always possible to choose the coordinate z of X^2 in such a manner that X^7 coordinates are holomorphic functions of z since a consistency of inherent complex structure of X^2 with that induced from X^7 is required. Geometrically this is like meeting of two points in the space of moduli.

Lorentz boosts produce new inequivalent choices of S^2 with their own complex coordinate: this set of complex structures is parameterized by the hyperboloid of future light cone (Lobatchevski space or

mass shell), but even this is not enough. The most plausible manner to circumvent the problem is that only the maxima of Kähler function correspond to the holomorphic situation so that super-symplectic algebra representing quantum fluctuations would induce conformal anomaly.

The isometries of δM_+^4 are in one-one correspondence with conformal transformations

For CP_2 factor the isometries reduce to $SU(3)$ group acting also as symplectic transformations. For $\delta M_+^4 = S^2 \times R_+$ one might expect that isometries reduce to Lorentz group containing rotation group of $SO(3)$ as conformal isometries. If r_M corresponds to a macroscopic length scale, then X^2 has a finite sized S^2 projection which spans a rather small solid angle so that group $SO(3)$ reduces in a good approximation to the group $E^2 \times SO(2)$ of translations and rotations of plane.

This expectation is however wrong! The light-likeness of δM_+^4 allows a dramatic generalization of the notion of isometry. The point is that the conformal transformations of S^2 induce a conformal factor $|df/dw|^2$ to the metric of δM_+^4 and the local radial scaling $r_M \rightarrow r_M/|df/dw|$ compensates it. Hence the group of conformal isometries consists of conformal transformations of S^2 with compensating radial scalings. This compensation of two kinds of conformal transformations is the deep geometric phenomenon which translates to the condition $L_{SC} - L_{SKM} = 0$ in the sub-space of physical states. Note that an analogous phenomenon occurs also for the light-like CDs X_l^3 with respect to the metrically 2-dimensional induced metric.

The X^2 -local radial scalings $r_M \rightarrow r_M(z, \bar{z})$ respect the conditions $g_{zz} = g_{\bar{z}\bar{z}} = 0$ so that a mere Weyl scaling leaving moduli invariant results. By multiplying the conformal isometries of δM_+^4 by z^n (z is used as a complex coordinate for X^2 and w as a complex coordinate for S^2) a conformal localization of conformal isometries would result. Kind of double conformal transformations would be in question. Note however that this requires that X^7 coordinates are holomorphic functions of X^2 coordinate. These transformations deform X^2 unlike the conformal transformations of X^2 . For X_l^3 similar local scalings of the light like coordinate leave the moduli invariant but lead out of X^7 .

Symplectic transformations break the conformal invariance

In general, infinitesimal symplectic transformations induce non-vanishing components $g_{zz}, g_{\bar{z}\bar{z}}$ of the induced metric and can thus change the moduli of X^2 . Thus the quantum fluctuations represented by super-symplectic algebra and contributing to the configuration space metric are in general moduli changing. It would be interesting to know explicitly the conditions (the number of which is the dimension of moduli space for a given genus), which guarantee that the infinitesimal symplectic transformation is moduli preserving.

4.4.2 The physical origin of the genus dependent contribution to the mass squared

Different p-adic length scales are not enough to explain the charged lepton mass ratios and an additional genus dependent contribution in the fermionic mass formula is required. The general form of this contribution can be guessed by regarding elementary particle vacuum functionals in the modular degrees of freedom as an analog of partition function and the modular contribution to the conformal weight as an analog of thermal energy obtained by averaging over moduli. p-Adic length scale hypothesis determines the overall scale of the contribution.

The exact physical origin of this contribution has remained mysterious but super-symplectic degrees of freedom represent a good candidate for the physical origin of this contribution. This would mean a sigh of relief since there would be no need to assign conformal weights, super-algebra, Dirac operators, Laplacians, etc.. with these degrees of freedom.

Thermodynamics in super-symplectic degrees of freedom as the origin of the modular contribution to the mass squared

The following general picture is the simplest found hitherto.

1. Elementary particle vacuum functionals are defined in the space of moduli of surfaces X^2 corresponding to the maxima of Kähler function. There some restrictions on X^2 . In particular, p-adic length scale poses restrictions on the size of X^2 . There is an infinite hierarchy of elementary

particle vacuum functionals satisfying the general constraints but only the lowest elementary particle vacuum functionals are assumed to contribute significantly to the vacuum expectation value of conformal weight determining the mass squared value.

2. The contribution of Super-Kac Moody thermodynamics to the vacuum conformal weight h coming from Virasoro excitations of the $h = 0$ massless state is estimated in the previous calculations and does not depend on moduli. The new element is that for a partonic 2-surface X^2 with given moduli, Virasoro thermodynamics is present also in super-symplectic degrees of freedom.

Super-symplectic thermodynamics means that, besides the ground state with $h_{gr} = -h_{SC}$ with minimal value of super-symplectic conformal weight h_{SC} , also thermal excitations of this state by super-symplectic Virasoro algebra having $h_{gr} = -h_{SC} - n$ are possible. For these ground states the SKM Virasoro generators creating states with net conformal weight $h = h_{SKM} - h_{SC} - n \geq 0$ have larger conformal weight so that the SKM thermal average h depends on n . It depends also on the moduli M of X^2 since the Beltrami differentials representing a tangent space basis for the moduli space \mathcal{M} do not commute with the super-symplectic algebra. Hence the thermally averaged SKM conformal weight h_{SKM} for given values of moduli satisfies

$$h_{SKM} = h(n, M) . \quad (4.4.2)$$

3. The average conformal weight induced by this double thermodynamics can be expressed as a super-symplectic thermal average $\langle \cdot \rangle_{SC}$ of the SKM thermal average $h(n, M)$:

$$h(M) = \langle h(n, M) \rangle_{SC} = \sum p_n(M) h(n) , \quad (4.4.3)$$

where the moduli dependent probability $p_n(M)$ of the super-symplectic Virasoro excitation with conformal weight n should be consistent with the p-adic thermodynamics. It is convenient to write $h(M)$ as

$$h(M) = h_0 + \Delta h(M) , \quad (4.4.4)$$

where h_0 is the minimum value of $h(M)$ in the space of moduli. The form of the elementary particle vacuum functionals suggest that h_0 corresponds to moduli with $Im(\Omega_{ij}) = 0$ and thus to singular configurations for which handles degenerate to one-dimensional lines attached to a sphere.

4. There is a further averaging of $\Delta h(M)$ over the moduli space \mathcal{M} by using the modulus squared of elementary particle vacuum functional so that one has

$$h = h_0 + \langle \Delta h(M) \rangle_{\mathcal{M}} . \quad (4.4.5)$$

Modular invariance allows to pose very strong conditions on the functional form of $\Delta h(M)$. The simplest assumption guaranteeing this and thermodynamical interpretation is that $\Delta h(M)$ is proportional to the logarithm of the vacuum functional Ω :

$$\Delta h(M) \propto -\log\left(\frac{\Omega(M)}{\Omega_{max}}\right) . \quad (4.4.6)$$

Here Ω_{max} corresponds to the maximum of Ω for which $\Delta h(M)$ vanishes.

Justification for the general form of the mass formula

The proposed general ansatz for $\Delta h(M)$ provides a justification for the general form of the mass formula deduced by intuitive arguments.

1. The factorization of the elementary particle vacuum functional Ω into a product of $2N(g) = 2^g(2^g + 1)$ terms and the logarithmic expression for $\Delta h(M)$ imply that the thermal expectation values is a sum over thermal expectation values over $2N(g)$ terms associated with various even characteristics (a, b) , where a and b are g -dimensional vectors with components equal to $1/2$ or 0 and the inner product $4a \cdot b$ is an even integer. If each term gives the same result in the averaging using Ω_{vac} as a partition function, the proportionality to $2N_g$ follows.
2. For genus $g \geq 2$ the partition function defines an average in $3g - 3$ complex-dimensional space of moduli. The analogy of $\langle \Delta h \rangle$ and thermal energy suggests that the contribution is proportional to the complex dimension $3g - 3$ of this space. For $g \leq 1$ the contribution the complex dimension of moduli space is g and the contribution would be proportional to g .

$$\begin{aligned} \langle \Delta h \rangle &\propto g \times X(g) \text{ for } g \leq 1 \text{ ,} \\ \langle \Delta h \rangle &\propto (3g - 3) \times X(g) \text{ for } g \geq 2 \text{ ,} \\ X(g) &= 2^g(2^g + 1) \text{ .} \end{aligned} \tag{4.4.7}$$

If X^2 is hyper-elliptic for the maxima of Kähler function, this expression makes sense only for $g \leq 2$ since vacuum functionals vanish for hyper-elliptic surfaces.

3. The earlier argument, inspired by the interpretation of elementary particle vacuum functional as a partition function, was that each factor of the elementary particle vacuum functional gives the same contribution to $\langle \Delta h \rangle$, and that this contribution is proportional to g since each handle behaves like a particle:

$$\langle \Delta h \rangle \propto g \times X(g) \text{ .} \tag{4.4.8}$$

The prediction following from the previous differs by a factor $(3g - 3)/g$ for $g \geq 2$. This would scale up the dominant modular contribution to the masses of the third $g = 2$ fermionic generation by a factor $\sqrt{3/2} \simeq 1.22$. One must of course remember, that these rough arguments allow g -dependent numerical factors of order one so that it is not possible to exclude either argument.

4.4.3 Generalization of Θ functions and quantization of p-adic moduli

The task is to find p-adic counterparts for theta functions and elementary particle vacuum functionals. The constraints come from the p-adic existence of the exponentials appearing as the summands of the theta functions and from the convergence of the sum. The exponentials must be proportional to powers of p just as the Boltzmann weights defining the p-adic partition function. The outcome is a quantization of moduli so that integration can be replaced with a summation and the average of $\Delta h(M)$ over moduli is well defined.

It is instructive to study the problem for torus in parallel with the general case. The ordinary moduli space of torus is parameterized by single complex number τ . The points related by $SL(2, Z)$ are equivalent, which means that the transformation $\tau \rightarrow (A\tau + B)/(C\tau + D)$ produces a point equivalent with τ . These transformations are generated by the shift $\tau \rightarrow \tau + 1$ and $\tau \rightarrow -1/\tau$. One can choose the fundamental domain of moduli space to be the intersection of the slice $Re(\tau) \in [-1/2, 1/2]$ with the exterior of unit circle $|\tau| = 1$. The idea is to start directly from physics and to look whether one might some define p-adic version of elementary particle vacuum functionals in the p-adic counter part of this set or in some modular invariant subset of this set.

Elementary particle vacuum functionals are expressible in terms of theta functions using the functions $\Theta^4[a, b] \overline{\Theta}^4[a, b]$ as a building block. The general expression for the theta function reads as

$$\Theta[a, b](\Omega) = \sum_n \exp(i\pi(n+a) \cdot \Omega \cdot (n+a)) \exp(2i\pi(n+a) \cdot b) . \quad (4.4.9)$$

The latter exponential phase gives only a factor $\pm i$ or ± 1 since $4a \cdot b$ is integer. For $p \bmod 4 = 3$ imaginary unit exists in an algebraic extension of p-adic numbers. In the case of torus (a, b) has the values $(0, 0)$, $(1/2, 0)$ and $(0, 1/2)$ for torus since only even characteristics are allowed.

Concerning the p-adicization of the first exponential appearing in the summands in Eq. 4.4.9, the obvious problem is that π does not exist p-adically unless one allows infinite-dimensional extension.

1. Consider first the real part of Ω . In this case the proper manner to treat the situation is to introduce an algebraic extension involving roots of unity so that $Re(\Omega)$ rational. This approach is proposed as a general approach to the p-adicization of quantum TGD in terms of harmonic analysis in symmetric spaces allowing to define integration also in p-adic context in a physically acceptable manner by reducing it to Fourier analysis. The simplest situation corresponds to integer values for $Re(\Omega)$ and in this case the phase are equal to $\pm i$ or ± 1 since a is half-integer valued. One can consider a hierarchy of variants of moduli space characterized by the allowed roots of unity. The physical interpretation for this hierarchy would be in terms of a hierarchy of measurement resolutions. Note that the real parts of Ω can be assumed to be rationals of form m/n where n is constructed as a product of finite number of primes and therefore the allowed rationals are linear combinations of inverses $1/p_i$ for a subset $\{p_i\}$ of primes.
2. For the imaginary part of Ω different approach is required. One wants a rapid convergence of the sum formula and this requires that the exponents reduces in this case to positive powers of p . This is achieved if one has

$$Im(\Omega) = -n \frac{\log(p)}{\pi} , \quad (4.4.10)$$

Unfortunately this condition is not consistent with the condition $Im(\Omega) > 0$. A manner to circumvent the difficulty is to replace Ω with its complex conjugate. Second approach is to define the real discretized variant of theta function first and then map it by canonical identification to its p-adic counterpart: this would map phase to phases and powers of p to their inverses. Note that a similar change of sign must be performed in p-adic thermodynamics for powers of p to map p-adic probabilities to real ones. By rescaling $Im(\Omega) \rightarrow \frac{\log(p)}{\pi} Im(\Omega)$ one has non-negative integer valued spectrum for $Im(\Omega)$ making possible to reduce integration in moduli space to a summation over finite number of rationals associated with the real part of Ω and powers of p associated with the imaginary part of Ω .

3. Since the exponents appearing in

$$p^{(n+a) \cdot Im(\Omega_{ij,p}) \cdot (n+a)} = p^{a \cdot Im(\Omega) \cdot a} \times p^{2a \cdot Im(\Omega) \cdot n} \times p^{+n \cdot Im(\Omega_{ij,p}) \cdot n}$$

are positive integers valued, $\Theta_{[a,b]}$ exist in R_p and converges. The problematic factor is the first exponent since the components of the vector a can have values $1/2$ and 0 and its existence implies a quantization of $Im(\Omega_{ij})$ as

$$Im(\Omega) = -Kn \frac{\log(p)}{p} , \quad n \in Z , \quad n \geq 1 , \quad (4.4.11)$$

In p-adic context this condition must be formulated for the exponent of Ω defining the natural coordinate. $K = 4$ guarantees the existence of Θ functions and $K = 1$ the existence of the building blocks $\Theta^4[a, b] \bar{\Theta}^4[a, b]$ of elementary particle vacuum functionals in R_p . The extension to higher genera means only replacement of Ω with the elements of a matrix.

4. One can criticize this approach for the loss of the full modular covariance in the definition of theta functions. The modular transformations $\Omega \rightarrow \Omega + n$ are consistent with the number theoretic constraints but the transformations $\Omega \rightarrow -1/\Omega$ do not respect them. It seem that one can circumvent the difficulty by restricting the consideration to a fundamental domain satisfying the number theoretic constraints.

This variant of moduli space is discrete and p-adicity is reflected only in the sense that the moduli space makes sense also p-adically. One can consider also a continuum variant of the p-adic moduli space using the same prescription as in the construction of p-adic symmetric spaces [21].

1. One can introduce $\exp(i\pi Re(\Omega))$ as the counterpart of $Re(\Omega)$ as a coordinate of the Teichmueller space. This coordinate makes sense only as a local coordinate since it does not differentiate between $Re(\Omega)$ and $Re(\Omega + 2n)$. On the other hand, modular invariance states that Ω and $\Omega + n$ correspond to the same moduli so that nothing is lost. In the similar manner one can introduce $\exp(\pi Im(\Omega)) \in \{p^n, n > 0\}$ as the counterpart of discretized version of $Im(\Omega)$.
2. The extension to continuum would mean in the case of $Re(\Omega)$ the extension of the phase $\exp(i\pi Re(\Omega))$ to a product $\exp(i\pi Re(\Omega))\exp(ipx) = \exp(i\pi Re(\Omega) + exp(ipx))$, where x is p-adic integer which can be also infinite as a real integer. This would mean that each root of unity representing allowed value $Re(\Omega)$ would have a p-adic neighborhood consisting of p-adic integers. This neighborhood would be the p-adic counterpart for the angular integral $\Delta\phi$ for a given root of unity and would not make itself visible in p-adic integration.
3. For the imaginary part one can also consider the extension of $\exp(\pi Im(\Omega))$ to $p^n \times \exp(npix)$ where x is a p-adic integer. This would assign to each point p^n a p-adic neighborhood defined by p-adic integers. This neighborhood is same all integers n with same p-adic norm. When n is proportional to p^k one has $\exp(npix) - 1 \propto p^k$.

The quantization of moduli characterizes precisely the conformal properties of the partonic 2-surfaces corresponding to different p-adic primes. In the real context -that is in the intersection of real and p-adic worlds- the quantization of moduli of torus would correspond to

$$\tau = K \left[\sum q + i \times n \frac{\log(p)}{\pi} \right], \quad (4.4.12)$$

where q is a rational number expressible as linear combination of inverses of a finite fixed set of primes defining the allowed roots of unity. $K = 1$ guarantees the existence of elementary particle vacuum functionals and $K = 4$ the existence of Theta functions. The ratio for the complex vectors defining the sides of the plane parallelogram defining torus via the identification of the parallel sides is quantized. In other words, the angles Φ between the sides and the ratios of the sides given by $|\tau|$ have quantized values.

The quantization rules for the moduli of the higher genera is of exactly same form

$$\Omega_{ij} = K \left[\sum q_{ij} + i \times n_{ij} \times \frac{\log(p)}{\pi} \right], \quad (4.4.13)$$

If the quantization rules hold true also for the maxima of Kähler function in the real context or more precisely- in the intersection of real and p-adic variants of the "world of classical worlds" identified as partonic 2-surfaces at the boundaries of causal diamond plus the data about their 4-D tangent space, there are good hopes that the p-adicized expression for Δh is obtained by a simple algebraic continuation of the real formula. Thus p-adic length scale would characterize partonic surface X^2 rather than the light like causal determinant X_l^3 containing X^2 . Therefore the idea that various p-adic primes label various X_l^3 connecting fixed partonic surfaces X_i^2 would not be correct.

Quite generally, the quantization of moduli means that the allowed 2-dimensional shapes form a lattice and are thus additive. It also means that the maxima of Kähler function would obey a linear superposition in an extreme abstract sense. The proposed number theoretical quantization is

expected to apply for any complex space allowing some preferred complex coordinates. In particular, configuration space of 2-surfaces could allow this kind of quantization in the complex coordinates naturally associated with isometries and this could allow to define configuration space integration, at least the counterpart of integration in zero mode degrees of freedom, as a summation.

Number theoretic vision leads to the notion of multi-p-adicity in the sense that the same partonic 2-surface can correspond to several p-adic primes and that infinite primes code for these primes [17, 55]. At the level of the moduli space this corresponds to the replacement of p with an integer in the formulas so that one can interpret the formulas both in real sense and p-adic sense for the primes p dividing the integer. Also the exponent of given prime in the integer matters. The construction of generalized eigen modes of Chern-Simons Dirac operator leads to the proposal that the collection of infinite primes characterizing infinite prime characterizes the geometry of the orbit of partonic 2-surface [55]. It would not be too surprising if this connection would reduce to the proposed discretization of the modular parameters of the partonic 2-surface.

4.4.4 The calculation of the modular contribution $\langle \Delta h \rangle$ to the conformal weight

The quantization of the moduli implies that the integral over moduli can be defined as a sum over moduli. The theta function $\Theta[a, b](\Omega)_p(\tau_p)$ is proportional to $p^{a \cdot a I m(\Omega_{ij,p})} = p^{K n_{ij} m(a)/4}$ for $a \cdot a = m(a)/4$, where $K = 1$ resp. $K = 4$ corresponds to the existence of elementary particle vacuum functionals resp. theta functions in R_p . These powers of p can be extracted from the thetas defining the vacuum functional. The numerator of the vacuum functional gives $(p^n)^{2K \sum_{a,b} m(a)}$. The denominator gives $(p^n)^{2K \sum_{a,b} m(a_0)}$, where a_0 corresponds to the minimum value of $m(a)$. $a_0 = (0, 0, \dots, 0)$ is allowed and gives $m(a_0) = 0$ so that the p-adic norm of the denominator equals to one. Hence one has

$$|\Omega_{vac}(\Omega_p)|_p = p^{-2nK \sum_{a,b} m(a)} \quad (4.4.14)$$

The sum converges extremely rapidly for large values of p as function of n so that in practice only few moduli contribute.

The definition of $\log(\Omega_{vac})$ poses however problems since in $\log(p)$ does not exist as a p-adic number in any p-adic number field. The argument of the logarithm should have a unit p-adic norm. The simplest manner to circumvent the difficulty is to use the fact that the p-adic norm $|\Omega_p|_p$ is also a modular invariant, and assume that the contribution to conformal weight depends on moduli as

$$\Delta h_p(\Omega_p) \propto \log\left(\frac{\Omega_{vac}}{|\Omega_{vac}|_p}\right) . \quad (4.4.15)$$

The sum defining $\langle \Delta h_p \rangle$ converges extremely rapidly and gives a result of order $O(p)$ p-adically as required.

The p-adic expression for $\langle \Delta h_p \rangle$ should result from the corresponding real expression by an algebraic continuation. This encourages the conjecture that the allowed moduli are quantized for the maxima of Kähler function, so that the integral over the moduli space is replaced with a sum also in the real case, and that Δh given by the double thermodynamics as a function of moduli can be defined as in the p-adic case. The positive power of p multiplying the numerator could be interpreted as a degeneracy factor. In fact, the moduli are not primary dynamical variables in the case of the induced metric, and there must be a modular invariant weight factor telling how many 2-surfaces correspond to given values of moduli. The power of p could correspond to this factor.

4.5 General mass formulas for non-Higgisy contributions

In the sequel various contributions to the mass squared are discussed.

4.5.1 General mass squared formula

The thermal independence of Super Virasoro and modular degrees of freedom implies that mass squared for elementary particle is the sum of Super Virasoro, modular and Higgsy contributions:

$$M^2 = M^2(\text{color}) + M^2(\text{SV}) + M^2(\text{mod}) + M^2(\text{Higgsy}) . \quad (4.5.1)$$

Also small renormalization correction contributions might be possible.

4.5.2 Color contribution to the mass squared

The mass squared contains a non-thermal color contribution to the ground state conformal weight coming from the mass squared of CP_2 spinor harmonic. The color contribution is an integer multiple of $m_0^2/3$, where $m_0^2 = 2\Lambda$ denotes the 'cosmological constant' of CP_2 (CP_2 satisfies Einstein equations $G^{\alpha\beta} = \Lambda g^{\alpha\beta}$).

The color contribution to the p-adic mass squared is integer valued only if $m_0^2/3$ is taken as a fundamental p-adic unit of mass squared. This choice has an obvious relevance for p-adic mass calculations since the simplest form of the canonical identification does not commute with a division by integer. More precisely, the image of number xp in canonical identification has a value of order 1 when x is a non-trivial rational number whereas for $x = np$ the value is n/p and extremely is small for physically interesting primes.

The choice of the p-adic mass squared unit are no effects on zeroth order contribution which must vanish for light states: this requirement eliminates quark and lepton states for which the CP_2 contribution to the mass squared is not integer valued using m_0^2 as a unit. There can be a dramatic effect on the first order contribution. The mass squared $m^2 = p/3$ using $m_0^2/3$ means that the particle is light. The mass squared becomes $m^2 = p/3$ when m_0^2 is used as a unit and the particle has mass of order 10^{-4} Planck masses. In the case of W and Z^0 bosons this problem is actually encountered. For light states using $m_0^2/3$ as a unit only the second order contribution to the mass squared is affected by this choice.

4.5.3 Modular contribution to the mass of elementary particle

The general form of the modular contribution is derivable from p-adic partition function for conformally invariant degrees of freedom associated with the boundary components. The general form of the vacuum functionals as modular invariant functions of Teichmuller parameters was derived in [22] and the square of the elementary particle vacuum functional can be identified as a partition function. Even theta functions serve as basic building blocks and the functionals are proportional to the product of all even theta functions and their complex conjugates. The number of theta functions for genus $g > 0$ is given by

$$N(g) = 2^{g-1}(2^g + 1) . \quad (4.5.2)$$

One has $N(1) = 3$ for muon and $N(2) = 10$ for τ .

1. Single theta function is analogous to a partition function. This implies that the modular contribution to the mass squared must be proportional to $2N(g)$. The factor two follows from the presence of both theta functions and their conjugates in the partition function.
2. The factorization properties of the vacuum functionals imply that handles behave effectively as particles. For example, at the limit, when the surface splits into two pieces with g_1 and $g - g_1$ handles, the partition function reduces to a product of g_1 and $g - g_1$ partition functions. This implies that the contribution to the mass squared is proportional to the genus of the surface. Altogether one has

$$\begin{aligned} M^2(\text{mod}, g) &= 2k(\text{mod})N(g)g \frac{m_0^2}{p} , \\ k(\text{mod}) &= 1 . \end{aligned} \quad (4.5.3)$$

Here $k(mod)$ is some integer valued constant (in order to avoid ultra heavy mass) to be determined. $k(mod) = 1$ turns out to be the correct choice for this parameter.

Summarizing, the real counterpart of the modular contribution to the mass of a particle belonging to $g + 1$:th generation reads as

$$\begin{aligned} M^2(mod) &= 0 \text{ for } e, \nu_e, u, d \text{ ,} \\ M^2(mod) &= 9 \frac{m_0^2}{p(X)} \text{ for } X = \mu, \nu_\mu, c, s \text{ ,} \\ M^2(mod) &= 60 \frac{m_0^2}{p(X)} \text{ for } X = \tau, \nu_\tau, t, b \text{ .} \end{aligned} \quad (4.5.4)$$

The requirement that hadronic mass spectrum and CKM matrix are sensible however forces the modular contribution to be the same for quarks, leptons and bosons. The higher order modular contributions to the mass squared are completely negligible if the degeneracy of massless state is $D(0, mod, g) = 1$ in the modular degrees of freedom as is in fact required by $k(mod) = 1$.

4.5.4 Thermal contribution to the mass squared

One can deduce the value of the thermal mass squared in order $O(p^2)$ (an excellent approximation) using the general mass formula given by p-adic thermodynamics. Assuming maximal p-adic temperature $T_p = 1$ one has

$$\begin{aligned} M^2 &= k(sp + Xp^2 + O(p^3)) \text{ ,} \\ s_\Delta &= \frac{D(\Delta + 1)}{D(\Delta)} \text{ ,} \\ X_\Delta &= 2 \frac{D(\Delta + 2)}{D(\Delta)} - \frac{D^2(\Delta + 1)}{D^2(\Delta)} \text{ ,} \\ k &= 1 \text{ .} \end{aligned} \quad (4.5.5)$$

Δ is the conformal weight of the operator creating massless state from the ground state.

The ratios $r_n = D(n+1)/D(n)$ allowing to deduce the values of s and X have been deduced from p-adic thermodynamics in [26]. Light state is obtained only provided $r(\Delta)$ is an integer. The remarkable result is that for lowest lying states this is the case. For instance, for Ramond representations the values of r_n are given by

$$(r_0, r_1, r_2, r_3) = (8, 5, 4, \frac{55}{16}) \text{ .} \quad (4.5.6)$$

The values of s and X are

$$\begin{aligned} (s_0, s_1, s_2) &= (8, 5, 4) \text{ ,} \\ (X_0, X_1, X_2) &= (16, 15, 11 + 1/2) \text{ .} \end{aligned} \quad (4.5.7)$$

The result means that second order contribution is extremely small for quarks and charged leptons having $\Delta < 2$. For neutrinos having $\Delta = 2$ the second order contribution is non-vanishing.

4.5.5 The contribution from the deviation of ground state conformal weight from negative integer

The interpretation inspired by p-adic mass calculations is that the squares λ_i^2 of the eigenvalues of the modified Dirac operator correspond to the conformal weights of ground states. Another natural physical interpretation of λ is as an analog of the Higgs vacuum expectation. The instability of the Higgs=0 phase would corresponds to the fact that $\lambda = 0$ mode is not localized to any region in which

ew magnetic field or induced Kähler field is non-vanishing. A good guess is that induced Kähler magnetic field B_K dictates the magnitude of the eigenvalues which is thus of order $h_0 = \sqrt{B_K R}$, R CP_2 radius. The first guess is that eigenvalues in the first approximation come as $(n + 1/2)h_0$. Each region where induced Kähler field is non-vanishing would correspond to different scale mass scale h_0 .

1. The vacuum expectation value of Higgs is only proportional to an eigenvalue λ , not equal to it. Indeed, Higgs and gauge bosons as elementary particles correspond to wormhole contacts carrying fermion and antifermion at the two wormhole throats and must be distinguished from the space-time correlate of its vacuum expectation as something proportional to λ . In the fermionic case the vacuum expectation value of Higgs does not seem to be even possible since fermions do not correspond to wormhole contacts between two space-time sheets but possess only single wormhole throat (p-adic mass calculations are consistent with this).
2. Physical considerations suggest that the vacuum expectation of Higgs field corresponds to a particular eigenvalue λ_i of modified Dirac operator so that the eigenvalues λ_i would define TGD counterparts for the minima of Higgs potential. Since the vacuum expectation of Higgs corresponds to a condensate of wormhole contacts giving rise to a coherent state, the vacuum expectation cannot be present for topologically condensed CP_2 type vacuum extremals representing fermions since only single wormhole throat is involved. This raises a hen-egg question about whether Higgs contributes to the mass or whether Higgs is only a correlate for massivation having description using more profound concepts. From TGD point of view the most elegant option is that Higgs does not give rise to mass but Higgs vacuum expectation value accompanies bosonic states and is naturally proportional to λ_i . With this interpretation λ_i could give a contribution to both fermionic and bosonic masses.
3. If the coset construction for super-symplectic and super Kac-Moody algebra implying Equivalence Principle is accepted, one encounters what looks like a problem. p-Adic mass calculations require negative ground state conformal weight compensated by Super Virasoro generators in order to obtain massless states. The tachyonicity of the ground states would mean a close analogy with both string models and Higgs mechanism. λ_i^2 is very natural candidate for the ground state conformal weights identified but would have wrong sign if the effective metric of X_I^3 defined by the inner products $T_K^{k\alpha} T_K^{l\beta} h_{kl}$ of the Kähler energy momentum tensor $T^{k\alpha} = h^{kl} \partial L_K / \partial h_\alpha^l$ and appearing in the modified Dirac operator D_K has Minkowskian signature.

The situation changes if the effective metric has Euclidian signature. This seems to be the case for the light-like surfaces assignable to the known extremals such as MEs and cosmic strings. In this kind of situation light-like coordinate possesses Euclidian signature and real eigenvalue spectrum is replaced with a purely imaginary one. Since Dirac operator is in question both signs for eigenvalues are possible and one obtains both exponentially increasing and decreasing solutions. This is essential for having solutions extending from the past end of X_I^3 to its future end. Non-unitary time evolution is possible because X_I^3 does not strictly speaking represent the time evolution of 2-D dynamical object but actual dynamical objects (by light-likeness both interpretation as dynamical evolution and dynamical object are present). The Euclidian signature of the effective metric would be a direct analog for the tachyonicity of the Higgs in unstable minimum and the generation of Higgs vacuum expectation would correspond to the compensation of ground state conformal weight by conformal weights of Super Virasoro generators.

4. In accordance with this λ_i^2 would give constant contribution to the ground state conformal weight. What contributes to the thermal mass squared is the deviation of the ground state conformal weight from half-odd integer since the negative integer part of the total conformal weight can be compensated by applying Virasoro generators to the ground state. The first guess motivated by cyclotron energy analogy is that the lowest conformal weights are of form $h_c = \lambda_i^2 = -1/2 - n + \Delta h_c$ so that lowest ground state conformal weight would be $h_c = -1/2$ in the first approximation. The negative integer part of the net conformal weight can be canceled using Super Virasoro generators but Δh_c would give to mass squared a contribution analogous to Higgs contribution. The mapping of the real ground state conformal weight to a p-adic number by canonical identification involves some delicacies.

5. p-Adic mass calculations are consistent with the assumption that Higgs type contribution is vanishing (that is small) for fermions and dominates for gauge bosons. This requires that the deviation of λ_i^2 with smallest magnitude from half-odd integer value in the case of fermions is considerably smaller than in the case of gauge bosons in the scale defined by p-adic mass scale $1/L(k)$ in question. Somehow this difference could relate to the fact that bosons correspond to pairs of wormhole throats.

4.5.6 General mass formula for Ramond representations

By taking the modular contribution from the boundaries into account the general p-adic mass formulas for the Ramond type states read for states for which the color contribution to the conformal weight is integer valued as

$$\begin{aligned}
\frac{m^2(\Delta = 0)}{m_0^2} &= (8 + n(g))p + Yp^2 , \\
\frac{m^2(\Delta = 1)}{m_0^2} &= (5 + n(g))p + Yp^2 , \\
\frac{m^2(\Delta = 2)}{m_0^2} &= (4 + n(g))p + (Y + \frac{23}{2})p^2 , \\
n(g) &= 3g \cdot 2^{g-1}(2^g + 1) .
\end{aligned} \tag{4.5.8}$$

Here Δ denotes the conformal weight of the operators creating massless states from the ground state and g denotes the genus of the boundary component. The values of $n(g)$ for the three lowest generations are $n(0) = 0$, $n(1) = 9$ and $n(2) = 60$. The value of second order thermal contribution is nontrivial for neutrinos only. The value of the rational number Y can, which corresponds to the renormalization correction to the mass, can be determined using experimental inputs.

Using m_0^2 as a unit, the expression for the mass of a Ramond type state reads in terms of the electron mass as

$$\begin{aligned}
M(\Delta, g, p)_R &= K(\Delta, g, p) \sqrt{\frac{M_{127}}{p}} m_e \\
K(0, g, p) &= \sqrt{\frac{n(g) + 8 + Y_R}{X}} \\
K(1, g, p) &= \sqrt{\frac{n(g) + 5 + Y_R}{X}} \\
K(2, g, p) &= \sqrt{\frac{n(g) + 4 + Y_R}{X}} , \\
X &= \sqrt{5 + Y(e)_R} .
\end{aligned} \tag{4.5.9}$$

Y can be assumed to depend on the electromagnetic charge and color representation of the state and is therefore same for all fermion families. Mathematica provides modules for calculating the real counterpart of the second order contribution and for finding realistic values of Y .

4.5.7 General mass formulas for NS representations

Using $m_0^2/3$ as a unit, the expression for the mass of a light NS type state for $T_p = 1$ ad $k_B = 1$ reads in terms of the electron mass as

$$\begin{aligned}
M(\Delta, g, p, N)_R &= K(\Delta, g, p, N) \sqrt{\frac{M_{127}}{p}} m_e \\
K(0, g, p, 1) &= \sqrt{\frac{n(g) + Y_R}{X}} , \\
K(0, g, p, 2) &= \sqrt{\frac{n(g) + 1 + Y_R}{X}} , \\
K(1, g, p, 3) &= \sqrt{\frac{n(g) + 3 + Y_R}{X}} , \\
K(2, g, p, 4) &= \sqrt{\frac{n(g) + 5 + Y_R}{X}} , \\
K(2, g, p, 5) &= \sqrt{\frac{n(g) + 10 + Y_R}{X}} , \\
X &= \sqrt{5 + Y(e)_R} .
\end{aligned} \tag{4.5.10}$$

Here N is the number of the 'active' NS sectors (sectors for which the conformal weight of the massless state is non-vanishing). Y denotes the renormalization correction to the boson mass and in general depends on the electro-weak and color quantum numbers of the boson.

The thermal contribution to the mass of W boson is too large by roughly a factor $\sqrt{3}$ for $T_p = 1$. Hence $T_p = 1/2$ must hold true for gauge bosons and their masses must have a non-thermal origin perhaps analogous to Higgs mechanism. Alternatively, the non-covariant constancy of charge matrices could induce the boson mass [26].

It is interesting to notice that the minimum mass squared for gauge boson corresponds to the p-adic mass unit $M^2 = m_0^2 p/3$ and this just what is needed in the case of W boson. This forces to ask whether $m_0^2/3$ is the correct choice for the mass squared unit so that non-thermally induced W mass would be the minimal $m_W^2 = p$ in the lowest order. This choice would mean the replacement

$$Y_R \rightarrow \frac{(3Y)_R}{3}$$

in the preceding formulas and would affect only neutrino mass in the fermionic sector. $m_0^2/3$ option is excluded by charged lepton mass calculation. This point will be discussed later.

4.5.8 Primary condensation levels from p-adic length scale hypothesis

p-Adic length scale hypothesis states that the primary condensation levels correspond to primes near prime powers of two $p \simeq 2^k$, k integer with prime values preferred. Black hole-elementary particle analogy [24] suggests a generalization of this hypothesis by allowing k to be a power of prime. The general number theoretical vision discussed in [21] provides a first principle justification for p-adic length scale hypothesis in its most general form. The best fit for the neutrino mass squared differences is obtained for $k = 13^2 = 169$ so that the generalization of the hypothesis might be necessary.

A particle primarily condensed on the level k can suffer secondary condensation on a level with the same value of k : for instance, electron ($k = 127$) suffers secondary condensation on $k = 127$ level. u, d, s quarks ($k = 107$) suffer secondary condensation on nuclear space-time sheet having $k = 113$. All quarks feed their color gauge fluxes at $k = 107$ space-time sheet. There is no deep reason forbidding the condensation of p on p . Primary and secondary condensation levels could also correspond to different but nearly identical values of p with the same value of k .

4.6 Fermion masses

In the earlier model the coefficient of $M^2 = kL_0$ had to be assumed to be different for various particle states. $k = 1$ was assumed for bosons and leptons and $k = 2/3$ for quarks. The fact that $k = 1$ holds true for all particles in the model including also super-symplectic invariance forces to modify the earlier construction of quark states. This turns out to be possible without affecting the earlier

p-adic mass calculations whose outcome depend in an essential manner on the ground state conformal weights h_{gr} of the fermions (h_{gr} can be negative). The structure of lepton and quark states in color degrees of freedom was discussed in [26].

4.6.1 Charged lepton mass ratios

The overall mass scale for lepton and quark masses is determined by the condensation level given by prime $p \simeq 2^k$, k prime by length scale hypothesis. For charged leptons k must correspond to $k = 127$ for electron, $k = 113$ for muon and $k = 107$ for τ . For muon $p = 2^{113} - 1 - 4 * 378$ is assumed (smallest prime below 2^{113} allowing $\sqrt{2}$ but not $\sqrt{3}$). So called Gaussian primes are to complex integers what primes are for the ordinary integers and the Gaussian counterparts of the Mersenne primes are Gaussian primes of form $(1 \pm i)^k - 1$. Rather interestingly, $k = 113$ corresponds to a Gaussian Mersenne so that all charged leptons correspond to generalized Mersenne primes.

For $k = 1$ the leptonic mass squared is integer valued in units of m_0^2 only for the states satisfying

$$p \bmod 3 \neq 2 .$$

Only these representations can give rise to massless states. Neutrinos correspond to (p, p) representations with $p \geq 1$ whereas charged leptons correspond to $(p, p + 3)$ representations. The earlier mass calculations demonstrate that leptonic masses can be understood if the ground state conformal weight is $h_{gr} = -1$ for charged leptons and $h_{gr} = -2$ for neutrinos.

The contribution of color partial wave to conformal weight is $h_c = (p^2 + 2p)/3$, $p \geq 1$, for neutrinos and $p = 1$ gives $h_c = 1$ (octet). For charged leptons $h_c = (p^2 + 5p + 6)/3$ gives $h_c = 2$ for $p = 0$ (decuplet). In both cases super-symplectic operator O must have a net conformal weight $h_{sc} = -3$ to produce a correct conformal weight for the ground state. p-adic considerations suggests the use of operators O with super-symplectic conformal weight $z = -1/2 - i \sum n_k y_k$, where $s_k = 1/2 + i y_k$ corresponds to zero of Riemann ζ . If the operators in question are color Hamiltonians in octet representation net super-symplectic conformal weight $h_{sc} = -3$ results. The tensor product of two octets with conjugate super-symplectic conformal weights contains both octet and decuplet so that singlets are obtained. What strengthens the hopes that the construction is not adhoc is that the same operator appears in the construction of quark states too.

Using CP_2 mass scale m_0^2 [26] as a p-adic unit, the mass formulas for the charged leptons read as

$$\begin{aligned} M^2(L) &= A(\nu) \frac{m_0^2}{p(L)} , \\ A(e) &= 5 + X(p(e)) , \\ A(\mu) &= 14 + X(p(\mu)) , \\ A(\tau) &= 65 + X(p(\tau)) . \end{aligned} \tag{4.6.1}$$

$X(\cdot)$ corresponds to the yet unknown second order corrections to the mass squared.

The following table gives the basic parameters as determined from the mass of electron for some values of Y_e . The mass of top quark favors as maximal value of CP_2 mass which corresponds to $Y_e = 0$.

Y_e	0	.5	.7798
$(m_0/m_{Pl}) \times 10^3$.2437	.2323	.2266
$K \times 10^{-7}$	2.5262	2.7788	2.9202
$(L_R/\sqrt{G}) \times 10^{-4}$	3.1580	3.3122	3.3954

Table 1. Table gives the values of CP_2 mass m_0 using Planck mass $m_{Pl} = 1/\sqrt{G}$ as unit, the ratio $K = R^2/G$ and CP_2 geodesic length $L = 2\pi R$ for $Y_e \in \{0, 0.5, 0.7798\}$.

The following table lists the lower and upper bounds for the charged lepton mass ratios obtained by taking second order contribution to zero or allowing it to have maximum possible value. The values of lepton masses are $m_e = .510999$ MeV, $m_\mu = 105.76583$ MeV, $m_\tau = 1775$ MeV.

$$\begin{aligned}
\frac{m(\mu)_+}{m(\mu)} &= \sqrt{\frac{15}{5}} 2^7 \frac{m_e}{m(\mu)} \simeq 1.0722 \ , \\
\frac{m(\mu)_-}{m(\mu)} &= \sqrt{\frac{14}{6}} 2^7 \frac{m_e}{m(\mu)} \simeq 0.9456 \ , \\
\frac{m(\tau)_+}{m(\tau)} &= \sqrt{\frac{66}{5}} 2^{10} \frac{m_e}{m(\tau)} \simeq 1.0710 \ , \\
\frac{m(\tau)_-}{m(\tau)} &= \sqrt{\frac{65}{6}} 2^{10} \frac{m_e}{m(\tau)} \simeq .9703 \ .
\end{aligned}
\tag{4.6.2}$$

For the maximal value of CP_2 mass the predictions for the mass ratio are systematically too large by a few per cent. From the formulas above it is clear that the second order corrections to mass squared can be such that correct masses result.

τ mass is least sensitive to $X(p(e)) \equiv Y_e$ and the maximum value of $Y_e \equiv Y_{e,max}$ consistent with τ mass corresponds to $Y_{e,max} = .7357$ and $Y_\tau = 1$. This means that the CP_2 mass is at least a fraction .9337 of its maximal value. If Y_L is same for all charged leptons and has the maximal value $Y_{e,max} = .7357$, the predictions for the mass ratios are

$$\begin{aligned}
\frac{m(\mu)_{pr}}{m(\mu)} &= \sqrt{\frac{14 + Y_{e,max}}{5 + Y_{e,max}}} \times 2^7 \frac{m_e}{m(\mu)} \simeq .9922 \ , \\
\frac{m(\tau)_{pr}}{m(\tau)} &= \sqrt{\frac{65 + Y_{e,max}}{5 + Y_{e,max}}} \times 2^{10} \frac{m_e}{m(\tau)} \simeq .9980 \ .
\end{aligned}
\tag{4.6.3}$$

The error is .8 per cent *resp.* .2 per cent for muon *resp.* τ .

The argument leading to estimate for the modular contribution to the mass squared [26] leaves two options for the coefficient of the modular contribution for $g = 2$ fermions: the value of coefficient is either $X = g$ for $g \leq 1$, $X = 3g - 3$ for $g \geq 2$ or $X = g$ always. For $g = 2$ the predictions are $X = 2$ and $X = 3$ in the two cases. The option $X = 3$ allows slightly larger maximal value of Y_e equal to $Y_{e,max}^1 = Y_{e,max} + (5 + Y_{e,max})/66$.

4.6.2 Neutrino masses

The estimation of neutrino masses is difficult at this stage since the prediction of the primary condensation level is not yet possible and neutrino mixing cannot yet be predicted from the basic principles. The cosmological bounds for neutrino masses however help to put upper bounds on the masses. If one takes seriously the LSND data on neutrino mass measurement of [44, 46] and the explanation of the atmospheric ν -deficit in terms of $\nu_\mu - \nu_\tau$ mixing [45, 48] one can deduce that the most plausible condensation level of μ and τ neutrinos is $k = 167$ or $k = 13^2 = 169$ allowed by the more general form of the p-adic length scale hypothesis suggested by the blackhole-elementary particle analogy. One can also deduce information about the mixing matrix associated with the neutrinos so that mass predictions become rather precise. In particular, the mass splitting of μ and τ neutrinos is predicted correctly if one assumes that the mixing matrix is a rational unitary matrix.

Super Virasoro contribution

Using $m_0^2/3$ as a p-adic unit, the expression for the Super Virasoro contribution to the mass squared of neutrinos is given by the formula

$$\begin{aligned}
M^2(SV) &= (s + (3Yp)_R/3) \frac{m_0^2}{p} , \\
s &= 4 \text{ or } 5 , \\
Y &= \frac{23}{2} + Y_1 ,
\end{aligned} \tag{4.6.4}$$

where m_0^2 is universal mass scale. One can consider two possible identifications of neutrinos corresponding to $s(\nu) = 4$ with $\Delta = 2$ and $s(\nu) = 5$ with $\Delta = 1$. The requirement that CKM matrix is sensible forces the asymmetric scenario in which quarks and, by symmetry, also leptons correspond to lowest possible excitation so that one must have $s(\nu) = 4$. Y_1 represents second order contribution to the neutrino mass coming from renormalization effects coming from self energy diagrams involving intermediate gauge bosons. Physical intuition suggest that this contribution is very small so that the precise measurement of the neutrino masses should give an excellent test for the theory.

With the above described assumptions and for $s = 4$, one has the following mass formula for neutrinos

$$\begin{aligned}
M^2(\nu) &= A(\nu) \frac{m_0^2}{p(\nu)} , \\
A(\nu_e) &= 4 + \frac{(3Y(p(\nu_e)))_R}{3} , \\
A(\nu_\mu) &= 13 + \frac{(3Y(p(\nu_\mu)))_R}{3} , \\
A(\nu_\tau) &= 64 + \frac{(3Y(p(\nu_\tau)))_R}{3} , \\
3Y &\simeq \frac{1}{2} .
\end{aligned} \tag{4.6.5}$$

The predictions must be consistent with the recent upper bounds [37] of order 10 eV, 270 keV and 0.3 MeV for ν_e , ν_μ and ν_τ respectively. The recently reported results of LSND measurement [46] for $\nu_e - \nu_\mu$ mixing gives string limits for $\Delta m^2(\nu_e, \nu_\mu)$ and the parameter $\sin^2(2\theta)$ characterizing the mixing: the limits are given in the figure 30 of [46]. The results suggests that the masses of both electron and muon neutrinos are below 5 eV and that mass squared difference $\Delta m^2 = m^2(\nu_\mu) - m^2(\nu_e)$ is between .25 – 25 eV². The simplest possibility is that ν_μ and ν_e have common condensation level (in analogy with d and s quarks). There are three candidates for the primary condensation level: namely $k = 163, 167$ and $k = 169$. The p-adic prime associated with the primary condensation level is assumed to be the nearest prime below 2^k allowing p-adic $\sqrt{2}$ but not $\sqrt{3}$ and satisfying $p \bmod 4 = 3$. The following table gives the values of various parameters and unmixed neutrino masses in various cases of interest.

k	p	$(3Y)_R/3$	$m(\nu_e)/eV$	$m(\nu_\mu)/eV$	$m(\nu_\tau)/eV$
163	$2^{163} - 4 * 144 - 1$	1.36	1.78	3.16	6.98
167	$2^{167} - 4 * 144 - 1$.34	.45	.79	1.75
169	$2^{169} - 4 * 210 - 1$.17	.22	.40	.87

Could neutrino topologically condense also in other p-adic length scales than $k = 169$?

One must keep mind open for the possibility that there are several p-adic length scales at which neutrinos can condense topologically. Biological length scales are especially interesting in this respect. In fact, all intermediate p-adic length scales $k = 151, 157, 163, 167$ could correspond to metastable neutrino states. The point is that these p-adic lengths scales are number theoretically completely exceptional in the sense that there exist Gaussian Mersenne $2^k \pm i$ (prime in the ring of complex integers) for all these values of k . Since charged leptons, atomic nuclei ($k = 113$), hadrons and intermediate gauge bosons correspond to ordinary or Gaussian Mersennes, it would not be surprising if the biologically important Gaussian Mersennes would correspond to length scales giving rise to metastable neutrino states. Of course, one can keep mind open for the possibility that $k = 167$ rather than $k = 13^2 = 169$ is the length scale defining the stable neutrino physics.

Neutrino mixing

Consider next the neutrino mixing. A quite general form of the neutrino mixing matrix D given by the table below will be considered.

	ν_e	ν_μ	ν_τ
ν_e	c_1	$s_1 c_3$	$s_1 s_3$
ν_μ	$-s_1 c_2$	$c_1 c_2 c_3 - s_2 s_3 \exp(i\delta)$	$c_1 c_2 s_3 + s_2 c_3 \exp(i\delta)$
ν_τ	$-s_1 s_2$	$c_1 s_2 c_3 + c_2 s_3 \exp(i\delta)$	$c_1 s_2 s_3 - c_2 c_3 \exp(i\delta)$

Physical intuition suggests that the angle δ related to CP breaking is small and will be assumed to be vanishing. Topological mixing is active only in modular degrees of freedom and one obtains for the first order terms of mixed masses the expressions

$$\begin{aligned}
 s(\nu_e) &= 4 + 9|U_{12}|^2 + 60|U_{13}|^2 = 4 + n_1 , \\
 s(\nu_\mu) &= 4 + 9|U_{22}|^2 + 60|U_{23}|^2 = 4 + n_2 , \\
 s(\nu_\tau) &= 4 + 9|U_{32}|^2 + 60|U_{33}|^2 = 4 + n_3 .
 \end{aligned}
 \tag{4.6.6}$$

The requirement that resulting masses are not ultraheavy implies that $s(\nu)$ must be small integers. The condition $n_1 + n_2 + n_3 = 69$ follows from unitarity. The simplest possibility is that the mixing matrix is a rational unitary matrix. The same ansatz was used successfully to deduce information about the mixing matrices of quarks. If neutrinos are condensed on the same condensation level, rationality implies that $\nu_\mu - \nu_\tau$ mass squared difference must come from the first order contribution to the mass squared and is therefore quantized and bounded from below.

The first piece of information is the atmospheric ν_μ/ν_e ratio, which is roughly by a factor 2 smaller than predicted by standard model [45]. A possible explanation is the CKM mixing of muon neutrino with τ -neutrino, whereas the mixing with electron neutrino is excluded as an explanation. The latest results from Kamiokande [45] are in accordance with the mixing $m^2(\nu_\tau) - m^2(\nu_\mu) \simeq 1.6 \cdot 10^{-2} eV^2$ and mixing angle $\sin^2(2\theta) = 1.0$: also the zenith angle dependence of the ratio is in accordance with the mixing interpretation. If mixing matrix is assumed to be rational then only $k = 169$ condensation level is allowed for ν_μ and ν_τ . For this level $\nu_\mu - \nu_\tau$ mass squared difference turns out to be $\Delta m^2 \simeq 10^{-2} eV^2$ for $\Delta s \equiv s(\nu_\tau) - s(\nu_\mu) = 1$, which is the only acceptable possibility and predicts $\nu_\mu - \nu_\tau$ mass squared difference correctly within experimental uncertainties! The fact that the predictions for mass squared differences are practically exact, provides a precision test for the rationality assumption.

What is measured in LSND experiment is the probability $P(t, E)$ that ν_μ transforms to ν_e in time t after its production in muon decay as a function of energy E of ν_μ . In the limit that ν_τ and ν_μ masses are identical, the expression of $P(t, E)$ is given by

$$\begin{aligned}
 P(t, E) &= \sin^2(2\theta) \sin^2\left(\frac{\Delta E t}{2}\right) , \\
 \sin^2(2\theta) &= 4c_1^2 s_1^2 c_2^2 ,
 \end{aligned}
 \tag{4.6.7}$$

where ΔE is energy difference of ν_μ and ν_e neutrinos and t denotes time. LSND experiment gives stringent conditions on the value of $\sin^2(2\theta)$ as the figure 30 of [46] shows. In particular, it seems that $\sin^2(2\theta)$ must be considerably below 10^{-1} and this implies that s_1^2 must be small enough.

The study of the mass formulas shows that the only possibility to satisfy the constraints for the mass squared and $\sin^2(2\theta)$ given by LSND experiment is to assume that the mixing of the electron neutrino with the tau neutrino is much larger than its mixing with the muon neutrino. This means that s_3 is quite near to unity. At the limit $s_3 = 1$ one obtains the following (nonrational) solution of

the mass squared conditions for $n_3 = n_2 + 1$ (forced by the atmospheric neutrino data)

$$\begin{aligned} s_1^2 &= \frac{69 - 2n_2 - 1}{60} , \\ c_2^2 &= \frac{n_2 - 9}{2n_2 - 17} , \\ \sin^2(2\theta) &= \frac{4(n_2 - 9)(34 - n_2)(n_2 - 4)}{51 \cdot 30^2} , \\ s(\nu_\mu) - s(\nu_e) &= 3n_2 - 68 . \end{aligned} \quad (4.6.8)$$

The study of the LSND data shows that there is only one acceptable solution to the conditions obtained by assuming maximal mass squared difference for ν_e and ν_μ

$$\begin{aligned} n_1 &= 2 \quad n_2 = 33 \quad n_3 = 34 , \\ s_1^2 &= \frac{1}{30} \quad c_2^2 = \frac{24}{49} , \\ \sin^2(2\theta) &= \frac{24}{49} \frac{2}{15} \frac{29}{30} \simeq .0631 , \\ s(\nu_\mu) - s(\nu_e) &= 31 \leftrightarrow .32 \text{ eV}^2 . \end{aligned} \quad (4.6.9)$$

That c_2^2 is near $1/2$ is not surprise taking into account the almost mass degeneracy of ν_{mu} and ν_τ . From the figure 30 of [46] it is clear that this solution belongs to 90 per cent likelihood region of LSND experiment but $\sin^2(2\theta)$ is about two times larger than the value allowed by Bugey reactor experiment. The study of various constraints given in [46] shows that the solution is consistent with bounds from all other experiments. If one assumes that $k > 169$ for $\nu_e \nu_\mu - \nu_e$ mass difference increases, implying slightly poorer consistency with LSND data.

There are reasons to hope that the actual rational solution can be regarded as a small deformation of this solution obtained by assuming that c_3 is non-vanishing. $s_1^2 = \frac{69-2n_2-1}{60-51c_3^2}$ increases in the deformation by $O(c_3^2)$ term but if c_3 is positive the value of $c_2^2 \simeq \frac{24-102c_1^0 c_2^0 s_2^0 c_3}{49} \sim \frac{24-61c_3}{49}$ decreases by $O(c_3)$ term so that it should be possible to reduce the value of $\sin^2(2\theta)$. Consistency with Bugey reactor experiment requires $.030 \leq \sin^2(2\theta) < .033$. $\sin^2(2\theta) = .032$ is achieved for $s_1^2 \simeq .035, s_2^2 \simeq .51$ and $c_3^2 \simeq .068$. The construction of U and D matrices for quarks shows that very stringent number theoretic conditions are obtained and as in case of quarks it might be necessary to allow complex CP breaking phase in the mixing matrix. One might even hope that the solution to the conditions is unique.

For the minimal rational mixing one has $s(\nu_e) = 5$, $s(\nu_\mu) = 36$ and $s(\nu_\tau) = 37$ if unmixed ν_e corresponds to $s = 4$. For $s = 5$ first order contributions are shifted by one unit. The masses ($s = 4$ case) and mass squared differences are given by the following table.

k	$m(\nu_e)$	$m(\nu_\mu)$	$m(\nu_\tau)$	$\Delta m^2(\nu_\mu - \nu_e)$	$\Delta m^2(\nu_\tau - \nu_e)$
169	.27 eV	.66 eV	.67 eV	.32 eV ²	.01 eV ²

Predictions for neutrino masses and mass squared splittings for $k = 169$ case.

Evidence for the dynamical mass scale of neutrinos

In recent years (I am writing this towards the end of year 2004 and much later than previous lines) a great progress has been made in the understanding of neutrino masses and neutrino mixing. The pleasant news from TGD perspective is that there is a strong evidence that neutrino masses depend on environment [88]. In TGD framework this translates to the statement that neutrinos can suffer topological condensation in several p-adic length scales. Not only in the p-adic length scales suggested by the number theoretical considerations but also in longer length scales, as will be found.

The experiments giving information about mass squared differences can be divided into three categories [88].

i) There along baseline experiments, which include solar neutrino experiments [40], KamLAND [43], K2K [42], and SuperK [41] as well as earlier studies of solar neutrinos. These experiments see

evidence for the neutrino mixing and involve significant propagation through dense matter. For the solar neutrinos and KamLAND the mass splittings are estimated to be of order $O(8 \times 10^{-5}) \text{ eV}^2$ or more cautiously $8 \times 10^{-5} \text{ eV}^2 < \delta m^2 < 2 \times 10^{-3} \text{ eV}^2$. For K2K and atmospheric neutrinos the mass splittings are of order $O(2 \times 10^{-3}) \text{ eV}^2$ or more cautiously $\delta m^2 > 10^{-3} \text{ eV}^2$. Thus the scale of mass splitting seems to be smaller for neutrinos in matter than in air, which would suggest that neutrinos able to propagate through a dense matter travel at space-time sheets corresponding to a larger p-adic length scale than in air.

ii) There are null short baseline experiments including CHOOZ, Bugey, and Palo Verde reactor experiments, and the higher energy CDHS, JARME, CHORUS, and NOMAD experiments, which involve muonic neutrinos (for references see [88]). No evidence for neutrino oscillations have been seen in these experiments.

iii) The results of LSND experiment[46] are consistent with oscillations with a mass splitting greater than $3 \times 10^{-2} \text{ eV}^2$. LSND has been generally been interpreted as necessitating a mixing with sterile neutrino. If neutrino mass scale is dynamical, situation however changes.

If one assumes that the p-adic length scale for the space-time sheets at which neutrinos can propagate is different for matter and air, the situation changes. According to [88] a mass $3 \times 10^{-2} \text{ eV}$ in air could explain the atmospheric results whereas mass of order $.1 \text{ eV}$ and $.07 \text{ eV}^2 < \delta m^2 < .26 \text{ eV}^2$ would explain the LSND result. These limits are of the same order as the order of magnitude predicted by $k = 169$ topological condensation.

Assuming that the scale of the mass splitting is proportional to the p-adic mass scale squared, one can consider candidates for the topological condensation levels involved.

1. Suppose that $k = 169 = 13^2$ is indeed the condensation level for LSND neutrinos. $k = 173$ would predict $m_{\nu_e} \sim 7 \times 10^{-2} \text{ eV}$ and $\delta m^2 \sim .02 \text{ eV}^2$. This could correspond to the masses of neutrinos propagating through air. For $k = 179$ one has $m_{\nu_e} \sim .8 \times 10^{-2} \text{ eV}$ and $\delta m^2 \sim 3 \times 10^{-4} \text{ eV}^2$ which could be associated with solar neutrinos and KamLAND neutrinos.
2. The primes $k = 157, 163, 167$ associated with Gaussian Mersennes would give $\delta m^2(157) = 2^6 \delta m^2(163) = 2^{10} \delta m^2(167) = 2^{12} \delta m^2(169)$ and mass scales $m(157) \sim 22.8 \text{ eV}$, $m(163) \sim 3.6 \text{ eV}$, $m(167) \sim .54 \text{ eV}$. These mass scales are unrealistic or propagating neutrinos. The interpretation consistent with TGD inspired model of condensed matter in which neutrinos screen the classical Z^0 force generated by nucleons would be that condensed matter neutrinos are confined inside these space-time sheets whereas the neutrinos able to propagate through condensed matter travel along $k > 167$ space-time sheets.

The results of MiniBooNE group as a support for the energy dependence of p-adic mass scale of neutrino

The basic prediction of TGD is that neutrino mass scale can depend on neutrino energy and the experimental determinations of neutrino mixing parameters support this prediction. The newest results (11 April 2007) about neutrino oscillations come from MiniBooNE group which has published its first findings [49] concerning neutrino oscillations in the mass range studied in LSND experiments [47].

1. The motivation for MiniBooNE

Neutrino oscillations are not well-understood. Three experiments LSND, atmospheric neutrinos, and solar neutrinos show oscillations but in widely different mass regions (1 eV^2 , $3 \times 10^{-3} \text{ eV}^2$, and $8 \times 10^{-5} \text{ eV}^2$).

In TGD framework the explanation would be that neutrinos can appear in several p-adically scaled up variants with different mass scales and therefore different scales for the differences Δm^2 for neutrino masses so that one should not try to explain the results of these experiments using single neutrino mass scale. In single-sheeted space-time it is very difficult to imagine that neutrino mass scale would depend on neutrino energy since neutrinos interact so extremely weakly with matter. The best known attempt to assign single mass to all neutrinos has been based on the use of so called sterile neutrinos which do not have electro-weak couplings. This approach is an ad hoc trick and rather ugly mathematically and excluded by the results of MiniBooNE experiments.

2. The result of MiniBooNE experiment

The purpose of the MiniBooNE experiment was to check whether LSND result $\Delta m^2 = 1\text{eV}^2$ is genuine. The group used muon neutrino beam and looked whether the transformations of muonic neutrinos to electron neutrinos occur in the mass squared region $\Delta m^2 \simeq 1\text{eV}^2$. No such transitions were found but there was evidence for transformations at low neutrino energies.

What looks first as an over-diplomatic formulation of the result was *MiniBooNE researchers showed conclusively that the LSND results could not be due to simple neutrino oscillation, a phenomenon in which one type of neutrino transforms into another type and back again.* rather than direct refutation of LSND results.

3. LSND and MiniBooNE are consistent in TGD Universe

The habitant of the many-sheeted space-time would not regard the previous statement as a mere diplomatic use of language. It is quite possible that neutrinos studied in MiniBooNE have suffered topological condensation at different space-time sheet than those in LSND if they are in different energy range (the preferred rest system fixed by the space-time sheet of the laboratory or Earth). To see whether this is the case let us look more carefully the experimental arrangements.

1. In LSND experiment 800 MeV proton beam entering in water target and the muon neutrinos resulted in the decay of produced pions. Muonic neutrinos had energies in 60-200 MeV range [47].
2. In MiniBooNE experiment [49] 8 GeV muon beam entered Beryllium target and muon neutrinos resulted in the decay of resulting pions and kaons. The resulting muonic neutrinos had energies the range 300-1500 GeV to be compared with 60-200 MeV.

Let us try to make this more explicit.

1. Neutrino energy ranges are quite different so that the experiments need not be directly comparable. The mixing obeys the analog of Schrödinger equation for free particle with energy replaced with $\Delta m^2/E$, where E is neutrino energy. The mixing probability as a function of distance L from the source of muon neutrinos is in 2-component model given by

$$P = \sin^2(\theta)\sin^2(1.27\Delta m^2 L/E) .$$

The characteristic length scale for mixing is $L = E/\Delta m^2$. If L is sufficiently small, the mixing is fifty-fifty already before the muon neutrinos enter the system, where the measurement is carried out and no mixing is detected. If L is considerably longer than the size of the measuring system, no mixing is observed either. Therefore the result can be understood if Δm^2 is much larger or much smaller than E/L , where L is the size of the measuring system and E is the typical neutrino energy.

2. MiniBooNE experiment found evidence for the appearance of electron neutrinos at low neutrino energies (below 500 MeV) which means direct support for the LSND findings and for the dependence of neutron mass scale on its energy relative to the rest system defined by the space-time sheet of laboratory.
3. Uncertainty Principle inspires the guess $L_p \propto 1/E$ implying $m_p \propto E$. Here E is the energy of the neutrino with respect to the rest system defined by the space-time sheet of the laboratory. Solar neutrinos indeed have the lowest energy (below 20 MeV) and the lowest value of Δm^2 . However, atmospheric neutrinos have energies starting from few hundreds of MeV and Δm^2 is by a factor of order 10 higher. This suggests that the the growth of Δm^2 with E^2 is slower than linear. It is perhaps not the energy alone which matters but the space-time sheet at which neutrinos topologically condense. For instance, MiniBooNE neutrinos above 500 MeV would topologically condense at space-time sheets for which the p-adic mass scale is higher than in LSND experiments and one would have $\Delta m^2 \gg 1\text{eV}^2$ implying maximal mixing in length scale much shorter than the size of experimental apparatus.
4. One could also argue that topological condensation occurs in condensed matter and that no topological condensation occurs for high enough neutrino energies so that neutrinos remain massless. One can even consider the possibility that the p-adic length scale L_p is proportional

to E/m_0^2 , where m_0 is proportional to the mass scale associated with non-relativistic neutrinos. The p-adic mass scale would obey $m_p \propto m_0^2/E$ so that the characteristic mixing length would be by a factor of order 100 longer in MiniBooNE experiment than in LSND.

Comments

Some comments on the proposed scenario are in order: some of the are written much later than the previous text.

1. Mass predictions are consistent with the bound $\Delta m(\nu_\mu, \nu_e) < 2 eV^2$ coming from the requirement that neutrino mixing does not spoil the so called r-process producing heavy elements in Super Novae [50].
2. TGD neutrinos cannot solve the dark matter problem: the total neutrino mass required by the cold+hot dark matter models would be about 5 eV. In [24] a model of galaxies based on string like objects of galaxy size and providing a more exotic source of dark matter, is discussed.
3. One could also consider the explanation of LSND data in terms of the interaction of ν_μ and nucleon via the exchange of $g = 1$ W boson. The fraction of the reactions $\bar{\nu}_\mu + p \rightarrow e^+ + n$ is at low neutrino energies $P \sim \frac{m_W^4(g=0)}{m_W^4(g=1)} \sin^2(\theta_c)$, where θ_c denotes Cabibbo angle. Even if the condensation level of $W(g = 1)$ is $k = 89$, the ratio is by a factor of order .05 too small to explain the average $\nu_\mu \rightarrow \nu_e$ transformation probability $P \simeq .003$ extracted from LSND data.
4. The predicted masses exclude MSW and vacuum oscillation solutions to the solar neutrino problem unless one assumes that several condensation levels and thus mass scales are possible for neutrinos. This is indeed suggested by the previous considerations.

4.6.3 Quark masses

The prediction of quark masses is more difficult due to the facts that the deduction of even the p-adic length scale determining the masses of these quarks is a non-trivial task, and the original identification was indeed wrong. Second difficulty is related to the topological mixing of quarks. The new scenario leads to a unique identification of masses with top quark mass as an empirical input and the thermodynamical model of topological mixing as a new theoretical input. Also CKM matrix is predicted highly uniquely.

Basic mass formulas

By the earlier mass calculations and construction of CKM matrix the ground state conformal weights of U and D type quarks must be $h_{gr}(U) = -1$ and $h_{gr}(D) = 0$. The formulas for the eigenvalues of CP_2 spinor Laplacian imply that if m_0^2 is used as a unit, color conformal weight $h_c \equiv m_{CP_2}^2$ is integer for $p \bmod = \pm 1$ for U type quark belonging to $(p + 1, p)$ type representation and obeying $h_c(U) = (p^2 + 3p + 2)/3$ and for $p \bmod 3 = 1$ for D type quark belonging $(p, p + 2)$ type representation and obeying $h_c(D) = (p^2 + 4p + 4)/3$. Only these states can be massless since color Hamiltonians have integer valued conformal weights.

In the recent case the minimal $p = 1$ states correspond to $h_c(U) = 2$ and $h_c(D) = 3$. $h_{gr}(U) = -1$ and $h_{gr}(D) = 0$ reproduce the previous results for quark masses required by the construction of CKM matrix. This requires super-symplectic operators O with a net conformal weight $h_{sc} = -3$ just as in the leptonic case. The facts that the values of p are minimal for spinor harmonics and the super-symplectic operator is same for both quarks and leptons suggest that the construction is not had hoc. The real justification would come from the demonstration that $h_{sc} = -3$ defines null state for SCV: this would also explain why h_{sc} would be same for all fermions.

Consider now the mass squared values for quarks. For $h(D) = 0$ and $h(U) = -1$ and using $m_0^2/3$ as a unit the expression for the thermal contribution to the mass squared of quark is given by the formula

$$\begin{aligned}
M^2 &= (s + X) \frac{m_0^2}{p} , \\
s(U) &= 5 , \quad s(D) = 8 , \\
X &\equiv \frac{(3Yp)_R}{3} ,
\end{aligned} \tag{4.6.10}$$

where the second order contribution Y corresponds to renormalization effects coming and depending on the isospin of the quark. When m_0^2 is used as a unit X is replaced by $X = (Y_p)_R$.

With the above described assumptions one has the following mass formula for quarks

$$\begin{aligned}
M^2(q) &= A(q) \frac{m_0^2}{p(q)} , \\
A(u) &= 5 + X_U(p(u)) , \quad A(c) = 14 + X_U(p(c)) , \quad A(t) = 65 + X_U(p(t)) , \\
A(d) &= 8 + X_D(p(d)) , \quad A(s) = 17 + X_D(p(s)) , \quad A(b) = 68 + X_D(p(b)) .
\end{aligned} \tag{4.6.11}$$

p-Adic length scale hypothesis allows to identify the p-adic primes labelling quarks whereas topological mixing of U and D quarks allows to deduce topological mixing matrices U and D and CKM matrix V and precise values of the masses apart from effects like color magnetic spin orbit splitting, color Coulombic energy, etc..

Integers n_{q_i} satisfying $\sum_i n(U_i) = \sum_i n(D_i) = 69$ characterize the masses of the quarks and also the topological mixing to high degree. The reason that modular contributions remain integers is that in the p-adic context non-trivial rationals would give CP_2 mass scale for the real counterpart of the mass squared. In the absence of mixing the values of integers are $n_d = n_u = 0$, $n_s = n_c = 9$, $n_b = n_t = 60$.

The fact that CKM matrix V expressible as a product $V = U^\dagger D$ of topological mixing matrices is near to a direct sum of 2×2 unit matrix and 1×1 unit matrix motivates the approximation $n_b \simeq n_t$. The large masses of top quark and of $t\bar{t}$ meson encourage to consider a scenario in which $n_t = n_b = n \leq 60$ holds true.

The model for topological mixing matrices and CKM matrix predicts U and D matrices highly uniquely and allows to understand quark and hadron masses in surprisingly detailed level.

1. $n_d = n_u = 60$ is not allowed by number theoretical conditions for U and D matrices and by the basic facts about CKM matrix but $n_t = n_b = 59$ allows almost maximal masses for b and t . This is not yet a complete hit. The unitarity of the mixing matrices and the construction of CKM matrix to be discussed in the next section forces the assignments

$$(n_d, n_s, n_b) = (5, 5, 59) , \quad (n_u, n_c, n_t) = (5, 6, 58) . \tag{4.6.12}$$

fixing completely the quark masses apart possible Higgs contribution [17]. Note that top quark mass is still rather near to its maximal value.

2. The constraint that valence quark contribution to pion mass does not exceed pion mass implies the constraint $n(d) \leq 6$ and $n(u) \leq 6$ in accordance with the predictions of the model of topological mixing. $u - d$ mass difference does not affect $\pi^+ - \pi^0$ mass difference and the quark contribution to $m(\pi)$ is predicted to be $\sqrt{(n_d + n_u + 13)/24} \times 136.9$ MeV for the maximal value of CP_2 mass (second order p-adic contribution to electron mass squared vanishes).

The p-adic length scales associated with quarks and quark masses

The identification of p-adic length scales associated with the quarks has turned to be a highly non-trivial problem. The reasons are that for light quarks it is difficult to deduce information about quark masses for hadron masses and that the unknown details of the topological mixing (unknown until the

advent of the thermodynamical model [17]) made possible several p-adic length scales for quarks. It has also become clear that the p-adic length scale can be different for free quark and bound quark and that bound quark p-adic scale can depend on hadron.

Two natural constraints have however emerged from the recent work.

1. Quark contribution to the hadron mass cannot be larger than color contribution and for quarks having $k_q \neq 107$ quark contribution to mass is added to color contribution to the mass. For quarks with same value of k conformal weight rather than mass is additive whereas for quarks with different value of k masses are additive. An important implication is that for diagonal mesons $M = q\bar{q}$ having $k(q) \neq 107$ the condition $m(M) \geq \sqrt{2}m_q$ must hold true. This gives strong constraints on quark masses.
2. The realization that scaled up variants of quarks explain elegantly the masses of light hadrons allows to understand large mass splittings of light hadrons without the introduction of strong isospin-isospin interaction.

The new model for quark masses is based on the following identifications of the p-adic length scales.

1. The nuclear p-adic length scale $L(k)$, $k = 113$, corresponds to the p-adic length scale determining the masses of u, d, and s quarks. Note that $k = 113$ corresponds to a so called Gaussian Mersenne. The interpretation is that quark massivation occurs at nuclear space-time sheet at which quarks feed their em fluxes. At $k = 107$ space-time sheet, where quarks feed their color gauge fluxes, the quark masses are vanishing in the first p-adic order. This could be due to the fact that the p-adic temperature is $T_p = 1/2$ at this space-time sheet so that the thermal contribution to the mass squared is negligible. This would reflect the fact that color interactions do not involve any counterpart of Higgs mechanism.

p-Adic mass calculations turn out to work remarkably well for massive quarks. The reason could be that M_{107} hadron physics means that *all* quarks feed their color gauge fluxes to $k = 107$ space-time sheets so that color contribution to the masses becomes negligible for heavy quarks as compared to Super-Kac Moody and modular contributions corresponding to em gauge flux feeded to $k > 107$ space-time sheets in case of heavy quarks. Note that Z^0 gauge flux is feeded to space-time sheets at which neutrinos reside and screen the flux and their size corresponds to the neutrino mass scale. This picture might throw some light to the question of whether and how it might be possible to demonstrate the existence of M_{89} hadron physics.

One might argue that $k = 107$ is not allowed as a condensation level in accordance with the idea that color and electro-weak gauge fluxes cannot be feeded at the space-time space time sheet since the classical color and electro-weak fields are functionally independent. The identification of η' meson as a bound state of scaled up $k = 107$ quarks is not however consistent with this idea unless one assumes that $k = 107$ space-time sheets in question are separate.

2. The requirement that the masses of diagonal pseudoscalar mesons of type $M = q\bar{q}$ are larger but as near as possible to the quark contribution $\sqrt{2}m_q$ to the valence quark mass, fixes the p-adic primes $p \simeq 2^k$ associated with c , b quarks but not t since toponium does not exist. These values of k are "nominal" since k seems to be dynamical. c quark corresponds to the p-adic length scale $k(c) = 104 = 2^3 \times 13$. b quark corresponds to $k(b) = 103$ for $n(b) = 5$. Direct determination of p-adic scale from top quark mass gives $k(t) = 94 = 2 \times 47$ so that secondary p-adic length scale is in question.

Top quark mass tends to be slightly too low as compared to the most recent experimental value of $m(t) = 169.1$ GeV with the allowed range being [164.7, 175.5] GeV [50]. The optimal situation corresponds to $Y_e = 0$ and $Y_t = 1$ and happens to give top mass exactly equal to the most probable experimental value. It must be emphasized that top quark is experimentally in a unique position since toponium does not exist and top quark mass is that of free top.

In the case of light quarks there are good reasons to believe that the p-adic mass scale of quark is different for free quark and bound state quark and that in case of bound quark it can also depend on hadron. This would explain the notions of valence (constituent) quark and current quark mass as

masses of bound state quark and free quark and leads also to a TGD counterpart of Gell-Mann-Okubo mass formula [17].

1. Constituent quark masses

Constituent quark masses correspond to masses derived assuming that they are bound to hadrons. If the value of k is assumed to depend on hadron one obtains nice mass formula for light hadrons as will be found later. The following table summarizes constituent quark masses as predicted by this model.

q	d	u	s	c	b	t
n_q	4	5	6	6	59	58
s_q	12	10	14	11	67	63
$k(q)$	113	113	113	104	103	94
$m(q)/GeV$.105	.092	.105	2.191	7.647	167.8

Table 2. Constituent quark masses predicted for diagonal mesons assuming $(n_d, n_s, n_b) = (5, 5, 59)$ and $(n_u, n_c, n_t) = (5, 6, 58)$, maximal CP_2 mass scale ($Y_e = 0$), and vanishing of second order contributions.

2. Current quark masses

Current quark masses would correspond to masses of free quarks which tend to be lower than valence quark masses. Hence k could be larger in the case of light quarks. The table of quark masses in Wikipedia [42] gives the value ranges for current quark masses depicted in the table below together with TGD predictions for the spectrum of current quark masses.

q	d	u	s
$m(q)_{exp}/MeV$	4-8	1.5-4	80-130
$k(q)$	(122,121,120)	(125,124,123,122)	(114,113,112)
$m(q)/MeV$	(4.5,6.6,9.3)	(1.4,2.0,2.9,4.1)	(74,105,149)
q	c	b	t
$m(q)_{exp}/MeV$	1150-1350	4100-4400	1691
$k(q)$	(106,105)	(105,104)	92
$m(q)/MeV$	(1045,1477)	(3823,5407)	167.8×10^3

Table 3. The experimental value ranges for current quark masses [42] and TGD predictions for their values assuming $(n_d, n_s, n_b) = (5, 5, 59)$, $(n_u, n_c, n_t) = (5, 6, 58)$, and $Y_e = 0$. For top quark $Y_t = 0$ is assumed. $Y_t = 1$ would give 169.2 GeV.

Some comments are in order.

1. The long p-adic length associated with light quarks seem to be in conflict with the idea that quarks have sizes smaller than hadron size. The paradox disappears when one realized that $k(q)$ characterizes the electromagnetic "field body" of quark having much larger size than hadron.
2. u and d current quarks correspond to a mass scale not much higher than that of electron and the ranges for mass estimates suggest that u could correspond to scales $k(u) \in (125, 124, 123, 122) = (5^3, 4 \times 31, 3 \times 41, 2 \times 61)$, whereas d would correspond to $k(d) \in (122, 121, 120) = (2 \times 61, 11^2, 3 \times 5 \times 8)$.
3. The TGD based model for nuclei based on the notion of nuclear string leads to the conclusion that exotic copies of $k = 113$ quarks having $k = 127$ are present in nuclei and are responsible for the color binding of nuclei [23, 47].
4. The predicted values for c and b masses are slightly too low for $(k(c), k(b)) = (106, 105) = (2 \times 53, 3 \times 5 \times 7)$. Second order Higgs contribution could increase the c mass into the range given in [42] but not that of b .

5. The mass of top quark has been slightly below the experimental estimate for long time. The experimental value has been coming down slowly and the most recent value obtained by CDF [51] is $m_t = 165.1 \pm 3.3 \pm 3.1$ GeV and consistent with the TGD prediction for $Y_e = Y_t = 0$.

One can talk about constituent and current quark masses simultaneously only if they correspond to dual descriptions. $M^8 - H$ duality [26] has been indeed suggested to relate the old fashioned low energy description of hadrons in terms of $SO(4)$ symmetry (Skyrme model) and higher energy description of hadrons based on QCD. In QCD description the mass of say baryon would be dominated by the mass associated with super-symplectic quanta carrying color. In $SO(4)$ description constituent quarks would carry most of the hadron mass.

Can Higgs field develop a vacuum expectation in fermionic sector at all?

An important conclusion following from the calculation of lepton and quark masses is that if Higgs contribution is present, it can be of second order p-adically and even negligible, perhaps even vanishing. There is indeed an argument forcing to consider this possibility seriously. The recent view about elementary particles is following.

1. Fermions correspond to CP_2 type vacuum extremals topologically condensed at positive/negative energy space-time sheets carrying quantum numbers at light-like wormhole throat. Higgs and gauge bosons correspond to wormhole contacts connecting positive and negative energy space-time sheets and carrying fermion and anti-fermion quantum numbers at the two light-like wormhole throats.
2. If the values of p-adic temperature are $T_p = 1$ and $T_p = 1/n$, $n > 1$ for fermions and bosons the thermodynamical contribution to the gauge boson mass is negligible.
3. Different p-adic temperatures and Kähler coupling strengths for fermions and bosons make sense if bosonic and fermionic partonic 3-surfaces meet only along their ends at the vertices of generalized Feynman diagrams but have no other common points [19]. This forces to consider the possibility that fermions cannot develop Higgs vacuum expectation value although they can couple to Higgs. This is not in contradiction with the modification of sigma model of hadrons based on the assumption that vacuum expectation of σ field gives a small contribution to hadron mass [20] since this field can be assigned to some bosonic space-time sheet pair associated with hadron.
4. Perhaps the most elegant interpretation is that ground state conformal is equal to the square of the eigenvalue of the modified Dirac operator. The ground state conformal weight is negative and its deviation from half odd integer value gives contribution to both fermion and boson masses. The Higgs expectation associated with coherent state of Higgs like wormhole contacts is naturally proportional to this parameter since no other parameter with dimensions of mass is present. Higgs vacuum expectation determines gauge boson masses only apparently if this interpretation is correct. The contribution of the ground state conformal weight to fermion mass square is near to zero. This means that λ is very near to negative half odd integer and therefore no significant difference between fermions and gauge bosons is implied.

4.7 Higgsy aspects of particle massivation

4.7.1 Can p-adic thermodynamics explain the masses of intermediate gauge bosons?

The requirement that the electron-intermediate gauge boson mass ratios are sensible, serves as a stringent test for the hypothesis that intermediate gauge boson masses result from the p-adic thermodynamics. It seems that the only possible option is that the parameter k has same value for both bosons, leptons, and quarks:

$$k_B = k_L = k_q = 1 \ .$$

In this case all gauge bosons have $D(0) = 1$ and there are good chances to obtain boson masses correctly. $k = 1$ together with $T_p = 1$ implies that the thermal masses of very many boson states are extremely heavy so that the spectrum of the boson exotics is reduced drastically. For $T_p = 1/2$ the thermal contribution to the mass squared is completely negligible.

Contrary to the original optimistic beliefs based on calculational error, it turned out impossible to predict W/e and Z/e mass ratios correctly in the original p-adic thermodynamics scenario. Although the errors are of order 20-30 percent, they seemed to exclude the explanation for the massivation of gauge bosons using p-adic thermodynamics.

1. The thermal mass squared for a boson state with N active sectors (non-vanishing vacuum weight) is determined by the partition function for the tensor product of N NS type Super Virasoro algebras. The degeneracies of the excited states as a function of N and the weight Δ of the operator creating the massless state are given in the table below.
2. Both W and Z must correspond to $N = 2$ active Super Virasoro sectors for which $D(1) = 1$ and $D(2) = 3$ so that (using the formulas of p-adic thermodynamics the thermal mass squared is $m^2 = k_B(p + 5p^2)$ for $T_p = 1$. The second order contribution to the thermal mass squared is extremely small so that Weinberg angle vanishes in the thermal approximation. $k_B = 1$ gives Z/e mass-ratio which is about 22 per cent too high. For $T_p = 1/2$ thermal masses are completely negligible.
3. The thermal prediction for W -boson mass is the same as for Z^0 mass and thus even worse since the two masses are related $M_W^2 = M_Z^2 \cos^2(\theta_W)$.

4.7.2 Comparison of TGD Higgs and with MSSM Higgs

The notion of Higgs in TGD framework differs from that of standard model and super-symmetric extension in several respects. Very concisely, the two complex $SU(2)_V$ doublets are replaced with scalar and pseudoscalar triplet and singlet so that the number of field components is same. The Higgs possibly developing vacuum expectation is now uniquely the scalar singlet unless one allows parity breaking. The number of remaining Higgs field components is 5 as in the minimal supersymmetric extension of the standard model.

TGD based particle concept very briefly

Before attempt to clarify the differences between TGD and standard model Higgs it is good to list the basic ideas behind TGD based notion of particle.

1. Bosonic emergence means that gauge bosons and Higgs and their super partners can be in the first approximation regarded as wormhole contacts with the throats carrying quantum numbers of fermion and antifermion. A given throat carrying fermionic quantum numbers. Also many fermion states are possible and have interpretation in terms of a supersymmetry extending the ordinary space-time supersymmetry in which super-generators are simply the fermionic oscillator operators assignable to the partonic 2-surface. These generators can be used to construct various super-conformal algebras. Right-handed neutrinos define the analog of ordinary space-time super-supersymmetry as it is encountered in MSSM. In topological condensation also fermions become wormhole contacts with second throat carrying purely bosonic quantum numbers.
2. The weak form of electric magnetic duality forces the conclusion that wormhole throats carry Kähler magnetic charges which much be neutralized by opposite Kähler magnetic charge. The natural idea is that monopole confinement is also behind color confinement and electroweak screening. In the case of color confinement the valence quarks would form wormhole throats connected by color magnetic flux tubes having total Kähler magnetic charge. Weak screening would mean that the throat compensating the Kähler magnetic charge of fermionic throat contains a neutrino-antineutrino pairs screening the weak isospin. This leaves to Z^0 coupling $I_L^3 + \sin^2(\theta_W)Q_{em}$ and if classical Z^0 field is present this leads to an interaction distinguishing between TGD and standard model.

3. Particle massivation is described by p-adic thermodynamics. p-Adic thermodynamics cannot explain gauge boson masses and if it contributes the contribution is small and corresponds to low p-adic temperatures $T_p = 1/n$. It is not yet completely clear whether the generation of vacuum contribution to ground state conformal weight implying deviation from half-integer value is responsible for weak gauge boson masses. It might be sensible to speak about coherent state of Higgs bosons in zero energy ontology and also in the case of fermions if interacting fermions have suffered topological condensation. If this is the case Higgs vacuum expectation value defining the coherent state can contribute to the particle mass but only in the case of weak gauge bosons give a dominating contribution. It is not clear whether the generation of non-half-integer vacuum conformal weight and Higgs mechanisms could be seen descriptions of one and same thing.

Scalar and pseudo-scalar triplet and singlet instead of two doublets

TGD based notion of Higgs differs from its standard model and MSSM counterpart because the notion of spinor is different. If one believes on the following arguments, the basic implication is that two Higgs doublets of MSSM are replaced with scalar and pseudo-scalar triplet and singlet.

1. In TGD framework space-time spinors are induced spinors and therefore spinors of 8-D space $M^4 \times CP_2$. The mixing of M^4 chiralities in the modified Dirac equation in the space-time interior serves as a tell-tale signature for the massivation and does not imply mixing of the imbedding space chiralities identified in terms of leptons and quarks.
2. Group theoretically gauge bosons and Higgs itself corresponds to a tensor product of two $M^4 \times CP_2$ spinors giving rise to a spin singlet. In electroweak degrees of freedom one has a tensor product of right and left handed doublets decomposing to triplet and singlet under $SU(2)_V$. The first guess would be that one obtains just triplet 3 and singlet 1 whereas in standard model one has a complex $SU(2)_V$ doublet. In MSSM the cancellation of anomalies requires two doublets. As noticed, TGD allows supersymmetry generalizing the usual space-time supersymmetry and also no anomaly cancellation argument allows to expect a pairs of triplets and singlets.
3. One can assign fermion with "upper" throat and antifermion with the "lower" throat or vice versa and one can have both the sum or difference of these two states. This does not however imply additional degeneracy. Fermionic statistics requires the antisymmetry of the state with respect to the exchange of all quantum numbers. Spin and isospin triplets (singlets) are symmetric (antisymmetric) under the exchange of spin quantum numbers and singlets antisymmetric. In the case of Higgs triplet (singlet) the sum (difference) of these states must be assumed and there is no additional degeneracy.
4. One can construct gauge bosons and Higgs type particles from both quarks and leptons. The requirement that the gauge bosons couple to both quarks and leptons implies that they correspond to sums of these Higgses and behave like H -vectors for one has $\Gamma_9 = 1$. One can however ask whether also H -axial vector gauge bosons and Higgs with $\Gamma_9 = -1$ should be allowed. They are not suggested by the study of the modified Dirac equation and it seems that this leads to physically non-sensical results. First of all, the exchanges of vectorial and axial Higgses between leptons and quarks would be of opposite sign and at high energies the sum over these exchanges would approach zero so that quark and lepton sectors would separate into non-interacting worlds. It is also difficult to imagine how one could avoid H -axial massless photon. p-Adic thermodynamics would allow the H -axial photon to become massive but it is not possible to understand how the H -axial scalar Higgs could transform to a longitudinal degree of freedom of the resulting H -axial photon.
5. One can construct the most general candidate for a Higgs particle using as charge matrix contracted between spinors associated with the opposite wormhole throats the product of a vector in the tangent space of CP_2 represented as sum of constant gamma matrices γ_A and electroweak charge matrix. One can express the products of the CP_2 gamma matrices and charge matrices in terms of CP_2 gamma matrices γ_A and $\gamma_5(CP_2)\gamma_A$. The action of CP_2 gamma matrix γ_5 however reduces to that of $\epsilon\gamma_5(M^4)$, where the sign factor $\epsilon = \pm 1$ depends on H-chirality. Therefore one would have scalar Higgs and pseudo-scalar Higgs and the couplings of pseudo-scalar

Higgs are of opposite sign for quarks and leptons. In unitary gauge one would have neutral scalar Higgs and 4 pseudo-scalar Higgses with the same charge spectrum as in MSSM. One can indeed construct Higgs particles as fermion-antifermion pairs by using products of charge matrices and CP_2 tangent space vector and transform them to scalar and pseudoscalar multiplets.

6. In Higgs mechanism the key idea is that one can represent the directional degrees of freedom of Higgs field in terms of coset space G/H , now $SU(2)_L \times U(1)/U(1)_{em}$. Therefore Higgs field can be written as in the form $exp(\sum_{T_a \in t} T^a \xi_a / v)(\rho + v)$, $t = g - h$, where v is the expectation value of the Higgs field fixing a preferred direction. The gauge transformation $g = exp(-\sum_{T_a \in t} T^a \xi_a / v)$ transforms Higgs to $\rho + v$ so that the degrees of freedom corresponding to the direction of Higgs are "eaten" by charge gauge potentials. In the resulting gauge the action contains only the YM part and Higgs term restricted to the fluctuations of Higgs around vacuum in the direction of v .
In the recent case the coset space would be the coset space of the holonomy group of CP_2 divided by the subgroup defined by electromagnetic charge commuting with the vacuum expectation value which is therefore linear combination of γ_0 and γ_3 in the most general case. The condition that entire $SU(2)_V$ leaves invariant the preferred direction fixes this direction to γ_0 which corresponds to the radial coordinate of CP_2 in the standard vielbein basis. In the recent case CP_2 holonomy group naturally defines a preferred direction of Higgs field and it seems that vacuum expectation value is not necessary for the elimination of the charged Higgs. Neutral Higgs would essentially correspond to the magnitude of the Higgs field.
7. If the TGD based description of radiative corrections relying on the notion of generalized Feynman diagram is approximately equivalent with QFT based description and if should not differ too dramatically from those of MSSM in the approximation of $N = 1$ supersymmetry meaning that only the super partners obtained using right handed neutrinos and antineutrinos are taken into account. At high energies the the action of γ_5 gives only a minus sign telling the M^4 chirality of approximately massless particle and one has right to expect that the effects of pseudo-scalar exchange in loops do not differ dramatically from those of a scalar exchange.

Can one identify a classical correlate for the Higgs?

The natural question is whether one can identify classical correlates for the Higgs field and massivation. Kähler action does not allow to identify any obvious correlates whereas Kähler Dirac action does.

1. Kähler Dirac action in the interior of space-time surface should contain the counterpart of Higgs term whose signature is that it mixes M^4 chiralities. The interaction term analogous to that appearing in the ordinary Dirac action coupled to gauge fields is

$$\begin{aligned}
 L_{int} &= \bar{\Psi} \hat{\Gamma}^\alpha A_\alpha \Psi , \\
 \hat{\Gamma}^\alpha &= T^{\alpha k} \gamma_k = T^{\alpha k} \gamma_k(M^4) + T^{\alpha k} \gamma_k(CP_2) , \\
 T^{\alpha k} &= \frac{\partial L_K}{\partial(\partial_\alpha h^k)} .
 \end{aligned} \tag{4.7.1}$$

Here A_α are the components of the induced spinor connection. $T^{\alpha k}$ denotes canonical momentum densities and conserved momentum and color currents are closely related to them. They are required by internal consistency (in particular, by the consistency with the vacuum degeneracy of Kähler action) and super-symmetry. If action were defined by the volume of space-time surface in the induced metric, modified gamma matrices would reduce to induced gamma matrices coding information about classical gravitational fields. Also now information about gravitation is coded besides the dynamics of Kähler action associated with zero modes. Kähler field can indeed be said to characterize zero modes locally whereas quantum fluctuating degrees contributing to the WCW metric and therefore identifiable as gravitational degrees of freedom in generalized sense of the word [22].

The modified gamma matrices decompose to two parts corresponding to M^4 and CP_2 gamma matrices and the presence of CP_2 gamma matrices implies the mixing of M^4 chiralities so that

massivation is unavoidable once one has a space-time surface which does not correspond to the canonically imbedded M^4 . Also the kinetic part of $\hat{\Gamma}^\alpha \partial_\alpha$ contains a term mixing M^4 chiralities having no obvious counterpart in the ordinary Dirac equation. The important conclusion is that whatever the dynamical details of massivation are it must take place.

2. The interaction term $T^{\alpha k} \gamma_k (CP_2) A_\alpha$ of the modified Dirac action defined by the contraction of canonically conjugate momenta with gauge potentials mixes M^4 chiralities so that it is in this sense analogous to Higgs coupling. In gauge transformations the gauge potentials however transform inhomogeneously. Does this mean that the term in question can be interpreted only as a signature for the presence of particle massivation or is also the identification as the classical counterpart of Higgs field sensical?

Optimist could argue that there is a natural preferred gauge associated with the classical spinor connection. For instance, the Coulomb interaction term for Kähler action vanishes in preferred gauge for the general solution ansatz implying the reduction of Kähler function to Chern-Simons term for extremal in presence of a constraint expressing the weak form of electric-magnetic duality. For Kähler gauge potential this gauge is highly unique. Also, if one imagines adding to the induced gauge potential quantum fluctuating part representing the quantum field, one could say that the classical Higgs field transforms homogeneously and that quantum part is gauge transformed inhomogeneously. The situation remains unsettled.

3. The classical correlate for the Higgs field in TGD is not a genuine scalar field but defines a vector in the 4-D tangent space of CP_2 . This allows to speak about CP_2 polarization. If the notion of unitary gauge meaning that an electro-weak gauge rotation takes Higgs to a standard direction invariant under $SU(2)_V$ rotations - in particular those induced by the vectorial isospin I_V^3 appearing in electromagnetic charge- then one can say that CP_2 polarization is always in the same direction for the scalar Higgs. In the case of pseudo-scalar Higgs all four CP_2 polarizations are possible.

4.7.3 How TGD based description of particle massivation relates to Higgs mechanism

In TGD framework p-adic thermodynamics gives the dominating contribution to fermion masses, which is something completely new. In the case of gauge bosons thermodynamic contribution is small since the inverse integer valued p-adic temperature is $T = 1/2$ for bosons or even lower: for fermions one has $T = 1$.

Whether Higgs can contribute to the masses is not completely clear. In TGD framework Mexican hat potential however looks like trick. One must however keep in mind that any other mechanism must explain the ratio of W and Z^0 masses and how these bosons receive their longitudinal polarizations. One must also consider seriously the possibility that all components for the TGD counterpart of Higgs boson are transformed to the longitudinal polarizations of the gauge bosons. Twistorial approach to TGD indeed strongly suggests that also the gauge bosons regarded usually as massless have a small mass guaranteeing cancellation of IR singularities. As I started write to write this piece of text I believed that photon does not eat Higgs but had to challenge my beliefs. Maybe there is no Higgs to be found at LHC! Only pseudo-scalar partner of Higgs would remain to be discovered.

The weak form of electric magnetic duality implying that each wormhole throat carrying fermionic quantum numbers is accompanied by a second wormhole throat carrying opposite magnetic charge and neutrino pair screening weak isospin and making gauge bosons massive. Concerning the implications the following view looks the most plausible one at this moment.

1. Neutral Higgs-if not eaten by photon- could develop a coherent state meaning vacuum expectation value and this is naturally proportional to the inverse of the p-adic length scale as are boson masses. This contribution can be assigned to the magnetic flux tube mentioned above since it screens weak force - or equivalently - makes them massive. Higgs expectation would not cause boson massivation. Rather, massivation and Higgs vacuum expectation would be caused by the presence of the magnetic flux tubes. Standard model would suffer from a causal illusion. Even a worse illusion is possible if the photon eats the neutral Higgs.

2. The "stringy" magnetic flux tube connecting fermion wormhole throat and the wormhole throat containing neutrino pair would give to the vacuum conformal weight a small contribution and therefore to the mass squared of both fermions and gauge bosons (dominating one for the latter). This contribution would be small in the p-adic sense (proportional $1/p^2$ rather than $1/p$). I cannot calculate this "stringy" contribution but stringy formula in weak scale is very suggestive.
3. In the case of light fermions and massless gauge bosons the stringy contribution must vanish and therefore must correspond to $n = 0$ string excitation (string does not vibrate at all) : otherwise the mass of fermion would be of order weak boson mass. For weak bosons $n = 1$ would look like a natural identification but also $n = 0$ makes sense since $h \pm 1$ states corresponds opposite three-momenta for massless fermion and antifermion so that the state is massive. The mechanism bringing in the $h = 0$ helicity of gauge boson would be the TGD counterpart for the transformation of Higgs component to a longitudinal polarization. $n \geq 0$ excited states of fermions and $n \geq 1$ excitations of bosons having masses above weak boson masses are predicted and would mean new physics becoming possibly visible at LHC.

Consider now the identification of Higgs in TGD framework.

1. In TGD framework Higgs particles do not correspond to complex $SU(2)$ doublets but to triplet and singlet having same quantum numbers as gauge bosons. Therefore the idea that photon eats neutral Higgs is suggestive. Also a pseudo-scalar variant of Higgs is predicted. Let us see how these states emerge from weak strings.
2. The two kinds of massive states corresponding to $n = 0$ and $n = 1$ give rise to massive spin 1 and spin 2 particles. First of all, the helicity doublet $(1, -1)$ is necessarily massive since the 3-momenta for massless fermion and anti-fermion are opposite. For $n = L = 0$ this gives two states but helicity zero component is lacking. For $n = L = 1$ one has tensor product of doublet $(1, -1)$ and angular momentum triplet formed by $L = 1$ rotational state of the weak string. This gives 2×3 states corresponding to $J = 0$ and $J = 2$ multiplets. Note however than in spin degrees of freedom the Higgs candidate is not a genuine elementary scalar particle.
3. Fermion and antifermion can have parallel three momenta summing up to a massless 4-momentum. Spin vanishes so that one has Higgs like particle also now. This particle is however pseudo-scalar being group theoretically analogous to meson formed as a pair of quark and antiquark. p-Adic thermodynamics gives a contribution to the mass squared. By taking a tensor product with rotational states of strings one would obtain Regge trajectory containing pseudoscalar Higgs as the lowest state.

Consider now the problem how the gauge bosons can eat the Higgs boson to get their longitudinal component.

1. ($J = 0, n = 1$) Higgs state can be combined with $n = 0$ $h = \pm 1$ doublet to give spin 1 massive triplet provided the masses of the two states are same. This will be discussed below.
2. Also gauge bosons usually regarded as massless can eat the scalar Higgs so that Higgs like particle could disappear completely. There would be no Higgs to be discovered at LHC! But is this a real prediction? Could it be that it is not possible to have exactly massless photons and gluons? The mixing of M^4 chiralities for Chern-Simons Dirac equation implies that also collinear massless fermion and antifermion can have helicity ± 1 . The problem is that the mixing of the chiralities is a signature of massivation!

Could it really be that even the gauge bosons regarded as massless have a small mass characterized by the length scale of the causal diamond defining the physical IR cutoff and that the remaining Higgs component would correspond to the longitudinal component of photon? This would mean the number of particles in the final states for a particle reaction with a fixed initial state is always bounded from above. This is important for the twistorial aesthetics of generalized Feynman diagrammatics implied by zero energy ontology. Also the vanishing of IR divergences is guaranteed by a small physical mass [19]. Maybe internal consistency allows only pseudo-scalar Higgs.

The weak form of electric-magnetic duality suggests strongly the existence of weak Regge trajectories.

1. The most general mass squared formula with spin-orbit interaction term $M_{L-S}^2 L \cdot S$ reads as

$$M^2 = nM_1^2 + M_0^2 + M_{L-S}^2 L \cdot S, \quad n = 0, 2, 4 \text{ or } n = 1, 3, 5, \dots, \quad (4.7.2)$$

M_1^2 corresponds to string tension and M_0^2 corresponds to the thermodynamical mass squared and possible other contributions. For a given trajectory even (odd) values of n have same parity and can correspond to excitations of same ground state. From ancient books written about hadronic string model one vaguely recalls that one can have several trajectories (satellites) and if one has something called exchange degeneracy, the even and odd trajectories define single line in $M^2 - J$ plane. As already noticed TGD variant of Higgs mechanism combines together $n = 0$ states and $n = 1$ states to form massive gauge bosons so that the trajectories are not independent.

2. For fermions, possible Higgs, and pseudo-scalar Higgs and their super partners also p-adic thermodynamical contributions are present. M_0^2 must be non-vanishing also for gauge bosons and be equal to the mass squared for the $n = L = 1$ spin singlet. By applying the formula to $h = \pm 1$ states one obtains

$$M_0^2 = M^2(\text{boson}) . \quad (4.7.3)$$

The mass squared for transversal polarizations with $(h, n, L) = (\pm 1, n = L = 0, S = 1)$ should be same as for the longitudinal polarization with $(h = 0, n = L = 1, S = 1, J = 0)$ state. This gives

$$M_1^2 + M_0^2 + M_{L-S}^2 L \cdot S = M_0^2 . \quad (4.7.4)$$

From $L \cdot S = [J(J+1) - L(L+1) - S(S+1)]/2 = -2$ for $J = 0, L = S = 1$ one has

$$M_{L-S}^2 = -\frac{M_1^2}{2} . \quad (4.7.5)$$

Only the value of weak string tension M_1^2 remains open.

3. If one applies this formula to arbitrary $n = L$ one obtains total spins $J = L + 1$ and $L - 1$ from the tensor product. For $J = L - 1$ one obtains

$$M^2 = (2n + 1)M_1^2 + M_0^2 .$$

For $J = L + 1$ only M_0^2 contribution remains so that one would have infinite degeneracy of the lightest states. Therefore stringy mass formula must contain a non-linear term making Regge trajectory curved. The simplest possible generalization which does not affect $n=0$ and $n=1$ states is of from

$$M^2 = n(n-1)M_2^2 + \left(n - \frac{L \cdot S}{2}\right)M_1^2 + M_0^2 . \quad (4.7.6)$$

The challenge is to understand the ratio of W and Z^0 masses, which is purely group theoretic and provides a strong support for the massivation by Higgs mechanism.

1. The above formula and empirical facts require

$$\frac{M_0^2(W)}{M_0^2(Z)} = \frac{M^2(W)}{M^2(Z)} = \cos^2(\theta_W) . \quad (4.7.7)$$

in excellent approximation. Since this parameter measures the interaction energy of the fermion and antifermion decomposing the gauge boson depending on the net quantum numbers of the pair, it would look very natural that one would have

$$M_0^2(W) = g_W^2 M_{SU(2)}^2 , \quad M_0^2(Z) = g_Z^2 M_{SU(2)}^2 . \quad (4.7.8)$$

Here $M_{SU(2)}^2$ would be the fundamental mass squared parameter for $SU(2)$ gauge bosons. p-Adic thermodynamics of course gives additional contribution which is vanishing or very small for gauge bosons.

2. The required mass ratio would result in an excellent approximation if one assumes that the mass scales associated with $SU(2)$ and $U(1)$ factors suffer a mixing completely analogous to the mixing of $U(1)$ gauge boson and neutral $SU(2)$ gauge boson W_3 leading to γ and Z^0 . Also Higgs, which consists of $SU(2)$ triplet and singlet in TGD Universe, would very naturally suffer similar mixing. Hence $M_0(B)$ for gauge boson B would be analogous to the vacuum expectation of corresponding mixed Higgs component. More precisely, one would have

$$\begin{aligned} M_0(W) &= M_{SU(2)} , \\ M_0(Z) &= \cos(\theta_W) M_{SU(2)} + \sin(\theta_W) M_{U(1)} , \\ M_0(\gamma) &= -\sin(\theta_W) M_{SU(2)} + \cos(\theta_W) M_{U(1)} . \end{aligned} \quad (4.7.9)$$

The condition that photon mass is very small and corresponds to IR cutoff mass scale gives $M_0(\gamma) = \epsilon \cos(\theta_W) M_{SU(2)}$, where ϵ is very small number, and implies

$$\begin{aligned} \frac{M_{U(1)}}{M(W)} &= \tan(\theta_W) + \epsilon , \\ \frac{M(\gamma)}{M(W)} &= \epsilon \times \cos(\theta_W) , \\ \frac{M(Z)}{M(W)} &= \frac{1 + \epsilon \times \sin(\theta_W) \cos(\theta_W)}{\cos(\theta_W)} . \end{aligned} \quad (4.7.10)$$

There is a small deviation from the prediction of the standard model for W/Z mass ratio but by the smallness of photon mass the deviation is so small that there is no hope of measuring it. One can of course keep mind open for $\epsilon = 0$. The formulas allow also an interpretation in terms of Higgs vacuum expectations as it must. The vacuum expectation would most naturally correspond to interaction energy between the massless fermion and antifermion with opposite 3-momenta at the throats of the wormhole contact and the challenge is to show that the proposed formulas characterize this interaction energy. Since CP_2 geometry codes for standard model symmetries and their breaking, it would not be surprising if this would happen. One cannot exclude the possibility that p-adic thermodynamics contributes to $M_0^2(boson)$. For instance, ϵ might characterize the p-adic thermal mass of photon.

If the mixing applies to the entire Regge trajectories, the above formulas would apply also to weak string tensions, and also photons would belong to Regge trajectories containing high spin excitations.

3. What one can one say about the value of the weak string tension M_1^2 ? The naive order of magnitude estimate is $M_1^2 \simeq m_W^2 \simeq 10^4 \text{ GeV}^2$ is by a factor 1/25 smaller than the direct scaling up of the hadronic string tension about 1 GeV^2 scaled up by a factor 2^{18} . The above argument however allows also the identification as the scaled up variant of hadronic string tension in which case the higher states at weak Regge trajectories would not be easy to discover since the mass scale defined by string tension would be 512 GeV to be compared with the recent beam energy 7 TeV. Weak string tension need of course not be equal to the scaled up hadronic string tension. Weak string tension - unlike its hadronic counterpart- could also depend on the electromagnetic charge and other characteristics of the particle.

Bibliography

Books about TGD

- [1] M. Pitkänen (2006), *Topological Geometroynamics: Overview*.
http://tgd.wippiespace.com/public_html/tgdview/tgdview.html.
- [2] M. Pitkänen (2006), *Quantum Physics as Infinite-Dimensional Geometry*.
http://tgd.wippiespace.com/public_html/tgdgeom/tgdgeom.html.
- [3] M. Pitkänen (2006), *Physics in Many-Sheeted Space-Time*.
http://tgd.wippiespace.com/public_html/tgdclass/tgdclass.html.
- [4] M. Pitkänen (2006), *p-Adic length Scale Hypothesis and Dark Matter Hierarchy*.
http://tgd.wippiespace.com/public_html/paddark/paddark.html.
- [5] M. Pitkänen (2006), *Quantum TGD*.
http://tgd.wippiespace.com/public_html/tgdquant/tgdquant.html.
- [6] M. Pitkänen (2006), *TGD as a Generalized Number Theory*.
http://tgd.wippiespace.com/public_html/tgdnumber/tgdnumber.html.
- [7] M. Pitkänen (2006), *TGD and Fringe Physics*.
http://tgd.wippiespace.com/public_html/freenergy/freenergy.html.

Books about TGD Inspired Theory of Consciousness and Quantum Biology

- [8] M. Pitkänen (2006), *TGD Inspired Theory of Consciousness*.
http://tgd.wippiespace.com/public_html/tgdconsc/tgdconsc.html.
- [9] M. Pitkänen (2006), *Bio-Systems as Self-Organizing Quantum Systems*.
http://tgd.wippiespace.com/public_html/bioselforg/bioselforg.html.
- [10] M. Pitkänen (2006), *Quantum Hardware of Living Matter*.
http://tgd.wippiespace.com/public_html/bioware/bioware.html.
- [11] M. Pitkänen (2006), *Bio-Systems as Conscious Holograms*.
http://tgd.wippiespace.com/public_html/hologram/hologram.html.
- [12] M. Pitkänen (2006), *Genes and Memes*.
http://tgd.wippiespace.com/public_html/genememe/genememe.html.
- [13] M. Pitkänen (2006), *Magnetospheric Consciousness*.
http://tgd.wippiespace.com/public_html/magnconsc/magnconsc.html.
- [14] M. Pitkänen (2006), *Mathematical Aspects of Consciousness Theory*.
http://tgd.wippiespace.com/public_html/mathconsc/mathconsc.html.
- [15] M. Pitkänen (2006), *TGD and EEG*.
http://tgd.wippiespace.com/public_html/tgdeeg/tgdeeg.html.

References to the chapters of the books about TGD

- [16] The chapter *Construction of Configuration Space Kähler Geometry from Symmetry Principles* of [2].
http://tgd.wippiespace.com/public_html/tgdgeom/tgdgeom.html#compl1.
- [17] The chapter *Identification of the Configuration Space Kähler Function* of [2].
http://tgd.wippiespace.com/public_html/tgdgeom/tgdgeom.html#kahler.
- [18] The chapter *Does the Modified Dirac Equation Define the Fundamental Action Principle?* of [2].
http://tgd.wippiespace.com/public_html/tgdgeom/tgdgeom.html#Dirac.
- [19] The chapter *Cosmic Strings* of [3].
http://tgd.wippiespace.com/public_html/tgdclass/tgdclass.html#cstrings.
- [20] The chapter *p-Adic Particle Massivation: Hadron Masses* of [4].
http://tgd.wippiespace.com/public_html/paddark/paddark.html#mass3.
- [21] The chapter *p-Adic Particle Massivation: New Physics* of [4].
http://tgd.wippiespace.com/public_html/paddark/paddark.html#mass4.
- [22] The chapter *TGD and Nuclear Physics* of [4].
http://tgd.wippiespace.com/public_html/paddark/paddark.html#padnucl.
- [23] The chapter *Nuclear String Model* of [4].
http://tgd.wippiespace.com/public_html/paddark/paddark.html#nuclstring.
- [24] The chapter *TGD as a Generalized Number Theory: p-Adicization Program* of [6].
http://tgd.wippiespace.com/public_html/tgdnumber/tgdnumber.html#visiona.
- [25] The chapter *TGD as a Generalized Number Theory: Infinite Primes* of [6].
http://tgd.wippiespace.com/public_html/tgdnumber/tgdnumber.html#visionc.
- [26] The chapter *Riemann Hypothesis and Physics* of [6].
http://tgd.wippiespace.com/public_html/tgdnumber/tgdnumber.html#riema.
- [27] The chapter *p-Adic Physics: Physical Ideas* of [6].
http://tgd.wippiespace.com/public_html/tgdnumber/tgdnumber.html#phblocks.
- [28] The chapter *Elementary Particle Vacuum Functionals* of [4].
http://tgd.wippiespace.com/public_html/paddark/paddark.html#elvafu.
- [29] The chapter *Massless States and Particle Massivation* of [4].
http://tgd.wippiespace.com/public_html/paddark/paddark.html#mless.
- [30] The chapter *Does the QFT Limit of TGD Have Space-Time Super-Symmetry?* of [5].
http://tgd.wippiespace.com/public_html/tgdquant/tgdquant.html#susy.
- [31] The chapter *Construction of Quantum Theory: S-matrix* of [5].
http://tgd.wippiespace.com/public_html/tgdquant/tgdquant.html#towards.
- [32] The chapter *Yangian Symmetry, Twistors, and TGD* of [5].
http://tgd.wippiespace.com/public_html/tgdquant/tgdquant.html#Yangian.
- [33] The chapter *Was von Neumann Right After All* of [5].
http://tgd.wippiespace.com/public_html/tgdquant/tgdquant.html#vNeumann.

Articles related to TGD

- [34] M. Pitkänen (2010), Article series in *Prespacetime Journal* Vol 1, No 3.

Mathematics

- [35] *Yangian symmetry*. <http://en.wikipedia.org/wiki/Yangian>.
- [36] M. Redei and M. Stöltzner (eds) (2001), *John von Neumann and the Foundations of Quantum Physics*. Vol. 8, Dordrecht: Kluwer Academic Publishers. V. S. Sunder (1987), *An Invitation to von Neumann Algebras*. New York: Springer-Verlag.

Particle and nuclear physics

- [37] A. D. Dolgov and I. Z. Rothstein, (1993), Phys. Rev. Lett. vol 71, No 4.
- [38] Denegri, D. *et al*(1989): *The number of neutrino species*. CERN EP/89-72, preprint.
- [39] *Rumsfeld hadrons*,
<http://dorigo.wordpress.com/2007/06/20/rumsfeld-hadrons/>.
- [40] SNO: Q. R Ahmad *et al*(2002), Phys. Rev. Lett. 89 011301, nucl-ex/0204008.
- [41] M. B. Smy (Super-Kamiokande)(2003), Nucl. Phys. Proc. Suppl. 118, 25. hep-ex/0208004.
- [42] R. J. Wilkes (K2K)(2002), ECONF C020805, TTH02, hep-ex/0212035.
- [43] K. Eguchi *et al* (KamLAND) (2003), Phys. Rev. Lett. 90, 021802, hep-ex/0212021.
- [44] W. C. Louis (1994), in Proceedings of the XVI Conference on Neutrino Physics and Astrophysics, Eilat, Israel.
- [45] Y. Fukuda *et al*(1994), Phys. Lett. B 335, p. 237.
- [46] C. Athanassopoulos *et al* (LSND collaboration) (1996), *Evidence for Neutrino Oscillations from Muon Decay at Rest*, nucl-ex/9605001.
- [47] LSND Collaboration (1997), *Evidence for $\nu_\mu - \nu_e$ oscillations from LSND*, arXiv:nucl-ex/9709006.
- [48] L. Borodovsky *et al* (1992), Phys. Rev. Lett. 68, p. 274.
- [49] MiniBooNE collaboration (2007), *A Search for Electron Neutrino in $\Delta m^2 = 1 \text{ eV}^2$ scale*,
<http://www-boone.fnal.gov/publicpages/pr18.pdf>.
See also the press release at http://www.fnal.gov/pub/presspass/press_releases/BooNE-box.html.
- [50] Q. -Z. Qian and G. M. Fuller (1995), Phys. Rev. D 51, 1479.
- [51] D. B. Kaplan, A. E. Nelson and N. Weiner (2004), *Neutrino Oscillations as a Probe of Dark Energy*, hep-ph/0401099.
- [52] *Quark*, http://en.wikipedia.org/wiki/Current_quark_mass.
- [53] Tommaso Dorigo (2008), *Top quark mass measured with neutrino phi weighting*. Blog posting about latest CDF measurement of top quark mass. <http://dorigo.wordpress.com/2008/12/08/top-quark-mass-measured-with-neutrino-phi-weighting/>.
- [54] Decamp *et al* (Aleph Collaboration)(1989):CERN-EP/89-141, preprint.

Chapter 5

p-Adic Particle Massivation: Hadron Masses

5.1 Introduction

In this chapter the results of the calculation of elementary particle masses will be used to construct a model predicting hadron masses. The new elements are a revised identification for the p-adic length scales of quarks and the realization that number theoretical constraints on topological mixing can be realized by assuming that topological mixing leads to a thermodynamical equilibrium. This gives an upper bound of 1200 for the number of different U and D matrices and the input from top quark mass and $\pi^+ - \pi^0$ mass difference implies that physical U and D matrices can be constructed as small perturbations of matrices expressible as a direct sum of essentially unique 2×2 and 1×1 matrices.

The assumption about the presence of scaled up variants of light quarks in light hadrons leads to a surprisingly successful model for pseudo scalar meson masses in terms of only quark masses. This conforms with the idea that at least light pseudo scalar mesons are Goldstone bosons in the sense that color Coulombic and magnetic contributions to the mass cancel each other. Also the mass differences between baryons containing different numbers of strange quarks can be understood if s quark appears as three scaled up versions. The earlier model for the purely hadronic contributions to hadron masses simplifies dramatically and only the color Coulombic and magnetic contributions to color conformal weight are needed.

5.1.1 Construction of U and D matrices

The basic constraint on the topological mixing that the modular contributions to the conformal weight defining the mass squared remain integer valued in the proper units: if this condition does not hold true, the order of magnitude for the real counterpart of the p-adic mass squared corresponds to 10^{-4} Planck masses.

Number theory gives strong constraints on CKM matrix. p-Adicization requires that U and D matrix elements are algebraic numbers. A strong constraint would be that the mixing probabilities are rational numbers implying that matrices defined by the moduli of U and D involve only square roots of rationals. The phases of matrix elements should belong to a finite extension of complex rationals.

Little can be said about the details of the dynamics of topological mixing. Nothing however prevents for constructing a thermodynamical model for the mixing. A thermodynamical model for U and D matrices maximizing the entropy defined by the mixing probabilities subject to the constraints fixing the values of n_{q_i} and the sums of row/column probabilities to one gives a thermodynamical ensemble with two quantized temperatures and two quantized chemical potentials. The resulting polynomial equations allow at most 1200 different solutions so that the number of U and D matrices is relatively small. The fact that matrix elements are algebraic numbers guarantees that the matrices are continuable to p-adic number fields as required.

The detailed study of quark mass spectrum leads to a tentative identification $(n_d, n_s, n_b) = (5, 5, 59)$ and $(n_u, n_c, n_t) = (5, 6, 58)$ of the modular contributions of conformal weights of quarks: note that

in absence of mixing the contributions would be $(0, 9, 60)$ for both U and D type quarks. That b and t quark masses are nearly maximal and thus mix very little with lighter quarks is forced by the masses of t quark and $t\bar{t}$ meson. The values of n_{q_i} for light quarks follow by considering $\pi^+ - \pi^0$ mass difference.

One might consider the possibility that n_{q_i} for slightly dynamical and can vary in light mesons in order to guarantee that $u\bar{u}$, $d\bar{d}$ and $s\bar{s}$ give identical modular contributions to the conformal weight in states which are linear combinations of quark pairs. It turns out that unitarity does not allow the choices $(n_1 = 4, n_2 < 9)$, and that the choice $(n_d, n_s) = (5, 5)$, $(n_u, n_c) = (5, 6)$ is the unique choice producing a realistic CKM matrix. The requirement that quark contribution to pseudo scalar meson mass is smaller than meson mass is possible to satisfy and gives a constraint on CP_2 mass scale consistent with the prediction of leptonic masses when second order p-adic contribution to lepton mass is allowed to be non-vanishing.

The small mixing with b and t quarks is natural since the modular conformal weight of unmixed state having spectrum $\{0, 9, 60\}$ is analogous to energy so that Boltzmann weight for $n(g = 3)$ thermal excitation is small for $g = 1, 2$ ground states.

The maximally entropic solutions can be found numerically by using the fact that only the probabilities p_{11} and p_{21} can be varied freely. The solutions are unique in the accuracy used, which suggests that the system allows only single thermodynamical phase.

The matrices U and D associated with the probability matrices can be deduced straightforwardly in the standard gauge. The U and D matrices derived from the probabilities determined by the entropy maximization turn out to be unitary for most values of n_1 and n_2 . This is a highly non-trivial result and means that mass and probability constraints together with entropy maximization define a sub-manifold of $SU(3)$ regarded as a sub-manifold in 9-D complex space. The choice $(n_u, n_c) = (4, n)$, $n < 9$, does not allow unitary U whereas $(n_u, n_c) = (5, 6)$ does. This choice is still consistent with top quark mass and together with $n_d = n_s = 5$ it leads to a rather reasonable CKM matrix with a value of CP breaking invariant within experimental limits. The elements V_{i3} and V_{3i} , $i = 1, 2$ are however roughly twice larger than their experimental values deduced assuming standard model. V_{31} is too large by a factor 1.6. The possibility of scaled up variants of light quarks could lead to too small experimental estimates for these matrix elements. The whole parameter space has not been scanned so that better candidates for CKM matrices might well exist.

5.1.2 Observations crucial for the model of hadron masses

The evolution of the model for hadron masses involves several key observations made during the more decade that I have been working with p-adic mass calculations.

The p-adic mass scales of quarks are dynamical

The existence of scaled up variants of quarks is suggested by various anomalies such as Aleph anomaly [44] and the strange bumpy structure of the distribution of the mass of the top quark candidate. This leads to the idea that the integer $k(q)$ characterizing the p-adic mass scale of quark is different for free quarks and bound quarks and that $k(q)$ can depend on hadron. Hence one can understand not only the notions of current quark mass and constituent quark mass but reproduce also the p-adic counterpart of Gell-Mann-Okubo mass formula. Indeed, the assumption about scaled up variants of u, d, s, and even c quarks in light hadrons leads to an excellent fit of meson masses with quark contribution explaining almost all of meson mass.

Quarks give dominating contribution to the masses of pseudoscalar mesons

The interpretation is that color Coulombic and color magnetic interaction conformal weights (rather than interaction energies) cancel each other in a approximation for pseudoscalar mesons in accordance with the idea that pseudo scalar mesons are massless as far as color interactions are considered. In the case of baryons the assumption that s quark appears in three different scaled up versions (which are Λ , $\{\Sigma, \Xi\}$, and Ω) allows to understand the mass differences between baryons with different s quark content. The dominating contribution to baryon mass has however remained hitherto unidentified.

What it means that Higgs like contribution to fermion masses is negligible?

The failure of the simplest form of p-adic thermodynamics for intermediate gauge bosons led to the unsatisfactory conclusion that p-adic thermodynamics is not enough and the coupling to Higgs bosons contributes to the gauge boson masses. This option had its own problems.

1. There are good, purely topological - reasons to believe that Higgs expectation for the fermionic space-time sheets is vanishing although fermions couple to Higgs. p-Adic thermodynamics would explain fermion masses completely: this indeed turns out to be the case within experimental uncertainties. The absence of Higgs contribution to fermion masses would however mean asymmetry between fermions and bosons.
2. After the understanding of the spectrum of the modified Dirac operator it became clear that ground state conformal weight is proportional to the square of the eigenvalue of the Dirac operator, and that it is the deviation of the ground state conformal weight from negative half odd integer which is responsible for the Higgs type contribution. This contribution to the mass squared is present for both fermions and bosons but the contribution must be small for fermions and dominate for gauge bosons.
3. In the case of gauge bosons Higgs vacuum expectation is proportional to this deviation for the simple reason that there is no other fundamental parameters with dimensions of mass available. Hence the role of Higgs boson would be misunderstood in standard model framework.

The fact that the prediction of the model for the top quark mass is consistent with the most recent limits on it [46], fixes the CP_2 mass scale with a high accuracy to the maximal one obtained if second order contribution to electron's p-adic mass squared vanishes. This is very valuable constraint on the model.

Conformal weights are additive for quarks with same p-adic prime

An essential element of the new understanding is that conformal weight (mass squared is additive) for quarks with the same p-adic length scale whereas mass is additive for quarks with different values of p . For instance, the masses of heavy $q\bar{q}$ mesons are equal to $\sqrt{2} \times m(q)$ rather than $2m(q)$. Since $k = 107$ for hadronic space-time sheet, for quarks with $k(q) \neq 107$, additivity holds true for the quark and color contributions for mass rather than mass squared.

This hypothesis yields surprisingly good fit for meson masses but for some mesons the predicted mass is slightly too high. The reduction of CP_2 mass scale to cure the situation is not possible since top quark mass would become too low. In case of diagonal mesons for which quarks correspond to same p-adic prime, quark contribution to mass squared can be reduced by ordinary color interactions and in case of non-diagonal mesons one can require that quark contribution is not larger than meson mass.

A remark about terminology

Before continuing a remark about terminology is in order.

1. In the generalized coset construction the symplectic algebra of $\delta M_{\pm}^4 \times CP_2$ and Super-Kac Moody algebras at light-like partonic surfaces X^3 are lifted to hyper-complex algebras inside the causal diamond of $M^4 \times CP_2$ carrying the zero energy states. SKM is identified as a subalgebra of SC and the differences of SC and SKM Super-Virasoro generators annihilate the physical states. All purely geometric contributions and their super-counterparts can be regarded as SC contributions. The fermionic contributions in electro-weak and spin degrees of freedom responsible also for color partial waves are trivially one and same. One could say that there is no other contribution than SC which can be however divided into a contribution from imbedded SKM subalgebra and a genuine SC contribution.
2. In the coset construction a tachyonic ground state of negative SC conformal weight from which SKM generators create massless states must have a negative conformal weight also in SKM sense. Therefore the earlier idea that genuine SC generators create the ground states with a negative conformal weight assignable to elementary particles does not work anymore: the

negative conformal weight must be due to SKM generators with conformal weight which is most naturally of form $h = -1/2 + iy$.

3. super-symplectic contribution with a positive conformal weight can be regarded also as a product of genuine SC contribution with a vanishing conformal weight and a contribution having also interpretation as SKM contribution. What motivates the term "super-symplectic bosons" used in the sequel is that in a non-perturbative situation this contribution is most naturally calculated by regarding it as a super-symplectic contribution. This contribution is highly constrained since it comes solely from generators which are color octets and singlets have spin one or spin zero. Genuine SC contribution with a zero conformal weight comes from the products of super-Hamiltonians in higher representations of $SU(3) \times SO(3)$ containing both positive and negative conformal weights compensating each other. This contribution must have vanishing color quantum numbers and spin since otherwise Dirac operators of H in SKM and SC degrees of freedom could not act on it in the same manner. Note that gluons do not correspond to SKM generators but to pairs of quark and antiquark at throats of a wormhole contact.

Super-symplectic bosons at hadronic space-time sheet can explain the constant contribution to baryonic masses

Quarks explain only a small fraction of the baryon mass and that there is an additional contribution which in a good approximation does not depend on baryon. This contribution should correspond to the non-perturbative aspects of QCD.

A possible identification of this contribution is in terms of super-symplectic gluons predicted by TGD. Baryonic space-time sheet with $k = 107$ would contain a many-particle state of super-symplectic gluons with net conformal weight of 16 units. This leads to a model of baryons masses in which masses are predicted with an accuracy better than 1 per cent. super-symplectic gluons also provide a possible solution to the spin puzzle of proton.

Hadronic string model provides a phenomenological description of non-perturbative aspects of QCD and a connection with the hadronic string model indeed emerges. Hadronic string tension is predicted correctly from the additivity of mass squared for $J = 2$ bound states of super-symplectic quanta. If the topological mixing for super-symplectic bosons is equal to that for U type quarks then a 3-particle state formed by 2 super-symplectic quanta from the first generation and 1 quantum from the second generation would define baryonic ground state with 16 units of conformal weight.

In the case of mesons pion could contain super-symplectic boson of first generation preventing the large negative contribution of the color magnetic spin-spin interaction to make pion a tachyon. For heavier bosons super-symplectic boson is not absolutely necessary but a very precise prediction for hadron masses results by assuming that the spin of hadron correlates with its super-symplectic particle content.

Color magnetic spin-spin splitting formulated in terms of conformal weight

What remains to be understood are the contributions of color Coulombic and magnetic interactions to the mass squared. There are several delicate points to be taken into account.

1. The QCD based formula for the color magnetic interaction energy fails completely since the dependence of color magnetic spin-spin splittings on quark mass scale is nearer to logarithmic dependence on p-adic length scale than being of form $1/m(q_i)m(q_j) \propto L(k_i)L(k_j)$. This finding supports the decade old idea that the proper notion is not color interaction energy but color conformal weight. A model based on this assumption is constructed assuming that all pseudoscalars are Goldstone boson like states. The predictions for the masses of mesons are not so good than for baryons, and one might criticize the application of the format of perturbative QCD in an essentially non-perturbative situation.
2. The comparison of the super-symplectic conformal weights associated with spin 0 and spin 1 states and spin 1/2 and spin 3/2 states shows that the different masses of these states could be understood in terms of the super-symplectic particle contents of the state correlating with the total quark spin. The resulting model allows excellent predictions also for the meson masses and implies that only pion and kaon can be regarded as Goldstone boson like states. The model based on spin-spin splittings is consistent with the model.

To sum up, the model provides an excellent understanding of baryon and meson masses. This success is highly non-trivial since the fit involves only the integers characterizing the p-adic length scales of quarks and the integers characterizing color magnetic spin-spin splitting plus p-adic thermodynamics and topological mixing for super-symplectic gluons. The next challenge would be to predict the correlation of hadron spin with super-symplectic particle content in the case of long-lived hadrons.

5.1.3 A possible model for hadron

These findings suggest that the following model for hadrons deserves a testing. Hadron can be characterized in terms of $k \geq 113$ partonic 2-surfaces $X^2(q_i)$ connected by join along boundaries bonds (JABs, flux tubes) to $k = 107$ 2-surface $X^2(H)$ corresponding to hadron. These flux tubes which for $k = 113$ have size much larger than hadron can be regarded as "field bodies" of quarks which themselves have sub-hadronic size. Color flux tubes between quarks are replaced with pairs of flux tubes from $X^2(q_1) \rightarrow X^2(H) \rightarrow X^2(q_2)$ mediating color Coulombic and magnetic interactions between quarks. In contrast to the standard model, mesons are characterized by two flux tubes rather than only one flux tube. Certainly this model gives nice predictions for hadron masses and even the large color Coulombic contribution to baryon masses can be deduced from $\rho - \pi$ mass splitting in a good approximation.

5.2 Quark masses

The prediction of quark masses is more difficult due to the facts that the deduction of even the p-adic length scale determining the masses of these quarks is a non-trivial task, and the original identification was indeed wrong. Second difficulty is related to the topological mixing of quarks. The new scenario leads to a unique identification of masses with top quark mass as an empirical input and the thermodynamical model of topological mixing as a new theoretical input. Also CKM matrix is predicted highly uniquely.

5.2.1 Basic mass formulas

By the earlier mass calculations and construction of CKM matrix the ground state conformal weights of U and D type quarks must be $h_{gr}(U) = -1$ and $h_{gr}(D) = 0$. The formulas for the eigenvalues of CP_2 spinor Laplacian imply that if m_0^2 is used as a unit, color conformal weight $h_c \equiv m_{CP_2}^2$ is integer for $p \bmod = \pm 1$ for U type quark belonging to $(p+1, p)$ type representation and obeying $h_c(U) = (p^2 + 3p + 2)/3$ and for $p \bmod 3 = 1$ for D type quark belonging to $(p, p+2)$ type representation and obeying $h_c(D) = (p^2 + 4p + 4)/3$. Only these states can be massless since color Hamiltonians have integer valued conformal weights.

In the recent case the minimal $p = 1$ states correspond to $h_c(U) = 2$ and $h_c(D) = 3$. $h_{gr}(U) = -1$ and $h_{gr}(D) = 0$ reproduce the previous results for quark masses required by the construction of CKM matrix. This requires super-symplectic operators O with a net conformal weight $h_{sc} = -3$ to compensate the anomalous color just as in the leptonic case. The facts that the values of p are minimal for spinor harmonics and the super-symplectic operator is same for both quarks and leptons suggest that the construction is not had hoc.

Consider now the mass squared values for quarks. For $h(D) = 0$ and $h(U) = -1$ and using $m_0^2/3$ as a unit the expression for the thermal contribution to the mass squared of quark is given by the formula

$$\begin{aligned} M^2 &= (s + X) \frac{m_0^2}{p} , \\ s(U) &= 5 , \quad s(D) = 8 , \\ X &\equiv \frac{(3Yp)_R}{3} , \end{aligned} \tag{5.2.1}$$

where the second order contribution Y corresponds to renormalization effects coming and depending on the isospin of the quark.

With the above described assumptions one has the following mass formula for quarks

$$M^2(q) = A(q) \frac{m_0^2}{p(q)} ,$$

$$\begin{aligned} A(u) &= 5 + X_U(p(u)) , & A(c) &= 14 + X_U(p(c)) , & A(t) &= 65 + X_U(p(t)) , \\ A(d) &= 8 + X_D(p(d)) , & A(s) &= 17 + X_D(p(s)) , & A(b) &= 68 + X_D(p(b)) . \end{aligned} \tag{5.2.2}$$

p-Adic length scale hypothesis allows to identify the p-adic primes labeling quarks whereas topological mixing of U and D quarks allows to deduce topological mixing matrices U and D and CKM matrix V and precise values of the masses apart from effects like color magnetic spin orbit splitting, color Coulombic energy, etc..

Integers n_{q_i} satisfying $\sum_i n(U_i) = \sum_i n(D_i) = 69$ characterize the masses of the quarks and also the topological mixing to high degree. The reason that modular contributions remain integers is that in the p-adic context non-trivial rationals would give CP_2 mass scale for the real counterpart of the mass squared. In the absence of mixing the values of integers are $n_d = n_u = 0$, $n_s = n_c = 9$, $n_b = n_t = 60$.

The fact that CKM matrix V expressible as a product $V = U^\dagger D$ of topological mixing matrices is near to a direct sum of 2×2 unit matrix and 1×1 unit matrix motivates the approximation $n_b \simeq n_t$.

The model for topological mixing matrices and CKM matrix predicts U and D matrices highly uniquely and allows to understand quark and hadron masses in surprisingly detailed level.

The large masses of top quark and of $t\bar{t}$ meson encourage to consider a scenario in which $n_t = n_b = n \leq 60$ holds true.

1. $n_d = n_u = 60$ is not allowed by number theoretical conditions for U and D matrices and by the basic facts about CKM matrix but $n_t = n_b = 59$ allows almost maximal masses for b and t . This is not yet a complete hit. The unitarity of the mixing matrices and the construction of CKM matrix to be discussed in the next section forces the assignments

$$(n_d, n_s, n_b) = (5, 5, 59) , \quad (n_u, n_c, n_t) = (5, 6, 58) . \tag{5.2.3}$$

fixing completely the quark masses apart from a possible few per cent renormalization effects of hadronic mass scale in topological condensation which seem to be present and will be discussed later ¹. Note that top quark mass is still rather near to its maximal value.

2. The constraint that quark contribution to pion mass does not exceed pion mass implies the constraint $n(d) \leq 6$ and $n(u) \leq 6$ in accordance with the predictions of the model of topological mixing. It is important to notice that $u - d$ mass difference does not affect $\pi^+ - \pi^0$ mass difference and the quark contribution to $m(\pi)$ is predicted to be $\sqrt{(n_d + n_u + 13)/24} \times 136.9$ MeV for the maximal value of CP_2 mass (second order p-adic contribution to electron mass squared vanishes).

5.2.2 The p-adic length scales associated with quarks and quark masses

The identification of p-adic length scales associated with the quarks has turned to be a highly non-trivial problem. The reasons are that for light quarks it is difficult to deduce information about quark masses for hadron masses and that the unknown details of the topological mixing (unknown until the advent of the thermodynamical model) made possible several p-adic length scales for quarks. It has also become clear that the p-adic length scale can be different from free quark and bound quark and that bound quark p-adic scale can depend on hadron.

Two natural constraints have however emerged from the recent work.

¹As this was written I had not realized that there is also a Higgs contribution which tends to increase top quark mass

1. Quark contribution to the hadron mass cannot be larger than color contribution and for quarks having $k_q \neq 107$ quark contribution to mass is added to color contribution to the mass. For quarks with same value of k conformal weight rather than mass is additive whereas for quarks with different value of k masses are additive. An important implication is that for diagonal mesons $M = q\bar{q}$ having $k(q) \neq 107$ the condition $m(M) \geq \sqrt{2}m_q$ must hold true. This gives strong constraints on quark masses.
2. The realization that scaled up variants of quarks explain elegantly the masses of light hadrons allows to understand large mass splittings of light hadrons without the introduction of strong isospin-isospin interaction.

The new model for quark masses is based on the following identifications of the p-adic length scales.

1. The nuclear p-adic length scale $L(k)$, $k = 113$, corresponds to the p-adic length scale determining the masses of u, d, and s quarks. Note that $k = 113$ corresponds to a so called Gaussian Mersenne. The interpretation is that quark massivation occurs at nuclear space-time sheet at which quarks feed their em fluxes. At $k = 107$ space-time sheet, where quarks feed their color gauge fluxes, the quark masses are vanishing in the first p-adic order. This could be due to the fact that the p-adic temperature is $T_p = 1/2$ at this space-time sheet so that the thermal contribution to the mass squared is negligible. This would reflect the fact that color interactions do not involve any counterpart of Higgs mechanism.

p-Adic mass calculations turn out to work remarkably well for massive quarks. The reason could be that M_{107} hadron physics means that *all* quarks feed their color gauge fluxes to $k = 107$ space-time sheets so that color contribution to the masses becomes negligible for heavy quarks as compared to Super-Kac Moody and modular contributions corresponding to em gauge flux feeded to $k > 107$ space-time sheets in case of heavy quarks. Note that Z^0 gauge flux is feeded to space-time sheets at which neutrinos reside and screen the flux and their size corresponds to the neutrino mass scale. This picture might throw some light to the question of whether and how it might be possible to demonstrate the existence of M_{89} hadron physics.

One might argue that $k = 107$ is not allowed as a condensation level in accordance with the idea that color and electro-weak gauge fluxes cannot be feeded at the space-time space time sheet since the classical color and electro-weak fields are functionally independent. The identification of η' meson as a bound state of scaled up $k = 107$ quarks is not however consistent with this idea unless one assumes that $k = 107$ space-time sheets in question are separate.

2. The requirement that the masses of diagonal pseudoscalar mesons of type $M = q\bar{q}$ are larger but as near as possible to the quark contribution $\sqrt{2}m_q$ to the valence quark mass, fixes the p-adic primes $p \simeq 2^k$ associated with c , b quarks but not t since toponium does not exist. These values of k are "nominal" since k seems to be dynamical. c quark corresponds to the p-adic length scale $k(c) = 104 = 2^3 \times 13$. b quark corresponds to $k(b) = 103$ for $n(b) = 5$. Direct determination of p-adic scale from top quark mass gives $k(t) = 94 = 2 \times 47$ so that secondary p-adic length scale is in question.
3. Top quark is experimentally in a unique position since toponium does not exist and top quark mass is that of free top. The prediction for top quark mass (see Table 1 below) is 167.8 GeV for $Y_t = Y_e = 0$ (second order contributions to mass vanish) and 169.1 GeV for $Y_t = 1$ and $Y_e = 0$ (maximal possible mass for top). The experimental estimate for m_t remained for a long time somewhat higher than the prediction but the estimates have gradually reduced. The previous experimental average value was $m(t) = 169.1$ GeV with the allowed range being [164.7, 175.5] GeV [46, 42]. The fine tuning $Y_e = 0, Y_t = 1$ giving 169.1 GeV is somewhat un-natural. The most recent value obtained by CDF and discussed in detail by Tommaso Dorigo [51] is $m_t = 165.1 \pm 3.3 \pm 3.1$ GeV. This is value is consistent with the lower bound predicted by TGD for $Y_e = Y_t = 0$ and increase of Y_t increases the value of the predicted mass. Clearly, TGD passes the stringent test posed by top quark.
4. There are good reasons to believe that the p-adic mass scale of quark is different for free quark and bound state quark and that in case of bound quark it can also depend on hadron. This

would explain the notions of valence (constituent) quark and current quark mass as masses of bound state quark and free quark and leads also to a TGD counterpart of Gell-Mann-Okubo mass formula.

1. Constituent quark masses

Constituent quark masses correspond to masses derived assuming that they are bound to hadrons. If the value of k is assumed to depend on hadron one obtains nice mass formula for light hadrons as will be found later. The following table summarizes constituent quark masses labelled by k_q deduced from the masses of diagonal mesons.

q	d	u	s	c	b	t
n_q	4	5	6	6	59	58
s_q	12	10	14	11	67	63
$k(q)$	113	113	113	104	103	94
$m(q)/GeV$.105	.0923	.105	2.191	7.647	167.8

Table 1. Constituent quark masses predicted for diagonal mesons assuming $(n_d, n_s, n_b) = (5, 5, 59)$ and $(n_u, n_c, n_t) = (5, 6, 58)$, maximal CP_2 mass scale ($Y_e = 0$), and vanishing of second order contributions.

2. Current quark masses

Current quark masses would correspond to masses of free quarks which tend to be lower than valence quark masses. Hence k could be larger in the case of light quarks. The table of quark masses in Wikipedia [42] gives the value ranges for current quark masses depicted in the table below together with TGD predictions for the spectrum of current quark masses.

q	d	u	s
$m(q)_{exp}/MeV$	4-8	1.5-4	80-130
$k(q)$	(122,121,120)	(125,124,123,122)	(114,113,112)
$m(q)/MeV$	(4.5,6.6,9.3)	(1.4,2.0,2.9,4.1)	(74,105,149)
q	c	b	t
$m(q)_{exp}/MeV$	1150-1350	4100-4400	1691
$k(q)$	(106,105)	(105,104)	92
$m(q)/MeV$	(1045,1477)	(3823,5407)	167.8

Table 2. The experimental value ranges for current quark masses [42] and TGD predictions for their values assuming $(n_d, n_s, n_b) = (5, 5, 59)$, $(n_u, n_c, n_t) = (5, 6, 58)$, $Y_e = 0$, and vanishing of second order contributions.

Some comments are in order.

1. The long p-adic length associated with light quarks seem to be in conflict with the idea that quarks have sizes smaller than hadron size. The paradox disappears when one realized that $k(q)$ characterizes the electromagnetic "field body" of quark having much larger size than hadron.
2. u and d current quarks correspond to a mass scale not much higher than that of electron and the ranges for mass estimates suggest that u could correspond to scales $k(u) \in (125, 124, 123, 122) = (5^3, 4 \times 31, 3 \times 41, 2 \times 61)$, whereas d would correspond to $k(d) \in (122, 121, 120) = (2 \times 61, 11^2, 3 \times 5 \times 8)$.
3. The TGD based model for nuclei based on the notion of nuclear string leads to the conclusion that exotic copies of $k = 113$ quarks having $k = 127$ are present in nuclei and are responsible for the color binding of nuclei [23, 47].
4. The predicted values for c and b masses are slightly too low for $(k(c), k(b)) = (106, 105) = (2 \times 53, 3 \times 5 \times 7)$. Second order Higgs contribution could increase the c mass into the range given in [42] but not that of b .

One can talk about constituent and current quark masses simultaneously only if they correspond to dual descriptions. $M^8 - H$ duality [26] has been indeed suggested to relate the old fashioned low energy description of hadrons in terms of $SO(4)$ symmetry (Skyrme model) and higher energy description of hadrons based on QCD. In QCD description the mass of say baryon would be dominated by the mass associated with super-symplectic quanta carrying color. In $SO(4)$ description constituent quarks would carry most of the hadron mass.

5.2.3 Are scaled up variants of quarks also there?

The following arguments suggest that p-adically scaled up variants of quarks might appear not only at very high energies but even in low energy hadron physics.

Aleph anomaly and scaled up copy of b quark

The prediction for the b quark mass is consistent with the explanation of the Aleph anomaly [44] inspired by the finding that neutrinos seem to condense at several p-adic length scales [88]. If b quark condenses at $k(b) = 97$ level, the predicted mass is $m(b, 97) = 52.3$ GeV for $n_b = 59$ for the maximal CP_2 mass consistent with η' mass. If the the mass of the particle candidate is defined experimentally as one half of the mass of resonance, b quark mass is actually by a factor $\sqrt{2}$ higher and scaled up b corresponds to $k(b) = 96 = 2^5 \times 3$. The prediction is consistent with the estimate 55 GeV for the mass of the Aleph particle and gives additional support for the model of topological mixing. Also the decay characteristics of Aleph particle are consistent with the interpretation as a scaled up b quark.

Scaled variants of top quark

Tony Smith has emphasized the fact that the distribution for the mass of the top quark candidate has a clear structure suggesting the existence of several states, which he interprets as excited states of top quark [49]. According to the figures 5.2.3 and 5.2.3 representing published FermiLab data, this structure is indeed clearly visible.

There is evidence for a sharp peak in the mass distribution of the top quark in 140-150 GeV range (Fig. 5.2.3). There is also a peak slightly below 120 GeV, which could correspond to a p-adically scaled down variant t quark with $k = 95$ having mass 119.6 GeV for $(Y_e = 0, Y_t = 1)$ There is also a small peak also around 265 GeV which could relate to $m(t(93)) = 240.4$ GeV. There top could appear at least for the p-adic scales $k = 93, 94, 95$ as also u and d quarks seem to appear as current quarks.

Scaled up variants of d, s, u, c in top quark mass scale

The fact that all neutrinos seem to appear as scaled up versions in several scales, encourages to look whether also $u, d, s,$ and c could appear as scaled up variants transforming to the more stable variants by a stepwise increase of the size scale involving the emission of electro-weak gauge bosons. In the following the scenario in which t and b quarks mix minimally is considered.

q	$m(92)/GeV$	$m(91)/GeV$	$m(90)/GeV$
u	134	189	267
d	152	216	304
c	140	198	280
s	152	216	304

Table 3. The masses of $k = 92, 91$ and $k = 90$ scaled up variants of u, d, c, s quarks assuming same integers n_{q_i} as for ordinary quarks in the scenario $(n_d, n_s, n_b) = (5, 5, 59)$ and $(n_u, n_c, n_t) = (5, 6, 58)$ and maximal CP_2 mass consistent with the η' mass.

1. For $k = 92$, the masses would be $m(q, 92) = 134, 140, 152, 152$ GeV in the order $q = u, c, d, s$ so that all these quarks might appear in the critical region where the top quark mass has been wandering.

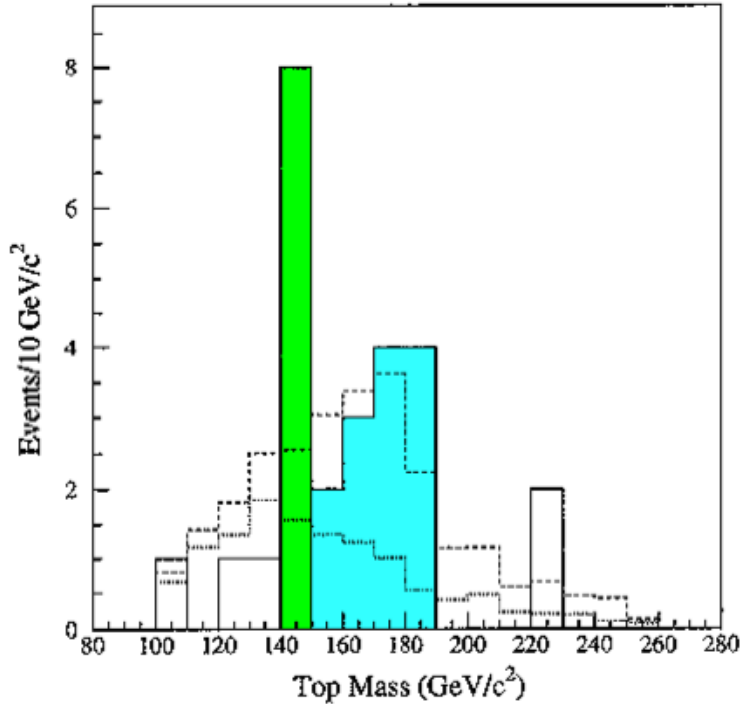


Figure 5.1: Fermilab semileptonic histogram for the distribution of the mass of top quark candidate (FERMILAB-PUB-94/097-E).

2. For $k = 91$ copies would have masses $m(q, 91) = 189, 198, 256, 256$ GeV in the order $q = u, c, d, s$. The masses of u and c are somewhat above the value of latest estimate 170 GeV for top quark mass [46].

Note that it is possible to distinguish between scaled up quarks of M_{107} hadron physics and the quarks of M_{89} hadron physics since the unique signature of M_{89} hadron physics would be the increase of the scale of color Coulombic and magnetic energies by a factor of 512. As will be found, this allows to estimate the masses of corresponding mesons and baryons by a direct scaling. For instance, M_{89} pion and nucleon would have masses 71.7 GeV and 481 GeV.

It must be added that the detailed identifications are sensitive to the exact value of the CP_2 mass scale. The possibility of at most 2.5 per cent downward scaling of masses occurs is allowed by the recent value range for top quark mass.

Fractally scaled up copies of light quarks and low mass hadrons?

One can of course ask, whether the fractally scaled up quarks could appear also in low lying hadrons. The arguments to be developed in detail later suggest that u , d , and s quark masses could be dynamical in the sense that several fractally scaled up copies can appear in low mass hadrons and explain the mass differences between hadrons.

In this picture the mass splittings of low lying hadrons with different flavors would result from fractally scaled up excitations of s and also u and d quarks in case of mesons. This notion would also throw light into the paradoxical presence of two kinds of quark masses: constituent quark masses and current quark masses having much smaller values than constituent quarks masses. That color spin-spin splittings are of same order of magnitude for all mesons supports the view that color gauge fluxes are feeded to $k = 107$ space-time sheet.

The alert reader has probably already asked whether also proton mass could be understood in terms of scaled up copies of u and d quarks. This does not seem to be the case, and an argument

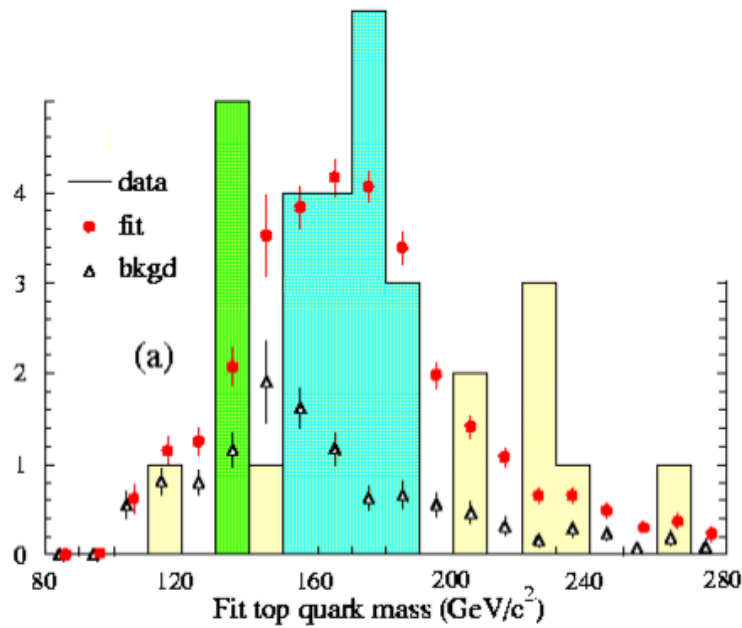


Figure 5.2: Fermilab D0 semileptonic histogram for the distribution of the mass of top quark candidate (hep-ex/9703008, April 26, 1994)

predicting with 23 per cent error proton mass scale from $\rho - \pi$ and $\Delta - N$ color magnetic splittings emerges.

To sum up, it seems quite possible that the scaled up quarks predicted by TGD have been observed for decade ago in FermiLab about that the prevailing dogmas has led to their neglect as statistical fluctuations. Even more, scaled up variants of s quarks might have been in front of our eyes for half century! Phenomenon is an existing phenomenon only if it is an understood phenomenon.

The mystery of two Ω_b baryons

Tommaso Dorigo has three interesting postings [48] about the discovery of Ω_b baryon containing two strange quarks and one bottom quark. Ω_b has been discovered -even twice. This is not a problem. The problem is that the masses of these Ω_b s differ quite too much. D0 collaboration discovered Ω_b with a significance of 5.4 sigma and a mass of 6165 ± 16.4 MeV [52]. Later CDF collaboration announced the discovery of the same particle with a significance of 5.5 sigma and a mass of 6054.4 ± 6.9 MeV. Both D0 and CDF agree that the particle is there at better than 5 sigma significance and also that the other collaboration is wrong. They cant both be right Or could they? In some other Universe that that of standard model and all its standard generalizations, maybe in some less theoretically respected Universe, say TGD Universe?

The mass difference between the two Ω_b candidates is 111 MeV, which represents the mass scale of strange quark. TDG inspired model for quark masses relies on p-adic thermodynamics and predicts that quarks can appear in several p-adic mass scales forming a hierarchy of half octaves - in other words mass scales comes as powers of square root of two. This property is absolutely essential for the TGD based model for masses of even low lying baryons and mesons where strange quarks indeed appear with several different p-adic mass scales. It also explains the large difference of the mass scales assigned to current quarks and constituent quarks. Light variants of quarks appear also in nuclear string model where nucleons are connected by color bonds containing light quark and antiquark at their ends.

Ω_b contains two strange quarks and the mass difference between the two candidates is of order of mass of strange quark. Could it be that both Ω_b s are real and the discrepancy provides additional

support for p-adic length scale hypothesis? The prediction of p-adic mass calculations for the mass of s quark is 105 MeV (see Table 1) so that the mass difference can be understood if the second s-quark in Ω_b has mass which is twice the "standard" value. Therefore the strange finding about Ω_b could give additional support for quantum TGD. Before buying a bottle of champagne, one should however understand why D0 and CDF collaborations only one Ω_b instead of both of them.

5.3 Topological mixing of quarks

The requirement that hadronic mass spectrum is physical requires mixing of U and D type boundary topologies. In this section quark masses and the mixing of the boundary topologies are considered on the general level and CKM matrix is derived using the existing empirical information plus the constraints on the quark masses to be derived from the hadronic mass spectrum in the later sections.

5.3.1 Mixing of the boundary topologies

In TGD the different mixings of the boundary topologies for U and D type quarks provide the fundamental mechanism for CKM mixing and also CP breaking. In the determination of CKM matrix one can use following conditions.

1. Mass squared expectation values in order $O(p)$ for the topologically mixed states must be integers and the study of the hadron mass spectrum leads to very stringent conditions on the values of these integers. Physical values for these integers imply essentially correct value for Cabibbo angle provided U and D matrices differ only slightly from the mixing matrices mixing only the two lowest generations.
2. The matrices U and D describing the mixing of U and D type boundary topologies are unitary in the p-adic sense. The requirement that the moduli squared of the matrix elements are rational numbers, is very attractive since it suggests equivalence of p-adic and real probability concepts and therefore could solve some conceptual problems related to the transition from the p-adic to real regime. It must be however immediately added that rationality assumption for the probabilities defined by S-matrix turns out to be non-physical. It turns out that the mixing scenario reproducing a physical CKM matrix is consistent with the rationality of the moduli squared of the matrix elements of U and D matrices but not with the rationality of the matrix elements themselves. The phase angles appearing in U and D matrix can be rational and in this case they correspond to Pythagorean triangles. In principle the rationality of the CKM matrix is possible.
3. The requirements that Cabibbo angle has correct value and that the elements $V(t, d)$ and $V(u, b)$ of the CKM matrix have small values not larger than 10^{-2} fixes the integers n_i characterizing quark masses to a very high degree and in a good approximation one can estimate the angle parameters analytically. remains open at this stage. The requirement of a realistic CKM matrix leads to a scenario for the values of n_i , which seems to be essentially unique.

The mass squared constraints give for the D matrix the following conditions

$$\begin{aligned}
 9|D_{12}|^2 + 60|D_{13}|^2 &= n_1(D) \equiv n_d , \\
 9|D_{22}|^2 + 60|D_{23}|^2 &= n_2(D) \equiv n_s , \\
 9|D_{32}|^2 + 60|D_{33}|^2 &= n_3(D) \equiv n_b = 69 - n_2(D) - n_1(D) .
 \end{aligned}
 \tag{5.3.1}$$

The third condition is not independent since the sum of the conditions is identically true by unitarity. For U matrix one has similar conditions:

$$\begin{aligned}
 9|U_{12}|^2 + 60|U_{13}|^2 &= n_1(U) \equiv n_u , \\
 9|U_{22}|^2 + 60|U_{23}|^2 &= n_2(U) \equiv n_c , \\
 9|U_{32}|^2 + 60|U_{33}|^2 &= n_3(U) \equiv n_t = 69 - n_2(U) - n_1(U) .
 \end{aligned}
 \tag{5.3.2}$$

The integers n_d, n_s and n_u, n_c characterize the masses of the physical quarks and the task is to derive the values of these integers by studying the spectrum of the hadronic masses. The second task is to find unitary mixing matrices satisfying these conditions.

The general form of U and D matrices can be deduced from the standard parametrization of the CKM matrix given by

$$V = \begin{bmatrix} c_1 & s_1 c_3 & s_1 s_3 \\ -s_1 c_2 & c_1 c_2 c_3 - s_2 s_3 \exp(i\delta_{CP}) & c_1 c_2 s_3 + s_2 c_3 \exp(i\delta_{CP}) \\ -s_1 s_2 & c_1 s_2 c_3 + c_2 s_3 \exp(i\delta_{CP}) & c_1 s_2 s_3 - c_2 c_3 \exp(i\delta_{CP}) \end{bmatrix} \quad (5.3.3)$$

This form of the CKM matrix is always possible to achieve by multiplying each U and D type quark fields with a suitable phase factor: this induces a multiplication U and D from left by a diagonal phase factor matrix inducing the multiplication of the columns of U and D by phase factors:

$$\begin{aligned} U &\rightarrow U \times d(\phi_1, \phi_2, \phi_3) , \\ D &\rightarrow D \times d(\chi_1, \chi_2, \chi_3) , \\ d(\phi_1, \phi_2, \phi_3) &\equiv \text{diag}(\exp(i\phi_1), \exp(i\phi_2), \exp(i\phi_3)) . \end{aligned}$$

The multiplication of the columns by the phase factors affects CKM matrix defined as

$$V = U^\dagger D \rightarrow d(-\phi_1, -\phi_2, -\phi_3) V d(\chi_1, \chi_2, \chi_3) . \quad (5.3.4)$$

By a suitable choice of the phases, the first row and column of V can be made real. The multiplication of the rows of U and D from the left by the same phase factors does not affect the elements of V. One can always choose D to be of the same general form as the CKM matrix but must allow U to have nontrivial phase overall factors on the second and third row so that the most general U matrix is parameterized by six parameters.

Mass squared conditions give two independent conditions on the values of the moduli of the matrix elements of U and D. This eliminates two coordinates so that the most general D matrix can be chosen to depend on 2 parameters, which can be taken to be $r_{11} \equiv |D_{11}|$ and $r_{21} \equiv |D_{21}|$. U matrix contains also the overall phase angles associated with the second and third row and hence depends on four parameters altogether.

5.3.2 The constraints on U and D matrices from quark masses

The new view about quark masses allows a surprisingly simple model for U and D matrices predicting in the lowest order approximation that the probabilities defined by these matrices are identical and that the integers characterizing the masses of U and D type quarks are identical.

The constraints on |U| and |D| matrices from quark masses

The understanding of quark masses pose strong constraints on U and D matrices. The constraints are identical in the approximation that V-matrix is identity matrix and read in the case of D-matrix as

$$\begin{aligned} n_d &= 13 = P_{12}^D \times 9 + P_{13}^D \times 60 , \\ n_s &= 31 = P_{22}^D \times 9 + P_{23}^D \times 60 . \end{aligned} \quad (5.3.5)$$

The conditions for b quark give nothing new. The extreme cases when only $g = 1$ or $g = 2$ contributes to n_q gives the bounds

$$\begin{aligned} \frac{15}{36} &\leq P_{13}^D \leq \frac{15}{60} , \\ \frac{22}{60} &\leq P_{23}^D \leq \frac{31}{60} . \end{aligned} \quad (5.3.6)$$

Unitarity conditions

The condition $D = VU$ and the fact that V is in not too far from unit matrix being in a good approximation a direct sum of 2×2 matrix and 1×1 identity matrix, imply together that U and D cannot differ much from each other. At least the probabilities defined by the moduli squared of matrix elements are near to each other.

1. Instead of trying numerically to solve U and D matrices by a direct numerical search, it is more appropriate to try to deduce estimates for the probabilities $P_{ij}^U = |U_{ij}|^2$ and $P_{ij}^D = |D_{ij}|^2$ determined by the moduli squared of the matrix elements and satisfying the unitarity conditions $\sum_j P_{ij}^X = 1$ and $\sum_i P_{ij}^X = 1$.
2. The formula $D = UV$ using the fact that V_{i3} is small for $i = 1, 2$ implies $|D_{i3}| \simeq |U_{i3}|$. By probability conservation also the condition $|D_{33}| \simeq |U_{33}|$ must hold true so that the third columns of U and D are same in a reasonable approximation.

1. Parametrization of $|U|$ and $|D|$ matrices

The following parametrization is natural for the matrices P_{ij}^X .

$$\begin{aligned} P_{12}^D &= \frac{k_D}{9} \quad , \quad P_{13}^D = \frac{n_d - k_D}{9} \quad , \\ P_{22}^D &= \frac{l_D}{9} \quad , \quad P_{23}^D = \frac{n_s - l_D}{60} \quad , \\ P_{32}^D &= \frac{9 - k_D - l_D}{9} \quad , \quad P_{33}^D = \frac{60 - n_s - n_d - k_D - l_D}{60} \quad . \end{aligned} \quad (5.3.7)$$

A similar parametrization holds true for P_{ij}^U but with $n_d = n_u$ and $n_s = n_c$ but possibly different values of k_U and l_U . Since $l_D \ll n_s$ is expected to hold true, P_{23}^D is in a good approximation equal to $P_{23}^D = n_s/60 = 31/60$. Same applies to P_{23}^U .

$k_X = 2$ (k_X need not be an integer) gives a good first estimate for mixing probabilities of u and d quark. Thus only the parameter l_X remains free if $k_D = 2$ is accepted.

The approximation $P_{i3}^U = P_{i3}^D$ motivated by the near unit matrix property of V , gives the parametrization

$$P_{12}^D = P_{12}^U = \frac{k}{9} \quad , \quad P_{13}^D = P_{13}^U = \frac{n_d - k}{60} \quad . \quad (5.3.8)$$

2. Constraints from CKM matrix in $|U| = |D|$ approximation

The condition $D_{12} = (UV)_{12}$ when feeded to the condition

$$P_{12}^U = P_{12}^D \quad (5.3.9)$$

using the approximation $k_D = k_U = k$ $l_D = l_U = l$ gives

$$|U_{i2}|^2 - |U_{i1}V_{12} + U_{i2}V_{22} + U_{i3}V_{32}|^2 = 0 \quad . \quad (5.3.10)$$

$i = 1, 2, 3$ In the approximation that the small V_{32} term does not contribute, this gives

$$|U_{i1}V_{12} + U_{i2}V_{22}|^2 = |U_{i2}|^2 \quad . \quad (5.3.11)$$

By dividing with $|U_{i1}|^2|V_{22}|^2$ and using the approximation $|V_{22}|^2 = 1$ this gives

$$\begin{aligned} v_i^2 + 2u_i v_i \cos(\Psi_i) &= 0 \quad , \\ \Psi_i &= \arg(V_{i2}) - \arg(V_{32}) + \arg(U_{i1}) - \arg(U_{i2}) \quad . \\ u_i &= \left| \frac{U_{i2}}{U_{i1}} \right| \quad , \quad v_i = \left| \frac{V_{i2}}{V_{22}} \right| \quad . \end{aligned} \quad (5.3.12)$$

This gives

$$\begin{aligned}
\cos(\Psi_i) &= -\frac{v_i}{2u_i} = -\frac{v_i}{2} \sqrt{\frac{9x_i}{k_i}} , \\
x_i &= P_{ii}^D = 1 - \frac{k_i}{9} - \frac{n(i) - k(i)}{60} , \\
k(1) &= k , \quad k(2) = l , \quad n(1) = n_d , \quad n(2) \equiv n_s .
\end{aligned} \tag{5.3.13}$$

The condition $|\cos(\Psi)| \leq 1$ is trivially satisfied. For $n_d = 13$ and $k = 2$ the condition gives $x = .59$ and $\cos(\Psi_1) = .185$. $k = 1.45$ gives $x = .65$ and $\cos(\Psi) = .226$, which is rather near to V_{12} .

5.3.3 Constraints from CKM matrix

Besides the constraints from hadron masses, there are constraints from CKM matrix $V = U^\dagger D$ on U and D matrices.

1. The fact that CKM matrix is near unit matrix implies that U and D matrix are near to each other and the assumption $n(U_i) = n(D_i)$ predicting quark masses correctly is consistent with this.
2. Cabibbo angle allows to derive the estimate for the difference $|U_{11}| - |D_{11}|$. Together with other conditions this difference fixes the scenario essentially uniquely.
3. The requirement that CP breaking invariant J has a correct order of magnitude gives a very strong constraint on D matrix. The smallness of J implies that V is nearly orthogonal matrix and same assumption can be made about U and D matrices.
4. The requirement that the moduli the first row (column) of CKM matrix are predicted correctly makes it possible to deduce for given D (U) U (D) matrix essentially uniquely. Unitarity requirement poses very strong additional constraints. It must be emphasized that the constraints from the moduli of the CKM alone are sufficient to determine U and D matrices and hence also quark masses and hadron masses to very high degree.

1. Bounds on CKM matrix elements

The most recent experimental information [38] concerning CKM matrix elements is summarized in table below

$ V_{13} \equiv V_{ub} = (0.087 \pm 0.075)V_{cb} : 0.42 \cdot 10^{-3} < V_{ub} < 6.98 \cdot 10^{-3}$
$ V_{23} \equiv V_{cb} = (41.2 \pm 4.5) \cdot 10^{-3}$
$ V_{31} \equiv V_{td} = (9.6 \pm 0.9) \cdot 10^{-3}$
$ V_{32} \equiv V_{ts} = (40.2 \pm 4.4) \cdot 10^{-3}$
$s_{Cab} = 0.226 \pm 0.002$

Table 4. The experimental constraints on the absolute values of the CKM matrix elements.

$$\begin{aligned}
s_1 &= .226 \pm .002 , \\
s_1 s_2 &= V_{31} = (9.6 \pm .9) \cdot 10^{-3} , \\
s_1 s_3 &= V_{13} = (.087 \pm .075) \cdot V_{23} , \\
V_{23} &= (40.2 \pm 4.4) \cdot 10^{-3} .
\end{aligned} \tag{5.3.14}$$

The remaining parameter is $\sin(\delta)$ or equivalently the CP breaking parameter J :

$$J = \text{Im}(V_{11}V_{22}\bar{V}_{12}\bar{V}_{21}) = c_1 c_2 c_3 s_2 s_3 s_1^2 \sin(\delta) , \tag{5.3.15}$$

where the upper bound is for $\sin(\delta) = 1$ and the previous average values of the parameters s_i, c_i (note that the poor knowledge of s_3 affects on the upper bound for J considerably). Unitary triangle [93] gives for the CP breaking parameter the limits

$$1.0 \times 10^{-4} \leq J \leq 1.7 \times 10^{-4} . \quad (5.3.16)$$

2. CP breaking in $M - \bar{M}$ systems as a source of information about CP breaking phase

Information about the value of $\sin(\delta)$ as well as on the range of possible top quark masses comes from CP breaking in $K - \bar{K}$ and $B - \bar{B}$ systems.

The observables in $K_L \rightarrow 2\pi$ system [106]

$$\begin{aligned} \eta_{+-} &= \frac{A(K_L \rightarrow \pi^+\pi^-)}{A(K_S \rightarrow \pi^+\pi^-)} = \epsilon + \frac{\epsilon'}{1 + \omega/\sqrt{2}} , \\ \eta_{00} &= \frac{A(K_L \rightarrow \pi^0\pi^0)}{A(K_S \rightarrow \pi^0\pi^0)} = \epsilon - 2\frac{\epsilon'}{1 - \sqrt{2}\omega} , \\ \omega &\sim \frac{1}{20} , \\ \epsilon &= (2.27 \pm .02) \cdot 10^{-3} \cdot \exp(i43.7^\circ) , \\ \left| \frac{\epsilon'}{\epsilon} \right| &= (3.3 \pm 1.1) \cdot 10^{-3} . \end{aligned} \quad (5.3.17)$$

The phases of ϵ and ϵ' are in good approximation identical. CP breaking in $K - \bar{K}$ mass matrix comes from the CP breaking imaginary part of $\bar{s}d \rightarrow s\bar{d}$ amplitude M_{12} (via the decay to intermediate W^+W^- pair) whereas $K^0\bar{K}^0$ mass difference Δm_K comes from the real part of this amplitude: the calculation of the real part cannot be done reliably for kaon since perturbative QCD does not work in the energy region in question. On can however relate the real part to the known mass difference between K_L and K_S : $2\text{Re}(M_{12}) = \Delta m_K$.

Using the results of [106]) one can express ϵ and ϵ'/ϵ in the following numerical form

$$\begin{aligned} |\epsilon| &= \frac{1}{\sqrt{2}} \frac{\text{Im}(M_{12}^{sd})}{\Delta m_K} - .05 \cdot \left| \frac{\epsilon'}{\epsilon} \right| = 2J(22.2B_K \cdot X(m_t) - .28B'_K) , \\ \left| \frac{\epsilon'}{\epsilon} \right| &= C \cdot J \cdot B'_K , \\ X(m_t) &= \frac{H(m_t)}{H(m_t = 60 \text{ GeV})} , \\ H(m_t) &= -\eta_1 F(x_c) + \eta_2 F(x_t)K + \eta_3 G(x_c, x_t) , \\ x_q &= \frac{m(q)^2}{m_W^2} , \\ K &= s_2^2 + s_2 s_3 \cos(\delta) . \end{aligned} \quad (5.3.13)$$

Here the values of QCD parameters η_i depend on top mass slightly. B'_K and B_K are strong interaction matrix elements and vary between 1/3 and 1. The functions F and G [106] are given by

$$\begin{aligned} F(x) &= x \left[\frac{1}{4} + \frac{9}{4} \frac{1}{1-x} - \frac{3}{2} \frac{1}{(1-x)^2} \right] + \frac{3}{2} \left(\frac{x}{x-1} \right)^3 \log(x) , \\ G(x, y) &= xy \left[\frac{1}{x-y} \left[\frac{1}{4} + \frac{3}{2} \frac{1}{1-x} - \frac{3}{4} \frac{1}{(1-x)^2} \right] \log(x) + (y \rightarrow x) - \frac{3}{4} \frac{1}{(1-x)(1-y)} \right] . \end{aligned} \quad (5.3.12)$$

One can solve parameter B'_K by requiring that the value of ϵ'/ϵ corresponds to the experimental mean value:

$$B'_K = \frac{1}{C \times J} \frac{\epsilon'}{\epsilon} . \quad (5.3.13)$$

The most recent measurements by KTeV collaboration in Fermi Lab [34] give for the ratio $|\epsilon'/\epsilon|$ the value $|\epsilon'/\epsilon| = (28 \pm 1) \times 10^{-4}$. The proposed standard model explanation for the large value of B'_K is that s-quark has running mass about $m_s(m_c) \simeq .1$ GeV at m_c [100]. The explanation is marginally consistent with the TGD prediction $m(s) = 127$ MeV for the mass of s quark. Also the effects caused by the predicted higher gluon generations having masses around 33 GeV can increase the value of ϵ'/ϵ by a factor 3 in the lowest approximation since the corrections involve sum over three different one-gluon loop diagrams with gluon mass small respect to intermediate boson mass scale [20].

A second source of information comes from $B - \bar{B}$ mass difference. At the energies in question perturbative QCD is expected to be applicable for the calculation of the mass difference and mass difference is predicted correctly if the mass of the top quark is essentially the mass of the observed top candidate [35].

3. U and D matrices could be nearly orthogonal matrices

The smallness of the CP breaking phase angle δ_{CP} means that V is very near to an orthogonal matrix. This raises the hope that in a suitable gauge also U and D are nearly orthogonal matrices and would be thus almost determined by single angle parameter θ_X , $X = U, D$. Cabibbo angle $s_c = \sin(\theta_c) = .226$ which is not too far from $\sin^2(\theta_W) \simeq .23$ and appears in V matrix rotating the rows of U to those of D . In very vague sense this angle would characterize between the difference of angle parameters characterizing U and D matrices. If U is orthogonal matrix then the decomposition

$$V = V_1 V_2 = \begin{bmatrix} c_1 & s_1 & 0 \\ -s_1 c_2 & c_1 c_2 & s_2 \exp(i\delta_{CP}) \\ -s_1 s_2 & c_1 s_2 & -c_2 \exp(i\delta_{CP}) \end{bmatrix} \times \begin{bmatrix} 1 & 0 & 0 \\ 0 & c_3 & s_3 \\ 0 & -s_3 & c_3 \end{bmatrix} \quad (5.3.14)$$

suggests that CP breaking can be visualized as a process in which first s and b quarks are slightly mixed to s' and b' by V_2 ($s_3 \simeq 1.4 \times 10^{-2}$) after which V_1 induces a slightly CP-breaking mixing of d and s' with b' ($s_2 \simeq .04$).

4. How the large mixing between u and c results

The prediction that u quark spends roughly 1/3 of time in $g = 0$ state looks bizarre and it is desirable to understand this from basic principles. The basic observations are following.

1. V matrix is in good approximation direct sum of 2×2 matrix inducing relatively large rotation with $\sin(\theta_c) \simeq .23$ and unit matrix. In particular, V_{i3} are very small for $i = 1, 2$. Using the formula $D = UV$ one finds that $|U_{i3}| = |D_{i3}|$ in a good approximation for $i = 1, 2$ and by unitarity also for $I = 3$. Thus the third columns of U and D are identical in a good approximation.
2. Assume that also U_{i3} and D_{i3} are small for $i = 1, 2$. A stronger assumption is that even the contribution of D_{13} and U_{13} are so small that they do not affect u and d masses. This implies

$$\begin{aligned} n_d &= 9|D_{12}|^2 + 60|D_{13}|^2 \simeq 9|D_{12}|^2 , \\ n_u &\simeq 9|U_{12}|^2 . \end{aligned} \quad (5.3.14)$$

Unitarity implies in this approximation

$$\begin{aligned} |U_{11}|^2 &\leq 1 - \frac{n_u}{9} = \frac{1}{3} , \\ |D_{11}|^2 &\leq 1 - \frac{n_d}{9} = \frac{5}{9} . \end{aligned} \quad (5.3.14)$$

3. It might be that there are also solutions for which mixing of u resp. d quark is mostly with t resp. b quarks but numerical experimentation does not favor this idea since CP breaking becomes extremely small. Since mixing presumably involves topology change, it seems obvious that topological mixing involving a creation or annihilation of two handles is improbable.

5.4 Construction of U , D , and CKM matrices

In this section it will be found that various mathematical and experimental constraints on U and D matrices determine them essentially uniquely.

5.4.1 The constraints from CKM matrix and number theoretical conditions

The requirement that U , D and V allow an algebraic continuation to finite-dimensional extensions of various p-adic number fields provides a very strong additional constraints. The mathematical problem is to understand how many unitary V matrices acting on U as $U \rightarrow D = UV$ respect the number theoretic constraints plus the constraints $n_u = n_d + 2$ and $n_c = n_d - 2$.

It is instructive to what happens in much simpler 2-dimensional case. In this case the conditions boil down to the conditions on $n(i)$ imply $|U| = |D|$ and this condition is equivalent with (say) the condition $|U_{11}| = |D_{11}|$. U and D can be parameterized as

$$U = \begin{pmatrix} \cos(\theta)\exp(i\psi) & \sin(\theta)\exp(i\phi) \\ -\sin(\theta)\exp(-i\phi) & \cos(\theta)\exp(-i\psi) \end{pmatrix}.$$

If $\cos(\theta)^2$ and $\sin(\theta)^2$ are rational numbers, $\exp(i\theta)$ is associated with a Gaussian integer. A more general requirement is that $\exp(i\theta)$ belongs to a finite-dimensional extension of rational numbers and thus corresponds to a products of a phase associated with Gaussian integer and a phase in a finite-dimensional algebraic extension of rational numbers.

Eliminating the trivial multiplicative phases gives a set of matrices U identifiable as a double coset space $X^2 = SU(2)/U(1)_R \times U(1)_L$. The value of $\cos(\theta) = |U_{11}|$ serving as a coordinate for X^2 is respected by the right multiplication with V . Eliminating trivial $U(1)_R$ phase multiplication, the space of V 's reduces to $S^2 = SU(2)/U(1)_R$. The condition that $\cos(\theta)$ is not changed leaves one parameter set of allowed matrices V .

The translation of these results to 3-dimensional case is rather straightforward. In the 3-dimensional case the probabilities P_{i2}, P_{i3} , $i = 1, 2$ characterize a general matrix $|U|$, and V can affect these probabilities subject to constraints on $n(I)$. When trivial phases affecting the probabilities are eliminated, the matrices U correspond naturally to points of the 4-dimensional double coset space $X^4 = SU(3)/(U(1) \times U(1))_R \times U(1) \times U(1)_L$ having dimension $D = 4$.

The two constraints on the probabilities mean that allowed solutions for given values of $n(I)$ define a 2-dimensional surface X^2 in X^4 . The allowed unitary transformations V must be such that they move U along this surface. Certainly they exist since X^2 can be regarded as a local section in $SU(3) \rightarrow X^2$ bundle obtained as a restriction of $SU(3) \rightarrow X^4$ bundle. The action of V on rows of U is ordinary unitary transformation plus a 2-dimensional unitary transformation preserving the Hermitian degenerate lengths $L_i = 9|U_{i2}|^2 + 60|U_{i3}|^2 = n_i$ defining the sub-bundle $SU(3) \rightarrow X^2$. Note for $L_1 = 0$ ($L_2 = 0$) the situation becomes 2-dimensional and solutions correspond to points in S^2 . Thus these points seem to represent a conical singularity of X^2 .

The 2-dimensionality of the solution space means that two moduli (probabilities) of any row or column of U or D matrix characterize the matrix apart from the non-uniqueness due to the gauge choice allowing $U(1)_L \times U(1)_R$ transformation of U . Of course, discrete sign degeneracy might be present.

A highly non-trivial problem is whether the set X^2 contains rational points and what is the number of these points. For instance, Fermat's theorem says that no rational solutions to the equation $x^n + y^n - z^n = 0$ exist for $n > 2$. The fact that the degenerate situation allows infinite number of rational solutions suggest that they exist also in the general case. Note also that the additional conditions are second order polynomial equations with rational coefficients so that $SU(3, Q)$ should contain non-trivial solutions to the equations.

It is possible to write $|U|$ in a form containing minimal number of square roots:

$$\begin{aligned}
|U_{11}| &= \sqrt{n_u} \frac{p_1}{N_1} , & |U_{12}| &= \sqrt{\frac{n_u}{9}} \frac{r_1}{N_1} , & |U_{13}| &= \sqrt{\frac{n_u}{60}} \frac{s_1}{N_1} , \\
|U_{21}| &= \sqrt{n_c} \frac{p_2}{N_2} , & |U_{22}| &= \sqrt{\frac{n_c}{9}} \frac{r_2}{N_2} , & |U_{23}| &= \sqrt{\frac{n_c}{60}} \frac{s_2}{N_2} , \\
|U_{31}| &= \sqrt{n_t} \frac{p_3}{N_3} , & |U_{32}| &= \sqrt{\frac{n_t}{9}} \frac{r_3}{N_3} , & |U_{33}| &= \sqrt{\frac{n_t}{60}} \frac{s_3}{N_3} .
\end{aligned} \tag{5.4.1}$$

Completely analogous expression holds true for D . r_i , s_i and N_i are integers, and the defining equations reduce in both cases to equations generalizing those satisfied by Pythagorean triangles

$$\begin{aligned}
r_1^2 + s_1^2 &= N_1^2 , \\
r_2^2 + s_2^2 &= N_2^2 , \\
r_3^2 + s_3^2 &= N_3^2 .
\end{aligned} \tag{5.4.0}$$

The square roots of n_i are also eliminated from the unitarity conditions which become equations with rational coefficients for the phases appearing in U and D . Hence there are good hopes that even rational solutions to the conditions might exist.

5.4.2 How strong number theoretic conditions one can pose on U and D matrices?

It is not quite clear how strong the number theoretic conditions on U and D matrices are. An attractive working hypothesis is that mixing probabilities are rational. This leaves a lot of freedom concerning the mixing matrices themselves since square roots of rationals, Pythagorean phases, and finite roots of unity can appear in the mixing matrices.

1. The most stringent requirement would be that U and D matrices are rational unitary matrices. p-Adicization without algebraic extension allows only matrices for which various phases and trigonometric functions are products of Pythagorean phases. This option will be found to be too restrictive. The minimal extension allows square roots requiring a finite-dimensional extension of p-adic numbers: geometrically this means a generalization Pythagorean triangles to triangles for which short sides are integer valued and long side is square root of integer. Pythagorean phases and their generalizations span infinite discrete subgroups of $SU(3)$.
2. Both the phases and also cosines and sines appearing in the mixing matrices could be restricted to algebraic roots of unit that is of form $exp(i2\pi/N)$ requiring finite algebraic extension of rationals and p-adic numbers. Roots of unity could define finite discrete subgroup of $SU(3)$ implying rather stringent conditions on the model. Root of unity option is highly suggestive in light of the most recent developments (more than decade after development of the model) related to the p-adicization in terms of harmonic analysis in symmetric spaces relying on the counterparts of plane waves defined in terms of roots of unity and leading to a p-adic version of real symmetric space [21]. Finite roots of unity define as a special case discrete subgroups of $SU(3)$ implying rather stringent conditions on the model. For instance, in case of $SU(2)$ these finite groups are well-known.

5.4.3 Could rational unitarity make sense?

In this section the considerations are restricted mostly to rational unitarity which at the time of writing of this chapter looked more attractive than the allowance of algebraic roots of unity. The number theoretic conditions following from the rational unitarity on the moduli of the U and D matrices are not completely independent of the parametrization used. The reason is that the products of the parameters in some algebraic extension of the rationals can combine to give a rational number. The safest parametrization to use is the one based on the moduli of the U and D matrix.

Parameterization of moduli in the case of rational unitarity

If one assumes rationality for the mixing matrix then all moduli can be written in the form

$$|D_{ij}| = \frac{n_{ij}}{N} . \quad (5.4.1)$$

If only moduli squared are required to be rational, the condition is replaced with a milder one:

$$|D_{ij}| = \frac{n_{ij}}{\sqrt{N}} . \quad (5.4.2)$$

Here \sqrt{N} belongs to square root allowing algebraic extension of the p-adic numbers but is not an integer itself. An even milder condition is

$$|D_{ij}| = \sqrt{\frac{n_{ij}}{N}} . \quad (5.4.3)$$

The following arguments show that only this option or more general option allowing roots of unity with rational mixing probabilities is allowed. These options is also natural in light or preceding general considerations.

Unitary and mass conditions modulo 8 for rational unitarity

For $p_{ij} = (\sqrt{\frac{n_{ij}}{N}})^k$, $k = 1$ or 2 , the requirement that the rows are unit vectors implies

$$\begin{aligned} \sum_j n_{i,j}^k &= N^k , \\ k &= 1 \text{ or } 2 . \end{aligned} \quad (5.4.3)$$

The problem of finding vectors with integer valued components and with a given integer valued length squared m ($k = 2$ case) is a well known and well understood problem of the number theory [28]. The basic idea is to write the conditions modulo 8 and use the fact that the square of odd (even) integer is 1 (0 or 4) modulo 8. The result is that one must have

$$m \in \{1, 2, 3, 5, 6\} , \quad (5.4.4)$$

for the conditions to possess nontrivial solutions. For $m = N$ case this is the only condition needed. In $m = N^2$ case the condition implies that N must be odd.

Using this result one can write the mass squared conditions modulo 8 for $k = 2$ as

$$\begin{aligned} 3n_{i,2}^2 + 4n_{i,3}^2 &= n_i X , \\ X &= 1 \text{ for } m = N^2 , \\ X &\in \{1, 2, 3, 5, 6\} \text{ for } m = N . \end{aligned} \quad (5.4.3)$$

Here modulo 8 arithmetics is understood. In $m = N^2$ case one must have $n_i \in \{0, 3, 4\}$ modulo 8. These conditions are not satisfied in general. For $m = N$ conditions allow considerably more general set of solutions. By summing the equations and using probability conservation one however obtains $7N = 5N$ implying $2N = 0$ so that the non-allowed value $N = 4$ or 0 results.

For $k = 1$ no obvious conditions result on the values of n_i and only this option is allowed by mass conditions for the physical masses.

Rational unitarity cannot hold true for U and D matrices separately

The mixing scenario is not consistent with the assumption that the matrix elements of U and D matrix are complex rational numbers. If this were the case then matrix elements had to be proportional to a common denominator $1/N$ such that N is odd integer (otherwise the conditions stating that the unit vector property of the rows is not satisfied). The conditions

$$\begin{aligned} \sum_j r_{ij} &= 1 , \\ 9r_{12} + 60r_{13} &= n_d , \\ 9r_{22} + 60r_{23} &= n_s , \\ 9r_{32} + 60r_{33} &= n_b , \\ r_{ij} &= \frac{n_{ij}}{N_i} , \end{aligned} \tag{5.4-1}$$

can be written modulo 8 as

$$\begin{aligned} \sum_j n_{ij}^k &= N^k , \\ n_{12}^k + 4n_{13}^k &= n_d N^k , \\ n_{22}^k + 4n_{23}^k &= n_s N^k , \\ n_{32}^k + 4n_{33}^k &= n_b N^k , \\ r_{ij} &= \left(\frac{n_{ij}}{N}\right)^{k/2} , \quad k = 1 \text{ or } 2 . \end{aligned} \tag{5.4-5}$$

1. Consider first the case $k = 2$. For odd n $n^2 = 1$ holds true and for even n $n^2 = 4$ or 0 holds true. It is easy to see that the conditions can be satisfied only if all integers are proportional to 4 but this cannot be possible since it would be possible since n_{ij} and N cannot contain common factors. Thus at least an extension allowing square roots is needed. Quite generally from $N^2 = 1 \pmod{8}$ the above equations give

$$n_{q_i} \pmod{8} \in \{0, 3, 4, 7\} .$$

This condition fails to be satisfied by in the general case.

2. For the option $k = 1$ for which only the probabilities are rational the sum of all three equations gives $5N = 5N$ so that equations are consistent.

The result favors the possibility that roots of unity are the basic building bricks of the mixing matrices. This does not exclude the possibility that mixing probabilities are rational numbers.

Rational unitarity for phase factors

The phase factors associated with the rows of the mixing matrix are rational provided the corresponding angles correspond to Pythagorean triangles. It must be however emphasized that roots of unit are highly suggestive in the recent vision about p-adicization. Combining this property with the orthogonality conditions for the rows of the U matrix, one obtains highly nontrivial conditions relating the integers characterizing the sides of the Pythagorean triangle to the integers n_{ij} . The requirement that the imaginary parts of the inner product vanish, gives the conditions

$$\frac{s_{i,2}}{s_{i3}} = \frac{n_{13}n_{i3}}{n_{12}n_{22}} , \quad i = 2, 3 . \tag{5.4-4}$$

Combining this conditions with the general representation for the sines of the Pythagorean triangle

$$\sin(\phi) = \frac{2rs}{r^2 + s^2} \text{ or } \frac{r^2 - s^2}{r^2 + s^2} , \quad (5.4-3)$$

one obtains conditions relating the integers appearing characterizing the triangle to the integers on the right hand side.

An interesting possibility is that the lengths of the hypotenusae of the triangles associated with $s(i, 2)$ ($(r(i), s(i))$) and s_{i3} ($(r_1(i), s_1(i))$) are the same and sines correspond to the products $2rs$:

$$\begin{aligned} r^2(i) + s^2(i) &= r_1^2(i) + s_1^2(i) , \\ s_{i,2} &= 2r(i)s(i)/(r^2(i) + s^2(i)) , \\ s_{i,3} &= 2r_1(i)s_1(i)/(r_1^2(i) + s_1^2(i)) . \end{aligned} \quad (5.4-4)$$

In this case the conditions give

$$\frac{r(i)s(i)}{r_1(i)s_1(i)} = \frac{n_{13}n_{i3}}{n_{12}n_{22}} . \quad (5.4-3)$$

The conditions are satisfied if one has

$$\begin{aligned} r(i)s(i) &= n_{13}n_{i3} , \\ r_1(i)s_1(i) &= n_{12}n_{22} . \end{aligned} \quad (5.4-3)$$

This implies that $r(i)$ and $s(i)$ are products of the factors contained in the product $n_{13}n_{i3}$. Analogous conclusion applies to $r_1(i)$ and $s_1(i)$.

Additional number theoretic conditions are obtained from the requirement that the real parts of the inner products between first row and second and third rows vanish:

$$n_{11}n_{i1} + c_{i,2}n_{12}n_{i2} + c_{i,3}n_{13}n_{i3} = 0 , \quad i = 2, 3 . \quad (5.4-2)$$

5.4.4 The parametrization suggested by the mass squared conditions

To understand the consequences of the mass squared conditions, it is useful to use a parametrization, which is more natural for the treatment of the mass squared conditions than the standard parametrization:

$$U = \begin{bmatrix} r_{11} & r_{12} & r_{13} \\ r_{21}x_2 & r_{22}x_2 \exp(i\phi_{22}) & r_{23}x_2 \exp(i\phi_{23}) \\ r_{31}x_3 & r_{32}x_3 \exp(i\phi_{32}) & r_{33}x_3 \exp(i\phi_{33}) \end{bmatrix} \quad (5.4-1)$$

$$\begin{aligned} x_2 &= \exp(i\phi_2) , \\ x_3 &= \exp(i\phi_3) . \end{aligned}$$

In case of D matrix, the phase factors x_2 and x_3 can be chosen to be trivial. As far as the treatment of the mass conditions and unitarity conditions for the rows is considered, one can restrict the consideration to the case, when the overall phase factors are trivial. The remaining parameters are not independent and one can deduce the formulas relating the moduli r_{ij} as well as the phase angles ϕ_{ij} to the parameters r_{11} and r_{12} . In general, the resulting parameters are not real and unitarity is broken.

Mass squared conditions and the requirement that the rows are unit vectors:

$$\begin{aligned} 9r_{i2}^2 + 60r_{i3}^2 &= n_i , \quad i = 1, 2 , \\ \sum_k r_{ik}^2 &= 1 , \end{aligned} \quad (5.4-1)$$

allows one to express r_{i2} and r_{i3} in terms of r_{i1}

$$\begin{aligned} r_{i2} &= \sqrt{\left[-\frac{n_i}{51} + \frac{20}{17}(1 - r_{i1}^2)\right]} , \\ r_{i3} &= \sqrt{\left[\frac{n_i}{51} - \frac{3}{17}(1 - r_{i1}^2)\right]} . \end{aligned} \quad (5.4-1)$$

The requirement that the rows are orthogonal to each other, relates the phase angles ϕ_{ij} in terms to r_{11} and r_{21} . Using the notations $\sin(\phi_{ij}) = s_{ij}$ and $\cos(\phi_{ij}) = c_{ij}$, one has

$$\begin{aligned} c_{i2} &= \frac{a_i}{b_i} , & c_{i3} &= -\frac{(A_{1i} + c_{i2}A_{2i})}{A_{3i}} , \\ s_{i2} &= \epsilon(i)\sqrt{1 - c_{i2}^2} , & s_{i3} &= -\frac{A_{2i}}{A_{3i}}s_{i2} , \\ A_{1i} &= r_{11}r_{i1} , & A_{2i} &= r_{12}r_{i2} \\ A_{3i} &= r_{13}r_{i3} , & \epsilon(i) &= \pm 1 . \\ a_i &= A_{3i}^2 - A_{1i}^2 - A_{2i}^2 , & b_i &= 2A_{1i}A_{2i} , \end{aligned} \quad (5.4.0)$$

The sign factors $\epsilon(i)$ are not completely free and must be chosen so that the second and third row are orthogonal.

The mass conditions imply the following bounds for the parameters r_{i1}

$$\begin{aligned} m_i &\leq r_{i1} \leq M_i , \\ m_i &= \sqrt{1 - \frac{n_i}{9}} \text{ for } n_i \leq 9 , \\ m_i &= 0 \text{ for } n_i \geq 9 , \\ M_i &= \sqrt{1 - \frac{n_i}{60}} . \end{aligned} \quad (5.4-2)$$

The boundaries for the regions of the solution manifold in (r_{11}, r_{21}) plane can be understood as follows. For given values of r_{11} and r_{21} there are in general two solutions corresponding to the sign factor $\epsilon(i)$ appearing in the equations defining the solutions of the mass squared conditions. This means just that complex conjugation gives a new solution from a given one. These two branches become degenerate, when the phase factors become ± 1 so that (s_{i2}, s_{i3}) vanishes for $i = 2$ or $i = 3$. Thus the curves at which one has $(s_{i2} = 0, s_{i3} = 0)$ define the boundaries of the projection of the solution manifold to (r_{11}, r_{21}) plane. At the boundaries the orthogonality conditions reduce to the form

$$\begin{aligned} r_{11}r_{i1} + \epsilon(i, 2)r_{12}r_{i2} + \epsilon_{i3}r_{13}r_{i3} &= 0 , \quad i = 2 \text{ or } 3 , \\ \epsilon_{22} &= \epsilon_{32} , \\ \epsilon_{23} &= -\epsilon_{33} \end{aligned} \quad (5.4-1)$$

where ϵ_{ij} corresponds to the value of the cosine of the phase angle in question. Consistency requires that either second or third row becomes real on the boundary of the unitarity region and that the matrices reduce to orthogonal matrices at the dip of the region allowed by unitarity.

5.4.5 Thermodynamical model for the topological mixing

What would be needed is a physical model for the topological mixing allowing to deduce U and D matrices from first principles. The physical mechanism behind the mixing is change of the topology of X^2 in the dynamical evolution defined by the light like 2-surface X_l^3 defining parton orbit. This suggests that the topology changes $g \rightarrow g \pm 1$ dominate the dynamics so that matrix elements U_{13} and D_{13} should be indeed small so that the weird looking result $P_{11}^U \simeq 1/3$ follows from the requirement $n_u = 6$. This model however suggests that the matrix elements U_{23} and D_{23} could be large unlike in the original model for U and D matrices.

Solution of thermodynamical model

A possible approach to the construction of mixing matrices is based on the idea that the interactions causing the mixing lead to a thermal equilibrium so that the entropies for the ensemble defined by the probabilities p_{ij}^U and p_{ij}^D matrix is maximized (the subscripts U and D are dropped in the sequel).

1. The elements in the three rows of the mixing matrix represent probabilities for three states of the system with energies $(E_{i1}, E_{i2}, E_{i3}) = (0, 9, 60)$ and average energy is fixed to $\langle E \rangle = 69$.
2. There are usual constraints from probability conservation for each row plus two independent constraints from columns. The latter constraints can be regarded as a constraint on a second quantity equal to 1 for each column and brings in variable analogous to chemical potential besides temperature.

The constraint from mass squared for the third row follows from these constraints. The independent constraints can be chosen to be the following ones

$$\begin{aligned} \sum_j p_{ij} - 1 = 0, \quad i = 1, 2, 3 & \quad \sum_i p_{ij} - 1 = 0, \quad j = 1, 2, \\ 9p_{i2} + 60p_{i3} - n_{q_i} = 0, \quad i = 1, 2. \end{aligned} \quad (5.4.0)$$

The obvious notations $(q_1, q_2) = (d, s)$ and $(q_1, 2_2) = (u, c)$ are introduced. The conditions on mass squared are completely analogous to the conditions fixing the energy of the ensemble and thus its temperature, and thermodynamical intuition suggests that the probabilities p_{ij} decrease exponentially as function of E_j in the absence of additional constraints coming from the probability conservation for the columns and meaning presence of chemical potential.

The variational principle maximizing entropy in presence of these constraints can be expressed as

$$\begin{aligned} L &= S + S_c \\ S &= \sum_{i,j} p_{ij} \times \log(p_{ij}) \\ S_c &= \sum_i \lambda_i (\sum_j p_{ij} - 1) + \sum_{j=1,2} \mu_j (\sum_i p_{ij} - 1) + \sum_{i=1,2} \sigma_i (9p_{i2} + 60p_{i3} - n_{q_i}). \end{aligned} \quad (5.4.-2)$$

The variational equation is

$$\partial_{p_{ij}} L = 0, \quad (5.4.-1)$$

and gives the probabilities as

$$\begin{aligned} p_{11} &= \frac{1}{Z_1}, \quad p_{12} = \frac{xx_1^3}{Z_1^3}, \quad p_{13} = \frac{yx_1^{20}}{Z_1^{20}}, \\ p_{21} &= \frac{1}{Z_2}, \quad p_{22} = \frac{xx_2^3}{Z_2^3}, \quad p_{23} = \frac{yx_2^{20}}{Z_2^{20}}, \\ p_{31} &= \frac{1}{Z_3}, \quad p_{32} = \frac{x}{Z_3}, \quad p_{33} = \frac{y}{Z_3}, \end{aligned} \quad (5.4.-1)$$

Here the parameters x, y, x_1, x_2 are defined as

$$\begin{aligned} x &= \exp(-\mu_2), \quad y = \exp(-\mu_3), \\ x_1 &= \exp(-3\sigma_1), \quad x_2 = \exp(-3\sigma_2). \end{aligned} \quad (5.4.-1)$$

whereas the row partition functions Z_i are defined as

$$Z_1 = 1 + xx_1^3 + yx_1^{20} \quad , \quad Z_2 = 1 + xx_2^3 + yx_2^{20} \quad , \quad Z_3 = 1 + x + y \quad . \quad (5.4.0)$$

Note that the parameters λ_i have been eliminated. There are four parameters $\mu_2, \mu_3, \sigma_2, \sigma_3$ and 2 conditions from columns and 2 mass conditions so that the number of solutions is discrete and only finite number of U and D matrices are possible in the thermodynamical approximation.

Mass squared conditions

The mass squared conditions read as

$$9xx_1^3 + 60yx_1^{20} = n(q_1)Z_1 \quad , \quad 9xx_2^3 + 60yx_2^{20} = n(q_2)Z_2 \quad . \quad (5.4.1)$$

These equations allow to solve y as a simple linear function of x

$$y = \frac{n(q_1) - xx_1^3(9 - n(q_1))}{(60 - n(q_1))x_1^{20}} \equiv kx + l \quad , \quad y = \frac{n(q_2) - xx_2^3(9 - n(q_2))}{(60 - n(q_2))x_2^{20}} \quad . \quad (5.4.2)$$

The identification of the two expressions for y allows to solve x_1 in terms of x_2 using equation of form $x_1^{20} - bx_1^3 + c = 0$:

$$\begin{aligned} & [60 - n(q_2)x_2^{20}] [n(q_1) - xx_1^3(9 - n(q_1))] \\ &= [60 - n(q_1))x_1^{20}] [n(q_2) - xx_2^3(9 - n(q_2))] \quad . \end{aligned} \quad (5.4.2)$$

In the most general case the equation allows 20 roots $x_1 = x_2(x_1)$.

Probability conservation

Probability conditions give additional information. By solving $1/Z_3$ from the first column gives

$$Z_1Z_2Z_3 - Z_1Z_2 - Z_2Z_3 - Z_1Z_3 = 0 \quad , \quad (5.4.3)$$

$$(5.4.4)$$

This equation is a polynomial equation for in x_1 and x_2 with degree 20 and together with Eq. 5.4.2 having same degree determines and (x_1, x_2) the possible values of x_1 and x_2 as function of x . The number of real positive roots is at most $20^2 = 400$.

Probability conservation for the second column gives

$$x [(1 - x_1^3)Z_2 + (1 - x_2^3)Z_1] + (1 - x)Z_1Z_2 = 0 \quad . \quad (5.4.5)$$

The row partition functions Z_i are linear functions of x and y and mass squared conditions give $y = kx + l$ (see Eq. 5.4.2) so that a third order polynomial equation for x results and gives the roots as functions of control parameters x_1 and x_2 . Either 1 or 3 real roots are obtained for x . The values of x_1 and x_2 are determined by the probability constraint Eq. 5.4.4 for the first column and Eq. 5.4.2 relating x_1 and x_2 .

The analogy with spontaneous magnetization

Physically the situation is analogous to a spontaneous symmetry breaking with y representing the external magnetizing field and x linear magnetization or vice versa. x_1 and x_2 are control parameters characterizing the interaction between spins. For single real root for x no spontaneous magnetization occurs but for 3 real roots there are two directions of spontaneous magnetization plus unstable state. In the recent case the roots must be positive. Since the maximal number of roots for (x_1, x_2) is 400, the maximal number of real roots is 1200. The trivial solution to the conditions is $p_{11} = 1, p_{22} = 1, p_{33} = 1$ with $x = y = 0$ represents corresponds to the absence of external magnetizing field and of magnetization.

Catastrophe theoretic description of the system

In the catastrophe theoretic approach one can see that situation as a cusp catastrophe with x as a behavior variable and x_1, x_2 in the role of control variables. In the standard parametrization of the cusp catastrophe [27] the conditions correspond to the equation

$$x^3 - a - bx = 0 , \quad (5.4.5)$$

In the recent case a more general polynomial $P_3(x)$ easily transformable to the standard form is in question. The coefficients of the polynomial $P_3(x) = Dx^3 + Cx^2 + Bx + A$ are

$$\begin{aligned} A &= Q(x_1)Q(x_2) , \\ B &= P(x_1)Q(x_2) + P(x_2)Q(x_1) + R(x_2) + R(x_1) , \\ C &= P(x_1)R(x_2) + P(x_2)R(x_1) - R(x_1)Q(x_2) - R(x_2)Q(x_1) , \\ D &= R(x_1)R(x_2) , \\ P(u) &= 1 - u^3 , \quad Q(u) = 1 + lu^{20} , \quad R(u) = u^3 + ku^{20} . \end{aligned} \quad (5.4.2)$$

The trivial scaling transformation $A \rightarrow A/D = \hat{A}$, $B \rightarrow B/D = \hat{B}$, $C \rightarrow C/D = \hat{C}$ and the shift $x \rightarrow x + \hat{C}/3$ casts the equation in the standard form and gives

$$\begin{aligned} a &= -\hat{A} + \frac{\hat{C}^3}{9} , \\ b &= -\hat{B} + \frac{\hat{C}^2}{3} . \end{aligned} \quad (5.4.1)$$

The curve

$$a = \pm 2\left(\frac{b}{3}\right)^{3/2} , b \geq 0 \quad (5.4.2)$$

represents the bifurcation set for the solutions. For $b \geq 0$, $|a| \leq (\frac{b}{3})^{3/2}$ three roots are obtained for x . $a = b = 0$ corresponds to the dip of the cusp. Three solutions result under the conditions

$$\begin{aligned} \frac{\hat{C}^2}{3} &\geq 3\hat{B} , \\ \left(-\hat{B} + \frac{\hat{C}^2}{3}\right)^3 &\leq \frac{(-\hat{A} + \frac{\hat{C}^3}{9})^2}{4} , \\ \hat{A} &= \frac{Q(x_1)Q(x_2)}{R(x_1)R(x_2)} , \\ \hat{B} &= \frac{P(x_1)Q(x_2) + P(x_2)Q(x_1) + R(x_2) + R(x_1)}{R(x_1)R(x_2)} , \\ \hat{C} &= \frac{P(x_1)R(x_2) + P(x_2)R(x_1) - R(x_1)Q(x_2) - R(x_2)Q(x_1)}{R(x_1)R(x_2)} , \\ P(u) &= 1 - u^3 , \quad Q(u) = 1 + lu^{20} , \quad R(u) = u^3 + ku^{20} . \end{aligned} \quad (5.4.2)$$

The boundaries of the regions are defined by polynomial equations for x_1 and x_2 . . The two mass squared conditions and the probability conservation for the first row select a discrete set of parameter combinations.

One might ask whether U and D matrices could correspond to different solutions of these equations for same values of n_{q_i} . This cannot be the case since this would predict too large $u - d$ mass difference.

Orthogonalization conditions for the rows should determine the phases more or less uniquely and could force CP breaking. The requirement that probabilities are rational valued implies that x_1 , x_2 , x and y are rational and poses very strong additional conditions to the solutions. The roots should correspond to very special solutions possessing symmetries so that the solutions of polynomial equations give probabilities as rational numbers. Note however that the solutions of polynomial equations with integer coefficients are in question and the solutions are algebraic numbers: this is enough as far as the p-adicization of the theory is considered.

Maximization of entropy solving constraint equations explicitly

The mass squared conditions allow to express the probabilities p_{ij} in terms of p_{11} and p_{21} (for instance) and this allows a rather concise representation for the solution to the maximization the entropy of topological mixing. The key formulas are following.

$$\begin{aligned} p_{31} &= 1 - p_{11} - p_{12} \ , \\ p_{i2} &= -\frac{n_i}{51} + \frac{20}{17}(1 - p_{i1}) \ , \quad i = 1, 2 \ , \\ p_{i3} &= \frac{n_i}{51} - \frac{3}{17}(1 - p_{i1}) \ , \quad i = 1, 2 \ . \end{aligned} \quad (5.4-3)$$

Expressing entropy directly in terms of p_{11} and p_{21} , the conditions for the maximization of entropy imply the equations

$$\log(p_{ij})X^{ij} = 0 \ , \quad \log(p_{ij})Y^{ij} = 0 \ , \quad (5.4-2)$$

where a summation over repeated indices is carried out. The matrices $X^{ij} = \partial_{p_{11}} p_{ij}$ and $Y^{ij} = \partial_{p_{21}} p_{ij}$ are given by

$$\begin{aligned} X &= \begin{pmatrix} 1 & -\frac{20}{17} & \frac{3}{17} \\ 0 & 0 & 0 \\ -1 & \frac{20}{17} & -\frac{3}{17} \end{pmatrix} \\ Y &= \begin{pmatrix} 0 & 0 & 0 \\ 1 & -\frac{20}{17} & \frac{3}{17} \\ -1 & \frac{20}{17} & -\frac{3}{17} \end{pmatrix} \end{aligned} \quad (5.4-3)$$

The equations can be transformed into the form

$$\prod_{ij} p_{ij}^{X_{ij}} = 1 \ , \quad \prod_{ij} p_{ij}^{Y_{ij}} = 1 \ . \quad (5.4-2)$$

When written explicitly, these equations read as

$$\begin{aligned} \frac{p_{11}}{1-p_{11}-p_{21}} \times \left(\frac{-n_1+60(1-p_{11})}{-n_3+60(p_{11}+p_{21})} \right)^{-20/17} \times \left(\frac{n_1-9(1-p_{11})}{n_3-9(p_{11}+p_{21})} \right)^{3/17} &= 1 \ , \\ \frac{p_{21}}{1-p_{11}-p_{21}} \times \left(\frac{-n_2+60(1-p_{21})}{-n_3+60(p_{11}+p_{21})} \right)^{-20/17} \times \left(\frac{n_2-9(1-p_{21})}{n_3-9(p_{11}+p_{21})} \right)^{3/17} &= 1 \ . \end{aligned} \quad (5.4-2)$$

The equations can be cast into polynomial equations in p_{11} and p_{21} by taking 17:th power of both equations. This gives polynomial equations of degree $d = 17 + 20 + 3 = 40$. The total number of solutions to the equations is at most $40 \times 40 = 1600$. The previous estimate gave upper bound $3 \times 20 \times 20 = 1200$ for the number of solution. It might be that some symmetry is involved and reduces the upper bound by a factor $3/4$.

The solutions can be sought using gradient dynamics in which system in (p_{11}, p_{21}) plane drifts in the force field defined by the gradient ∇S of the entropy $S = -\sum_{ij} p_{ij} \log(p_{ij})$ and ends up to the maximum of S , $S = -\sum_{ij} p_{ij} \log(p_{ij})$.

$$\begin{aligned} \frac{dp_{11}}{dt} &= \partial_{p_{11}} S = -X^{ij} \log(p_{ij}) \quad , \\ \frac{dp_{21}}{dt} &= \partial_{p_{21}} S = -Y^{ij} \log(p_{ij}) \quad , \end{aligned} \tag{5.4.-2}$$

The conditions that the probabilities are positive give the constraints

$$\begin{aligned} 1 - \frac{n_1}{9} &\leq p_{11} \leq 1 - \frac{n_1}{60} \quad , \\ 1 - \frac{n_2}{9} &\leq p_{21} \leq 1 - \frac{n_2}{60} \quad , \\ 0 &\leq p_{21} \leq 1 - p_{11} \quad , \\ \frac{69 - n_1 - n_2}{60} - p_{11} &\leq p_{21} \leq \frac{69 - n_1 - n_2}{9} - p_{11} \end{aligned} \tag{5.4.-5}$$

on the region containing the solutions.

5.4.6 U and D matrices from the knowledge of top quark mass alone?

As already found, a possible resolution to the problems created by top quark is based on the additivity of mass squared so that top quark mass would be about 230 GeV, which indeed corresponds to a peak in mass distribution of top candidate, whereas $t\bar{t}$ meson mass would be 163 GeV. This requires that top quark mass changes very little in topological mixing. It is easy to see that the mass constraints imply that for $n_t = n_b = 60$ the smallness of V_{i3} and $V(3i)$ matrix elements implies that both U and D must be direct sums of 2×2 matrix and 1×1 unit matrix and that V matrix would have also similar decomposition. Therefore $n_b = n_t = 59$ seems to be the only number theoretically acceptable option. The comparison with the predictions with pion mass led to a unique identification $(n_d, n_b, n_s) = (5, 5, 59), (n_u, n_c, n_t) = (4, 6, 59)$.

U and D matrices as perturbations of matrices mixing only the first two genera

This picture suggests that U and D matrices could be seen as small perturbations of very simple U and D matrices satisfying $|U| = |D|$ corresponding to $n = 60$ and having $(n_d, n_b, n_s) = (4, 5, 60), (n_u, n_c, n_t) = (4, 5, 60)$ predicting V matrix characterized by Cabibbo angle alone. For instance, CP breaking parameter would characterize this perturbation. The perturbed matrices should obey thermodynamical constraints and it could be possible to linearize the thermodynamical conditions and in this manner to predict realistic mixing matrices from first principles. The existence of small perturbations yielding acceptable matrices implies also that these matrices be near a point at which two different matrices resulting as a solution to the thermodynamical conditions coincide.

D matrix can be deduced from U matrix since $9|D_{12}|^2 \simeq n_d$ fixes the value of the relative phase of the two terms in the expression of D_{12} .

$$\begin{aligned} |D_{12}|^2 &= |U_{11}V_{12} + U_{12}V_{22}|^2 \\ &= |U_{11}|^2|V_{12}|^2 + |U_{12}|^2|V_{22}|^2 \\ &\quad + 2|U_{11}||V_{12}||U_{12}||V_{22}|\cos(\Psi) = \frac{n_d}{9} \quad , \\ \Psi &= \arg(U_{11}) + \arg(V_{12}) - \arg(U_{12}) - \arg(V_{22}) \quad . \end{aligned} \tag{5.4.-8}$$

Using the values of the moduli of U_{ij} and the approximation $|V_{22}| = 1$ this gives for $\cos(\Psi)$

$$\begin{aligned}
\cos(\Psi) &= \frac{A}{B} , \\
A &= \frac{n_d - n_u}{9} - \frac{9 - n_u}{9} |V_{12}|^2 , \\
B &= \frac{2}{9|V_{12}|} \sqrt{n_u(9 - n_u)} .
\end{aligned} \tag{5.4-9}$$

The experimentation with different values of n_d and n_u shows that $n_u = 6, n_d = 4$ gives $\cos(\Psi) = -1.123$. Of course, $n_u = 6, n_d = 4$ option is not even allowed by $n_t = 60$. For $n_d = 4, n_u = 5$ one has $\cos(\Psi) = -0.5958$. $n_d = 5, n_u = 6$ corresponding to the perturbed solution gives $\cos(\Psi) = -0.6014$.

Hence the initial situation could be $(n_u = 5, n_s = 4, n_b = 60)$, $(n_d = 4, n_s = 5, n_t = 60)$ and the physical U and D matrices result from U and D matrices by a small perturbation as one unit of t (b) mass squared is transferred to u (s) quark and produces symmetry breaking as $(n_d = 5, n_s = 5, n_b = 59)$, $(n_u = 6, n_c = 4, n_t = 59)$.

The unperturbed matrices $|U|$ and $|D|$ would be identical with $|U|$ given by

$$|U_{11}| = |U_{22}| = \frac{2}{3} , \quad |U_{12}| = |U_{21}| = \frac{\sqrt{5}}{3} , \tag{5.4-8}$$

The thermodynamical model allows solutions reducing to a direct sum of 2×2 and 1×1 matrices, and since $|U|$ matrix is fixed completely by the mass constraints, it is trivially consistent with the thermodynamical model.

Direct search of U and D matrices

The general formulas for p^U and p^D in terms of the probabilities p_{11} and p_{21} allow straightforward search for the probability matrices having maximum entropy just by scanning the (p_{11}, p_{21}) plane constrained by the conditions that all probabilities are positive and smaller than 1. In the physically interesting case the solution is sought near a solution for which the non-vanishing probabilities are $p_{11} = p_{22} = (9 - n_1)/9$, $p_{12} = p_{21} = n_1/9$, $p_{33} = 1$, $n_1 = 4$ or 5. The inequalities allow to consider only the values $p_{11} \geq (9 - n_1)/9$.

1. Probability matrices p^U and p^D

The direct search leads to maximally entropic p^D matrix with $(n_d, n_s) = (5, 5)$:

$$p^D = \begin{pmatrix} 0.4982 & 0.4923 & 0.0095 \\ 0.4981 & 0.4924 & 0.0095 \\ 0.0037 & 0.0153 & 0.9810 \end{pmatrix} , \quad p_0^D = \begin{pmatrix} 0.5556 & 0.4444 & 0 \\ 0.4444 & 0.5556 & 0 \\ 0 & 0 & 1 \end{pmatrix} . \tag{5.4-8}$$

p_0^D represents the unperturbed matrix p_0^D with $n(d=4), n_s = 5$ and is included for the purpose of comparison. The entropy $S(p^D) = 1.5603$ is larger than the entropy $S(p_0^D) = 1.3739$. A possible interpretation is in terms of the spontaneous symmetry breaking induced by entropy maximization in presence of constraints.

A maximally entropic p^U matrix with $(n_u, n_c) = (5, 6)$ is given by

$$p^U = \begin{pmatrix} 0.5137 & 0.4741 & 0.0122 \\ 0.4775 & 0.4970 & 0.0254 \\ 0.0088 & 0.0289 & 0.9623 \end{pmatrix} \tag{5.4-8}$$

The value of entropy is $S(p^U) = 1.7246$. There could be also other maxima of entropy but in the range covering almost completely the allowed range of the parameters and in the accuracy used only single maximum appears.

The probabilities p_{ii}^D resp. p_{ii}^U satisfy the constraint $p(i, i) \geq .492$ resp. $p_{ii} \geq .497$ so that the earlier proposal for the solution of proton spin crisis must be given up and the solution discussed in [28] remains the proposal in TGD framework.

2. Near orthogonality of U and D matrices

An interesting question whether U and D matrices can be transformed to approximately orthogonal matrices by a suitable $(U(1) \times U(1))_L \times (U(1) \times U(1))_R$ transformation and whether CP breaking phase appearing in CKM matrix could reflect the small breaking of orthogonality. If this expectation is correct, it should be possible to construct from $|U|$ ($|D|$) an approximately orthogonal matrix by multiplying the matrix elements $|U_{ij}|$, $i, j \in \{2, 3\}$ by appropriate sign factors. A convenient manner to achieve this is to multiply $|U|$ ($|D|$) in an element wise manner $((A \circ B)_{ij} = A_{ij}B_{ij})$ by a sign factor matrix S .

1. In the case of $|U|$ the matrix $U = S \circ |U|$, $S(2, 2) = S(2, 3) = S(3, 2) = -1$, $S_{ij} = 1$ otherwise, is approximately orthogonal as the fact that the matrix $U^T U$ given by

$$U^T U = \begin{pmatrix} 1.0000 & 0.0006 & -0.0075 \\ 0.0006 & 1.0000 & -0.0038 \\ -0.0075 & -0.0038 & 1.0000 \end{pmatrix}$$

is near unit matrix, demonstrates.

2. For D matrix there are two nearly orthogonal variants. For $D = S \circ |D|$, $S(2, 2) = S(2, 3) = S(3, 2) = -1$, $S_{ij} = 1$ otherwise, one has

$$D^T D = \begin{pmatrix} 1.0000 & -0.0075 & 0.0604 \\ -0.0075 & 1.0000 & 0.0143 \\ 0.0604 & 0.0143 & 1.0000 \end{pmatrix} .$$

The choice $D = S \circ D$, $S(2, 2) = S(2, 3) = S(3, 3) = -1$, $S_{ij} = 1$ otherwise, is slightly better

$$D^T D = \begin{pmatrix} 1.0000 & -0.0075 & 0.0604 \\ -0.0075 & 1.0000 & 0.0143 \\ 0.0601 & 0.0143 & 1.0000 \end{pmatrix} .$$

3. The matrices U and D in the standard gauge

Entropy maximization indeed yields probability matrices associated with unitary matrices. 8 phase factors are possible for the matrix elements but only 4 are relevant as far as the unitarity conditions are considered. The vanishing of the inner products between row vectors, gives 6 conditions altogether so that the system seems to be over-determined. The values of the parameters s_1, s_2, s_3 and phase angle δ in the "standard gauge" can be solved in terms of r_{11} and r_{21} .

The requirement that the norms of the parameters c_i are not larger than unity poses non-trivial constraints on the probability matrices. This should be the case since the number of unitarity conditions is 9 whereas probability conservation for columns and rows gives only 5 conditions so that not every probability matrix can define unitary matrix. It would seem that the constraints are satisfied only if the 2 mass squared conditions and 2 conditions from the entropy maximization are equivalent with 4 unitarity conditions so that the number of conditions becomes $5+4=9$. Therefore entropy maximization and mass squared conditions would force the points of complex 9-dimensional space defined by 3×3 matrices to a 9-dimensional surface representing group $U(3)$ so that these conditions would have a group theoretic meaning.

The formulas

$$\begin{aligned} r_{i2} &= \sqrt{\left[-\frac{n_i}{51} + \frac{20}{17}(1 - r_{i1}^2)\right]} , \\ r_{i3} &= \sqrt{\left[\frac{n_i}{51} - \frac{3}{17}(1 - r_{i1}^2)\right]} . \end{aligned} \tag{5.4.-8}$$

and

$$U = \begin{bmatrix} c_1 & s_1 c_3 & s_1 s_3 \\ -s_1 c_2 & c_1 c_2 c_3 - s_2 s_3 \exp(i\delta) & c_1 c_2 s_3 + s_2 c_3 \exp(i\delta) \\ -s_1 s_2 & c_1 s_2 c_3 + c_2 s_3 \exp(i\delta) & c_1 s_2 s_3 - c_2 c_3 \exp(i\delta) \end{bmatrix} \quad (5.4-7)$$

give

$$\begin{aligned} c_1 &= r_{11} \quad , \quad c_2 = \frac{r_{21}}{\sqrt{1-r_{11}^2}} \quad , \\ s_3 &= \frac{r_{13}}{\sqrt{1-r_{11}^2}} \quad , \quad \cos(\delta) = \frac{c_1^2 c_2^2 c_3^2 + s_2^2 s_3^2 - r_{22}^2}{2c_1 c_2 c_3 s_2 s_3} \quad . \end{aligned} \quad (5.4-6)$$

Preliminary calculations show that for $n_1 = n_2 = 5$ case the matrix of moduli allows a continuation to a unitary matrix but that for $n_1 = 4, n_2 = 6$ the value of $\cos(\delta)$ is larger than one. This would suggest that unitarity indeed gives additional constraints on the integers n_i . The unitary (in the numerical accuracy used) $(n_d, n_s) = (5, 5)$ D matrix is given by

$$D = \begin{pmatrix} 0.7059 & 0.7016 & 0.0975 \\ -0.7057 & 0.7017 - 0.0106i & 0.0599 + 0.0766i \\ -0.0608 & 0.0005 + 0.1235i & 0.4366 - 0.8890i \end{pmatrix} .$$

The unitarity of this matrix supports the view that for certain integers n_i the mass squared conditions and entropy maximization reduce to group theoretic conditions. The numerical experimentation shows that the necessary condition for the unitarity is $n_1 > 4$ for $n_2 < 9$ whereas for $n_2 \geq 9$ the unitarity is achieved also for $n_1 = 4$.

Direct search for CKM matrices

The standard gauge in which the first row and first column of unitary matrix are real provides a convenient representation for the topological mixing matrices: it is convenient to refer to these representations as U_0 and D_0 . The possibility to multiply the rows of U_0 and D_0 by phase factors ($U(1) \times U(1)$) $_R$ transformations) provides 2 independent phases affecting the values of $|V|$. The phases $\exp(i\phi_j)$, $j = 2, 3$ multiplying the second and third row of D_0 can be estimated from the matrix elements of $|V|$, say from the elements $|V_{11}| = \cos(\theta_c) \equiv v_{11}$, $\sin\theta_c = .226 \pm .002$ and $|V_{31}| = (9.6 \pm .9) \cdot 10^{-3} \equiv v_{31}$. Hence the model would predict two parameters of the CKM matrix, say s_3 and δ_{CP} , in its standard representation.

The fact that the existing empirical bounds on the matrix elements of V are based on the standard model physics raises the question about how seriously they should be taken. The possible existence of fractally scaled up versions of light quarks could effectively reduce the matrix elements for the electro-weak decays $b \rightarrow c + W$, $b \rightarrow u + W$ resp. $t \rightarrow s + W$, $t \rightarrow d + W$ since the decays involving scaled up versions of light quarks can be counted as decays $W \rightarrow bc$ resp. $W \rightarrow tb$. This would favor too small experimental estimates for the matrix elements V_{i3} and V_{3i} , $i = 1, 2$. In particular, the matrix element $V_{31} = V_{td}$ could be larger than the accepted value.

Various constraints do not leave much freedom to choose the parameters n_{q_i} . The preliminary numerical experimentation shows that the choice $(n_d, n_s) = (5, 5)$ and $(n_u, n_c) = (5, 6)$ yields realistic U and D matrices. In particular, the conditions $|U(1, 1)| > .7$ and $|D(1, 1)| > .7$ hold true and mean that the original proposal for the solution of spin puzzle of proton must be given up. In [28] an alternative proposal based on more recent findings is discussed. Only for this choice reasonably realistic CKM matrices have been found.

1. The requirement that the parameters $|V_{11}|$ (or equivalently, Cabibbo angle and $|V_{31}|$) are produced correctly, yields CKM matrices for which CP breaking parameter J is roughly one half of its accepted value. The matrix elements $V_{23} \equiv V_{cb}$, $V_{32} \equiv V_{tc}$, and $V_{13} \equiv V_{ub}$ are roughly twice their accepted value. This suggests that the condition on V_{31} should be loosened.
2. The following tables summarize the results of the search requiring that
 - i) the value of the Cabibbo angle s_{Cab} is within the experimental limits $s_{Cab} = .223 \pm .002$,
 - ii) $V_{31} = (9.6 \pm .9) \cdot 10^{-3}$, is allowed to have value at most twice its upper bound,

iii) V_{13} whose upper bound is determined by probability conservation, is within the experimental limits $.42 \cdot 10^{-3} < |V_{ub}| < 6.98 \cdot 10^{-3}$ whereas $V_{23} \simeq 4 \times 10^{-3}$ should come out as a prediction, iv) the CP breaking parameter satisfies the condition $|(J - J_0)/J_0| < .6$, where $J_0 = 10^{-4}$ represents the lower bound for J (the experimental bounds for J are $J \times 10^4 \in (1 - 1.7)$).

The pairs of the phase angles (ϕ_1, ϕ_2) defining the phases ($\exp(i\phi_1), \exp(i\phi_2)$) are listed below

$$\begin{array}{l}
 \text{class 1: } \begin{array}{ccccc} \phi_1 & 0.1005 & 0.1005 & 4.8129 & 4.8129 \\ \phi_2 & 0.0754 & 1.4828 & 4.7878 & 6.1952 \end{array} \\
 \text{class 2: } \begin{array}{ccccc} \phi_1 & 0.1005 & 0.1005 & 4.8129 & 4.8129 \\ \phi_2 & 2.3122 & 5.5292 & 0.7414 & 3.9584 \end{array}
 \end{array} \tag{5.4.-6}$$

The phase angle pairs correspond to two different classes of U , D , and V matrices. The U , D and V matrices inside each class are identical at least up to 11 digits(!). Very probably the phase angle pairs are related by some kind of symmetry.

The values of the fitted parameters for the two classes are given by

$$\begin{array}{l}
 \begin{array}{cccc} & |V_{11}| & |V_{31}| & |V_{13}| & J/10^{-4} \\
 \text{class 1} & 0.9740 & 0.0157 & 0.0069 & .93953 \\
 \text{class 2} & 0.9740 & 0.0164 & 0.0067 & 1.0267 \end{array}
 \end{array}$$

V_{31} is predicted to be about 1.6 times larger than the experimental upper bound and for both classes V_{23} and V_{32} are roughly too times too large. Otherwise the fit is consistent with the experimental limits for class 2. For class 1 the CP breaking parameter is 7 per cent below the experimental lower bound. In fact, the value of J is fixed already by the constraints on V_{31} and V_{11} and reduces by a factor of one half if V_{31} is required to be within its experimental limits.

U , D and $|V|$ matrices for class 1 are given by

$$\begin{array}{l}
 U = \begin{bmatrix} 0.7167 & 0.6885 & 0.1105 \\ -0.6910 & 0.7047 - 0.0210i & 0.0909 + 0.1310i \\ -0.0938 & 0.0696 + 0.1550i & 0.1747 - 0.9653i \end{bmatrix} \\
 D = \begin{bmatrix} 0.7059 & 0.7016 & 0.0975 \\ -0.6347 - 0.3085i & 0.6358 + 0.2972i & 0.0203 + 0.0951i \\ -0.0587 - 0.0159i & -0.0317 + 0.1194i & 0.6534 - 0.7444i \end{bmatrix} \\
 |V| = \begin{bmatrix} 0.9740 & 0.2265 & 0.0069 \\ 0.2261 & 0.9703 & 0.0862 \\ 0.0157 & 0.0850 & 0.9963 \end{bmatrix}
 \end{array} \tag{5.4.-8}$$

U , D and $|V|$ matrices for class 2 are given by

$$\begin{array}{l}
 U = \begin{bmatrix} 0.7167 & 0.6885 & 0.1105 \\ -0.6910 & 0.7047 - 0.0210i & 0.0909 + 0.1310i \\ -0.0938 & 0.0696 + 0.1550i & 0.1747 - 0.9653i \end{bmatrix} \\
 D = \begin{bmatrix} 0.7059 & 0.7016 & 0.0975 \\ -0.6347 - 0.3085i & 0.6358 + 0.2972i & 0.0203 + 0.0951i \\ -0.0589 - 0.0151i & -0.0302 + 0.1198i & 0.6440 - 0.7525i \end{bmatrix} \\
 |V| = \begin{bmatrix} 0.9740 & 0.2265 & 0.0067 \\ 0.2260 & 0.9704 & 0.0851 \\ 0.0164 & 0.0838 & 0.9963 \end{bmatrix}
 \end{array} \tag{5.4.-10}$$

What raises worries is that the values of $|V_{23}| = |V_{cb}|$ and $|V_{32}| = |V_{ts}|$ are roughly twice their experimental estimates. This, as well as the discrepancy related to V_{31} , might be understood in terms of the electro-weak decays of b and t to scaled up quarks causing a reduction of the branching ratios

$b \rightarrow c + W$, $t \rightarrow s + W$ and $t \rightarrow t + d$. The attempts to find more successful integer combinations n_i has failed hitherto. The model for pseudoscalar meson masses, the predicted relatively small masses of light quarks, and the explanation for $t\bar{t}$ meson mass supports this mixing scenario.

5.5 Hadron masses

Besides the quark contributions already discussed, hadron mass squared can contain several other contributions and the task is to find a model allowing to identify and estimate these contributions. There are several guidelines for the numerical experimentation.

1. Conformal weight, that is mass squared, is assumed to be additive for quarks corresponding to the same p-adic prime. For instance, in case of $q\bar{q}$ mesons the mass would be $\sqrt{2}m(q)$ and the contribution of $k = 113$ u, d, s quarks to nucleon mass would be $< \sqrt{3} \times 100$ MeV and thus surprisingly small. For cd meson quark masses would be additive.
2. Old fashioned quark model explains reasonably well hadron masses in terms of constituent quark masses. Effective 2-dimensionality of partons suggests an interpretation for the constituent quark as a composite structure formed by the current quark identified as a partonic 2-surface X^2 characterized by $k(q)$ and by join along boundaries bond, kind of a gluonic "rubber band" characterized by $k = 107$ and connecting X^2 to the $k = 107$ hadronic 2-surface $X^2(H)$ representing hadron. $X^2(q_i)$ could be perhaps regarded as a hole in $k = k(q)$ 3-surface. The 2-dimensional visualization for a 3-dimensional topological condensation would become much more than a mere visualization. This view about hadrons brings in mind unavoidably the surreal 2-dimensional structures formed by organs like retina. Of course, effective 2-dimensionality allows to characterize the entire Universe as an extremely complex fractal 2-surface.

The large mass of the constituent quark would be due to the color Coulombic and spin-spin interaction conformal weights of join along boundaries bond. Quark mass and the mass due to the color interaction conformal weight would be additive unless $k = 107$ for the quark (it seems that for η' this is indeed the case!). Classical color gauge fluxes would flow between $k = 107$ and $k \neq 107$ space-time sheets along the bonds. Color dynamics would take place at $k = 107$ space-time sheet in the sense that color gauge flux between quarks q_1 and q_2 flows first from $X^2(k(q_1))$ to the hadronic 2-surface $X^2(k = 107)$ and then back to $X^2(k(q_2))$. The induced Kähler field is always accompanied by a classical color gauge field and the classical color gauge flux would represent non-perturbative aspects of color interactions at space-time level.

3. A crucial observation is that the mass of η meson is rather precisely 4 times the pion mass whereas the mass of its spin excited companion ω is very nearly the same as the mass of ρ meson. This suggests that u, d quarks correspond to $k = 109$ inside η but to $k = 113$ inside ω . This inspires the idea that the p-adic mass scale of quarks is dynamical and sensitive to small perturbations as the fact that for CP_2 type extremals the operators corresponding to different p-adic primes reduce to one and same operator forces to suspect. If k characterizes the length scale associated with the elementary particle horizon as \sqrt{k} multiple of CP_2 length scale, quark mass would be characterized by the size of elementary particle horizon sensitive to the dynamics in hadronic mass scale.

The physical states would result as small perturbations of this degenerate ground state and the value of $k(q)$ would be sensitive to the perturbation. A rather nice fit for meson and baryon masses results by assuming that the p-adic length scale of the quark is dynamical.

4. In the case of pseudoscalar mesons the scaled up versions of light quarks identifiable as constituent quarks, turn out to explain almost all of the pseudo scalar meson mass, and this inspires a new formulation for the old vision about pseudoscalar mesons as Goldstone bosons. At least light pseudoscalar mesons are Goldstone bosons in the sense that the color Coulombic and spin-spin interaction energies cancel in a good approximation so that quarks at $k \neq 107$ space-time sheets are responsible for most of the meson mass. The assumption that only $k(s)$ is dynamical for light baryons is enough to understand the mass differences between baryons having different numbers of strange quarks.

5. Color magnetic spin-spin interaction energies are indeed surprisingly constant among baryons. Also for mesons spin-spin interaction energies vary much less than the scaling of quark masses would predict on basis of QCD formula. This motivates the replacement of the interaction energy with interaction conformal weight in the case of color interactions. The interaction conformal weight is assignable to $k = 107$ space-time sheet, and the fact that spin-spin splittings of also heavy hadrons can be measured in few hundred MeVs, supports this identification. The mild dependence of color Coulombic conformal weight and spin-spin interaction conformal weight on hadron would be due to their dependence on the primes $k(q_i)$ and $k = 107$ characterizing space-time sheets connected by the the color bonds $q_i \rightarrow 107$ and $107 \rightarrow q_j$.
6. The values for the parameters s_{ij}^c and S_{ij} characterizing color Coulombic and color magnetic interaction conformal weights can be deduced from the mass squared differences for hadrons and assuming definite values for the parameters $k(q_i)$ characterizing quark masses. It seems that no other sources to meson mass (or at least pion mass) are needed.
7. In the case of nucleons the understanding of nucleon mass requires a large additional contribution about 780 MeV since quarks contribute only about 160 MeV to the mass of nucleon. This contribution can be assumed to be same for all baryons as the possibility to understand baryon mass differences in terms of quark masses demonstrates. The most plausible identification of this contribution is in terms of 2- or 3-particle state formed by super-symplectic gluons assignable to $k = 107$ hadronic space-time sheet and having conformal weight $s = 16$ corresponding to mass 934.2 MeV (rather near to nucleon mass and η' mass). This leads to a vision about non-perturbative aspects of color interactions and allows to understand baryon masses with accuracy better than one per cent. Also a connection with hadronic string model emerges and hadronic string tension is predicted correctly.

5.5.1 The definition of the model for hadron masses

The defining assumptions of the model of hadron masses are following. CP_2 mass defines the overall elementary particle mass scale. Electron mass determines this mass only in certain limits.

Model for hadronic quarks

The numerical construction of U and D matrices using the thermodynamical model for the topological mixing justifies the assumptions $n_d = n_s = 5, n_b = 59$ and $n_u = 5, n_c = 6, n_t = 58$.

Quarks can appear both as free quarks and bound state quarks and the value of $k(q)$ is in general different for free and bound state quarks and can depend on hadron in case of bound state quarks. This allows to understand satisfactorily the masses of low lying hadrons.

Quark mass contribution to the mass of the hadron

Quark mass squared is p-adically additive for quarks with same value of p-adic prime. In the case of meson one has

$$m_M^2(p_1 = p_2) = m_{q_1}^2 + m_{q_2}^2 . \quad (5.5.1)$$

m_q denotes constituent quark mass which is larger than current quark mass due to the smaller value of k .

Masses are additive for different values of p .

$$m_M(p_1 \neq p_2) = m_{q_1} + m_{q_2} . \quad (5.5.2)$$

The generalization of these formulas to the case of baryons is trivial.

Super-symplectic gluons and non-perturbative aspects of hadron physics

At least in the case of light pseudoscalar mesons the contribution of quark masses to the mass squared of meson dominates whereas spin 1 mesons contain a large contribution identified as color interaction conformal weight (color magnetic spin-spin interaction conformal weight and color Coulombic conformal weight). This conformal weight cannot however correspond to the ordinary color interactions alone and is negative for pseudoscalars and compensated by some unknown contribution in the case of pion in order to avoid tachyonic mass. Quite generally this realizes the idea about light pseudoscalar mesons as Goldstone bosons. Analogous mass formulas hold for baryons but in this case the additional contribution which dominates.

The unknown contribution can be assigned to the $k = 107$ hadronic space-time sheet and must correspond to the non-perturbative aspects of QCD and the failure of the quantum field theory approach at low energies. In TGD the failure of QFT picture corresponds to the presence of configuration space degrees of freedom ("world of classical worlds") in which super-symplectic algebra acts. The failure of the approximation assuming single fixed background space-time is in question.

The purely bosonic generators carry color and spin quantum numbers: spin has however the character of orbital angular momentum. The only electro-weak quantum numbers of super-generators are those of right-handed neutrino. If the super-generators degrees carry the quark spin at high energies, a solution of proton spin puzzle emerges [20].

The presence of these degrees of freedom means that there are two contributions to color interaction energies corresponding to the ordinary gluon exchanges and exchanges of super-symplectic gluons. For $g = 0$ these gluons are massless and in absence of topological mixing could form a contribution analogous to sea or Bose-Einstein condensate. For $g = 1$ their mass can be calculated. It turns out the model assuming same topological mixing as in case of U quarks leads to excellent understanding of baryon masses assuming that hadron spin correlates with the super-symplectic particle content of the hadronic space-time sheet.

Top quark mass as a fundamental constraint

CP_2 mass is an important parameter of the model. The vanishing second order contribution to electron mass gives an upper bound for CP_2 mass. The bound $Y_e \leq .7357$ can be derived from the requirement that it is possible to reproduce τ mass in p-adic thermodynamics. Maximal second order contribution corresponds to a minimal CP_2 mass reduced by a factor $\sqrt{5/6} = .9129$ from its maximal value. There is a natural mechanism making second order contribution negligible. Leptonic masses tend to be predicted to be few per cent too high [26] if the second order contribution from p-adic thermodynamics to the electron mass vanishes, which suggests that second order contribution might be there.

For $Y_e = 0$ and $Y_t = 1$ the most recent experimental best estimate 169.1 GeV [46] for top quark mass is reproduced exactly. Even $Y_t = 0$ allows a prediction in the allowed range. For too large Y_e top quark mass is predicted to be too small unless one allows first order Higgs contribution to the top quark mass. This means that CP_2 mass can be scaled down from its maximal value at most 2.5 per cent. This translates to the condition $Y_e < .26$. It is possible to understand quark masses satisfactorily by assuming that Higgs contribution is second order p-adically and even negligible. In fact, there are good arguments suggesting that Higgs does not develop vacuum expectation at fermionic space-time sheets [26]. If this is the case, top quark mass gives a very strong constraint to the model.

The super-symplectic color interactions associated with $k = 107$ space-time sheet give rise to the dominant reduction of the color conformal weight having interpretation in terms of color magnetic and electric conformal weights. Canonical correspondence implies that this contribution is always non-negative. Therefore the simple additive formula can lead to a situation in which the contribution of quarks to the meson mass can be slightly larger than meson mass and it is not obvious whether it is possible to reduce this contribution by any means since the reduction of CP_2 mass scale makes top quark mass too small.

For diagonal mesons for which quarks have the same value of p-adic prime, ordinary color interaction between quarks can contribute negative conformal weight reducing the contribution to the mass squared. In the case of non-diagonal mesons it is not clear whether this kind of color interaction exists. This kind of gluons would correspond to pairs of light-like partonic 3-surfaces for which throats correspond to different values of p-adic prime p . These are in principle possible but could couple weakly

to matter. It seems that the parameters of the model, essentially CP_2 mass scale strongly constrained by the top quark mass, allow the quark contributions of non-diagonal mesons to be below the mass of the meson.

The fact that standard QCD model for color binding energies works rather well for heavy mesons suggests that the notion of negative color binding energy might make sense and could explain the discrepancy. The mixing of real and p-adic physics descriptions is however aesthetically very unappealing but might be the only way out of the problem. The p-adic counterpart of this description in case of heavy diagonal mesons would be based on the introduction of a negative color Coulombic contribution to the the conformal weight of quark pair.

Smallness of isospin splittings

The smallness of isospin splittings inside $I_s = 1/2$ doublets poses an further constraint. $d_{113} - u_{113}$ mass difference is about $\Delta m_{d-u} = 13$ MeV and larger than typical isospin splitting. The repulsive Coulomb interaction between quarks typically tends to reduce the mass differences due to Δm_{d-u} and the the sign of Δm_{d-u} explains the "wrong" sign of n-p mass difference equal to $\Delta m_{n-p} = 1.3$ MeV. Non-diagonal hadrons containing scaled up u and d quarks would have anomalously large isospin splittings. On the other hand, for a diagonal meson containing b quark and scaled up u and d quark isospin splitting is proportional to $(m_d^2 - m_u^2)/m_b$ and small. B meson corresponds to this kind of situation.

5.5.2 The anatomy of hadronic space-time sheet

Although the presence of the hadronic space-time sheet having $k = 107$ has been obvious from the beginning, the questions about its anatomy emerged only quite recently after the vision about the spectrum of Kähler coupling strength had emerged [26, 20].

In the case of pseudoscalar mesons quarks give the dominating contribution to the meson mass. This is not true for spin 1/2 baryons and the dominating contribution must have some other origin. TGD allows to identify this contribution in terms of states created by purely bosonic generators of super-symplectic algebra and having as a space-time correlate CP_2 type vacuum extremals topologically condensed at $k = 107$ hadronic space-time sheet (or having this space-time sheet as field body). Proton and neutron masses are predicted with .5 per cent accuracy and $\Delta - N$ mass splitting with .6 per cent accuracy. A further outcome is a possible solution to the spin puzzle of proton proposed already earlier [20].

Quark contribution cannot dominate light baryon mass

The first guess would be that the masses give dominating contribution to the mass of baryon. Since mass squared is additive, this would require rather large quark masses for proton and neutron. $k(d) = k(u) = k(s) = 108$ would give $(m(d), m(u), m(s)) = (571.3, 520.4, 616.6)$ MeV and $(m(n), m(p)) = (961.1, 931.7)$ MeV to be compared with the actual masses $(m(n), m(p)) = (939.6, 938.3)$ MeV. The difference looks too large to be explainable in terms of Coulombic self-interaction energy. $\lambda - n$ mass splitting would be 27.6 MeV for $k(s) = 108$ which is much smaller than the real mass splitting 176.0 MeV. For $k(s) = 110$ one would have 120.0 MeV.

Does $k = 107$ hadronic space-time sheet give the large contribution to baryon mass?

In the sigma model for baryons the dominating contribution to the mass of baryon results as a vacuum expectation value of scalar field and light pseudoscalar mesons are analogous to Goldstone bosons whose masses are basically due to the masses of light quarks.

This would suggest that $k = 107$ gluonic/hadronic space-time sheet gives a large contribution to the mass squared of baryon. p-Adic thermodynamics allows to expect that the contribution to the mass squared is in a good approximation of form

$$\Delta m^2 = nm^2(107) ,$$

where $m^2(107)$ is the minimum possible p-adic mass mass squared and n a positive integer. One has $m(107) = 2^{10}m(127) = 2^{10}m_e/\sqrt{5} = 233.55$ MeV for $Y_e = 0$ favored by the top quark mass.

1. $n = 11$ predicts $(m(n), m(p)) = (944.5, 939.3)$ MeV for $k = 113$ quarks: the actual masses are $(m(n), m(p)) = (939.6, 938.3)$ MeV. Coulombic repulsion between u quarks could reduce the p-n difference to a realistic value.
2. $\lambda - n$ mass splitting would be 184.7 MeV for $k(s) = 111$ to be compared with the real difference which is 176.0 MeV. Note however that color magnetic spin-spin splitting requires that the ground state mass squared is larger than $11m_0^2(107)$.

What is responsible for the large ground state mass of the baryon?

The observations made above do not leave much room for alternative models. The basic problem is the identification of the large contribution to the mass squared coming from the hadronic space-time sheet with $k = 107$. This contribution could have the energy of classical color field as a space-time correlate.

1. The assignment of the energy to the vacuum expectation value of sigma boson does not look very promising since the very existence sigma boson is questionable and it does not relate naturally to classical color gauge fields. More generally, since no gauge symmetry breaking is involved, the counterpart of Higgs mechanism as a development of a coherent state of scalar bosons does not look a plausible idea.
2. One can however consider the possibility of a Bose-Einstein condensate or of a more general many-particle state of massive bosons possibly carrying color quantum numbers. A many-boson state of exotic bosons at $k = 107$ space-time sheet having net mass squared

$$m^2 = nm_0^2(107) \quad , \quad n = \sum_i n_i$$

could explain the baryonic ground state mass. Note that the possible values of n_i are predicted by p-adic thermodynamics with $T_p = 1$.

Glueballs cannot be in question

Glueballs [32, 43] define the first candidate for the exotic boson in question. There are however several objections against this idea.

1. QCD predicts that lightest glue-balls consisting of two gluons have $J^{PC} = 0^{++}$ and 2^{++} and have mass 1650 MeV [43]. If one takes QCD seriously, one must exclude this option. One can also argue that light glue balls should have been observed long ago and wonder why their Bose-Einstein condensate is not associated with mesons.
2. There are also theoretical objections in TGD framework.
 - i) Can one really apply p-adic thermodynamics to the bound states of gluons? Even if this is possible, can one assume the p-adic temperature $T_p = 1$ for them if $T_p < 1$ holds true for gauge bosons consisting of fermion-antifermion pairs [20, 26].
 - ii) Baryons are fermions and one can argue that they must correspond to single space-time sheet rather than a pair of positive and negative energy space-time sheets required by the glueball Bose-Einstein condensate realized as wormhole contacts connecting these space-time sheets. This argument should be taken with a big grain of salt.

Do exotic colored bosons give rise to the ground state mass of baryon?

The objections listed above lead to an identification of bosons responsible for the ground state mass, which looks much more promising.

1. Super-symplectic gluons

TGD predicts exotic bosons and their super-conformal partners. The bosons created by the purely bosonic part of super-symplectic algebra [22, 33], whose generators belong to the representations of the color group and 3-D rotation group but have vanishing electro-weak quantum numbers. Their

spin is analogous to orbital angular momentum whereas the spin of ordinary gauge bosons reduces to fermionic spin. The super-partners of the super-symplectic bosons have quantum numbers of a right handed neutrino and have no electro-weak couplings. Recall that super-symplectic algebra is crucial for the construction of configuration space Kähler geometry.

Exotic bosons are single-sheeted structures meaning that they correspond to a single wormhole throat associated with a CP_2 type vacuum extremal. The assignment of these bosons to hadronic space-time is an attractive idea. The only contribution to the mass would come from the genus and $g = 0$ state would be massless in absence of topological mixing. In this case $g = 0$ bosons could condense on the ground state and define the analog of gluonic contribution to the parton sea. If they mix situation changes.

$g = 1$ unmixed super-symplectic boson would have mass squared $9m_0^2(k)$ (mass would be 700.7 MeV). For a ground state containing two $g = 1$ exotic bosons, one would have ground state mass squared $M_0^2 = 18m_0^2$ corresponding to $(m(n), m(p)) = (1160.8, 1155.6)$ MeV. Negative color Coulombic conformal and color magnetic spin-spin splitting can reduce the mass of system as well as. Electromagnetic Coulomb interaction energy can reduce the p-n mass splitting to a realistic value.

1. Color magnetic spin-spin splitting for baryons gives a test for this hypothesis. The splitting of the conformal weight is by group theoretic arguments of the same general form as that of color magnetic energy and given by $(m^2(N), m^2(\Delta)) = (18m_0^2 - X, 18m_0^2 + X)$ in absence of topological mixing. $n = 11$ for nucleon mass implies $X = 7$ and $m(\Delta) = 5m_0(107) = 1338$ MeV to be compared with the actual mass $m(\Delta) = 1232$ MeV. The prediction is too large by about 8.6 per cent.

If one allows negative color Coulombic conformal weight $\Delta s = -2$ the mass squared reduces by 2 units. The alternative is topological mixing one can have $m^2 = 8m_0^2$ instead of $9m_0^2$. This gives $m(\Delta) = 1240$ MeV so that the error is only .6 per cent. The mass of topologically mixed exotic boson would be 660.6 MeV and equals to m_{104} . Amusingly, $k = 104$ happens to corresponds to the inverse of α_K for gauge bosons.

2. One must consider also the possibility that super-symplectic gluons suffer topological mixing identical with that suffered by say U type quarks in which the conformal weights would be (5,6,58) for the three lowest generations. The ground state of baryon could consist of 2 gluons of lowest generation and one gluon of second generation ($5 + 5 + 6 = 16$). If mixing is same as for D type quarks with weights (5,5,59), one can have only $s = 15$ state. It turns out that this option allows to predict hadron masses with amazing precision if one assumes correlation between hadron spin and its super-symplectic particle content.
3. The conclusion is that a many-particle state of super-symplectic bosons could be responsible for the ground state mass of baryon. Also the baryonic spin puzzle caused by the fact that quarks give only a small contribution to the spin of baryons, could find a natural solution since these bosons could give to the spin of baryon an angular momentum like contribution having nothing to do with the angular momentum of quarks.

2. A connection with hadronic string model

Hadronic string model provides a phenomenological description of the non-perturbative aspects of hadron physics, and TGD was born also as a generalization of the hadronic string model. Hence one can ask whether something resembling hadronic string model might emerge from the super-symplectic sector. TGD allows string like objects but the fundamental string tension is gigantic, roughly a factor 10^{-8} of that defined by Planck constant. The hypothesis motivated by the p-adic length scale hypothesis is that vacuum extremals deformed to non-vacuum extremals give to a hierarchy of string like structures with string tension $T \propto 1/L_p^2$, L_p the p-adic length scale. The challenge has been the identification of quantum counterpart of this picture.

The fundamental mass formula of the string model relates mass squared and angular momentum of the stringy state. It has the form

$$M^2 = kJ, \quad k \simeq .9 \text{ GeV}^2. \quad (5.5.3)$$

A more general formula is $M^2 = kn$.

This kind of formula results from the additivity of the conformal weight (and thus mass squared) if one constructs a many particle state from $g = 1$ super-symplectic bosons with a thermal mass squared $M^2 = M_0^2 n$, $M_0^2 = n_0 m_{107}^2$. The angular momentum of the building blocks has some spectrum fixed by Virasoro conditions. If the basic building block has angular momentum J_0 and mass squared M_0^2 , one obtains $M^2 = M_0^2 J$, $k = M_0^2$, $J = nJ_0$. The values of n are even in old fashioned string model for a Regge trajectory with a fixed parity. $J_0 = 2$ implies the same result so that basic unit might be called "strong graviton".

One can consider several candidates for the values of n_0 . In the absence of topological mixing one has $n_0 = 9$ for super-symplectic gluons. The bound state of two super-symplectic $g = 1$ bosons with mass squared $M_0^2 = 16m_{107}^2$ (two units of color binding conformal weight) could be responsible for the ground state mass of baryons. If topological mixing occurs and is same as for U type quarks then also a bound state of 2 gluons of first generation and 1 gluon of second generation gives $M_0^2 = 16m_{107}^2$.

The table below summarizes the prediction for the string tension in various cases. The identification of the basic excitations as many-particle states from bound states of super-symplectic gluons with $M_0^2 = 16m_{107}^2$ predicts the nominal value of the .9 GeV with 3 per cent accuracy.

n_0	5	9	16	18
M_0^2/GeV^2	.273	.490	0.872	0.982

Table 6. The prediction for the hadronic string tension for some values of the mass squared of super-symplectic particle used to construct hadronic excitations.

Pomeron [72] represented an anomaly of the hadronic string model as a hadron like particle which was not accompanied by a Regge trajectory. A natural interpretation would be as a space-time sheet containing valence quarks as a structure connected by color flux tubes to single structure. There is recent quite direct experimental evidence for the existence of Pomeron [63, 107, 92] in proton photon collisions: Pomeron seems to leave the hadronic space-time sheet for a moment and collide with photon after which it topologically condenses back to the hadronic space-time sheet. For a more detailed discussion see [20].

This picture allows also to consider a possible mechanism explaining spin puzzle of proton and I have already earlier considered an explanation in terms of super-symplectic spin [20] assuming that state is superposition of ordinary ($J = 0, J_q = 1/2$) state and ($J = 2, J_q = 3/2$) state in which super-symplectic bound state has spin 2.

3. Some implications

If one accepts this picture, it becomes possible to derive general mass formulas also for the baryons of scaled up copies of QCD possibly associated with various Mersenne primes and Gaussian Mersennes. In particular, the mass formulas for leptobaryons, in particular "electro-baryons", can be deduced [24]. Good estimates for the masses of the mesons and baryons of M_{89} hadron physics are also obtained by simple scaling of the ordinary hadron masses by factor 512. Scaled up isospin splittings would be one signature of M_{89} hadron physics: for instance, n-p splitting of 1.3 MeV would scale up to 665.6 MeV.

What about mesons?

The original short-lived belief was that only baryons are accompanied by a pair of super-symplectic bosons condensed at hadronic $k = 107$ space-time sheet. By noticing that color magnetic spin-spin splitting requires an additional contribution to the mass conformal weight of meson cancelled by spin-spin splitting conformal weight in the case of pseudoscalar mesons to first order in p , one ends up with the conclusion that also mesons could possess the hadronic space-time sheet.

It however turns out that the contribution of super-symplectic massive boson is necessarily only in the case of $\pi - \rho$ system and produces mere nuisance in the case of heavier mesons. The special role of $\pi - \rho$ system could be understood in terms of color confinement which would make pion $k = 107$ tachyon without the presence of additional mass squared.

The super-symplectic contribution must correspond to a conformal weight of 5 units in the case of pion and thus to *single* super-symplectic boson with $m^2 = 5m_{107}^2$ instead of $9m_{107}^2$ as for $g = 1$ super-symplectic bosons. A possible interpretation is in terms of $g = 0$ boson which has suffered a topological mixing. That 5 units of conformal weight result also in the topological mixing of u and d quarks supports this option and forces to ask whether also super-symplectic topological mixing is

same inside baryons and mesons. If it is same for U type quarks and super-symplectic bosons one has $(s_1, s_2, s_3) = (5, 6, 58)$ for the super-symplectic gluons. As noticed, $S_{SC} = 16$ for baryons is obtained if one has a bound state of 2 bosons of first generation and one boson of second generation giving $s_{SC} = 5 + 5 + 6 = 16$. One can wonder how tightly the super-symplectic gluons are associated with baryonic valence quarks.

5.5.3 Pseudoscalar meson masses

The requirement that all contributions to the meson masses have p-adic origin allows to fix the model uniquely and also constraints on the value of the parameter Y_e emerge. In the following only pseudoscalar mesons will be considered.

Light pseudoscalar mesons as analogs of Goldstone bosons

Fractally scaled up versions of light quarks allow a rather simple model for hadron masses. In the old fashioned $SU(3)$ based quark model η meson is regarded as a combination $u\bar{u} + d\bar{d} - 2s\bar{s}$. The basic observation is that η mass is rather precisely 4 times the mass of π whereas the mass of ω is very near to ρ mass. This suggests that η results by a fractal scaling of quark masses obtained by the replacement $k(q) = 113 \rightarrow 109$ for the quarks appearing in η . This inspires the idea that mesonic quarks are scaled up variants of light quarks and at least light pseudoscalar mesons are almost Goldstone bosons in the sense that quark contribution to the mass is as large as possible but smaller than meson mass. This idea must of course be taken as an interesting ansatz and in the end of the chapter it will be found that this idea might work only in the case of pion and kaon systems.

Quark contributions to meson masses

The following table summarizes the predictions for quark contributions to the masses of mesons assuming $k(q)$ depending on meson and assuming $Y_e = 0$ guaranteeing maximum value of top quark mass.

Meson	scaled quarks	$m_q(M)/MeV$	m_{exp}/MeV
π^0	d_{113}, u_{113}	140.0	135.0
π^+	d_{113}, u_{113}	140.0	139.6
K^0	d_{114}, s_{109}	495.5	497.7
K^+	u_{114}, s_{109}	486.3	493.7
η	$u_{109}, d_{109}, s_{109}$	522.2	548.9
η'	$u_{107}, d_{107}, s_{107}, c_{107}$	1144.2	957.6
$\eta' = B_{SC} + \sum_i q_i \bar{q}_i$	q_{118}	959.2	957.6
η_c	c_{104}	3098	2980
D^0	c_{105}, u_{113}	1642	1865
D^+	c_{105}, d_{113}	1654	1870
Υ	b_{103}	10814	9460
B	$b_{104}, d_{104}, u_{104}$	5909	5270

Table 7. Summary of the model for contribution of quarks to the masses of mesons containing scaled up u,d, and s quarks. The model assumes the maximal value of CP_2 mass allowed by η' mass and the condition $Y_e = 0$ favored by top quark mass.

1. The quark contribution to pion mass is predicted to be 140 MeV, which is by few percent above the pion mass. Ordinary color interactions between pionic quarks can however reduce the conformal weight of pion by one unit. The reduction of CP_2 mass scaled cannot be considered since it would reduce top quark mass to 163.3 GeV which is slightly below the favored range of values [46].
2. The success of the fit requires that spin-spin splitting cancels the mass of super-symplectic boson in a good approximation for pseudoscalar mesons. This would be in accordance with the

Goldstone boson interpretation of pseudoscalar mesons in the sense that color contribution to the mass from $k = 107$ space-time sheet vanishes in the lowest p-adic order.

3. In the case of η *resp.* η' meson it has been assumed that the states have form $(u\bar{u} + \bar{d} - 2s\bar{s})/\sqrt{6}$ *resp.* $(u\bar{u} + \bar{d} + s\bar{s})/\sqrt{3}$.
4. B mesons have anomalously large coupling to $\eta'K$ and $\eta'X$ [39], which indicates an anomalously large coupling of η' to gluons [37]. The interpretation has been in terms of a considerable mixing η' with gluon-gluon bound state.

η' mass is only 2.5 per cent higher than the mass $4m_{107}$ of super-symplectic boson B_{SC} associated with the hadronic space-time sheet of hadron. Large mixing scenario is however not consistent with the existence of Φ with nearly the same mass. This encourages to consider the possibility that η' corresponds to a super-symplectic boson B_{SC} plus quark pair with $k(d) = k(u) = k(s) = k(c) = 118$ with maximal mixing. In this case the contribution of quarks to the mass would be 25.1 MeV and one would have $m(\eta') = 959.2$ MeV which coincides with the actual mass with 1 per mille accuracy. Note that this model predicts identical couplings to various quark pairs as does also the model assuming that $\eta' - \Phi$ system is singlet with respect to flavor $SU(3)$ (having no fundamental status in TGD).

It is clear from the above table that the quark contributions to the masses of π , η' and B are slightly above the meson masses. In the case of B the discrepancy is largest and about 12 per cent. If one assumes that all contributions to the mass have p-adic origin, they are necessarily non-negative.

1. In the case of diagonal mesons the ordinary color interactions can reduce the contribution of quark masses to the mass of the meson. In the case of η' baruyonic super-symplectic gluon B_{SC} could resolve the problem.
2. In the case of non-diagonal mesons the only possible solution of the problem is that $Y_e > 0$ holds true so that mass scale is reduced by a factor $1 - P = \sqrt{5}/(5 + Y_e)$ giving $Y_e \simeq .056$. The prediction for top quark mass is reduced by 1.1 per cent to 167.2 GeV which belongs to the allowed range [46].
3. In the case of B meson one is forced to assume $k_b = k_d = k_u = 104$ although it would be possible to achieve smaller quark contribution by an alternative choice. This choice explains the observed very small isospin splitting and diagonality allows the ordinary color interaction to reduce the quark contribution to the B meson mass.
4. At the end of the chapter an alternative scenario in which quark masses give in good approximation only the masses of pion and kaon will be considered.

An example about how the mesonic mass formula works

The mass of the B_c meson (bound state of b and c quark) has been measured with a precision by CDF (see the blog posting by Tommaso Dorigo [50]) and is found to be $M(B_c) = 6276.5 \pm 4.8$ MeV. Dorigo notices that there is a strange "crackpottian" co-incidence involved. Take the masses of the fundamental mesons made of $c\bar{c}$ (Ψ) and $b\bar{b}$ (Υ), add them, and divide by two. The value of mass turns out to be 6278.6 MeV, less than one part per mille away from the B_c mass!

The general p-adic mass formulas and the dependence of k_q on hadron explain the co-incidence. The mass of B_c is given as $m(B_c) = m(c, k_c(B_c)) + m(b, k_b(B_c))$, whereas the masses of Ψ and Υ are given by $m(\Psi) = \sqrt{2}m(c, k_\Psi)$ and $m(\Upsilon) = \sqrt{2}m(b, k_\Upsilon)$. Assuming $k_c(B_c) = k_c(\Psi)$ and $k_b(B_c) = k_b(\Upsilon)$ would give $m(B_c) = [m(\Psi) + m(\Upsilon)]/\sqrt{2}$ which is by a factor $\sqrt{2}$ higher than the prediction of the "crackpot" formula. $k_c(B_c) = k_c(\Psi) + 1$ and $k_b(B_c) = k_b(\Upsilon) + 1$ however gives the correct result.

As such the formula makes sense but the one part per mille accuracy must be an accident in TGD framework.

1. The predictions for Ψ and Υ masses are too small by 2 *resp.* 5 per cent in the model assuming no effective scaling down of CP_2 mass.

2. The formula makes sense if the quarks are effectively free inside hadrons and the only effect of the binding is the change of the mass scale of the quark. This makes sense if the contribution of the color interactions, in particular color magnetic spin-spin splitting, to the heavy meson masses are small enough. Ψ and η_c correspond to spin 1 and spin 0 states and their masses by 3.7 per cent ($m(\eta_c) = 2980$ MeV and $m(\Psi) = 3096.9$) so that color magnetic spin-spin splitting is measured using per cent as natural unit.

5.5.4 Baryonic mass differences as a source of information

The first step in the development of the model for the baryon masses was the observations that $B - n$ mass differences can be understood if baryons are assumed to contain scaled versions of strange and heavy quarks. The deduction of precise values of $k(q)$ is however not quite straightforward since the color magnetic contribution to the mass affects the situation. Thus a working hypothesis worth of studying is that ground state contribution is same for all baryons and that for spin 1/2 baryons quark contribution to the mass added to this contribution is near as possible to the real mass but smaller than it.

The purpose of the following explicit is to to convince the reader that baryon mass difference can be indeed understood in terms of quark mass differences.

1. $\Lambda - n$ mass difference is 176 MeV and ($k(s) = 111, k(d) = 114$) for λ would predict the mass difference $m(\lambda) - m(n) = m_q(\lambda) - m_q(n)$, where one has $m_q(\lambda) = m(s_{111}) + \sqrt{2}m(d_{114}) - m(n)$, $m_q(n) = \sqrt{m(u_{113})^2 + 2m(d_{113})^2}$. The prediction equals to 141 MeV. It is possible to achieve smaller discrepancy but more precise considerations support this identification. Note that the spin-spin interaction energy is same if u and d quark form the paired quark system which is in $J = 0$ or $J = 1$ state so that the mass difference indeed can be regarded as quark mass difference.
2. $\Sigma - n$ mass difference is 257 MeV. If sigma contains s_{111}, u_{114} and d_{114} , the mass difference is predicted to be $m_q(\Sigma) - m_q(n)$, $m_q(\Sigma) = m(s_{111}) + \sqrt{2}m(d_{114})$ and comes out as 228 MeV.
3. If Ξ contains two s_{110} quarks and u_{113} (d_{113}), he mass difference comes out as 351 MeV to be compared with the experimental value 381 MeV.
4. Even single hadron, such as Ω , could contain several scaled up variants of s quark. $s_{108} + 2s_{111}$ decomposition would give mass difference 718 MeV to be compared with the real mass difference 734 MeV.
5. For Λ_c the mass is 2282 MeV. For $k(c) = 105$ instead of $k(c) = 104$ the predicted $\Lambda_c - n$ mass difference is 1341 MeV whereas the experimental difference is 1344 MeV.
6. For Λ_b the mass is 5425 MeV. For $k(b) = 104$ instead of $k(b) = 103$ the predicted $\Lambda_b - n$ mass difference is 4403 MeV. The experimental difference is 4485 MeV.

Baryon	s content	$\Delta m/MeV$	$\Delta m_{exp}/MeV$
Λ	s_{111}	141	176
Σ	s_{110}	228	257
Ξ	$s_{110} + s_{111}$	351	381
Ω	$s_{108} + 2s_{110}$	718	734
Λ_c	$c_{105}, d_{112}, u_{112}$	1341	1344
Λ_b	$b_{105}, u_{106}, d_{106}$	4403	4485

Table 8. Summary of the model for the quark contribution to the masses of baryons containing strange quarks deduced from mass differences and neglecting second order contributions to the mass. Δm denotes the predicted $B - n$ mass difference $m(B) - m(n)$. The subscript 'exp' refer to experimental value of the quantity in question.

5.5.5 Color magnetic spin-spin splitting

Color magnetic hyperfine splitting makes it possible to understand the $\rho - \pi$, $K^* - K$, $\Delta - N$, etc. mass differences [29]. That the order of magnitude for the splittings remains same over the entire spectrum of hadrons serves as a support for the idea that color fluxes are feeded to $k = 107$ space-time sheet. This would suggest that color coupling strength does not run for the physical states and runs only for the intermediate states appearing in parton description of the hadron reactions. A possible manner to see the situation in terms of intermediate states feeding color gauge flux to space-time sheets with $k > 107$ so that the additive color Coulombic interaction conformal weights $s(q_i, q_j)$ would depend only on the integers $k(q_i), k(q_j)$. It will be found that the dependence is roughly of form $1/(k(q_i) + k(q_j))$, which brings in mind a logarithmic dependence of α_s on p-adic length scales involved.

There are two approaches to the problem of estimating spin-spin splitting: the first one is based on spin-spin interaction energy and the second one on spin-spin interaction conformal weight. The latter one turns out to be the only working one.

The model based on spin-spin interaction energy fails

Classical model would apply real number based physics to estimate the splittings and calculate color magnetic interaction energies. Standard QCD approach predicts that the color magnetic interaction energy is of form

$$\Delta E = S \sum_{pairs} \frac{\bar{s}_i \cdot \bar{s}_j}{m_i m_j r_{ij}^3} . \quad (5.5.4)$$

The mass differences for hadrons allow to deduce information about the nature of color magnetic interaction and make some conclusions about the applicability this model.

1. For mesons the spin-spin splitting varies from 630 MeV for $\rho - \pi$ system to 120 MeV $\Psi - \eta_c$ excludes the classical model predicting that the splitting should be proportional to $1/m(q_1)m(q_2)$ (variation by a factor $2^{113-106} = 128$ instead of 5 would be predicted if the size of the hadron remains same). Also the predicted ratio of $K^* - K$ splitting to $\rho - \pi$ splitting would be 1/4 rather than .63. The ratio of $\eta - \omega$ splitting to $\rho - \pi$ splitting would be 1/16 rather than .34. The ratio of $\Phi - \eta'$ splitting to $\rho - \pi$ splitting would be $1/32 \simeq .03$ instead of .11.

The inspection of the spin-spin interaction energies would suggest that the interaction energy scales $E(i, j)$ obey roughly the formula

$$\begin{aligned} E(i, j) &\sim \frac{5}{2} \times \frac{1}{(\Delta k(q_1) + \Delta k(q_2))} = \\ &5 \times \frac{1}{\log_2 \{ [L(113)/L(k(q_1))] \times [L(113)/L(k(q_2))] \}} \\ \Delta k(q) &= 113 - k(q) \end{aligned}$$

rather than being proportional to $2^{-k(q_1) - k(q_2)}$. The hypothesis that p-adic length scale $L(k)$ of order CP_2 length scale range corresponds to the size of elementary particle horizon associated with wormhole contacts feeding gauge fluxes of the CP_2 type extremal representing particle to the larger space-time sheet with $p \simeq 2^k$ might allow to understand this dependence.

2. $\Delta - N$, $\Sigma^* - \Sigma$, and $\Xi^* - \Xi$ mass differences are 291 MeV, 194 MeV, 220 MeV. If strange quark inside Σ corresponds to $k = 110$, the ratio of $\Sigma^* - \Sigma$ splitting to $\Delta - N$ splitting is predicted to be by a factor 1.17 larger than experimental ratio. $\Xi^* - \Xi$ splitting assuming $k(s) = 109$ the ratio would be .19 and quite too small. Assuming that s, u, d quarks have more or less same mass, the model would predict reasonably well the ratios of the splittings. Either the idea about scaled up variants of s is wrong or the notion of interaction energy must be replaced with interaction conformal weight in order to calculate the effects of color interactions to hadron masses.

The modelling of color magnetic spin-spin interaction in terms of conformal weight

The model based on the notion of interaction conformal weight generalizes the formula for color magnetic interaction energy to the p-adic context so that color magnetic interaction contributes directly to the conformal weight rather than rest mass. The effect is so large that it must be p-adically first order (the maximal contribution in second order to hadron mass would be however only 224 MeV) and the generalization of the mass splitting formula is rather obvious:

$$\Delta s = \sum_{\text{pairs}} S_{ij} \bar{s}_i \cdot \bar{s}_j . \quad (5.5.5)$$

The coefficients S_{ij} depend must be such that integer valued Δs results and CP_2 masses are avoided: this makes the model highly predictive. Coefficients can depend both on quark pair and on hadron since the size of hadron need not be constant. In any case, very limited range of possibilities remains for the coefficients.

This might be understood if the color flux carrying JAB connecting quark to $k = 107$ hadronic space-time sheet is also characterized by a value of $k \geq 113$. This fixes practically completely the model in the case of mesons. If the interaction strengths $s_c(i, j)$ characterizing color Coulombic interaction conformal weight between two quarks depends only on the flux tube pair connecting the quarks via $k = 107$ space-time sheet via the integers $k(q_i)$, the model contains only very few parameters.

The modelling of color magnetic- spin-spin splitting in terms of super-symplectic boson content

The recent variant for the model of the color magnetic spin-spin splitting replacing energy with conformal weight is considerably simpler than the earlier one. Still one can argue that a model using perturbative QCD as a format is not the optimal one in a genuinely non-perturbative situation.

The explicit comparison of the super-symplectic conformal weights associated with spin 0 and spin 1 states on one hand and spin 1/2 and spin 3/2 states on the other hand is carried out at the end of the chapter. The comparison demonstrates that the difference between these states could be understood in terms of super-symplectic particle contents of the states by introducing only single additional negative conformal weight s_c describing color Coulombic binding . s_c is constant for baryons ($s_c = -4$) and in the case of mesons non-vanishing only for pions ($s_c = -5$) and kaons ($s_c = -12$). This leads to an excellent prediction for the masses also in the meson sector since pseudoscalar mesons heavier than kaon are not Goldstone boson like states in this model.

The correlation of the spin of quark-system with the particle content of the super-symplectic sector increases dramatically the predictive power of the model since the allowed conformal weights of super-symplectic bosons are (5,6,58). One can even consider the possibility that also exotic hadrons with different super-symplectic particle content exist: this means a natural generalization of the notion of Regge trajectories. This description will be summarized at the end of the chapter.

5.5.6 Color magnetic spin-spin interaction and super-symplectic contribution to the mass of hadron

Since $k = 107$ contribution to hadron mass is always non-negative, spin-spin interaction conformal weight and also color Coulombic conformal weight must be subtracted from some additional contribution both in the case of pseudo-scalars and spin 1/2 baryons.

Baryonic case

In the case of baryons the additional contribution could be identified as a 2-particle state of super-symplectic bosons with mass squared $9m_{107}^2$ in case of baryons. The net mass is $s_{CS} = 18m_{107}^2$. The study of $N - \Delta$ system shows that color Coulombic interaction energy for single super-symplectic structural unit corresponds to $\Delta s_{SC} = -2$ in the case of nucleon system so that one has $s_{SC} = 18 \rightarrow 16$. If topological mixing for super-symplectic bosons is same as for U type quarks with conformal weights (5,6,58), the already discussed three-particle state of would give $s_{SC} = 5 + 5 + 6 = 16$.

The basic requirement is that the the sum of spin-spin interaction conformal weight and s_{CS} reduces to the conformal weight corresponding to the difference of nucleon mass and quark contribution to 774.6 MeV and correspond to $s = 11$.

One might hope that the situation could be the same for all baryons but it is safer to introduce an additional color Coulombic conformal weight $s_c(B)$ which vanishes for $N - \Delta$ system and hope that it is small as suggested by the fact that quark contributions explain quite satisfactorily the mass differences of baryons. This conformal weight could be assigned to the interaction of quarks via super-symplectic gluons and would represent a correction to the simplest model. Strictly speaking, the term "color Coulombic" should be taken as a mere convenient letter sequence.

Pseudo scalars

In the case of pseudoscalars the situation is not so simple. What is clear that quark masses determine the meson mass in good accuracy.

In this case s_{CS} can be determined uniquely from the requirement that in case of pion it is cancelled the conformal weight characterizing $\rho - \pi$ color magnetic spin-spin splitting:

$$s_{SC} = |\Delta s(\pi, spin - spin)| . \quad (5.5.6)$$

This gives $s_{SC} = 21/4 \simeq 5$.

The interpretation as a bound state of super-symplectic $g = 1$ and $g = 0$ gluon would require binding conformal weight by 4 units which looks somewhat strange. The masslessness of $g = 0$ gluon does not support the formation of this kind of bound state. An alternative option is in terms of topological mixing in which case $g = 0$ boson should receive 5 units of conformal weight.

Explicit calculations demonstrate that for mesons heavier than pion the role of s_c is to compensate s_{SC} . This suggests that the boson of lowest generation is present only inside $\pi - \rho$ system and prevents the large and negative color magnetic spin-spin interaction conformal weight to make pion a tachyon. The special role of pion could be understood in terms of a phase transition to color confining phase. Note however that the mass of η' could be understood by assuming baryonic super-symplectic boson of conformal weight $s_{SC} = 16$ and fully mixed $k = 118$ quarks.

Formulas for $s_c(H)$ for mesons

For option I one has $s_{SC} = 5$ for all mesons. For option II s_{CS} vanishes for all mesons except π and ρ . For option I one obtains the formula

$$s_c(M) = -s_{SC} - \Delta s(M_0, spin - spin) = -5 + |\Delta s(M_0, spin - spin)| . \quad (5.5.6)$$

For option II one has

$$s_c(M) = -5 + |\Delta s(M_0, spin - spin)| , \quad M = \pi, \rho , \quad (5.5.6)$$

$$s_c(M) = |\Delta s(M_0, spin - spin)| , \quad M \neq \pi, \rho . \quad (5.5.7)$$

M_0 refers to the pseudoscalar.

Formulas for $s_c(H)$ for baryons

In the case of spin 1/2 baryons the requirement that the sum of color Coulombic and color magnetic conformal weights is same as for nucleons fixes the values of $s_c(B)$:

$$\begin{aligned}
s_c(B) &= s_0 - s_{SC} - \Delta s(B_{1/2}, \text{spin} - \text{spin}) = -5 + |\Delta s(B_{1/2}, \text{spin} - \text{spin})| , \\
s_{SC} &= 16 , \\
s_0 &= S(m(n) - m_q(n), 107) , \\
m_q(n) &= \sqrt{2m_d^2 + m_u^2} , \\
S(x, 107) &\equiv \left[\left(\frac{x}{m_{107}} \right)^2 \right] .
\end{aligned} \tag{5.5.4}$$

$s_0 = 11$ corresponds to the contribution difference of (say) neutron mass and quark contribution to the nucleon mass. s_{SC} corresponds to the conformal weight due to super-symplectic bosons. In the defining formula for $S(x, 107)$ $[x]$ denotes the integer closest to x .

The conformal weights associated with spin-spin splitting

The general formula for the spin-spin splitting allowing to determine the parameters S_{ij} from the masses of a pair $H^* - H$ of hadrons (say $\rho - \pi$ or $\Delta - N$). The parameters can be deduced from the observation that the mass difference $m(M^*) - m(M)$ for mesons corresponds to the difference of spin-splitting contributions to the mass:

$$\Delta s(M^*) - \Delta s(M) = S(m(M^*) - m(M), 107) . \tag{5.5.5}$$

For baryons one has

$$\begin{aligned}
\Delta s(B^*) - \Delta s(B) &= X_1 - X_0 , \\
X_1 &= S(m(B^*) - m_q(B), 107) = , \\
X_0 &= S(m(B) - m_q(B), 107) .
\end{aligned} \tag{5.5.4}$$

Here $m_q(B) = m_q(B^*)$ denotes the quark contribution to the nucleon mass. The possibility to understand the mass differences of spin 1/2 baryons in terms of differences for $m_q(B)$ inspires the hypothesis that X_0 is constant also for baryons (it vanishes for mesons). If so X_0 can be determined from neutron mass as

$$\begin{aligned}
X_0 &= S(m(n) - m_q(n), 107) , \\
m_q(n) &= \sqrt{2m_d^2 + m_u^2} .
\end{aligned} \tag{5.5.4}$$

Here $m_q(n)$ is the contribution of quarks to neutron mass.

These formulas are *not* identical with those used in the earlier calculations and the difference is due to the fact that $k = 107$ contributions and quark contributions are calculated separately unless quarks correspond $k = 107$. The formula allows to calculate second order contribution to the mass splitting.

p-Adicization brings in additional constraints. The requirement that the predicted mass of spin 1 boson and spin 3/2 fermion is not larger than than the experimental mass can pose strong constraints the scaling factor $\sqrt{5/(5 + Y_e)}$ in the case of non-diagonal hadrons unless one is willing to modify the model for spin-spin splittings. It was already found that in case of $\rho - \pi$ system this implies that top quark mass is at the lower limit of the allowed mass interval. One cannot take these constraints so seriously as the constraints that quark mass contribution is lower than meson mass in the case the quarks do not correspond to $k = 107$.

General mass formula

The general formula for the mass of hadron can be written as a sum of perturbative and non-perturbative contributions as

$$m(H) = m_P + m_{NP} . \quad (5.5.5)$$

Preceding considerations lead to a simple formula for the non-perturbative contribution m_{NP} to the masses of spin 0 and spin 1 doublet of mesons:

$$\begin{aligned} m_{NP}(M) &= \sqrt{s_{NP}(M)} \times m_{107} , \\ s_{NP}(M_0) &= 0 , \\ s_{NP}(M_1) &= S(m(M^*) - m(M), 107) . \end{aligned} \quad (5.5.4)$$

For spin 1/2 and 3/2 doublet of baryons one has

$$\begin{aligned} m_{NP}(B) &= \sqrt{s_{NP}(B)} \times m_{107} , \\ s_{NP}(B_{1/2}) &= S(m_n - \sqrt{2m_d^2 + m_u^2}, 107) , \\ s_{NP}(B_{3/2}) &= S(m(B^*) - m_q(B), 107) . \end{aligned} \quad (5.5.3)$$

Perturbative contribution m_P contains in the lowest order approximation only the contribution of quark masses. In the case of diagonal mesons also a contribution from the ordinary color-Coulombic force and color magnetic spin-spin splitting can be present. For heavy mesons this contribution seems necessary since pure quark contribution is exceeds by few per cent the mass of meson.

Spin-spin interaction conformal weights for baryons

Consider now the determination of S_{ij} in the case of baryons. The general splitting pattern for baryons resulting from color Coulombic, and spin-spin interactions is given by the following table. The following equations summarize spin-spin splittings for baryons in a form of a table.

<i>baryon</i>	J	J_{12}	ΔS^{spin}
N	$\frac{1}{2}$	0	$-\frac{3}{4}S_{d,d}$
Δ	$\frac{3}{2}$	1	$\frac{3}{4}S_{d,d}$
Λ	$\frac{1}{2}$	0	$-\frac{3}{4}S_{d,d}$
Σ	$\frac{1}{2}$	0	$-\frac{3}{4}S_{d,d}$
Σ^*	$\frac{1}{2}$	0	$\frac{1}{4}S_{d,d}$ $+\frac{1}{2}S_{d,s}$
Ξ	$\frac{1}{2}$	0	$-\frac{3}{4}S_{s,s}$
Ξ^*	$\frac{1}{2}$	0	$\frac{1}{4}S_{s,s}$ $+\frac{1}{2}S_{d,s}$
Ω	$\frac{3}{2}$	1	$\frac{3}{4}S_{s,s}$

(5.5.3)

Spin-spin splittings are deduced from the formulas

$$\begin{aligned} \Delta S^{spin} &= S_{q_1, q_2} \left(\frac{J_{12}(J_{12} + 1)}{2} - \frac{3}{4} \right) , \\ &+ \frac{1}{4} (S_{q_1, q_3} + S_{q_2, q_3}) (J(J + 1) - J_{12}(J_{12} + 1) - \frac{3}{4}) , \end{aligned} \quad (5.5.2)$$

where J_{12} is the angular momentum eigenvalue of the 'first two quarks', whose value is fixed by the requirement that magnetic moments are of correct sign.

The masses determine the values of the parameters uniquely if one assumes that color binding energy is constant as indeed suggested by the very notion of M_{107} hadron physics. The requirement is that the mass difference squared for $\Delta - N$, $\Sigma^* - \Sigma$, and $\Xi^* - \Xi$ come out correctly.

Consider now the values of S_{ij} for the models assuming $k = 113$ light quarks and dynamical $k(s)$.

1. For $N - \Delta$ system the equation is

$$S_{d_{113},d_{113}} = \frac{1}{3}S(m(\Delta) - m_q(N), 107) - S(m(N) - m_q(N), 107) .$$

Here $m_q(N)$ refers to the quark contribution to the baryon mass.

2. For $\Sigma^* - \Sigma$ system the basic equation can be written as

$$S_{d_{114},s_{110}} = 2[S(m(\Sigma^*) - m_q(\Sigma), 107) - S(m(\Sigma) - m_q(\Sigma), 107) - S(d_{114}, d_{114})] .$$

One must make some assumption in order to find a unique solution. The simplest assumption is that $S_{d_{114},d_{114}} = S_{d_{114},s_{110}}$. This implies

$$S_{d_{114},d_{114}} = \frac{1}{3}[S(m(\Sigma^*) - m_q(\Sigma), 107) - S(m(\Sigma) - m_q(\Sigma), 107)] .$$

3. In the case of $\Xi^* - \Xi$ system the equation is

$$S_{s_{110},s_{110}} = -\frac{1}{2}S_{d_{113},s_{110}} + [S(m(\Xi^*) - m_q(\Xi), 107) - S(m(\Xi) - m_q(\Xi), 107)] .$$

If one assumes $S_{s_{110},s_{110}} = S_{d_{113},s_{110}}$ one obtains

$$S_{s_{110},s_{110}} = \frac{1}{3}[S(m(\Xi^*) - m_q(\Xi), 107) - S(m(\Xi) - m_q(\Xi), 107)] .$$

The resulting values of the parameters characterizing baryonic spin-spin splittings are in the table below. The parameters rela

$S_{d_{113},d_{113}}$	$S_{d_{114},d_{114}}$	$S_{d_{114},s_{110}}$	$S_{s_{110},s_{110}}$	$S_{d_{113},s_{110}}$	(5.5.3)
7	6	6	$\frac{8}{3}$	$\frac{8}{3}$	

The mass squared unit used is m_0^2 and $k = 107$ defines the p-adic length scale used. The elements of $S_{i,j}$ between different p-adic primes are assumed to be vanishing. The matrix elements are quite near to each other which raises the hope that the model indeed makes sense.

Color Coulombic binding conformal weights are given by the expression $s_c = -5 + |\Delta s(B_{1/2}, spin - spin)|$. The weights are given in the following table

<i>baryon</i>	N	Σ	Ξ	(5.5.3)
s_c	$\frac{1}{4}$	$-\frac{1}{2}$	-3	

Some remarks are in order.

1. A good sign is that the values of s_c are small as compared to the value of $s_{CS} = 18$ in all baryons so that only a small correction is in question.
2. The magnitude of s_c increases with the mass of baryon which does not conform with the expectations raised by ordinary QCD evolution. Could this mean that asymptotic freedom means that the color interaction between quarks occurs increasingly via super-symplectic gluons? For $N - \Delta$ system the actual value of s_c should vanish.
3. One might worry about the fact the color binding conformal weights are not integral valued. The total conformal weights determining the mass squared are however integers.

Spin-spin interaction conformal weights for mesons

The values of mesonic interaction strengths $S_{i,j}$ can in principle be deduced from the observed mass splittings. The following equations summarize the spin-spin splitting pattern for mesons in a form of table.

<i>meson</i>	Δs^{spin}
π	$-\frac{3}{4}S_{d,d}$
ρ	$\frac{1}{4}S_{d,d}$
η	$-\frac{3}{4}S_{d,d}$
ω	$\frac{1}{4}S_{d,d}$
$K^\pm, K^0(CP = 1)$	$-\frac{3}{4}S_{d,s}$
$K^0(CP = -1)$	$-\frac{3}{4}S_{d,s}$
$K^{*,\pm}, K^{*,0}(CP = 1)$	$\frac{1}{4}S_{d,s}$
$K^{*,0}(CP = -1)$	$\frac{1}{4}S_{d,s}$
η'	$-\frac{3}{4}S_{s,s}$
Φ	$\frac{1}{4}S_{s,s}$
η_c	$-\frac{3}{4}S_{c,c}$
Ψ	$\frac{1}{4}S_{c,c}$
$D^\pm, D^0(CP = 1)$	$-\frac{3}{4}S_{d,c}$
$D^0(CP = -1)$	$-\frac{3}{4}S_{d,c}$
$D^{*,\pm}, D^{*0}(CP = 1)$	$\frac{1}{4}S_{d,c}$
$D^{*0}(CP = -1)$	$\frac{1}{4}S_{d,c}$

(5.5.3)

Consider the spin-spin interaction for mesons.

1. For $\rho - \pi$ system one has

$$S_{d_{113},d_{113}} = s(m(\rho) - m_q(\pi)) .$$

Using $s(\rho) = 14$ and $s(\pi) = 0$ gives $S(d_{113}, d_{113}) = 13$.

2. $\omega - \eta$ system one obtains

$$S_{q_{109},q_{109}} = S(m(\omega) - m_q(\eta), 107)$$

3. $K^* - K$ -splitting gives $S_{d_{114},s_{109}} = S(m(K^*) - m_q(K), 107)$.
4. $\Phi - \eta'$ splitting gives $S_{q_{107},q_{107}} = S(m(\Phi) - m_q(\eta'), 107)$.
5. $D^* - D$ mass splitting gives $S_{d_{113},c_{105}} = S(m(D^*) - m_q(D), 107)$.
6. $\Psi - \eta_c$ mass difference gives $S_{c_{104},c_{104}} = s(m(\Psi) - m_q(\eta_c), 107)$.

The results for the spin-spin interaction strengths S_{ij} are summarized in the table below. q_{109} refers to u , d , and s quarks.

$S_{d_{113},d_{113}}$	$S_{q_{109},q_{109}}$	$S_{q_{107},q_{107}}$	$S_{d_{114},s_{109}}$	$S_{d_{113},c_{105}}$	$S_{c_{104},c_{104}}$
7	1	0	3	2	0

(5.5.3)

Note that interaction strengths tend to be weaker for mesons than for baryons. For scaled up quarks the value of interaction strength tends to decrease and is smaller for non-diagonal than diagonal interactions. Since the values of $k(q_i)$ maximize the quark contribution to hadron masses, the interaction strength produce a satisfactory mass fit for hadrons with errors of not larger than about five cent.

The color Coulombic binding conformal weights for meson states are given in the following table:

<i>meson</i>	π	K	η	η'	D	ψ
$s_c(I)$	+1/4	-4 - 1/4	-6	-3 - 1/4	-4 - 1/2	-5
$s_c(II)$	1/4	3/4	1	1 + 3/4	1/2	0

(5.5.3)

For option I $g = 1$ boson is present in all mesons. The magnitude of s_c increases with the mass of the meson and more or less compensates $s_{CS} = 5$. This forces to consider the possibility that only pion contains the super-symplectic boson compensating the large and negative spin-spin interaction conformal weight making the state tachyon otherwise. For option II s_c is relatively small and positive for this option.

5.5.7 Summary about the predictions for hadron masses

The following tables summarize the predictions for baryon masses following from the proposed model with optimal choices of the integers $k(q)$ characterizing the mass scales of quarks and requiring that the predicted isospin splittings are of same order than the observed splittings. This condition is non-trivial: for instance, in case of B meson the smallness of splitting forces the condition $k(b) = k(d) = k(u) = 104$ so that mass squared is additive and the large contribution of b quark minimizes the isospin splitting.

Meson masses assuming that all pseudoscalars are Goldstone bosons

<i>Meson</i>	<i>quarks</i>	$m_{pr}(M)/MeV$	m_{exp}/MeV
π^0	$B_{SC,1} + d_{113}, u_{113}$	140.0	135.0
π^+	d_{113}, u_{113}	140.0	139.6
ρ^0	d_{113}, u_{113}	756	772
ρ^+	d_{113}, u_{113}	756	770
K^0	d_{114}, s_{109}	496	498
K^+	u_{114}, s_{109}	486	494
K^{0*}	d_{114}, s_{109}	896	900
K^{+*}	u_{114}, s_{109}	892	891
η	$u_{109}, d_{109}, s_{109}$	522	549
ω^0	$u_{109}, d_{109}, s_{109}$	817	783
η'	$u_{107}, d_{107}, s_{107}, c_{107}$	1144	958
Φ	$u_{107}, d_{107}, s_{107}, c_{107}$	1144	1019
η_c	c_{104}	3098	2980
D^0	c_{105}, u_{113}	1642	1865
D^+	c_{105}, d_{113}	1655	1870
D^{*0}	c_{105}, u_{114}	1971	2007
D^{*+}	c_{105}, d_{114}	1985	2010
F	$c_{105}, s(106)$	1954	2021
Υ	b_{103}	10814	9460
B	$b_{104}, d_{104}, u_{104}$	5909	5270

Table 9. The prediction of meson masses. The model assumes the maximal value of CP_2 mass allowed by η' mass and the condition $Y_e = 0$ favored by top quark mass.

In the case of meson masses the predictions for masses are not so good as for baryons. Errors are at worst about 5 per cent. For non-diagonal mesons the predicted masses are smaller than actual masses and in the case of kaons excellent. Also the prediction of pion mass is good but about 5 per cent too large. In the case of diagonal mesons ordinary color interactions could reduce the predicted masses in case that they are larger than actual ones.

Meson masses assuming that only pion and kaon are Goldstone bosons

The Goldstone boson interpretation does not seem completely satisfactory. In order to make progress one can check whether the masses associated with super-symplectic bosons could serve as basic units for pseudoscalar and vector boson masses. A more general fit would be based on the use of fictive boson B_{107} with mass m_{107} as a basic unit in $k = 107$ contribution to the mass. The table below gives very accurate formulas for the meson masses in terms of the scale m_{107} and quark contribution to the masses.

Meson	quarks	$m_{pr}(M)/MeV$	m_{exp}/MeV
π^0	d_{113}, u_{113}	140.0	135.0
π^+	d_{113}, u_{113}	140.0	139.6
ρ^0	$6B_{107} + d_{113}, u_{113}$	758	772
ρ^+	$6B_{107} + d_{113}, u_{113}$	758	770
K^0	d_{114}, s_{109}	496	498
K^+	u_{114}, s_{109}	486	494
K^{0*}	$3B_{107} + d_{114}, s_{109}$	901	900
K^{+*}	$3B_{107} + u_{114}, s_{109}$	891	891
η	$B_{SC,1} + u_{118}, d_{118}, s_{118}$	548	549
ω^0	$2B_{SC,1} + u_{118}, d_{118}, s_{118}$	803	783
η'	$2B_{SC,1} + B_{SC,2} + q_{118}$	959	958
Φ	$2B_{SC,1} + B_{SC,2} + q_{118}$	959	1019
η_c	$2B_{SC,1} + c_{105}$	2929	2980
Ψ	$3B_{SC,1} + c_{105}$	3098	3100
D^0	$2m_{SC,1} + c_{106}, u_{118}$	1853	1865
D^+	$2m_{SC,1} + c_{106}, d_{118}$	1850	1870
D^{*0}	$3m_{SC,1} + c_{106}, u_{118}$	2019	2007
D^{*+}	$3m_{SC,1} + c_{106}, d_{118}$	2016	2010
F	$3m_{SC,2} + c_{105}, s(113)$	2010	2021
Υ	$B_{SC,3} + b_{104}$	9441	9460
B^\pm	$3B_{SC,2} + b_{105}, d_{105}, u_{105}$	5169	5270

Table 10. Table demonstrates that scalar and vector meson masses can be effectively regarded as expressible in terms of quark contribution and contribution coming from many particle states of super-symplectic bosons $B_{SC,k}$, $k = 1, 2, 3$, with conformal weights (5,6,28) associated also with U type quarks. B_{107} denotes effective super-symplectic boson with mass conformal weight 1 and mass m_{107} . $Y_e = 0$ favored by top quark mass is assumed.

The table demonstrates following.

1. For mesons heavier than kaons, the masses are effective sums of masses for quarks and many-particle state formed by super-symplectic bosons allowed by the topological mixing of U type quarks.
2. For $\pi - \rho$ resp. $K - K^*$ systems the masses can be expressed using effective $7B_{107}$ state resp. $3B_{107}$ state. Second order contribution to the conformal weight from the super-symplectic color interaction can explain the too small mass of ρ and too large mass of π if it interferes with the corresponding quark mass contribution.
3. For pseudo-scalars heavier than kaon the mass of the super-symplectic meson is not completely compensated by spin-spin splitting for the pseudoscalar state so that Goldstone boson interpretation does not make sense anymore. In the case of heavy mesons the predicted masses of pseudoscalars are slightly below the actual mass.
4. The predicted masses are not larger than actual masses (ω_0 is the troublemaker) if one assumes 2.5 per cent reduction of CP_2 mass scale for which top quark mass is at the lower bound of the allowed mass range.

5. Color magnetic spin-spin splitting parameters can be deduced from the differences of super-symplectic conformal weights for pseudoscalar and spin one boson. There is however no absolute need for this perturbative construct.
6. One can consider the possibility that the super-symplectic boson content is actual and correlates with the spin of quark-antiquark system for mesons heavier than kaons. The point would be that the representability in terms of super-symplectic bosons would make the model for the color magnetic spin-spin splittings highly predictive. This interpretation makes sense in the case of $\pi - \rho$ and $K - K^*$ systems only if one introduces negative color Coulombic conformal weight s_c . For heavier mesons only this contribution would be second order in p which is more or less consistent with the view about color coupling evolution. $\pi - \rho$ would correspond to B_1 ($s = 5$) and $2B_2$ ($s = 12$) ground states with color Coulombic conformal weight $s_c = -12$. $K - K^*$ would correspond to $2B_2$ ($s = 12$) and $3B_1$ with $s_c = -12$. The presence of ground state bosons saves π and K from becoming tachyons.

Whatever the correct physical interpretation of the mass formulas represented by the table above is, it is clear that m_{107} defines a fundamental mass scale also for meson systems.

Baryon masses

One can ask whether the representability of spin-spin splitting in terms of super-symplectic conformal boson content is possible also in the case of baryons so that perturbative formulas altogether would not be necessary. The physical interpretation would be that the total spin of baryonic quarks correlates with the content of super-symplectic bosons. The existence of this kind of representation would be one step towards understanding of also spin-spin splitting from first principles.

This is indeed the case if one accepts negative color Coulombic conformal weight $s_c = -4$. Spin 1/2 ground states would correspond to $3B_1$ with conformal weight $s = 15$, one B_1 for each valence quark. Spin 3/2 states would correspond to $5B_1$ with $s = 25$ in the case of Δ , to $2B_1 + B_2$ in the case of Σ^* with $s = 23$, and to $B_1 + 3B_2$ with $s = 24$ in case of Ξ^* .

Baryon	quarks	$m_{pr}(B)/MeV$	m_{exp}/MeV
p	$3B_1 + u_{113}, d_{113}$	942.3	938.3
n	$3B_1 + u_{113}, d_{113}$	949.8	939.6
Δ^{++}	$5B_1 + u_{113}$	1230	1231
Δ^+	$5B_1 + u_{113}, d_{113}$	1238	1235
Δ^0	$5B_1 + u_{113}, d_{113}$	1245	1237
Δ^-	$5B_1 + d_{113}$	1253	≤ 1238
Λ	$3B_1 + u_{114}, d_{114}, s_{111}$	1090	1116
Σ^+	$3B_1 + u_{114}, s_{110}$	1165	1189
Σ^0	$3B_1 + u_{114}, d_{113}, s_{110}$	1171	1192
Σ^-	$3B_1 + d_{114}, s_{110}$	1178	1197
Σ^{*+}	$2B_1 + 2B_2 + u_{114}, s_{110}$	1381	1385
Ξ^0	$2B_1 + 2B_2 + u_{113}, s_{110}, s_{111}$	1301	1315
Ξ^-	$3B_1 + d_{113}, s_{110}$	1288	1321
Ξ^{*0}	$B_1 + 3B_2 + u_{113}, s_{110}$	1531	1532
Ξ^{*-}	$B_1 + 3B_2 + d_{113}, s_{110}$	1505	1535
Ω^-	$3B_1 + s_{108}, s_{111}$	1667	1672
Λ_c	$3B_1 + d_{110}, u_{110}, c_{106}$	2261	2282
Λ_b	$3B_1 + d_{108}, u_{108}, b_{105}$	5390	5425

Table11. The predictions for baryon masses assuming $Y_c = 0$.

From the table for the predicted baryon masses one finds that the predicted masses are slightly below the experimental masses for all baryons except for some baryons in $N - \Delta$ multiplet and for Ω . The reduction of the CP_2 mass scale by a factor of order per cent consistent with what is known about top quark mass cures this problem (also ordinary color interactions could take of the problem).

In principle the quark contribution to the hadron mass is measurable. Suppose that color binding conformal weight can be assigned to the color interaction in super-symplectic degrees of freedom alone. Above the "ionization" energy, which corresponds to the contribution of quarks to the mass of hadron, valence quark space-time sheet can separate from the hadronic space-time sheet in the collisions of hadrons. This threshold might be visible in the collision cross sections for say nucleon-nucleon collisions. For nucleons this energy corresponds to 170 MeV.

5.5.8 Some critical comments

The number theoretical model for quark masses and topological mixing matrices and CKM matrix as well as the simple model for hadron masses give strong support for the belief that the general vision is correct. One must bear in mind that the scenario need not be final so that the basic objections deserve an explicit articulation.

Is the canonical identification the only manner to map mass squared values to their real counterparts

In p-adic thermodynamics p-adic particle mass squared is mapped to its real counterpart by the canonical identification. If the $O(p)$ contribution corresponds to non-trivial rational number, the real mass is of order CP_2 mass. This allows to eliminate a large number of exotics. In particular, it implies that the modular contribution to the mass squared must be of form np rather than $(r/s)p$. This assumption is absolutely crucial in the model of topological mixing matrices and CKM matrix.

One can however question the use of the standard form of the canonical identification to map p-adic mass squared to its real counterpart. The requirement that p-adic and real S-matrix elements (in particular coupling constants) are related in a realistic manner, forces a modification of the canonical identification. Instead of a direct identification of real and p-adic rationals, the p-adic rationals in R_p are mapped to real rationals (or vice versa) using a variant of the canonical identification $I_{R \rightarrow R_p}$ in which the expansion of rational number $q = r/s = \sum r_n p^n / \sum s_n p^n$ is replaced with the rational number $q_1 = r_1/s_1 = \sum r_n p^{-n} / \sum s_n p^{-n}$ interpreted as a p-adic number:

$$q = \frac{r}{s} = \frac{\sum_n r_n p^n}{\sum_m s_m p^m} \rightarrow q_1 = \frac{\sum_n r_n p^{-n}}{\sum_m s_m p^{-m}} = \frac{I(r)}{I(s)} . \quad (5.5.4)$$

The nice feature of this variant of the canonical identification is that it respects quantitative behavior of amplitudes, respects symmetries, and maps unitary matrices to unitary matrices if the matrix elements correspond to rationals (or generalized rationals in algebraic extension of rationals) if the p-adic integers involved are smaller than p . At the limit of infinitely large p this is always satisfied.

Quite generally, the thermodynamical contribution to the particle mass squared is in the lowest p-adic order of form rp/s , where r is the number of excitations with conformal weight 1 and s the number of massless excitations with vanishing conformal weight. The real counterpart of mass squared for the ordinary canonical identification is of order CP_2 mass by $r/s = R + r_1 p + \dots$ with $R < p$ near to p . Hence the states for which massless state is degenerate become ultra heavy if r is not divisible by s . For the new variant of canonical identification these states would be light.

Even worse, the new form does not require the modular contribution to the p-adic mass squared to be of form np . Some other justification for this assumption would be needed. The first guess is that the conditions on mass squared plus probability conservation might not be consistent with unitarity unless the modular contribution to the mass squared remains integer valued in the mixing (note that all integer values are not possible). Direct numerical experimentation however shows that that this is not the case.

The predicted integer valued contributions to the mass squared are minimal in the case of u and d quarks and very nearly maximal in the case t and b quarks. This suggests a possible way out of the difficulty. Perhaps the rational valued p-adic mass squared of u and d quarks are minimal and those of b and t quarks maximal or nearly maximal. This might also allow to improve the prediction for the CKM matrix.

The objection against the use of the new variant of canonical identification is that the predictions of p-adic thermodynamics for mass squared are not rational numbers but infinite power series. p-Adic thermodynamics itself however defines a unique representation of probabilities as ratios of generalized

Boltzmann weights and partition function and thus the variant of canonical identification might indeed generalize. If this representation generalizes to the sum of modular and Virasoro contributions, then the new form of canonical identification becomes very attractive. Also an elegant model for the masses of intermediate gauge bosons results if $O(p)$ contribution to mass squared is allowed to be a rational number.

Uncertainties related to the CP_2 length scale

The uncertainties related to the CP_2 length scale mean that one cannot take the detailed model for hadron masses too literally unless one takes the recent value of top quark mass at face value and requiring ($Y_e = 0, Y_t = 1$) in rather high accuracy. This constraint allows at most 2.5 per cent reduction of the fundamental mass scale and baryonic masses suggest a 1 per cent reduction. The accurate knowledge of top quark mass is therefore of fundamental importance from the point of view of TGD.

Bibliography

Books about TGD

- [1] M. Pitkänen (2006), *Topological Geometroynamics: Overview*.
http://tgd.wippiespace.com/public_html/tgdview/tgdview.html.
- [2] M. Pitkänen (2006), *Quantum Physics as Infinite-Dimensional Geometry*.
http://tgd.wippiespace.com/public_html/tgdgeom/tgdgeom.html.
- [3] M. Pitkänen (2006), *Physics in Many-Sheeted Space-Time*.
http://tgd.wippiespace.com/public_html/tgdclass/tgdclass.html.
- [4] M. Pitkänen (2006), *p-Adic length Scale Hypothesis and Dark Matter Hierarchy*.
http://tgd.wippiespace.com/public_html/paddark/paddark.html.
- [5] M. Pitkänen (2006), *Quantum TGD*.
http://tgd.wippiespace.com/public_html/tgdquant/tgdquant.html.
- [6] M. Pitkänen (2006), *TGD as a Generalized Number Theory*.
http://tgd.wippiespace.com/public_html/tgdnumber/tgdnumber.html.
- [7] M. Pitkänen (2006), *TGD and Fringe Physics*.
http://tgd.wippiespace.com/public_html/freenergy/freenergy.html.

Books about TGD Inspired Theory of Consciousness and Quantum Biology

- [8] M. Pitkänen (2006), *TGD Inspired Theory of Consciousness*.
http://tgd.wippiespace.com/public_html/tgdconsc/tgdconsc.html.
- [9] M. Pitkänen (2006), *Bio-Systems as Self-Organizing Quantum Systems*.
http://tgd.wippiespace.com/public_html/bioselforg/bioselforg.html.
- [10] M. Pitkänen (2006), *Quantum Hardware of Living Matter*.
http://tgd.wippiespace.com/public_html/bioware/bioware.html.
- [11] M. Pitkänen (2006), *Bio-Systems as Conscious Holograms*.
http://tgd.wippiespace.com/public_html/hologram/hologram.html.
- [12] M. Pitkänen (2006), *Genes and Memes*.
http://tgd.wippiespace.com/public_html/genememe/genememe.html.
- [13] M. Pitkänen (2006), *Magnetospheric Consciousness*.
http://tgd.wippiespace.com/public_html/magnconsc/magnconsc.html.
- [14] M. Pitkänen (2006), *Mathematical Aspects of Consciousness Theory*.
http://tgd.wippiespace.com/public_html/mathconsc/mathconsc.html.
- [15] M. Pitkänen (2006), *TGD and EEG*.
http://tgd.wippiespace.com/public_html/tgdeeg/tgdeeg.html.

References to the chapters of the books about TGD

- [16] The chapter *p-Adic Particle Massivation: Elementary particle Masses* of [4].
http://tgd.wippiespace.com/public_html/paddark/paddark.html#mass2.
- [17] The chapter *p-Adic Particle Massivation: New Physics* of [4].
http://tgd.wippiespace.com/public_html/paddark/paddark.html#mass4.
- [18] The chapter *TGD as a Generalized Number Theory: p-Adicization Program* of [6].
http://tgd.wippiespace.com/public_html/tgdnumber/tgdnumber.html#visiona.
- [19] The chapter *Construction of Configuration Space Kähler Geometry from Symmetry Principles* of [2].
http://tgd.wippiespace.com/public_html/tgdgeom/tgdgeom.html#compl1.
- [20] The chapter *TGD and Nuclear Physics* of [4].
http://tgd.wippiespace.com/public_html/paddark/paddark.html#padnucl.
- [21] The chapter *The Recent Status of Leptohadron Hypothesis* of [4].
http://tgd.wippiespace.com/public_html/paddark/paddark.html#leptc.
- [22] The chapter *Nuclear String Model* of [4].
http://tgd.wippiespace.com/public_html/paddark/paddark.html#nuclstring.
- [23] The chapter *Configuration Space Spinor Structure* of [2].
http://tgd.wippiespace.com/public_html/tgdgeom/tgdgeom.html#cspin.
- [24] The chapter *Is it Possible to Understand Coupling Constant Evolution at Space-Time Level?* of [5].
http://tgd.wippiespace.com/public_html/tgdquant/tgdquant.html#rgflow.
- [25] The chapter *General Ideas about Many-Sheeted Space-Time: Part I* of [3].
http://tgd.wippiespace.com/public_html/tgdclass/tgdclass.html#topcond.

Articles related to TGD

- [26] M. Pitkänen (2007), *Further Progress in Nuclear String Hypothesis*, http://tgd.wippiespace.com/public_html/articles/nuclstring.pdf.

Mathematics

- [27] E. C. Zeeman (ed.)(1977), *Catastrophe Theory*. Addison-Wessley Publishing Company.
- [28] G. Grosswald (1985), *Representations of Integers as Sums of Squares*. Springer Verlag, New York.

Theoretical physics

- [29] F.E.Close (1979), *An Introduction to Quarks and Partons*, Academic Press.

Particle and nuclear physics

- [30] A. Brandt *et al* (1992), Phys. Lett. B 297, p. 417.
- [31] D. B. Kaplan, A. E. Nelson and N. Weiner (2004), *Neutrino Oscillations as a Probe of Dark Energy*, hep-ph/0401099.

- [32] *Glueball*, <http://en.wikipedia.org/wiki/Glueballs>.
- [33] N. M. Queen, G. Violini (1974), *Dispersion Theory in High Energy Physics*, The Macmillan Press Limited.
- [34] <http://fnphyx-www.fnal.gov/experiments/ktev/epsprime/epsprime.html>.
- [35] A. Ali, D. London (1995), *Zeitschrift fur Phys. C* 65, p. 431.
- [36] A. M. Smith *et al*(1985), *Phys. Lett. B* 163, p. 267.
- [37] D. Atwood and A. Somi (1997), JLAB-THY-97;
ibid (1997), *Phys. Rev. Lett.* 79, 5206. See also
H. W. Pfaff (2000), *η' Meson Production*.
<http://pcweb.physik.uni-giessen.de/disto/papers/etaprime.htm>.
- [38] A.J. Buras (1944), *Phys. Lett. B.* 333, No 3,4, p. 476.
- [39] B. H. Behrens *et al* (1998), *Phys. Rev. Lett.* 80, 3710;
T. E. Browder *et al* (1998), *Phys. Rev. Lett.* 81, 1786.
- [40] G. Buchalla, A.J. Buras and M. Lautenbacher (1996), *Rev. Mod. Phys.* 68, p. 1125.
- [41] M. Derrick *et al*(1993), *Phys. Lett B* 315, p. 481.
- [42] *Quark*, http://en.wikipedia.org/wiki/Current_quark_mass.
- [43] *Non- $q\bar{q}$ mesons*,
http://pdg.lbl.gov/2006/reviews/nonqqbar_mxxx050.pdf.
- [44] H. Waschmuth (CERN, for the Aleph collaboration) (1996), *Results from e^+e^- collisions at 130, 136 and 140 GeV center of mass energies in the ALEPH Experiment*.
http://alephwww.cern.ch/ALPUB/pub/pub_96.html.
- [45] E. A. Paschos and U. Turke (1989), *Phys. Rep.*, Vol. 178, No 4.
- [46] *The top quark mass measured from its production rate*,
<http://dorigo.wordpress.com/2007/06/26/a-particle-mass-from-its-production-rate/#more-910>.
- [47] Y. Keum, U. Nierste and A. I. Sanda (1999), *A short look at ϵ'/ϵ* . hep-ph/9903230.
- [48] T. Dorigo (2009), *Nitpicking Ω_b discovery*.
http://www.scientificblogging.com/quantum_diaries_survivor/nitpicking_omega_b_discovery.
T. Dorigo (2009), *Nitpicking Ω_b discovery: part II*.
http://www.scientificblogging.com/quantum_diaries_survivor/nitpicking_omega_b_baryon_part_ii.
T. Dorigo (2009), *Real discovery of Ω_b released by CDF today*.
http://www.scientificblogging.com/quantum_diaries_survivor/real_discovery_omega_b_released_cdf_today.
- [49] T. Smith (2003), *Truth Quark, Higgs, and Vacua*,
<http://www.innerx.net/personal/tsmith/TQvacua.html> .
- [50] *Rumsfeld hadrons*,
<http://dorigo.wordpress.com/2007/06/20/rumsfeld-hadrons/>.
- [51] Tommaso Dorigo (2008), *Top quark mass measured with neutrino phi weighting*. Blog posting about latest CDF measurement of top quark mass.
<http://dorigo.wordpress.com/2008/12/08/top-quark-mass-measured-with-neutrino-phi-weighting>
- [52] D0 collaboration. (2008), *Observation of the doubly strange b baryon Ω_b^-* . <http://arxiv.org/abs/0808.4142>.

Chapter 6

p-Adic Particle Massivation: New Physics

6.1 Introduction

TGD certainly predicts a lot of new physics, actually infinite hierarchies of fractal copies of standard model physics, but the precise characterization of predictions has varied as the interpretation of the theory has evolved during years.

6.1.1 Basic new physics predictions

Concerning new physics the basic predictions are following. TGD predicts a rich spectrum of massless states for which ground states of negative super-symplectic conformal weight are created by colored super-generators. By color confinement these states do not however give rise to macroscopic long range forces. A hierarchy color and weak physics is predicted. Also dark matter hierarchy corresponding to a hierarchy of Planck constants brings in a hierarchy of variants of standard model physics labeled by the values of Planck constant. Thus in TGD the question is not about predicting some exotic particles but an entire fractal hierarchies of copies of standard model physics.

The family replication for fermions correspond in case of gauge bosons prediction of bosons labelled by genera of the two light-like wormhole throats associated with the wormhole contact representing boson. There are very general arguments predicting that the number of fermionic genera is three and this means that gauge bosons can be arranged into genus-SU(3) singlet and octet. Octet corresponds to exotic gauge bosons and its members should develop Higgs expectation value. Completely symmetric coupling between Higgs octet and boson octet allows also the bosons with vanishing genus-SU(3) quantum numbers to develop mass.

Higgs field is predicted and its vacuum expectation value explains boson masses. By a general argument p-adic temperature for bosons is low and this means that Higgs contribution to the gauge boson mass dominates. Only p-adic thermodynamics is needed to explain fermion masses and the masses of super-symplectic bosons and their super counterparts. There is an argument suggesting that vacuum expectation value of Higgs at fermion space-time sheets is not possible. Almost universality of the topological mixing inducing also CKM mixing allows to predict mass spectrum of these states.

6.1.2 Outline of the topics of the chapter

Summary of new physics effects

Various new physics effects related to the predicted exotic particles are discussed. No attempt to discuss systematically the spectrum of various exotic bosons and fermions, basically due to the ground states created by color super-symplectic and Kac-Moody generators, will be made. Rather, the attempt is to summarize the new physics expected on basis of recent interpretation of quantum TGD.

1. There is a brief discussion of family replication phenomenon in the case of gauge bosons based on the identification of gauge bosons as wormhole contacts. Also an argument forcing the

identification of partonic vertices as branchings of partonic 2-surfaces is developed.

2. Fractal copies of quarks is basic prediction and now a key part of the model for hadron masses. ALEPH anomaly is interpreted in terms of a fractal copy of b-quark corresponding to $k=197$.
3. The possible signatures of M_{89} hadron physics in e^+e^- annihilation experiments are discussed using a naive scaling of ordinary hadron physics.
4. The possibility that the newly born concept of Pomeron of Regge theory might be identified as the sea of perturbative QCD is considered.
5. In p-adic context exotic representations of Super Virasoro with $M^2 \propto p^k$, $k = 1, 2, \dots$ are possible. For $k = 1$ the states of these representations have same mass scale as elementary particles although in real context the masses would be gigantic. This inspires the question whether non-perturbative aspects of hadron physics could be assigned to the presence of these representations. The prospects for this are promising. Pion mass is almost exactly equal to the mass of lowest state of the exotic representation for $k = 107$ and Regge slope for rotational excitations of hadrons is predicted with three per cent accuracy assuming that they correspond to the states of $k = 101$ exotic Super Virasoro representations. This leads to the idea that hadronization and fragmentation correspond to phase transitions between ordinary and exotic Super Virasoro representations and that there is entire fractal hierarchy of hadrons inside hadrons and QCD:s inside QCD:s corresponding to p-adic length scales $L(k)$, $k = 107, 103, 101, 97, \dots$

Cosmic primes and Mersenne primes

p-Adic length scale hypothesis suggests the existence of a scaled up copy of hadron physics associated with each Mersenne prime $M_n = 2^n - 1, n$ prime: M_{107} corresponds to ordinary hadron physics. There is some evidence for exotic hadrons. Centauro events and the peculiar events associated with $E > 10^5$ GeV radiation from Cygnus X-3 could be understood as due to the decay of gamma rays to M_{89} hadron pair in the atmosphere. The decay $\pi_n \rightarrow \gamma\gamma$ produces a peak in the spectrum of the cosmic gamma rays at energy $\frac{m(\pi_n)}{2}$ and there is evidence for the peaks at energies $E_{89} \simeq 34$ GeV and $E_{31} \simeq 3.5 \cdot 10^{10}$ GeV. The absence of the peak at $E_{61} \simeq 1.5 \cdot 10^6$ GeV can be understood as due to the strong absorption caused by the e^+e^- pair creation with photons of the cosmic microwave background. Cosmic string decays $cosmic\ string \rightarrow M_2\ hadrons \rightarrow M_3\ hadrons \dots \rightarrow M_{107}\ hadrons$ is a new source of cosmic rays. The mechanism could explain the change of the slope in the hadronic cosmic ray spectrum at M_{61} pion rest energy $3 \cdot 10^6$ GeV. The cosmic ray radiation at energies near 10^9 GeV apparently consisting of protons and nuclei not lighter than Fe might be actually dominated by gamma rays: at these energies γ and p induced showers have same muon content and the decays of gamma rays to M_{89} and M_{61} hadrons in the atmosphere can mimic the presence of heavy nuclei in the cosmic radiation.

Anomalously large direct CP breaking in $K - \bar{K}$ system and exotic gluons

The recently observed anomalously large direct CP breaking in $K_L \rightarrow \pi\pi$ decays is explained in terms of loop corrections due to the predicted 2 exotic gluons having masses around 33.6 GeV. It will be also found that the TGD version of the chiral field theory believed to provide a phenomenological low energy description of QCD differs from its standard model version in that quark masses are replaced in TGD framework with shifts of quark masses induced by the vacuum expectation values of the scalar meson fields. This conforms with the TGD view about Higgs mechanism as causing only small mass shifts. It must be however emphasized that there is an argument suggesting that the vacuum expectation value of Higgs in fermionic case does not even make sense.

6.2 Exotic particles predicted by TGD

Besides lepto-hadrons and M_{89} hadrons TGD suggests also other new physics effects such as higher generations for bosons and fractally scaled up versions of quarks. The basic challenge is to decide on experimental grounds whether partonic vertices correspond to fusions or branchings and the physics of $M\bar{M}$ systems allows to do this. More exotic effects are related to the new concept of space

time: for example the concept of topological evaporation (formation of Baby Universes in elementary particle length scale) suggests an explanation for the Pomeron. Also exotic p-adic Super Virasoro representations for which the CP_2 mass scale is replaced effectively divided by a power of p can be considered as possible associated with non-perturbative aspects of hadronic physics.

6.2.1 Higher gauge boson families

TGD predicts that also gauge bosons, with gravitons included, should be characterized by family replication phenomenon but not quite in the expected manner. The first expectation was that these gauge bosons would have at least 3 light generations just like quarks and leptons.

Only within last two years it has become clear that there is a deep difference between fermions and gauge bosons. Elementary fermions and particles super-conformally related to elementary fermions correspond to single throat of a wormhole contact assignable to a topologically condensed CP_2 type vacuum extremal whereas gauge bosons would correspond to a wormhole throat pair assignable to wormhole contact connecting two space-time sheets. Wormhole throats correspond to light-like partonic 3-surfaces at which the signature of the induced metric changes.

In the case of 3 generations gauge bosons can be arranged to octet and singlet representations of a dynamical $SU(3)$ and octet bosons for which wormhole throats have different genus could be massive and effectively absent from the spectrum.

Exotic gauge boson octet would induce particle reactions in which conserved handle number would be exchanged between incoming particles such that total handle number of boson would be difference of the handle numbers of positive and negative energy throat. These gauge bosons would induce flavor changing but genus conserving neutral current. There is no evidence for this kind of currents at low energies which suggests that octet mesons are heavy. Typical reaction would be $\mu + e \rightarrow e + \mu$ scattering by exchange of $\Delta g = 1$ exotic photon.

New view about interaction vertices and bosons

There are two options for the identification of particle vertices as topological vertices.

1. Option a)

The original assumption was that one can assign also to bosons a partonic 2-surface X^2 with more or less well defined genus g . The hypothesis is consistent with the view that particle reactions are described by smooth 4-surfaces with vertices being singular 3-surfaces intermediate between two three-topologies. The basic objection against this option is that it can induce too high rates for flavor changing currents. In particular $g > 0$ gluons could induce these currents. Second counter argument is that stable $n > 4$ -particle vertices are not possible.

2. Option b)

According to the new vision (option 2)), particle decays correspond to branchings of the partonic 2-surfaces in the same sense as the vertices of the ordinary Feynman diagrams do correspond to branchings of lines. The basic mathematical justification for this vision is the enormous simplification caused by the fact that vertices correspond to non-singular 2-manifolds. This option allows also $n > 3$ -vertices as stable vertices.

A consistency with the experimental facts is achieved if the observed gauge bosons have each value of $g(X^2)$ with the same probability. Hence the general boson state would correspond to a phase $\exp(in2\pi g/3)$, $n = 0, 1, 2$, in the discrete space of 3 lowest topologies $g = 0, 1, 2$. The observed bosons would correspond to $n = 0$ state and exotic higher states to $n = 1, 2$.

The nice feature of this option is that no flavor changing neutral electro-weak or color currents are predicted. This conforms with the fact that CKM mixing can be understood as electro-weak phenomenon described most naturally by causal determinants X_l^3 (appearing as lines of generalized Feynman diagram) connecting fermionic 2-surfaces of different genus.

Consider now objections against this scenario.

1. Since the modular contribution does not depend on the gradient of the elementary particle vacuum functional but only on its logarithm, all three boson states should have mass squared which is the average of the mass squared values $M^2(g)$ associated with three generations. The fact that

modular contribution to the mass squared is due to the super-symplectic thermodynamics allows to circumvent this objection. If the super-symplectic p-adic temperature is small, say $T_p = 1/2$, then the modular contribution to the mass squared is completely negligible also for $g > 0$ and photon, graviton, and gluons could remain massless. The wiggling of the elementary particle vacuum functionals at the boundaries of the moduli spaces \mathcal{M}_g corresponding to 2-surfaces intermediate between different 2-topologies (say pinched torus and self-touching sphere) caused by the change of overall phase might relate to the higher p-adic temperature T_p for exotic bosons.

2. If photon states had a 3-fold degeneracy, the energy density of black body radiation would be three times higher than it is. This problem is avoided if the the super-symplectic temperature for $n = 1, 2$ states is higher than for $n = 0$ states, and same as for fermions, say $T_p = 1$. In this case two mass degenerate bosons would be predicted with mass squared being the average over the three genera. In this kind of situation the factor $1/3$ could make the real mass squared very large, or order CP_2 mass squared, unless the sum of the modular contributions to the mass squared values $M_{mod}^2(g) \propto n(g)$ is divisible by 3. This would make also photon, graviton, and gluons massive. Fortunately, $n(g)$ is divisible by 3 as is clear from $n(0) = 0$, $n(1) = 9$, $n(2) = 60$.

Masses of genus-octet bosons

For option 1) ordinary bosons are accompanied by $g > 0$ massive partners. For option 2) both ordinary gauge bosons and their exotic partners have suffered maximal topological mixing in the case that they are singlets with respect to the dynamical $SU(3)$. There are good reasons to expect that Higgs mechanism for ordinary gauge bosons generalizes as such and that $1/T_p > 1$ means that the contribution of p-adic thermodynamics to the mass is negligible. The scale of Higgs boson expectation would be given by p-adic length scale and mass degeneracy of octet is expected. A good guess is obtained by scaling the masses of electro-weak bosons by the factor $2^{(k-89)/2}$. Also the masses of genus-octet of gluons and photon should be non-vanishing and induced by a vacuum expectation of Higgs particle which is electro-weak singlet but genus-octet.

Indications for genus-generation correspondence for gauge bosons

Tommaso Dorigo is a highly inspiring blogger since he writes from the point of view of experimental physicist without the burden of theoretical dogmas. I share with him also the symptoms of splitting of personality to fluctuation-enthusiast and die-hard skeptic. This makes life interesting but not easy. This time Tommaso told about the evidence for new neutral gauge boson states in $p\bar{p}$ collisions. The title of the posting was "A New Z' Boson at 240 GeV? No, Wait, at 720!?" [97].

1. The findings

The title tells that the tentative interpretation of these states are as excited states of Z^0 boson and that the masses of the states are around 240 GeV and 720 GeV. The evidence for the new states comes from electron-positron pairs in relatively narrow energy interval produced by the decays of the might-be-there gauge boson. This kind of decay is an especially clean signature since strong interaction effects are not present and it appears at sharp energy.

240 GeV bump was reported by CDF last year [104] CDF last year in $p\bar{p}$ collisions at $\sqrt{s} = 1.96$ TeV. The probability that it is a fluctuation is .6 per cent. What is encouraging that also D0 found the same bump. If the particle in question is analogous to Z^0 , it should decay also to muons. CDF checked this and found a negative result. This made Tommaso rather skeptic.

Also indications for 720 GeV resonance (720 GeV is just a nominal value, the mass could be somewhere between 700-800 GeV) was reported by D0 collaboration: the report is titled as "Search for high-mass narrow resonances in the di-electron channel at D0" [75]. There are just 2 events above 700 GeV but background is small: just three events above 600 GeV. It is easy to guess what skeptic would say.

Before continuing I want to make clear that I refuse to be blind believer or die-hard skeptic and that I am unable to say anything serious about the experimental side. I am just interested to see whether these events might be interpreted in TGD framework. TGD indeed predicts -or should I say strongly suggests- a lot of new physics above intermediate boson length scale.

2. Are exotic Z^0 bosons p-adically scaled up variants of ordinary Z^0 boson?

p-Adic length scale hypothesis allows the p-adic length scale characterized by prime $p \simeq 2^k$ vary since k can have several integer values. The TGD counterpart of Gell-Mann-Okubo mass formula involves varying value of k for quark masses. Several anomalies reported by Tommaso during years could be resolved if k can have several values. Last anomaly was the discovery that Ω_b baryon containing two strange quarks and bottom quark seems to appear with two masses differing by about 100 MeV. TGD explains the mass difference correctly by assuming that strange quark can have besides ordinary mass scale mass differing by factor of 2. The prediction is 105 MeV.

One can look whether p-adic length scale hypothesis could explain the masses of exotic Z^0 candidates as multiples of half octaves of Z^0 mass which is 91 GeV. $k=3$ would give 257 GeV, not too far from 240 GeV. $k=6$ would give 728 GeV consistent with the nominal value of the mass. Also other masses are predicted and this could serve as a test for the theory. This option does not however explain why muon pairs are not produced in the case of 240 GeV resonance.

3. Support for topological explanation of family replication phenomenon?

The improved explanation is based on TGD based view about family replication phenomenon [22].

1. In TGD the explanation of family replication is in terms of genus of 2-dimensional partonic surface representing fermion. Fermions correspond to SU(3) triplet of a dynamical symmetry assignable to the three lowest genera (sphere, torus, sphere with two handles). Bosons as wormhole contacts have two wormhole throats carrying fermion numbers and correspond to SU(3) singlet and octet. Sooner or later the members of the octet - presumably heavier than singlet - should be observed (maybe this has been done now;-)).
2. The exchange of these particles predicts also charged flavor changing currents respecting conservation of corresponding "isospin" and "hypercharge." For instance, lepton quark scattering $e + s \rightarrow \mu + d$ would be possible. The most dramatic signature of these states is production of muon-positron pairs (for instance) via decays.
3. Since the Z^0 or photon like boson in question has vanishing "isospin" and "hypercharge", it must be orthogonal to the ordinary Z^0 which couples identically to all families. There are two states of this kind and they correspond to superpositions of fermion pairs of different generations in TGD framework. The two bosons - very optimistically identified as 240 GeV and 720 GeV Z^0 , must be orthogonal to the ordinary Z^0 . This requires that the phase factors in superposition of pairs adjust themselves properly. Also mixing effects breaking color symmetry are possible and expected to occur since the SU(3) in question is not an exact symmetry. Hence the exotic Z^0 bosons *could* couple preferentially to some fermion generation. This kind of mixing might be used to explain the absence of muon pair signal in the case of 240 GeV resonance.
4. The prediction for the masses is same as for the first option if the octet and singlet bosons have identical masses for same p-adic mass scale so that mass splitting between different representations would take place via the choice of the mass scale alone.

4. Could scaled up copy of hadron physics involved?

One can also ask whether these particles could come from the decays of hadrons of a scaled up copy of hadron physics strongly suggested by p-Adic length scale hypothesis.

1. Various hadron physics would correspond to Mersenne primes: standard hadron physics to M_{107} and new hadron physics to Mersenne prime $M_{89} = 2^{89} - 1$. The first guess for the mass scale of "light" M_{89} hadrons would be $2^{(107-89)/2} = 512$ times that for ordinary hadrons. The electron pairs might result in a decay of scaled up variant of pseudoscalar mesons π , η , or of η' or spin one ρ and ω mesons with nearly the same mass. Only scaled up ρ and ω mesons remains under consideration if one assumes spin 1.
2. The scaling of pion mass about 140 MeV gives 72 GeV. This is three times smaller than 240 GeV but this is extremely rough estimate. Actually it is the p-adic mass scale of quarks involved which matters rather than that of hadronic space-time sheet characterized by M_{89} . The naive scaling of the mass of η meson with mass 548 MeV would give about 281 GeV. η' would give 490 GeV. ρ meson with mass would give 396 GeV. The estimates are just order of magnitude estimates since the mass splitting between pseudoscalar and corresponding vector meson is sensitive to quark mass scale.

3. This option does not provide any explanation for the lack of muon pairs in decays of 240 GeV resonance.

To conclude, family replication phenomenon for gauge bosons is consistent with the claimed masses and also absence of muon pairs might be understood and it remains to be seen whether only statistical fluctuations are in question.

6.2.2 Does TGD allow the counterpart of space-time super-symmetry

The question whether TGD allows space-time super-symmetry or something akin to it has been a longstanding problem. A considerable progress in the respect became possible with the better understanding of the modified Dirac equation. At the same time I learned about almost 15 year old striking $e\bar{e}\gamma\gamma + \cancel{E}$ detected by CDF collaboration [70, 89] from Tommaso Dorigo's blog [101].

Basic data bits

Let us first summarize the data bits about possible relevance of super-symmetry for TGD before the addition of the 3-D measurement interaction term to the modified Dirac action [33, 55].

1. Right-handed covariantly constant neutrino spinor ν_R defines a super-symmetry in CP_2 degrees of freedom in the sense that Dirac equation is satisfied by covariant constancy and there is no need for the usual ansatz $\Psi = D\Psi_0$ giving $D^2\Psi = 0$. This super-symmetry allows to construct solutions of Dirac equation in CP_2 [44, 17, 47, 45].
2. In $M^4 \times CP_2$ this means the existence of massless modes $\Psi = \cancel{p}\Psi_0$, where Ψ_0 is the tensor product of M^4 and CP_2 spinors. For these solutions M^4 chiralities are not mixed unlike for all other modes which are massive and carry color quantum numbers depending on the CP_2 chirality and charge. As matter fact, covariantly constant right-handed neutrino spinor mode is the only color singlet. The mechanism leading to non-colored states for fermions is based on super-conformal representations for which the color is neutralized [26, 26]. The negative conformal weight of the vacuum also cancels the enormous contribution to mass squared coming from mass in CP_2 degrees of freedom.
3. Right-handed covariantly constant neutrino allows to construct the gamma matrices of the world of classical worlds (WCW) as fermionic counterparts of Hamiltonians of WCW. This gives rise super-symplectic symmetry algebra having interpretation also as a conformal algebra. Also more general super-conformal symmetries exist.
4. Space-time (in the sense of Minkowski space M^4) super-symmetry in the conventional sense of the word is impossible in TGD framework since it would require Majorana spinors. In 8-D space-time with Minkowski signature of metric Majorana spinors are definitely ruled out by the standard argument leading to super string model. Majorana spinors would also break separate conservation of lepton and baryon numbers in TGD framework.

Could one generalize super-symmetry?

Could one then consider a more general space-time super-symmetry with "space-time" identified as space-time surface rather than Minkowski space?

1. The TGD variant of the super-symmetry could correspond quite concretely to the addition to fermion and boson states right-handed neutrinos. Since right-handed neutrinos do not have electro-weak interactions, the addition might not appreciably affect the mass formula although it could affect the p-adic prime defining the mass scale.
2. The problem is to understand what this addition of the right-handed neutrino means. To begin with, notice that in TGD Universe fermions reside at light-like 3-surfaces at which the signature of induced metric changes. Bosons correspond to pairs of light-like wormhole throats with wormhole contact having Euclidian signature of the induced metric. It is essential that either fermion or antifermion in the boson state carries what might be called un-physical polarization

in the standard conceptual framework. Only in this manner the helicities can come out correctly. The assumption that the bosonic wormhole throats correspond to positive and negative energy space-time sheets realizes this constraint in the framework of zero energy ontology.

3. The super-symmetry as an addition to the fermion state a second wormhole throats carrying right handed neutrino quantum numbers does not make sense since the resulting state cannot be distinguished from gauge boson or Higgs type particle. The light-like 3-surfaces can however carry fermion numbers up to the number of modes of the induced spinor field, which is expected to be infinite inside string like objects having wormhole throats at ends and finite when one has space time sheets containing the throats [55]. In very general sense one could say that each mode defines a very large broken N -super-symmetry with the value of N depending on state and light-like 3-surface. The breaking of this super-symmetry would come from electro-weak -, color -, and gravitational interactions. Right-handed neutrino would by its electro-weak and color inertness define a minimally broken super-symmetry.
4. What this addition of the right handed neutrinos or more general fermion modes could precisely mean? One cannot assign fermionic oscillator operators to right handed neutrinos which are covariantly constant in both M^4 and CP_2 degrees of freedom since the modes with vanishing energy (frequency) cannot correspond to fermionic oscillator operator creating a physical state since one would have $a = a^\dagger$. The intuitive view is that all the spinor modes move in an exactly collinear manner -somewhat like quarks inside hadron do approximately.

Modified Dirac equation briefly

The answer to the question what "collinear motion" means mathematically emerged from the recent progress in the understanding of the modified Dirac equation.

1. The modified Dirac action involves two terms. Besides the original 4-D modified Dirac action there is measurement interaction which can be localized to wormhole throat or to any light-like 3-surfaces "parallel" to it in the slicing of space-time sheet by light-like 3-surfaces. This term correlates space-time geometry with quantum numbers assignable to super-conformal representations and is also necessary to obtain almost-stringy propagator.
2. The modified Dirac equation with measurement action added reads as

$$\begin{aligned}
 D_K \Psi &= 0 , \\
 D_3 \Psi &= (D_{C-S} + Q \times O) \Psi = 0 , \\
 [D_3, D_K] \Psi &= 0 .
 \end{aligned}
 \tag{6.2.-1}$$

- (a) D_K corresponds formally to 4-D massless Dirac equation in X^4 . D_3 realizes measurement interaction. D_{C-S} is the 3-D modified Dirac action defined by Chern-Simons action.
- (b) Q is linear in Cartan algebra generators of the isometry algebra of imbedding space (color isospin and hypercharge plus four-momentum or two components of four momentum and spin and boost in direction of 3-momentum). Q is expressible as

$$Q = Q_A \partial_\alpha h^k g^{AB} j_{Bk} \hat{\Gamma}_{CS}^\alpha .
 \tag{6.2.0}$$

Here Q_A is Cartan algebra generator acting on physical states. Physical states must be eigen states of Q_A since otherwise the equations do not make sense. g^{AB} is the inverse of the matrix defined by the imbedding space inner product of Killing vector fields j_A^k and j_B^l : its existence allows only Cartan algebra charges. $\hat{\Gamma}_{CS}^\alpha$ is the modified gamma matrix associated with the Chern-Simons action.

(c) In general case the modified gamma matrices are defined in terms of action density L as

$$\hat{\Gamma}^\alpha = \frac{\partial L}{\partial_\alpha h^k} \gamma^k . \quad (6.2.1)$$

γ^k denotes imbedding space gamma matrices.

- (d) The operator O characterizes the conserved fermionic current to which Cartan algebra generators of isometries couple. The simplest conserved currents correspond to quark or lepton currents and corresponding vectorial isospin- and spin currents [55]. Besides this there is an infinite hierarchy of conserved currents relating to quantum criticality and in one-one correspondence with vanishing second variations of Kähler action for preferred extremal. These couplings allow to represent measurement interaction for any observable.
3. The equation $D_3\nu_R = 0$ would reduce for vanishing color charges and covariantly constant spinor to the analog of algebraic fermionic on mass shell condition $p_A\gamma^A\nu_R = 0$ since Q is obtained by projecting the total four-momentum of the parton state interpreted as a vector-field of H to the space-time surface and by replacing ordinary gamma matrices with the modified ones. This equation cannot be exact since Q depends on the point of the light-like 3-surface so that covariant constancy fails and D_{C-S} cannot annihilate the state. This is the space-time correlate for the breaking of super-symmetry. The action of the Cartan algebra generators is purely algebraic and on the state of super-conformal representations rather than that of a differential operator on spinor field. The modified equation implies that all spinor modes represent fermions moving collinearly in the sense an equation with the same total four-momentum and total color quantum numbers is satisfied by all of them. Note that p_A represents the total four-momentum of the state rather than individual four-momenta of fermions.

TGD counterpart of space-time super-symmetry

This picture allows to define more precisely what one means with the approximate super-symmetries in TGD framework.

1. One can in principle construct many-fermion states containing both fermions and anti-fermions at given light-like 3-surface. The four-momenta of states related by super-symmetry need not be same. Super-symmetry breaking is present and has as the space-time correlate the deviation of the modified gamma matrices from the ordinary M^4 gamma matrices. In particular, the fact that $\hat{\Gamma}^\alpha$ possesses CP_2 part in general means that different M^4 chiralities are mixed: a space-time correlate for the massivation of the elementary particles.
2. For right-handed neutrino super-symmetry breaking is expected to be smallest but also in the case of the right-handed neutrino mode mixing of M^4 chiralities takes place and breaks the TGD counterpart of super-symmetry.
3. The fact that all helicities in the state are physical for a given light-like 3-surface has important implications. For instance, the addition of a right-handed antineutrino to right-handed (left-handed) electron state gives scalar (spin 1) state. Also states with fermion number two are obtained from fermions. For instance, for e_R one obtains the states $\{e_R, e_R\nu_R\bar{\nu}_R, e_R\bar{\nu}_R, e_R\nu_R\}$ with lepton numbers $(1, 1, 0, 2)$ and spins $(1/2, 1/2, 0, 1)$. For e_L one obtains the states $\{e_L, e_L\nu_R\bar{\nu}_R, e_L\bar{\nu}_R, e_L\nu_R\}$ with lepton numbers $(1, 1, 0, 2)$ and spins $(1/2, 1/2, 1, 0)$. In the case of gauge boson and Higgs type particles -allowed by TGD but not required by p-adic mass calculations- gauge boson has 15 super partners with fermion numbers $[2, 1, 0, -1, -2]$.

The cautious conclusion is that the recent view about quantum TGD allows the analog of super-symmetry which is necessary broken and for which the multiplets are much more general than for the ordinary super-symmetry. Right-handed neutrinos might however define something resembling ordinary super-symmetry to a high extent. The question is how strong prediction one can deduce using quantum TGD and proposed super-symmetry.

1. For a minimal breaking of super-symmetry only the p-adic length scale characterizing the super-partner differs from that for partner but the mass of the state is same. This would allow only a discrete set of masses for various super-partners coming as half octaves of the mass of the particle in question. A highly predictive model results.
2. The quantum field theoretic description should be based on QFT limit of TGD formulated in terms of bosonic emergence [25]. This formulation should allow to calculate the propagators of the super-partners in terms of fermionic loops.
3. This TGD variant of space-time super-symmetry resembles ordinary super-symmetry in the sense that selection rules due to the right-handed neutrino number conservation and analogous to the conservation of R-parity hold true. The states inside super-multiplets have identical electro-weak and color quantum numbers but their p-adic mass scales can be different. It should be possible to estimate reaction rates using rules very similar to those of super-symmetric gauge theories.
4. It might be even possible to find some simple generalization of standard super-symmetric gauge theory to get rough estimates for the reaction rates. There are however problems. The fact that spins $J = 0, 1, 2, 3/2, 2$ are possible for super-partners of gauge bosons forces to ask whether these additional states define an analog of non-stringy strong gravitation. Note that graviton in TGD framework corresponds to a pair of wormhole throats connected by flux tube (counterpart of string) and for gravitons one obtains 2^8 -fold degeneracy.

Experimental indication for space-time super-symmetry

There is experimental indication for super-symmetry dating back to 1995 [70]. The event involves $e^+e^-\gamma\gamma$ plus missing transverse energy \cancel{E}_T . The electron-positron pair has transversal energies $E_T = (36, 59)$ GeV and invariant mass $M_{ee} = 165$ GeV. The two photons have transversal energies (30,38) GeV. The missing transverse energy is $\cancel{E}_T = 53$ GeV. The cross sections for these events in standard model are too small to be observed. Statistical fluctuation could be in question but one could also consider the event as an indication for super-symmetry.

In [89] an explanation of the event in terms of minimal super-symmetric standard model (MSSM) was proposed.

1. The collision of proton and antiproton would induce an annihilation of quark and antiquark to selectron pair $\tilde{e}^-\tilde{e}^+$ via virtual photon or Z^0 boson with the mass of \tilde{e} in the range (80,130) GeV (the upper bound comes from the total energy of the particles involved).
2. \tilde{e}^\pm would in turn decay to e^\pm and neutralino χ_2^0 ad χ_2^0 to the lightest super-symmetric particle χ_1^0 and photon. The neutralinos are in principle mixtures of the super partners associated with γ , Z^0 , and neutral higgs h (there are two of them in minimal super-symmetric generalization of standard model). The highest probability for the chain is obtained if χ_2^0 is gluino and χ_1^0 is higgsino.
3. The kinematics of the event allows to deduce the bounds

$$\begin{aligned}
 80 &< m(\tilde{e})/GeV < 130 \quad , \\
 38 &\leq m(\chi_2^0)/GeV \leq \min [1.12m(\tilde{e})/GeV - 37, 95 + 0.17m(\chi_1^0)/GeV] \quad , \\
 m(\chi_1^0)/GeV &\leq m(\chi_2^0)/GeV \leq \min [1.4m(\tilde{e})/GeV - 105, 1.6m(\chi_2^0)/GeV - 60] \quad .
 \end{aligned}
 \tag{6.2.-1}$$

4. Sfermion production rate depends only on masses of the sfermions, so that slepton production cross section decouples from the analysis of particular scenarios. The cross section is at the level of $\sigma = 10$ fb and consistent with data (one event!). The parameters of MSSM are super-symmetric soft-breaking parameters, super-potential parameters, and the parameter $\tan(\beta)$. This allows to derive more stringent limits on the masses and parameters of MSSM.

Consider now the explanation of the event in TGD framework.

1. By the properties of super-partners the production rate for $\tilde{e}^- \tilde{e}^+$ is predicted to be same as in MSSM for $\tilde{e} = e_R \tilde{\nu}_R$. Same order of magnitude is predicted also for more exotic super-partners such as $e_L \tilde{\nu}_R$ with spin 1.
2. In TGD framework it is safest to use just the kinematical bounds on the masses and p-adic length scale hypothesis. If super-symmetry breaking means same mass formula from p-adic thermodynamics but in a different p-adic mass scale, $m(\tilde{e})$ is related by a power of $\sqrt{2}$ to $m(e)$. Using $m(\tilde{e}) = 2^{(127-k(\tilde{e}))/2} m(e)$ one finds that the mass range [80, 130] GeV allows two possible masses for selectron corresponding to $p \simeq 2^k$, $k = 91$ with $m(\tilde{e}) = 131.1$ GeV and $k = 92$ with $m(\tilde{e}) = 92.7$ GeV. The bounds on $m(Z)$ leave only the option $m(\tilde{Z}) = m(Z) = 91.2$ GeV and $m(\tilde{e}) = 131.1$ GeV.
3. The indirect determinations of Higgs masses from experimental data seem to converge to two different values. The first one would correspond to $m(h) = 129$ GeV and $k(h) = 94$ and second one to $m(h) = 91$ GeV with $k(h) = 95$ [26]. The fact that already the TGD counterpart for the Gell-Mann-Okubo mass formula in TGD framework requires quarks to exist at several p-adic mass scales [17], suggests that Higgs can exist in both of these mass scales depending on the experimental situation. The mass of Higgsino would correspond to some half octave of $m(h)$. Note that the model allows to conclude that Higgs indeed exists also in TGD Universe although it does not seem to play the same role in particle massivation as in the standard model. The bounds allow only $k(\tilde{h}) = k(h) + 3 = 97$ and $m(\tilde{h}) = 45.6$ GeV for $m(h) = 129$ GeV. The same mass is obtained for $m(h) = 91$ GeV. Therefore the kinematic limits plus super-symmetry breaking at the level of p-adic mass scale fix completely the masses of the super-particles involved in absence of mixing effects for sneutralinos. To sum up, the masses of sparticles involved are predicted to be

$$m(\tilde{e}) = 131 \text{ GeV} , \quad m(\tilde{Z}^0) = 91.2 \text{ GeV} , \quad m(\tilde{h}) = 45.6 \text{ GeV} . \quad (6.2.0)$$

6.2.3 The physics of $M - \bar{M}$ systems forces the identification of vertices as branchings of partonic 2-surfaces

For option 2) gluons are superpositions of $g = 0, 1, 2$ states with identical probabilities and vertices correspond to branchings of partonic 2-surfaces. Exotic gluons do not induce mixing of quark families and genus changing transitions correspond to light like 3-surfaces connecting partonic 2-surfaces with different genera. CKM mixing is induced by this topological mixing. The basic testable predictions relate to the physics of $M\bar{M}$ systems and are due to the contribution of exotic gluons and large direct CP breaking effects in $K - \bar{K}$ favor this option.

For option 1) vertices correspond to fusions rather than branchings of the partonic 2-surfaces. The prediction that quarks can exchange handle number by exchanging $g > 0$ gluons (to be denoted by G_g in the sequel) could be in conflict with the experimental facts.

1. CP breaking in $K - \bar{K}$ as a basic test

CP breaking physics in kaon-antikaon and other neutral pseudoscalar meson systems is very sensitive to the new physics. What makes the situation especially interesting, is the recently reported high precision value for the parameter ϵ'/ϵ describing direct CP breaking in kaon-antikaon system [65]. The value is almost by an order of magnitude larger than the standard model expectation. $K - \bar{K}$ mass difference predicted by perturbative standard model is 30 per cent smaller than the the experimental value and one cannot exclude the possibility that new physics instead of/besides non-perturbative QCD might be involved.

In standard model the low energy effective action is determined by box and penguin diagrams. $\Delta S = 2$ piece of the effective weak Lagrangian, which describes processes like $s\bar{d} \rightarrow d\bar{s}$, determines the value of the $K - \bar{K}$ mass difference Δm_K and since this piece determines $K \rightarrow \bar{K}$ amplitude it also contributes to the parameter ϵ characterizing indirect CP breaking. $\Delta S = 2$ part of the weak effective action corresponds to box diagrams involving two W boson exchanges.

2. Δm_K kills option a

For option 1) box diagrams involving Z and $g > 0$ exchanges are allowed provided exchanges correspond to exchange of both Z and $g > 0$ gluon. The most obvious objection is that the exchanges of $g > 0$ gluons make strong $\Delta S > 0$ decays of mesons possible: $K_S \rightarrow \pi\pi$ is a good example of this kind of decay. The enhancement of the decay rate would be of order $(\alpha_s(g=1)/\alpha_{em})^2(m_W/m_G(g=1))^2 \sim 10^3$. Also other $\Delta S = 1$ decay rates would be enhanced by this factor. The real killer prediction is a gigantic value of Δm_K for kaon-antikaon system resulting from the possibility of $\bar{s}d \rightarrow \bar{d}s$ decay by single $g = 1$ gluon exchange. This prediction alone excludes option 1).

3. Option 2) could explain direct CP breaking

For option 2) box diagrams are not affected in the lowest order by exotic gluons. The standard model contributions to Δm_K and indirect CP breaking are correct for the observed value of the top quark mass which results if top corresponds to a secondary padic length scale $L(2, k)$ associated with $k = 47$ (Appendix). Higher order gluonic contribution could increase the value of Δm_K predicted to be about 30 per cent too small by the standard model.

In standard model penguin diagrams contribute to $\Delta S = 1$ piece of the weak Lagrangian, which determines the direct CP breaking characterized by the parameter ϵ'/ϵ . Penguin diagrams, which describe processes like $s\bar{d} \rightarrow d\bar{d}$, are characterized by effective vertices dsB , where B denotes photon, gluon or Z boson. dsB vertices give the dominant contribution to direct CP breaking in standard model. The new penguin diagrams are obtained from ordinary penguin diagrams by replacing ordinary gluons with exotic gluons.

For option 2) the contributions predicted by the standard model are multiplied by a factor 3 in the approximation that exotic gluon mass is negligible in the mass scale of intermediate gauge boson. These diagrams affect the value of the parameter ϵ'/ϵ characterizing direct CP breaking in $K - \bar{K}$ system found experimentally to be almost order of magnitude larger than standard model expectation [65].

6.2.4 Super-symplectic bosons

TGD predicts also exotic bosons which are analogous to fermion in the sense that they correspond to single wormhole throat associated with CP_2 type vacuum extremal whereas ordinary gauge bosons corresponds to a pair of wormhole contacts assignable to wormhole contact connecting positive and negative energy space-time sheets. These bosons have super-conformal partners with quantum numbers of right handed neutrino and thus having no electro-weak couplings. The bosons are created by the purely bosonic part of super-symplectic algebra [22, 33], whose generators belong to the representations of the color group and 3-D rotation group but have vanishing electro-weak quantum numbers. Their spin is analogous to orbital angular momentum whereas the spin of ordinary gauge bosons reduces to fermionic spin. Recall that super-symplectic algebra is crucial for the construction of configuration space Kähler geometry. If one assumes that super-symplectic gluons suffer topological mixing identical with that suffered by say U type quarks, the conformal weights would be (5,6,58) for the three lowest generations. The application of super-symplectic bosons in TGD based model of hadron masses is discussed in [17] and here only a brief summary is given.

As explained in [17], the assignment of these bosons to hadronic space-time sheet is an attractive idea.

1. Quarks explain only a small fraction of the baryon mass and that there is an additional contribution which in a good approximation does not depend on baryon. This contribution should correspond to the non-perturbative aspects of QCD. A possible identification of this contribution is in terms of super-symplectic gluons. Baryonic space-time sheet with $k = 107$ would contain a many-particle state of super-symplectic gluons with net conformal weight of 16 units. This leads to a model of baryons masses in which masses are predicted with an accuracy better than 1 per cent.
2. Hadronic string model provides a phenomenological description of non-perturbative aspects of QCD and a connection with the hadronic string model indeed emerges. Hadronic string tension is predicted correctly from the additivity of mass squared for $J = 2$ bound states of super-symplectic quanta. If the topological mixing for super-symplectic bosons is equal to that for U

type quarks then a 3-particle state formed by 2 super-symplectic quanta from the first generation and 1 quantum from the second generation would define baryonic ground state with 16 units of conformal weight. A very precise prediction for hadron masses results by assuming that the spin of hadron correlates with its super-symplectic particle content.

3. Also the baryonic spin puzzle caused by the fact that quarks give only a small contribution to the spin of baryons, could find a natural solution since these bosons could give to the spin of baryon an angular momentum like contribution having nothing to do with the angular momentum of quarks.
4. Super-symplectic bosons suggest a solution to several other anomalies related to hadron physics. The events observed for a couple of years ago in RHIC [77] suggest a creation of a black-hole like state in the collision of heavy nuclei and inspire the notion of color glass condensate of gluons, whose natural identification in TGD framework would be in terms of a fusion of hadronic space-time sheets containing super-symplectic matter materialized also from the collision energy. In the collision, valence quarks connected together by color bonds to form separate units would evaporate from their hadronic space-time sheets in the collision, and would define TGD counterpart of Pomeron, which experienced a reincarnation for few years ago [63]. The strange features of the events related to the collisions of high energy cosmic rays with hadrons of atmosphere (the particles in question are hadron like but the penetration length is anomalously long and the rate for the production of hadrons increases as one approaches surface of Earth) could be also understood in terms of the same general mechanism.

6.2.5 A new twist in the spin puzzle of proton

The so called proton spin crisis or spin puzzle of proton was an outcome of the experimental finding that the quarks contribute only 13-17 per cent of proton spin [62, 60] whereas the simplest valence quark model predicts that quarks contribute about 75 per cent to the spin of proton with the remaining 25 per cent being due to the orbital motion of quarks. Besides the orbital motion of valence quarks also gluons could contribute to the spin of proton. Also polarized sea quarks can be considered as a source of proton spin.

Quite recently, the spin crisis got a new twist [99]. One of the few absolute predictions of perturbative QCD (pQCD) is that at the limit, when the momentum fraction of quark approaches unity, quark spin should be parallel to the proton spin. This is due to the helicity conservation predicted by pQCD in the lowest order. The findings are consistent with this expectation in the case of protonic u quarks but not in the case of protonic d quark. The discovery is of a special interest from the point of view of TGD since it might have an explanation involving the notions of many-sheeted space-time, of color-magnetic flux tubes, the predicted super-symplectic "vacuum" spin, and also the concept of quantum parallel dissipation.

The experimental findings

In the experiment performed in Jefferson Lab [99] neutron spin asymmetries A_1^n and polarized structure functions $g_{1,2}^n$ were deduced for three kinematic configurations in the deep inelastic region from $e^{-3}\text{He}$ scattering using 5.7 GeV longitudinally polarized electron beam and a polarized ^3He target. A_1^n and $g_{1,2}^n$ were deduced for $x = .33, .47$, and $.60$ and $Q^2 = 2.7, 3.5$ and 4.8 $(\text{GeV}/c)^2$. A_1^n and g_1^n at $x = .33$ are consistent with the world data. At $x = .47$ A_1^n crosses zero and is significantly positive at $x = 0.60$. This finding agrees with the next-to-leading order QCD analysis of previous world data without the helicity conservation constraint. The trend of the data agrees with the predictions of the constituent quark model but disagrees with the leading order pQCD assuming hadron helicity conservation.

By isospin symmetry one can translate the result to the case of proton by the replacement $u \leftrightarrow d$. By using world proton data, the polarized quark distribution functions were deduced for proton using isospin symmetry between neutron and proton. It was found that $\Delta u/u$ agrees with the predictions of various models while $\Delta d/d$ disagrees with the leading-order pQCD.

Let us denote by $q(x) = q^\uparrow + q^\downarrow(x)$ the spin independent quark distribution function. The difference $\Delta q(x) = q^\uparrow - q^\downarrow(x)$ measures the contribution of quark q to the spin of hadron. The measurement allowed to deduce estimates for the ratios $(\Delta q(x) + \Delta \bar{q}(x))/(q(x) + \bar{q}(x))$.

The conclusion of [99] is that for proton one has

$$\frac{\Delta u(x) + \Delta \bar{u}(x)}{u(x) + \bar{u}(x)} \simeq .737 \pm .007 \quad , \quad \text{for } x = .6 \quad .$$

This is consistent with the pQCD prediction. For d quark the experiment gives

$$\frac{\Delta d(x) + \Delta \bar{d}(x)}{d(x) + \bar{d}(x)} \simeq -.324 \pm .083 \quad \text{for } x = .6 \quad .$$

The interpretation is that d quark with momentum fraction $x > .6$ in proton spends a considerable fraction of time in a state in which its spin is opposite to the spin of proton so that the helicity conservation predicted by first order pQCD fails. This prediction is of special importance as one of the few absolute predictions of pQCD.

The finding is consistent with the relativistic $SU(6)$ symmetry broken by spin-spin interaction and the QCD based model interpolated from data but giving up helicity conservation [99]. $SU(6)$ is however not a fundamental symmetry so that its success is probably accidental.

It has been also proposed that the spin crisis might be illusory [98] and due to the fact that the vector sum of quark spins is not a Lorentz invariant quantity so that the sum of quark spins in infinite-momentum frame where quark distribution functions are defined is not same as, and could thus be smaller than, the spin sum in the rest frame. The correction due to the transverse momentum of the quark brings in a non-negative numerical correction factor which is in the range $(0, 1)$. The negative sign of $\Delta d/d$ is not consistent with this proposal.

TGD based model for the findings

The TGD based explanation for the finding involves the following elements.

1. TGD predicts the possibility of vacuum spin due to the super-symplectic symmetry. Valence quarks can be modelled as a star like formation of magnetic flux tubes emanating from a vertex with the conservation of color magnetic flux forcing the valence quarks to form a single coherent structure. A good guess is that the super-symplectic spin corresponds classically to the rotation of the the star like structure.
2. By parity conservation only even values of super-symplectic spin J are allowed and the simplest assumption is that the valence quark state is a superposition of ordinary $J = 0$ states predicted by pQCD and $J = 2$ state in which all quarks have spin which is in a direction opposite to the direction of the proton spin. The state of $J = 1/2$ baryon is thus replaced by a new one:

$$\begin{aligned} |B, \frac{1}{2}, \uparrow\rangle &= a|B, 1/2, \frac{1}{2}\rangle |J = J_z = 0\rangle + b|B, \frac{3}{2}, -\frac{3}{2}\rangle |J = J_z = 2\rangle \quad , \\ |B, 1/2, \frac{1}{2}\rangle &= \sum_{q_1, q_2, q_3} c_{q_1, q_2, q_3} q_1^\uparrow q_2^\uparrow q_3^\downarrow \quad , \\ |B, \frac{3}{2}, -\frac{3}{2}\rangle &= d_{q_1, q_2, q_3} q_1^\downarrow q_2^\downarrow q_3^\downarrow \quad . \end{aligned} \tag{6.2.-1}$$

$|B, 1/2, \frac{1}{2}\rangle$ is in a good approximation the baryon state as predicted by pQCD. The coefficients c_{q_1, q_2, q_3} and d_{q_1, q_2, q_3} depend on momentum fractions of quarks and the states are normalized so that $|a|^2 + |b|^2 = 1$ is satisfied: the notation $p = |a|^2$ will be used in the sequel. The quark parts of $J = 0$ and $J = 2$ have quantum numbers of proton and Δ resonance. $J = 2$ part need not however have the quark distribution functions of Δ .

3. The introduction of $J = 0$ and $J = 2$ ground states with a simultaneous use of quark distribution functions makes sense if one allows quantum parallel dissipation. Although the system is coherent in the super-symplectic degrees of freedom which correspond to the hadron size scale, there is a de-coherence in quark degrees of freedom which correspond to a shorter p-adic length scale and smaller space-time sheets.

4. Consider now the detailed structure of the $J = 2$ state in the case of proton. If the d quark is at the rotation axis, the rotating part of the triangular flux tube structure resembles a string containing u -quarks at its ends and forming a di-quark like structure. Di-quark structure is taken to mean correlations between u -quarks in the sense that they have nearly the same value of x so that $x < 1/2$ holds true for them whereas the d -quark behaving more like a free quark can have $x > 1/2$.

A stronger assumption is that di-quark behaves like a single colored hadron with a small value of x and only the d -quark behaves as a free quark able to have large values of x . Certainly this would be achieved if u quarks reside at their own string like space-time sheet having $J = 2$.

From these assumptions it follows that if u quark has $x > 1/2$, the state effectively reduces to a state predicted by pQCD and $u(x) \rightarrow 1$ for $x \rightarrow 1$ is predicted. For the d quark the situation is different and introducing distribution functions $q^J(x)$ for $J = 0, 2$ separately, one can write the spin asymmetry at the limit $x \rightarrow 1$ as

$$\begin{aligned} A_d &\equiv \frac{\Delta d(x) + \Delta \bar{d}(x)}{d(x) + \bar{d}(x)} = \frac{p(\Delta d_0 + \Delta \bar{d}_0) + (1-p)(\Delta d_2 + \Delta \bar{d}_2)}{p(d_0 + \bar{d}_0) + (1-p)(d_2 + \bar{d}_2)}, \\ p &= |a|^2. \end{aligned} \quad (6.2-1)$$

Helicity conservation gives $\Delta d_0/d_0 \rightarrow 1$ at the limit $x \rightarrow 1$ and one has trivially $\Delta d_2/d_2 = -1$. Taking the ratio

$$y = \frac{d_2}{d_0}$$

as a parameter, one can write

$$A_d \rightarrow \frac{p - (1-p)y}{p + (1-p)y} \quad (6.2.0)$$

at the limit $x \rightarrow 1$. This allows to deduce the value of the parameter y once the value of p is known:

$$y = \frac{p}{1-p} \times \frac{1 - A_d}{1 + A_d}. \quad (6.2.1)$$

From the requirement that quarks contribute a fraction $\Sigma = \sum_q \Delta q \in (13, 17)$ per cent to proton spin, one can deduce the value of p using

$$\frac{p \times \frac{1}{2} - (1-p) \times \frac{3}{2}}{\frac{1}{2}} = \Sigma \quad (6.2.2)$$

giving $p = (3 + \Sigma)/4 \simeq .75$.

Eq. 6.2.1 allows estimate the value of y . In the range $\Sigma \in (.13, .30)$ defined by the lower and upper bounds for the contribution of quarks to the proton spin, $A_d = -.32$ gives $y \in (6.98, 9.15)$. $d_2(x)$ would be more strongly concentrated at high values of x than $d_0(x)$. This conforms with the assumption that u quarks tend to carry a small fraction of proton momentum in $J = 2$ state for which uu can be regarded as a string like di-quark state.

A further input to the model comes from the ratio of neutron and proton F_2 structure functions expressible in terms of quark distribution functions of proton as

$$R^{np} \equiv \frac{F_2^n}{F_2^p} = \frac{u(x) + 4d(x)}{4u(x) + d(x)}. \quad (6.2.3)$$

According to [99] $R^{np}(x)$ is a straight line starting with $R^{np}(x \rightarrow 0) \simeq 1$ and dropping below $1/2$ as $x \rightarrow 1$. The behavior for small x can be understood in terms of sea quark dominance. The pQCD

prediction for R^{np} is $R^{np} \rightarrow 3/7$ for $x \rightarrow 1$, which corresponds to $d/u \rightarrow z = 1/5$. TGD prediction for R^{np} for $x \rightarrow 1$

$$\begin{aligned} R^{np} &\equiv \frac{F_2^n}{F_2^p} = \frac{pu_0 + 4(pd_0 + (1-p)d_2)}{4pu_0 + pd_0 + (1-p)d_2} \\ &= \frac{p + 4z(p + (1-p)y)}{4p + z(p + (1-p)y)}. \end{aligned} \quad (6.2.3)$$

In the range $\Sigma \in (.13, .30)$ which corresponds to $y \in (6.98, 9.15)$ for $A_d = -.32$ $R^{np} = 1/2$ gives $z \simeq .1$, which is 20 per cent of pQCD prediction. 80 percent of d -quarks with large x predicted to be in $J = 0$ state by pQCD would be in $J = 2$ state.

6.2.6 Fractally scaled up versions of quarks

The strange anomalies of neutrino oscillations [88] suggesting that neutrino mass scale depends on environment can be understood if neutrinos can suffer topological condensation in several p-adic length scales [26]. The obvious question whether this could occur also in the case of quarks led to a very fruitful developments leading to the understanding of hadronic mass spectrum in terms of scaled up variants of quarks. Also the mass distribution of top quark candidate exhibits structure which could be interpreted in terms of heavy variants of light quarks. The ALEPH anomaly [105], which I first erratically explained in terms of a light top quark has a nice explanation in terms of b quark condensed at $k = 97$ level and having mass ~ 55 GeV. These points are discussed in detail in [17].

The emergence of ALEPH results [105] meant a an important twist in the development of ideas related to the identification of top quark. In the LEP 1.5 run with $E_{cm} = 130 - 140$ GeV, ALEPH found 14 e^+e^- annihilation events, which pass their 4-jet criteria whereas 7.1 events are expected from standard model physics. Pairs of dijets with vanishing mass difference are in question and dijets could result from the decay of a new particle with mass about 55 GeV.

The data do not allow to conclude whether the new particle candidate is a fermion or boson. Top quark pairs produced in e^+e^- annihilation could produce 4-jets via gluon emission but this mechanism does not lead to an enhancement of 4-jet fraction. No $b\bar{b}b\bar{b}$ jets have been observed and only one event containing b has been identified so that the interpretation in terms of top quark is not possible unless there exists some new decay channel, which dominates in decays and leads to hadronic jets not initiated by b quarks. For option 2), which seems to be the only sensible option, this kind of decay channels are absent.

Super symmetrized standard model suggests the interpretation in terms of super partners of quarks or/and gauge bosons [113]. It seems now safe to conclude that TGD does not predict sparticles. If the exotic particles are gluons their presence does not affect Z^0 and W decay widths. If the condensation level of gluons is $k = 97$ and mixing is absent the gluon masses are given by $m_g(0) = 0$, $m_g(1) = 19.2$ GeV and $m_g(2) = 49.5$ GeV for option 1) and assuming $k = 97$ and hadronic mass renormalization. It is however very difficult to understand how a pair of $g = 2$ gluons could be created in e^+e^- annihilation. Moreover, for option 2), which seems to be the only sensible option, the gluon masses are $m_g(0) = 0$, $m_g(1) = m_g(2) = 30.6$ GeV for $k = 97$. In this case also other values of k are possible since strong decays of quarks are not possible.

The strong variations in the order of magnitude of mass squared differences between neutrino families [88] can be understood if they can suffer a topological condensation in several p-adic length scales. One can ask whether also t and b quark could do the same. In absence of mixing effects the masses of $k = 97$ t and b quarks would be given by $m_t \simeq 48.7$ GeV and $m_b \simeq 52.3$ GeV taking into account the hadronic mass renormalization. Topological mixing reduces the masses somewhat. The fact that b quarks are not observed in the final state leaves only $b(97)$ as a realistic option. Since Z^0 boson mass is ~ 94 GeV, $b(97)$ does not appreciably affect Z^0 boson decay width. The observed anomalies concentrate at cm energy about 105 GeV. This energy is 15 percent smaller than the total mass of top pair. The discrepancy could be understood as resulting from the binding energy of the $b(97)\bar{b}(97)$ bound states. Binding energy should be a fraction of order $\alpha_s \simeq .1$ of the total energy and about ten per cent so that consistency is achieved.

6.2.7 What M_{89} Hadron Physics would look like?

TGD suggests the existence of the scaled up copies of hadron physics corresponding to the Mersenne primes $M_n = 89, 61, 31, \dots$ at least in the sense that α_s has maximum at these length scales. The assumption of QCD:s decoupling completely from each other seems more unrealistic.

The requirement of unitarity forces the existence of Higgs particle in gauge theories. The failure of the p-adic mass calculations to predict intermediate gauge boson masses correctly forces to give up the idea that boson masses are of purely thermodynamical origin. A possible TGD counterpart for the Higgs fields is as the fields defined by the Kac-Moody generators associated with the complement of the $u(2)$ algebra of $su(3)$ associated with the conserved charges Q_J defined by the variation of the modified Dirac action with respect to the induced Kähler form. As found in the [26], the small coupling of the Higgs to fermionic masses resolves the paradoxical situation created by the failure to detect Higgs boson. Also the fact that left handed electro-weak charge matrices are not covariantly constant could explain Higgs vacuum expectation value without an introduction of an elementary scalar field.

One could of course, consider also other explanations for Higgs. The only scalar mesons with masses in intermediate boson mass scale allowed by TGD are bound states of quark and antiquark of M_{89} hadron physics such that quark and antiquark have parallel spins and relative angular momentum $L = 1$. The effective couplings of these states to leptons and quarks could mimic the couplings of Higgs boson to some degree. Scalar bound states of heavy quarks are also present in ordinary hadron physics. The coherent states formed by these particles could mimic the effects caused by a fundamental Higgs field.

M_{89} would be obtained in the first approximation by scaling the ordinary hadron physics by the ratio $\sqrt{\frac{M_{89}}{M_{107}}}$. This implies that QCD Λ , string tension, etc. get scaled by the appropriate power of this factor. If one estimates the u_{89} mass as $m(u_{89}) = m(\rho_{89})/2$ one obtains the TGD prediction for its mass as $m(u_{89}) = 512m(\rho_{107})/2 \simeq 197 \text{ GeV}$. Defining $u(89)$ mass by scaling the mass of ordinary u quark defined as one third of proton mass one obtains u_{89} mass about 160 GeV . This estimate for u_{89} mass happened to be within experimental uncertainties equal to the mass of the top candidate discovered just when the mass calculations were carried out and led to a tentative identification of the top candidate as u_{89} .

The fact that top candidate turned out to have production and decay characteristics of the real top forced to give up this hypothesis. Also the study of CKM matrix led to the cautious conclusion that only the mass of the experimental top candidate is consistent with CP breaking observed in $K - \bar{K}$ and $B - \bar{B}$ system (Appendix). Even more, the direct calculation of the u_{89} mass from p-adic thermodynamics gives $m(u_{89}) \simeq 262 \text{ GeV}$ and demonstrates the the idea about identifying top quark as u_{89} quark was a result of sloppy order of magnitude thinking. The relatively high mass however leaves open the possibility that M_{89} physics exists.

M_{89} physics means the emergence of a new condensate level in the hadronic physics. One can visualize M_{89} hadrons as very tiny objects possibly condensed on the quarks and gluons of M_{107} hadron physics. The New Physics begins to reveal itself, when the collision energy is so high that M_{89} hadrons inside quarks and gluons can exist as on mass shell particles (M_{89} hadron inside M_{107} hadron is comparable to a bee of size of one cm in a room of size about 5 meters!).

The new Physics at the energies not much above the energy scale of top is essentially the counterpart of ordinary hadron physics at cm energies of the order of ρ/ω meson mass. Therefore M_{89} meson resonances and their interactions described rather satisfactorily by the old fashioned string model with string tension scaled by factor 2^{18} should describe the situation. The electro-weak interactions should be in turn describable using generalization of current algebra ideas, such as PCAC and vector dominance model. If M_{89} hadrons condense on quarks and gluons this physics must be convoluted with the distribution functions of M_{89} hadrons inside quarks and gluons. The resonance structures are partially smeared out by the convolution process.

M_{89} vector mesons should be observed as resonances in e^+e^- annihilation and charged M_{89} pion should be pair produced at e^+e^- collision energies achievable in near future at LEP. Gamma pairs form unique signature of neutral leptopion. The following table gives the naive scaling estimate for the masses of lowest lying M_{89} hadrons.

meson	m/GeV	baryon	m/GeV
π^0	69.1	p	480.4
π^+	71.5	n	481.0
K^+	252.8	Λ	571.2
K^0	254.8	Σ^+	609.0
η	281.0	Σ^0	610.4
η'	490.5	Σ^-	610.5
ρ	394.2	Ξ^0	673.2
ω	400.9	Ξ^-	676.5
K^*	456.7	Ω^-	856.2
Φ	522		

Table 3. Masses of low lying hadrons for M_{89} hadron physics obtained by scaling ordinary hadron masses by a factor of 512.

Consider next the estimation of the production and decay rates for $\rho(89)/\omega(89)$ and more generally M_{89} mesons. In e^+e^- annihilation vector boson resonances are produced via the decay of virtual photon or Z^0 . Since low energies are in question at M_{89} level the scaled up version of vector dominance model described in the nice book of Feynman [48] should give a satisfactory description for the production of M_{89} mesons via resonance mechanism. The idea is to introduce direct coupling $F_V = m_V^2/g_V$ of photon (or gauge boson) to vector boson (ρ, ω, ϕ). The diagrams describing the production of mesons via decay of vector boson contain vector boson propagator $\frac{1}{p^2 - m_V^2 + im_V \Delta}$ and the production rate is enhanced by a factor $R = 4\pi m_V^2/(\Delta^2 g_V^2)$ in the resonance: the factor should be same in M_{89} physics as in ordinary hadron physics. The ratio $r = \alpha_{em} R/\alpha_s$ gives a rough measure for the ratio of the rates of production for $u(89)$ and ordinary top quark. A rough estimate for what is to be expected is obtained by scaling the results of ordinary hadron physics. The table below gives the estimates for the quantity r and one has $r = 15.1$ for ω .

meson	$m/512 MeV$	$\Delta/512 MeV$	$g_V^2/4\pi$	r
ρ	770	150	2.27	0.52
ω	783	10	18.3	15.1
Φ	1019	4.2	13.3	230.8

Table 4. Scaled up resonance production parameters for ρ, ω and Φ . The last column of the table gives the value of the quantity $r = \alpha_{em} R/\alpha_s$, which should give a measure for the ratio of production rate of $u(89)$ and of the production of ordinary top quark pair.

Centauro type events [57] might find nice explanation in terms of M_{89} hadron physics. If electro-weak decay channels dominate over hadronic decay channels for M_{89} mesons this might lead to anomalously small abundance of ordinary pions in Centauro events. In particular, neutral M_{89} pions are expected to decay dominantly to photon pairs and since monoenergetic gamma pairs are used as a signature of pions the observed abundance of ordinary pions becomes small. Evidence for M_{89} pions comes from anomalous gamma pairs detected in the decays of Z^0 bosons[58] with total energy of about $60 GeV$. The pairs might be related to the decay of M_{89} exotic pion predicted to have mass $m_{89} \simeq 2^9 m_\pi \simeq 67.5 GeV$.

The resonance production of M_{89} vector mesons via the graph $q\bar{q} \rightarrow \gamma(virt) \rightarrow M(M_{89})$ and their decay to dijets gives small contribution to dijet production rate.

At high enough cm energies, presumably of order $\sqrt{s} \sim 10 TeV$ in $p\bar{p}$ collisions the jets of M_{89} hadron physics should begin to manifest themselves. The unique signature of M_{89} jets is that the p_T spectrum for the hadrons of the jet, which is of form $exp(-kp_T^2/\Lambda(89))$, is by factor 512 wider than the p_T spectrum of hadrons for ordinary jets.

Following list gives some of the unique signatures of New Physics.

1. At higher energies exotic pions are produced abundantly and might be detectable via annihilation to monoenergetic photon pair. π^0 of the New Physics should have mass $69.1 GeV$ and $\gamma\gamma$ annihilation width $512 \cdot 7.63 eV = 3.9 MeV$ (obtained by scaling from that for ordinary pion). The width for the decay by W emission from either quark of $\pi^0(89)$ (the second is assumed to act as spectator) is of order $G_F^2 m(u(89))^5/(192\pi^3)$ and of order 2.5 MeV.

2. The scaling of mass splittings inside isopin multiplets with the scale factor 512 as compared to ordinary hadron physics is a unique signature of M_{89} hadrons.
3. The scaled up versions of ρ and ω meson should be found at nearby energies. Kaon (and s quark) of the New Physics should be seen as a decay product of $\Phi(522 \text{ GeV}) \rightarrow K + \bar{K}$: from table 6.2.7 one finds that that Φ should have rather small hadronic width $\Delta \simeq 2.2 \text{ GeV}$ so that the parameter measuring its production rate to the production rate of ordinary quark is as high as $r \simeq 230.8$ at resonance.

6.2.8 Could neutrinos appear in several p-adic mass scales?

There are some indications that neutrinos can appear in several mass scales from neutrino oscillations [82]. These oscillations can be classified to vacuum oscillations and to solar neutrino oscillations believed to be due to the so called MSW effect in the dense matter of Sun. There are also indications that the mixing is different for neutrinos and antineutrinos [103, 59].

In TGD framework p-adic length scale hypothesis might explain these findings. The basic vision is that the p-adic length scale of neutrino can vary so that the mass squared scale comes as octaves. Mixing matrices would be universal. The large discrepancy between LSND and MiniBoone results [103] contra solar neutrino results could be understood if electron and muon neutrinos have same p-adic mass scale for solar neutrinos but for LSND and MiniBoone the mass scale of either neutrino type is scaled up. The existence of a sterile neutrino [74] suggested as an explanation of the findings would be replaced by p-adically scaled up variant of ordinary neutrino having standard weak interactions. This scaling up can be different for neutrinos and antineutrinos as suggested by the fact that the anomaly is present only for antineutrinos.

The different values of Δm^2 for neutrinos and antineutrinos in MINOS experiment [59] can be understood if the p-adic mass scale for neutrinos increases by one unit. The breaking of CP and CPT would be spontaneous and realized as a choice of different p-adic mass scales and could be understood in zero energy ontology. Similar mechanism would break supersymmetry and explain large differences between the mass scales of elementary fermions, which for same p-adic prime would have mass scales differing not too much.

Experimental results

There several different type of experimental approaches to study the oscillations. One can study the deficit of electron type solar electron neutrinos (Kamiokande, Super-Kamiokande); one can measure the deficit of muon to electron flux ratio measuring the rate for the transformation of ν_μ to ν_τ (super-Kamiokande); one can study directly the deficit of ν_e ($\bar{\nu}_e$) neutrinos due to transformation to ν_μ ν_μ coming from nuclear reactor with energies in the same range as for solar neutrinos (KamLAND); and one can also study neutrinos from particle accelerators in much higher energy range such as solar neutrino oscillations (K2K,LSND,Miniboone,Minos).

1. Solar neutrino experiments and atmospheric neutrino experiments

The rate of neutrino oscillations is sensitive to the mass squared differences Δm_{12}^2 , Δm_{12}^2 , Δm_{13}^2 and corresponding mixing angles θ_{12} , θ_{13} , θ_{23} between ν_e , ν_μ , and ν_τ (ordered in obvious manner). Solar neutrino experiments allow to determine $\sin^2(2\theta_{12})$ and Δm_{12}^2 . The experiments involving atmospheric neutrino oscillations allow to determine $\sin^2(2\theta_{23})$ and Δm_{23}^2 .

The estimates of the mixing parameters obtained from solar neutrino experiments and atmospheric neutrino experiments are $\sin^2(2\theta_{13}) = 0.08$, $\sin^2(2\theta_{23}) = 0.95$, and $\sin^2(2\theta_{12}) = 0.86$. The mixing between ν_e and ν_τ is very small. The mixing between ν_e and ν_μ , and ν_μ and ν_τ tends is rather near to maximal. The estimates for the mass squared differences are $\Delta m_{12}^2 = 8 \times 10^{-5} \text{ eV}^2$, $\Delta m_{23}^2 \simeq \Delta m_{13}^2 = 2.4 \times 10^{-3} \text{ eV}^2$. The mass squared differences have obviously very different scale but this need not means that the same is true for mass squared values.

2. The results of LSND and MiniBoone

LSND experiment measuring the transformation of $\bar{\nu}_\mu$ to $\bar{\nu}_e$ gave a totally different estimate for Δm_{12}^2 than solar neutrino experiments [103, 74]. If one assumes same value of $\sin^2(\theta_{12})^2 \simeq .86$ one obtains $\Delta m_{23}^2 \sim .1 \text{ eV}^2$ to be compared with $\Delta m_{12}^2 = 8 \times 10^{-5} \text{ eV}^2$. This result is known as LSND

anomaly and led to the hypothesis that there exists a sterile neutrino having no weak interactions and mixing with the ordinary electron neutrino and inducing a rapid mixing caused by the large value of Δm^2 . The purpose of MiniBoone experiment [103] was to test LSND anomaly.

1. It was found that the two-neutrino fit for the oscillations for $\nu_\mu \rightarrow \nu_e$ is not consistent with LSND results. There is an unexplained 3σ electron excess for $E < 475$ MeV. For $E > 475$ MeV the two-neutrino fit is not consistent with LSND fit. The estimate for Δm^2 is in the range $.1 - 1$ eV² and differs dramatically from the solar neutrino data.
2. For antineutrinos there is a small 1.3σ electron excess for $E < 475$ MeV. For $E > 475$ MeV the excess is 3 per cent consistent with null. Two-neutrino oscillation fits are consistent with LSND. The best fit gives $(\Delta m_{12}^2, \sin^2(2\theta_{12})) = (0.064 \text{ eV}^2, 0.96)$. The value of Δm_{12}^2 is by a factor 800 larger than that estimated from solar neutrino experiments.

All other experiments (see the table of the summary of [74] about sterile neutrino hypothesis) are consistent with the absence of $\nu_\mu \rightarrow \nu_e$ and $\bar{\nu}_\mu \rightarrow \bar{\nu}_e$ mixing and only LSND and MiniBoone report an indication for a signal. If one however takes these findings seriously they suggest that neutrinos and antineutrinos behave differently in the experimental situations considered. Two-neutrino scenarios for the mixing (no sterile neutrinos) are consistent with data for either neutrinos or antineutrinos but not both [74].

3. The results of MINOS group

The MINOS group at Fermi National Accelerator Laboratory has reported evidence that the mass squared differences between neutrinos are not same for neutrinos and antineutrinos [59]. In this case one measures the disappearance of ν_μ and $\bar{\nu}_\mu$ neutrinos from high energy beam in the range .5-1 GeV and the dominating contribution comes from the transformation to τ neutrinos. Δm_{23}^2 is reported to be about 40 percent larger for antineutrinos than for neutrinos. There is 5 percent probability that the mass squared differences are same. The best fits for the basic parameters are $(\Delta m_{23}^2 = 2.35 \times 10^{-3}, \sin^2(2\theta_{23}) = 1)$ for neutrinos with error margin for Δm^2 being about 5 per cent and $(\Delta m_{23}^2 = 3.36 \times 10^{-3}, \sin^2(2\theta_{23}) = .86)$ for antineutrinos with errors margin around 10 per cent. The ratio of mass squared differences is $r \equiv \Delta m^2(\bar{\nu})/\Delta m^2(\nu) = 1.42$. If one assumes $\sin^2(2\theta_{23}) = 1$ in both cases the ratio comes as $r = 1.3$.

Explanation of findings in terms of p-adic length scale hypothesis

p-Adic length scale hypothesis predicts that fermions can correspond to several values of p-adic prime meaning that the mass squared comes as octaves (powers of two). The simplest model for the neutrino mixing assumes universal topological mixing matrices and therefore for CKM matrices so that the results should be understood in terms of different p-adic mass scales. Even CP breaking and CPT breaking at fundamental level is un-necessary although it would occur spontaneously in the experimental situation selecting different p-adic mass scales for neutrinos and antineutrinos. The expression for the mixing probability a function of neutrino energy in two-neutrino model for the mixing is of form

$$P(E) = \sin^2(2\theta)\sin^2(X) \ , \ X = k \times \Delta m^2 \times \frac{L}{E} \ .$$

Here k is a numerical constant, L is the length travelled, and E is neutrino energy.

1. LSND and MiniBoone results

LSND and MiniBoone results are inconsistent with solar neutrino data since the value of Δm_{12}^2 is by a factor 800 larger than that estimated from solar neutrino experiments. This could be understood if in solar neutrino experiments ν_μ and ν_w correspond to the same p-adic mass scale $k = k_0$ and have very nearly identical masses so that Δm^2 scale is much smaller than the mass squared scale. If either p-adic scale is changed from k_0 to $k_0 + k$, the mass squared difference increases dramatically. The counterpart of the sterile neutrino would be a p-adically scaled up version of the ordinary neutrino having standard electro-weak interactions. The p-adic mass scale would correspond to the mass scale defined by Δm^2 in LSND and MiniBoone experiments and therefore a mass scale in the range .3-1 eV. The p-adic length scale assignable to eV mass scale could correspond to $k = 167$, which corresponds

to cell length scale of $2.5 \mu\text{m}$. $k = 167$ defines one of the Gaussian Mersennes $M_{G,k} = (1+i)^k - 1$ $k = 151, 157, 163, 167$ varying in the range 10 nm (celle membrane thickness) and $2.5 \mu\text{m}$ defining the size of cell nucleus proposed to be fundamental for the understanding of living matter [43].

2. MINOS results

One must assume also now that the p-adic mass scales for ν_τ and $\bar{\nu}_\tau$ are near to each other in the "normal" experimental situation. Assuming that the mass squared scales of ν_μ or $\bar{\nu}_\mu$ come as 2^{-k} powers of $m_{\nu_\mu}^2 = m_{\nu_\tau}^2 + \Delta m^2$, one obtains

$$m_{\nu_\tau}^2(k_0) - m_{\bar{\nu}_\mu}^2(k_0 + k) = (1 - 2^{-k})m_{\nu_\tau}^2 - 2^{-k}\Delta m_0^2 .$$

For $k = 1$ this gives

$$r = \frac{\Delta m^2(k=2)}{\Delta m^2(k=1)} = \frac{\frac{3}{2} - \frac{2r}{3}}{1-r} , \quad r = \frac{\Delta m_0^2}{m_{\nu_\tau}^2} . \quad (6.2.4)$$

One has $r \geq 3/2$ for $r > 0$ if one has $m_{\nu_\tau} > m_{\nu_\mu}$ for the same p-adic length scale. The experimental ratio $r \simeq 1.3$ could be understood for $r \simeq -.31$. The experimental uncertainties certainly allow the value $r = 1.5$ for $k(\bar{\nu}_\mu) = 1$ and $k(\nu_\mu) = 2$.

This result implies that the mass scale of ν_μ and ν_τ differ by a factor $1/2$ in the "normal" situation so that mass squared scale of ν_τ would be of order $5 \times 10^{-3} \text{ eV}^2$. The mass scales for $\bar{\nu}_\tau$ and ν_τ would about $.07 \text{ eV}$ and $.05 \text{ eV}$. In the LSND and MiniBoone experiments the p-adic mass scale of other neutrino would be around $.1-1 \text{ eV}$ so that different p-adic mass scale large by a factor $2^{k/2}$, $2 \leq k \leq 7$ would be in question. The different results from various experiments could be perhaps understood in terms of the sensitivity of the p-adic mass scale to the experimental situation. Neutrino energy could serve as a control parameter.

CP and CPT breaking

Different values of Δm_{ij}^2 for neutrinos and antineutrinos would require in standard QFT framework not only the violation of CP but also CP [49, 114] which is the cherished symmetry of quantum field theories. CPT symmetry states that when one reverses time's arrow, reverses the signs of momenta and replaces particles with their antiparticles, the resulting Universe obeys the same laws as the original one. CPT invariance follows from Lorentz invariance, Lorentz invariance of vacuum state, and from the assumption that energy is bounded from below. On the other hand, CPT violation requires the breaking of Lorentz invariance.

In TGD framework this kind of violation does not seem to be necessary at fundamental level since p-adic scale hypothesis allowing neutrinos and also other fermions to have several mass scales coming as half-octaves of a basic mass scale for given quantum numbers. In fact, even in TGD inspired low energy hadron physics quarks appear in several mass scales. One could explain the different choice of the p-adic mass scales as being due to the experimental arrangement which selects different p-adic length scales for neutrinos and antineutrinos so that one could speak about spontaneous breaking of CP and possibly CPT. The CP breaking at the fundamental level which is however expected to be small in the case considered. The basic prediction of TGD and relates to the CP breaking of Chern-Simons action inducing CP breaking in the modified Dirac action defining the fermionic propagator [42].

One can indeed consider the possibility of a spontaneous breaking of CPT symmetry in TGD framework since for a given CD (causal diamond defined as the intersection of future and past directed light-cones whose size scales are assumed to come as octaves) the Lorentz invariance is broken due to the preferred time direction (rest system) defined by the time-like line connecting the tips of CD . Since the world of classical worlds is union of CD s with all boosts included the Lorentz invariance is not violated at the level of WCW. Spontaneous symmetry breaking would be analogous to that for the solutions of field equations possessing the symmetry themselves. The mechanism of breaking would be same as that for supersymmetry. For same p-adic length scale particles and their super-partners would have same masses and only the selection of the p-adic mass scale would induces the mass splitting.

There is an article about CPT violation[50] of the dynamics defined by what the authors also call Chern-Simons term. This term is not identical with the measurement interaction term introduced

in TGD framework. It is however linear in momentum as is also the measurement interaction term added to Chern-Simons Dirac action and this is what is essential from the point of view of CPT. The measurement interaction term has a formal interpretation as $U(1)$ gauge transform but having non-trivial physical effect since it is added only to the Chern-Simons Dirac action term but not to Kähler-Dirac action. The linearity with respect to momentum suggests CPT oddness of the measurement interaction term. In absence of the measurement interaction CPT would be intact but the change of the sign of the measurement interaction term in PT would bring in CPT violation. One must however notice that in TGD framework both imbedding space level and space-time level are involved and this does not allow straightforward application of standard arguments.

6.2.9 Topological evaporation and the concept of Pomeron

Topological evaporation provides an explanation for the mysterious concept of Pomeron originally introduced to describe hadronic diffractive scattering as the exchange of Pomeron Regge trajectory [72]. No hadrons belonging to Pomeron trajectory were however found and via the advent of QCD Pomeron was almost forgotten. Pomeron has recently experienced reincarnation [63, 107, 92]. In Hera [63] $e - p$ collisions, where proton scatters essentially elastically whereas jets in the direction of incoming virtual photon emitted by electron are observed. These events can be understood by assuming that proton emits color singlet particle carrying small fraction of proton's momentum. This particle in turn collides with virtual photon (antiproton) whereas proton scatters essentially elastically.

The identification of the color singlet particle as Pomeron looks natural since Pomeron emission describes nicely diffractive scattering of hadrons. Analogous hard diffractive scattering events in pX diffractive scattering with $X = \bar{p}$ [107] or $X = p$ [92] have also been observed. What happens is that proton scatters essentially elastically and emitted Pomeron collides with X and suffers hard scattering so that large rapidity gap jets in the direction of X are observed. These results suggest that Pomeron is real and consists of ordinary partons.

TGD framework leads to two alternative identifications of Pomeron relying on same geometric picture in which Pomeron corresponds to a space-time sheet separating from hadronic space-time sheet and colliding with photon.

Earlier model

The earlier model is based on the assumption that baryonic quarks carry the entire four-momentum of baryon. p-Adic mass calculations have shown that this assumption is wrong. The modification of the model requires however to change only wordings so that I will represent the earlier model first.

The TGD based identification of Pomeron is very economical: Pomeron corresponds to sea partons, when valence quarks are in vapor phase. In TGD inspired phenomenology events involving Pomeron correspond to pX collisions, where incoming X collides with proton, when valence quarks have suffered coherent simultaneous (by color confinement) evaporation into vapor phase. System X sees only the sea left behind in evaporation and scatters from it whereas valence quarks continue without noticing X and condense later to form quasi-elastically scattered proton. If X suffers hard scattering from the sea the peculiar hard diffractive scattering events are observed. The fraction of these events is equal to the fraction f of time spent by valence quarks in vapor phase.

Dimensional argument can be used to derive a rough order of magnitude estimate for f as $f \sim 1/\alpha = 1/137 \sim 10^{-2}$ for f : f is of same order of magnitude as the fraction (about 5 per cent) of peculiar events from all deep inelastic scattering events in Hera. The time spent in condensate is by dimensional arguments of the order of the p-adic length scale $L(M_{107})$, not far from proton Compton length. Time dilation effects at high collision energies guarantee that valence quarks indeed stay in vapor phase during the collision. The identification of Pomeron as sea explains also why Pomeron Regge trajectory does not correspond to actual on mass shell particles.

The existing detailed knowledge about the properties of sea structure functions provides a stringent test for the TGD scenario. According to [107] Pomeron structure function seems to consist of soft $((1-x)^5)$, hard $((1-x))$ and super-hard component (delta function like component at $x = 1$). The peculiar super hard component finds explanation in TGD based picture. The structure function $q_P(x, z)$ of parton in Pomeron contains the longitudinal momentum fraction z of the Pomeron as a parameter and $q_P(x, z)$ is obtained by scaling from the sea structure function $q(x)$ for proton

$q_P(x, z) = q(zx)$. The value of structure function at $x = 1$ is non-vanishing: $q_P(x = 1, z) = q(z)$ and this explains the necessity to introduce super hard delta function component in the fit of [107].

Updated model

The recent developments in the understanding of hadron mass spectrum involve the realization that hadronic $k = 107$ space-time sheet is a carrier of super-symplectic bosons (and possibly their super-counterparts with quantum numbers of right handed neutrino) [17]. The model leads to amazingly simple and accurate mass formulas for hadrons. Most of the baryonic momentum is carried by super-symplectic quanta: valence quarks correspond in proton to a relatively small fraction of total mass: about 170 MeV. The counterparts of string excitations correspond to super-symplectic many-particle states and the additivity of conformal weight proportional to mass squared implies stringy mass formula and generalization of Regge trajectory picture. Hadronic string tension is predicted correctly. Model also provides a solution to the proton spin puzzle.

In this framework valence quarks would naturally correspond to a color singlet state formed by space-time sheets connected by color flux tubes having no Regge trajectories and carrying a relatively small fraction of baryonic momentum. In the collisions discussed valence quarks would leave the hadronic space-time sheet and suffer a collision with photon. The lightness of Pomeron and electro-weak neutrality of Pomeron support the view that photon stripes valence quarks from Pomeron, which continues its flight more or less unperturbed. Instead of an actual topological evaporation the bonds connecting valence quarks to the hadronic space-time sheet could be stretched during the collision with photon.

The large value of $\alpha_K = 1/4$ for super-symplectic matter suggests that the criterion for a phase transition increasing the value of Planck constant [39] and leading to a phase, where $\alpha_K \propto 1/\hbar$ is reduced, could occur. For α_K to remain invariant, $\hbar_0 \rightarrow 26\hbar_0$ would be required. In this case, the size of hadronic space-time sheet, "color field body of the hadron", would be $26 \times L(107) = 46$ fm, roughly the size of the heaviest nuclei. Hence a natural expectation is that the dark side of nuclei plays a role in the formation of atomic nuclei. Note that the sizes of electromagnetic field bodies of current quarks u and d with masses of order few MeV is not much smaller than the Compton length of electron. This would mean that super-symplectic bosons would represent dark matter in a well-defined sense and Pomeron exchange would represent temporary separation of ordinary and dark matter.

Note however that the fact that super-symplectic bosons have no electro-weak interactions, implies their dark matter character even for the ordinary value of Planck constant: this could be taken as an objection against dark matter hierarchy. My own interpretation is that super-symplectic matter is dark matter in the strongest sense of the world whereas ordinary matter in the large \hbar phase is only apparently dark matter because standard interactions do not reveal themselves in the expected manner.

Astrophysical counterpart of Pomeron events

Pomeron events have direct analogy in astrophysical length scales. In the collision of two galaxies dark and visible matter parts of the colliding galaxies have been found to separate by Chandra X-ray Observatory [85].

Imagine a collision between two galaxies. The ordinary matter in them collides and gets interlocked due to the mutual gravitational attraction. Dark matter, however, just keeps its momentum and keeps going on leaving behind the colliding galaxies. This kind of event has been detected by the Chandra X-Ray Observatory by using an ingenious manner to detect dark matter. Collisions of ordinary matter produces a lot of X-rays and the dark matter outside the galaxies acts as a gravitational lens.

6.2.10 Wild speculations about non-perturbative aspects of hadron physics and exotic Super Virasoro representations

If the canonical correspondence mapping the p-adic mass squared values to real numbers is taken completely seriously, then TGD predicts infinite hierarchy of exotic light representations of Super Virasoro. These exotic states are created by sub-algebras of Super Kac-Moody and SKM algebras whose generators have conformal weights divisible by p^n , $n = 1, 2, \dots$. Ordinary representations would correspond to $n = 0$.

For the exotic representations the p-adic mass squared of the particle is proportional to Virasoro p^n . When the value of the p-adic mass squared is power of p : $M^2 \propto p^n$, $n = 1, 2, \dots$, the real counterpart of the mass squared in canonical identification is extremely small since it is proportional to $1/p^n$ in this case. It is of course not at all clear whether these representations have any real counterpart and if even this the case the could be thermally unstable in an environment with higher p-adic temperature.

Also ordinary low temperature ($T_p = 1/n$) Super Virasoro representations allow extremely light states but in this case there is no subalgebra generating these states. If these representations exist they could correspond to low energy-long length scale fractal copies of elementary particles. Due to the state degeneracy providing an enormous information storage capacity associated with these states these representations, if realized in nature, might have biological relevance [45, 40].

There is however an objection against this idea: these representations are possible also in elementary particle length scales and for $M^2 \propto L_0 = n p m_0^2$ the representations have same mass scale as ordinary elementary particles. These representations couple to ordinary elementary particles via classical gauge fields and could therefore be present also in elementary particle physics. For reasons which become clear below, exotic Super Virasoro representations might provide a model for low energy hadron physics.

1. The formula

$$M_R^2 = \frac{n m_0^2}{p}$$

is generalization of the mass formula of hadronic string models and reduces to it when the angular momentum

$$J = \alpha' M^2$$

of the hadronic state satisfies $J = n$. From this Regge slope α' and string tension T are given by

$$T = \frac{1}{2\pi\alpha'} \quad , \quad \frac{1}{\alpha'} = \frac{m_0^2}{p} \quad .$$

The observed value of the Regge slope is $\alpha' = .9/GeV^2$.

2. The value of the predicted string tension is easily found. The prediction of TGD based mass calculations for the value of the p-adic pion mass squared is

$$m_\pi^2 = p m_0^2 + O(p^2) \simeq p m_0^2 \quad , \quad p = M_{107} \quad .$$

$m_\pi \geq m_0/\sqrt{M_{107}}$ and $m_\pi = 134$ MeV gives upper bound for m_0 which is consistent with the prediction for the mass of electron. For $k = 107$ the value of α' would be roughly 64 times too large as simple calculation shows. For $k = 101$ one has

$$\alpha' = \frac{.87}{GeV^2} \quad ,$$

which deviates from the value $\alpha' = .9/GeV^2$ determined from ρ Regge trajectory only by three per cent.

3. This would suggest that excited states of ordinary hadrons contain $k = 101$ space-time sheets with p-adic length scale of .3 fm condensed on $k = 107$ hadronic space-time sheet with 8 times larger p-adic length scale and that the angular momentum of these excitations is not assignable to the ordinary quarks but to the states of $k = 101$ exotic Super Virasoro representation. The slight deviation from $.9/GeV^2$ could be explained if the contribution of quarks and gluons to the mass squared decreases as a function of J so that the effective value of α' increases and effective string tension increases. This might be due to the transformation of parton mass squared to the mass squared associated with $k = 101$ exotic Super Virasoro states. Note that $n = 1$ excitation

of $k = 101$ Super Virasoro has mass $m_1 = 1.07$ GeV, which is larger than proton mass: therefore the spin of these excitations cannot resolve the spin crisis of proton.

4. For $k = 103$ the predicted value of string tension is by a factor $1/4$ smaller. An interesting question is whether $k = 107$ and $k = 103$ excitations might be observable in low energy hadron physics.

The second thought provoking observation is that pion mass squared corresponds in excellent approximation to that for $n = 1$ state of exotic Super Virasoro representation for $k = 107$. This suggests that in case of pion quark masses are compensated apart from $O(p^2)$ contributions completely by various interaction energy and the energy associated with exotic Super Virasoro representation contributes to the mass squared. This would be p-adic articulation for the statement that pion is massless Goldstone boson. Since pion represents essentially non-perturbative aspects of QCD, this raises the possibility that exotic Super Virasoro representations could provide the long sought first principle theory of low energy hadronic physics.

1. In this theory hadrons would correspond to exotic Super Virasoro representations whereas quark-gluon plasma would correspond to ordinary p-adic Super Virasoro representations. In color confined phase p-adic α_c would have increased to the critical value $\alpha_c = p + O(p^2)$ implying dramatic drop of the real counterpart of α_c to $\alpha_c^R \simeq 1/p$ so that color interactions would disappear effectively and only electro-weak interactions and the geometric interactions between the space-time sheets would remain. What is important is that these phases can exist inside hadron for several values of p . This suggests a fractal hierarchy of hadrons inside hadrons and QCD:s inside QCD:s with the values of $\Lambda(k) \propto 1/L^2(k)$, $k = 107, 103, 101, \dots$. In particular, rotational excitations would mean generation of $k = 101$ hadrons inside $k = 107$ hadrons.
2. Hadronization and fragmentation are semi-phenomenological aspects of QCD and would correspond at fundamental level to the phase transitions between the exotic Super Virasoro representations and ordinary Super Virasoro representations. Also the concepts of sea and Pomeron could be reduced the states of exotic Super Virasoro representations associated with $k = 107, 103, 101, 97, \dots$

In light of the successes of the hadron model based on super-symplectic many-particle states assigned to hadrons [17] the exotic Super Virasoro representations do not look attractive from the point of view of ordinary hadron physics. Also the thermal instability is a good objection against them.

6.3 The incredibly shrinking proton

The discovery that the charge radius of proton deduced from the muonic version of hydrogen atom is about 4 per cent smaller than from the radius deduced from hydrogen atom [91, 55] is in complete conflict with the cherished belief that atomic physics belongs to the museum of science. The title of the article *Quantum electrodynamics-a chink in the armour?* of the article published in Nature [84] expresses well the possible implications, which might actually go well extend beyond QED.

The finding is a problem of QED or to the standard view about what proton is. Lamb shift [54] is the effect distinguishing between the states hydrogen atom having otherwise the same energy but different angular momentum. The effect is due to the quantum fluctuations of the electromagnetic field. The energy shift factorizes to a product of two expressions. The first one describes the effect of these zero point fluctuations on the position of electron or muon and the second one characterizes the average of nuclear charge density as "seen" by electron or muon. The latter one should be same as in the case of ordinary hydrogen atom but it is not. Does this mean that the presence of muon reduces the charge radius of proton as determined from muon wave function? This of course looks implausible since the radius of proton is so small. Note that the compression of the muon's wave function has the same effect.

Before continuing it is good to recall that QED and quantum field theories in general have difficulties with the description of bound states: something which has not received too much attention. For instance, van der Waals force at molecular scales is a problem. A possible TGD based explanation and a possible solution of difficulties proposed for two decades ago is that for bound states

the two charged particles (say nucleus and electron or two atoms) correspond to two 3-D surfaces glued by flux tubes rather than being idealized to points of Minkowski space. This would make the non-relativistic description based on Schrödinger amplitude natural and replace the description based on Bethe-Salpeter equation having horrible mathematical properties.

6.3.1 Basic facts and notions

In this section the basic TGD inspired ideas and notions - in particular the notion of field body- are introduced and the general mechanism possibly explaining the reduction of the effective charge radius relying on the leakage of muon wave function to the flux tubes associated with u quarks is introduced. After this the value of leakage probability is estimated from the standard formula for the Lamb shift in the experimental situation considered.

Basic notions of TGD which might be relevant for the problem

Can one say anything interesting about the possible mechanism behind the anomaly if one accepts TGD framework? How the presence of muon could reduce the charge radius of proton? Let us first list the basic facts and notions.

1. One can say that the size of muonic hydrogen characterized by Bohr radius is by factor $m_e/m_\mu = 1/211.4 = 4.7 \times 10^{-4}$ smaller than for hydrogen atom and equals to 250 fm. Hydrogen atom Bohr radius is .53 Angstroms.
2. Proton contains 2 quarks with charge $2e/3$ and one d quark which charge $-e/3$. These quarks are light. The last determination of u and d quark masses[43] gives masses, which are $m_u = 2$ MeV and $m_d = 5$ MeV (I leave out the error bars). The standard view is that the contribution of quarks to proton mass is of same order of magnitude. This would mean that quarks are not too relativistic meaning that one can assign to them a size of order Compton wave length of order $4 \times r_e \simeq 600$ fm in the case of u quark (roughly twice the Bohr radius of muonic hydrogen) and $10 \times r_e \simeq 24$ fm in the case of d quark. These wavelengths are much longer than the proton charge radius and for u quark more than twice longer than the Bohr radius of the muonic hydrogen. That parts of proton would be hundreds of times larger than proton itself sounds a rather weird idea. One could of course argue that the scales in question do not correspond to anything geometric. In TGD framework this is not the way out since quantum classical correspondence requires this geometric correlate.
3. There is also the notion of classical radius of electron and quark. It is given by $r = \alpha\hbar/m$ and is in the case of electron this radius is 2.8 fm whereas proton charge radius is .877 fm and smaller. The dependence on Planck constant is only apparent as it should be since classical radius is in question. For u quark the classical radius is .52 fm and smaller than proton charge radius. The constraint that the classical radii of quarks are smaller than proton charge radius gives a lower bound of quark masses: p-adic scaling of u quark mass by $2^{-1/2}$ would give classical radius .73 fm which still satisfies the bound. TGD framework the proper generalization would be $r = \alpha_K\hbar/m$, where α_K is Kähler coupling strength defining the fundamental coupling constant of the theory and quantized from quantum criticality. Its value is very near or equal to fine structure constant in electron length scale.
4. The intuitive picture is that light-like 3-surfaces assignable to quarks describe random motion of partonic 2-surfaces with light-velocity. This is analogous to zitterbewegung assigned classically to the ordinary Dirac equation. The notion of braid emerging from Chern-Simons Dirac equation via periodic boundary conditions means that the orbits of partonic 2-surface effectively reduces to braids carrying fermionic quantum numbers. These braids in turn define higher level braids which would move inside a structure characterizing the particle geometrically. Internal consistency suggests that the classical radius $r = \alpha_K\hbar/m$ characterizes the size scale of the zitterbewegung orbits of quarks.

I cannot resist the temptation to emphasize the fact that Bohr orbitology is now reasonably well understood. The solutions of field equations with higher than 3-D CP_2 projection describing

radiation fields allow only generalizations of plane waves but not their superpositions in accordance with the fact it is these modes that are observed. For massless extremals with 2-D CP_2 projection superposition is possible only for parallel light-like wave vectors. Furthermore, the restriction of the solutions of the Chern-Simons Dirac equation at light-like 3-surfaces to braid strands gives the analogs of Bohr orbits. Wave functions of -say electron in atom- are wave functions for the position of wormhole throat and thus for braid strands so that Bohr's theory becomes part of quantum theory.

5. In TGD framework quantum classical correspondence requires -or at least strongly suggests- that also the p-adic length scales assignable to u and d quarks have geometrical correlates. That quarks would have sizes much larger than proton itself how sounds rather paradoxical and could be used as an objection against p-adic length scale hypothesis. Topological field quantization however leads to the notion of field body as a structure consisting of flux tubes and the identification of this geometric correlate would be in terms of Kähler (or color-, or electro-) magnetic body of proton consisting of color flux tubes beginning from space-time sheets of valence quarks and having length scale of order Compton wavelength much longer than the size of proton itself. Magnetic loops and electric flux tubes would be in question. Also secondary p-adic length scale characterizes field body. For instance, in the case of electron the causal diamond assigned to electron would correspond to the time scale of .1 seconds defining an important bio-rhythm.

Could the notion of field body explain the anomaly?

The large Compton radii of quarks and the notion of field body encourage the attempt to imagine a mechanism affecting the charge radius of proton as determined from electron's or muon's wave function.

1. Muon's wave function is compressed to a volume which is about 8 million times smaller than the corresponding volume in the case of electron. The Compton radius of u quark more that twice larger than the Bohr radius of muonic hydrogen so that muon should interact directly with the field body of u quark. The field body of d quark would have size 24 fm which is about ten times smaller than the Bohr radius so that one can say that the volume in which muons sees the field body of d quark is only one thousandth of the total volume. The main effect would be therefore due to the two u quarks having total charge of $4e/3$.

One can say that muon begins to "see" the field bodies of u quarks and interacts directly with u quarks rather than with proton via its electromagnetic field body. With d quarks it would still interact via protons field body to which d quark should feed its electromagnetic flux. This could be quite enough to explain why the charge radius of proton determined from the expectation value defined by its wave function wave function is smaller than for electron. One must of course notice that this brings in also direct magnetic interactions with u quarks.

2. What could be the basic mechanism for the reduction of charge radius? Could it be that the electron is caught with some probability into the flux tubes of u quarks and that Schrödinger amplitude for this kind state vanishes near the origin? If so, this portion of state would not contribute to the charge radius and the since the portion ordinary state would smaller, this would imply an effective reduction of the charge radius determined from experimental data using the standard theory since the reduction of the norm of the standard part of the state would be erratically interpreted as a reduction of the charge radius.
3. This effect would be of course present also in the case of electron but in this case the u quarks correspond to a volume which million times smaller than the volume defined by Bohr radius so that electron does not in practice "see" the quark sub-structure of proton. The probability P for getting caught would be in a good approximation proportional to the value of $|\Psi(r_u)|^2$ and in the first approximation one would have

$$\frac{P_e}{P_\mu} \sim (a_\mu/a_e)^3 = (m_e/m_\mu)^3 \sim 10^{-7} .$$

from the proportionality $\Psi_i \propto 1/a_i^{3/2}$, $i=e,\mu$.

A general formula for Lamb shift in terms of proton charge radius

The charge radius of proton is determined from the Lamb shift between 2S- and 2P states of muonic hydrogen. Without this effect resulting from vacuum polarization of photon Dirac equation for hydrogen would predict identical energies for these states. The calculation reduces to the calculation of vacuum polarization of photon inducing to the Coulomb potential and an additional vacuum polarization term. Besides this effect one must also take into account the finite size of the proton which can be coded in terms of the form factor deducible from scattering data. It is just this correction which makes it possible to determine the charge radius of proton from the Lamb shift.

1. In the article [90] the basic theoretical results related to the Lamb shift in terms of the vacuum polarization of photon are discussed. Proton's charge density in this representation is expressed in terms of proton form factor in principle deducible from the scattering data. Two special cases can be distinguished corresponding to the point like proton for which Lamb shift is non-vanishing only for S wave states and non-point like proton for which energy shift is present also for other states. The theoretical expression for the Lamb shift involves very refined calculations. Between 2P and 2S states the expression for the Lamb shift is of form

$$\Delta E(2P_{3/2}^{F=2} 2S_{1/2}^{F=1}) = a - br_p^2 + cr_p^3 = 209.968(5)5.2248 \times r_p^2 + 0.0347 \times r_p^3 \text{ meV} . \quad (6.3.1)$$

where the charge radius $r_p = .8750$ is expressed in femtometers and energy in meVs.

2. The general expression of Lamb shift is given in terms of the form factor by

$$E(2P - 2S) = \int \frac{d^3q}{(2\pi)^3} \times (-4\pi\alpha) \frac{F(q^2)}{q^2} \frac{\Pi(q^2)}{q^2} \times \int (|\Psi_{2P}(r)|^2 - |\Psi_{2S}(r)|^2) \exp(iq \cdot r) dV . \quad (6.3.1)$$

Here Π is a scalar representing vacuum polarization due to decay of photon to virtual pairs.

The model to be discussed predicts that the effect is due to a leakage from "standard" state to what I call flux tube state. This means a multiplication of $|\Psi_{2P}|^2$ with the normalization factor $1/N$ of the standard state orthogonalized with respect to flux tube state. It is essential that $1/N$ is larger than unity so that the effect is a genuine quantum effect not understandable in terms of classical probability.

The modification of the formula is due to the normalization of the 2P and 2S states. These are in general different. The normalization factor $1/N$ is same for all terms in the expression of Lamb shift for a given state but in general different for 2S and 2P states. Since the lowest order term dominates by a factor of ~ 40 over the second one, one can conclude that the modification should affect the lowest order term by about 4 per cent. Since the second term is negative and the modification of the first term is interpreted as a modification of the second term when r_p is estimated from the standard formula, the first term must increase by about 4 per cent. This is achieved if this state is orthogonalized with respect to the flux tube state. For states Ψ_0 and Ψ_{tube} with unit norm this means the modification

$$\begin{aligned} \Psi_0 &\rightarrow \frac{1}{1 - |C|^2} \times (\Psi_i - C\Psi_{tube}) , \\ C &= \langle \Psi_{tube} | \Psi_0 \rangle . \end{aligned} \quad (6.3.1)$$

In the lowest order approximation one obtains

$$a - br_p^2 + cr_p^3 \rightarrow (1 + |C|^2)a - br_p^2 + cr_p^3 . \quad (6.3.2)$$

Using instead of this expression the standard formula gives a wrong estimate r_p from the condition

$$a - br_p^2 + cr_p^3 \rightarrow (1 + |C|^2)a - br_p^2 + cr_p^3 . \quad (6.3.3)$$

This gives the equivalent conditions

$$\begin{aligned} \hat{r}_p^2 &= r_p^2 - \frac{|C|^2 a}{b} , \\ P_{tube} &\equiv |C|^2 \simeq 2 \frac{b}{a} \times r_p^2 \times \frac{(r_p - \hat{r}_p)}{r_p} . \end{aligned} \quad (6.3.3)$$

The resulting estimate for the leakage probability is $P_{tube} \simeq .0015$. The model should be able to reproduce this probability.

6.3.2 A model for the coupling between standard states and flux tube states

Just for fun one can look whether the idea about confinement of muon to quark flux tube carrying electric flux could make sense.

1. Assume that the quark is accompanied by a flux tube carrying electric flux $\int EdS = -\int \nabla \Phi \cdot dS = q$, where $q = 2e/3 = ke$ is the u quark charge. The potential created by the u quark at the proton end of the flux tube with transversal area $S = \pi R^2$ idealized as effectively 1-D structure is

$$\Phi = -\frac{ke}{\pi R^2} |x| + \Phi_0 . \quad (6.3.4)$$

The normalization factor comes from the condition that the total electric flux is q . The value of the additive constant V_0 is fixed by the condition that the potential coincides with Coulomb potential at $r = r_u$, where r_u is u quark Compton length. This gives

$$e\Phi_0 = \frac{e^2}{r_u} + Kr_u , \quad K = \frac{ke^2}{\pi R^2} . \quad (6.3.5)$$

2. Parameter R should be of order of magnitude of charge radius $\alpha_K r_u$ of u quark is free parameter in some limits. $\alpha_K = \alpha$ is expected to hold true in excellent approximation. Therefore a convenient parametrization is

$$R = z\alpha r_u . \quad (6.3.6)$$

This gives

$$K = \frac{4k}{\alpha r_u^2} , \quad e\Phi_0 = 4\left(\pi\alpha + \frac{k}{\alpha}\right) \frac{1}{r_u} . \quad (6.3.7)$$

3. The requirement that electron with four times larger charge radius that u quark can topologically condensed inside the flux tube without a change in the average radius of the flux tube (and thus in a reduction in p-adic length scale increasing its mass by a factor 4!) suggests that $z \geq 4$ holds true at least far away from proton. Near proton the condition that the radius of the flux tube is smaller than electron's charge radius is satisfied for $z = 1$.

Reduction of Schrödinger equation at flux tube to Airy equation

The 1-D Schrödinger equation at flux tube has as its solutions Airy functions and the related functions known as "Bairy" functions.

1. What one has is a one-dimensional Schrödinger equation of general form

$$-\frac{\hbar^2}{2m_\mu} \frac{d^2\Psi}{dx^2} + (Kx - e\Phi_0)\Psi = E\Psi, \quad K = \frac{ke^2}{\pi R^2}. \quad (6.3.8)$$

By performing a linear coordinate change

$$u = \left(\frac{2m_\mu K}{\hbar^2}\right)^{1/3}(x - x_E), \quad x_E = \frac{-|E| + e\Phi_0}{K}, \quad (6.3.9)$$

one obtains

$$\frac{d^2\Psi}{du^2} - u\Psi = 0. \quad (6.3.10)$$

This differential equation is known as Airy equation (or Stokes equation) and defines special functions $Ai(x)$ known as Airy functions and related functions $Bi(x)$ referred to as "Bairy" functions [52]. Airy functions characterize the intensity near an optical directional caustic such as that of rainbow.

2. The explicit expressions for $Ai(u)$ and $Bi(u)$ are is given by

$$\begin{aligned} Ai(u) &= \frac{1}{\pi} \int_0^\infty \cos\left(\frac{1}{3}t^3 + ut\right) dt, \\ Bi(u) &= \frac{1}{\pi} \int_0^\infty \left[\exp\left(-\frac{1}{3}t^3\right) + \sin\left(\frac{1}{3}t^3 + ut\right) \right] dt. \end{aligned} \quad (6.3.10)$$

$Ai(u)$ oscillates rapidly for negative values of u having interpretation in terms of real wave vector and goes exponentially to zero for $u > 0$. $Bi(u)$ oscillates also for negative values of x but increases exponentially for positive values of u . The oscillatory behavior and its character become obvious by noticing that stationary phase approximation is possible for $x < 0$.

The approximate expressions of $Ai(u)$ and $Bi(u)$ for $u > 0$ are given by

$$\begin{aligned} Ai(u) &\sim \frac{1}{2\pi^{1/2}} \exp\left(-\frac{2}{3}u^{3/2}\right) u^{-1/4}, \\ Bi(u) &\sim \frac{1}{\pi^{1/2}} \exp\left(\frac{2}{3}u^{3/2}\right) u^{-1/4}. \end{aligned} \quad (6.3.10)$$

For $u < 0$ one has

$$\begin{aligned} Ai(u) &\sim \frac{1}{\pi^{1/2}} \sin\left(\frac{2}{3}(-u)^{3/2}\right) (-u)^{-1/4}, \\ Bi(u) &\sim \frac{1}{\pi^{1/2}} \cos\left(\frac{2}{3}(-u)^{3/2}\right) (-u)^{-1/4}. \end{aligned} \quad (6.3.10)$$

3. $u = 0$ corresponds to the turning point of the classical motion where the kinetic energy changes sign. $x = 0$ and $x = r_u$ correspond to the points

$$\begin{aligned} u_{min} \equiv u(0) &= -\left(\frac{2m_\mu K}{\hbar^2}\right)^{1/3} x_E , \\ u_{max} \equiv u(r_u) &= \left(\frac{2m_\mu K}{\hbar^2}\right)^{1/3} (r_u - x_E) , \\ x_E &= \frac{-|E| + e\Phi_0}{K} . \end{aligned} \quad (6.3.9)$$

4. The general solution is

$$\Psi = aAi(u) + bBi(u) . \quad (6.3.10)$$

The natural boundary condition is the vanishing of Ψ at the lower end of the flux tube giving

$$\frac{b}{a} = -\frac{Ai(u(0))}{Bi(u(0))} . \quad (6.3.11)$$

A non-vanishing value of b implies that the solution increases exponentially for positive values of the argument and the solution can be regarded as being concentrated in an excellent approximation near the upper end of the flux tube.

Second boundary condition is perhaps most naturally the condition that the energy is same for the flux tube amplitude as for the standard solution. Alternative boundary conditions would require the vanishing of the solution at both ends of the flux tube and in this case one obtains very large number of solutions as WKB approximation demonstrates. The normalization of the state so that it has a unit norm fixes the magnitude of the coefficients a and b since one can choose them to be real.

Estimate for the probability that muon is caught to the flux tube

The simplest estimate for the muon to be caught to the flux tube state characterized by the same energy as standard state is the overlap integral of the ordinary hydrogen wave function of muon and of the effectively one-dimensional flux tube. What one means with overlap integral is however not quite obvious.

1. The basic condition is that the modified "standard" state is orthogonal to the flux tube state. One can write the expression of a general state as

$$\begin{aligned} \Psi_{nlm} &\rightarrow N \times (\Psi_{nlm} - C(E, nlm)\Phi_{nlm}) , \\ \Phi_{nlm} &= Y_{lm}\Psi_E , \\ C(E, nlm) &= \langle \Psi_E | \Psi_{nlm} \rangle . \end{aligned} \quad (6.3.10)$$

Here Φ_{nlm} depends a flux tube state in which spherical harmonics is wave function in the space of orientations of the flux tube and Ψ_E is flux tube state with same energy as standard state. Here an inner product between standard states and flux tube states is introduced.

2. Assuming same energy for flux tube state and standard state, the expression for the total total probability for ending up to single flux tube would be determined from the orthogonality condition as

$$P_{nlm} = \frac{|C(E, nlm)|^2}{1 - |C(E, lmn)|^2} . \quad (6.3.11)$$

Here E refers to the common energy of flux tube state and standard state. The fact that flux tube states vanish at the lower end of the flux tube implies that they do not contribute to the expression for average charge density. The reduced contribution of the standard part implies that the attempt to interpret the experimental results in "standard model" gives a reduced value of the charge radius. The size of the contribution is given by P_{nlm} whose value should be about 4 per cent.

One can consider two alternative forms for the inner product between standard states and flux tube states. Intuitively it is clear that an overlap between the two wave functions must be in question.

1. The simplest possibility is that one takes only overlap at the upper end of the flux tube which defines 2-D surface. Second possibility is that that the overlap is over entire flux tube projection at the space-time sheet of atom.

$$\begin{aligned} \langle \Psi_E | \Psi_{nlm} \rangle &= \int_{end} \bar{\Psi}_r \Psi_{nlm} dS \quad (\text{Option I}) , \\ \langle \Psi_E | \Psi_{nlm} \rangle &= \int_{tube} \bar{\Psi}_r \Psi_{nlm} dV \quad (\text{Option II}) . \end{aligned} \quad (6.3.11)$$

2. For option I the inner product is non-vanishing only if Ψ_E is non-vanishing at the end of the flux tube. This would mean that electron ends up to the flux tube through its end. The inner product is dimensionless without introduction of a dimensional coupling parameter if the inner product for flux tube states is defined by 1-dimensional integral: one might criticize this assumption as illogical. Unitarity might be a problem since the local behaviour of the flux tube wave function at the end of the flux tube could imply that the contribution of the flux tube state in the quantum state dominates and this does not look plausible. One can of course consider the introduction to the inner product a coefficient representing coupling constant but this would mean loss of predictivity. Schrödinger equation at the end of the flux tubes guarantees the conservation of the probability current only if the energy of flux tube state is same as that of standard state or if the flux tube Schrödinger amplitude vanishes at the end of the flux tube.
3. For option II there are no problems with unitary since the overlap probability is always smaller than unity. Option II however involves overlap between standard states and flux tube states even when the wave function at the upper end of the flux tube vanishes. One can however consider the possibility that the possible flux tube states are orthogonalized with respect to standard states with leakage to flux tubes. The interpretation for the overlap integral would be that electron ends up to the flux tube via the formation of wormhole contact.

Option I fails

The considerations will be first restricted to the simpler option I. The generalization of the results of calculation to option II is rather straightforward. It turns out that option II gives correct order of magnitude for the reduction of charge radius for reasonable parameter values.

1. In a good approximation one can express the overlap integrals over the flux tube end (option I) as

$$\begin{aligned}
C(E, nlm) &= \int_{tube} \bar{\Psi}_E \Psi_{nlm} dS \simeq \pi R^2 \times Y_{lm} \times C(E, nl) , \\
C(E, nl) &= \bar{\Psi}_E(r_u) R_{nl}(r_u) .
\end{aligned} \tag{6.3.11}$$

An explicit expression for the coefficients can be deduced by using expression for Ψ_E as a superposition of Airy and Bairy functions. This gives

$$\begin{aligned}
C(E, nl) &= \bar{\Psi}_E(r_u) R_{nl}(r_u) , \\
\Psi_E(x) &= a_E Ai(u_E) + b Bi(u_E) , \quad \frac{a_E}{b_E} = -\frac{Bi(u_E(0))}{Ai(u_E(0))} , \\
u_E(x) &= \left(\frac{2m_\mu K}{\hbar^2}\right)^{1/3} (x - x_E) , \quad x_E = \frac{|E| - e\Phi_0}{K} , \\
K &= \frac{ke^2}{\pi R^2} , \quad R = z\alpha_K r_u , \quad k = \frac{2}{3} .
\end{aligned} \tag{6.3.8}$$

The normalization of the coefficients is fixed from the condition that a and b chosen in such a manner that Ψ has unit norm. For these boundary conditions Bi is expected to dominate completely in the sum and the solution can be regarded as exponentially decreasing function concentrated around the upper end of the flux tube.

In order to get a quantitative view about the situation one can express the parameters u_{min} and u_{max} in terms of the basic dimensionless parameters of the problem.

1. One obtains

$$\begin{aligned}
u_{min} \equiv u(0) &= -2\left(\frac{k}{z\alpha}\right)^{1/3} \left[1 + \pi \frac{z}{k} \alpha^2 \left(1 - \frac{1}{2} \alpha r\right)\right] \times r^{1/3} , \\
u_{max} \equiv u(r_u) &= u(0) + 2\frac{k}{z\alpha} \times r^{1/3} , \\
r &= \frac{m_\mu}{m_u} , \quad R = z\alpha r_u .
\end{aligned} \tag{6.3.7}$$

Using the numerical values of the parameters one obtains for $z = 1$ and $\alpha = 1/137$ the values $u_{min} = -33.807$ and $u_{max} = 651.69$. The value of u_{max} is so large that the normalization is in practice fixed by the exponential behavior of Bi for the suggested boundary conditions.

2. The normalization constant is in good approximation defined by the integral of the approximate form of Bi^2 over positive values of u and one has

$$N^2 \simeq \frac{dx}{du} \times \int_{u_{min}}^{u_{max}} Bi(u)^2 du , \quad \frac{dx}{du} = \frac{1}{2} \left(\frac{z^2 \alpha}{k}\right)^{1/3} \times r^{1/3} r_u , \tag{6.3.7}$$

By taking $t = \exp(\frac{4}{3}u^{3/2})$ as integration variable one obtains

$$\begin{aligned}
\int_{u_{min}}^{u_{max}} Bi(u)^2 du &\simeq \pi^{-1} \int_{u_{min}}^{u_{max}} \exp\left(\frac{4}{3}u^{3/2}\right) u^{-1/2} du \\
&= \left(\frac{4}{3}\right)^{2/3} \pi^{-1} \int_{t_{min}}^{t_{max}} \frac{dt}{\log(t)^{2/3}} \simeq \frac{1}{\pi} \frac{\exp(\frac{4}{3}u_{max}^{3/2})}{u_{max}} .
\end{aligned} \tag{6.3.7}$$

This gives for the normalization factor the expression

$$N \simeq \frac{1}{2} \left(\frac{z^2 \alpha}{k} \right)^{2/3} r^{1/3} r_u^{1/2} \exp\left(\frac{2}{3} u_{max}^{3/2}\right) . \quad (6.3.8)$$

3. One obtains for the value of Ψ_E at the end of the flux tube the estimate

$$\Psi_E(r_u) = \frac{Bi(u_{max})}{N} \simeq 2\pi^{-1/2} \times \left(\frac{k}{z^2 \alpha} \right)^{2/3} r^{1/3} r_u^{-1/2} , \quad r = \frac{r_u}{r_\mu} . \quad (6.3.9)$$

4. The inner product defined as overlap integral gives for the ground state

$$\begin{aligned} C_{E,00} &= \Psi_E(r_u) \times \Psi_{1,0,0}(r_u) \times \pi R^2 \\ &= 2\pi^{-1/2} \left(\frac{k}{z^2 \alpha} \right)^{2/3} r^{1/3} r_u^{-1/2} \times \left(\frac{1}{\pi a(\mu)^3} \right)^{1/2} \times \exp(-\alpha r) \times \pi z^2 \alpha^2 r_u^2 \\ &= 2\pi^{1/2} k^{2/3} z^{2/3} r^{11/6} \alpha^{17/6} \exp(-\alpha r) . \end{aligned} \quad (6.3.8)$$

The relative reduction of charge radius equals to $P = C_{E,00}^2$. For $z = 1$ one obtains $P = C_{E,00}^2 = 5.5 \times 10^{-6}$, which is by three orders of magnitude smaller than the value needed for $P_{tube} = C_{E,20}^2 = .0015$. The obvious explanation for the smallness is the α^2 factor coming from the area of flux tube in the inner product.

Option II could work

The failure of the simplest model is essentially due to the inner product. For option II the inner product for the flux tube states involves the integral over the area of flux tube so that the normalization factor for the state is obtained from the previous one by the replacement $N \rightarrow N/\sqrt{\pi R^2}$. In the integral over the flux tube the exponent function is in the first approximation equal to constant since the wave function for ground state is at the end of the flux tube only by a factor .678 smaller than at the origin and the wave function is strongly concentrated near the end of the flux tube. The inner product defined by the overlap integral over the flux tube implies $N \rightarrow NS^{1/2}$, $S = \pi R^2 = z^2 \alpha^2 r_u^2$. In good approximation the inner product for option II means the replacement

$$\begin{aligned} C_{E,n0} &\rightarrow A \times B \times C_{E,n0} , \\ A &= \frac{\frac{dx}{du}}{\sqrt{\pi R^2}} = \frac{1}{2\sqrt{\pi}} z^{-1/3} k^{-1/3} \alpha^{-2/3} r^{1/3} , \\ B &= \frac{\int Bi(u) du}{\sqrt{Bi(u_{max})}} = u_{max}^{-1/4} = 2^{-1/4} z^{1/2} k^{-1/4} \alpha^{1/4} r^{-1/12} . \end{aligned} \quad (6.3.7)$$

Using the expression

$$R_{20}(r_u) = \frac{1}{2\sqrt{2}} \times \left(\frac{1}{a_\mu} \right)^{3/2} \times (2 - r\alpha) \times \exp(-r\alpha) , \quad r = \frac{r_u}{r_\mu} \quad (6.3.8)$$

one obtains for $C_{E,20}$ the expression

$$C_{E,20} = 2^{-3/4} z^{5/6} k^{1/12} \alpha^{29/12} r^{25/12} \times (2 - r\alpha) \times \exp(-r\alpha) . \quad (6.3.9)$$

By the earlier general argument one should have $P_{tube} = |C_{E,20}|^2 \simeq .0015$. $P_{tube} = .0015$ is obtained for $z = 1$ and $N = 2$ corresponding to single flux tube per u quark. If the flux tubes are in opposite

directions, the leakage into 2P state vanishes. Note that this leakage does not affect the value of the coefficient a in the general formula for the Lamb shift. The radius of the flux tube is by a factor $1/4$ smaller than the classical radius of electron and one could argue that this makes it impossible for electron to topologically condense at the flux tube. For $z = 4$ one would have $P_{tube} = .015$ which is 10 times too large a value. Note that the nucleus possess a wave function for the orientation of the flux tube. If this corresponds to S-wave state then only the leakage between S-wave states and standard states is possible.

6.3.3 Are exotic flux tube bound states possible?

There seems to be no deep reason forbidding the possibility of genuine flux tube states decoupling from the standard states completely. To get some idea about the energy eigenvalues one can apply WKB approximation. This approach should work now: in fact, the study on WKB approximation near turning point by using linearization of the the potential leads always to Airy equation so that the linear potential represents an ideal situation for WKB approximation. As noticed these states do not seem to be directly relevant for the recent situation. The fact that these states have larger binding energies than the ordinary states of hydrogen atom might make possible to liberate energy by inducing transitions to these states.

1. Assume that a bound state with a negative energy E is formed inside the flux tube. This means that the condition $p^2 = 2m(E - V) \geq 0$, $V = -e\Phi$, holds true in the region $x \leq x_{max} < r_u$ and $p^2 = 2m(E - V) < 0$ in the region $r_u > x \geq x_{max}$. The expression for x_{max} is

$$x_{max} = \frac{\pi R^2}{k} \left(-\frac{|E|}{e^2} + \frac{1}{r_u} + \frac{kr_u}{\pi R^2} \right) \hbar . \quad (6.3.10)$$

$x_{max} < r_u$ holds true if one has

$$|E| < \frac{e^2}{r_u} = E_{max} . \quad (6.3.11)$$

The ratio of this energy to the ground state energy of muonic hydrogen is from $E(1) = e^2/2a(\mu)$ and $a = \hbar/\alpha m$ given by

$$\frac{E_{max}}{E(n=1)} = \frac{2m_u}{\alpha m_\mu} \simeq 5.185 . \quad (6.3.12)$$

This encourages to think that the ground state energy could be reduced by the formation of this kind of bound state if it is possible to find a value of n in the allowed range. The physical state would of course contain only a small fraction of this state. In the case of electron the increase of the binding energy is even more dramatic since one has

$$\frac{E_{max}}{E(n=1)} = \frac{2m_u}{\alpha m_e} = \frac{8}{\alpha} \simeq 1096 . \quad (6.3.13)$$

2. One can apply WKB quantization in the region where the momentum is real to get the condition

$$I = \int_0^{x_{max}} \sqrt{2m(E + e\Phi)} \frac{dx}{\hbar} = n + \frac{1}{2} . \quad (6.3.14)$$

By performing the integral one obtains the quantization condition

$$\begin{aligned}
 I &= k^{-1}(8\pi\alpha)^{1/2} \times \frac{R^2}{r_u^{3/2}r_\mu} \times A^{3/2} = n + \frac{1}{2} , \\
 A &= 1 + kx^2 - \frac{|E|r_u}{e^2} , \\
 x &= \frac{r_u}{R} , \quad k = \frac{2}{3\pi} , \quad r_i = \frac{\hbar}{m_i} .
 \end{aligned} \tag{6.3.13}$$

3. Parameter R should be of order of magnitude of charge radius $\alpha_K r_u$ of u quark is free parameter in some limits. $\alpha_K = \alpha$ is expected to hold true in excellent approximation. Therefore a convenient parametrization is

$$R = z\alpha r_u . \tag{6.3.14}$$

This gives for the binding energy the general expression in terms of the ground state binding energy $E(1, \mu)$ of muonic hydrogen as

$$\begin{aligned}
 |E| &= C \times E(1, \mu) , \\
 C &= D \times (1 + Kz^{-2}\alpha^{-2} - (\frac{y}{z^2})^{2/3} \times (n + 1/2)^{2/3}) , \\
 D &= 2y \times (\frac{K^2}{8\pi\alpha})^{1/3} , \\
 y &= \frac{m_u}{m_\mu} , \quad K = \frac{2}{3\pi} .
 \end{aligned} \tag{6.3.12}$$

4. There is a finite number of bound states. The above mentioned consistency conditions coming from $0 < x_{max} < r_\mu$ give $0 < C < C_{max} = 5.185$ restricting the allowed value of n to some interval. One obtains the estimates

$$\begin{aligned}
 n_{min} &\simeq \frac{z^2}{y} (1 + Kz^{-2}\alpha^{-2} - \frac{C_{max}}{D})^{3/2} - \frac{1}{2} , \\
 n_{max} &= \frac{z^2}{y} (1 + Kz^{-2}\alpha^{-2})^{3/2} - \frac{1}{2} .
 \end{aligned} \tag{6.3.12}$$

Very large value of n is required by the consistency condition. The calculation gives $n_{min} \in \{1.22 \times 10^7, 4.59 \times 10^6, 1.48 \times 10^5\}$ and $n_{max} \in \{1.33 \times 10^7, 6.66 \times 10^6, 3.34 \times 10^6\}$ for $z \in \{1, 2, 4\}$. This would be a very large number of allowed bound states -about 3.2×10^6 for $z = 1$.

The WKB state behaves as a plane wave below x_{max} and sum of exponentially decaying and increasing amplitudes above x_{max} :

$$\begin{aligned}
 &\frac{1}{\sqrt{k(x)}} \left[A \exp(i \int_0^x k(y) dy) + B \exp(-i \int_0^x k(y) dy) \right] , \\
 &\frac{1}{\sqrt{\kappa(x)}} \left[C \exp(- \int_{x_{max}}^x \kappa(y) dy) + D \exp(\int_{x_{max}}^x \kappa(y) dy) \right] , \\
 &k(x) = \sqrt{2m(-|E| + e\Phi)} , \quad \kappa(x) = \sqrt{2m(|E| - e\Phi)} .
 \end{aligned} \tag{6.3.9}$$

At the classical turning point these two amplitudes must be identical.

The next task is to decide about natural boundary conditions. Two types of boundary conditions must be considered. The basic condition is that genuine flux tube states are in question. This requires that the inner product between flux tube states and standard states defined by the integral over flux tube ends vanishes. This is guaranteed if the Schrödinger amplitude for the flux tube state vanishes at the ends of the flux tube so that flux tube behaves like an infinite potential well. The condition $\Psi(0) = 0$ at the lower end of the flux tube would give $A = -B$. Combined with the continuity condition at the turning point these conditions imply that Ψ can be assumed to be real. The $\Psi(r_u) = 0$ gives a condition leading to the quantization of energy.

The wave function over the directions of flux tube with a given value of n is given by the spherical harmonics assigned to the state (n, l, m) .

6.4 Comments about new physics predicted by TGD at LHC

The situation in particle physics is extremely interesting from TGD point of view since the accuracy of the picture about particles has increased dramatically after the discovery of the weak form of electric-magnetic duality and the understanding of how twistor program could be realized in TGD framework. Among other things, the findings from LHC make it possible to test whether this picture is realistic and exclude alternatives. In the following I summarize the recent picture without any guarantee that it would be modified as data from LHC arrives. I will also half-seriously consider the rumors about the first super partners in TGD framework.

6.4.1 Particles as wormhole contacts

The assumption that partonic 2-surfaces correspond to representations of Super Virasoro algebra has been an unchallenged assumption of the p-adic mass calculations for a long time although one might argue that these objects do not possess stringy characteristics, in particular they do not possess two ends. The progress in the understanding of the modified Dirac equation and the introduction of the weak form of electric magnetic duality [55] however forces to modify the picture about the origin of the string mass spectrum.

1. The weak form of electric-magnetic duality, the basic facts about modified Dirac equation and the proposed twistorialization of quantum TGD [19] force to conclude that both strings and bosons and their super-counterparts emerge from massless fermions moving collinearly at partonic two-surfaces. Stringy mass spectrum is consistent with this only if p-adic thermodynamics describes wormhole contacts as analogs of stringy objects having quantum numbers at the throats playing the role of string ends. For instance, the three-momenta of massless wormhole throats could be in opposite direction so that wormhole contact would become massive. The fundamental string like objects would therefore correspond to the wormhole contacts with size scale of order CP_2 length. Already these objects must have a correct correlation between color and electroweak quantum numbers. The colored super-generators taking care that anomalous color is compensated can be assigned with purely bosonic quanta associated with the wormhole throats which carry no fermion number.
2. Second modification comes from the necessity to assume weak confinement in the sense that each wormhole throat carrying fermionic numbers is accompanied by a second wormhole throat carrying neutrino pair cancelling the net weak isospin so that only electromagnetic charge remains unscreened. This screening must take place in weak length scale so that ordinary elementary particles are predicted to be string like objects. This string tension has however nothing to do with the fundamental string tension responsible for the mass spectrum. This picture is forced also by the fact that fermionic wormhole throats necessarily carry Kähler magnetic charge [55] so that in the case of leptons the second wormhole throat must carry a compensating Kähler magnetic charge. In the case of quarks one can consider the possibility that magnetic charges are not neutralized completely in weak scale and that the compensation occurs in QCD length scale so that Kähler magnetic confinement would accompany color confinement. This means color magnetic confinement since classical color gauge fields are proportional to induced Kähler field.

These modifications do not seem to appreciably affect the results of calculations, which depend only on the number of tensor factors in super Virasoro representation, they are not taken explicitly into account in the calculations. The predictions of the general theory are consistent with the earliest mass calculations, and the earlier ad hoc parameters disappear. In particular, optimal lowest order predictions for the charged lepton masses are obtained and photon, gluon and graviton appear as essentially massless particles. What is new is the possibility to describe the massivation of gauge bosons by including the contribution from the string tension of weak string like objects: weak boson masses have indeed been the trouble makers and have forced to conclude that Higgs expectation might be needed unless some other mechanism contributes to the conformal vacuum weight of the ground state.

6.4.2 New physics at LHC is approximately unavoidable

Tommaso Dorigo has written a summary [118] about a highly interesting conference talk by Guido Altarelli in 2010 LHC Days in Split [119]. This talk provides new insights to the developing ideas about the relationship of electric-magnetic magnetic duality and particle massivation.

The talk begins with the question "Is it possible that Higgs will not be found?". The general conclusion is that if Higgs is not found then some other new physics is "approximately unavoidable". One very general reason is that the unitarity of electroweak theory is otherwise spoiled. Altarelli saw also a reason for worry. The new physics should emerge rather abruptly: the general view is that there is no evidence for its existence from the previous experimental work. How can it be possible that the new physics lurking just behind the corner manages to hide itself so completely?

TGD predict Higgs and supersymmetry and also weak confinement

This touched something inside me since the questions whether TGD predicts Higgs and standard space-time super-symmetry have shadowed my life for a long time. When the notions of bosonic emergence and understanding of super-conformal symmetry in terms of partons identified as wormhole throats emerged, it became clear that boson with quantum numbers of Higgs identified as wormhole contact with opposite throats carrying fermion and antifermion quantum numbers is bound to exist. Also an appropriate generalization of broken space-time supersymmetry exists and reduces to $\mathcal{N} = 1$ super-symmetry at low energy limit.

The emergence of the weak form of electric-magnetic duality during this year led to the realization that the wormhole throats behave like magnetic monopoles since the CP_2 projections of these 2-surfaces are homologically non-trivial. The only manner to avoid macroscopic magnetic monopole fields is magnetic confinement appearing as a side product of electro-weak symmetry breaking and possibly also of color confinement. In the case of electroweak symmetry breaking this would mean that a wormhole throat carrying lepton or quark quantum numbers is accompanied by second throat with opposite Kähler magnetic charge and carrying quantum numbers of neutrino and antineutrino neutralizing the weak charge of the elementary fermion and screening of weak force. One can speak of weak confinement. For quarks the neutralization of magnetic charge need not be complete and valence quarks could be Kähler magnetic monopoles giving rise to hadrons which have neither magnetic nor color charges.

Physical elementary particles would be string like objects with length of order weak length scale. This would certainly represent new physics which could become visible at LHC. This piece of new physics (TGD predicts also many other pieces) would resemble the good old hadron physics for which the predecessor of the recent super string theory provided a satisfactory description. Regge trajectories would be one striking signature of this physics both at the level of states and scattering amplitudes. The string tension of these trajectories would be enormous: in the first estimate $2^{107-89=18}$ times higher than that for low energy hadrons. Mass scale would be about .512 TeV to be compared with the collision energy of 7 TeV of LHC. The proton of this physics would have mass of about .512 TeV (if one believes on naive p-adic scaling) and is expected to be unstable against decay to ordinary hadrons. Lifetime should be long since otherwise also the ordinary proton is expected to be unstable against decay to scaled down hadrons with say p-adic length scale of electron (, which corresponds to the largest Mersenne prime which does not define super-astrophysical p-adic length scale).

p-Adic thermodynamics and the emergence of string like objects from massless partons

While reading the summary about Altarelli's representation I realized that I have been talking for years about scaled up copy of hadron physics at electroweak length scale. What distinguishes the string like objects of this hadronic physics from those of electroweak physics? Or do they represent two different aspects of something more general? The obvious answer would be that color confinement is not involved with weak strings and that this is the basic distinction. This answer seems to be correct.

1. Dirac equation in $M^4 \times CP_2$ predicts that free fermions -also leptons- in general correspond to in non-trivial color partial waves of CP_2 and that the correlation between color and electroweak quantum numbers is wrong although quarks correspond to triality $t=1$ and leptons to triality $t=0$. This was a strong objection against TGD until I realized that super-conformal invariance could resolve the problem. The lightest leptonic (quark) states are color singlets (triplets) and colored super-conformal generators can generate the anomalous color so that lightest leptons and quarks are color singlets and triplets. p-Adic mass calculations are consistent with this picture. The contributions from enormous bare mass squared (conformal weight) whose values are dictated by the color partial waves of quarks and leptons are compensated by negative tachyonic mass squared (conformal weight) of the vacuum state.
2. p-Adic thermodynamics assumes that elementary particles correspond to representations of super-conformal algebra characterized by enormous string tension. Elementary particle mass scales emerge thermodynamically from a fundamental mass scale which corresponds to CP_2 mass, which is roughly $10^{-4} - 10^{-3}$ times Planck mass. Massless states with vanishing conformal weight are thermally mixed with those with non-vanishing conformal weight and enormous value of mass squared given by string mass formula.
3. Weak form of electric-magnetic duality, the basic facts about modified Dirac equation, and also twistorialization of quantum TGD force to conclude that both strings and bosons and their super-counterparts emerge from massless fermions moving collinearly at partonic two-surfaces. Stringy mass spectrum is consistent with this only if p-Adic thermodynamics describes wormhole contacts. For instance, the three-momenta of massless wormhole throats could be in opposite direction so that wormhole contact would become massive. String like objects would therefore correspond to the wormhole contacts with size scale of order CP_2 length. Wormhole contacts would be the fundamental stringy objects and already these have the correct correlation between color and electroweak quantum numbers.
4. One can of course ask whether the anomalous color could be neutralized in the weak scale? This is not possible. p-Adic thermodynamics with string tension defined by electro-weak length scale would make completely unrealistic predictions.

How the new physics around the corner manages to hide so well?

The basic worry of Guido Altarelli is expressed by the question of the title and it seems that the new physics predicted TGD might provide a satisfactory answer to the question.

1. What seems to be a prediction is that the weak length scale serves as the confinement scale for the string like objects with second end containing neutrino pairs with electroweak isospin. Regge trajectories of weak bosons and Higgs is one consequence. The new physics would be behind the corner would be made virtually invisible by weak confinement. The replacement of these neutrino pairs with more general states would give a lot of new physics.
2. Of course, Nature could choose to scale up the weak scale to say Mersenne prime M_{61} meaning weak bosons with mass scale 512 higher than weak scale. This would be more or less equivalent with the disappearance of weak interactions and the new weak physics would emerge in discontinuous manner via phase transition. That an entire weak physics would just disappear from existence without any warning sounds of course weird! In reality of course the phase transition would take place for a small portion of the stuff created in the collisions. The scaled up weak bosons would also decay in time scale which is by a factor $1/512$ shorter than the life time of weak bosons. The challenge is therefore to detect very small signals from background.

3. Whether a scaled up counterpart of hadron physics exists at weak scale remains an open question. There is evidence for scaled up variants of leptohadrons for which both ends would contain charged leptons in color partial waves. For these states at p-adic mass scales characterizing ordinary leptons there indeed exists experimental evidence.

6.4.3 How TGD based description of particle massivation relates to Higgs mechanism?

In TGD framework p-adic thermodynamics gives the dominating contribution to fermion masses, which is something completely new. In the case of gauge bosons thermodynamic contribution is small since the inverse integer valued p-adic temperature is $T = 1/2$ for bosons or even lower: for fermions one has $T = 1$.

Whether Higgs can contribute to the masses is not completely clear. In TGD framework Mexican hat potential however looks like trick. One must however keep in mind that any other mechanism must explain the ratio of W and Z^0 masses and how these bosons receive their longitudinal polarizations. One must also consider seriously the possibility that all components for the TGD counterpart of Higgs boson are transformed to the longitudinal polarizations of the gauge bosons. Twistorial approach to TGD indeed strongly suggests that also the gauge bosons regarded usually as massless have a small mass guaranteeing cancellation of IR singularities. As I started write to write this piece of text I believed that photon does not eat Higgs but had to challenge my beliefs. Maybe there is no Higgs to be found at LHC! Only pseudo-scalar partner of Higgs would remain to be discovered.

The weak form of electric magnetic duality implying that each wormhole throat carrying fermionic quantum numbers is accompanied by a second wormhole throat carrying opposite magnetic charge and neutrino pair screening weak isospin and making gauge bosons massive. Concerning the implications the following view looks the most plausible one at this moment.

1. Neutral Higgs-if not eaten by photon- could develop a coherent state meaning vacuum expectation value and this is naturally proportional to the inverse of the p-adic length scale as are boson masses. This contribution can be assigned to the magnetic flux tube mentioned above since it screens weak force - or equivalently - makes them massive. Higgs expectation would not cause boson massivation. Rather, massivation and Higgs vacuum expectation would be caused by the presence of the magnetic flux tubes. Standard model would suffer from a causal illusion. Even a worse illusion is possible if the photon eats the neutral Higgs.
2. The "stringy" magnetic flux tube connecting fermion wormhole throat and the wormhole throat containing neutrino pair would give to the vacuum conformal weight a small contribution and therefore to the mass squared of both fermions and gauge bosons (dominating one for the latter). This contribution would be small in the p-adic sense (proportional $1/p^2$ rather than $1/p$). I cannot calculate this "stringy" contribution but stringy formula in weak scale is very suggestive.
3. In the case of light fermions and massless gauge bosons the stringy contribution must vanish and therefore must correspond to $n = 0$ string excitation (string does not vibrate at all) : otherwise the mass of fermion would be of order weak boson mass. For weak bosons $n = 1$ would look like a natural identification but also $n = 0$ makes sense since $h \pm 1$ states corresponds opposite three-momenta for massless fermion and antifermion so that the state is massive. The mechanism bringing in the $h = 0$ helicity of gauge boson would be the TGD counterpart for the transformation of Higgs component to a longitudinal polarization. $n \geq 0$ excited states of fermions and $n \geq 1$ excitations of bosons having masses above weak boson masses are predicted and would mean new physics becoming possibly visible at LHC.

Consider now the identification of Higgs in TGD framework.

1. In TGD framework Higgs particles do not correspond to complex $SU(2)$ doublets but to triplet and singlet having same quantum numbers as gauge bosons. Therefore the idea that photon eats neutral Higgs is suggestive. Also a pseudo-scalar variant of Higgs is predicted. Let us see how these states emerge from weak strings.

2. The two kinds of massive states corresponding to $n = 0$ and $n = 1$ give rise to massive spin 1 and spin 2 particles. First of all, the helicity doublet $(1, -1)$ is necessarily massive since the 3-momenta for massless fermion and anti-fermion are opposite. For $n = L = 0$ this gives two states but helicity zero component is lacking. For $n = L = 1$ one has tensor product of doublet $(1, -1)$ and angular momentum triplet formed by $L = 1$ rotational state of the weak string. This gives 2×3 states corresponding to $J = 0$ and $J = 2$ multiplets. Note however than in spin degrees of freedom the Higgs candidate is not a genuine elementary scalar particle.
3. Fermion and antifermion can have parallel three momenta summing up to a massless 4-momentum. Spin vanishes so that one has Higgs like particle also now. This particle is however pseudo-scalar being group theoretically analogous to meson formed as a pair of quark and antiquark. p-Adic thermodynamics gives a contribution to the mass squared. By taking a tensor product with rotational states of strings one would obtain Regge trajectory containing pseudoscalar Higgs as the lowest state.

Consider now the problem how the gauge bosons can eat the Higgs boson to get their longitudinal component.

1. ($J = 0, n = 1$) Higgs state can be combined with $n = 0$ $h = \pm 1$ doublet to give spin 1 massive triplet provided the masses of the two states are same. This will be discussed below.
2. Also gauge bosons usually regarded as massless can eat the scalar Higgs so that Higgs like particle could disappear completely. There would be no Higgs to be discovered at LHC! But is this a real prediction? Could it be that it is not possible to have exactly massless photons and gluons? The mixing of M^4 chiralities for Chern-Simons Dirac equation implies that also collinear massless fermion and antifermion can have helicity ± 1 . The problem is that the mixing of the chiralities is a signature of massivation!

Could it really be that even the gauge bosons regarded as massless have a small mass characterized by the length scale of the causal diamond defining the physical IR cutoff and that the remaining Higgs component would correspond to the longitudinal component of photon? This would mean the number of particles in the final states for a particle reaction with a fixed initial state is always bounded from above. This is important for the twistorial aesthetics of generalized Feynman diagrammatics implied by zero energy ontology. Also the vanishing of IR divergences is guaranteed by a small physical mass [19]. Maybe internal consistency allows only pseudo-scalar Higgs.

The weak form of electric-magnetic duality suggests strongly the existence of weak Regge trajectories.

1. The most general mass squared formula with spin-orbit interaction term $M_{L-S}^2 L \cdot S$ reads as

$$M^2 = nM_1^2 + M_0^2 + M_{L-S}^2 L \cdot S, \quad n = 0, 2, 4 \quad \text{or} \quad n = 1, 3, 5, \dots, \quad (6.4.1)$$

M_1^2 corresponds to string tension and M_0^2 corresponds to the thermodynamical mass squared and possible other contributions. For a given trajectory even (odd) values of n have same parity and can correspond to excitations of same ground state. From ancient books written about hadronic string model one vaguely recalls that one can have several trajectories (satellites) and if one has something called exchange degeneracy, the even and odd trajectories define single line in $M^2 - J$ plane. As already noticed TGD variant of Higgs mechanism combines together $n = 0$ states and $n = 1$ states to form massive gauge bosons so that the trajectories are not independent.

2. For fermions, possible Higgs, and pseudo-scalar Higgs and their super partners also p-adic thermodynamical contributions are present. M_0^2 must be non-vanishing also for gauge bosons and be equal to the mass squared for the $n = L = 1$ spin singlet. By applying the formula to $h = \pm 1$ states one obtains

$$M_0^2 = M^2(\text{boson}) . \quad (6.4.2)$$

The mass squared for transversal polarizations with $(h, n, L) = (\pm 1, n = L = 0, S = 1)$ should be same as for the longitudinal polarization with $(h = 0, n = L = 1, S = 1, J = 0)$ state. This gives

$$M_1^2 + M_0^2 + M_{L-S}^2 L \cdot S = M_0^2 . \quad (6.4.3)$$

From $L \cdot S = [J(J + 1) - L(L + 1) - S(S + 1)] / 2 = -2$ for $J = 0, L = S = 1$ one has

$$M_{L-S}^2 = -\frac{M_1^2}{2} . \quad (6.4.4)$$

Only the value of weak string tension M_1^2 remains open.

3. If one applies this formula to arbitrary $n = L$ one obtains total spins $J = L + 1$ and $L - 1$ from the tensor product. For $J = L - 1$ one obtains

$$M^2 = (2n + 1)M_1^2 + M_0^2 .$$

For $J = L + 1$ only M_0^2 contribution remains so that one would have infinite degeneracy of the lightest states. Therefore stringy mass formula must contain a non-linear term making Regge trajectory curved. The simplest possible generalization which does not affect $n=0$ and $n=1$ states is of from

$$M^2 = n(n - 1)M_2^2 + (n - \frac{L \cdot S}{2})M_1^2 + M_0^2 . \quad (6.4.5)$$

The challenge is to understand the ratio of W and Z⁰ masses, which is purely group theoretic and provides a strong support for the massivation by Higgs mechanism.

1. The above formula and empirical facts require

$$\frac{M_0^2(W)}{M_0^2(Z)} = \frac{M^2(W)}{M^2(Z)} = \cos^2(\theta_W) . \quad (6.4.6)$$

in excellent approximation. Since this parameter measures the interaction energy of the fermion and antifermion decomposing the gauge boson depending on the net quantum numbers of the pair, it would look very natural that one would have

$$M_0^2(W) = g_W^2 M_{SU(2)}^2 , \quad M_0^2(Z) = g_Z^2 M_{SU(2)}^2 . \quad (6.4.7)$$

Here $M_{SU(2)}^2$ would be the fundamental mass squared parameter for $SU(2)$ gauge bosons. p-Adic thermodynamics of course gives additional contribution which is vanishing or very small for gauge bosons.

2. The required mass ratio would result in an excellent approximation if one assumes that the mass scales associated with $SU(2)$ and $U(1)$ factors suffer a mixing completely analogous to the mixing of $U(1)$ gauge boson and neutral $SU(2)$ gauge boson W_3 leading to γ and Z^0 . Also Higgs, which consists of $SU(2)$ triplet and singlet in TGD Universe, would very naturally suffer similar mixing. Hence $M_0(B)$ for gauge boson B would be analogous to the vacuum expectation of corresponding mixed Higgs component. More precisely, one would have

$$\begin{aligned} M_0(W) &= M_{SU(2)} , \\ M_0(Z) &= \cos(\theta_W)M_{SU(2)} + \sin(\theta_W)M_{U(1)} , \\ M_0(\gamma) &= -\sin(\theta_W)M_{SU(2)} + \cos(\theta_W)M_{U(1)} . \end{aligned} \quad (6.4.6)$$

The condition that photon mass is very small and corresponds to IR cutoff mass scale gives $M_0(\gamma) = \epsilon \cos(\theta_W)M_{SU(2)}$, where ϵ is very small number, and implies

$$\begin{aligned} \frac{M_{U(1)}}{M(W)} &= \tan(\theta_W) + \epsilon , \\ \frac{M(\gamma)}{M(W)} &= \epsilon \times \cos(\theta_W) , \\ \frac{M(Z)}{M(W)} &= \frac{1 + \epsilon \times \sin(\theta_W)\cos(\theta_W)}{\cos(\theta_W)} . \end{aligned} \quad (6.4.5)$$

There is a small deviation from the prediction of the standard model for W/Z mass ratio but by the smallness of photon mass the deviation is so small that there is no hope of measuring it. One can of course keep mind open for $\epsilon = 0$. The formulas allow also an interpretation in terms of Higgs vacuum expectations as it must. The vacuum expectation would most naturally correspond to interaction energy between the massless fermion and antifermion with opposite 3-momenta at the throats of the wormhole contact and the challenge is to show that the proposed formulas characterize this interaction energy. Since CP_2 geometry codes for standard model symmetries and their breaking, it would not be surprising if this would happen. One cannot exclude the possibility that p-adic thermodynamics contributes to $M_0^2(boson)$. For instance, ϵ might characterize the p-adic thermal mass of photon.

If the mixing applies to the entire Regge trajectories, the above formulas would apply also to weak string tensions, and also photons would belong to Regge trajectories containing high spin excitations.

3. What one can one say about the value of the weak string tension M_1^2 ? The naive order of magnitude estimate is $M_1^2 \simeq m_W^2 \simeq 10^4 \text{ GeV}^2$ is by a factor $1/25$ smaller than the direct scaling up of the hadronic string tension about 1 GeV^2 scaled up by a factor 2^{18} . The above argument however allows also the identification as the scaled up variant of hadronic string tension in which case the higher states at weak Regge trajectories would not be easy to discover since the mass scale defined by string tension would be 512 GeV to be compared with the recent beam energy 7 TeV . Weak string tension need of course not be equal to the scaled up hadronic string tension. Weak string tension - unlike its hadronic counterpart- could also depend on the electromagnetic charge and other characteristics of the particle.

6.4.4 First rumors about supersymmetric partners from LHC

Lubos Motl has reported the first rumors from LHC concerning super-partners [120]. The estimates for the masses are 200 GeV for a scalar super partner of fermion and 160 GeV for a fermionic superpartner of gauge boson or Higgs. Being an incurable optimist I suppose that the rumors from LHC are more trustworthy than the physics blog rumors usually. If so, can one understand these masses in TGD framework and what can one conclude about them?

Consider first the theoretical background in light p-adic mass calculations, the weak form of electric-magnetic duality, and TGD based view about supersymmetry.

1. The simplest possibility is that the p-adic length scale of the super-partner differs from that of partner but the p-adic thermodynamical contributions to the mass squared obey the same formula.
2. If the p-adic prime $p \simeq 2^k$ of super-partner is smaller than $M_{89} = 2^{89} - 1$, the weak length scale must be scaled down and $M_{61} = 2^{61} - 1$ is the next Mersenne prime. Scaled up variant of QCD for M_{89} would naturally correspond to M_{61} weak physics and would have hadronic string tension about 2^{18} GeV² by scaling the ordinary hadronic string tension of about 1 GeV². This scaled up variant of hadronic physics is an old prediction of TGD. As noticed, also weak string tension could have the same value. Quite generally, the pairs of weak and hadronic scales predicted to form a hierarchy could correspond to pairs of subsequent (possibly Gaussian) Mersenne primes.
3. What happens for $k = 89$? Can the particle topologically condense at the same p-adic scale that characterizes its weak flux tube? Or should one assume that the p-adic prime corresponds to $k \leq 89$ assuming that the particle has standard weak interactions. If so then the superpartners of light fermions would have $k \leq 89$. This is a strong prediction if superpartners obey the same mass formula as particles. In the case of weak gluinos and also QCD gluinos the bound would be $k \leq 89$ and even stronger bound would be $k = 89$ so that the masses of wino and zino would be same as W and Z⁰.

One must be however very cautious with this kind of arguments since one is dealing with quantum theory. For instance, quarks inside proton have masses in 10 MeV scale and their Compton lengths are much larger than the Compton size of proton and even atomic nucleus. The interpretation is that for the corresponding space-time sheets is in terms of the color magnetic body of quark. These large space-time sheets are essential in the model of the Lamb shift anomaly of muonic hydrogen discussed in the section "The incredibly shrinking proton".

4. In TGD framework Higgs and its pseudo-scalar companion define electroweak triplet and singlet and Higgs could be eaten completely by electro-weak gauge bosons if the TGD based mechanism of massivation is correct. The condition of exact Yangian symmetry demands the cancellation of IR divergences requiring a small mass for all gauge bosons and graviton. The twistorially natural assumption that gauge bosons are bound states of massless fermion and antifermion implies that the three-momenta of fermion and antifermion are in opposite directions so that all gauge bosons -even photon- and graviton would be massive. Super-symmetry strongly suggests that gauginos eat Higgsinos as they become massive so that only massive gauge bosons and gauginos and possible pseudoscalar Higgs and its superpartner would remain to be discovered at LHC. Similar mechanism can indeed work also in the case of gluons expected to have colored scalar counterparts. Gluon would be massless below the scale corresponding to QCD Λ and massive above this scale.

What does this picture give when compared with the rumors about super-partners of fermion and scalar. If selectron corresponds to the not necessarily allowed $M_{89} = 2^{89} - 1$, and obeys otherwise the same mass formula as electron, the mass should be 250 GeV, which is too large. For $k = 88$ which is the smallest value allowed by the above argument, one would obtain 177 GeV not far from 160 GeV. Therefore the interpretation as selectron could make sense.

In the case of super-partner of scalar one can consider several options.

1. The first observation is that 200 GeV mass does not satisfy the proposed upper bound $k \geq 89$ for higgsinos and gauginos suggested by the condition that the weak string cannot have p-adic length scale longer than the p-adic length scale at which the particle condensed topologically. Hence neither higgsino nor longitudinal polarization of gaugino can be in question.
2. If one gives up the upper bound $m_Z = 91.2$ GeV on mass but takes the twistorially motivated and mathematically beautiful horror scenario for LHC seriously, the 200 GeV particle can only correspond to a longitudinal polarization of Zino or photino.

One can of course forget the upper bound on mass and give up the horror scenario for a moment and look what one obtains.

1. If photonic Higgs is not eaten by photon, one would obtain $k(\text{Higgs}) = k(\text{Higgsino}) + n$. $n = 1, 2, 3$ would give Higgs mass equal to (141, 100, 71) GeV for $m(\text{Higgsino}) = 200$ GeV. On basis of experimental data mildly suggesting that neutral Higgs appears in two mass scales I have considered the possibility that Higgs indeed appears at two p-adic length scales corresponding to about 130 GeV and 92 GeV related by square root of two factor. 130 GeV would give $m(\text{Higgsino}) = 184$ GeV: I dare guess that this is consistent with the estimate 200 GeV.
2. For W and Z^0 Higgsinos the mass would be p-adically scaled up variant of W or Z^0 mass and for Z^0 mass about 91.2 GeV Z^0 Higgsino mass would be 182.4 GeV for $n = 2$. For W Higgsino the mass would be around 160.8 GeV.

I have already earlier considered the predictions of p-adic length scale hypothesis for super partners on basis of single very strange scattering event (see the section "Experimental indication for space-time supersymmetry"). This kind of considerations must of course be taken as a mere blog entertainment. The hypothesis assuming that the mass formulas for particles and sparticles are same but p-adic length scale is possibly different, combined with kinematical constraints fixes the masses of TGD counterparts of selectron, higgsino, and Z^0 -gluino to be 131 GeV (just at the upper bound allowed kinematically), 45.6 GeV, and 91.2 GeV (Z^0 mass) respectively. The masses are consistent with the bounds predicted by the MSSM inspired model.

Selectron mass would be by a factor $2^{-1/2}$ smaller than 177 GeV and presumably consistent with the 160 GeV rumor. Higgsino mass would be one half of Z^0 mass and would satisfy the proposed constraint $k \leq 89$. Z^0 gluino mass would be equal to Z^0 mass also in accordance with the proposed constraint. W gluino is predicted to have same mass as W. In the case of photino the upper bound to the mass would be given by weak boson mass scale. Could it be that the life would be so simple? Could these predictions make it easy to discover super partners at LHC? Well-informed reader might be able to answer these questions.

6.5 Simulating Big Bang in laboratory

Ultra-high energy collisions of heavy nuclei at Relativistic Heavy Ion Collider (RHIC) can create so high temperatures that there are hopes of simulating Big Bang in laboratory. The experiment with PHOBOS detector [94] probed the nature of the strong nuclear force by smashing two Gold atoms together at ultrahigh energies. The analysis of the experimental data has been carried out by Prof. Manly and his collaborators at RHIC in Brookhaven, NY [77]. The surprise was that the hydrodynamical flow for non-head-on collisions did not possess the expected longitudinal boost invariance.

This finding stimulates in TGD framework the idea that something much deeper might be involved.

1. The quantum criticality of the TGD inspired very early cosmology predicts the flatness of 3-space as do also inflationary cosmologies. The TGD inspired cosmology is 'silent whisper amplified to big bang' since the matter gradually topologically condenses from decaying cosmic string to the space-time sheet representing the cosmology. This suggests that one could model also the evolution of the quark-gluon plasma in an analogous manner. Now the matter condensing to the quark-gluon plasma space-time sheet would flow from other space-time sheets. The evolution of the quark-gluon plasma would very literally look like the very early critical cosmology.
2. What is so remarkable is that critical cosmology is not a small perturbation of the empty cosmology represented by the future light cone. By perturbing this cosmology so that the spherical symmetry is broken, it might possible to understand qualitatively the findings of [77]. Maybe even the breaking of the spherical symmetry in the collision might be understood as a strong gravitational effect on distances transforming the spherical shape of the plasma ball to a non-spherical shape without affecting the spherical shape of its M_+^4 projection.
3. The model seems to work at qualitative level and predicts strong gravitational effects in elementary particle length scales so that TGD based gravitational physics would differ dramatically from that predicted by the competing theories. Standard cosmology cannot produce these effects without a large breaking of the cherished Lorentz and rotational symmetries forming the basis of elementary particle physics. Thus the the PHOBOS experiment gives direct support for

the view that Poincare symmetry is symmetry of the imbedding space rather than that of the space-time.

4. This picture was completed a couple of years later by the progress made in hadronic mass calculations [17]. It has already earlier been clear that quarks are responsible only for a small part of the mass of baryons (170 GeV in case of nucleons). The assumption that hadronic $k = 107$ space-time sheet carries a many-particle state of super-symplectic particles with vanishing electro-weak quantum numbers (meaning darkness in the strongest sense of the word.)
5. TGD allows a model of hadrons predicting their masses with accuracy better than one per cent. In this framework color glass condensate can be identified as a state formed when the hadronic space-time sheets of colliding hadrons fuse to single long stringy object and collision energy is transformed to super-symplectic hadrons.

What I have written above reflects the situation around 2005 when RHIC was in blogs. After 5 years later (2010) LHC gave its first results suggesting similar phenomena in proton-proton collisions. These results provide support for the idea that the formation of long entangled hadronic strings by a fusion of hadronic strings forming a structure analogous to black hole or initial string dominated phase of the cosmology are responsible for the RHIC findings. In the LHC case the mechanism leading to this kind of strings must be different since initial state contains only two protons. I would not anymore distinguish between hadrons and super-symplectic hadrons since in the recent picture super-symplectic excitations are responsible for most of the mass of the hadron. The view about dark matter as macroscopic quantum phase with large Planck constant has also evolved a lot from what it was at that time and I have polished reference to some short lived ideas for the benefit of the reader and me. I did not speak about zero energy ontology at that time and the understanding of the general mathematical structure of TGD has improved dramatically during these years.

6.5.1 Experimental arrangement and findings

Heuristic description of the findings

In the experiments using PHOBOS detector ultrahigh energy Au+Au collisions at center of mass energy for which nucleon-nucleon center of mass energy is $\sqrt{s_{NN}} = 130$ GeV, were studied [94].

1. In the analyzed collisions the Au nuclei did not collide quite head-on. In classical picture the collision region, where quark gluon plasma is created, can be modelled as the intersection of two colliding balls, and its intersection with plane orthogonal to the colliding beams going through the center of mass of the system is defined by two pieces of circles, whose intersection points are sharp tips. Thus rotational symmetry is broken for the initial state in this picture.
2. The particles in quark-gluon plasma can be compared to a persons in a crowded room trying to get out. The particles collide many times with the particles of the quark gluon plasma before reaching the surface of the plasma. The distance $d(z, \phi)$ from the point $(z, 0)$ at the beam axis to the point $(0, \phi)$ at the plasma surface depends on ϕ . Obviously, the distance is longest to the tips $\phi = \pm\pi/2$ and shortest to the points $\phi = 0, \phi = \phi$ of the surface at the sides of the collision region. The time $\tau(z, \phi)$ spent by a particle to the travel to the plasma surface should be a monotonically increasing function $f(d)$ of d :

$$\tau(z, \phi) = f(d(z, \phi)) .$$

For instance, for diffusion one would have $\tau \propto d^2$ and $\tau \propto d$ for a pure drift.

3. What was observed that for $z = 0$ the difference

$$\Delta\tau = \tau(z = 0, \pi/2) - \tau(z = 0, 0)$$

was indeed non-vanishing but that for larger values of z the difference tended to zero. Since the variation of z correspond that for the rapidity variable y for a given particle energy, this means that particle distributions depend on rapidity which means a breaking of the longitudinal boost invariance assumed in hydrodynamical models of the plasma. It was also found that the difference vanishes for large values of y : this finding is also important for what follows.

A more detailed description

Consider now the situation in a more quantitative manner.

1. Let z -axis be in the direction of the beam and ϕ the angle coordinate in the plane E^2 orthogonal to the beam. The kinematical variables are the rapidity of the detected particle defined as $y = \log[(E + p_z)/(E - p_z)]/2$ (E and p_z denote energy and longitudinal momentum), Feynman scaling variable $x_F \simeq 2E/\sqrt{s}$, and transversal momentum p_T .
2. By quantum-classical correspondence, one can translate the components of momentum to space-time coordinates since classically one has $x^\mu = p^\mu a/m$. Here a is proper time for a future light cone, whose tip defines the point where the quark gluon plasma begins to be generated, and $v^\mu = p^\mu/m$ is the four-velocity of the particle. Momentum space is thus mapped to an $a = \text{constant}$ hyperboloid of the future light cone for each value of a .

In this correspondence the rapidity variable y is mapped to $y = \log[(t + z)/(t - z)]$, $|z| \leq t$ and non-vanishing values for y correspond to particles which emerge, not from the collision point defining the origin of the plane E^2 , but from a point above or below E^2 . $|z| \leq t$ tells the coordinate along the beam direction for the vertex, where the particle was created. The limit $y \rightarrow 0$ corresponds to the limit $a \rightarrow \infty$ and the limit $y \rightarrow \pm\infty$ to $a \rightarrow 0$ (light cone boundary).

3. Quark-parton models predict at low energies an exponential cutoff in transverse momentum p_T ; Feynman scaling $dN/dx_F = f(x_F)$ independent of s ; and longitudinal boost invariance, that is rapidity plateau meaning that the distributions of particles do not depend on y . In the space-time picture this means that the space-time is effectively two-dimensional and that particle distributions are Lorentz invariant: string like space-time sheets provide a possible geometric description of this situation.
4. In the case of an ideal quark-gluon plasma, the system completely forgets that it was created in a collision and particle distributions do not contain any information about the beam direction. In a head-on collision there is a full rotational symmetry and even Lorentz invariance so that transverse momentum cutoff disappears. Rapidity plateau is predicted in all directions.
5. The collisions studied were not quite head-on collisions and were characterized by an impact parameter vector with length b and direction angle ψ_2 in the plane E^2 . The particle distribution at the boundary of the plane E^2 was studied as a function of the angle coordinate $\phi - \psi_2$ and rapidity y which corresponds for given energy distance to a definite point of beam axis.

The hydrodynamical view about the situation looks like follows.

1. The particle distributions $N(p^\mu)$ as function of momentum components are mapped to space-time distributions $N(x^\mu, a)$ of particles. This leads to the idea that one could model the situation using Robertson-Walker type cosmology. Co-moving Lorentz invariant particle currents depending on the cosmic time only would correspond in this picture to Lorentz invariant momentum distributions.
2. Hydrodynamical models assign to the particle distribution $d^2N/dyd\phi$ a hydrodynamical flow characterized by four-velocity $v^\mu(y, \phi)$ for each value of the rapidity variable y . Longitudinal boost invariance predicting rapidity plateau states that the hydrodynamical flow does not depend on y at all. Because of the breaking of the rotational symmetry in the plane orthogonal to the beam, the hydrodynamical flow v depends on the angle coordinate $\phi - \psi_2$. It is possible to Fourier analyze this dependence and the second Fourier coefficient v_2 of $\cos(2(\phi - \psi_2))$ in the expansion

$$\frac{dN}{d\phi} \simeq 1 + \sum_n v_n \cos(n(\phi - \psi_2)) \quad (6.5.1)$$

was analyzed in [77].

3. It was found that the Fourier component v_2 depends on rapidity y , which means a breaking of the longitudinal boost invariance. v_2 also vanishes for large values of y . If this is true for all Fourier coefficients v_n , the situation becomes effectively Lorentz invariant for large values of y since one has $v(y, \phi) \rightarrow 1$.

Large values of y correspond to small values of a and to the initial moment of big bang in cosmological analogy. Hence the finding could be interpreted as a cosmological Lorentz invariance inside the light cone cosmology emerging from the collision point. Small values of y in turn correspond to large values of a so that the breaking of the spherical symmetry of the cosmology should be manifest only at $a \rightarrow \infty$ limit. These observations suggest a radical re-consideration of what happens in the collision: the breaking of the spherical symmetry would not be a property of the initial state but of the final state.

6.5.2 TGD based model for the quark-gluon plasma

Consider now the general assumptions the TGD based model for the quark gluon plasma region in the approximation that spherical symmetry is not broken.

1. Quantum-classical correspondence supports the mapping of the momentum space of a particle to a hyperboloid of future light cone. Thus the symmetries of the particle distributions with respect to momentum variables correspond directly to space-time symmetries.
2. The M_+^4 projection of a Robertson-Walker cosmology imbedded to $H = M_+^4 \times CP_2$ is future light cone. Hence it is natural to model the hydrodynamical flow as a mini-cosmology. Even more, one can assume that the collision quite literally creates a space-time sheet which locally obeys Robertson-Walker type cosmology. This assumption is sensible in many-sheeted space-time and conforms with the fractality of TGD inspired cosmology (cosmologies inside cosmologies).
3. If the space-time sheet containing the quark-gluon plasma is gradually filled with matter, one can quite well consider the possibility that the breaking of the spherical symmetry develops gradually, as suggested by the finding $v_2 \rightarrow 1$ for large values of $|y|$ (small values of a). To achieve Lorentz invariance at the limit $a \rightarrow 0$, one must assume that the expanding region corresponds to $r = \text{constant}$ "coordinate ball" in Robertson-Walker cosmology, and that the breaking of the spherical symmetry for the induced metric leads for large values of a to a situation described as a "not head-on collision".
4. Critical cosmology is by definition unstable, and one can model the Au+Au collision as a perturbation of the critical cosmology breaking the spherical symmetry. The shape of $r = \text{constant}$ sphere defined by the induced metric is changed by strong gravitational interactions such that it corresponds to the shape for the intersection of the colliding nuclei. One can view the collision as a spontaneous symmetry breaking process in which a critical quark-gluon plasma cosmology develops a quantum fluctuation leading to a situation described in terms of impact parameter. This kind of modelling is not natural for a hyperbolic cosmology, which is a small perturbation of the empty M_+^4 cosmology.

The imbedding of the critical cosmology

Any Robertson-Walker cosmology can be imbedded as a space-time sheet, whose M_+^4 projection is future light cone. The line element is

$$ds^2 = f(a)da^2 - a^2(K(r)dr^2 + r^2d\Omega^2) . \quad (6.5.2)$$

Here a is the scaling factor of the cosmology and for the imbedding as surface corresponds to the future light cone proper time.

This light cone has its tip at the point, where the formation of quark gluon plasma starts. (θ, ϕ) are the spherical coordinates and appear in $d\Omega^2$ defining the line element of the unit sphere. a and r are related to the spherical Minkowski coordinates (m^0, r_M, θ, ϕ) by $(a = \sqrt{(m^0)^2 - r_M^2}, r = r_M/a)$. If hyperbolic cosmology is in question, the function $K(r)$ is given by $K(r) = 1/(1 + r^2)$. For the critical cosmology 3-space is flat and one has $K(r) = 1$.

1. The critical cosmologies imbeddable to $H = M_+^4 \times CP_2$ are unique apart from a single parameter defining the duration of this cosmology. Eventually the critical cosmology must transform to a hyperbolic cosmology. Critical cosmology breaks Lorentz symmetry at space-time level since Lorentz group is replaced by the group of rotations and translations acting as symmetries of the flat Euclidian space.
2. Critical cosmology replaces Big Bang with a silent whisper amplified to a big but not infinitely big bang. The silent whisper aspect makes the cosmology ideal for the space-time sheet associated with the quark gluon plasma: the interpretation is that the quark gluon plasma is gradually transferred to the plasma space-time sheet from the other space-time sheets. In the real cosmology the condensing matter corresponds to the decay products of cosmic string in 'vapor phase'. The density of the quark gluon plasma cannot increase without limit and after some critical period the transition to a hyperbolic cosmology occurs. This transition could, but need not, correspond to the hadronization.
3. The imbedding of the critical cosmology to $M_+^4 \times S^2$ is given by

$$\begin{aligned} \sin(\Theta) &= \frac{a}{a_m} , \\ \Phi &= g(r) . \end{aligned} \tag{6.5.2}$$

Here Θ and Φ denote the spherical coordinates of the geodesic sphere S^2 of CP_2 . One has

$$\begin{aligned} f(a) &= 1 - \frac{R^2 k^2}{(1 - (a/a_m)^2)} , \\ (\partial_r \Phi)^2 &= \frac{a_m^2}{R^2} \times \frac{r^2}{1 + r^2} . \end{aligned} \tag{6.5.2}$$

Here R denotes the radius of S^2 . From the expression for the gradient of Φ it is clear that gravitational effects are very strong. The imbedding becomes singular for $a = a_m$. The transition to a hyperbolic cosmology must occur before this.

This model for the quark-gluon plasma would predict Lorentz symmetry and $v = 1$ (and $v_n = 0$) corresponding to head-on collision so that it is not yet a realistic model.

TGD based model for the quark-gluon plasma without breaking of spherical symmetry

There is a highly unique deformation of the critical cosmology transforming metric spheres to highly non-spherical structures purely gravitationally. The deformation can be characterized by the following formula

$$\sin^2(\Theta) = \left(\frac{a}{a_m}\right)^2 \times (1 + \Delta(a, \theta, \phi)^2) . \tag{6.5.3}$$

1. This induces deformation of the g_{rr} component of the induced metric given by

$$g_{rr} = -a^2 \left[1 + \Delta^2(a, \theta, \phi) \frac{r^2}{1 + r^2} \right] . \tag{6.5.4}$$

Remarkably, g_{rr} does not depend at all on CP_2 size and the parameter a_m determining the duration of the critical cosmology. The disappearance of the dimensional parameters can be understood to reflect the criticality. Thus a strong gravitational effect independent of the gravitational constant (proportional to R^2) results. This implies that the expanding plasma space-time sheet having sphere as M_+^4 projection differs radically from sphere in the induced metric for large values of a . Thus one can understand why the parameter v_2 is non-vanishing for small values of the rapidity y .

2. The line element contains also the components g_{ij} , $i, j \in \{a, \theta, \phi\}$. These components are proportional to the factor

$$\frac{1}{1 - (a/a_m)^2(1 + \Delta^2)} , \quad (6.5.5)$$

which diverges for

$$a_m(\theta, \phi) = \frac{a_m}{\sqrt{1 + \Delta^2}} . \quad (6.5.6)$$

Presumably quark-gluon plasma phase begins to hadronize first at the points of the plasma surface for which $\Delta(\theta, \phi)$ is maximum, that is at the tips of the intersection region of the colliding nuclei. A phase transition producing string like objects is one possible space-time description of the process.

6.5.3 Further experimental findings and theoretical ideas

The interaction between experiment and theory is pure magic. Although experimenter and theorist are often working without any direct interaction (as in case of TGD), I have the strong feeling that this disjointness is only apparent and there is higher organizing intellect behind this coherence. Again and again it has turned out that just few experimental findings allow to organize separate and loosely related physical ideas to a consistent scheme. The physics done in RHIC has played completely unique role in this respect.

Super-symplectic matter as the TGD counterpart of CGC?

The model discussed above explained the strange breaking of longitudinal Lorentz invariance in terms of a hadronic mini bang cosmology. The next twist in the story was the shocking finding, compared to Columbus's discovery of America, was that, rather than behaving as a dilute gas, the plasma behaved like a liquid with strong correlations between partons, and having density 30-50 times higher than predicted by QCD calculations [66]. When I learned about these findings towards the end of 2004, I proposed how TGD might explain them in terms of what I called conformal confinement [26]. This idea - although not wrong for any obvious reason - did not however have any obvious implications. After the progress made in p-adic mass calculations of hadrons leading to highly successful model for both hadron and meson masses [17], the idea was replaced with the hypothesis that the condensate in question is Bose-Einstein condensate like state of super-symplectic particles formed when the hadronic space-time sheets of colliding nucleons fuse together to form a long string like object.

A further refinement of the idea comes from the hypothesis that quark gluon plasma is formed by the topological condensation of quarks to hadronic strings identified as color flux tubes. This would explain the high density of the plasma. The highly entangled hadronic string would be analogous to the initial state of TGD inspired cosmology with the only difference that string tension is extremely small in the hadronic context. This structure would possess also characteristics of blackhole.

Fireballs behaving like black hole like objects

The latest discovery in RHIC is that fireball, which lasts a mere 10^{-23} seconds, can be detected because it absorbs jets of particles produced by the collision [71]. The association with the notion black hole is unavoidable and there indeed exists a rather esoteric M-theory inspired model "The RHIC fireball as a dual black hole" by Hortiu Nastase [64] for the strange findings.

The Physics Today article [59] "What Have We Learned From the Relativistic Heavy Ion Collider?" gives a nice account about experimental findings. Extremely high collision energies are in question: Gold nuclei contain energy of about 100 GeV per nucleon: 100 times proton mass. The expectation was that a large volume of thermalized Quark-Gluon Plasma (QGP) is formed in which partons lose rapidly their transverse momentum. The great surprise was the suppression of high transverse

momentum collisions suggesting that in this phase strong collective interactions are present. This has inspired the proposal that quark gluon plasma is preceded by liquid like phase which has been christened as Color Glass Condensate (CGC) thought to contain Bose-Einstein condensate of gluons.

The theoretical ideas relating CGC to gravitational interactions

Color glass condensate relates naturally to several gravitation related theoretical ideas discovered during the last year.

1. Classical gravitation and color confinement

Just some time ago it became clear that strong classical gravitation might play a key role in the understanding of color confinement [19]. Whether the situation looks confinement or asymptotic freedom would be in the eyes of beholder: this is one example of dualities filling TGD Universe. If one looks the situation at the hadronic space-time sheet or one has asymptotic freedom, particles move essentially like free massless particles. But - and this is absolutely essential- in the induced metric of hadronic space-time sheet. This metric represents classical gravitational field becoming extremely strong near hadronic boundary. From the point of view of outsider, the motion of quarks slows down to rest when they approach hadronic boundary: confinement. The distance to hadron surface is infinite or at least very large since the induced metric becomes singular at the light-like boundary! Also hadronic time ceases to run near the boundary and finite hadronic time corresponds to infinite time of observer. When you look from outside you find that this light-like 3-surface is just static surface like a black hole horizon which is also a light-like 3-surface. This gives confinement.

2. Dark matter in TGD

The evidence for hadronic black hole like structures is especially fascinating. In TGD Universe dark matter can be (not always) ordinary matter at larger space-time sheets in particular magnetic flux tubes. The mere fact that the particles are at larger space-time sheets might make them more or less invisible.

Matter can be however dark in much stronger sense, should I use the word "black"! The findings suggesting that planetary orbits obey Bohr rules with a gigantic Planck constant [78, 38] would suggest quantum coherence of dark matter even in astrophysical length scales and this raises the fascinating possibility that Planck constant is dynamical so that fine structure constant. Dark matter would correspond to phases with non-standard value of Planck constant. This quantization saves from black hole collapse just as the quantization of hydrogen atom saves from the infrared catastrophe.

The basic criterion for the transition to this phase would be that it occurs when some coupling strength - say fine structure constant multiplied by appropriate charges or gravitational constant multiplied by masses- becomes so large that the perturbation series for scattering amplitudes fails to converge. The phase transition increases Planck constant so that convergence is achieved. The attempts to build a detailed view about what might happen led to a generalization of the imbedding space concept by replacing M^4 (or rather the causal diamond) and CP_2 with their singular coverings. During 2010 it turned out that this generalization could be regarded as a conventional manner to describe a situation in which space-time surface becomes analogous to a multi-sheeted Riemann surface. If so, then Planck constant would be replaced by its integer multiple only in effective sense.

The obvious questions are following. Could black hole like objects/magnetic flux tubes/cosmic strings consist of quantum coherent dark matter? Does this dark matter consist dominantly from hadronic space-time sheets which have fused together and contain super-symplectic bosons and their super-partners (with quantum numbers of right handed neutrino) having therefore no electro-weak interactions. Electro-weak charges would be at different space-time sheets.

1. Gravitational interaction cannot force the transition to dark phase in a purely hadronic system at RHIC energies since the product GM_1M_2 characterizing the interaction strength of two masses must be larger than unity ($\hbar = c = 1$) for the phase transition increasing Planck constant to occur. Hence the collision energy should be above Planck mass for the phase transition to occur if gravitational interactions are responsible for the transition.
2. The criterion for the transition to dark phase is however much more general and states that the system does its best to stay perturbative by increasing its Planck constant in discrete steps and applies thus also in the case of color interactions and governs the phase transition to the TGD

counterpart of non-perturbative QCD. Criterion would be roughly $\alpha_s Q_s^2 > 1$ for two color charges of opposite sign. Hadronic string picture would suggest that the criterion is equivalent to the generalization of the gravitational criterion to its strong gravity analog $nL_p^2 M^2 > 1$, where L_p is the p-adic length scale characterizing color magnetic energy density (hadronic string tension) and M is the mass of the color magnetic flux tube and n is a numerical constant. Presumably L_p , $p = M_{107} = 2^{107} - 1$, is the p-adic length scale since Mersenne prime M_{107} labels the space-time sheet at which partons feed their color gauge fluxes. The temperature during this phase could correspond to Hagedorn temperature (for the history and various interpretations of Hagedorn temperature see the CERN Courier article [53]) for strings and is determined by string tension and would naturally correspond also to the temperature during the critical phase determined by its duration as well as corresponding black-hole temperature. This temperature is expected to be somewhat higher than hadronization temperature found to be about $\simeq 176$ MeV. The density of inertial mass would be maximal during this phase as also the density of gravitational mass during the critical phase.

Lepto-hadron physics [24], one of the predictions of TGD, is one instance of a similar situation. In this case electromagnetic interaction strength defined in an analogous manner becomes larger than unity in heavy ion collisions just above the Coulomb wall and leads to the appearance of mysterious states having a natural interpretation in terms of lepto-pion condensate. Lepto-pions are pairs of color octet excitations of electron and positron.

3. Description of collisions using analogy with black holes

The following view about RHIC events represents my immediate reaction to the latest RHIC news in terms of black-hole physics instead of notions related to big bang. Since black hole collapse is roughly the time reversal of big bang, the description is complementary to the earliest one.

In TGD context one can ask whether the fireballs possibly detected at RHIC are produced when a portion of quark-gluon plasma in the collision region formed by two Gold nuclei separates from hadronic space-time sheets which in turn fuse to form a larger space-time sheet separated from the remaining collision region by a light-like 3-D surface (I have used to speak about light-like causal determinants) mathematically completely analogous to a black hole horizon. This larger space-time sheet would contain color glass condensate of super-symplectic gluons formed from the collision energy. A formation of an analog of black hole would indeed be in question.

The valence quarks forming structures connected by color bonds would in the first step of the collision separate from their hadronic space-time sheets which fuse together to form color glass condensate. Similar process has been observed experimentally in the collisions demonstrating the experimental reality of Pomeron, a color singlet state having no Regge trajectory [63] and identifiable as a structure formed by valence quarks connected by color bonds. In the collision it temporarily separates from the hadronic space-time sheet. Later the Pomeron and the new mesonic and baryonic Pomerons created in the collision suffer a topological condensation to the color glass condensate: this process would be analogous to a process in which black hole sucks matter from environment.

Of course, the relationship between mass and radius would be completely different with gravitational constant presumably replaced by the square of appropriate p-adic length scale presumably of order pion Compton length: this is very natural if TGD counterparts of black-holes are formed by color magnetic flux tubes. This gravitational constant expressible in terms of hadronic string tension of $.9 \text{ GeV}^2$ predicted correctly by super-symplectic picture would characterize the strong gravitational interaction assignable to super-symplectic $J = 2$ gravitons. I have long time ago in the context of p-adic mass calculations formulated quantitatively the notion of elementary particle black hole analogy making the notion of elementary particle horizon and generalization of Hawking-Bekenstein law [24].

The size L of the "hadronic black hole" would be relatively large using protonic Compton radius as a unit of length. For instance, for $\hbar = 26\hbar_0$ the size would be $26 \times L(107) = 46$ fm and correspond to a size of a heavy nucleus. This large size would fit nicely with the idea about nuclear sized color glass condensate. The density of partons (possibly gluons) would be very high and large fraction of them would have been materialized from the brehmstrahlung produced by the de-accelerating nuclei. Partons would be gravitationally confined inside this region. The interactions of partons would lead to a generation of a liquid like dense phase and a rapid thermalization would occur. The collisions of partons producing high transverse momentum partons occurring inside this region would yield no

detectable high p_T jets since the matter coming out from this region would be somewhat like a thermal radiation from an evaporating black hole identified as a highly entangled hadronic string in Hagedorn temperature. This space-time sheet would expand and cool down to QQP and crystallize into hadrons.

4. Quantitative comparison with experimental data

Consider now a quantitative comparison of the model with experimental data. The estimated freeze-out temperature of quark gluon plasma is $T_f \simeq 175.76$ MeV [59, 64], not far from the total contribution of quarks to the mass of nucleon, which is 170 MeV [17]. Hagedorn temperature identified as black-hole temperature should be higher than this temperature. The experimental estimate for the hadronic Hagedorn temperature from the transversal momentum distribution of baryons is $\simeq 160$ MeV. On the other hand, according to the estimates of hep-ph/0006020 the values of Hagedorn temperatures for mesons and baryons are $T_H(M) = 195$ MeV and $T_H(B) = 141$ MeV respectively.

D-dimensional bosonic string model for hadrons gives for the mesonic Hagedorn temperature the expression [53]

$$T_H = \frac{\sqrt{6}}{2\pi(D-2)\alpha'} , \quad (6.5.7)$$

For a string in $D = 4$ -dimensional space-time and for the value $\alpha' \sim 1 \text{ GeV}^{-2}$ of Regge slope, this would give $T_H = 195$ MeV, which is slightly larger than the freezing out temperature as it indeed should be, and in an excellent agreement with the experimental value of [51]. It deserves to be noticed that in the model for fireball as a dual 10-D black-hole the rough estimate for the temperature of color glass condensate becomes too low by a factor 1/8 [64]. In light of this I would not yet rush to conclude that the fireball is actually a 10-dimensional black hole.

Note that the baryonic Hagedorn temperature is smaller than mesonic one by a factor of about $\sqrt{2}$. According to [51] this could be qualitatively understood from the fact that the number of degrees of freedom is larger so that the effective value of D in the mesonic formula is larger. $D_{eff} = 6$ would give $T_H = 138$ MeV to be compared with $T_H(B) = 141$ MeV. On the other hand, TGD based model for hadronic masses [17] assumes that quarks feed their color fluxes to $k = 107$ space-time sheets. For mesons there are two color flux tubes and for baryons three. Using the same logic as in [51], one would have $D_{eff}(B)/D_{eff}(M) = 3/2$. This predicts $T_H(B) = 159$ MeV to be compared with 160 MeV deduced from the distribution of transversal momenta in p-p collisions.

6.5.4 Are ordinary black-holes replaced with super-symplectic black-holes in TGD Universe?

Some variants of super string model predict the production of small black-holes at LHC. I have never taken this idea seriously but in a well-defined sense TGD predicts black-holes associated with super-symplectic gravitons with strong gravitational constant defined by the hadronic string tension. The proposal is that super-symplectic black-holes have been already seen in Hera, RHIC, and the strange cosmic ray events.

Baryonic super-symplectic black-holes of the ordinary M_{107} hadron physics would have mass 934.2 MeV, very near to proton mass. The mass of their M_{89} counterparts would be 512 times higher, about 478 GeV if quark masses scale also by this factor. This need not be the case: if one has $k = 113 \rightarrow 103$ instead of 105 one has 434 GeV mass. "Ionization energy" for Pomeron, the structure formed by valence quarks connected by color bonds separating from the space-time sheet of super-symplectic black-hole in the production process, corresponds to the total quark mass and is about 170 MeV for ordinary proton and 87 GeV for M_{89} proton. This kind of picture about black-hole formation expected to occur in LHC differs from the stringy picture since a fusion of the hadronic mini black-holes to a larger black-hole is in question.

An interesting question is whether the ultrahigh energy cosmic rays having energies larger than the GZK cut-off of 5×10^{10} GeV are baryons, which have lost their valence quarks in a collision with hadron and therefore have no interactions with the microwave background so that they are able to propagate through long distances.

In neutron stars the hadronic space-time sheets could form a gigantic super-symplectic black-hole and ordinary black-holes would be naturally replaced with super-symplectic black-holes in TGD

framework (only a small part of black-hole interior metric is representable as an induced metric). This obviously means a profound difference between TGD and string models.

1. Hawking-Bekenstein black-hole entropy would be replaced with its p-adic counterpart given by

$$S_p = \left(\frac{M}{m(CP_2)}\right)^2 \times \log(p) , \quad (6.5.8)$$

where $m(CP_2)$ is CP_2 mass, which is roughly 10^{-4} times Planck mass. M is the contribution of p-adic thermodynamics to the mass. This contribution is extremely small for gauge bosons but for fermions and super-symplectic particles it gives the entire mass.

2. If p-adic length scale hypothesis $p \simeq 2^k$ holds true, one obtains

$$S_p = k \log(2) \times \left(\frac{M}{m(CP_2)}\right)^2, \quad (6.5.9)$$

$m(CP_2) = \hbar/R$, R the "radius" of CP_2 , corresponds to the standard value of \hbar_0 for all values of \hbar .

3. Hawking-Bekenstein area law gives in the case of Schwarzschild black-hole

$$S = \frac{A}{4G} \times \hbar = \pi GM^2 \times \hbar . \quad (6.5.10)$$

For the p-adic variant of the law Planck mass is replaced with CP_2 mass and $k \log(2) \simeq \log(p)$ appears as an additional factor. Area law is obtained in the case of elementary particles if k is prime and wormhole throats have M^4 radius given by p-adic length scale $L_k = \sqrt{k}R$ which is exponentially smaller than L_p . For macroscopic super-symplectic black-holes modified area law results if the radius of the large wormhole throat equals to Schwarzschild radius. Schwarzschild radius is indeed natural: in [35] I have shown that a simple deformation of the Schwarzschild exterior metric to a metric representing rotating star transforms Schwarzschild horizon to a light-like 3-surface at which the signature of the induced metric is transformed from Minkowskian to Euclidian.

4. The formula for the gravitational Planck constant appearing in the Bohr quantization of planetary orbits and characterizing the gravitational field body mediating gravitational interaction between masses M and m [38] reads as

$$\hbar_{gr} = \frac{GMm}{v_0} \hbar_0 .$$

$v_0 = 2^{-11}$ is the preferred value of v_0 . One could argue that the value of gravitational Planck constant is such that the Compton length \hbar_{gr}/M of the black-hole equals to its Schwarzschild radius. This would give

$$\hbar_{gr} = \frac{GM^2}{v_0} \hbar_0 , \quad v_0 = 1/2 . \quad (6.5.11)$$

The requirement that \hbar_{gr} is a ratio of ruler-and-compass integers expressible as a product of distinct Fermat primes (only four of them are known) and power of 2 would quantize the mass spectrum of black hole [38]. Even without this constraint M^2 is integer valued using p-adic mass squared unit and if p-adic length scale hypothesis holds true this unit is in an excellent approximation power of two.

5. The gravitational collapse of a star would correspond to a process in which the initial value of v_0 , say $v_0 = 2^{-11}$, increases in a stepwise manner to some value $v_0 \leq 1/2$. For a supernova with solar mass with radius of 9 km the final value of v_0 would be $v_0 = 1/6$. The star could have an onion like structure with largest values of v_0 at the core as suggested by the model of planetary system. Powers of two would be favored values of v_0 . If the formula holds true also for Sun one obtains $1/v_0 = 3 \times 17 \times 2^{13}$ with 10 per cent error.
6. Black-hole evaporation could be seen as means for the super-symplectic black-hole to get rid of its electro-weak charges and fermion numbers (except right handed neutrino number) as the antiparticles of the emitted particles annihilate with the particles inside super-symplectic black-hole. This kind of minimally interacting state is a natural final state of star. Ideal super-symplectic black-hole would have only angular momentum and right handed neutrino number.
7. In TGD light-like partonic 3-surfaces are the fundamental objects and space-time interior defines only the classical correlates of quantum physics. The space-time sheet containing the highly entangled cosmic string might be separated from environment by a wormhole contact with size of black-hole horizon.

This looks the most plausible option but one can of course ask whether the large partonic 3-surface defining the horizon of the black-hole actually contains all super-symplectic particles so that super-symplectic black-hole would be single gigantic super-symplectic parton. The interior of super-symplectic black-hole would be a space-like region of space-time, perhaps resulting as a large deformation of CP_2 type vacuum extremal. Black-hole sized wormhole contact would define a gauge boson like variant of the black-hole connecting two space-time sheets and getting its mass through Higgs mechanism. A good guess is that these states are extremely light.

6.5.5 Very cautious conclusions

The model for quark-gluon plasma in terms of valence quark space-time sheets separated from hadronic space-time sheets forming a color glass condensate relies on quantum criticality and implies gravitation like effects due to the presence of super-symplectic strong gravitons. At space-time level the change of the distances due to strong gravitation affects the metric so that the breaking of spherical symmetry is caused by gravitational interaction. TGD encourages to think that this mechanism is quite generally at work in the collisions of nuclei. One must take seriously the possibility that strong gravitation is present also in longer length scales (say biological), in particular in processes in which new space-time sheets are generated. Critical cosmology might provide a universal model for the emergence of a new space-time sheet.

The model supports TGD based early cosmology and quantum criticality. In standard physics framework the cosmology in question is not sensible since it would predict a large breaking of the Lorentz invariance, and would mean the breakdown of the entire conceptual framework underlying elementary particle physics. In TGD framework Lorentz invariance is not lost at the level of imbedding space, and the experiments provide support for the view about space-time as a surface and for the notion of many-sheeted space-time.

The attempts to understand later strange events reported by RHIC have led to a dramatic increase of understanding of TGD and allow to fuse together separate threads of TGD.

1. The description of RHIC events in terms of the formation of hadronic black hole and its evaporation seems to be also possible and essentially identical with description as a mini bang.
2. It took some time to realize that scaled down TGD inspired cosmology as a model for quark gluon plasma predicts a new phase identifiable as color glass condensate and still a couple of years to realize the proper interpretation of it in terms of super-symplectic bosons having no counterpart in QCD framework.
3. There is also a connection with the dramatic findings suggesting that Planck constant for dark matter has a gigantic value.
4. Black holes and their scaled counterparts would not be merciless information destroyers in TGD Universe. The entanglement of particles having particle like integrity would make black hole

like states ideal candidates for quantum computer like systems. One could even imagine that the galactic black hole is a highly tangled cosmic string in Hagedorn temperature performing quantum computations the complexity of which is totally out of reach of human intellect! Indeed, TGD inspired consciousness predicts that evolution leads to the increase of information and intelligence, and the evolution of stars should not form exception to this. Also the interpretation of black hole as consisting of dark matter follows from this picture.

Summarizing, it seems that thanks to some crucial experimental inputs the new physics predicted by TGD is becoming testable in laboratory.

6.5.6 Five years later

The emergence of the first interesting findings from LHC by CMS collaboration [116, 115] provide new insights to the TGD picture about the phase transition from QCD plasma to hadronic phase and inspired also the updating of the model of RHIC events (mainly elimination of some remnants from the time when the ideas about hierarchy of Planck constants had just born).

In some proton-proton collisions more than hundred particles are produced suggesting a single object from which they are produced. Since the density of matter approaches to that observed in heavy ion collisions for five years ago at RHIC, a formation of quark gluon plasma and its subsequent decay is what one would expect. The observations are not however quite what QCD plasma picture would allow to expect. Of course, already the RHIC results disagreed with what QCD expectations. What is so striking is the evolution of long range correlations between particles in events containing more than 90 particles as the transverse momentum of the particles increases in the range 1-3 GeV (see the excellent description of the correlations by Lubos Motl in his blog [117]).

One studies correlation function for two particles as a function of two variables. The first variable is the difference $\Delta\phi$ for the emission angles and second is essentially the difference for the velocities described relativistically by the difference $\Delta\eta$ for hyperbolic angles. As the transverse momentum p_T increases the correlation function develops structure. Around origin of $\Delta\eta$ axis a widening plateau develops near $\Delta\phi = 0$. Also a wide ridge with almost constant value as function of $\Delta\eta$ develops near $\Delta\phi = \pi$. The interpretation is that particles tend to move collinearly and or in opposite directions. In the latter case their velocity differences are large since they move in opposite directions so that a long ridge develops in $\Delta\eta$ direction in the graph.

Ideal QCD plasma would predict no correlations between particles and therefore no structures like this. The radiation of particles would be like blackbody radiation with no correlations between photons. The description in terms of string like object proposed also by Lubos on basis of analysis of the graph showing the distributions as an explanation of correlations looks attractive. The decay of a string like structure producing particles at its both ends moving nearly parallel to the string to opposite directions could be in question.

Since the densities of particles approach those at RHIC, I would bet that the explanation (whatever it is!) of the hydrodynamical behavior observed at RHIC for some years ago should apply also now. The introduction of string like objects in this model was natural since in TGD framework even ordinary nuclei are string like objects with nucleons connected by color flux tubes [47]: this predicts a lot of new nuclear physics for which there is evidence. The basic idea was that in the high density hadronic color flux tubes associated with the colliding nucleon connect to form long highly entangled hadronic strings containing quark gluon plasma. The decay of these structures would explain the strange correlations. It must be however emphasized that in the recent case the initial state consists of two protons rather than heavy nuclei so that the long hadronic string could form from the QCD like quark gluon plasma at criticality when long range fluctuations emerge.

The main assumptions of the model for the RHIC events and those observed now deserve to be summarized. Consider first the "macroscopic description".

1. A critical system associated with confinement-deconfinement transition of the quark-gluon plasma formed in the collision and inhibiting long range correlations would be in question.
2. The proposed hydrodynamic space-time description was in terms of a scaled variant of what I call critical cosmology defining a universal space-time correlate for criticality: the specific property of this cosmology is that the mass contained by comoving volume approaches to zero at the the initial moment so that Big Bang begins as a silent whisper and is not so scaring;-). Criticality

means flat 3-space instead of Lobatchevski space and means breaking of Lorentz invariance to $SO(4)$. Breaking of Lorentz invariance was indeed observed for particle distributions but now I am not so sure whether it has much to do with this.

The microscopic level the description would be like follows.

1. A highly entangled long hadronic string like object (color-magnetic flux tube) would be formed at high density of nucleons via the fusion of ordinary hadronic color-magnetic flux tubes to much longer one and containing quark gluon plasma. In QCD world plasma would not be at flux tube.
2. This geometrically (and perhaps also quantally!) entangled string like object would straighten and split to hadrons in the subsequent "cosmological evolution" and yield large numbers of almost collinear particles. The initial situation should be apart from scaling similar as in cosmology where a highly entangled soup of cosmic strings (magnetic flux tubes) precedes the space-time as we understand it. Maybe ordinary cosmology could provide analogy as galaxies arranged to form linear structures?
3. This structure would have also black hole like aspects but in totally different sense as the 10-D hadronic black-hole proposed by Nastase to describe the findings. Note that M-theorists identify black holes as highly entangled strings: in TGD 1-D strings are replaced by 3-D string like objects.

TGD suggests the existence of a scaled up copy of hadron physics associated with each Mersenne prime $M_n = 2^n - 1$, n prime: M_{107} corresponds to ordinary hadron physics. There is some evidence for exotic hadrons. Also Gaussian Mersennes $(1+i)^k - 1$, could correspond to hadron physics. Four of them ($k = 151, 157, 163, 167$) are in the biologically interesting length scale range between cell membrane thickness and the size of cell nucleus.

Centauro events and the peculiar events associated with $E > 10^5$ GeV radiation from Cygnus X-3 could be understood as due to the decay of gamma rays to M_{89} hadron pair in the atmosphere. The decay $\pi_n \rightarrow \gamma\gamma$ produces a peak in the spectrum of the cosmic gamma rays at energy $\frac{m(\pi_n)}{2}$ and there is evidence for the peaks at energies $E_{89} \simeq 34$ GeV and $E_{31} \simeq 3.5 \cdot 10^{10}$ GeV. The absence of the peak at $E_{61} \simeq 1.5 \cdot 10^6$ GeV can be understood as due to the strong absorption caused by the e^+e^- pair creation with photons of the cosmic microwave background.

Cosmic string decays $\text{cosmic string} \rightarrow M_2 \text{ hadrons} \rightarrow M_3 \text{ hadrons} \dots \rightarrow M_{107} \text{ hadrons}$ is a new source of cosmic rays. The mechanism could explain the change of the slope in the hadronic cosmic ray spectrum at $3 \cdot 10^6$ GeV which is not far from M_{61} pion rest energy $1.2 \cdot 10^6$ GeV.

The cosmic ray radiation at energies near 10^9 GeV apparently consisting of protons and nuclei not lighter than Fe might be actually dominated by gamma rays: at these energies γ and p induced showers have same muon content and the decays of gamma rays to M_{89} and M_{61} hadrons in the atmosphere can mimic the presence of heavy nuclei in the cosmic radiation.

The identification of the hadronic space-time sheet as a super-symplectic mini black-hole [17] suggests that part of ultra-high energy cosmic rays could be protons which have lost their valence quarks. These particles would have essentially same mass as proton and would behave like mini black-holes consisting of dark matter. They could even give a dominating contribution to the dark matter. Since electro-weak interactions are absent, the scattering from microwave background is absent, and they could propagate over much longer distances than ordinary particles. An interesting question is whether the ultrahigh energy cosmic rays having energies larger than the GZK cut-off of 5×10^{10} GeV are super-symplectic mini black-holes associated with M_{107} hadron physics or some other copy of hadron physics.

6.5.7 Mersenne primes and mass scales

p-Adic mass calculations lead to quite detailed predictions for elementary particle masses. In particular, there are reasons to believe that the most important fundamental elementary particle mass scales correspond to Mersenne primes $M_n = 2^n - 1$, $n = 2, 3, 7, 13, 17, 19, \dots$

$$\begin{aligned}
m_n^2 &= \frac{m_0^2}{M_n} , \\
m_0 &\simeq 1.41 \cdot \frac{10^{-4}}{\sqrt{G}} ,
\end{aligned} \tag{6.5.11}$$

where \sqrt{G} is Planck length. The lower bound for n can be of course larger than $n = 2$. The known elementary particle mass scales were identified as mass scales associated identified with Mersenne primes $M_{127} \simeq 10^{38}$ (leptons), M_{107} (hadrons) and M_{89} (intermediate gauge bosons). Of course, also other p-adic length scales are possible and it is quite possible that not all Mersenne primes are realized. On the other hand, also Gaussian Mersennes could be important (muon and atomic nuclei corresponds to Gaussian Mersenne $(1+i)^k - 1$ with $k = 113$).

Theory predicts also some higher mass scales corresponding to the Mersenne primes M_n for $n = 89, 61, 31, 19, 17, 13, 7, 3$ and suggests the existence of a scaled up copy of hadron physics with each of these mass scales. In particular, masses should be related by simple scalings to the masses of the ordinary hadrons.

An attractive hypothesis is that the color interactions of the particles of level M_n can be described using the ordinary QCD scaled up to the level M_n so that that masses and the confinement mass scale Λ is scaled up by the factor $\sqrt{M_n/M_{107}}$.

$$\Lambda_n = \sqrt{\frac{M_n}{M_{107}}} \Lambda . \tag{6.5.12}$$

In particular, the naive scaling prediction for the masses of the exotic pions associated with M_n is given by

$$m(\pi_n) = \sqrt{\frac{M_n}{M_{107}}} m_\pi . \tag{6.5.13}$$

Here $m_\pi \simeq 135 \text{ MeV}$ is the mass of the ordinary pion.

The interactions between the different level hadrons are mediated by the emission of electro-weak gauge bosons and by gluons with cm energies larger than the energy defined by the confinement scale of level with smaller p . The decay of the exotic hadrons at level M_{n_k} to exotic hadrons at level $M_{n_{k+1}}$ must take place by a transition sequence leading from the effective M_{n_k} -adic space-time topology to effective $M_{n_{k+1}}$ -adic topology. All intermediate p-adic topologies might be involved.

6.5.8 Cosmic strings and cosmic rays

Cosmic strings are fundamental objects in quantum TGD and dominated during early cosmology.

Cosmic strings

Cosmic strings (not quite the same thing in TGD as in GUTs) are basic objects in TGD inspired cosmology [16, 24].

1. In TGD inspired galaxy model galaxies are regarded as mass concentrations around cosmic strings and the energy of the string corresponds to the dark energy whereas the particles condensed at cosmic strings and magnetic flux tubes resulting from them during cosmic expansion correspond to dark matter [16, 24]. The galactic nuclei, often regarded as candidates for black holes, are the most probable seats for decaying highly entangled cosmic strings.
2. Galaxies are known to organize to form larger linear structures. This can be understood if the highly entangled galactic strings organize around long strings like pearls in necklace. Long strings could correspond to galactic jets and their gravitational field could explain the constant velocity spectrum of distant stars in the galactic halo.

3. In [16, 24, 38] it is suggested that decaying cosmic strings might provide a common explanation for the energy production of quasars, galactic jets and gamma ray bursters and that the visible matter in galaxies could be regarded as decay products of cosmic strings. The magnetic and Z^0 magnetic flux tubes resulting during the cosmic expansion from cosmic strings allow to assign at least part of gamma ray bursts to neutron stars. Hot spots (with temperature even as high as $T \sim \frac{10^{-3.5}}{\sqrt{G}}$) in the cosmic string emitting ultra high energy cosmic rays might be created under the violent conditions prevailing in the galactic nucleus.

The decay of the cosmic strings provides a possible mechanism for the production of the exotic hadrons and in particular, exotic pions. In [68] the idea that cosmic strings might produce gamma rays by decaying first into 'X' particles with mass of order 10^{15} GeV and then to gamma rays, was proposed. As authors notice this model has some potential difficulties resulting from the direct production of gamma rays in the source region and the presence of intensive electromagnetic fields near the source. These difficulties are overcome if cosmic strings decay first into exotic hadrons of type M_{n_0} , $n_0 \geq 3$ of energy of order $2^{-n_0+2} 10^{25} \text{ GeV}$, which in turn decay to exotic hadrons corresponding to M_k , $k > n_0$ via ordinary color interaction, and so on so that a sequence of M_k :s starting some value of n_0 in $n = 2, 3, 7, 13, 17, 19, 31, 61, 89, 107$ is obtained. The value of n remains open at this stage and depends on the temperature of the hot spot and much smaller temperatures than the $T \sim m_0$ are possible: favored temperatures are the temperatures $T_n \sim m_n$ at which M_n hadrons become unstable against thermal decay.

Decays of cosmic strings as producer of high energy cosmic gamma rays

In [69] the gamma ray signatures from ordinary cosmic strings were considered and a dynamical QCD based model for the decay of cosmic string was developed. In this model the final state particles were assumed to be ordinary hadrons and final state interactions were neglected. In present case the string decays first to M_{n_0} hadrons and the time scale of for color interaction between M_{n_0} hadrons is extremely short (given by the length scale defined by the inverse of π_{n_0} mass) as compared to the time time scale in case of ordinary hadrons. Therefore the interactions between the final state particles must be taken into account and there are good reasons to expect that thermal equilibrium sets on and much simpler thermodynamic description of the process becomes possible.

A possible description for the decaying part of the highly tangled cosmic string is as a 'fireball' containing various M_{n_0} ($n \geq 3$) partons in thermal equilibrium at Hagedorn temperature T_{n_0} of order $T_{n_0} \sim m_{n_0} = 2^{-2+n_0} \frac{10^{-4}}{k\sqrt{G}}$, $k \simeq 1.288$. The experimental discoveries made in RHIC suggest [59] that high energy nuclear collisions create instead of quark gluon plasma a liquid like phase involving gluonic BE condensate christened as color glass condensate. Also black hole like behavior is suggested by the experiments.

RHIC findings inspire a TGD based model for this phase as a macroscopic quantum phase condensed on a highly tangled color magnetic string at Hagedorn temperature. The model relies also on the notion of dynamical but quantized \hbar [16] and its recent form to the realization that super-symplectic many-particle states at hadronic space-time sheets give dominating contribution to the baryonic mass and explain hadronic masses with an excellent accuracy.

This phase has no direct gauge interactions with ordinary matter and is identified in TGD framework as a particular instance of dark matter. Quite generally, quantum coherent dark matter would reside at magnetic flux tubes idealizable as string like objects with string tension determined by the p-adic length scale and thus outside the "ordinary" space-time. This suggests that color glass condensate forms when hadronic space-time sheets fuse to single long string like object containing large number of super-symplectic bosons.

Color glass condensate has black-hole like properties by its electro-weak darkness and there are excellent reasons to believe that also ordinary black holes could by their large density correspond to states in which super-symplectic matter would form single connected string like structure (if Planck constant is larger for super-symplectic hadrons, this fusion is even more probable).

This inspires the following mechanism for the decay of exotic boson.

1. The tangled cosmic string begins to cool down and when the temperature becomes smaller than $m(\pi_{n_0})$ mass it has decayed to M_{n_1} matter which in turn continues to decay to M_{n_2} matter. The decay to M_{n_1} matter could occur via a sequence $n_0 \rightarrow n_0 - 1 \rightarrow \dots n_1$ of phase

transitions corresponding to the intermediate p-adic length scales $p \simeq 2^k$, $n_1 \geq k > n_0$. Of course, all intermediate p-adic length scales are in principle possible so that the process would be practically continuous and analogous to p-adic length scale evolution with $p \simeq 2^k$ representing more stable intermediate states.

2. The first possibility is that virtual hadrons decay to virtual hadrons in the transition $k \rightarrow k - 1$. The alternative option is that the density of final state hadrons is so high that they fuse to form a single highly entangled hadronic string at Hagedorn temperature T_{k-1} so that the process would resemble an evaporation of a hadronic black hole staying in quark plasma phase without freezing to hadrons in the intermediate states. This entangled string would contain partons as "color glass condensate".
3. The process continues until all particles have decayed to ordinary hadrons. Part of the M_n low energy thermal pions decay to gamma ray pairs and produce a characteristic peak in cosmic gamma ray spectrum at energies $E_n = \frac{m(\pi_n)}{2}$ (possibly red-shifted by the expansion of the Universe). The decay of the cosmic string generates also ultra high energy hadronic cosmic rays, say protons. Since the creation of ordinary hadron with ultra high energy is certainly a rare process there are good hopes of avoiding the problems related to the direct production of protons by cosmic strings (these protons produce two high flux of low energy gamma rays, when interacting with cosmic microwave background [68]).

Topologically condensed cosmic strings as analogs super-symplectic black-holes?

Super-symplectic matter has very stringy character. For instance, it obeys stringy mass formula due the additivity and quantization of mass squared as multiples of p-adic mass scale squared [17]. The ensuing additivity of mass squared defines a universal formula for binding energy having no independence on interaction mechanism. Highly entangled strings carrying super-symplectic dark matter are indeed excellent candidates for TGD variants of black-holes. The space-time sheet containing the highly entangled cosmic string is separated from environment by a wormhole contact with a radius of black-hole horizon. Schwarzschild radius has also interpretation as Compton length with Planck constant equal to gravitational Planck constant $\hbar/\hbar_0 = 2GM^2$. In this framework the proposed decay of cosmic strings would represent nothing but the TGD counterpart of Hawking radiation. Presumably the value of p-adic prime in primordial stage was as small as possible, even $p = 2$ can be considered.

Exotic cosmic ray events and exotic hadrons

One signature of the exotic hadrons is related to the interaction of the ultra high energy gamma rays with the atmosphere. What can happen is that gamma rays in the presence of an atmospheric nucleus decay to virtual exotic quark pair associated with M_{n_k} , which in turn produces a cascade of exotic hadrons associated with M_{n_k} through the ordinary scaled up color interaction. These hadrons in turn decay $M_{n_{k+1}}$ type hadrons via mechanisms to be discussed later. At the last step ordinary hadrons are produced. The collision creates in the atmospheric nucleus the analog of quark gluon plasma which forms a second kind of fireball decaying to ordinary hadrons. RHIC experiments have already discovered these fireballs and identified them as color glass condensates [59]. It must be emphasized that it is far from clear whether QCD really predicts this phase.

These showers differ from ordinary gamma ray showers in several respects.

1. Exotic hadrons can have small momenta and the decay products can have isotropic angular distribution so that the shower created by gamma rays looks like that created by a massive particle.
2. The muon content is expected to be similar to that of a typical hadronic shower generated by proton and larger than the muon content of ordinary gamma ray shower [67].
3. Due to the kinematics of the reactions of type $\gamma + p \rightarrow H_{M_n} + \dots + p$ the only possibility at the available gamma ray energies is that M_{89} hadrons are produced at gamma ray energies above 10 TeV . The masses of these hadrons are predicted to be above 70 GeV and this suggests that these hadrons might be identified incorrectly as heavy nuclei (heavier than ^{56}Fe). These signatures will be discussed in more detail in the sequel in relation to Centauro type events,

Cygnus X-3 events and other exotic cosmic ray events. For a good review for these events and models form them see the review article [87].

Some cosmic ray events [86, 95] have total laboratory energy as high as 3000 TeV which suggests that the shower contains hadron like particles, which are more penetrating than ordinary hadrons.

1. One might argue that exotic hadrons corresponding M_k , $k > 107$ with interact only electro-weakly (color is confined in the length scale associated with M_n) with the atmosphere one might argue that they are more penetrating than the ordinary hadrons.
2. The observed highly penetrating fireballs could also correspond super-symplectic dark matter part of incoming, possibly exotic, hadron fused with that for a hadron of atmosphere. Both hadrons would have lost their valence quarks in the collision just as in the case of Pomeron events. Large fraction of the collision energy would be transformed to super-symplectic quanta in the process and give rise to a large color spin glass condensate. These condensates would have no direct electro-weak interactions with ordinary matter which would explain their long penetration lengths in the atmosphere. Sooner or later the color glass condensate would decay to hadrons by the analog of blackhole evaporation. This process is different from QCD type hadronization process occurring in hadronic collisions and this might allow to understand the anomalously low production of neutral pions.

Exotic mesons can also decay to lepton pairs and neutral exotic pions produce gamma pairs. These gamma pairs in principle provide a signature for the presence of exotic pions in the cosmic ray shower. If M_{89} proton is sufficiently long-lived enough they might be detectable. The properties of Centauro type events however suggest that M_{89} protons are short lived.

6.5.9 Centauro type events, Cygnus X-3 and M_{89} hadrons

The results reported by Brazil-Japan Emulsion Chamber Collaboration [86, 61] on multiple production of hadrons induced by cosmic rays with energies $E_{lab} > 10^5$ GeV provide evidence for new Physics. The distributions for the transverse momentum p_T and longitudinal momentum fraction x for pions were found to differ from the distributions extrapolated from lower energies. The widening of the transversal momentum distributions has also been observed at accelerator energies (*ISR* above $\sqrt{s} = 63$ GeV and CERN SPS-p \bar{p} Collider at $\sqrt{s} = 540$ GeV). Furthermore, exotic events called Geminion, Centauro, Chiron with emission of $n_B \leq 100$ hundred baryons but practically no pions were detected. There are also peculiar events associated with the radiation coming from Cygnus X-3. A recent summary about peculiar events is given in the review article [87].

Mirim, Acu and Quacu

The exotic cosmic ray events are described in the review article of [86]. In [86] the multiple production of pions is classified into 3 jet types called Mirim, Acu and Quacu. Although the transverse momentum distributions for pions observed at low energies are universal, Acu and Quacu jets are characterized by wider transverse momentum distributions with larger value of average transverse momentum p_T than in low energy pionization: this widening is in accordance with accelerator results. The distributions for the longitudinal momentum fraction x scale but differ from the low energy situation for Acu and Quacu jets.

In [86, 78, 57] a description of these events in terms of 'fireballs' decaying into ordinary hadrons were considered. The p_T distribution associated with Mirim is just the ordinary low energy transverse momentum distribution whereas the distributions associated with Acu and Quacu are wider. The masses of the fireballs were assumed to be discrete and were found to be $M_0 \sim 2 - 3$ GeV (Mirim), $M_1 \sim 15 - 30$ GeV (Acu), $M_2 \sim 100 - 300$ GeV (Quacu). It should be noticed that the upper bounds for the masses associated with Acu and Quacu fireballs are roughly by a factor of two smaller than the naive mass estimates 69 GeV and 481 GeV associated with M_{89} pion and M_{89} proton. The temperatures were found to be in range 0.4–10 GeV for Acu and Quacu fireball and to be substantially larger than the ordinary Hagedorn temperature $T_H \simeq 0.16$ GeV.

Chirons, Centauros, anti-Centauros, and Geminions

For the second class of events consisting of Chirons, Centauros and Geminions observed at laboratory energies $100 - 1000 \text{ TeV}$ pion production is strongly suppressed (gamma pairs resulting from the decay of neutral pions are almost absent) [86]. The primary event takes place few hundred meters above the detector and decay products are known to be hadrons and mostly baryons: about 15 (100) for Mini-Centauros (Centauros). This excludes the possibility that exotic hadrons decay in emulsion chamber and implies also that the decay mechanism of the primary particle is such that very few mesons are produced.

The fireball hypothesis has been applied also to Centauro type events assuming that fireballs corresponds to a different phase than in the case of Mirim, Acu and Quacu [86, 57]. The fireball masses associated with Mini-Centauro and Centauro are according to the estimate of [86] $M_{mini} = 35 \text{ GeV}$ and $M_{Centauro} = 230 \text{ GeV}$. These masses are almost exactly one half of the masses of the M_{89} pion (70 GeV) and proton (470 GeV) respectively!

$$\begin{aligned} M_{Mini} &\simeq \frac{m(\pi_{89})}{2} , \\ M_{Centauro} &\simeq \frac{m(p_{89})}{2} . \end{aligned} \tag{6.5.13}$$

This suggests that the decay of cosmic gamma ray to M_{89} quark pair which in turn hadronizes to (possibly virtual) M_{89} hadrons induced by the interaction with the nucleon of atmosphere is the origin of Mini-Centauro/Centauro events.

The basic difference between the decaying fireballs in Acu/Quacu events and Centauro type events is that Acu/Quacu decays produce neutral pions unlike Centauros.

The appearance of the factor of 1/2 in the mass estimates needs an explanation. One explanation is systematic error in the evaluation of hadronic energy: for instance, the gamma inelasticity k_γ telling which fraction of hadronic energy is transformed to electromagnetic energy might be actually smaller than believed by a factor of order two. An alternative explanation is related to the decay mechanism of M_{89} particle: if the decay takes place via a decay to two off mass shell M_{89} hadrons decaying in turn to hadrons then the average rest energy of the fireball is indeed one half of the mass of the decaying on mass shell particle. The reason for the necessity of off mass shell intermediate states is perhaps the stability of the on mass shell exotic hadrons against the direct decay to ordinary hadrons.

Anti-Centauros are much like Centauros except that neutral pions are over-abundant [87]. The speculative model [45] relies on the notion of chiral condensates consisting of neutral pions in the case of Centauros and charged pions in the case of anti-Centauros. If one wants to explain Anti-Centauros in terms of M_{89} physics should be able to explain the over abundance of neutral pions in terms of decay products of ordinary hadrons at later stages of the decay cascade.

The case of Cygnus X-3

There are peculiar events associated with the cosmic rays coming from Cygnus X-3 at gamma ray energies above 10^5 GeV [79]. The primary particle must be massless particle and is most probably ordinary gamma ray. The structure of the shower however suggests that the decaying particle is very massive! Furthermore, the muon content of the shower is larger than that associated with gamma ray shower. A possible explanation is that the gamma rays coming from Cygnus X-3 with energy above the threshold 10^4 GeV produce M_{89} hadrons, which in turn create the cosmic ray shower through the decay to M_{89} hadrons and the decay of these to the ordinary M_{107} hadrons: this indeed means that the gamma rays behave like a massive particles in the atmosphere.

6.5.10 TGD based explanation of the exotic events

The TGD based model for exotic events involve p-adic length scale hierarchy, many-sheeted space-time, and TGD inspired view about dark matter. A decisive empirical input comes from RHIC events suggesting that quark gluon plasma is actually a liquid like "macroscopic" quantum phase identifiable as a particular instance of dark matter.

General considerations

The mass estimates for the fireballs and the absence of neutral pions suggest that Mini-Centauro/Centauro type events correspond to the decay of M_{89} hadrons (pion/proton) to ordinary hadrons. The general model for the exotic events would be following.

1. Cosmic gamma ray decays first into M_{89} quark pair via electromagnetic interaction with the nucleon of the atmosphere. Pairs of Centauros/anti-Centauros and quark-gluon-plasma blobs explaining Mirim/Qcu/Quacu events would be naturally created in these collisions.
2. The quark pair in turn hadronizes to M_{89} hadrons decaying to virtual $k > 89$ hadrons which in turn end up via a sequential decay process to ordinary hadrons. This process is kinematically possible if the condition $E_{tot} > 2M^2/m_p$, is satisfied (M is the mass of the exotic hadron). For example, the energy of the gamma ray must be larger than 500 TeV for exotic proton pair production. For the exotic pion the corresponding lower bound is about 10 TeV . The energies of the exotic events are indeed above 100 TeV in accordance with these bounds. The average total energy is about $E_{tot} = 1740 \text{ TeV}$ for Centauros and $E_{tot} \simeq 903 \text{ TeV}$ for Mini-Centauros [57]. The mechanism implies that two M_{89} fireballs are produced. 'Binocular' events (Geminions) consisting of two widely separated fireballs have indeed been observed [86].
3. If anti-Centauros result via the same mechanism there must be a mechanism explaining why the production of neutral pions varies from event to event. One proposal is that the difference is due to a formation of pion condensates consisting of neutral *resp.* charged pions in the two situations [45]. This hypothesis would unify Centauro events with anti-Centauro events in which the production of neutral pions is abnormally high [87].
4. Mirim/Acu/Quacu events could correspond to the decay of a high temperature quark-gluon plasma blob, or rather color glass condensate, to hadrons (recall that the estimated plasma temperatures are much lower than for Centauros). The collision of M_{89} hadron possibly generated in the interaction of the cosmic gamma ray with ordinary nucleon could induce both the decay of M_{89} hadron to virtual hadrons and generate quark-gluon plasma blob in the atmospheric target nucleus. Hagedorn temperature $T(k)$, $89 < k \leq 107$ is a good guess for the temperature of this plasma blob. RHIC findings [59] suggest that the blob corresponds to highly tangled hadronic string containing super-symplectic dark matter and decaying by de-coherence to ordinary hadrons [16].

Connection with TGD based model for RHIC events

The counterparts of Centauros and other exotic events have not been observed in accelerator experiments. More than a decade after writing the first version of the model for Centauros came however data from RHIC experiment [59], which seems to provide a connection between laboratory and cosmic ray data. In RHIC collisions of very energetic Gold nuclei are studied. The collisions were expected to create a quark gluon plasma freezing to ordinary hadrons. The surprise was that the resulting state behaves like an ideal liquid and has also black hole like properties [59].

Recall that the TGD based model [38, 16] for RHIC findings is following.

1. The state in question corresponds to a highly entangled hadronic string at Hagedorn temperature defining the analog of black hole and decaying by evaporation. The gravitational constant defined by Planck length is effectively replaced by a hadronic gravitational constant defined by the hadronic length scale. p-Adic length scale hypothesis predicts entire hierarchy of Hagedorn temperatures.
2. Bose-Einstein condensate of gluons referred to as color glass condensate has been proposed as an explanation for the liquid like behavior of the quark-gluon phase. TGD based explanation for the liquid like state is that that the state in question corresponds to a large Bose-Einstein condensate like state of super-symplectic particles resulting as hadronic space-time sheets fuse. Super-symplectic bosons have vanishing electro-weak quantum numbers since super-symplectic generators are either purely bosonic or possess quantum numbers of right handed neutrino. Dark matter is in question.

3. LHC has already produce evidence for quark gluon plasma possessing anomalous properties but created in collisions of protons rather than those of heavy nuclei. The TGD based explanation is in formation of long highly entangled color flux tube producing hadrons as it decays [20]. It might be that the creation of these objects in the decays of M_{89} hadrons are responsible for some aspects of the exotic cosmic ray events.

A more precise model for exotic events

A more detailed formulation necessitates a rough model for the transformation of M_{89} hadrons to M_{107} hadrons.

1. On mass shell exotic hadrons can be assumed to be stable against direct decay to ordinary hadrons so that their decay must take place via a sequential decay to off mass shell exotic hadrons characterized by $107 > k > 89$, which eventually decay to ordinary hadrons. The simplest decay mode is the decay to two virtual exotic hadrons with average mass, which is one half of the mass of the decaying exotic hadron in accordance with observations.
2. M_{89} hadron decays to virtual hadrons with $p \simeq 2^k > M_{89}$ dominate over electro-weak decays since the characteristic time scale is defined by $\Lambda(QCD, M_{89}) = 512\Lambda(QCD, 107)$. This means that most of the energy in the process goes to virtual $k > 89$ virtual mesons. Neutral $k > 89$ virtual pions, if created, can decay to gamma pairs so that the problem of understanding the absence of neutral pions remains.
3. M_{89} hadronic space-time sheet suffers a topological phase transition to M_{107} hadronic space-time sheet via several steps $k = 89 \rightarrow k_1 > 89 \dots \rightarrow k_n = 107$. In the process the size of hadronic surface suffers a $2^9 = 512$ -fold expansion meaning the increase of volume by a factor for $2^{27} \sim 10^9/8$ so that a small scale Big Bang is really in question! The expansion brings in mind liquid-vapor phase transition but the freezing to hadrons (due to the properties of color coupling constant evolution) makes the transition more like a liquid-solid phase transition.

As noticed, all p-adic length scales in the range involved could be present but $p \simeq 2^k$ would define more stable intermediate states. A possible experimental signature for the sequence of the phase transitions labeled by $89 \leq k \leq 107$ is a bumpy structure of the detected hadronic cascades with a maximum of 17 maxima. This kind of structure with a constant distance between maxima and 11 maxima has been indeed observed for some cascades (see Fig. 8 of [87]).

A good guess for the critical temperature of the Big Bang like phase transition to occur is $T_{cr}(89) = km_{89}$, where k is some numerical factor. TGD inspired model for the early cosmology provides a universal hydrodynamics model for this period as a mini Big Bang, or rather "a soft whisper amplified to a relatively big bang", containing the duration of the period as the only parameter [16].

4. If the decay process is fast enough, the density of virtual hadrons in the final state becomes so high that they form single highly tangled cosmic string in Hagedorn temperature $T(k)$. An entire sequence of $T(k) = km_k$, $107 > k > 89$ of phase transition temperatures could be involved without intermediate freezing to hadrons. Since the transformation of $k = 89$ hadrons to $k = 107$ hadrons would be essentially a decay process, the distribution of decay products is isotropic in the center of mass frame of $k = 89$ hadron (Centaurus/anti-Centaurus). The same conclusion holds true for the decay of quark gluon plasma (Mirim/Qcu/Quacu).

How to understand the anomalous production of pions?

One can imagine two different explanations for the varying number of pions in the events.

1. M_{89} hadrons produce M_{89} pions

This model would explain the special features of Centaurus. To Anti-Centaurus the model does not apply. One could hope that the decay cascade of Centauro leads at later stages to color glass phases for ordinary hadrons producing surplus of neutral pions.

2. *Restoration of electro-weak symmetry?*

The anomalous production of pions might relate to the restoration of electro-weak symmetry in case of M_{89} hadrons. For M_{89} hadrons the restoration of the electro-weak symmetry would be natural since in TGD framework classical induced gauge fields are massless for known non-vacuum extremals below the p-adic length scale $L(89)$ defining the fundamental electro-weak length scale. The finite size of the space-time sheet carrying these fields brings in the length scale determining the boson mass when the space-time sheet in question looks point like in the length scale resolution used. The model of elementary particles as weak strings (Kähler magnetic flux tubes) suggests that electroweak symmetry restoration takes place inside weak magnetic flux tubes and that one might have Bose-Einstein condensate with negative and positive net charges in turn implying the abundance of charged pions. One might argue that for particles topologically condensed to space-time sheets with $k > 89$ M_{61} defines the weak scale so that weak interactions effectively disappear.

In zero energy ontology zero energy states are characterized by time-like entanglement coefficients defining M -matrices in turn identifiable as the rows of the unitary U -matrix coding for physics in TGD Universe. The superposition of zero energy states for which positive energy parts have varying values of conserved charges (say electromagnetic charge) do not break conservation laws. Note that also in super-conductors coherent states of Cooper pairs make sense in zero energy ontology without breaking the conservation of fermion number. Therefore one can consider generation of coherent states of pions with non-standard direction of isospin in the collisions of cosmic rays with the nuclei of atmosphere. The TGD inspired model for leptohadrons [24] assumes that the coherent states of leptopions consisting of pionlike bound states of colored excitations of leptons are created in the strong non-orthogonal magnetic and electric fields of the colliding heavy nuclei or other charged particles. Similar situation might be encountered in the collision of high energy cosmic rays with the nuclei of the atmosphere.

Both Centauros and anti-Centauros could be understood if the transformation of M_{89} hadrons to ordinary hadrons generates "mis-aligned" pionic BE condensates. $U(2)_{ew}$ symmetry is restored for M_{89} hadrons and there is no preferred isospin direction for the order parameter of M_{89} pionic BE condensate. This BE condensate is however excluded by energetic considerations. The sequence of phase transitions leading to M_{107} hadrons involving intermediate p-adic length scales could however generate this kind of BE condensate.

If an overcooling occurs in the sense that electro-weak symmetry is not lost, the first intermediate pion condensate can correspond to π_+, π_- or π_0 . Charged π condensates would be created in pairs with opposite charges. In this kind of situation the number of gamma rays produced in the decay to ordinary hadrons would vary from event to event.

The presence of pionic BE condensates favors the decay to M_{107} hadrons via hadronic intermediate states rather than via the cooling of partonic phase condensed on single tangled string whose length grows. This and the idea that $U(2)_{ew}$ symmetry could be exact for the dark matter phase, encourages to consider also the possibility that M_{89} hadron decays to a state consisting of dark M_{107} hadrons forming a BE condensate like state behaving like single coherent unit and interacting with the ordinary matter only via emission of dark gauge boson BE condensates de-cohering to ordinary gauge bosons.

Dark pionic BE condensates with various charges could be present. These dark π condensates would decay coherently to pairs of dark ew boson "laser beams", which can interact with the ordinary matter only after they have de-cohered to ordinary ew gauge bosons and remain undetected if the de-coherence time for dark bosons is long enough, probably not so. Dark hadron option could thus explain also the abnormally long penetration lengths.

3. Is long range charge entanglement involved?

The variation for the number of pions could involve electromagnetic charge entanglement between particles produced in the event and ordinary matter. This would guarantee strict charge conservation when the quantization axis for weak isospin for the resulting hadrons differs from that for the ordinary matter. The decay of the pion to gamma pair becomes possible only after the entanglement is reduced and if de-coherence time is long enough it is possible to understand the variation.

6.5.11 Cosmic ray spectrum and exotic hadrons

The hierarchy of M_n hadron physics provides also a mechanism producing ultra high energy cosmic gamma rays and hadrons.

Do gamma rays dominate the spectrum at ultrahigh energies?

A possible piece of evidence for M_{89} hadrons is related to the analysis [108] of the cosmic ray composition near 10^9 GeV. The analysis was based on the assumption that the spectrum consists of nuclei. The assumptions and conclusions of the analysis can be criticized:

1. There is argument [110], which states that the interaction of protons having energy above 10^9 GeV with the cosmic microwave background implies pion pair creation and a rapid loss of proton energy so that the contribution of protons should be strongly suppressed in the cosmic ray spectrum above $E = 7 \cdot 10^{10}$ GeV. If protons dominate, cosmic ray spectrum should effectively terminate at energy of order $7 \cdot 10^{10}$ GeV: some events above $E = 10^{11}$ GeV have been however detected [66].
2. It is not obvious whether one can distinguish between protons and gamma rays at these energies since the muon content of the photon and proton showers are near to each other at these energies [68]. Therefore the particles identified as protons might well be gamma rays.
3. The spectrum can be fitted assuming that cosmic ray spectrum has two components. Light component ('protons') can be identified as protons and He nuclei. The heavy component ('Fe') corresponds to Fe and heavier nuclei. The nuclei between He and Fe seem to be peculiarly absent. Furthermore, there are also indications that spectrum contains only light nuclei in the range $3 \cdot 10^7 - 10^{11}$ GeV [76].

An alternative interpretation suggested also in [68] is that cosmic ray flux is dominated by gamma rays at these energies. 'Protons' correspond to gamma rays interacting ordinarily with matter. 'Fe nuclei' correspond to the fraction of gamma rays decaying first into M_{89} exotic quark pair producing corresponding exotic hadrons, which then decay to ordinary hadrons and produce showers resembling ordinary heavy nucleus shower. Super-symplectic vision allows to consider the possibility that 'protons' correspond to super-symplectic part of proton having essentially the same mass.

Hadronic component of the cosmic ray spectrum

The properties of the hadronic cosmic ray spectrum above $4 \cdot 10^5$ GeV are not well understood.

1. It has turned out difficult to invent acceleration mechanisms producing hadronic cosmic rays having energies above 10^5 GeV [108].
2. The spectrum contains a 'knee' (power $E^{-2.7}$ changes to about E^{-3} at the knee), which is at the energy $3 \cdot 10^6$ GeV [108] and equals to the mass of M_{61} pion. It is difficult to understand how the knee is generated although several explanations have been proposed (these are reviewed shortly in [108]).

A possible solution of the problems is that part of the hadronic cosmic rays are generated in the decay of string like objects rather than by some acceleration mechanism. Assume that M_{n_k} hadron is created in the decay cascade. Since M_{n_k+m} , $m = 1, 2, ..$ hadrons can have rest masses above M_{n_k} threshold mass, one can consider the possibility that M_{n_k} hadron decays sequentially to ordinary M_{107} hadron with arbitrary large rest mass (even larger than M_{n_k} pion mass) and that this ordinary hadron in turn produces some very energetic low mass hadrons, say proton and antiproton, identifiable as cosmic rays. The most efficient producers of hadrons are M_{n_k} pions since these are produced most abundantly in the decay of M_{n_k+1} hadrons. M_{n_k} pion at rest cannot however decay to ordinary hadrons with energy above M_{n_k} pion mass. Therefore the slope of the cosmic ray energy flux should become steeper above M_{n_k} , in particular M_{61} , threshold.

The problem of relic quarks and hierarchy of QCD:s

Baryon and lepton numbers are conserved separately in TGD and one of the basic problems of the gauge theories with conserved baryon number is the problem of relic quarks. Hadronization starts in temperature of the order of quark mass and since hadronization is basically many quark process it continues until the expansion rate of the Universe becomes larger than the rate of the hadronization. As a consequence the number density of relic quarks is much larger than the upper bound $n_{relic} <$

$\rho_B/m_q = 10^{-9}n_\gamma m_p/m_q$ obtained from the requirement that the contribution of relic quarks to mass density is smaller than the baryonic mass density. There is also an experimental upper bound $n_{relic} < 10^{-28}n_\gamma$.

The assumption about the existence of QCD:s with a hierarchy of increasing scales $\Lambda_{QCD}(M_n)$ implies that the length scale $L(n) \sim 1/\sqrt{\Lambda_{QCD}(M_n)}$ below which quarks are free, decreases with increasing cosmic temperature and therefore the problem of the relic quarks disappears.

6.5.12 Ultrahigh energy cosmic rays as super-symplectic quanta?

Near the end of year 2007 Pierre Auger Collaboration made a very important announcement relating to ultrahigh energy cosmic rays. I glue below a popular summary of the findings [124].

Scientists of the Pierre Auger Collaboration announced today (8 Nov. 2007) that active galactic nuclei are the most likely candidate for the source of the highest-energy cosmic rays that hit Earth. Using the Pierre Auger Observatory in Argentina, the largest cosmic-ray observatory in the world, a team of scientists from 17 countries found that the sources of the highest-energy particles are not distributed uniformly across the sky. Instead, the Auger results link the origins of these mysterious particles to the locations of nearby galaxies that have active nuclei in their centers. The results appear in the Nov. 9 issue of the journal Science.

Active Galactic Nuclei (AGN) are thought to be powered by supermassive black holes that are devouring large amounts of matter. They have long been considered sites where high-energy particle production might take place. They swallow gas, dust and other matter from their host galaxies and spew out particles and energy. While most galaxies have black holes at their center, only a fraction of all galaxies have an AGN. The exact mechanism of how AGNs can accelerate particles to energies 100 million times higher than the most powerful particle accelerator on Earth is still a mystery.

What has been found?

About million cosmic ray events have been recorded and 80 of them correspond to particles with energy above the so called GKZ bound, which is $.54 \times 10^{11}$ GeV. Electromagnetically interacting particles with these energies from distant galaxies should not be able to reach Earth. This would be due to the scattering from the photons of the microwave background. About 20 particles of this kind however comes from the direction of distant active galactic nuclei and the probability that this is an accident is about 1 per cent. Particles having only strong interactions would be in question. The problem is that this kind of particles are not predicted by the standard model (gluons are confined).

What does TGD say about the finding?

TGD provides an explanation for the new kind of particles.

1. The original TGD based model for the galactic nucleus is as a highly tangled cosmic string (in TGD sense of course [24]. Much later it became clear that also TGD based model for black-hole is as this kind of string like object near Hagedorn temperature [24]. Ultrahigh energy particles could result as decay products of a decaying split cosmic string as an extremely energetic galactic jet. Kind of cosmic fire cracker would be in question. Originally I proposed this decay as an explanation for the gamma ray bursts. It seems that gamma ray bursts however come from thickened cosmic strings having weaker magnetic field and much lower energy density [38].
2. TGD predicts particles having only strong interactions [26]. I have christened these particles super-symplectic quanta. These particles correspond to the vibrational degrees of freedom of partonic 2-surface and are not visible at the quantum field theory limit for which partonic 2-surfaces become points.

What super-symplectic quanta are?

Super-symplectic quanta are created by the elements of super-symplectic algebra, which creates quantum states besides the super Kac-Moody algebra present also in super string model. Both algebras relate closely to the conformal invariance of light-like 3-surfaces.

1. The elements of super-symplectic algebra are in one-one correspondence with the Hamiltonians generating symplectic transformations of $\delta M_{\pm}^4 \times CP_2$. Note that the 3-D light-cone boundary is metrically 2-dimensional and possesses degenerate symplectic and Kähler structures so that one can indeed speak about symplectic (canonical) transformations.
2. This algebra is the analog of Kac-Moody algebra with finite-dimensional Lie group replaced with the infinite-dimensional group of symplectic transformations [22]. This should give an idea about how gigantic a symmetry is in question. This is as it should be since these symmetries act as the largest possible symmetry group for the Kähler geometry of the world of classical worlds (WCW) consisting of light-like 3-surfaces in 8-D imbedding space for given values of zero modes (labeling the spaces in the union of infinite-dimensional symmetric spaces). This implies that for the given values of zero modes all points of WCW are metrically equivalent: a generalization of the perfect cosmological principle making theory calculable and guaranteeing that WCW metric exists mathematically. Super-symplectic generators correspond to gamma matrices of WCW and have the quantum numbers of right handed neutrino (no electro-weak interactions). Note that a geometrization of fermionic statistics is achieved.
3. The Hamiltonians and super-Hamiltonians have only color and angular momentum quantum numbers and no electro-weak quantum numbers so that electro-weak interactions are absent. Super-symplectic quanta however interact strongly.

Also hadrons contain super-symplectic quanta

One can say that TGD based model for hadron is at space-time level kind of combination of QCD and old fashioned string model forgotten when QCD came in fashion and then transformed to the highly unsuccessful but equally fashionable theory of everything.

1. At quantum level the energy corresponding to string tension explaining about 70 per cent of proton mass corresponds to super-symplectic quanta [17]. super-symplectic quanta allow to understand hadron masses with a precision better than 1 per cent.
2. Super-symplectic degrees of freedom allow also to solve spin puzzle of the proton: the average quark spin would be zero since same net angular momentum of hadron can be obtained by coupling quarks of opposite spin with angular momentum eigen states with different projection to the direction of quantization axis.
3. If one considers proton without valence quarks and gluons, one obtains a boson with mass very nearly equal to that of proton (for proton super-symplectic binding energy compensates quark masses with high precision). These kind of pseudo protons might be created in high energy collisions when the space-time sheets carrying valence quarks and super-symplectic space-time sheet separate from each other. Super-symplectic quanta might be produced in accelerators in this manner and there is actually experimental support for this from Hera.
4. The exotic particles could correspond to some p-adic copy of hadron physics predicted by TGD and have very large mass smaller however than the energy. Mersenne primes $M_n = 2^n - 1$ define excellent candidates for these copies. Ordinary hadrons correspond to M_{107} . The protons of M_{31} hadron physics would have the mass of proton scaled up by a factor $2^{(107-31)/2} = 2^{38} \simeq 2.6 \times 10^{11}$. Energy should be above 2.6×10^{11} GeV and is above $.54 \times 10^{11}$ GeV for the particles above the GKZ limit. Even super-symplectic quanta associated with proton of this kind could be in question. Note that CP_2 mass corresponds roughly to about 10^{14} proton masses.
5. Ideal blackholes would be very long highly tangled string like objects, scaled up hadrons, containing only super-symplectic quanta. Hence it would not be surprising if they would emit super-symplectic quanta. The transformation of supernovas to neutron stars and possibly blackholes would involve the fusion of hadronic strings to longer strings and eventual annihilation and evaporation of the ordinary matter so that only super-symplectic matter would remain eventually. A wide variety of intermediate states with different values of string tension would be possible and the ultimate blackhole would correspond to highly tangled cosmic string. Dark matter would be in question in the sense that Planck constant could be very large.

6.6 TGD based explanation for the anomalously large direct CP violation in $K \rightarrow 2\pi$ decay

KTev collaboration in Fermilab [65] has measured the parameter $|\epsilon'/\epsilon|$ characterizing the size of the direct CP violation in the decays of kaons to two pions. The value of the parameter was found to be $|\epsilon'/\epsilon| = (2.8 \pm .1)10^{-3}$ and is almost by an order of magnitude larger than the naive standard model expectations based on the hypothesis that direct CP breaking is induced by CKM matrix. In [100] it was shown that the value of the parameter could be understood without introducing any new physics if the value of running strange quark mass at m_c is about $m_s(m_c) = .1$ GeV and $m_d \ll m_s$ holds true.

6.6.1 How to solve the problems in TGD framework

Problems

Also in TGD framework the situation looks confusing.

1. The TGD based prediction for the value of the CP breaking parameter for CKM matrices satisfying the constraints coming from p-adicity is within the experimental constraints $1.0 \times 10^{-4} \leq J \leq 1.7 \times 10^{-4}$ coming from the standard model so that J produces no problems (see [17] or Appendix for the CKM matrix as predicted by TGD).
2. The dominating contributions of the chiral field theory to $Re(\epsilon'/\epsilon)$ are proportional to $1/(m_s + m_d)^2$. The predictions of p-adic thermodynamics for s and d quark masses for $k(d) = k(s) = 113$ are $m_d(113) = m_s(113) = 90$ MeV and if this mass can be interpreted as $m_s(m_c) \simeq 0.1$ GeV, the prediction is too small by a factor 1/4. Even worse, if m_s corresponds to the scaled up mass $m_s(109) \simeq 360$ MeV of the s quark inside kaon, the situation changes completely and ϵ'/ϵ is too small by a factor $\sim 1/4.5^2 \simeq .05$.
3. TGD predicts that family replication phenomenon has also a bosonic counterpart. In the original scenario gauge bosons had single light-like wormhole throat as space-time correlate just like fermions and two exotic gluons were predicted corresponding to $g = 1$ and $g = 2$. The assumption that fermions at partonic space-time sheets are free fermions however forces to identify gauge bosons as wormhole contacts such that the two light-like wormhole throats carry quantum numbers of fermion and antifermion. Gauge bosons can be arranged into SU(3) singlet corresponding to ordinary gauge bosons and octet, where SU(3) states correspond to pairs (g_1, g_2) of handle numbers $0 \leq g_i \leq 2$.

The experimental non-existence of flavor changing currents suggest strongly that the masses of octet gauge bosons are high. This requires that they correspond to $L(89)$ or even shorter p-adic length scale. Hence these gauge bosons are not interesting from the point of view of CP breaking.

4. The recent breakthrough in p-adic mass calculations for hadrons [17] led also the understanding of non-perturbative aspects of hadron physics in terms of super-symplectic bosons which correspond to single light-like wormhole throat so that they couplings to quarks in the sense of generalized Feynman diagrams do not imply flavor changing neutral currents.

The basic prediction is that topologically mixed super-symplectic bosons are responsible for the most of the mass of proton and that it is possible to deduce the super-symplectic content of hadrons from their masses if their topological mixing is assumed to be same as for U type quarks. The masses of these bosons correspond to p-adic length scale $L(107)$ and are small in length scale $L(89)$ relevant for CP breaking. These observations suggest that higher gluon genera of the earlier model should be replaced with super-symplectic gluons.

In the standard diagrammatic expression for the CP breaking parameter gluon propagators are replaced by a sum of ordinary massless and two exotic gluon massive gluon propagators. The fact that the matrix elements relevant for the estimation of the CP breaking parameter are estimated at momentum transfer of order $\mu = m_W$, implies that gluon masses do not significantly change the contribution of the super-symplectic gluons to the amplitude apart from the change in value of color

coupling strength. Hence the penguin amplitudes are simply multiplied by some factor X determined by the number of super-symplectic gluons light in length scale $L(89)$ and by the coupling constants of these gluons and the ratio ϵ'/ϵ is multiplied by a factor X . Unfortunately, it is not possible to calculate this factor at this stage.

The model based on exotic gluons and current quarks

It is essential that exotic gluons correspond to single light-like wormhole throat and thus have family replication phenomenon analogous to that of fermions. Two models can be considered.

1. The original model based on the assumption that ordinary gauge bosons correspond to single wormhole throat. There are good reasons to believe that this interpretation is wrong.
2. The new model based on super-symplectic exotic gluons whose number is not known but is multiple of 3. The couplings to quarks are not known. Also color single super-symplectic bosons could be also present.

1. The difficulty of the original model

The problem of this model is that assuming exotic gluons in sense 1) ϵ'/ϵ would be still by a factor .15 too small for $m_s(109)$ relevant for kaons.

The basic observation is that the gluon contribution is proportional to $1/(m_s + m_d)^2$ and for $m_s(113)$ instead of $m_s(119)$ ϵ'/ϵ would be a fraction $(16+1)/2 = 8.5$ large and by a factor 1.275 larger than the experimental value since $m_d = m_s$ rather than $m_d \ll m_s$ holds true.

This observation stimulated the idea that a transition $s_{109} \rightarrow s_{113}$ occurs before electro-weak process and would have an interpretation as a transformation of a constituent quark to current quark. This requires that the amplitudes for the transition $s(109) \rightarrow s(113)$ and its reversal are near to unity.

The question is why $s(109) \rightarrow s(113)$ constituent-current transformation should occur in electro-weak interactions and why it occurs with amplitude $A \sim 1$. Of course it could also be that also d quark is transformed to a very low mass variant with mass about 4 MeV predicted by chiral field theory. This would correspond to $k = 125$. As a result the amplitude would be multiplied by a factor 4 and $A = 1/2$ would become possible.

For some reason the join along boundaries bonds feeding em gauge flux of s quark to $k = 109$ space-time sheet would be transferred to nuclear space-time sheets with $k = 113$ before the electro-weak scattering process responsible for the CP breaking. Note that the value of strange quark mass about 176 MeV deduced from τ lepton decay rate corresponds to $m_s(111)$ in a good approximation. Also this indicates that various scaled up variants of quark masses can appear in the electro-weak dynamics as intermediate states.

The assumption for the proportionality $\epsilon'/\epsilon \propto 1/(m_s + m_d)^2$ derivable from chiral field theory can be criticized. Finding a justification for this assumption seems to be a non-trivial challenge since it is not at all clear that chiral field theory based on $SU(3)$ flavor symmetry makes sense in TGD context.

2. Super-symplectic variant of the original model

For super-symplectic gluons one can predict only that the relevant gluon exchange amplitude increases by a factor

$$X = \sum_{i,j} \alpha_s(B_{i,j}) \ ,$$

where $\alpha_s(B_{i,j})$ is the color coupling strength to j :th generation of the super-symplectic gluon B_i . In principle also color neutral super-symplectic bosons having spin might contribute.

For $\alpha_s(B_{i,j}) = \alpha_s(B_i)$ one would have

$$X = 3 \sum_i \alpha_s(B_i) \ .$$

If the number of light super-symplectic gluons large enough, it is possible to have a large enough value of X to compensate for the factor .14 so that the assumption about the transformation $s(109) \rightarrow s(113)$ from constituent quark to current quark would become un-necessary. $X \sim 8$ would be needed.

Recall that super-symplectic algebra is analogous to Kac-Moody algebra in the sense that finite-dimensional Lie-group is replaced with symplectic group. Super-symplectic gluons correspond to states created by super-algebra generators, which are in one-one correspondence Hamiltonians of $\delta M_+^4 \times CP_2$ subject to some additional conditions making subset of states zero norm states. Therefore more than single octet of super-symplectic bosons and also higher dimensional representations might be possible.

All depends on which of these super-symplectic states correspond to light particles. This in turn depends on the details of super-symplectic representations (they correspond to the states of negative conformal weight annihilated by Virasoro generators $L_n, n < 0$ [37]). Here the help of a mathematician specialized to the representations of super-conformal algebras would be needed.

At this moment it is not possible to know whether the transformation to current quark is needed or even possible and this motivates the following discussion of the basic notions and chiral field theory approach in more detail in order to clarify what is involved.

6.6.2 Basic notations and concepts

Until 1963 CP symmetry was believed to be an exact symmetry of Nature. In this year it was however observed by Christensen, Cronin, Fitch and Turlay that CP symmetry is violated in hadronic decays of neutral kaons. In order to interpret the experimental evidence one must consider the strong Hamiltonian eigen states K^0 and its CP conjugate \bar{K}^0 as a mixture of physical short lived K_S decaying predominantly to two pions and long-lived K_L decaying mostly semi-leptonically and into 3 pion states. Two- and three pion final states have odd and even CP parity. In absence of CP breaking one would identify K_S and K_L as the CP even and CP odd states

$$\begin{aligned} K_1 &= (K^0 + \bar{K}^0)/\sqrt{2} \ , \\ K_2 &= (K^0 - \bar{K}^0)/\sqrt{2} \ . \end{aligned} \tag{6.6.0}$$

What was observed in 1963 was that K_L decays also to two-pion final states.

There are two mechanisms of CP violation. The indirect mechanism involves a slight mixing of K^1 and K^2 characterized by a complex mixing parameter $\bar{\epsilon}$

$$\begin{aligned} K_S &= \frac{K_1 + \bar{\epsilon}K_2}{1 + |\bar{\epsilon}|^2} \ , \\ K_L &= \frac{K_2 + \bar{\epsilon}K_1}{1 + |\bar{\epsilon}|^2} \ . \end{aligned} \tag{6.6.0}$$

Direct mechanism involves the direct decay of K_2 to two pion state and is induced by the weak interaction Lagrangian L_W directly. Both mechanisms can be parameterized in terms of the small ratios

$$\begin{aligned} \eta_{00} &= \frac{\langle \pi^0 \pi^0 | L_W | K_L \rangle}{\langle \pi^0 \pi^0 | L_W | K_S \rangle} \ , \\ \eta_{+-} &= \frac{\langle \pi^+ \pi^- | L_W | K_L \rangle}{\langle \pi^+ \pi^- | L_W | K_S \rangle} \ . \end{aligned} \tag{6.6.-1}$$

Here L_W represents the $\Delta S = 1$ part of the weak Lagrangian. The equations for η parameters can be also written as

$$\begin{aligned} \eta_{00} &= \epsilon - \frac{2\epsilon'}{1 - \omega/\sqrt{2}} \simeq \epsilon - 2\epsilon' \ , \\ \eta_{+-} &= \epsilon - \frac{2\epsilon'}{1 + \omega/\sqrt{2}} \simeq \epsilon + \epsilon' \ . \end{aligned} \tag{6.6.-1}$$

Parameter $\bar{\epsilon}$ is simply related to ϵ . The parameter ω measures the ratio

$$|\omega| = \frac{|\langle(\pi\pi)_{I=2}|L_W|K_S\rangle|}{|\langle(\pi\pi)_{I=0}|L_W|K_S\rangle|} \simeq 1/22.2 \quad (6.6.0)$$

$I = 0$ and $I = 2$ denote the isospin states of final state pions.

The CP violating parameters are expressible in terms of $K_{S,L}$ decay amplitudes as

$$\begin{aligned} \epsilon &= \frac{\langle(\pi\pi)_{I=0}|L_W|K_L\rangle}{\langle(\pi\pi)_{I=0}|L_W|K_S\rangle} \quad , \\ \epsilon' &= \frac{\epsilon}{\sqrt{2}} \left[\frac{\langle(\pi\pi)_{I=2}|L_W|K_L\rangle}{\langle(\pi\pi)_{I=0}|L_W|K_L\rangle} - \frac{\langle(\pi\pi)_{I=2}|L_W|K_S\rangle}{\langle(\pi\pi)_{I=0}|L_W|K_S\rangle} \right] \quad . \end{aligned} \quad (6.6.0)$$

By Watson's theorem one can write the generic amplitudes for K^0 and \bar{K}^0 decay as

$$\begin{aligned} \langle(\pi\pi)_I|L_W|K^0\rangle &= -iA_I \exp(i\delta_I) \quad , \\ \langle(\pi\pi)_I|L_W|\bar{K}^0\rangle &= -iA_I^* \exp(i\delta_I) \quad , \end{aligned} \quad (6.6.0)$$

where the phases δ_I arise from the pion final state interactions. In good approximation ($|\bar{\epsilon}ImA_0| \ll |ReA_0|$, $|\bar{\epsilon}|^2 \ll 1$) one can write

$$\begin{aligned} \epsilon' &= \exp(i(\pi/2 + \delta_2 - \delta_1)) \times \frac{\omega}{\sqrt{2}} \times \left(\frac{ImA_2}{ReA_2} - \frac{ImA_0}{ReA_0} \right) \quad , \\ \omega &= \frac{ReA_2}{ReA_0} \quad . \end{aligned} \quad (6.6.0)$$

With the approximations used one obtains a relationship

$$\epsilon' = \bar{\epsilon} + i \frac{ImA_0}{ReA_0} \quad . \quad (6.6.1)$$

One can find a more detailed representation of the subject in various review articles [106, 125]. The standard model of CP breaking is based on the presence of complex phases in CKM matrix.

The value of the parameter ϵ describing indirect CP violation is well established and given by

$$|\epsilon| = (2.266 \pm .017) \times 10^{-3} \quad .$$

The phases of ϵ and ϵ' are in good approximation identical so that their signs are same. The value of $Re(\epsilon'/\epsilon)$ was finally established by KTeV collaboration at Fermi Lab to be

$$Re\left(\frac{\epsilon'}{\epsilon}\right) = (2.8 \pm .01) \times 10^{-3} \quad .$$

The measurement is consistent with the result of the CERN experiment NA31, which has also found a non-vanishing value for this parameter.

There are several theories of CP violation. The so called milliweak theory predicts vanishing value of ϵ' . The model based on the presence of CP breaking phases in three-generation CKM matrix predicts non-vanishing value for the parameter. Also Higgs particles can effect the value of the parameter in standard model. Standard model predicts this parameter to be nonzero but the expectation has been that the value is roughly ten times smaller than the measured value.

A possible explanation of the effect which does not introduce new physics is based on the hypothesis that the mass of s quark is smaller than the mass of d quark: the running mass $m_s(2 \text{ GeV}) \simeq .1 \text{ GeV}$ is needed to explain the anomaly if CP breaking parameter J is taken to be in the range $(1 - 1.7) \times 10^{-4}$ claimed in [93] to follow from unitarity. There is however experimental evidence from τ decays for $m_s(m(\tau)) = (172 \pm 31) \text{ MeV}$. This suggests that some new short length scale physics is involved.

Standard model prediction for $Re(\epsilon'/\epsilon)$ [100] can be summarized in a handy formula

$$\begin{aligned}
Re\left(\frac{\epsilon'}{\epsilon}\right) &= J \times \left[-1.35 + R_s \left(A_6 B_6^{1/2} + A_8 B_8^{3/2} \right) \right] , \\
A_6 &= 1.1 |r_Z^8| , \\
A_8 &= 1.0 - .67 |r_Z^8| .
\end{aligned} \tag{6.6.0}$$

The subscript Z refers to renormalization mass m_Z . The parameter R_s is given by

$$R_s \simeq \left[\frac{150 \text{ MeV}}{m_s(m_c) + m_d(m_c)} \right]^2 . \tag{6.6.1}$$

The dominating contributions to $Re(\frac{\epsilon'}{\epsilon})$ come from second (A_6) and third terms (A_8). These terms correspond to gluonic and electro-weak penguin diagram contributions to the CP breaking decays and of opposite sign. Clearly, the sum of the two terms is roughly one third of the gluonic term alone.

6.6.3 Separation of short and long distance physics using operator product expansion

The calculation of CP breaking parameters involves physics in very wide energy scale. The strategy is to derive low energy effective action by functionally integrating over the short distance effects coming from energies larger than m_c . This leads to Wilson expansion for the low energy electro-weak effective Lagrangian

$$L_{low,W} = - \sum_i C_i(\mu, m_c, m_b, m_t, m_W, \dots) Q_i(\mu) . \tag{6.6.2}$$

The coefficients C_i of the operators Q_i in the low energy effective action for light quarks (u, d, s) are functionals of various parameters characterizing short distance physics. The coefficients $C_i(\mu)$ in Wilson expansion of electro-weak effective action can be written as

$$C_i(\mu) = \frac{G_F}{\sqrt{2}} V_{ud} V_{us}^* [x_i(\mu) + \tau y_i(\mu)] . \tag{6.6.3}$$

Here x_i and y_i are Wilson coefficients. V_{ij} denotes CKM matrix and τ is defined as $\tau = V_{td} V_{ts}^* / V_{ud} V_{us}^*$. $V_{td} V_{ts}^*$ is identical with CP breaking invariant J in standard parametrization. Coefficients $y_i(\mu)$ summarize short distance CP breaking physics and in order to determine CP breaking one needs to consider only the coefficients y_i .

Long distance physics is the difficult part of the calculation since it involves calculation of matrix elements of the quark operators Q_i between initial kaon state and final two-pion state. There are several approaches to the problem. Chiral field theory [102] is phenomenological approach and relies on the idea that low energy effective action for quarks can be expressed in a good approximation using meson fields. Lattice QCD is believed to provide a more fundamental direct method for the calculation of the correlation functions of Q_i .

Short distance physics

In present initial states are kaons and μ denotes the momentum exchange for a typical diagram associated with the scattering of $d\bar{s}$ quark to final state consisting of of light quarks. μ is taken to be of order m_W and by using renormalization group equations one can deduce the values of the coefficients $C_i(\mu)$ at energy scales, typically of order 1 GeV.

The basic standard diagrams contributing to the $\Delta S = 1$ and $\Delta S = 2$ processes are given by the figure below.

The quark operators Q_i appearing in the expansion can be classified. In present case the list of relevant operators correspond to various terms possible in four-fermion Fermi interaction and are given by the following list.

$$Q_1 = (\bar{s}_\alpha u_\beta)_{V-A} (\bar{u}_\beta d_\alpha)_{V-A} , \quad (6.6.3)$$

$$Q_2 = (\bar{s}u)_{V-A} (\bar{u}d)_{V-A} , \quad (6.6.3)$$

$$Q_{3,5} = (\bar{s}d)_{V-A} \sum_q (\bar{q}q)_{V\mp A} ,$$

$$Q_{4,6} = (\bar{s}_\alpha d_\beta)_{V-A} \sum_q (\bar{q}_\beta q_\alpha)_{V\mp A} ,$$

$$Q_{7,9} = \frac{3}{2} (\bar{s}d)_{V-A} \sum_q \hat{e}_q (\bar{q}q)_{V\pm A} ,$$

$$Q_{8,10} = \frac{3}{2} (\bar{s}_\alpha d_\beta)_{V-A} \sum_q \hat{e}_q (\bar{q}_\beta q_\alpha)_{V\pm A} . \quad (6.6.1)$$

α, β denote color indices and \hat{e}_q denote quark charges. $V \pm A$ refers to the Dirac structure $\gamma_\mu (1 \pm \gamma_5)$. Q_2 is induced by mere W exchange whereas gluonic loop corrections to Q_2 induce Q_1 . QCD through penguin loop induces the penguin operators Q_{3-6} . Electro-weak loops, in which penguin gluon is replaced with electro-weak gauge boson, induce $Q_{7,9}$ and part of Q_3 . The operators $Q_{8,10}$ are induced by the QCD renormalization of the electro-weak loop operators $Q_{7,9}$.

As far as the calculation of ϵ'/ϵ is considered, the dominating contributions come from the penguin diagrams, which are proportional to the vertices $s\bar{d}V$, where V is either gluon or electro-weak gauge boson and to the propagator denominator of V with momentum squared equal to momentum exchange between initial state quarks, which equals to $(p_i - p_j)^2 = \mu^2$. For option 2) the standard gluon contribution is replaced with a sum over contributions of ordinary and exotic gluons. For option 1) situation is more complicated since $g > 0$ gluons can change the genus of the fermion.

The operators Q_6 and Q_8 give the dominating contributions to ϵ'/ϵ and these contributions are competing. Q_6 and Q_8 differ only by the fact that in Q_8 penguin gluon is replaced with penguin electro-weak boson γ or Z^0 . For neutral kaon initial state electro-weak penguin diagram is proportional to the product $e_q e_{\bar{q}} = -e_q^2$ of the virtual quark whereas in case of gluons the factor $Tr(T^a T^a) > 0$ appears. Therefore the contributions associated with Q_6 and Q_8 are of opposite sign and mutually competing.

Detailed calculations lead to the formula already described:

$$Re\left(\frac{\epsilon'}{\epsilon}\right) = J \times \left[-1.35 + R_s \left(A_6 B_6^{1/2} + A_8 B_8^{3/2} \right) \right] ,$$

$$A_6 = 1.1 |r_Z^8| ,$$

$$A_8 = 1.0 - .67 |r_Z^8| . \quad (6.6.0)$$

for $Re(\epsilon'/\epsilon)$. The coefficients B_6 and B_8 code the long distance physics and their values do not differ too much from $B_6 = B_8 = 1$. Clearly, the sum of Q_6 and Q_8 contributions is roughly one third of the Q_6 contribution alone. From the general structure of Feynman diagrams it is clear that for option 2) the effect caused by the introduction of exotic gluons is in a good approximation a simple scaling of the Q_6 contribution by a factor 3 in the approximation that gluon masses are negligible as compared to W mass, and that this new contribution can enhance direct CP breaking dramatically.

Chiral field theory approach

The basic problem is to calculate electro-weak matrix elements of the quark effective action between hadronic states. These matrix elements reduce to vacuum expectation values of various quark bilinears appearing in four-fermion Fermi interaction Lagrangian. This problem is very difficult since non-perturbative QCD is involved in an essential manner. An attempt to circumvent this problem [102] is based on the hypothesis that low energy effective action for quarks is essentially equivalent with the low energy effective action, where pseudoscalar meson fields as dynamical fields and scalar, vector and axial vector meson fields occur as external fields not subject to variations. Quark masses

are identified as vacuum expectation values of the external scalar meson field. The approximate symmetry of the chiral field theory is flavor $SU(3)_L \times SU(3)_R$ which is exact symmetry at the limit of massless quarks. This symmetry can be realized if mesons are represented by an element U of $SU(3)$ regarded as a dynamical field: the two $SU(3)$:s act on U from left and right respectively. For small perturbations around ground state mesons correspond to various Lie-algebra generators of $SU(3)$. Chiral field develops vacuum expectation value. If vacuum expectation is not proportional to unit matrix it corresponds to the presence of coherent states associated with the neutral components of the pseudo scalar meson field.

The basic formulation of the chiral field theory approach is described in [102] whereas its application to the calculation of ϵ'/ϵ is described in [96]. The strong part of the chiral action [102] is given by the formula

$$\begin{aligned} L_S &= \frac{f^2}{4} [Tr\{D_\mu U^\dagger D^\mu U\} + 2B_0 Tr\{(s - ip)U\} + 2B_0^* Tr\{(s + ip)U^\dagger\}] \\ &+ \frac{1}{12} H_0 D_\mu \theta D^\mu \theta . \end{aligned} \quad (6.6.0)$$

D_μ denotes the covariant derivative defined by the couplings to the left and right handed gauge bosons L_μ and R_μ defined as superpositions $R_\mu = v_\mu + a_\mu$ and $L_\mu = v_\mu - a_\mu$ of the vector and axial vector mesons fields v and a . Action contains three coupling constant parameters: f , B_0 and H_0 , which is present because the presence of color instantons can lead to a non-vanishing value of the θ parameter in QCD. In lowest order f is pion decay constant f_π and B_0 sets the scale in the formula $M_M^2 = B_0(\sum_i m(q_i))$ inspired by broken $SU(3)$ symmetry and resulting as a prediction of the model. The components for the non-vanishing vacuum expectation value for the external scalar field are identified as quark masses. The generation of vacuum expectation value of s implies that quark condensates are developed:

$$\begin{aligned} \langle \bar{q}_i q_j \rangle &= B_0 f^2 \delta_{i,j} , \\ B_0 f^2 &= \frac{f_\pi^2 m_\pi^2}{(m_u + m_d)} = \frac{f_K^2 m_K^2}{(m_s + m_d)} . \end{aligned} \quad (6.6.0)$$

Note that the strong part of the chiral Lagrangian is invariant under the overall scaling of quark masses.

The weak part of the chiral action corresponds to the sigma model counterpart of the most general electro-weak four-fermion action. The recipe for constructing this action is described in more detail in [96] and can be summarized as rules associating with various fermionic bi-linears appearing in the generalized Fermi action corresponding terms of the weak part of the chiral action. In particular, the following rules hold true:

$$\begin{aligned} \bar{q}_L^j \gamma^\mu q_L^i &\rightarrow -i f_\pi^2 (U^\dagger D_\mu U)_{ij} , \\ \bar{q}_R^j \gamma^\mu q_R^i &\rightarrow -i f_\pi^2 (U D_\mu U^\dagger)_{ij} , \\ \bar{q}_L^j \gamma^\mu q_R^i &\rightarrow -2B_0 \left[\frac{f^2}{4} U + \text{higher order terms} \right]_{ij} , \\ \bar{q}_R^j \gamma^\mu q_L^i &\rightarrow -2B_0 \left[\frac{f^2}{4} U^\dagger + \text{higher order terms} \right]_{ij} . \end{aligned} \quad (6.6.-2)$$

The chiral counterparts of the left and right handed currents are proportional to BM and depend on the ratios of quark masses only. The terms giving dominating contribution to the $\Delta S = 1$ part of the weak effective action involve the chiral counterparts of terms $\bar{q}_L^j q_R^i$ breaking chiral invariance. The chiral counterparts of these terms are proportional to B and, in accordance with expectations, fail to be invariant under the overall scaling of quark masses. The higher order contributions to these terms are important for the calculations of direct CP breaking effects but are not written explicitly here because they are not needed in the estimate for how the predictions of the standard model are

modified in TGD framework. The terms breaking chiral symmetry give rise to ϵ'/ϵ a contribution, which is proportional to $1/(m_s + m_d)^2$.

The $\Delta S = 2$ part of effective quark action is involved with $K^0 \rightarrow \bar{K}^0$ transitions and the corresponding quark operator is given by

$$Q_{S2} = (\bar{s}_L \gamma^\mu d_L)(\bar{s}_L \gamma^\mu d_L) . \quad (6.6-1)$$

The chiral counterpart of this operator is obviously invariant under overall scaling of quark masses.

Does chiral theory approach make sense in TGD framework?

The TGD based model for the large direct CP breaking based on exotic gluons and on the transformation of s_{109} to s_{113} has been already discussed. The open question is whether the $1/(m_s + m_d)^2$ proportionality of the CP breaking amplitude can be justified in TGD context where it is not at all clear that chiral theory approach makes sense.

In standard model framework chiral field theory provides a phenomenological description of the low energy hadron physics and makes possible the calculation of various hadronic matrix elements needed to derive the predictions for CP breaking effect.

Chiral field theory limit however involves some questionable assumptions about the relationship between QCD and low energy hadron physics.

1. $SU(3)$ symmetry is assumed and allows description of light mesons in terms of $SU(3)$ valued chiral field U possessing $SU(3)_R \times SU(3)_R$ symmetry broken only by quark mass matrix. In TGD framework $SU(3)$ symmetry is purely phenomenological symmetry since the fundamental gauge group is the gauge group of the standard model.
2. The generation of quark masses is described as effective spontaneous symmetry breaking caused by the vacuum expectation value of $SU(3)$ Lie-algebra valued external scalar field s . Quark masses are identified as the components of the diagonal vacuum expectation value of this field. Physically the scalar field corresponds to scalar meson field so that quark masses would result from the coupling of the quarks to coherent states of scalar mesons. This cannot be a correct physical description in TGD framework, where p-adic thermodynamics gives rise to quark masses. Of course, the presence of the scalar field can give rise to a small shift in the values of the quark masses. Also Higgs field could be in question.
3. The coupling of the field s to chiral field U implies in the standard model context that the mass squared values of mesons are proportional to the sums of masses of the mesonic quarks: for instance, $M_\pi^2 = B_0(m_u + m_d)$ and $M_K^2 = B_0(m_s + m_d)$, where B_0 is one of the basic coupling constants of the chiral field theory. This formula is not consistent with the p-adic mass calculations, where quark mass squared is additive for quarks with the same value of k_q and quark mass for different values of k_q . Indeed, the formulas $M_\pi^2 = m_u^2 + m_d^2$ and $M_K^2 = (m_s + m_d)^2$ are true. The chiral field formula predicts $m_s/m_d \simeq 24$ requiring $m_u = m_d \simeq 13$ MeV ($k = 121$) for $m_s(113) = 320$ MeV whereas TGD predicts $m_s(109)/m_d(107) = 4$. For $m_s \simeq 100$ MeV the prediction is $m_d \simeq 4.2$ MeV. This looks suspiciously small.

To sum up, although the basic assumptions of chiral field theory limit look too specific in TGD framework, its predictions for low energy hadron physics are well-tested and TGD could be consistent with them. If this the case, the assumption about $s_{109} \rightarrow s_{107}$ transition allows a correct prediction of direct CP breaking amplitude using chiral field theory limit.

6.7 Appendix

6.7.1 Effective Feynman rules and the effect of top quark mass on the effective action

The effective low energy field theory relevant for $K - \bar{K}$ systems is in the standard model context summarized elegantly using the Feynman rules of effective field theory deriving from box and penguin

diagrams. The rules in t'Hooft-Feynman gauge are summarized in excellent review article of Buras and Fleischer [73]. For box diagrams the rules are following:

$$\begin{aligned}
Box(\Delta S = 2) &= \lambda_i^2 \frac{G_F^2}{16\pi^2} M_W^2 S_0(x_i) (\bar{s}d)_{V-A} (\bar{s}d)_{V-A} , \\
Box(T_3 = -1/2) &= \lambda_i \frac{G_F}{\sqrt{2}} \frac{\alpha}{\sin^2(\theta_W)} B_0(x_i) (\bar{s}d)_{V-A} (\bar{\mu}\mu)_{V-A} , \\
Box(T_3 = 1/2) &= \lambda_i \frac{G_F}{\sqrt{2}} \frac{\alpha}{\sin^2(\theta_W)} [-4B_0(x_i)] (\bar{s}d)_{V-A} (\bar{\nu}\nu)_{V-A} , \\
\lambda_i &= V_{is}^* V_{id} .
\end{aligned} \tag{6.7.-2}$$

The box vertices listed here describe the decays $K_0 \rightarrow \bar{K}_0$ and contribute to $K_0 \rightarrow \bar{\mu}\mu$ and $K_0 \rightarrow \bar{\nu}\nu$ decays. $(\bar{q}_1 q_2)_{V-A}$ is shorthand notation for the left handed weak current involving gamma matrices and the products of fermionic bi-linears actually involve contraction of the gamma matrix indices.

Penguin diagrams can be characterized by the effective vertices $\bar{s}dB$, where B is photon, Z boson or gluon, which is treated as usual in effective field theory

$$\begin{aligned}
\bar{s}Zd &= i\lambda_i \frac{G_F}{\sqrt{2}} \frac{g_Z}{2\pi^2} M_Z^2 g_Z C_0(x_i) \bar{s}\gamma^\mu (1 - \gamma_5) d , \\
\bar{s}\gamma d &= -i\lambda_i \frac{G_F}{\sqrt{2}} \frac{e}{8\pi^2} D_0(x_i) \bar{s}(q^2\gamma^\mu - q^\mu q^\nu \gamma_\nu) (1 - \gamma_5) d , \\
\bar{s}G^a d &= -i\lambda_i \frac{G_F}{\sqrt{2}} \frac{g_s}{8\pi^2} E_0(x_i) \bar{s}(q^2\gamma^\mu - q^\mu q^\nu \gamma_\nu) (1 - \gamma_5) T^a d .
\end{aligned} \tag{6.7.-3}$$

The vertices above correspond to the exchange of Z , photon and gluon between the quarks. Boson propagator and second vertex is constructed using the standard Feynman rules. The counterparts of the sdB vertices are easily constructed for $g > 0$ gluons. The orthogonality of single hadron states requires that flavor is conserved for $g > 0$ exchanges.

The functions B_0, C_0, \dots characterize the low energy effective action at mass scale $\mu = m_W$. The subscript '0' refers to the values of these functions without QCD corrections, which are taken into account using renormalization group equations to deduced the functions at mass scale of order 1 GeV. The functions are listed below:

$$\begin{aligned}
B_0(x_t) &= \frac{1}{4} \left[\frac{x_t}{y_t} + \frac{x_t \log(x_t)}{y_t^2} \right] , \\
C_0(x_t) &= \frac{x_t}{8} \left[-\frac{x_t - 6}{y_t} + \frac{3x_t + 2}{y_t^2} \log(x_t) \right] , \\
D_0(x_t) &= -\frac{4}{9} \log(x_t) - \frac{25x_t^2 - 19x_t^3}{36y_t^3} + \frac{x_t^2(-6 - 2x_t + 5x_t^2)}{18y_t^3} \log(x_t) , \\
E_0(x_t) &= -\frac{2}{3} \log(x_t) + \frac{x_t^2(15 - 16x_t - 4x_t^2)}{6y_t^4} \log(x_t) + \frac{x_t(18 - 11x_t - x_t^2)}{12y_t^3} , \\
S_0(x_t) &= \frac{4x_t - 11x_t^2 + x_t^3}{4y_t^2} - \frac{3x_t^2 \log(x_t)}{2y_t^3} , \\
S_0(x_c, x_t) &= x_c \left[\log\left(\frac{x_t}{x_c}\right) - \frac{3x_t}{4y_t} - \frac{3x_t^2 \log(x_t)}{4y_t^2} \right] , \\
x_c &= \left(\frac{m_c}{m_W}\right)^2 \quad x_t = \left(\frac{m_t}{m_W}\right)^2 , \quad y_t = 1 - x_t .
\end{aligned} \tag{6.7.-8}$$

Although x_t , being the interesting parameter, appears as the only argument of these functions, also the contributions coming from light quarks propagating in the loops are included. For comparison purposes it is useful to give the explicit relations between electro-weak coupling parameters and G_F .

$$\begin{aligned}
\frac{G_F}{\sqrt{2}} &= \frac{g_W^2}{8m_W^2} , \\
g_W &= \frac{e}{\sin(\theta_W)} , \\
g_Z &= \frac{e}{\sin(\theta_W)\cos(\theta_W)} .
\end{aligned} \tag{6.7.-9}$$

The following table summarizes the effect of the change of the top quark mass on the functions B_0, C_0, \dots . What is given are the ratios $r(f) = f(55)/f(175)$ of the functions B_0, C_0, \dots evaluated for top quark masses 55 GeV and 175 GeV respectively.

f	$B_0(x_t)$	$C_0(x_t)$	$D_0(x_t)$	$E_0(x_t)$	$S_0(x_t)$	$S_0(x_c, x_t)$	(6.7.-8)
r	.51	.09	-.70	3.44	.15	.81	

These results leave allow only the identification of the experimental candidate as a realistic candidate for top quark.

1. The function B_0 is reduced only by a factor of 1/2 and there are no new physics contributions to B_0 in the lowest order. The function C_0 characterizing Z penguin diagrams is reduced by an order of magnitude. The coefficient $C_0(x_t) - 4B_0(x_t)$ characterizes the dominating contribution to $K \rightarrow \mu^+\mu^-$ decay in standard model and the decay amplitude is reduced by a factor .27 so that this decay would provide a stringent test selecting between 55 GeV top quark and 175 GeV top quark. Unfortunately, the predicted $K \rightarrow \mu^+\mu^-$ rate is still by several orders of magnitude below the experimental upper bound.
2. The function $S_0(x_t)$ characterizing $B - \bar{B}$ and $K - \bar{K}$ mass differences is reduced almost by an order of magnitude. Note that in case of Δm_K the ratio $r(tt/ct)$ of the WW box diagram amplitudes with two top quarks and c and t in internal fermion lines is $r(tt/ct) \sim 738$ for $m_t = 175$ GeV and $r(tt/ct) \sim 138$ for $m_t = 55$ GeV (the moduli of the factors coming from CKM matrix are taken into account). Thus $m_t = 175$ GeV is the only sensible choice.

6.7.2 U and D matrices from the knowledge of top quark mass alone?

As already found, a possible resolution to the problems created by top quark is based on the additivity of mass squared so that top quark mass would be about 230 GeV, which indeed corresponds to a peak in mass distribution of top candidate, whereas $t\bar{t}$ meson mass would be 163 GeV. This requires that top quark mass changes very little in topological mixing. It is easy to see that the mass constraints imply that for $n_t = n_b = 60$ the smallness of V_{i3} and $V(3i)$ matrix elements implies that both U and D must be direct sums of 2×2 matrix and 1×1 unit matrix and that V matrix would have also similar decomposition. Therefore $n_b = n_t = 59$ seems to be the only number theoretically acceptable option. The comparison with the predictions with pion mass led to a unique identification $(n_d, n_b, n_s) = (5, 5, 59), (n_u, n_c, n_t) = (4, 6, 59)$.

U and D matrices as perturbations of matrices mixing only the first two genera

This picture suggests that U and D matrices could be seen as small perturbations of very simple U and D matrices satisfying $|U| = |D|$ corresponding to $n = 60$ and having $(n_d, n_b, n_s) = (4, 5, 60), (n_u, n_c, n_t) = (4, 5, 60)$ predicting V matrix characterized by Cabibbo angle alone. For instance, CP breaking parameter would characterize this perturbation. The perturbed matrices should obey thermodynamical constraints and it could be possible to linearize the thermodynamical conditions and in this manner to predict realistic mixing matrices from first principles. The existence of small perturbations yielding acceptable matrices implies also that these matrices be near a point at which two different matrices resulting as a solution to the thermodynamical conditions coincide.

D matrix can be deduced from U matrix since $9|D_{12}|^2 \simeq n_d$ fixes the value of the relative phase of the two terms in the expression of D_{12} .

$$\begin{aligned}
|D_{12}|^2 &= |U_{11}V_{12} + U_{12}V_{22}|^2 \\
&= |U_{11}|^2|V_{12}|^2 + |U_{12}|^2|V_{22}|^2 \\
&\quad + 2|U_{11}||V_{12}||U_{12}||V_{22}|\cos(\Psi) = \frac{n_d}{9} , \\
\Psi &= \arg(U_{11}) + \arg(V_{12}) - \arg(U_{12}) - \arg(V_{22}) .
\end{aligned} \tag{6.7.-11}$$

Using the values of the moduli of U_{ij} and the approximation $|V_{22}| = 1$ this gives for $\cos(\Psi)$

$$\begin{aligned}
\cos(\Psi) &= \frac{A}{B} , \\
A &= \frac{n_d - n_u}{9} - \frac{9 - n_u}{9}|V_{12}|^2 , \\
B &= \frac{2}{9|V_{12}|} \sqrt{n_u(9 - n_u)} .
\end{aligned} \tag{6.7.-12}$$

The experimentation with different values of n_d and n_u shows that $n_u = 6, n_d = 4$ gives $\cos(\Psi) = -1.123$. Of course, $n_u = 6, n_d = 4$ option is not even allowed by $n_t = 60$. For $n_d = 4, n_u = 5$ one has $\cos(\Psi) = -0.5958$. $n_d = 5, n_u = 6$ corresponding to the perturbed solution gives $\cos(\Psi) = -0.6014$.

Hence the initial situation could be $(n_u = 5, n_s = 4, n_b = 60)$, $(n_d = 4, n_s = 5, n_t = 60)$ and the physical U and D matrices result from U and D matrices by a small perturbation as one unit of t (b) mass squared is transferred to u (s) quark and produces symmetry breaking as $(n_d = 5, n_s = t, n_b = 59)$, $(n_u = 6, n_c = 4, n_t = 59)$.

The unperturbed matrices $|U|$ and $|D|$ would be identical with $|U|$ given by

$$|U_{11}| = |U_{22}| = \frac{2}{3} , \quad |U_{12}| = |U_{21}| = \frac{\sqrt{5}}{3} , \tag{6.7.-11}$$

The thermodynamical model allows solutions reducing to a direct sum of 2×2 and 1×1 matrices, and since $|U|$ matrix is fixed completely by the mass constraints, it is trivially consistent with the thermodynamical model.

Direct search of U and D matrices

The general formulas for p^U and p^D in terms of the probabilities p_{11} and p_{21} allow straightforward search for the probability matrices having maximum entropy just by scanning the (p_{11}, p_{21}) plane constrained by the conditions that all probabilities are positive and smaller than 1. In the physically interesting case the solution is sought near a solution for which the non-vanishing probabilities are $p_{11} = p_{22} = (9 - n_1)/9$, $p_{12} = p_{21} = n_1/9$, $p_{33} = 1$, $n_1 = 4$ or 5 . The inequalities allow to consider only the values $p_{11} \geq (9 - n_1)/9$.

1. Probability matrices p^U and p^D

The direct search leads to maximally entropic p^D matrix with $(n_d, n_s) = (5, 5)$:

$$p^D = \begin{pmatrix} 0.4982 & 0.4923 & 0.0095 \\ 0.4981 & 0.4924 & 0.0095 \\ 0.0037 & 0.0153 & 0.9810 \end{pmatrix} , \quad p_0^D = \begin{pmatrix} 0.5556 & 0.4444 & 0 \\ 0.4444 & 0.5556 & 0 \\ 0 & 0 & 1 \end{pmatrix} . \tag{6.7.-11}$$

p_0^D represents the unperturbed matrix p_0^D with $n(d=4), n_s = 5$ and is included for the purpose of comparison. The entropy $S(p^D) = 1.5603$ is larger than the entropy $S(p_0^D) = 1.3739$. A possible interpretation is in terms of the spontaneous symmetry breaking induced by entropy maximization in presence of constraints.

A maximally entropic p^U matrix with $(n_u, n_c) = (5, 6)$ is given by

$$p^U = \begin{pmatrix} 0.5137 & 0.4741 & 0.0122 \\ 0.4775 & 0.4970 & 0.0254 \\ 0.0088 & 0.0289 & 0.9623 \end{pmatrix}$$

(6.7.-11)

The value of entropy is $S(p^U) = 1.7246$. There could be also other maxima of entropy but in the range covering almost completely the allowed range of the parameters and in the accuracy used only single maximum appears.

The probabilities p_{ii}^D resp. p_{ii}^U satisfy the constraint $p(i, i) \geq .492$ resp. $p_{ii} \geq .497$ so that the earlier proposal for the solution of proton spin crisis must be given up and the solution discussed in [28] remains the proposal in TGD framework.

2. Near orthogonality of U and D matrices

An interesting question whether U and D matrices can be transformed to approximately orthogonal matrices by a suitable $(U(1) \times U(1))_L \times (U(1) \times U(1))_R$ transformation and whether CP breaking phase appearing in CKM matrix could reflect the small breaking of orthogonality. If this expectation is correct, it should be possible to construct from $|U|$ ($|D|$) an approximately orthogonal matrix by multiplying the matrix elements $|U_{ij}|$, $i, j \in \{2, 3\}$ by appropriate sign factors. A convenient manner to achieve this is to multiply $|U|$ ($|D|$) in an element wise manner $((A \circ B)_{ij} = A_{ij}B_{ij})$ by a sign factor matrix S .

1. In the case of $|U|$ the matrix $U = S \circ |U|$, $S(2, 2) = S(2, 3) = S(3, 2) = -1$, $S_{ij} = 1$ otherwise, is approximately orthogonal as the fact that the matrix $U^T U$ given by

$$U^T U = \begin{pmatrix} 1.0000 & 0.0006 & -0.0075 \\ 0.0006 & 1.0000 & -0.0038 \\ -0.0075 & -0.0038 & 1.0000 \end{pmatrix}$$

is near unit matrix, demonstrates.

2. For D matrix there are two nearly orthogonal variants. For $D = S \circ |D|$, $S(2, 2) = S(2, 3) = S(3, 2) = -1$, $S_{ij} = 1$ otherwise, one has

$$D^T D = \begin{pmatrix} 1.0000 & -0.0075 & 0.0604 \\ -0.0075 & 1.0000 & 0.0143 \\ 0.0604 & 0.0143 & 1.0000 \end{pmatrix} .$$

The choice $D = S \circ D$, $S(2, 2) = S(2, 3) = S(3, 3) = -1$, $S_{ij} = 1$ otherwise, is slightly better

$$D^T D = \begin{pmatrix} 1.0000 & -0.0075 & 0.0604 \\ -0.0075 & 1.0000 & 0.0143 \\ 0.0601 & 0.0143 & 1.0000 \end{pmatrix} .$$

3. The matrices U and D in the standard gauge

Entropy maximization indeed yields probability matrices associated with unitary matrices. 8 phase factors are possible for the matrix elements but only 4 are relevant as far as the unitarity conditions are considered. The vanishing of the inner products between row vectors, gives 6 conditions altogether so that the system seems to be over-determined. The values of the parameters s_1, s_2, s_3 and phase angle δ in the "standard gauge" can be solved in terms of r_{11} and r_{21} .

The requirement that the norms of the parameters c_i are not larger than unity poses non-trivial constraints on the probability matrices. This should be the case since the number of unitarity conditions is 9 whereas probability conservation for columns and rows gives only 5 conditions so that not every probability matrix can define unitary matrix. It would seem that that the constraints are satisfied only if the the 2 mass squared conditions and 2 conditions from the entropy maximization are equivalent with 4 unitarity conditions so that the number of conditions becomes $5+4=9$. Therefore

entropy maximization and mass squared conditions would force the points of complex 9-dimensional space defined by 3×3 matrices to a 9-dimensional surface representing group $U(3)$ so that these conditions would have a group theoretic meaning.

The formulas

$$\begin{aligned} r_{i2} &= \sqrt{\left[-\frac{n_i}{51} + \frac{20}{17}(1 - r_{i1}^2)\right]}, \\ r_{i3} &= \sqrt{\left[\frac{n_i}{51} - \frac{3}{17}(1 - r_{i1}^2)\right]}. \end{aligned} \quad (6.7-11)$$

and

$$U = \begin{bmatrix} c_1 & s_1 c_3 & s_1 s_3 \\ -s_1 c_2 & c_1 c_2 c_3 - s_2 s_3 \exp(i\delta) & c_1 c_2 s_3 + s_2 c_3 \exp(i\delta) \\ -s_1 s_2 & c_1 s_2 c_3 + c_2 s_3 \exp(i\delta) & c_1 s_2 s_3 - c_2 c_3 \exp(i\delta) \end{bmatrix} \quad (6.7-10)$$

give

$$\begin{aligned} c_1 &= r_{11}, & c_2 &= \frac{r_{21}}{\sqrt{1 - r_{11}^2}}, \\ s_3 &= \frac{r_{13}}{\sqrt{1 - r_{11}^2}}, & \cos(\delta) &= \frac{c_1^2 c_2^2 c_3^2 + s_2^2 s_3^2 - r_{22}^2}{2c_1 c_2 c_3 s_2 s_3}. \end{aligned} \quad (6.7-9)$$

Preliminary calculations show that for $n_1 = n_2 = 5$ case the matrix of moduli allows a continuation to a unitary matrix but that for $n_1 = 4, n_2 = 6$ the value of $\cos(\delta)$ is larger than one. This would suggest that unitarity indeed gives additional constraints on the integers n_i . The unitary (in the numerical accuracy used) $(n_d, n_s) = (5, 5)$ D matrix is given by

$$D = \begin{pmatrix} 0.7059 & 0.7016 & 0.0975 \\ -0.7057 & 0.7017 - 0.0106i & 0.0599 + 0.0766i \\ -0.0608 & 0.0005 + 0.1235i & 0.4366 - 0.8890i \end{pmatrix}.$$

The unitarity of this matrix supports the view that for certain integers n_i the mass squared conditions and entropy maximization reduce to group theoretic conditions. The numerical experimentation shows that the necessary condition for the unitarity is $n_1 > 4$ for $n_2 < 9$ whereas for $n_2 \geq 9$ the unitarity is achieved also for $n_1 = 4$.

Direct search for CKM matrices

The standard gauge in which the first row and first column of unitary matrix are real provides a convenient representation for the topological mixing matrices: it is convenient to refer to these representations as U_0 and D_0 . The possibility to multiply the rows of U_0 and D_0 by phase factors ($U(1) \times U(1)$) $_R$ transformations) provides 2 independent phases affecting the values of $|V|$. The phases $\exp(i\phi_j)$, $j = 2, 3$ multiplying the second and third row of D_0 can be estimated from the matrix elements of $|V|$, say from the elements $|V_{11}| = \cos(\theta_c) \equiv v_{11}$, $\sin\theta_c = .226 \pm .002$ and $|V_{31}| = (9.6 \pm .9) \cdot 10^{-3} \equiv v_{31}$. Hence the model would predict two parameters of the CKM matrix, say s_3 and δ_{CP} , in its standard representation.

The fact that the existing empirical bounds on the matrix elements of V are based on the standard model physics raises the question about how seriously they should be taken. The possible existence of fractally scaled up versions of light quarks could effectively reduce the matrix elements for the electro-weak decays $b \rightarrow c + W$, $b \rightarrow u + W$ resp. $t \rightarrow s + W$, $t \rightarrow d + W$ since the decays involving scaled up versions of light quarks can be counted as decays $W \rightarrow bc$ resp. $W \rightarrow tb$. This would favor too small experimental estimates for the matrix elements V_{i3} and V_{3i} , $i = 1, 2$. In particular, the matrix element $V_{31} = V_{td}$ could be larger than the accepted value.

Various constraints do not leave much freedom to choose the parameters n_{q_i} . The preliminary numerical experimentation shows that the choice $(n_d, n_s) = (5, 5)$ and $(n_u, n_c) = (5, 6)$ yields realistic U and D matrices. In particular, the conditions $|U(1, 1)| > .7$ and $|D(1, 1)| > .7$ hold true and

mean that the original proposal for the solution of spin puzzle of proton must be given up. In [28] an alternative proposal based on more recent findings is discussed. Only for this choice reasonably realistic CKM matrices have been found. For $n_t = 58$ the mass of $t\bar{t}$ meson mass is reduced by one percent from 2×163 GeV for $n(5) = 59$ so that $n_t = 58$ is still acceptable if the additivity of conformal weight rather than mass is accepted for diagonal mesons.

1. The requirement that the parameters $|V_{11}|$ (or equivalently, Cabibbo angle) and $|V_{31}|$ are produced correctly, yields CKM matrices for which CP breaking parameter J is roughly one half of its accepted value. The matrix elements $V_{23} \equiv V_{cb}$, $V_{32} \equiv V_{tc}$, and $V_{13} \equiv V_{ub}$ are roughly twice their accepted value. This suggests that the condition on V_{31} should be loosened.
2. The following tables summarize the results of the search requiring that
 - i) the value of the Cabibbo angle s_{Cab} is within the experimental limits $s_{Cab} = .223 \pm .002$,
 - ii) $V_{31} = (9.6 \pm .9) \cdot 10^{-3}$, is allowed to have value at most twice its upper bound,
 - iii) V_{13} whose upper bound is determined by probability conservation, is within the experimental limits $.42 \cdot 10^{-3} < |V_{ub}| < 6.98 \cdot 10^{-3}$ whereas $V_{23} \simeq 4 \times 10^{-3}$ should come out as a prediction,
 - iv) the CP breaking parameter satisfies the condition $|(J - J_0)/J_0| < .6$, where $J_0 = 10^{-4}$ represents the lower bound for J (the experimental bounds for J are $J \times 10^4 \in (1 - 1.7)$).

The pairs of the phase angles (ϕ_1, ϕ_2) defining the phases ($exp(i\phi_1), exp(i\phi_2)$) are listed below

$$\begin{array}{l}
 \text{class 1 : } \begin{array}{cccccc} \phi_1 & 0.1005 & 0.1005 & 4.8129 & 4.8129 & \\ \phi_2 & 0.0754 & 1.4828 & 4.7878 & 6.1952 & \end{array} \\
 \text{class 2 : } \begin{array}{cccccc} \phi_1 & 0.1005 & 0.1005 & 4.8129 & 4.8129 & \\ \phi_2 & 2.3122 & 5.5292 & 0.7414 & 3.9584 & \end{array}
 \end{array} \tag{6.7-9}$$

The phase angle pairs correspond to two different classes of U , D , and V matrices. The U , D and V matrices inside each class are identical at least up to 11 digits(!). Very probably the phase angle pairs are related by some kind of symmetry.

The values of the fitted parameters for the two classes are given by

$$\begin{array}{l}
 \begin{array}{cccccc} & |V_{11}| & |V_{31}| & |V_{13}| & J/10^{-4} & \\ \text{class 1} & 0.9740 & 0.0157 & 0.0069 & .93953 & \\ \text{class 2} & 0.9740 & 0.0164 & 0.0067 & 1.0267 & \end{array}
 \end{array}$$

V_{31} is predicted to be about 1.6 times larger than the experimental upper bound and for both classes V_{23} and V_{32} are roughly too times too large. Otherwise the fit is consistent with the experimental limits for class 2. For class 1 the CP breaking parameter is 7 per cent below the experimental lower bound. In fact, the value of J is fixed already by the constraints on V_{31} and V_{11} and reduces by a factor of one half if V_{31} is required to be within its experimental limits.

U , D and $|V|$ matrices for class 1 are given by

$$\begin{array}{l}
 U = \begin{bmatrix} 0.7167 & 0.6885 & 0.1105 \\ -0.6910 & 0.7047 - 0.0210i & 0.0909 + 0.1310i \\ -0.0938 & 0.0696 + 0.1550i & 0.1747 - 0.9653i \end{bmatrix} \\
 D = \begin{bmatrix} 0.7059 & 0.7016 & 0.0975 \\ -0.6347 - 0.3085i & 0.6358 + 0.2972i & 0.0203 + 0.0951i \\ -0.0587 - 0.0159i & -0.0317 + 0.1194i & 0.6534 - 0.7444i \end{bmatrix} \\
 |V| = \begin{bmatrix} 0.9740 & 0.2265 & 0.0069 \\ 0.2261 & 0.9703 & 0.0862 \\ 0.0157 & 0.0850 & 0.9963 \end{bmatrix}
 \end{array} \tag{6.7-11}$$

U , D and $|V|$ matrices for class 2 are given by

$$\begin{aligned}
 U &= \begin{bmatrix} 0.7167 & 0.6885 & 0.1105 \\ -0.6910 & 0.7047 - 0.0210i & 0.0909 + 0.1310i \\ -0.0938 & 0.0696 + 0.1550i & 0.1747 - 0.9653i \end{bmatrix} \\
 D &= \begin{bmatrix} 0.7059 & 0.7016 & 0.0975 \\ -0.6347 - 0.3085i & 0.6358 + 0.2972i & 0.0203 + 0.0951i \\ -0.0589 - 0.0151i & -0.0302 + 0.1198i & 0.6440 - 0.7525i \end{bmatrix} \\
 |V| &= \begin{bmatrix} 0.9740 & 0.2265 & 0.0067 \\ 0.2260 & 0.9704 & 0.0851 \\ 0.0164 & 0.0838 & 0.9963 \end{bmatrix}
 \end{aligned}
 \tag{6.7.-13}$$

What raises worries is that the values of $|V_{23}| = |V_{cb}|$ and $|V_{32}| = |V_{ts}|$ are roughly twice their experimental estimates. This, as well as the discrepancy related to V_{31} , might be understood in terms of the electro-weak decays of b and t to scaled up quarks causing a reduction of the branching ratios $b \rightarrow c + W$, $t \rightarrow s + W$ and $t \rightarrow t + d$. The attempts to find more successful integer combinations n_i has failed hitherto. The model for pseudoscalar meson masses, the predicted relatively small masses of light quarks, and the explanation for $t\bar{t}$ meson mass supports this mixing scenario.

Bibliography

Books about TGD

- [1] M. Pitkänen (2006), *Topological Geometroynamics: Overview*.
http://tgd.wippiespace.com/public_html/tgdview/tgdview.html.
- [2] M. Pitkänen (2006), *Quantum Physics as Infinite-Dimensional Geometry*.
http://tgd.wippiespace.com/public_html/tgdgeom/tgdgeom.html.
- [3] M. Pitkänen (2006), *Physics in Many-Sheeted Space-Time*.
http://tgd.wippiespace.com/public_html/tgdclass/tgdclass.html.
- [4] M. Pitkänen (2006), *p-Adic length Scale Hypothesis and Dark Matter Hierarchy*.
http://tgd.wippiespace.com/public_html/paddark/paddark.html.
- [5] M. Pitkänen (2006), *Quantum TGD*.
http://tgd.wippiespace.com/public_html/tgdquant/tgdquant.html.
- [6] M. Pitkänen (2006), *TGD as a Generalized Number Theory*.
http://tgd.wippiespace.com/public_html/tgdnumber/tgdnumber.html.
- [7] M. Pitkänen (2006), *TGD and Fringe Physics*.
http://tgd.wippiespace.com/public_html/freenergy/freenergy.html.

Books about TGD Inspired Theory of Consciousness and Quantum Biology

- [8] M. Pitkänen (2006), *TGD Inspired Theory of Consciousness*.
http://tgd.wippiespace.com/public_html/tgdconsc/tgdconsc.html.
- [9] M. Pitkänen (2006), *Bio-Systems as Self-Organizing Quantum Systems*.
http://tgd.wippiespace.com/public_html/bioselforg/bioselforg.html.
- [10] M. Pitkänen (2006), *Quantum Hardware of Living Matter*.
http://tgd.wippiespace.com/public_html/bioware/bioware.html.
- [11] M. Pitkänen (2006), *Bio-Systems as Conscious Holograms*.
http://tgd.wippiespace.com/public_html/hologram/hologram.html.
- [12] M. Pitkänen (2006), *Genes and Memes*.
http://tgd.wippiespace.com/public_html/genememe/genememe.html.
- [13] M. Pitkänen (2006), *Magnetospheric Consciousness*.
http://tgd.wippiespace.com/public_html/magnconsc/magnconsc.html.
- [14] M. Pitkänen (2006), *Mathematical Aspects of Consciousness Theory*.
http://tgd.wippiespace.com/public_html/mathconsc/mathconsc.html.
- [15] M. Pitkänen (2006), *TGD and EEG*.
http://tgd.wippiespace.com/public_html/tgdeeg/tgdeeg.html.

References to the chapters of the books about TGD

- [16] The chapter *Dark Forces and Living Matter* of [4].
http://tgd.wippiespace.com/public_html/paddark/paddark.html#darkforces.
- [17] The chapter *Construction of Configuration Space Kähler Geometry from Symmetry Principles* of [2].
http://tgd.wippiespace.com/public_html/tgdgeom/tgdgeom.html#compl1.
- [18] The chapter *Does the Modified Dirac Equation Define the Fundamental Action Principle?* of [2].
http://tgd.wippiespace.com/public_html/tgdgeom/tgdgeom.html#Dirac.
- [19] The chapter *Yangian Symmetry, Twistors, and TGD* of [5].
http://tgd.wippiespace.com/public_html/tgdquant/tgdquant.html#Yangian.
- [20] The chapter *Quantum Field Theory Limit of TGD from Bosonic Emergence* of [5].
http://tgd.wippiespace.com/public_html/tgdquant/tgdquant.html#emergence.
- [21] The chapter *Nuclear String Model* of [4].
http://tgd.wippiespace.com/public_html/paddark/paddark.html#nuclstring.
- [22] The chapter *Elementary Particle Vacuum Functionals* of [4].
http://tgd.wippiespace.com/public_html/paddark/paddark.html#elvafu.
- [23] The chapter *General Ideas about Many-Sheeted Space-Time: Part I* of [3].
http://tgd.wippiespace.com/public_html/tgdclass/tgdclass.html#topcond.
- [24] The chapter *p-Adic Physics: Physical Ideas* of [6].
http://tgd.wippiespace.com/public_html/tgdnumber/tgdnumber.html#phblocks.
- [25] The chapter *Is it Possible to Understand Coupling Constant Evolution at Space-Time Level?* of [5].
http://tgd.wippiespace.com/public_html/tgdquant/tgdquant.html#rgflow.
- [26] The chapter *Cosmic Strings* of [3].
http://tgd.wippiespace.com/public_html/tgdclass/tgdclass.html#cstrings.
- [27] The chapter *p-Adic Particle Massivation: Hadron Masses* of [4].
http://tgd.wippiespace.com/public_html/paddark/paddark.html#mass3.
- [28] The chapter *p-Adic Particle Massivation: Elementary particle Masses* of [4].
http://tgd.wippiespace.com/public_html/paddark/paddark.html#mass2.
- [29] The chapter *TGD as a Generalized Number Theory: Quaternions, Octonions, and their Hyper Counterparts* of [6].
http://tgd.wippiespace.com/public_html/tgdnumber/tgdnumber.html#visionb.
- [30] The chapter *TGD and Cosmology* of [3].
http://tgd.wippiespace.com/public_html/tgdclass/tgdclass.html#cosmo.
- [31] The chapter *The Recent Status of Leptohadron Hypothesis* of [4].
http://tgd.wippiespace.com/public_html/paddark/paddark.html#leptc.
- [32] The chapter *The Notion of Free Energy and Many-Sheeted Space-Time Concept* of [7].
http://tgd.wippiespace.com/public_html/freenergy/freenergy.html#freenergy.
- [33] The chapter *Configuration Space Spinor Structure* of [2].
http://tgd.wippiespace.com/public_html/tgdgeom/tgdgeom.html#cspin.
- [34] The chapter *The Relationship Between TGD and GRT* of [3].
http://tgd.wippiespace.com/public_html/tgdclass/tgdclass.html#tgdgrt.
- [35] The chapter *Does TGD Predict the Spectrum of Planck Constants?* of [5].
http://tgd.wippiespace.com/public_html/tgdquant/tgdquant.html#Planck.

- [36] The chapter *Massless States and Particle Massivation* of [4].
http://tgd.wippiespace.com/public_html/paddark/paddark.html#mless.
- [37] The chapter *Construction of Quantum Theory: Symmetries* of [5].
http://tgd.wippiespace.com/public_html/tgdquant/tgdquant.html#quthe.
- [38] The chapter *TGD and Astrophysics* of [3].
http://tgd.wippiespace.com/public_html/tgdclass/tgdclass.html#astro.

References to the chapters of the books about TGD Inspired Theory of Consciousness and Quantum Biology

- [39] The chapter *Dark Matter Hierarchy and Hierarchy of EEGs* of [15].
http://tgd.wippiespace.com/public_html/tgdeeg/tgdeeg.html#eegdark.
- [40] The chapter *Quantum Antenna Hypothesis* of [10].
http://tgd.wippiespace.com/public_html/bioware/bioware.html#tubuc.
- [41] The chapter *Negentropy Maximization Principle* of [8].
http://tgd.wippiespace.com/public_html/tgdconsc/tgdconsc.html#nmpc.

Articles related to TGD

- [42] M. Pitkänen (2010), *Construction of Configuration Space Spinor Structure*. http://tgd.wippiespace.com/public_html/articles/spinstructure.pdf.

Mathematics

- [43] P. A. M. Dirac (1939), *A New Notation for Quantum Mechanics*. Proceedings of the Cambridge Philosophical Society, 35: 416-418.
 J. E. Roberts (1966), *The Dirac Bra and Ket Formalism*. Journal of Mathematical Physics, 7: 1097-1104.
 Halvorson, Hans and Clifton, Rob (2001).
- [44] Hawking, S.,W. and Pope, C., N. (1978): *Generalized Spin Structures in Quantum Gravity*. Physics Letters Vol 73 B, no 1.
- [45] T. Eguchi, B. Gilkey, J. Hanson (1980). Phys. Rep. 66, 6, 1980.
- [46] Pope, C., N. (1980): *Eigenfunctions and Spin^c Structures on CP₂* D.A.M.T.P. preprint.
- [47] G. W. Gibbons, C. N. Pope (1977): *CP₂ as gravitational instanton*. Commun. Math. Phys. 55, 53.

Theoretical physics

- [48] R.P. Feynman (1972), *Photon-Hadron Interactions*, W.A. Benjamin Inc.
- [49] *CPT symmetry*. http://en.wikipedia.org/wiki/CPT_symmetry.
- [50] N. Li, Yi-Fu Cai, X. Wang, X. Zhang (2009), *CPT Violating Electrodynamics and Chern-Simons Modified Gravity*. <http://arxiv.org/abs/0907.5159>.
- [51] W. Broniowski (2002), *Two Hagedorn temperatures*, hep-ph/0006020.
- [52] *Airy functions*. http://en.wikipedia.org/wiki/Airy_function.
- [53] T. Ericson and J. Rafelski (2002), *The tale of the Hagedorn temperature*, Cern Courier, vol 43, No 7. <http://www.cerncourier.com/main/toc/43/7>.

Particle and nuclear physics

- [54] *Lamb shift*. http://en.wikipedia.org/wiki/Lamb_shift.
- [55] J. Flowers (2010), *Quantum electrodynamics: A chink in the armour?*. Nature 466. 195-196. <http://www.nature.com/nature/journal/v466/n7303/pdf/466195a.pdf>.
- [56] R. Baltrusaitis *et al* (1984), Astrophys. J. 281, L9, R. Baltrusaitis *et al* (1985), Phys. Rev. Lett. 54, 1875.
- [57] C. M. G. Lattes. Y. Fujimoto and S. Hasegava (1980), Phys. Rep., Vol. 65, No 3.
- [58] L3 collaboration (1992), *High mass photon pairs in $l^+l^- \gamma\gamma$ events at LEP*, Phys. Lett. B., vol 295, No 3, 4.
- [59] *Minos for Scientists*. <http://www-numi.fnal.gov/PublicInfo/forscientists.html>.
Neutrinos and Antineutrinos Differ in Key Property, Experiment Suggests. <http://www.sciencedaily.com/releases/2010/06/100614121606.htm>.
- [60] M. J. Alguard *et al* (1978), Phys. Rev. Lett. 41, 70; G. Baum *et al* (1983), Phys. Rev.Lett. 51, 1135.
- [61] Brazil-Japan Collaboration on Chacaltaya Emulsion Chamber Experiments (J. A. Chinellato *et al*): in Proton-Antiproton Collider Physics, 1981, Madison, Wis. (New York, N.Y. 1982)
- [62] J. Ashman *et al* (1988), Phys. Lett. B 206, 364; J. Ashman *et al* (1989), Nucl. Phys. B 328, 1.
- [63] M. Derrick *et al*(1993), Phys. Lett B 315, p. 481.
- [64] H. Nastase (2005), *The RHIC fireball as a dual black hole*, hep-th/0501068.
- [65] <http://fnphyx-www.fnal.gov/experiments/ktev/epsprime/epsprime.html>.
- [66] P. Sokolsky, P. Sommers and B. R. Dawson (1992), *Extremely High Energy Cosmic Rays*, Phys. Rep. Vol. 217, No 5.
- [67] J. Wdowczyk (1965), Proc. 9th Int. Conf. Cosmic Rays, Vol 2 , p. 691.
- [68] X. Chi, C. Dahanayake, J. Wdowczyk and A. W. Wolfendale (1993), *Cosmic rays and cosmic strings and Gamma rays from collapsing cosmic strings*, Astroparticle Physics 1, 129-131 and 239-243.
- [69] J. H. MacGibbon and R. H. Brandenberger (1993), *Gamma-ray signatures for ordinary cosmic strings*, Phys. Rev. D, Vol 47, No 6, p. 2883.
- [70] Seongwan Park (1995), *Search for New Phenomena in CDF-I: Z' , W' , and leptoquarks*. Proceedings for the 10th Topical Workshop on Proton-Antiproton Collider Physics. Fermilab, Batavia, Illinois, 1995. Fermilab-Conf-95/155-E.<http://lss.fnal.gov/archive/1995/conf/Conf-95-155-E.pdf>.
- [71] E. S. Reich (2005), *Black hole like phenomenon created by collider*, New Scientist 19, issue 2491.
- [72] N. M. Queen, G. Violini (1974), *Dispersion Theory in High Energy Physics*, The Macmillan Press Limited.
- [73] A. J. Buras and R. Fleischer (1997), *Quark mixing, CP violation and Rare Decays After the Top Quark Discovery*. hep-ph/9704376.
- [74] G. Karagiorgi (2010), *Towards Solution of MiniBoone-LSND anomalies*. <http://indico.cern.ch/contributionDisplay.py?contribId=209&sessionId=3&confId=73981>.
- [75] D0 collaboration (2009), *Search for high-mass narrow resonances in the di-electron channel at D0*. <http://www-d0.fnal.gov/Run2Physics/WWW/results/prelim/NP/N66/>.

- [76] J. Linsley and A. A. Watson (1981), Phys. Rev. Lett. 436, 459.
- [77] B. B. Back *et al*(2002), Phys. Rev. Lett. Vol. 89, No 22, 25 November. See also <http://www.scienceblog.com/community/modules.php?name=News&file=article&sid=357>.
- [78] P. Ammiraju, E. Recami, W. A. Rodriguez Jr. (1983), *Chirons, Geminions, Centauros, Decays into Pions:a Phenomenological and Theoretical Analysis*, Il Nuovo Cimento, vol. 78 A, No 2, p. 173.
- [79] J. M. Bonnet-Bidaud and G. Chardin (1988), *Cygnus X-3. a critical review*, Phys. Rep. Vol 170, No 6.
- [80] M. T. Ressel and M. S. Turner (1990), Comments Astrophys. 14, 323.
- [81] J. D. Bjorken (1997), Acta Phys. Polonica B. V. 28. p. 2773.
- [82] *Neutrino oscillation*. http://en.wikipedia.org/wiki/Neutrino_oscillation.
- [83] C. T. Hill and D. N. Schramm(1984), Phys. Rev. D 31, p. 564.
- [84] R. Pohl *et al* (2010), *The size of proton*. Nature 466. 213-216. <http://www.nature.com/nature/journal/v466/n7303/full/nature09250.html>.
- [85] *NASA announces dark matter discovery*, http://www.nasa.gov/home/hqnews/2006/aug/HQ_M06128_dark_matter.html.
- [86] C. M. G. Lattes. Y. Fujimoto and S. Hasegava (1980), Phys. Rep., Vol. 65, No 3.
- [87] D. Gladysz-Dziadus (), *Are Centauros Exotic Signals of Quark-Gluon Plasma*. <http://www1.jinr.ru/Archive/Pepan/v-34-3/v-34-3-3.pdf>.
- [88] D. B. Kaplan, A. E. Nelson and N. Weiner (2004), *Neutrino Oscillations as a Probe of Dark Energy*, hep-ph/0401099.
- [89] S. Ambrosanio *et al* (1996), *Supersymmetric analysis and predictions based on the CDF $ee\gamma\gamma + E_T$ event*. arXiv:hep-ph/9602239v2.<http://arxiv.org/abs/hep-ph/9602239>.
- [90] A. S. Antognini (2005), *The Lamb shift Experiment in Muonic Hydrogen* . http://edoc.ub.uni-muenchen.de/5044/1/Antognini_Aldo.pdf.
- [91] K. McAlpine (2010), *Incredible shrinking proton raises eyebrows*.<http://www.newscientist.com/article/dn19141-incredible-shrinking-proton-raises-eyebrows.html>.
- [92] A. M. Smith *et al*(1985), Phys. Lett. B 163, p. 267.
- [93] G. Buchalla, A.J. Buras and M. Lautenbacher (1996), Rev. Mod. Phys. 68, p. 1125.
- [94] B. B. Back *et al*(2002), Nucl. Phys. A698, 416 (2002).
- [95] Pamir Collaboration (1979), Proc. 16:th Intern. Cosmic Ray Conf. Vol. 7, p. 279.
- [96] S. Bertolini, Marco Fabbrichesi and Jan. O. Eeg (1998). *Estimating ϵ'/ϵ . A review*. hep-ph/9802405.
- [97] Tommaso Dorigo (2009), *A New Z' Boson at 240 GeV? No, Wait, at 720!?*. http://www.scientificblogging.com/quantum_diaries_survivor/new_z_boson_240_gev_no_wait_720.
- [98] Bo-Ciang Ma (2000), *The spin structure of the proton*, RIKEN Review No. 28.
- [99] X. Zheng *et al* (2004), The Jefferson Lab Hall A Collaboration, *Precision Measurement of the Neutron Spin Asymmetries and Spin-Dependent Structure Functions in the Valence Quark Region*, arXiv:nucl-ex/0405006 .
- [100] Y. Keum, U. Nierste and A. I. Sanda (1999), *A short look at ϵ'/ϵ* . hep-ph/9903230.

- [101] Tommaso Dorigo (2009), *CDF Kisses Another New Physics Effect Bye-Bye*. http://www.scientificblogging.com/quantum_diaries_survivor/cdf_kisses_another_new_physics_effect_byebye.
- [102] J. Gasser and H. Luytweyler (1985), *Chiral perturbation theory: expansions the the mass of the strange quark*, Nucl. Phys. B 250, p. 465.
- [103] R. Van de Water (2010), *Updated Anti-neutrino Oscillation Results from Mini-BooNE*. <http://indico.cern.ch/getFile.py/access?contribId=208&sessionId=3&resId=0&materialId=slides&confId=73981>.
- [104] CDF collaboration (2008), *High-mass Di-electron Resonance Research in $p\bar{p}$ Collisions at $s = 1.96$ TeV*. http://www-cdf.fnal.gov/physics/exotic/r2a/20080306.dielelectron_duke/pub25/cdfnote9160_pub.pdf.
- [105] H. Waschmuth (CERN, for the Aleph collaboration) (1996), *Results from e^+e^- collisions at 130, 136 and 140 GeV center of mass energies in the ALEPH Experiment*. http://alephwww.cern.ch/ALPUB/pub/pub_96.html.
- [106] E. A. Paschos and U. Turke (1989), Phys. Rep., Vol. 178, No 4.
- [107] A. Brandt *et al* (1992), Phys. Lett. B 297, p. 417.
- [108] T. K. Gaiser *et al* (1993), *Cosmic ray composition around 10^{18} eV*, Phys. Rev. D, vol 47, no 5.
- [109] D. T. H. Davies *et al* (2010), *Precise Charm to Strange Mass Ratio and Light Quark Masses from Full Lattice QCD*. Phys. Rev. Lett. 104, 132003. <http://prl.aps.org/abstract/PRL/v104/i13/e132003>.
A. Cho (2010), *Mass of the common quark finally nailed down*. <http://news.sciencemag.org/sciencenow/2010/04/mass-of-the-common-quark-finally.html>.
- [110] K. Greisen (1966), Phys. Rev. Lett. 16, 748.
- [111] T. Ludham and L. McLerran (2003), *What Have We Learned From the Relativistic Heavy Ion Collider?*, Physics Today, October issue. <http://www.physicstoday.org/vol-56/iss-10/p48.html>.
- [112] E. Samuel (2002), *Ghost in the Atom*, New Scientist, vol 176 issue 2366 - 26 October 2002, page 30.
- [113] G. R. Farrar (1995), *New Signatures of Squarks*, hep-ph/9512306.
- [114] Lubos Motl (2010), *MINOS: hints of CPT-violation in the neutrino sector*. <http://motls.blogspot.com/2010/06/minos-hints-of-cpt-violation-in.html>.
- [115] CMS Collaboration (2010), *Observation of Long-Range, Near-Side Angular Correlations in Proton-Proton Collisions at the LHC*. <http://cms.web.cern.ch/cms/News/2010/QCD-10-002/QCD-10-002.pdf>.
- [116] *CMS observes a potentially new and interesting effect*. <http://user.web.cern.ch/user/news/2010/100921.html>.
- [117] L. Motl (2010), *LHC probably sees new shocking physics*. <http://motls.blogspot.com/2010/09/lhc-probably-sees-new-shocking-physics.html>.
- [118] Tommaso Dorigo (2010), *Altarelli: "Approximately Impossible" That LHC Fails*. http://www.science20.com/quantum_diaries_survivor/altarelli_approximately_impossible_lhc_fails.
- [119] G. Altarelli (2010), *LHC Physics in the SM and Beyond*. <http://indico.cern.ch/conferenceOtherViews.py?view=standard&confId=89312>.
- [120] L. Motl (2010), *CMS SUSY group working hard*. <http://motls.blogspot.com/2010/10/cms-susy-group-working-hard.html>.

Condensed matter physics

- [121] R. Mills *et al*(2003), *Spectroscopic and NMR identification of novel hybrid ions in fractional quantum energy states formed by an exothermic reaction of atomic hydrogen with certain catalysts*. <http://www.blacklightpower.com/techpapers.html> .
- [122] *First images of heavy electrons in action*. Energy Daily. http://www.energy-daily.com/reports/First_Images_Of_Heavy_Electrons_In_Action_999.html.

Cosmology and astrophysics

- [123] D. Da Roacha and L. Nottale (2003), *Gravitational Structure Formation in Scale Relativity*. astro-ph/0310036.
- [124] The Pierre Auger Collaboration (2007), *Correlation of Highest Energy Cosmic Rays with Nearby Galactic Objects*. Science, 9 November, 938-943.
A. Cho (2007), *Universe's Highest-Energy Particles Traced Back to Other Galaxies*. Science, 9 November, 896-897.
See also http://www.auger.org/news/PRagn/AGN_correlation.html.

Consciousness related references

- [125] N. Cherry (2000), Conference report on effects of ELF fields on brain, <http://www.tassie.net.au/emfacts/icnirp.txt>.

6.8 Figures and Illustrations

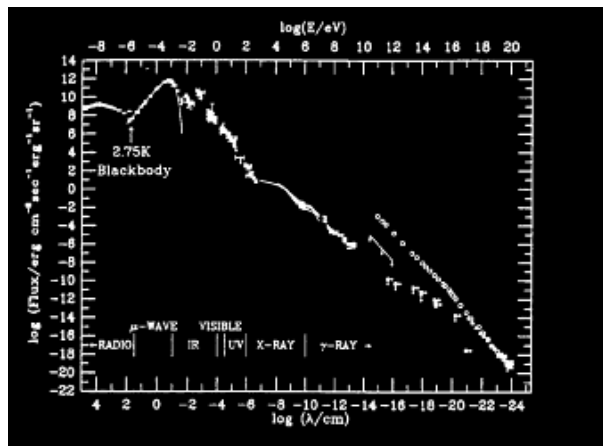


Figure 6.1: There are some indications that cosmic gamma ray flux contains a peak in the energy interval $10^{10} - 10^{11}$ eV. Figure is taken from [80].

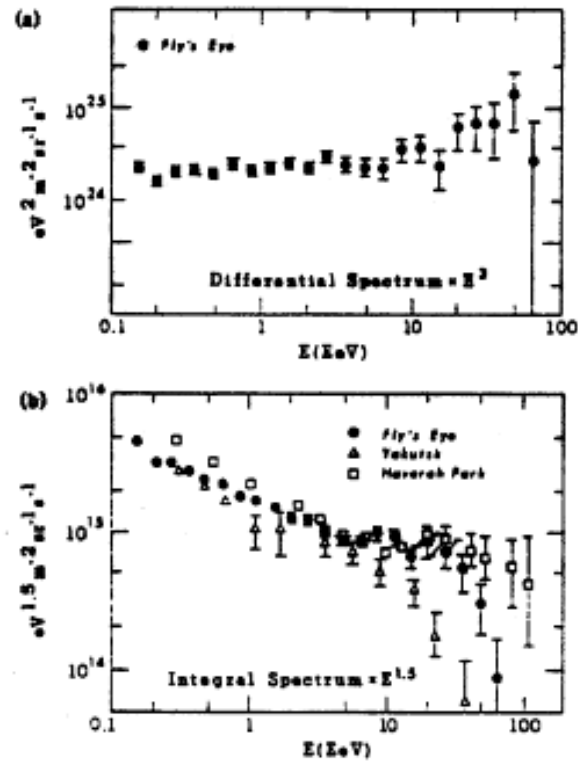


FIG. 2. (a) Differential spectrum $j(E)$ plotted as $E^2 j(E)$. A power-law best fit of the form $j(E) = aE^{-\gamma}$ yields $a = 109.6 \pm 2.2 \text{ EeV}^{-1} \text{ km}^{-2} \text{ sr}^{-1} \text{ yr}^{-1}$ and $\gamma = 2.94 \pm 0.02$ for events at $E < 10 \text{ EeV}$. Between 10 and 50 EeV we obtain $a = 34 \pm 17 \text{ EeV}^{-1} \text{ km}^{-2} \text{ sr}^{-1} \text{ yr}^{-1}$ and $\gamma = 2.42 \pm 0.27$. The lack of events above 50 EeV indicates that the flattened slope does not continue. (b) Integral spectrum $I(>E)$ plotted as $E^{1.5} I(>E)$. Data from both Haverah Park and Yakutsk (Refs. 10, 12, and 13) experiments are also shown.

Figure 6.2:

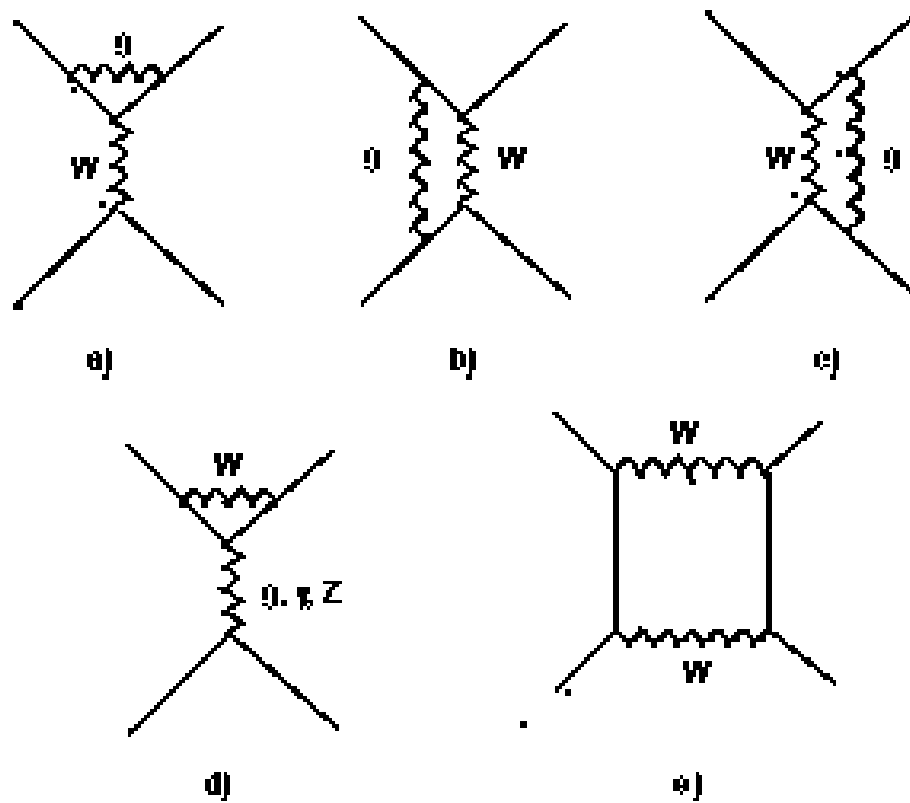


Figure 6.3: Standard model contributions to the matching of the quark operators in the effective flavor-changing Lagrangian

Part II

**P-ADIC LENGTH SCALE
HYPOTHESIS AND DARK
MATTER HIERARCHY**

Chapter 7

Recent Status of Lepto-Hadron Hypothesis

7.1 Introduction

TGD suggest strongly ('predicts' is perhaps too strong expression) the existence of color excited leptons. The mass calculations based on p-adic thermodynamics and p-adic conformal invariance lead to a rather detailed picture about color excited leptons.

1. The simplest color excited neutrinos and charged leptons belong to the color octets ν_8 and L_{10} and $L_{\bar{10}}$ decuplet representations respectively and lepto-hadrons are formed as the color singlet bound states of these and possible other representations. Electro-weak symmetry suggests strongly that the minimal representation content is octet and decuplets for both neutrinos and charged leptons.
2. The basic mass scale for lepto-hadron physics is completely fixed by p-adic length scale hypothesis. The first guess is that color excited leptons have the levels $k = 127, 113, 107, \dots$ ($p \simeq 2^k$, k prime or power of prime) associated with charged leptons as primary condensation levels. p-Adic length scale hypothesis allows however also the level $k = 11^2 = 121$ in case of electronic lepto-hadrons. Thus both $k = 127$ and $k = 121$ must be considered as a candidate for the level associated with the observed lepto-hadrons. If also lepto-hadrons correspond non-perturbatively to exotic Super Virasoro representations, lepto-pion mass relates to pion mass by the scaling factor $L(107)/L(k) = k^{(107-k)/2}$. For $k = 121$ one has $m_{\pi_L} \simeq 1.057$ MeV which compares favorably with the mass $m_{\pi_L} \simeq 1.062$ MeV of the lowest observed state: thus $k = 121$ is the best candidate contrary to the earlier beliefs. The mass spectrum of lepto-hadrons is expected to have same general characteristics as hadronic mass spectrum and a satisfactory description should be based on string tension concept. Regge slope is predicted to be of order $\alpha' \simeq 1.02/MeV^2$ for $k = 121$. The masses of ground state lepto-hadrons are calculable once primary condensation levels for colored leptons and the CKM matrix describing the mixing of color excited lepton families is known.

The strongest counter arguments against color excited leptons are the following ones.

1. The decay widths of Z^0 and W boson allow only $N = 3$ light particles with neutrino quantum numbers. The introduction of new light elementary particles seems to make the decay widths of Z^0 and W intolerably large.
2. Lepto-hadrons should have been seen in e^+e^- scattering at energies above few MeV . In particular, lepto-hadronic counterparts of hadron jets should have been observed.

A possible resolution of these problems is provided by the loss of asymptotic freedom in lepto-hadron physics. Lepto-hadron physics would effectively exist in a rather limited energy range about one MeV.

The development of the ideas about dark matter hierarchy [28, 23, 27, 16] led however to a much more elegant solution of the problem.

1. TGD predicts an infinite hierarchy of various kinds of dark matters which in particular means a hierarchy of color and electro-weak physics with weak mass scales labelled by appropriate p-adic primes different from M_{89} : the simplest option is that also ordinary photons and gluons are labelled by M_{89} .
2. There are number theoretical selection rules telling which particles can interact with each other. The assignment of a collection of primes to elementary particle as characterizer of p-adic primes characterizing the particles coupling directly to it, is inspired by the notion of infinite primes [17], and discussed in [28]. Only particles characterized by integers having common prime factors can interact by the exchange of elementary bosons: the p-adic length scale of boson corresponds to a common primes.
3. Also the physics characterized by different values of \hbar are dark with respect to each other as far quantum coherent gauge interactions are considered. Laser beams might well correspond to photons characterized by p-adic prime different from M_{89} and de-coherence for the beam would mean decay to ordinary photons. De-coherence interaction involves scaling down of the Compton length characterizing the size of the space-time of particle implying that particles do not anymore overlap so that macroscopic quantum coherence is lost.
4. Those dark physics which are dark relative to each other can interact only via graviton exchange. If lepto-hadrons correspond to a physics for which weak bosons correspond to a p-adic prime different from M_{89} , intermediate gauge bosons cannot have direct decays to colored excitations of leptons irrespective of whether the QCD in question is asymptotically free or not. Neither are there direct interactions between the QED:s and QCD:s in question if M_{89} characterizes also ordinary photons and gluons. These ideas are discussed and applied in detail in [28, 23, 27].

Skeptic reader might stop the reading after these counter arguments unless there were definite experimental evidence supporting the lepto-hadron hypothesis.

1. The production of anomalous e^+e^- pairs in heavy ion collisions (energies just above the Coulomb barrier) suggests the existence of pseudoscalar particles decaying to e^+e^- pairs. A natural identification is as lepto-pions that is bound states of color octet excitations of e^+ and e^- .
2. The second puzzle, Karmen anomaly, is quite recent [40]. It has been found that in charge pion decay the distribution for the number of neutrinos accompanying muon in decay $\pi \rightarrow \mu + \nu_\mu$ as a function of time seems to have a small shoulder at $t_0 \sim ms$. A possible explanation is the decay of charged pion to muon plus some new weakly interacting particle with mass of order $30 MeV$ [31]: the production and decay of this particle would proceed via mixing with muon neutrino. TGD suggests the identification of this state as color singlet leptobaryon of, say type $L_B = f_{abc}L_8^a L_8^b \bar{L}_8^c$, having electro-weak quantum numbers of neutrino.
3. The third puzzle is the anomalously high decay rate of orto-positronium. [60]. e^+e^- annihilation to virtual photon followed by the decay to real photon plus virtual lepto-pion followed by the decay of the virtual lepto-pion to real photon pair, $\pi_L \gamma \gamma$ coupling being determined by axial anomaly, provides a possible explanation of the puzzle.
4. There exists also evidence for anomalously large production of low energy e^+e^- pairs [39, 35, 36, 61] in hadronic collisions, which might be basically due to the production of lepto-hadrons via the decay of virtual photons to colored leptons.

In this chapter a revised form of lepto-hadron hypothesis is described.

1. Sigma model realization of PCAC hypothesis allows to determine the decay widths of lepto-pion and lepto-sigma to photon pairs and e^+e^- pairs. Ortopositronium anomaly determines the value of $f(\pi_L)$ and therefore the value of lepto-pion-lepto-nucleon coupling and the decay rate of lepto-pion to two photons. Various decay widths are in accordance with the experimental data and corrections to electro-weak decay rates of neutron and muon are small.
2. One can consider several alternative interpretations for the resonances.

Option 1: For the minimal color representation content, three lepto-pions are predicted corresponding to 8, 10, $\overline{10}$ representations of the color group. If the lightest lepto-nucleons e_{ex} have masses only slightly larger than electron mass, the anomalous e^+e^- could be actually $e_{ex}^+ + e_{ex}^-$ pairs produced in the decays of lepto-pions. One could identify 1.062, 1.63 and 1.77 MeV states as the three lepto-pions corresponding to 8, 10, $\overline{10}$ representations and also understand why the latter two resonances have nearly degenerate masses. Since d and s quarks have same primary condensation level and same weak quantum numbers as colored e and μ , one might argue that also colored e and μ correspond to $k = 121$. From the mass ratio of the colored e and μ , as predicted by TGD, the mass of the muonic lepto-pion should be about 1.8 MeV in the absence of topological mixing. This suggests that 1.83 MeV state corresponds to the lightest $g = 1$ lepto-pion.

Option 2: If one believes sigma model (in ordinary hadron physics the existence of sigma meson is not established and its width is certainly very large if it exists), then lepto-pions are accompanied by sigma scalars. If lepto-sigmas decay dominantly to e^+e^- pairs (this might be forced by kinematics) then one could adopt the previous scenario and could identify 1.062 state as lepto-pion and 1.63, 1.77 and 1.83 MeV states as lepto-sigmas rather than lepto-pions. The fact that muonic lepto-pion should have mass about 1.8 MeV in the absence of topological mixing, suggests that the masses of lepto-sigma and lepto-pion should be rather close to each other.

Option 3: One could also interpret the resonances as string model 'satellite states' having interpretation as radial excitations of the ground state lepto-pion and lepto-sigma. This identification is not however so plausible as the genuinely TGD based identification and will not be discussed in the sequel.

3. PCAC hypothesis and sigma model leads to a general model for lepto-hadron production in the electromagnetic fields of the colliding nuclei and production rates for lepto-pion and other lepto-hadrons are closely related to the Fourier transform of the instanton density $\vec{E} \cdot \vec{B}$ of the electromagnetic field created by nuclei. The first source of anomalous e^+e^- pairs is the production of $\sigma_L\pi_L$ pairs from vacuum followed by $\sigma_L \rightarrow e^+e^-$ decay. If $e_{ex}^+e_{ex}^-$ pairs rather than genuine e^+e^- pairs are in question, the production is production of lepto-pions from vacuum followed by lepto-pion decay to lepto-nucleon pair.

Option 1: For the production of lepto-nucleon pairs the cross section is only slightly below the experimental upper bound for the production of the anomalous e^+e^- pairs and the decay rate of lepto-pion to lepto-nucleon pair is of correct order of magnitude.

Option 2: The rough order of magnitude estimate for the production cross section of anomalous e^+e^- pairs via $\sigma_L\pi_L$ pair creation followed by $\sigma_L \rightarrow e^+e^-$ decay, is by a factor of order $1/\sum N_c^2$ (N_c is the total number of states for a given colour representation and sum over the representations contributing to the orthopositronium anomaly appears) smaller than the reported cross section in case of 1.8 MeV resonance. The discrepancy could be due to the neglect of the large radiative corrections (the coupling $g(\pi_L\pi_L\sigma_L) = g(\sigma_L\sigma_L\sigma_L)$ is very large) and also due to the uncertainties in the value of the measured cross section.

Given the unclear status of sigma in hadron physics, one has a temptation to conclude that anomalous e^+e^- pairs actually correspond to lepto-nucleon pairs.

4. The vision about dark matter suggests that direct couplings between leptons and lepto-hadrons are absent in which case no new effects in the direct interactions of ordinary leptons are predicted. If colored leptons couple directly to ordinary leptons, several new physics effects such as resonances in photon-photon scattering at cm energy equal to lepto-pion masses and the production of $e_{ex}\bar{e}_{ex}$ (e_{ex} is lepton with quantum numbers of electron) and $e_{ex}\bar{e}$ pairs in heavy ion collisions, are possible. Lepto-pion exchange would give dominating contribution to $\nu - e$ and $\bar{\nu} - e$ scattering at low energies. Lepto-hadron jets should be observed in e^+e^- annihilation at energies above few MeV:s unless the loss of asymptotic freedom restricts lepto-hadronic physics to a very narrow energy range and perhaps to entirely non-perturbative regime of lepto-hadronic QCD.

This chapter is a revised version of the earlier chapter [26] and still a work in progress. I apologize for the reader for possible inconvenience. The motivation for the re-writing came from the evidence for

the production of τ -pions in high energy proton-antiproton collisions [57, 54]. Since the kinematics of these collisions differs dramatically from that for heavy ion collisions, a critical re-examination of the earlier model - which had admittedly somewhat ad hoc character- became necessary. As a consequence the earlier model simplified dramatically. As far as basic calculations are considered, the modification makes itself visible only at the level of coefficients. Even more remarkably, it turned out possible to calculate exactly the lepto-pion production amplitude under a very natural approximation, which can be also generalized so that the calculation of production amplitude can be made analytically in high accuracy and only the integration over lepto-pion momentum must be carried out numerically. As a consequence, a rough analytic estimate for the production cross section follows and turns out to be of correct order of magnitude. It must be however stressed that the cross section is highly sensitive to the value of the cutoff parameter (at least in this naive estimate) and only a precise calculation can settle the situation.

7.2 Lepto-hadron hypothesis

7.2.1 Anomalous e^+e^- pairs in heavy ion collisions

Heavy ion collision experiments carried out at the Gesellschaft für Schwerionenforschung in Darmstadt, West Germany [41, 49, 55, 42] have yielded a rather puzzling set of results. The expectation was that in heavy ion collisions in which the combined charge of the two colliding ions exceeds 173, a composite nucleus with $Z > Z_{cr}$ would form and the probability for spontaneous positron emission would become appreciable.

Indeed, narrow peaks of widths of roughly 50-70 keV and energies about 350 ± 50 keV were observed in the positron spectra but it turned out that the position of the peaks seems to be a constant function of Z rather than vary as Z^{20} as expected and that peaks are generated also for Z smaller than the critical Z . The collision energies at which peaks occur lie in the neighborhood of 5.7-6 MeV/nucleon. Also it was found that positrons are accompanied by e^- - emission. Data are consistent with the assumption that some structure at rest in cm is formed and decays subsequently to e^+e^- pair.

Various theoretical explanations for these peaks have been suggested [46, 48]. For example, lines might be created by pair conversion in the presence of heavy nuclei. In nuclear physics explanations the lines are due to some nuclear transition that occurs in the compound nucleus formed in the collision or in the fragments formed. The Z -independence of the peaks seems however to exclude both atomic and nuclear physics explanations [46]. Elementary particle physics explanations [46, 48] seem to be excluded already by the fact that several peaks have been observed in the range 1.6 – 1.8 MeV with widths of order $10^1 - 10^2$ keV. These states decay to e^+e^- pairs. There is evidence for one narrow peak with width of order one keV at 1.062 MeV [46]: this state decays to photon-photon pairs.

Thus it seems that the structures produced might be composite, perhaps resonances in e^+e^- system. The difficulty of this explanation is that conventional QED seems to offer no natural explanation for the strong force needed to explain the energy scale of the states. One idea is that the strong electromagnetic fields create a new phase of QED [46] and that the resonances are analogous to pseudoscalar mesons appearing as resonances in strongly interacting systems.

TGD based explanation relies on the following hypothesis motivated by Topological Geometro-dynamics.

1. Ordinary leptons are not point like particles and can have colored excitations, which form color singlet bound states. A natural identification for the primary condensate level is $k = 121$ so that the mass scale is of order one MeV for the states containing lowest generation colored leptons. The fact that d and s quarks, having the same weak quantum numbers as charged leptons, have same primary condensation level, suggests that both colored electron and muon condense to the same level. The expectation that lepto-hadron physics exists in a narrow energy interval only, suggests that also colored τ should condense on the same level.
2. The states in question are lepto-hadrons, that is color confined states formed from the colored excitations of e^+ and e^- . The decay rate to lepto-nucleon pairs $e_{ex}^+e_{ex}^-$ is large and turns out to give rise to correct order of magnitude for the decay width. Hence two options emerge.

Option 1: Lepto-nucleons e_{ex} have masses only slightly above the electron mass and since they behave like electrons, anomalous e^+e^- pairs could actually correspond to lepto-nucleon pairs

created in the decays of lepto-pions. 1.062, 1.63 and 1.77 MeV states can be identified as lowest generation lepto-pions correspond to octet and two decuplets. 1.83 MeV state could be identified as the second generation lepto-pion corresponding to colored muon. The small branching fraction to gamma pairs explains why the decays of the higher mass lepto-pions to gamma pairs has not been observed. $g = 0$ lepto-pion decays to lepto-nucleon pairs can be visualized as occurring via dual diagrams obeying Zweig's rule (annihilation is not allowed inside incoming or outgoing particle states). The decay of $g = 1$ colored muon pair occurs via Zweig rule violating annihilation to two gluon intermediate state, which transforms back to virtual $g = 0$ colored electron pair decaying via dual diagram: the violation of Zweig's rule suggests that the decay rate for 1.8 MeV state is smaller than for the lighter states. Quantitative model shows that this scenario is the most plausible one.

Option 2: Lepto-sigmas, which are the scalar partners of lepto-pions predicted by sigma model, are the source of anomalous (and genuine) e^+e^- pairs. In this case 1.062 state must correspond to lepto-pion whereas higher states must be identified as lepto-sigmas. Also now new lepto-pion states decaying to gamma pairs are predicted and one could hence argue that this prediction is not consistent with what has been observed. A crucial assumption is that lepto-sigmas are light and cannot decay to other lepto-mesons. Ordinary hadronic physics suggests that this need not be the case: the hadronic decay width of the ordinary sigma, if it exists, is very large.

The program of the section is following:

1. PCAC hypothesis, successful in low energy pion physics, is generalized to the case of lepto-pion. Hypothesis allows to deduce the coupling of lepto-pion to leptons and lepto-baryons in terms of leptobaryon-lepton mixing angles. Orthopositronium anomaly allows to deduce precise value of $f(\pi_L)$ characterizing the decay rate of lepto-pion so that the crucial parameters of the model are completely fixed. The decay rates of lepto-pion to photon pair and of lepto-sigma to ordinary e^+e^- pairs are within experimental bounds and corrections to muon and beta decay rates are small. New calculable resonance contributions to photon-photon scattering at cm energy equal to lepto-pion masses are predicted.
2. If anomalous e^+e^- pairs are actually lepto-nucleon pairs, only a model for the creation of lepto-pions from vacuum is needed. In an external electromagnetic field lepto-pion develops a vacuum expectation value proportional to electromagnetic anomaly term [28] so that the production amplitude for the lepto-pion is essentially the Fourier transform of the scalar product of the electric field of the stationary target nucleus with the magnetic field of the colliding nucleus.
3. If anomalous e^+e^- pairs are produced in the decays of lepto-sigmas, the starting point is sigma model providing a realization of PCAC hypothesis. Sigma model makes it possible to relate the production amplitude for $\sigma_L\pi_L$ pairs to the lepto-pion production amplitude: the key element of the model is the large value of the $\sigma\pi_L\pi_L$ coupling constant.
4. Lepto-hadron production amplitudes are proportional to lepto-pion production amplitude and this motivates a detailed study of lepto-pion production. Two models for lepto-pion production are developed: in classical model colliding nucleus is treated classically whereas in quantum model the colliding nucleus is described quantum mechanically. It turns out that classical model explains the peculiar production characteristics of lepto-pion but that production cross section is too small by several orders of magnitude. Quantum mechanical model predicts also diffractive effects: production cross section varies rapidly as a function of the scattering angle and for a fixed value of scattering angle there is a rapid variation with the collision velocity. The estimate for the total lepto-pion production cross section increases by several orders of magnitude due to the coherent summation of the contributions to the amplitude from different values of the impact parameter at the peak.
5. The production rate for lepto-nucleon pairs is only slightly smaller than the experimental upper bound but the e^+e^- production rate predicted by sigma model approach is still by a factor of order $1/\sum N_c^2$ smaller than the reported maximum cross section. A possible explanation for this discrepancy is the huge value of the coupling $g(\pi_L, \pi_L, \sigma_L) = g(\sigma_L, \sigma_L, \sigma_L)$ implying that the diagram involving the exchange of virtual sigma can give the dominant contribution to the production cross section of $\sigma_L\pi_L$ pair.

7.2.2 Lepto-pions and generalized PCAC hypothesis

One can say that the PCAC hypothesis predicts the existence of pions and a connection between the pion nucleon coupling strength and the pion decay rate to leptons. In the following we give the PCAC argument and its generalization and consider various consequences.

PCAC for ordinary pions

The PCAC argument for ordinary pions goes as follows [30]:

1. Consider the contribution of the hadronic axial current to the matrix element describing lepton nucleon scattering (say $N + \nu \rightarrow P + e^-$) by weak interactions. The contribution in question reduces to the well-known current-current form

$$\begin{aligned} M &= \frac{G_F}{\sqrt{2}} g_A L_\alpha \langle P | A^\alpha | P \rangle , \\ L_\alpha &= \bar{e} \gamma_\alpha (1 + \gamma_5) \nu , \\ \langle P | A^\alpha | P \rangle &= \bar{P} \gamma^\alpha N , \end{aligned} \quad (7.2-1)$$

where $G_F = \frac{\pi\alpha}{2m_W^2 \sin^2(\theta_W)} \simeq 10^{-5}/m_p^2$ denotes the dimensional weak interaction coupling strength and g_A is the nucleon axial form factor: $g_A \simeq 1.253$.

2. The matrix element of the hadronic axial current is not divergenceless, due to the non-vanishing nucleon mass,

$$a_\alpha \langle P | A^\alpha | P \rangle \simeq 2m_p \bar{P} \gamma_5 N . \quad (7.2.0)$$

Here q^α denotes the momentum transfer vector. In order to obtain divergenceless current, one can modify the expression for the matrix element of the axial current

$$\langle P | A^\alpha | N \rangle \rightarrow \langle P | A^\alpha | N \rangle - q^\alpha 2m_p \bar{P} \gamma_5 N \frac{1}{q^2} . \quad (7.2.1)$$

3. The modification introduces a new term to the lepton-hadron scattering amplitude identifiable as an exchange of a massless pseudoscalar particle

$$\delta T = \frac{G_F g_A}{\sqrt{2}} L_\alpha \frac{2m_p q^\alpha}{q^2} \bar{P} \gamma_5 N . \quad (7.2.2)$$

The amplitude is identifiable as the amplitude describing the exchange of the pion, which gets its mass via the breaking of chiral invariance and one obtains by the straightforward replacement $q^2 \rightarrow q^2 - m_\pi^2$ the correct form of the amplitude.

4. The nontrivial point is that the interpretations as pion exchange is indeed possible since the amplitude obtained is to a good approximation identical to that obtained from the Feynman diagram describing pion exchange, where the pion nucleon coupling constant and pion decay amplitude appear

$$T_2 = \frac{G}{\sqrt{2}} f_\pi q^\alpha L_\alpha \frac{1}{q^2 - m_\pi^2} g \sqrt{2} \bar{P} \gamma_5 N . \quad (7.2.3)$$

The condition $\delta T \sim T_2$ gives from Goldberger-Treiman [30]

$$g_A (\simeq 1.25) = \sqrt{2} \frac{f_\pi g}{2m_p} (\simeq 1.3) , \quad (7.2.4)$$

satisfied in a good accuracy experimentally.

PCAC in leptonic sector

A natural question is why not generalize the previous argument to the leptonic sector and look at what one obtains. The generalization is based on following general picture.

1. There are two levels to be considered: the level of ordinary leptons and the level of leptobaryons of, say type $f_{ABC} \nu_8^A \nu_8^B \bar{L}_{10}^C$, possessing same quantum numbers as leptons. The interaction transforming these states to each other causes in mass eigenstates mixing of leptobaryons with ordinary leptons described by mixing angles. The masses of lepton and corresponding leptobaryon could be quite near to each other and in case of electron this should be the case as it turns out.
2. A counterargument against the applications of PCAC hypothesis at level of ordinary leptons is that baryons and mesons are both bound states of quarks whereas ordinary leptons are not bound states of colored leptons. The divergence of the axial current is however completely independent of the possible internal structure of leptons and microscopic emission mechanism. Ordinary lepton cannot emit lepto-pion directly but must first transform to leptobaryon with same quantum numbers: phenomenologically this process can be described using mixing angle $\sin(\theta_B)$. The emission of lepto-pion proceeds as $L \rightarrow B_L : B_L \rightarrow B_L + \pi_L : B_L \rightarrow L$, where B_L denotes leptobaryon of type structure $f_{ABC} L_8^A L_8^B \bar{L}_8^C$. The transformation amplitude $L \rightarrow B_L$ is proportional to the mixing angle $\sin(\theta_L)$.

Three different PCAC type identities are assumed to hold true:

PCAC1) The vertex for the emission of lepto-pion by ordinary lepton is equivalent with the graph in which lepton L transforms to leptobaryon L^{ex} with same quantum numbers, emits lepto-pion and transforms back to ordinary lepton. The assumption relates the couplings $g(L_1, L_2)$ and $g(L_1^{ex}, L_2^{ex})$ (analogous to strong coupling) and mixing angles to each other

$$g(L_1, L_2) = g(L_1^{ex}, L_2^{ex}) \sin(\theta_1) \sin(\theta_2) . \quad (7.2.5)$$

The condition implies that in electro-weak interactions ordinary leptons do not transform to their exotic counterparts.

PCAC2) The generalization of the ordinary Goldberger-Treiman argument holds true, when ordinary baryons are replaced with leptobaryons. This gives the condition expressing the coupling $f(\pi_L)$ of the lepto-pion state to axial current defined as

$$\langle vac | A_\alpha | \pi_L \rangle = i p_\alpha f(\pi_L) , \quad (7.2.6)$$

in terms of the masses of leptobaryons and strong coupling g .

$$f(\pi_L) = \sqrt{2} g_A \frac{(m_{ex}(1) + m_{ex}(2)) \sin(\theta_1) \sin(\theta_2)}{g(L_1, L_2)} , \quad (7.2.7)$$

where g_A is parameter characterizing the deviation of weak coupling strength associated with leptobaryon from ideal value: $g_A \sim 1$ holds true in good approximation.

PCAC3) The elimination of leptonic axial anomaly from leptonic current fixes the values of $g(L_i, L_j)$.

1. The standard contribution to the scattering of leptons by weak interactions given by the expression

$$\begin{aligned} T &= \frac{G_F}{\sqrt{2}} \langle L_1 | A^\alpha | L_2 \rangle \langle L_3 | A_\alpha | L_4 \rangle , \\ \langle L_i | A^\alpha | L_j \rangle &= \bar{L}_i \gamma^\alpha \gamma_5 L_j . \end{aligned} \quad (7.2.7)$$

2. The elimination of the leptonic axial anomaly

$$q_\alpha \langle L_i | A^\alpha | L_j \rangle = (m(L_i) + m(L_j)) \bar{L}_i \gamma_5 L_j , \quad (7.2.8)$$

by modifying the axial current by the anomaly term

$$\langle L_i | A^\alpha | L_j \rangle \rightarrow \langle L_i | A^\alpha | L_j \rangle - (m(L_i) + m(L_j)) \frac{q^\alpha}{q^2} \bar{L}_i \gamma_5 L_j , \quad (7.2.9)$$

induces a new interaction term in the scattering of ordinary leptons.

3. It is assumed that this term is equivalent with the exchange of lepto-pion. This fixes the value of the coupling constant $g(L_1, L_2)$ to

$$\begin{aligned} g(L_1, L_2) &= 2^{1/4} \sqrt{G_F} (m(L_1) + m(L_2)) \xi , \\ \xi(\text{charged}) &= 1 , \\ \xi(\text{neutral}) &= \cos(\theta_W) . \end{aligned} \quad (7.2.8)$$

Here the coefficient ξ is related to different values of masses for gauge bosons W and Z appearing in charged and neutral current interactions. An important factor 2 comes from the modification of the axial current in both matrix elements of the axial current.

Lepto-pion exchange interaction couples right and left handed leptons to each other and its strength is of the same order of magnitude as the strength of the ordinary weak interaction at energies not considerably large than the mass of the lepto-pion. At high energies this interaction is negligible and the existence of the lepto-pion predicts no corrections to the parameters of the standard model since these are determined from weak interactions at much higher energies. If lepto-pion mass is sufficiently small (as found, $m(\pi_L) < 2m_e$ is allowed by the experimental data), the interaction mediated by lepto-pion exchange can become quite strong due to the presence of the lepto-pion propagator. The value of the lepton-lepto-pion coupling is $g(e, e) \equiv g \sim 5.6 \cdot 10^{-6}$. It is perhaps worth noticing that the value of the coupling constant is of the same order as lepton-Higgs coupling constant and also proportional to the mass of the lepton.

PCAC identities fix the values of coupling constants apart from the values of mixing angles. If one assumes that the strong interaction mediated by lepto-pions is really strong and the coupling strength $g(L_{ex}, L_{ex})$ is of same order of magnitude as the ordinary pion nucleon coupling strength $g(\pi NN) \simeq 13.5$ one obtains an estimate for the value of the mixing angle $\sin(\theta_e)$ $\sin^2(\theta_e) \sim \frac{g(\pi NN)}{g(L, L)} \sim 2.4 \cdot 10^{-6}$. This implies the order of magnitude $f(\pi_L) \sim 10^{-6} m_W \sim 10^2 \text{ keV}$ for $f(\pi_L)$. The order of magnitude is correct as will be found. Ortopositronium decay rate anomaly $\Delta\Gamma/\Gamma \sim 10^{-3}$ and the assumption $m_{ex} \geq 1.3 \text{ MeV}$ (so that $e_{ex}\bar{e}$ decay is not possible) gives the upper bound $\sin(\theta_e) \leq x \cdot \sqrt{N_c} \cdot 10^{-4}$, where the value of $x \sim 1$ depends on the number of the lepto-pion type states and on the precise value of the Op anomaly.

7.2.3 Lepto-pion decays and PCAC hypothesis

The PCAC argument makes it possible to predict the lepto-pion coupling and decay rates of the lepto-pion to various channels. Actually the orders of magnitude for the decay rates of the lepto-sigma and other lepto-mesons can be deduced also. The comparison with the experimental data is made difficult by the uncertainty of the identifications. The lightest candidate has mass 1.062 MeV and decay width of order 1 keV [46]: only photon photon decay has been observed for this state. The next lepto-meson candidates are in the mass range $1.6 - 1.8 \text{ MeV}$. Perhaps the best status is possessed by 'Darmstadtium' with mass 1.8 MeV . For these states decays to final states identified as e^+e^- pairs dominate: if indeed e^+e^- pairs, these states probably correspond to the decay products of lepto-sigma. Another possibility is that pairs are actually lepto-nucleon pairs with the mass of the lepto-nucleon only slightly larger than electron mass. Hadron physics experience suggests that the decay widths of the lepto-hadrons (lepto-pion forming a possible exception) should be about 1-10 per cent of particle mass as in hadron physics. The upper bounds for the widths are indeed in the range $50 - 70 \text{ keV}$ [46].

$$\Gamma(\pi_L \rightarrow \gamma\gamma)$$

As in the case of the ordinary pion, anomaly considerations give the following approximate expression for the decay rate of the lepto-pion to two-photon final states [28])

$$\Gamma(\pi_L \rightarrow \gamma\gamma) = \frac{N_c^2 \alpha^2 m^3(\pi_L)}{64 f(\pi_L)^2 \pi^3} . \quad (7.2.9)$$

$N_c = 8, 10$ is the number of the colored lepton states coming from the axial anomaly loop. For $m(\pi_L) = 1.062 \text{ MeV}$ and $f(\pi_L) = N_c \cdot 7.9 \text{ keV}$ implied by the orthopositronium decay rate anomaly $\Delta\Gamma/\Gamma = 10^{-3}$ one has $\Gamma(\gamma\gamma) = .52 \text{ keV}$, which is consistent with the experimental estimate of order 1 keV [46].

In fact, several lepto-pion states could exist (4 at least corresponding to the resonances at 1.062, 1.63, 1.77 and 1.83 MeV). Since all these lepto-pion states contribute to Op decay rate, the actual value of $f(\pi_L)$ assumed to scale as $m(\pi_L)$, is actually larger in this case: it turns out that $f(\pi_L)$ for the lightest lepto-pion increases to $f(\pi_L)(\text{lightest}) = N_c \cdot 15 \text{ keV}$ and gives $\Gamma(\gamma\gamma) \simeq .13 \text{ keV}$ in case of the lightest lepto-pion if lepto-pions are assumed to correspond the resonances. Note that the order of magnitude for $f(\pi_L)$ is same as deduced from the assumption that lepto-hadronic counterpart of $g(\pi NN)$ equals to the ordinary $g(\pi NN)$. The increase of the orthopositronium anomaly by a factor of, say 4, implies corresponding decrease in $f(\pi_L)^2$. The value of $f(\pi_L)$ is also sensitive to the precise value of the mass of the lightest lepto-pion.

Lepto-pion-lepton coupling

The value of the lepto-pion-lepton coupling can be used to predict the decay rate of lepto-pion to leptons. One obtains for the decay rate $\pi_L^0 \rightarrow e^+e^-$ the estimate

$$\begin{aligned} \Gamma(\pi_L \rightarrow e^+e^-) &= 4 \frac{g(e, e)^2 \pi}{2(2\pi)^2} (1 - 4x^2) m(\pi_L) \\ &= 16 G m_e^2 \cos^2(\theta_W) \frac{\sqrt{2}}{4\pi} (1 - 4x^2) m(\pi_L) , \\ x &= \frac{m_e}{m(\pi_L)} . \end{aligned} \quad (7.2.8)$$

for the decay rate of the lepto-pion: for lepto-pion mass $m(\pi_L) \simeq 1.062 \text{ MeV}$ one obtains for the decay rate the estimate $\Gamma \sim 1/(1.3 \cdot 10^{-8} \text{ sec})$: the low decay rate is partly due to the phase space suppression and implies that e^+e^- decay products cannot be observed in the measurement volume. The low decay rate is in accordance with the identification of the lepto-pion as the $m = 1.062 \text{ MeV}$ lepto-pion candidate. In sigma model lepto-pion and lepto-sigma have identical lifetimes and for lepto-sigma mass of order 1.8 MeV one obtains $\Gamma(\sigma_L \rightarrow e^+e^-) \simeq 1/(8.2 \cdot 10^{-10} \text{ sec})$: the prediction is larger than the lower limit $\sim 1/(10^{-9} \text{ sec})$ for the decay rate implied by the requirement that σ_L decays

inside the measurement volume. The estimates of the lifetime obtained from heavy ion collisions [32] give the estimate $\tau \geq 10^{-10}$ sec. The large value of the lifetime is in accordance with the limits for the lifetime obtained from Bhabha scattering [52], which indicate that the lifetime must be longer than 10^{-12} sec.

For lepto-meson candidates with mass above 1.6 MeV no experimental evidence for other decay modes than $X \rightarrow e^+e^-$ has been found and the empirical upper limit for $\gamma\gamma/e^+e^-$ branching ratio [59] is $\Gamma(\gamma\gamma)/\Gamma(e^+e^-) \leq 10^{-3}$. If the identification of the decay products as e^+e^- pairs is correct then the only possible conclusion is that these states cannot correspond to lepto-pion since lepto-pion should decay dominantly into photon photon pairs. Situation changes if pairs of lepton-ucleons $e_{ex}\bar{e}_{ex}$ of type $e_{ex} = e_8\nu_8\bar{\nu}_8$ pair are in question.

I realized that this conclusion might be questioned for more than decade after writing the above text as I developed a model for CDF anomaly suggesting the existence of τ -pions. Since colored leptons are color octets, anomalous magnetic moment type coupling of form $\overline{L}Tr(F^{\mu\nu}\Sigma_{\mu\nu}L_8)$ (the trace is over the Lie-algebra generators of $SU(3)$ and $F^{\mu\nu}$ denotes color gauge field) between ordinary lepton, colored lepton and lepto-gluon is possible. The exchange of a virtual lepto-gluon allows lepto-pion to decay by lepto-strong interactions to electron-positron pairs. The decay rate is limited by the kinematics for the lightest state very near to the final state mass and might make decay rate to in this case very small. If the rate for the decay to electron-positron pair is comparable to that for the decay to two photons the production rate for electron-positron pairs could be of the same order of magnitude as lepton production rate. The anomalous magnetic moment of electron however poses strong limitations on this coupling and it might be that the coupling is too small. This coupling could however induce the mixing of e_{ex} with e .

$$\Gamma(\pi_L \rightarrow e + \bar{\nu}_e)$$

The expression for the decay rate $\pi_L \rightarrow e + \bar{\nu}_e$ reads as

$$\begin{aligned} \Gamma(\pi_L^- \rightarrow e\nu_e) &= 8Gm_e^2 \frac{(1-x^2)^2}{2(1+x^2)} \frac{\sqrt{2}}{(2\pi)^5} m(\pi_L) , \\ &= \frac{4}{\cos^2(\theta_W)} \frac{(1-x^2)}{(1+x^2)(1-4x^2)} \Gamma(\pi_L^0 \rightarrow e^+e^-) , \end{aligned} \quad (7.2.8)$$

and gives $\Gamma(\pi_L^- \rightarrow e\nu_e) \simeq 1/(3.6 \cdot 10^{-10} \text{ sec})$ for $m(\pi_L) = 1.062 \text{ MeV}$.

$$\Gamma(\pi_L/\sigma_L \rightarrow e_{ex}\bar{e}_{ex}) \text{ and } \Gamma(\pi_L/\sigma_L \rightarrow e_{ex}\bar{e})$$

Sigma model predicts lepto-pion and lepto-sigma to have same coupling to lepto-nucleon e_{ex} pair so that in the sequel only lepto-pion decay rates are considered. One must consider also the possibility that lepto-pion decay products are either $e_{ex}\bar{e}_{ex}$ or $e_{ex}\bar{e}$ pairs with e_{ex} having mass of near the mass of electron so that it could be misidentified as electron. If the mass of lepto-nucleon e_{ex} with quantum numbers of electron is smaller than $m(\pi_L)/2$ it can be produced in lepto-pion annihilation. One must also assume $m(e_{ex}) > m_e$: otherwise electrons would spontaneously decay to lepto-nucleons via photon emission. The production rate to lepto-nucleon pair can be written as

$$\begin{aligned} \Gamma(\pi_L \rightarrow e_{ex}^+e_{ex}^-) &= \frac{1}{\sin^4(\theta_e)} \frac{(1-4y^2)}{(1-4x^2)} \Gamma(\pi_L \rightarrow e^+e^-) , \\ y &= \frac{m(e_{ex})}{m(\pi_L)} . \end{aligned} \quad (7.2.8)$$

If $e - e_{ex}$ mass difference is sufficiently small the kinematic suppression does not differ significantly from that for e^+e^- pair. The limits from Bhabha scattering give no bounds on the rate of $\pi_L \rightarrow e_{ex}^+e_{ex}^-$ decay. The decay rate $\Gamma \sim 10^{20}/\text{sec}$ implied by $\sin(\theta_e) \sim 10^{-4}$ implies decay width of order .1 MeV: the order of magnitude is the naively expected one and means that the decay to $e_{ex}^+e_{ex}^-$ pairs dominates over the decay to gamma pairs except in the case of the lightest lepto-pion state for which the decay is kinematically forbidden.

The decay rate of the lepto-pion to $\bar{e}e_{ex}$ pair has sensible order of magnitude: for $\sin(\theta_e) = 1.2 \cdot 10^{-3}$, $m_{\sigma_L} = 1.8 \text{ MeV}$ and $m_{e_{ex}} = 1.3 \text{ MeV}$ one has $\Gamma \simeq 60 \text{ eV}$ allowed by the experimental limits. This decay is kinematically possible only provided the mass of e_{ex} is in below 1.3 MeV . These decays should dominate by a factor $1/\sin^2(\theta_e)$ over e^+e^- decays if kinematically allowed.

A signature of these events, if identified erratically as electron positron pairs, is the non-vanishing value of the energy difference in the cm frame of the pair: $E(e^-) - E(e^+) \simeq (m^2(e_{ex}) - m_e^2)/2E > 160 \text{ keV}$ for $E = 1.8 \text{ MeV}$. If the decay $e_{ex} \rightarrow e + \gamma$ takes place before the detection the energy asymmetry changes its sign. Energy asymmetry [45] increasing with the rest energy of the decaying object has indeed been observed: the proposed interpretation has been that electron forms a bound state with the second nucleus so that its energy is lowered. Also a deviation from the momentum distribution implied by the decay of neutral particle to e^+e^- pair (momenta are opposite in the rest frame) results from the emission of photon. This kind of deviation has also been observed [45]: the proposed explanation is that third object is involved in the decay. A possible alternative explanation for the asymmetries is the production mechanism ($\sigma_L\pi_L$ pairs instead of single particle states).

$$\Gamma(e_{ex} \rightarrow e + \gamma)$$

The decay to electron and photon would be a unique signature of e_{ex} . The general feature of fermion family mixing is that mixing takes place in charged currents. In present case mixing is of different type so that $e_{ex} \rightarrow e + \gamma$ might be allowed. If this is not the case then the decay takes place as weak decay via the emission of virtual W boson: $e_{ex} \rightarrow e + \nu_e + \bar{\nu}_e$ and is very slow due to the presence of mixing angle and kinematical suppression. The energy of the emitted photon is $E_\gamma = (m_{e_{ex}}^2 - m_e^2)/2m_e$. The decay rate $\Gamma(e_{ex} \rightarrow e + \gamma)$ is given by

$$\begin{aligned} \Gamma(e_{ex} \rightarrow e + \gamma) &= \alpha_{em} \sin^2(\theta_e) X m_e , \\ X &= \frac{(m_1 - m_e)^3 (m_1 + m_e) m_e}{(m_1^2 + m_e^2)^2 m_1} . \end{aligned} \tag{7.2.7}$$

For $m(e_{ex}) = 1.3 \text{ MeV}$ the decay of order $1/(1.4 \cdot 10^{-12} \text{ sec})$ for $\sin(\theta_e) = 1.2 \cdot 10^{-3}$ so that leptonucleons would decay to electrons in the measurement volume. In the experiments positrons are identified via pair annihilation and since pair annihilation rate for $\bar{e}e_{ex}$ is by a factor $\sin^2(\theta_e)$ slower than for e^+ the particles identified as positrons must indeed be positrons. For sufficiently small mass difference $m(e_{ex}) - m_e$ the particles identified as electron could actually be e_{ex} . The decay of e_{ex} to electron plus photon before its detection seems however more reasonable alternative since it could explain the observed energy asymmetry [45].

Some implications

The results have several implications as far as the decays of on mass shell states are considered:

1. For $m(e_{ex}) > 1.3 \text{ MeV}$ the only kinematically possible decay mode is the decay to e^+e^- pair. Production mechanism might explain the asymmetries [45]. The decay rate of on mass shell π_L and σ_L (or η_L, ρ_L, \dots) is above the lower limit allowed by the detection in the measurement volume.
2. If the mass of e_{ex} is larger than $.9 \text{ MeV}$ but smaller than 1.3 MeV $e_{ex}\bar{e}$ decays dominate over e^+e^- decays. The decay $e_{ex} \rightarrow e + \gamma$ before detection could explain the observed energy asymmetry.
3. It will be found that the direct production of $e_{ex}\bar{e}$ pairs is also possible in the heavy ion collision but the rate is much smaller due to the smaller phase space volume in two-particle case. The annihilation rate of $\bar{e}e_{ex}$ in matter is by a factor $\sin^2(\theta_e)$ smaller than the annihilation rate of positron. This provides a unique signature of e_{ex} if e^+ annihilation rate in matter is larger than the decay rate of $\bar{e}e_{ex}$. In lead the lifetime of positron is $\tau \sim 10^{-10} \text{ sec}$ and indeed larger than e_{ex} lifetime.

Karmen anomaly

A brief comment on the Karmen anomaly [40] observed in the decays of π^+ is in order. The anomaly suggests the existence [31] of new weakly interacting neutral particle x , which mixes with muon neutrino. Since $g = 1$ neutrino corresponds to charmed quark in hadron physics context having $k = 103$ rather than $k = 107$ as primary condensation level, a natural guess for its primary condensation level is $k = 113$, which would mean that the mass scale would be of order muon mass: the particle candidate indeed has mass of order 30 MeV. One class of solutions to laboratory constraints, which might evade also cosmological and astrophysical constraints, corresponds to object x mixing with muon type neutrino and decaying radiatively to $\gamma + \nu_\mu$ via the emission of virtual W boson. The value of the mixing parameter $U(\mu, x)$ describing $\nu_{\mu x} - x$ mixing satisfies $|U_{\mu, x}|^4 \simeq .8 \cdot 10^{-10}$.

The following naive PCAC argument gives order of magnitude estimate for $|U(\mu, x)| \sim \sin(\theta_\mu)$. The value of $g(\mu, \mu)$ is by a factor $m(\mu)/m_e$ larger than $g(e, e)$. If the lepto-hadronic couplings $g(\mu_{ex}, \mu_{ex})$ and $g(e_{ex}, e_{ex})$ are of same order of magnitude then one has $\sin(\theta_\mu) \leq .02$ (3 lepto-pion states and Op anomaly equal to $Op = 5 \cdot 10^{-3}$): the lower bound is 6.5 times larger than the value .003 deduced in [31]. The actual value could be considerably smaller since e_{ex} mass could be larger than 1.3 MeV by a factor of order 10.

7.2.4 Lepto-pions and weak decays

The couplings of lepto-meson to electro-weak gauge bosons can be estimated using PCAC and CVC hypothesis [28]. The effective $m_{\pi_L} - W$ vertex is the matrix element of electro-weak axial current between vacuum and charged lepto-meson state and can be deduced using same arguments as in the case of ordinary charged pion

$$\langle 0 | J_A^\alpha | \pi_L^- \rangle = K m(\pi_L) p^\alpha, \quad (7.2.7)$$

where K is some numerical factor and p^α denotes the momentum of lepto-pion. For neutral lepto-pion the same argument gives vanishing coupling to photon by the conservation of vector current. This has the important consequence that lepto-pion cannot be observed as resonance in e^+e^- annihilation in single photon channel. In two photon channel lepto-pion should appear as resonance. The effective interaction Lagrangian is the 'instanton' density of electromagnetic field giving additional contribution to the divergence of the axial current and was used to derive a model for lepto-pion production in heavy ion collisions.

Lepto-hadrons and lepton decays

The lifetime of charged lepto-pion is from PCAC estimates larger than 10^{-10} seconds by the previous PCAC estimates. Therefore lepto-pions are practically stable particles and can appear in the final states of particle reactions. In particular, lepto-pion atoms are possible and by Bose statistics have the peculiar property that ground state can contain many lepto-pions.

Lepton decays $L \rightarrow \nu_\mu + H_L$, $L = e, \mu, \tau$ via emission of virtual W are kinematically allowed and an anomalous resonance peak in the neutrino energy spectrum at energy

$$E(\nu_L) = \frac{m(L)}{2} - \frac{m_H^2}{2m(L)}, \quad (7.2.8)$$

provides a unique test for the lepto-hadron hypothesis. If lepto-pion is too light electrons would decay to charged lepto-pions and neutrinos unless the condition $m(\pi_L) > m_e$ holds true.

The existence of a new decay channel for muon is an obvious danger to the lepto-hadron scenario: large changes in muon decay rate are not allowed.

Consider first the decay $\mu \rightarrow \nu_\mu + \pi_L$ where π_L is on mass shell lepto-pion. Lepto-pion has energy $\sim m(\mu)/2$ in muon rest system and is highly relativistic so that in the muon rest system the lifetime of lepto-pion is of order $\frac{m(\mu)}{2m(\pi_L)} \tau(\pi_L)$ and the average length traveled by lepto-pion before decay is of order 10^8 meters! This means that lepto-pion can be treated as stable particle. The presence of a new

decay channel changes the lifetime of muon although the rate for events using $e\nu_e$ pair as signature is not changed. The effective $H_L - W$ vertex was deduced above. The rate for the decay via lepto-pion emission and its ratio to ordinary rate for muon decay are given by

$$\begin{aligned}\Gamma(\mu \rightarrow \nu_\mu + H_L) &= \frac{G^2 K^2}{2^5 \pi} m^4(\mu) m^2(H_L) \left(1 - \frac{m^2(H_L)}{m^2(\mu)}\right) \frac{(m^2(\mu) - m^2(H_L))}{(m^2(\mu) + m^2(H_L))} , \\ \frac{\Gamma(\mu \rightarrow \nu_\mu + H_L)}{\Gamma(\mu \rightarrow \nu_\mu + e + \bar{\nu}_e)} &= 6 \cdot (2\pi^4) K^2 \frac{m^2(H_L)}{m^2(\mu)} \frac{(m^2(\mu) - m^2(H_L))}{(m^2(\mu) + m^2(H_L))} ,\end{aligned}\tag{7.2.7}$$

and is of order $.93K^2$ in case of lepto-pion. As far as the determination of G_F or equivalently m_W^2 from muon decay rate is considered the situation seems to be good since the change introduced to G_F is of order $\Delta G_F/G_F \simeq 0.93K^2$ so that K must be considerably smaller than one. For the physical value of K : $K \leq 10^{-2}$ the contribution to the muon decay rate is negligible.

Lepto-hadrons can appear also as virtual particles in the decay amplitude $\mu \rightarrow \nu_\mu + e\nu_e$ and this changes the value of muon decay rate. The correction is however extremely small since the decay vertex of intermediate off mass shell lepto-pion is proportional to its decay rate.

Lepto-pions and beta decay

If lepto-pions are allowed as final state particles lepto-pion emission provides a new channel $n \rightarrow p + \pi_L$ for beta decay of nuclei since the invariant mass of virtual W boson varies within the range ($m_e = 0.511 \text{ MeV}$, $m_n - m_p = 1.293 \text{ MeV}$). The resonance peak for $m(\pi_L) \simeq 1 \text{ MeV}$ is extremely sharp due to the long lifetime of the charged lepto-pion. The energy of the lepto-pion at resonance is

$$E(\pi_L) = (m_n - m_p) \frac{(m_n + m_p)}{2m_n} + \frac{m(\pi_L)^2}{2m_n} \simeq m_n - m_p .\tag{7.2.8}$$

Together with long lifetime this lepto-pions escape the detector volume without decaying (the exact knowledge of the energy of charged lepto-pion might make possible its direct detection).

The contribution of lepto-pion to neutron decay rate is not negligible. Decay amplitude is proportional to superposition of divergences of axial and vector currents between proton and neutron states.

$$M = \frac{G}{\sqrt{2}} K m(\pi_L) (q^\alpha V_\alpha + q^\alpha A_\alpha) .\tag{7.2.9}$$

For exactly conserved vector current the contribution of vector current vanishes identically. The matrix element of the divergence of axial vector current at small momentum transfer (approximately zero) is in good approximation given by

$$\begin{aligned}\langle p | q^\alpha A_\alpha | n \rangle &= g_A (m_p + m_n) \bar{u}_p \gamma_5 u_n , \\ g_A &\simeq 1.253 .\end{aligned}\tag{7.2.9}$$

Straightforward calculation shows that the ratio for the decay rate via lepto-pion emission and ordinary beta decay rate is in good approximation given by

$$\begin{aligned}\frac{\Gamma(n \rightarrow p + \pi_L)}{\Gamma(n \rightarrow p + e + \bar{\nu}_e)} &= \frac{30\pi^2 g_A^2 K^2}{0.47 \cdot (1 + 3g_A^2)} \frac{m_{\pi_L}^2 (\Delta^2 - m_{\pi_L}^2)^2}{\Delta^6} , \\ \Delta &= m(n) - m(p) .\end{aligned}\tag{7.2.9}$$

Lepto-pion contribution is smaller than ordinary contribution if the condition

$$K < \left[\frac{.47 \cdot (1 + 3g_A^2)}{30\pi^2 g_A^2} \frac{\Delta^6}{(\Delta^2 - m_{\pi_L}^2)^2 m_{\pi_L}^2} \right]^{1/2} \simeq .28 ,\tag{7.2.10}$$

is satisfied. The upper bound $K \leq 10^{-2}$ coming from the lepto-pion decay width and Op anomaly implies that the contribution of the lepto-pion to beta decay rate is very small.

7.2.5 Ortopositronium puzzle and lepto-pion in photon photon scattering

The decay rate of orpositronium (Op) has been found to be slightly larger than the rate predicted by QED [60, 58]: the discrepancy is of order $\Delta\Gamma/\Gamma \sim 10^{-3}$. For parapositronium no anomaly has been observed. Most of the proposed explanations [58] are based on the decay mode $Op \rightarrow X + \gamma$, where X is some exotic particle. The experimental limits on the branching ratio $\Gamma(Op \rightarrow X + \gamma)$ are below the required value of order 10^{-3} . This explanation is excluded also by the standard cosmology [58].

Lepto-pion hypothesis suggests an obvious solution of the Op-puzzle. The increase in annihilation rate is due to the additional contribution to $Op \rightarrow 3\gamma$ decay coming from the decay $Op \rightarrow \gamma_V$ (V denotes 'virtual') followed by the decay $\gamma_V \rightarrow \gamma + \pi_L^V$ followed by the decay $\pi_L^V \rightarrow \gamma + \gamma$ of the virtual lepto-pion to two photon state. $\gamma\gamma\pi_L$ vertices are induced by the axial current anomaly $\propto E \cdot B$. Also a modification of parapositronium decay rate is predicted. The first contribution comes from the decay $Op \rightarrow \pi_L^V \rightarrow \gamma + \gamma$ but the contribution is very small due the smallness of the coupling $g(e, e)$. The second contribution obtained from orpositronium contribution by replacing one outgoing photon with a loop photon is also small. Since the production of a real lepto-pion is impossible, the mechanism is consistent with the experimental constraints.

The modification to the Op annihilation amplitude comes in a good approximation from the interference term between the ordinary e^+e^- annihilation amplitude F_{st} and lepto-pion induced annihilation amplitude F_{new} :

$$\Delta\Gamma \propto 2Re(F_{st}\bar{F}_{new}) , \quad (7.2.11)$$

and rough order of magnitude estimate suggests $\Delta\Gamma/\Gamma \sim K^2/e^2 = \alpha^2/4\pi \sim 10^{-3}$. It turns out that the sign and the order of magnitude of the new contribution are correct for $f(\pi_L) \sim 2 \text{ keV}$ deduced also from the anomalous e^+e^- production rate.

The new contribution to $e^+e^- \rightarrow 3\gamma$ decay amplitude is most easily derivable using for lepto-pion-photon interaction the effective action

$$\begin{aligned} L_1 &= K\pi_L F \wedge F , \\ K &= \frac{\alpha_{em} N_c}{8\pi f(\pi_L)} , \end{aligned} \quad (7.2.11)$$

where F is quantized electromagnetic field. The calculation of the lepto-pion contribution proceeds in manner described in [28], where the expression for the standard contribution and an elegant method for treating the average over e^+e^- spin triplet states and sum over photon polarizations, can be found. The contribution to the decay rate can be written as

$$\begin{aligned} \frac{\Delta\Gamma}{\Gamma} &\simeq K_1 I_0 , \\ K_1 &= \frac{3\alpha N_c^2}{(\pi^2 - 9)2^9 (2\pi)^3} \left(\frac{m_e}{f(\pi_L)}\right)^2 , \\ I_0 &= \int_0^1 \int_{-1}^{umax} \frac{f}{v+f-1-x^2} v^2 (2(f-v)u + 2 - v - f) dv du , \\ f &\equiv f(v, u) = 1 - \frac{v}{2} - \sqrt{\left(1 - \frac{v}{2}\right)^2 - \frac{1-v}{1-u}} , \\ u &= \bar{n}_1 \cdot \bar{n}_2 , \quad \bar{n}_i = \frac{\bar{k}_i}{\omega_i} , \quad umax = \frac{(\frac{v}{2})^2}{(1 - \frac{v}{2})^2} , \\ v &= \frac{\omega_3}{m_e} , \quad x = \frac{m_{\pi_L}}{2m_e} . \end{aligned} \quad (7.2.7)$$

ω_i and \bar{k}_i denote the energies of photons, u denotes the cosine of the angle between first and second photon and v is the energy of the third photon using electron mass as unit. The condition $\Delta\Gamma/\Gamma = 10^{-3}$ gives for the parameter $f(\pi_L)$ the value $f(\pi_L)(1.062 \text{ MeV}) \simeq N_c \cdot 7.9 \text{ keV}$. If there are several lepto-pion states, they contribute to the decay anomaly additively. If the four known resonances correspond

directly to lepto-pions decaying to lepto-nucleon pairs and $f(\pi_L)$ is assumed to scale as $N_c m_{\pi_L}$, one obtains $f(\pi_L)(1.062 \text{ MeV}) \simeq N_c \cdot 14.7 \text{ keV}$. From the PCAC relation one obtains for $\sin(\theta_e)$ the upper bound $\sin(\theta_e) \leq x \cdot \sqrt{N_c} 10^{-4}$ assuming $m_{ex} \geq 1.3 \text{ MeV}$ (so that $e_{ex}\bar{e}$ decay is not possible), where $x = 1.2$ for single lepto-pion state and $x = 1.36$ for four lepto-pion states identified as the observed resonances.

Lepto-pion photon interaction implies also a new contribution to photon-photon scattering. Just at the threshold $E = m_{\pi_L}/2$ the creation of lepto-pion in photon photon scattering is possible and the appearance of lepto-pion as virtual particle gives resonance type behaviour to photon photon scattering near $s = m_{\pi_L}^2$. The total photon-photon cross section in zero decay width approximation is given by

$$\sigma = \frac{\alpha^4 N_c^2}{2^{14} (2\pi)^6} \frac{E^6}{f_{\pi_L}^4 (E^2 - \frac{m_{\pi_L}^2}{4})^2} . \quad (7.2.8)$$

N	$Op/10^{-3}$	$f(\pi_L)/(N_c \text{ keV})$	$\sin(\theta_e)(m_{ex}/1.3 \text{ MeV})^{1/2}$	$\Gamma(\pi_L)/\text{keV}$
1	1	7.9	$1.2 \cdot 10^{-4} \sqrt{N_c}$.51
3	1	14.7	$1.7 \cdot 10^{-4} \sqrt{N_c}$.13
3	5	6.5	$3.6 \cdot 10^{-4} \sqrt{N_c}$.73

Table 1: The dependence of various quantities on the number of lepto-pion type states and Op anomaly, whose value is varied assuming the proportionality $f(\pi_L) \propto N_c m_{\pi_L}$. N_c refers to the number of lepto-pion states in given representation and Op denotes lepto-pion anomaly.

7.2.6 Spontaneous vacuum expectation of lepto-pion field as source of lepto-pions

The basic assumption in the model of lepto-pion and lepto-hadron production is the spontaneous generation of lepto-pion vacuum expectation value in strong nonorthogonal electric and magnetic fields. This assumption is in fact very natural in TGD ¹.

1. The well known relation [28] expressing pion field as a sum of the divergence of axial vector current and anomaly term generalizes to the case of lepto-pion

$$\pi_L = \frac{1}{f(\pi_L)m^2(\pi_L)} (\nabla \cdot j^A + \frac{\alpha_{em} N_c}{2\pi} E \cdot B) . \quad (7.2.9)$$

In the case of lepto-pion case the value of $f(\pi_L)$ has been already deduced from PCAC argument. Anomaly term gives rise to pion decay to two photons so that one obtains an estimate for the lifetime of the lepto-pion.

This relation is taken as the basis for the model describing also the production of lepto-pion in external electromagnetic field. The idea is that the presence of external electromagnetic field gives rise to a vacuum expectation value of lepto-pion field. Vacuum expectation is obtained by assuming that the vacuum expectation value of axial vector current vanishes.

$$\begin{aligned} \langle vac | \pi | vac \rangle &= K E \cdot B , \\ K &= \frac{\alpha_{em} N_c}{2\pi f(\pi_L)m^2(\pi_L)} . \end{aligned} \quad (7.2.9)$$

Some comments concerning this hypothesis are in order here:

¹ 'Instanton density' generates coherent state of lepto-pions just like classical em current generates coherent state of photons

- (a) The basic hypothesis making possible to avoid large parity breaking effects in atomic and molecular physics is that p-adic condensation levels with length scale $L(n) < 10^{-6} m$ are purely electromagnetic in the sense that nuclei feed their Z^0 charges on condensate levels with $L(n) \geq 10^{-6} m$. The absence of Z^0 charges does not however exclude the possibility of the classical Z^0 fields induced by the nonorthogonality of the ordinary electric and magnetic fields (if Z^0 fields vanish E and B are orthogonal in TGD).
- (b) The non-vanishing vacuum expectation value of the lepto-pion field implies parity breaking in atomic length scales. This is understandable from basic principles of TGD since classical Z^0 field has parity breaking axial coupling to electrons and protons. The non-vanishing classical lepto-pion field is in fact more or less equivalent with the presence of classical Z^0 field.
2. The amplitude for the production of lepto-pion with four momentum $p = (p_0, \vec{p})$ in an external electromagnetic field can be deduced by writing lepto-pion field as sum of classical and quantum parts: $\pi_L = \pi_L(class) + \pi_L(quant)$ and by decomposing the mass term into interaction term plus c-number term and standard mass term:

$$\begin{aligned} \frac{m^2(\pi_L)\pi_L^2}{2} &= L_{int} + L_0 , \\ L_0 &= \frac{m^2(\pi_L)}{2}(\pi_L^2(class) + \pi_L^2(quant)) , \\ L_{int} &= m^2(\pi_L)\pi_L(class)\pi_L(quant) . \end{aligned} \quad (7.2.8)$$

Interaction Lagrangian corresponds to L_{int} linear in lepto-pion oscillator operators. Using standard LSZ reduction formula and normalization conventions of [28] one obtains for the probability amplitude for creating lepto-pion of momentum p from vacuum the expression

$$\begin{aligned} A(p) &\equiv \langle a(p)\pi_L \rangle = (2\pi)^3 m^2(\pi_L) \int f_p(x) \langle vac | \pi | vac \rangle d^4x , \\ f_p &= e^{ip \cdot x} . \end{aligned} \quad (7.2.8)$$

The probability for the production of lepto-pion in phase space volume element d^3p is obtained by multiplying with the density of states factor $d^3n = V \frac{d^3p}{(2\pi)^3}$:

$$\begin{aligned} dP &= A|U|^2 V d^3p , \\ A &= \left(\frac{\alpha_{em} N_c^2 m^2(\pi_L)}{2\pi f(\pi_L)} \right)^2 , \\ U &= \int e^{ip \cdot x} E \cdot B d^4x . \end{aligned} \quad (7.2.7)$$

The first conclusion that one can draw is that nonstatic electromagnetic fields are required for lepto-pion creation since in static fields energy conservation forces lepto-pion to have zero energy and thus prohibits real lepto-pion production. In particular, the spontaneous creation lepto-pion in static Coulombic and magnetic dipole fields of nucleus is impossible.

7.2.7 Sigma model and creation of lepto-hadrons in electromagnetic fields

Why sigma model approach?

For several reasons it is necessary to generalize the model for lepto-pion production to a model for lepto-hadron production.

1. Sigma model approach is necessary if one assumes that anomalous e^+e^- pairs are genuine e^+e^- pairs rather lepto-nucleon pairs produced in the decays of lepto-sigmas.
2. A model for the production of lepto-hadrons is obtained from an effective action describing the strong and electromagnetic interactions between lepto-hadrons. The simplest model is sigma model describing the interaction between lepto-nucleons, lepto-pion and a hypothetical scalar particle σ_L [28]. This model realizes lepto-pion field as a divergence of the axial current and gives the standard relation between $f(\pi_L)$, g and m_{ex} . All couplings of the model are related to the masses of e_{ex} , π_L and σ_L . The generation of lepto-pion vacuum expectation value in the proposed manner takes place via triangle anomaly diagrams in the external electromagnetic field.
3. If needed the model can be generalized to contain terms describing also other lepto-hadrons. The generalized model should contain also vector bosons ρ_L and ω_L as well as pseudoscalars η_L and η'_L and radial excitations of π_L and σ_L . An open question is whether also η and η' generate vacuum expectation value proportional to $E \cdot B$. Actually all these states appear as 3-fold degenerate for the minimal color representation content of the theory.
4. The following observations are useful for what follows.
 - (a) Orthopositronium decay width anomaly gives the estimate $f(\pi_L) \sim N_c \cdot 7.9 \text{ keV}$ and from this one can deduce an upper bound for lepto-pion production cross section in an external electromagnetic field. The calculation of lepto-pion production cross section shows that lepto-pion production cross section is somewhat smaller than the upper bound for the observed anomalous e^+e^- production cross section, even when one tunes the values of the various parameters. This is consistent with the idea that lepto-nucleon pairs, with lepto-nucleon mass being only slightly larger than electron mass, are in question.
 - (b) Also the direct production of the lepto-nucleon pairs via the interaction term $g \cos(\theta_e) \bar{e}_{ex} \gamma_5 e_{ex} \pi_L (cl)$ is possible but gives rise to continuum mass squared spectrum rather than resonant structures. The direct production of the pairs via the interaction term $g \sin(\theta_e) \bar{e} \gamma_5 e_{ex} \pi_L (cl)$ from is much slower process than the production via the meson decays and does not give rise to resonant structures since Also the production via the $\bar{e} e_{ex}$ decay of virtual lepto-pion created from classical field is slow process since it involves $\sin^2(\theta_e)$.
 - (c) e^+e^- production can also proceed also via the creation of many particle states. The simplest candidates are $V_L + \pi_L$ states created via $\partial_\alpha \pi_L V^\alpha \pi_L (class)$ term in action and $\sigma_L + \pi_L$ states created via the the $k \sigma_L \pi_L \pi_L (class)$ term in the sigma model action. The production cross section via the decays of vector mesons is certainly very small since the production vertex involves the inner product of vector boson 3 momentum with its polarization vector and the situation is non-relativistic.
 - (d) If the strong decay of σ_L to lepto-mesons is kinematically forbidden (this is not suggested by the experience with the ordinary hadron physics), the production rate for σ_L meson is large since the coupling k turns out to be given by $k = (m_{\sigma_L}^2 - m_{\pi_L}^2)/2f(\pi_L)$ and is anomalously large for the value of $f(\pi_L) \geq 7.9 \cdot N_c \text{ keV}$ derived from orthopositronium anomaly: $k \sim 336m(\pi_L)/N_c$ for $f(\pi_L) \sim N_c \cdot 7.9 \text{ keV}$. The resulting additional factor in the production cross section compensates the reduction factor coming from two-particle phase space volume. Despite this the estimate for the production cross section of anomalous e^+e^- pairs is roughly by a factor $1/N_c^2$ smaller than the maximum experimental cross section. The radiative corrections are huge and should give the dominant contribution to the cross section. It is however questionable very the assumed small lepto-hadronic decay width and mass of σ_L is consistent with the extremely strong interactions of σ_L .

Simplest sigma model

A detailed description of the sigma model can be found in [28] and it suffices to outline only the crucial features here.

1. The action of lepto-hadronic sigma model reads as

$$\begin{aligned}
L &= L_S + c\sigma_L , \\
L_S &= \bar{\psi}_L(i\gamma^k\partial_k + g(\sigma_L + i\pi_L \cdot \tau\gamma_5))\psi_L + \frac{1}{2}((\partial\pi_L)^2 + (\partial\sigma_L)^2) \\
&\quad - \frac{\mu^2}{2}(\sigma_L^2 + \pi_L^2) - \frac{\lambda}{4}(\sigma_L^2 + \pi_L^2)^2 .
\end{aligned} \tag{7.2.6}$$

π_L is isospin triplet and σ_L isospin singlet. ψ_L is isospin doublet with electro-weak quantum numbers of electron and neutrino (e_{ex} and ν_{ex}). The model allows $so(4)$ symmetry. Vector current is conserved but for $c \neq 0$ axial current generates divergence, which is proportional to pion field: $\partial^\alpha A_\alpha = -c\pi_L$.

2. The presence of the linear term implies that σ_L field generates vacuum expectation value $\langle 0|\sigma_L|0\rangle = v$. When the action is written in terms of new quantum field $\sigma'_L = \sigma_L - v$ one has

$$\begin{aligned}
L &= \bar{\psi}_L(i\gamma^k\partial_k + m + g(\sigma'_L + i\pi_L \cdot \tau\gamma_5))\psi_L + \frac{1}{2}((\partial\pi_L)^2 + (\partial\sigma'_L)^2) \\
&\quad - \frac{1}{2}m_{\sigma_L}^2(\sigma'_L)^2 - \frac{m_{\pi_L}^2}{2}\pi_L^2 \\
&\quad - \lambda v\sigma'_L((\sigma'_L)^2 + \pi_L^2) - \frac{\lambda}{4}((\sigma'_L)^2 + \pi_L^2)^2 ,
\end{aligned} \tag{7.2.4}$$

The masses are given by

$$\begin{aligned}
m_{\pi_L}^2 &= \mu^2 + \lambda v^2 , \\
m_{\sigma_L}^2 &= \mu^2 + 3\lambda v^2 , \\
m &= -gv .
\end{aligned} \tag{7.2.3}$$

These formulas relate the parameters μ, v, g to lepto-hadrons masses.

3. The requirement that σ'_L has vanishing vacuum expectation implies in Born approximation

$$c - \mu^2 v - \lambda v^3 = 0 , \tag{7.2.4}$$

which implies

$$\begin{aligned}
f(\pi_L) &= -v = -\frac{c}{m^2(\pi_L)} , \\
m_{ex} &= gf(\pi_L) .
\end{aligned} \tag{7.2.4}$$

Note that e_{ex} and ν_{ex} are predicted to have identical masses in this approximation. The value of the strong coupling constant g of lepto-hadronic physics is indeed strong from $m_{ex} > m_e$ and $f(\pi_L) < N_c \cdot 10$ keV.

4. A new feature is the generation of the lepto-pion vacuum expectation value in an external electromagnetic field (of course, this is possible for the ordinary pion field, too!). The vacuum expectation is generated via the triangle anomaly diagram in a manner identical to the generation of a non-vanishing photon-photon decay amplitude and is proportional to the instanton density of the electromagnetic field. By redefining the pion field as a sum $\pi_L = \pi_L(cl) + \pi'_L$ one obtains effective action describing the creation of the lepto-hadrons in strong electromagnetic fields.
5. As far as the production of $\sigma_L\pi_L$ pairs is considered, the interaction term $\lambda v\sigma'_L\pi_L^2$ is especially interesting since it leads to the creation of $\sigma_L\pi_L$ pairs via the interaction term $k\lambda v\sigma'_L\pi_L(qu)\pi_L(cl)$. The coefficient of this term can be expressed in terms of the lepto-meson masses and $f(\pi_L)$:

$$\begin{aligned}
 k &\equiv 2\lambda v = \frac{m_{\sigma_L}^2 - m_{\pi_L}^2}{2f(\pi_L)} = xm_{\pi_L} \ , \\
 x &= \frac{1}{2} \left(\frac{m_{\sigma_L}^2}{m_{\pi_L}^2} - 1 \right) \frac{m_{\pi_L}}{f(\pi_L)} \ .
 \end{aligned}
 \tag{7.2.4}$$

The large value of the coupling deriving from $f(\pi_L) = N_c \cdot 7.9 \text{ keV}$ compensates the reduction of the production rate coming from the smallness of two-particle phase space volume as compared with single particle-phase space volume but fails to produce large enough production cross section. The large value of $g(\sigma_L, \sigma_L, \sigma_L) = g(\sigma_L, \pi_L, \pi_L)$ however implies that the radiative contribution to the production cross section coming from the emission of a virtual sigma in the production vertex is much larger than the lowest order production cross section and with a rather small value of the relative $\sigma_L - \pi_L$ mass difference correct order of magnitude of cross section should be possible.

7.2.8 Classical model for lepto-pion production

The nice feature of both quantum and classical model is that the production amplitudes associated with all lepto-hadron production reactions in external electromagnetic field are proportional to the lepto-pion production amplitude and apart from phase space volume factors production cross sections are expected to be given by lepto-pion production cross section. Therefore it makes sense to construct a detailed model for lepto-pion production despite the fact that lepto-pion decays probably contribute only a very small fraction to the observed e^+e^- pairs.

General considerations

Angular momentum barrier makes the production of lepto-mesons with orbital angular momentum $L > 0$ improbable. Therefore the observed resonances are expected to be $L = 0$ pseudoscalar states. Lepto-pion production has two signatures which any realistic model should reproduce.

1. Data are consistent with the assumption that states are produced at rest in cm frame.
2. The production probability has a peak in a narrow region of velocities of colliding nucleus around the velocity needed to overcome Coulomb barrier in head on collision. The relative width of the velocity peak is of order $\Delta\beta/\beta \simeq \cdot 10^{-2}$ [55]. In Th-Th system [70] two peaks at projectile energies 5.70 MeV and 5.75 MeV per nucleon have been observed. This suggests that some kind of diffraction mechanism based on the finite size of nuclei is at work.
In this section a model treating nuclei as point like charges and nucleus-nucleus collision purely classically is developed. This model yields qualitative predictions in agreement with the signature 1) but fails to reproduce the possible diffraction behavior although one can develop argument for understanding the behavior above Coulomb wall.

The general expression for the amplitude for creation of lepton in external electric and magnetic fields has been derived in Appendix. Let us now specialize to the case of heavy ion collision. We consider the situation, where the scattering angle of the colliding nucleus is measured. Treating the collision completely classically we can assume that collision occurs with a well defined value of the

impact parameter in a fixed scattering plane. The coordinates are chosen so that target nucleus is at rest at the origin of the coordinates and colliding nucleus moves in z-direction in $y=0$ plane with velocity β . The scattering angle of the scattered nucleus is denoted by α , the velocity of the lepton by v and the direction angles of lepton velocity by (θ, ϕ) .

The minimum value of the impact parameter for the Coulomb collision of point like charges is given by the expression

$$\begin{aligned} b &= \frac{b_0 \cot(\alpha/2)}{2} , \\ b_0 &= \frac{2Z_1 Z_2 \alpha_{em}}{M_R \beta^2} , \end{aligned} \quad (7.2.4)$$

where b_0 is the expression for the distance of the closest approach in head on collision. M_R denotes the reduced mass of the nucleus-nucleus system.

To estimate the amplitude for lepton production the following simplifying assumptions are made.

1. Nuclei can be treated as point like charges. This assumption is well motivated, when the impact parameter of the collision is larger than the critical impact parameter given by the sum of radii of the colliding nuclei:

$$b_{cr} = R_1 + R_2 . \quad (7.2.5)$$

For scattering angles that are sufficiently large the values of the impact parameter do not satisfy the above condition in the region of the velocity peak. p-Adic considerations lead to the conclusion that nuclear condensation level corresponds to prime $p \sim 2^k$, $k = 113$ (k is prime). This suggest that nuclear radius should be replaced by the size $L(113)$ of the p-adic convergence cube associated with nucleus (see the chapter "TGD and Nuclear Physics": $L(113) \sim 1.7 \cdot 10^{-14} m$ implies that cutoff radius is $b_{cr} \sim 2L(113) \sim 3.4 \cdot 10^{-14} m$.

2. Since the velocities are non-relativistic (about $0.12c$) one can treat the motion of the nuclei non-relativistically and the non-retarded electromagnetic fields associated with the exactly known classical orbits can be used. The use of classical orbit doesn't take into account recoil effect caused by lepton production. Since the mass ratio of lepton and the reduced mass of heavy nucleus system is of order 10^{-5} the recoil effect is however negligible.
3. The model simplifies considerably, when the orbit is idealized with a straight line with impact parameter determined from the condition expressing scattering angle in terms of the impact parameter. This approximation is certainly well founded for large values of impact parameter. For small values of impact parameter the situation is quite different and an interesting problem is whether the contributions of long range radiation fields created by accelerating nuclei in head-on collision could give large contribution to lepton production rate. On the line connecting the nuclei the electric part of the radiation field created by first nucleus is indeed parallel to the magnetic part of the radiation field created by second nucleus. In this approximation the instanton density in the rest frame of the target nucleus is just the scalar product of the Coulombic electric field E of the target nucleus and of the magnetic field B of the colliding nucleus obtained by boosting it from the Coulomb field of nucleus at rest.

Expression of the classical cross section

First some kinematical notations. lepton four-momentum in the rest system of target nucleus is given by the following expression

$$\begin{aligned} p &= (p_0, \vec{p}) = m\gamma_1(1, v\sin(\theta)\cos(\phi), v\sin(\theta)\sin(\phi), v\cos(\theta)) , \\ \gamma_1 &= 1/(1-v^2)^{1/2} . \end{aligned} \quad (7.2.5)$$

The velocity and Lorentz boost factor of the projectile nucleus are denoted by β and $\gamma = 1/\sqrt{1-\beta^2}$. The double differential cross section in the classical model can be written as

$$\begin{aligned}
 d\sigma &= dP 2\pi b db , \\
 dP &= K |A(b,p)|^2 d^3n , \text{ per } d^3n = V \frac{d^3p}{(2\pi)^3} , \\
 K &= (Z_1 Z_2)^2 (\alpha_{em})^4 \times N_c^2 \left(\frac{m(\pi_L)}{f(\pi_L)} \right)^2 \frac{1}{2\pi^{13}} , \\
 A(b,p) &= N_0 \frac{4\pi}{Z_1 Z_2 \alpha_{em}} \times U(b,p) , \\
 U(b,p) &= \int e^{ip \cdot x} E \cdot B d^4x , \\
 N_0 &= \frac{(2\pi)^7}{i} .
 \end{aligned} \tag{7.2.1}$$

where b denotes impact parameter. The formula generalizes the classical formula for the cross section of Coulomb scattering. In the calculation of the total cross section one must introduce some cutoff radii and the presence of the volume factor V brings in the cutoff volume explicitly (particle in the box description for leptopions). Obviously the cutoff length must be longer than leptopion Compton length. Normalization factor N_0 has been introduced in order to extract out large powers of 2π .

From this one obtains differential cross section as

$$\begin{aligned}
 d\sigma &= P 2\pi b db , \\
 P &= \int K |A(b,p)|^2 V \frac{d^3p}{(2\pi)^3} , .
 \end{aligned} \tag{7.2.1}$$

The first objection is the need to explicitly introduce the reaction volume: this obviously breaks manifest Lorentz invariance. The cross section was estimated in the earlier version of the model [26] and turned to be too small by several orders of magnitude. This inspired the idea that constructive interference for the production amplitudes for different values of impact parameter could increase the cross section.

7.2.9 Quantum model for leptopion production

There are good reasons for considering the quantum model. First, the leptopion production cross section is by several orders of magnitude too small in classical model. Secondly, in Th-Th collisions there are indications about the presence of two velocity peaks with separation $\delta\beta/\beta \sim 10^{-2}$ [55] and this suggests that quantum mechanical diffraction effects might be in question. These effects could come from the upper and/or lower length scale cutoff and from the delocalization of the wave function of incoming nucleus.

The question is what quantum model means. The most natural thing is to start from Coulomb scattering and multiply Coulomb scattering amplitude for a given impact parameter value b with the amplitude for leptopion production. This because the classical differential cross section given by $2\pi b db$ in Coulomb scattering equals to the quantum cross section. One might however argue that on basis of $S = 1 + T$ decomposition of S-matrix the lowest order contribution to leptopion production in quantum situation corresponds to the absence of any scattering. The leptopion production amplitude is indeed non-vanishing also for the free motion of nuclei. The resolution of what looks like a paradox could come from many-sheeted space-time concept: if no scattering occurs, the space-time sheets representing colliding nuclei do not touch and all and there is no interference of em fields so that there is no leptopion production. It turns however that lowest order contribution indeed corresponds to the absence of scattering in the model that works.

Two possible approaches

One can imagine two approaches to the construction of the model for production amplitude in quantum case.

The first approach is based on eikonal approximation [29]. Eikonal approximation applies at high energy limit when the scattering angle is small and one can approximate the orbit of the projectile with a straight orbit.

The expression for the scattering amplitude in eikonal approximation reads as

$$\begin{aligned} f(\theta, \phi) &= \frac{k}{2\pi i} \int d^2b \exp(-ik \cdot b) \exp(i\xi(b)) - 1 , \\ \xi(b) &= \frac{-m}{k\hbar^2} \int_{z=-\infty}^{z=\infty} dz V(z, b) , \\ \frac{d\sigma}{d\Omega} &= |f^2| . \end{aligned} \quad (7.2.0)$$

as one expands the exponential in lowest in spherically symmetric potential order one obtains the

$$f(\theta, \phi) \simeq -\frac{m}{2\pi\hbar^2} \int J_0(k_T b) \xi(b) b db . \quad (7.2.0)$$

The challenge is to find whether it is possible to generalize this expression so that it applies to the production of leptopions.

1. The simplest guess is that one should multiply the eikonal amplitude with the dimensionless amplitude $A(b)$:

$$\begin{aligned} f(\theta, \phi) &\rightarrow f(\theta, \phi, p) = \frac{k}{2\pi i} \int d^2b \exp(-ik \cdot b) \exp(i\xi(b)) - 1 A(b, p) \\ &\simeq -\frac{m}{2\pi\hbar^2} \int J_0(k_T b) \xi(b) A(b, p) b db . \end{aligned} \quad (7.2.0)$$

2. Amplitude squared must give differential cross section for leptopion production and scattering

$$\begin{aligned} d\sigma &= |f(\theta, \phi, p)|^2 d\Omega d^3n , \\ d^3n &= V d^3p . \end{aligned} \quad (7.2.0)$$

This requires an explicit introduction of a volume factor V via a spatial cutoff. This cutoff is necessary for the coordinate z in the case of Coulomb potential, and would have interpretation in terms of a finite spatio-temporal volume in which the space-time sheets of the colliding particles are in contact and fields interfere.

3. There are several objections against this approach. The loss of a manifest relativistic invariance in the density of states factor for leptopion does not look nice. One must keep count about the scattering of the projectile which means a considerable complication from the point of view of numerical calculations. In classical picture for orbits the scattering angle in principle is fixed once impact parameter is known so that the introduction of scattering angles does not look logical.

Second approach starts from the classical picture in which each impact parameter corresponds to a definite scattering angle so that the resulting amplitude describes leptopion production amplitude and says nothing about the scattering of the projectile. This approach is more in spirit with TGD since classical physics is exact part of quantum TGD and classical orbit is absolutely real from the point of view of leptopion production amplitude.

1. The counterpart of the eikonal exponent has interpretation as the exponent of classical action associated with the Coulomb interaction

$$S(b) = \int_{\gamma} V ds \quad (7.2.1)$$

along the orbit γ of the particle, which can be taken also as a real classical orbit but will be approximated with rectilinear orbit in sequel.

2. The first guess for the production amplitude is

$$\begin{aligned} f(p) &= \int d^2b \exp(-i\Delta k(b) \cdot b) \exp\left[\frac{i}{\hbar} S(b)\right] A(b, p) \\ &= \int J_0(k_T(b)b) \left(1 + \frac{i}{\hbar} \int_{z=-a}^{z=a} dz V(z, b) + \dots\right) A(b, p) . \end{aligned} \quad (7.2.1)$$

Δk is the change of the momentum in the classical scattering and in the scattering plane. The cutoff $|z| \leq a$ in the longitudinal direction corresponds to a finite imbedding space volume inside which the space-time sheets of target and projectile are in contact.

3. The production amplitude is non-trivial even if the interaction potential vanishes being given by

$$f(p) = \int d^2b \exp(-ik \cdot b) A(b, p) = 2\pi i n t J_0(k_T(b)b) \times A(b, p) b db . \quad (7.2.2)$$

This formula can be seen as a generalization of quantum formula in the sense that incoherent integral over production probabilities at various values of b is replaced by an integral over production amplitude over b so that interference effects become possible.

4. This result could be seen as a problem. On basis of $S = 1 + iT$ decomposition corresponding to free motion and genuine interaction, one could argue that since the exponent of action corresponds to S , $A(p, b)$ vanishes when the space-time sheets are not in contact. The improved guess for the amplitude is

$$\begin{aligned} f(p) &= \int d^2b \exp(-ik \cdot b) \exp\left(\frac{i}{\hbar} S(b)\right) A(b, p) \\ &= \int J_0(k_T(b)b) \left(\frac{i}{\hbar} \int_{z=-a}^{z=a} V(z, b) + \dots\right) A(b, p) . \end{aligned} \quad (7.2.2)$$

This would mean that there would be no classical limit when coherence is assumed to be lost. At this stage one must keep mind open for both options.

5. The dimension of $f(p)$ is L^2/\hbar

$$d\sigma = |f(p)|^2 \frac{d^3p}{2E_p (2\pi)^3} . \quad (7.2.3)$$

has correct dimension. This model will be considered in sequel. The earlier work in [26] was however based on the first option.

Production amplitude

The Fourier transform of $E \cdot B$ can be expressed as a convolution of Fourier transforms of E and B and the resulting expression for the amplitude reduces by residue calculus (see APPENDIX) to the following general form

$$\begin{aligned} A(b, p) &\equiv N_0 \times \frac{4\pi}{Z_1 Z_2 \alpha_{em}} \times U(b, p) = 2\pi i (CUT_1 + CUT_2) , \\ N_0 &= \frac{(2\pi)^7}{i} . \end{aligned} \quad (7.2.3)$$

where nuclear charges are such that Coulomb potential is $1/r$. The motivation for the strange looking notation is to extract all powers of 2π so that the resulting amplitudes contain only factors of order unity.

The contribution of the first cut for $\phi \in [0, \pi/2]$ is given by the expression

$$\begin{aligned} CUT_1 &= D_1 \times \int_0^{\pi/2} \exp\left(-\frac{b}{b_0} \cos(\psi)\right) A_1 d\psi , \\ D_1 &= -\frac{1}{2} \frac{\sin(\phi)}{\sin(\theta)} , \quad b_0 = \frac{\hbar \beta \gamma}{m \gamma_1} , \\ A_1 &= \frac{A + iB \cos(\psi)}{\cos^2(\psi) + 2iC \cos(\psi) + D} , \\ A &= \sin(\theta) \cos(\phi) , \quad B = K , \\ C &= K \frac{\cos(\phi)}{\sin(\theta)} , \quad D = -\sin^2(\phi) - \frac{K^2}{\sin^2(\theta)} , \\ K &= \beta \gamma \left(1 - \frac{v_{cm}}{\beta} \cos(\theta)\right) , \quad v_{cm} = \frac{2v}{1+v^2} . \end{aligned} \quad (7.2.-2)$$

The definitions of the various kinematical variables are given in previous formulas. The notation is tailored to express the facts that A_1 is rational function of $\cos(\psi)$ and that integrand depends exponentially on the impact parameter.

The expression for CUT_2 reads as

$$\begin{aligned} CUT_2 &= D_2 \times \int_0^{\pi/2} \exp\left(i \frac{b}{b_1} \cos(\psi)\right) A_2 d\psi , \\ D_2 &= -\frac{\sin(\frac{\phi}{2})}{u \sin(\theta)} \times \exp\left(-\frac{b}{b_2}\right) , \\ b_1 &= \frac{\hbar \beta}{m \gamma_1} , \quad b_2 = \frac{\hbar}{mb \gamma_1 \times \sin(\theta) \cos(\phi)} \\ A_2 &= \frac{A \cos(\psi) + B}{\cos^2(\psi) + C \cos(\psi) + D} , \\ A &= \sin(\theta) \cos(\phi) u , \quad B = \frac{w}{v_{cm}} + \frac{v}{\beta} \sin^2(\theta) [\sin^2(\phi) - \cos^2(\phi)] , \\ C &= 2i \frac{\beta w \cos(\phi)}{u v_{cm} \sin(\theta)} , \quad D = -\frac{1}{u^2} \left(\frac{\sin^2(\phi)}{\gamma^2} + \beta^2 (v^2 \sin^2(\theta) - \frac{2vw}{v_{cm}}) \cos^2(\phi)\right) \\ &\quad + \frac{w^2}{v_{cm}^2 u^2 \sin^2(\theta)} + 2i \frac{\beta v}{u} \sin(\theta) \cos(\phi) , \\ u &= 1 - \beta v \cos(\theta) , \quad w = 1 - \frac{v_{cm}}{\beta} \cos(\theta) . \end{aligned} \quad (7.2.-8)$$

$$(7.2.-7)$$

The denominator X_2 has no poles and the contribution of the second cut is therefore always finite. Again the expression is tailored to make clear the functional dependence of the integrand on $\cos(\psi)$

and on impact parameter. Besides this the exponential damping makes in non-relativistic situation the integrand small everywhere except in the vicinity of $\cos(\Psi) = 0$ and for small values of the impact parameter.

Using the symmetries

$$\begin{aligned} U(b, p_x, -p_y) &= -U(b, p_x, p_y) , \\ U(b, -p_x, -p_y) &= \bar{U}(b, p_x, p_y) , \end{aligned} \quad (7.2-7)$$

of the amplitude one can calculate the amplitude for other values of ϕ .

CUT_1 gives the singular contribution to the amplitude. The reason is that the factor X_1 appearing in denominator of cut term vanishes, when the conditions

$$\begin{aligned} \cos(\theta) &= \frac{\beta}{v_{cm}} , \\ \sin(\phi) &= \cos(\psi) , \end{aligned} \quad (7.2-7)$$

are satisfied. In forward direction this condition tells that z- component of the lepton momentum in velocity center of mass coordinate system vanishes. In laboratory this condition means that the lepton moves in certain cone defined by the value of its velocity. The condition is possible to satisfy only above the threshold $v_{cm} \geq \beta$.

For $K = 0$ the integral reduces to the form

$$CUT_1 = \frac{1}{2} \cos(\phi) \sin(\phi) \lim_{\varepsilon \rightarrow 0} \frac{\int_0^{\pi/2} \exp\left(-\frac{\cos(\psi)}{\sin(\phi_0)}\right) d\psi}{(\sin^2(\phi) - \cos^2\psi + i\varepsilon)} . \quad (7.2-7)$$

One can estimate the singular part of the integral by replacing the exponent term with its value at the pole. The integral contains two parts: the first part is principal value integral and second part can be regarded as integral over a small semicircle going around the pole of integrand in upper half plane. The remaining integrations can be performed using elementary calculus and one obtains for the singular cut contribution the approximate expression

$$\begin{aligned} CUT_1 &\simeq e^{-(b/a)(\sin(\phi)/\sin(\phi_0))} \left(\frac{\ln(X)}{2} + \frac{i\pi}{2} \right) , \\ X &= \frac{((1+s)^{1/2} + (1-s)^{1/2})}{((1+s)^{1/2} - (1-s)^{1/2})} , \\ s &= \sin(\phi) , \\ \sin(\phi_0) &= \frac{\beta\gamma}{\gamma_1 m(\pi_L) a} . \end{aligned} \quad (7.2-9)$$

The principal value contribution to the amplitude diverges logarithmically for $\phi = 0$ and dominates over 'pole' contribution for small values of ϕ . For finite values of impact parameter the amplitude decreases exponentially as a function of ϕ .

If the singular term appearing in CUT_1 indeed gives the dominant contribution to the lepton production one can make some conclusions concerning the properties of the production amplitude. For given lepton cm velocity v_{cm} the production associated with the singular peak is predicted to occur mainly in the cone $\cos(\theta) = \beta/v_{cm}$: in forward direction this corresponds to the vanishing of the z-component of the lepton momentum in velocity center of mass frame. Since the values of $\sin(\theta)$ are of order .1 the transversal momentum is small and production occurs almost at rest in cm frame as observed. In addition, the singular production cross section is concentrated in the production plane ($\phi = 0$) due to the exponential dependence of the singular production amplitude on the angle ϕ and impact parameter and the presence of the logarithmic singularity. The observed lepton velocities are in the range $\Delta v/v \simeq 0.2$ [55] and this corresponds to the angular width $\Delta\theta \simeq 34$ degrees.

Differential cross section in the quantum model

There are two options to consider depending on whether one uses $\exp(iS)$ or $\exp(iS) - 1$ to define the production amplitude.

1. For the $\exp(iS)$ option the expression for the differential cross section reads in the lowest order as

$$\begin{aligned} d\sigma &= K |f_B|^2 \frac{d^3p}{2E_p} , \\ f_B &\simeq i \int \exp(-i\Delta k \cdot r) (CUT_1 + CUT_2) bdbdzd\phi , \\ K &= (Z_1 Z_2)^2 \alpha_{em}^4 N_c^2 \left(\frac{m(\pi_L)}{f(\pi_L)} \right)^2 \frac{1}{(2\pi)^{15}} . \end{aligned} \quad (7.2.-10)$$

Here Δk is the momentum exchange in Coulomb scattering and a vector in the scattering plane so that the above described formula is obtained for the linear orbits.

2. For the $\exp(iS) - 1$ option the differential production cross section for leptopion is in the lowest non-trivial approximation for the exponent of action S given by the expression

$$\begin{aligned} d\sigma &= K |f_B|^2 \frac{d^3p}{2E_p} , \\ f_B &\simeq \int \exp(-i\Delta k \cdot r) V(z, b) (CUT_1 + CUT_2) bdbdzd\phi , \\ V(z, b) &= \frac{1}{r} , \\ K &= (Z_1 Z_2)^4 \alpha_{em}^6 N_c^2 \left(\frac{m(\pi_L)}{f(\pi_L)} \right)^2 \frac{1}{(2\pi)^{15}} . \end{aligned} \quad (7.2.-12)$$

Effectively the Coulomb potential is replaced with the product of the Coulomb potential and leptopion production amplitude $A(b, p)$. Since α_{em} is assumed to correspond to relate to its standard value by a scaling \hbar_0/\hbar factor.

3. Coulomb potential brings in an additional $(Z_1 Z_2 \alpha_{em})^2$ factor to the differential cross section, which in the case of heavy ion scattering increases the contribution to the cross section by a factor of order 3×10^3 but reduces it by a factor of order 5×10^{-5} in the case of proton-antiproton scattering. The increase of \hbar expected to be forced by the requirement that perturbation theory is not lost however reduces the contribution from higher orders in V . It should be possible to distinguish between the two options on basis of these differences.

The scattering amplitude can be reduced to a simpler form by using the defining integral representation

$$J_0(x) = \frac{1}{2\pi} \int_0^{2\pi} \exp(-ix \sin(\phi)) d\phi$$

of Bessel functions.

1. For $\exp(iS)$ option this gives

$$\begin{aligned} f_B &= 2\pi i \int J_0(\Delta k b) (CUT_1 + CUT_2) bdb , \\ \Delta k &= 2k \sin\left(\frac{\alpha}{2}\right) , \quad k = M_R \beta , \\ M_R &\simeq A_R m_p , \quad A_R = \frac{A_1 A_2}{A_1 + A_2} , \end{aligned} \quad (7.2.-13)$$

where the length scale cutoffs in various integrations are not written explicitly. The value of α can be deduced once the value of impact parameter is known in the case of the classical Coulomb scattering.

2. For $\exp(iS) - 1$ option one has

$$\begin{aligned} f_B &= 2\pi i \int F(b) J_0(\Delta kb) (CUT_1 + CUT_2) b db , \\ F(b \geq b_{cr}) &= 2 \int dz \frac{1}{\sqrt{z^2 + b^2}} = \ln\left(\frac{\sqrt{a^2 - b^2} + a}{b}\right) , \end{aligned} \quad (7.2.-14)$$

Note that the factors K appearing in the different cross section are different in these two cases.

Calculation of the lepton production amplitude in the quantum model

The details related to the calculation of the production amplitude can be found in appendix and it suffices to describe only the general treatment here. The production amplitude of the quantum model contains integrations over the impact parameter and angle parameter ψ associated with the cut. The integrands appearing in the definition of the contributions CUT_1 and CUT_2 to the scattering amplitude have simple exponential dependence on impact parameter. The function F appearing in the definition of the scattering amplitude is a rather slow varying function as compared to the Bessel function, which allows trigonometric approximation and for small values of scattering angle equals to its value at origin. This motivates the division of the impact parameter range into pieces so that F can be approximated with its mean value inside each piece so that integration over cutoff parameters can be performed exactly inside each piece.

In Appendix the explicit expansion in power series with respect to impact parameter is derived by assuming $J_0(k_T b) \simeq 1$ and $F(b) = F = \text{constant}$. These formulas can be easily generalized by assuming a piecewise constancy of these two functions. This means that the only integration over the lepton phase space must be carried out numerically.

CUT_1 becomes also singular at $\cos(\theta) = \beta/v_{cm}$, $\cos(\psi) = \sin(\phi)$. The singular contribution of the production amplitude can be extracted by putting $\cos(\psi) = \sin(\phi)$ in the arguments of the exponent functions appearing in the amplitude so that one obtains a rational function of $\cos(\psi)$ and $\sin(\psi)$ integrable analytically. The remaining nonsingular contribution can be integrated numerically.

Formula for the production cross section

In the case of heavy ion collisions the rectilinear motion is not an excellent approximation since the anomalous events are observed near Coulomb wall and $\beta \simeq .1$ holds true. Despite this this can be taken as a first approximation.

The expression for the differential cross section for lepton production in heavy ion collisions is given by

$$d\sigma = KF^2 \left| \int (CUT_1 + CUT_2) b db \right|^2 \frac{d^3p}{2E} , \quad (7.2.-14)$$

This expression and also the expressions of the integrals of CUT_1 and CUT_2 are calculated explicitly as powers series of the impact parameter in the Appendix.

1. For $\exp(iS)$ option one has

$$\begin{aligned} K &= (Z_1 Z_2)^2 \alpha_{em}^4 N_c^2 \left[\frac{m(\pi_L)}{f(\pi_L)} \right]^2 \frac{1}{(2\pi)^{13}} , \\ F &= 1 . \end{aligned} \quad (7.2.-14)$$

2. For $\exp(iS) - 1$ option one has

$$\begin{aligned} K &= (Z_1 Z_2)^4 \alpha_{em}^6 N_c^2 \left[\frac{m(\pi_L)}{f(\pi_L)} \right]^2 \frac{1}{(2\pi)^{13}} , \\ F &= 2 \langle \ln \left(\frac{\sqrt{a^2 - b^2} + a}{b} \right) \rangle . \end{aligned} \quad (7.2.-14)$$

In the approximation that F is constant the two lowest order predictions are related by a scaling factor

$$R = (Z_1 Z_2 \alpha_{em})^2 F^2 . \quad (7.2.-13)$$

It is interesting to get a rough order of magnitude feeling about the situation assuming that the contributions of CUT_1 and CUT_2 are of order unity. For $Z_1 = Z_2 = 92$ and $m(\pi_L)/f(\pi_L) \simeq 1.5$ -as in the case of ordinary pion- one obtains following results. It must be emphasized that these estimates are extremely sensitive to the over all scaling of f_B and to the choice of the cutoff parameter a and cannot be taken too seriously.

1. From $\beta \simeq .1$ one has $b_0 \simeq .1/m(\pi_L)$. One can argue that the impact parameter cutoff $a = x b_0$ should satisfy $a \geq 1/m_{\pi_L}$ so that $x \geq 10$ should hold true.
2. For $\exp(iS) - 1$ option one has $K = 4.7 \times 10^{-6}$. From the classical model the allowed phase space volume is of order $\frac{1}{3} \Delta v^3 \sim 10^{-4}$. By using $a = m(\pi_L)$ as a cutoff and $m(\pi_L) \simeq 2m_e$ one obtains $\sigma \sim 4 \mu\text{b}$, which is of same order of magnitude as the experimental estimate $5 \mu\text{b}$.
3. For $\exp(iS)$ option one has $K = 1.2 \times 10^{-9}$ and the estimate for cross section is 1.1 nb for $a = 1/m(\pi_L)$. A correct order of magnitude is obtained by assuming $a = 5.5/m(\pi_L)$ and that a^4 scaling holds true. At larger values of impact parameter a^2 scaling sets on and would require $a \sim 30/m(\pi_L)$ which would correspond to $.36 \text{ \AA}$ and to atomic length scale. It is not possible to distinguish between the two options.
4. The singular contribution near to production plane at the cone $v_{cm} \cos(\theta) = \beta$ is expected to enhance the total cross section. The strong sensitivity of the cross section to the choice of the cutoff parameter allows to reproduce the experimental findings easily and it would be important to establish strong bounds on the value of the impact parameter.

Dominating contribution to production cross section and diffractive effects

Consider now the behavior of the dominating singular contribution to the production amplitude at the cone $\cos(\theta) = \beta/v_{cm}$ depending on b via the exponent factor . This amplitude factorizes into a product

$$\begin{aligned} f_{B,sing} &= K_0 a^2 B(\Delta k) A_{sing}(b, p) , \\ B(\Delta k) &= \int F(ax) J_0(\Delta k ax) \exp\left(-\frac{\sin(\phi)}{\sin(\phi_0)} x\right) x dx , \\ &\sim \sqrt{\frac{2}{\pi \Delta k a}} \int F(ax) \cos\left(\Delta k ax - \frac{\pi}{4}\right) \exp\left(-\frac{\sin(\phi)}{\sin(\phi_0)} x\right) \sqrt{x} dx , \\ x &= \frac{b}{a} . \end{aligned} \quad (7.2.-15)$$

The factor $A_{sing}(b, p) \equiv (4\pi/(Z_1 Z_2 \alpha_{em}) U_{sing}(b, p)$ is the analytically calculable singular and dominating part of the leptopion production amplitude (see appendix) with the exponential factor excluded. The factor B is responsible for diffractive effects. The contribution of the peak to the total production cross section is of same order of magnitude as the classical production cross section.

At the peak $\phi \sim 0$ the contribution the exponent of the production amplitude is constant at this limit one obtains product of the Fourier transform of Coulomb potential with cutoffs with the production amplitude. One can calculate the Fourier transform of the Coulomb potential analytically to obtain

$$\begin{aligned} f_{B,sing} &\simeq 4\pi K_0 \frac{(\cos(\Delta ka) - \cos(\Delta kb_{cr}))}{\Delta k^2} CUT_1 \\ \Delta k &= 2\beta \sin\left(\frac{\alpha}{2}\right) . \end{aligned} \quad (7.2.-15)$$

One obtains oscillatory behavior as a function of the collision velocity in fixed angle scattering and the period of oscillation depends on scattering angle and varies in wide limits.

The relationship between scattering angle α and impact parameter in Coulomb scattering translates the impact parameter cutoffs to the scattering angle cutoffs

$$\begin{aligned} a &= \frac{Z_1 Z_2 \alpha_{em}}{M_R \beta^2} \cot(\alpha(min)/2) , \\ b_{cr} &= \frac{Z_1 Z_2 \alpha_{em}}{M_R \beta^2} \cot(\alpha(max)/2) . \end{aligned} \quad (7.2.-15)$$

This gives for the argument Δkb of the Bessel function at lower and upper cutoffs the approximate expressions

$$\begin{aligned} \Delta ka &\simeq \frac{2Z_1 Z_2 \alpha_{em}}{\beta} \sim \frac{124}{\beta} , \\ \Delta kb_{cr} &\simeq x_0 \frac{2Z_1 Z_2 \alpha_{em}}{\beta} \sim \frac{124x_0}{\beta} . \end{aligned} \quad (7.2.-15)$$

The numerical values are for $Z_1 = Z_2 = 92$ (U-U collision). What is remarkable that the argument Δka at upper momentum cutoff does not depend at all on the value of the cutoff length. The resulting oscillation at minimum scattering angle is more rapid than allowed by the width of the observed peak: $\Delta\beta/\beta \sim 3 \cdot 10^{-3}$ instead of $\Delta\beta/\beta \sim 10^{-2}$: of course, the measured value need not correspond to minimum scattering angle. The oscillation associated with the lower cutoff comes from $\cos(2M_R b_{cr} \beta \sin(\alpha/2))$ and is slow for small scattering angles $\alpha < 1/A_R \sim 10^{-2}$. For $\alpha(max)$ the oscillation is rapid: $\delta\beta/\beta \sim 10^{-3}$.

In the total production cross section integrated over all scattering angles (or finite angular range) diffractive effects disappear. This might explain why the peak has not been observed in some experiments [55].

Cutoff length scales

Consider next the constraints on the upper cutoff length scale.

1. The production amplitude turns out to decrease exponentially as a function of impact parameter b unless lepton is produced in scattering plane. The contribution of leptons produced in scattering plane however gives divergent contribution to the total cross section integrated over all impact parameter values and upper cutoff length scale a is necessary. If one considers scattering with scattering angle between specified limits this is of course not a problem of classical model.
2. Upper cutoff length scale must be longer than the Compton length of lepton.
3. Upper cutoff length scale a should be certainly smaller than the interatomic distance. For partially ionized atoms a more stringent upper bound for a is the size r of atom defined as the distance above which atom looks essentially neutral: a rough extrapolation from hydrogen atom gives $r \sim a_0/Z^{1/3} \sim 1.5 \cdot 10^{-11} m$ (a_0 is Bohr radius of hydrogen atom). Therefore cutoff scale would be between Bohr radius $a_0/Z \sim .5 \cdot 10^{-12} m$ and r . In the recent case however atoms are completely ionized so that cutoff length scale can be longer. It turns out that 10 A reproduces the empirical estimate for the cross section correctly.

Numerical estimate for the electro-pion production cross section

The numerical estimate for the electro-pion production cross section is carried out for thorium with ($Z = 90, A = 232$). The value of the collision velocity of the incoming nucleus in the rest frame of the second nucleus is taken as $\beta = .1$. From the width $\delta v/v = .2$ of velocity distribution in the same frame the upper bound $\gamma \leq 1 + \delta$, $\delta \simeq 2 \times 10^{-3}$ for the Lorentz boost factor of electro-pion in cm system is deduced. The cutoff is necessary because energy conservation is not coded to the structure of the model.

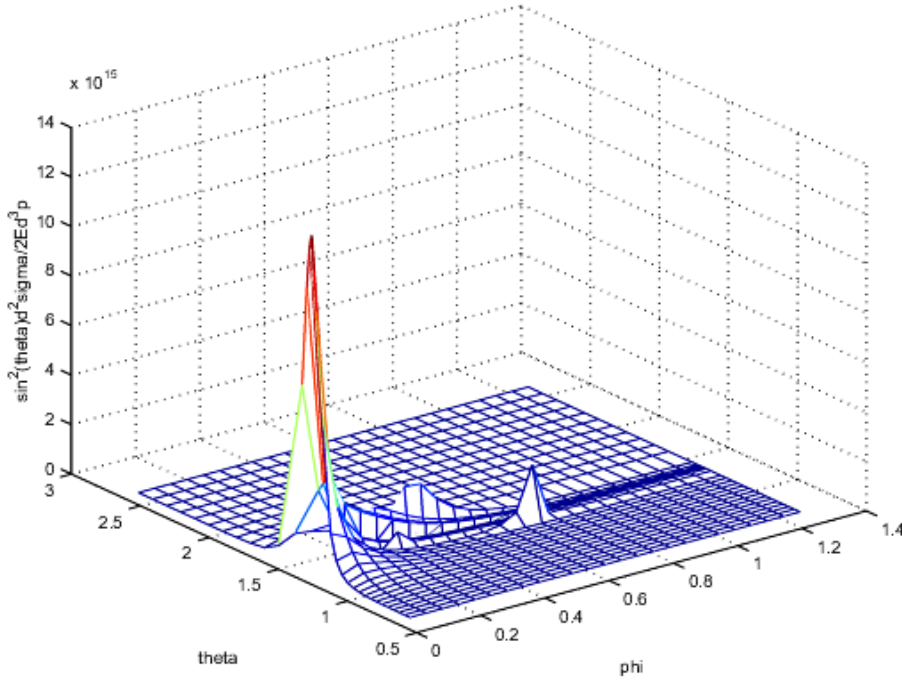


Figure 7.1: Differential cross section $\sin^2(\theta) \times \frac{d^2 \sigma}{2E d^3 p}$ for τ -pion production for $\gamma_1 = 1.0319 \times 10^3$ in the rest system of antiproton for $\delta = 1.5$. $m(\pi_\tau)$ defines the unit of energy and nb is the unit for cross section. The ranges of θ and ϕ are $(0, \pi)$ and $(0, \pi/2)$.

As expected, the singular contribution from the cone $v_{cm} \cos(\theta) = \beta$, $v_{cm} = 2v/(1 + v^2)$ gives the dominating contribution to the cross section. This contribution is proportional to the value of b_{max}^2 at the limit $\phi = 0$. Cutoff radius is taken to be $b_{max} = 150 \times \gamma_{cm} \hbar / m(\pi_e) = 1.04$ A. The numerical estimate for the cross section using the parameter values listed comes out as $\sigma = 5.6 \mu b$ to be compared with the rough experimental estimate of about $5 \mu b$. The interpretation would be that the space-time sheet associated with colliding nuclei during the collision has this transversal size in cm system. At this space-time sheet the electric and magnetic fields of the nuclei interfere.

From this one can cautiously conclude that leptopion model is consistent with both electro-pion production and τ -pion production in proton antiproton collisions. One can of course criticize the large value of impact parameter and a good justification for 1 Angstrom should be found. One could also worry about the singular character of the amplitude making the integration of total cross section somewhat risky business using the rather meager numerical facilities available. The rigorous method to calculate the contribution near the singularity relies on stepwise halving of the increment $\Delta\theta$ as one approaches the singularity. The calculation gives essentially the same result as that with constant value of $\Delta\theta$. Hence it seems that one can trust on the result of calculation.

Figure 2. gives the differential production cross section for $\gamma_1 = 1.0319$. Obviously the differential cross section is strongly concentrated at the cone due to singularity of the production amplitude for fixed b .

The important conclusion is that the same model can reproduce the value of production cross section for both electro-pions explaining the old electron-positron anomaly of heavy ion collisions and τ -pions explaining the CDF anomaly of proton-antiproton collisions at cm energy $\sqrt{s} = 1.96$ TeV (to be discussed later) with essentially same and rather reasonable assumptions (do not however forget the large maximal value of the impact parameter!).

In the case of electro-pions one must notice that depending on situation the final states are gamma pairs for the electron-pion with mass very nearly equal to electron mass. In the case of neutral tau-pion the strong decay to three p-adically scaled down versions of τ -pion proceeds faster or at least rate comparable to that for the decay to gamma pair. For higher mass variants of electro-pion for which there is evidence (for instance, one with mass 1.6 MeV) the final states are dominated by electron-positron pairs. This is true if the primary decay products are electro-baryons of form (say) $e_{ex} = e_8 \nu_8 \nu_{c,8}$ resulting via electro-strong decays instead of electrons and having slightly larger mass than electron. Otherwise the decay to gamma pair would dominate also the decays of higher mass states. A small magnetic moment type coupling between e, e_{ex} and electro-gluon field made possible by the color octet character of colored leptons induces the mixing of e and e_{ex} so that e_{ex} can transform to e by the emission of photon. The anomalous magnetic moment of electron poses restrictions on the color magnetic coupling.

$e_{ex}^+ e_{ex}^-$ pairs from leptopions or $e^+ e^-$ pairs from lepto-sigmas?

If one assumes that anomalous $e^+ e^-$ pairs correspond to lepto-nucleon pairs, then leptopion production cross section gives a direct estimate for the production rate of $e^+ e^-$ pairs. The results of the table 3 show that in case of 1.8 MeV state, the predicted cross section is roughly by a factor 5 smaller than the experimental upper bound for the cross section. Since this leptopion state is rather massive, positron decay width allows smaller $f(\pi_L)$ in this case and the production cross section could be larger than the estimate used by the $1/f(\pi_L)^2$ proportionality of the cross section. Both the simplicity and predictive power of this option and the satisfactory agreement with the experimental data suggest that this option provides the most plausible explanation of the anomalous $e^+ e^-$ pairs.

N	$Op/10^{-3}$	$\Gamma(\pi_L)/keV$	$\sigma(\pi_L)/\mu b$	$\sigma(\pi_L)/\mu b$
			$a = .01$	$a = .1$
1	1	.51	.13	1.4
3	1	.13	.04	.41
3	5	.73	.19	2.1

Table 2. The table summarizes leptopion lifetime and the upper bounds for leptopion (and lepto-nucleon pair) production cross sections for the lightest leptopion. N refers to the number of leptopion states and $Op = \Delta\Gamma/\Gamma$ refers to orthopositronium decay anomaly. The values of upper cutoff length a are in units of $10^{-10} m$.

If one assumes that anomalous $e^+ e^-$ pairs result from the decays of lepto-sigmas, the value of $e^+ e^-$ production cross section can be estimated as follows. $e^+ e^-$ pairs are produced from via the creation of $\sigma_L \pi_L$ pairs from vacuum and subsequent decay σ_L to $e^+ e^-$ pairs. The estimate for (or rather for the upper bound of) $\pi_L \sigma_L$ production cross section is obtained as

$$\begin{aligned}
 \sigma(e^+ e^-) &\simeq X \sigma(\pi_L) , \\
 X &= \frac{V_2}{V_1} \left(\frac{k m_{\sigma_L}}{m_{\pi_L}^2} \right)^2 , \\
 \frac{V_2}{V_1} &= V_{rel} = \frac{v_{12}^3}{3(2\pi)^2} \sim 1.1 \cdot 10^{-5} , \\
 \frac{k}{m_{p\pi_L}} &= \frac{(m_{\sigma}^2 - m_{\pi_L}^2)}{2m_{\pi_L} f(\pi_L)} .
 \end{aligned} \tag{7.2.-17}$$

Here V_2/V_1 of two-particle and single particle phase space volumes. V_2 is in good approximation the product $V_1(cm)V_1(rel)$ of single particle phase space volumes associated with cm coordinate and

relative coordinate and one has $V_2/V_1 \sim V_{rel} = \frac{v_{12}^3}{3(2\pi)^2} \simeq 1.1 \cdot 10^{-5}$ if the maximum value of the relative velocity is $v_{12} \sim .1$.

Situation is partially saved by the anomalously large value of $\sigma_L \pi_L \pi_L$ coupling constant k appearing in the production vertex $k \sigma_L \pi_L \pi_L$ (*class*). Production cross section is very sensitive to the value of $f(\pi_L)$ and Op anomaly $\Delta\Gamma/\Gamma = 5 \cdot 10^{-3}$ gives upper bound $2 \mu b/N_c^2$ for $a = 10^{-11} m$, which is considerably smaller than the experimental upper bound $5 \mu b$. The huge value of the $g(\pi_L, \pi_L, \sigma_L)$ and $g(\sigma_L, \sigma_L, \sigma_L)$, however implies that radiative corrections to the cross section given by σ exchange are much larger than the lowest order contribution to the cross section! If this is the case then lepto-sigma option might survive but perturbative approach probably would not make sense. On the other hand, one could argue that sigma model action should be regarded as an effective action giving only tree diagrams so that radiative corrections cannot save the situation. There are also purely physical counter arguments against lepto-sigma option: hadronic physics experience suggests that the mass of lepto-sigma is much larger than lepton mass so that lepto-sigma becomes very wide resonance decaying strongly and having negligibly small branching ratio to e^+e^- pairs.

It must be emphasized that the estimates are very rough (the replacement of the integral over the angle α with rough upper bound, estimate for the phase space volume, the values of cutoff radii, the neglect of the velocity dependence of the production cross section, the estimate for the minimum scattering angle, ...). Also the measured production cross section is subject to considerable uncertainties (even the issue whether or not anomalous pairs are produced is not yet completely settled!).

Summary

The usefulness of the modeling lepton production is that the knowledge of lepton production rate makes it possible to estimate also the production rates for other lepto-hadrons and even for many particle states consisting of lepto-hadrons using some effective action describing the strong interactions between lepto-hadrons. One can consider two basic models for lepton production. The models contain no free parameters unless one regards cutoff length scales as such. Classical model predicts the singular production characteristics of lepton. Quantum model predicts several velocity peaks at fixed scattering angle and the distance between the peaks of the production cross section depends sensitively on the value of the scattering angle. Production cross section depends sensitively on the value of the scattering angle for a fixed collision velocity. In both models the reduction of the lepton production rate above Coulomb wall could be understood as a threshold effect: for the collisions with impact parameter smaller than two times nuclear radius, the production amplitude becomes very small since $E \cdot B$ is more or less random for these collisions in the interaction region. The effect is visible for fixed sufficiently large scattering angle only. The value of the anomalous e^+e^- production cross section is of nearly the observed order of magnitude provided that e^+e^- pairs are actually lepto-nucleon pairs originating from the decays of the leptons. Alternative mechanism, in which anomalous pairs originate from the creation of $\sigma_L \pi_L$ pairs from vacuum followed by the decay $\sigma_L \rightarrow e^+e^-$ gives too small production cross section by a factor of order $1/N_c^2$ in lowest order calculation. This alternative works only provided that radiative corrections give the dominant contribution to the production rate of $\pi_L \sigma_L$ pairs as is the case if $\pi_L \sigma_L$ mass difference is of order ten per cent. The existence of at least three colored leptons and family replication provide the most plausible explanation the appearance of several peaks.

The proposed models are certainly over idealizations: in particular the approximation that nuclear motion is free motion fails for those values of the impact parameter, which are most important in the classical model. To improve the models one should calculate the Fourier transform of $E \cdot B$ using the fields of nuclei for classical orbits in Coulomb field rather than free motion. The second improvement is related to the more precise modelling of the situation at length scales below b_{cr} , where nuclei do not behave like point like charges. A peculiar feature of the model from the point of view of standard physics is the appearance of the classical electromagnetic fields associated with the classical orbits of the colliding nuclei in the definition of the quantum model. This is in spirit with Quantum TGD: Quantum TGD associates a unique space-time surface (classical history) to a given 3-surface (counterpart of quantum state).

7.3 Further developments

This section represents further developments of leptohadron model which have emerged during years after the first version of the model published in International Journal of Theoretical Physics.

7.3.1 How to observe leptonic color?

The most obvious argument against lepto-hadrons is that their production via the decay of virtual photons to lepto-mesons has not been observed in hadronic collisions. The argument is wrong. Anomalously large production of low energy e^+e^- pairs [39, 35, 36, 61] in hadronic collisions has been actually observed. The most natural source for photons and e^+e^- pairs are lepto-hadrons. There are two possibilities for the basic production mechanism.

1. Colored leptons result directly from the decay of hadronic gluons. Internal consistency excludes this alternative.
2. Colored leptons result from the decay of virtual photons. This hypothesis is in accordance with the general idea that the QCD:s associated with different condensate levels of p-adic topological condensate do not communicate. More precisely, in TGD framework leptons and quarks correspond to different chiralities of configuration space spinors: this implies that baryon and lepton numbers are conserved exactly and therefore the stability of proton. In particular, leptons and quarks correspond to different Kac Moody representations: important difference as compared with typical unified theory, where leptons and quarks share common multiplets of the unifying group. The special feature of TGD is that there are several gluons since it is possible to associate to each Kac-Moody representation gluons, which are "irreducible" in the sense that they couple only to a single Kac Moody representation. It is clear that if the physical gluons are "irreducible" the world separates into different Kac Moody representations having their own color interactions and communicating only via electro-weak and gravitational interactions. In particular, no strong interactions between leptons and hadrons occur. Since colored lepton corresponds to colored ground state of Kac-Moody representations the gluonic color coupling between ordinary lepton and colored lepton vanishes.

If this picture is correct then lepto-hadrons are produced only via the ordinary electro-weak interactions: at higher energies via the decay of virtual photon to colored lepton pair and at low energies via the emission of leptopion by photon. Consider next various manners to observe the effects of lepton color.

1. Resonance structure in the photon-photon scattering and energy near leptopion mass is a unique signature of leptopion.
2. The production of lepto-mesons in strong classical electromagnetic fields (of nuclei, for example) is one possibility. There are several important constraints for the production of leptopions in this kind of situation.
 - i) The scalar product $E \cdot B$ must be large. Faraway from the source region this scalar product tends to vanish: consider only Coulomb field.
 - ii) The region, where $E \cdot B$ has considerable size cannot be too small as compared with leptopion de Broglie wavelength (large when compared with the size of nuclei for example). If this condition doesn't hold true the plane wave appearing in Fourier amplitude is essentially constant spatially and since the fields are approximately static the Fourier component of $E \cdot B$ is expressible as a spatial divergence, which reduces to a surface integral over a surface faraway from the source region. Resulting amplitude is small since fields in faraway region have essentially vanishing $E \cdot B$.
 - iii) If fields are exactly static, then energy conservation prohibits lepto-hadron production.
3. Also the production of $e_{ex}^+e_{ex}^-$ and $e^+e_{ex}^-$ pairs in nuclear electromagnetic fields with nonvanishing $E \cdot B$ is possible either directly or as decay products of leptopions. In the direct production, the predicted cross section is small due to the presence of two-particle phase space factor. One signature of e_{ex}^- is emission line accompanying the decay $e_{ex}^- \rightarrow e^- + \gamma$. The collisions of nuclei in highly ionized (perhaps astrophysical) plasmas provide a possible source of leptobaryons.

4. The interaction of quantized em field with classical electromagnetic fields is one experimental arrangement to come into mind. The simplest arrangement consisting of linearly polarized photons with energy near leptopion mass plus constant classical em field does not however work. The direct production of $\pi_L - \gamma$ pairs in rapidly varying classical electromagnetic field with frequency near leptopion mass is perhaps a more realistic possibility. An interesting possibility is that violent collisions inside astrophysical objects could lead to gamma ray bursts via the production of pions and leptopions in rapidly varying classical E and B fields.
5. In the collisions of hadrons, virtual photon produced in collision can decay to lepto-hadrons, which in turn produce leptopions decaying to lepton-nucleon pairs. As already noticed, anomalous production of low energy e^+e^- pairs (actually lepton-nucleon pairs!) [39] in hadronic collisions has been observed.
6. $e - \nu_e$ and $e - \bar{\nu}_e$ scattering at energies below one MeV provide a unique signature of leptopion. In $e - \bar{\nu}_e$ scattering π_L appears as resonance.
7. If leptonic color coupling strength has sufficiently small value in the energy range at which lepto-hadronic QCD exists, e^+e^- annihilation at energies above few MeV should produce colored pairs and lepto-hadronic counterparts of the hadron jets should be observed. The fact that nothing like this has been observed, suggests that lepto-hadronic coupling constant evolution does not allow the perturbative QCD phase.

7.3.2 New experimental evidence

After writing this chapter astrophysical support for the notion of leptopions has appeared. There is also experimental evidence for the existence of colored muons

Could lepto-hadrons correspond to dark matter?

The proposed identification of cosmic strings (in TGD sense) as the ultimate source of both visible and dark matter discussed in [24] does not exclude the possibility that a considerable portion of topologically condensed cosmic strings have decayed to some light particles. In particular, this could be the situation in the galactic nuclei.

The idea that lepto-hadrons might have something to do with the dark matter has popped up now and then during the last decade but for some reason I have not taken it seriously. Situation changed towards the end of the year 2003. There exist now detailed maps of the dark matter in the center of galaxy and it has been found that the density of dark matter correlates strongly with the intensity of monochromatic photons with energy equal to the rest mass of electron [69].

The only explanation for the radiation is that some yet unidentified particle of mass very nearly equal to $2m_e$ decays to an electron-positron pair. Electron and positron are almost at rest and this implies a high rate for the annihilation to a pair of gamma rays. A natural identification for the particle in question would be as a leptopion (or rather, electro-pion). By their low mass leptopions, just like ordinary pions, would be produced in high abundance, in lepto-hadronic strong reactions and therefore the intensity of the monochromatic photons resulting in their decays would serve as a measure for the density of the lepto-hadronic matter. Also the presence of leptopionic condensates can be considered.

These findings force to take seriously the identification of the dark matter as lepto-hadrons. This is however not the only possibility. The TGD based model for tetra-neutrons discussed in [23] is based on the hypothesis that mesons made of scaled down versions of quarks corresponding to Mersenne prime M_{127} (ordinary quarks correspond to $k = 107$) and having masses around one MeV could correspond to the color electric flux tubes binding the neutrons to form a tetra-neutron. The same force would be also relevant for the understanding of alpha particles.

There are also good theoretical arguments for why lepto-hadrons should be dark matter in the sense of having a non-standard value of Planck constant.

1. Since particles with different Planck constant correspond to different pages of the book like structure defining the generalization of the imbedding space, the decays of intermediate gauge bosons to colored excitations of leptons would not occur and would thus not contribute to their decay widths.

2. In the case of electro-pions the large value of the coupling parameter $Z_1 Z_2 \alpha_{em} > 1$ combined with the hypothesis that a phase transition increasing Planck constant occurs as perturbative QFT like description fails would predict that electro-pions represent dark matter. Indeed, the power series expansion of the $exp(iS)$ term might well fail to converge in this case since S is proportional to $Z_1 Z_2$. For τ -pion production one has $Z_1 = -Z_2 = 1$ and in this case one can consider also the possibility that τ -pions are not dark in the sense of having large Planck constant. Contrary to the original expectations darkness does not affect the lowest order prediction for the production cross section of leptopion.

The proposed identification raises several questions.

1. Why the ratio of the leptohadronic mass density to the mass density of the ordinary hadrons would be so high, of order 7? Could an entire hierarchy of asymptotically non-free QCDs be responsible for the dark matter so that leptohadrons would explain only a small portion of the dark matter?
2. Under what conditions one can regard leptohadronic matter as a dark matter? Could short life-times of leptohadrons make them effectively dark matter in the sense that there would be no stable enough atom like structures consisting of say charged leptobaryons bound electromagnetically to the ordinary nuclei or electrons? But what would be the mechanism producing leptohadrons in this case (nuclear collisions produce leptopions only under very special conditions)?
3. What would be the role of the many-sheeted space-time: could leptohadrons and atomic nuclei reside at different space-time sheets so that leptobaryons could be long-lived? Could dark matter quite generally correspond to the matter at different space-time sheets and thus serve as a direct signature of the many-sheeted space-time topology?

Lightnings and leptopions

The latest discovery of Fermi space-telescope [64] is the finding of .511 MeV gamma rays in the the spectrum of photons associated with lightnings. It was discovered already years ago that lightnings are accompanied by X-rays [43] and even gamma rays [44]. For instance, the strong electric fields created by a positively charged region of cloud could accelerate electron from both downwards and upwards to this region. The problem is that atmosphere is not empty and dissipation would restrict the energies to be much lower than gamma ray energies which are in MeV range. Note that the temperatures in lightning are about 3×10^4 K and correspond to electron energy of 2.6 eV which is by a factor 10^5 smaller than electron mass and gamma ray energy scale!

Situation changes if dissipation is absent so that the electrons are accelerated without any energy losses. This is the case if the electrons reside in large \hbar quantum phase at magnetic flux tubes so that dissipative losses are small and electrons can reach relativistic energies. This is the explanation that I provided years ago for the [16].

Fermi however observed also something completely new. There is also a peaking of gamma rays around energy .511 MeV. The decay of electro-pion is an obvious explanation for this peaking. If electro-pions are there, collisions of highly energetic particles lasting for time of about $\tau \sim \hbar/\text{MeV}$ are expected. The natural candidates for the colliding charged particles are electrons. The center of mass system -the system in which total momentum of colliding electron pair vanishes- should be in a good approximation at rest with respect to Fermi space telescope. Otherwise the energy of gamma rays would be higher or lower than .511 MeV.

The only possibility that I can imagine is that the second electron comes from below and second from above the positively charged region of the thunder cloud. Both arrive as dark electrons with a large value of \hbar and are accelerated to relativistic energies since dissipation is very small. They could collide as dark electrons (the more probable option as will be found below) or suffer a phase transition transforming them to ordinary electrons before the collision. Electro-pion coherent state is created in the strong $E \cdot B$ created for a a period of time of order $\tau \sim \hbar_0/\text{MeV}$. This state annihilates rapidly to pairs of gamma rays which are ordinary or transform to ordinary ones depending on whether electrons where dark or not.

What the phase transition of dark electrons to ordinary electrons means, needs some explaining. The generalized imbedding space is obtained by gluing almost copies of 8-D imbedding space $M^4 \times CP_2$

along their common back to get a book like structure. Particles at different pages of the book are dark with respect to each other in the sense that they have no local interactions. This is enough to explain what is actually known about dark matter. Particles at different pages can however interact via classical fields and photon exchange (for instance). The phase transition of electron from dark to visible form preceding the collision of dark electrons would simply mean the leakage from large \hbar page to the "visible" page with ordinary value of Planck constant.

Alert reader might be ready to ask the obvious question. Why not to test the hypothesis in laboratory? It should not be too difficult to allow two electrons to collide with a relativistic energy and find whether gamma pairs with energy .511 MeV are produced in rest system. Maybe gamma ray pairs have been missed for some reason? If not (the probable option), then colored electrons and leptopions are always dark. This would explain why the colored leptons do not contribute to the decay widths of weak gauge bosons which pose very strong constraints for the existence of light exotic particles.

Experimental evidence for colored muons

Also μ and τ should possess colored excitations. About fifteen years after this prediction was made. Direct experimental evidence for these states finally emerges (the year I am adding this comment is 2007) [43, 44]. The mass of the new particle, which is either scalar or pseudoscalar, is 214.4 MeV whereas muon mass is 105.6 MeV. The mass is about 1.5 per cent higher than two times muon mass. The proposed interpretation is as a light Higgs. I do not immediately resonate with this interpretation although p-adically scaled up variants of also Higgs bosons live happily in the fractal Universe of TGD. The most natural TGD inspired interpretation is as a pion like bound state of colored excitations of muon completely analogous to leptopion (or rather, electro-pion).

Scaled up variants of QCD appear also in nuclear string model [23, 47], where scaled variant of QCD for exotic quarks in p-adic length scale of electron is responsible for the binding of ${}^4\text{He}$ nuclei to nuclear strings. One cannot exclude the possibility that the fermion and anti-fermion at the ends of color flux tubes connecting nucleons are actually colored leptons although the working hypothesis is that they are exotic quark and anti-quark. One can of course also turn around the argument: could it be that leptopions are "leptonuclei", that is bound states of ordinary leptons bound by color flux tubes for a QCD in length scale considerably shorter than the p-adic length scale of lepton.

7.3.3 Evidence for τ -hadrons

The evidence for τ -leptons came in somewhat funny but very pleasant manner. During my friday morning blog walk, the day next to my birthday October 30, I found that Peter Woit had told in his blog about a possible discovery of a new long-lived particle by CDF experiment [62] emphasizing how revolutionary finding is if it is real. There is a detailed paper [57] with title *Study of multi-muon events produced in p-pbar collisions at $\sqrt{s} = 1.96 \text{ TeV}$* by CDF collaboration added to the ArXiv October 29 - the eve of my birthday. I got even second gift posted to arXiv the very same day and reporting an anomalously high abundance of positrons in cosmic ray radiation [63]. Both of these article give support for basic predictions of TGD differentiating between TGD and standard model and its generalizations.

The first gift

A brief summary of Peter Woit about the finding gives good idea about what is involved.

The article originates in studies designed to determine the b-bbar cross-section by looking for events, where a b-bbar pair is produced, each component of the pair decaying into a muon. The b-quark lifetime is of order a picosecond, so b-quarks travel a millimeter or so before decaying. The tracks from these decays can be reconstructed using the inner silicon detectors surrounding the beam-pipe, which has a radius of 1.5 cm. They can be characterized by their impact parameter, the closest distance between the extrapolated track and the primary interaction vertex, in the plane transverse to the beam.

If one looks at events where the b-quark vertices are directly reconstructed, fitting a secondary vertex, the cross-section for b-bbar production comes out about as expected. On the other hand, if one just tries to identify b-quarks by their semi-leptonic decays, one gets a value for the b-bbar cross-section

that is too large by a factor of two. In the second case, presumably there is some background being misidentified as b - $b\bar{b}$ production.

The new result is based on a study of this background using a sample of events containing two muons, varying the tightness of the requirements on observed tracks in the layers of the silicon detector. The background being searched for should appear as the requirements are loosened. It turns out that such events seem to contain an anomalous component with unexpected properties that disagree with those of the known possible sources of background. The number of these anomalous events is large (tens of thousands), so this cannot just be a statistical fluctuation.

One of the anomalous properties of these events is that they contain tracks with large impact parameters, of order a centimeter rather than the hundreds of microns characteristic of b -quark decays. Fitting this tail by an exponential, one gets what one would expect to see from the decay of a new, unknown particle with a lifetime of about 20 picoseconds. These events have further unusual properties, including an anomalously high number of additional muons in small angular cones about the primary ones.

The lifetime is estimated to be considerably longer than b quark life time and below the lifetime 89.5 ps of $K_{0,s}$ mesons. The fit to the tail of "ghost" muons gives the estimate of 20 picoseconds.

The second gift

In October 29 also another remarkable paper [63] had appeared in arXiv. It was titled *Observation of an anomalous positron abundance in the cosmic radiation*. PAMELA collaboration finds an excess of cosmic ray positron at energies $10 \rightarrow 50$ GeV. PAMELA anomaly is discussed in Resonaances blog [38]. ATIC collaboration in turn sees an excess of electrons and positrons going all the way up to energies of order 500-800 GeV [33].

Also Peter Woit refers to these cosmic ray anomalies and also to the article *LHC Signals for a SuperUnified Theory of Dark Matter* by Nima Arkadi-Hamed and Neal Weiner [37], where a model of dark matter inspired by these anomalies is proposed together with a prediction of lepton jets with invariant masses with mass scale of order GeV. The model assumes a new gauge interaction for dark matter particles with Higgs and gauge boson masses around GeV. The prediction is that LHC should detect "lepton jets" with smaller angular separations and GeV scale invariant masses.

Explanation of the CDF anomaly

Consider first the CDF anomaly. TGD predicts a fractal hierarchy of QCD type physics. In particular, colored excitations of leptons are predicted to exist. Neutral leptopions would have mass only slightly above two times the charged lepton mass. Also charged leptopions are predicted and their masses depend on what is the p -adic mass scale of neutrino and it is not clear whether it is much longer than that for charge colored lepton as in the case of ordinary leptons.

1. There exists a considerable evidence for colored electrons as already found. The anomalous production of electron positron pairs discovered in heavy ion collisions can be understood in terms of decays of electro-pions produced in the strong non-orthogonal electric and magnetic fields created in these collisions. The action determining the production rate would be proportional to the product of the leptopion field and highly unique "instanton" action for electromagnetic field determined by anomaly arguments so that the model is highly predictive.
2. Also the .511 MeV emission line [56, 47] from the galactic center can be understood in terms of decays of neutral electro-pions to photon pairs. Electro-pions would reside at magnetic flux tubes of strong galactic magnetic fields. It is also possible that these particles are dark in TGD sense.
3. There is also evidence for colored excitations of muon and muo-pion [43, 44]. Muo-pions could be produced by the same mechanism as electro-pions in high energy collisions of charged particles when strong non-orthogonal magnetic and electric fields are generated.

Also τ -hadrons are possible and CDF anomaly can be understood in terms of a production of higher energy τ -hadrons as the following argument demonstrates.

1. τ -QCD at high energies would produce "lepton jets" just as ordinary QCD. In particular, muon pairs with invariant energy below $2m(\tau) \sim 3.6$ GeV would be produced by the decays of neutral τ -pions. The production of monochromatic gamma ray pairs is predicted to dominate the decays. Note that the space-time sheet associated with both ordinary hadrons and τ lepton correspond to the p-adic prime $M_{107} = 2^{107} - 1$.
2. The model for the production of electro-pions in heavy ion collisions suggests that the production of τ -pions could take place in higher energy collisions of protons generating very strong non-orthogonal magnetic and electric fields. This This would reduce the model to the quantum model for electro-pion production.
3. One can imagine several options for the detailed production mechanism.
 - (a) The decay of *virtual* τ -pions created in these fields to pairs of leptobaryons generates lepton jets. Since colored leptons correspond to color octets, leptobaryons could correspond to states of form LLL or $L\bar{L}L$.
 - (b) The option inspired by a blog discussion with Ervin Goldfein is that a coherent state of τ -pions is created first and is then heated to QCD plasma like state producing the lepton jets like in QCD. The linear coupling to $E \cdot B$ defined by em fields of colliding nucleons would be analogous to the coupling of harmonic oscillator to constant force and generate the coherent state.
 - (c) The option inspired by CDF model [54] is that a p-adically scaled up variant of *on mass shell* neutral τ -pion having $k = 103$ and 4 times larger mass than $k = 107$ τ -pion is produced and decays to three $k = 105$ τ -pions with $k = 105$ neutral τ -pion in turn decaying to three $k = 107$ τ -pions.
4. The basic characteristics of the anomalous muon pair prediction seems to fit with what one would expect from a jet generating a cascade of τ -pions. Muons with both charges would be produced democratically from neutral τ -pions; the number of muons would be anomalously high; and the invariant masses of muon pairs would be below 3.6 GeV for neutral τ -pions and below 1.8 GeV for charged τ -pions if colored neutrinos are light.
5. The lifetime of 20 ps can be assigned with charged τ -pion decaying weakly only into muon and neutrino. This provides a killer test for the hypothesis. In absence of CKM mixing for colored neutrinos, the decay rate to lepton and its antineutrino is given by

$$\Gamma(\pi_\tau \rightarrow L + \bar{\nu}_L) = \frac{G^2 m(L)^2 f^2(\pi) (m(\pi_\tau)^2 - m(L)^2)^2}{4\pi m^3(\pi_\tau)} . \quad (7.3.1)$$

The parameter $f(\pi_\tau)$ characterizing the coupling of pion to the axial current can be written as $f(\pi_\tau) = r(\pi_\tau)m(\pi_\tau)$. For ordinary pion one has $f(\pi) = 93$ MeV and $r(\pi) = .67$. The decay rate for charged τ -pion is obtained by simple scaling giving

$$\begin{aligned} \Gamma(\pi_\tau \rightarrow L + \bar{\nu}_L) &= 8x^2 u^2 y^3 (1 - z^2) \frac{1}{\cos^2(\theta_c)} \Gamma(\pi \rightarrow \mu + \bar{\nu}_\mu) , \\ x &= \frac{m(L)}{m(\mu)} , \quad y = \frac{m(\tau)}{m(\pi)} , \quad z = \frac{m(L)}{2m(\tau)} , \quad u = \frac{r(\pi_\tau)}{r(\pi)} . \end{aligned} \quad (7.3.0)$$

If the p-adic mass scale of the colored neutrino is same as for ordinary neutrinos, the mass of charged leptopion is in good approximation equal to the mass of τ and the decay rates to τ and electron are for the lack of phase space much slower than to muons so that muons are produced preferentially.

6. For $m(\tau) = 1.8$ GeV and $m(\pi) = .14$ GeV and the same value for f_π as for ordinary pion the lifetime is obtained by scaling from the lifetime of charged pion about 2.6×10^{-8} s. The prediction is 3.31×10^{-12} s to be compared with the experimental estimate about 20×10^{-12} s. $r(\pi_\tau) = .41r_\pi$ gives a correct prediction. Hence the explanation in terms of τ -pions seems to be rather convincing unless one is willing to believe in really nasty miracles.
7. Neutral τ -pion would decay dominantly to monochromatic pairs of gamma rays. The decay rate is dictated by the product of τ -pion field and "instanton" action, essentially the inner product of electric and magnetic fields and reducing to total divergence of instanton current locally. The rate is given by

$$\begin{aligned} \Gamma(\pi_\tau \rightarrow \gamma + \gamma) &= \frac{\alpha_{em}^2 m^3(\pi_\tau)}{64\pi^3 f(\pi_\tau)^2} = 2x^{-2}y \times \Gamma(\pi \rightarrow \gamma + \gamma) , \\ x &= \frac{f(\pi_\tau)}{m(\pi_\tau)} , \quad y = \frac{m(\tau)}{m(\pi)} . \Gamma(\pi \rightarrow \gamma + \gamma) = 7.37 \text{ eV} . \end{aligned} \tag{7.3.-1}$$

The predicted lifetime is 1.17×10^{-17} seconds.

8. Second decay channel is to lepton pairs, with muon pair production dominating for kinematical reasons. The invariant mass of the pairs is 3.6 GeV if no other particles are produced. Whether the mass of colored neutrino is essentially the same as that of charged lepton or corresponds to the same p-adic scale as the mass of the ordinary neutrino remains an open question. If colored neutrino is light, the invariant mass of muon-neutrino pair is below 1.78 GeV.

PAMELA and ATIC anomalies

TGD predicts also a hierarchy of hadron physics assignable to Mersenne primes. The mass scale of M_{89} hadron physics is by a factor 512 higher than that of ordinary hadron physics. Therefore a very rough estimate for the nucleons of this physics is 512 GeV. This suggests that the decays of M_{89} hadrons are responsible for the anomalous positrons and electrons up to energies 500-800 GeV reported by ATIC collaboration. An equally naive scaling for the mass of pion predicts that M_{89} pion has mass 72 GeV. This could relate to the anomalous cosmic ray positrons in the energy interval 10-50 GeV reported by PAMELA collaboration. Be as it may, the prediction is that M_{89} hadron physics exists and could make itself visible in LHC.

The surprising finding is that positron fraction (the ratio of flux of positrons to the sum of electron and positron fluxes) increases above 10 GeV. If positrons emerge from secondary production during the propagation of cosmic ray-nuclei, this ratio should decrease if only standard physics is involved with the collisions. This is taken as evidence for the production of electron-positron pairs, possibly in the decays of dark matter particles.

Leptohadron hypothesis predicts that in high energy collisions of charged nuclei with charged particles of matter it is possible to produce also charged electro-pions, which decay to electrons or positrons depending on their charge and produce the electronic counterparts of the jets discovered in CDF. This proposal - and more generally leptohadron hypothesis - could be tested by trying to find whether also electronic jets can be found in proton-proton collisions. They should be present at considerably lower energies than muon jets. I decided to check whether I have said something about this earlier and found that I have noticed years ago that there is evidence for the production of anomalous electron-positron pairs in hadronic reactions [39, 35, 36, 61]: some of it dates back to seventies.

The first guess is that the center of mass energy at which the jet formation begins to make itself visible is in a constant ratio to the mass of charged lepton. From CDF data this ratio satisfies $\sqrt{s}/m_\tau = x < 10^3$. For electro-pions the threshold energy would be around $10^{-3}x \times .5$ GeV and for muo-pions around $10^{-3}x \times 100$ GeV.

Comparison of TGD model with the model of CDF collaboration

Few days after the experimental a theoretical paper by CDF collaboration proposing a phenomenological model for the CDF anomaly appeared in the arXiv [54], and it is interesting to compare the model with TGD based model (or rather, one of them corresponding to the third option mentioned above).

The paper proposes that three new particles are involved. The masses for the particles - christened h_3 , h_2 , and h_1 - are assumed to be 3.6 GeV, 7.3 GeV, and 15 GeV. h_1 is assumed to be pair produced and decay to h_2 pair decaying to h_3 pair decaying to a τ pair.

h_3 is assumed to have mass 3.6 GeV and life-time of 20×10^{-12} seconds. The mass is same as the TGD based prediction for neutral τ -pion mass, whose lifetime however equals to 1.12×10^{-17} seconds ($\gamma + \gamma$ decay dominates). The correct prediction for the lifetime provides a strong support for the identification of long-lived state as charged τ -pion with mass near τ mass so that the decay to μ and its antineutrino dominates. Hence the model is not consistent with leptohadronic model.

p-Adic length scale hypothesis predicts that allowed mass scales come as powers of $\sqrt{2}$ and these masses indeed come in good approximation as powers of 2. Several p-adic scales appear in low energy hadron physics for quarks and this replaces Gell-Mann formula for low-lying hadron masses. Therefore one can ask whether the proposed masses correspond to neutral tau-pion with $p = M_k = 2^k - 1$, $k = 107$, and its p-adically scaled up variants with $p \simeq 2^k$, $k = 105$, and $k = 103$ (also prime). The prediction for masses would be 3.6 GeV, 7.2 GeV, 14.4 GeV.

This co-incidence cannot of course be taken too seriously since the powers of two in CDF model have a rather mundane origin: they follow from the assumed production mechanism producing 8 τ -leptons from h_1 . One can however spend some time by looking whether it could be realized somehow allowing p-adically scaled up variants of τ -pion.

1. The proposed model for the production of muon jets is based on production of $k=103$ neutral τ -pion (or several of them) having 8 times larger mass than $k=107$ τ -pion in strong EB background of the colliding proton and antiproton and decaying via strong interactions to $k=105$ and $k=107$ τ -pions.
2. The first step would be

$$\pi_{\tau}^0(103) \rightarrow \pi_{\tau}^0(105) + \pi_{\tau}^+(105) + \pi_{\tau}^-(105) .$$

This step is not kinematically possible if masses are obtained by exact scaling and if $m(\pi_{\tau}^0) < m(\pi_{\tau}^{\pm})$ holds true as for ordinary pion. p-Adic mass formulas do not however predict exact scaling. In the case that reaction is not kinematically possible, it must be replaced with a reaction in which second charged $k=105$ pion is virtual and decays weakly. This option however reduces the rate of the process dramatically and might be excluded.

3. Second step would consist of a scaled variant of the first step

$$\pi_{\tau}^0(105) \rightarrow \pi_{\tau}^0(107) + \pi_{\tau}^+(107) + \pi_{\tau}^-(107) ,$$

where second charged pion also can be virtual and decay weakly, and the weak decays of the $\pi_{\tau}^{\pm}(105)$ with mass $2m(\tau)$ to lepton pairs. The rates for these are obtained from previous formulas by scaling.

4. The last step would involve the decays of both charged and neutral $\pi_{\tau}(107)$. The signature of the mechanism would be anomalous γ pairs with invariant masses $2^k \times m(\tau)$, $k = 1, 2, 3$ coming from the decays of neutral τ -pions.
5. Dimensionless four-pion coupling λ determines the decay rates for neutral τ -pions appearing in the cascade. Rates are proportional to phase space-volumes, which are rather small by kinetic reasons.

The total cross section for producing single leptopion can be estimated by using the quantum model for leptopion production. Production amplitude is essentially Coulomb scattering amplitude for a given value of the impact parameter b for colliding proton and anti-proton multiplied by the

amplitude $U(b, p)$ for producing on mass shell $k = 103$ lepton with given four-momentum in the fields E and B and given essentially by the Fourier transform of $E \cdot B$. The replacement of the motion with free motion should be a good approximation.

UV and IR cutoffs for the impact parameter appear in the model and are identifiable as appropriate p-adic length scales. UV cutoff could correspond to the Compton size of nucleon ($k = 107$) and IR cutoff to the size of the space-time sheets representing topologically quantized electromagnetic fields of colliding nucleons (perhaps $k = 113$ corresponding to nuclear p-adic length scale and size for color magnetic body of constituent quarks or $k = 127$ for the magnetic body of current quarks with mass scale of order MeV). If one has $\hbar/\hbar_0 = 2^7$ one could also guess that the IR cutoff corresponds to the size of dark em space-time sheet equal to $2^7 L(113) = L(127)$ (or $2^7 L(127) = L(141)$), which corresponds to electron's p-adic length scale. These are of course rough guesses.

Quantitatively the jet-likeness of muons means that the additional muons are contained in the cone $\theta < 36.8$ degrees around the initial muon direction. If the decay of $\pi_\tau^0(k)$ can occur to on mass shell $\pi_\tau^0(k+2)$, $k = 103, 105$, it is possible to understand jets as a consequence of the decay kinematics forcing the pions resulting as decay products to be almost at rest.

1. Suppose that the decays to three pions can take place as on mass shell decays so that pions are very nearly at rest. The distribution of decay products $\mu\bar{\nu}$ in the decays of $\pi^\pm(105)$ is spherically symmetric in the rest frame and the energy and momentum of the muon are given by

$$[E, p] = [m(\tau) + \frac{m^2(\mu)}{4m(\tau)}, m(\tau) - \frac{m^2(\mu)}{4m(\tau)}] .$$

The boost factor $\gamma = 1/\sqrt{1-v^2}$ to the rest system of muon is $\gamma = \frac{m(\tau)}{m(\mu)} + \frac{m(\mu)}{4m(\tau)} \sim 18$.

2. The momentum distribution for μ^+ coming from π_τ^+ is spherically symmetric in the rest system of π^+ . In the rest system of μ^- the momentum distribution is non-vanishing only for when the angle θ between the direction of velocity of μ^- is below a maximum value of given by $\tan(\theta_{max}) = 1$ corresponding to a situation in which the momentum μ^+ is orthogonal to the momentum of μ^- (the maximum transverse momentum equals to $m(\mu)v\gamma$ and longitudinal momentum becomes $m(\mu)v\gamma$ in the boost). This angle corresponds to 45 degrees and is not too far from 36.8 degrees.
3. At the next step the energy of muons resulting in the decays of $\pi^\pm(103)$

$$[E, p] = [\frac{m(\tau)}{2} + \frac{m^2(\mu)}{2m(\tau)}, \frac{m(\tau)}{2} - \frac{m^2(\mu)}{2m(\tau)}] ,$$

and the boost factor is $\gamma_1 = \frac{m(\tau)}{2m(\mu)} + \frac{m(\mu)}{2m(\tau)} \sim 9$. θ_{max} satisfies the condition $\tan(\theta_{max}) = \gamma_1 v_1 / \gamma v \simeq 1/2$ giving $\theta_{max} \simeq 26.6$ degrees.

If on mass shell decays are not allowed the situation changes since either of the charged pions is off mass shell. In order to obtain similar result the virtual should occur dominantly via states near to on mass shell pion. Since four-pion coupling is just constant, this option does not seem to be realized.

Quantitatively the jet-likeness of muons means that the additional muons are contained in the cone $\theta < 36.8$ degrees around the initial muon direction. If the decay of $\pi_\tau^0(k)$ can occur to on mass shell $\pi_\tau^0(k+2)$, $k = 103, 105$, it is possible to understand jets as a consequence of the decay kinematics forcing the pions resulting as decay products to be almost at rest.

1. Suppose that the decays to three pions can take place as on mass shell decays so that pions are very nearly at rest. The distribution of decay products $\mu\bar{\nu}$ in the decays of $\pi^\pm(105)$ is spherically symmetric in the rest frame and the energy and momentum of the muon are given by

$$[E, p] = [m(\tau) + \frac{m^2(\mu)}{4m(\tau)}, m(\tau) - \frac{m^2(\mu)}{4m(\tau)}] .$$

The boost factor $\gamma = 1/\sqrt{1-v^2}$ to the rest system of muon is $\gamma = \frac{m(\tau)}{m(\mu)} + \frac{m(\mu)}{4m(\tau)} \sim 18$.

2. The momentum distribution for μ^+ coming from π_τ^+ is spherically symmetric in the rest system of π^+ . In the rest system of μ^- the momentum distribution is non-vanishing only for when the angle θ between the direction of velocity of μ^- is below a maximum value of given by $\tan(\theta_{max}) = 1$ corresponding to a situation in which the momentum μ^+ is orthogonal to the momentum of μ^- (the maximum transverse momentum equals to $m(\mu)v\gamma$ and longitudinal momentum becomes $m(\mu)v\gamma$ in the boost). This angle corresponds to 45 degrees and is not too far from 36.8 degrees.
3. At the next step the energy of muons resulting in the decays of π^\pm (103)

$$[E, p] = \left[\frac{m(\tau)}{2} + \frac{m^2(\mu)}{2m(\tau)}, \frac{m(\tau)}{2} - \frac{m^2(\mu)}{2m(\tau)} \right],$$

and the boost factor is $\gamma_1 = \frac{m(\tau)}{2m(\mu)} + \frac{m(\mu)}{2m(\tau)} \sim 9$. θ_{max} satisfies the condition $\tan(\theta_{max}) = \gamma_1 v_1 / \gamma v \simeq 1/2$ giving $\theta_{max} \simeq 26.6$ degrees.

If on mass shell decays are not possible, the situation changes since either of the charged pions is off mass shell. In order to obtain similar result the virtual should occur dominantly via states near to on mass shell pion. Since four-pion coupling is just constant, this option does not seem to be realized.

Numerical estimate for the production cross section

The numerical estimate of the cross section involves some delicacies. The model has purely physical cutoffs which must be formulated in a precise manner.

1. Since energy conservation is not coded into the model, some assumption about the maximal τ -pion energy in cm system expressed as a fraction ϵ of proton's center of mass energy is necessary. Maximal fraction corresponds to the condition $m(\pi_\tau) \leq m(\pi_\tau)\gamma_1 \leq \epsilon m_p \gamma_{cm}$ in cm system giving $[m(\pi_\tau)/(m_p \gamma_{cm})] \leq \epsilon \leq 1$. γ_{cm} can be deduced from the center of mass energy of proton as $\gamma_{cm} = \sqrt{s} 2m_p$, $\sqrt{s} = 1.96$ TeV. This gives $1.6 \times 10^{-2} < \epsilon < 1$ in a reasonable approximation. It is convenient to parameterize ϵ as

$$\epsilon = (1 + \delta) \times \frac{m(\pi_\tau)}{m_p} \times \frac{1}{\gamma_{cm}}.$$

The coordinate system in which the calculations are carried out is taken to be the rest system of (say) antiproton so that one must perform a Lorentz boost to obtain upper and lower limits for the velocity of τ -pion in this system. In this system the range of γ_1 is fixed by the maximal cm velocity fixed by ϵ and the upper/lower limit of γ_1 corresponds to a direction parallel/opposite to the velocity of proton.

2. By Lorentz invariance the value of the impact parameter cutoff b_{max} should be expressible in terms τ -pion Compton length and the center of mass energy of the colliding proton and the assumption is that $b_{max} = \gamma_{cm} \times \hbar/m(\pi_\tau)$, where it is assumed $m(\pi_\tau) = 8m(\tau)$. The production cross section does not depend much on the precise choice of the impact parameter cutoff b_{max} unless it is un-physically large in which case b_{max}^2 proportionality is predicted.

The numerical estimate for the production cross section involves some delicacies.

1. The power series expansion of the integral of CUT_1 using partial fraction representation does not converge since that roots c_\pm are very large in the entire integration region. Instead the approximation $A_1 \simeq iB \cos(\psi)/D$ simplifying considerably the calculations can be used. Also the value of $b_1 L$ is rather small and one can use stationary phase approximation for CUT_2 . It turns out that the contribution of CUT_2 is negligible as compared to that of CUT_1 .
2. Since the situation is singular for $\theta = 0$ and $\phi = 0$ and $\phi = \pi/2$ (by symmetry it is enough to calculate the cross section only for this kinematical region), cutoffs

$$\theta \in [\epsilon_1, (1 - \epsilon_1)] \times \pi, \quad \phi \in [\epsilon_1, (1 - \epsilon_1)] \times \pi/2, \quad \epsilon_1 = 10^{-3}.$$

The result of the calculation is not very sensitive to the value of the cutoff.

- Since the available numerical environment was rather primitive (MATLAB in personal computer), the requirement of a reasonable calculation time restricted the number of intervals in the discretization for the three kinematical variables γ, θ, ϕ to be below $N_{max} = 80$. The result of calculation did not depend appreciably on the number of intervals above $N = 40$ for γ_1 integral and for θ and ϕ integrals even $N = 10$ gave a good estimate.

The calculations were carried for the $exp(iS)$ option since in good approximation the estimate for $exp(iS) - 1$ model is obtained by a simple scaling. $exp(iS)$ model produces a correct order of magnitude for the cross section whereas $exp(iS) - 1$ variant predicts a cross section, which is by several orders of magnitude smaller by downwards α_{em}^2 scaling. As I asked Tommaso Dorigo for an estimate for the production cross section in his first blog posting [34], he mentioned that authors refer to a production cross section is 100 nb which looks to me suspiciously large (too large by three orders of magnitude), when compared with the production rate of muon pairs from b-bbar. $\delta = 1.5$ which corresponds to τ -pion energy 36 GeV gives the estimate $\sigma = 351$ nb. The energy is suspiciously high.

In fact, in the recent blog posting of Tommaso Dorigo [53] a value of order .1 nb for the production cross section was mentioned. Electro-pions in heavy ion collisions are produced almost at rest and one has $\Delta v/v \simeq .2$ giving $\delta = \Delta E/m(\pi) \simeq 2 \times 10^{-3}$. If one believes in fractal scaling, this should be at least the order of magnitude also in the case of τ -pion. This would give the estimate $\sigma = 1$ nb. For $\delta = \Delta E/m(\pi) \simeq 10^{-3}$ a cross section $\sigma = .16$ nb would result.

One must of course take the estimate cautiously but there are reasons to hope that large systematic errors are not present anymore. In any case, the model can explain also the order of magnitude of the production cross section under reasonable assumptions about cutoffs.

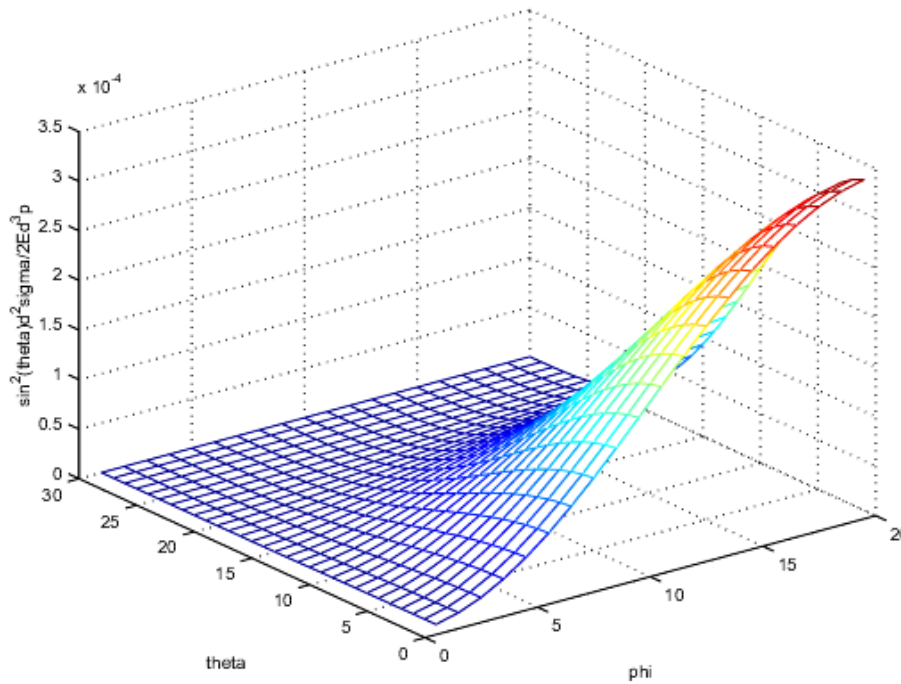


Figure 7.2: Differential cross section $\sin^2(\theta) \times \frac{d^2\sigma}{2E d^3p}$ for τ -pion production for $\gamma_1 = 1.090 \times 10^3$ in the rest system of antiproton for $\delta = 1.5$. $m(\pi_\tau)$ defines the unit of energy and nb is the unit for cross section. The ranges of θ and ϕ are $(0, \pi)$ and $(0, \pi/2)$.

Does the production of leptopions involve a phase transition increasing Planck constant?

The critical argument of Tommaso Dorigo in his blog inspired an attempt to formulate more precisely the hypothesis $\sqrt{s}/m_\tau > x < 10^3$. This led to the realization that a phase transition increasing Planck

constant might happen in the production process as also the model for the production of electro-pions requires.

Suppose that the instanton coupling gives rise to *virtual* neutral leptopions which ultimately produce the jets (this is first of the three models that one can imagine). E and B could be associated with the colliding proton and antiproton or quarks.

1. The amplitude for leptopion production is essentially Fourier transform of $E \cdot B$, where E and B are the non-orthogonal electric and magnetic fields of the colliding charges. At the level of scales one has $\tau \sim \hbar/E$, where τ is the time during which $E \cdot B$ is large enough during collision and E is the energy scale of the virtual leptopion giving rise to the jet.
2. In order to have jets one must have $m(\pi_\tau) \ll E$. If the scaling law $E \propto \sqrt{s}$ hold true, one indeed has $\sqrt{s}/m(\pi_\tau) > x < 10^3$.
3. If proton and antiproton would move freely, τ would be of the order of the time for proton to move through a distance, which is 2 times the Lorentz contracted radius of proton: $\tau_{free} = 2 \times \sqrt{1 - v^2} R_p / v = 2\hbar/E_p$. This would give for the energy scale of virtual τ -pion the estimate $E = \hbar/\tau_{free} = \sqrt{s}/4$. $x = 4$ is certainly quite too small value. Actually $\tau > \tau_{free}$ holds true but one can argue that without new physics the time for the preservation of $E \cdot B$ cannot be by a factor of order 2^8 longer than for free collision.
4. For a colliding quark pair one would have $\tau_{free} = 4\hbar/\sqrt{s_{pair}(s)}$, where $\sqrt{s_{pair}(s)}$ would be the typical invariant energy of the pair which is exponentially smaller than \sqrt{s} . Somewhat paradoxically from classical physics point of view, the time scale would be much longer for the collision of quarks than that for proton and antiproton.

The possible new physics relates to the possibility that leptopions are dark matter in the sense that they have Planck constant larger than the standard value.

1. Suppose that the produced leptopions have Planck constant larger than its standard value \hbar_0 . Originally the idea was that larger value of \hbar would scale up the production cross section. It turned out that this is not the case. For $exp(iS)$ option the lowest order contribution is not affected by the scaling of \hbar and for $exp(iS) - 1$ option the lowest order contribution scales down as $1/\hbar^2$. The improved formulation of the model however led to a correct order of magnitude estimates for the production cross section.
2. Assume that a phase transition increasing Planck constant occurs during the collision. Hence τ is scaled up by a factor $y = \hbar/\hbar_0$. The inverse of the leptopion mass scale is a natural candidate for the scaled up dark time scale. $\tau(\hbar_0) \sim \tau_{free}$, one obtains $y \sim \sqrt{s_{min}}/4m(\pi_\tau) \leq 2^8$ giving for proton-antiproton option the first guess $\sqrt{s}/m(\pi_\tau) > x < 2^{10}$. If the value of y does not depend on the type of leptopion, the proposed estimates for muo- and electro-pion follow.
3. If the fields E and B are associated with colliding quarks, only colliding quark pairs with $\sqrt{s_{pair}(s)} > (>)m(\pi_\tau)$ contribute giving $y_q(s) = \sqrt{s_{pair}(s)}/s \times y$.

If the τ -pions produced in the magnetic field are on-mass shell τ -pions with $k = 113$, the value of \hbar would satisfy $\hbar/\hbar_0 < 2^5$ and $\sqrt{s}/m(\pi_\tau) > x < 2^7$.

Tau-pions again but now as dark matter candidate in galactic center

The standard view about dark matter is that it has only gravitational interactions with ordinary matter so that high densities of dark matter are required to detect its signatures. On the average the density of dark matter is about 80 per cent of ordinary matter. Clearly, Milky Way's center is an excellent place for detecting the signatures of dark matter. The annihilation of pairs of dark matter particles to gamma rays is one possible signature and one could study the anomalous features of gamma ray spectrum from the galactic center (a region with radius about 100 light years).

Europe's INTEGRAL satellite launched in 2002 indeed found bright gamma ray radiations coming from the center of galaxy with energy of .511 MeV, which is slightly above electron mass (see the references below). The official interpretation is that the gammas are produced in the annihilations of particles of positrons and electrons in turn created in dark matter annihilations. TGD suggests much

simpler mechanism. Gamma rays would be produced in the decay of what I call electropions having mass which is slightly larger than $m = 2m_e$.

The news of the day [66] was that the data from Fermi Gamma Ray telescope give analyzed by Dan Hooper and Lisa Goodenough [65] gives evidence for a dark matter candidate with mass between 7.3-9.2 GeV decaying predominantly into a pair of τ leptons. The estimate for the mass region is roughly 4 times τ mass. What puts bells ringing that a mass of a charged lepton appears again!

1. Explanation in TGD framework

The new finding fits nicely to a bigger story based on TGD.

1. TGD predicts that both quarks and leptons should have colored excitations devoted to the lepto-hadron model). In the case of leptons lowest excitations are color octets. In the case of electro-pion this hypothesis finds support from the anomalous production of electron positron pairs in heavy ion collisions discovered already at seventies but forgotten for long ago since the existence of light particle at this mass scale simply was in total complete with standard model and what was known about the decay widths of intermediate gauge bosons. Also orthopositronium decay width anomaly -forgotten also-has explanation in terms of lepton hypothesis [60, 58].
2. The colored leptons would be dark in TGD sense, which means that they live in dark sector of the "world of classical worlds" (WCW) meaning that they have no direct interactions (common vertices of Feynman diagrams) with ordinary matter. They simply live at different space-time sheets. A phase transition which is geometrically a leakage between dark sector and ordinary sector are possible and make possible interactions between ordinary and dark matter based on exchanged particles suffering this phase transition. Therefore the decay widths of intermediate gauge bosons do not kill the model. TGD based model of dark matter in terms of hierarchy of values of Planck constants coming as multiples of its smallest possible value (the simplest option) need not to be postulated separately and can be regarded as a prediction of quantum TGD reflecting directly the vacuum degeneracy and extreme non-linearity of Kähler action (Maxwell action for induced CP_2 Kähler form).
3. CDF anomaly which created a lot of discussion in blogs for two years ago can be understood in terms of taupion. Taupion and its p-adically scaled up versions with masses about $2^k m_\tau$, $k = 1, 2, 3$ and $m_\tau \simeq 1.8$ GeV explains the findings reported by CDF in TGD framework. The masses of taupions would be 3.6 GeV, 7.2 GeV, and 14.2 GeV in good approximation and come as octaves of the mass of tau-lepton pair.

2. Predictions

The mass estimate for the dark matter particle suggests by Fermi Gamma Ray telescope corresponds to $k = 2$ octave for taupion and the predict mass is about 7.2 GeV which at the lower boundary of the range 7.3-9.2 GeV. Also dark matter particles decaying to tau pairs and having masses 3.6 GeV and 14.2 GeV should be found.

Also muo-pion should exist there and should have mass slightly above $2m_\mu = 210.4$ MeV so that a gamma rays peak slightly above the energy $m_\mu = 105.2$ MeV should be discovered. Also octaves of this mass can be imagined. There is also evidence also for the existence of muo-pion [?, ?].

LHC should provide excellent opportunities to test tau-pion and muo-pion hypothesis. Electropion was discovered in heavy ion collisions and also at LHC they study heavy ion collisions but at much higher energies generating the required very strong non-orthogonal electric and magnetic fields for which the "instanton density" defined as the inner product of electric and magnetic fields is large and rapidly varying. As an optimist I hope that muo-pion and tau-pion could be discovered despite the fact that their decay signatures are very different from those for ordinary particles and despite that fact that at these energies one must know precisely what one is trying to find in order to disentangle it from the enormous background.

3. Also DAMA, CoGeNT, and PAMELA give indications for tau-pion

Note that also DAMA experiment [67] suggests the existence of dark matter particle in this mass range but it is not clear whether it can have anything to do with tau-pion state. One could of course imagine that dark tau-pions are created in the collisions of highly energetic cosmic rays with the

nuclei of atmosphere. Also Coherent Germanium Neutrino Technology (CoGeNT) experiment [68] has released data that are best explained in terms of a dark matter particle with mass in the range 7-11 GeV.

The decay of tau-pions produce lepton pairs, mostly tau but also muons and electrons. The subsequent decays of tau-leptons to muons and electrons produce also electrons and positrons. This relates interestingly to the positron excess reported by PAMELA collaboration [63] at the same time as CDF anomaly was reported. The anomaly started at positron energy about 3.6 GeV, which is one just one half of 7. 2 GeV for tau-pion mass! What was remarkable that no antiproton excess predicted by standard dark matter candidates was observed. Therefore the interpretation as decay products of tau-pions seems to make sense!

Could it have been otherwise?

To sum up, the probability that a correct prediction for the lifetime of the new particle using only known lepton masses and standard formulas for weak decay rates follows by accident is extremely low. Throwing billion times coin and getting the same result every time might be something comparable to this. Therefore my sincere hope is that colleagues would be finally mature to take TGD seriously. If TGD based explanation of the anomalous production of electron positron pairs in heavy ion collisions would have been taken seriously for fifteen years ago, particle physics might look quite different now.

7.3.4 Could lepto-hadrons be replaced with bound states of exotic quarks?

Can one then exclude the possibility that electron-hadrons correspond to colored quarks condensed around $k = 127$ hadronic space-time sheet: that is M_{127} hadron physics? There are several objections against this identification.

1. The recent empirical evidence for the colored counterpart of μ and τ supports the view that colored excitations of leptons are in question.
2. The octet character of color representation makes possible the mixing of leptons with lepto-baryons of form $L\nu_L\bar{\nu}_L$ by color magnetic coupling between leptogluons and ordinary and colored lepton. This is essential for understanding the production of electron-positron pairs.
3. In the case CDF anomaly also the assumption that colored variant of τ neutrino is very light is essential. In the case of colored quarks this assumption is not natural.

7.3.5 About the masses of lepto-hadrons

The progress made in understanding of dark matter hierarchy [39] and non-perturbative aspects of hadron physics [17, 20] allow to sharpen also the model of lepto-hadrons.

The model for the masses of ordinary hadrons [17] applies also to the scaled up variants of the hadron physics. The two contributions to the hadron mass correspond to quark contribution and a contribution from super-symplectic bosons. For quarks labeled identical p-adic primes mass squared is additive and for quarks labeled by different primes mass is additive. Quark contribution is calculable once the p-adic primes of quarks are fixed.

super-symplectic contribution comes from super-symplectic bosons at hadronic space-time sheet labeled by Mersenne prime and is universal if one assumes that the topological mixing of the super-symplectic bosons is universal. If this mixing is same as for U type quarks, hadron masses can be reproduced in an excellent approximation if the super-symplectic boson content of hadron is assumed to correlate with the net spin of quarks.

In the case of baryons and pion and kaon one must assume the presence of a negative color conformal weight characterizing color binding. The value of this conformal weight is same for all baryons and super-symplectic contribution dominates over quark contribution for nucleons. In the case of mesons binding conformal weight can be assumed to vanish for mesons heavier than kaon and one can regard pion and kaon as Golstone bosons in the sense that quark contribution gives the mass of the meson.

This picture generalizes to the case of lepto-hadrons.

1. By the additivity of the mass squared leptonic contribution to lepton mass would be $\sqrt{2}m_e(k)$, where k characterizes the p-adic length scale of colored electron. For $k = 127$ the mass of lepton would be .702 MeV and too small. For $k = 126$ the mass would be $2m_e = 1.02$ MeV and is very near to the mass of the lepton. Note that for ordinary hadrons quarks can appear in several scaled up variants inside hadrons and the value of k depends on hadron. The prediction for the mass of lepton would be $m_{\pi_L} + \sqrt{7}m_{127} \simeq 1.62$ MeV ($m_{127} = m_e/\sqrt{5}$).
2. The state consisting of three colored electrons would correspond to leptonic variant of Δ_{++} having charge $q = -3$. The quark contribution to the mass of $\Delta_L \equiv \Delta_{L,3-}$ would be by the additivity of mass squared $\sqrt{3} \times m_e(k = 126) = 1.25$ MeV. If super-symplectic particle content is same as for Δ_L , super-symplectic contribution would be $m_{SC} = 5 \times m_{127}$, and equal to $m_{SC} = .765$ MeV so that the mass of Δ_L would be $m_{\Delta_L} = 2.34$ MeV. If colored neutrino corresponds to the same p-adic prime as colored electron, also lepton has mass in MeV scale.

7.4 APPENDIX

7.4.1 Evaluation of lepton production amplitude

General form of the integral

The amplitude for lepton production with four momentum

$$\begin{aligned} p &= (p_0, \vec{p}) = m\gamma_1(1, v\sin(\theta)\cos(\phi), v\sin(\theta)\sin(\phi), v\cos(\theta)) , \\ \gamma_1 &= 1/(1-v^2)^{1/2} , \end{aligned} \quad (7.4.0)$$

is essentially the Fourier component of the instanton density

$$U(b, p) = \int e^{ip \cdot x} E \cdot B d^4x \quad (7.4.1)$$

associated with the electromagnetic field of the colliding nuclei.

In order to avoid cumbersome numerical factors, it is convenient to introduce the amplitude $A(b, p)$ as

$$\begin{aligned} A(b, p) &= N_0 \times \frac{4\pi}{Z_1 Z_2 \alpha_{em}} \times U(b, p) , \\ N_0 &= \frac{(2\pi)^7}{i} \end{aligned} \quad (7.4.1)$$

Coordinates are chosen so that target nucleus is at rest at the origin of coordinates and colliding nucleus moves along positive z direction in $y = 0$ plane with velocity β . The orbit is approximated with straight line with impact parameter b .

Instanton density is just the scalar product of the static electric field E of the target nucleus and magnetic field B the magnetic field associated with the colliding nucleus, which is obtained by boosting the Coulomb field of static nucleus to velocity β . The flux lines of the magnetic field rotate around the direction of the velocity of the colliding nucleus so that instanton density is indeed non vanishing.

The Fourier transforms of E and B for nuclear charge 4π (chose for convenience) giving rise to Coulomb potential $1/r$ are given by the expressions

$$\begin{aligned} E_i(k) &= N\delta(k_0)k_i/k^2 , \\ B_i(k) &= N\delta(\gamma(k_0 - \beta k_z))k_j \varepsilon_{ijz} e^{ik_x b} / ((\frac{k_z}{\gamma})^2 + k_T^2) , \\ N &= \frac{1}{(2\pi)^2} . \end{aligned} \quad (7.4.0)$$

The normalization factor corresponds to momentum space integration measure d^4p . The Fourier transform of the instanton density can be expressed as a convolution of the Fourier transforms of E and B.

$$\begin{aligned} A(b, p) &\equiv = N_0 N_1 \int E(p-k) \cdot B(k) d^4k , \\ N_1 &= \frac{1}{(2\pi)^4} . \end{aligned} \quad (7.4.0)$$

Where the fields correspond to charges $\pm 4\pi$. In the convolution the presence of two delta functions makes it possible to integrate over k_0 and k_z and the expression for U reduces to a two-fold integral

$$\begin{aligned} A(b, p) &= \beta\gamma \int dk_x dk_y \exp(ik_x b) (k_x p_y - k_y p_x) / AB , \\ A &= (p_z - \frac{p_0}{\beta})^2 + p_T^2 + k_T^2 - 2k_T \cdot p_T \\ B &= k_T^2 + (\frac{p_0}{\beta\gamma})^2 , \\ p_T &= (p_x, p_y) . \end{aligned} \quad (7.4.-2)$$

To carry out the remaining integrations one can apply residue calculus.

1. k_y integral is expressed as a sum of two pole contributions
2. k_x integral is expressed as a sum of two pole contributions plus two cut contributions.

k_y -integration

Integration over k_y can be performed by completing the integration contour along real axis to a half circle in upper half plane (see Fig. 7.4.1).

The poles of the integrand come from the two factors A and B in denominator and are given by the expressions

$$\begin{aligned} k_y^1 &= i(k_x^2 + (\frac{p_0}{\beta\gamma})^2)^{1/2} , \\ k_y^2 &= p_y + i((p_z - \frac{p_0}{\beta})^2 + p_x^2 + k_x^2 - 2p_x k_x)^{1/2} . \end{aligned} \quad (7.4.-2)$$

One obtains for the amplitude an expression as a sum of two terms

$$A(b, p) = 2\pi i \int e^{ik_x b} (U_1 + U_2) dk_x , \quad (7.4.-1)$$

corresponding to two poles in upper half plane.

The explicit expression for the first term is given by

$$\begin{aligned} U_1 &= RE_1 + iIM_1 , \\ RE_1 &= (k_x \frac{p_0}{\beta} y - p_x r e_1 / 2) / (r e_1^2 + i m_1^2) , \\ IM_1 &= (-k_x p_y r e_1 / 2 K_1^{1/2} - p_x p_y K_1^{1/2}) / (r e_1^2 + i m_1^2) , \\ r e_1 &= (p_z - \frac{p_0}{\beta})^2 + p_T^2 - (\frac{p_0}{\beta\gamma})^2 - 2p_x k_x , \\ i m_1 &= -2K_1^{1/2} p_y , \\ K_1 &= k_x^2 + (\frac{p_0}{\beta\gamma})^2 . \end{aligned} \quad (7.4.-5)$$

The expression for the second term is given by

$$\begin{aligned}
U_2 &= RE_2 + iIM_2 , \\
RE_2 &= -((k_x p_y - p_x p_y)p_y + p_x r e_2/2)/(r e_2^2 + i m_2^2) , \\
IM_2 &= -(k_x p_y - p_x p_y)r e_2/2K_2^{1/2} + p_x p_y K_2^{1/2}/(r e_2^2 + i m_2^2) , \\
r e_2 &= -(p_z - \frac{p_0}{\beta})^2 + (\frac{p_0}{\beta\gamma})^2 + 2p_x k_x + \frac{p_0}{\beta}y - \frac{p_0}{\beta}x , \\
i m_2 &= 2p_y K_2^{1/2} , \\
K_2 &= (p_z - \frac{p_0}{\beta})^2 + \frac{p_0}{\beta}x + k_x^2 - 2p_x k_x .
\end{aligned} \tag{7.4.-9}$$

A little inspection shows that the real parts cancel each other: $RE_1 + RE_2 = 0$. A further useful result is the identity $i m_1^2 + r e_1^2 = r e_2^2 + i m_2^2$ and the identity $r e_2 = -r e_1 + 2p_y^2$.

k_x -integration

One cannot perform k_x -integration completely using residue calculus. The reason is that the terms IM_1 and IM_2 have cuts in complex plane. One can however reduce the integral to a sum of pole terms plus integrals over the cuts.

The poles of U_1 and U_2 come from the denominators and are in fact common for the two integrands. The explicit expressions for the pole in upper half plane, where integrand converges exponentially are given by

$$\begin{aligned}
r e_i^2 + i m_i^2 &= 0 , \quad i = 1, 2 , \\
k_x &= (-b + i(-b^2 + 4ac)^{1/2})/2a , \\
a &= 4p_T^2 , \\
b &= -4((p_z - \frac{p_0}{\beta})^2 + p_T^2 - (\frac{p_0}{\beta\gamma})^2)p_x , \\
c &= ((p_z - \frac{p_0}{\beta})^2 + p_T^2 - (\frac{p_0}{\beta\gamma})^2)^2 + 4(\frac{p_0}{\beta\gamma})^2 p_y^2 .
\end{aligned} \tag{7.4.-12}$$

A straightforward calculation using the previous identities shows that the contributions of IM_1 and IM_2 at pole have opposite signs and the contribution from poles vanishes identically!

The cuts associated with U_1 and U_2 come from the square root terms K_1 and K_2 . The condition for the appearance of the cut is that K_1 (K_2) is real and positive. In case of K_1 this condition gives

$$k_x = it, \quad t \in (0, \frac{p_0}{\beta\gamma}) . \tag{7.4.-11}$$

In case of K_2 the same condition gives

$$k_x = p_x + it, \quad t \in (0, \frac{p_0}{\beta} - p_z) . \tag{7.4.-10}$$

Both cuts are in the direction of imaginary axis.

The integral over real axis can be completed to an integral over semi-circle and this integral in turn can be expressed as a sum of two terms (see Fig. 7.4.1).

$$A(b, p) = 2\pi i(CUT_1 + CUT_2) . \tag{7.4.-9}$$

The first term corresponds to contour, which avoids the cuts and reduces to a sum of pole contributions. Second term corresponds to the addition of the cut contributions.

In the following we shall give the expressions of various terms in the region $\phi \in [0, \pi/2]$. Using the symmetries

$$\begin{aligned} A(b, p_x, -p_y) &= -A(b, p_x, p_y) , \\ A(b, -p_x, -p_y) &= \bar{A}(b, p_x, p_y) . \end{aligned} \quad (7.4.-9)$$

of the amplitude one can calculate the amplitude for other values of ϕ .

The integration variable for cuts is the imaginary part t of complexified k_x . To get a more convenient form for cut integrals one can perform a change of the integration variable

$$\begin{aligned} \cos(\psi) &= \frac{t}{\left(\frac{p_0}{\beta\gamma}\right)} , \\ \cos(\psi) &= \frac{t}{\left(\frac{p_0}{\beta} - p_z\right)} , \\ \psi &\in [0, \pi/2] . \end{aligned} \quad (7.4.-10)$$

1. The contribution of the first cut

By a painstaking calculation one verifies that the expression for the contribution of the first cut is given by

$$\begin{aligned} CUT_1 &= D_1 \times \int_0^{\pi/2} \exp\left(-\frac{b}{b_0} \cos(\psi)\right) A_1 d\psi , \\ D_1 &= -\frac{1}{2} \frac{\sin(\phi)}{\sin(\theta)} , \quad b_0 = \frac{\hbar \beta\gamma}{m \gamma_1} , \\ A_1 &= \frac{A + iB \cos(\psi)}{\cos^2(\psi) + 2iC \cos(\psi) + D} , \\ A &= \sin(\theta) \cos(\phi) , \quad B = K , \\ C &= K \frac{\cos(\phi)}{\sin(\theta)} , \quad D = -\sin^2(\phi) - \frac{K^2}{\sin^2(\theta)} , \\ K &= \beta\gamma \left(1 - \frac{v_{cm}}{\beta} \cos(\theta)\right) , \quad v_{cm} = \frac{2v}{1 + v^2} . \end{aligned} \quad (7.4.-15)$$

The definitions of the various kinematical variables are given in previous formulas. The notation is tailored to express that A_1 is rational function of $\cos(\psi)$.

1. The exponential $\exp(-bcos(\psi)/b_0)$ is very small in the condition

$$\cos(\psi) \geq \cos(\psi_0) \equiv \frac{\hbar \beta\gamma}{mb \gamma_1 \cos(\phi)} \quad (7.4.-14)$$

holds true. Here $\hbar = 1$ convention has been given up to make clear that the increase of the Compton length of leptopion due to the scaling of \hbar increase the magnitude of the contribution. If the condition $\cos(\psi_0) \ll 1$ holds true, the integral over ψ receives contributions only from narrow range of values near the upper boundary $\psi = \pi/2$ plus the contribution corresponding to the pole of X_1 . The practical condition is in terms of critical parameter b_{max} above which exponential approaches zero very rapidly.

2. For $\cos(\psi_0) \ll 1$, that is for $b > b_{max}$ and in the approximation that the function multiplying the exponent is replaced with its value for $\psi = \pi/2$, one obtains for CUT_1 the expression

$$\begin{aligned} CUT_1 &\simeq D_1 A_1(\psi = \pi/2) \frac{\hbar}{mb} \\ &= \frac{1}{2} \times \frac{\beta\gamma}{\gamma_1} \times \frac{\hbar}{mb} \times \frac{\sin^2(\theta) \cos(\phi) \sin(\phi)}{\sin^2(\theta) \sin^2(\phi) + K^2} . \end{aligned} \quad (7.4.-14)$$

3. For $\cos(\psi_0) \gg 1$ exponential factor can be replaced by unity in good approximation and the integral reduces to an integral of rational function of $\cos(\psi)$ having the form

$$D_1 \frac{A + iB \cos(\psi)}{\cos^2(\psi) + 2iC \times \cos(\psi) + D} \quad (7.4.-14)$$

which can be expressed in terms of the roots c_{\pm} of the denominator as

$$D_1 \times \sum_{\pm} \frac{A \mp iBc_{\pm}}{\cos(\psi) - c_{\pm}}, \quad c_{\pm} = -iC \pm \sqrt{-C^2 - D} \quad (7.4.-13)$$

Integral reduces to an integral of rational function over the interval $[0, 1]$ by the standard substitution $\tan(\psi/2) = t$, $d\psi = 2dt/(1+t^2)$, $\cos(\psi) = (1-t^2)/(1+t^2)$, $\sin(\psi) = 2t/(1+t^2)$.

$$I = 2D_1 \sum_{\pm} \int_0^1 dt \frac{A \mp iBc_{\pm}}{1 - c_{\pm} - (1 + c_{\pm})t^2} \quad (7.4.-12)$$

This gives

$$I = 2D_1 \sum_{\pm} \frac{A \mp iBc_{\pm}}{s_{\pm}} \times \arctan\left(\frac{1 + c_{\pm}}{1 - c_{\pm}}\right) \quad (7.4.-12)$$

s_{\pm} is defined as $\sqrt{1 - c_{\pm}^2}$ and one must be careful with the signs. This gives for CUT_1 the approximate expression

$$\begin{aligned} CUT_1 &= D_1 \sum_{\pm} \frac{\sin(\theta) \cos(\phi) \mp iKc_{\pm}}{s_{\pm}} \times \arctan\left(\frac{1 + c_{\pm}}{1 - c_{\pm}}\right), \\ c_{\pm} &= \frac{-iK \cos(\phi) \pm \sin(\phi) \sqrt{\sin^2(\theta) + K^2}}{\sin(\theta)}. \end{aligned} \quad (7.4.-12)$$

Arcus tangent function must be defined in terms of logarithm functions since the argument is complex.

4. In the intermediate region, where the exponential differs from unity one can use expansion in Taylor polynomial to sum over integrals of rational functions of $\cos(\psi)$ and one obtains the expression

$$\begin{aligned} CUT_1 &= D_1 \sum_{n=0}^{\infty} \frac{(-1)^n}{n!} \left(\frac{b}{b_0}\right)^n I_n, \\ I_n &= \sum_{\pm} (A \mp iBc_{\pm}) I_n(c_{\pm}), \\ I_n(c) &= \int_0^{\pi/2} \frac{\cos^n(\psi)}{\cos(\psi) - c} \quad (7.4.-14) \end{aligned}$$

$I_n(c)$ can be calculated explicitly by expanding in the integrand $\cos(\psi)^n$ to polynomial with respect to $\cos(\psi) - c$, $c \equiv c_{\pm}$

$$\frac{\cos^n(\psi)}{\cos(\psi) - c} = \sum_{m=0}^{n-1} \binom{n}{m} c^m (\cos(\psi) - c)^{n-m-1} + \frac{c^n}{\cos(\psi) - c} . \quad (7.4.-14)$$

After the change of the integration variable the integral reads as

$$\begin{aligned} I_n(c) &= \sum_{m=0}^{n-1} \sum_{k=0}^{n-m-1} \binom{n}{m} \binom{n-m-1}{k} (-1)^k (1-c)^{n-m-1-k} (1+c)^k c^m I(k, n-m) \\ &+ \frac{c^n}{1-c} \times \log \left[\frac{\sqrt{1-c} + \sqrt{1+c}}{\sqrt{1-c} - \sqrt{1+c}} \right] , \\ I(k, n) &= 2 \int dt \frac{t^{2k}}{(1+t^2)^n} . \end{aligned} \quad (7.4.-15)$$

Partial integration for $I(k, n)$ gives the recursion formula

$$I(k, n) = -\frac{2^{-n+1}}{n-1} + \frac{2k-1}{2(n-1)} \times I(k-1, n-1) . \quad (7.4.-14)$$

The lowest term in the recursion formula corresponds to $I(0, n-k)$, can be calculated by using the expression

$$\begin{aligned} (1+t^2)^{-n} &= \sum_{k=0}^n c(n, k) [(1+it)^{-k} + (1-it)^{-k}] , \\ c(n, k) &= \sum_{l=0}^{n-k-1} c(n-1, k+l) 2^{-l-2} + c(n-1, n-1) 2^{-n+k-1} . \end{aligned} \quad (7.4.-14)$$

The formula is deducible by assuming the expression to be known for n and multiplying the expression with $(1+t^2)^{-1} = [(1+it)^{-1} + (1-it)^{-1}]/2$ and applying this identity to the resulting products of $(1+it)^{-1}$ and $(1-it)^{-1}$. This gives

$$I(0, n) = -2i \sum_{k=2, n} \frac{c(n, k)}{(k-1)} [1 + 2^{(k-1)/2} \sin((k-1)\pi/4)] + c(n, 1) \log \left(\frac{1+i}{1-i} \right) . \quad (7.4.-13)$$

This boils down to the following expression for CUT_1

$$\begin{aligned}
CUT_1 &= D_1 \sum_{n=0}^{\infty} \frac{(-1)^n}{n!} \left(\frac{b}{b_0}\right)^n I_n , \\
I_n &= \sum_{\pm} [A \mp iBc_{\pm}] I_n(\cos(c_{\pm})) , \\
I_n(c) &= \sum_{m=1}^{n-1} \sum_{k=0}^{n-m-1} \binom{n}{m} \binom{n-m-1}{k} (1-c)^{n-m-1-k} (1+c)^k c^m I(k, n-m-1) \\
&\quad + \frac{c^n}{1-c} \times \log \left[\frac{\sqrt{1-c} + \sqrt{1+c}}{\sqrt{1-c} - \sqrt{1+c}} \right] , \\
I(k, n) &= -\frac{2^{-n+1}}{n-1} + \frac{2k-1}{2(n-1)} \times I(k-1, n-1) , \\
I(0, n) &= -2i \sum_{k=2}^n \frac{c(n, k)}{(k-1)} [1 + 2^{(k-1)/2} \sin((k-1)\pi/4)] - c(n, 1) , \\
c(n, k) &= \sum_{l=0}^{n-k-1} c(n-1, k+l) 2^{-l-2} + c(n-1, n-1) 2^{-n+k-1} . \tag{7.4.-18}
\end{aligned}$$

This expansion in powers of c_{\pm} fails to converge when their values are very large. This happens in the case of τ -pion production amplitude. In this case one typically has however the situation in which the conditions $A_1 \simeq iB\cos(\psi)/D$ holds true in excellent approximation and one can write

$$\begin{aligned}
CUT_1 &\simeq i \frac{D_1 B}{D} \times \sum_{n=0,1,\dots} \frac{(-1)^n}{n! 2^n} \left(\frac{b}{b_0}\right)^n I_n \times , \\
I_n &= \int_0^{\pi/2} \cos(\psi)^{n+1} d\psi = \sum_{k=0}^{n+1} \binom{n+1}{k} \frac{i^{n-2k} - 1}{n+1-2k} . \tag{7.4.-18}
\end{aligned}$$

The denominator X_1 vanishes, when the conditions

$$\begin{aligned}
\cos(\theta) &= \frac{\beta}{v_{cm}} , \\
\sin(\phi) &= \cos(\psi) \tag{7.4.-18}
\end{aligned}$$

hold. In forward direction the conditions express the vanishing of the z-component of the lepton velocity in velocity cm frame as one can realize by noticing that condition reduces to the condition $v = \beta/2$ in non-relativistic limit. This corresponds to the production of lepton with momentum in scattering plane and with direction angle $\cos(\theta) = \beta/v_{cm}$.

CUT_1 diverges logarithmically for these values of kinematical variables at the limit $\phi \rightarrow 0$ as is easy to see by studying the behavior of the integral near as K approaches zero so that X_1 approaches zero at $\sin(\phi) = \cos(\Phi)$ and the integral over a small interval of length $\Delta\Psi$ around $\cos(\Psi) = \sin(\phi)$ gives a contribution proportional to $\log(A + B\Delta\Psi)/B$, $A = K[K - 2i\sin(\theta)\sin^2(\phi)]$ and $B = 2\sin(\theta)\cos(\phi)[\sin(\theta)\sin(\phi) - iK\cos(\phi)]$. Both A and B vanish at the limit $\phi \rightarrow 0$, $K \rightarrow 0$. The exponential damping reduces the magnitude of the singular contribution for large values of $\sin(\phi)$ as is clear from the first formula.

2. The contribution of the second cut

The expression for CUT_2 reads as

$$\begin{aligned}
CUT_2 &= D_2 \exp\left(-\frac{b}{b_2}\right) \times \int_0^{\pi/2} \exp\left(i\frac{b}{b_1} \cos(\psi)\right) A_2 d\psi , \\
D_2 &= -\frac{\sin(\frac{\phi}{2})}{u \sin(\theta)} , \\
b_1 &= \frac{\hbar \beta}{m \gamma_1} , \quad b_2 = \frac{\hbar}{mb \gamma_1 \times \sin(\theta) \cos(\phi)} \\
A_2 &= \frac{A \cos(\psi) + B}{\cos^2(\psi) + 2iC \cos(\psi) + D} , \\
A &= \sin(\theta) \cos(\phi) u , \quad B = \frac{w}{v_{cm}} + \frac{v}{\beta} \sin^2(\theta) [\sin^2(\phi) - \cos^2(\phi)] , \\
C &= \frac{\beta w \cos(\phi)}{u v_{cm} \sin(\theta)} , \quad D = -\frac{1}{u^2} \left(\frac{\sin^2(\phi)}{\gamma^2} + \beta^2 (v^2 \sin^2(\theta) - \frac{2vw}{v_{cm}}) \cos^2(\phi) \right) \\
&\quad + \frac{w^2}{v_{cm}^2 u^2 \sin^2(\theta)} + 2i \frac{\beta v}{u} \sin(\theta) \cos(\phi) , \\
u &= 1 - \beta v \cos(\theta) , \quad w = 1 - \frac{v_{cm}}{\beta} \cos(\theta) .
\end{aligned} \tag{7.4.-24}$$

(7.4.-23)

The denominator X_2 has no poles and the contribution of the second cut is therefore always finite.

1. The factor $\exp(-b/b_2)$ gives an exponential reduction and the contribution of CUT_2 is large only when the criterion

$$b < \frac{\hbar}{m} \times \frac{1}{v \gamma_1 \sin(\theta) \cos(\phi)}$$

for the impact parameter b is satisfied. Large values of \hbar increase the range of allowed impact parameters since the Compton length of lepton increases.

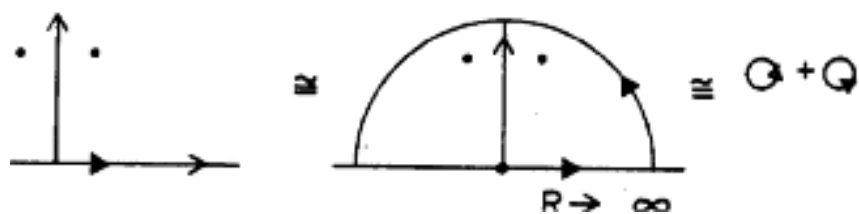
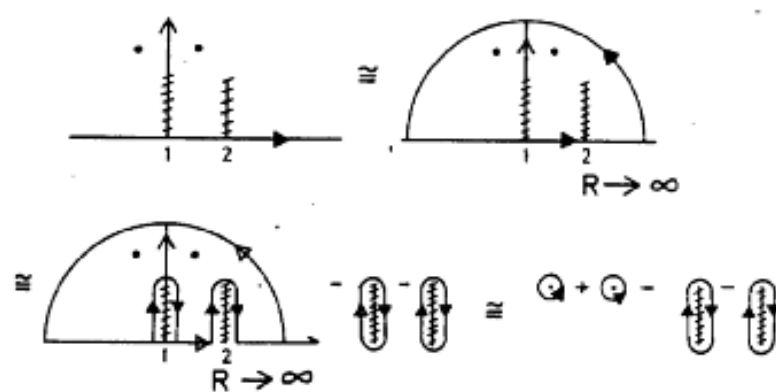
2. At the limit when the exponent becomes very large the variation of the phase factor implies destructive interference and one can perform stationary phase approximation around $\psi = \pi/2$. This gives

$$\begin{aligned}
CUT_2 &\simeq \sqrt{\frac{2\pi b_1}{b}} \times D_2 \times \exp\left(\frac{b}{b_2}\right) A_2(\psi = 0) , \\
D_2 &= -\frac{\sin(\frac{\phi}{2})}{u \sin(\theta)} , \quad A_2 = \frac{A}{D} .
\end{aligned} \tag{7.4.-23}$$

3. As for CUT_1 , the integral over ψ can be expressed as a finite sum of integrals of rational functions, when the value of $(b/b_1) \cos(\psi)$ is so small that $\exp(i(b/b_1) \cos(\psi))$ can be approximated by a Taylor polynomial. More generally, one obtains the expansion

$$\begin{aligned}
CUT_2 &= D_2 \exp\left(-\frac{b}{b_2}\right) \times \sum_{n=0}^{\infty} \frac{1}{n!} i^n \left(\frac{b}{b_1}\right)^n I_n(A, B, C, D) , \\
I_n(A, B, C, D) &= \int_0^{\pi/2} \cos(\psi)^n \frac{A + iB \cos(\psi)}{\cos^2(\psi) + C \cos(\psi) + D} .
\end{aligned} \tag{7.4.-23}$$

The integrand of $I_n(A, B, C, D)$ is same rational function as in the case of CUT_1 but the parameters A, B, C, D given in the expression for CUT_2 are different functions of the kinematical variables. The functions appearing in the expression for integrals $I_n(c)$ correspond to the roots of the denominator of A_2 and are given by $c_{\pm} = -iC \pm \sqrt{-C^2 - D}$, where C and D are the function appearing in the general expression for CUT_2 in Eq. 7.4.-23.

Figure 7.3: Evaluation of k_y -integral using residue calculus.Figure 7.4: Evaluation of k_x -integral using residue calculus.

7.4.2 Production amplitude in quantum model

The previous expressions for CUT_1 and CUT_2 as such give the production amplitude for given b in the classical model and the cross section can be calculated by integrating over the values of b . The finite Taylor expansion of the amplitude in powers of b allows explicit formulas when impact parameter cutoff is assumed.

General expression of the production amplitude

In quantum model the production amplitude can be reduced to simpler form by using the defining integral representation of Bessel functions

$$\begin{aligned}
 f_B &= i \int F(b) J_0(\Delta kb) (CUT_1 + CUT_2) b db , \\
 F &= 1 \text{ for } \exp(i(S)) \text{ option} , \\
 F(b \geq b_{cr}) &= \int dz \frac{1}{\sqrt{z^2 + b^2}} = 2 \ln\left(\frac{\sqrt{a^2 - b^2} + a}{b}\right) \text{ for } \exp(i(S)) - 1 \text{ option} , \\
 \Delta k &= 2k \sin\left(\frac{\alpha}{2}\right) , \quad k = M_R \beta .
 \end{aligned} \tag{7.4.-25}$$

Note that F is a rather slowly varying function of b and in good approximation can be replaced by its average value $A(b, p)$, which has been already explicitly calculated as power series in b . α_{em} corresponds to the value of α_{em} for the standard value of Planck constant.

The limit $\Delta k = 0$

The integral of the contribution of CUT_1 over the impact parameter b involves integrals of the form

$$\begin{aligned}
 J_{1,n} &= b_0^2 \int J_0(\Delta kb) F(b) x^{n+1} dx , \\
 x &= \frac{b}{b_0} .
 \end{aligned} \tag{7.4.-25}$$

Here a is the upper impact parameter cutoff. For CUT_2 one has integrals of the form

$$\begin{aligned}
 J_{2,n} &= b_1^2 \left(\frac{b_2}{b_1}\right)^{n+2} \int J_0(\Delta kb) F(b) \exp(-x) x^{n+1} dx , \\
 x &= \frac{b}{b_2} .
 \end{aligned} \tag{7.4.-25}$$

Using the following approximations it is possible to estimate the integrals analytically.

1. The logarithmic term is slowly varying function and can be replaced with its average value

$$F(b) \rightarrow \langle F(b) \rangle \equiv F . \tag{7.4.-24}$$

2. Δk is fixed once the value of the impact parameter is known. At the limit $\Delta k = 0$ making sense for very high energy collisions one can but the value of Bessel function to $J_0(0) = 1$. Hence it is advantageous to calculate the integrals of $\int CUT_i b db$.

Consider first the integral $\int CUT_1 b db$. If exponential series converges rapidly one can use Taylor polynomial and calculate the integrals explicitly. When this is not the case one can calculate integral approximately and the total integral is sum over two contributions:

$$\int CUT_1 b db = I_a + I_b . \tag{7.4.-23}$$

1. The region in which Taylor expansion converges rapidly gives rise integrals

$$\begin{aligned} I_{1,n} &\simeq b_0^2 \int x^{n+1} dx = b_0^2 \frac{1}{n+2} \left[\left(\frac{b_{max}}{b_0} \right)^{n+2} - \left(\frac{b_{cr}}{b_0} \right)^{n+2} \right] \simeq b_0^2 \frac{1}{n+2} \left(\frac{b_{max}}{b_0} \right)^{n+2} , \\ I_{2,n} &\simeq b_1^2 \left(\frac{b_2}{b_1} \right)^{n+2} \int exp(-x) x^{n+1} dx = b_1^2 \left(\frac{b_2}{b_1} \right)^{n+2} (n+1)! . \end{aligned} \quad (7.4.-24)$$

2. For the perturbative part of CUT_1 one obtains the expression

$$\begin{aligned} I_a &= \int_0^{b_{max}} CUT_1 b db = D_1 \times b_0^2 \times \sum_{n=0}^{\infty} \frac{1}{n!(n+2)} \left(\frac{b_{max}}{b_0} \right)^{n+2} I_n(A, B, C, D) , \\ D_1 &= -\frac{1}{2} \frac{\sin(\phi)}{\sin(\theta)} , \quad b_0 = \frac{\hbar\beta\gamma}{m\gamma_1} . \end{aligned} \quad (7.4.-25)$$

There b_{max} is the largest value of b for which the series converges sufficiently rapidly.

3. The convergence of the exponential series is poor for large values of b/b_0 , that is for $b > b_m$. In this case one can use the approximation in which the multiplier of exponent function in the integrand is replaced with its value at $\psi = \pi/2$ so that amplitude becomes proportional to b_0/b . In this case the integral over b gives a factor proportional to ab_0 , where a is the impact parameter cutoff.

$$\begin{aligned} I_b &\equiv \int_{b_m}^a CUT_1 b db \simeq b_0(a - b_m) D_1 \times A_1(\psi = \pi/2) \\ &= \frac{\beta\gamma}{\gamma_1} \times \frac{\hbar}{m} \times \frac{\sin^2(\theta) \cos(\phi) \sin(\phi)}{\sin^2(\theta) \sin^2(\phi) + K^2} , \\ D_1 &= -\frac{1}{2} \frac{\sin(\phi)}{\sin(\theta)} , \quad A_1(\psi = \pi/2) = \frac{A}{D} . \end{aligned} \quad (7.4.-27)$$

4. As already explained, the expansion based on partial fractions does not converge, when the roots c_{\pm} have very large values. This indeed occurs in the case of τ -pion production cross section. In this case one has $A_1 \simeq iB \cos(\psi)/D$ in excellent approximation and one can calculate CUT_1 in much easier manner. Using the formula of Eq. 7.4.-18 for CUT_1 , one obtains

$$\begin{aligned} \int CUT_1 b db &\simeq b_0^2 \frac{D_1 B}{D} \times \sum_{n=0,1,\dots} \frac{(-1)^n}{n!(n+2)2^n} \times \sum_{k=0}^{n+1} \binom{n+1}{k} c_{n,k} \times \left(\frac{b_{max}}{b_0} \right)^n , \\ c_{n,k} &= \frac{i^{n+1-2k} - 1}{n+1-2k} \text{ for } n \neq 2k-1 , \quad c_{n,k} = \frac{i\pi}{2} \text{ for } n = 2k-1 , \end{aligned} \quad (7.4.-27)$$

Note that for $n = 2k + 1 = k$ the coefficient diverges formally and actua

Highly analogous treatment applies to the integral of CUT_2 .

1. For the perturbative contribution to $\int CUT_2 bdb$ one obtains

$$\begin{aligned} I_a &= \int_0^{b_{1,max}} CUT_2 bdb = b_1^2 D_2 \sum_{n=0}^{\infty} (n+1) i^n I_n(A, B, C, D) \times \left(\frac{b_2}{b_1}\right)^{n+2} , \\ D_2 &= -\frac{\sin(\frac{\phi}{2})}{u \sin(\theta)} , \\ b_1 &= \frac{\hbar\beta}{m\gamma_1} , \quad b_2 = \frac{\hbar}{m\gamma_1} \frac{1}{\sin(\theta)\cos(\phi)} . \end{aligned} \quad (7.4.-28)$$

2. Taylor series converges slowly for

$$\frac{b_1}{b_2} = \frac{\sin(\theta)\cos(\phi)}{\beta} \rightarrow 0 .$$

In this case one can replace $\exp(-b/b_2)$ with unity or expand it as Taylor series taking only few terms. This gives the expression for the integral which is of the same general form as in the case of CUT_1

$$I_a = \int_0^{b_{max}} CUT_2 bdb = b_1^2 D_2 \sum_{n=0}^{\infty} \frac{i^n}{n!(n+2)} I_n(A, B, C, D) \left(\frac{b_{max}}{b_1}\right)^{n+1} . \quad (7.4.-28)$$

3. Also when b/b_1 becomes very large, one must apply stationary phase approximation to calculate the contribution of CUT_2 which gives a result proportional to $\sqrt{b_1/b}$. Assume that $b_m \gg b_1$ is the value of impact parameter above which stationary phase approximation is good. This gives for the non-perturbative contribution to the production amplitude the expression

$$\begin{aligned} I_b &= \int_{b_m}^a CUT_2 bdb = k \sqrt{\frac{2\pi b_1}{b_2}} b_2^2 \times D_2 \times A_2(\psi = \pi/2) , \\ k &= \int_{x_1}^{x_2} \exp(-x) x^{1/2} dx = 2 \int_{\sqrt{x_1}}^{\sqrt{x_2}} \exp(-u^2) u^2 du , \\ x_1 &= \frac{b_m}{b_2} , \quad x_2 = \frac{a}{b_2} . \end{aligned} \quad (7.4.-29)$$

In good approximation one can take $x_2 = \infty$. $x_1 = 0$ gives the upper bound $k \leq \sqrt{\pi}$ for the integral.

Some remarks relating to the numerics are in order.

1. The contributions of both CUT_1 and CUT_2 are proportional to $1/\sin(\theta)$ in the forward direction. The denominators of A_i however behave like $1/\sin^2(\theta)$ at this limit so that the amplitude behaves as $\sin(\theta)$ at this limit and the amplitude approaches to zero like $\sin(\theta)$. Therefore the singularity is only apparent but must be taken into account in the calculation since one has $c_{\pm} \rightarrow i\infty$ at this limit for CUT_2 and for CUT_1 the roots approach to $c_+ = c_- = i\infty$. One must pose a cutoff θ_{min} below which the contribution of CUT_1 and CUT_2 are calculated directly using approximate he expressions for $D_i A_i$.

$$\begin{aligned} D_1 A_1 &\rightarrow -\frac{i}{K} \cos(\psi) \times \sin(\theta) \rightarrow 0 \\ D_2 A_2 &\rightarrow -\frac{wv_{cm}}{w} \times \sin(\theta) \rightarrow 0 . \end{aligned} \quad (7.4.-29)$$

In good approximation both contributions vanish since also $\sin^2(\theta)$ factor from the phase space integration reduces the contribution.

2. A second numerical problem is posed by the possible vanishing of

$$K = \beta\gamma\left(1 - \frac{v_c m}{\beta} \cos(\theta)\right) .$$

In this case the roots $c_{\pm} = \pm \sin(\phi)$ are real and c_+ gives rise to a pole in the integrand.

The singularity to the amplitude comes from the logarithmic contributions in the Taylor series expansion of the amplitude. The sum of the singular contributions coming from c_+ and c_- are of form

$$\frac{c_n}{2} (\sqrt{1 - \sin(\phi)} + \sqrt{1 + \sin(\phi)}) \log\left(\frac{1+u}{1-u}\right) , \quad u = \sqrt{\frac{1 + \sin(\phi)}{1 - \sin(\phi)}} .$$

Here c_n characterizes the $1/(\cos(\psi) - c_{\pm})$ term of associated with the $\cos(\psi)^n$ term in the Taylor expansion. Logarithm becomes singular for the two terms in the sum at the limit $\phi \rightarrow 0$. The sum however behaves as

$$\frac{c_n}{2} \sin(\phi) \log\left(\frac{\sin(\phi)}{2}\right) .$$

so that the net result vanishes at the limit $\phi \rightarrow 0$. It is essential that the logarithmic singularities corresponding to the roots c_+ and c_- cancel each other and this must be taken into account in numerics. There is also apparent singularity at $\phi = \pi/2$ canceled by $\cos(\phi)$ factor in D_1 . The simplest manner to get rid of the problem is to exclude small intervals $[0, \epsilon]$ and $[\pi/2 - \epsilon, \pi/2]$ from the phase space volume.

Improved approximation to the production cross section

The approximation $J_0(\Delta k_T(b)b) = 1$ and $F(b) = F = \text{constant}$ allows to perform the integrations over impact parameter explicitly (for $\exp(iS)$ option $F = 1$ holds true identically in the lowest order approximation). An improved approximation is obtained by dividing the range of impact parameters to pieces and performing the integrals over the impact parameter ranges exactly using the average values of these functions. This requires only a straightforward generalization of the formulas derived above involving integrals of the functions x^n and $\exp(-x)x^n$ over finite range. Obviously this is still numerically well-controlled procedure.

7.4.3 Evaluation of the singular parts of the amplitudes

The singular parts of the amplitudes $CUT_{1,sing}$ and $B_{1,sing}$ are rational functions of $\cos(\psi)$ and the integrals over ψ can be evaluated exactly.

In the classical model the expression for $U_{1,sing}$ appearing as integrand in the expression of $CUT_{1,sing}$ reads as

$$\begin{aligned}
A_{1,sing} &= -\frac{1}{2\sqrt{K^2 + \sin^2(\theta)}}(\sin(\theta)\cos(\phi)A_a + iKA_b) , \\
A_a &= I_1(\beta, \pi/2) = \int_0^{\pi/2} d\psi f_1 , \\
A_b &= I_2(\beta, \pi/2) = \int_0^{\pi/2} d\psi f_2 , \\
f_1 &= \frac{1}{(\cos(\psi) - c_1)(\cos(\psi) - c_2)} , \\
f_2 &= \cos(\psi)f_1 , \\
c_1 &= \frac{-iK\cos(\phi) + \sin(\phi)\sqrt{K^2 + \sin^2(\theta)}}{\sin(\theta)} , \\
c_2 &= -\bar{c}_1 .
\end{aligned} \tag{7.4.-34}$$

Here c_i are the roots of the polynomial X_1 appearing in the denominator of the integrand.

In quantum model the approximate expression for the singular contribution to the production amplitude can be written as

$$\begin{aligned}
B_{1,sing} &\simeq k_1 \frac{\sin(\theta)\sin(\phi)}{2\sqrt{K^2 + \sin^2(\theta)}} \sum_n \langle F \rangle_n (I(x(n+1)) - I(x(n))) , \\
I(x) &= \exp\left(-\frac{\sin(\phi)x}{\sin(\phi_0)}\right) (\sin(\theta)\cos(\phi)A_a(\Delta ka, x) + iKA_b(\Delta ka, x)) , \\
k_1 &= 2\pi^2 M_R Z_1 Z_2 \alpha_{em} \frac{\sqrt{2}}{\sqrt{\Delta k \pi}} \sin(\phi_0) .
\end{aligned} \tag{7.4.-36}$$

The expressions for the amplitudes $A_a(k, x)$ and $A_b(k, x)$ read as

$$\begin{aligned}
A_a(k, x) &= \cos(kx)I_3(k, 0, \pi/2) + i\sin(\phi_0)k\sin(kx)I_5(k, 0, \pi/2) , \\
A_b(k, x) &= \cos(kx)I_4(k, 0, \pi/2) + i\sin(\phi_0)k\sin(kx)I_3(k, 0, \pi/2) , \\
I_i(k, \alpha, \beta) &= \int_\alpha^\beta f_i(k)d\psi , \\
f_3(k) &= \frac{\cos(\psi)}{(\cos^2(\psi) + \sin^2(\phi_0)k^2)} f_1(k) , \\
f_4(k) &= \cos(\psi)f_3(k) , \\
f_5(k) &= \frac{1}{(\cos^2(\psi) + \sin^2(\phi_0)k^2)} f_1(k) .
\end{aligned} \tag{7.4.-41}$$

The expressions for the integrals I_i as functions of the endpoints α and β can be written as

$$\begin{aligned}
I_1(k, \alpha, \beta) &= I_0(c_1, \alpha, \beta) - I_0(c_2, \alpha, \beta) , \\
I_2(\alpha, \beta) &= c_1 I_0(c_1, \alpha, \beta) - c_2 I_0(c_2, \alpha, \beta) , \\
I_3 &= C_{34} \sum_{i=1,2,j=3,4} \frac{1}{(c_i - c_j)} (c_i I_0(c_i, \alpha, \beta) - c_j I_0(c_j, \alpha, \beta)) , \\
I_4 &= C_{34} \sum_{i=1,2,j=3,4} \frac{1}{(c_i - c_j)} ((c_i - c_j)(\beta - \alpha) - c_i^2 I_0(c_i, \alpha, \beta) + c_j^2 I_0(c_j, \alpha, \beta)) , \\
I_5 &= C_{34} \sum_{i=1,2,j=3,4} \frac{1}{(c_i - c_j)} (I_0(c_i, \alpha, \beta) - I_0(c_j, \alpha, \beta)) , \\
C_{34} &= \frac{1}{c_3 - c_4} = \frac{1}{2ikas\sin(\phi_0)} .
\end{aligned} \tag{7.4.-45}$$

The parameters c_1 and c_2 are the zeros of X_1 as function of $\cos(\psi)$ and c_3 and c_4 the zeros of the function $\cos^2(\psi) + k^2 a^2 \sin^2(\phi_0)$:

$$\begin{aligned}
c_1 &= \frac{-iK\cos(\phi) + \sin(\phi)\sqrt{K^2 + \sin^2(\theta)}}{\sin(\theta)} , \\
c_2 &= \frac{-iK\cos(\phi) - \sin(\phi)\sqrt{K^2 + \sin^2(\theta)}}{\sin(\theta)} , \\
c_3 &= ikas\sin(\phi_0) , \\
c_4 &= -ikas\sin(\phi_0) .
\end{aligned} \tag{7.4.-48}$$

The basic integral $I_0(c, \alpha, \beta)$ appearing in the formulas is given by

$$\begin{aligned}
I_0(c, \alpha, \beta) &= \int_{\alpha}^{\beta} d\psi \frac{1}{(\cos(\psi) - c)} , \\
&= \frac{1}{\sqrt{1 - c^2}} (f(\alpha) - f(\beta)) , \\
f(x) &= \ln\left(\frac{1 + \tan(x/2)t_0}{1 - \tan(x/2)t_0}\right) , \\
t_0 &= \sqrt{\frac{1 - c}{1 + c}} .
\end{aligned} \tag{7.4.-50}$$

From the expression of I_0 one discovers that scattering amplitude has logarithmic singularity, when the condition $\tan(\alpha/2) = 1/t_0$ or $\tan(\beta/2) = 1/t_0$ is satisfied and appears, when c_1 and c_2 are real. This happens at the cone $K = 0$ ($\theta = \theta_0$), when the condition

$$\begin{aligned}
\sqrt{\frac{1 - \sin(\phi)}{1 + \sin(\phi)}} &= \tan(x/2) , \\
x &= \alpha \text{ or } \beta .
\end{aligned} \tag{7.4.-50}$$

holds true. The condition is satisfied for $\phi \simeq x/2$. $x = 0$ is the only interesting case and gives singularity at $\phi = 0$. In the classical case this gives logarithmic singularity in production amplitude for all scattering angles.

Bibliography

Books about TGD

- [1] M. Pitkänen (2006), *Topological Geometrostatics: Overview*.
http://tgd.wippiespace.com/public_html/tgdview/tgdview.html.
- [2] M. Pitkänen (2006), *Quantum Physics as Infinite-Dimensional Geometry*.
http://tgd.wippiespace.com/public_html/tgdgeom/tgdgeom.html.
- [3] M. Pitkänen (2006), *Physics in Many-Sheeted Space-Time*.
http://tgd.wippiespace.com/public_html/tgdclass/tgdclass.html.
- [4] M. Pitkänen (2006), *p-Adic length Scale Hypothesis and Dark Matter Hierarchy*.
http://tgd.wippiespace.com/public_html/paddark/paddark.html.
- [5] M. Pitkänen (2006), *Quantum TGD*.
http://tgd.wippiespace.com/public_html/tgdquant/tgdquant.html.
- [6] M. Pitkänen (2006), *TGD as a Generalized Number Theory*.
http://tgd.wippiespace.com/public_html/tgdnumber/tgdnumber.html.
- [7] M. Pitkänen (2006), *TGD and Fringe Physics*.
http://tgd.wippiespace.com/public_html/freenergy/freenergy.html.

Books about TGD Inspired Theory of Consciousness and Quantum Biology

- [8] M. Pitkänen (2006), *TGD Inspired Theory of Consciousness*.
http://tgd.wippiespace.com/public_html/tgdconsc/tgdconsc.html.
- [9] M. Pitkänen (2006), *Bio-Systems as Self-Organizing Quantum Systems*.
http://tgd.wippiespace.com/public_html/bioselforg/bioselforg.html.
- [10] M. Pitkänen (2006), *Quantum Hardware of Living Matter*.
http://tgd.wippiespace.com/public_html/bioware/bioware.html.
- [11] M. Pitkänen (2006), *Bio-Systems as Conscious Holograms*.
http://tgd.wippiespace.com/public_html/hologram/hologram.html.
- [12] M. Pitkänen (2006), *Genes and Memes*.
http://tgd.wippiespace.com/public_html/genememe/genememe.html.
- [13] M. Pitkänen (2006), *Magnetospheric Consciousness*.
http://tgd.wippiespace.com/public_html/magnconsc/magnconsc.html.
- [14] M. Pitkänen (2006), *Mathematical Aspects of Consciousness Theory*.
http://tgd.wippiespace.com/public_html/mathconsc/mathconsc.html.
- [15] M. Pitkänen (2006), *TGD and EEG*.
http://tgd.wippiespace.com/public_html/tgdeeg/tgdeeg.html.

References to the chapters of the books about TGD

- [16] The chapter *p-Adic Particle Massivation: Hadron Masses* of [4].
http://tgd.wippiespace.com/public_html/paddark/paddark.html#mass3.
- [17] The chapter *TGD as a Generalized Number Theory: Infinite Primes* of [6].
http://tgd.wippiespace.com/public_html/tgdnumber/tgdnumber.html#visionc.
- [18] The chapter *Nuclear String Model* of [4].
http://tgd.wippiespace.com/public_html/paddark/paddark.html#nuclstring.
- [19] The chapter *Dark Forces and Living Matter* of [4].
http://tgd.wippiespace.com/public_html/paddark/paddark.html#darkforces.
- [20] The chapter *TGD and Nuclear Physics* of [4].
http://tgd.wippiespace.com/public_html/paddark/paddark.html#padnucl.
- [21] The chapter *p-Adic Particle Massivation: New Physics* of [4].
http://tgd.wippiespace.com/public_html/paddark/paddark.html#mass4.
- [22] The chapter *Dark Nuclear Physics and Condensed Matter* of [4].
http://tgd.wippiespace.com/public_html/paddark/paddark.html#exonuclear.
- [23] The chapter *General Ideas about Many-Sheeted Space-Time: Part I* of [3].
http://tgd.wippiespace.com/public_html/tgdclass/tgdclass.html#topcond.
- [24] The chapter *Does TGD Predict the Spectrum of Planck Constants?* of [5].
http://tgd.wippiespace.com/public_html/tgdquant/tgdquant.html#Planck.
- [25] The chapter *Cosmic Strings* of [3].
http://tgd.wippiespace.com/public_html/tgdclass/tgdclass.html#cstrings.

Appendices and references to some older books

- [26] The chapter *The Status of Lepto-pion Hypothesis* of "TGD and p-Adic Numbers".
http://tgd.wippiespace.com/public_html/padtgd/padtgd.html#leptc.

Articles related to TGD

- [27] M. Pitkänen (2007), *Further Progress in Nuclear String Hypothesis*, http://tgd.wippiespace.com/public_html/articles/nuclstring.pdf.

Theoretical physics

- [28] C. Itzykson, J.-B. Zuber (1980), *Quantum Field Theory*, 549, New York: Mc Graw- Hill Inc.
- [29] K. V. Shajesh (2008), *Eikonal approximation*, <http://www.nhn.ou.edu/~shajesh/eikonal/sp.pdf>.
- [30] L. B. Okun (1982) , *Leptons and Quarks*, North-Holland, Amsterdam.

Particle and nuclear physics

- [31] V. Barger, R. J. N. Phillips, S. Sarkar (1995), Phys. Lett. B 352,365-371.
- [32] W. Koenig *et al*(1987), Zeitschrift fur Physik A, 3288, 1297.
- [33] J. Chang *et al.* (ATIC) (2005), prepared for 29th International Cosmic Ray Conferences (ICRC 2005), Pune, India, 31 Aug 03 - 10 2005.
- [34] T. Dorigo (2008), *Some notes on the multi-muon analysis - part I*.
<http://dorigo.wordpress.com/2008/11/08/some-notes-on-the-multi-muon-analysis-part-i/>.
- [35] A.T. Goshaw *et al*(1979), Phys. Rev. Lett. 43, 1065.
- [36] P.V. Chliapnikov *et al*(1984), Phys. Lett. B 141, 276.
- [37] N. Arkani-Hamed and N. Weiner (2008), *LHC Signals for a SuperUnified Theory of Dark Matter*, arXiv:0810.0714arXiv.org.
- [38] *Pamela is coming out* (2008), <http://resonaances.blogspot.com/2008/10/pamelas-coming-out.html>.
- [39] T. Akesson *et al*(1987), Phys. Lett. B192, 463, T. Akesson *et al*(1987), Phys. Rev. D36, 2615.
- [40] KARMEN Collaboration, B. Armbruster *et al* (1995) , Phys. Lett. B 348, 19.
- [41] J.Schweppe *et al.*(1983), Phys. Rev. Lett. 51, 2261.
- [42] H.Tsertos *et al.* (1985) , Phys. Lett. 162B, 273, H.Tsertos *et al.*(1987) , Z. Phys. A 326, 235.
- [43] N. Jones (2003), *Lightning strikes release powerful X-ray bursts*, New Scientist, February 2003, issue 2381.
<http://www.newscientist.com/article.ns?id=mg17723811.500>.
- [44] M. McKee (2005), *Earth creates powerful gamma-ray flashes* NewScientist.com news service, 17 February,
<http://www.newscientist.com/channel/space/dn7025>.
- [45] P. Salabura *et al* (1990), Phys. Lett. B 245, 2, 153.
- [46] A. Chodos (1987) , Comments Nucl. Part. Phys., Vol 17, No 4, pp. 211, 223.
- [47] G. Weidenspointner *et al* (2006), *The sky distribution of positronium annihilation continuum emission measured with SPI/INTEGRAL*, Astron. Astrophys. 450, 1013, astro-ph/0601673.
- [48] L. Kraus and M. Zeller (1986), Phys. Rev. D 34, 3385.
- [49] M. Clemente *et al.* (1984), Phys. Rev. Lett. 137B, 41.
- [50] X.-G. He, J. Tandean, G. Valencia (2007), *Has HyperCP Observed a Light Higgs Boson?*, Phys. Rev. D74.
<http://arxiv.org/abs/hep-ph/0610274>.
- [51] X.-G. He, J. Tandean, G. Valencia (2007), *Light Higgs Production in Hyperon Decay*, Phys. Rev. Lett. 98.
<http://arxiv.org/abs/hep-ph/0610362>.
- [52] S. Judge *et al* (1990) , Phys.Rev. Lett., 65(8), 972.
- [53] T. Dorigo (2008), *Saving a good text from a few mistakes*.
<http://dorigo.wordpress.com/2008/11/21/saving-a-good-text-from-a-few-mistakes/>.
- [54] CDF: T. Daniels *et al* (1994), Fermilab-Conf-94/136-E; Fermilab-Conf-94/212-E.

- [55] T. Cowan et al.(1985), Phys. Rev. Lett. 54, 1761 and T. Cowan et al.(1986), Phys. Rev. Lett. 56, 444.
- [56] E. Churazov, R. Sunyaev, S. Sazonov, M. Revnivtsev, and D. Varshalovich, *Positron annihilation spectrum from the Galactic Center region observed by SPI/INTEGRAL*, Mon. Not. Roy. Astron. Soc. 357, 1377 (2005), astro-ph/0411351.
- [57] CDF Collaboration (2008), *Study of multi-muon events produced in p-pbar collisions at $\sqrt{s}=1.96$ TeV*. http://arxiv.org/PS_cache/arxiv/pdf/0810/0810.0714v1.pdf.
- [58] R. Escrivabno,E. Masso, R. Toldra (1995), Phys. Lett. B. 356, 313-318.
- [59] K. Dantzman *et al* (1989), Phys. Rev. Lett., 62, 2353.
- [60] C. I. Westbrook ,D. W Kidley, R. S. Gidley, R. S Conti and A. Rich (1987), Phys. Rev. Lett. 58, 1328.
- [61] S. Barshay (1992) , Mod. Phys. Lett. A, Vol 7, No 20, p. 1843.
- [62] Peter Woit (2008), *A new long-lived particle by CDF experiment*, <http://www.math.columbia.edu/~woit/wordpress/?p=1045>.
- [63] PAMELA Collaboration (2008), *Observation of an anomalous positron abundance in the cosmic radiation*. http://arxiv.org/PS_cache/arxiv/pdf/0810/0810.4995v1.pdf.
M. Boexio (2008), talk represented at IDM 2008, Stockholm, Sweden.
- [64] C. Cofield (2009), *Antimatter from lightning flashes the Fermi space telescope*. Popular article in Symmetry Breaking (joint Fermilab/SLAC publication), vol 6, issue 5, October.
<http://www.symmetrymagazine.org/breaking/2009/11/06/antimatter-from-lightning-flashes-the-fermi-space-telescope>
See also <http://motls.blogspot.com/2009/11/fermi-lightnings-produce-positrons.html>.
- [65] D. Hooper and L. Goodenough (2010), *Dark Matter Annihilation in The Galactic Center As Seen by the Fermi Gamma Ray Space Telescope*. <http://arxiv.org/pdf/1010.2752v1>.
- [66] R. Courtland (2010), *Hints of lightweight dark matter particle found in space*. <http://www.newscientist.com/article/dn19655-hints-of-lightweight-dark-matter-particle-found-in-space.html>.
- [67] DAMA collaboration (2010), *Results from DAMA/LIBRA at Gran Sasso*, Found. Phys. 40, p. 900. <http://people.roma2.infn.it/~dama/web/publ10.html>.
- [68] CoGENT collaboration (2010), *Results from a Search for Light-Mass Dark Matter with a P-type Point Contact Germanium Detector*. <http://arxiv.org/abs/1002.4703>.

Cosmology and astrophysics

- [69] C. Boehm, D. Hooper, J. Silk, M. Casse (2003), *MeV Dark Matter: Has It Been Detected?*. arXiv:astro-ph/0309686. See also *Astronomers claim dark matter breakthrough*. New Scientist, 6 October, 2003. <http://www.newscientist.com/news/news.jsp?id=ns99994214>.

Neuroscience

- [70] J. D. Cowan (1982), *Spontaneous symmetry breaking in large-scale nervous activity*. International Journal of Quantum Chemistry, 22:1059-1082.

Chapter 8

TGD and Nuclear Physics

8.1 Introduction

Despite the immense amount of data about nuclear properties, the first principle understanding of the nuclear strong force is still lacking. The conventional meson exchange description works at qualitative level only and does not provide a viable perturbative approach to the description of the strong force. The new concept of atomic nucleus forced by TGD suggests quite different approach to the quantitative description of the strong force in terms of the notion of field body, join along boundaries bond concept, long ranged color gauge fields associated with dark hadronic matter, and p-adic length scale hierarchy.

8.1.1 p-Adic length scale hierarchy

p-Adic length scale hypothesis

The concept of the p-adic topological condensate is the corner stone of p-adic TGD. Various levels of the topological condensate obey effective p-adic topology and are assumed to form a p-adic hierarchy ($p_1 \leq p_2$ can condense on p_2). By the length scale hypothesis, the physically interesting length scales should come as square roots of powers of 2: $L(k) \simeq 2^{\frac{k}{2}} l$, $l \simeq 1.288E + 4\sqrt{G}$ and prime powers of k are especially interesting.

For nuclear physics applications the most interesting values of k are: $k = 107$ (hadronic space-time sheet at which quarks feed their color gauge fluxes), $k = 109$ (radius of light nucleus such as alpha particle), $k = 113$ (the space-time at which quarks feed their electromagnetic gauge fluxes), $k = k_{em} = 127$ or 131 (electronic or atomic space-time sheet receiving electromagnetic gauge fluxes of nuclei).

The so called Gaussian primes are to complex integers what primes are for the ordinary integers and the Gaussian counterparts of the Mersenne primes are Gaussian primes of form $(1 \pm i)^k - 1$. Rather interestingly, $k = 113$ corresponds to a Gaussian Mersenne. Also the primes $k = 151, 157, 163, 167$ defining biologically important length scales correspond to Gaussian Mersennes. Thus the electromagnetic p-adic length scales associated with quarks, hadrons, and nuclear physics as well as with muon are in well defined sense also Mersenne length scales. A possible interpretation for complex primes is in terms of complex conformal weights for elementary particles. If the net conformal weights of physical states are required to be real this gives rise to conformal confinement.

There are however arguments suggesting the conformal weights can be complex for particles and that the imaginary part of the conformal weight defines a new kind of conserved quantum number, "scaling momentum", whose sign distinguishes between particles and their phase conjugates which can be regarded as particles of negative energy traveling to the direction of geometric past. There would be inherent arrow of geometric time associated with particles with complex conformal weight. For instance, the strange properties of phase conjugate photons could be understood since second law of thermodynamics would hold true in a reversed direction of geometric time for them.

Particles are characterized by a collection of p-adic primes

It seems that is not correct to speak about particle as a space-time sheet characterized by single p-adic prime. Already p-adic mass calculations suggest that there are several sizes corresponding to space-time sheets at which particle feeds its gauge charges. p-Adic length scale hypothesis provides further insight: the length scale is more like the size of field body and possibly also delocalization volume of particle determining the p-adic mass scale in p-adic thermodynamics rather than the geometric size for the elementary particle.

What one can definitely say that each particle is characterized by a collection of p-adic primes and one of them characterizes the mass scale of the particle whereas other characterize its interactions. There are two possible interpretations and both of them allow to resolve objections against p-adic hierarchies of color and electro-weak physics.

1. These primes characterize the space-time sheets at which it feeds its gauge fluxes and particles can interact only via their common space-time sheets and are otherwise dark with respect to each other.
2. Number theoretical vision supports the notion of multi-p p-adicity and the idea that elementary particles correspond to infinite primes, integers, or perhaps even rationals [17, 28]. To infinite primes, integers, and rationals it is possible to associate a finite rational $q = m/n$ by a homomorphism. q defines an effective q-adic topology of space-time sheet consistent with p-adic topologies defined by the primes dividing m and n (1/p-adic topology is homeomorphic to p-adic topology). The largest prime dividing m determines the mass scale of the space-time sheet in p-adic thermodynamics. m and n are exchanged by super-symmetry and the primes dividing m (n) correspond to space-time sheets with positive (negative) time orientation. Two space-time sheets characterized by rationals having common prime factors can be connected by a $\#_B$ contact and can interact by the exchange of particles characterized by divisors of m or n .

The nice feature of this option is that single multi-p p-adic space-time sheet rather than a collection of them characterizes elementary particle. Concerning the description of interaction vertices as generalization of vertices of Feynman graphs (vertices as branchings of 3-surfaces) this option is decisively simpler than option 1) and is consistent with earlier number theoretic argument allowing to evaluate gravitational coupling strength [17, 28]. It is also easier to understand why the largest prime in the collection determines the mass scale of elementary particle.

Interestingly, these two options are not necessarily mutually exclusive: single multi-p p-adic space-time sheet could correspond to many-sheeted structure with respect to real topology.

What is the proper interpretation of p-adic length scales

One of the surprises of p-adic mass calculations was that for u and d quarks electromagnetic size corresponds to $k = 113$ which corresponds to the length scale of 2×10^{-14} m. This leads to the view that also hadrons and nuclei have this size in some sense. The charge radii of even largest nuclei without neutron halo are smaller than this.

1. If electromagnetic charges of quarks inside nucleons were separately delocalized in the scale $L(113)$, also the distributions of electromagnetic charges of nuclei would be non-trivial in surprisingly long length scale. Em charges would exhibit fractionality in this length scale and Rutherford scattering cross sections would be modified. The fact that the height of the Coulomb wall at $L(113)$ is lower than the observed heights of the Coulomb wall would lead to a paradox. This suggests that the p-adic length scale $L(113)$ does not characterize the geometric size of neither nucleons nor nuclei but to the size, perhaps height, of the electromagnetic field body associated with quark/hadron/nucleus.
2. If protons feed their electric em gauge fluxes to the same space-time sheet, there is an electromagnetic harmonic oscillator potential contributing to the nuclear energies. The Mersenne prime M_{127} as a characterizer of the field body of nucleus is natural and it also corresponds to the space-time sheet of electron.

3. For weak forces the size of the field body would be given by electro-weak length scale $L(89)$. The size scale would also correspond to the p-adic delocalization length scale of ordinary sized nucleons and nuclei.
4. It turns out that the identification of nuclear strong interactions in terms of dark QCD with large value of \hbar and color length scale scaled up to $L_c \simeq 2^{11}L(107) \simeq .5 \times 10^{-11}$ m (!) predicts for the nuclei same electromagnetic sizes as in the conventional theory: scaled up sizes appear only in the dark sector and characterize the size of color field body so that paradoxes are avoided. There are also reasons to believe that dark quarks are dark also with respect to electromagnetic and weak interactions so that the sizes of corresponding field bodies are scaled up by a factor $1/v_0$.

The hypothesis that the collection of primes corresponds to multi-p p-adicity rather than collection of space-time sheets implies this. For this option various field bodies could form single field body in q-adic sense with superposed p-adic fractalities much like waves of shorter wavelength scale superposed on waves of longer wavelength scale. As noticed, this might be consistent with the existence of several p-adic field bodies with respect to real topology.

Field/magnetic bodies would represent the space-time correlate for the formation of bound states. It is even possible to think that bound state entanglement corresponds to the linking of magnetic flux tubes. The contributions of say color interactions between nucleons to the binding energy would be estimated using the field magnitudes at position of exotic quarks and the hypothesis is made that these intensities correlate with the shortest distance between dark quarks although the distance along the field body is of order L_c .

This picture finds experimental support.

1. Neutron proton scattering at low energies gives however surprisingly clear evidence for the presence of the p-adic length scales $L(109)$ ($k = 109$ is prime) and $L(113)$ in nuclear physics. The scattering lengths for s and p waves are $a_s = -2.37 \times 10^{-14}$ m and $a_t = 5.4 \times 10^{-15}$ m [54]. a_s is anomalously large and the standard explanation is that deuteron almost allows singlet wave bound state. a_t is near to $L(109) = 2L(107) \simeq 5.0 \times 10^{-15}$ m, which is in accordance with the assumption that in triplet state neutron and proton are glued by color bond together to form structure with size or order $L(109) = 2L(107)$. a_s is of same order of magnitude as $L(113) = 2 \times 10^{-14}$ m so that the interpretation in terms of the $k = 113$ space-time sheet is suggestive.
2. Neutron halos at distance of about 2.5×10^{-14} m longer than even $L(113) = 2 \times 10^{-14}$ m are difficult to understand in the standard nuclear physics framework and provide support for the large value of L_c . They could be understood in terms of delocalization of quarks in the length scale $L(113)$ and color charges in the length scale of L_c . For instance, the nucleus in the center could be color charged and neutron halo would be analogous to a colored matter around the central halo.

8.1.2 TGD based view about dark matter

TGD suggests an explanation of dark matter as a macroscopically quantum coherent phase residing at larger space-time sheets [16].

1. TGD suggests that \hbar is dynamical and possesses a spectrum expressible in terms of generalized Beraha numbers $B_r = 4\cos^2(\pi/r)$, where $r > 3$ is a rational number [34, 16]. Just above $r = 3$ arbitrarily large values of \hbar and thus also macroscopic quantum phases are possible. The criterion for transition to large \hbar phase is the failure of perturbative expansion so that Mother Nature takes care of the problems of theoretician. A good guess is that the criticality condition reads as $Q_1 Q_2 \alpha \simeq 1$ where Q_i are gauge charges and α gauge coupling strength. This leads to universal properties of the large \hbar phase. For instance, \hbar is scaled in the transition to dark phase by a harmonic or subharmonic of parameter $1/v_0 \simeq 2^{11}$ which is essentially the ratio of CP_2 length scale and Planck length [38, 16]. The criticality condition can be applied also to dark matter itself and entire hierarchy of dark matters is predicted corresponding to the spectrum of values of \hbar .

2. The particles of dark matter can also carry phase carry complex conformal weights but the net conformal weights for blocks of this kind of dark matter would be real. This implies macroscopic quantum coherence. It is not absolutely necessary that \hbar is large for this phase.
3. From the point of view of nuclear physics application of this hypothesis is to QCD. The prediction is that the electromagnetic Compton sizes of dark quarks are scaled from $L(107)$ to about $2^{11}L(107) = L(129) = 2L(127)$, which is larger than the p-adic electromagnetic size of electron! The classical scattering cross sections are not changed but changes the geometric sizes of dark quarks, hadrons, and nuclei. The original hypothesis that ordinary valence quarks are dark whereas sea quarks correspond to ordinary value of \hbar is taken as a starting point. In accordance with the earlier model, nucleons in atomic nuclei are assumed to be accompanied by color bonds connecting exotic quark and anti-quark characterized p-adic length scale $L(127)$ with ordinary value of \hbar and having thus scaled down mass of order MeV. The strong binding would be due the color bonds having exotic quark and anti-quark at their ends.
4. Quantum classical correspondence suggests that classical long ranged electro-weak gauge fields serve as classical space-time correlates for dark electro-weak gauge bosons, which are massless. This hypothesis could explain the special properties of bio-matter, in particular the chiral selection as resulting from the coupling to dark Z^0 quanta. Long range weak forces present in TGD counterpart of Higgs=0 phase should allow to understand the differences between biochemistry and the chemistry of dead matter.

The basic implication of the new view is that the earlier view about nuclear physics applies now to dark nuclear physics and large parity breaking effects and contribution of Z^0 force to scattering and interaction energy are not anymore a nuisance.

5. For ordinary condensed matter quarks and leptons Z^0 charge are screened in electro-weak length scale whereas in dark matter $k = 89$ electro-weak space-time sheet have suffered a phase transition to a p-adic topology with a larger value of k . Gaussian Mersennes, in particular those associated with $k = 113, 151, 157, 163, 167$ are excellent candidates in this respect. The particles of this exotic phase of matter would have complex conformal weights closely related to the zeros of Riemann Zeta. The simplest possibility is that they correspond to a single non-trivial zero of Zeta and there is infinite hierarchy of particles of this kind.

In dark matter phase weak gauge fluxes could be feeded to say $k = k_Z = 169$ space-time sheet corresponding to neutrino Compton length and having size of cell. For this scenario to make sense it is essential that p-adic thermodynamics predicts for dark quarks and leptons essentially the same masses as for their ordinary counterparts [26].

8.1.3 The identification of long range classical weak gauge fields as correlates for dark massless weak bosons

Long ranged electro-weak gauge fields are unavoidably present when the dimension D of the CP_2 projection of the space-time sheet is larger than 2. Classical color gauge fields are non-vanishing for all non-vacuum extremals. This poses deep interpretational problems. If ordinary quarks and leptons are assumed to carry weak charges feeded to larger space-time sheets within electro-weak length scale, large hadronic, nuclear, and atomic parity breaking effects, large contributions of the classical Z^0 force to Rutherford scattering, and strong isotopic effects, are expected. If weak charges are screened within electro-weak length scale, the question about the interpretation of long ranged classical weak fields remains.

During years I have discussed several solutions to these problems.

Option I: The trivial solution of the constraints is that Z^0 charges are neutralized at electro-weak length scale. The problem is that this option leaves open the interpretation of classical long ranged electro-weak gauge fields unavoidably present in all length scales when the dimension for the CP_2 projection of the space-time surface satisfies $D > 2$.

Option II: Second option involves several variants but the basic assumption is that nuclei or even quarks feed their Z^0 charges to a space-time sheet with size of order neutrino Compton length. The large parity breaking effects in hadronic, atomic, and nuclear length scales is not the only difficulty. The scattering of electrons, neutrons and protons in the classical long range Z^0 force contributes to the

Rutherford cross section and it is very difficult to see how neutrino screening could make these effects small enough. Strong isotopic effects in condensed matter due to the classical Z^0 interaction energy are expected. It is far from clear whether all these constraints can be satisfied by any assumptions about the structure of topological condensate.

Option III: During 2005 third option solving the problems emerged based on the progress in the understanding of the basic mathematics behind TGD.

In ordinary phase the Z^0 charges of elementary particles are indeed neutralized in intermediate boson length scale so that the problems related to the parity breaking, the large contributions of classical Z^0 force to Rutherford scattering, and large isotopic effects in condensed matter, trivialize.

Classical electro-weak gauge fields in macroscopic length scales are identified as space-time correlates for the gauge fields created by dark matter, which corresponds to a macroscopically quantum coherent phase for which elementary particles possess complex conformal weights such that the net conformal weight of the system is real.

In this phase $U(2)_{ew}$ symmetry is not broken below the scaled up weak scale except for fermions so that gauge bosons are massless below this length scale whereas fermion masses are essentially the same as for ordinary matter. By charge screening gauge bosons look massive in length scales much longer than the relevant p-adic length scale. The large parity breaking effects in living matter (chiral selection for bio-molecules) support the view that dark matter is what makes living matter living.

Classical long ranged color gauge fields always present for non-vacuum extremals are interpreted as space-time correlates of gluon fields associated with dark copies of hadron physics. It seems that this picture is indeed what TGD predicts.

8.1.4 Dark color force as a space-time correlate for the strong nuclear force?

Color confinement suggests a basic application of the basic criteria for the transition to large \hbar phase. The obvious guess is that valence quarks are dark [16, 27]. Dark matter phase for quarks does not change the lowest order classical strong interaction cross sections but reduces dramatically higher order perturbative corrections and resolves the problems created by the large value of QCD coupling strength in the hadronic phase.

The challenge is to understand the strong binding solely in terms of dark QCD with large value of \hbar reducing color coupling strength of valence quarks to $v_0 \simeq 2^{-11}$. The best manner to introduce the basic ideas is as a series of not so frequently asked questions and answers.

Rubber band model of strong nuclear force as starting point

The first question is what is the vision for nuclear strong interaction that one can start from. The sticky toffee model of Chris Illert [53] is based on the paradox created by the fact alpha particles can tunnel from the nucleus but that the reversal of this process in nuclear collisions does not occur. Illert proposes a classical model for the tunnelling of alpha particles from nucleus based on dynamical electromagnetic charge. Illert is forced to assume that virtual pions inside nuclei have considerably larger size than predicted by QCD and the model. Strikingly, the model favors fractional alpha particle charges at the nuclear surface. The TGD based interpretation would be based on the identification of the rubber bands of Illert as long color bonds having exotic light quark and anti-quark at their ends and connecting escaping alpha particle to the mother nucleus. The challenge is to give meaning to the attribute "exotic".

How the darkness of valence quarks can be consistent with the known sizes of nuclei?

The assumption about darkness of valence quarks in the sense of large \hbar ($\hbar_s = \hbar/v_0$) is very natural if one takes the basic criterion for darkness seriously. The obvious question is how the dark color force can bind the nucleons to nuclei of ordinary size if the strength of color force is v_0 and color sizes of valence quarks are about $L(129)$?

It seems also obvious that $L(107)$ in some sense defines the size for nucleons, and somehow this should be consistent with scaled up size $L(k_{eff} = 129)$ implied by the valence quarks with large \hbar . The proposal of [16, 27] inspired by RHIC findings [59] is that valence quarks are dark in the sense of

having large value of \hbar and thus correspond to $k_{eff} = 129$ whereas sea quarks correspond to ordinary value for \hbar and give rise to the QCD size $\sim L(107)$ of nucleon.

If one assumes that the typical distances between sea quark space-time sheets of nucleons is obtained by scaling down the size scale of valence quarks, the size scale of nuclei comes out correctly.

Valence quarks and exotic quarks cannot be identical

The hypothesis is that nucleons contain or there are associated with them pairs of exotic quarks and flux tubes of color field bodies of size $\sim L(129)$ connecting the exotic quark and anti-quark in separate nuclei. Nucleons would be structures with the size of ordinary nucleus formed as densely packed structures of size $L(129)$ identifiable as the size of color magnetic body.

The masses of exotic quarks must be however small so that they must differ from valence quarks. The simplest possibility is that exotic quarks are not dark but p-adically scaled down versions of sea quarks with ordinary value of \hbar having $k = 127$ so that masses are scaled down by a factor 2^{-10} .

Energetic considerations favor the option that exotic quarks associate with nucleons via the $k_{eff} = 111$ space-time sheets containing nucleons and dark quarks. Encouragingly, the assumption that nucleons topologically condense at the weak $k_{eff} = 111$ space-time sheet of size $L(111) \simeq 10^{-14}$ m of exotic quarks predicts essentially correctly the mass number of the highest known super-massive nucleus. Neutron halos are outside this radius and can be understood in terms color Coulombic binding by dark gluons. Tetraneutron can be identified as alpha particle containing two negatively charged color bonds.

What determines the binding energy per nucleon?

The binding energies per nucleon for $A \geq 4$ do not vary too much from 7 MeV but the lighter nuclei have anomalously small binding energies. The color bond defined by a color magnetic flux tube of length $\sim L(k = 127)$ or $\sim L(k_{eff} = 129)$ connecting exotic quark and anti-quark in separate nucleons with scaled down masses $m_q(dark) \sim xm_q$, with $x = 2^{-10}$ for option for $k = 127$, is a good candidate in this respect. Color magnetic spin-spin interaction would give the dominant contribution to the interaction energy as in the case of hadrons. This interaction energy is expected to depend on exotic quark pair only. The large zero point kinetic energy of light nuclei topologically condensed at $k_{eff} = 111$ space-time sheet having possible identification as the dark variant of $k = 89$ weak space-time sheet explains why the binding energies of D and ${}^3\text{He}$ are anomalously small.

What can one assume about the color bonds?

Can one allow only quark anti-quark type color bonds? Can one allow the bonds to be also electromagnetically charged as the earlier model for tetra-neutron suggests (tetra-neutron would be alpha particle containing two negatively charged color bonds so that the problems with the Fermi statistics are circumvented). Can one apply Fermi statistics simultaneously to exotic quarks and anti-quarks and dark valence quarks?

Option I: Assume that exotic and dark valence quarks are identical in the sense of Fermi statistics. This assumption sounds somewhat non-convincing but is favored by p-adic mass calculations supporting the view that the p-adic mass scale of hadronic quarks can vary. If this hypothesis holds true at least effectively, very few color bonds from a given nucleon are allowed by statistics and there are good reasons to argue that nucleons are arranged to highly tangled string like structures filling nuclear volume with two nucleons being connected by color bonds having of length of order $L(129)$. The organization into closed strings is also favored by the conservation of magnetic flux.

The notion of nuclear string is strongly supported by the resulting model explaining the nuclear binding energies per nucleon. It is essential that nucleons form what might be called nuclear strings rather than more general tangles. Attractive p-p and n-n bonds must correspond to colored ρ_0 type bonds with spin one and attractive p-n type bonds to color singlet pion type bonds. The quantitative estimates for the spin-spin interaction energy of the lightest nuclei lead to more precise estimates for the lengths of color bonds. The resulting net color quantum numbers must be compensated by dark gluon condensate, the existence of which is suggested by RHIC experiments [59]. This option is strongly favored by the estimate of nuclear binding energies.

Option II: If Fermi statistics is not assumed to apply in the proposed manner, then color magnetic flux tubes bonds between any pair of nucleons are possible. The identification of color isospin as

strong isospin still effective removes color degree of freedom. As many as 8 color tubes can leave the nucleus if exotic quarks and anti-quarks are in the same orbital state and a cubic lattice like structure would become possible. This picture would be consistent with the idea that in ordinary field theory all particle pairs contribute to the interaction energy. The large scale of the magnetic flux tubes would suggest that the contributions cannot depend much on particle pair. The behavior of the binding energies favors strongly the idea of nuclear string and reduces this option to the first one.

What is the origin of strong force and strong isospin?

Here the answer is motivated by the geometry of CP_2 allowing to identify the holonomy group of electro-weak spinor connection as $U(2)$ subgroup of color group. Strong isospin group $SU(2)$ is identified as subgroup of isotropy group $U(2)$ for space-time surfaces in a sub-theory defined by $M^4 \times S^2$, S^2 a homologically non-trivial geodesic sphere of CP_2 and second factor of $U(1) \times U(1)$ subgroup of the holonomies for the induced Abelian gauge fields corresponds to strong isospin component I_3 . The extremely tight correlations between various classical fields lead to the hypothesis that the strong isospin identifiable as color isospin I_3 of exotic quarks at the ends of color bonds attached to a given nucleon is identical with the weak isospin of the nucleon. Note that this does not require that exotic and valence quarks are identical particles in the sense of Fermi statistics.

Does the model explain the strong spin orbit coupling ($L \cdot S$ force)? This force can be identified as an effect due to the motion of fermion string containing the effectively color charged nucleons in the color magnetic field $v \times E$ induced by the motion of string in the color electric field at the dark $k = 107$ space-time sheet.

How the phenomenological shell model with harmonic oscillator potential emerges?

Nucleus can be seen as a collection of long color magnetic flux tubes glued to nucleons with the mediation of exotic quarks and anti-quarks. If nuclei form closed string, as one expects in the case of Fermi statistics constraint, also this string defines a closed string or possibly a collection of linked and knotted closed strings. If Fermi statistics constraint is not applied, the nuclear strings form a more complex knotted and linked tangle. The stringy space-time sheets would be the color magnetic flux tubes connecting exotic quarks belonging to different nucleons.

The color bonds between the nucleons are indeed strings connecting them and the averaged interaction between neighboring nucleons in the nuclear string gives in the lowest order approximation 3-D harmonic oscillator potential although strings have $D = 2$ transversal degrees of freedom. Even in the case that nucleons for nuclear strings and thus have only two bonds to neighbors the average force around equilibrium position is expected to be a harmonic force in a good approximation. The nuclear wave functions fix the restrictions of stringy wave functionals to the positions of nucleons at the nuclear strings. Using M-theory language, nucleons would represent branes connected by color magnetic flux tubes representing strings whose ends co-move with branes.

Which nuclei are the most stable ones and what is the origin of magic numbers?

$P = N$ closed strings correspond to energy minima and their deformations obtained by adding or subtracting nucleons in general correspond to smaller binding energy per nucleon. Thus the observed strong correlation between P and N finds a natural explanation unlike in the harmonic oscillator model. For large values of A the generation of dark gluon condensate and corresponding color Coulombic binding energy favors the surplus of neutrons and the generation of neutron halos. The model explains also the spectrum of light nuclei, in particular the absence of pp , nn , ppp , and nnn nuclei.

In the standard framework spin-orbit coupling explains the magic nuclei and color Coulombic force gives rise to this kind of force in the same manner as in atomic physics context. Besides the standard magic numbers there are also non-standard ones (such as $Z, N = 6, 12$) if the maximum of binding energy is taken as a definition of magic, there are also other magic numbers than the standard ones. Hence can consider also alternative explanations for magic numbers. The geometric view about nucleus suggests that the five Platonic regular solids might defined favor nuclear configurations and it indeed turns that they explain non-standard magic numbers for light nuclei.

New magic nuclei might be obtained by linking strings representing doubly magic nuclei. An entire hierarchy of linkings becomes possible and could explain the new magic numbers 14, 16, 30, 32 discovered for neutrons [58]. Linking of the nuclear strings could be rather stable by Pauli Exclusion

Principle. For instance, ^{16}O would correspond to linked ^4He and ^{12}C nuclei. Higher magic numbers 28, 50, ... allow partitions to sums of lower magic numbers which encourages to consider the geometric interpretation as linked nuclei. p-Adic length scale hypothesis in turn suggests the existence of magic numbers coming as powers of 2^3 .

What about the description of nuclear reactions?

The identification of nuclei as linked and knotted strings filling the nuclear volume for constant nuclear density leads to a topological description for the nuclear reactions with simplest reactions corresponding to fusion and fission of closed nuclear strings. The microscopic description is in terms of nucleon collisions in which exotic quarks and anti-quarks are re-shared between nucleons and also new pairs are created. The distinction to ordinary string model is that the topological reactions for strings can occur only when the points at which they are attached to nucleons collide.

The old fashioned description of the nuclear strong force is based on the meson exchange picture. The perturbation theory based on the exchange of pions doesn't however make sense in practice. In the hadronic string model this description would be replaced by hadronic string diagrams. The description of nuclear scattering in terms of nuclear strings allows phenomenological interpretation in terms of stringy diagrams but color bonds between nucleons do not correspond to meson exchanges but are something genuinely new.

8.1.5 Tritium beta decay anomaly

The proposed model explains the anomaly associated with the tritium beta decay. What has been observed [44, 66] is that the spectrum intensity of electrons has a narrow bump near the endpoint energy. Also the maximum energy E_0 of electrons is shifted downwards.

I have considered two explanations for the anomaly. The original models are based on TGD variants of original models [51, 56] involving belt of dark neutrinos or antineutrinos along the orbit of Earth. Only recently (towards the end of year 2008) I realized that nuclear string model provides much more elegant explanation of the anomaly and has also the potential to explain much more general anomalies [42, 36, 63].

8.1.6 Cold fusion and Trojan horse mechanism

Cold fusion [39] has not been taken seriously by the physics community but the situation has begun to change gradually. There is an increasing evidence for the occurrence of nuclear transmutations of heavier elements besides the production of ^4He and ^3H whereas the production rate of ^3He and neutrons is very low. These characteristics are not consistent with the standard nuclear physics predictions. Also Coulomb wall and the absence of gamma rays and the lack of a mechanism transferring nuclear energy to the electrolyte have been used as an argument against cold fusion.

An additional piece to the puzzle came when Ditmire *et al* [57] observed that the spectrum of electron energies in laser induced explosions of ion clusters extends up to energies of order MeV (rather than 10^2 eV!): this suggests that strong interactions are involved.

The possibility of charged color bonds explaining tetra-neutron allows to construct a model explaining both the observations of Ditmire *et al* and cold fusion and nuclear transmutations. 'Trojan horse mechanism' allows to circumvent the Coulomb wall, and explains various selection rules and the absence of gamma rays, and also provides a mechanism for the heating of electrolyte.

8.2 Model for the nucleus based on exotic quarks

The challenge is to understand the strong binding solely in terms of the color bonds and large value of \hbar for valence quarks reducing color coupling strength to v_0 and scaling their sizes to $L(107)/v_0 = L(129)$. There are many questions to be answered. How exotic quarks with scaled down masses differ from dark valence quarks? How the model can be consistent with the known nuclear radii of nuclei if valence quarks have Compton length of order $L(129)$?

8.2.1 The notion of color bond

The basic notion is that of color bond having exotic quark and anti-quark at its ends. Color bonds connecting nucleons make them effectively color charged so that nuclei can be regarded as color bound states of nucleons glued together using color bonds.

The motivation for the notion of color bond comes from the hypothesis that valence quarks are in large \hbar phase, and also from the ideas inspired by the work of Chris Illert [53] suggesting that long virtual pions act as "rubber bands" connecting nucleons to each other. There are indications that the quark distribution functions for the nucleons inside nuclei differ from those for free nucleons [44, 36]. QCD based estimates show that color van der Waals force is not involved [36]. The contribution of the quark pairs associated with color bonds is a possible explanation for this phenomenon.

8.2.2 Are the quarks associated with color bonds dark or p-adically scaled down quarks?

What seems clear is that color bonds with light quark and antiquark, to be referred as exotic quarks in the sequel, at their ends could explain strong nuclear force. Concerning the identification of the exotic quarks there are frustratingly many options. In lack of deeper understanding, the only manner to proceed is to try to make a detailed comparison of various alternatives in hope of identifying a unique internally consistent option.

The basic observation is that if four-momentum is conserved in the phase transition to the dark phase, the masses of quarks in large \hbar phase should not differ from those in ordinary phase, which means that Compton lengths and p-adic length scale are scaled up by a factor $1/v_0$. This assumption explains elegantly cold fusion and many other anomalies [27, 16]. The quarks at the ends of color bonds must however have scaled down masses to not affect too much the masses of nuclei. This option would also allow to identify valence and possibly also sea quarks as dark quarks in accordance with the general criterion for the transition to dark phase as proposed in the model for RHIC events [59, 16].

Exotic quarks must be light. Hence there should be some difference between exotic and valence quarks. This leaves two options to consider.

Are the exotic quarks p-adically scaled down versions of ordinary quarks with ordinary value of \hbar ?

Exotic quarks could simply correspond to longer p-adic length scale, say M_{127} and thus having masses scaled down by a factor 2^{-10} but ordinary value of \hbar . One can also consider the possibility that they correspond to a QCD associated with M_{127} as proposed earlier. They could also correspond to their own weak length scale and weak bosons. This would resolve the objections against new elementary particles coming from the decay widths of intermediate gauge bosons even without assumption about the loss of asymptotic freedom implying that the QCD in question effectively exists only in finite length scale range.

p-Adic mass calculations indeed support the view to that hadronic quarks appear as several scaled up variants and there is no reason to assume that also scaled down variants could not appear. This hypothesis leads to correct order of magnitude estimates for the color magnetic spin-spin interaction energy.

For this option valence (and possibly also sea) quarks could be dark and have color sizes of order $L(k_{eff} = 129)$ as suggested by the criterion $\alpha_s Q_c^2 \simeq 1$ for color confinement as a transition to a dark phase.

Do exotic quarks correspond to large \hbar and reduced c ?

If valence quarks are dark one can wonder why not also exotic quarks are dark and whether there exists a mechanism reducing their masses by a factor v_0 .

If one questions the assumption that \hbar is a fundamental constant, sooner or later also the question "What about c ?" pops up. There are indeed motivations for expecting that c has a discrete spectrum in a well-defined sense. TGD predicts an infinite variety of warped vacuum extremals defining imbeddings of M^4 to $M^4 \times CP_2$ with $g_{tt} = \sqrt{1 - R^2\omega^2}$, $g_{ij} = -\delta_{ij}$, and if common M^4 time coordinate is used for them the maximal signal velocity is for them given by $c_{\#}/c = \sqrt{1 - R^2\omega^2}$.

Physically this means that the time taken for light to travel between point A and B depends on what space-time sheet the light travels even in the case that gravitational and gauge fields are absent. The fact that the analog of Bohr quantization occurs for the deformed vacuum extremals of Kähler action suggests that $c_{\#}$ has a discrete spectrum.

This inspires the question whether also light velocity c besides \hbar is quantized in powers of v_0 so that the rest energies of dark quarks would be given by $E_0 = \hbar_s c_{\#} / L(k_{eff} = k + 22) = \hbar c_{\#} / L(k)$ and scale down because of the scaling $c \rightarrow v_0 \times c$. A distinction between rest mass and rest energy should be made since rest mass is scaled up as $M \rightarrow M/v_0$. Compton time would be by a factor $1/v_0^2$ longer than the ordinary Compton time.

If c and \hbar can scale up separately but in powers of v_0 (or its harmonics and sub-harmonics) it is possible to have a situation in which $\hbar c$ remains invariant because mass scale is reduced v_0 and \hbar is increased by $1/v_0$. In the case of dark quarks this would mean that light would propagate with velocity $2^{-11}c$ along various space-time sheets associated with dark quarks.

This admittedly complex looking option would mean that valence quarks have large \hbar but ordinary c and exotic quarks have large \hbar but small c due to the warping of their space-time sheet in time direction.

8.2.3 Electro-weak properties of exotic and dark quarks

Are exotic quarks scaled down with respect to electromagnetic interactions?

The earlier models involving large \hbar rely on the assumption that the transition to large \hbar phase with respect to electromagnetic interactions occurs only under special conditions (models for cold fusion and structure of water represent basic examples). Hence valence quarks can be in large \hbar phase only with respect to strong and possibly weak interactions.

1. For p-adically scaled down exotic quarks also the electromagnetic space-time sheet should correspond to scaled up value of k since $k = 113$ would give too large contribution to the quark mass. It is not clear whether both em and color space-time sheets can correspond to $k = 127$ or whether one must have $k_{em} = 131$.
2. For exotic quarks with large \hbar and small c the situation can be different $k = 107$ contribution to quark mass is scaled down by v_0 factor: $m_q(\text{dark}) = v_0 m_q \sim .05$ MeV. Since $k = 113$ contributes a considerable fraction to hadron mass, one can argue that also the $k = 113$ contribution to the mass must be scaled down so that dark quarks would be also electromagnetically dark. If so, the size of $k = 113$ dark electromagnetic field body would be of order atomic size and nuclei would represent in their structure also atomic length scale.

Are exotic and dark quarks scaled down with respect to weak interactions?

What about darkness of exotic and dark quarks with respect to weak interactions? The qualitative behavior of the binding energies of $A \leq 4$ nuclei can be understood if they possess zero point kinetic energy associated with space-time sheet with size characterized by $L(k = 111 = 3 \times 37) \simeq 10^{-14}$ m. Also the maximal mass number of super-heavy nuclei without neutron halo is predicted correctly. $k_{eff} = 111$ happens to correspond to the scaled weak length scale M_{89} which raises the possibility that dark quarks correspond to large value of \hbar with respect to weak interactions. This could be the case for dark valence quarks and both identifications of exotic quarks.

1. For $k = 127$ quarks with dark weak interactions no large parity breaking effects are induced neither below mass scale m_W .
2. For large \hbar -small c option the scale invariance of gauge interactions would mean that the masses of the corresponding weak bosons are of order 50 MeV but the weak interaction rates are scaled down by a factor v_0^2 since the ratios m_q/m_W invariant under the transition to dark phase appear in the rates: this at energy scale smaller than $v_0 m_w$. This disfavors this option.

8.2.4 How the statistics of exotic and ordinary quarks relate to each other?

Exotic and ordinary quarks should be identical or in some sense effectively identical in order that nuclear string picture would result.

Can one regard exotic quarks and ordinary quarks as identical fermions?

The first guess would be that this is not the case. One must be however cautious. The fact that p-adically scaled up variants of quarks appear in the model of hadrons suggested by p-adic mass calculations, suggests that the scaled up versions must be regarded as identical fermions. Since also the scaling of \hbar induces only a scaling up of length scale, one might argue that this conclusion holds true quite generally.

Identity is also favored by a physical argument. If identity holds true, Fermi statistics forces the nucleons to form closed nuclear strings to maximize their binding energies. The notion nuclear string explains nicely the behavior nuclear binding energies per nucleon and also suggests that linking and knotting could define mechanisms for nuclear binding.

Could dark quarks and ordinary quarks be only effectively identical?

The idea of regarding quarks and dark quarks as identical fermions does not sound convincing, and one can ask the idea could make sense in some effective sense only.

1. The effective identity follows from a model for matter antimatter symmetry assuming that ordinary quarks form strongly correlated pairs with dark anti-quarks so that nucleons would be accompanied by dark antinucleons and quarks and dark quarks would be effectively identical. This option looks however rather science fictive and involves un-necessarily strong assumption.
2. A weaker hypothesis is inspired by the model of topological condensation based on $\#$ (/worm-hole/ topological sum) contacts [28]. $\#$ contact can be modelled as a CP_2 type extremal with Euclidian signature of induced metric forming topological sum with the two space-time sheets having Minkowskian signature of induced metric. $\#$ contact is thus accompanied by two light-like 3-D causal horizons at which the metric determinant vanishes. These causal horizons carry of quantum numbers and are identified as partons. If the contact is passive in the sense that it mediates only gauge fluxes, the quantum numbers of the two partons cancel each other. This can be true also for four-momentum in the case that time orientations of the space-time sheets are opposite.

This kind of $\#$ contacts between $k_{eff} = 129$ and $k = 127$ space-time sheets would force effective identity of $k = 127$ and $k_{eff} = 129$ quarks. The implication would be that in many-sheeted sense nucleons inside nuclei would have ordinary quantum numbers whereas in single sheeted point sense they would carry quantum numbers of quark or anti-quark.

8.3 Model of strong nuclear force based on color bonds between exotic quarks

In this section the color bond model of strong nuclear force is developed in more detail.

8.3.1 A model for color bonds in terms of color flux tubes

Simple model for color bond

Consider next a simple model for color bond.

1. The first guess would be that the color bond has quantum numbers of neutral pion so that also the pair of nucleons connected by a color bond would behave like a pion. This gives attractive color magnetic interaction energy and an attractive identification is as p-n bond.
2. Also the bonds with identical spins and identical color charges at the ends of the bond yield an attractive color magnetic spin-spin interaction energy. This kind of bonds would be responsible for p-p and n-n pairing. In this case color magnetic energy is however by a factor 1/3 smaller and could explain the non-existence of pp and nn bound states. An even number of neutral ρ type bonds could be allowed without anomalous contribution to the spin. High spin nuclei could contain many ρ type bonds so that antimatter would play important role in the physics of heavy nuclei.

3. A further generalization by allowing also electromagnetically charged color bonds with em quantum numbers of pion and ρ would explain tetra-neutron [55, 54] as alpha particle (pnpn) with two π_- type color bonds. This would predict a rich variety of exotic nuclei. Long color bonds connecting quark and anti-quark attached to different nucleons would also allow to understand the observation of Chris Illert [53] that the classical description of quantum tunneling suggests that nucleons at the surface of nucleus have charges which are fractional.

This picture would suggest that the color isospin of the quark at the end of the bond equals to the weak isospin of the nucleon and is also identifiable as the strong isospin of the nucleon inside nucleus. To achieve an overall color neutrality the presence a dark gluon condensate compensating for the net color charge of colored bonds must be assumed. This could also compensate the net spin of the colored bonds.

The surplus of neutrons in nuclei would tend to create a non-vanishing color isospin which could be cancelled by the dark gluon condensate. The results of RHIC experiment [59] can be understood in TGD framework as a generation of a highly tangled string like structure containing large number of p-p and n-n type bonds and thus also dark gluon condensate neutralizing the net color charge. This would suggest that in a good approximation the nuclei could be seen as tangled string like structures formed from protons and neutrons. If the distances between nuclei are indeed what standard nuclear physics suggests, kind of nuclear strings would be in question.

Simple model for color magnetic flux tubes

Color magnetic flux tubes carrying also color electric fields would define the color magnetic body of the nucleus having size of order $L(129)$. Dark quarks would have also weak and electromagnetic field bodies with sizes $L(111)$ and $L(135)$. The color magnetic body codes information about nucleus itself but also has independent degrees of freedom, in particular those associated with linking and knotting of the flux tubes (braiding plays a key role in the models of topological quantum computation [42]).

Color flux tubes carry a non-trivial color magnetic flux and one can wonder whether the color flux tubes can end or whether they form closed circuits. Since CP_2 geometry allows homological magnetic charges, color magnetic flux tubes could have ends with quarks and anti-quark at them acting as sources of the color magnetic field. The model for binding energies however favors closed strings. In the general case the color magnetic flux tubes would have a complex sub-manifold of CP_2 with boundary as a CP_2 projection.

The spin-spin interaction energies depend crucially on the value of the color magnetic field strength experienced by the exotic quark at the end of color flux tube, and one can at least try make educated guesses about it. The conservation of the color magnetic flux gives the condition $g_s B \propto 1/S$, where S is the area of the cross section of the tube. $S \geq L^2(107)$ is the first guess for the area if valence quarks are ordinary. $S \geq L^2(k_{eff} = 129)$ is the natural guess if valence quarks are dark.

The quantization of the color magnetic flux using the scaled up value of \hbar would give $\int g_s B dS = n/v_0$ implying $g_s B \simeq n/v_0 S$. When applied to $S \sim L^2(107)$ the quantization condition would give quite too large estimate for the spin-spin interaction energy. For $S \sim L^2(129)$ the scale of the interaction energy would come out correctly. For $k = 127$ option $S \sim L^2(127)$ is forced by the quantization condition.

This observation favors strongly dark valence quarks for both options. The magnetic flux of exotic quarks would be feeded to flux tubes of transverse area $\sim L^2(k)$, $k = 127$ or $k = 129$, coupling naturally with the color magnetic flux tubes of valence quarks with size $L(129)$.

A further constraint could come from the requirement that the flux tubes is such that locally the magnetic field looks like a dipole field. This would mean that the flux tube would become thicker at larger distances roughly as $S(r) \propto r^3$. An alternative restriction would come from the requirement that the energy of the color magnetic flux tube is same irrespective of its cross section at dark quark position. This would give $S \propto L$ where L is the length of the flux tube.

Quantum classical correspondence requires color bonds

Non-vacuum extremals are always accompanied by a non-vanishing classical electro-weak and color gauge fields. This is an obvious challenge for quantum classical correspondence. The presence of a suitable configuration of color bonds with dark quarks at their ends starting from nucleon gives hopes

of resolving this interpretational problem. Dark quarks and anti-quarks would serve as sources of the color and weak electric gauge fluxes and quarks and nucleons would create the classical em field.

The requirement that classical Abelian gauge fluxes are equal to the quantum charges would pose very strong conditions on the physical states. For instance, quantization condition for Weinberg angle is expected to appear. The fact that classical fluxes are inversely proportional to the inverse of the corresponding gauge coupling strength $1/\alpha_i$ gives additional flexibility and with a proper choice of gauge coupling strengths the conditions might be satisfied and space-time description would also code for the values of gauge coupling strengths. Color bonds should be present in all length scales for non-vacuum extremals encouraging the hypothesis about the p-adic hierarchy of dark QCD type phases.

Identification of dark quarks and valence quarks as identical fermions forces the organization of nucleons to nuclear strings?

Quantum classical correspondence in strong form gives strong constraints on the construction. The model explaining the nuclear binding energies per nucleon strongly favors the option in which nucleons arrange to form closed nuclear strings. If dark quarks and ordinary valence quarks can be regarded as identical fermions this hypothesis follows as a prediction. Therefore this hypothesis, which admittedly looks ad hoc and might make sense only effectively (see the discussion below), deserves a detailed consideration.

Fermi statistics implies that the quark at the end of the color bond must be in a spin state which is different from the spin state of the nucleon (spin of d quark in the case of p=uud and u quark in the case of n) to allow local S-wave. For anti-quarks there are no constraints. Only d (u) quark with spin opposite to that of p (n) can be associated with p (n) end of the color bond. Hence at most five different bonds can begin from a given nucleon. In the case of proton p_\downarrow they are give by $d_\uparrow\bar{d}_\downarrow$, $\bar{q}_\downarrow q_\uparrow$, $q = u, d$.

Only two bonds between given nuclei are possible as following examples demonstrate.

1. $p_\downarrow - n_\uparrow$: $d_\uparrow\bar{d}_\downarrow, \bar{u}_\downarrow u_\uparrow$.
2. $p_\downarrow - p_\uparrow$: $d_\uparrow\bar{d}_\uparrow, \bar{d}_\uparrow d_\uparrow$.

The experimentation with the rules in case of neutral color bonds supports the view that although branchings are possible, they do not allow more than $A = Z + N$ bonds. One example is 6 nucleon state with p at center connected by 5 bonds to p+ 4n at periphery and an additional bond connecting peripheral p and n. This kind of configuration could be considered as one possible configuration in the case of ${}^6\text{Li}$ and ${}^6\text{He}$. It would seem that there is always a closed string structure with A bonds maximizing the color magnetic binding energy. The allowance of also charged color bonds makes possible to understand tetra-neutron as alpha particle with two charged color bonds.

The fact that neutron number for nuclei tends to be larger than proton number implies that the number of n-n type ρ bonds for stringy configurations is higher than p-p type bonds so that net color isospin equal equal to $I_3 = -(A - 2Z)$ is generated in case of stringy nuclei and is most naturally cancelled by a dark gluon condensate. Neutralizing gluon condensate allows neutron halo with a non-vanishing value of I_3 .

8.3.2 About the energetics of color bonds

To build a more quantitative picture about the anatomy of the color bond it is necessary to consider its energetics. The assumption that in lowest order in \hbar the binding energy transforms as rest energy under the p-adic scaling and scaling of \hbar makes it easy to make order of magnitude estimates by scaling from the hadronic case.

Color field energy of the bond

At the microscopic level the harmonic oscillator description should correspond to the color energy associated with color bonds having u or d type quark and corresponding anti-quarks at their ends. For simplicity restrict the consideration in the sequel to electromagnetically neutral color bonds.

Besides spin-spin interaction energy and color Coulombic interaction energy there are contributions of color fields coded by the string tension $T_d = v_0 T$ of the color bond, where $T \simeq 1/\text{GeV}^2$ is hadronic

string tension. The energy of string with given length remains invariant in the combined scaling of \hbar , string tension, and length L of the color bond represented by color magnetic flux tube (which contain also color electric fields).

1. The mass of the color bonds between valence quarks assumed to have $\hbar_s = \hbar/v_0$ of length $L = xL(129)$ are given by $M(107) \sim x \times \hbar/L(107) \sim x \times .5 \text{ GeV}$ and correspond naturally to the energy scale of hadronic strong interactions.
2. The rest energy of the color bonds between $k = 127$ quarks with ordinary value of \hbar having length $L = xL(127)$ are given by $M(127) \sim x \times \hbar/L(127) = 2^{-10}M(107)$ so that the order of magnitude is $x \times .5 \text{ MeV}$.
3. The rest energy of the color bonds between $k_{eff} = 129$ dark quarks with $c_{\#} = v_0c$ is given by the same expression. Note however that rest mass would be scaled up by a factor $1/v_0$.

The resulting picture seems to be in a dramatic conflict with the electromagnetic size of nucleus which favors the $L \sim L(107) < 2 \text{ fm}$ rather than $L \sim L(129)$ and which is smaller by a factor 2^{-11} and which favors also the notion of nuclear string. The resolution of the paradox is based on the notion of color magnetic body. Color bonds behave like color magnetic dipoles and bonds correspond to flux tubes of a topologically quantized dipole type color magnetic field having length of order $L(129) \simeq 5 \times 10^{-12} \text{ m}$ connecting nucleons at distance $L < L(107)$.

Color magnetic spin-spin interaction energy, the structure of color bonds, and the size scale of the nucleus

Color magnetic spin-spin interaction allows to understand $\rho - \pi$ mass splitting in terms of color magnetic spin-spin interaction expected to give the dominating contribution to the nuclear binding energy. The quantitative formulation of this idea requiring consistency with p-adic mass calculations and with existing view about typical electromagnetic nuclear size scale fixed by the height of Coulomb wall leads to a rather unique picture about color magnetic bonds.

1. Questions

One can pose several questions helping to develop a detailed model for the structure of the color bond.

1. The contributions $k = 113$ and $k = 107$ space-time sheets to the mass squared are of same order of magnitude [17]. The contributions to the mass squared add coherently inside a given space-time sheet. This requires that nucleonic space-time sheet are not directly connected by join along boundaries bonds and the assumption that color bond connect dark quarks is consistent with this. This means that it makes sense to estimate contributions to the mass squared at single nucleon level.
2. The contribution of color magnetic spin-spin interaction to the mass squared of nucleon can be regarded as coming from $k = 107$ space-time sheets as p-adic contribution but with a large value of \hbar . If $k = 107$ contribution would vanish, only a positive contribution to mass would be possible since the real counterpart Δm_R^2 of p-adic Δm^2 is always positive whereas $(m^2 + \Delta m^2)_R < m_R^2$ can hold true.
3. What has been said about color magnetic body and color bonds applies also to electromagnetic field body characterized by $k = 113$. The usual electromagnetic size of nucleus is defined by the relative distances of nucleons in M^4 can be much smaller than $L(113)$ so that the prediction for Coulomb wall is not reduced to the Coulomb potential at distance $L(113)$. Nucleon mass could be seen as due to p-adic thermodynamics for mass squared (or rather, conformal weight) with the real counterpart of the temperature being determined by p-adic length scale $L(113)$.
4. The model inspired by p-adic mass calculations [17] forced the conclusion that valence quarks have join along boundaries bonds between $k = 107$ and $k = 113$ space-time sheets possibly feeding color fluxes so that closed flux loops between the two space-time sheets result. The counter intuitive conclusion was that roughly half of quark mass is contributed by the $k = 113$

space-time sheet which is by a scale factor 8 larger than the color size of quarks. If valence quarks are dark, scaled up $k = 107$ space-time sheet having $k_{eff} = 129$ becomes the larger space-time sheet, and the situation would not look so counter-intuitive anymore.

5. How the ends of the color bonds are attached to the $k = 113$ nucleon space-time sheets? The simplest assumption is that color bonds correspond to color magnetic flux tubes of length scale $L(129)$ starting at or being closely associated with $k = 107$ space-time sheets of nucleons. Hence the contribution to the mass squared would come from scaled up $k_{eff} = 129$ space-time sheet and add coherently to the dominating p-adic $k = 107$ contribution to the mass squared of nucleon.
6. If exotic quarks are $k = 127$ quarks with ordinary value of \hbar , one encounters the problem how their contributions can add coherently with $k_{eff} = 129$ color contribution to reduce the rest energy of nucleus. One possibility allowed by the appearance of harmonics of v_0 is that \hbar is scaled up by $1/(2v_0) \simeq 2^{10}$ so that space-time sheets have same size or that p-adic additivity of mass squared is possible for effective p-adic topologies which do not differ too much from each other.

2. Estimate for color magnetic spin-spin interaction energy

Suppose the scaling invariance in the sense that the binding energies transform in the lowest order just like rest masses so that one can estimate the color magnetic spin-spin splittings from the corresponding splittings for hadrons without any detailed modelling. This hypothesis is very attractive predicts for both options that the scale of color magnetic spin-spin splitting is 2^{-n} times lower than for $\pi - \rho$ system, where $n = 10$ for $n = 127$ option and $n = 11$ for $k_{eff} = 129$ option. For scaled down spin-spin interaction energy for π type bond is $E \sim .4$ MeV for $k = 127$ and $\sim .2$ MeV for $k_{eff} = 11$, which would mean that the bond is shorter than scaled up length $L(\pi)$ of color bond between valence quarks of pion.

The further assumption that color magnetic spin-spin interaction energy behaves as $\alpha_s/m_q^2 L^3$, $L = x2^n L(\pi)$. This gives $E \simeq x^{-3}2^{-n}E(107)$. The value of x can be estimated from the requirement that the energy is of order few MeV. This gives $x \sim 10^{-1/3}$ for $k = 127$ option and $x \sim (20)^{-1/3}$ for $k_{eff} = 129$ option.

8.4 How the color bond model relates to the ordinary description of nuclear strong interactions?

How the notion of strong isospin emerges from the color bond model? What about shell model description based on harmonic oscillator potential? Does the model predict spin-orbit interaction? Is it possible to understand the general behavior of the nuclear binding energies, in particular the anomalously small binding energies of light nuclei? What about magic numbers? The following discussion tries to answer these questions.

8.4.1 How strong isospin emerges?

The notion of strong isospin is a crucial piece of standard nuclear physics. Could it emerge naturally in the transition to the phase involving dark quarks? Could the transition to color confined phase mean a reduction of color group as isotropy group of CP_2 type extremals representing elementary particles to $U(2)$ identifiable as strong isospin group. Could $U(1)_Y \times U(1)_{I_3}$ or $U(1)_{I_3}$ be identifiable as the Abelian holonomy group of the classical color field responsible for the selection of a preferred direction of strong isospin?

This picture would not mean breaking of the color symmetry at the configuration space level where it would rotate space-time surfaces in CP_2 like rigid bodies. Rather, the breaking would be analogous to the breaking of rotational symmetry of individual particles by particle interactions. Strong isospin would correspond to the isotropy group of the space-time surface and the preferred quantization direction to the holonomy group of the induced color gauge field. The topological condensation of quarks and gluons at hadronic and nuclear space-time surfaces would freeze the color rotational degrees of freedom apart from isotropies providing thus the appropriate description for the reduced color symmetries.

Mathematical support for the picture from classical TGD

There is mathematical support for the proposed view and closely relating to the long-standing interpretational problems of TGD.

1. CP_2 holonomy group is identifiable as $U(2)$ subgroup of color group and well as electro-weak gauge group. Hitherto the possible physical meaning of this connection has remained poorly understood. $U(2)$ subgroup as isotropies of space-time surfaces with $D = 2$ -dimensional CP_2 projection, which belongs to a homologically non-trivial geodesic sphere S^2 , and defines a sub-theory for which all induced gauge fields are Abelian and a natural selection of a preferred strong isospin direction occurs. Thus one might identify strong isospin symmetry as the $SU(2)$ subgroup of color group acting as the isotropy group of the space-time surface and strong isospin would not correspond to the group of isometries but to space-time isotropies.
2. Color isospin component of gluon field, em field and Z^0 field which corresponds to weak isospin, are proportional to each other for solutions having 2-dimensional CP_2 projection. In fact, both Z^0 and I_3 component of gluon field are proportional to the induced Kähler form with a positive coefficient. If the proposed quantum classical correspondence for color bonds holds true, this means that the signs of these charges are indeed correlated also for nucleon and quark/ anti-quark. The ratios of these charges are fixed for the extremals for which CP_2 projection is homologically non-trivial geodesic sphere S^2 .
3. It is far from clear whether the classical Z^0 field can vanish for any non-vacuum extremals. If this is not the case, dark weak bosons would be unavoidable and strong isospin could be identifiable as color isospin and dark weak isospin. The predicted parity breaking effects need not be easily detectable since dark quarks would be indeed dark matter. An open question is whether some kind of duality holds true in the sense that either color field or vectorial part of Z^0 field could be used to describe the nuclear interaction. This duality brings in mind the $SO(4) \leftrightarrow SU(3)$ duality motivated by the number theoretical vision [22, 26, 21, 19].
4. The minimal form of the quantum classical correspondence is that at least the signs of the I_3 and Y components of the color electric flux correlate with the dark quark at the end of color bond and the signs of the Z^0 field and Kähler field correlate with the sign of weak isospin and weak hyper-charge of nucleon. A stronger condition is that these classical gauge fluxes are identical with a proper choice of the values of gauge coupling strengths and that in the case of color fluxes the quark at the end of the bond determines the color gauge fluxes in the bond whereas electromagnetic would distribute freely between the bonds.

Correlation between weak isospin and color isospin

The weakest assumption motivated by this picture would be that the sign of color isospin correlates with the sign of weak isospin so that the quarks at the ends of color bonds starting from nucleon would have color isospin equal to the weak isospin of the nucleon:

$$I_{3,s} = I_{3,w} = I_{3,c} .$$

This assumption would allow to interpret the attractive strong interaction between nucleons in terms of color magnetic interaction. p-n bond would be neutral π_0 type color singlet bonds. n-n and p-p bonds would have spin ± 1 and color isospin equal to strong iso-spin of ρ_{\pm} . Note that QCD type color singlet states invariant under $I_3 \rightarrow -I_3$ would not be possible. Color magnetic interaction mediated by the pion type color bond would be attractive for p and n since color isospins would be opposite sign but repulsive for pp and nn since color isospins would have same sign. The ρ type color bond with identical spins and color isospins I_3 would generate attractive interaction between identical nucleons. The color magnetic spin-spin interaction energy would be 3 times larger for π type bond so that the formation of deuterium as bound state of p and n and absence of pp and nn bound states might be understood.

It is not possible to exclude charged color bonds, and as will be found, their presence provides an elegant explanation for tetra-neutron [55, 54].

8.4.2 How to understand the emergence of harmonic oscillator potential and spin-orbit interaction?

Shell model based on harmonic oscillator potential and spin-orbit interaction provide rather satisfactory model of nuclei explaining among other things magic numbers.

Harmonic oscillator potential as a phenomenological description

It would be a mistake to interpret nuclear harmonic oscillator potential in terms Coulomb potential for the I_3 component of the classical gluon field having color isospin as its source. Interaction energy would have correct sign only for proton+quark/ anti-quark or neutron+quark/ anti-quark at the end of the color bond so that only neutrons or protons would experience an attractive force.

Rather, the harmonic oscillator potential codes for the presence of color Coulombic and color magnetic interaction energies and is thus only a phenomenological notion. Harmonic oscillator potential emerges indeed naturally since the nucleus can be regarded as a collection of nucleons connected by color flux tubes acting rather literally as strings. The expansion the interaction energy around equilibrium position naturally gives a collection of harmonic oscillators. The average force experience by a nucleon is expected to be radial and this justifies the introduction of external harmonic oscillator potential depending on A via the oscillator frequency.

At the deeper level the system could be seen as a tangle formed by bosonic strings represented by magnetic flux tubes connecting $k = 111$ space-time sheets containing dark quarks closely associated with nucleons. The oscillations of nucleons in harmonic oscillator potential induce the motion of dark quark space-time sheets play the role of branes in turn inducing motion of the ends of flux tubes fix the boundary values for the vibrations of the flux tubes. The average force experienced by nucleons around equilibrium configuration is expected to define radial harmonic force. This holds true even in the case of nuclear string.

In this picture $k = 111$ space-time sheets could contain the nucleons of even heaviest nuclei if the nucleon size is taken to be $2L(107)/3 \simeq 1.5$ fm. The prediction for the highest possible mass number without neutron halo, which is at radius $2.5 \times L(111)$, would be $A = 296$ assuming that nuclear radius is $R = 1.4$ fm. $A = 298$ is the mass number of the heaviest known superheavy nucleus [41] so that the prediction can be regarded as a victory of the model.

Could conformal invariance play a key role in nuclear physics?

The behavior the binding energies of $A \leq 4$ nucleons strongly suggest that nucleons are arranged to closed string like structure and have thus only two color bonds to the neighboring nucleons in the nuclear string. The thickness of the string at the positions of fermions defines the length scale cutoff defining the minimal volume taken by a single localized fermion characterized by given p-adic prime.

The conformal invariance for the sections of the string defined by color bonds is should allow a deeper formulation of the model in terms of conformal field theory. The harmonic oscillator spectrum for single particle states could be interpreted in terms of stringy mass squared formula $M^2 = M_0^2 + m_1^2 n$ which gives in good approximation

$$M = m_0 + \frac{m_1^2}{2M_0} n . \tag{8.4.1}$$

The force constant would be determined by M_0 which would be equal to nucleon mass.

Presumably this would bring to the mind of M-theorist nucleus as a system of A branes connected by strings. The restriction of the wave functional of the string consisting of portions connecting nucleons to each other at the junction points would be induced by the wave functions of nucleons. The bosonic excitations of the color magnetic strings would contribute to color magnetic energy of the string characterized by its string tension. This energy scale might be considerably smaller than the fermionic energy scale determined by the color magnetic spin-spin interaction.

Dark color force as the origin of spin-orbit interaction

The deviation of the magic numbers associated with protons ($Z = 2, 8, 20, 28, 40, 82$) and neutrons ($A - Z = 2, 8, 20, 28, 50, 82, 126$) from the predictions of harmonic oscillator model provided the

motivation for the introduction of the spin orbit interaction V_{L-S} [36] with the following general form

$$V_{L-S}(r) = \bar{L} \cdot \bar{S} \frac{1}{r} \left(\frac{dV_s}{dr} + \frac{dV_I}{dr} \bar{\tau}_1 \cdot \bar{\tau}_2 \right) . \quad (8.4.2)$$

The interaction implies the splitting of (j, l, s) eigen states so that states $j, l = j \pm \frac{1}{2}$ have different energies. If the energy splitting is large enough, some states belonging to a higher shell come down and combine with the states of the lower shell to form a new shell with a larger magic number. This is what should happen for both proton and neutron single particle states.

The origin of spin-orbit interaction would be the classical color field created by the color isospin in p-p and n-n color bonds and dark gluons compensating the color charge. Spin-orbit interaction results in the atomic physics context from the motion of electrons in the electric field of the nucleus. The moving particle experiences in its rest frame a magnetic field $\bar{B} = \bar{v} \times \bar{E}$, which in the spherically symmetric case can by little manipulations can be cast into the form

$$\bar{B} = \frac{\bar{p}}{m} \times \frac{\bar{r}}{r} \frac{dV}{dr} = \bar{L} \frac{1}{m} \frac{1}{r} \frac{dV}{dr} .$$

The interaction energy is given by

$$E = -\bar{\mu} \cdot \bar{B} = -\frac{ge}{2m^2} \bar{S} \cdot \bar{L} \times \frac{1}{r} \frac{dV}{dr} . \quad (8.4.3)$$

Here magnetic moment is expressed in terms of spin using the standard definitions. g denotes Lande factor and equals in good approximation to $g = 2$ for point like fermion.

Classical color field can be assumed to contain only I_3 component and be derivable from spherically symmetric potential. In the recent case the color bonds moving made from two quarks and moving with nuclear string experience the force.

The color magnetic moments of the quark and anti-quark are of same sign in for both ρ and π type bond so that the isospin component of the net color magnetic moment can be written as

$$\bar{\mu}_c = g \frac{g_s}{m_q(\text{dark})} I_3 \bar{S} . \quad (8.4.4)$$

Here g_s denotes color coupling constant, g is the Lande factor equal to $g = 2$ in ideal case, and m is mass parameter. Since the color bond is color magnetic flux tube attached from its ends to dark quarks it seems that the mass parameter $m_q(\text{dark})$ in the magnetic moment is that of dark quark and should be $m_q(\text{dark}) = v_0 m_q$.

An additional factor of 2 is present because both quark and anti-quark of the bond give same contribution to the color moment of the bond. I_3 equals to the strong isospin of the nucleon to which the quark is attached and spin is opposite to the spin of this quark so that a complete correlation with the quantum numbers of the second nucleon results and one can effectively assign the spin orbit interaction with nucleons. The net interaction energy is small for spin paired states. The sign of the interaction is same for both neutrons and protons.

Using the general form of the spin orbit interaction potential in the non-relativistic limit, one can cast the $L - S$ interaction term in a the form

$$V_{L-S}(r) = \frac{16\pi\mu_c}{m_q(\text{dark})} \bar{L} \cdot \bar{S} \frac{1}{r} \frac{dV_{I_3}}{dr} . \quad (8.4.5)$$

In the first order perturbation theory the energy change for (j, l, s) eigen state with $l = j + \epsilon \frac{1}{2}$, $\epsilon = \pm 1$ and spherically symmetric electromagnetic gauge potential $V(r)$ [33] given by

$$\begin{aligned} \Delta E(j, l = j + \epsilon \frac{1}{2}) &= \frac{4g_s^2}{m_q^2(\text{dark})L^3} (N - P) c(l) \left[\epsilon(j + \frac{1}{2}) + 1 \right] , \\ c(l) &= -\frac{4\pi L^3}{g_s(N - P)} \langle l | \frac{1}{r} \frac{dV_{I_3}}{dr} | l \rangle . \end{aligned} \quad (8.4.4)$$

The coefficient $g_s/4\pi$ and factor $N - P$ have been extracted from the color gauge potential in the expression of $a(l)$ to get a more kinematical expression. $N - P$ -proportionality is expected since the system has net nuclear color isospin proportional to $N - P$ neutralized by dark gluons which can be thought of as creating the potential in which the nuclear string moves. The constant $c(l)$ contains information about the detailed distribution of the color isospin. $c(l)$ depends also on the details of the model (the behavior of single particle radial wave function $R_{n,l}(r)$ in case of wave mechanical model and now on its analog defined by the wave function of nucleon induced by nuclear string). R denotes the nuclear charge radius.

The general order of magnitude of L is $L \sim L(129)$. What comes in mind first is the scaling $L \sim v_0^{-1}R_0$, $R_0 \sim (3/5) \times L(107) \simeq 1.5 \times 10^{-15}$ m. This is not consistent with the fact that for light nuclei with $A \leq 4$ L decreases with A but conforms with the fact that spin-spin interaction energies which are very sensitive to L can depend only slightly on A so that L must be more or less independent on A . Assume $g_s^2/4\pi = .1$ and $m_q = m_u \sim .1$ GeV, $g = 1$ in the formula for the color magnetic moment. By using $2\pi/L(107) \simeq .5$ GeV these assumptions lead to the estimate

$$\begin{aligned} \Delta E(j, l = j + \epsilon \frac{1}{2}) &= \frac{4g_s^2}{m_q^2 L^3(107)} \left(\frac{5}{3}\right)^3 \times v_0 \times (N - P) \times c(l) \times \left[\epsilon(j + \frac{1}{2}) + 1 \right] \\ &\simeq \left(\epsilon(j + \frac{1}{2}) + 1 \right) \times (N - P) \times c(l) \times 2.9 \text{ MeV} . \end{aligned} \tag{8.4.3}$$

The splitting is predicted to be same for protons and neutrons and also the magnitude looks reasonable. If the dark gluons are at the center and create a potential which is gradually screened by the dark quark pairs, the sign of the spin-orbit interaction term is correct meaning that the contribution to binding energy is positive for $j + 1/2$ state. In the case of neutron halo the unscreened remainder of the dark gluon color charge would define $1/r$ potential at the halo possibly responsible for the stability.

This estimate should be compared to the general estimate for the energy scale in the harmonic oscillator model given by $\omega_0 \simeq 41 \cdot A^{-1/3}$ MeV [36] so that the general orders of magnitude make sense.

8.4.3 Binding energies and stability of light nuclei

Some examples are in order to see whether the proposed picture might have something to do with reality.

Binding energies of light nuclei

The estimate for the binding energies of light nuclei is based on the following assumptions.

1. Neglect the contribution of the string tension and dark gluon condensate to the binding energy.
2. Suppose that the number of bonds equals to A for $A \leq 4$ nuclei and that the the bonds are arranged to maximize color magnetic spin-spin interaction energy. A possible interpretation is in terms of a closed color magnetic flux tube connecting nucleons. The presence of close color magnetic flux tubes is necessary unless one allows homological color magnetic monopoles. This option favors the maximization of the number of n-p type bonds since their spin-spin interaction energy is 3 times higher than that for p-p and n-n type bonds. This is just a working hypothesis and would mean that nuclei could be seen as nuclear strings.

The alternative interpretation is that the number bonds per nucleon is constant so that the binding energy would not depend on nucleon. The number of bonds could be quite large. Scaling the c quark mass of about 4 GeV gives gives dark mass of about 2 MeV so that two dark generations might be possible. For two dark quark generations 8+8 different quarks can appear at the ends of color flux tubes and 64 different color bonds are in principle possible (which brings in mind the idea of nuclear genetic code and TGD proposal for quantum computation utilizing braided flux tubes!). Also in this case the bond energy can depend on whether p or n is question for $P \neq N$ nuclei since p-p and n-n bonds have smaller bind energy than p-n type bonds.

3. Assume that the nucleons are topologically condensed at $k = 111$ space-time sheet with zero point kinetic energy

$$E_0(A) \sim \frac{3n}{2} \frac{\pi^2}{Am_p L^2(111)} \equiv \frac{n}{A} \times E_0(A=1) ,$$

where n is a numerical factor and $E_0(A=1) \simeq 23$ MeV. Let ΔE denote the color magnetic spin-spin interaction energy per nucleon for π type bond. The zero point kinetic energy is largest for $A \leq 3$ and explains why the binding energy is so small. For $n = 1$ the zero point kinetic energy would be 5.8 MeV for $A = 4$, 7.7 MeV for $A = 3$, and 11.5 MeV for $A = 2$.

With these assumptions the binding energy per bond can be written for $A \leq 4$ as

$$E = r \times \Delta E - \frac{nE_0(p)}{A^2} ,$$

where Δ denotes the color magnetic spin-spin interaction energy per bond. The parameter r codes for the fact that color magnetic spin-spin interaction energy depends on whether p-p or n-n type bond is in question. The values of r are $r(^4He) = 1, r(^3He) = 7/9, r(^2H) = 1$.

Estimates for n and Δ can be deduced from the binding energies of 2H and 3He . The result is $n = 1.0296$ and $\Delta E = 7.03$ MeV. The prediction for 4He binding energy is 6.71 MeV which is slightly smaller than the actual energy 7.07 MeV. The value of the binding energy per nucleon is in the range 7.4-8.8 MeV for heavier nuclei which compares favorably with the prediction 7.66 MeV at the limit $A \rightarrow \infty$. The generation of dark gluon condensate and color Coulombic energy per nucleon increasing with the number of nucleons could explain the discrepancy.

(A,Z)	(2,1)	(3,1)	(3,2)	(4,2)
E_B/MeV	1.111	2.826	2.572	7.0720

Table 1. The binding energies per nucleon for the lightest nuclei.

Why certain light nuclei do not exist?

The model should also explain why some light nuclei do not exist. In the case of proton rich nuclei electromagnetic Coulomb interaction acts as un-stabilizer. For heavy nuclei with non-vanishing value of $P - N$ the positive contribution of dark gluons to the energy tends to in-stabilize the nuclei. The color Coulombic interaction energy is expected to behave as $(N - P)^2$ whereas the energy of dark gluons behaves as $|N - P|$. Hence one expects that for some critical value of $|N - P|$ color Coulombic interaction is able to compensate the contribution of dark gluon energy. On the other hand, the larger number of nn type bonds tends reduced the color magnetic spin-spin interaction energy.

1. Coulomb repulsion for pp is estimated to be .76 MeV from $^3He - ^3H$ mass difference whereas the color magnetic binding energy would be $E_D/3 = .74$ MeV from the fact that the energy of ρ type bond is 1/3 from that for π type bond. Hence pp bound state would not be possible. The fact that nn bound state does not exist, suggests that the energy of the color neutralizing dark gluon overcomes the color Coulombic interaction energy of dark gluon and dark quarks and spin-spin interaction energy of ρ_0 type bond.
2. For ppp and nnn protons cannot be in S wave. The color magnetic bond energy per nucleon would be predicted to be $E_D = 2.233$ MeV whereas a rough order of magnitude estimate for Coulombic repulsion as

$$E_{em} = Z(Z-1) \times [E_B(^3H) - E_B(^3He)] = Z(Z-1) \times .76 \text{ MeV}$$

gives $E_{em} \simeq 4.56$ MeV so that ppp bound state is not possible. nnn bound state would not be possible because three dark gluons would not be able to create high enough color Coulomb interaction energy E_c which together with color magnetic spin-spin interaction energy E_D would compensate their own negative contribution $3E_g$:

$$3E_g > E_D + E_c .$$

3. For pppp and nnnn Fermi statistics forces two nucleons to higher partial waves so that the states are not stable. Tetraneutron need not correspond to nnnn state in TGD framework but has more natural interpretation as an alpha particle containing two negatively charged dark quark pairs.

8.4.4 Strong correlation between proton and neutron numbers and magic numbers

The estimates for the binding energies suggest that nucleons arrange into closed nuclear strings in which nucleons are connected by long color magnetics with one dark quark anti-quark pair per nucleon. Nuclear string approach allows to understand the strong correlation between proton and neutron numbers as well as magic numbers.

Strong correlation between Z and N

$N = Z$ nuclei with maximal color magnetic spin-spin interaction energy arranged into closed nuclear strings contain only colored π type bonds between p and n and should be especially stable. The question is how to create minimum energy configurations with $N \neq Z$.

1. If only stringy configurations are allowed, the removal of the proton would create ρ type n-n bond and lead to a reduction of binding energy per nucleon. This would predict that (Z,Z) type isotopes correspond to maxima of binding energy per nucleon. The increase of the Coulombic energy disfavors the removal of neutrons and addition of protons.
2. For a given closed string structure one can always link any given proton by $\bar{u}u$ bond to neutron and by $\bar{d}d$ bonds to two protons (same for neutron). The addition of only neutron to a branch from proton gives nuclei $(Z,N=Z+k)$, $k = 1, \dots, Z$, having only π type bonds. In a similar manner nuclei with $(Z+k, Z)$, $k = 1, \dots, Z$, containing only π type bonds are obtained. This mechanism would predict isotopes in the ranges $(Z,Z)-(Z,2Z)$ and $(Z,Z)-(2Z,Z)$ with the same strong binding energy per nucleon apart from increase of the binding energy caused by the generation of dark gluon condensate which in the case of protons seems to be overcome by Coulomb repulsion. Very many of these isotopes are not observed so that this mechanism is not favored.

Consider how this picture compares with experimental facts.

1. Most $Z = N$ with $Z \leq 29$ nuclei exist and are stable against strong decays but can decay weakly. The interpretation for the absence of $Z > 29$ $Z = N$ nuclei would be in terms of Coulomb repulsion. Binding energy per nucleon is usually maximum for $N = Z$ or $N = Z + 1$ for nuclei lighter than Si. The tendency $N > Z$ for heavier nuclei could be perhaps understood in terms of the color Coulombic interaction energy of dark gluon condensate with color charges in n-n type color bonds. This would allow also to understand why for $Z = 20$ all isotopes with $(Z = 20, N > 20)$ have higher binding energy per nucleon than $(Z = 20, N = 20)$ isotope in conflict with the idea that doubly magic nucleus should have a maximal binding energy.

The addition of neutrons to ^{40}Ca nucleus, besides increasing the binding energy per nucleon, also decreases the charge radius of the nucleus contrary to the expectation that the radius of the nucleus should be proportional to $A^{1/3}$ [36]. A possible interpretation is in terms of the color Coulombic interaction energy due to the generation of dark gluon condensate, the presence of which reduces the equilibrium charge radius of the nucleus.

2. ^8Be having $(Z, N) = (4, 4)$ decaying by alpha emission (to two alpha particles) is an exception to the rule. The binding energy per nucleon 7.0603 MeV of Be is slightly lower than the binding energy 7.0720 MeV of alpha particle and the pinching of the Be string to form two alpha strings could be a possible topological decay mechanism.

Magic nuclei in shell model and TGD context

Spin-spin pairing for identical nucleons in the harmonic oscillator potential is an essential element of the harmonic oscillator model explaining among other things shell structure and lowest magic numbers 2, 8, 20 but failing for higher magic numbers 28, 50, 82, 126 (the prediction is 2,8,20 and 40, 68, 82, 122). Spin-orbit coupling [52] reproduces effectively the desired shell structure by drawing some states of the higher shell to the lower shell, and it is indeed possible to reproduce the magic numbers in this manner for 3-D harmonic oscillator model.

This picture works nicely if magic nuclei are identified as nuclei which have exceptionally high abundances. ^{28}Fe , the most abundant element, is however an exception to the rule since neither Z nor N are magic in this case. The standard explanation for the stable nuclei of this kind is as endpoints of radioactive series. This explanation does not however remove the problem of understanding their large binding energy, which is after all what matters.

The surprise of recent years has been that even for neutron rich unstable nuclei 28 appears as a magic number for unstable neutrons in very neutron rich nuclei such as $\text{Si}(14,28)$ [58] so that the notion of magic number does not seem to be so dependent on spin-orbit interactions with the nuclear environment as believed. Also new magic numbers such as $N=14,16,30,32$ have been discovered in the neutron sector [58]. Already the stable isotope $\text{Mg}(12,14)$ has larger binding energy per nucleon than doubly magic $\text{Mg}(12,12)$ and could be perhaps understood in terms of dark gluons. ^{56}Fe and ^{58}Fe correspond to $N=30$ and 32 . The linking of two $N=8$ magic nuclei would give $N=16$ and various linkings of $N=14$ and $N=16$ nuclei would reduce the stability $N = 28, 30, 32$ magic nuclei to the stability of their building blocks. Perhaps these findings could provide motivations for considering whether the stringy picture might provide an alternative approach to understanding of the magic numbers.

1. The identification of magic nuclei as minima of binding energy predicts new magic numbers

The identification of the magic nuclei as minima of the binding energy as function of Z and N provides an alternative definition for magic numbers but this would predict among other things that also $Z = N = 4, 6, 12$ also correspond to doubly magic nuclei in the sense that $E_b(^8\text{Be}) = 7.0603$, $E_b(^{12}\text{C}) = 7.677$ MeV and $E_B(^{24}\text{Mg}) = 8.2526$ are maxima for the binding energy per nucleon as a function of Z and N . For higher nuclei addition of neutrons to a doubly magic nucleus typically increases the binding energy up to some critical number of added neutrons (the generation of the dark gluon condensate would explain this in TGD framework). The maximum for the excitation energy of the first excitation seems to be the definition of magic in the shell model.

2. Platonic solids and magic numbers

The TGD picture suggest that light magic nuclei could have a different, purely geometric, interpretation in terms of five regular Platonic solids. $Z = N = 4, 6, 8, 12, 20$ could correspond to tetrahedron, octahedron (6 vertices), hexahedron (8 vertices), dodecahedron (12 vertices), and icosahedron (20) vertices. Each vertex would contain a bonded neutron and proton in the case of doubly magic nucleus. This model would predict correctly all the maxima of the binding energy per nucleon for $Z, N \leq 20$.

3. p-Adic length scale hypothesis and magic numbers

$Z = N = 8$ could be also interpreted as a maximal number of nucleons which $k = 109$ space-time sheet associated with dark quarks can contain. p-Adic length scale hypothesis would suggest that strings with length coming as p-adic length scale $L(k)$ are especially stable. Strings with thickness $L(109)$ would correspond to $Z=N=2$ for length $L = L(109)$, $L(k = 109 + 2n)$ would correspond to $Z = 2^{n+1}$ explaining $N = 2, 8, 16, 32$.

4. Could the linking of magic nuclei produce new magic nuclei?

Nuclear strings can become knotted and linked with fermion statistics guaranteing that the links cannot be destroyed by a 3-dimensional topological transition.

An interesting question is whether the magic numbers $N = 14, 16, 30, 32$ could be interpreted in terms of lower level magic numbers: $14=8+6, 16=8+8, 30=16+40, 32=16+16$. This would make sense if $k = 111$ space-time sheets containing $Z, N \leq 4, 6, 8$ neutrons and protons define basic nucleon clusters forming closed nuclear strings. The linking these structures could give rise to higher magic nuclei whose stability would reduce that of the building blocks, and it would be possible to interpret

magic number $Z, N = 28 = 20 + 8$ as linked lower level magic nuclei.

The partitions $28=20+8$, $50=20+2+28 = 20+2+8+20$, $82=50+2+28$, $126=50+50+20+6=82+28+8+8$ inspire the question whether higher doubly magic nuclei and their deformations could correspond to linked lower level magic nuclei so that a linking hierarchy would result.

Could the transition to the electromagnetically dark matter cause the absence of higher shells?

Spin orbit coupling explains the failure of the shell model as an explanation of the magic numbers. Transition to electromagnetic dark matter at critical charge number $Z = 12$ suggests an alternative explanation for the failure in the case of protons. The phase transition of Pd nuclei ($Z=46$) to electromagnetically dark nuclear phase inducing in turn the transition of D nuclei to dark matter phase has been proposed as an explanation for cold fusion [16].

On basis of $Z^2\alpha_{em} \simeq 1$ criterion $Z = 12$ would correspond to the critical value for the nuclear charge causing this transition. One can argue that due to the Fermi statistics nuclear shells behave as weakly interacting units and the transition occurs for the first time for $Z = 20$ nucleus, which corresponds to Ca, one of the most important ions biologically and neurophysiologically. These necessarily completely filled structures would become structural units of nuclei at electromagnetically dark level.

An alternative interpretation is that the criterion to dark matter phase applies only to a pair of two systems and reads thus $Z_1Z_2\alpha_{em} \simeq 1$ implying that only the nuclei $Z, N \geq 40$ can perform the transition to the dark phase (what this really means is an interesting question). This would explain why Pd with $Z = 46$ has so special role in cold fusion.

Interestingly, the number of protons at $n = 2$ shell of harmonic oscillator is $Z = 12$ and thus corresponds to a critical value for em charge above which a transition to an electromagnetic dark matter phase increasing the size of the electromagnetic $k = 113$ space-time sheet of nucleus by a factor $\simeq 2^{11}$ could occur. This could explain why $n = 2$ represents the highest allowed harmonic oscillator shell with higher level structures consisting of clusters of $n < 3$ shells. Neutrons halos could however allow higher shells.

Could only the hadronic space-time sheet be scaled up for light nuclei?

The model discussed in this chapter is based on guess work and leaves a lot of room for different scenarios. One of them emerged only after a couple of months finishing the work with this chapter.

1. Is only the \hbar associated with hadronic space-time sheet large?

The surprising and poorly understood conclusion from the p-adic mass calculations was that the p-adic primes characterizing light quarks u,d,s satisfy $k_q < 107$, where $k = 107$ characterizes hadronic space-time sheet [17].

1. The interpretation of $k = 107$ space-time sheet as a hadronic space-time sheet implies that quarks topologically condense at this space-time sheet so that $k = 107$ cannot belong to the collection of primes characterizing quark.
2. Since hadron is expected to be larger than quark, quark space-time sheets should satisfy $k_q < 107$ unless \hbar is large for the hadronic space-time sheet so that one has $k_{eff} = 107 + 22 = 129$. This would predict two kinds of hadrons. Low energy hadrons consists of u, d, and s quarks with $k_q < 107$ so that hadronic space-time sheet must correspond to $k_{eff} = 129$ and large value of \hbar . One can speak of confined phase. This allows also $k = 127$ light variants of quarks appearing in the model of atomic nucleus. The hadrons consisting of c,t,b and the p-adically scaled up variants of u,d,s having $k_q > 107$, \hbar has its ordinary value in accordance with the idea about asymptotic freedom and the view that the states in question correspond to short-lived resonances.

This picture is very elegant but would mean that it would be light *hadron* rather than quark which should have large \hbar and scaled up Compton length. This does not affect appreciably the model of atomic nucleus since the crucial length scales $L(127)$ and $L(129)$ are still present.

2. Under what conditions quarks correspond to large \hbar phase?

What creates worries is that the scaling up of $k = 113$ quark space-time sheets of quarks forms an essential ingredient of condensed matter applications [27] assuming also that these scaled up space-time sheets couple to scaled up $k = 113$ variants of weak bosons. Thus one must ask under what conditions $k = 113$ quarks, and more generally, all quarks can make a transition to a dark phase accompanying a simultaneous transition of hadron to a doubly dark phase.

The criterion for the transition to a large \hbar phase at the level of valence quarks would require that the criticality criterion is satisfied at $k = 111$ space-time sheet and would be expressible as $Z^2\alpha_{em} = 1$ or some variant of this condition discussed above.

The scaled up $k = 127$ quark would correspond to $k = 149$, the thickness of the lipid layer of cell membrane. The scaled up hadron would correspond to $k = 151$, the thickness of cell membrane. This would mean that already the magnetic bodies of hadrons would have size of cell membrane thickness so that the formation of macroscopic quantum phases would be a necessity since the average distance between hadrons is much smaller than their Compton length.

8.4.5 A remark about stringy description of strong reactions

If nucleons are arranged into possibly linked and knotted closed nuclear strings, nuclear reactions could be described in terms of basic string diagrams for closed nuclear strings.

The simplest fusion/fission reactions $A_1 + A_2 \leftrightarrow (A_1 + A_2)$, $A_i > 2$, could correspond to reactions in which the $k = 111$ dark space-time sheets fuse or decay and re-distribution of dark quarks and anti-quarks between nucleons occurs so that system can form a new nucleus or decay to a new nuclei. This also means re-organizes the linking and knotting of the color flux tubes.

The reactions $p/n + A \rightarrow ..$ would involve the topological condensation of the nucleon to $k = 111$ space-time sheet after which it can receive quark anti-quark pair, which can be also created by dark gluon emission followed by annihilation to a dark quark pair.

8.4.6 Nuclear strings and DNA strands

Nuclear strings consisting of protons and neutrons bring in mind bit arrays. Their dark mirror counterparts in turn brings in mind the structure of DNA double strand. This idea does not look so weird once one fully accepts the hierarchies associated with TGD. The hierarchy of space-time sheets quantified by p-adic fractality, the hierarchy of infinite primes representable as a repeated second quantization of a super-symmetric arithmetic quantum field theory, the self hierarchy predicted by TGD inspired theory of consciousness, the Jones inclusion hierarchy for von Neumann factors of type II_1 appearing in quantum TGD and allowing to formulate what might be called Feynman rules for cognition, and the hierarchy of dark matters would all reflect the same reflective hierarchy.

The experience with DNA suggests that nuclear strings could form coiled tight double helices for which only transversal degrees of freedom would appear as collective degrees of freedom. DNA allows a hierarchy of coilings and DNA molecules can also link and this could happen also now. Nuclei as collections of linked nuclear strings could perhaps be said to code the electromagnetic and color field bodies and it is difficult to avoid the idea that DNA would code in the same manner field bodies at which matter condenses to form much larger structures. The hierarchy of dark matters would give rise to a hierarchy of this kind of codings.

The linking and knotting of string like structures is the key element in the model of topological quantum computation and the large value of \hbar for dark matter makes it ideal for this purpose. I have already earlier proposed a model of DNA based topological quantum computation inspired by some strange numerical co-incidences [42]. If dark matter is the essence of intelligent and intentional life at the level of molecular physics, it is difficult to see how it could not serve a similar role even at the level of elementary particle physics and provide kind of zoomed up "cognitive" representation for the ordinary matter.

The precise dark-visible correspondence might fail at the level of nuclei and nucleons because the lifetimes of the scaled down dark matter nucleons and nuclei are different from those of ordinary nucleons if dark matter is dark also with respect to weak interactions. The weak interaction rates in the lowest order are scaled up by the presence of $1/m_W^4$ factors by a factor 2^{-44} so that weak interactions are not so weak anymore. If dark electron and neutrino have their ordinary masses, dark proton and neutron would be stable. If also they appear as scaled down versions situation changes, but only a small change of the mass ratio of dark proton and neutron can make the weak decay of free

dark neutron impossible kinematically and the one-to-one correspondence would make sense for stable nuclei. The beta decays of dark nuclei could however as a third order process with a considerable rate and change dramatically the weak decay rates of dark nuclei.

8.5 Neutron halos, tetra-neutron, and "sticky toffee" model of nucleus

Neutron halos and tetra neutron represent two poorly understood features of nuclear physics which all have been seen as suggesting the existence of an unknown long range force or forces.

8.5.1 Tetra-neutron

There is evidence for the existence of tetra-neutrons [55]. Standard theory does not support their existence [54] so that the evidence for them came as a complete experimental surprise. Tetra-neutrons are believed to consist of 4 neutrons. In particular their lifetime, which is about 100 nanoseconds, is almost an eternity in the natural time scale of nuclear physics. The reason why the existing theory of nuclear force does not allow tetra-neutrons relates to Fermi statistics: the second pair of neutrons is necessarily in a highly energetic state so that a bound state is not possible.

Exotic quarks and charged color bonds provide perhaps the most natural explanation for tetra-neutron in TGD framework. In the model discussed hitherto only electromagnetically neutral color bonds have been considered but one can consider also charged color bonds in analogy allowing instead of neutral π and ρ also their charged companions. This would make possible to construct from two protons and neutrons the analog of alpha particle by replacing two neutral color bonds with negatively charged bonds so that one would have two $\bar{u}d$ p-n bonds and two $\bar{u}u$ p-n bonds. Statistics difficulty would be circumvented and the state would decay to four neutrons via W boson exchange between quark of charged p-n bonds and protons. The model suggests the existence of also neutral variant of deuteron.

One can consider two options according to whether the exotic quarks have large \hbar but small c (Option II) or whether they are just p-adically scaled up quarks with $k = 127$ (Option I). I have considered earlier a model analogous to option II but based on the hypothesis about existence of scaled down variant of QCD associated with Mersenne prime M_{127} . The so called leptohadron physics would also be associated with M_{127} and involve colored excitations of leptons [24] which might also represent dark matter: in this case dark valence leptons with color would correspond to $k\ell f = 149$, which happens to correspond to the thickness of the lipid layer of cell membrane.

The notion of many-sheeted space-time predicts the possibility of fractal scaled up/down versions of QCD which, by the loss of asymptotic freedom, exist only in certain length scale range and energy range. Thus the prediction does not lead to contradictions elementary particle physics limits for the number of colored elementary particles. The scaled up dark variants of QCD like theory allow to circumvent these problems even when asymptotic freedom is assumed.

In particular, pions and other mesons could exist for $k = 127$ option as scaled down versions having much smaller masses. This led to the earlier model of tetra-neutron as an ordinary alpha particle bound with two exotic pions with negative charges and having very small masses. This state looks like tetra-neutron and decays to neutrons weakly. The statistics problem is thus circumvented and the model makes precise quantitative predictions.

8.5.2 The formation of neutron halo and TGD

One counter argument against TGD inspired nuclear model is the short range of the nuclear forces: the introduction of the p-adic length scale $L(113) \simeq 1.6E^{-14}$ m is in conflict with this classical wisdom. There exists however direct evidence for the proposed length scale besides the evidence from the p-n low energy scattering. Some light nuclei such as ${}^8\text{He}$, ${}^{11}\text{Li}$ and ${}^{11}\text{Be}$ possess neutron halo with radius of size $\sim 2.5E^{-14}$ m [68]. The width of the halo is rather large if the usual nuclear length scale is used as unit and the neutrons in the halo seem to behave as free particles. The short range of the nuclear forces makes it rather difficult to understand the formation of the neutron halo although the existing models can circumvent this difficulty. The proposed picture of the nucleus suggests a rather simple model for the halo.

For ordinary nuclei the densities of nucleons tend to be concentrated near the center of the nucleus. One can however consider the possibility of adding nucleons in vicinity of the boundary of the $k = 111$ space-time sheet associated with the nucleus itself. The binding force would be color interaction between the color charges of color bonds and neutralizing color charge of colored gluons in the center (or in halo itself). Neutron halo would define a separate nucleus in the sense that states could be constructed by starting from the ground state. Halo would correspond to a quantum delocalized cluster of size of alpha particle.

The case ^{11}Be provides support for the theory. Standard shell model suggests that six neutrons of ^{11}Be fill completely $1s_{\frac{1}{2}}$ and $1p_{\frac{3}{2}}$ states while $1p_{\frac{1}{2}}$ state holds one neutron so that ^{11}Be ground state has $J^\pi = \frac{1}{2}^-$ whereas experimentally ground state is known to have $J^\pi = \frac{1}{2}^+$. The system can be regarded as $^{10}\text{Be} + \text{halo neutron}$. The first guess is that the state could be simply of the following form

$$|0^+\rangle \times |2s_{1/2}\rangle . \quad (8.5.1)$$

Color force would stabilize this state. A more general state is a superposition of higher $ns_{1/2}$ states in order to achieve more sharp localization near boundary. This increases the kinetic energy of the neutron and the small binding energy of the halo neutron about 2.5 MeV implies that the kinetic energy should be of order $5 - 6 \text{ MeV}$. For instance, in the model described in [61] the halo neutron property and correct spin-parity for ^{11}Be can be realized if the state is superposition of form

$$\begin{aligned} |^{11}\text{Be}\rangle &= a|0^+\rangle \times |2s_{1/2}\rangle + ba|2^+\rangle \times |21d_{5/2}\rangle , \\ a &\simeq .74 , \\ b &\simeq .63 . \end{aligned} \quad (8.5.0)$$

The correlation between the core and halo neutron is necessary in the model of [61] to produce bound $1/2^+$ state. The halo neutron must also rotate.

The second example is provided by two-neutron halo nuclei, such as ^{11}Li and ^{12}Be , which do not bind single neutron but bind two neutrons. This looks mysterious since free neutrons do not allow bound states. A possible explanation is that the increase of the color Coulombic interaction energy of neutron color bonds with at least N-P dark gluons makes possible binding of neutron halo to the center nucleus. The situation would be analogous to the formation of planetary system. Order of magnitude estimate for color Coulombic interaction energy of halo neutron is $E \sim (N-P)\alpha_s/L(113) \simeq (N-P) \times .8 \text{ MeV}$. For $N-P=3$ the binding energy would be about 2.3 MeV and smaller than the experimental estimate 2.5 MeV . For $N-P=4$ this gives 3.2 MeV and larger than 2.5 MeV so that there is some room for the reduction of binding energy by the contribution from kinetic energy.

8.5.3 The "sticky toffee" model of Chris Illert for alpha decays

Chris Illert [53] has proposed what he calls "sticky toffee" model of alpha decay. The starting point of the work is a criticism of the wave-mechanical model for alpha decay of nuclei as occurring through tunneling. The proposal is that tunneling might allow a classical particle description after all. Quantum classical correspondence suggests the same in TGD framework.

The proposed description is based on the idea that the tunneling alpha particle has abnormally small charge inside the tunneling region. This reduces the electrostatic interaction of alpha particle with nucleus so that it can penetrate to otherwise classically non-allowed region separating it from the external world and can leak out of the parent nucleus. More quantitatively, the momentum given by $p = \sqrt{2m(E-V)}$ of alpha particle remains real during tunneling. As the alpha particle escapes, it gradually increases its charge to its full value of 2 units possessed by the ordinary alpha particle.

What is interesting is that the model predicts the charge of the proto-alpha particle at the surface of the decaying nucleus from the knowledge of alpha particle energy, nuclear radius, and charge by using just energy conservation in Coulombic field. What is assumed that the charge of the particle is such that Coulombic energy remains equal to the alpha particle energy all the way from the nuclear surface through the Coulomb wall to the distance where alpha particle can have full charge. This is a slight idealization since it would mean that the alpha particle kinetic energy vanishes.

To my opinion, the dynamical charge of alpha particle is a manner to articulate what happens in the tunneling. Thus the model cannot replace quantum description but only become a part of it. In particular, the successful prediction of the decay rates exponentially sensitive to the alpha particle energy cannot be deduced from a purely classical theory.

The charges at the surface of the nucleus tend to be near $1/3$ and $2/3$. What is amazing is that these charges correspond to the charges of the quark and anti-quark composing pion. That quarks should reveal themselves in the classical model for alpha decay is a complete surprise.

From this finding Illert concludes that during the decay the alpha particle is connected to the parent nucleus by rubber band like strings having quark and anti-quark at their ends, that is color flux tubes. These strings are interpreted as virtual pions. These strings get stretched and eventually must split since the color force between the quark and anti-quark at the ends of the string grows very strong.

This model is very attractive but has a deep problem: color forces mediate very short ranged and rapidly occurring interactions and should not be important for alpha decay which is a very slow process involving electromagnetic interactions in an essential manner. This does not diminish the pioneering value of Illert's work, just the opposite: pioneers must often have the courage to go against rationality as defined by the existing dogmas.

My earlier suggestion was that these pions serving as "rubber strings" are not ordinary pions but fractal copies of ordinary pions being much lighter and having much larger size. TGD indeed predicts the possibility of fractal copies of quantum chromo-dynamics (QCD). Thus there would exist a fractal copy of ordinary hadron physics operating in much longer length scales and having its own, much lighter, particle spectrum. The proposal was that this QCD corresponds to Mersenne prime M_{127} .

The dark QCD based on scaled up copies of ordinary quarks leads to a more elegant model in which virtual are replaced by π and ρ type color bonds, the latter being colored. Also an explanation of tetra-neutron emerges as a by-product since two pionic bonds can have negative charges. The identification of the nucleus as a nuclear string predicts the decay mechanism in which alpha particle pinches off and indeed has quarks and/or anti-quark attached to the ends of two nucleons.

Summarizing, although the model discussed in [53] does not predict tetra-neutron, it represents findings and ideas, which might be of crucial importance in the topological and geometric modeling of nuclear decays. The finding that alpha decay could be described in terms of pions, although wrong as such, opens the way to a realization that ordinary pions and thus also ordinary hadron and nuclear physics might have lighter fractal copies.

8.6 Tritium beta decay anomaly

The determination of neutrino mass from the beta decay of tritium leads to a tachyonic mass squared [44, 66]. I have considered several alternative explanations for this long standing anomaly.

1. ${}^3\text{He}$ nucleus resulting in the decay could be fake (tritium nucleus with one positively charged color bond making it to look like ${}^3\text{He}$). The idea that slightly smaller mass of the fake ${}^3\text{He}$ might explain the anomaly: it however turned out that the model cannot explain the variation of the anomaly from experiment to experiment.
2. Much later I realized that also the initial ${}^3\text{H}$ nucleus could be fake (${}^3\text{He}$ nucleus with one negatively charged color bond). It turned out that fake tritium option can explain all aspects of the anomaly and also other anomalies related to radioactive and alpha decays of nuclei.
3. The alternative based on the assumption of dark neutrino or antineutrino belt surrounding Earth's orbit and explain satisfactorily several aspects of the anomaly but fails in its simplest form to explain the dependence of the anomaly on experiment. Since the fake tritium scenario is based only on the basic assumptions of the nuclear string model [47] and brings in only new values of kinematical parameters it is definitely favored.

8.6.1 Tritium beta decay anomaly

A brief summary of experimental data before going to the detailed models is in order.

Is neutrino tachyonic?

Nuclear beta decay allows in principle to determine the value of the neutrino mass since the energy distribution function for electrons is sensitive to neutrino mass at the boundary of the kinematically allowed region corresponding to the situation in which final neutrino energy goes to zero [47].

The most useful quantity for measuring the neutrino mass is the so called Kurie plot for the function

$$K(E) \equiv \left[\frac{d\Gamma/dE}{pEF(Z, E)} \right]^{1/2} \sim (E_\nu k_\nu)^{1/2} = \left[E_\nu \sqrt{E_\nu^2 - m(\nu)^2} \right]^{1/2},$$

$$E_\nu = E_0 - E, \quad E_0 = M_i - M_f - m(\nu). \quad (8.6.0)$$

Here E denotes electron energy and E_0 is its upper bound from energy and momentum conservation (for a configuration in which final state nucleon is at rest). Mass shell condition lowers the upper bound to $E \leq E_0 - m(\nu)$. For $m(\nu) = 0$ Kurie plot is straight line near its endpoint. For $m(\nu) > 0$ the end point is shifted to $E_0 - m(\nu)$ and $K(E)$ behaves as $m(\nu)^{1/2} k_\nu^{1/2}$ near the end point.

The problem is that the determination of $m(\nu)$ from this parametrization in tritium beta decay experiments gives a negative mass squared varies and is $m(\nu)^2 = -147 \pm 68 \pm 41 \text{ eV}^2$ according to [47]! This behavior means that the derivative of $K(E)$ is infinite at the end point E_0 and $K(E)$ increases much faster near end point than it should. One can quite safely argue that tachyonicity gives only an ad hoc parametrization for the change of the shape of the function K deriving from some unidentified physical effect: in particular, the value of the tachyonic mass must correspond to a parameter related to new physics and need not have anything to do with neutrino mass.

More detailed experimental data

The results of Troitsk and Mainz experiments can be taken as constraints of the model. In Troitsk experiments [44] gas phase tritium is used whereas in Mainz experiments [66] liquid tritium film is used.

Troitsk experiments are described in [44]. In 1944 Troitsk experiment, the enhancement of the spectrum intensity was found to begin roughly at $V_b \simeq 7.6 \text{ eV}$ below E_0 . The conclusion was that the rise of the spectrum intensity below 18,300 eV with respect to the standard model prediction takes place (this is illustrated in fig. 4 of [44]). No bump was claimed in this paper. In the analysis of 1996 experiment Troitsk group however concluded that the trapping of electrons gives rise to the enrichment of the low energy spectrum intensity of electrons and that when takes this effect into account, a narrow bump results.

Figure 4 of [44] demonstrates that spectrum intensity is below the theoretical value near the endpoint (right from the bump). In [44] the reduction of the spectrum intensity was assumed to be due to non-vanishing neutrino mass in [44]. The determination of $m(\nu)$ from the data near the end point assuming that beta decay is in question [44] gives $m(\nu) \sim 5 \text{ eV}$.

The data can be parameterized by a parameter V_b which in the model context can be interpreted as repulsive interaction energy of antineutrinos with condensed matter suggested to explain the bump. Accordingly, the parametrization of $K(E)$ near the end point is

$$K(E) \sim (E - E_0)\theta(E - E_0) \rightarrow (E - E_0)\theta(E - E_0 + V_b) .$$

The end point is shifted to energy $E_\nu = V_b$ and $K(E)$ drops from the value V_b to zero at at this energy.

The values of V_b deduced from Troitsk and Mainz experiments are in the range 5 – 100 eV. The value of V_b observed in Troitsk experiments using gas phase tritium [44] was of order 10 eV. In Mainz experiment [66] tritium film was used and the excess of counts around energy $V_b \simeq 100 \text{ eV}$ below E_0 was observed.

There is also a time variation involved with the value of V_b . In 1944 experiment [44] the bump was roughly $V_b \simeq 7.6 \text{ eV}$ below E_0 . In 1996 experiment [44] the value of V_b was found to be $V_b \simeq 12.3 \text{ eV}$ [66]. Time variation was observed also in the Mainz experiment. In 'Neutrino 98' conference an oscillatory time variation for the position of the peak with a period of 1/2 years in the amplitude was reported by Troitsk group.

8.6.2 Could TGD based exotic nuclear physics explain the anomaly?

Nuclear string model explains tetra-neutron as alpha particle with two negatively charged color bonds. This inspires the question whether some fraction of decays could correspond to the decays of tritium to fake ${}^3\text{He}$ (tritium with one positively charged color bond) or fake tritium (${}^3\text{He}$ with one negatively charged color bond) to ${}^3\text{He}$.

Could the decays of tritium decay to fake ${}^3\text{He}$ explain the anomaly?

Consider first the fake ${}^3\text{He}$ option. Tritium (pnn) would decay with some rate to a fake ${}^3\text{He}$, call it ${}^3\text{He}_f$, which is actually tritium nucleus containing one positively charged color bond and possessing mass slightly different than that of ${}^3\text{He}$ (ppn).

1. In this kind of situation the expression for the function $K(E, k)$ differs from $K(\text{stand})$ since the upper bound E_0 for the maximal electron energy is modified:

$$\begin{aligned} E_0 &\rightarrow E_1 = M({}^3\text{H}) - M({}^3\text{He}_f) - m_\mu = M({}^3\text{H}) - M({}^3\text{He}) + \Delta M - m_\mu , \\ \Delta M &= M({}^3\text{He}) - M({}^3\text{He}_f) . \end{aligned} \quad (8.6.0)$$

Depending on whether ${}^3\text{He}_f$ is heavier/lighter than ${}^3\text{He}$ E_0 decreases/increases. From $V_b \in [5 - 100]$ eV and from the TGD based prediction order $m(\bar{\nu}) \sim .27$ eV one can conclude that ΔM should be in the range 10-200 eV.

2. In the lowest approximation $K(E)$ can be written as

$$K(E) = K_0(E, E_1, k)\theta(E_1 - E) \simeq (E_1 - E)\theta(E_1 - E) . \quad (8.6.1)$$

Here $\theta(x)$ denotes step function and $K_0(E, E_0, k)$ corresponds to the massless antineutrino.

3. If a fraction p of the final state nuclei correspond to a fake ${}^3\text{He}$ the function $K(E)$ deduced from data is a linear combination of functions $K(E, {}^3\text{He})$ and $K(E, {}^3\text{He}_f)$ and given by

$$\begin{aligned} K(E) &= (1 - p)K(E, {}^3\text{He}) + pK(E, {}^3\text{He}_f) \\ &\simeq (1 - p)(E_0 - E)\theta(E_0 - E) + p(E_1 - E)\theta(E_1 - E) \end{aligned} \quad (8.6.1)$$

in the approximation $m_\nu = 0$.

For $m({}^3\text{He}_f) < m({}^3\text{He})$ one has $E_1 > E_0$ giving

$$K(E) = (E_0 - E)\theta(E_0 - E) + p(E_1 - E_0)\theta(E_1 - E)\theta(E - E_0) . \quad (8.6.2)$$

$K(E, E_0)$ is shifted upwards by a constant term $p\Delta M$ in the region $E_0 > E$. At $E = E_0$ the derivative of $K(E)$ is infinite which corresponds to the divergence of the derivative of square root function in the simpler parametrization using tachyonic mass. The prediction of the model is the presence of a tail corresponding to the region $E_0 < E < E_1$.

4. The model does not as such explain the bump near the end point of the spectrum. The decay ${}^3\text{H} \rightarrow {}^3\text{He}_f$ can be interpreted in terms of an exotic weak decay $d \rightarrow u + W^-$ of the exotic d quark at the end of color bond connecting nucleons inside ${}^3\text{H}$. The rate for these interactions cannot differ too much from that for ordinary weak interactions and W boson must transform to its ordinary variant before the decay $W \rightarrow e + \bar{\nu}$. Either the weak decay at quark level or the phase transition could take place with a considerable rate only for low enough virtual W boson energies, say for energies for which the Compton length of massless W boson correspond to the size scale of color flux tubes predicted to be much longer than nuclear size. Is so the anomaly would be absent for higher energies and a bump would result.

5. The value of $K(E)$ at $E = E_0$ is $V_b \equiv p(E_1 - E_0)$. The variation of the fraction p could explain the observed dependence of V_b on experiment as well as its time variation. It is however difficult to understand how p could vary.

Could the decays of fake tritium to ${}^3\text{He}$ explain the anomaly?

Second option is that fraction p of the tritium nuclei are fake and correspond to ${}^3\text{He}$ nuclei with one negatively charged color bond.

1. By repeating the previous calculation exactly the same expression for $K(E)$ in the approximation $m_\nu = 0$ but with the replacement

$$\Delta M = M({}^3\text{He}) - M({}^3\text{He}_f) \rightarrow M({}^3\text{H}_f) - M({}^3\text{H}) . \quad (8.6.3)$$

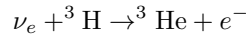
2. In this case it is possible to understand the variations in the shape of $K(E)$ if the fraction of ${}^3\text{H}_f$ varies in time and from experiment to experiment. A possible mechanism inducing this variation is a transition inducing the transformation ${}^3\text{H}_f \rightarrow {}^3\text{H}$ by an exotic weak decay $d + p \rightarrow u + n$, where u and d correspond to the quarks at the ends of color flux tubes. This kind of transition could be induced by the absorption of X-rays, say artificial X-rays or X-rays from Sun. The inverse of this process in Sun could generate X rays which induce this process in resonant manner at the surface of Earth.
3. The well-known poorly understood X-ray bursts from Sun during solar flares in the wavelength range 1-8 Å [46] corresponds to energies in the range 1.6-12.4 keV, 3 octaves in good approximation. This radiation could be partly due to transitions between ordinary and exotic states of nuclei rather than brehmstrahlung resulting in the acceleration of charged particles to relativistic energies. The energy range suggests the presence of three p-adic length scales: nuclear string model indeed predicts several p-adic length scales for color bonds corresponding to different mass scales for quarks at the ends of the bonds [47]. This energy range is considerably above the energy range 5 – 100 eV and suggests the range $[4 \times 10^{-4}, 6 \times 10^{-2}]$ for the values of p . The existence of these excitations would mean a new branch of low energy nuclear physics, which might be dubbed X-ray nuclear physics. The energy scale of for the excitation energies of exotic nuclei could corresponds to Coulomb interaction energy $\alpha_{em}m$, where m is mass scale of the exotic quark. This means energy scale of 10 keV for MeV mass scale.
4. The approximately 1/2 year period of the temporal variation would naturally correspond to the $1/R^2$ dependence of the intensity of X-ray radiation from Sun. There is evidence that the period is few hours longer than 1/2 years which supports the view that the origin of periodicity is not purely geometric but relates to the dynamics of X-ray radiation from Sun. Note that for 2 hours one would have $\Delta T/T \simeq 2^{-11}$, which defines a fundamental constant in TGD Universe and is also near to the electron proton mass ratio.
5. All nuclei could appear as similar anomalous variants. Since both weak and strong decay rates are sensitive to the binding energy, it is possible to test this prediction by finding whether nuclear decay rates show anomalous time variation.
6. The model could explain also other anomalies of radioactive reaction rates including the findings of Shnoll [42] and the unexplained fluctuations in the decay rates of ${}^{32}\text{Si}$ and ${}^{226}\text{Ra}$ reported quite recently [36] and correlating with $1/R^2$, R distance between Earth and Sun. ${}^{226}\text{Ra}$ decays by alpha emission but the sensitive dependence of alpha decay rate on binding energy means that the temporal variation of the fraction of fake ${}^{226}\text{Ra}$ isotopes could explain the variation of the decay rates. The intensity of the X-ray radiation from Sun is proportional to $1/R^2$ so that the correlation of the fluctuation with distance would emerge naturally.
7. Also a dip in the decay rates of ${}^{54}\text{Mn}$ coincident with a peak in proton and X-ray fluxes during solar flare [63] has been observed: the proposal is that neutrino flux from Sun is also enhanced during the solar flare and induces the effect. A peak in X-ray flux is a more natural explanation in TGD framework.

8. The model predicts interaction between atomic physics and nuclear physics, which might be of relevance in biology. For instance, the transitions between exotic and ordinary variants of nuclei could yield X-rays inducing atomic transitions or ionization. The wave length range 1-8 Angstroms for anomalous X-rays corresponds to the range $Z \in [11, 30]$ for ionization energies. The biologically important ions Na^+ , Mg^{++} , P^- , Cl^- , K^+ , Ca^{++} have $Z = (11, 15, 17, 19, 20)$. I have proposed that Na^+ , Cl^- , K^+ (fermions) are actually bosonic exotic ions forming Bose-Einstein condensates at magnetic flux tubes [27]. The exchange of W bosons between neutral Ne and A(rgon) atoms (bosons) could yield exotic bosonic variants of Na^+ (perhaps even Mg^{++} , which is boson also as ordinary ion) and Cl^- ions. Similar exchange between A atoms could yield exotic bosonic variants of Cl^- and K^+ (and even Ca^{++} , which is also boson as ordinary variant). This hypothesis is testable by measuring the nuclear weights of these ions. X-rays from Sun are not present during night time and this could relate to the night-day cycle of living organisms. Note that magnetic bodies are of size scale of Earth and even larger so that the exotic ions inside them could be subject to intense X-ray radiation. X-rays could also be dark X-rays with large Planck constant and thus with much lower frequency than ordinary X-rays so that control could be possible.

8.6.3 The model based on dark neutrinos

A common origin of the tritium beta decay anomaly was independently suggested by several groups (see [51]): a broad spike or bump like excess of counts centered 5 – 100 eV below the end point energy E_0 . In [51] it was suggested that a repulsive interaction of antineutrinos with condensed matter with interaction energy of order $V_b \simeq 5 - 100$ eV could explain the bump.

It has been pointed out by Stevenson [56] that the process in which neutrinos are absorbed from a background of electron neutrinos



leads to electrons in the anomalous endpoint region. This gives an essentially constant addition to the region $E_0 - E_F < E < E_0$. The density of cosmic neutrino background is however far too small to give the required large background density of order $1/m(\nu)^3$.

The earlier -wrong- hypothesis that nuclei are Z^0 charged are consistent with both options described above as explanations of the anomaly. One can modify these models to apply also in the new framework. The problem of these models is that one is forced to make ad hoc assumptions about dynamics in long length scales. They might make sense in TGD Universe but would require experimental justification. These models in their simplest form fail also to explain the dependence of V_b on experiment and fail to provide provide insights about more general time variations of nuclear decay rates.

Neutrino belt or antineutrino belt?

The model corresponding to mechanism of [51] is that the belt consists of dark antineutrinos and the repulsive interaction energy of antineutrino with the these neutrinos explains the anomaly. The model based on dark neutrinos assumes that Earth's orbit is surrounded by a belt of dark neutrinos and that the mechanism proposed in [56] could be at work. The periodic variation of the dark neutrino density along the orbit of Earth around Sun could also explain the periodic variations of the bump.

1. The first mechanism corresponds to that suggested in [51]. The antineutrino emitted in the beta decay can transform to a dark neutrino by mixing and experiences a repulsive Z^0 force which effectively shifts the electron energy spectrum downwards. In this case the repulsive interaction energy V_b of dark anti-neutrinos with the dark antineutrinos of the solar belt would replace ΔM in the previous formula:

$$E_0 = M({}^3\text{H}) - M({}^3\text{He}) - m(\nu) \rightarrow M({}^3\text{H}) - M({}^3\text{He}) - V_b - m(\nu_d) . \quad (8.6.3)$$

2. Second option corresponds to the mechanism proposed in [56]. Dark neutrino transforms to ordinary one and induces by ordinary W exchange ordinary tritium beta decay. In this case the Fermi energy E_F of dark neutrino determines the width of the bump and one has $V_b = E_F$:

$$E_0 = M(^3\text{H}) - M(^3\text{He}) - m(\nu) \rightarrow M(^3\text{H}) - M(^3\text{He}) - E_F + m(\nu_d) . \quad (8.6.3)$$

The rate of the process would be given by the standard model and only the density of dark neutrinos and the ratio $M^2(\nu, \nu(\text{dark}))/M^2(\nu)$ appear as free parameters.

Notice that these models are simpler than the original models which assumed that the interaction of neutrinos with condensed matter carrying Z^0 charge is involved. The explanation for the dependence of V_b on experiment poses a difficulty for both models. For the antineutrino belt the repulsive interaction energy is proportional to the density of antineutrinos. For neutrino belt V_b corresponds to the Fermi energy proportional to the density of neutrinos. In both cases large variation of V_b requires a large variation of the density of antineutrinos (neutrinos) of the belt in the scale smaller than Earth size. This does not look too plausible.

Can one understand time variation of V_b ?

The periodic variation of the density of neutrinos or antineutrinos in the belt should induce the variation of V_b . The ordering of the two models trying to explain this variation reflects the evolution of the general ideas about quantum TGD.

1. First model

The value of the period and the fact that maximum shift occurs when Earth is near to its position nearest to Sun suggests that the physics of solar system must be involved somehow. The simplest explanation is that gravitational acceleration tends to drive dark neutrinos (antineutrinos) as near as possible to Sun inside the belt. In thermal equilibrium with temperature T the Boltzmann factor

$$\exp\left(-\frac{V_{gr}}{T}\right) = \exp\left(-\frac{GMm(\nu_d)}{rT}\right) \quad (8.6.4)$$

for the dark neutrino would determine the density profile of dark neutrinos along the belt as function of the distance r to the Sun.

The existence of the dark neutrino belt conforms with the model of for the formation of solar system from dark matter with a gigantic value of Planck constant discussed in [38, 16]. The model indeed assumes that the dark matter is located at space-time sheet surrounding the orbit of Earth. The requirement that dark neutrino density is few neutrinos per atomic volume in the belt leads to a lower bound for the mass of the belt:

$$M(\text{belt}) \simeq m(\nu_d) \frac{\text{Vol}(\text{belt})}{a^3} > 10^{-11} M(\text{Sun}) \quad (a \simeq 10^{-10} \text{ meters}) . \quad (8.6.5)$$

Here it is assumed that the dark neutrino mass is same as neutrino mass, which of course is an unnecessarily strong assumption. If the belt is at rest, the time period for the variation of the tritium beta decay anomaly is exactly half year. The period seems to be few hours longer than one half year (as reported in Neutrino98 conference in Tokyo by Lobashev *et al*) [44], which suggests that belt rotates slowly relative to Earth in the same direction as Earth.

2. Second model

The model for radioactive decay rate anomalies requires that neutrinos and Earth move respect to each other and that the density of neutrinos in the laboratory volume varies along the orbit.

1. Assume first that ordinary quantum mechanics applies and neutrinos are ordinary. The simplest expectation from Equivalence Principle assuming that neutrinos and Earth move independently along geodesic lines is that the velocity is same for Earth and neutrinos. No effect results even if the density of neutrinos along the orbit varies.
2. Suppose that the neutrinos are dark in the sense of having gigantic gravitational Planck constant and are in a macroscopically quantum coherent phase delocalized along the entire orbit and described by a wave function (also neutrino Cooper pairs can be considered). If the neutrino ring is exactly circular as Bohr orbit picture suggests and contains Earth's orbit, the thickness of the ring must be at least $d = a - b$, where a and b are major and minor axis. Exact rotational symmetry implies that dark neutrinos are characterized by a phase factor characterizing the angular momentum eigen state in question (the unit of the quantized angular momentum is now very large). Thus neutrino density depends only on the transversal coordinates of the tube and vanishes at the boundary of the tube. Since the Earth's orbit is ellipse, the transversal variation of the neutrino density inside the tube induces periodic variations of the neutrino density in the detector and could explain the effects on radioactive decay rates.

Although the model might explain the time variation of V_b it does not provide any obvious explanation for beta decay rates in general and fails to explain the variation of the alpha decay rate of ^{226}Ra nor the correlation of decay rates with solar flares. Hence it is clear that the model involving only the notion of nuclear string is favored.

8.6.4 Some other apparent anomalies made possible by dark neutrinos

The appearance of dark neutrinos in the final states of beta decays allow to imagine also some other apparent anomalies.

Apparent anomaly in the inverse beta decay

For the antineutrino belt option one can consider also the possibility of an apparent anomaly in the inverse beta decay in which positron and neutrino are emitted but only electron observed. The apparent anomaly would result from the absorption of a dark antineutrino with repulsive Z^0 interaction energy with condensed matter.

In this case the value of E_0 increases

$$E_0 = M_i - M_f - m(\nu) \rightarrow \hat{E}_0 = M_i - M_f + m(\nu_d) + V_b \quad , \quad (8.6.6)$$

which means that positron spectrum extends above the kinematic limit if V_b has the value predicted by the explanation of tritium beta decay anomaly.

A second anomalous situation results if the emitted neutrino transforms to a dark neutrino with negative binding energy. In this case the value of E_0 would change as

$$E_0 \rightarrow \hat{E}_0 = M_i - M_f - m(\nu_d) + V_b \quad . \quad (8.6.7)$$

Apparently neutrinoless beta decay and double beta decay

Neutrinoless double beta decay (NDB) is certainly one of the most significant nuclear physics processes from the point of view of unified theories (the popular article of New Scientist [79] provides a good view of NDB and the recent rather exciting experimental situation). In the standard physics framework NDB can occur only if neutrinos are Majorana neutrinos so that neutrino number is conserved only modulo 2 meaning that neutrino and antineutrino are one and the same particle. Since no antineutrinos are emitted in the NDB, the total energy of the two electrons is larger than in the normal double beta decay, and serves as an experimental signature of the process.

There are several collaborations studying NDB. The team formed by Hans Klapdor-Kleingrothaus and colleagues from the the Max Planck Insitute for Nuclear Physics in Heidelberg have been studying this process since 1990 in Gran Sasso laboratory. The decays studied are decays of Germanium-76 isotope known to be one of the few isotopes undergoing ordinary double beta decay transforming it

into Selenium. The energy of the emitted two electrons is absorbed by the surrounding Ge atoms. The total energy which is larger for NDB decay serves as a signature of the process.

Three years ago came the first paper of the Heidelberg group reporting the observation of 15 NDB decays [53]. The analysis of the experiments however received a very critical response from colleagues. The Kurchatov Institute quitted the collaboration at 2001 and represented its own analysis with the conclusion that the data do not support NDB. Three years later Heidelberg group represented 14 new candidates for NDB and a new analysis [65]. It is now admitted that the team is not obviously wrong but that there are still doubts whether the background radioactivity has been handled correctly.

In TGD Universe neutrinos are Dirac neutrinos and NDB is not possible. The possibility of dark neutrinos however allow to consider the possibility of apparently neutrinoless beta decay and double beta decay.

What would happen that the ordinary neutrino emitted in the beta decay of proton transforms into a dark neutrino by mixing. The dark neutrino would not be observed so that apparently neutrinoless beta decay would be in question. Dark neutrino has a negative interaction energy with condensed matter assuming that the explanation of tritium beta decay anomaly is correct so that electron would have an anomalously high energy. The process cannot occur if the negative energy states of the Fermi sea are filled as indeed suggested by energetic considerations.

The generalization of this process would be double beta decay involving strong interaction between decaying neutrons mediated by color bond between them and the transformation of second neutrino to dark neutrino with negative energy so that the electrons would have anomalously high energy. The same objection applies to this process as to the apparently neutrinoless beta decay.

8.7 Cold fusion and Trojan horse mechanism

The model for cold fusion has developed gradually as the understanding of quantum TGD and many-sheeted space-time has developed. Trojan horse mechanism has served as the connecting thread between various models. The last step of progress relates to the new vision about nuclear physics but it is still impossible to fix the model completely unless one poses the condition of minimality and the requirement that single mechanism is behind various anomalies.

8.7.1 Exotic quarks and charged color bonds as a common denominator of anomalous phenomena

There should exist a common denominator for anomalous behavior of water, cold fusion, the findings of Ditmire suggesting cold fusion, sono-fusion, exotic chemistries, strange properties of living matter including chiral selection, and also phenomena like low compressibility of condensed matter which standard physicist would not be worried about.

It seems that compression inducing the generation of charged color bonds between nucleons and leading to a formation of super-nuclei with atomic distances between building blocks might be the sought for common denominator. For super nuclei the repulsive weak interactions between exotic quark and anti-quark belonging to the two bonded nuclei would compensate the attractive color force so that a stable configuration of atomic size would result. Note that the weak coupling strength would be actually strong by the general criterion for transition to the large \hbar phase.

The charging of color bonds would occur via W boson exchange between exotic and valence quarks with exotic W boson transforming to ordinary W via mixing.

The alternative option is a phase transition of nuclei transforming $k = 113$ em space-time sheets of valence quarks to em dark space-time sheets with a large value of \hbar suggested for heavier nuclei by the general criteria. This phase transition could be avoided if the criticality forces surplus protons to transfer the electromagnetic charge of valence quarks to color bonds so that the situation reduces to the first option. In this picture standard nuclear physics would remain almost untouched and nothing new expect exotic quarks and charged color bonds is introduced.

The following examples suggest that this general picture indeed might unify a large class of phenomena.

1. The super-nuclei formed by the dark protons of water would be a basic example about this phenomenon. The occurrence of the process is plausible if also nucleons possess or can generate

closed loops with exotic quark and anti-quark at the ends of the loop belonging to the same nucleon. The fact that these protons are dark with respect to electromagnetic interactions suggests that the charge of protons is transferred to the color bonds so that the outcome is a nuclear string formed from neutrons connected by positively charged color bonds. Darkness with respect to weak interactions suggests that valence quarks are doubly dark. This would mean that the p-adic length scale of color bonds would correspond to $k_{eff} = 107 + 2 \times 22 = 151$ for $\hbar_s = n^2 \hbar / v_0^2$, $n = 1$. This corresponds to the thickness of cell membrane so that the structure of water would contain information about the basic biological length scale.

2. In condensed matter the super-nuclei would form at some critical pressure when weakly charged color bonds between neighboring nuclei become possible and compensate the attractive color force. This would explain the low compressibility of condensed matter.
3. Bio-polymers in vivo might correspond to super-nuclei connected by charged color bonds whose weak charges would explain the large parity breaking involve with chiral selection. Hydrogen bond might be a basic example of a charged color bond. It could be that the value of integer n in $\hbar_s = n\hbar/v_0$ is $n = 3$ in living matter and $n = 1$ in ordinary condensed matter.

Trojan horse mechanism might work also at the level of chemistry making possible to circumvent electronic Coulomb wall and might be an essential characteristic of the catalytic action. Note that Pd is also a powerful catalyst. $n = 1$ might however distinguish it from bio-catalysts. In separate context I have dubbed this mechanism as 'Houdini effect'.

The reported occurrence of nuclear transmutations [40, 41] such as $^{23}\text{Na} + ^{16}\text{O} \rightarrow ^{39}\text{K}$ in living matter allowing growing cells to regenerate elements K, Mg, Ca, or Fe, could be understood as fusion of neighboring nuclei connected by charged color bond which becomes neutral by W emission so that collapse to single nucleus results in absence of the repulsive weak force. Perhaps it is someday possible to produce metabolic energy by bio-fusion or perhaps Nature has already discovered the trick!

4. In cold fusion the nuclei of target D and Pd would combine to form super-nuclei connected by charged color bonds. This would explain why the heavy loading of Pd nuclei with D (for a review of loading process see [60]) does not generate enormous pressures. Cold fusion would occur in some critical interval of loadings allowing ordinary and exotic nuclei to transform to each other. The transfer of the em charge of D to the color bond connecting D and Pd would make D effectively nn state. Together with the fact that the color bond would have length of order atomic radius would mean that the Coulomb wall of Pd and D is not felt by beam nuclei and Trojan horse mechanism would become possible. The prediction is that Coulomb wall disappears only when deuterium or tritium target is used. If nuclei can transform to dark em phase cold fusion could occur for arbitrary target nuclei. That it is observed only for D and possibly H does not support this option.

If valence quarks are doubly dark, their magnetic bodies have size of order $L(151) = 10$ nm, which is also the size scale of the nano-scaled Pd particles, color force would become long ranged. In sono-luminescence and son-fusion and also in nuclear transmutations similar formation of super-nuclei would occur and the collapse of super-nucleus to single nucleus could occur by the proposed mechanism.

5. In the experiments of Ditmire *et al* laser pulse induces very dense phase of Xenon atoms having $Z = 54$ which is heated to energies in which electron energies extend to MeV region and expands rapidly. $Z = 54$ means that Xe satisfies the most stringent condition of criticality for the transition to electromagnetic large \hbar phase. This transition does not occur if protons feed the surplus em charge to the color bonds so that Xe nuclei also weakly charged. Assume that some fraction of Xe is in this kind of phase. The compression of Xe gas by laser pulse compresses Xe super-nuclei. If the connecting charged color bonds emit their em and weak charge by emission of W boson the super-nuclei collapse to single nucleus and nuclear fusion reactions become possible. The repulsive weak force becoming manifest in the compression generates brehmstrahlung heating the system and induces a violent explosion much like in sono-fusion.

In the sequel the experiments Ditmire *et al* and cold fusion are discussed in detail using this model.

8.7.2 The experiments of Ditmire *et al*

An important stimulation in the development of the model for cold fusion came from the observations of Ditmire *et al* [57] published in Nature. The discovery was that the energy spectrum of electrons in ionic explosions induced by the laser heating of ionic clusters extends up to energies of order MeV (rather 10^2 eV(!)): this suggests strongly a mechanism making strong interactions possible.

In the experimental arrangement of Ditmire *et al* clusters of Xenon atoms are hit by ultrashort (150 fsec), high-intensity (2×10^{16} W/cm²) laser pulses[57]. This leads to superheating and production of high energy ions in the explosions of the superheated clusters. The highest ion energies are by 4 orders of magnitude larger than expected and of order MeV, the typical energy scale of nuclear strong interaction. The average ion energy is 45 ± 5 keV for cluster size of 6.5 nm and decreases slowly with the size of the cluster. No hot ions are produced for small clusters containing less than ~ 100 Xe atoms. It is not yet understood why the clusters explode so much more violently than molecules (producing 1 MeV ions as opposed to 100 eV ions) and small clusters. Another striking feature of the laser-cluster interaction is ionization to very high charge states, much higher than in the ionization, which can be produced by simple field ionization.

Consider first a more detailed model of the superheating as it is described in [57].

In an intensely irradiated cluster, optically and collisionally ionized electrons undergo rapid collisional heating for the short time ($< ps$) before the cluster disassembles in the laser field. Our recent studies of the electron energy spectra produced by the high intensity irradiation of large Xe clusters with 150 fs laser pulse indicate that collisional heating within the cluster can produce electrons with energy up to 3 keV, an energy much higher than that typical of solid target plasmas.

A sharp peak in the measured electron energy spectrum suggested that the cluster micro-plasma exhibited a resonance in the heating by laser pulse similar to the giant resonance seen in metallic clusters. A small amount of cluster expansion during the laser pulse lowers the electron density to bring the near-infrared laser light into resonance with the free-electron plasma frequency in the cluster. This resonance greatly increases the laser electric field density within the cluster, and the laser absorption rate is enhanced, rapidly heating the electrons on a very fast (< 10 fs) time scale to a highly non-equilibrium superheated state with mean energies of many keV. Charge separation of hot electrons inevitably leads to a very fast expansion of the cluster ions. This process is fundamentally different from low-intensity photo-fragmentation of cluster and far more energetic than the Coulomb explosion of small molecules.

Authors believe (rather naturally!) that the production of hot ions is made possible by the high ion-temperatures produced by the not yet properly understood heating mechanism and suggest that this mechanism might make even table-top fusion possible.

In TGD framework the proposed general vision suggests following picture.

1. Laser pulse induces a compression of clusters of Xe atoms already containing super-nuclei with charged color bonds so that repulsive weak interaction compensated by color force in equilibrium situation becomes manifest and induces the expansion of the system much like the expansion of the bubble in sono-luminescence. The resulting brehmstrahlung heats the system.
2. The critical cluster size 6.5 nm could correspond to the p-adic length length scale $L(k_{eff} = 151) = 10$ nm for doubly dark valence quarks with $n = 1$.
3. The nuclear fusions resulting when color bonds between nuclei become neutral and induce collapse to single nucleus. Anomalously high charge states could be a byproduct of violent and very rapid fusions of neighboring color bonded Xe nuclei tearing Xe nuclei and outer electrons apart. These fusions would generate quantum coherent dark gamma ray beams transforming to ordinary gamma rays by de-coherence transition reducing the wavelength of gamma rays by a factor of 2^{-11} for $\hbar_s = \hbar/v_0$. It is also possible that dark gamma rays are absorbed by Pd super-nuclei. The wavelengths of dark gamma rays with energy of MeV would of order 2 nanometers in this case so that a coherent heating would happen in rather large volume.

8.7.3 Brief summary of cold fusion

In the following history and signatures of cold fusion are briefly summarized.

History of cold fusion

The first claim for cold fusion [77] dates back to March 23, 1989, when Pons and Fleischmann announced that nuclear fusion, producing usable amounts of heat, could be induced to take place on a table-top by electrolyzing heavy water and using electrodes made of Pd and platinum. Various laboratories all-over the world tried to reproduce the experiments. The poor reproducibility and the absence of the typical side products of nuclear fusion (gamma rays and neutrons) led soon to the conclusion (represented in the dramatic session of American Physical Society May 1, 1989) that nuclear fusion cannot explain the heat production. Main stream scientists made final conclusions about the subject of 'cold fusion' and cold fusion people became a pariah class of the scientific community.

The work with cold fusion however continued and gradually situation has changed. It became clear that nuclear reaction products, mainly ${}^4\text{He}$, are present. Gradually also the reasons for the poor reproducibility of the experiments became better understood. A representative example about the change of the attitudes is the article of Schwinger [26] in which cold fusion is taken seriously. The article also demonstrates that the counter arguments of hot fusion people are based on the implicit assumption that hot fusion theory describes cold fusion despite the fact that the physical situations are radically different.

The development on the experimental side has been based on techniques involving the use of catalysis, nanotechnology, electrolysis, glow discharge and ultrasonic cavitation. There are now public demonstrations of cold fusion reactors, whose output energy far exceeds input energy and commercial applications are under intensive development, see for instance the home page of Russ George [59], for whom I am grateful for informing me about the recent state of cold fusion.

Rather remarkably, also the production of heavier elements has been detected [62] and this makes the explanation of the effect even more difficult in standard physics context and definitely excludes the explanations claiming that some chemical process is the source of the excess heat. The possibility of nuclear transmutation also suggests the possibility to transform ordinary nuclear wastes into non-radioactive nuclei and the first method achieving this has already been reported [64]. There are claims [40, 41] that cold fusion indeed occurs in bio-systems.

There is also some evidence for high temperature super conductivity associated with deuterium loaded palladium [62]. Good representations about the subject of cold fusion and references to the experimental work can be found at various cold fusion web-sites [50, 40, 68, 59]. Also the articles of J. Rothwell [62] and the excellent review article of E. Storms [61] are recommended.

It has become clear that cold fusion differs from hot fusion in several respects: gamma rays are not produced and the flux of neutrons is much lower than predicted by standard nuclear physics (these features are very well-come from the point of view of the technological applications). Together with the fact that Coulomb wall does not allow the occurrence of cold fusion at all in the standard physics context, this forces the conclusion that new physics must be involved.

It seems that TGD indeed could provide this new physics. The key elements of the model to be discussed are Trojan horse mechanism and coherent photon exchange action of D nuclei with Cooper pairs of the exotic super conductor formed by the D-loaded cathode material (say Palladium).

In the sequel the consideration is restricted to the case of Pd cathode: the model generalizes trivially to the case of a more general cathode material.

Signatures of cold fusion

In the following the consideration is restricted to cold fusion in which two deuterium nuclei react strongly since this is the basic reaction type studied.

In hot fusion there are three reaction types:

- 1) $D + D \rightarrow {}^4\text{He} + \gamma$ (23.8MeV)
- 2) $D + D \rightarrow {}^3\text{He} + n$
- 3) $D + D \rightarrow {}^3\text{H} + p$.

The rate for the process 1) predicted by standard nuclear physics is more than 10^{-3} times lower than for the processes 2) and 3) [39]. The reason is that the emission of the gamma ray involves the relatively weak electromagnetic interaction whereas the latter two processes are strong.

The most obvious objection against cold fusion is that the Coulomb wall between the nuclei makes the mentioned processes extremely improbable at room temperature. Of course, this alone implies

that one should not apply the rules of hot fusion to cold fusion. Cold fusion indeed differs from hot fusion in several other aspects.

1. No gamma rays are seen.
2. The flux of energetic neutrons is much lower than expected on basis of the heat production rate an by interpolating hot fusion physics to the recent case.

These signatures can also be (and have been!) used to claim that no real fusion process occurs. It has however become clear that the isotopes of Helium and also some tritium accumulate to the Pd target during the reaction and already now prototype reactors for which the output energy exceeds input energy have been built and commercial applications are under development, see for instance [59]. Therefore the situation has turned around. The rules of standard physics do not apply so that some new nuclear physics must be involved and it has become an exciting intellectual challenge to understand what is happening. A representative example of this attitude and an enjoyable analysis of the counter arguments against cold fusion is provided by the article 'Energy transfer in cold fusion and sono-luminescence' of Julian Schwinger [26]. This article should be contrasted with the ultra-skeptical article 'ESP and Cold Fusion: parallels in pseudoscience' of V. J. Stenger [32].

Cold fusion has also other features, which serve as valuable constraints for the model building.

1. Cold fusion is not a bulk phenomenon. It seems that fusion occurs most effectively in nano-particles of Pd and the development of the required nano-technology has made possible to produce fusion energy in controlled manner. Concerning applications this is a good news since there is no fear that the process could run out of control.
2. The ratio x of D atoms to Pd atoms in Pd particle must lie the critical range [.85, .90] for the production of ${}^4\text{He}$ to occur [45]. This explains the poor repeatability of the earlier experiments and also the fact that fusion occurred sporadically.
3. Also the transmutations of Pd nuclei are observed [62].

Below a list of questions that any theory of cold fusion should be able to answer.

1. Why cold fusion is not a bulk phenomenon?
2. Why cold fusion of the light nuclei seems to occur only above the critical value $x \simeq .85$ of D concentration?
3. How fusing nuclei are able to effectively circumvent the Coulomb wall?
4. How the energy is transferred from nuclear degrees of freedom to much longer condensed matter degrees of freedom?
5. Why gamma rays are not produced, why the flux of high energy neutrons is so low and why the production of ${}^4\text{He}$ dominates (also some tritium is produced)?
6. How nuclear transmutations are possible?

8.7.4 TGD inspired model of cold fusion

The model to be discussed is based on Trojan horse mechanism and explains elegantly all those aspects of cold fusion which are in conflict with standard nuclear physics. The reaction mechanism explains also the sensitivity of the occurrence of cold fusion to small external perturbations.

Model for D-loaded Pd nano-particle

It seems that cold fusion is a critical phenomenon. The average D/Pd ratio must be in the interval (.85, .90). The current must be over-critical and must flow a time longer than a critical time. The effect occurs in a small fraction of samples. Deuterium at the surface of the cathode is found to be important and activity tends to concentrate in patches. The generation of fractures leads to the loss of the anomalous energy production. Even the shaking of the sample can have the same effect. The addition of even a small amount of H_2O to the electrolyte (protons to the cathode) stops the anomalous energy production.

All these findings support the catastrophe theoretic picture according to which the decomposition into patches corresponds to criticality allowing the presence of ordinary and exotic phase whose transformation to the ordinary phases makes possible cold fusion reactions. The added ordinary protons and fractures could serve as a seed for a phase transition leading to a region where only single phase is possible.

In TGD framework Pd nano-particles correspond to space-time sheets of size of order $10^{-9} - 10^{-8}$ m and fusion is restricted inside these structures. Cold fusion can be regarded as a fusion of incoming ordinary D with target D attached to the surface of Pd rather than between two free D:s as suggested by the standard nuclear physics wisdom. Thus cold fusion could be regarded as 'burning' of D associated with a finite space-time sheets so that cold fusion is not a bulk phenomenon and is very sensitive to the in-homogenities of the Pd particle. Note that this in principle makes the control of cold fusion easier.

The critical loading fraction varies in the range .85 – .90. This value is so large that enormous pressures would be generated unless the deuterium nuclei lose their translational degrees of freedom by forming some kind of bound states with Pd nuclei. The guess is that the bound states correspond to the formation of super-nuclei with em and weakly charged color bonds connecting Pd and D nuclei. $k = 113$ dark weak force, which is actually strong by the criticality condition, compensates the color force between the exotic quarks. This makes D nuclei effectively nn nuclei so that Coulomb wall does not produce difficulties.

The challenge is to understand the origin of the criticality condition for super-nucleus. The question is why the number of D nuclei per Pd nuclei varies in so narrow range for the phase transition leading to the formation of super-nuclei to occur. Catastrophe theoretic thinking suggests that a cusp catastrophe typical for phase transitions is in question. In the critical range there are two phases, exotic and ordinary phase, which can easily transform to each other. Criticality is essential for the cold fusion reactions to occur since initial state involves exotic D+Pd complex and final state involves ordinary nuclei.

The ratio x would correspond to the variable which varies in a direction transversal to cusp and whose variation therefore leads to a catastrophic jump inducing the phase transition or its reverse. x would be a pressure type variable which plays similar role also in phase transitions like liquid-gas phase transition. The critical range for x would correspond to the critical range of pressure in which liquid and gas are in equilibrium.

Second variable varies along the cusp so that the transition is possible above certain critical value. This variable presumably relates to the energetics of the transition so that transition would liberate energy above critical value of the parameter. Temperature is a natural candidate for this variable. Catastrophe theoretic model implies that for a given value x in catastrophe region both ordinary phase and exotic phase are possible. In these regions cold fusion can occur. In regions where the system is outside the catastrophe region so that system is stably in either phase, cold fusion cannot occur. This explains why Pd contains only patches where cold fusion occurs. The control variable, be it local temperature or something else, could be perhaps identified by studying the local conditions guaranteeing the occurrence of cold fusion. It is indeed known that the increase of temperature favors the occurrence of cold fusion.

The behavior variable could distinguish between the two phases and could correspond to the surface density n of D nuclei bound to Pd nuclei and transformed to fake D. The potential function could be free energy minimized when the system is in constant temperature and the two phases would correspond to local minima of free energy.

Anomalous reaction kinetics of cold fusion

One can deduce a more detailed model for cold fusion from observations, which are discussed systematically in [39] and in the references discussed therein.

1. When D_2O is used as an electrolyte, the process occurs when PdD acts as a cathode but does not seem to occur when it is used as anode. This suggests that the basic reaction is between the ordinary deuterium $D = pn$ of electrolyte with the exotic $D=nn + \text{charged color bond}$ attached to Pd in the cathode.
2. For ordinary nuclei fusions to tritium and ${}^3\text{He}$ occur with approximately identical rates. The first reaction produces neutron and ${}^3\text{He}$ via $D + D \rightarrow n + {}^3\text{He}$, whereas second reaction produces proton and tritium via $D + D \rightarrow p + {}^3\text{H}$. The standard nuclear physics prediction is that one neutron per each tritium nucleus should be produced. Tritium can be observed by its beta decay to ${}^3\text{He}$ and the ratio of neutron flux is several orders of magnitude smaller than tritium flux as found for instance by Tadahiko Mizuno and his collaborators (Mizuno describes the experimental process leading to this discovery in his book [70]). Hence the reaction producing ${}^3\text{He}$ cannot occur significantly in cold fusion which means a conflict with the basic predictions of the standard nuclear physics.

The explanation is following. If D is fake D ($nn + \text{charged color bond}$ connecting it with Pd), one expects that the production of ${}^3\text{He}$ is hindered since there is no proton directly available. Also in the case that the reaction $n + \text{color bond} \rightarrow p$ occurs, one expects that Coulomb wall makes the process slow.

3. The production of ${}^4\text{He}$, which should not occur practically at all, is reported to dominate and the fraction of tritium is below .1 per cent. The explanation could be that also multiple attachments to target can occur such that D attaches to (D+Pd) by forming a charged color bond. Thus would have $nnnn$ state with two charged color bonds attached to Pd. This state could split from Pd and transform via exchange of two light weak bosons between exotic and valence quarks to ${}^4\text{He}$ (assuming that dark $W(113)$ can mix with $W(89)$). It is also possible that the super-nuclear string formed by Pd and D splits and emits ${}^4\text{He}$ as in ordinary alpha decay. Gamma rays need not be generated since the recoil momentum could be transferred to the Pd target like in Mössbauer effect.
4. Also more complex reactions between D and Pd and between Pd nuclei can occur. These can lead to the reactions transforming the nuclear charge of Pd and thus to nuclear transmutations.
5. The mechanism also explains why the cold fusion producing ${}^3\text{He}$ and neutrons does not occur using water instead of heavy water. There are reports about cold fusion also in this case [61]. If one fourth of protons in water are arranged to nuclear strings consisting of neutrons connected by positively charged color bonds as the TGD based model explaining the anomalies of water suggests [27], these strings could attach to fake D and induce cold fusion reactions.
6. The proposed reaction mechanism explains why neutrons are not produced in amounts consistent with the anomalous energy production. The addition of water to the electrolyte however induces neutron bursts. Suppose that one fourth of protons in water forms similar dark phase being transformed to neutrons connected by positively charged color bonds, as assumed in the model of water explaining various anomalies of water [27]. What comes in mind is that neutrons are generated when a neutron string from H_2O containing only charged color bonds attaches to $D + Pd$ ($nn + \text{charged color bond} + Pd$). Neutrons of nn are connected by a neutral color bond. If charged color bonds between neutrons are energetically more favorable than neutral color bonds, nn could emit a free neutron in the process so that the outcome would be a neutron string containing only charged color bonds attached to Pd.

How objections against cold fusion are circumvented?

It has already become clear that the model allows to circumvent the basic reaction kinetic arguments against cold fusion [39].

1. Coulomb wall makes nuclear fusions impossible.

2. ${}^3\text{He}$ and ${}^3\text{H}$ should be produced in equal amounts. The fraction of ${}^4\text{He}$ should be smaller than 10^{-3} .
3. The claimed nuclear transmutation reactions (reported to occur also in living matter [40]) should not occur.

Consider next the objections related to energetics.

1. Gamma rays, which should be produced in most nuclear reactions such as ${}^4\text{He}$ production to guarantee momentum conservation are not observed. The explanation is that the recoil momentum goes to the macroscopic quantum phase defined by the Pd lattice as in Mössbauer effect, and eventually heats the electrolyte system. This provides the mechanism by which the liberated nuclear energy is transferred to the electrolyte difficult to imagine in standard nuclear physics framework.
2. If a nuclear reaction should occur, the immediate release of energy can not be communicated to the lattice in the time available. In the recent case the time scale is however multiplied by the factor $r = \hbar_s/\hbar$ giving scaling factor 2^{11} so that the situation changes dramatically.

8.7.5 Do nuclear reaction rates depend on environment?

Claus Rolfs and his group have found experimental evidence for the dependence of the rates of nuclear reactions on the condensed matter environment [67]. For instance, the rates for the reactions ${}^{50}\text{V}(p,n){}^{50}\text{Cr}$ and ${}^{176}\text{Lu}(p,n)$ are fastest in conductors. The model explaining the findings has been tested for elements covering a large portion of the periodic table.

Debye screening of nuclear charge by electrons as an explanation for the findings

The proposed theoretical explanation [67] is that conduction electrons screen the nuclear charge or equivalently that incoming proton gets additional acceleration in the attractive Coulomb field of electrons so that the effective collision energy increases so that reaction rates below Coulomb wall increase since the thickness of the Coulomb barrier is reduced.

The resulting Debye radius

$$R_D = 69 \sqrt{\frac{T}{n_{eff}\rho_a}} \quad , \quad (8.7.1)$$

where ρ_a is the density of atoms per cubic meter and T is measured in Kelvins. R_D is of order .01 Angstroms for $T = 373$ K for $n_{eff} = 1$, $a = 10^{-10}$ m. The theoretical model [65, 64] predicts that the cross section below Coulomb barrier for $X(p, n)$ collisions is enhanced by the factor

$$f(E) = \frac{E}{E + U_e} \exp\left(\frac{\pi\eta U_e}{E}\right) \quad . \quad (8.7.2)$$

E is center of mass energy and η so called Sommerfeld parameter and

$$U_e \equiv U_D = 2.09 \times 10^{-11} (Z(Z+1))^{1/2} \times \left(\frac{n_{eff}\rho_a}{T}\right)^{1/2} \text{ eV} \quad (8.7.3)$$

is the screening energy defined as the Coulomb interaction energy of electron cloud responsible for Debye screening and projectile nucleus. The idea is that at R_D nuclear charge is nearly completely screened so that the energy of projectile is $E + U_e$ at this radius which means effectively higher collision energy.

The experimental findings from the study of 52 metals support the expression for the screening factor across the periodic table.

1. The linear dependence of U_e on Z and $T^{-1/2}$ dependence on temperature conforms with the prediction. Also the predicted dependence on energy has been tested [67].

- The value of the effective number n_{eff} of screening electrons deduced from the experimental data is consistent with $n_{eff}(Hall)$ deduced from quantum Hall effect.

The model suggests that also the decay rates of nuclei, say beta and alpha decay rates, could be affected by electron screening. There is already preliminary evidence for the reduction of beta decay rate of ^{22}Na β decay rate in Pd [58], metal which is utilized also in cold fusion experiments. This might have quite far reaching technological implications. For instance, the artificial reduction of half-lives of the radioactive nuclei could allow an effective treatment of radio-active wastes. An interesting question is whether screening effect could explain cold fusion [39] and sono-fusion [63].

Electron screening and Trojan horse mechanism

These experimental findings allow to quantify the Trojan horse mechanism. The idea is that projectile nucleus enters the region of the target nucleus along a larger space-time sheet and in this manner avoids the Coulomb wall. The nuclear reaction itself occurs conventionally. In conductors the space-time sheet of conduction electrons is a natural candidate for the larger space-time sheet.

At conduction electron space-time sheet there is a constant charged density consisting of n_{eff} electrons in the atomic volume $V = 1/n_a$. This creates harmonic oscillator potential in which incoming proton accelerates towards origin. The interaction energy at radius r is given by

$$V(r) = \alpha n_{eff} \frac{r^2}{2a^3}, \quad (8.7.4)$$

where a is atomic radius.

The proton ends up to this space-time sheet by a thermal kick compensating the harmonic oscillator energy. This occurs below with a high probability below radius R for which the thermal energy $E = T/2$ of electron corresponds to the energy in the harmonic oscillator potential. This gives the condition

$$R = \sqrt{\frac{Ta}{n_{eff}\alpha}} a. \quad (8.7.5)$$

This condition is exactly of the same form as the condition given by Debye model for electron screening but has a completely different physical interpretation.

Since the proton need not travel through the nuclear Coulomb potential, it effectively gains the energy

$$E_e = Z \frac{\alpha}{R} = \frac{Z\alpha^{3/2}}{a} \sqrt{\frac{n_{eff}}{Ta}}. \quad (8.7.6)$$

which would be otherwise lost in the repulsive nuclear Coulomb potential. Note that the contribution of the thermal energy to E_e is neglected. The dependence on the parameters involved is exactly the same as in the case of Debye model. For $T = 373$ K in the ^{176}Lu experiment and $n_{eff}(Lu) = 2.2 \pm 1.2$, and $a = a_0 = .52 \times 10^{-10}$ m (Bohr radius of hydrogen as estimate for atomic radius), one has $E_e = 28.0$ keV to be compared with $U_e = 21 \pm 6$ keV of [67] ($a = 10^{-10}$ m corresponds to 1.24×10^4 eV and 1 K to 10^{-4} eV). A slightly larger atomic radius allows to achieve consistency. The value of \hbar does not play any role in this model since the considerations are purely classical.

An interesting question is what the model says about the decay rates of nuclei in conductors. For instance, if the proton from the decaying nucleus can enter directly to the space-time sheet of the conduction electrons, the Coulomb wall corresponds to the Coulomb interaction energy of proton with conduction electrons at atomic radius and is equal to $\alpha n_{eff}/a$ so that the decay rate should be enhanced.

Trojan horse mechanism realized in this manner does not seem to explain the basic findings about cold fusion. Trojan horse mechanism applied to deuterium projectile and D-Pd target would predict standard nuclear physics. The reported strong suppression of ^3He production with respect to ^3H production however requires non-standard nuclear physics and the model discussed in the previous subsection provides this physics. Both mechanisms could of course be involved.

Bibliography

Books about TGD

- [1] M. Pitkänen (2006), *Topological Geometroynamics: Overview*.
http://tgd.wippiespace.com/public_html/tgdview/tgdview.html.
- [2] M. Pitkänen (2006), *Quantum Physics as Infinite-Dimensional Geometry*.
http://tgd.wippiespace.com/public_html/tgdgeom/tgdgeom.html.
- [3] M. Pitkänen (2006), *Physics in Many-Sheeted Space-Time*.
http://tgd.wippiespace.com/public_html/tgdclass/tgdclass.html.
- [4] M. Pitkänen (2006), *p-Adic length Scale Hypothesis and Dark Matter Hierarchy*.
http://tgd.wippiespace.com/public_html/paddark/paddark.html.
- [5] M. Pitkänen (2006), *Quantum TGD*.
http://tgd.wippiespace.com/public_html/tgdquant/tgdquant.html.
- [6] M. Pitkänen (2006), *TGD as a Generalized Number Theory*.
http://tgd.wippiespace.com/public_html/tgdnumber/tgdnumber.html.
- [7] M. Pitkänen (2006), *TGD and Fringe Physics*.
http://tgd.wippiespace.com/public_html/freenergy/freenergy.html.

Books about TGD Inspired Theory of Consciousness and Quantum Biology

- [8] M. Pitkänen (2006), *TGD Inspired Theory of Consciousness*.
http://tgd.wippiespace.com/public_html/tgdconsc/tgdconsc.html.
- [9] M. Pitkänen (2006), *Bio-Systems as Self-Organizing Quantum Systems*.
http://tgd.wippiespace.com/public_html/bioselforg/bioselforg.html.
- [10] M. Pitkänen (2006), *Quantum Hardware of Living Matter*.
http://tgd.wippiespace.com/public_html/bioware/bioware.html.
- [11] M. Pitkänen (2006), *Bio-Systems as Conscious Holograms*.
http://tgd.wippiespace.com/public_html/hologram/hologram.html.
- [12] M. Pitkänen (2006), *Genes and Memes*.
http://tgd.wippiespace.com/public_html/genememe/genememe.html.
- [13] M. Pitkänen (2006), *Magnetospheric Consciousness*.
http://tgd.wippiespace.com/public_html/magnconsc/magnconsc.html.
- [14] M. Pitkänen (2006), *Mathematical Aspects of Consciousness Theory*.
http://tgd.wippiespace.com/public_html/mathconsc/mathconsc.html.
- [15] M. Pitkänen (2006), *TGD and EEG*.
http://tgd.wippiespace.com/public_html/tgdeeg/tgdeeg.html.

References to the chapters of the books about TGD

- [16] The chapter *Dark Forces and Living Matter* of [4].
http://tgd.wippiespace.com/public_html/paddark/paddark.html#darkforces.
- [17] The chapter *p-Adic Particle Massivation: Hadron Masses* of [4].
http://tgd.wippiespace.com/public_html/paddark/paddark.html#mass3.
- [18] The chapter *p-Adic Particle Massivation: Elementary particle Masses* of [4].
http://tgd.wippiespace.com/public_html/paddark/paddark.html#mass2.
- [19] The chapter *TGD as a Generalized Number Theory: Quaternions, Octonions, and their Hyper Counterparts* of [6].
http://tgd.wippiespace.com/public_html/tgdnumber/tgdnumber.html#visionb.
- [20] The chapter *Nuclear String Model* of [4].
http://tgd.wippiespace.com/public_html/paddark/paddark.html#nuclstring.
- [21] The chapter *TGD and M-Theory* of [1].
http://tgd.wippiespace.com/public_html/tgdview/tgdview.html#MTGD.
- [22] The chapter *An Overview about the Evolution of Quantum TGD* of [1].
http://tgd.wippiespace.com/public_html/tgdview/tgdview.html#evoI.
- [23] The chapter *The Recent Status of Leptohadron Hypothesis* of [4].
http://tgd.wippiespace.com/public_html/paddark/paddark.html#leptc.
- [24] The chapter *TGD as a Generalized Number Theory: Infinite Primes* of [6].
http://tgd.wippiespace.com/public_html/tgdnumber/tgdnumber.html#visionc.
- [25] The chapter *TGD and Astrophysics* of [3].
http://tgd.wippiespace.com/public_html/tgdclass/tgdclass.html#astro.
- [26] The chapter *An Overview about Quantum TGD: Part I* of [1].
http://tgd.wippiespace.com/public_html/tgdview/tgdview.html#evoII.
- [27] The chapter *Was von Neumann Right After All* of [5].
http://tgd.wippiespace.com/public_html/tgdquant/tgdquant.html#vNeumann.
- [28] The chapter *Dark Nuclear Physics and Condensed Matter* of [4].
http://tgd.wippiespace.com/public_html/paddark/paddark.html#exonuclear.
- [29] The chapter *General Ideas about Many-Sheeted Space-Time: Part I* of [3].
http://tgd.wippiespace.com/public_html/tgdclass/tgdclass.html#topcond.

References to the chapters of the books about TGD Inspired Theory of Consciousness and Quantum Biology

- [30] The chapter *Quantum Model for Nerve Pulse* of [15].
http://tgd.wippiespace.com/public_html//tgdeeg/tgdeeg/tgdeeg.html#pulse.
- [31] The chapter *Topological Quantum Computation in TGD Universe* of [12].
http://tgd.wippiespace.com/public_html/genememe/genememe.html#tqc.

Articles related to TGD

- [32] M. Pitkänen (2007), *Further Progress in Nuclear String Hypothesis*, http://tgd.wippiespace.com/public_html/articles/nuclstring.pdf.

Theoretical physics

- [33] E. M. Lifshitz and L. P. Pitaevski (1974), *Relativistic Quantum Theory: Part 2*, Pergamon Press.

Particle and nuclear physics

- [34] Russ George's homepage,
<http://www.hooked.net/~rgeorge/saturnahome.html> .
- [35] V. J. Stenger (1995), *ESP and Cold Fusion: parallels in pseudoscience*, <http://www.phys.hawaii.edu/vjs/www/cold.txt>.
- [36] J. H. Jenkins *et al* (2008), *Evidence for Correlations Between Nuclear Decay Rates and Earth-Sun Distance*. arXiv:0808.3283v1 [astro-ph], <http://arxiv.org/abs/0808.3283>.
- [37] C. Rolfs and W. S. Rodney (1988), *Cauldrons in the Cosmos* (Chicago, IL: University of Chicago Press).
- [38] E. Storms (2001), *Cold fusion, an objective assessment*,
<http://home.netcom.com/~storms2/review8.html>.
- [39] J. Schwinger (1992), *Energy Transfer In Cold Fusion and Sonoluminescence*, <http://jcbmac.chem.brown.edu/baird/coldfusion/schwinger.html>.
- [40] *Infinite energy magazine* homepage. <http://www.mv.com/ipusers/zeropoint/>.
- [41] P. H Heenen and N. Nazarewicz (2002), *Quest for superheavy nuclei*, vol. 33, No 1. Europhysics News,
<http://www.europhysicsnews.com/full/13/article2/article2.html>.
- [42] C. L. Kervran (1972), *Biological transmutations, and their applications in chemistry, physics, biology, ecology, medicine, nutrition, agriculture, geology*, Swan House Publishing Co.
- [43] P. Tompkins and C. Bird (1973), *The secret life of plants*, Harper & Row, New York.
- [44] Aubert *et al* (1983), Phys. Lett. 123B, p. 275.
- [45] S. E. Shnoll *et al* (1998), *Realization of discrete states during fluctuations in macroscopic processes*, Uspekhi Fisicheskikh Nauk, Vol. 41, No. 10, pp. 1025-1035.
- [46] *GOES X-ray flux plot*. http://www.swpc.noaa.gov/rt_plots/xray_5m.html.
- [47] C. W. Kim and A. Pevsner (1993), *Neutrinos in Physics and Astrophysics*, Harwood Academic Publishers, USA.
- [48] S. M. Wong(1990), *Introductory Nuclear Physics*, Prentice-Hall Inc.
- [49] C. Rolfs *et al* (2006), *First hints on a change of the ^{22}Na β decay half-life in the metal Pd*, Eur. Phys. J. A 28, 251.
- [50] *Cold fusion links* homepage.
<http://www.teleport.com/~genel/coldf.html>.
- [51] J. I. Collar (1996), *Endpoint Structure in Beta Decay from Coherent Weak-Interaction of the Neutrino*, hep-ph/9611420.
- [52] P. G. Hansen(1993), *Nuclear structure at the drip lines*, Nuclear Phys. A, Vol. 553.
- [53] H. V. Klapdor-Kleingrothaus *et al* (2001), Eur. Phys. J. A 12, 147 and hep-ph/0103062.
- [54] R. Serber (1987), *Serber Says: About Nuclear Physis*, World Scientific.

- [55] T. Ludham and L. McLerran (2003), *What Have We Learned From the Relativistic Heavy Ion Collider?*, Physics Today, October issue.
<http://www.physicstoday.org/vol-56/iss-10/p48.html>.
- [56] G. J. Stephenson Jr. (1993), *Perspectives in Neutrinos, Atomic Physics and Gravitation*, ed. J. T. Thanh Van, T. Darmour, E. Hinds and J. Wilkerson (Editions Frontieres, Gif-sur-Yvette), p.31.
- [57] T. Ditmire *et al* (1997), *High energy ions produced in explosions of superheated atomic clusters*, Nature vol. 386, March 6, p. 55.
- [58] T. Mizuno *et al* (2002), *Hydrogen Evolution by Plasma Electolysis in Aqueous solution*, Japanese Journal of Applied Physics, Vol. 44, No 1A, pp. 396-401.
- [59] V. M. Lobashev *et al*(1996), in *Neutrino 96* (Ed. K. Enqvist, K. Huitu, J. Maalampi). World Scientific, Singapore.
- [60] E. Storms (1998), *Formation of b-PdD Containing High Deuterium Concentration Using Electrolysis of Heavy-Water*. <http://home.netcom.com/~storms2/review4.html>.
- [61] T. Otsuka, N. Fukunishi, H. Sagawa (1993), Phys. Rev. Lett, Vol 70, No 10, p. 1385.
- [62] E. Storms (1996), *Review of cold fusion effect*.
<http://www.jse.com/storms/1.html>.
E. Storms (1998), *Cold Fusion Revisited*,
<http://home.netcom.com/~storms2/review5.html>.
- [63] J. H. Jenkins and E. Fischbach (2008) *Perturbation of Nuclear Decay Rates During the Solar Flare of 13 December 2006*, arXiv:0808.3156v1 [astro-ph].
- [64] Robert Bass (1997), *Cincinnati group announces transmutation of radiation waste into useful metals using "table-top" energy levels!*. News Release: July, '97 New Energy News (monthly newsletter of the Institute for New Energy), Vol. 5, No. 3.
- [65] H. V. Klapdor-Kleingrothaus, I. V. Jrivosheina, A. Dietz, and O. Chkvorets (2004), *Search for Neutrinoless Double Beta Decay with Enriched ^{76}Ge in Gran Sasso 1990-2003*, hep-ph/0404088. -Art Library.
- [66] Ch. Weinheimer *et al* (1993), Phys. Lett. 300B, 210.
- [67] S. Moszkowski (1996), *Maria Goeppert Mayer*, Talk Presented at APS meeting Indianapolis, May 4, 1996.
<http://www.physics.ucla.edu/~moszkows/mgm/mgmso.htm>. See also "*Magic Numbers*" in *Nuclear Structure*,
<http://hyperphysics.phy-astr.gsu.edu/hbase/nuclear/shell.html#c2>. *Enhanced abundance of magic number nuclei*,
<http://hyperphysics.phy-astr.gsu.edu/hbase/nuclear/shell2.html>.
- [68] Bibliography of Cold Fusion - Chemistry Dept., Aarhus University. <http://www.kemi.aau.dk/~db/fusion/fusion.html>.
- [69] C. Illert (1993), *ALCHEMY TODAY-Platonic Geometries in Nuclear Physics*, Volume 1. ISBN 0 949357 13 8, second edition. Science-Art Library.
- [70] H. J. Assenbaum, K. Langanke and C. Rolfs (1987), Z. Phys. A 327, 461.
- [71] C.A. Bertulani, V. Zelevinsky (2002), *Is the tetra-neutron a bound dineutron-dineutron molecule?*, J.Phys. G29, 2431-2437. arXiv:nucl-th/0212060.
- [72] F. M. Marquez *et al* (2003), Phys. Rev. C65, 044006.

- [73] Jed Rothwell(1996).
Some recent developments in cold fusion,
<http://ourworld.compuserve.com/homepages/JedRothwell/brieftec.htm>.
Report on The Second International Low Energy Nuclear Reactions Conference Holiday Inn, College Station, Texas, September 13-14, 1996.
<http://ourworld.compuserve.com/homepages/JedRothwell/ilenrc2s.htm>,
Review of the Sixth International Conference on Cold Fusion (ICCF6),
<http://ourworld.compuserve.com/homepages/JedRothwell/iccf6rev.htm>.
- [74] B. Dume (2005), "*Magic*" numbers remain magic, Physics Web. <http://physicsweb.org/articles/news/9/6/9/1>. (Si(14,28) is magic unstable nucleus.)
B. Ray (2005), *FSU researchers find 'magic' at the subatomic level*,
http://www.fsu.com/pages/2005/07/05/magic_subatomic.html. (Magic Number N=14.)
New Magic Number "16" Where Nuclei Exist Stably Discovered, <http://www.mext.go.jp/english/news/2000/06/s000606.html>.
A. Ozawa *et al* (2000), Phys. Rev. Lett.84, 5493. (Magic number N=16).
A. Ozawa *et al* (2001), *Observation of new proton and neutron magic numbers*, http://lbl.confex.com/lbl/2001/program/abstract_97.htm. (Magic numbers N=16,20,32.)
- [75] C. Rolfs *et al* (2006), *High-Z electron screening, the cases $^{50}\text{V}(p,n)^{50}\text{Cr}$ and $^{176}\text{Lu}(p,n)$* , J. Phys. G: Nuclear. Part Phys. 32 489. Eur. Phys. J. A 28, 251-252.
- [76] R. P. Taleyarkhan *et al* (2006), *Nuclear Emissions During Self-Nucleated Acoustic Cavitation*.
<http://adsabs.harvard.edu/abs/2006PhRvL..96c4301T>.
For material about sono-fusion see <http://members.nuvox.net/~on.jwclymer/snf/>.
- [77] Fleischmann, M., Pons, S. and Hawkins, M. (1989). *Electrochemically induced nuclear fusion of deuterium*, J. Electroanal. Chem., 261, 301. See also: *ibid*, 263, 187.

Condensed matter physics

- [78] F. Levy, I. Sheikin, B. Grenier, and A. D. Huxley (2005), *Magnetic Field-Induced Superconductivity in the Ferromagnet URhGe*. Science 26, August, 1343-1346.
See also P. Rogers (2005), *Critical breakthrough*. Physics Web. <http://physicsweb.org/articles/news/9/8/17>.

Cosmology and astrophysics

- [79] E. Cartlidge (2004), *Half the Universe is Missing*. a popular article about claimed identification of NPDs. New Scientist Vol 182, No 2463.

Chapter 9

Nuclear String Hypothesis

9.1 Introduction

Nuclear string hypothesis [23] is one of the most dramatic almost-predictions of TGD [5]. The hypothesis in its original form assumes that nucleons inside nucleus organize to closed nuclear strings with neighboring nuclei of the string connected by exotic meson bonds consisting of color magnetic flux tube with quark and anti-quark at its ends. The lengths of flux tubes correspond to the p-adic length scale of electron and therefore the mass scale of the exotic mesons is around 1 MeV in accordance with the general scale of nuclear binding energies. The long lengths of em flux tubes increase the distance between nucleons and reduce Coulomb repulsion. A fractally scaled up variant of ordinary QCD with respect to p-adic length scale would be in question and the usual wisdom about ordinary pions and other mesons as the origin of nuclear force would be simply wrong in TGD framework as the large mass scale of ordinary pion indeed suggests. The presence of exotic light mesons in nuclei has been proposed also by Illert [53] based on evidence for charge fractionization effects in nuclear decays.

9.1.1 $A > 4$ nuclei as nuclear strings consisting of $A \leq 4$ nuclei

In the sequel a more refined version of nuclear string hypothesis is developed.

1. The first refinement of the hypothesis is that ${}^4\text{He}$ nuclei and $A < 4$ nuclei and possibly also nucleons appear as basic building blocks of nuclear strings instead of nucleons which in turn can be regarded as strings of nucleons. Large number of stable lightest isotopes of form $A = 4n$ supports the hypothesis that the number of ${}^4\text{He}$ nuclei is maximal. One can hope that even also weak decay characteristics could be reduced to those for $A < 4$ nuclei using this hypothesis.
2. One can understand the behavior of nuclear binding energies surprisingly well from the assumptions that total *strong* binding energy associated with $A \leq 4$ building blocks is *additive* for nuclear strings and that the addition of neutrons tends to reduce Coulombic energy per string length by increasing the length of the nuclear string implying increase binding energy and stabilization of the nucleus. This picture does not explain the variation of binding energy per nucleon and its maximum appearing for ${}^{56}\text{Fe}$.
3. In TGD framework tetra-neutron [55, 54] is interpreted as a variant of alpha particle obtained by replacing two meson-like stringy bonds connecting neighboring nucleons of the nuclear string with their negatively charged variants [23]. For heavier nuclei tetra-neutron is needed as an additional building brick and the local maxima of binding energy E_B per nucleon as function of neutron number are consistent with the presence of tetra-neutrons. The additivity of magic numbers 2, 8, 20, 28, 50, 82, 126 predicted by nuclear string hypothesis is also consistent with experimental facts and new magic numbers are predicted [52, 58].

9.1.2 Bose-Einstein condensation of color bonds as a mechanism of nuclear binding

The attempt to understand the variation of the nuclear binding energy and its maximum for Fe leads to a quantitative model of nuclei lighter than Fe as color bound Bose-Einstein condensates of 4He nuclei or rather, of pion like colored states associated with color flux tubes connecting 4He nuclei. The crucial element of the model is that color contribution to the binding energy is proportional to n^2 where n is the number of color bonds. Fermi statistics explains the reduction of E_B for the nuclei heavier than Fe . Detailed estimate favors harmonic oscillator model over free nucleon model with oscillator strength having interpretation in terms of string tension.

Fractal scaling argument allows to understand 4He and lighter nuclei as strings formed from nucleons with nucleons bound together by color bonds. Three fractally scaled variants of QCD corresponding $A > 4$ nuclei, $A = 4$ nuclei and $A < 4$ nuclei are thus involved. The binding energies of also lighter nuclei are predicted surprisingly accurately by applying simple p-adic scaling to the parameters of model for the electromagnetic and color binding energies in heavier nuclei.

9.1.3 Giant dipole resonance as de-coherence of Bose-Einstein condensate of color bonds

Giant (dipole) resonances [28, 57, 33], and so called pygmy resonances [40, 41] interpreted in terms of de-coherence of the Bose-Einstein condensates associated with $A \leq 4$ nuclei and with the nuclear string formed from $A \leq 4$ nuclei provide a unique test for the model. The key observation is that the splitting of the Bose-Einstein condensate to pieces costs a precisely defined energy due to the n^2 dependence of the total binding energy. For 4He de-coherence the model predicts singlet line at 12.74 MeV and triplet (25.48, 27.30, 29.12) MeV at ~ 27 MeV spanning 4 MeV wide range which is of the same order as the width of the giant dipole resonance for nuclei with full shells.

The de-coherence at the level of nuclear string predicts 1 MeV wide bands 1.4 MeV above the basic lines. Bands decompose to lines with precisely predicted energies. Also these contribute to the width. The predictions are in a surprisingly good agreement with experimental values. The so called pygmy resonance appearing in neutron rich nuclei can be understood as a de-coherence for $A = 3$ nuclei. A doublet (7.520, 8.4600) MeV at ~ 8 MeV is predicted. At least the prediction for the position is correct.

9.1.4 Dark nuclear strings as analogs of as analogs of DNA-, RNA- and amino-acid sequences and baryonic realization of genetic code

One biological speculation [41] inspired by the dark matter hierarchy is that genetic code as well as DNA-, RNA- and amino-acid sequences should have representation in terms of dark nuclear strings. The model for dark baryons indeed leads to an identification of these analogs and the basic numbers of genetic code including also the numbers of aminoacids coded by a given number of codons are predicted correctly. Hence it seems that genetic code is universal rather than being an accidental outcome of the biological evolution.

9.2 Some variants of the nuclear string hypothesis

The basic assumptions of the nuclear string model could be made stronger in several testable ways. One can make several alternative hypothesis.

9.2.1 Could linking of nuclear strings give rise to heavier stable nuclei?

Nuclear strings (Z_1, N_1) and (Z_2, N_2) could link to form larger nuclei $(Z_1 + Z_2, N_1 + N_2)$. If one can neglect the interactions between linked nuclei, the properties of the resulting nuclei should be determined by those of composites. Linking should however be the confining interaction forbidding the decay of the stable composite. The objection against this option is that it is difficult to characterize the constraint that strings are not allowed to touch and there is no good reason forbidding the touching.

The basic prediction would be that if the nuclei (Z_1, N_1) and (Z_2, N_2) which are stable, very long-lived, or possess exceptionally large binding energy then also the nucleus $(Z_1 + Z_2, N_1 + N_2)$ has this

property. If the linked nuclear strings are essentially free then the expectation is that the half-life of a composite of unstable nuclei is that of the shorter lived nucleus. This kind of regularity would have been probably observed long time ago.

9.2.2 Nuclear strings as connected sums of shorter nuclear strings?

Nuclear strings can form connected sum of the shorter nuclear strings. Connected sum means that one deletes very short portions of nuclear string A and B and connects the resulting ends of string A and B together. In other words: A is inserted inside B or vice versa or A and B are cut to open strings and connected and closed again. This outcome would result when A and B touch each other at some point. If touching occurs at several points more complex fusion of nuclei to a larger nucleus to a composite occurs with piece of A followed by a piece of B followed... For this option there is a non-trivial interaction between strings and the properties of nuclei need not be simply additive but one might still hope that stable nuclei fuse to form stable nuclei. In particular, the prediction for the half-life based on binding by linking does not hold true anymore.

Classical picture would suggest that the two strings cannot rotate with respect to each other unless they correspond to rather simple symmetric configurations: this applies also to linked strings. If so then the relative angular momentum L of nuclear strings vanishes and total angular momentum J of the resulting nucleus satisfies $|J_1 - J_2| \leq J \leq J_1 + J_2$.

9.2.3 Is knotting of nuclear strings possible?

One can consider also the knotting of nuclear strings as a mechanism giving rise to exotic excitations of nuclear. Knots decompose to prime knots so that kind of prime nuclei identified in terms of prime knots might appear. Fractal thinking suggests an analogy with the poorly understood phenomenon of protein folding. It is known that proteins always end up to a unique highly folded configuration and one might think that also nuclear ground states correspond to unique configurations to which quantum system (also proteins would be such if dark matter is present) ends up via quantum tunnelling unlike classical system which would stick into some valley representing a state of higher energy. The spin glass degeneracy suggests an fractal landscape of ground state configurations characterized by knotting and possibly also linking.

9.3 Could nuclear strings be connected sums of alpha strings and lighter nuclear strings?

The attempt to kill the composite string model leads to a stronger formulation in which nuclear string consists of alpha particles plus a minimum number of lighter nuclei. To test the basic predictions of the model I have used the rather old tables of [47] for binding energies of stable and long-lived isotopes and more modern tables [51] for basic data about isotopes known recently.

9.3.1 Does the notion of elementary nucleus make sense?

The simplest formulation of the model assumes some minimal set of *stable* "elementary nuclei" from which more complex *stable* nuclei can be constructed.

1. If heavier nuclei are formed by *linking* then alpha particle ${}^4\text{He} = (Z, N) = (2, 2)$ suggests itself as the lightest stable composite allowing interpretation as a closed string. For connected sum option even single nucleon n or p can appear as a composite. This option turns out to be the more plausible one.
2. In the model based on linking ${}^6\text{Li} = (3, 3)$ and ${}^7\text{Li} = (3, 4)$ would also act as "elementary nuclei" as well as ${}^9\text{Be} = (4, 5)$ and ${}^{10}\text{Be} = (4, 6)$. For the model based on connected sum these nuclei might be regarded as composites ${}^6\text{Li} = (3, 3) = (2, 2) + (1, 1)$, ${}^7\text{Li} = (3, 4) = (2, 2) + (1, 2)$, ${}^9\text{Be} = (4, 5) = 2 \times (2, 2) + (0, 1)$ and ${}^{10}\text{Be} = (4, 6) = (2, 2) + 2 \times (1, 2)$. The study of binding energies supports the connected sum option.

3. ^{10}B has total nuclear spin $J = 3$ and $^{10}B = (5, 5) = (3, 3) + (2, 2) = {}^6Li + {}^4He$ makes sense if the composites can be in relative $L = 2$ state (6Li has $J = 1$ and 4He has $J = 0$). ^{11}B has $J = 3/2$ so that $^{11}B = (5, 6) = (3, 4) + (2, 2) = {}^7Li + {}^4He$ makes sense because 7Li has $J = 3/2$. For the model based on disjoint linking also ^{10}B would be also regarded as "elementary nucleus". This asymmetry disfavors the model based on linking.

9.3.2 Stable nuclei need not fuse to form stable nuclei

The question is whether the simplest model predicts stable nuclei which do not exist. In particular, are the linked 4He composites stable? The simplest case corresponds to ${}^8B = (4, 4) = {}^4He + {}^4He$ which is not stable against alpha decay. Thus stable nuclei need not fuse to form stable nuclei. On the other hand, the very instability against alpha decay suggests that 4B can be indeed regarded as composite of two alpha particles. A good explanation for the instability against alpha decay is the exceptionally large binding energy $E = 7.07$ MeV per nucleon of alpha particle. The fact that the binding energy per nucleon for 8Be is also exceptionally large and equal to 7.06 MeV $< E_B({}^4He)$ supports the interpretation as a composite of alpha particles.

For heavier nuclei binding energy per nucleon increases and has maximum 8.78 MeV for Fe. This encourages to consider the possibility that alpha particle acts as a fundamental composite of nuclear strings with minimum number of lighter isotopes guaranteeing correct neutron number. Indeed, the decomposition to a maximum number of alpha particles allows a qualitative understanding of binding energies assuming that additional contribution not larger than 1.8 MeV per nucleon is present.

The nuclei ${}^{12}C$, ${}^{16}O$, ${}^{20}Ne$, ${}^{24}Mg$, ${}^{28}Si$, ${}^{32}S$, ${}^{36}A$, and ${}^{40}Ca$ are lightest stable isotopes of form $(Z, Z) = n \times {}^4He$, $n = 3, \dots, 10$, for which E_B is larger than for 4He . For the first four nuclei E_B has a local maximum as function of N . For the remaining the maximum of E_B is obtained for $(Z, Z + 1)$. ${}^{44}Ti = (22, 22)$ does not exist as a long-lived isotope whereas ${}^{45}Ti$ does. The addition of neutron could increase E_B by increasing the length of nuclear string and thus reducing the Coulomb interaction energy per nucleon. This mechanism would provide an explanation also for neutron halos [68].

Also the fact that stable nuclei in general have $N \geq Z$ supports the view that $N = Z$ state corresponds to string consisting of alpha particles and that $N > Z$ states are obtained by adding something between. $N < Z$ states would necessarily contain at least one stable nucleus lighter than 4He with smaller binding energy. 3He is the only possible candidate as the only stable nucleus with $N < Z$. ($E_B({}^2H) = 1.11$ MeV and $E_B({}^3He) = 2.57$ MeV). Individual nucleons are also possible in principle but not favored. This together with increase of Coulomb interaction energy per nucleon due to the greater density of em charge per string length would explain their smaller binding energy and instability.

9.3.3 Formula for binding energy per nucleon as a test for the model

The study of 8B inspires the hypothesis that the total binding energy for the nucleus $(Z_1 + Z_2, N_1 + N_2)$ is in the first approximation the sum of total binding energies of composites so that one would have for the binding energy per nucleon the prediction

$$E_B = \frac{A_1}{A_1 + A_2} \times E_{B_1} + \frac{A_2}{A_1 + A_2} \times E_{B_2}$$

in the case of 2-nucleus composite. The generalization to N-nucleus composite would be

$$E_B = \sum_k \frac{A_k}{\sum_r A_r} \times E_{B_k} .$$

This prediction would apply also to the unstable composites. The increase of binding energy with the increase of nuclear weight indeed suggests a decomposition of nuclear string to a sequence alpha strings plus some minimum number of shorter strings.

The first objection is that for both Li , B , and Be which all having two stable isotopes, the lighter stable isotope has a slightly smaller binding energy contrary to the expectation based on additivity of the total binding energy. This can be however understood in terms of the reduction of Coulomb energy per string length resulting in the addition of neutron (protons have larger average distance

along nuclear string along mediating the electric flux). The reduction of Coulomb energy per unit length of nuclear string could also partially explain why one has $E_B > E_B(^4He)$ for heavier nuclei.

The composition ${}^6Li = (3, 3) = (2, 2) + (1, 1)$ predicts $E_B \simeq 5.0$ MeV not too far from 5.3 MeV. The decomposition ${}^7Li = (3, 4) = (2, 2) + (1, 2)$ predicts $E_B = 5.2$ MeV to be compared with 5.6 MeV so that the agreement is satisfactory. The decomposition ${}^8Be = (4, 4) = 2 \times {}^4He$ predicts $E_B = 7.07$ MeV to be compared with the experimental value 7.06 MeV. 9Be and ${}^{10}Be$ have $E_B = 6.46$ MeV and $E_B = 6.50$ MeV. The fact that binding energy slightly increases in addition of neutron can be understood since the addition of neutrons to 8Be reduces the Coulomb interaction energy per unit length. Also neutron spin pairing reduces E_B . The additive formula for E_B is satisfied with an accuracy better than 1 MeV also for ${}^{10}B$ and ${}^{11}B$.

9.3.4 Decay characteristics and binding energies as signatures of the decomposition of nuclear string

One might hope of reducing the weak decay characteristics to those of shortest unstable nuclear strings appearing in the decomposition. Alternatively, one could deduce the decomposition from the weak decay characteristics and binding energy using the previous formulas. The picture of nucleus as a string of alpha particles plus minimum number of lighter nuclei 3He having $E_B = 2.57$ MeV, 3H unstable against beta decay with half-life of 12.26 years and having $E_B = 2.83$ MeV, and 2H having $E_B = 1.1$ MeV gives hopes of modelling weak decays in terms of decays for these light composites.

1. β^- decay could be seen as a signature for the presence of 3H string and alpha decay as a signature for the presence of 4He string.
2. β^+ decay might be interpreted as a signature for the presence of 3He string which decays to 3H (the mass of 3H is only .018 MeV higher than that of 3He). For instance, ${}^8B = (5, 3) = (3, 2) + (2, 1) = {}^5Li + {}^3He$ suffers β^+ decay to ${}^8Be = (4, 4)$ which in turn decays by alpha emission which suggests the re-arrangement to $(3, 2) + (1, 2) \rightarrow (2, 2) + (2, 2)$ maximizing binding energy.
3. Also individual nucleons can appear in the decomposition and give rise to β^- and possible also β^+ decays.

9.3.5 Are magic numbers additive?

The magic numbers 2, 8, 20, 28, 50, 82, 126 [52] for protons and neutrons are usually regarded as a support for the harmonic oscillator model. There are also other possible explanations for magic nuclei and there are deviations from the naive predictions. One can also consider several different criteria for what it is to be magic. Binding energy is the most natural criterion but need not always mean stability. For instance ${}^8B = (4, 4) = {}^4He + {}^4He$ has high binding energy but is unstable against alpha decay.

Nuclear string model suggests that the fusion of magic nuclear strings by connected sum yields new kind of highly stable nuclei so that also $(Z_1 + Z_2, N_1 + N_2)$ is a magic nucleus if (Z_i, N_i) is such. One has $N = 28 = 20 + 8$, $50 = 28 + 20 + 2$, and $N = 82 = 50 + 28 + 2 \times 2$. Also other magic numbers are predicted. There is evidence for them [58].

1. ${}^{16}O = (8, 8)$ and ${}^{40}Ca = (20, 20)$ corresponds to doubly magic nuclei and ${}^{60}Ni = (28, 32) = (20, 20) + (8, 8) + {}^4n$ has a local maximum of binding energy as function of neutron number. This is not true for ${}^{56}Ni$ so that the idea of magic nucleus in neutron sector is not supported by this case. The explanation would be in terms of the reduction of E_B due to the reduction of Coulomb energy per string length as neutrons are added.
2. Also ${}^{80}Kr = (36, 44) = (36, 36) + {}^4n = (20, 20) + (8, 8) + (8, 8) + {}^4n$ corresponds to a local maximum of binding energy per nucleon as also does ${}^{84}Kr = {}^{80}Kr + {}^4n$ containing two tetra-neutrons. Note however that ${}^{88}Zr = (40, 48)$ is not a stable isotope although it can be regarded as a composite of doubly magic nucleus and of two tetra-neutrons.

9.3.6 Stable nuclei as composites of lighter nuclei and necessity of tetra-neutron?

The obvious test is to look whether stable nuclei can be constructed as composites of lighter ones. In particular, one can check whether tetra-neutron 4n interpreted as a variant of alpha particle obtained by replacing two meson-like stringy bonds connecting neighboring nucleons of the nuclear string with their negatively charged variants is necessary for the understanding of heavier nuclei.

1. ${}^{48}Ca = (20, 28)$ with half-life $> 2 \times 10^{16}$ years has neutron excess of 8 units and the only reasonable interpretation seems to be as a composite of the lightest stable Ca isotope $Ca(20, 20)$, which is doubly magic nucleus and two tetra-neutrons: ${}^{48}Ca = (20, 28) = {}^{40}Ca + 2 \times {}^4n$.
2. The next problematic nucleus is ${}^{49}Ti$.
 - i) ${}^{49}Ti = (22, 27)$ having neutron excess of 5 one cannot be expressed as a composite of lighter nuclei unless one assumes non-vanishing and large relative angular momentum for the composites. For ${}^{50}Ti = (22, 28)$ no decomposition can be found. The presence of tetra-neutron would reduce the situation to ${}^{49}Ti = (22, 27) = {}^{45}Ti + {}^4n$. Note that ${}^{45}Ti$ is the lightest Ti isotope with relatively long half-life of 3.10 hours so that the addition of tetra-neutron would stabilize the system since Coulomb energy per length of string would be reduced.
 - ii) ${}^{48}Ti$ could not involve tetra-neutron by this criterion. It indeed allows decomposition to standard nuclei is also possible as ${}^{48}Ti = (22, 26) = {}^{41}K + {}^7Li$.
 - iii) The heaviest stable Ti isotope would have the decomposition ${}^{50}Ti = {}^{46}Ti + {}^4n$, where ${}^{46}Ti$ is the lightest stable Ti isotope.
3. The heavier stable nuclei ${}^{50+k}V = (23, 27 + k)$, $k = 0, 1$, ${}^{52+k}Cr = (24, 28 + k)$, $k = 0, 1, 2$, ${}^{55}Mn = (25, 30)$ and ${}^{56+k}Fe = (26, 30 + k)$, $k = 0, 1, 2$ would have similar interpretation. The stable isotopes ${}^{50}Cr = (24, 26)$ and ${}^{54}Fe = (26, 28)$ would not contain tetra-neutron. Also for heavier nuclei both kinds of stable states appear and tetra-neutron would explain this.
4. ${}^{112}Sn = (50, 62) = (50, 50) + 3 \times {}^4n$, ${}^{116}Sn$, ${}^{120}Sn$, and ${}^{124}Sn$ are local maxima of E_B as a function of neutron number and the interpretation in terms of tetra-neutrons looks rather natural. Note that $Z = 50$ is a magic number.

Nuclear string model looks surprisingly promising and it would be interesting to compare systematically the predictions for E_B with its actual values and look whether the beta decays could be understood in terms of those of composites lighter than 4He .

9.3.7 What are the building blocks of nuclear strings?

One can also consider several options for the more detailed structure of nuclear strings. The original model assumed that proton and neutron are basic building blocks but this model is too simple.

Option Ia)

A more detailed work in attempt to understand binding energies led to the idea that there is fractal structure involved. At the highest level the building blocks of nuclear strings are $A \leq 4$ nuclei. These nuclei in turn would be constructed as short nuclear strings of ordinary nucleons.

The basic objection against the model is the experimental absence of stable $n - n$ bound state analogous to deuteron favored by lacking Coulomb repulsion and attractive electromagnetic spin-spin interaction in spin 1 state. Same applies to tri-neutron states and possibly also tetra-neutron state. There has been however speculation about the existence of di-neutron and poly-neutron states [48, 34].

The standard explanation is that strong force couples to strong isospin and that the repulsive strong force in nn and pp states makes bound states of this kind impossible. This force, if really present, should correspond to shorter length scale than the isospin independent forces in the model under consideration. In space-time description these forces would correspond to forces mediated between nucleons along the space-time sheet of the nucleus whereas exotic color forces would be mediated along the color magnetic flux tubes having much longer length scale. Even for this option one cannot exclude exotic di-neutron obtained from deuteron by allowing color bond to carry negative em charge.

Since em charges 0, 1, -1 are possible for color bonds, a nucleus with mass number $A > 2$ extends to a multiplet containing $3A$ exotic charge states.

Option Ib)

One might ask whether it is possible to get rid of isospin dependent strong forces and exotic charge states in the proposed framework. One can indeed consider also other explanations for the absence of genuine poly-neutrons.

1. The formation of negatively charged bonds with neutrons replaced by protons would minimize both nuclear mass and Coulomb energy although binding energy per nucleon would be reduced and the increase of neutron number in heavy nuclei would be only apparent.
2. The strongest hypothesis is that mass minimization forces protons and negatively charged color bonds to serve as the basic building bricks of all nuclei. If this were the case, deuteron would be a di-proton having negatively charged color bond. The total binding energy would be only $2.222 - 1.293 = .9290$ MeV. Di-neutron would be impossible for this option since only one color bond can be present in this state.

The small mass difference $m(^3He) - m(^3H) = .018$ MeV would have a natural interpretation as Coulomb interaction energy. Tri-neutron would be allowed. Alpha particle would consist of four protons and two negatively charged color bonds and the actual binding energy per nucleon would be by $(m_n - m_p)/2$ smaller than believed. Tetra-neutron would also consist of four protons and the binding energy per nucleon would be smaller by $m_n - m_p$ than what obtains in the standard model of nucleus. Beta decays would be basically beta decays of exotic quarks associated with color bonds.

Note that the mere assumption that the di-neutrons appearing inside nuclei have protons as building bricks means a rather large apparent binding energy this might explain why di-neutrons have not been detected. An interesting question is whether also higher n-deuteron states than 4He consisting of strings of deuteron nuclei and other $A \leq 3$ nuclei could exist and play some role in the nuclear physics of $Z \neq N$ nuclei.

If protons are the basic building bricks, the binding energy per nucleon is replaced in the calculations with its actual value

$$E_B \rightarrow E_B - \frac{N}{A} \Delta m \quad , \quad \Delta m = m_n - m_p = 1.2930 \text{ MeV} \quad . \quad (9.3.1)$$

This replacement does not affect at all the parameters of the of $Z = 2n$ nuclei identified as 4He strings.

One can of course consider also the option that nuclei containing ordinary neutrons are possible but that are unstable against beta decay to nuclei containing only protons and negatively charged bonds. This would suggest that di-neutron exists but is not appreciably produced in nuclear reactions and has not been therefore detected.

Options IIa) and IIb)

It is not clear whether the fermions at the ends of color bonds are exotic quarks or leptons. Lepto-pion (or electro-pion) hypothesis [24] was inspired by the anomalous e^+e^- production in heavy ion collisions near Coulomb wall and states that electro-pions which are bound states of colored excitations of electrons with ground state mass 1.062 MeV are responsible for the effect. The model predicts that also other charged leptons have color excitations and give rise to exotic counterpart of QCD.

Also μ and τ should possess colored excitations. About fifteen years after this prediction was made, direct experimental evidence for these states finally emerges [43, 44]. The mass of the new particle, which is either scalar or pseudoscalar, is 214.4 MeV whereas muon mass is 105.6 MeV. The mass is about 1.5 per cent higher than two times muon mass. The most natural TGD inspired interpretation is as a pion like bound state of colored excitations of muon completely analogous to lepto-pion (or rather, electro-pion) [24].

One cannot exclude the possibility that the fermion and anti-fermion at the ends of color flux tubes connecting nucleons are actually colored leptons although the working hypothesis is that they

are exotic quark and anti-quark. One can of course also turn around the argument: could it be that lepto-pions are "leptonuclei", that is bound states of ordinary leptons bound by color flux tubes for a QCD in length scale considerably shorter than the p-adic length scale of lepton.

Scaling argument applied to ordinary pion mass suggests that the masses of exotic quarks at the ends of color bonds are considerably below MeV scale. One can however consider the possibility that colored electrons with mass of ordinary electron are in question in which case color bonds identifiable as colored variants of electro-pions could be assumed to contribute in the first guess the mass $m(\pi) = 1.062$ MeV per each nucleon for $A > 2$ nuclei. This implies the general replacement

$$\begin{aligned} E_B &\rightarrow E_B + m(\pi_L) - \frac{N}{A} \Delta m \text{ for } A > 2, \\ E_B &\rightarrow E_B + \frac{m(\pi_L)}{2} - \frac{N}{A} \Delta m \text{ for } A = 2. \end{aligned} \quad (9.3.1)$$

This option will be referred to as option IIb). One can also consider the option IIa) in which nucleons are ordinary but lepto-pion mass $m(\pi_L) = 1.062$ MeV gives the mass associated with color bond.

These options are equivalent for $N = Z = 2n$ nuclei with $A > 4$ but for $A \leq 4$ nuclei assumed to form nucleon string they options differ.

9.4 Light nuclei as color bound Bose-Einstein condensates of 4He nuclei

The attempt to understand the variation of nuclear binding energy and its maximum for Fe leads to a model of nuclei lighter than Fe as color bound Bose-Einstein condensates of 4He nuclei or meson-like structures associated with them. Fractal scaling argument allows to understand 4He itself as analogous state formed from nucleons.

9.4.1 How to explain the maximum of E_B for iron?

The simplest model predicts that the binding energy per nucleon equals to $E_B({}^4He)$ for all $Z = N = 2n$ nuclei. The actual binding energy grows slowly, has a maximum at ${}^{52}Fe$, and then begins to decrease but remains above $E_B({}^4He)$. The following values give representative examples for $Z = N$ nuclei.

nucleus	4He	8Be	${}^{40}Ca$	${}^{52}Fe$
E_B/MeV	7.0720	7.0603	8.5504	8.6104

For nuclei heavier than Fe there are no long-lived $Z = N = 2n$ isotopes and the natural reason would be alpha decay to ${}^{52}Fe$. If tetra-neutron is what TGD suggests it to be one can guess that tetra-neutron mass is very nearly equal to the mass of the alpha particle. This would allow to regard states $N = Z + 4n$ as states as analogous to unstable states $N_1 = Z_1 = Z + 2n$ consisting of alpha particles. This gives estimate for E_B for unstable $N = Z$ states. For ${}^{256}Fm = (100, 156)$ one has $E_B = 7.433$ MeV which is still above $E_B({}^4He) = 7.0720$ MeV. The challenge is to understand the variation of the binding energy per nucleon and its maximum for Fe .

9.4.2 Scaled up QCD with Bose-Einstein condensate of 4He nuclei explains the growth of E_B

The first thing to come in mind is that repulsive Coulomb contribution would cause the variation of the binding energy. Since alpha particles are building blocks for $Z = N$ nuclei, 8Be provides a test for this idea. If the difference between binding energies per nucleon for 8Be and 4He were due to Coulomb repulsion alone, one would have $E_c = E_B({}^4He) - E_B({}^8Be) = .0117$ MeV, which is of order $\alpha_{em}/L(127)$. This would conform with the idea that flux tubes mediating em interaction have length of order electron Compton length. Long flux tubes would provide the mechanism minimizing Coulomb energy. A more realistic interpretation consistent with this mechanism would be that Coulombic and

color interaction energies compensate each other: this can of course occur to some degree but it seems safe to assume that Coulomb contribution is small.

The basic question is how one could understand the behavior of E_B if its variation corresponds to that for color binding energy per nucleon. The natural scale of energy is MeV and this conforms with the fact that the range of variation for color binding energy associated with $L(127)$ QCD is about 1.5 MeV. By a naive scaling the value of M_{127} pion mass is by a factor $2^{(127-107)/2} = 10^{-3}$ times smaller than that of ordinary pion and thus .14 MeV. The scaling of QCD Λ is a more reliable estimate for the binding energy scale and gives a slightly larger value but of the same order of magnitude. The total variation of E_B is large in the natural energy scale of M_{127} QCD and suggests strong non-linear effects.

In the absence of other contributions em and color contributions to E_B cancel for 8Be . If color and Coulomb contributions on total binding energy depend roughly linearly on the number of 4He nuclei, the cancellation to E_B should occur in a good approximation also for them. This does not happen which means that color contribution to E_B is in lowest approximation linear in n meaning n^2 -dependence of the total color binding energy. This non-linear behavior suggests strongly the presence of Bose-Einstein condensate of 4He nuclei or structures associated with them. The most natural candidates are the meson like colored strings connecting 4He nuclei together.

The additivity of n color magnetic (and/or electric) fluxes would imply that classical field energy is n^2 -fold. This does not yet imply same for binding energy unless the value of α_s is negative which it can be below confinement length scale. An alternative interpretation could be in terms of color magnetic interaction energy. The number of quarks and anti-quarks would be proportional to n as would be also the color magnetic flux so that n^2 -proportionality would result also in this manner.

If the addition of single alpha particle corresponds to an addition of a constant color contribution E_s to E_B (the color binding energy per nucleon, not the total binding energy!) one has $E_B({}^{52}Fe) = E_B({}^4He) + 13E_s$ giving $E_s = .1834$ MeV, which conforms with the order of magnitude estimate given by M_{127} QCD.

The task is to find whether this picture could explain the behavior of E_B . The simplest formula for $E_B(Z = N = 2n)$ would be given by

$$E_B(n) = -\frac{n(n-1)}{L(A)n}k_s + nE_s . \quad (9.4.1)$$

Here the first term corresponds to the Coulomb interaction energy of n 4He nuclei proportional to $n(n-1)$ and inversely proportional to the length $L(A)$ of nuclear string. Second term is color binding energy per nucleon proportional to n .

The simplest assumption is that each 4He corresponds always to same length of nuclear string so that one has $L \propto A$ and one can write

$$E_B(n) = E_B({}^4He) - \frac{n(n-1)}{n^2}E_c + nE_s . \quad (9.4.2)$$

The value of $E_B({}^8Be) \simeq E_B({}^4He)$ ($n = 2$) gives for the unit of Coulomb energy

$$E_c = 4E_s + 2[E_B({}^4He) - E_B({}^8Be)] \simeq 4E_s . \quad (9.4.3)$$

The general formula for the binding energy reads as

$$\begin{aligned} E_B(n) &= E_B({}^4He) - 2\frac{n(n-1)}{n^2}[E_B({}^4He) - E_B({}^8Be)] \\ &+ [-4\frac{n(n-1)}{n^2} + n]E_s . \end{aligned} \quad (9.4.3)$$

The condition that $E_B({}^{52}Fe)$ ($n = 13$) comes out correctly gives

$$E_s = \frac{13}{121}(E_B({}^{52}Fe) - E_B({}^4He)) + \frac{13 \times 24}{121}[E_B({}^4He) - E_B({}^8Be)] . \quad (9.4.4)$$

This gives $E_s \simeq .1955$ MeV which conforms with M_{127} QCD estimate. For the E_c one obtains $E_c = 1.6104$ MeV and for Coulomb energy of ${}^4\text{He}$ nuclei in ${}^8\text{Be}$ one obtains $E = E_c/2 = .8052$ MeV. The order of magnitude is consistent with the mass difference of proton and neutron. The scale suggests that electromagnetic flux tubes are shorter than color flux tubes and correspond to the secondary p-adic length scale $L(2, 61) = L(127)/2^{5/2}$ associated with Mersenne prime M_{61} . The scaling factor for the energy scale would be $2^{5/2} \simeq 5.657$.

The calculations have been carried out without assuming which are actual composites of ${}^4\text{He}$ nuclei (neutrons and protons plus neutral color bonds or protons and neutral and negatively charged color bonds) and assuming the masses of color bonds are negligible. As a matter fact, the mass of color bond does not affect the estimates if one uses only nuclei heavier than ${}^4\text{He}$ to estimate the parameters. The estimates above however involve ${}^4\text{He}$ so that small change on the parameters is induced.

9.4.3 Why E_B decreases for heavier nuclei?

The prediction that E_B increases as $(A/4)^2$ for $Z = N$ nuclei is unrealistic since E_B decreases slowly for $A \geq 52$ nuclei. Fermi statistics provides a convincing explanation assuming that fermions move in an effective harmonic oscillator potential due to the string tension whereas free nucleon model predicts too large size for the nucleus. The splitting of the Bose-Einstein condensate to pieces is second explanation that one can imagine but fails at the level of details.

Fermi statistics as a reason for the reduction of the binding energy

The failure of the model is at least partially due to the neglect of the Fermi statistics. For the lighter nuclei description as many boson state with few fermions is expected to work. As the length of nuclear string grows in fixed nuclear volume, the probability of self intersection increases and Fermi statistics forces the wave function for stringy configurations to wiggle which reduces binding energy.

1. For the estimation purposes consider $A = 256$ nucleus ${}^{256}\text{Mv}$ having $Z = 101$ and $E_B = 7.4241$ MeV. Assume that this unstable nucleus is nearly equivalent with a nucleus consisting of $n = 64$ ${}^4\text{He}$ nuclei ($Z = N$). Assuming single color condensate this would give the color contribution

$$E_s^{tot} = (Z/2)^2 \times E_s = 64^2 \times E_s$$

with color contribution to E_B equal to $(Z/2)E_s \simeq 12.51$ MeV.

2. Suppose that color binding energy is canceled by the energy of nucleon identified as kinetic energy in the case of free nucleon model and as harmonic oscillator energy in the case of harmonic oscillator model.
3. The number of states with a given principal quantum number n for both free nucleons in a spherical box and harmonic oscillator model is by spherical symmetry $2n^2$ and the number of protons/neutrons for a full shell nuclei behaves as $N_1 \simeq 2n_{max}^3/3$. The estimate for the average energy per nucleon is given in the two cases as

$$\begin{aligned} \langle E \rangle_H &= 2^{-4/3} \times N^{1/3} E_0, \quad E_0 = \omega_0, \\ \langle E \rangle_F &= \frac{2}{5} \left(\frac{3}{2}\right)^{5/3} N^{2/3} E_0, \quad E_0 = \frac{\pi^2}{2m_p L^2}. \end{aligned} \quad (9.4.3)$$

Harmonic oscillator energy $\langle E \rangle_H$ increases as $N^{1/3}$ and $\langle E \rangle_F$ as $N^{2/3}$. Neither of these cannot win the contribution of the color binding energy increasing as N .

4. Equating this energy with the total color binding energy gives an estimate for E_0 as

$$\begin{aligned}
E_0 &= (2/3)^{1/3} \times Z^{-4/3} \times (Z/2)^2 \times E_s , \\
E_0 &= \frac{5}{4} \left(\frac{2}{3}\right)^{5/3} \times Z^{-5/3} \times (Z/2)^2 \times E_s , \\
E_s &= .1955 \text{ MeV} .
\end{aligned} \tag{9.4.2}$$

The first case corresponds to harmonic oscillator model and second to free nucleon model.

5. For the harmonic oscillator model one obtains the estimate $E_0 = \hbar\omega_0 \simeq 2.73 \text{ MeV}$. The general estimate for the energy scale in the harmonic oscillator model given by $\omega_0 \simeq 41 \cdot A^{-1/3} \text{ MeV}$ [36] giving $\omega_0 = 6.5 \text{ MeV}$ for $A = 256$ (this estimate implies that harmonic oscillator energy per nucleon is approximately constant and would suggest that string tension tends to reduce as the length of string increases). Harmonic oscillator potential would have roughly twice too strong strength but the order of magnitude is correct. Color contribution to the binding energy might relate the reduction of the oscillator strength in TGD framework.
6. Free nucleon model gives the estimate $E_0 = .0626 \text{ MeV}$. For the size of a $A = 256$ nucleus one obtains $L \simeq 3.8L(113) \simeq 76 \text{ fm}$. This is by one order of magnitude larger than the size predicted by the standard formula $r = r_0 A^{1/3}$, $r_0 = 1.25 \text{ fm}$ and 8 fm for $A = 256$.

Harmonic oscillator picture is clearly favored and string tension explains the origin of the harmonic oscillator potential. Harmonic oscillator picture is expected to emerge at the limit of heavy nuclei for which nuclear string more or less fills the nuclear volume whereas for light nuclei the description in terms of bosonic 4He nuclei should make sense. For heavy nuclei Fermi statistics at nuclear level would begin to be visible and excite vibrational modes of the nuclear string mapped to the excited states of harmonic oscillator in the shell model description.

Could upper limit for the size of 4He Bose-Einstein condensate explain the maximum of binding energy per nucleon?

One can imagine also an alternative explanation for why E_B to decrease after $A = 52$. One might that $A = 52$ represents the largest 4He Bose-Einstein condensate and that for heavier nuclei Bose-Einstein condensate de-coheres into two parts. Bose-Einstein condensate of $n = 13$ 4He nuclei would be the best that one can achieve.

This could explain the reduction of the binding energy and also the emergence of tetra-neutrons as well as the instability of $Z = N$ nuclei heavier than ${}^{52}Fe$. A number theoretical interpretation related to the p-adic length scale hypothesis suggests also itself: as the size of the tangled nuclear string becomes larger than the next p-adic length scale, Bose-Einstein condensate might lose its coherence and split into two.

If one assumes that 4He Bose-Einstein condensate has an upper size corresponding to $n = 13$, the prediction is that after $A = 52$ second Bose-Einstein condensate begins to form. E_B is obtained as the average

$$E_B(Z, N) = \frac{52}{A} E_B({}^{52}Fe) + \frac{A - 52}{A} E_B({}^{A-52}X(Z, N)) .$$

The derivative

$$dE_B/dA = (52/A)[-E_B({}^{52}Fe) + E_B({}^{A-52}X)] + \frac{A - 52}{A} dE_B({}^{A-52}X(Z, N))/dA$$

is first negative but its sign must change since the nuclei consisting of two copies of ${}^{52}Fe$ condensates have same E_B as ${}^{52}Fe$. This is an un-physical result. This does not exclude the splitting of Bose-Einstein condensate but the dominant contribution to the reduction of E_B must be due to Fermi statistics.

9.5 What QCD binds nucleons to $A \leq 4$ nuclei?

The obvious question is whether scaled variant(s) of color force could bind nucleons to form $A \leq 4$ nuclei which in turn bind to form heavier nuclei. Since the binding energy scale for ${}^3\text{He}$ is much smaller than for ${}^4\text{He}$ one might consider the possibility that the p-adic length scale for QCD associated with ${}^4\text{He}$ is different from that for $A < 4$ nuclei.

9.5.1 The QCD associated with nuclei lighter than ${}^4\text{He}$

It would be nice if one could understand the binding energies of also $A \leq 4$ nuclei in terms of a scaled variant of QCD applied at the level of nucleons. Here one has several options to test.

Various options to consider

Assume that neutral color bonds have negligible fermion masses at their ends: this is expected if the exotic quarks appear at the ends of color bonds and by the naive scaling of pion mass. One can also consider the possibility that the p-adic temperature for the quarks satisfies $T = 1/n \leq 1/2$ so that quarks would be massless in excellent approximation. $T = 1/n < 1$ holds true for gauge bosons and one might argue that color bonds as bosonic particles indeed have $T < 1$.

Option Ia): Building bricks are ordinary nucleons.

Option IIa): Building blocks are protons and neutral and negatively charged color bonds. This means the replacement $E_B \rightarrow E_B - \Delta m$ for $A > 2$ nuclei and $E_B \rightarrow E_B - \Delta m/2$ for $A = 2$ with $\Delta m = n_n - m_p = 1.2930$ MeV.

Options Ib and IIb are obtained by assuming that the masses of fermions at the ends of color bonds are non-negligible. Electro-pion mass $m(\pi_L) = 1.062$ MeV is a good candidate for the mass of the color bond. Option Ia allow 3 per cent accuracy for the predicted binding energies. Option IIb works satisfactorily but the errors are below 22 per cent only.

Ordinary nucleons and massless color bonds

It turns out that for the option Ia), ordinary nucleons and massless color bonds, is the most plausible candidate for $A < 4$ QCD is the secondary p-adic length scale $L(2, 59)$ associated with prime $p \simeq 2^k$, $k = 59$ with $k_{eff} = 2 \times 59 = 118$. The proper scaling of the electromagnetic p-adic length scale corresponds to a scaling factor 2^3 meaning that one has $k_{eff} = 122 \rightarrow k_{eff} - 6 = 116 = 4 \times 29$ corresponding to $L(4, 29)$.

1. Direct p-adic scaling of the parameters

E_s would be scaled up p-adically by a factor $2^{(127-118)/2} = 2^{9/2}$. E_c would be scaled up by a factor $2^{(122-116)/2} = 2^3$. There is also a scaling of E_c by a factor $1/4$ due to the reduction of charge unit and scaling of both E_c and E_s by a factor $1/4$ since the basic units are now nucleons. This gives

$$\hat{E}_s = 2^{5/2} E_s = 1.1056 \text{ MeV} , \quad \hat{E}_c = 2^{-1} E_c = .8056 \text{ MeV} . \quad (9.5.1)$$

The value of electromagnetic energy unit is quite reasonable.

The basic formula for the binding energy reads now

$$E_B = -\frac{(n(p)(n(p)-1))}{A^2} \hat{E}_c + n \hat{E}_s , \quad (9.5.2)$$

where $n(p)$ is the number of protons $n = A$ holds true for $A > 2$. For deuteron one has $n = 1$ since deuteron has only single color bond. This delicacy is a crucial prediction and the model fails to work without it.

This gives

$$E_B({}^2\text{H}) = \hat{E}_s , \quad E_B({}^3\text{H}) = 3\hat{E}_s , \quad E_B({}^3\text{He}) = -\frac{2}{9} \hat{E}_c + 3\hat{E}_s . \quad (9.5.2)$$

The predictions are given by the third row of the table below. The predicted values given are too large by about 15 per cent in the worst case.

The reduction of the value of α_s in the p-adic scaling would improve the situation. The requirement that $E_B(^3H)$ comes out correctly predicts a reduction factor .8520 for α_s . The predictions are given in the fourth row of the table below. Errors are below 15 per cent.

nucleus	2H	3H	3He
$E_B(exp)/MeV$	1.111	2.826	2.572
$E_B(pred_1)/MeV$	1.106	3.317	3.138
$E_B(pred_2)/MeV$.942	2.826	2.647

The discrepancy is 15 per cent for 2H . By a small scaling of E_c the fit for 3He can be made perfect. Agreement is rather good but requires that conventional strong force transmitted along nuclear space-time sheet is present and makes nn and pp states unstable. Isospin dependent strong interaction energy would be only .17 MeV in isospin singlet state which suggests that a large cancelation between scalar and vector contributions occurs. pnn and ppn could be regarded as Dn and Dp states with no strong force between D and nucleon. The contribution of isospin dependent strong force to E_B is scaled down by a factor 2/3 in $A = 3$ states from that for deuteron and is almost negligible. This option seems to allow an almost perfect fit of the binding energies. Note that one cannot exclude exotic nn-state obtained from deuteron by giving color bond negative em charge.

Other options

Consider next other options.

1. Option IIb

For option IIb) the basic building bricks are protons and $m(\pi) = 1.062$ is assumed. The basic objection against this option is that for protons as constituents *real* binding energies satisfy $E_B(^3He) < E_B(^3H)$ whereas Coulombic repulsion would suggest $E_B(^3He) > E_B(^3H)$ unless magnetic spin-spin interaction effects affect the situation. One can however look how good a fit one can obtain in this manner.

As found, the predictions of direct scaling are too large for $E_B(^3H)$ and $E_B(^3He)$ (slight reduction of α_s cures the situation). Since the actual binding energy increases by $m(\pi_L) - (2/3)(m_n - m_p)$ for 3H and by $m(\pi_L) - (1/3)(m_n - m_p)$ for 3He , it is clear that the assumption that lepto-pion mass is of order 1 MeV improves the fit. The results are given by the table below.

nucleus	2H	3H	3He
$E_B(exp)/MeV$	1.111	2.826	2.572
$E_B(pred)/MeV$.875	3.117	2.507

Here $E_B(pred)$ corresponds to the effective value of binding energy assuming that nuclei effectively consist of ordinary protons and neutrons. The discrepancies are below 22 percent.

What is troublesome that neither the scaling of α_s nor modification of E_c improves the situation for 2H and 3H . Moreover, magnetic spin-spin interaction energy for deuteron is expected to reduce $E_B(pred)$ further in triplet state. Thus option IIb) does not look promising.

2. Option Ib)

For option Ib) with $m(\pi) = 1.062$ MeV and ordinary nucleons the actual binding $E_B(act)$ energy increases by $m(\pi)$ for $A = 3$ nuclei and by $m(\pi)/2$ for deuteron. Direct scaling gives a reasonably good fit for the p-adic length scale $L(9, 13)$ with $k_{eff} = 117$ meaning $\sqrt{2}$ scaling of E_s . For deuteron the predicted E_B is too low by 30 per cent. One might argue that isospin dependent strong force between nucleons becomes important in this p-adic length scale and reduces deuteron binding energy by 30 per cent. This option is not un-necessary complex as compared to the option Ia).

nucleus	2H	3H	3He
$E_B(act)/MeV$	1.642	3.880	3.634
$E_B(pred)/MeV$	1.3322	3.997	3.743

For option IIa) with $m(\pi) = 0$ and protons as building blocks the fit gets worse for $A = 3$ nuclei.

9.5.2 The QCD associated with 4He

4He must somehow differ from $A \leq 3$ nucleons. If one takes the argument based on isospin dependence strong force seriously, the reasonable looking conclusion would be that 4He is at the space-time sheet of nucleons a bound state of two deuterons which induce no isospin dependent strong nuclear force. One could regard the system also as a closed string of four nucleons such that neighboring p and n form strong iso-spin singlets. The previous treatment applies as such.

For 4He option Ia) with a direct scaling would predict $E_B({}^4He) < 4 \times \hat{E}_s = 3.720$ MeV which is by a factor of order 2 too small. The natural explanation would be that for 4He both color and em field body correspond to the p-adic length scale $L(4, 29)$ ($k_{eff} = 116$) so that E_s would increase by a factor of 2 to 1.860 MeV. Somewhat surprisingly, $A \leq 3$ nuclei would have "color field bodies" by a factor 2 larger than 4He .

1. For option Ia) this would predict $E_B({}^4He) = 7.32867$ MeV to be compared with the real value 7.0720 MeV. A reduction of α_s by 3.5 per cent would explain the discrepancy. That α_s decreases in the transition sequence $k_{eff} = 127 \rightarrow 118 \rightarrow 116$ which is consistent with the general vision about evolution of color coupling strength.
2. If one assumes option Ib) with $m(\pi) = 1.062$ MeV the actual binding energy increases to 8.13 MeV. The strong binding energy of deuteron units would give an additional .15 MeV binding energy per nucleon so that one would have $E_B({}^4He) = 7.47$ MeV so that 10 per cent accuracy is achieved. Obviously this option does not work so well as Ia).
3. If one assumes option IIb), the actual binding energy would increase by .415 MeV to 7.4827 MeV which would make fit somewhat poorer. A small reduction of E_c could allow to achieve a perfect fit.

9.5.3 What about tetra-neutron?

One can estimate the value of $E_B({}^4n)$ from binding energies of nuclei (Z, N) and $(Z, N+4)$ ($A = Z+N$) as

$$E_B({}^4n) = \frac{A+4}{4} [E_B(A+4) - \frac{A}{A+4} E_B(A)] .$$

In the table below there are some estimate for $E_B({}^4n)$.

(Z, N)	$(26,26)$ (${}^{52}Fe$)	$(50,70)$ (${}^{120}Sn$)	$(82,124)$ (${}^{206}Pb$)
$E_B({}^4n)/MeV$	6.280	7.3916	5.8031

The prediction of the above model would be $E({}^4n) = 4\hat{E}_s = 3.760$ MeV for $\hat{E}_s = .940$ MeV associated with $A < 4$ nuclei and $k_{eff} = 118 = 2 \times 59$ associated with $A < 4$ nuclei. For $k_{eff} = 116$ associated with 4He $E_s({}^4n) = E_s({}^4He) = 1.82$ MeV the prediction would be 7.28 MeV. 14 percent reduction of α_s would give the estimated value for of E_s for ${}^{52}Fe$.

If tetra-neutron is ppnn bound state with two negatively charged color bonds, this estimate is not quite correct since the actual binding energy per nucleon is $E_B({}^4He) - (m_n - m_p)/2$. This implies a small correction $E_B(A+4) \rightarrow E_B(A+4) - 2(m_n - m_p)/(A+4)$. The correction is negligible.

One can make also a direct estimate of 4n binding energy assuming tetra-neutron to be ppnn bound state. If the masses of charged color bonds do not differ appreciably from those of neutral bonds (as the p-adic scaling of $\pi + -\pi^0$ mass difference of about 4.9 MeV strongly suggests) then model Ia) with $E_s = E_B({}^3H)/3$ implies that the actual binding energy $E_B({}^4n) = 4E_s = E_B({}^3H)/3$ (see the table below). The apparent binding energy is $E_{B,app} = E_B({}^4n) + (m_n - m_p)/2$. Binding energy differs

dramatically from what one can imagine in more conventional models of strong interactions in which even the existence of tetra-neutron is highly questionable.

k_{eff}	2×59	4×29
$E_B(ack)(^4n)/MeV$	3.7680	
$E_{B,app}(4n)/MeV$	4.4135	8.1825

The higher binding energy per nucleon for tetra-neutron might directly relate to the neutron richness of heavy nuclei in accordance with the vision that Coulomb energy is what disfavors proton rich nuclei.

According to [42], tetra-neutron might have been observed in the decay ${}^8He \rightarrow {}^4He + {}^4n$ and the accepted value for the mass of 8He isotope gives the upper bound of $E(^4n) < 3.1$ MeV, which is one half of the the estimate. One can of course consider the possibility that free tetra-neutron corresponds to $L(2, 59)$ and nuclear tetra-neutron corresponds to the length scale $L(4, 29)$ of 4He . Also light quarks appear as several p-adically scaled up variants in the TGD based model for low-lying hadrons and there is also evidence that neutrinos appear in several scales.

9.5.4 What could be the general mass formula?

In the proposed model nucleus consists of $A \leq 4$ nuclei. Concerning the details of the model there are several questions to be answered. Do $A \leq 3$ nuclei and $A = 4$ nuclei 4He and tetra-neutron form separate nuclear strings carrying their own color magnetic fields as the different p-adic length scale for the corresponding "color magnetic bodies" would suggest? Or do they combine by a connected sum operation to single closed string? Is there single Bose-Einstein condensate or several ones.

Certainly the Bose-Einstein condensates associated with nucleons forming $A < 4$ nuclei are separate from those for $A = 4$ nuclei. The behavior of E_B in turn can be understood if 4He nuclei and tetra-neutrons form separate Bose-Einstein condensates. For $Z > N$ nuclei poly-protons constructed as exotic charge states of stable $A \leq 4$ nuclei could give rise to the proton excess.

Before continuing it is appropriate to list the apparent binding energies for poly-neutrons and poly-protons.

poly-neutron	n	2n	3n	4n
$E_{B,app}/MeV$	0	$E_B({}^2H) + \frac{\Delta}{2}$	$E_B({}^3H) + \frac{2\Delta}{3}$	$E_B({}^4He) + \frac{\Delta}{2}$
poly-proton	p	2p	3p	4p
$E_{B,app}/MeV$	0	$E_B({}^2H) - \frac{\Delta}{2}$	$E_B({}^3He) - \frac{\Delta}{3}$	$E_B({}^4He) - \frac{\Delta}{2}$

For heavier nuclei $E_{B,app}({}^4n)$ is smaller than $E_B({}^4He) + (m_p - m_n)/2$.

The first guess for the general formula for the binding energy for nucleus (Z, N) is obtained by assuming that for maximum number of 4He nuclei and tetra-neutrons/tetra-protons identified as 4H nuclei with 2 negatively/positively charged color bonds are present.

1. $N \geq Z$ nuclei

Even- Z nuclei with $N \geq Z$ can be expressed as $(Z = 2n, N = 2(n + k) + m)$, $m = 0, 1, 2$ or 3 . For $Z \leq 26$ (only single Bose-Einstein condensate) this gives for the apparent binding energy per nucleon (assuming that all neutrons are indeed neutrons) the formula

$$\begin{aligned}
 E_B(2n, 2(n + k) + m) &= \frac{n}{A} E_B({}^4He) + \frac{k}{A} E_{B,app}({}^4n) + \frac{1}{A} E_{B,app}({}^m n) \\
 &+ \frac{n^2 + k^2}{n + k} E_s - \frac{Z(Z - 1)}{A^2} E_c .
 \end{aligned}
 \tag{9.5.2}$$

The situation for the odd- Z nuclei $(Z, N) = (2n + 1, 2(n + k) + m)$ can be reduced to that for even- Z nuclei if one can assume that the $(2n + 1)^{th}$ proton combines with 2 neutrons to form 3He nucleus so that one has still $2(k - 1) + m$ neutrons combining to $A \leq 4$ poly-neutrons in above described manner.

2. $Z \geq N$ nuclei

For the nuclei having $Z > N$ the formation of a maximal number of ${}^4\text{He}$ nuclei leaves k excess protons. For long-lived nuclei $k \leq 2$ is satisfied. One could think of decomposing the excess protons to exotic variants of $A \leq 4$ nuclei by assuming that some charged bonds carry positive charge with an obvious generalization of the above formula.

The only differences with respect to a nucleus with neutron excess would be that the apparent binding energy is smaller than the actual one and positive charge would give rise to Coulomb interaction energy reducing the binding energy (but only very slightly). The change of the binding energy in the subtraction of single neutron from $Z = N = 2n$ nucleus is predicted to be approximately $\Delta E_B = -E_B({}^4\text{He})/A$. In the case of ${}^{32}\text{S}$ this predicts $\Delta E_B = .2209$ MeV. The real value is .2110 MeV. The fact that the general order of magnitude for the change of the binding energy as Z or N changes by one unit supports the proposed picture.

9.5.5 Nuclear strings and cold fusion

To summarize, option Ia) assuming that strong isospin dependent force acts on the nuclear space-time sheet and binds pn pairs to singlets such that the strong binding energy is very nearly zero in singlet state by the cancelation of scalar and vector contributions, is the most promising one. It predicts the existence of exotic di-,tri-, and tetra-neutron like particles and even negatively charged exotics obtained from ${}^2\text{H}, {}^3\text{H}, {}^3\text{He}$, and ${}^4\text{He}$ by adding negatively charged color bond. For instance, ${}^3\text{H}$ extends to a multiplet with em charges 1, 0, -1, -2. Of course, heavy nuclei with proton neutron excess could actually be such nuclei.

The exotic states are stable under beta decay for $m(\pi) < m_e$. The simplest neutral exotic nucleus corresponds to exotic deuteron with single negatively charged color bond. Using this as target it would be possible to achieve cold fusion since Coulomb wall would be absent. The empirical evidence for cold fusion thus supports the prediction of exotic charged states.

Signatures of cold fusion

In the following the consideration is restricted to cold fusion in which two deuterium nuclei react strongly since this is the basic reaction type studied.

In hot fusion there are three reaction types:

- 1) $D + D \rightarrow {}^4\text{He} + \gamma$ (23.8MeV)
- 2) $D + D \rightarrow {}^3\text{He} + n$
- 3) $D + D \rightarrow {}^3\text{H} + p$.

The rate for the process 1) predicted by standard nuclear physics is more than 10^{-3} times lower than for the processes 2) and 3) [39]. The reason is that the emission of the gamma ray involves the relatively weak electromagnetic interaction whereas the latter two processes are strong.

The most obvious objection against cold fusion is that the Coulomb wall between the nuclei makes the mentioned processes extremely improbable at room temperature. Of course, this alone implies that one should not apply the rules of hot fusion to cold fusion. Cold fusion indeed differs from hot fusion in several other aspects.

1. No gamma rays are seen.
2. The flux of energetic neutrons is much lower than expected on basis of the heat production rate an by interpolating hot fusion physics to the recent case.

These signatures can also be (and have been!) used to claim that no real fusion process occurs. It has however become clear that the isotopes of Helium and also some tritium accumulate to the Pd target during the reaction and already now prototype reactors for which the output energy exceeds input energy have been built and commercial applications are under development, see for instance [59]. Therefore the situation has turned around. The rules of standard physics do not apply so that some new nuclear physics must be involved and it has become an exciting intellectual challenge to understand what is happening. A representative example of this attitude and an enjoyable analysis of the counter arguments against cold fusion is provided by the article 'Energy transfer in cold fusion and sono-luminescence' of Julian Schwinger [26]. This article should be contrasted with the ultra-skeptical article 'ESP and Cold Fusion: parallels in pseudoscience' of V. J. Stenger [32].

Cold fusion has also other features, which serve as valuable constraints for the model building.

1. Cold fusion is not a bulk phenomenon. It seems that fusion occurs most effectively in nanoparticles of Pd and the development of the required nano-technology has made possible to produce fusion energy in controlled manner. Concerning applications this is a good news since there is no fear that the process could run out of control.
2. The ratio x of D atoms to Pd atoms in Pd particle must lie the critical range $[\.85, .90]$ for the production of ${}^4\text{He}$ to occur [45]. This explains the poor repeatability of the earlier experiments and also the fact that fusion occurred sporadically.
3. Also the transmutations of Pd nuclei are observed [62].

Below a list of questions that any theory of cold fusion should be able to answer.

1. Why cold fusion is not a bulk phenomenon?
2. Why cold fusion of the light nuclei seems to occur only above the critical value $x \simeq .85$ of D concentration?
3. How fusing nuclei are able to effectively circumvent the Coulomb wall?
4. How the energy is transferred from nuclear degrees of freedom to much longer condensed matter degrees of freedom?
5. Why gamma rays are not produced, why the flux of high energy neutrons is so low and why the production of ${}^4\text{He}$ dominates (also some tritium is produced)?
6. How nuclear transmutations are possible?

Could exotic deuterium make cold fusion possible?

One model of cold fusion has been already discussed in [23] and the recent model is very similar to that. The basic idea is that only the neutrons of incoming and target nuclei can interact strongly, that is their space-time sheets can fuse. One might hope that neutral deuterium having single negatively charged color bond could allow to realize this mechanism.

1. Suppose that part of the deuterium in Pd catalyst corresponds to exotic deuterium with neutral nuclei so that cold fusion would occur between neutral exotic D nuclei in the target and charged incoming D nuclei and Coulomb wall in the nuclear scale would be absent.
2. The exotic variant of the ordinary $D + D$ reaction yields final states in which ${}^4\text{He}$, ${}^3\text{He}$ and ${}^3\text{H}$ are replaced with their exotic counterparts with charge lowered by one unit. In particular, exotic ${}^3\text{H}$ is neutral and there is no Coulomb wall hindering its fusion with Pd nuclei so that nuclear transmutations can occur.

Why the neutron and gamma fluxes are low might be understood if for some reason only exotic ${}^3\text{H}$ is produced, that is the production of charged final state nuclei is suppressed. The explanation relies on Coulomb wall at the nucleon level.

1. Initial state contains one charged and one neutral color bond and final state $A = 3$ or $A = 4$ color bonds. Additional neutral color bonds must be created in the reaction (one for the production $A = 3$ final states and two for $A = 4$ final state). The process involves the creation of neural fermion pairs. The emission of one exotic gluon per bond decaying to a neutral pair is necessary to achieve this. This requires that nucleon space-time sheets fuse together. Exotic D certainly belongs to the final state nucleus since charged color bond is not expected to be split in the process.
2. The process necessarily involves a temporary fusion of nucleon space-time sheets. One can understand the selection rules if only neutron space-time sheets can fuse appreciably so that only ${}^3\text{H}$ would be produced. Here Coulomb wall at nucleon level should enter into the game.

3. Protonic space-time sheets have the same positive sign of charge always so that there is a Coulomb wall between them. This explains why the reactions producing exotic ${}^4\text{He}$ do not occur appreciably. If the quark/antiquark at the neutron end of the color bond of ordinary D has positive charge, there is Coulomb attraction between proton and corresponding negatively charged quark. Thus energy minimization implies that the neutron space-time sheet of ordinary D has positive net charge and Coulomb repulsion prevents it from fusing with the proton space-time sheet of target D . The desired selection rules would thus be due to Coulomb wall at the nucleon level.

About the phase transition transforming ordinary deuterium to exotic deuterium

The exotic deuterium at the surface of Pd target seems to form patches (for a detailed summary see [23]). This suggests that a condensed matter phase transition involving also nuclei is involved. A possible mechanism giving rise to this kind of phase would be a local phase transition in the Pd target involving both D and Pd . In [23] it was suggested that deuterium nuclei transform in this phase transition to "ordinary" di-neutrons connected by a charged color bond to Pd nuclei. In the recent case di-neutron could be replaced by neutral D .

The phase transition transforming neutral color bond to a negatively charged one would certainly involve the emission of W^+ boson, which must be exotic in the sense that its Compton length is of order atomic size so that it could be treated as a massless particle and the rate for the process would be of the same order of magnitude as for electro-magnetic processes. One can imagine two options.

1. Exotic W^+ boson emission generates a positively charged color bond between Pd nucleus and exotic deuteron as in the previous model.
2. The exchange of exotic W^+ bosons between ordinary D nuclei and Pd induces the transformation $Z \rightarrow Z + 1$ inducing an alchemic phase transition $Pd \rightarrow Ag$. The most abundant Pd isotopes with $A = 105$ and 106 would transform to a state of same mass but chemically equivalent with the two lightest long-lived Ag isotopes. ${}^{106}\text{Ag}$ is unstable against β^+ decay to Pd and ${}^{105}\text{Ag}$ transforms to Pd via electron capture. For ${}^{106}\text{Ag}$ (${}^{105}\text{Ag}$) the rest energy is 4 MeV (2.2 MeV) higher than for ${}^{106}\text{Pd}$ (${}^{105}\text{Pd}$), which suggests that the resulting silver cannot be genuine.

This phase transition need not be favored energetically since the energy loaded into electrolyte could induce it. The energies should (and could in the recent scenario) correspond to energies typical for condensed matter physics. The densities of Ag and Pd are 10.49 gcm^{-3} and 12.023 gcm^{-3} so that the phase transition would expand the volume by a factor 1.0465. The porous character of Pd would allow this. The needed critical packing fraction for Pd would guarantee one D nucleus per one Pd nucleus with a sufficient accuracy.

Exotic weak bosons seem to be necessary

The proposed phase transition cannot proceed via the exchange of the ordinary W bosons. Rather, W bosons having Compton length of order atomic size are needed. These W bosons could correspond to a scaled up variant of ordinary W bosons having smaller mass, perhaps even of the order of electron mass. They could be also dark in the sense that Planck constant for them would have the value $\hbar = n\hbar_0$ implying scaling up of their Compton size by n . For $n \sim 2^{48}$ the Compton length of ordinary W boson would be of the order of atomic size so that for interactions below this length scale weak bosons would be effectively massless. p-Adically scaled up copy of weak physics with a large value of Planck constant could be in question. For instance, W bosons could correspond to the nuclear p-adic length scale $L(k = 113)$ and $n = 2^{11}$.

Few weeks after having written this chapter I learned that cold fusion is in news again: both Nature and New Scientists commented the latest results [45]. It seems that the emission of highly energetic charged particles which cannot be due to chemical reactions and could emerge from cold fusion has been demonstrated beyond doubt by Frank Cordon's team [27] using detectors known as CR-39 plastics of size scale of coin used already earlier in hot fusion research. The method is both cheap and simple. The idea is that travelling charged particles shatter the bonds of the plastic's polymers leaving pits or tracks in the plastic. Under the conditions claimed to make cold fusion possible (1 deuterium per 1 Pd nucleus making in TGD based model possible the phase transition of

D to its neutral variant by the emission of exotic dark W boson with interaction range of order atomic radius) tracks and pits appear during short period of time to the detector.

9.5.6 Strong force as a scaled and dark electro-weak force?

The fiddling with the nuclear string model has led to following conclusions.

1. Strong isospin dependent nuclear force, which does not reduce to color force, is necessary in order to eliminate polynutron and polyproton states. This force contributes practically nothing to the energies of bound states. This can be understood as being due to the cancelation of isospin scalar and vector parts of this force for them. Only strong isospin singlets and their composites with isospin doublet (n,p) are allowed for $A \leq 4$ nuclei serving as building bricks of the nuclear strings. Only *effective* polynutron states are allowed and they are strong isospin singlets or doublets containing charged color bonds.
2. The force could act in the length scalar of nuclear space-time sheets: $k = 113$ nuclear p-adic length scale is a good candidate for this length scale. One must be however cautious: the contribution to the energy of nuclei is so small that length scale could be much longer and perhaps same as in case of exotic color bonds. Color bonds connecting nuclei correspond to much longer p-adic length scale and appear in three p-adically scaled up variants corresponding to $A < 4$ nuclei, $A = 4$ nuclei and $A > 4$ nuclei.
3. The prediction of exotic deuterons with vanishing nuclear em charge leads to a simplification of the earlier model of cold fusion explaining its basic selection rules elegantly but requires a scaled variant of electro-weak force in the length scale of atom.

What is then this mysterious strong force? And how abundant these copies of color and electro-weak force actually are? Is there some unifying principle telling which of them are realized?

From foregoing plus TGD inspired model for quantum biology involving also dark and scaled variants of electro-weak and color forces it is becoming more and more obvious that the scaled up variants of both QCD and electro-weak physics appear in various space-time sheets of TGD Universe. This raises the following questions.

1. Could the isospin dependent strong force between nucleons be nothing but a p-adically scaled up (with respect to length scale) version of the electro-weak interactions in the p-adic length scale defined by Mersenne prime M_{89} with new length scale assigned with gluons and characterized by Mersenne prime M_{107} ? Strong force would be electro-weak force but in the length scale of hadron! Or possibly in length scale of nucleus ($k_{eff} = 107 + 6 = 113$) if a dark variant of strong force with $h = nh_0 = 2^3 h_0$ is in question.
2. Why shouldn't there be a scaled up variant of electro-weak force also in the p-adic length scale of the nuclear color flux tubes?
3. Could it be that all Mersenne primes and also other preferred p-adic primes correspond to entire standard model physics including also gravitation? Could be kind of natural selection which selects the p-adic survivors as proposed long time ago?

Positive answers to the last questions would clean the air and have quite a strong unifying power in the rather speculative and very-many-sheeted TGD Universe.

1. The prediction for new QCD type physics at M_{89} would get additional support. Perhaps also LHC provides it within the next half decade.
2. Electro-weak physics for Mersenne prime M_{127} assigned to electron and exotic quarks and color excited leptons would be predicted. This would predict the exotic quarks appearing in nuclear string model and conform with the 15 year old leptohadron hypothesis [24]. M_{127} dark weak physics would also make possible the phase transition transforming ordinary deuterium in Pd target to exotic deuterium with vanishing nuclear charge.

The most obvious objection against this unifying vision is that hadrons decay only according to the electro-weak physics corresponding to M_{89} . If they would decay according to M_{107} weak physics, the decay rates would be much much faster since the mass scale of electro-weak bosons would be reduced by a factor 2^{-9} (this would give increase of decay rates by a factor 2^{36} from the propagator of weak boson). This is however not a problem if strong force is a dark with say $n = 8$ giving corresponding to nuclear length scale. This crazy conjecture might work if one accepts the dark Bohr rules!

9.6 Giant dipole resonance as a dynamical signature for the existence of Bose-Einstein condensates?

The basic characteristic of the Bose-Einstein condensate model is the non-linearity of the color contribution to the binding energy. The implication is that the de-coherence of the Bose-Einstein condensate of the nuclear string consisting of 4He nuclei costs energy. This de-coherence need not involve a splitting of nuclear strings although also this is possible. Similar de-coherence can occur for 4He $A < 4$ nuclei. It turns out that these three de-coherence mechanisms explain quite nicely the basic aspects of giant dipole resonance (GDR) and its variants both qualitatively and quantitatively and that precise predictions for the fine structure of GDR emerge.

9.6.1 De-coherence at the level of 4He nuclear string

The de-coherence of a nucleus having n 4He nuclei to a nucleus containing two Bose-Einstein condensates having $n - k$ and $k > 2$ 4He nuclei requires energy given by

$$\begin{aligned}\Delta E &= (n^2 - (n - k)^2 - k^2)E_s = 2k(n - k)E_s, \quad k > 2, \\ \Delta E &= (n^2 - (n - 2)^2 - 1)E_s = (4n - 5)E_s, \quad k = 2, \\ E_s &\simeq .1955 \text{ MeV}.\end{aligned}\tag{9.6.-1}$$

Bose-Einstein condensate could also split into several pieces with some of them consisting of single 4He nucleus in which case there is no contribution to the color binding energy. A more general formula for the resonance energy reads as

$$\begin{aligned}\Delta E &= (n^2 - \sum_i k^2(n_i))E_s, \quad \sum_i n_i = n, \\ k(n_i) &= \begin{cases} n_i & \text{for } n_i > 2, \\ 1 & \text{for } n_i = 2, \\ 0 & \text{for } n_i = 1. \end{cases}\end{aligned}\tag{9.6.-2}$$

The table below lists the resonance energies for four manners of ${}^{16}O$ nucleus ($n = 4$) to lose its coherence.

final state	3+1	2+2	2+1+1	1+1+1+1
$\Delta E/MeV$	1.3685	2.7370	2.9325	3.1280

Rather small energies are involved. More generally, the minimum and maximum resonance energy would vary as $\Delta E_{min} = (2n - 1)E_s$ and $\Delta E_{max} = n^2E_s$ (total de-coherence). For $n = n_{max} = 13$ one would have $\Delta E_{min} = 2.3640$ MeV and $\Delta E_{max} = 33.099$ MeV.

Clearly, the loss of coherence at this level is a low energy collective phenomenon but certainly testable. For nuclei with $A > 60$ one can imagine also double resonance when both coherent Bose-Einstein condensates possibly present split into pieces. For $A \geq 120$ also triple resonance is possible.

9.6.2 De-coherence inside 4He nuclei

One can consider also the loss of coherence occurring at the level 4He nuclei. Predictions for resonance energies and for the dependence of GR cross sections on mass number follow.

Resonance energies

For ${}^4\text{He}$ nuclei one has $E_s = 1.820$ MeV. In this case de-coherence would mean the decomposition of Bose-Einstein condensate to $n = 4 \rightarrow \sum n_i = n$ with $\Delta E = n^2 - \sum_{n_i} k^1(n_i) = 16 - \sum_{n_i} k^2(n_i)$. The table below gives the resonance energies for the four options $n \rightarrow \sum_i n_i$ for the loss of coherence.

final state	3+1	2+2	2+1+1	1+1+1+1
$\Delta E/\text{MeV}$	12.74	25.48	27.30	29.12

These energies span the range at which the cross section for ${}^{16}\text{O}(\gamma, xn)$ reaction has giant dipole resonances [28]. Quite generally, GDR is a broad bump with substructure beginning around 10 MeV and ranging to 30 MeV. The average position of the bump as a function of atomic number can be parameterized by the following formula

$$E(A)/\text{MeV} = 31.2A^{-1/3} + 20.6A^{-1/6} \quad (9.6-1)$$

given in [57]. The energy varies from 36.6 MeV for $A = 4$ (the fit is probably not good for very low values of A) to 13.75 MeV for $A = 206$. The width of GDR ranges from 4-5 MeV for closed shell nuclei up to 8 MeV for nuclei between closed shells.

The observation raises the question whether the de-coherence of Bose-Einstein condensates associated with ${}^4\text{He}$ and nuclear string could relate to GDR and its variants. If so, GR proper would be a collective phenomenon both at the level of single ${}^4\text{He}$ nucleus (main contribution to the resonance energy) and entire nucleus (width of the resonance). The killer prediction is that even ${}^4\text{He}$ should exhibit giant dipole resonance and its variants: GDR in ${}^4\text{He}$ has been reported [50].

Some tests

This hypothesis seems to survive the basic qualitative and quantitative tests.

1. The basic prediction of the model peak at 12.74 MeV and at triplet of closely located peaks at (25.48, 27.30, 29.12) MeV spanning a range of about 4 MeV, which is slightly smaller than the width of GDR. According to [33] there are two peaks identified as iso-scalar GMR at $13.7 \pm .3$ MeV and iso-vector GMR at 26 ± 3 MeV. The 6 MeV uncertainty related to the position of iso-vector peak suggests that it corresponds to the triplet (25.48, 27.30, 29.12) MeV whereas singlet would correspond to the iso-scalar peak. According to the interpretation represented in [33] iso-scalar *resp.* iso-vector peak would correspond to oscillations of proton and neutron densities in same *resp.* opposite phase. This interpretation can make sense in TGD framework only inside single ${}^4\text{He}$ nucleus and would apply to the transverse oscillations of ${}^4\text{He}$ string rather than radial oscillations of entire nucleus.
2. The presence of triplet structure seems to explain most of the width of iso-vector GR. The combination of GDR internal to ${}^4\text{He}$ with GDR for the entire nucleus (for which resonance energies vary from $\Delta E_{min} = (2n - 1)E_s$ to $\Delta E_{max} = n^2E_s$ ($n = A/4$)) predicts that also latter contributes to the width of GDR and give it additional fine structure. The order of magnitude for ΔE_{min} is in the range [1.3685, 2.3640] MeV which is consistent with the width of GDR and predicts a band of width 1 MeV located 1.4 MeV above the basic peak.
3. The de-coherence of $A < 4$ nuclei could increase the width of the peaks for nuclei with partially filled shells: maximum and minimum values of resonance energy are $9E_s({}^4\text{He})/2 = 8.19$ MeV and $4E_s({}^4\text{He}) = 7.28$ MeV for ${}^3\text{He}$ and ${}^3\text{H}$ which conforms with the upper bound 8 MeV for the width.
4. It is also possible that n ${}^4\text{He}$ nuclei simultaneously lose their coherence. If multiplet de-coherence occurs coherently it gives rise to harmonics of GDR. For de-coherent decoherence so that the emitted photons should correspond to those associated with single ${}^4\text{He}$ GDR combined with nuclear GDR. If absorption occurs for $n \leq 13$ nuclei simultaneously, one obtains a convoluted spectrum for resonant absorption energy

$$\Delta E = [16n - \sum_{j=1}^n \sum_{i_j} k^2(n_{i_j})] E_s . \quad (9.6.0)$$

The maximum value of ΔE given by $\Delta E_{max} = n \times 29.12$ MeV. For $n = 13$ this would give $\Delta E_{max} = 378.56$ MeV for the upper bound for the range of excitation energies for GDR. For heavy nuclei [57] GDR occurs in the range 30-130 MeV of excitation energies so that the order of magnitude is correct. Lower bound in turn corresponds to a total loss of coherence for single ${}^4\text{He}$ nucleus.

5. That the width of GDR increases with the excitation energy [57] is consistent with the excitation of higher GDR resonances associated with the entire nuclear string. $n \leq n_{max}$ for GDR at the level of the entire nucleus means saturation of the GDR peak with excitation energy which has been indeed observed [28].

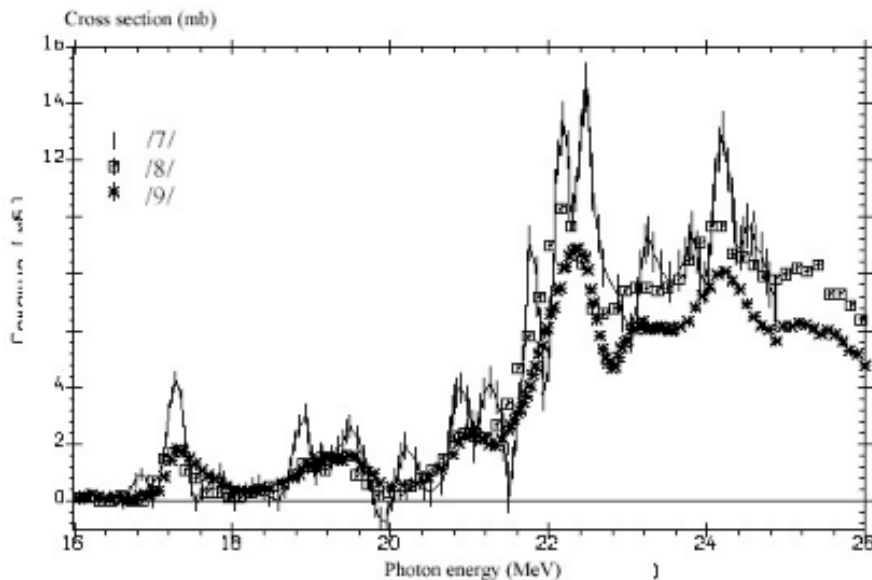


Figure 9.1: The comparison of photon neutron cross sections ${}^{16}\text{O}(\gamma, xn)$ obtained in one BR-experiment (Moscow State University) and two QMA experiments carried out at Saclay (France) Livermore (USA). Figure is taken from [28] where also references to experiments can be found.

One can look whether the model might work even at the level of details. Figure 3 of [28] compares total photon neutron reaction cross sections for ${}^{16}\text{O}(\gamma, xn)$ in the range 16-26 MeV from some experiments so that the possible structure at 12.74 MeV is not visible in it. It is obvious that the resonance structure is more complex than predicted by the simplest model. It seems however possible to explain this.

1. The main part of the resonance is a high bump above 22 MeV spanning an interval of about 4 MeV just as the triplet at (25.48, 27.30, 29.12) MeV does. This suggest a shift of the predicted 3-peak structure in the range 25-30 MeV range downwards by about 3 MeV. This happens if the photo excitation inducing the de-coherence involves a dropping from a state with excitation energy of 3 MeV to the ground state. The peak structure has peaks roughly at the shifted energies but there is also an additional structure which might be understood in terms of the bands of width 1 MeV located 1.4 MeV above the basic line.

2. There are three smaller bumps below the main bump which also span a range of 4 MeV which suggests that also they correspond to a shifted variant of the basic three-peak structure. This can be understood if the photo excitation inducing de-coherence leads from an excited state with excitation energy 8.3 MeV to ground state shifting the resonance triplet (25.48, 27.30, 29.12) MeV to resonance triplet at (17.2, 19.00, 20.82) MeV.

On basis of these arguments it seems that the proposed mechanism might explain GR and its variants. The basic prediction would be the presence of singlet and triplet resonance peaks corresponding to the four manners to lose the coherence. Second signature is the precise prediction for the fine structure of resonance peaks.

Predictions for cross sections

The estimation of collision cross sections in nuclear string model would require detailed numerical models. One approach to modelling would be to treat the colliding nuclear strings as random coils with finite thickness defined by the size of $A \leq 4$ strings. The intersections of colliding strings would induce fusion reactions and self intersections fissions. Simple statistical models for the intersections based on geometric probability are possible and allow to estimate branching ratios to various channels.

In the case of GR the reduction to 4He level means strong testable predictions for the dependence of GR cross sections on the mass number. GR involves formation of eye-glass type configuration at level of single 4He and in the collision of nuclei with mass numbers A_1 and A_2 GR means formation of these configurations for some $A = 4$ unit associated with either nucleus. Hence the GR cross section should be in a reasonable approximation proportional to $n_1 + n_2$ where n_i are the numbers of $A = 4$ sub-units, which can be either 4He , tetra-neutron, or possible other variants of 4He having charged color bonds. For $Z_i = 2m_i$, $N = 2n_i$, $A_i = 4(m_i + n_i)$ nuclei one has $n_1 + n_2 = (A_1 + A_2)/4$. Also a characteristic oscillatory behavior as a function of A is expected if the number of $A = 4$ units is maximal. If GR reactions are induced by the touching of 4He units of nuclear string implying transfer of kinetic energy between units then the GR cross sections should depend only on the energy per 4He nucleus in cm system, which is also a strong prediction.

9.6.3 De-coherence inside $A = 3$ nuclei and pygmy resonances

For neutron rich nuclei the loss of coherence is expected to occur inside 4He , tetra-neutron, 3He and possibly also 3n which might be stable in the nuclear environment. The de-coherence of tetra-neutron gives in the first approximation the same resonance energy spectrum as that for 4He since $E_B({}^4n) \sim E_B({}^4He)$ roughly consistent with the previous estimates for $E_B({}^4n)$ implies $E_s({}^4n) \sim E_s({}^4He)$.

The de-coherence inside $A = 3$ nuclei might explain the so called pygmy resonance appearing in neutron rich nuclei, which according to [40] is wide bump around $E \sim 8$ MeV. For $A = 3$ nuclei only two de-coherence transitions are possible: $3 \rightarrow 2 + 1$ and $3 \rightarrow 1 + 1 + 1$ and $E_s = E_B({}^3H) = .940$ MeV the corresponding energies are $8E_s = 7.520$ MeV and $9 * E_s = 8.4600$ MeV. Mean energy is indeed ~ 8 MeV and the separation of peaks about 1 MeV. The de-coherence at level of 4He string might add to this 1 MeV wide bands about 1.4 MeV above the basic lines.

The figure of [41] illustrating photo-absorption cross section in ${}^{44}Ca$ and ${}^{48}Ca$ shows three peaks at 6.8, 7.3, 7.8 and 8 MeV in ${}^{44}Ca$. The additional two peaks might be assigned with the excitation of initial or final states. This suggests also the presence of also $A = 3$ nuclear strings in ${}^{44}Ca$ besides H4 and 4n strings. Perhaps neutron halo wave function contains ${}^3n + n$ component besides 4n . For ${}^{48}Ca$ these peaks are much weaker suggesting the dominance of $2 \times {}^4n$ component.

9.6.4 De-coherence and the differential topology of nuclear reactions

Nuclear string model allows a topological description of nuclear decays in terms of closed string diagrams and it is interesting to look what characteristic predictions follow without going to detailed quantitative modelling of stringy collisions possibly using some variant of string models.

In the de-coherence eye-glass type singularities of the closed nuclear string appear and make possible nuclear decays.

1. At the level of 4He sub-strings the simplest singularities correspond to $4 \rightarrow 3 + 1$ and $4 \rightarrow 2 + 2$ eye-glass singularities. The first one corresponds to low energy GR and second to one of higher

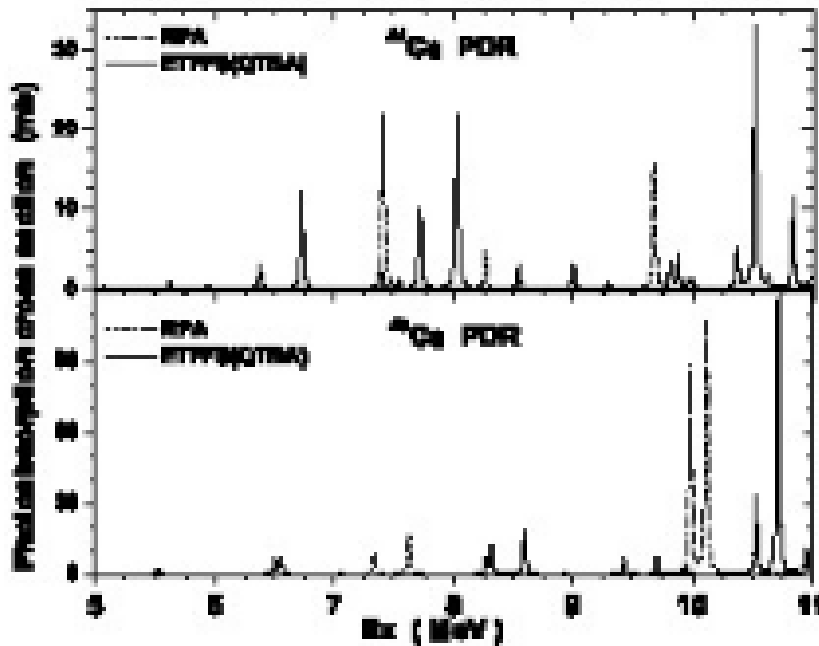


Figure 9.2: Pygmy resonances in ^{44}Ca and ^{48}Ca up to 11 MeV. Figure is taken from [41].

energy GRs. They can naturally lead to decays in which nucleon or deuteron is emitted in decay process. The singularities $4 \rightarrow 2 + 1 + 1$ resp. $4 \rightarrow 1 + 1 + 1 + 1$ correspond to eye-glasses with 3 resp. four lenses and mean the decay of ^4He to deuteron and two nucleons resp. 4 nucleons. The prediction is that the emission of deuteron requires a considerably larger excitation energy than the emission of single nucleon. For GR at level of $A = 3$ nuclei analogous considerations apply. Taking into account the possible tunnelling of the nuclear strings from the nuclear space-time sheet modifies this simple picture.

2. For GR in the scale of entire nuclei the corresponding singular configurations typically make possible the emission of alpha particle. Considerably smaller collision energies should be able to induce the emission of alpha particles than the emission of nucleons if only stringy excitations matter. The excitation energy needed for the emission of α particle is predicted to increase with A since the number n of ^4He nuclei increases with A . For instance, for $Z = N = 2n$ nuclei $n \rightarrow n - 1 + 1$ would require the excitation energy $(2n - 1)E_c = (A/2 - 1)E_c$, $E_c \simeq .2$ MeV. The tunnelling of the alpha particle from the nuclear space-time sheet can modify the situation.

The decay process allows a differential topological description. Quite generally, in the de-coherence process $n \rightarrow (n - k) + k$ the color magnetic flux through the closed string must be reduced from n to $n - k$ units through the first closed string and to k units through the second one. The reduction of the color color magnetic fluxes means the reduction of the total color binding energy from $n^2 E_c$ $((n - k)^2 + k^2) E_c$ and the kinetic energy of the colliding nucleons should provide this energy.

Faraday's law, which is essentially a differential topological statement, requires the presence of a time dependent color electric field making possible the reduction of the color magnetic fluxes. The holonomy group of the classical color gauge field $G_{\alpha\beta}^A$ is always Abelian in TGD framework being proportional to $H^A J_{\alpha\beta}$, where H^A are color Hamiltonians and $J_{\alpha\beta}$ is the induced Kähler form. Hence it should be possible to treat the situation in terms of the induced Kähler field alone. Obviously, the change of the Kähler (color) electric flux in the reaction corresponds to the change of (color) Kähler (color) magnetic flux. The change of color electric flux occurs naturally in a collision situation involving changing induced gauge fields.

9.7 Cold fusion, plasma electrolysis, biological transmutations, and burning salt water

The article of Kanarev and Mizuno [72] reports findings supporting the occurrence of cold fusion in NaOH and KOH hydrolysis. The situation is different from standard cold fusion where heavy water D_2O is used instead of H_2O .

One can understand the cold fusion reactions reported by Mizuno as nuclear reactions in which part of what I call dark proton string having negatively charged color bonds (essentially a zoomed up variant of ordinary nucleus with large Planck constant) suffers a phase transition to ordinary matter and experiences ordinary strong interactions with the nuclei at the cathode. In the simplest model the final state would contain only ordinary nuclear matter. The generation of plasma in plasma electrolysis can be seen as a process analogous to the positive feedback loop in ordinary nuclear reactions.

Rather encouragingly, the model allows to understand also deuterium cold fusion and leads to a solution of several other anomalies.

1. The so called lithium problem of cosmology (the observed abundance of lithium is by a factor 2.5 lower than predicted by standard cosmology [76]) can be resolved if lithium nuclei transform partially to dark lithium nuclei.
2. The so called $H_{1.5}O$ anomaly of water [47, 51, 49, 50] can be understood if 1/4 of protons of water forms dark lithium nuclei or heavier dark nuclei formed as sequences of these just as ordinary nuclei are constructed as sequences of 4He and lighter nuclei in nuclear string model. The results force to consider the possibility that nuclear isotopes unstable as ordinary matter can be stable dark matter.
3. The mysterious behavior burning salt water [79] can be also understood in the same framework.
4. The model explains the nuclear transmutations observed in Kanarev's plasma electrolysis. Intriguingly, several biologically important ions belong to the reaction products in the case of NaOH electrolysis. This raises the question whether cold nuclear reactions occur in living matter and are responsible for generation of biologically most important ions.

9.7.1 The data

Findings of Kanarev

Kanarev has found that the volume of produced H_2 and O_2 gases is much larger than the volume resulting in the electrolysis of the water used in the process. If one knows the values of p and T one can estimate the volumes of H_2 and O_2 using the equation of state $V = nT/p$ of ideal gas. This gives

$$V(H_2; p, T) = \frac{A(H_2)}{A(H_2O)} \times \frac{M(H_2O)}{m_p} = \frac{1}{9} \frac{M(H_2O)}{m_p} \times \frac{T}{p} .$$

Here $M(H_2O)$ is the total mass of the water (.272 kg for KOH and .445 kg for NaOH).

In the situation considered one should be able to produce from one liter of water 1220 liters of hydrogen and 622 liters of oxygen giving

$$V(H_2)/V(H_2O) = 1.220 \times 10^3 , \quad V(O_2)/V(H_2O) = .622 \times 10^3 ,$$

$$r(gas) = V(H_2 + O_2)/V(H_2O) = 1.844 \times 10^3 , \quad V(H_2)/V(O_2) \simeq 1.96 .$$

$V(H_2)/V(O_2) \simeq 1.96$ is 4 per cent smaller than the prediction $V(H_2)/V(O_2) = 2$ of the ideal gas approximation.

The volumes of O_2 and H_2 are not reported separately. The table gives the total volumes of gas produced and ratios to the volume of water used.

	$M(H_2O)/kg$	$V(gas)/m^3$	$\frac{V(gas)}{V(H_2O)}$	$\frac{[V(gas)/V(H_2O)]}{r(gas)}$
KOH	.272	8.75	3.2×10^4	17.4
NaOH	.445	12.66	2.8×10^4	15.2

Table 1. The weight of water used in the electrolysis and the total volume of gas produced for KOH and NaOH electrolysis. $r(gas)$ denotes the naive prediction for the total volume of gas per water volume appearing in previous table. For KOH *resp.* NaOH the volume ratio $[V(gas)/V(H_2O)]$ is by a factor $r = 17.4$ *resp.* $r = 15.2$ higher than the naive estimate.

Findings of Mizuno

Mizuno in turn found that the Fe cathode contains Si, K, Cr, Fe, Cu for both KOH and NaOH electrolysis and in case of NaOH also Al, Si, Ca. The fraction of these nuclei is of order one per cent. The table below gives the fractions for both KOH and NaOH.

KOH				
Element(Z,N)	Al(13,27)	Si(14,28)	Cl(17,18)	K(19,20)
%		0.94		4.50
Element(Z,N)	Ca(20,20)	Cr(24,28)	Fe(26,29)	Cu(29,34)
%		1.90	93.0	0.45
NaOH				
Element(Z,N)	Al(13,27)	Si(14,28)	Cl(17,18)	K(19,20)
%	1.10	0.55	0.20	0.60
Element(Z,N)	Ca(20,20)	Cr(24,28)	Fe(26,29)	Cu(29,34)
%	0.40	1.60	94.0	0.65

Table 2. The per cent of various nuclei in cathode for KOH and NaOH electrolysis.

The results supports the view that nuclear reactions involving new nuclear physics are involved and that part of H_2 and O_2 could be produced by nuclear reactions at the cathode.

1. For *Si*, *K*, *Cr*, *Fe*, and *Cu* the mechanism could be common for both *NaOH* and *KOH* electrolysis and presumably involve fission of *Fe* nuclei. The percent of *K* in *KOH* is considerably larger than in *NaOH* case and this is presumably due to the absorption of K^+ ions by the cathode.
2. For *Al*, *Si*, and *Ca* the reaction occurring only for *Na* should involve *Na* ions absorbed by the cathode and suffering cold fusion with some particles -call them just *X* - to be identified.
3. *Cu* is the only element heavier than *Fe* and is expected to be produced by fusion with *X*. Quite generally, the fractions are of order one per cent.
4. The authors suggests that the extra volume of H_2 and O_2 molecules is due to nuclear reactions in the cathode. A test for this hypothesis would be the ratio of H_2 and O_2 volumes. Large deviation from value 2 would support the hypothesis. The value near 2 would in turn support the hypothesis that the water produced by electrolysis is considerably denser than ordinary water.

9.7.2 $H_{1.5}O$ anomaly and nuclear string model

It would seem that some exotic nuclei, perhaps consisting of protons, should be involved with the cold fusion. Concerning the identification of these exotic particles there are several guidelines. $H_{1.5}O$ anomaly, anomalous production of e^+e^- pairs in heavy ion collisions, and nuclear string model.

$H_{1.5}O$ anomaly and anomalous production of electron-positron pairs in heavy ion collisions

There exists an anomaly which could be explained in terms of long open nuclear strings. The explanation of $H_{1.5}O$ anomaly [47, 51, 49, 50] discussed in [27] as a manifestation of dark protons was one of the first applications of TGD based ideas about dark matter. The proposed explanation is that the fraction of 1/4 of protons is in attosecond time scale dark and invisible in electron scattering and neutron diffraction. Note that attosecond time scale corresponds to the time during which light travels a length of order atomic size.

A natural identification of the dark protons would be in terms of protonic strings behaving like nuclei having anomalously large size, which would be due to the anomalously large value of Planck constant. A partial neutralization by negatively charge color bonds would make these states stable.

The TGD based explanation of anomalous production of electron-positron pairs in the collisions of heavy nuclei just above the Coulomb wall [24] is in terms of lepto-pions consisting of pairs of color octet electron and positron allowed by TGD and having mass slightly below $2m_e \simeq 1$ MeV. The strong electromagnetic fields created in collision create coherent state of leptopions decaying into electron positron pairs.

Nuclear string model

The nuclear string model describes nuclei as string like structures with nucleons connected by color magnetic flux tubes whose length is of order electron Compton length about 10^{-12} meters and even longer and thus much longer than the size scale of nuclei themselves which is below 10^{-14} meters. Color magnetic flux tubes define the color magnetic body of nucleus and each flux tube has colored fermion and antifermion at its ends. The net color of pair is non-vanishing so that color confinement binds the nucleons to the nuclear string. Nuclei can be visualized as structures analogous to plants with nucleus taking the role of seed and color magnetic body of much larger size taking the role of plant with color flux tubes however returning back to another nucleon inside nucleus.

One can imagine two basic identifications of the fermions.

1. For the first option fermions are identified as quarks. The color flux tube can have three charge states $q = +1, 0, -1$ according to whether it corresponds to $u\bar{d}, u\bar{u} + d\bar{d}$, or $\bar{u}d$ type state for quarks. This predicts a rich spectrum of exotic nuclei in which neutrons consist actually of proton plus negatively charged flux tube. The small mass difference between neutron and proton and small mass of the quarks (of order MeV) could quite well mean that these exotic nuclei are identified as ordinary nuclei. The findings of Illert [53] support the identification as quarks.
2. Lepto-hadron hypothesis [24] encourages to consider also the possibility that color bonds have color octet electrons at their ends. This would make it easier to understand why lepto-pions are produced in the collisions of heavy nuclei.
3. One can also consider the possibility that the color bonds are superpositions of quark-antiquark pairs and colored electron-positron pairs.

Two options

One can consider two options for protonic strings. Either their correspond to open strings connected by color magnetic flux tubes or protons are dark so that giant nuclei are in question.

1. Protonic strings as open strings?

Color flux tubes connecting nucleons are long and one can ask whether it might be possible also open nuclear strings with long color flux tubes connecting widely separate nucleons even at atomic distance. These kind of structures would be favored if the ends of nuclear string are charged.

Even without assumption of large values of Planck constant for the color magnetic body and quarks the net length of flux tubes could be of the order of atomic size. Large value \hbar would imply an additional scaling.

The simplest giant nuclei constructible in this manner would consist of protons connected by color magnetic flux tubes to form an open string. Stability suggest that the charge per length is not too high so that some minimum fraction of the color bonds would be negatively charged. One could speak of exotic counterparts of ordinary nuclei differing from them only in the sense that size scale is much larger. A natural assumption is that the distance between charged protonic space-time sheets along string is constant.

In the sequel the notation $X(z, n)$ will be used for the protonic string containing net charge z and n negatively charged bonds. $a = z + n$ will denote the number of protons. z, n and a are analogous to nuclear charge Z , neutron number N , and mass number A . For open strings the charge is $z \geq 1$ and for closed strings $z \geq 0$ holds true.

This option has however problem. It is difficult imagine how the nuclear reactions could take place. One can imagine ordinary stringy diagrams in which touching of strings means that proton of

protonic string and ordinary nucleus interact strongly in ordinary sense of the word. It is however difficult to imagine how entire protonic string could be absorbed into the ordinary nucleus.

2. *Are protons of the protonic string dark?*

Second option is that protonic strings consist of dark protons so that nuclear space-time-sheet has scale up size, perhaps of order atomic size. This means that fermionic charge is distributed in much larger volume and possibly also the fermions associated with color magnetic flux tubes have scaled up sized. The value $\hbar = 2^{11}\hbar_0$ would predict Compton length of order 10^{-12} m for nucleon and upper size of order 10^{-11} for nuclei.

Cold nuclear reactions require a transformation of dark protons to ordinary ones and this requires leakage to the sector of the imbedding space in which the ordinary nuclei reside (here the book metaphor for imbedding space is very useful). This process can take place for a neutral part of protonic string and involves a reduction of proton and fermion sizes to normal ones. The phase transition could occur first only for a neutral piece of the protonic string having charges at its ends and initiate the nuclear reaction. Part of protonic string could remain dark and remaining part could be "eaten" by the ordinary nucleus or dark protonic string could "eat" part of the ordinary nuclear string. If the leakage occurs for the entire dark proton string, the nuclear reaction itself is just ordinary nuclear reaction and is expected to give out ordinary nuclei. What is important that apart from the crucial phase transition steps in the beginning and perhaps also in the end of the reaction, the model reduces to ordinary nuclear physics and is in principle testable.

The basic question is how plasma phase resulting in electrolysis leads to the formation of dark protons. The proposal [39] that the transition takes place with perturbative description of the plasma phase fails, might be more or less correct. Later a more detailed nuclear physics picture about the situation emerges.

3. *What happens to electrons in the formation of protonic strings?*

One should answer two questions.

1. What happens to the electrons of hydrogen atoms in the formation of dark protonic strings?
2. In plasma electrolysis the increase of the input voltage implies a mysterious reduction of the electron current with the simultaneous increase of the size of the plasma region near the cathode [70]. This means reduction of conductance with voltage and thus non-linear behavior. Where does electronic charge go?

Obviously the negatively charged color bond created by adding one proton to a protonic string could take the charge of electron and transform electrons as charge carriers to color bonds of dark *Li* isotopes which charge $Z = 3$ by gluing to existing protons sequence proton and negatively charged color bond. If the proton comes from H_2O OH^- replaces electron as a charge carrier. This would reduced the conductivity since OH^- is much heavier than electron. This kind of process and its reversal would take place in the transformation of hydrogen atoms to dark proton strings and back in atto-second time scale.

The color bond could be either $\bar{u}d$ pair or $e_8\bar{\nu}_8$ pair or quantum superposition of these. The basic vertex would involve the exchange of color octet super-symplectic bosons and their neutrino counterparts. Lepton number conservation requires creation of color singlet states formed of color octet neutrinos which are bosons and carrying lepton number -2. One color confined neutrino pair would be created for each electron pair consumed in the process and might escape the system: if this happens, the process is not reversible above the time scale defined by colored neutrino mass scale of order .1 eV which happens to be of order .1 attoseconds for ordinary neutrinos. Also ordinary nuclei could consist of nucleons connected by identical neutral color bonds (mostly).

The exchange of light counterparts of charged ρ mesons having mass of order MeV could lead to the transformation of neutral color bonds to charged ones. In deuterium cold fusion the exchange of charged ρ mesons between D and Pd nuclei could transform D nuclei to states behaving like di-neutrons so that cold fusion for D could take place. In the earlier proposal exchange of W^+ boson of scaled variant of weak interactions was proposed as a mechanism.

The formation of charged color bonds binding new dark protons to existing protonic nuclear strings or giving rise to the formation of completely new protonic strings would also increase of the rates of cold nuclear reactions.

Note that this picture leaves open the question whether the fermions associated with color bonds are quarks or electrons.

Nuclei and their dark variants must have same binding energy scale at nuclear quantum criticality

The basic question is what happens to the scale of binding energy of nuclei in the zooming up of nuclear space-time sheet. Quantum criticality requires that the binding energies scales must be same.

1. Consider first the binding energy of the nuclear strings. The highly non-trivial prediction of the nuclear string model is that the contributions of strong contact interactions at nuclear space-time sheet (having size $L < 10^{-14}$ m) to the binding energy vanish in good approximation for ground states with vanishing strong isospin. This means that the binding energy comes from the binding energy assignable to color bonds connecting nucleons together.
2. Suppose that this holds true in a good approximation also for dark nuclei for which the distances of nucleons at zoomed up nuclear space-time sheet (having originally size below 10^{-14} meters) are scaled up. As a matter fact, since the scale of binding energy for contact interactions is expected to reduce, the situation is expected to improve. Suppose that color bonds with length of order 10^{-12} m preserve their lengths. Under these assumptions the nuclear binding energy scale is not affected appreciably and one can have nuclear quantum criticality. Note that the length for the color bonds poses upper limit of order 100 for the scaling of Planck constant.

It is essential that the length of color bonds is not changed and only the size of the nuclear space-time sheet changes. If also the length and thickness of color bonds is scaled up then a naive scaling argument assuming that color binding energy related to the interaction of transforms as color Coulombic binding energy would predict that the energy scales like $1/\hbar$. The binding energies of dark nuclei would be much smaller and transformation of ordinary nuclei to dark nuclei would not take place spontaneously. Quantum criticality would not hold true and the argument explaining the transformation of ordinary Li to its dark counterpart and the model for the deuterium cold fusion would be lost.

9.7.3 A model for the observations of Mizuno

The basic objection against cold nuclear reactions is that Coulomb wall makes it impossible for the incoming nuclei to reach the range of strong interactions. In order that the particle gets to the cathode from electrolyte it should be positively charged. Positive charge however implies Coulomb wall which cannot be overcome with the low energies involved.

These two contradictory conditions can be satisfied if the electrolysis produces exotic phase of water satisfying the chemical formula $H_{1.5}O$ with 1/4 of protons in the form of almost neutral protonic strings can possess only few neutral color bonds. The neutral portions of the protonic string, which have suffered phase transition to a phase with ordinary Planck constant could get very near to the target nucleus since the charges of proton can be neutralized in the size scale of proton by the charges \bar{u} and \bar{d} quarks or e and $\bar{\nu}$ associated with the two bonds connecting proton to the two neighboring protons. This could make possible cold nuclear reactions.

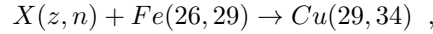
It turns out that the model fixes protonic strings to isotopes of dark Lithium (with neutrons replaced with proton plus negatively charged color bond). What is intriguing is that the biologically most important ions (besides Na^+) Cl^- , K^+ , and Ca^{++} appear at the cathode in Kanarev's plasma electrolysis actually result as outcomes of cold nuclear reactions between dark Li and Na^+ .

General assumptions of the model

The general assumptions of the model are following.

1. Ordinary nuclei are nuclear strings, which can contain besides neutrons also "pseudo-neutrons" consisting of pairs of protons and negatively charged color bonds. The model for D cold fusion requires that the Pd nuclei contain also "pseudo-neutrons".
2. Reaction products resulting in the fusion of exotic protonic string transforming partially to ordinary nuclear matter (if originally in dark phase) consist of the nuclei detected in the cathode plus possibly also nuclei which form gases or noble gases and leak out from the cathode.

3. *Si*, *K*, *Cr*, and *Cu* are produced by the same mechanism in both KOH and NaOH electrolysis.
4. *Al*, *Cl*, and *Ca* is produced by a mechanism which must involve cold nuclear reaction between protonic string and Na ions condensed on the cathode.
5. $Cu(Z, N) = Cu(29, 34)$ is the only product nucleus heavier than $Fe(26, 29)$. If no other nuclei are involved and Cu is produced by cold fusion



the anatomy of protonic string must be

$$X(z, n) = X(3, 5)$$

so that dark variant $Li(3, 5)$ having charge 3 and mass number 8 would be in question. $X(3, 5)$ would have 2 neutral color bonds and 5 negatively charged color bonds. To minimize Coulomb interaction the neutral color bonds must reside at the ends of the string. For quark option one would have charge $1 + 2/3$ at the first end and $1 + 1/3$ at the second end and charges of all protons between them would be neutralized. For color octet lepton color bond one would have charge 2 at the other end and zero at the other end.

For quark option the net protonic charge at the ends of the string causing repulsive interaction between the ends could make protonic string unstable against transition to dark phase in which the distance between ends is much longer even if the ends are closed within scaled up variant of the nuclear volume.

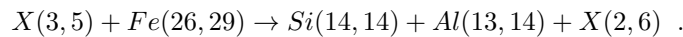
Arbitrarily long strings $X(3, n)$ having neutral bonds only at their ends are possible and their fusions lead to neutron rich isotopes of *Cu* nucleus decaying to the stable isotope. Hence the prediction that only *Cu* is produced is very general.

The simplest dark protonic strings $X(3, n)$ have quantum numbers of $Li(3, n)$. One of the hard problems of Big Bang cosmology is that the measured abundance of lithium is by a factor of about 2.5 lower than the predicted abundance [76]. The spontaneous transformation of $Li(3, n)$ isotopes to their dark variants could explain the discrepancy. Just by passing notice that *Li* has mood stabilizing effect [35]: the spontaneous transformation of Li^+ to its dark variant might relate to this effect.

Production mechanisms for the light nuclei common to *Na* and *K*

These nuclei must be produced by a fission of *Fe* nuclei.

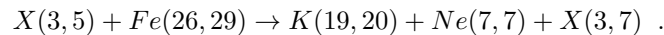
1. For $Si(14, 14)$ production the mechanism would be cold fission of *Fe* nucleus to two parts in the collision with the protonic string:



$X(2, 6)$ represent dark or ordinary $He(2, 6)$. As a noble gas *He* isotope would leave the cathode.

Note that arbitrarily long proton strings with two neutral bonds at their ends give neutron rich isotope of *Si* and exotic or ordinary isotope of *He* so that again the prediction is very general.

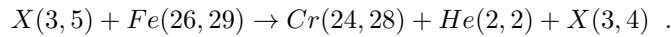
2. $K(19, 20)$ is produced much more in KOH which most probably means that part of K^+ is absorbed from the electrolyte. In this case the reaction could proceed as follows:



Note that the neutron number could be distributed in many manners between final states. For arbitrarily long proton string with two neutral bonds at ends higher neutron rich isotopes of *K* and *Ne* are produced. As noble gas *Ne* would leak out from the cathode.

Ordinary $Li(3, 7)$ would decay by neutron emission to stable isotopes of Li . The temperature of the system determines whether Li boils out (1615 K under normal pressure). Li is not reported to appear in the cathode. In plasma electrolysis the temperature is in the interval $.5 \times 10^4$ - 10^4 C and around 10^3 C in the ordinary electrolysis so that the high temperature might explain the absence of Li . Also the in-stability of Li isotopes against transition to dark Li in electrolyte would imply the absence of Li .

3. For $Cr(24, 28)$ production the simplest reaction would be



Helium would leak out as noble gas. Proton string would shorten by one unit and keep its charge. $X(3, 4)$ would represent the stable isotope $Li(3, 4)$ or its dark counterpart and what has been said in 2) applies also now.

How to understand the difference between KOH and NOH?

One should understand why Al , Cl , and Ca are not detected in the case of KOH electrolysis.

Al , Cl , and Ca would be created in the fusion of protonic strings with $Na(11, 12)$ nuclei absorbed by the cathode. With this assumption the rates are expected to be of same order of magnitude for all these processes as suggested by the one per cent order of magnitude for all fractions.

One can imagine two reaction mechanisms.

I: One could understand the production assuming only $X(3, 5)$ protonic strings if the number of $X(3, 5)$ strings absorbed by single Na nucleus can be $k = 1, 2, 3$ and that nuclear fission can take place after each step with a rate which is slow as compared to the rate of absorptions involving also the phase transition to dark matter. This is however highly implausible since ordinary nuclear interactions are in question.

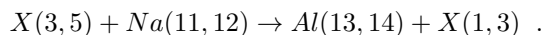
II: Second possibility is that the protonic strings appearing with the highest probability are obtained by fusing copies of the basic string $X(3, 5)$ by using neutral color bond between the strings. The minimization of electrostatic energy requires that that neutral color bonds are equally spaced so that there are three completely neutralized protons between non-neutralized protons.

One would have thus at least the strings $X(3, 5)$, $X(6, 10)$, and $X(9, 15)$, which correspond to dark $Li(3, 5)$ and dark variants of the unstable isotopes $C(6, 10)$ and $F(9, 15)$. In nuclear string model also ordinary nuclei are constructed from $He(2, 2)$ strings and lighter strings in completely analogous manner, and one could perhaps see the dark nuclei constructed from $Li(3, 5)$ as the next level of hierarchy realized only at the level of dark matter.

The charge per nucleon would be $3/8$ and the length of the string would be a multiple of 8. Interestingly, the numbers 3, 5, and 8 are subsequent Fibonacci numbers appearing very frequently also in biology (micro-tubules, sunflower patterns). The model predicts also the occurrence of cold fusions $X(z = 3k, n = 5k) + Fe(26, 29) \rightarrow (Z, N) = (26 + 3k, 29 + 5k)$. For $k = 2$ this would give $Ge(32, 39)$ which is stable isotope of Ge . For $k = 3$ one would have $(Z, N) = (35, 44)$ which is stable isotope of Br [47, 51].

Consider now detailed description of the reactions explaining the nuclei detected in the cathode.

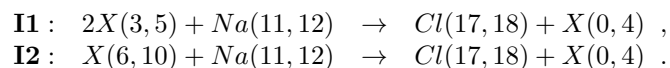
1. $Al(13, 14)$ would be produced in the reaction



$H(1, 3)$ or its dark variant could be in question. Also the reaction $X(3, 5) + Na(11, 12) \rightarrow Al(13, 17) + p$, where $Al(12, 17)$ is an unstable isotope of Al is possible.

The full absorption of protonic string would yield $Si(14, 17)$ beta-decaying to $P(15, 16)$, which is stable. Either P leaks out from the cathode or full absorption does not take place appreciably.

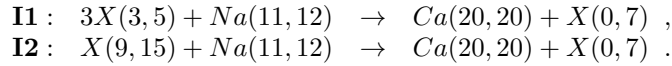
2. $Cl(17, 18)$ would be produced by the sequence



$X(0, 4)$ represents ordinary or dark tetra-neutron [55, 54, 42]. The instability of the transformation of tetra-neutron to dark matter could explain why its existence has remained controversial.

If the protonic string were absorbed completely, the resulting $Cl(17, 22)$ - if equivalent to ordinary nucleus - would transform via beta-decays to $A(18, 23)$ and then to $K(19, 22)$, which is stable and detected in the target.

3. $Ca(20, 20)$ would be produced in the reaction



$X(0, 7)$ would be dark counterpart of "septa-neutron". The complete absorption of nuclear string would produce $Ca(20, 27)$, which (if ordinary nucleus) transforms via beta decays to $Sc(21, 26)$ and then to $Ti(22, 25)$, which is stable.

9.7.4 Comparison with the model of deuterium cold fusion

It is interesting to compare the model with the model for cold fusion [62, 45] reported using deuterium target and D_2O instead of water.

Earlier model

1. The model is based on the assumption that D nuclei in the target suffer a phase transition to a state in which D nuclei become neutral so that the color bond between neutron and proton becomes negatively charged: one has effectively di-neutrons.
2. The mechanism of charging of color bond must either involve weak interactions or exchange of lepto- ρ mesons already discussed briefly. The proposal is that the exchange of W bosons of scaled up version of weak physics is involved with the range of interactions given by atomic length scale. The exchange of W^+ bosons was assumed to take place between Pd and D nuclei. This mechanism could lead to the formation of negatively charged color bonds in also ordinary nuclei.
3. The neutrality of exotic D nuclei allows to overcome Coulomb wall. One can understand the reported selection rules: in particular the absence of Helium isotopes (only isotopes of H are detected). The absence of gamma rays can be understood if the resulting gamma rays are dark and leak out before a transformation to ordinary gamma rays.

Are D nuclei in Pd target dark or not?

The question whether the exotic D nuclei are dark was left pending. The recent model suggests that the answer is affirmative.

1. The basic difference between the two experiments would be that in Kanarev's experiments incoming nuclei are dark whereas in D fusion cathode contains the dark nuclei and cold nuclear reactions occur at the "dark side" and is preceded by ordinary-to-dark phase transition for incoming D .
2. D cold fusion occurs for a very restricted range of parameters characterizing target: the first parameter is doping ratio: essentially one D nucleus per one Pd nucleus is needed which would fit with the assumption that scaled up size is of the order of atom size. Temperature is second parameter. This and the fact that the situation is highly sensitive to perturbations conforms with the interpretation as a phase transition to dark matter occurring at quantum criticality.
3. The model for Kanarev's findings forces to consider the possibility that dark D nuclei combine to form longer strings and can also give rise to dark $Li(3, 5)$ explaining the observed nuclear transmutations in the target.

4. In cold nuclear reactions incoming nuclei would transform to dark nuclei (the picture as a leakage between different pages of a book like structure defined by the generalized imbedding space is helpful). The reaction would take place for dark nuclei in zoomed up nuclear physics and the reaction products would be unstable against phase transition to ordinary nuclei.
5. Is it then necessary to assume that target D nuclei are transformed to neutral ones (di-neutrons effectively) in order to have cold nuclear reactions? Nuclear space-time sheets are scaled up. If nucleon space-time sheets are not scaled up, p and n are connected by color magnetic flux tubes of same length as in the case of ordinary nuclei but located at much larger nuclear space-time sheet. The classical analog for the quantal distribution of nucleon charges is even charge distribution in a sphere of radius R defined by the charge of the scaled up nucleus. The height of the Coulomb wall is $E_c = e^2/R$. If $R = a$, a the atomic radius, one has $E_c \sim .1$ keV. The wall is by a factor 10^{-4} lower than in ordinary nuclear collision so that the incoming D nucleus might overcome the Coulomb wall.

If Coulomb wall can be overcome, all dark variants of $D+D$ reaction are possible. Helium nuclei have not been however detected, which supports the view that D in target is transformed to its neutral variant. Gamma rays would be dark and could leak out without detection which would explain the absence of gamma rays.

Nuclear quantum criticality is essential

A note about the energetics of cold nuclear reactions is in order. The nuclear quantum criticality deriving from the cancelation of the contact interaction energies between nucleons for isospin singlets and scaling up of *only* nuclear space-time sheet is an absolutely essential assumption. Otherwise dark D would have much smaller binding energy scale than the visible one, and ordinary D in the Pd target could not transform to dark "di-neutron" state. Also the transformation of incoming D to its dark variant D at cathode could not take place.

9.7.5 What happens to OH bonds in plasma electrolysis?

For an innocent novice one strange aspect of hydrolysis is how the OH bonds having energies of order 8 eV can be split in temperatures corresponding to photon energies of order .5 eV. Kanarev has suggested his own theory for how this could happen [60]. TGD suggests that OH bonds are transformed to their dark variants with scaled down bond energy and that there might be no essential difference between OH bond and hydrogen bond.

The reduction of energy of OH bonds in plasma electrolysis

Kanarev has found that in plasma electrolysis the energy of OH bonds is reduced from roughly 8 eV to about .5 eV, which corresponds to the fundamental metabolic energy quantum identifiable as the zero point kinetic energy liberate as proton drops from $k = 137$ space-time sheet to much larger space-time sheet. In pyrolysis [71] similar reduction could occur since the pyrolysis occurs above temperature about 4000 C conforming with the energy scale of hydrogen bond.

The explanation discussed in [39] is that there is some mechanism exciting the bonds to a state with much lower bond energy. Dark matter hierarchy [39] suggests that the excitation corresponds to the transformation of OH bond to dark bond so that the energy scale of the state is reduced.

Also in the ordinary electrolysis of water [73] the energy of OH bonds is reduced to about 3.3 eV meaning a reduction factor of order 2. The simplest interpretation would be as a transformation of OH bonds to dark OH bond with $\hbar \rightarrow 2\hbar$ (the scaling could be also by some other integer or even rational). The energy needed to transform the bond to dark bond could come from remote metabolism via the dropping of dark protons from a dark variant of some sub-atomic space-time sheet with size not smaller than the size of the atomic space-time sheet to a larger space-time sheet.

$H_{1.5}O$ anomaly suggests that 1/4 of protons of water are dark in atto-second time scale [27] and one can imagine that both protons of water molecule can become dark under conditions defined by plasma electrolysis. Also the atomic space-time sheets and electron associated with OH bonds could become dark.

Atomic binding energies transform as $1/\hbar^2$. If the energy of hydrogen bond transforms like Coulombic interaction energy as given by the perturbative calculation, it is scaled down as $1/\hbar$ since the length

of the bond scales up like \hbar . Effectively $\alpha_{em} \propto 1/\hbar$ is replaced by its scaled down value. For $\hbar \rightarrow 2^4 \hbar_0$ the energy would scale from 8 eV to .5 eV and the standard metabolic energy quantum could induce the splitting of the dark OH bond. If 2^4 is the scale factor of \hbar for dark nuclear space-time sheets, their size would be of order 10^{-3} meters. The model for cold fusion is consistent with this since what matters is different value of Planck constant for the dark nuclear space-time sheets.

There is an objection against the reduction of OH bond energy. The bonds could be split by a process in which dark nuclear reactions kick protons to $k = 133$ dark space-time sheet. In this case the maximal zero point kinetic energy liberated in the dropping back would be 8 eV and could induce breaking of OH bond. For $\hbar/\hbar_0 \geq 4$ the size of $k = 133$ dark space-time sheet would be larger than the size of $k = 137$ atomic space-time sheet.

Are hydrogen bonds dark OH bonds?

The fact that the energy of hydrogen bonds [70] is typically around .5 eV forces to ask what distinguishes hydrogen bond from dark OH bond. Could it be that the two bonds are one and the same thing so that dark OH bonds would form standard part of the standard chemistry and molecular biology? In hydrogen bond same hydrogen would be shared by the oxygen atoms of the neighboring atoms. For the first O the bond would be ordinary OH bond and for the second O its dark variant with scaled down Coulomb energy. Under conditions making possible pyrolysis and plasma electrolysis both bonds would become dark. The variation of the hydrogen bond energy could reflect the variation of the scaling factor of \hbar .

The concentration of the spectrum of bond energies on integer multiples of fundamental energy scale - or even better, on powers of 2 - would provide support for the identification. There is evidence for two kinds of hydrogen bonds with bond energies in ratio 1:2 [46, 56]: the TGD based model is discussed in [27].

Mechanism transforming OH bonds to their dark counterparts

The transformation of OH bonds to dark bonds would occur both in ordinary and plasma electrolysis and only the change of Planck constant would distinguish between the two situations.

1. Whatever the mechanism transforming OH bonds to their dark counterparts is, metabolic energy is needed to achieve this. Kanarev also claims over-unity energy production [60]. Cold fusion researchers make the same claim about ordinary electrolysis. Cold nuclear reactions between Na^+ (K^+) and dark protons and dark Li could obviously serve as the primary energy source. This would provide the fundamental reason for why $NaOH$ or KOH must be present. Cold nuclear reactions would thus occur also in the ordinary electrolysis of water and provide the energy inducing the transition of OH bonds to dark ones by (say) $\hbar \rightarrow 2\hbar$ transition.
2. One can imagine several metabolic mechanisms for the visible-to-dark transformation of HO bonds. The energy spectrum of cold nuclear reactions forms a continuum whereas the energies needed to transform OH bonds to their dark variants presumably are in narrow bands. Therefore the energy liberated in cold nuclear reactions is not probably used as such. It is more plausible that standard metabolic energy quanta liberated in the dropping of protons (most naturally) to larger space-time sheets are utilized. The most important metabolic energy quanta for the dropping of proton come as $E_k = 2^{k-137} k E_0$: $E_0 = .5$ eV is liberated in the dropping of proton from atomic space-time sheet ($k = 137$) to much larger space-time sheet (the discrete spectrum of increments of the vacuum energy in the dropping approaches this energy [27]). The energy liberated in the dark nuclear reactions would "load metabolic batteries" by kicking the dark protons to the dark variants of $k < 137$ space-time sheet (the size of dark atomic space-time sheet scales like \hbar). Their dropping to larger space-time sheets would liberate photons with energies near to those transforming OH bonds to hydrogen bonds.
3. A signature for the standard metabolic energy quanta would be visible light at $2eV$ and also discrete lines below it accumulating to $2eV$. Kanarev's indeed reports the presence of red light [60] as a signature for the occurrence of process.

9.7.6 A model for plasma electrolysis

Kanarev's experiments involve also other strange aspects which lead to the view that cold nuclear reactions and dark matter physics are essential aspects of not only plasma electrolysis of Kanarev but also of ordinary electrolysis and responsible for the claimed over unity energy production. Biologically important ions are produced in reactions of dark Li and Na^+ and there is very strong electric voltage over the cell membrane. This inspires the question whether cold nuclear reactions serve as a metabolic energy source in living cell and are also responsible for production of ions heavier than Na^+ .

Brief description of plasma electrolysis

Electrolysis [73], pyrolysis [71], and plasma electrolysis [60, 70] of water are methods of producing free hydrogen. In pyrolysis the temperature above 4000 C leads to hydrogen and oxygen production. Oxygen production occurs also at cathode and hydrogen yield is higher than given by Faraday law for ordinary electrolysis [73].

The article of Mizuno and collaborators [70] about hydrogen production by plasma electrolysis contains a brief description of plasma electrolysis. A glow discharge occurs as the input voltage used in electrolysis is above a critical value and plasma is formed near cathode. In the arrangement of [70] plasma state is easily achieved above 140 V. If the values of temperature and current density are right, hydrogen generation in excess of Faraday's law as well as a production of oxygen at cathode (not possible in ideal electrolysis) are observed. Above 350 V the control of the process becomes difficult.

What really happens in electrolysis and plasma electrolysis?

1. Ordinary electrolysis

To understand what might happen in the plasma electrolysis consider first the ordinary electrolysis of water.

1. The arrangement involves typically the electrolyte consisting of water plus $NaOH$ or KOH without which hydrolysis is impossible for thermodynamical reasons.
2. Electronic current flows from the anode to cathode along a wire. In electrolyte there is a current of positively charged ions from anode to cathode. At the cathode the reaction $2H_2O + 2e^- \rightarrow 2H_2 + 2OH^-$ yields hydrogen molecules seen as bubbles in water. At the anode the reaction $2H_2O \rightarrow O_2 + 4H^+ + 4e^-$ is followed by the reaction $2H^+ + 2e^- \rightarrow H_2$ and the flow of $2e^-$ to the cathode along wire. The net outcome is hydrolysis: $H_2O \rightarrow 2H_2 + 2O_2$. Note that O_2 is produced only at anode and H_2 at both anode and cathode.

2. What happens in plasma electrolysis?

In plasma electrolysis something different might happen.

1. Cold nuclear reactions should take place at cathode in presence of Na^+ ions plus dark Li and should be in equilibrium under ordinary conditions and contribute mainly to the formation of dark OH bonds. The rate of cold nuclear reactions increases with input voltage V since the currents of Na^+ and dark Li to the cathode increase. Obviously the increased rate of energy yield from dark nuclear reactions could be the real reason for the formation of plasma phase above critical voltage.
2. By previous considerations the reduction of electron current above critical voltage has interpretation as a transition in which electronic charge is transferred to negative charge of color bonds of dark proton strings. Existing protonic strings could grow longer and also new strings could be created from the ionized hydrogen resulting in the electrolysis of water. The increase of the size of the dark nuclei would mean increase of the cross sections for cold nuclear reactions. The liberated energy would ionize hydrogen atoms and give rise to a positive feedback loop somewhat like in ordinary nuclear reactions.

3. The increased energy yield in cold nuclear reactions suggests that OH bonds are transformed very effectively to dark OH bonds in the plasma region. This means that the thermal radiation can split the hydrogen bonds and induce the splitting of two water molecules to $4H$ and $2O$ and therefore production of $2H_2 + O_2$ everywhere in this kind of region. The temperature used by Kanarev corresponds to energy between .5-1 eV [60] which conforms with the fact that OH bond energy is reduced to about .5 eV. Note that the presence of anode and cathode is not absolutely necessary if cold nuclear reactions can take place in the entire electrolyte volume and generate plasma phase by positive feedback loop.
4. The prediction is that Faraday's law for hydrogen production does not hold true. O/H ratio has the value $r = O/H = 0$ for the ordinary electrolysis at cathode. $r = 1/2$ holds true if local dissociation of water molecules dominates. According to [70] r increases from electrolysis value $r = .066$ above $V = 140$ V achieving the value $r = .45$ for $V = 350$ V where the system becomes unstable. Also cold nuclear reactions could contribute to hydrogen and oxygen production and affect the value of r as suggested by the large volume of gas produced in Kanarev's experiments [72].

Over-unity energy production?

Over-unity energy production with output power 2- or even 3-fold as compared with input power has been reported from plasma electrolysis. The effectiveness is deduced from the heating of of the system. Note that Mizuno reports in [70] that 10 per cent effectiveness but this is for the storage of energy to hydrogen and does not take into account the energy going to the heating of water.

The formation of higher isotopes of Li by fusing dark protons to existing dark proton strings is a good candidate for the dominant energy production mechanism. An estimate for the energy liberate in single process $Li(3, n) + m_p + e \rightarrow Li(3, n + 1) + 2\nu_8$ is obtained by using energy conservation. Here $2\nu_8$ denotes color singlet bound state of two color octet excitations of neutrino.

Since e_8 and ν_8 are analogous to u and d quarks one expects that their masses are very nearly the same. This gives as the first guess $m_{\nu_8} = m_e$ and since leptopion (color bound state of color octet electrons, [24]) has mass $m = 2m_e$ a good guess is $m(2\nu_8) = 2m_{\nu_8} = 2m_e$. The energy conservation would give

$$m(Li(3, n)) + m_p = m(Li(3, n + 1)) + m_e + T(2\nu_8) + E(\gamma) . \quad (9.7.1)$$

Here $T(2\nu_8)$ is the kinetic energy of $2\nu_8$ state and E_γ is the energy of photon possibly also emitted in the process.

The process is kinematically possible if the condition

$$\Delta m = m(Li(3, n)) + m_p - m(Li(3, n + 1)) \geq m_e . \quad (9.7.2)$$

is satisfied. All incoming particles are approximated to be at rest, which is a good approximation taking into account that chemical energy scales are much lower than nuclear ones. For the left hand side one obtains from the mass difference of $Li(3, n = 4)$ and $Li(3, 5)$ isotopes the estimate $\Delta m = 1.2312$ MeV for the liberated binding energy which is considerably larger than $m_e = .51$ MeV. Hence the process is kinematically possible and $2\nu_8$ would move with a relativistic velocity $v = .81c$ and presumably leave the system without interacting with it.

The process can involve also the emission of photons and the maximal amount of energy that photon can carry out corresponds to $E = \Delta m = 1.2312$ MeV. Let us denote by $\langle E \rangle < \Delta m$ the average photonic energy emitted in the process and express it as

$$\langle E \rangle = z\Delta m , \quad z < 1. \quad (9.7.3)$$

One obtains an estimate for the production rate of photon energy (only this heats the system) from the incoming electron current I . If a fraction $x(V)$ of the current is transformed to negatively charged color bonds the rate for energy production becomes by a little manipulation

$$\frac{P/kW}{I/A} = x(V)z \times 3.5945 . \tag{9.7.4}$$

This formula allows to estimate the value of the parameter $x(V)z$ from experimental data. Since simplest Feynman graph producing also photons is obtained by adding photon line to the basic graph, one expects that z is of order fine structure constant:

$$z \sim \alpha_{em} = 1/137 . \tag{9.7.5}$$

The ratios of the excess power for a pair of (V, I) values should satisfy the condition

$$\frac{P(V_1)I(V_2)}{P(V_2)I(V_1)} = \frac{x(V_1)}{x(V_2)} . \tag{9.7.6}$$

$x(V)$ should be deducible as a function of voltage using these formulas if the model is correct.

These formulae allow to compare the predictions of the model with the experimental results of Naudin for Mizuno-Omori Cold Fusion reactor [37]. The following table gives the values of $\epsilon = x(V)z$ and ratios $x(V(n))/x(V(n_1))$ deduced from the data tabulated by Naudin [46] for the various series of experiments using the formulae above.

1. Most values of $x(V)z$ are in the range .03 – .12. $z = 1/137$ would give $x(V)z \leq 1/137$ so that order of magnitude is predicted correctly. One cannot over-emphasize this result.

2. Apart from some exceptions the values look rather reasonable and do not vary too much. If one neglects the exceptional values, ones has $x_{max}(V)/x_{min}(V) < 4$. $n = 1, 5, 8, 9, 29$ correspond to exceptionally small values of $x(V)$. Perhaps cold fusion is not present for some reason. The output power is smaller than input power for $n = 9$ and $n = 29$.

n	Voltage/V	Current/A	$x(V)z$	$x(V(n))/x(V(2))$
1	185	8.56	0.005	.145
2	147	2.45	0.036	1.00
3	215	2.10	0.046	1.30
4	220	9.32	0.044	1.22
5	145	1.06	0.001	.03
6	213	1.40	0.05	1.34
7	236	1.73	0.08	2.18
8	148	.83	0.01	.21
9	148	1.01	-0.00	-0.008
10	221	1.31	0.03	.87
11	279	3.03	0.05	1.46
12	200	8.58	0.03	0.89
13	199	7.03	0.07	1.91
14	215	9.78	0.04	1.07
15	207	8.34	0.03	0.74
16	247	2.19	0.06	1.69
17	260	2.20	0.02	0.55
18	257	2.08	0.03	0.71
19	195	2.95	0.06	1.59
20	198	2.62	0.07	1.98
21	182	2.40	0.05	1.26
22	212	2.27	0.06	1.74
23	259	2.13	0.12	3.22
24	260	4.83	0.04	1.05
25	209	3.53	0.04	1.16
26	230	4.99	0.10	2.79
27	231	5.46	0.09	2.53
28	233	5.16	0.10	2.85
29	155	4.60	-0.00	-0.04
30	220	4.44	0.11	2.95
31	256	5.25	0.05	1.36
32	211	3.68	0.03	.97
33	201	3.82	0.04	1.06

Table 3. The values of $x(V)z$ and $x(V(n))/x(V(1))$ deduced from the data of *Cold Fusion reaction-Experimental test results on June 25, 2003 by JL Naudin* at <http://jlnlabs.online.fr/cfr/html/cfrdatas.htm>.

Has living matter invented cold nuclear physics?

Intriguingly, the ions Na^+ , Cl^- , K^+ , Ca^{++} detected by Mizuno in the cathode in Kanarev's experiments [72] correspond to the most important biological ions. There is also a considerable evidence for the occurrence of nuclear transmutations in living matter [40, 41]. For instance, Kervran claims that it is not possible to understand where the Ca needed to form the shells of eggs comes from. A possible explanation is that dark nuclear reactions between Na^+ and dark Lithium produced the needed Ca .

There is extremely strong electric field through cell membrane (resting voltage is about .06 V). The acceleration of electrons in this field could generate plasma phase and creation of dark Li nuclei via a positive feedback loop. This could mean that cold nuclear reactions serve also in living cell as a basic metabolic energy source (possibly in the dark sector) and that also biologically important ions result as products of cold nuclear reactions.

9.7.7 Comparison with the reports about biological transmutations

Kervran's book "Biological Transmutations" [40] contains a surprisingly detailed summary about his work with biological transmutations and it is interesting to find whether the proposed model could explain the findings of Kervran. TGD suggests two general mechanisms.

1. The nuclear reactions involving dark Li , C , and F predicted to be present in living matter.
2. Nuclear fusions made possible by a temporary transformation of ordinary nuclear space-time sheets to dark ones with much larger size so that Coulomb wall is reduced considerably. The nuclear reaction might proceed if it is energetically possible. Almost any reaction $A + B \rightarrow C$ is possible via this mechanism unless the nuclei are not too heavy.

Fortuitous observations

In his childhood Kervran started to wonder why hens living in a limestone poor region containing thus very little calcium in ground and receiving no calcium in their nutrition could develop the calcium required by eggs and by their own bones. He noticed that hens had the habit of eating mica, which contains silicon. Later this led to the idea that Si could somehow transmute to Ca in living matter. In the proposed model this could correspond to fusion of $Si(14, 14) + \mathbf{C}(6, 6) \rightarrow Ca(20, 20)$ which occurs spontaneously.

Second fortuitous observation were the mysterious CO poisonings by welders working in factory. After careful studies Kervran concluded that CO must be produced endogenously and proposed that the inhaled air which had been in contact with incandescent iron induces the transformation $N_2 \rightarrow CO$ conserving both neutron and neutron number. This transformation might be understood in TGD context if the nuclear space-time sheets are part of time in dark with much larger size so that a direct contact becomes possible for nuclear space-time sheets and Coulomb wall is reduced so that the reaction can proceed with some probability if energetically possible. The thermal energy received from hot iron might help to overcome the Coulomb barrier. The mass difference $m(2N) - m(O) - m(C) = 10.45$ MeV allows this reaction to occur spontaneously.

Examples of various anomalies

Kervran discusses several plant anomalies. The ashes of plants growing in Si rich soil contain more Ca than they should: this transmutation has been already discussed. The ashes of a plant growing on Cu fibres contain no copper but 17 per cent of iron oxides in addition to other elements which could not have come from the rain water. The reaction $Cu(58) + \mathbf{Li}(3, 4) \rightarrow Fe(26, 32) + \mathbf{C}(6, 6)$ would liberate energy of 11.5 MeV.

There are several mineral anomalies.

1. Dolomite rock is formed inside limestone rocks which would suggest the transmutation of $Ca(20, 20)$ into $Mg(12, 12)$. The nuclear reaction $Ca(20, 20) + \mathbf{Li}(3, 4) \rightarrow Mg(12, 12) + Na(11, 12)$ would liberate energy of 3.46 MeV. Ca emerges from Si in soil and in what Kervran refers to a "sickness of stone". The candidate reaction has been already discussed.
2. Graphite is found in siliceous rocks. Kervran proposes the reaction $Si \rightarrow C + O$. $m(Si) - m(C) - m(O) = -16.798$ MeV does not allow this reaction to proceed spontaneously but the reaction $Si + \mathbf{Li} \rightarrow C + Na$ liberates the energy 2.8880 MeV.
3. Kervran mentions the reaction $O + O \rightarrow S$ as a manner to produce sulphur from oxygen. This reaction is obviously energetically favored.

Kervran discusses the transmutations $Na \rightarrow K$ and $Na \rightarrow Ca$ occurring also in plasma electrolysis and explained by TGD based model. Further transmutations are $Na \rightarrow Mg$ and $Mg \rightarrow Ca$. $Na \rightarrow Mg$ could correspond to the reaction $Na(11, 12) + \mathbf{Li}(3, 2) \rightarrow Mg(12, 12) + He(2, 2)$ favored by the high binding energy per nucleon for 4He (7.072 MeV). $Mg \rightarrow Ca$ would correspond to the reaction $Mg + O \rightarrow Ca$, which obviously liberates energy.

9.7.8 Are the abundances of heavier elements determined by cold fusion in interstellar medium?

According to the standard model, elements not heavier than *Li* were created in Big Bang. Heavier elements were produced in stars by nuclear fusion and ended up to the interstellar space in super-nova explosions and were gradually enriched in this process. Lithium problem forces to take this theoretical framework with a grain of salt.

The work of Kervran [40] suggests that cold nuclear reactions are occurring with considerable rates, not only in living matter but also in non-organic matter. Kervran indeed proposes that also the abundances of elements at Earth and planets are to high degree determined by nuclear transmutations and discusses some examples. For instance, new mechanisms for generation of *O* and *Si* would change dramatically the existing views about evolution of planets and prebiotic evolution of Earth.

Are heavier nuclei produced in the interstellar space?

TGD based model is consistent with the findings of Kervran and encourages to a consider a simple model for the generation of heavier elements in interstellar medium. The assumptions are following.

1. Dark nuclei $X(3k, n)$, that is nuclear strings of form $Li(3, n)$, $C(6, n)$, $F(9, n)$, $Mg(12, n)$, $P(15, n)$, $A(18, n)$, etc..., form as a fusion of *Li* strings. $n = Z$ is the most plausible value of n . There is also 4He present but as a noble gas it need not play an important role in condensed matter phase (say interstellar dust). The presence of water necessitates that of $Li(3, n)$ if one accepts the proposed model as such.
2. The resulting nuclei are in general stable against spontaneous fission by energy conservation. The binding energy of $He(2, 2)$ is however exceptionally high so that alpha decay can occur in dark nuclear reactions between $X(3k, n)$ allowed by the considerable reduction of the Coulomb wall. The induced fissions $X(3k, n) \rightarrow X(3k - 2, n - 2) + He(2, 2)$ produces nuclei with atomic number $Z \bmod 3 = 1$ such as $Be(4, 5)$, $N(7, 7)$, $Ne(10, 10)$, $Al(13, 14)$, $S(16, 16)$, $K(19, 20)$,... Similar nuclear reactions make possible a further alpha decay of $Z \bmod 3 = 1$ nuclei to give nuclei with $Z \bmod 2$ such as $B(5, 6)$, $O(8, 8)$, $Na(11, 12)$, $Si(14, 14)$, $Cl(17, 18)$, $Ca(20, 20)$,... so that most stable isotopes of light nuclei could result in these fissions.
3. The dark nuclear fusions of already existing nuclei can create also heavier *Fe*. Only the gradual decrease of the binding energy per nucleon for nuclei heavier than *Fe* poses restrictions on this process.

The table below allows the reader to build a more concrete view about how the heavier nuclei might be generated via the proposed mechanisms.

H(1,0)							He(2,2)
Li(3,4)	Be(4,5)	B(5,6)	C(6,6)	N(7,7)	O(8,8)	F(9,10)	Ne(10,10)
Na(11,12)	Mg(12,12)	Al(13,14)	Si(14,14)	P(15,16)	S(16,16)	Cl(17,18)	A(18,22)
K(19,20)	Ca(20,20)						

Table 4. The table gives the most abundant isotopes of stable nuclei.

The abundances of nuclei in interstellar space should not depend on time

The basic prediction of TGD inspired model is that the abundances of the nuclei in the interstellar space should not depend on time if the rates are so high that equilibrium situation is reached rapidly. The \hbar increasing phase transformation of the nuclear space-time sheet determines the time scale in which equilibrium sets on. Standard model makes different prediction: the abundances of the heavier nuclei should gradually increase as the nuclei are repeatedly re-processed in stars and blown out to the interstellar space in super-nova explosion.

Amazingly, there is empirical support for this highly non-trivial prediction [75]. Quite surprisingly, the 25 measured elemental abundances (elements up to $Sn(50, 70)$ (tin) and $Pb(82, 124)$ (lead)) of a 12 billion years old galaxy turned out to be very nearly the same as those for Sun. For instance, oxygen abundance was 1/3 from that from that estimated for Sun. Standard model would predict that the abundances should be .01-.1 from that for Sun as measured for stars in our galaxy. The conjecture was that there must be some unknown law guaranteing that the distribution of stars of various masses

is time independent. The alternative conclusion would be that heavier elements are created mostly in interstellar gas and dust.

Could also "ordinary" nuclei consist of protons and negatively charged color bonds?

The model would strongly suggest that also ordinary stable nuclei consist of protons with proton and negatively charged color bond behaving effectively like neutron. Note however that I have also consider the possibility that neutron halo consists of protons connected by negatively charged color bonds to main nucleus. The smaller mass of proton would favor it as a fundamental building block of nucleus and negatively charged color bonds would be a natural manner to minimize Coulomb energy. The fact that neutron does not suffer a beta decay to proton in nuclear environment provided by stable nuclei would also find an explanation.

1. Ordinary shell model of nucleus would make sense in length scales in which proton plus negatively charged color bond looks like neutron.
2. The strictly nucleonic strong nuclear isospin is not vanishing for the ground state nuclei if all nucleons are protons. This assumption of the nuclear string model is crucial for quantum criticality since it implies that binding energies are not changed in the scaling of \hbar if the length of the color bonds is not changed. The quarks of charged color bond however give rise to a compensating strong isospin and color bond plus proton behaves in a good approximation like neutron.
3. Beta decays might pose a problem for this model. The electrons resulting in beta decays of this kind nuclei consisting of protons should come from the beta decay of the d -quark neutralizing negatively charged color bond. The nuclei generated in high energy nuclear reactions would presumably contain genuine neutrons and suffer beta decay in which d quark is nucleonic quark. The question is whether how much the rates for these two kinds of beta decays differ and whether existing facts about beta decays could kill the model.

9.7.9 Tests and improvements

Test for the hypothesis about new physics of water

The model involves hypothesis about new physics and chemistry related to water.

1. The identification of hydrogen bond as dark OH bond could be tested. One could check whether the qualitative properties of bonds are consistent with each. One could try to find evidence for quantization of bond energies as integer multiples of same energy (possible power of two multiples).
2. $H_{1.5}O$ formula in atto-second scale should be tested further and one could look whether similar formula holds true for heavy water so that sequences of dark protons might be replaced with sequences of dark deuterons.
3. One could find whether plasma electrolysis takes place in heavy water.

Testing of the nuclear physics predictions

The model in its simplest form assumes that only dark Li , C , F , etc. are present in water. This predicts quite specific nuclear reactions in electrolyte and target and reaction product. For both target and electrolyte isotopes of nuclei with atomic number $Z + k3$ are predicted to result in cold fusion reactions if energetically possible. For a target heavier than Fe also fission reactions might take place.

The estimates for the liberated energies are obtained assuming that dark nuclei have same binding energies as ordinary ones. In some cases the liberated energy is estimated using the binding energy per nucleon for a lighter isotope. Ordinary nuclei with maximal binding energy correspond to nuclear strings having 4He or its variants containing negatively charged color bonds as a basic structural unit. One could argue that gluing $nLi(3,5)$ or its isotope does not give rise to a ground state so that the actual energy liberated in the process is reduced so that process might be even impossible

energetically. This could explain the absence of *Ge* from *Fe* cathode and the absence of *Ti*, *Mn*, and *Ni* in *KOH* plasma electrolysis [72].

Cathode: For cathode *Fe* and *W* have been used. For *Fe* the fusions $Fe + Li \rightarrow Cu + 28.84 \text{ MeV}$ and $Fe + C \rightarrow Ge + 21.64 \text{ MeV}$ are possible energetically. Mizuno does not report the presence of *Ge* in *Fe* target. The reduction of the binding energy of dark $C(6, 10)$ by 21.64 MeV (1.35 MeV per nucleon) would make second reaction impossible but would still allow $Li + C$ and $Na + C$ fusion. Second possibility is that *Ge* containing negatively charged color bonds has smaller binding energy per nucleon than ordinary *Ge*. $W + Li \rightarrow Ir$ would liberate 8.7 MeV if binding energy of dark *Li* is same as of ordinary *Li*.

Electrolyte: Consider electrolytes containing ions X^+ with atomic number Z . If X is lighter than *Fe*, the isotopes of nuclei with atomic number $Z + 3k$ might be produced in fusion reactions $nLi + X$. $X = Li, K, Na$ has one electron at s-shell whereas *B*, *Al*, *Cr*, ... has one electron at p-shell.

Reaction	Li + <i>Li</i> → <i>C</i>	C + <i>Li</i> → <i>F</i>	F + <i>Li</i> → <i>Mg</i>
<i>E/MeV</i>	27.1	24.0	31.5
	Li + <i>Na</i> → <i>Si</i>	C + <i>Na</i> → <i>Cl</i>	F + <i>Na</i> → <i>Ca</i>
<i>E/MeV</i>	34.4	30.5	33.7
	Li + <i>K</i> → <i>Ti</i>	C + <i>K</i> → <i>Mn</i>	F + <i>K</i> → <i>Ni</i>
<i>E/MeV</i>	32.2	33.6	32.7

Table 5. The estimates for the energies liberated in fusions of dark nuclei of water and the ion of electrolyte. Boldface refers to dark nuclei $Li(3, 5)$, $C(6, 10)$, and $F(9, 15)$.

Relationship to the model of Widom and Larsen and further tests

W. Guglinski kindly informed me about the theory of cold fusion by Widom and Larsen [49]. This theory relies on standard nuclear physics. The theory is reported to explain cold fusion reaction products nicely in terms of the transformation of electrons and protons to very low energy neutrons which can overcome the Coulomb barrier. The problem of the theory is that very high energy electrons are required since one has $Q = .78 \text{ MeV}$ for $e + p \rightarrow n$ and $Q = -3.0 \text{ MeV}$ for $e + D \rightarrow n + n$. It is difficult to understand how so energetic electrons could result in ordinary condensed matter.

Since proton plus color bond is from the point of view of nuclear physics neutron and the fusion reactions would obey ordinary nuclear physics rules, the predictions of TGD are not expected to deviate too much from those of the model of Widom and Larsen.

An important class of predictions relate to ordinary nuclear physics. Tetra-neutron could be alpha particle with two negatively charged color bonds and neutron halos could consist of protons connected to nucleus by negatively charged color bonds. This could reduce the binding energy considerably.

Cold nuclear fusion might also provide an in situ mechanism for the formation of ores. Nuclear ores in places where they should not exist but involving remnants of organic matter would be the prediction. Cold fusion has a potential for a technology allowing to generate some metals artificially.

How to optimize the energy production?

The proposed model for the plasma electrolysis suggests following improvements to the experimental arrangement.

The production of energy in process is due to three reactions: 1) $Li + p$ in plasma. 2) $Li + Fe/W...$ in target, and 3) $Li + Na/K...$ in plasma. The model suggests that 1) dominates so that basic process would occur in plasma rather than cathode.

1. Since *W* does not evaporate so easily, it is better material for cathode if the production of dark *Li* dominates energy production.
2. Cathode could be replaced with a planar electrode with fractal peaky structure generating the required strong electric fields. This could increase the effectiveness of the energy production by increasing the effective area used.

3. Since $H_2O \rightarrow OH^- + p$ is required by the generation of dark Li sequences. The energy feed must be able to follow the rapidly growing energy needs of this reaction which seems to occur as bursts.
4. The prediction is that the output power is proportional to electron current rather than input power. This suggests minimization of input power by minimizing voltage. This requires maximization of electron conductivity. Unfortunately, the transformation of electrons to OH^- ions as charge carriers reduces conductivity.

9.7.10 Burning salt water by radio-waves and cold fusion by plasma electrolysis

John Kanzius has made a strange discovery [79]: salt water in the test tube radiated by radio waves at harmonics of a frequency $f=13.56$ MHz burns. Temperatures about 1500 C, which correspond to .17 eV energy have been reported. One can radiate also hand but nothing happens. The original discovery of Kanzius was the finding that radio waves could be used to cure cancer by destroying the cancer cells. The proposal is that this effect might provide new energy source by liberating chemical energy in an exceptionally effective manner. The power is about 200 W so that the power used could explain the effect if it is absorbed in resonance like manner by salt water. In the following it is proposed that the cold nuclear reactions are the source of the energy.

Do radio waves of large Planck constant transform to microwave photons or visible photons in the process?

The energies of photons involved are very small, multiples of 5.6×10^{-8} eV and their effect should be very small since it is difficult to imagine what resonant molecular transition could cause the effect. This leads to the question whether the radio wave beam could contain a considerable fraction of dark photons for which Planck constant is larger so that the energy of photons is much larger. The underlying mechanism would be phase transition of dark photons with large Planck constant to ordinary photons with shorter wavelength coupling resonantly to some molecular degrees of freedom and inducing the heating. Microwave oven of course comes in mind immediately. The fact that photosynthesis means burning of water and the fact that visible light is emitted in turn suggests that the radiowave photons are transformed to visible or nearly visible photons corresponding to the energy scale of photons involved with photosynthesis.

The original argument inspired by the analogy with microwave oven is discussed below. The generalization to the case of visible photons is rather straightforward and is discussed in [27].

1. The fact that the effects occur at harmonics of the fundamental frequency suggests that rotational states of molecules are in question as in microwave heating. The formula for the rotational energies [67] is

$$E(l) = E_0 \times (l(l+1)) \quad , \quad E_0 = \hbar_0^2 / 2\mu R^2 \quad , \quad \mu = m_1 m_2 / (m_1 + m_2) \quad .$$

Here R is molecular radius which by definition is deduced from the rotational energy spectrum. The energy inducing the transition $l \rightarrow l+1$ is $\Delta E(l) = 2E_0 \times (l+1)$.

2. $NaCl$ molecules crystallize to solid so that the rotational heating of $NaCl$ molecules cannot be in question.
3. The microwave frequency used in microwave ovens is 2.45 GHz giving for the Planck constant the estimate 180.67 equal to 180 with error of .4 per cent. The values of Planck constants for $(\hat{M}^4/G_a) \times \hat{C}P_2 \hat{\times} G_b$ option (factor space of M^4 and covering space of CP_2 maximizing Planck constant for given G_a and G_b) are given by $\hbar/\hbar_0 = n_a n_b$. $n_a n_b = 4 \times 9 \times 5 = 180$ can result from the number theoretically simple values of quantum phases $exp(i2\pi/n_i)$ corresponding to polygons constructible using only ruler and compass. For instance, one could have $n_a = 2 \times 3$ and $n_b = 2 \times 3 \times 5$.

Connection with plasma electrolysis?

The burning of salt water involves also the production of O_2 and H_2 gases. Usually this happens in the electrolysis of water [73]. The arrangement involves typically electrolyte consisting of water plus $NaOH$ or KOH present also now but anode, cathode and electronic current absent. The proposed mechanism of electrolysis involving cold nuclear reactions however allows the splitting of water molecules to H_2 and O_2 even without these prerequisites.

The thermal radiation from the plasma created in the process has temperature about 1500 C which correspond to energy about .17 eV: this is not enough for splitting of bonds with energy .5 eV. The temperature in salt water could be however considerably higher.

The presence of visible light suggests that plasma phase is created as in plasma electrolysis. Dark nuclear reactions would provide the energy leading to ionization of hydrogen atoms and subsequent transformation of the electronic charge to that of charged color bonds in protonic strings. This in turn would increase the rate of cold nuclear reactions and the liberated energy would ionize more hydrogen atoms so that a positive feedback loop would result.

Cold nuclear reactions should provide the energy transforming hydrogen bonds to dark bonds with energy scaled down by a factor of about 2^{-6} from say 8 eV to .125 eV if $T = 1500C$ is accepted as temperature of water. If Planck constant is scaled up by the factor $r = 180$ suggested by the interpretation in terms of microwave heating, the scaling of the Planck constant would reduce the energy of OH bonds to about .04 eV, which happens to be slightly below the energy assignable to the cell membrane resting potential. The scaling of the size of nuclear space-time sheets of D by factor $r = 180$ is consistent with the length of color bonds of order 10^{-12} m. The role of microwave heating would be to preserve this temperature so that the electrolysis of water can continue. Note that the energy from cold nuclear reactions could partially escape as dark photons.

There are some questions to be answered.

1. Are the radio wave photons dark or does water - which is a very special kind of liquid - induce the transformation of ordinary radio wave photons to dark photons by fusing 180 radio wave massless extremals (MEs) to single ME. Does this transformation occur for all frequencies? This kind of transformation might play a key role in transforming ordinary EEG photons to dark photons and partially explain the special role of water in living systems.
2. Why the radiation does not induce a spontaneous combustion of living matter which also contains Na^+ and other ions. A possible reason is that \hbar corresponds to Planck constant of dark Li which is much higher in living water. Hence the energies of dark photons do not induce microwave heating.
3. The visible light generated in the process has yellow color. The mundane explanation is that the introduction Na or its compounds into flame yields bright yellow color due to so called sodium D-lines [48] at 588.9950 and 589.5924 nm emitted in transition from 3p to 3s level. Visible light could result as dark photons from the dropping of dark protons from dark space-time sheets of size at least atomic size to larger dark space-time sheets or to ordinary space-time sheets of same size and de-cohere to ordinary light. Yellow light corresponds roughly to the rather narrow energy range .96-2.1 eV (.59 - .63 μm). The metabolic quanta correspond to jumps to space-time sheets of increasing size give rise to the fractal series $E/eV = 2 \times (1 - 2^{-n})$ for transitions $k = 135 \rightarrow 135 + n$, $n = 1, 2, \dots$ [27]. For $n = 3, 4, 5$ the lines have energies 1.74, 1.87, 1.93 eV and are in the visible red ($\lambda/\mu m = .71, .66, .64$). For $n > 5$ the color is yellow. In Kanarev's experiments the color is red which would mean the dominance of $n < 6$ lines: this color is regarded as a signature of the plasma electrolysis. In the burning of salt water the light is yellow [79], which allows to consider the possibility that yellow light is partially due to $n > 5$ lines. Yellow color could also result from the dropping $k = 134 \rightarrow 135$ ($n = 1$).

9.7.11 GSI anomaly

"Jester" wrote a nice blog posting titled *Hitchhikers-guide-to-ghosts-and-spooks in particle physics* summarizing quite a bundle of anomalies of particle physics and also one of nuclear physics- known as GSI anomaly. The abstract of the article *Observation of Non-Exponential Orbital Electron Capture Decays of Hydrogen-Like ^{140}Pr and ^{142}Pm Ions* [29] describing the anomaly is here.

We report on time-modulated two-body weak decays observed in the orbital electron capture of hydrogen-like ^{140}Pr and ^{142}Pm ions coasting in an ion storage ring. Using non-destructive single ion, time-resolved Schottky mass spectrometry we found that the expected exponential decay is modulated in time with a modulation period of about 7 seconds for both systems. Tentatively this observation is attributed to the coherent superposition of finite mass eigenstates of the electron neutrinos from the weak decay into a two-body final state.

This brings in mind the nuclear decay rate anomalies which I discussed earlier in the blog posting *Tritium beta decay anomaly and variations in the rates of radioactive processes* and in [23]. These variations in decay rates are in the scale of year and decay rate variation correlates with the distance from Sun. Also solar flares seem to induce decay rate variations.

The TGD based explanation [23] relies on nuclear string model in which nuclei are connected by color flux tubes having exotic variant quark and antiquark at their ends (TGD predicts fractal hierarchy of QCD like physics). These flux tubes can be also charged: the possible charges $\pm 1, 0$. This means a rich spectrum of exotic states and a lot of new low energy nuclear physics. The energy scale corresponds to Coulomb interaction energy $\alpha_{em}m$, where m is mass scale of the exotic quark. This means energy scale of 10 keV for MeV mass scale. The well-known poorly understood X-ray bursts from Sun during solar flares in the wavelength range 1-8 Å correspond to energies in the range 1.6-12.4 keV -3 octaves in good approximation- might relate to this new nuclear physics and in turn might excite nuclei from the ground state to these excited states and the small mixture of exotic nuclei with slightly different nuclear decay rates could cause the effective variation of the decay rate. The mass scale $m \sim 1$ MeV for exotic quarks would predict Coulombic energy of order $\alpha_{em}m$ which is of order 10 keV.

The question is whether there could be a flux of X rays in time scale of 7 seconds causing the rate fluctuation by the same mechanism also in GSI experiment. For instance, could this flux relate to synchrotron radiation. I could not identify any candidate for this periodicity from the article. In any case, the prediction is what might be called X ray nuclear physics and artificial X ray irradiation of nuclei would be an easy manner to kill or prove the general hypothesis.

One can imagine also another possibility.

1. The first guess is that the transitions between ordinary and exotic states of the ion are induced by the emission of exotic W boson between nucleon and exotic quark so that the charge of the color bond is changed. In standard model the objection would be that classical W fields do not make sense in the length scale in question. The basic prediction deriving from induced field concept (classical ew gauge fields correspond to the projection of CP_2 spinor curvature to the space-time surface) is however the existence of classical long range gauge fields- both ew and color. Classical W field can induce charge entanglement in all length scales and one of the control mechanisms of TGD inspired quantum biology relies on remote control of charge densities in this manner. Also the model of cold fusion could involve similar oscillating time like entanglement allowing the bombarding nucleus to penetrate to the nucleus when proton has transformed to neutron in good approximation and charge is delocalized to the color bond having much larger size.
2. In the approximation that one has two-state system, this interaction can be modelled by using as interaction Hamiltonian hermitian non-diagonal matrix V , which can be written as $V\sigma_x$, where σ_x is Pauli sigma matrix. If this process occurs coherently in time scales longer than \hbar/V , an oscillation with frequency $\omega = V/\hbar$ results. Since weak interactions are in question 7 second modulation period might make sense.

The hypothesis can be tested quantitatively.

1. The weak interaction Coulomb potential energy is of form

$$\frac{V(r)}{\hbar} = \alpha_W \frac{\exp(-m_W r)}{r}, \quad (9.7.7)$$

where r is the distance between nucleon center of mass and the end of color flux tube and therefore of order proton Compton length r_p so that one can write

$$r = x \times r_p \ .$$

where x should be of order unity but below it.

2. The frequency $\omega = 2\pi/\tau = V/\hbar$ must correspond to 14 seconds, twice the oscillation period of the varying reaction rate. By taking W boson Compton time t_W as time unit this condition can be written as

$$\begin{aligned} \frac{\alpha_W \exp(-y)}{y} &= \frac{t_W}{\tau} \ , \\ y &= x \frac{r_p}{r_W} = x \frac{m_W}{m_p} \simeq 80 \times x \ , \\ \alpha_W &= \alpha_{em} / \sin^2 \theta_W \ . \end{aligned}$$

3. This gives the condition

$$\frac{\exp(-y)}{y} = \frac{t_p}{\tau} \times \frac{\sin^2 \theta_W}{80 \times \alpha_{em}} \ . \quad (9.7.8)$$

This allows to solve y since the left hand side is known. Feeding in proton Compton length $r_p = 1.321 \times 10^{-15}$ m and $\sin^2 \theta_W = .23$ one obtains that the distance between flux tube end and proton cm is $x = .6446$ times proton Compton length, which compares favorably with the guess $x \simeq 1$ but smaller than 1. One must however notice that the oscillation period is exponentially sensitive to the value of x . For instance, if the charge entanglement were between nucleons, $x > 1$ would hold true and the time scale would be enormous. Hence the simple model requires new physics and predicts correctly the period of the oscillation under very reasonable assumptions.

4. One could criticize this by saying that the masses of two states differ by amount which is of order 10 keV or so. This does not however affect the argument since the mass corresponds to the diagonal non-interaction part of the Hamiltonian contributing only rapidly oscillating phases whereas interaction potential induces oscillating mixing as is easy to see in interaction picture.
5. If one believes in the hierarchy of Planck constants and p-adically scaled variants of weak interaction physics, charge entanglement would be possible in much longer length scales and the time scale of it raises the question whether qubits could be realized using proton and neutron in quantum computation purposes. I have also proposed that charge entanglement could serve as a mechanism of bio-control allowing to induce charge density gradients from distance in turn acting as switches inducing biological functions.

So: it happened again! Again I have given a good reason for my learned critics to argue that TGD explains everything so that I am a crackpot and so on and so on. Well... after a first feeling of deep shame I dare to defend myself. In the case of standard model explanatory power has not been regarded as an argument against the theory but my case is of course different since I do not have any academic position since my fate is to live in the arctic scientific environment of Finland. And if my name were Feynman, this little argument would be an instant classic. But most theoreticians are just little opportunists building their career and this does not leave much room for intellectual honesty.

9.8 Dark nuclear strings as analogs of DNA-, RNA- and amino-acid sequences and baryonic realization of genetic code?

Water memory is one of the ugly words in the vocabulary of a main stream scientist. The work of pioneers is however now carrying fruit. The group led by Jean-Luc Montagnier, who received Nobel prize for discovering HIV virus, has found strong evidence for water memory and detailed information about the mechanism involved [109, 41, 32]. The work leading to the discovery was motivated by the following mysterious finding. When the water solution containing human cells infected by bacteria

was filtered in purpose of sterilizing it, it indeed satisfied the criteria for the absence of infected cells immediately after the procedure. When one however adds human cells to the filtrate, infected cells appear within few weeks. If this is really the case and if the filter does what it is believed to do, this raises the question whether there might be a representation of genetic code based on nano-structures able to leak through the filter with pores size below 200 nm.

The question is whether dark nuclear strings might provide a representation of the genetic code. In fact, I posed this question year before the results of the experiment came with motivation coming from attempts to understand water memory. The outcome was a totally unexpected finding: the states of dark nucleons formed from three quarks can be naturally grouped to multiplets in one-one correspondence with 64 DNAs, 64 RNAs, and 20 aminoacids and there is natural mapping of DNA and RNA type states to aminoacid type states such that the numbers of DNAs/RNAs mapped to given aminoacid are same as for the vertebrate genetic code.

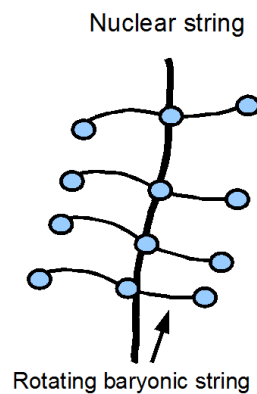


Figure 9.3: Illustration of a possible vision about dark nucleus as a nuclear string consisting of rotating baryonic strings.

The basic idea is simple. Since baryons consist of 3 quarks just as DNA codons consist of three nucleotides, one might ask whether codons could correspond to baryons obtained as open strings with quarks connected by two color flux tubes. This representation would be based on entanglement rather than letter sequences. The question is therefore whether the dark baryons constructed as string of 3 quarks using color flux tubes could realize 64 codons and whether 20 aminoacids could be identified as equivalence classes of some equivalence relation between 64 fundamental codons in a natural manner.

The following model indeed reproduces the genetic code directly from a model of dark neutral baryons as strings of 3 quarks connected by color flux tubes.

1. Dark nuclear baryons are considered as a fundamental realization of DNA codons and constructed as open strings of 3 dark quarks connected by two colored flux tubes, which can be also charged. The baryonic strings cannot combine to form a strictly linear structure since strict rotational invariance would not allow the quark strings to have angular momentum with respect to the quantization axis defined by the nuclear string. The independent rotation of quark strings and breaking of rotational symmetry from $SO(3)$ to $SO(2)$ induced by the direction of the nuclear string is essential for the model.
 - (a) Baryonic strings could form a helical nuclear string (stability might require this) locally parallel to DNA, RNA, or aminoacid) helix with rotations acting either along the axis of the DNA or along the local axis of DNA along helix. The rotation of a flux tube portion around an axis parallel to the local axis along DNA helix requires that magnetic flux tube has a kink in this portion. An interesting question is whether this kink has correlate at the level of DNA too. Notice that color bonds appear in two scales corresponding to these two strings. The model of DNA as topological quantum computer [44] allows a modification in which dark nuclear string of this kind is parallel to DNA and each codon has a flux tube connection to the lipid of cell membrane or possibly to some other bio-molecule.

- (b) The analogs of DNA -, RNA -, and of amino-acid sequences could also correspond to sequences of dark baryons in which baryons would be 3-quark strings in the plane transversal to the dark nuclear string and expected to rotate by stringy boundary conditions. Thus one would have nuclear string consisting of short baryonic strings not connected along their ends (see Fig. 9.8). In this case all baryons would be free to rotate.
2. The new element as compared to the standard quark model is that between both dark quarks and dark baryons can be charged carrying charge $0, \pm 1$. This is assumed also in nuclear string model and there is empirical support for the existence of exotic nuclei containing charged color bonds between nuclei.
 3. The net charge of the dark baryons in question is assumed to vanish to minimize Coulomb repulsion:

$$\sum_q Q_{em}(q) = - \sum_{flux\ tubes} Q_{em}(flux\ tube) . \quad (9.8.1)$$

This kind of selection is natural taking into account the breaking of isospin symmetry. In the recent case the breaking cannot however be as large as for ordinary baryons (implying large mass difference between Δ and nucleon states).

4. One can classify the states of the open 3-quark string by the total charges and spins associated with 3 quarks and to the two color bonds. Total em charges of quarks vary in the range $Z_B \in \{2, 1, 0, -1\}$ and total color bond charges in the range $Z_b \in \{2, 1, 0, -1, -2\}$. Only neutral states are allowed. Total quark spin projection varies in the range $J_B = 3/2, 1/2, -1/2, -3/2$ and the total flux tube spin projection in the range $J_b = 2, 1, -1, -2$. If one takes for a given total charge assumed to be vanishing one representative from each class (J_B, J_b) , one obtains $4 \times 5 = 20$ states which is the number of amino-acids. Thus genetic code might be realized at the level of baryons by mapping the neutral states with a given spin projection to single representative state with the same spin projection. The problem is to find whether one can identify the analogs of DNA, RNA and aminoacids as baryon like states.

9.8.1 States in the quark degrees of freedom

One must construct many-particle states both in quark and flux tube degrees of freedom. These states can be constructed as representations of rotation group $SU(2)$ and strong isospin group $SU(2)$ by using the standard tensor product rule $j_1 \times j_2 = j_1 + j_2 \oplus j_1 + j_2 - 1 \oplus \dots \oplus |j_1 - j_2|$ for the representation of $SU(2)$ and Fermi statistics and Bose-Einstein statistics are used to deduce correlations between total spin and total isospin (for instance, $J = I$ rule holds true in quark degrees of freedom). Charge neutrality is assumed and the breaking of rotational symmetry in the direction of nuclear string is assumed.

Consider first the states of dark baryons in quark degrees of freedom.

1. The tensor product $2 \otimes 2 \otimes 2$ is involved in both cases. Without any additional constraints this tensor product decomposes as $(3 \oplus 1) \otimes 2 = 4 \oplus 2 \oplus 2$: 8 states altogether. This is what one should have for DNA and RNA candidates. If one has only identical quarks uuu or ddd , Pauli exclusion rule allows only the 4-D spin $3/2$ representation corresponding to completely symmetric representation -just as in standard quark model. These 4 states correspond to a candidate for amino-acids. Thus RNA and DNA should correspond to states of type uud and ddu and aminoacids to states of type uuu or ddd . What this means physically will be considered later.
2. Due to spin-statistics constraint only the representations with $(J, I) = (3/2, 3/2)$ (Δ resonance) and the second $(J, I) = (1/2, 1/2)$ (proton and neutron) are realized as free baryons. Now of course a dark -possibly p-adically scaled up - variant of QCD is considered so that more general baryonic states are possible. By the way, the spin statistics problem which forced to introduce quark color strongly suggests that the construction of the codons as sequences of 3 nucleons - which one might also consider - is not a good idea.

3. Second nucleon like spin doublet - call it 2_{odd} - has wrong parity in the sense that it would require $L = 1$ ground state for two identical quarks (uu or dd pair). Dropping 2_{odd} and using only $4 \oplus 2$ for the rotation group would give degeneracies $(1, 2, 2, 1)$ and 6 states only. All the representations in $4 \oplus 2 \oplus 2_{odd}$ are needed to get 8 states with a given quark charge and one should transform the wrong parity doublet to positive parity doublet somehow. Since open string geometry breaks rotational symmetry to a subgroup $SO(2)$ of rotations acting along the direction of the string and since the boundary conditions on baryonic strings force their ends to rotate with light velocity, the attractive possibility is to add a baryonic stringy excitation with angular momentum projection $L_z = -1$ to the wrong parity doublet so that the parity comes out correctly. $L_z = -1$ orbital angular momentum for the relative motion of uu or dd quark pair in the open 3-quark string would be in question. The degeneracies for spin projection value $J_z = 3/2, \dots, -3/2$ are $(1, 2, 3, 2)$. Genetic code means spin projection mapping the states in $4 \oplus 2 \oplus 2_{odd}$ to 4.

9.8.2 States in the flux tube degrees of freedom

Consider next the states in flux tube degrees of freedom.

1. The situation is analogous to a construction of mesons from quarks and antiquarks and one obtains the analogs of π meson (pion) with spin 0 and ρ meson with spin 1 since spin statistics forces $J = I$ condition also now. States of a given charge for a flux tube correspond to the tensor product $2 \otimes 2 = 3 \oplus 1$ for the rotation group.
2. Without any further constraints the tensor product $3 \otimes 3 = 5 \oplus 3 \oplus 1$ for the flux tubes states gives $8+1$ states. By dropping the scalar state this gives 8 states required by DNA and RNA analogs. The degeneracies of the states for DNA/RNA type realization with a given spin projection for $5 \oplus 3$ are $(1, 2, 2, 2, 1)$. 8×8 states result altogether for both uud and udd for which color bonds have different charges. Also for ddd state with quark charge -1 one obtains $5 \oplus 3$ states giving 40 states altogether.
3. If the charges of the color bonds are identical as the are for uuu type states serving as candidates for the counterparts of aminoacids bosonic statistics allows only 5 states ($J = 2$ state). Hence 20 counterparts of aminoacids are obtained for uuu . Genetic code means the projection of the states of $5 \oplus 3$ to those of 5 with the same spin projection and same total charge.

9.8.3 Analogs of DNA, RNA, aminoacids, and of translation and transcription mechanisms

Consider next the identification of analogs of DNA, RNA and aminoacids and the baryonic realization of the genetic code, translation and transcription.

1. The analogs of DNA and RNA can be identified dark baryons with quark content uud , ddu with color bonds having different charges. There are 3 color bond pairs corresponding to charge pairs $(q_1, q_2) = (-1, 0), (-1, 1), (0, 1)$ (the order of charges does not matter). The condition that the total charge of dark baryon vanishes allows for uud only the bond pair $(-1, 0)$ and for udd only the pair $(-1, 1)$. These thus only single neutral dark baryon of type uud resp. udd : these would be the analogs of DNA and RNA codons. Amino-acids would correspond to uuu states with identical color bonds with charges $(-1, -1), (0, 0)$, or $(1, 1)$. uuu with color bond charges $(-1, -1)$ is the only neutral state. Hence only the analogs of DNA, RNA, and aminoacids are obtained, which is rather remarkable result.
2. The basic transcription and translation machinery could be realized as processes in which the analog of DNA can replicate, and can be transcribed to the analog of mRNA in turn translated to the analogs of amino-acids. In terms of flux tube connections the realization of genetic code, transcription, and translation, would mean that only dark baryons with same total quark spin and same total color bond spin can be connected by flux tubes. Charges are of course identical since they vanish.

- Genetic code maps of $(4 \oplus 2 \oplus 2) \otimes (5 \oplus 3)$ to the states of 4×5 . The most natural map takes the states with a given spin to a state with the same spin so that the code is unique. This would give the degeneracies $D(k)$ as products of numbers $D_B \in \{1, 2, 3, 2\}$ and $D_b \in \{1, 2, 2, 2, 1\}$: $D = D_B \times D_b$. Only the observed degeneracies $D = 1, 2, 3, 4, 6$ are predicted. The numbers $N(k)$ of aminoacids coded by D codons would be

$$[N(1), N(2), N(3), N(4), N(6)] = [2, 7, 2, 6, 3] .$$

The correct numbers for vertebrate nuclear code are $(N(1), N(2), N(3), N(4), N(6)) = (2, 9, 1, 5, 3)$. Some kind of symmetry breaking must take place and should relate to the emergence of stopping codons. If one codon in second 3-plet becomes stopping codon, the 3-plet becomes doublet. If 2 codons in 4-plet become stopping codons it also becomes doublet and one obtains the correct result $(2, 9, 1, 5, 3)!$

- Stopping codons would most naturally correspond to the codons, which involve the $L_z = -1$ relative rotational excitation of uu or dd type quark pair. For the 3-plet the two candidates for the stopping codon state are $|1/2, -1/2\rangle \otimes \{|2, k\rangle\}$, $k = 2, -2$. The total spins are $J_z = 3/2$ and $J_z = -7/2$. The three candidates for the 4-plet from which two states are thrown out are $|1/2, -3/2\rangle \otimes \{|2, k\rangle, |1, k\rangle\}$, $k = 1, 0, -1$. The total spins are now $J_z = -1/2, -3/2, -5/2$. One guess is that the states with smallest value of J_z are dropped which would mean that $J_z = -7/2$ states in 3-plet and $J_z = -5/2$ states 4-plet become stopping codons.
- One can ask why just vertebrate code? Why not vertebrate mitochondrial code, which has unbroken $A-G$ and $T-C$ symmetries with respect to the third nucleotide. And is it possible to understand the rarely occurring variants of the genetic code in this framework? One explanation is that the baryonic realization is the fundamental one and biochemical realization has gradually evolved from non-faithful realization to a faithful one as kind of emulation of dark nuclear physics. Also the role of tRNA in the realization of the code is crucial and could explain the fact that the code can be context sensitive for some codons.

9.8.4 Understanding the symmetries of the code

Quantum entanglement between quarks and color flux tubes would be essential for the baryonic realization of the genetic code whereas chemical realization could be said to be classical. Quantal aspect means that one cannot decompose to codon to letters anymore. This raises questions concerning the symmetries of the code.

- What is the counterpart for the conjugation $ZYZ \rightarrow X_c Y_c Z_c$ for the codons?
- The conjugation of the second nucleotide Y having chemical interpretation in terms of hydrophoby-hydrophily dichotomy in biology. In DNA as tqc model it corresponds to matter-antimatter conjugation for quarks associated with flux tubes connecting DNA nucleotides to the lipids of the cell membrane. What is the interpretation in now?
- The A-G, T-C symmetries with respect to the third nucleotide Z allow an interpretation as weak isospin symmetry in DNA as tqc model. Can one identify counterpart of this symmetry when the decomposition into individual nucleotides does not make sense?

Natural candidates for the building blocks of the analogs of these symmetries are the change of the sign of the spin direction for quarks and for flux tubes.

- For quarks the spin projections are always non-vanishing so that the map has no fixed points. For flux tube spin the states of spin $S_z = 0$ are fixed points. The change of the sign of quark spin projection must therefore be present for both $XYZ \rightarrow X_c Y_c Z_c$ and $Y \rightarrow Y_c$ but also something else might be needed. Note that without the symmetry breaking $(1, 3, 3, 1) \rightarrow (1, 2, 3, 2)$ the code table would be symmetric in the permutation of 2 first and 2 last columns of the code table induced by both full conjugation and conjugation of Y .

2. The analogs of the approximate $A - G$ and $T - C$ symmetries cannot involve the change of spin direction in neither quark nor flux tube sector. These symmetries act inside the A-G and T-C sub-2-columns of the 4-columns defining the rows of the code table. Hence this symmetry must permute the states of same spin inside 5 and 3 for flux tubes and 4 and 2 for quarks but leave 2_{odd} invariant. This guarantees that for the two non-degenerate codons coding for only single amino-acid and one of the codons inside triplet the action is trivial. Hence the baryonic analog of the approximate $A - G$ and $T - C$ symmetry would be exact symmetry and be due to the basic definition of the genetic code as a mapping states of same flux tube spin and quark spin to single representative state. The existence of full 4-columns coding for the same aminoacid would be due to the fact that states with same quark spin inside $(2, 3, 2)$ code for the same amino-acid.
3. A detailed comparison of the code table with the code table in spin representation should allow to fix their correspondence uniquely apart from permutations of n-plets and thus also the representation of the conjugations. What is clear that Y conjugation must involve the change of quark spin direction whereas Z conjugation which maps typically 2-plets to each other must involve the permutation of states with same J_z for the flux tubes. It is not quite clear what X conjugation correspond to.

9.8.5 Some comments about the physics behind the code

Consider next some particle physicist's objections against this picture.

1. The realization of the code requires the dark scaled variants of spin 3/2 baryons known as Δ resonance and the analogs (and only the analogs) of spin 1 mesons known as ρ mesons. The lifetime of these states is very short in ordinary hadron physics. Now one has a scaled up variant of hadron physics: possibly in both dark and p-adic senses with latter allowing arbitrarily small overall mass scales. Hence the lifetimes of states can be scaled up.
2. Both the absolute and relative mass differences between Δ and N resp. ρ and π are large in ordinary hadron physics and this makes the decays of Δ and ρ possible kinematically. This is due to color magnetic spin-spin splitting proportional to the color coupling strength $\alpha_s \sim .1$, which is large. In the recent case α_s could be considerably smaller - say of the same order of magnitude as fine structure constant $1/137$ - so that the mass splittings could be so small as to make decays impossible.
3. Dark hadrons could have lower mass scale than the ordinary ones if scaled up variants of quarks in p-adic sense are in question. Note that the model for cold fusion that inspired the idea about genetic code requires that dark nuclear strings have the same mass scale as ordinary baryons. In any case, the most general option inspired by the vision about hierarchy of conscious entities extended to a hierarchy of life forms is that several dark and p-adic scaled up variants of baryons realizing genetic code are possible.
4. The heaviest objection relates to the addition of $L_z = -1$ excitation to $S_z = |1/2, \pm 1/2\rangle_{odd}$ states which transforms the degeneracies of the quark spin states from $(1, 3, 3, 1)$ to $(1, 2, 3, 2)$. The only reasonable answer is that the breaking of the full rotation symmetry reduces $SO(3)$ to $SO(2)$. Also the fact that the states of massless particles are labeled by the representation of $SO(2)$ might be of some relevance. The deeper level explanation in TGD framework might be as follows. The generalized imbedding space is constructed by gluing almost copies of the 8-D imbedding space with different Planck constants together along a 4-D subspace like pages of book along a common back. The construction involves symmetry breaking in both rotational and color degrees of freedom to Cartan sub-group and the interpretation is as a geometric representation for the selection of the quantization axis. Quantum TGD is indeed meant to be a geometrization of the entire quantum physics as a physics of the classical spinor fields in the "world of classical worlds" so that also the choice of measurement axis must have a geometric description.

The conclusion is that genetic code can be understood as a map of stringy baryonic states induced by the projection of all states with same spin projection to a representative state with the same spin projection. Genetic code would be realized at the level of dark nuclear physics and biochemical

representation would be only one particular higher level representation of the code. A hierarchy of dark baryon realizations corresponding to p-adic and dark matter hierarchies can be considered. Translation and transcription machinery would be realized by flux tubes connecting only states with same quark spin and flux tube spin. Charge neutrality is essential for having only the analogs of DNA, RNA and aminoacids and would guarantee the em stability of the states.

Acknowledgements

I am grateful for Elio Conte for discussions which inspired further study of the nuclear string model.

Bibliography

Books about TGD

- [1] M. Pitkänen (2006), *Topological Geometroynamics: Overview*.
http://tgd.wippiespace.com/public_html/tgdview/tgdview.html.
- [2] M. Pitkänen (2006), *Quantum Physics as Infinite-Dimensional Geometry*.
http://tgd.wippiespace.com/public_html/tgdgeom/tgdgeom.html.
- [3] M. Pitkänen (2006), *Physics in Many-Sheeted Space-Time*.
http://tgd.wippiespace.com/public_html/tgdclass/tgdclass.html.
- [4] M. Pitkänen (2006), *p-Adic length Scale Hypothesis and Dark Matter Hierarchy*.
http://tgd.wippiespace.com/public_html/paddark/paddark.html.
- [5] M. Pitkänen (2006), *Quantum TGD*.
http://tgd.wippiespace.com/public_html/tgdquant/tgdquant.html.
- [6] M. Pitkänen (2006), *TGD as a Generalized Number Theory*.
http://tgd.wippiespace.com/public_html/tgdnumber/tgdnumber.html.
- [7] M. Pitkänen (2006), *TGD and Fringe Physics*.
http://tgd.wippiespace.com/public_html/freenergy/freenergy.html.

Books about TGD Inspired Theory of Consciousness and Quantum Biology

- [8] M. Pitkänen (2006), *TGD Inspired Theory of Consciousness*.
http://tgd.wippiespace.com/public_html/tgdconsc/tgdconsc.html.
- [9] M. Pitkänen (2006), *Bio-Systems as Self-Organizing Quantum Systems*.
http://tgd.wippiespace.com/public_html/bioselforg/bioselforg.html.
- [10] M. Pitkänen (2006), *Quantum Hardware of Living Matter*.
http://tgd.wippiespace.com/public_html/bioware/bioware.html.
- [11] M. Pitkänen (2006), *Bio-Systems as Conscious Holograms*.
http://tgd.wippiespace.com/public_html/hologram/hologram.html.
- [12] M. Pitkänen (2006), *Genes and Memes*.
http://tgd.wippiespace.com/public_html/genememe/genememe.html.
- [13] M. Pitkänen (2006), *Magnetospheric Consciousness*.
http://tgd.wippiespace.com/public_html/magnconsc/magnconsc.html.
- [14] M. Pitkänen (2006), *Mathematical Aspects of Consciousness Theory*.
http://tgd.wippiespace.com/public_html/mathconsc/mathconsc.html.
- [15] M. Pitkänen (2006), *TGD and EEG*.
http://tgd.wippiespace.com/public_html/tgdeeg/tgdeeg.html.

References to the chapters of the books about TGD

- [16] The chapter *The Recent Status of Leptohadron Hypothesis* of [4].
http://tgd.wippiespace.com/public_html/paddark/paddark.html#leptc.
- [17] The chapter *TGD and Nuclear Physics* of [4].
http://tgd.wippiespace.com/public_html/paddark/paddark.html#padnucl.
- [18] The chapter *Quantum Astrophysics* of [3].
http://tgd.wippiespace.com/public_html/tgdclass/tgdclass.html#qastro.
- [19] The chapter *The Notion of Free Energy and Many-Sheeted Space-Time Concept* of [7].
http://tgd.wippiespace.com/public_html/freenergy/freenergy.html#freenergy.
- [20] The chapter *Dark Nuclear Physics and Condensed Matter* of [4].
http://tgd.wippiespace.com/public_html/paddark/paddark.html#exonuclear.
- [21] The chapter *Does TGD Predict the Spectrum of Planck Constants?* of [5].
http://tgd.wippiespace.com/public_html/tgdquant/tgdquant.html#Planck.

References to the chapters of the books about TGD Inspired Theory of Consciousness and Quantum Biology

- [22] The chapter *The Notion of Wave-Genome and DNA as Topological Quantum Computer* of [12].
http://tgd.wippiespace.com/public_html/genememe/genememe.html#gari.
- [23] The chapter *Homeopathy in Many-Sheeted Space-Time* of [11].
http://tgd.wippiespace.com/public_html/hologram/hologram.html#homeoc.
- [24] The chapter *DNA as Topological Quantum Computer* of [12].
http://tgd.wippiespace.com/public_html/genememe/genememe.html#dnatqc.

Particle and nuclear physics

- [25] E. Storms (2001), *Cold fusion, an objective assessment*,
<http://home.netcom.com/~storms2/review8.html>.
- [26] J. Schwinger (1992), *Energy Transfer In Cold Fusion and Sonoluminescence*, <http://jcbmac.chem.brown.edu/baird/coldfusion/schwinger.html>.
- [27] *Extraordinary Evidence*. <http://newenergytimes.com/news/2006/NET19.htm#ee>.
- [28] B. S. Iskhanov, I. M. Kapitonov, V. V. Varlamov, *Giant Dipole Resonance: What is Known About?*,
<http://cdfc.sinp.msu.ru/publications/lshkhv-ELI03.pdf>.
- [29] GSI collaboration (2008), *Observation of Non-Exponential Orbital Electron Capture Decays of Hydrogen-Like ^{140}Pr and ^{142}Pm Ions*. <http://xxx.lanl.gov/abs/0801.2079>.
- [30] C. L. Kervran (1972), *Biological transmutations, and their applications in chemistry, physics, biology, ecology, medicine, nutrition, agriculture, geology*, Swan House Publishing Co.
- [31] P. Tompkins and C. Bird (1973), *The secret life of plants*, Harper & Row, New York.
- [32] V. J. Stenger (1995), *ESP and Cold Fusion: parallels in pseudoscience*, <http://www.phys.hawaii.edu/vjs/www/cold.txt>.
- [33] D. Vretenar, N. Paar, P. Ring, G. A. Lasazissis (1998), *Nonlinear dynamics of giant resonances in atomic nuclei*, arXiv:nucl-th/9809003.

- [34] *Polynutron*, <http://en.wikipedia.org/wiki/Polynutron>.
- [35] *Lithium*, <http://en.wikipedia.org/wiki/Lithium>.
- [36] S. M. Wong(1990), *Introductory Nuclear Physics*, Prentice-Hall Inc.
- [37] *Mizuno-Omori Cold Fusion Reactor*(1998), Infinite Energy Magazine, Vol4, Issue 20. <http://www.amasci.com/weird/anode.txt>.
- [38] T. Mizuno *et al* (2002), *Hydrogen Evolution by Plasma Electolysis in Aqueous solution*, Japanese Journal of Applied Physics, Vol. 44, No 1A, pp. 396-401.
- [39] P. G. Hansen(1993), *Nuclear structure at the drip lines*, Nuclear Phys. A, Vol. 553.
- [40] T. N. Leite, N. Teruya *Structure of the Isovector Dipole Resonance in Neutron-Rich ^{60}Ca Nucleus and Direct Decay from Pygmy Resonance*. arXiv:nucl-th/0308081.
- [41] G. Tertuchny *et al* (2006), *Microscopic description of the pygmy and giant electric dipole resonances in stable Ca isotopes*. arXiv:nucl-th/0603/0603051.
- [42] J. E. Ungar (1982), *Double Charge Exchange of pions on ^4He* , PhD thesis in California Institute of Technology, http://etd.caltech.edu/etd/available/etd-11032005-112918/unrestricted/Ungar_je_1983.pdf.
- [43] X.-G. He, J. Tandean, G. Valencia (2007), *Has HyperCP Observed a Light Higgs Boson?*, Phys. Rev. D74. <http://arxiv.org/abs/hep-ph/0610274>.
- [44] X.-G. He, J. Tandean, G. Valencia (2007), *Light Higgs Production in Hyperon Decay*, Phys. Rev. Lett. 98. <http://arxiv.org/abs/hep-ph/0610362>.
- [45] *Cold fusion is back at the American Chemical Society*, <http://www.nature.com/news/2007/070326/full/070326-12.html>.
Cold fusion - hot news again, <http://www.newscientist.com/channel/fundamentals/mg19426021.000-cold-fusion--hot-news-again.html>.
- [46] J. Naudin (2003), *Cold Fusion reactor experimental test results*. <http://jlnlabs.online.fr/cfr/html/cfrdatas.htm>.
- [47] R. Howard (1963), *Nuclear Physics*, Wadsworth Publishing Company, Inc..
- [48] *Dineutron*, <http://en.wikipedia.org/wiki/Dineutron>.
- [49] A. Widom and L. Larsen (2007), *Theoretical Standard Model Rates of Proton to Neutron Conversions Near Metallic Hydride Surfaces* nucl-th/0608059. <http://newenergytimes.com/Library/2006WidomLarsen-TheoreticalStandard-V2.pdf>.
- [50] T. Yamagata *et al* (2005), *Excitations of the Giant Dipole Resonances in ^4He and in the alpha Cluster of $^{6,7}\text{Li}$ via (p,p') Reactions*, EXOTIC NUCLEAR SYSTEMS: International Symposium on Exotic Nuclear Systems ENS'05. AIP Conference Proceedings, Volume 802, pp. 301-304.
- [51] *The Berkeley Laboratory Isotopes Project's Exploring the Table of Isotopes*, http://ie.lbl.gov/education/parent/Ti_iso.htm.
- [52] S. Moszkowski (1996), *Maria Goeppert Mayer*, Talk Presented at APS meeting Indianapolis, May 4, 1996. <http://www.physics.ucla.edu/~moszkows/mgm/mgmso.htm>. See also "Magic Numbers" in *Nuclear Structure*, <http://hyperphysics.phy-astr.gsu.edu/hbase/nuclear/shell.html#c2>. *Enhanced abundance of magic number nuclei*, <http://hyperphysics.phy-astr.gsu.edu/hbase/nuclear/shell2.html>.

- [53] C. Illert (1993), *ALCHEMY TODAY-Platonic Geometries in Nuclear Physics*, Volume 1. ISBN 0 949357 13 8, second edition. Science-Art Library.
- [54] C.A. Bertulani, V. Zelevinsky (2002), *Is the tetra-neutron a bound dineutron-dineutron molecule?*, J.Phys. G29, 2431-2437. arXiv:nucl-th/0212060.
- [55] F. M. Marquez *et al* (2003), Phys. Rev. C65, 044006.
- [56] Jed Rothwell(1996).
Some recent developments in cold fusion,
<http://ourworld.compuserve.com/homepages/JedRothwell/brieftec.htm>.
Report on The Second International Low Energy Nuclear Reactions Conference Holiday Inn, College Station, Texas, September 13-14, 1996.
<http://ourworld.compuserve.com/homepages/JedRothwell/ilenrc2s.htm>,
Review of the Sixth International Conference on Cold Fusion (ICCF6),
<http://ourworld.compuserve.com/homepages/JedRothwell/iccf6rev.htm>.
- [57] T. Baumann *et al* (1998), *Evolution of the Giant Dipole Resonance in Excited ^{120}Sn and ^{208}Pb Nuclei Populated by Inelastic Alpha Scattering*, Nucl. Phys. A 635, 428-445.
<http://www.phy.ornl.gov/progress/ribphys/reaction/rib031.pdf>.
- [58] B. Dume (2005), "Magic" numbers remain magic, Physics Web. <http://physicsweb.org/articles/news/9/6/9/1>. (Si(14,28) is magic unstable nucleus.)
 B. Ray (2005), *FSU researchers find 'magic' at the subatomic level*,
http://www.fsu.com/pages/2005/07/05/magic_subatomic.html. (Magic Number N=14.)
New Magic Number "16" Where Nuclei Exist Stably Discovered, <http://www.mext.go.jp/english/news/2000/06/s000606.html>.
 A. Ozawa *et al* (2000), Phys. Rev. Lett.84, 5493. (Magic number N=16).
 A. Ozawa *et al* (2001), *Observation of new proton and neutron magic numbers*, http://lbl.confex.com/lbl/2001/program/abstract_97.htm. (Magic numbers N=16,20,32.)
- [59] Russ George's homepage,
<http://www.hooked.net/~rgeorge/saturnahome.html> .

Condensed matter physics

- [60] P. Kanarev (2002) *Water is New Source of Energy*. Krasnodar.
- [61] J-C. Li and D.K. Ross (1993), *Evidence of Two Kinds of Hydrogen Bonds in Ices*. J-C. Li and D.K. Ross, Nature, 365, 327-329.
- [62] M. Chaplin (2005), *Water Structure and Behavior*. <http://www.lsbu.ac.uk/water/index.html>.
 For 41 anomalies see <http://www.lsbu.ac.uk/water/anmlies.html>.
 For the icosahedral clustering see <http://www.lsbu.ac.uk/water/clusters.html>.
- [63] W. D. Knight *et al* (1984), Phys.Rev. Lett. 52, 2141.
- [64] R. A. Cowley (2004), *Neutron-scattering experiments and quantum entanglement*. Physica B 350 (2004) 243-245.
- [65] J. K. Borchardt(2003), *The chemical formula H₂O - a misnomer*. The Alchemist 8 Aug (2003).
- [66] R. Moreh, R. C. Block, Y. Danon, and M. Neumann (2005), *Search for anomalous scattering of keV neutrons from H₂O-D₂O mixtures*. Phys. Rev. Lett. 94, 185301.
- [67] . *Rotational energies of molecules*. <http://hyperphysics.phy-astr.gsu.edu/HBASE/molecule/rotrig.html#c3>.
- [68] *Burning salt water*. <http://www.youtube.com/watch?v=aGg0ATfoBgo>.

- [69] F. Levy, I. Sheikin, B. Grenier, and A. D. Huxley (2005), *Magnetic Field-Induced Superconductivity in the Ferromagnet URhGe*. Science 26, August, 1343-1346.
See also P. Rogers (2005), *Critical breakthrough*. Physics Web. <http://physicsweb.org/articles/news/9/8/17>.
- [70] *Hydrogen bonds*. http://en.wikipedia.org/wiki/Hydrogen_bond.
- [71] *Pyrolysis*. <http://en.wikipedia.org/wiki/Pyrolysis>.
- [72] *Cold fusion by plasma electrolysis of water*. Ph. M. Kanarev and T. Mizuno (2002). <http://www.guns.connect.fi/innoplaza/energy/story/Kanarev/codlfusion/>.
- [73] *Electrolysis of water*.
http://en.wikipedia.org/wiki/Electrolysis_of_water.
- [74] R. Matthews (1997), *Wacky Water*. New Scientist 154 (2087):4043, 21 June.

Cosmology and astrophysics

- [75] J. Prochaska, J. C. Howk, A. M. Wolfe (2003), *The elemental abundance pattern in a galaxy at $z = 2.626$* . Nature 423, 57-59 (2003). See also *Distant elements of surprise*. <http://physicsworld.com/cws/article/print/17750>.
- [76] C. Charbonnel and F. Primas (2005), *The lithium content of the Galactic Halo stars*. astro-ph/0505247. http://www.arxiv.org/PS_cache/astro-ph/pdf/0505/0505247v2.pdf.

Biology related references

- [77] L. Montagnier, J. Aissa, S. Ferris, J.-L. Montagnier, and C. Lavall'e (2009). *Electromagnetic Signals Are Produced by Aqueous Nanostructures Derived from Bacterial DNA Sequences*. Interdiscip. Sci. Comput. Life Sci. <http://www.springerlink.com/content/0557v31188m3766x/>.

Chapter 10

Dark Nuclear Physics and Condensed Matter

10.1 Introduction

The unavoidable presence of classical long ranged weak (and also color) gauge fields in TGD Universe has been a continual source of worries for more than two decades. The basic question has been whether electro-weak charges of elementary particles are screened in electro-weak length scale or not. The TGD based view about dark matter assumes that weak charges are indeed screened for ordinary matter in electro-weak length scale but that dark electro-weak bosons correspond to much longer symmetry breaking length scale.

The large value of \hbar in dark matter phase implies that Compton lengths and -times are scaled up. In particular, the sizes of nucleons and nuclei become of order atom size so that dark nuclear physics would have direct relevance for condensed matter physics. It becomes impossible to make a reductionistic separation between nuclear physics and condensed matter physics and chemistry anymore.

In its original form this chapter was an attempt to concretize and develop ideas related to dark matter by using some experimental inputs with emphasis on the predicted interaction between the new nuclear physics and condensed matter. As the vision about dark matter became more coherent and the nuclear string model developed in its recent form, it became necessary to update the chapter and throw away the obsolete material. I have also divided the material to two chapters such that second chapter focuses to dark weak and color forces and their implications. I dare hope that the recent representation is more focused than the earlier one.

10.1.1 Dark rules

I have done a considerable amount of trials and errors in order to identify the basic rules allowing to understand what it means to be dark matter is and what happens in the phase transition to dark matter. It is good to try to summarize the basic rules of p-adic and dark physics allowing to avoid obvious contradictions.

Could basic quantum TGD imply the hierarchy of Planck constants?

The implications of the hierarchy of Planck constants depend on whether one assumes it as an independent additional postulate or as a consequence of basic quantum TGD. The first option originally motivated by physical anomalies would allow both singular coverings and factor spaces. The latter option, which emerged five years after the basic idea, would allow only singular coverings. They would provide only a convenient tool to describe the fact that the correspondence between canonical momentum densities and time derivatives of the imbedding space coordinates at the ends of space-time sheets is not one-to-one. As a matter fact, this observation forced the idea about quantum physics as classical physics in the "world of classical worlds" for two decades ago. The quantization of Planck constant as integer multiples of its standard value would be an effective phenomenon for this option

holding true at the sheets of the covering. These options lead to different predictions and one can in principle test whether either of them is correct.

The notion of field body

The notion of "field body" implied by topological field quantization is essential piece of classical TGD. It seems possible to assign to physical systems field identities- that is separate magnetic and electric field bodies identifiable as flux quanta. This is not possible in Maxwell's electrodynamics. The first naive guess was that one can speak of separate em, Z^0 , W , gluonic, and gravitonic field bodies, each characterized by its own p-adic prime. The tight constraints coming from the fact that the induced gauge fields are expressible in terms of CP_2 coordinates and their derivatives implies however strong correlations between classical gauge fields. For instance, the vanishing of classical Kähler field for vacuum extremals implies that em and Z^0 fields are proportional to each other. The non-vanishing of induced Kähler field in turn implies non-vanishing classical color fields. This gives rise at least to two basic types of field bodies predicting a lot of new physics even in macroscopic length scales. For instance, electric and magnetic flux tubes must have at their ends quarks and antiquarks serving as sources of classical color fields unless one believes that vacuum charge densities serve as sources of these fields. In the similar manner neutrinos and antineutrinos are needed to create classical Z^0 fields associated with almost vacuum extremal flux tubes. These fields could be interpreted also as vacuum polarization effects and one could distinguish them from fields created by genuine sources. For instance, the unavoidable classical color fields associated with the flux tubes of electromagnetic field body which is not vacuum extremal would represent vacuum polarization in macroscopic scale.

What is interesting that the conceptual separation of interactions to various types would have a direct correlate at the level of space-time topology. From a different perspective inspired by the general vision that many-sheeted space-time provides symbolic representations of quantum physics, the very fact that we make this conceptual separation of fundamental interactions could reflect the topological separation at space-time level.

The p-adic mass calculations for quarks encourage to think that the p-adic length scale characterizing the mass of particle is associated with its electromagnetic body and in the case of neutrinos with its Z^0 body. Z^0 body can contribute also to the mass of charged particles but the contribution would be small. It is also possible that these field bodies are purely magnetic for color and weak interactions. Color flux tubes would have exotic fermion and anti-fermion at their ends and define colored variants of pions. This would apply not only in the case of nuclear strings but also to molecules and larger structures so that scaled variants of elementary particles and standard model would appear in all length scales as indeed implied by the fact that classical electro-weak and color fields are unavoidable in TGD framework.

One can also go further and distinguish between magnetic field body of free particle for which flux quanta start and return to the particle and "relative field" bodies associated with pairs of particles. Very complex structures emerge and should be essential for the understanding the space-time correlates of various interactions. In a well-defined sense they would define space-time correlate for the conceptual analysis of the interactions into separate parts. In order to minimize confusion it should be emphasized that the notion of field body used in this chapter relates to those space-time correlates of interactions, which are more or less *static* and related to the formation of *bound states*.

What dark variant of elementary particle means

It is not at all clear what the notion of dark variant of elementary particle or of larger structures could mean.

1. Are only field bodies dark?

One variety of dark particle is obtained by making some of the field bodies dark by increasing the value of Planck constant. This hypothesis could be replaced with the stronger assumption that elementary particles are maximally quantum critical systems so that they are same irrespective of the value of the Planck constant. Elementary particles would be represented by partonic 2-surfaces, which belong to the universal orbifold singularities remaining invariant by all groups $G_a \times G_b$ for a given choice of quantization axes. If $G_a \times G_b$ is assumed to leave invariant the choice of the quantization axes, it must be of the form $Z_{n_a} \times Z_{n_b} \subset SO(3) \times SU(3)$. Partonic 2-surface would belong to

$M^2 \times CP_2/U(1) \times U(1)$, where M^2 is spanned by the quantization axis of angular momentum and the time axis defining the rest system.

A different manner to say this is that the CP_2 type extremal representing particle would suffer multiple topological condensation on its field bodies so that there would be no separate "particle space-time sheet".

Darkness would be restricted to particle interactions. The value of the Planck constant would be assigned to a particular interaction between systems rather than system itself. This conforms with the original finding that gravitational Planck constant satisfies $\hbar = GM_1M_2/v_0$, $v_0 \simeq 2^{-11}$. Since each interaction can give rise to a hierarchy dark phases, a rich variety of partially dark phases is predicted. The standard assumption that dark matter is visible only via gravitational interactions would mean that gravitational field body would not be dark for this particular dark matter.

Complex combinations of dark field bodies become possible and the dream is that one could understand various phases of matter in terms of these combinations. All phase transitions, including the familiar liquid-gas and solid-liquid phase transitions, could have a unified description in terms of dark phase transition for an appropriate field body. At mathematical level Jones inclusions would provide this description.

The book metaphor for the interactions at space-time level is very useful in this framework. Elementary particles correspond to ordinary value of Planck constant analogous to the ordinary sheets of a book and the field bodies mediating their interactions are the same space-time sheet or at dark sheets of the book.

2. Can also elementary particles be dark?

Also dark elementary particles themselves rather than only the flux quanta could correspond to dark space-time sheet defining multiple coverings of $H/G_a \times G_b$. This would mean giving up the maximal quantum criticality hypothesis in the case of elementary particles. These sheets would be exact copies of each other. If single sheet of the covering contains topologically condensed space-time sheet, also other sheets contain its exact copy.

The question is whether these copies of space-time sheet defining classical identical systems can carry different fermionic quantum numbers or only identical fermionic quantum numbers so that the dark particle would be exotic many-fermion system allowing an apparent violation of statistics (N fermions in the same state).

Even if one allows varying number of fermions in the same state with respect to a basic copy of sheet, one ends up with the notion of N -atom in which nuclei would be ordinary but electrons would reside at the sheets of the covering. The question is whether symbolic representations essential for understanding of living matter could emerge already at molecular level via the formation of N -atoms.

What happens in charge fractionization?

The hierarchy of Planck constants suggests strongly charge fractionization. What happens for binding energies is however not obvious. The first guess is that one just replaces \hbar with its scaled value in the standard formulas. One can however ask whether the resulting expression applies to single sheet of covering or to the sum of binding energies associated with the sheets of covering. In the case of factor space analogous problem is not encountered.

If the coverings follow from basic quantum TGD one can deduce unique rules for what happens. These rules can be assumed also in the more general case. Since the sheets of the singular covering coincide at the partonic 2-surfaces associated with ends of CD the time evolution and also "evolution" in space-like direction means instability of in the sense that partonic 2-surface decomposes to $r = \hbar/\hbar_0 = n_a n_b$ sheets. This implies fractionization of all total quantum numbers such as energy and momentum. From this one can also deduce what happens to various binding energies. For instance, the total (!) cyclotron energy is indeed multiplied by factor and the total(!) binding energy of dark hydrogen atom is what the naive scaling of \hbar would give. The reason is that the mass of particle is fractionized: $m \rightarrow m/n_a n_b$. Therefore the original guesses would be correct. In particular, the expression of the total gravitational binding energy essential for the original Bohr model of planetary orbits is consistent with the new more precise rules.

Criterion for the transition to dark phase

The naive criterion $\alpha Q_1 Q_2 > 1$ (or its generalization) for the transition to dark matter phase relates always to the interaction between two systems and the interpretation is that when the field strength characterizing the interaction becomes too strong, the interaction is mediated by dark space-time sheets which define $n = n(G_a) \times n(G_b)$ -fold covering of $M^4 \times CP_2/G_a \times G_b$. The sharing of flux between different space-time sheets reduces the field strength associated with single sheet below the critical value.

For the option in which singular coverings follow from basic quantum TGD this criterion or its appropriate generalization has very concrete interpretation. At the ends of CD the partonic 2-surface is unstable against decay to n_a sheets when some of the quantum numbers of the partonic 2-surface are too large. A similar decay to n_b sheets would happen also when one moves in space-like direction.

One can ask whether this instability could have something to do with N-vertices of generalized Feynman diagrams in which decay of a partonic 2-surfaces to N-1 surfaces takes place. For instance, could it be that 3-vertex- possibly the only fundamental vertex, correspond to this process and could higher vertices have an interpretation in terms of the hierarchy of Planck constants? This would mean analogy with Jones inclusions for which $n \geq 3$ holds true. The assumption that exact fractionization of quantum numbers takes place is not consistent with the identification in terms of Feynman diagrams. Also the huge values of $n_a n_b$ disfavor this identification unless one restricts it to $n_a n_b = 2$.

The considerations of [55] suggest that in the vertices of generalized Feynman diagrams a re-distribution of the sheets of the coverings can take place in such a manner that the total number of sheets is conserved. The leakage of between different sectors of WCW would in turn mean analogs of self-energy vertices in which n_a and n_b are replaced with their factors or with integers containing them as factors.

Mersenne hypothesis

The generalization of the imbedding space means a book like structure for which the pages are products of singular coverings or factor spaces of CD (causal diamond defined as intersection of future and past directed light-cones) and of CP_2 [39]. This predicts that Planck constants are rationals and that given value of Planck constant corresponds to an infinite number of different pages of the Big Book, which might be seen as a drawback. If only singular covering spaces are allowed the values of Planck constant are products of integers and given value of Planck constant corresponds to a finite number of pages given by the number of decompositions of the integer to two different integers.

TGD inspired quantum biology and number theoretical considerations suggest preferred values for $r = \hbar/\hbar_0$. For the most general option the values of \hbar are products and ratios of two integers n_a and n_b . Ruler and compass integers defined by the products of distinct Fermat primes and power of two are number theoretically favored values for these integers because the phases $\exp(i2\pi/n_i)$, $i \in \{a, b\}$, in this case are number theoretically very simple and should have emerged first in the number theoretical evolution via algebraic extensions of p-adics and of rationals. p-Adic length scale hypothesis favors powers of two as values of r .

One can however ask whether a more precise characterization of preferred Mersennes could exist and whether there could exist a stronger correlation between hierarchies of p-adic length scales and Planck constants. Mersenne primes $M_k = 2^k - 1$, $k \in \{89, 107, 127\}$, and Gaussian Mersennes $M_{G,k} = (1+i)k - 1$, $k \in \{113, 151, 157, 163, 167, 239, 241, \dots\}$ are expected to be physically highly interesting and up to $k = 127$ indeed correspond to elementary particles. The number theoretical miracle is that all the four p-adic length scales with $k \in \{151, 157, 163, 167\}$ are in the biologically highly interesting range 10 nm-2.5 μ m). The question has been whether these define scaled up copies of electro-weak and QCD type physics with ordinary value of \hbar . The proposal that this is the case and that these physics are in a well-defined sense induced by the dark scaled up variants of corresponding lower level physics leads to a prediction for the preferred values of $r = 2^{k_d}$, $k_d = k_i - k_j$.

What induction means is that dark variant of exotic nuclear physics induces exotic physics with ordinary value of Planck constant in the new scale in a resonant manner: dark gauge bosons transform to their ordinary variants with the same Compton length. This transformation is natural since in length scales below the Compton length the gauge bosons behave as massless and free particles. As a consequence, lighter variants of weak bosons emerge and QCD confinement scale becomes longer.

This proposal will be referred to as Mersenne hypothesis. It leads to strong predictions about EEG

[43] since it predicts a spectrum of preferred Josephson frequencies for a given value of membrane potential and also assigns to a given value of \hbar a fixed size scale having interpretation as the size scale of the body part or magnetic body. Also a vision about evolution of life emerges. Mersenne hypothesis is especially interesting as far as new physics in condensed matter length scales is considered: this includes exotic scaled up variants of the ordinary nuclear physics and their dark variants. Even dark nucleons are possible and this gives justification for the model of dark nucleons predicting the counterparts of DNA, RNA, tRNA, and aminoacids as well as realization of vertebrate genetic code [48].

These exotic nuclear physics with ordinary value of Planck constant could correspond to ground states that are almost vacuum extremals corresponding to homologically trivial geodesic sphere of CP_2 near criticality to a phase transition changing Planck constant. Ordinary nuclear physics would correspond to homologically non-trivial geodesic sphere and far from vacuum extremal property. For vacuum extremals of this kind classical Z^0 field proportional to electromagnetic field is present and this modifies dramatically the view about cell membrane as Josephson junction. The model for cell membrane as almost vacuum extremal indeed led to a quantitative breakthrough in TGD inspired model of EEG and is therefore something to be taken seriously. The safest option concerning empirical facts is that the copies of electro-weak and color physics with ordinary value of Planck constant are possible only for almost vacuum extremals - that is at criticality against phase transition changing Planck constant.

10.1.2 Some implications

As already noticed, the detailed implications of the hierarchy of Planck constants depend on whether one brings in the hierarchy of singular coverings and factor spaces of the imbedding space as an independent postulate or whether one assumes that singular coverings emerge as an effective description from basic quantum TGD

Dark variants of nuclear physics

One can imagine endless variety of dark variants of ordinary nuclei and every piece of data is well-come in attempts to avoid a complete inflation of speculative ideas. The book metaphor for the extended imbedding space is useful in the attempts to imagine various exotic phases of matter. For the minimal option atomic nuclei would be ordinary whereas field bodies could be dark and analogous to n -sheeted Riemann surfaces. One can imagine that the nuclei are at the "standard" page of the book and color bonds at different page with different p-adic length scale or having different Planck constant \hbar . This would give two hierarchies of nuclei with increasing size.

Color magnetic body of the structure would become a key element in understanding the nuclear binding energies, giant dipole resonances, and nuclear decays. Also other field bodies are in a key role and there seems to be a field body for every basic interaction (classical gauge fields are induced from spinor connection and only four independent field variables are involved so that this is indeed required).

Nothing prevents from generalizing the nuclear string picture so that color bonds could bind also atoms to molecules and molecules to larger structures analogous to nuclei. Even hydrogen bond might be interpreted in this manner. Molecular physics could be seen as a scaled up variant of nuclear physics in a well-defined sense. The exotic features would relate to the hierarchy of various field bodies, including color bonds, electric and weak bonds. These field bodies would play key role also in biology and replaced molecular randomness with coherence in much longer length scale.

In the attempt to make this vision quantitative the starting point is nuclear string model [47] and the model of cold fusion based on it forcing also to conclude the scaled variants of electro-weak bosons are involved. The model of cold fusion requires the presence of a variant electro-weak interactions for which weak bosons are effectively massless below the atomic length scale.

$k = 113$ p-adically scaled up variant of ordinary weak physics which is dark and corresponds to $\hbar = r\hbar_0$, $r = 2^{k_a}$, $k_d = 14 = 127 - 113$ is an option consistent with Mersenne hypothesis and gives weak bosons in electron length scale. Another possibility is defined by $k = 113$ and $k_d = 24 = 113 - 89 = 151 - 127$ and corresponds to the p-adic length scale $k = 137$ defining atomic length scale. This would give rise to weak bosons with masses in keV scale and these would be certainly relevant for the physics of condensed matter.

Anomalies of water could be understood if one assumes that color bonds can become dark with suitable values of $r = 2^{k_d}$ and if super-nuclei formed by connecting different nuclei by the color bonds are possible. Tetrahedral and icosahedral water clusters could be seen as magic super-nuclei in this framework. Color bonds could connect either proton nuclei or water molecules.

The model for partially dark condensed matter deriving from exotic nuclear physics and exotic weak interactions could allow to understand the low compressibility of the condensed matter as being due to the repulsive weak force between exotic quarks, explains large parity breaking effects in living matter (chiral selection), and suggests a profound modification of the notion of chemical bond having most important implications for bio-chemistry and understanding of bio-chemical evolution.

Could the notion of dark atom make sense?

One can also imagine several variants of dark atom. Book metaphor suggest one variant of dark atom.

1. Nuclei and electrons could be ordinary but classical electromagnetic interactions are mediated via dark space-time sheet "along different page of the book". The value of Planck constant would be scaled so that one would obtain a hierarchy of scaled variants of hydrogen atom. The findings of Mills [93] could find an explanation in terms of a reduced Planck constant if singular factor spaces are assumed to be possible. An alternative explanation is based on the notion of quantum-hydrogen atom obtained as q-deformation of the ordinary hydrogen atom.
2. A more exotic variant if atom is obtained by assuming ordinary nuclei but dark, not totally quantum critical, electrons. Dark space-time surface is analogous to n-sheeted Riemann surface and if one assumes that each sheet could carry electron, one ends up with the notion of N -atom. This variant of dark atom is more or less equivalent with that following from the option for which the singular coverings of imbedding space are effective manner to describe the many-valuedness of the time derivatives of the imbedding space coordinates as functions of canonical momentum densities.

10.2 A generalization of the notion of imbedding space as a realization of the hierarchy of Planck constants

10.2.1 Hierarchy of Planck constants and the generalization of the notion of imbedding space

In the following the recent view about structure of imbedding space forced by the quantization of Planck constant is summarized. The question is whether it might be possible in some sense to replace H or its Cartesian factors by their necessarily singular multiple coverings and factor spaces. One can consider two options: either M^4 or the causal diamond CD . The latter one is the more plausible option from the point of view of WCW geometry.

The evolution of physical ideas about hierarchy of Planck constants

The evolution of the physical ideas related to the hierarchy of Planck constants and dark matter as a hierarchy of phases of matter with non-standard value of Planck constants was much faster than the evolution of mathematical ideas and quite a number of applications have been developed during last five years.

1. The starting point was the proposal of Nottale [78] that the orbits of inner planets correspond to Bohr orbits with Planck constant $\hbar_{gr} = GMm/v_0$ and outer planets with Planck constant $\hbar_{gr} = 5GMm/v_0$, $v_0/c \simeq 2^{-11}$. The basic proposal [38] was that ordinary matter condenses around dark matter which is a phase of matter characterized by a non-standard value of Planck constant whose value is gigantic for the space-time sheets mediating gravitational interaction. The interpretation of these space-time sheets could be as magnetic flux quanta or as massless extremals assignable to gravitons.

2. Ordinary particles possibly residing at these space-time sheet have enormous value of Compton length meaning that the density of matter at these space-time sheets must be very slowly varying. The string tension of string like objects implies effective negative pressure characterizing dark energy so that the interpretation in terms of dark energy might make sense [16]. TGD predicted a one-parameter family of Robertson-Walker cosmologies with critical or over-critical mass density and the "pressure" associated with these cosmologies is negative.
3. The quantization of Planck constant does not make sense unless one modifies the view about standard space-time is. Particles with different Planck constant must belong to different worlds in the sense local interactions of particles with different values of \hbar are not possible. This inspires the idea about the book like structure of the imbedding space obtained by gluing almost copies of H together along common "back" and partially labeled by different values of Planck constant.
4. Darkness is a relative notion in this framework and due to the fact that particles at different pages of the book like structure cannot appear in the same vertex of the generalized Feynman diagram. The phase transitions in which partonic 2-surface X^2 during its travel along X_l^3 leads to another page of book are however possible and change Planck constant. Particle (say photon -) exchanges of this kind allow particles at different pages to interact. The interactions are strongly constrained by charge fractionization and are essentially phase transitions involving many particles. Classical interactions are also possible. It might be that we are actually observing dark matter via classical fields all the time and perhaps have even photographed it [41].
5. The realization that non-standard values of Planck constant give rise to charge and spin fractionization and anyonization led to the precise identification of the prerequisites of anyonic phase [24]. If the partonic 2-surface, which can have even astrophysical size, surrounds the tip of CD , the matter at the surface is anyonic and particles are confined at this surface. Dark matter could be confined inside this kind of light-like 3-surfaces around which ordinary matter condenses. If the radii of the basic pieces of these nearly spherical anyonic surfaces - glued to a connected structure by flux tubes mediating gravitational interaction - are given by Bohr rules, the findings of Nottale [78] can be understood. Dark matter would resemble to a high degree matter in black holes replaced in TGD framework by light-like partonic 2-surfaces with a minimum size of order Schwarzschild radius r_S of order scaled up Planck length $l_{Pl} = \sqrt{\hbar_{gr} G} = GM$. Black hole entropy is inversely proportional to \hbar and predicted to be of order unity so that dramatic modification of the picture about black holes is implied.
6. Perhaps the most fascinating applications are in biology. The anomalous behavior ionic currents through cell membrane (low dissipation, quantal character, no change when the membrane is replaced with artificial one) has a natural explanation in terms of dark supra currents. This leads to a vision about how dark matter and phase transitions changing the value of Planck constant could relate to the basic functions of cell, functioning of DNA and aminoacids, and to the mysteries of bio-catalysis. This leads also a model for EEG interpreted as a communication and control tool of magnetic body containing dark matter and using biological body as motor instrument and sensory receptor. One especially amazing outcome is the emergence of genetic code of vertebrates from the model of dark nuclei as nuclear strings [47, 41].

The most general option for the generalized imbedding space

Simple physical arguments pose constraints on the choice of the most general form of the imbedding space.

1. The fundamental group of the space for which one constructs a non-singular covering space or factor space should be non-trivial. This is certainly not possible for M^4 , CD , CP_2 , or H . One can however construct singular covering spaces. The fixing of the quantization axes implies a selection of the sub-space $H_4 = M^2 \times S^2 \subset M^4 \times CP_2$, where S^2 is geodesic sphere of CP_2 . $\hat{M}^4 = M^4 \setminus M^2$ and $\hat{CP}_2 = CP_2 \setminus S^2$ have fundamental group Z since the codimension of the excluded sub-manifold is equal to two and homotopically the situation is like that for a punctured plane. The exclusion of these sub-manifolds defined by the choice of quantization axes could naturally give rise to the desired situation.

2. CP_2 allows two geodesic spheres which left invariant by $U(2)$ resp. $SO(3)$. The first one is homologically non-trivial. For homologically non-trivial geodesic sphere $H_4 = M^2 \times S^2$ represents a straight cosmic string which is non-vacuum extremal of Kähler action (not necessarily preferred extremal). One can argue that the many-valuedness of \hbar is un-acceptable for non-vacuum extremals so that only homologically trivial geodesic sphere S^2 would be acceptable. One could go even further. If the extremals in $M^2 \times CP_2$ can be preferred non-vacuum extremals, the singular coverings of M^4 are not possible. Therefore only the singular coverings and factor spaces of CP_2 over the homologically trivial geodesic sphere S^2 would be possible. This however looks a non-physical outcome.
 - (a) The situation changes if the extremals of type $M^2 \times Y^2$, Y^2 a holomorphic surface of CP_3 , fail to be hyperquaternionic. The tangent space M^2 represents hypercomplex sub-space and the product of the modified gamma matrices associated with the tangent spaces of Y^2 should belong to M^2 algebra. This need not be the case in general.
 - (b) The situation changes also if one reinterprets the gluing procedure by introducing scaled up coordinates for M^4 so that metric is continuous at $M^2 \times CP_2$ but CD s with different size have different sizes differing by the ratio of Planck constants and would thus have only piece of lower or upper boundary in common.
3. For the more general option one would have four different options corresponding to the Cartesian products of singular coverings and factor spaces. These options can be denoted by $C-C$, $C-F$, $F-C$, and $F-F$, where C (F) signifies for covering (factor space) and first (second) letter signifies for CD (CP_2) and correspond to the spaces $(\hat{C}D \hat{\times} G_a) \times (\hat{C}P_2 \hat{\times} G_b)$, $(\hat{C}D \hat{\times} G_a) \times \hat{C}P_2/G_b$, $\hat{C}D/G_a \times (\hat{C}P_2 \hat{\times} G_b)$, and $\hat{C}D/G_a \times \hat{C}P_2/G_b$.
4. The groups G_i could correspond to cyclic groups Z_n . One can also consider an extension by replacing M^2 and S^2 with its orbit under more general group G (say tetrahedral, octahedral, or icosahedral group). One expects that the discrete subgroups of $SU(2)$ emerge naturally in this framework if one allows the action of these groups on the singular sub-manifolds M^2 or S^2 . This would replace the singular manifold with a set of its rotated copies in the case that the subgroups have genuinely 3-dimensional action (the subgroups which corresponds to exceptional groups in the ADE correspondence). For instance, in the case of M^2 the quantization axes for angular momentum would be replaced by the set of quantization axes going through the vertices of tetrahedron, octahedron, or icosahedron. This would bring non-commutative homotopy groups into the picture in a natural manner.

About the phase transitions changing Planck constant

There are several non-trivial questions related to the details of the gluing procedure and phase transition as motion of partonic 2-surface from one sector of the imbedding space to another one.

1. How the gluing of copies of imbedding space at $M^2 \times CP_2$ takes place? It would seem that the covariant metric of CD factor proportional to \hbar^2 must be discontinuous at the singular manifold since only in this manner the idea about different scaling factor of CD metric can make sense. On the other hand, one can always scale the M^4 coordinates so that the metric is continuous but the sizes of CD s with different Planck constants differ by the ratio of the Planck constants.
2. One might worry whether the phase transition changing Planck constant means an instantaneous change of the size of partonic 2-surface in M^4 degrees of freedom. This is not the case. Light-likeness in $M^2 \times S^2$ makes sense only for surfaces $X^1 \times D^2 \subset M^2 \times S^2$, where X^1 is light-like geodesic. The requirement that the partonic 2-surface X^2 moving from one sector of H to another one is light-like at $M^2 \times S^2$ irrespective of the value of Planck constant requires that X^2 has single point of M^2 as M^2 projection. Hence no sudden change of the size X^2 occurs.
3. A natural question is whether the phase transition changing the value of Planck constant can occur purely classically or whether it is analogous to quantum tunneling. Classical non-vacuum extremals of Chern-Simons action have two-dimensional CP_2 projection to homologically non-trivial geodesic sphere S^2_I . The deformation of the entire S^2_I to homologically trivial geodesic sphere S^2_{II} is not possible so that only combinations of partonic 2-surfaces with vanishing total

homology charge (Kähler magnetic charge) can in principle move from sector to another one, and this process involves fusion of these 2-surfaces such that CP_2 projection becomes single homologically trivial 2-surface. A piece of a non-trivial geodesic sphere S^2_I of CP_2 can be deformed to that of S^2_{II} using 2-dimensional homotopy flattening the piece of S^2 to curve. If this homotopy cannot be chosen to be light-like, the phase transitions changing Planck constant take place only via quantum tunnelling. Obviously the notions of light-like homotopies (cobordisms) are very relevant for the understanding of phase transitions changing Planck constant.

How one could fix the spectrum of Planck constants?

The question how the observed Planck constant relates to the integers n_a and n_b defining the covering and factors spaces, is far from trivial and I have considered several options. The basic physical inputs are the condition that scaling of Planck constant must correspond to the scaling of the metric of CD (that is Compton lengths) on one hand and the scaling of the gauge coupling strength $g^2/4\pi\hbar$ on the other hand.

1. One can assign to Planck constant to both CD and CP_2 by assuming that it appears in the commutation relations of corresponding symmetry algebras. Algebraist would argue that Planck constants $\hbar(CD)$ and $\hbar(CP_2)$ must define a homomorphism respecting multiplication and division (when possible) by G_i . This requires $r(X) = \hbar(X)\hbar_0 = n$ for covering and $r(X) = 1/n$ for factor space or vice versa.
2. If one assumes that $\hbar^2(X)$, $X = M^4$, CP_2 corresponds to the scaling of the covariant metric tensor g_{ij} and performs an over-all scaling of H -metric allowed by the Weyl invariance of Kähler action by dividing metric with $\hbar^2(CP_2)$, one obtains the scaling of M^4 covariant metric by $r^2 \equiv \hbar^2/\hbar_0^2 = \hbar^2(M^4)/\hbar^2(CP_2)$ whereas CP_2 metric is not scaled at all.
3. The condition that \hbar scales as n_a is guaranteed if one has $\hbar(CD) = n_a\hbar_0$. This does not fix the dependence of $\hbar(CP_2)$ on n_b and one could have $\hbar(CP_2) = n_b\hbar_0$ or $\hbar(CP_2) = \hbar_0/n_b$. The intuitive picture is that n_b - fold covering gives in good approximation rise to $n_a n_b$ sheets and multiplies YM action action by $n_a n_b$ which is equivalent with the $\hbar = n_a n_b \hbar_0$ if one effectively compresses the covering to $CD \times CP_2$. One would have $\hbar(CP_2) = \hbar_0/n_b$ and $\hbar = n_a n_b \hbar_0$. Note that the descriptions using ordinary Planck constant and coverings and scaled Planck constant but contracting the covering would be alternative descriptions.

This gives the following formulas $r \equiv \hbar/\hbar_0 = r(M^4)/r(CP_2)$ in various cases.

$$\begin{array}{ccccc}
 C - C & F - C & C - F & F - F & \\
 \hline
 r & n_a n_b & \frac{n_a}{n_b} & \frac{n_b}{n_a} & \frac{1}{n_a n_b}
 \end{array}$$

Preferred values of Planck constants

Number theoretic considerations favor the hypothesis that the integers corresponding to Fermat polygons constructible using only ruler and compass and given as products $n_F = 2^k \prod_s F_s$, where $F_s = 2^{2^s} + 1$ are distinct Fermat primes, are favored. The reason would be that quantum phase $q = \exp(i\pi/n)$ is in this case expressible using only iterated square root operation by starting from rationals. The known Fermat primes correspond to $s = 0, 1, 2, 3, 4$ so that the hypothesis is very strong and predicts that p-adic length scales have satellite length scales given as multiples of n_F of fundamental p-adic length scale. $n_F = 2^{11}$ corresponds in TGD framework to a fundamental constant expressible as a combination of Kähler coupling strength, CP_2 radius and Planck length appearing in the expression for the tension of cosmic strings, and the powers of 2^{11} was proposed to define favored as values of n_a in living matter [43].

The hypothesis that Mersenne primes $M_k = 2^k - 1$, $k \in \{89, 107, 127\}$, and Gaussian Mersennes $M_{G,k} = (1 + i)k - 1$, $k \in \{113, 151, 157, 163, 167, 239, 241.. \}$ (the number theoretical miracle is that all the four p-adic length scales with $k \in \{151, 157, 163, 167\}$ are in the biologically highly interesting range 10 nm-2.5 μm) define scaled up copies of electro-weak and QCD type physics with ordinary value of \hbar and that these physics are induced by dark variants of corresponding lower level physics leads to a prediction for the preferred values of $r = 2^{k_d}$, $k_d = k_i - k_j$, and the resulting picture finds

support from the ensuing models for biological evolution and for EEG [43]. This hypothesis - to be referred to as Mersenne hypothesis - replaces the rather ad hoc proposal $r = \hbar/\hbar_0 = 2^{11k}$ for the preferred values of Planck constant.

How Planck constants are visible in Kähler action?

$\hbar(M^4)$ and $\hbar(CP_2)$ appear in the commutation and anticommutation relations of various superconformal algebras. Only the ratio of M^4 and CP_2 Planck constants appears in Kähler action and is due to the fact that the M^4 and CP_2 metrics of the imbedding space sector with given values of Planck constants are proportional to the corresponding Planck. This implies that Kähler function codes for radiative corrections to the classical action, which makes possible to consider the possibility that higher order radiative corrections to functional integral vanish as one might expect at quantum criticality. For a given p-adic length scale space-time sheets with all allowed values of Planck constants are possible. Hence the spectrum of quantum critical fluctuations could in the ideal case correspond to the spectrum of \hbar coding for the scaled up values of Compton lengths and other quantal lengths and times. If so, large \hbar phases could be crucial for understanding of quantum critical superconductors, in particular high T_c superconductors.

A simple model for fractional quantum Hall effect

The generalization of the imbedding space suggests that it could be possible to understand fractional quantum Hall effect [67] at the level of basic quantum TGD as integer QHE for non-standard value of Planck constant.

The formula for the quantized Hall conductance is given by

$$\begin{aligned}\sigma &= \nu \times \frac{e^2}{h} , \\ \nu &= \frac{n}{m} .\end{aligned}\tag{10.2-1}$$

Series of fractions in $\nu = 1/3, 2/5, 3/7, 4/9, 5/11, 6/13, 7/15, \dots, 2/3, 3/5, 4/7, 5/9, 6/11, 7/13, \dots, 5/3, 8/5, 11/7, 14/9, \dots, 4/3, 7/5, 10/7, 13/9, \dots, 1/5, 2/9, 3/13, \dots, 2/7, 3/11, \dots, 1/7, \dots$ with odd denominator have been observed as are also $\nu = 1/2$ and $\nu = 5/2$ states with even denominator [67].

The model of Laughlin [74] cannot explain all aspects of FQHE. The best existing model proposed originally by Jain is based on composite fermions resulting as bound states of electron and even number of magnetic flux quanta [73]. Electrons remain integer charged but due to the effective magnetic field electrons appear to have fractional charges. Composite fermion picture predicts all the observed fractions and also their relative intensities and the order in which they appear as the quality of sample improves.

Before proposing the TGD based model of FQHE as IQHE with non-standard value of Planck constant, it is good to represent a simple explanation of IQHE effect. Choose the coordinates of the current carrying slab so that x varies in the direction of Hall current and y in the direction of the main current. For IQHE the value of Hall conductivity is given by $\sigma = j_y/E_x = n_e e v / v B = n_e e / B = N e^2 / h B S = N e^2 / m h$, where m characterizes the value of magnetized flux and N is the total number of electrons in the current. In the Landau gauge $A_y = x B$ one can assume that energy eigenstates are momentum eigenstates in the direction of current and harmonic oscillator Gaussians in x -direction in which Hall current runs. This gives

$$\Psi \propto \exp(iky) H_n(x + kl^2) \exp\left(-\frac{(x+kl^2)^2}{2l^2}\right) , \quad l^2 = \frac{\hbar}{eB} .\tag{10.2.0}$$

Only the states for which the oscillator Gaussian differs considerably from zero inside slab are important so that the momentum eigenvalues are in good approximation in the range $0 \leq k \leq k_{max} = L_x/l^2$. Using $N = (L_y/2\pi) \int_0^{k_{max}} dk$ one obtains that the total number of momentum eigenstates associated with the given value of n is $N = e B d L_x L_y / h = n$. If ν Landau states are filled, the value of σ is $\sigma = \nu e^2 / h$.

The interpretation of FQHE as IQHE with non standard value of Planck constant could explain also the fractionization of charge, spin, and electron number. There are $2 \times 2 = 4$ combinations of

covering and factor spaces of CP_2 and three of them can lead to the increase or at least fractionization of the Planck constant required by FQHE.

1. The prediction for the filling fraction in FQHE would be

$$\nu = \nu_0 \frac{\hbar_0}{\hbar} \quad , \quad \nu_0 = 1, 2, \dots \quad . \quad (10.2.1)$$

ν_0 denotes the number of filled Landau levels.

2. Let us denote the options as C-C, C-F, F-C, F-F, where the first (second) letter tells whether a singular covering or factor space of CD (CP_2) is in question. The observed filling fractions are consistent with options C-C, C-F, and F-C for which CD or CP_2 or both correspond to a singular covering space. The values of ν in various cases are given by the following table.

<i>Option</i>	<i>C – C</i>	<i>C – F</i>	<i>F – C</i>
ν	$\frac{\nu_0}{n_a n_b}$	$\frac{\nu_0 n_b}{n_a}$	$\frac{\nu_0 n_a}{n_b}$

(10.2.1)

There is a complete symmetry under the exchange of CD and CP_2 as far as values of ν are considered.

3. All three options are consistent with observations. Charge fractionization allows only the options $C – C$ and $F – C$. If one believes the general arguments stating that also spin is fractionized in FQHE then only the option $C – C$, for which charge and spin units are equal to $1/n_b$ and $1/n_a$ respectively, remains. For $C – C$ option one must allow $\nu_0 > 1$.
4. Both $\nu = 1/2$ and $\nu = 5/2$ state has been observed [67, 72]. The fractionized charge is believed to be $e/4$ in the latter case [75, 76]. This requires $n_b = 4$ allowing only (C, C) and (F, C) options. $n_i \geq 3$ holds true if coverings and factor spaces are correlates for Jones inclusions and this gives additional constraint. The minimal values of (ν_0, n_a, n_b) are $(2, 1, 4)$ for $\nu = 1/2$ and $(10, 1, 4)$ for $\nu = 5/2$ for both $C – C$ and $F – C$ option. Filling fraction $1/2$ corresponds in the composite fermion model and also experimentally to the limit of zero magnetic field [73]. $n_b = 2$ would be inconsistent with the observed fractionization of electric charge for $\nu = 5/2$ and with the vision inspired by Jones inclusions implying $n_i \geq 3$.
5. A possible problematic aspect of the TGD based model is the experimental absence of even values of m except $m = 2$ (Laughlin’s model predicts only odd values of m). A possible explanation is that by some symmetry condition possibly related to fermionic statistics (as in Laughlin model) both n_a and n_b must be odd. This would require that $m = 2$ case differs in some manner from the remaining cases.
6. Large values of m in $\nu = n/m$ emerge as B increases. This can be understood from flux quantization. One has $e \int B dS = n\hbar$. By using actual fractional charge $e_F = e/n_b$ in the flux factor would give for (C, C) option $e_F \int B dS = n n_a \hbar_0$. The interpretation is that each of the n_b sheets contributes one unit to the flux for e . Note that the value of magnetic field at given sheet is not affected so that the build-up of multiple covering seems to keep magnetic field strength below critical value.
7. The understanding of the thermal stability is not trivial. The original FQHE was observed in 80 mK temperature corresponding roughly to a thermal energy of $T \sim 10^{-5}$ eV. For graphene the effect is observed at room temperature. Cyclotron energy for electron is (from $f_e = 6 \times 10^5$ Hz at $B = .2$ Gauss) of order thermal energy at room temperature in a magnetic field varying in the range 1-10 Tesla. This raises the question why the original FQHE requires such

a low temperature. A possible explanation is that since FQHE involves several values of Planck constant, it is quantum critical phenomenon and is characterized by a critical temperature. The differences of single particle energies associated with the phase with ordinary Planck constant and phases with different Planck constant would characterize the transition temperature.

10.2.2 Could the dynamics of Kähler action predict the hierarchy of Planck constants?

The original justification for the hierarchy of Planck constants came from the indications that Planck constant could have large values in both astrophysical systems involving dark matter and also in biology. The realization of the hierarchy in terms of the singular coverings and possibly also factor spaces of CD and CP_2 emerged from consistency conditions. The formula for the Planck constant involves heuristic guess work and physical plausibility arguments. There are good arguments in favor of the hypothesis that only coverings are possible. Only a finite number of pages of the Big Book correspond to a given value of Planck constant, biological evolution corresponds to a gradual dispersion to the pages of the Big Book with larger Planck constant, and a connection with the hierarchy of infinite primes and p-adicization program based on the mathematical realization of finite measurement resolution emerges.

One can however ask whether this hierarchy could emerge directly from the basic quantum TGD rather than as a separate hypothesis. The following arguments suggest that this might be possible. One finds also a precise geometric interpretation of preferred extremal property interpreted as criticality in zero energy ontology.

1-1 correspondence between canonical momentum densities and time derivatives fails for Kähler action

The basic motivation for the geometrization program was the observation that canonical quantization for TGD fails. To see what is involved let us try to perform a canonical quantization in zero energy ontology at the 3-D surfaces located at the light-like boundaries of $CD \times CP_2$.

1. In canonical quantization canonical momentum densities $\pi_k^0 \equiv \pi_k = \partial L_K / \partial(\partial_0 h^k)$, where $\partial_0 h^k$ denotes the time derivative of imbedding space coordinate, are the physically natural quantities in terms of which to fix the initial values: once their value distribution is fixed also conserved charges are fixed. Also the weak form of electric-magnetic duality given by $J^{03} \sqrt{g_4} = 4\pi \alpha_K J_{12}$ and a mild generalization of this condition to be discussed below can be interpreted as a manner to fix the values of conserved gauge charges (not Noether charges) to their quantized values since Kähler magnetic flux equals to the integer giving the homology class of the (wormhole) throat. This condition alone need not characterize criticality, which requires an infinite number of deformations of X^4 for which the second variation of the Kähler action vanishes and implies infinite number conserved charges. This in fact gives hopes of replacing π_k with these conserved Noether charges.
2. Canonical quantization requires that $\partial_0 h^k$ in the energy is expressed in terms of π_k . The equation defining π_k in terms of $\partial_0 h^k$ is however highly non-linear although algebraic. By taking squares the equations reduces to equations for rational functions of $\partial_0 h^k$. $\partial_0 h^k$ appears in contravariant and covariant metric at most quadratically and in the induced Kähler electric field linearly and by multiplying the equations by $\det(g_4)^3$ one can transform the equations to a polynomial form so that in principle $\partial_0 h^k$ can be obtained as a solution of polynomial equations.
3. One can always eliminate one half of the coordinates by choosing 4 imbedding space coordinates as the coordinates of the spacetime surface so that the initial value conditions reduce to those for the canonical momentum densities associated with the remaining four coordinates. For instance, for space-time surfaces representable as map $M^4 \rightarrow CP_2$ M^4 coordinates are natural and the time derivatives $\partial_0 s^k$ of CP_2 coordinates are multivalued. One would obtain four polynomial equations with $\partial_0 s^k$ as unknowns. In regions where CP_2 projection is 4-dimensional -in particular for the deformations of CP_2 vacuum extremals the natural coordinates are CP_2 coordinates and one can regard $\partial_0 m^k$ as unknowns. For the deformations of cosmic strings, which are of form

$X^4 = X^2 \times Y^2 \subset M^4 \times CP_2$, one can use coordinates of $M^2 \times S^2$, where S^2 is geodesic sphere as natural coordinates and regard as unknowns E^2 coordinates and remaining CP_2 coordinates.

4. One can imagine solving one of the four polynomials equations for time derivatives in terms of other obtaining N roots. Then one would substitute these roots to the remaining 3 conditions to obtain algebraic equations from which one solves then second variable. Obviously situation is very complex without additional symmetries. The criticality of the preferred extremals might however give additional conditions allowing simplifications. The reasons for giving up the canonical quantization program was following. For the vacuum extremals of Kähler action π_k are however identically vanishing and this means that there is an infinite number of value distributions for $\partial_0 h^k$. For small deformations of vacuum extremals one might however hope a finite number of solutions to the conditions and thus finite number of space-time surfaces carrying same conserved charges.

If one assumes that physics is characterized by the values of the conserved charges one must treat the the many-valuedness of $\partial_0 h^k$. The most obvious guess is that one should replace the space of space-like 4-surfaces corresponding to different roots $\partial_0 h^k = F^k(\pi_l)$ with four-surfaces in the covering space of $CD \times CP_2$ corresponding to different branches of the many-valued function $\partial_0 h^k = F^k(\pi_l)$ co-inciding at the ends of CD .

Do the coverings forces by the many-valuedness of $\partial_0 h^k$ correspond to the coverings associated with the hierarchy of Planck constants?

The obvious question is whether this covering space actually corresponds to the covering spaces associated with the hierarchy of Planck constants. This would conform with quantum classical correspondence. The hierarchy of Planck constants and hierarchy of covering spaces was introduced to cure the failure of the perturbation theory at quantum level. At classical level the multivaluedness of $\partial_0 h^k$ means a failure of perturbative canonical quantization and forces the introduction of the covering spaces. The interpretation would be that when the density of matter becomes critical the space-time surface splits to several branches so that the density at each branches is sub-critical. It is of course not at all obvious whether the proposed structure of the Big Book is really consistent with this hypothesis and one also consider modifications of this structure if necessary. The manner to proceed is by making questions.

1. The proposed picture would give only single integer characterizing the covering. Two integers assignable to CD and CP_2 degrees of freedom are however needed. How these two coverings could emerge?
 - (a) One should fix also the values of $\pi_k^n = \partial L_K / \partial h_n^k$, where n refers to space-like normal coordinate at the wormhole throats. If one requires that charges do not flow between regions with different signatures of the metric the natural condition is $\pi_k^n = 0$ and allows also multi-valued solution. Since wormhole throats carry magnetic charge and since weak form of electric-magnetic duality is assumed, one can assume that CP_2 projection is four-dimensional so that one can use CP_2 coordinates and regard $\partial_0 m^k$ as unknowns. The basic idea about topological condensation in turn suggests that M^4 projection can be assumed to be 4-D inside space-like 3-surfaces so that here $\partial_0 s^k$ are the unknowns. At partonic 2-surfaces one would have conditions for both π_k^0 and π_k^n . One might hope that the numbers of solutions are finite for preferred extremals because of their symmetries and given by n_a for $\partial_0 m^k$ and by n_b for $\partial_0 s^k$. The optimistic guess is that n_a and n_b corresponds to the numbers of sheets for singular coverings of CD and CP_2 . The covering could be visualized as replacement of space-time surfaces with space-time surfaces which have $n_a n_b$ branches. n_b branches would degenerate to single branch at the ends of diagrams of the generated Feynman graph and n_a branches would degenerate to single one at wormhole throats.
 - (b) This picture is not quite correct yet. The fixing of π_k^0 and π_k^n should relate closely to the effective 2-dimensionality as an additional condition perhaps crucial for criticality. One could argue that both π_k^0 and π_k^n must be fixed at X^3 and X_l^3 in order to effectively bring in dynamics in two directions so that X^3 could be interpreted as a an orbit of partonic 2-surface in space-like direction and X_l^3 as its orbit in light-like direction. The additional

conditions could be seen as gauge conditions made possible by symplectic and Kac-Moody type conformal symmetries. The conditions for π_0^k would give n_b branches in CP_2 degrees of freedom and the conditions for π_k^n would split each of these branches to n_a branches.

- (c) The existence of these two kinds of conserved charges (possibly vanishing for π_k^n) could relate also very closely to the slicing of the space-time sheets by string world sheets and partonic 2-surfaces.
2. Should one then treat these branches as separate space-time surfaces or as a single space-time surface? The treatment as a single surface seems to be the correct thing to do. Classically the conserved charges would be $n_a n_b$ times larger than for single branch. Kähler action need not (but could!) be same for different branches but the total action is $n_a n_b$ times the average action and this effectively corresponds to the replacement of the \hbar_0/g_K^2 factor of the action with \hbar/g_K^2 , $r \equiv \hbar/\hbar_0 = n_a n_b$. Since the conserved quantum charges are proportional to \hbar one could argue that $r = n_a n_b$ tells only that the charge conserved charge is $n_a n_b$ times larger than without multi-valuedness. \hbar would be only effectively $n_a n_b$ fold. This is of course poor man's argument but might catch something essential about the situation.
 3. How could one interpret the condition $J^{03}\sqrt{g_4} = 4\pi\alpha_K J_{12}$ and its generalization to be discussed below in this framework? The first observation is that the total Kähler electric charge is by $\alpha_K \propto 1/(n_a n_b)$ same always. The interpretation would be in terms of charge fractionization meaning that each branch would carry Kähler electric charge $Q_K = ng_K/n_a n_b$. I have indeed suggested explanation of charge fractionization and quantum Hall effect based on this picture.
 4. The vision about the hierarchy of Planck constants involves also assumptions about imbedding space metric. The assumption that the M^4 covariant metric is proportional to \hbar^2 follows from the physical idea about \hbar scaling of quantum lengths as what Compton length is. One can always introduce scaled M^4 coordinates bringing M^4 metric into the standard form by scaling up the M^4 size of CD . It is not clear whether the scaling up of CD size follows automatically from the proposed scenario. The basic question is why the M^4 size scale of the critical extremals must scale like $n_a n_b$? This should somehow relate to the weak self-duality conditions implying that Kähler field at each branch is reduced by a factor $1/r$ at each branch. Field equations should possess a dynamical symmetry involving the scaling of CD by integer k and $J^{0\beta}\sqrt{g_4}$ and $J^{n\beta}\sqrt{g_4}$ by $1/k$. The scaling of CD should be due to the scaling up of the M^4 time interval during which the branched light-like 3-surface returns back to a non-branched one.
 5. The proposed view about hierarchy of Planck constants is that the singular coverings reduce to single-sheeted coverings at $M^2 \subset M^4$ for CD and to $S^2 \subset CP_2$ for CP_2 . Here S^2 is any homologically trivial geodesic sphere of CP_2 and has vanishing Kähler form. Weak self-duality condition is indeed consistent with any value of \hbar and implies that the vacuum property for the partonic 2-surface implies vacuum property for the entire space-time sheet as holography indeed requires. This condition however generalizes. In weak self-duality conditions the value of \hbar is free for any 2-D Lagrangian sub-manifold of CP_2 .

The branching along M^2 would mean that the branches of preferred extremals always collapse to single branch when their M^4 projection belongs to M^2 . Magnetically charged light-like throats cannot have M^4 projection in M^2 so that self-duality conditions for different values of \hbar do not lead to inconsistencies. For spacelike 3-surfaces at the boundaries of CD the condition would mean that the M^4 projection becomes light-like geodesic. Straight cosmic strings would have M^2 as M^4 projection. Also CP_2 type vacuum extremals for which the random light-like projection in M^4 belongs to M^2 would represent this of situation. One can ask whether the degeneration of branches actually takes place along any string like object $X^2 \times Y^2$, where X^2 defines a minimal surface in M^4 . For these the weak self-duality condition would imply $\hbar = \infty$ at the ends of the string. It is very plausible that string like objects feed their magnetic fluxes to larger space-times sheets through wormhole contacts so that these conditions are not encountered.

Connection with the criticality of preferred extremals

Also a connection with quantum criticality and the criticality of the preferred extremals suggests itself. Criticality for the preferred extremals must be a property of space-like 3-surfaces and light-like 3-surfaces with degenerate 4-metric and the degeneration of the $n_a n_b$ branches of the space-time surface at the its ends and at wormhole throats is exactly what happens at criticality. For instance, in catastrophe theory roots of the polynomial equation giving extrema of a potential as function of control parameters co-incide at criticality. If this picture is correct the hierarchy of Planck constants would be an outcome of criticality and of preferred extremal property and preferred extremals would be just those multi-branched space-time surfaces for which branches co-incide at the the boundaries of $CD \times CP_2$ and at the throats.

10.3 General ideas about dark matter

In the sequel general ideas about the role of dark matter in condensed matter physics are described.

10.3.1 How the scaling of \hbar affects physics and how to detect dark matter?

It is relatively easy to deduce the basic implications of the scaling of \hbar .

1. If the rate for the process is non-vanishing classically, it is not affected in the lowest order. For instance, scattering cross sections for say electron-electron scattering and e^+e^- annihilation are not affected in the lowest order since the increase of Compton length compensates for the reduction of α_{em} . Photon-photon scattering cross section, which vanishes classically and is proportional to $\alpha_{em}^4 \hbar^2/E^2$, scales down as $1/\hbar^2$.
2. Higher order corrections coming as powers of the gauge coupling strength α are reduced since $\alpha = g^2/4\pi\hbar$ is reduced. Since one has $\hbar_s/\hbar = \alpha Q_1 Q_2/v_0$, $\alpha Q_1 Q_2$ is effectively replaced with a universal coupling strength v_0 . In the case of QCD the paradoxical sounding implication is that α_s would become very small.

10.3.2 General view about dark matter hierarchy and interactions between relatively dark matters

The identification of the precise criterion characterizing dark matter phase is far from obvious. TGD actually suggests an infinite number of phases which are dark relative to each other in some sense and can transform to each other only via a phase transition which might be called de-coherence or its reversal and which should be also characterized precisely.

A possible solution of the problem comes from the general construction recipe for S-matrix. Fundamental vertices correspond to partonic 2-surfaces representing intersections of incoming and outgoing light-like partonic 3-surfaces.

1. If the characterization of the interaction vertices involves all points of partonic 2-surfaces, they must correspond to definite value of Planck constants and more precisely, definite groups G_a and G_b characterizing dark matter hierarchy. Particles of different G_b phases could not appear in the same vertex since the partons in question would correspond to vacuum extremals. Hence the phase transition changing the particles to each other analogous could not be described by a vertex and would be analogous to a de-coherence.

The phase transition could occur at the incoming or outgoing particle lines. At space-time level the phase transition would mean essentially a leakage between different sectors of imbedding space and means that partonic 2-surface at leakage point has CP_2 projection reducing to the orbifold point invariant under G or alternatively, its M_{\pm}^4 projection corresponds to the tip of M_{\pm}^4 . Relative darkness would certainly mean different groups G_a and G_b . Note that $\hbar(M^4)$ *resp.* $\hbar(CP_2)$ can be same for different groups G_a *resp.* G_b and that only the ratio of $\hbar(M^4)/\hbar(M^4)$ appears in the Kähler action.

2. One can represent a criticism against the idea that relatively dark matters cannot appear at the same interaction vertex. The point is that the construction of S-matrix for transitions transforming partonic 2-surfaces in different number fields involves only the rational (algebraic) points in the intersection of the 2-surfaces in question. This idea applies also to the case in which particles correspond to different values of Planck constant. What is only needed that all the common points correspond to the orbifold point in M^4 or CP_2 degrees of freedom and are thus intermediate between two sectors of imbedding space. In this picture phase transitions would occur through vertices and S-matrix would characterize their probabilities. It seems that this option is the correct one.

If the matrix elements for real-real transitions involve all or at least a circle of the partonic 2-surface as stringy considerations suggest [19], then one would have clear distinction between quantum phase transitions and ordinary quantum transitions. Note however that one could understand the weakness of the quantal interactions between relatively dark matters solely from the fact that the CP_2 type extremals providing space-time correlates for particle propagators must in this case go through an intermediate state with at most point-like CP_2 projection.

What does one mean with dark variants of elementary particle?

It is not at all clear what one means with the dark variant of elementary particle. In this respect p-adic mass calculations provide a valuable hint. According to the p-adic mass calculations [17], $k = 113$ characterizes electromagnetic size of u and d quarks, of nucleons, and nuclei. $k = 107$ characterizes the QCD size of hadrons. This is somewhat paradoxical situation since one would expect that quark space-time sheets would be smaller than hadronic space-time sheets.

The simplest resolution of the problem suggested by the basic characteristics of electro-weak symmetry breaking is that $k = 113$ characterizes the size of the electro-magnetic field body of the quark and that the prime characterizing p-adic mass scale labels the em field body of the particle. One can assign mass also the Z^0 body but this would be much smaller as the small scale of neutrino masses suggests. This size scale correspond to a length scale of order $10 \mu\text{m}$, which conforms with the expectation that classical Z^0 force is important in biological length scales. The size of Z^0 body of neutrino could relate directly to the chirality selection in living matter. An interesting question is whether the Z^0 field bodies of also other elementary fermions are of this size.

If this picture is correct then dark variant of elementary particle would differ from ordinary only in the sense that its field body would be dark. This conforms with the general working hypothesis is that only field bodies can be dark.

Are particles characterized by different p-adic primes relatively dark?

Each particle is characterized by a collection of p-adic primes corresponding to the partonic 2-surfaces associate with the particle like 3-surface. Number theoretical vision supports the notion of multi-p p-adicity and the idea that elementary particles correspond to infinite primes, integers, or perhaps even rationals [17, 28]. To infinite primes, integers, and rationals it is possible to associate a finite rational $q = m/n$ by a homomorphism. This would suggest generalization of p-adicity with q-adicity (q-adic topology does not correspond to number field) but this does not seem to be a promising idea.

The crucial observation is that one can decompose the infinite prime, call it P , to finite and infinite parts and distinguish between bosonic and fermionic finite primes of which infinite prime can be said to consist of [34, 17, 53]. The interpretation is that bosonic and fermionic finite primes in the *infinite* part of P code for p-adic topologies of light-like partonic 3-surfaces associated with a given *real* space-time sheet whereas the primes in the *finite* part of P code for p-adic lightlike partonic 3-surfaces.

This raises two options.

1. Two space-time sheets characterized by rationals having common prime factors can be connected by a $\#_B$ contact and can interact by the exchange of particles characterized by divisors of m or n since in this case partonic 2-surface with same p-adic or effective p-adic topology can be found. This is the only possible interaction between them.
2. The number theoretic vision about the construction of S-matrix however allows to construct S-matrix also in the case that partons belong to different number fields and one ends up with a

very elegant description involving only finite number of points of partonic 2-surfaces belonging to their intersection consisting of rational (algebraic points of imbedding space), which by algebraic universality could apply also to diagonal transitions. Also now the interactions mediated between propagators connecting partons with different effective p-adic topologies might be very slow so that this would give rise to relative darkness.

Hierarchy of infinite primes and dark matter hierarchy

In previous consideration only the simplest infinite primes at the lowest level of hierarchy were considered. Simple infinite primes allow a symmetry changing the sign of the finite part of infinite prime. A possible interpretation in terms of phase conjugation. One can consider also more complex infinite primes at this level and a possible interpretation in terms of bound states of several particles. One can also consider infinite integers and rationals: the interpretation would be as many particle states. Rationals might correspond to states containing particles and antiparticles. At the higher levels of the hierarchy infinite primes of previous take the role of finite primes at the previous level and physically these states correspond to higher level bound states of the particles of the previous level.

Thus TGD predicts an entire hierarchy of dark matters such that the many particle states at previous level become particles at the next level. This hierarchy would provide a concrete physical identification for the hierarchy of infinite primes identifiable in terms of a repeated second quantization of an arithmetic super-symmetric QFT [17] including both free many-particle states and their bound states. The finite primes about which infinite prime is in a well defined sense a composite of would correspond to the particles in the state forming a unit of dark matter. Particles belonging to different levels of this hierarchy would obviously correspond to different levels of dark matter hierarchy but their interactions must reduce to the fundamental partonic vertices.

10.3.3 How dark matter and visible matter interact?

The hypothesis that the value of \hbar is dynamical, quantized and becomes large at the verge of a transition to a non-perturbative phase in the ordinary sense of the word has fascinating implications. In particular, dark matter, would correspond to a large value of \hbar and could be responsible for the properties of the living matter. In order to test the idea experimentally, a more concrete model for the interaction of ordinary matter and dark matter must be developed and here of course experimental input and the consistency with the earlier quantum model of living matter is of considerable help.

How dark photons transform to ordinary photons?

The transitions of dark atoms naturally correspond to coherent transitions of the entire dark electron BE condensate and thus generate N_{cr} dark photons and behave thus like laser beams. Dark photons do not interact directly with the visible matter. An open question is whether even ordinary laser beams could be identified as beams of dark photons: the multiple covering property at the level of imbedding space and the fact that MEs are possible in all sectors suggests that this is not the case. Note that the transition from dark to ordinary photons implies the scaling of wave length and thus also of coherence length by a factor n_b/n_a .

Dark \leftrightarrow visible transition should have also a space-time correlate. The so called topological light rays or MEs ("massless extremals") represent a crucial deviation of TGD from Maxwell's ED and have all the properties characterizing macroscopic classical coherence. Therefore MEs are excellent candidates for the space-time correlate of BE condensate of dark photons.

MEs carry in general a superposition of harmonics of some basic frequency determined by the length of ME. A natural expectation is that the frequency of classical field corresponds to the generalized de Broglie frequency of dark photon and is thus \hbar/\hbar_s times lower than for ordinary photons. In completely analogous manner de Broglie wave length is scaled up by $k = \hbar_s/\hbar$. Classically the decay of dark photons to visible photons would mean that an oscillation with frequency f inside topological light ray transforms to an oscillation of frequency f/k such that the intensity of the oscillation is scaled up by a factor k . Furthermore, the ME in question could naturally decompose into $1 < N_{cr} \leq 137$ ordinary photons in the case that dark atoms are in question. Of course also MEs could decay to lower level MEs and this has an interpretation in terms of hierarchy of dark matters to be discussed next.

About the criterion for the transition increasing the value of Planck constant

An attractive assumption is that the transition to dark matter phase occurs when the interaction strength satisfies the criticality condition $Q_1 Q_2 \alpha \simeq 1$. A special case corresponds to self interaction with $Q_1 = Q_2$. This condition applies only to gauge interactions so that particles can be characterized by gauge charges. A more general characterization would be that transition occurs when perturbation theory ceases to converge. The criterion cannot be applied to phenomenological QFT description of strong force in terms of, say, pion exchange.

Some examples are in order to test this view.

1. Transition from perturbative phase in QCD to hadronic phase is the most obvious application. The identification of valence quarks and gluons as dark matter would predict for them QCD size ($k = 107$ space-time sheet) of about electron Compton length. This does not change the QCD cross sections in the lowest order perturbation theory but makes them excellent predictions. It also provides completely new view about how color force determines the nuclear strong force indeed manifesting itself as long ranged harmonic oscillator potential, the long range of which becomes manifest in the case of neutron halos of size of 2.5×10^{-14} m [68]. One can also understand tetra-neutron in this framework. This criterion applies also in QCD plasma and explains the formation of liquid like color glass condensate detected in RHIC [59]. A possible interpretation for QCD size would be as a length of the cylindrical magnetic walls defining the magnetic body associated with u and d type valence quarks, nucleons, and nuclei.
2. QCD size of quark must be distinguished from the electromagnetic size of quark associated with $k = 113$ space-time sheets of u and d quarks and assignable to the height of the magnetic body and defining the length scale of join along boundaries contacts feeding quark charges to $k = 113$ space-time sheets.
3. In the case of atomic nuclei the criterion would naturally apply to the electromagnetic interaction energy of two nucleon clusters inside nucleus or to self energy ($Q^2 \alpha_{em} = 1$). Quite generally, the size of the electromagnetic $k = 113$ space-time sheet would increase by a $n_F = 2^k \prod_s F_s$, where F_s are different Fermat primes (the known ones being 3, 5, 17, 257, $2^{16} + 1$), in the transition to large \hbar phase. Especially interesting values of n_F seem to be of form $n_F = 2^{k11}$ and possibly also $n_F = 2^{k11} \prod_s F_s$. Similar criterion would apply in the plasma phase. Note that many free energy anomalies involve the formation of cold plasma [39].

The criterion would give in the case of single nucleus and plasma $Z \geq 12$ if the charges are within single space-time sheet. This is consistent with cold fusion involving Palladium nuclei [39]. Since u and d quarks have $k = 113$, they both and thus both neutrons and protons could make a transition to large \hbar phase. This is consistent with the selection rules of cold fusion since the production of ${}^3\text{He}$ involves a phase transition $\text{pnp}_d \rightarrow \text{pnp}$ and the contraction of p_d to p is made un-probable by the Coulomb wall whereas the transition $\text{nnp}_d \rightarrow \text{nnp}$ producing tritium does not suffer from this restriction.

Strong and weak physics of nuclei would not be affected in the phase transition. Electromagnetic perturbative physics of nuclei would not be affected in the process in the lowest order in \hbar (classical approximation) but the height of the Coulomb wall would be reduced by a factor $1/n_F$ by the increase in the electromagnetic size of the nucleus. Also Pd nuclei could make the transition and Pd nuclei could catalyze the transition in the case the deuterium nuclei.

10.3.4 Could one demonstrate the existence of large Planck constant photons using ordinary camera or even bare eyes?

If ordinary light sources generate also dark photons with same energy but with scaled up wavelength, this might have effects detectable with camera and even with bare eyes. In the following I consider in a rather light-hearted and speculative spirit two possible effects of this kind appearing in both visual perception and in photos. For crackpotters I want to make clear that I love to play with ideas to see whether they work or not, and that I am ready to accept some convincing mundane explanation of these effects and I would be happy to hear about this kind of explanations. I was not able to find any such explanation from Wikipedia using words like camera, digital camera, lense, aberrations [104].

Why light from an intense light source seems to decompose into rays?

If one also assumes that ordinary radiation fields decompose in TGD Universe into topological light rays ("massless extremals", MEs) even stronger predictions follow. If Planck constant equals to $\hbar = q \times \hbar_0$, $q = n_a/n_b$, MEs should possess Z_{n_a} as an exact discrete symmetry group acting as rotations along the direction of propagation for the induced gauge fields inside ME.

The structure of MEs should somewhat realize this symmetry and one possibility is that MEs has a wheel like structure decomposing into radial spokes with angular distance $\Delta\phi = 2\pi/n_a$ related by the symmetries in question. This brings strongly in mind phenomenon which everyone can observe anytime: the light from a bright source decomposes into radial rays as if one were seeing the profile of the light rays emitted in a plane orthogonal to the line connecting eye and the light source. The effect is especially strong if eyes are stirred. It would seem that focusing makes the effect stronger.

Could this apparent decomposition to light rays reflect directly the structure of dark MEs and could one deduce the value of n_a by just counting the number of rays in camera picture, where the phenomenon turned to be also visible? Note that the size of these wheel like MEs would be macroscopic and diffractive effects do not seem to be involved. The simplest assumption is that most of photons giving rise to the wheel like appearance are transformed to ordinary photons before their detection.

The discussions about this led to a little experimentation with camera at the summer cottage of my friend Samppa Pentikäinen, quite a magician in technical affairs. When I mentioned the decomposition of light from an intense light source to rays at the level of visual percept and wondered whether the same occurs also in camera, Samppa decided to take photos with a digital camera directed to Sun. The effect occurred also in this case and might correspond to decomposition to MEs with various values of n_a but with same quantization axis so that the effect is not smoothed out.

What was interesting was the presence of some stronger almost vertical "rays" located symmetrically near the vertical axis of the camera. In old-fashioned cameras the shutter mechanism determining the exposure time is based on the opening of the first shutter followed by closing a second shutter after the exposure time so that every point of sensor receives input for equally long time. The area of the region determining input is bounded by a vertical line. If macroscopic MEs are involved, the contribution of vertical rays is either nothing or all unlike that of other rays and this might somehow explain why their contribution is enhanced. The shutter mechanism is un-necessary in digital cameras since the time for the reset of sensors is what matters. Something in the geometry of the camera or in the reset mechanism must select vertical direction in a preferred position. For instance, the outer "aperture" of the camera had the geometry of a flattened square.

Anomalous diffraction of dark photons

Second prediction is the possibility of diffractive effects in length scales where they should not occur. A good example is the diffraction of light coming from a small aperture of radius d . The diffraction pattern is determined by the Bessel function

$$J_1(x) \text{ , } x = kdsin(\theta) \text{ , } k = 2\pi/\lambda.$$

There is a strong light spot in the center and light rings around whose radii increase in size as the distance of the screen from the aperture increases. Dark rings correspond to the zeros of $J_1(x)$ at $x = x_n$ and the following scaling law for the nodes holds true

$$sin(\theta_n) = x_n \frac{\lambda}{2\pi d} per.$$

For very small wavelengths the central spot is almost point-like and contains most light intensity.

If photons of visible light correspond to large Planck constant $\hbar = q \times \hbar_0$ transformed to ordinary photons in the detector (say camera film or eye), their wavelength is scaled by q , and one has

$$sin(\theta_n) \rightarrow q \times sin(\theta_n)$$

The size of the diffraction pattern for visible light is scaled up by q .

This effect might make it possible to detect dark photons with energies of visible photons and possibly present in the ordinary light.

1. What is needed is an intense light source and Sun is an excellent candidate in this respect. Dark photon beam is also needed and n dark photons with a given visible wavelength λ could result when dark photon with $\hbar = n \times q \times \hbar_0$ decays to n dark photons with same wavelength but smaller Planck constant $\hbar = q \times \hbar_0$. If this beam enters the camera or eye one has a beam of n dark photons which forms a diffraction pattern producing camera picture in the de-coherence to ordinary photons.
2. In the case of an aperture with a geometry of a circular hole, the first dark ring for ordinary visible photons would be at $\sin(\theta) \simeq (\pi/36)\lambda/d$. For a distance of $r = 2$ cm between the sensor plane ("film") and effective circular hole this would mean radius of $R \simeq r \sin(\theta) \simeq 1.7$ micrometers for micron wave length. The actual size of spots is of order $R \simeq 1$ mm so that the value of q would be around 1000: $q = 2^{10}$ and $q = 2^{11}$ belong to the favored values for q .
3. One can imagine also an alternative situation. If photons responsible for the spot arrive along single ME, the transversal thickness R of ME is smaller than the radius of hole, say of order of wavelength, ME itself effectively defines the hole with radius R and the value of $\sin(\theta_n)$ does not depend on the value of d for $d > R$. Even ordinary photons arriving along MEs of this kind could give rise to an anomalous diffraction pattern. Note that the transversal thickness of ME need not be fixed however. It however seems that MEs are now macroscopic.
4. A similar effect results as one looks at an intense light source: bright spots appear in the visual field as one closes the eyes. If there is some more mundane explanation (I do not doubt this!), it must apply in both cases and explain also why the spots have precisely defined color rather than being white.
5. The only mention about effects of diffractive aberration effects are colored rings around say disk like objects analogous to colors around shadow of say disk like object. The radii of these diffraction rings in this case scale like wavelengths and distance from the object.
6. Wikipedia contains an article from which one learns that the effect in question is known as lens flares [102]. The article states that flares typically manifest as several starbursts, circles, and rings across the picture and result in internal reflection and scattering from material inhomogeneities in lens (such as multiple surfaces). The shape of the flares also depends on the shape of aperture. These features conform at least qualitatively with what one would expect from a diffraction if Planck constant is large enough for photons with energy of visible photon.

The article [82] defines flares in more restrictive manner: lense flares result when *non-image* forming light enters the lens and subsequently hits the camera's film or digital sensor and produces typically polygonal shape with sides which depend on the shape of lense diaphragm. The identification as a flare applies also to the apparent decomposition to rays and this dependence indeed fits with the observations.

The experimentation of Samppa using digital camera demonstrated the appearance of colored spots in the pictures. If I have understood correctly, the sensors defining the pixels of the picture are in the focal plane and the diffraction for large Planck constant might explain the phenomenon. Since I did not have the idea about diffractive mechanism in mind, I did not check whether fainter colored rings might surround the bright spot.

1. In any case, the readily testable prediction is that zooming to bright light source by reducing the size of the aperture should increase the size and number of the colored spots. As a matter fact, experimentation demonstrated that focusing brought in large number of these spots but we did not check whether the size was increased.
2. Standard explanation predicts that the bright spots are present also with weaker illumination but with so weak intensity that they are not detected by eye. The positions of spots should also depend only on the illumination and camera. The explanation in terms of beams of large Planck constant photons predicts this if the flux of dark photons from any light source is constant.

10.3.5 Dark matter and exotic color and electro-weak interactions

The presence of classical electro-weak and color gauge fields in all length scales is an unavoidable prediction of TGD and the interpretation in terms of p-adic and dark matter hierarchies is also more or less unavoidable. The new element in the interpretation is based on the observation that the quark and antiquarks at the ends of flux tubes serving as sources of classical color gauge fields could be seen as a vacuum polarization effect. In the same manner neutrino pairs at the ends of flux tubes serving as sources of classical Z^0 fields could be seen as a vacuum polarization effect.

One of the many open questions is whether also p-adic hierarchy defines a hierarchy of confinement scales for color interactions and screening scales for weak interactions or whether only the hierarchy of Planck constants gives rise to this kind of hierarchy. It would look strange if all flux tubes of macroscopic size scale would always correspond to a large value of \hbar and therefore singular covering and fractionized quantum numbers. Also the proposed dark rules involving hierarchy of Mersenne rules would support the view that both hierarchies are present and there is an interaction between them in the sense that phase transitions between dark and thus scaled up counterpart of p-adic length scale and non-dark scaled up p-adic length scale can take place. The proposed stability criteria certainly allow this.

Do p-adic and dark matter hierarchies provide a correct interpretation of long ranged classical electro-weak gauge fields?

For two decades one of the basic interpretational challenges of TGD has been to understand how the un-avoidable presence of long range classical electro-weak gauge fields can be consistent with the small parity breaking effects in atomic and nuclear length scales. Also classical color gauge fields are predicted, and I have proposed that color qualia correspond to increments of color quantum numbers [33]. The proposed model for screening cannot banish the unpleasant feeling that the screening cannot be complete enough to eliminate large parity breaking effects in atomic length scales so that one must keep mind open for alternatives.

p-Adic length scale hypothesis suggests the possibility that both electro-weak gauge bosons and gluons can appear as effectively massless particles in several length scales and there indeed exists evidence that neutrinos appear in several scaled variants [71] (for TGD based model see [26]).

This inspires the working hypothesis that long range classical electro-weak gauge and gluon fields are correlated for light or massless p-adically scaled up and dark electro-weak gauge bosons and gluons. Thus both p-adic and dark hierarchies would be involved. For the p-adic hierarchy the masses would be scaled up whereas for the dark hierarchy masses would be same. The essentially new element in the interpretation would be that these fields assignable to flux quanta could be seen as vacuum polarization effects in even macroscopic length scales. This vision would definitely mean new physics effects but the interpretation would be consistent with quantum field theoretic intuition.

1. In this kind of scenario ordinary quarks and leptons could be essentially identical with their standard counterparts with electro-weak charges screened in electro-weak length scale so that the problems related to the smallness of atomic parity breaking would be trivially resolved. The weak form of electric-magnetic duality allows to identify the screening mechanism as analog of confinement mechanism for weak isospin
2. In condensed matter blobs of size larger than neutrino Compton length (about $5 \mu\text{m}$ if $k = 169$ determines the p-adic length scale of condensed matter neutrinos) the situation could be different. Also the presence of dark matter phases with sizes and neutrino Compton lengths corresponding to the length scales $L(k)$, $k = 151, 157, 163, 167$ in the range $10 \text{ nm} - 2.5 \mu\text{m}$ are suggested by the number theoretic considerations (these values of k correspond to so called Gaussian Mersennes [51]). Only a fraction of the condensed matter consisting of regions of size $L(k)$ need to be in the dark phase.
3. Dark quarks and leptons would have masses essentially identical to their standard model counterparts. Only the electro-weak boson masses which are determined by a different mechanism than the dominating contribution to fermion masses [26, 26] would be small or vanishing. Below the dark or p-adic length scale in question gauge bosons would behave like massless quanta.

4. The large parity breaking effects in living matter would be due to the presence of dark nuclei and leptons. Later the idea that super-fluidity corresponds to Z^0 super-conductivity will be discussed it might be that also super-fluid phase corresponds to dark neutron phase.

The basic prediction of TGD based model of dark matter as a phase with a large value of Planck constant is the scaling up of various quantal length and time scales. Mersenne hypothesis allows a wide range of scales so that very rich structures are possible.

Dark photon many particle states behave like laser beams decaying to ordinary photons by decoherence meaning a transformation of dark photons to ordinary ones. Also dark electro-weak bosons and gluons would be massless or have small masses determined by the p-adic length scale in question. The decay products of dark electro-weak gauge bosons would be ordinary electro-weak bosons decaying rapidly via virtual electro-weak gauge boson states to ordinary leptons. Topological light rays ("massless extremals") for which all classical gauge fields are massless are natural space-time correlates for the dark boson laser beams. Obviously this means that the basic difference between the chemistries of living and non-living matter would be the absence of electro-weak symmetry breaking in living matter (which does not mean that elementary fermions would be massless).

Criterion for the presence of exotic electro-weak bosons and gluons

Classical gauge fields directly are space-time correlates of quantum states. The gauge fields associated with massless extremals ("topological light rays") decompose to free part and a part having non-vanishing divergence giving rise to a light-like Abelian gauge current. Free part would correspond to Bose-Einstein condensates and current would define a coherent state of dark photons.

The dimension D of the CP_2 projection of the space-time sheet serves as a criterion for the presence of long ranged classical electro-weak and gluon fields. D also classifies the (possibly asymptotic) solutions of field equations [36].

1. For $D = 2$ induced gauge fields are Abelian and induced Kähler form vanishes for vacuum extremals: in this case classical em and Z^0 fields are proportional to each other. The non-vanishing Kähler field implies that induced gluon fields are non-vanishing in general. This raises the question whether long ranged color fields and by quantum classical correspondence also long ranged QCD accompany non-vacuum extremals in all length scales. This makes one wonder whether color confinement is possible at all and whether scaled down variants of QCD appear in all length scales.

The possibility to add constants to color Hamiltonians appearing in the expression of the classical color gauge fields allows to have vanishing color charges in the case of an arbitrary space-time sheet. The requirement that color quantum numbers of the generator vanish allows to add the constant only to the Hamiltonians of color hyper charge and isospin so that for $D = 2$ extremals color charges can be made vanishing. This might allow to understand how color confinement is consistent with long ranged induced Kähler field.

2. For $D \geq 3$ all classical long ranged electro-weak fields and non-Abelian color fields are present. This condition is satisfied when electric and magnetic fields are not orthogonal and the instanton density $A \wedge J$ for induced Kähler form is non-vanishing. The rather strong conclusion is that in length scales in which exotic electro-weak bosons are not present, one has $D = 2$ and gauge fields are Abelian and correspond trivially to fixed points of renormalization group realized as a hydrodynamic flow at space-time sheets [26].

Quantum classical correspondence suggests the existence of electro-weak gauge bosons with mass scale determined by the size of the space-time sheets carrying classical long range electro-weak fields. This would mean the existence of new kind of gauge bosons.

The obvious objection is that the existence of these gauge bosons would be reflected in the decay widths of intermediate gauge bosons. The remedy of the problem is based on the notion of space-time democracy suggested strongly by the fact that the interactions between space-time sheets possessing different p-adic topologies proceed with very slow rates simply because the number of common rational (algebraic) points of partonic 2-surfaces appearing in the vertex is small.

For light exotic electro-weak bosons also the corresponding leptons and quarks would possess a large weak space-time sheet but lack the ordinary weak partonic 2-surface so that there would be no

direct coupling to electro-weak gauge bosons. These space-time sheets are dark in weak sense but need not have a large value of \hbar . This picture implies the notion of partial darkness since any space-time sheets with different ordinary of Gaussian primes are dark with respect to each other.

Do Gaussian Mersennes define a hierarchy of dark electro-weak physics?

Gaussian Mersennes are defined as Gaussian primes of form $g_n = (1+i)^n - 1$, where n must be prime. They have norm squared $g\bar{g} = 2^n - 1$. The list of the first Gaussian Mersennes corresponds to the following values of n .

2, 3, 5, 7, 11, 19, 29, 47, 73, 79, 113, 151, 157, 163, 167, 239, 241, 283, 353, 367, 379, 457, 997, 1367, 3041, 10141, 14699, 27529, 49207, 77291, 85237, 106693, 160423 and 203789.

The Gaussian primes $k = 113, 151, 157, 163, 167$ correspond to length scales which are of most obvious interest but in TGD framework one cannot exclude the twin prime 239, 241 corresponds to length scales $L(k) \simeq 160$ km and 320 km. Also larger primes could be of relevant for bio-systems and consciousness. Also the secondary and higher length scales associated with $k < 113$ could be of importance and their are several length scales of this kind in the range of biologically interesting length scales. Physics and biology inspired considerations suggests that particular Gaussian primes correspond to a particular kind of exotic matter, possibly also to large \hbar phase.

$k = 113$ corresponds to the electromagnetic length scale of u and d quarks and nuclear p-adic length scale. For dark matter these length scales are scaled up by a factor $r \sim 2^{k_d}$, with k_d fixed by Mersenne hypothesis.

On basis of biological considerations (large parity breaking in living matter) there is a temptation to assign to these length scales a scaled down copy of electro-weak physics and perhaps also of color physics. The mechanism giving rise to these states would be a phase transition transforming the ordinary $k = 89$ Mersenne of weak space-time sheets to a Gaussian Mersenne and thus increasing its size dramatically.

If given space-time sheet couples considerably only to space-time sheets characterized by same prime or Gaussian prime, the bosons of these physics do not couple directly to ordinary particles, and one avoids consistency problems due to the presence of new light particles (consider only the decay widths of intermediate gauge bosons [20]) even in the case that the loss of asymptotic freedom is not assumed.

A question arises about the interpretation of structures of the predicted size. The strong interaction size of u and d quarks, hadrons, and nuclei is smaller than $L(k = 113) \simeq 2 \times 10^{-4}$ m for even heaviest nuclei if one accepts the formula $R \sim A^{1/3} \times 1.5 \times 10^{-15}$ m. A natural interpretation for this length scale would be as the size of the field body/magnetic body of system defined by its topologically quantized gauge fields/magnetic parts of gauge fields. The (possibly dark) p-adic length scale characterizes also the lengths of join along boundaries bonds feeding gauge fluxes from elementary particle to the space-time sheet in question. The delocalization due these join along boundaries bonds in p-adic length scale in question would determine the scale of the contribution to the mass squared of the system as predicted by p-adic thermodynamics.

10.3.6 Anti-matter and dark matter

The usual view about matter anti-matter asymmetry is that during early cosmology matter-antimatter asymmetry characterized by the relative density difference of order $r = 10^{-9}$ was somehow generated and that the observed matter corresponds to what remained in the annihilation of quarks and leptons to bosons. A possible mechanism inducing the CP asymmetry is based on the CP breaking phase of CKM matrix.

The TGD based view about energy [35, 16] forces the conclusion that all conserved quantum numbers including the conserved inertial energy have vanishing densities in cosmological length scales. Therefore fermion numbers associated with matter and antimatter must compensate each other. Therefore the standard option seems to be excluded in TGD framework.

The way out could be based on the many-sheeted space-time and the possibility of cosmic strings. One particular TGD inspired model involves a small matter-antimatter asymmetry induced by the Kähler electric fields of cosmic strings [24]. The topological condensation of fermions and antifermions at space-time sheets carrying Kähler electric field of say cosmic string gives rise to a binding energy

which is of different sign for fermions and antifermions and therefore should induce the asymmetry. The outcome of the annihilation period would be matter outside cosmic strings and antimatter inside them.

One can also imagine that in a given Kähler electric field matter develops large binding energy and antimatter large positive interaction energy which induces instability leading to the splitting of partonic 2-surfaces to dark space-time sheets implying fractionization and reduction of the energy at given sheet of the covering. Dark antimatter would interact very weakly with ordinary matter so that the non-observability of antimatter would find an elegant explanation. One can imagine also the generation of local asymmetries inside Kähler electric flux tubes leading to flux tube states with matter and antimatter condensed at the opposite ends of the flux tubes.

10.4 Dark variants of nuclear physics

The book metaphor for the extended imbedding space can be utilized as a guideline as one tries to imagine various exotic phases of matter. For the minimal option atomic nuclei can be assumed to be ordinary (in the sense of nuclear string model [24]!) and only field bodies can be dark. If only singular coverings of M^4 and CP_2 are allowed the value of Planck constant is product of two integers. Ruler and compass hypothesis restricts these integers considerably and Mersenne hypothesis provides further constraints on the model. Nuclei can be visualized as residing at the "standard" pages of the book and dark color-/weak-/em- bonds are at different pages with different p-adic length scale or having different Planck constant. This would give two hierarchies of nuclei with increasing size.

10.4.1 Constraints from the nuclear string model

In the case of exotic nuclei nuclear string model [47] is a safe starting point. In this model nucleons are connected by color flux tubes having exotic light fermion and antifermion at their ends. Whether fermion is quark or colored excitation of lepton remains open question at this stage. The mass of the exotic fermion is much smaller than 1 MeV (p-adic temperature $T = 1/n < 1$). This model predicts large number of exotic states since color bonds, which can be regarded as colored pions, can have em charges (1,-1,0). In particular, neutral variant of deuterium is predicted and this leads to a model of cold fusion explaining its basic selection rules. The earlier model for cold fusion discussed in [23], which served as a constraint in the earlier speculations, is not so simple than the model of [47].

What is important that the model requires that weak bosons for which Compton length is of order atomic size are involved. Weak bosons would behave as massless particles below the Compton and the rates for the exchanges of weak bosons would be high in the length scales considered. Weak bosons would correspond to scaled up variants of the ordinary weak bosons: scaling could be p-adic in which mass scale is reduced and weak interaction rates even above Compton length would be scaled up as $1/M_W^4$. The scaling could result also from the scaling of Planck constant in which case masses of weak bosons nor weak interaction rates in the lowest order would not be affected. If only dark scaling is involved, weak interactions would be still extremely weak above dark Compton length of weak bosons. Of course, both scalings can be imagined.

The scale of the color binding energy is $E_s = .2$ MeV for ordinary 4He strings [24]. $k = 151, 157, 163, 167$ define Gaussian Mersennes $G_{M,k} = (1 + i)^k - 1$ and excellent candidates for biologically important p-adic length scales. There are also higher Gaussian Mersennes such as those corresponding to $k = 239, 241$ and also these seem to be interesting biologically (see [43] where a vision about evolution and generalized EEG based on Gaussian Mersennes is described). Let us assume that these scales and also those corresponding to $k = 89, 107, 113, 127$ allow scaled variants of electroweak and color interactions with ordinary value of Planck constant. If M_{127} is scaled up to Gaussian Mersenne $M_{G,167}$, one obtains cell-nucleus sized ($2.58 \mu m$) exotic nuclei and the unit of color binding energy is still .2 eV. For p-adic length scale of order $100 \mu m$ (size of large neuron) the energy scale is still around thermal energy at room temperature.

In the case of dark color bonds it is not quite clear how the unit E_s of the color binding energy scales. If color Coulombic energy is in question, one expects $1/\hbar^2$ scaling. Rather remarkably, this scaling predicts that the unit for the energy of $A < 4$ color bond scales down to .5 eV which is the energy of hydrogen bond so that hydrogen bonds, and also other molecular bonds, might involve color bonds between proton and oxygen.

10.4.2 Constraints from the anomalous behavior of water

$H_{1.5}O$ behavior of water with respect to neutron and electron scattering is observed in attosecond time scale which corresponds to 3 Angstrom length scale, defining an excellent candidate for the size scale of exotic nuclei and Compton length of exotic weak interactions.

What happens to the invisible protons?

A possible explanation for the findings is that one fourth of protons forms neutral multi-proton states connected by possibly negatively charged color bonds of length differing sufficiently from the length of ordinary O-H bond. Although the protons are ordinary, neutron diffraction reflecting the crystal like order of water in atomic length scales would not see these poly-proton super-nuclei if they form separate closed strings.

1. For the ordinary nuclei the p-adic length scale associated with the color bonds between 4He corresponds to M_{127} , and one can imagine exotic nuclear strings obtained by connecting two ordinary nuclei with color bonds. If second exotic nucleus is neutral (the model of cold fusion assumes that D nucleus is neutral) this could work since the Coulomb wall is absent. If the exotic nuclei have opposite em charges, the situation improves further. New super-dense phases of condensed matter would be predicted.

If one fourth of hydrogen nuclei of water combine to form possibly neutral nuclear strings with average distance of nuclei of order $L(127)$, they are not visible in diffraction at atomic length scale because the natural length scale is shortened by a factor of order 32 but could be revealed in neutron diffraction at higher momentum exchanges. The transition between this kind of phase and ordinary nuclei would be rather dramatic event and the exchanges of exotic weak bosons with Compton lengths of order atomic size induce the formation of this kind of nuclei (this exchange is assumed in the model of cold fusion).

2. If dark color magnetic bonds are allowed, a natural distance between the building blocks of super-nuclei is given by the size scale of the color magnetic body. In nuclear string model the size scales of color magnetic bodies associated with nuclear strings consisting of 4He and $A < 4$ nuclei color magnetic bodies correspond to $k = 127$ and $k = 118$ whereas em magnetic body corresponds to $k = 116$ [47]. For dark variants of magnetic bodies the sizes of these magnetic bodies are scaled. There are several options to consider: consider only $k_d = 113 - 89 = 24$, $k_d = 127 - 107 = 20$ and $k_d = 107 - 89 = 18$. Table 1 below summarizes the effective dark p-adic length scales involved.
3. Consider $k_d = 24$ as an example. From Table 1 the scaled up p-adic length scales of the magnetic bodies would be $L(127 + 24 = 151) = 10$ nm, $L(118 + 24 = 142) = 4.4$ Angstrom, and $L(116 + 24 = 140) = 2.2$ Angstrom. The first scale equals to the thickness of cell membrane which suggests a direct connection with biology. The latter two scales correspond to molecular length scales and it is not clear why the protons of dark nuclear strings of this kind would not be observed in electron and neutron scattering. This would leave only nuclear strings formed from 4He nuclei into consideration.

The crucial parameter is the the unit E_s of the color binding energy. Since this parameter should correspond to color Coulombic potential it could transform like the binding energy of hydrogen atom and therefore scale as $1/\hbar^2$. This would mean that $E_s = 2.2$ MeV deduced from the deuteron binding energy would scale down to .12 eV for $r = 2^{24}$.

k_d	24	20	18
$k_{eff} = 127 + k_d$	151	142	140
$k_{eff} = 118 + k_d$	142	138	136
$k_{eff} = 116 + k_d$	140	136	134

Table 1. The integers k_{eff} characterize the effective p-adic length scales for some dark variants of color magnetic bodies for 4He and $A < 4$ color magnetic bodies corresponding to $k \in \{127, 118\}$ and

for the dark variants of $k = 116$ electromagnetic body for nuclear strings. Dark variants correspond to $k_d \in \{24 = 113 - 89 = 151 - 127, 20 = 127 - 107, 18 = 107 - 89\}$ allowed by Mersenne hypothesis.

The transition between the dark and ordinary nuclei would be favored by the minimization of Coulomb energy and energy differences would be small because of darkness. The transitions in which ordinary proton becomes dark and fuses to super-nuclear string or vice versa could be the basic control mechanism of bio-catalysis. Metabolic energy quantum .5 eV should relate to this transition.

Magic nuclei could have fractally scaled up variants in molecular length scale and tetrahedral and icosahedral water clusters could correspond to $A = 8$ and $A = 20$ magic nuclei with color bonds connecting nucleons belonging to different dark nuclei.

About the identification of the exotic weak physics?

The model of cold fusion requires exotic weak physics with the range of weak interaction of order atomic radius.

One can consider the possibility of $k = 113$ dark weak physics with $r = 2^{24}$ ($89 \rightarrow 113$ in Mersenne hypothesis) implying that the dark weak scale corresponds to p-adic length scale $k = 137$. Weak Compton length for $k = 113$ dark weak bosons would be about 3 Angstrom. Below $L(137)$ weak bosons would behave as massless particles. Above $L(137)$ weak bosons would have the mass scale $2^{-12}m_W \sim 25$ MeV and weak rates would be scaled up by 2^{48} . Bohr radius would represent a critical transition length scale and exotic weak force could have dramatic implications for the behavior of the condensed matter in high pressures when exotic weak force would become visible. In particular, chiral selection in living matter could be understood in terms of large parity breaking implied. These physics would manifest themselves only at criticality for the phase transitions changing Planck constant and would correspond to almost vacuum extremals defining a phase different from that assignable to standard model physics.

To sum up, it would seem that the variant of ordinary nuclear physics obtained by making color bonds and weak bonds dark is the most promising approach to the $H_{1.5}O$ anomaly and cold fusion. Exotic weak bosons with Compton wave length of atomic size and the most natural assumption is that they are dark $k = 113$ weak bosons with $k_d = 24 = 113 - 89$. One variant of exotic atoms is as atoms for which electromagnetic interaction between ordinary nuclei and ordinary electrons is mediated along dark topological field quanta.

10.4.3 Exotic chemistries and electromagnetic nuclear darkness

The extremely hostile and highly un-intellectual attitude of skeptics stimulates fear in anyone possessing amygdala, and I am not an exception. Therefore it was a very pleasant surprise to receive an email telling about an article published in April 16, 2005 issue of New Scientist [52]. The article gives a popular summary about the work of the research group of Walter Knight with Na atom clusters [48] and of the research group of Welford Castleman with Al atom clusters [54].

The article tells that during last two decades a growing evidence for a new kind of chemistry have been emerging. Groups of atoms seem to be able to mimic the chemical behavior of single atom. For instance, clusters of 8, 20, 40, 58 or 92 sodium atoms mimic the behavior of noble gas atoms [48]. By using oxygen to strip away electrons one by one from clusters of Al atoms it is possible to make the cluster to mimic entire series of atoms [54]. For aluminium cluster-ions made of 13, 23 and 37 atoms plus an extra electron are chemically inert.

One can imagine two explanations for the findings.

1. The nuclei are dark in the sense that the sizes of nuclear space-time sheets are scaled up implying the smoothing out of the nuclear charge.
2. Only electrons are dark in the sense of having scaled up Compton lengths so that the size of multi-electron bound states is not smaller than electron Compton length and electrons "see" multi-nuclear charge distribution.

If darkness and Compton length is assigned with the em field body, it becomes a property of interaction, and it seems impossible to distinguish between options 1) and 2).

What one means with dark nuclei and electrons?

Can the idea about dark nuclei and electrons be consistent with the minimalist picture in which only field bodies are dark? Doesn't the darkness of nucleus or electron mean that also multi-electron states with n electrons are possible?

The proper re-interpretation of the notion Compton length would allow a consistency with the minimalist scenario. If the p-adic prime labelling the particle actually labels its electromagnetic body as p-adic mass calculations for quark masses encourage to believe, Compton length corresponds to the size scale of the electromagnetic field body and the models discussed below would be consistent with the minimal scenario. Electrons indeed "see" the external charge distribution by their electromagnetic field body and field body also carries this distribution since CP_2 extremals do not carry it. One could also defend this interpretation by saying that electrons is operationally only what can be observed about it through various interactions and therefore Compton length (various Compton length like parameters) must be assigned with its field body (bodies).

Also maximal quantum criticality implies that darkness is restricted to field bodies but does not exclude the possibility that elementary particle like structures can possess non-minimal quantum criticality and thus possess multi-sheeted character.

Option I: nuclei are electromagnetically dark

The general vision about nuclear dark matter suggests that the system consists of super-nuclei analogous to ordinary nuclei such that electrons are ordinary and do not screen the Coulomb potentials of atomic nuclei.

The simplest possibility is that the electromagnetic field bodies of nuclei or quarks become dark implying delocalization of nuclear charge. The valence electrons would form a kind of mini-conductor with electrons delocalized in the volume of the cluster. The electronic analog of the nuclear shell model predicts that full electron shells define stable configurations analogous to magic nuclei. The model explains the numbers of atoms in chemically inert Al and Ca clusters and generalizes the notion of valence to the level of cluster so that the cluster would behave like single super-atom.

The electromagnetic $k = 113$ space-time sheets (em field bodies) of quarks could have scaled up size $\sqrt{r}L(113) = L(113+k_d) = 2^{k_d/2} \times 2 \times 10^{-14}$ m. One would have atomic size scale .8 Angstroms for $r = 2^{k_d}$, $k_d = 24$ - an option already introduced. A suggestive interpretation is that the electric charge of nuclei or valence quarks assignable to their field bodies is delocalized quantum mechanically to atomic length scale. Electrons would in a good approximation experience quantum mechanically the nuclear charges as a constant background, jellium, whose effect is indeed modellable using harmonic oscillator potential.

One can test the proposed criterion for the phase transition to darkness. The unscreened electromagnetic interaction energy between a block of partially ionized nuclei with a net em charge Z with Z electrons would define the relevant parameter as $r \equiv Z^2\alpha$. For the total charge $Z \geq 12$ the condition $r \geq 1$ is satisfied. For a full shell with 8 electrons this condition is not satisfied.

Option II: Electrons are electro-magnetically dark

Since the energy spectrum of harmonic oscillator potential is invariant under the scaling of \hbar accompanied by the opposite scaling of the oscillator frequency ω , one must consider also the em bodies of electrons are in large \hbar phase (one can of course ask whether they could be observed in this phase!). The rule would be that the size of the bound states is larger than the scaled up electron Compton length.

The Compton wavelength of electrons would be scaled up by a factor r where r is product of different Fermat primes and power of 2 for ruler and compass hypothesis. For Mersenne hypothesis one would have $r = 2^{k_d}$. For $k_d = 24$ the effective p-adic scale of electron would be to about $L(151) = 10$ nm. The atomic cluster of this size would contain roughly $10^6 \times (a_0/a)^3$ atoms where a is atomic volume and $a_0 = 1$ Angstrom is the natural unit.

The shell model of nucleus is in TGD framework a phenomenological description justified by nuclear string model with string tension responsible for the oscillator potential. This leads to ask whether the electrons of jellium actually form analogs of nuclear strings with electrons connected by color bonds.

10.5 Has dark matter been observed?

In this section two examples about anomalies perhaps having interpretation in terms of quantized Planck constant are discussed. The first anomaly belongs to the realm of particle physics and hence does not quite fit the title of the chapter. Second anomaly relates to nuclear physics.

10.5.1 Optical rotation of a laser beam in a magnetic field

The group of G. Cantatore has reported an optical rotation of a laser beam in a magnetic field [91]. The experimental arrangement involves a magnetic field of strength $B = 5$ Tesla. Laser beam travels 22000 times forth and back in a direction orthogonal to the magnetic field travelling 1 m during each pass through the magnet. The wavelength of the laser light is 1064 nm (the energy is 1.1654 eV). A rotation of $(3.9 \pm .5) \times 10^{-12}$ rad/pass is observed.

Faraday effect [88] is optical rotation which occurs when photon beam propagates in a direction parallel to the magnetic field and requires parity breaking guaranteeing that the velocities of propagation for two circular polarizations are different. Now however the laser beam is orthogonal to the magnetic field so that Faraday effect cannot be in question.

The proposed interpretation for the rotation would be that the component of photon having polarization parallel to the magnetic field mixes with QCD axion, one of the many candidates for dark matter. The mass of the axion would be about 1 meV. Mixing would imply a reduction of the corresponding polarization component and thus in the generic case induce a rotation of the polarization direction. Note that the laser beam could partially transform to axions, travel through a non-transparent wall, and appear again as ordinary photons.

The disturbing finding is that the rate for the rotation is by a factor 2.8×10^4 higher than predicted. This would have catastrophic astrophysical implications since stars would rapidly lose their energy via axion radiation.

What explanations one could imagine for the observations in TGD framework if one accepts the hierarchy of Planck constants?

1. The simplest model that I have been able to imagine does not assume axion like states. The optical rotation would be due to the leakage of the laser photons to dark pages of the Big Book at the ends of the magnet where the space-time sheet carrying the magnetic field becomes locally a vacuum extremal. This explanation would not mean direct seeing of dark matter but the observation of a transformation of ordinary matter to dark matter. Quite generally, this experimental approach might be much better strategy to the experimental proof of the existence of the dark matter than the usual approaches and is especially attractive in living matter.
2. TGD could also provide a justification for the axion based explanation of the optical rotation involving parity breaking. TGD predicts the existence of a hierarchy of QCD type physics based on the predicted hierarchy of scaled up variants of quarks and also those of color excited leptons. The fact that these states are not seen in the decay widths of intermediate gauge bosons can be understood if the particles in question are dark matter with non-standard value of Planck constant and hence residing at different page of the book like structure formed by the imbedding space. I have discussed in detail the general model in the case of leptohadrons consisting of colored excitation of ordinary lepton and explaining quite an impressive bundle of anomalies [24]. Since leptopion has quantum numbers of axion and similar couplings, it is natural to propose that the claimed axion like particle -if it indeed exists- is a pion like state consisting either exotic light quarks or leptons.

The model would differ from the above model only in that the leakage to the dark sector would take place by a transformation of the laser photon to a pionlike state so that no parity breaking would take place. But the basic point is that vacuum extremals through which the leakage can occur, break the parity strongly by the presence of classical Z^0 fields. The idea about leakage together with the non-constancy of pion-type field appearing in the coupling to the instanton density imply that that the space-time sheet representing the magnetic field is vacuum extremal -at least in some regions- and this assumption looks un-necessarily strong. Also detailed assumptions about the dependence of the basic parameters appearing in PCAC hypothesis must be made.

What raised the hopes was the intriguing observation that the ratio of laser photon frequency to the cyclotron frequency of electron in the magnetic field considered equals to $r = 2^{11}$: this put bells ringing in the p-adically tuned mind and inspired the question whether one could have $\hbar/\hbar_0 = 2^{11}$. The assumption of cyclotron condensate of electron pairs at dark space-time sheet must be however justified and one must answer at least the question why it is needed. A possible answer would be that the leakage occurs via Bose-Einstein condensation to a coherent state of cyclotron photons. But this would mean return to the original model where laser photons leak! Obviously the model becomes too complicated for Occam and therefore I have dropped out the model.

The simplest model should start just from the finding that the linear polarization parallel to the magnetic field seems to leak with a certain rate as it traverses the magnet. The leakage of laser photons to a dark matter space-time sheet is what comes mind first in TGD context. A killer test for this explanation is to use polarization parallel to the magnetic field: in this case no optical rotation should take place.

1. The leakage should take place along the intersection of the pages of the Big Book which correspond to geodesically trivial geodesic sphere of CP_2 so that induced Kähler field vanishes and vacuum extremals or nearly vacuum extremals are in question. Leakage could occur within magnet or the ends of the magnet could involve this kind of critical membrane like region and as the photon passes through them the leakage could occur.
2. Since parity breaking takes place, the instanton density for the electromagnetic field provides a natural description of the situation. The interaction term is obtained by replacing either E in $E \cdot B$ with its quantized counterpart describing laser photons. This gives a linear coupling to photon oscillator operators completely analogous to a coupling to an external current and one can calculate the leakage rate using the standard rules.
3. The interaction term is total divergence and reduces to a 3-D Chern-Simons type term associated with the boundaries of the membrane like region or magnet in the general case and the leakage can be said to occur at the ends of the magnet for non-vacuum extremals.

One can ask whether one should use the instanton density of Kähler field rather than that of em field in the model. In this case Kähler gauge potential would couple the quantized em field via $U(1)$ part of em charge. One would not have gauge invariance since for the induced Kähler field gauge degeneracy is replaced with spin glass degeneracy and gauge transformations of the vacuum extremals induced by symplectic transformations of CP_2 deform the space-time surface. In this case E in $E \cdot A$ would be replaced with the radiation field at the ends of the magnet. In order to have a non-vanishing leakage the instanton density within magnet must be non-vanishing meaning that CP_2 projection of the magnet's space-time sheet must be 4-D at least somewhere. For the first option it can be 2-D.

The coefficient K of the instanton term defining the action should depend on the value of Planck constant. $1/e^2$ proportionality of the ordinary Maxwell action means that the coefficient of the instanton term could be proportional to \hbar . The most general dependence $K = k(e^2\hbar/4\pi)/e^2 \equiv f(\alpha_{em}r)/e^2$, $r = \hbar/\hbar_0$. Since non-perturbative effect is in question $k((\alpha_{em}r) \propto 1/(\alpha_{em}r))$ is suggestive and guarantees that the leakage probability becomes small for large values of Planck constant.

This option will not be discussed further but it might have also relevance to the parity breaking in biology. In fact, I have proposed that the realization of genetic code based on nucleotide dependent optical rotation of polarization of photons proposed by Gariaev [110] could be based on Faraday effect or its analogy [41].

One can consider also a generalization of this model by assuming that photon transforms to dark pion-like state in the leakage. In this case the action does not however reduce to a total divergence and the condition that the entire magnet corresponds to vacuum extremal seems to be unrealistic.

10.5.2 Do nuclear reaction rates depend on environment?

Claus Rolfs and his group have found experimental evidence for the dependence of the rates of nuclear reactions on the condensed matter environment [67]. For instance, the rates for the reactions $^{50}\text{V}(p,n)^{50}\text{Cr}$ and $^{176}\text{Lu}(p,n)$ are fastest in conductors. The model explaining the findings has been tested for elements covering a large portion of the periodic table.

Debye screening of nuclear charge by electrons as an explanation for the findings

The proposed theoretical explanation [67] is that conduction electrons screen the nuclear charge or equivalently that incoming proton gets additional acceleration in the attractive Coulomb field of electrons so that the effective collision energy increases so that reaction rates below Coulomb wall increase since the thickness of the Coulomb barrier is reduced.

The resulting Debye radius

$$R_D = 69 \sqrt{\frac{T}{n_{eff} \rho_a}}, \quad (10.5.1)$$

where ρ_a is the density of atoms per cubic meter and T is measured in Kelvins. R_D is of order .01 Angstroms for $T = 373$ K for $n_{eff} = 1$, $a = 10^{-10}$ m. The theoretical model [65, 64] predicts that the cross section below Coulomb barrier for $X(p, n)$ collisions is enhanced by the factor

$$f(E) = \frac{E}{E + U_e} \exp\left(\frac{\pi \eta U_e}{E}\right). \quad (10.5.2)$$

E is center of mass energy and η so called Sommerfeld parameter and

$$U_e \equiv U_D = 2.09 \times 10^{-11} (Z(Z+1))^{1/2} \times \left(\frac{n_{eff} \rho_a}{T}\right)^{1/2} \text{ eV} \quad (10.5.3)$$

is the screening energy defined as the Coulomb interaction energy of electron cloud responsible for Debye screening and projectile nucleus. The idea is that at R_D nuclear charge is nearly completely screened so that the energy of projectile is $E + U_e$ at this radius which means effectively higher collision energy.

The experimental findings from the study of 52 metals support the expression for the screening factor across the periodic table.

1. The linear dependence of U_e on Z and $T^{-1/2}$ dependence on temperature conforms with the prediction. Also the predicted dependence on energy has been tested [67].
2. The value of the effective number n_{eff} of screening electrons deduced from the experimental data is consistent with $n_{eff}(Hall)$ deduced from quantum Hall effect.

The model suggests that also the decay rates of nuclei, say beta and alpha decay rates, could be affected by electron screening. There is already preliminary evidence for the reduction of beta decay rate of ^{22}Na β decay rate in Pd [58], metal which is utilized also in cold fusion experiments. This might have quite far reaching technological implications. For instance, the artificial reduction of half-lives of the radioactive nuclei could allow an effective treatment of radio-active wastes. An interesting question is whether screening effect could explain cold fusion [39] and sono-fusion [63]: I have proposed a different model for cold fusion based on large \hbar in [23].

Could quantization of Planck constant explain why Debye model works?

The basic objection against the Debye model is that the thermodynamical treatment of electrons as classical particles below the atomic radius is in conflict with the basic assumptions of atomic physics. On the other hand, it is not trivial to invent models reproducing the predictions of the Debye model so that it makes sense to ask whether the quantization of Planck constant predicted by TGD could explain why Debye model works.

TGD predicts that Planck constant is quantized in integer multiples: $\hbar = n \hbar_0$, where \hbar_0 is the minimal value of Planck constant identified tentatively as the ordinary Planck constant. The preferred values for the scaling factors n of \hbar correspond to n-polygons constructible using ruler and compass. The values of n in question are given by $n_F = 2^k \prod_i F_{s_i}$, where the Fermat primes $F_s = 2^{2^s} + 1$ appearing in the product are distinct. The lowest Fermat primes are 3, 5, 17, 257, $2^{16} + 1$. In the model of living matter the especially favored values of \hbar come as powers $2^{k_{11}}$ [43, 16].

It is not quite obvious that ordinary nuclear physics and atomic physics should correspond to the minimum value \hbar_0 of Planck constant. The predictions for the favored values of n are not affected if one has $\hbar(\text{stand}) = 2^k \hbar_0$, $k \geq 0$. The non-perturbative character of strong force suggests that the Planck constant for nuclear physics is not actually the minimal one [23]. As a matter fact, TGD based model for nucleus implies that its "color magnetic body" has size of order electron Compton length. Also valence quarks inside hadrons have been proposed to correspond to non-minimal value of Planck constant since color confinement is definitely a non-perturbative effect. Since the lowest order classical predictions for the scattering cross sections in perturbative phase do not depend on the value of the Planck constant one can consider the testing of this issue is not trivial in the case of nuclear physics where perturbative approach does not really work.

Suppose that one has $n = n_0 = 2^{k_0} > 1$ for nuclei so that their quantum sizes are of order electron Compton length or perhaps even larger. One could even consider the possibility that both nuclei and atomic electrons correspond to $n = n_0$, and that conduction electrons can make a transition to a state with $n_1 < n_0$. This transition could actually explain how the electron conductivity is reduced to a finite value. In this state electrons would have Compton length scaled down by a factor n_0/n_1 .

For instance, if one has $n_0 = 2^{11k_0}$ as suggested by the model for quantum biology [43] and by the TGD based explanation of the claimed detection of dark matter [91], the Compton length $L_e = 2.4 \times 10^{-12}$ m for electron would reduce in the transition $k_0 \rightarrow k_0 - 1$ to $L_e = 2^{-11} L_e \simeq 1.17$ fm, which is rather near to the proton Compton length since one has $m_p/m_e \simeq .94 \times 2^{11}$. It is not too difficult to believe that electrons in this state could behave like classical particles with respect to their interaction with nuclei and atoms so that Debye model would work.

The basic objection against this model is that anyonic atoms should allow more states than ordinary atoms since very space-time sheet can carry up to n electrons with identical quantum numbers in conventional sense. This should have been seen.

Electron screening and Trojan horse mechanism

An alternative mechanism is based on Trojan horse mechanism suggested as a basic mechanism of cold fusion [23]. The idea is that projectile nucleus enters the region of the target nucleus along a larger space-time sheet and in this manner avoids the Coulomb wall. The nuclear reaction itself occurs conventionally. In conductors the space-time sheet of conduction electrons is a natural candidate for the larger space-time sheet.

At conduction electron space-time sheet there is a constant charged density consisting of n_{eff} electrons in the atomic volume $V = 1/n_a$. This creates harmonic oscillator potential in which incoming proton accelerates towards origin. The interaction energy at radius r is given by

$$V(r) = \alpha n_{eff} \frac{r^2}{2a^3} , \quad (10.5.4)$$

where a is atomic radius.

The proton ends up to this space-time sheet by a thermal kick compensating the harmonic oscillator energy. This occurs below with a high probability below radius R for which the thermal energy $E = T/2$ of electron corresponds to the energy in the harmonic oscillator potential. This gives the condition

$$R = \sqrt{\frac{Ta}{n_{eff}\alpha}} a . \quad (10.5.5)$$

This condition is exactly of the same form as the condition given by Debye model for electron screening but has a completely different physical interpretation.

Since the proton need not travel through the nuclear Coulomb potential, it effectively gains the energy

$$E_e = Z \frac{\alpha}{R} = \frac{Z\alpha^{3/2}}{a} \sqrt{\frac{n_{eff}}{Ta}} . \quad (10.5.6)$$

which would be otherwise lost in the repulsive nuclear Coulomb potential. Note that the contribution of the thermal energy to E_e is neglected. The dependence on the parameters involved is exactly the same as in the case of Debye model. For $T = 373$ K in the ^{176}Lu experiment and $n_{eff}(\text{Lu}) = 2.2 \pm 1.2$, and $a = a_0 = .52 \times 10^{-10}$ m (Bohr radius of hydrogen as estimate for atomic radius), one has $E_e = 28.0$ keV to be compared with $U_e = 21 \pm 6$ keV of [67] ($a = 10^{-10}$ m corresponds to 1.24×10^4 eV and 1 K to 10^{-4} eV). A slightly larger atomic radius allows to achieve consistency. The value of \hbar does not play any role in this model since the considerations are purely classical.

An interesting question is what the model says about the decay rates of nuclei in conductors. For instance, if the proton from the decaying nucleus can enter directly to the space-time sheet of the conduction electrons, the Coulomb wall corresponds to the Coulomb interaction energy of proton with conduction electrons at atomic radius and is equal to $\alpha n_{eff}/a$ so that the decay rate should be enhanced.

10.6 Water and new physics

In this section the previous ideas are applied in an attempt to understand the very special properties of water.

10.6.1 The 41 anomalies of water

The following list of 41 anomalies of water taken from [47] should convince the reader about the very special nature of water. The detailed descriptions of the anomalies can be found in [47]. As a matter of fact, the number of anomalies had grown to 63 when I made my last visit to the homepage of Chaplin.

The many anomalies of water need not be all due to the presence of the dark matter. As suggested already fifteen years ago, p-adic length scale hierarchy forces to replace ordinary thermodynamics with a p-adic fractal hierarchy of thermodynamics and this means that one must speak about thermodynamics in a given length scale rather than mere thermodynamics of continuous matter.

Instead of listing just the anomalies I suggest also a possible interpretation based on the assumption that some fraction of protons (and perhaps also OH^- ions) is dark. This hypothesis is motivated by the scattering data suggesting that $H_{1.5}O$ is the proper chemical formula for water in attosecond time scale and explained by assuming that about 1/4 of protons are dark in the experimental situation. It is natural to assume that the increase of temperature or pressure reduces the dark portion. Unless the establishment of equilibrium ratio for dark and ordinary phase is very fast process, water can be regarded as a two-phase system mathematically. A continuous spectrum of metastable forms of water and ice distinguished by the ratio of the densities of ordinary and dark phase is expected. Complex phase diagrams is also a natural outcome.

Dark portion is expected to induce long range correlations affecting melting/boiling/critical points, viscosity, and heats of vaporization and fusion. Anomalous behaviors under the changes of temperature and pressure and anomalies in compressibility and thermal expansivity are expected. Specific heats and transport properties are affected by the presence of dark degrees of freedom, and the coupling of electromagnetic radiation to dark degrees of freedom influences the dielectric properties of water.

In order to systemize the discussion I have classified the anomalous to different groups.

1. Anomalies suggesting the presence of dark phase inducing long range correlations.
 - (a) Water has unusually high melting point.
 - (b) Water has unusually high boiling point.
 - (c) Water has unusually high critical point.
 - (d) Water has unusually high surface tension and can bounce.
 - (e) Water has unusually high viscosity.
 - (f) Water has unusually high heat of vaporization.

Comment: The presence of dark portion implies long range correlations and they could help to restore solid/liquid phase, raise the the critical point, increase surface tension, increase viscosity and require more energy to achieve vaporization. The ability to bounce would suggest that dark

portion of water -at least near the surface- is in solid phase. Dark water is in rubber-like phase also in the interior below a length scale defined by the length of dark flux tubes.

2. Anomalies related to the effect of temperature increase.
 - (a) Water shrinks on melting.
 - (b) Water has a high density that increases on heating (up to 3.984°C).
 - (c) The number of nearest neighbors increases on melting.
 - (d) The number of nearest neighbors increases with temperature.
 - (e) Water shows an unusually large viscosity increase but diffusion decrease as the temperature is lowered.
 - (f) At low temperatures, the self-diffusion of water increases as the density and pressure increase.
 - (g) Water has a low coefficient of expansion (thermal expansivity).
 - (h) Water's thermal expansivity reduces increasingly (becoming negative) at low temperatures.

Comment: The increase of temperature induces shrinking of the flux tubes connecting water molecules in the phase transition reducing Planck constant and brings the molecules closer to each other. This could explain shrinking on melting, the increase of the density in some temperature range above which the normal thermal expansion would win the shrinking tendency, the increase of nearest neighbors on melting and with the increase of temperature. Concerning the shrinking on melting one can however argue that the regular lattice like structure of ice is not that with minimum volume per molecule so that no new physics would be needed unless it is needed to explain why the volume per molecule is not minimum.

The unusually large viscosity increase with reduce temperature would be due to the increase of the large \hbar portion inducing long range correlations. If the diffusion takes place only in the normal phase the anomalous reduction of diffusion could be due to the reduction of the density of the normal phase. Similar explanation applies to the behavior of self-diffusion.

The low value of coefficient of thermal expansion could be understood in terms of the phase transitions reducing the flux tube lengths and bringing the molecules near to each other and thus reducing the normal thermal expansion. At low enough temperatures the expansivity would become negative since this effect would overcome the normal thermal expansion.

3. Anomalies related to the effects of pressure.
 - (a) Pressure reduces its melting point (13.35 MPa about 133.5 times the standard atmospheric pressure) gives a melting point of -1°C)
 - (b) Pressure reduces the temperature of maximum density.
 - (c) D₂O and T₂O differ from H₂O in their physical properties much more than might be expected from their increased mass; e.g. they have increasing temperatures of maximum density (11.185°C and 13.4°C respectively).
 - (d) Water's viscosity decreases with pressure (at temperatures below 33°C).

Comment: The reduction of melting point, temperature of maximum density, and viscosity with pressure could be due to the reduction of the dark portion as pressure increases. Pressure would induce the phase transition reducing the value of Planck constant for the flux tubes connecting water molecules. That the situation is different for D₂O and T₂O could be understood if dark D and T are absent. The question is what happens in the transition to solid phase. The reduction of the density would conform with the idea that the portion of dark phase increases. The reduction of viscosity with pressure would follow from the reduction of dark phase causing long range correlations.

4. Anomalies related to compressibility.
 - (a) Water has unusually low compressibility.

- (b) The compressibility drops as temperature increases down to a minimum at about 46.5°C . Below this temperature, water is easier to compress as the temperature is lowered.

Comment: The anomalously high compressibility below 46.5°C could be understood if only the standard phase responds to pressure appreciably. In this case the effective density is smaller than the net density and make it easier to compress the water as the temperature is lowered. The increase of temperature would increase the effective density as dark matter is transformed to ordinary one and reduce the compressibility. Above 46.5°C the effect of dark matter would be overcome by the increase of compressibility due to the increase of temperature.

- (c) The speed of sound increases with temperature (up to a maximum at 73°C).

Comment: The speed of sound is given by the expression

$$c^2 = \frac{\partial p}{\partial \rho} .$$

Pressure p is essentially the density of thermal energy associated with the ordinary matter. When the fraction of ordinary matter increases the pressure effectively increases and this leads to the increase of c .

- (d) Under high pressure water molecules move further away from each other with increasing pressure.

Comment: The behavior under increasing high pressure is in conflict with the hypothesis that pressure tends to reduce the portion of dark phase. The question is why the increase of pressure at high enough pressures would induce phase transition increasing the value of Planck constant for the flux tubes connecting the molecules? If the dark matter does not respond to pressure appreciably, the increase of the portion of dark matter might allow the minimization of energy. Does this mean that the work done by the high enough pressure to reduce the volume is larger than the energy needed to induce the tunneling to the dark phase?

5. Anomalies related to the heat capacity.

- (a) Water has over twice the specific heat capacity of ice or steam.
 (b) The specific heat capacity (C_P and C_V) is unusually high.
 (c) Specific heat capacity C_P has a minimum.

Comment: The anomalously high heat capacity of water could be understood in terms of dark non-translational degrees of freedom even if the dark phase is rubber-like below the length scale of the dark flux tubes. The energy pumped to the system would go to these degrees of freedom. The small heat capacity of solid phase would suggest that the freezing means also freezing of these degrees of freedom meaning the reduction of the contribution to heat capacity.

6. Anomalies related to phase transitions

- (a) Supercooled water has two phases and a second critical point at about -91°C .
 (b) Liquid water may be supercooled, in tiny droplets, down to about -70°C . It may also be produced from glassy amorphous ice between -123°C and -149°C and may coexist with cubic ice up to -63°C .
 (c) Solid water exists in a wider variety of stable (and metastable) crystal and amorphous structures than other materials.
 (d) The heat of fusion of water with temperature exhibits a maximum at -17°C .

Comment: The presence of both dark and ordinary phase with varying ratio of densities could help to understand the richness of the structures below freezing point. For instance, one can imagine that either the ordinary or dark phase is super-cooled and the other freezes.

7. Anomalies of solutions of water.

- (a) Solutes have varying effects on properties such as density and viscosity.
- (b) None of its solutions even approach thermodynamic ideality; even D_2O in H_2O is not ideal.
- (c) The solubilities of non-polar gases in water decrease with temperature to a minimum and then rise.

Comment: The different interactions of solutes with the dark phase could explain these findings. For instance, the probability that the presence of solute induces a phase transition reducing the portion of the dark phase could depend on solute. The decrease of the solubilities of non-polar gases in water with temperature could be due to the fact that the solubility is at low temperatures basically due to the presence of the dark phase. At higher temperatures higher thermal energies of the solute molecules would increase the solubility.

8. Anomalies in transport properties.

- (a) NMR spin-lattice relaxation time is very short at low temperatures.

Comment: The transfer of magnetic energy to the dark degrees of freedom could dominate the relaxation process. If synchrotron Bose-Einstein condensates are present in dark degrees of freedom this might make sense.

- (b) Hot water may freeze faster than cold water; the Mpemba effect [74]. For instance, water sample in 100 C freezes faster than that in 35 C.

Comment: This effect seems to be in conflict with thermodynamics and remains poorly understood. The possibility of having continuum of metastable two-phase systems suggests a possible solution to the mystery. The freezing of the dark portion of water should occur slower than the freezing of the ordinary portion since the heat transfer rate is expected to be lower a larger value of Planck constant. The very naive just-for-definiteness estimate is that the transfer rate for energy to the cold system is inversely proportional to $1/\hbar$. If the formation of dark phase is a slow process as compared to the transfer of energy to the cold phase, the freezing of hot water would lead to a metastable ice consisting mostly of ordinary water molecules and takes place faster than the freezing of cold water already containing the slowly freezing dark portion.

- (c) Proton and hydroxide ion mobilities are anomalously fast in an electric field.

Comment: Mobility is of form $a\tau$, where a the acceleration a in the electric field times the characteristic time τ for motion without collisions. If part of protons move along dark flux tubes this time is longer. The high mobility of OH_- ions would suggest that also these can be in dark phase.

- (d) The electrical conductivity of water rises to a maximum at about 230°C and then falls.

Comment: Electrical conductivity is closely related to mobility so that the same argument applies.

- (e) The thermal conductivity of water is high and rises to a maximum at about 130°C.

Comment: The anomalously high thermal conductivity could be due to the motion of heat carriers along dark flux tubes with low dissipation.

- (f) Warm water vibrates longer than cold water.

Comment: This could be due to the faster transfer of vibrational energy to the dark vibrational of magnetic degrees of freedom. If the number of these degrees of freedom is higher than the number of ordinary degrees of freedom, one can understand also the anomalously high heat capacity. Vibration could continue in dark degrees of freedom in which case the effect would be apparent. If its only the ordinary water which vibrates in the original situation then equipartition of energy with dark degrees of freedom implies apparent dissipation.

9. Anomalous electromagnetic properties of water.

- (a) X-ray diffraction shows an unusually detailed structure.

Comment: This would not be surprising if two phases with possibly varying ratio are present. For instance, the different X-ray diffraction patterns for water obtained by a rapid

freezing from high and low temperatures could serve as a test for the proposed explanation of Mpemba effect.

- (b) The dielectric constant is high and behaves anomalously with temperature.

Comment: This could relate to the interaction of photons with dark portion of water. Dielectric constant characterizes the coupling of radiation to oscillatory degrees of freedom and is sum of terms proportional to $1/(\omega^2 - \omega_i^2)$, where ω_i is resonance frequency. If the resonance frequencies ω_i scale as $1/\hbar$, dark portion gives a larger contribution at frequencies $\omega < \omega_i$. In particular the static dielectric constant increases.

- (c) The refractive index of water has a maximum value at just below 0°C.

Comment: It is not quite clear whether this maximum corresponds to room pressure or appears quite generally. Let us assume the first option. In any case the dependence of the freezing temperature on pressure is very weak. The maximal interaction with the dark portion of water at freezing point combined with the above argument would predict that refractive index increases down to the freezing point. The reduction of the density at freezing point would reduce the refractive index since dynamic susceptibility is proportional to the density of atom so that a maximum would be the outcome.

These examples might serve as a motivation for an attempt to build a more detailed model for the dark portion of water. The model to be discussed was one of the first attempts to understand the implications of the idea about hierarchy of Planck constants. Since five years have passed is badly in need of updating.

10.6.2 The model

Networks of directed hydrogen bonds $H-O-H \cdots OH_2$ with positively charged H acting as a binding unit between negatively charged O (donor) and OH_2 (acceptor) bonds explaining clustering of water molecules can be used to explain qualitatively many of the anomalies at least qualitatively [47].

The anomaly giving evidence for anomalous nuclear physics is that the physical properties D_2O and T_2O differ much more from H_2O than one might expect on basis of increased masses of water molecules. This suggests that dark protons could be responsible for the anomalies. That heavy water in large concentrations acts as a poison is consistent with the view that the macroscopic quantum phase of dark protons is responsible for the special biological role of water.

What proton darkness could mean?

In the experimental situation one fourth of protons of water are not seen in neither electron nor neutron scattering in atto-second time scale which translates 3 Angstrom wavelength scale suggesting that in both cases diffraction scattering is in question. This of course does not mean that the fraction of dark protons is always 1/4 and it is indeed natural to assume that it is reduced at higher temperatures. Both nuclear strong interactions and magnetic scattering contribute to the diffraction which is sensitive to the intra-atomic distances. The minimal conclusion is that the protons form a separate phase with inter-proton distance sufficiently different from that between water molecules and are not seen in neutron and electron diffraction in the atto-second time scale at which protons of water molecule are visible. The stronger conclusion is that they are dark with respect to nuclear strong interactions.

The previous considerations inspired by the model of nuclei as nuclear strings suggests possible explanations.

1. Hydrogen atoms form analogs of nuclear strings connected by color bonds.
2. Nuclear protons form super-nuclei connected by dark color bonds or belong to such super-nuclei (possibly consisting of 4He nuclei). If color bonds are negatively charged, closed nuclear strings of this kind are neutral and not visible in electron scattering; this assumption is however unnecessarily strong for invisibility in diffractive scattering in atto-second time scale. Only the field bodies of proton carrying weak and color fields could be dark and electromagnetic field body has ordinary value of Planck constant so that dark protons could give rise to ordinary hydrogen atoms.

Could also the color flux tubes connecting quarks inside dark protons be dark?

The first option is that only the color flux tubes connecting protons are dark and of length of atomic size scale. The second possibility is that also the color flux tubes connecting quarks are dark and have length of order atomic size scale. Dark nucleons could be visualized as strings formed from three quarks of order atom size scale connected by color flux tubes. The generalization of the nuclear string model leads to a model of dark nucleon discussed in detail [47, 48, 32]. Dark nucleons would in turn form dark nuclei as string like objects.

The amazing finding is that the states of nucleon assumed to be neutral (for definiteness) are in one-one-correspondence with DNA, RNA, mRNA, tRNA and aminoacids and that a physically natural pairing of DNA codons and aminoacids exists and consistent with vertebrate genetic code. Same applies also to nucleons having the charge of proton. The nuclear strings formed from either dark neutrons or dark protons could in principle realize genetic code. This realization would be more fundamental than the usual chemical realization and would force to modify profoundly the ideas about prebiotic evolution. The prebiotic evolution could be evolution of water and the recent evolution could involve genetic engineering based on virtual world experimentation with the dark variant variant of the genetic apparatus. The minimum requirement would be the transcription of at dark DNA defined by nuclear strings to ordinary DNA. Dark nuclear strings could be able to diffuse without difficulties through cell membranes and the transcription of the dark genes to ordinary ones followed by gluing and pasting to genome could make possible the genetic engineering at the level of germ cells.

Another natural hypothesis is that the magnetic bodies assignable to the nuclear strings are responsible for water memory [32] and that the mechanism of water memory relies on the mimicry of biologically active molecules by dark proton strings. The frequencies involved with water memory are low and nothing to do with molecular energy levels. This is consistent with the identification as cyclotron frequencies so that it would be enough to mimic only the cyclotron spectrum. The mechanism would be similar to that of entrainment of brain to external frequencies and based on the variation of the thickness of magnetic flux tubes or sheets inducing the change of magnetic field and cyclotron frequency. One could perhaps say that magnetic bodies of dark genes as living creatures with some amount of intelligence and ability to planned actions. The evolution of cells up to the neurons of cortex could be accompanied by the evolution of the magnetic bodies of dark nuclear strings realized as the emergence of higher values of Planck constant.

Concerning the mechanism of the debated homeopathic effect itself the situation remains unclear. Homeopathic remedy is obtained by a repeated dilution and succussion of the solution containing the molecules causing the symptoms of the disease [32]. If the cyclotron frequencies of the magnetic body alone are responsible for the biological effect, one can wonder why the homeopathic remedy does not have the same undesired effects as the original molecule. A more reasonable hypothesis is that the cyclotron frequency spectrums serves only as a signature of the molecule and the homeopathic remedy only activates the immune system of the organism by cheating it to believe that the undesired molecules are present. The immune system is known to be subject to very fast genetic evolution, and dark nuclear strings forming representations of biologically active molecules and dark genome could be actively involved with this evolution.

What inspires to take these speculations more than as a poor quality entertainment is that the recent findings of the group led by HIV Nobelist Montagnier related to water memory provide support for the hypothesis that a nonstandard realization of genetic code indeed exists [109]. These findings will be discussed later in this section.

Model for super-nuclei formed from dark protons

Dark protons could form super nuclei with nucleons connected by dark color bonds with $\hbar = r\hbar_0$ with $r = 2^{k_d}$, $k_d = 151 - 127 = 24$. The large distance between protons would eliminate isospin dependent strong force so that multi-proton states are indeed possible. The interpretation would be that nuclear p-adic length scale is zoomed up to $L(113 + 24 = 137) \sim .78$ Angstroms. Dark color bonds could also connect different nuclei. The earlier hypothesis $r = 2^{11k}$ encourages to consider also $k_d = 22$, which is also one of the favored dark scalings allowed by Mersenne hypothesis ($22 = 18 + 4 = 107 - 89 + 167 - 163$) giving p-adic scale .39 Angstroms.

The predictions of the model for bond energy depend on the transformation properties of E_s under the scaling of \hbar .

1. For small perturbations harmonic oscillator approximation $V \propto kR^2/2 \propto \alpha R^2/2$ makes sense and is invariant under the scalings $\alpha_s \rightarrow \alpha_s/r$ and $R \rightarrow \sqrt{r}R$ -at least if the scalings are not too large. Bonds with different values of Planck constant have nearly identical energies, which would be indeed consistent with the idea about criticality against the change of Planck constant.

One can arrive the same conclusion follows also in different manner. The parameter ω corresponds to a quantity of form $\omega = v/L$, where L is a characteristic length scale and v a characteristic velocity. The scaling law of homeopathy [32] would suggest the dependence $v = c/\sqrt{r}$ and $L \propto \sqrt{r}L$ giving predicting that energy is invariant.

The result also conforms with the idea that classical perturbative theory does not involve Planck constant. This behavior does not however allow to identify hydrogen as color bonds since the resulting bond energies would be in MeV range.

2. The interpretation of E_s as color Coulombic potential energy α_s/R would suggest that E_s behaves under scaling like the binding energy of hydrogen atom ($1/r^2$ scaling). This interpretation implies non-perturbative effects since in semiclassical approximation energy should not depend on r . Color force is non-perturbative so that one can defend this assumption.

(a) For $k_d = 24$ E_s would be about .12 eV and considerably lower than the nominal energy of the hydrogen bond.

(b) For $k_d = 22$ one would obtain energy .48 eV. This energy is same as the universal metabolic energy quantum so that the basic metabolic processes might involve transitions dark-ordinary transition for protons. This would however suggest that the length of color bond is same as that of hydrogen bond so that the protons in question would not be invisible in diffraction in atto-second time scale. The interpretation of color bonds between atoms as hydrogen bonds is much more attractive. Of course, for large values of Planck the invariance of oscillator spectrum implies very large force constant so that the color bond would become very rigid.

These two interpretations are not contradictory if one interprets the non-perturbative contribution to the color binding energy as an additional constant contribution to the harmonic oscillator Hamiltonian which does not contribute the spectrum of excitations energies but only to the ground state energy.

The notion of flux tube state

An approach based more heavily on first principles than the above order of magnitude estimates is inspired by two steps of progress several years after these speculations.

1. Weak form of electric-magnetic duality

The weak form of electric magnetic duality led to an identification of a concrete mechanism of electroweak screening based on the pairing of homological Kähler magnetic monopoles formed by fermion wormhole throats with oppositely magnetically charged wormhole throats carrying quantum numbers of neutrino pair and screening the weak isospin and leaving only electromagnetic charge.

1. The size scale of the Kähler magnetic flux tubes connecting the magnetic monopoles would be of order intermediate gauge boson Compton length. For dark variants of elementary fermions it would be scaled up by $\sqrt{\hbar/\hbar_0}$. The new weak physics involving long range weak fields would be associated with magnetic flux tube like structures. Same conclusion applies also to new QCD type physics since also color confinement would be accompanied Kähler magnetic confinement. This allows to pose very strong restrictions on the models. For instance, it is quite possible that the notion of neutrino atom does not make sense expect if one can assume that the dark quarks feed their weak Z^0 gauge fluxes through a spherically symmetric flux collection of radial flux tubes allowing Coulombic Z^0 gauge potential as an approximate representation inside the radius defined by the length of the flux tubes.
2. It is important to notice that the screening leaves the vectorial coupling to classical Z^0 field proportional to $\sin^2(\theta_W)Q_{em}$. This could have non-trivial physical implications perhaps allowing to kill the model.

- (a) For space-time surfaces near vacuum extremals the classical Z^0 fields are strong due to the condition that the induced Kähler field is very weak []. More explicitly, from the equations for classical induced gauge fields in terms of Kähler form and classical Z^0 field [46]

$$\gamma = 3J - \frac{p}{2}Z^0, \quad Q_Z = I_L^3 - pQ_{em}, \quad p = \sin^2(\theta_W) \quad (10.6.1)$$

it follows that for the vacuum extremals the part of the classical electro-weak force proportional to the electromagnetic charge vanishes for $p = 0$ so that only the left-handed couplings to the weak gauge bosons remain. The vanishing of induced Kähler form gives

$$Z^0 = -\frac{2}{p}\gamma. \quad (10.6.2)$$

The condition implies very large effective coupling to the classical electromagnetic field since electromagnetic charge is effectively replaced with

$$Q_{em,eff} = Q_{em} - \frac{2}{p}(I_L^3 - pQ_{em}). \quad (10.6.3)$$

- (b) The proposed model for cell membrane as a Josephson junction relies on almost vacuum extremals and dark nuclei in the sense that the weak space-time sheet associated with the nuclei of biological important ions (at least) are dark [27]. It is assumed that quarks are dark in the length scale considered so that also their weak isospin remains unscreened. In the case of nuclei this means that there is contribution from the vectorial part of weak isospin given by $(Z - N)/4$ proportional to the difference of proton number and neutron number. The dominating contribution comes from Q_{em} term for heavier nuclei. It is essential that weak space-time sheets of electrons are assumed to be ordinary.
- (c) One can ask whether the nuclei could be ordinary nuclei. If so, one must still assume that the electrons of the nuclei do not couple to the classical fields assignable to the cell membrane space-time sheet since without this assumption the coupling to Z^0 field would be proportional to the total em charge of the ion rather than nuclear em charge. It is difficult to justify this assumption. In any case, for this option I_L^3 contribution would be totally absent. This affects the effective couplings of biologically important ions to the membrane potential somewhat and modifies the nice quantitative predictions of the model of photoreceptors predicting correctly the frequencies of visible light with maximal response.

2. The notion of flux tube state

The TGD inspired explanation for the finding that the measurement of Lamb shift for muonic hydrogen atom gives proton radius which is 4 per cent smaller than that deducible from ordinary hydrogen atom led to the notion of flux tube state in which muon or electric is confined inside flux tube [20]. In non-relativistic approximation based on Schrödinger equation, the model leads to wave functions expressible in terms of Airy and "Bairy" functions and WKB approximation allows to deduce an estimate for the energy eigenvalue spectrum. This model works as such also as a model for flux tubes states in which also classical electroweak and color fields are involved. Color holonomy is quite generally Abelian for classical color fields and for 2-D CP_2 projection electroweak fields are also Abelian so that the model is expected to be mathematically reasonably simple even when induced spinors are assumed.

The concept of flux tube state is very general and allow to model at least some chemical bonds. In particular, valence bonds might allow description as flux tube states of valence electrons. Hydrogen bonds are responsible for the clustering of water molecules and an obvious question is whether these bonds could be modeled as dark flux tube states of valence electrons. The model is testable since one can predict the energy spectrum of excited states for given thickness of the flux tube and the value of electric flux through it. Also the flux tube states of say electrons assignable to the magnetic flux tubes assumed to connect DNA nucleotides and lipids of cell membrane in the model of DNA as topological quantum computer [44] could be relevant.

Two kinds of bonds are predicted

Duppose that dark bonds are associated with the electro-magnetic field body. If classical Z^0 field vanishes, em field is proportional to Kähler field as are also the components of the classical color field. The bonds involving classical color gauge fields could have quark and antiquark at the opposite ends of the flux tube as the source of the color gauge field. This is indeed assumed in the model of DNA as topological quantum computer [44].

If one wants vanishing or very weak color gauge fields, one must allow almost vacuum extremals. This implies that classical Z^0 force is strong and the situation assumed to prevail for the cell membrane would hold also for hydrogen bonds. For almost vacuum extremals the ratio of electric and Z^0 fluxes is so small- of order $1/50$ for the small value of Weinberg angle $p = .0295$ (rather than $p \simeq .23$) if appearing as the parameter of the model. The molecule can serve as the source of classical Z^0 and electromagnetic fields in two manners.

1. The almost vacuum flux tubes could have many neutrino state and its conjugate at the opposite ends of the flux tube acting as the source of the classical Z^0 field. This kind of flux tubes would traverse through the cell membrane.
2. The molecule would be accompanied by two kinds of flux tubes. Some of them would be almost vacuum extremals carrying an electric flux much smaller than elementary charge e . Some of them would be accompanied by very weak Z^0 field and electromagnetic field plus color gauge fields generated by the above mechanism. These flux tubes would connect cell membrane and genome.

Two kinds of hydrogen bonds

There is experimental evidence for two different hydrogen bonds. Li and Ross represent experimental evidence for two kinds of hydrogen bonds in ice in an article published in Nature 1993 [46], and there is a popular article "Wacky Water" in New Scientist about this finding [56]. The ratio of the force constants K associated with the bonds is 1:2.

The proposed scaling law $\omega \rightarrow \omega/r$ predicts $\omega \propto 1/r$ so that $k_d \rightarrow k_d + 1$ would explain the reduction of the force constant by factor $1/2$. The presence of two kinds of bonds could be also seen as a reflection of quantum criticality against change of Planck constant.

Can one understand the finding in terms of dark color bonds?

1. The model is consistent with the identification of the two bonds in terms different values of Planck constant. The proposed scaling law for ω predicts $\omega \propto 1/r$ so that $k_d \rightarrow k_d + 1$ would explain the reduction of the force constant by factor $1/2$. above described general model for which bond energy contains perturbative harmonic oscillator contribution and non-perturbative Coulombic contribution.
2. The identification of hydrogen bond as dark color bond is however questionable. If bond energy contains a color binding energy scaling as $1/r^2$ contributing only constant shift to the harmonic oscillator Hamiltonian, the behavior of the force constant is consistent with the model. If one assumes that the harmonic oscillator spectrum remains invariant under large scalings of \hbar , the force constant becomes extremely strong and the color bond would be by a factor r^2 more rigid than hydrogen bond if one takes seriously the proposed estimates for the value of r . The alternative interpretation would be in terms of almost vacuum extremal property reducing the force constant to a very small value already from the beginning.

The possibility to divide the bonds to two kinds of bonds in an arbitrary manner brings in a large ground state degeneracy given by $D = 16!/(8!)^2$ unless additional symmetries are assumed and give for the system spin glass like character and explain large number of different amorphous phases for ice [47]. This degeneracy would also make possible information storage and provide water with memory.

Hydrogen bonds as color bonds between nuclei?

The original hypothesis was that there are two kinds of hydrogen bonds: dark and "ordinary". The finding that the estimate for the energy of dark nuclear color bond with $k_d = 22$ equals to the energy

of typical hydrogen bond raises the question whether all hydrogen bonds are associated with color bonds between nuclei. Color bond would bind the proton to electronegative nucleus and this would lead to the formation of hydrogen bond at the level of valence electrons as hydrogen donates its electron to the electronegative atom. The electronic contribution would explain the variation of the bond energy.

If hydrogen bonds connect H-atom to O-atom to acceptor nucleus, if E_s for p-O bond is same as for p-n color bond, and if color bonds are dark with $k_d = 22$, the bond energy $E_s = .5$ eV. Besides this one must assume that the oscillator energy is very small and comparable to the energy of hydrogen bond - this could be due to almost vacuum extremal property.

Dark -possibly (almost unavoidably) colored or weakly charged- bonds could serve as a prerequisite for the formation of electronic parts of hydrogen bonds and could be associated also with other molecular bonds so that dark nuclear physics might be essential part of molecular physics. Dark color bonds could be also charged which brings in additional exotic effects. The long range order of hydrogen bonded liquids could be due to the ordinary hydrogen bonds. An interesting question is whether nuclear color bonds could be responsible for the long range order of all liquids. If so dark nuclear physics would be also crucial for the understanding of the condensed matter.

In the case of water the presence of dark color bonds between dark protons would bring in additional long range order in length scale of order 10 Angstrom characteristic for DNA transversal scale: also hydrogen bonds play a crucial role in DNA double strand. Two kinds of bond networks could allow to understand why water is so different from other molecular liquids containing also hydrogen atoms and the long range order of water molecule clusters would reflect basically the long range order of two kinds of dark nuclei.

Recall that the model for dark nucleons predicts that nucleon states can be grouped to states in one-one correspondence with DNA, RNA, tRNA, and aminoacids and that the degeneracies of the vertebrate genetic code are predicted correctly. This led to suggestion that genetic code is realized already at the level of dark nuclei consisting of sequences of neutrons [47, 48]. Neutrons were assumed in order to achieve stability and could be replaced with protons.

Tetrahedral and icosahedral clusters of water molecules and dark color bonds

Water molecules form both tetrahedral and icosahedral clusters. 4He corresponds to tetrahedral symmetry so that tetrahedral cluster could be the condensed matter counterpart of 4He . In the nuclear string model nuclear strings consist of maximum number of 4He nuclei themselves closed strings in shorter length scale.

The p-adic length scales associated with 4He nuclei and nuclear string are $k = 116$ and $k = 127$. The color bond between 4He units has $E_s = .2$ MeV and $r = 2^{22}$ would give by scaling $E_s = .05$ eV which is the already familiar energy associated with cell membrane potential at the threshold for the nerve pulse generation. The binding energy associated with a string formed by n tetrahedral clusters would be $n^2 E_s$. This observation raises the question whether the neural firing is accompanied by the re-organization of strings formed by the tetrahedral clusters and possibly responsible for a representation of information and water memory.

The icosahedral model [47] for water clusters assumes that 20 tetrahedral clusters, each of them containing 14 molecules, combine to form icosahedral clusters containing 280 water molecules. Concerning the explanation of anomalies, the key observation is that icosahedral clusters have a smaller volume per water molecule than tetrahedral clusters but cannot form a lattice structure.

The number 20 for the dark magic dark nuclei forming the icosahedron is also a magic number and a possible interpretation for tetrahedral and icosahedral water clusters would be as magic super-nuclei and the prediction would be that binding energy behaves as $n^2 E_s$ rather than being just the sum of the binding energies of hydrogen bonds ($n E_s$).

It is interesting to compare this model with the model for hexagonal ice which assumes four hydrogen bonds per water molecule: for two of them the molecule acts as a donor and for two of them as an acceptor. Each water molecule in the vertices of a tetrahedron containing 14 hydrogen atoms has a hydrogen bond to a water molecule in the interior, each of which have 3 hydrogen bonds to molecules at the middle points of the edges of the tetrahedron. This makes 16 hydrogen bonds altogether. If all of them are of first type with bonding energy $E_s = .5$ eV and if the bond network is connected one would obtain total bond energy equal to $n^2 E_s = 258 \times .5$ eV rather than only $n E_s = 16 \times .5$ eV. Bonds of second type would have no role in the model.

Tetrahedral and icosahedral clusters and dark electrons

An interesting question is whether one could interpret tetrahedral and icosahedral symmetries in terms of symmetries of the singular coverings or factor spaces of CD . This does not seem to be the case.

1. One cannot understand discrete molecular symmetries for factor space-space option since the symmetry related points of CD would correspond to one and same space-time point.
2. For the option allowing only singular coverings of $CD \times CP_2$ interpreted in terms of many-valuedness of the time derivatives of the imbedding space coordinates as functions of canonical momentum densities this interpretation is not possible.
3. One can also consider the possibility that the singular coverings are over $(CD/G_a) \times (CP_2/G_b)$ rather than $CD \times CP_2$. This would predict Planck constant to be of form $r = n_a n_b$, with $n_a = 3$ for tetrahedral clusters and $n_a = 5$ for icosahedral clusters. n_a and n_b would correspond to the orders of maximal cyclic subgroups of the corresponding symmetry groups. There would be a deviation from the simplest proposal for preferred Planck constants. This option would require space-time surfaces to have exact discrete symmetries and this does not look plausible.

Note that synaptic contacts contain clathrin molecules which are truncated icosahedrons and form lattice structures and are speculated to be involved with quantum computation like activities possibly performed by microtubules. Many viruses have the shape of icosahedron.

It should be noticed that single nucleotide in DNA double strands corresponds to a twist of $2\pi/10$ per single DNA triplet so that 10 DNA strands corresponding to length $L(151) = 10$ nm (cell membrane thickness) correspond to $3 \times 2\pi$ twist. This could be perhaps interpreted as evidence for group C_{10} perhaps making possible quantum computation at the level of DNA.

10.6.3 Further comments on 41 anomalies

Some clarifying general comments -now in more standard conceptual framework- about the anomalies are in order. Quite generally, it seems that it is the presence of new degrees of freedom, the presence of icosahedral clusters, and possibly also macroscopic quantum coherence of dark matter, which are responsible for the peculiar properties of water.

The hydrogen bonds assigned to tetrahedral and icosahedral clusters should be same so that if the hydrogen bonds are assignable to dark protons this is the case for all clusters. Perhaps the number of dark protons and -perhaps equivalently- hydrogen bonds per volume is what distinguishes between these clusters and that the disappearance of dark protons leads to the disappearance of hydrogen bonds. Since it is quite possible that no new physics of proposed kind is involved, the following the explanation of anomalies uses only the notions of icosahedral and tetrahedral clusters and dark protons are mentioned only in passing.

1. Anomalies relating to the presence of icosahedral clusters

Icosahedral water clusters have a better packing ratio than tetrahedral lattice and thus correspond to a larger density. They also minimize energy but cannot form a lattice [47].

1. This explains the unusually high melting point, boiling point, critical point, surface tension, viscosity, heat of vaporization, shrinking on melting, high density increasing on heating, increase of the number of nearest neighbors in melting and with temperature. It is also possible to understand why X-ray diffraction shows an unusually detailed structure.

The presence of icosahedral clusters allows to understand why liquid water can be super-cooled, and why the distances of water molecules increase under high pressure. The spin glass degeneracy implied by dark and ordinary hydrogen bonds could explain why ice has many glassy amorphous phases. The two phases of super-cooled water could correspond to the binary degree of freedom brought in by two different hydrogen bonds. For the first phase both hydrogen atoms of a given water molecule would be either dark or ordinary. For the second phase the first hydrogen atom would be dark and second one ordinary.

Since icosahedral clusters have lower energy than a piece of ice of same size, they tend to super-cool and this slows down the transition to the solid phase. The reason why hot water cools

faster would be that the number of icosahedral clusters is smaller: if cooling is carried with a sufficient efficiency icosahedral clusters do not form.

2. Pressure can be visualized as a particle bombardment of water clusters tending to reduce their volume. The collisions with particles can induce local transitions of icosahedral structures to tetrahedral structures with a larger specific volume and energy. This would explain the low compressibility of water and why pressure reduces melting point and the temperature of maximum density and viscosity.
3. The increase of temperature is expected to reduce the number of icosahedral clusters so that the effect of pressure on these clusters is not so large. This explains the increase of compressibility with temperature below 46.5°C. The fact that the collapse of icosahedral clusters opposes the usual thermal expansion is consistent with the low thermal expansivity as well as the change of sign of expansivity near melting point. Since the square of sound velocity is inversely proportional to compressibility and density, also the increase of speed of sound with temperature can be understood.

2. *The presence of dark degrees of freedom and spin glass degeneracy*

The presence of dark degrees of freedom and the degeneracy of dark nucleus ground states could explain the high specific heat capacity of water. The reduction of dark matter degrees of freedom for ice and steam would explain why water has over twice the specific heat capacity of ice or steam. The possibility to relax by dissipating energy to the dark matter degrees of freedom would explain the short spin-lattice relaxation time. The fact that cold water has more degrees of freedom explains why warm water vibrates longer than cold water.

Also the high thermal and electric conductivity of water could be understood. The so called Grotthuss mechanism [47, 72] explaining OH₋ and H₊ mobilities (related closely to conductivities) is based on hopping of electron of OH₋ and H₊ in the network formed by hydrogen bonds and generalizes to the recent case. The reduction of conductivity with temperature would be due to the storage of the transferred energy/capture of charge carriers to the water molecule clusters.

3. *Macroscopic quantum coherence*

The high value of dielectric constant could derive from the fact that dark nuclei and super-nuclei are quantum coherent in a rather long length scale. For curl free electric fields potential difference must be same along space-time sheets of matter and dark matter. The synchronous quantum coherent collective motion of dark protons (and possible dark electrons) in an oscillating external electric field generates dark photon laser beams (it is not clear yet whether these dark laser beams are actually ordinary laser beams) de-cohering to ordinary photons and yield a large dynamical polarization. As the temperature is lowered the effect becomes stronger.

10.6.4 Genes and water memory

After long time I had opportunity to read a beautiful experimental article about experimental biology. Yolene Thomas, who worked with Benveniste, kindly sent the article to me. The freely loadable article is *Electromagnetic Signals Are Produced by Aqueous Nanostructures Derived from Bacterial DNA Sequences* by Luc Montagnier, Jamal Aissa, Stéphane Ferris, Jean-Luc Montagnier, and Claude Lavalley published in the journal *Interdiscip. Sci. Comput. Life Sci.* (2009) [109].

Basic findings at cell level

I try to list the essential points of the article. Apologies for biologists: I am not a specialist.

1. Certain pathogenic micro-organisms are objects of the study. The bacteria *Mycoplasma Pirum* and *E. Choli* belong to the targets of the study. The motivating observation was that some procedures aimed at sterilizing biological fluids can yield under some conditions the infectious micro-organism which was present before the filtration and absent immediately after it. For instance, one filtrates a culture of human lymphocytes infected by *M. Pirum*, which has infected human lymphocytes to make it sterile. The filters used have 100 nm and 20 nm porosities.

M. Pirum has size of 300 nm so that apparently sterile fluids results. However if this fluid is incubated with a mycoplasma negative culture of human lymphocytes, mycoplasma re-appears within 2 or 3 weeks! This sounds mysterious. Same happens as 20 nm filtration is applied to a minor infective fraction of HIV, whose viral particles have size in the range 100-120 nm.

2. These findings motivated a study of the filtrates and it was discovered that they have a capacity to produce low frequency electromagnetic waves with frequencies in good approximation coming as the first three harmonics of kHz frequency, which by the way plays also a central role in neural synchrony. What sounds mysterious is that the effect appeared after appropriate dilutions with water: positive dilution fraction varied between 10^{-7} and 10^{-12} . The uninfected eukaryotic cells used as controls did not show the emission. These signals appeared for both M. Pirum and E. Choli but for M. Pirum a filtration using 20 nm filter canceled the effect. Hence it seems that the nano-structures in question have size between 20 and 100 nm in this case.

A resonance phenomenon depending on excitation by the electromagnetic waves is suggested as an underlying mechanism. Stochastic resonance familiar to physicists suggests itself and also I have discussed it while developing ideas about quantum brain [52]. The proposed explanation for the necessity of the dilution could be kind of self-inhibition. Maybe a gel like phase which does not emit radiation is present in sufficiently low dilution but is destroyed in high dilutions after which emission begins. Note that the gel phase would not be present in healthy tissue. Also a destructive interference of radiation emitted by several sources can be imagined.

3. Also a cross talk between dilutions was discovered. The experiment involved two tubes. Donor tube was at a low dilution of E. Choli and "silent" (and carrying gel like phase if the above conjecture is right). Receiver tube was in high dilution (dilution fraction 10^{-9}) and "loud". Both tubes were placed in mu-metal box for 24 hours at room temperature. Both tubes were silent after his. After a further dilution made for the receiver tube it became loud again. This could be understood in terms of the formation of gel like phase in which the radiation does not take place. The effect disappeared when one interposed a sheath of mu-metal between the tubes. Emission of similar signals was observed for many other bacterial specials, all pathogenic. The transfer occurred only between identical bacterial species which suggests that the signals and possibly also frequencies are characteristic for the species and possibly code for DNA sequences characterizing the species.
4. A further surprising finding was that the signal appeared in dilution which was always the same irrespective of what was the original dilution.

Experimentation at gene level

The next step in experimentation was performed at gene level.

1. The killing of bacteria did not cancel the emission in appropriate dilutions unless the genetic material was destroyed. It turned out that the genetic material extracted from the bacteria filtered and diluted with water produced also an emission for sufficiently high dilutions.
2. The filtration step was essential for the emission also now. The filtration for 100 nm did not retain DNA which was indeed present in the filtrate. That effect occurred suggests that filtration destroyed a gel like structure inhibiting the effect. When 20 nm filtration was used the effect disappeared which suggests that the size of the structure was in the range 20-100 nm.
3. After the treatment by DNase enzyme inducing splitting of DNA to pieces the emission was absent. The treatment of DNA solution by restriction enzyme acting on many sites of DNA did not suppress the emission suggesting that the emission is linked with rather short sequences or with rare sequences.
4. The fact that pathogenic bacteria produce the emission but not "good" bacteria suggests that effect is caused by some specific gene. It was found that single gene - adhesin responsible for the adhesion of mycoplasma to human cells- was responsible for the effect. When the cloned gene was attached to two plasmids and the E. Choli DNA was transformed with the either plasmid, the emission was produced.

Some consequences

The findings could have rather interesting consequences.

1. The refinement of the analysis could make possible diagnostics of various diseases and suggests bacterial origin of diseases like Alzheimer disease, Parkinson disease, Multiple Sclerosis and Rheumatoid Arthritis since the emission signal could serve as a signature of the gene causing the disease. The signal can be detected also from RNA viruses such as HIV, influenza virus A, and Hepatitis C virus.
2. Emission could also play key role in the mechanism of adhesion to human cells making possible the infection perhaps acting as a kind of password.

The results are rather impressive. Some strongly conditioned skeptic might have already stopped reading after encountering the word "dilution" and associating it with a word which no skeptic scientist in his right mind should not say aloud: "homeopathy"! By reading carefully what I wrote above, it is easy to discover that the experimenters unashamedly manufactured a homeopathic remedy out of the filtrate! And the motivating finding was that although filtrate should not have contained the bacteria, they (according to authors), or at least the effects caused by them, appeared within weeks to it! This is of course impossible in the word of skeptic.

The next reaction of the skeptic is of course that this is fraud or the experimenters are miserable crackpots. Amusingly, one of the miserable crackpots is Nobelist Luc Montagnier, whose research group discovered AIDS virus.

How TGD could explain the findings?

Let us leave the raging skeptics for a moment and sketch possible explanations in TGD framework.

1. Skeptic would argue that the filtration allowed a small portion of infected cells to leak through the filter. Many-sheeted space-time suggests a science fictive variant of this explanation. During filtration part of the infected cells is "dropped" to large space-time sheets and diffused back to the original space-time sheets during the next week. This would explain why the micro-organisms were regenerated within few weeks. Same mechanism could work for ordinary molecules and explain homeopathy. This can be tested: look whether the molecules return back to the the diluted solution in the case of a homeopathic remedy.
2. If no cells remain in the filtrate, something really miraculous looking events are required to make possible the regeneration of the effects serving as the presence of cells. This even in the case that DNA fragments remain in the filtrate.
 - (a) The minimum option is that the presence of these structures contained only the relevant information about the infecting bacteria and this information coded in terms of frequencies was enough to induce the signatures of the infection as a kind of molecular conditioning. Experimentalists can probably immediately answer whether this can be the case.
 - (b) The most radical option is that the infecting bacteria were actually regenerated as experimenters claim! The information about their DNA was in some form present and was transcribed to DNA and/or RNA, which in turn transformed to proteins. Maybe the small fragment of DNA (adhesin) and this information should have been enough to regenerate the DNA of the bacterium and bacterium itself. A test for this hypothesis is whether the mere nanoparticles left from the DNA preparation to the filtrate can induce the regeneration of infecting molecules.

The notion of magnetic body carrying dark matter quantum controlling living matter forms the basic element of TGD inspired model of quantum biology and suggests a more concrete model. The discovery of nanotubes connecting cells with distance up to 300μ [111] provides experimental support for the notion .

1. If the matter at given layer of the onion-like structure formed by magnetic bodies has large \hbar , one can argue that the layer corresponds to a higher evolutionary level than ordinary matter

with longer time scale of memory and planned action. Hence it would not be surprising if the magnetic bodies were able to replicate and use ordinary molecules as kind of sensory receptors and motor organs. Perhaps the replication of magnetic bodies preceded the replication at DNA level and genetic code is realized already at this more fundamental level somehow. Perhaps the replication of magnetic bodies induces the replication of DNA as I have suggested.

2. The magnetic body of DNA could make DNA a topological quantum computer [44]. DNA itself would represent the hardware and magnetic bodies would carry the evolving quantum computer programs realized in terms of braidings of magnetic flux tubes. The natural communication and control tool would be cyclotron radiation besides Josephson radiation associated with cell membranes acting as Josephson junctions. Cyclotron frequencies are indeed the only natural frequencies that one can assign to molecules in kHz range. There would be an entire fractal hierarchy of analogs of EEG making possible the communication with and control by magnetic bodies.
3. The values of Planck constant would define a hierarchy of magnetic bodies which corresponds to evolutionary hierarchy and the emergence of a new level would mean jump in evolution. Gel like phases could serve as a correlate for the presence of the magnetic body. The phase transitions changing the value of Planck constant and scale up or down the size of the magnetic flux tubes. They are proposed to serve as a basic control mechanism making possible to understand the properties and the dynamics of the gel phases and how biomolecules can find each other in the thick molecular soup via a phase transition reducing the length of flux tubes connecting the biomolecules in question and thus forcing them to the vicinity of each other.

Consider now how this model could explain the findings.

1. Minimal option is that the the flux tubes correspond to "larger space-time sheets" and the infected cells managed to flow into the filtrate along magnetic flux tubes from the filter. This kind of transfer of DNA might be made possible by the recently discovered nanotubes already mentioned.
2. Maybe the radiation resulted as dark photons invisible for ordinary instruments transformed to ordinary photons as the gel phase assignable with the dark matter at magnetic flux tube network associated with the infected cells and corresponding DNA was destroyed in the filtration.

This is not the only possible guess. A phase conjugate cyclotron radiation with a large value of Planck constant could also allow for the nanostructures in dilute solute to gain metabolic energy by sending negative energy quanta to a system able to receive them. Indeed the presence of ambient radiation was necessary for the emission. Maybe that for sufficiently dilute solute this mechanism allows to the nanostructures to get metabolic energy from the ambient radiation whereas for the gel phase the metabolic needs are not so demanding. In the similar manner bacteria form colonies when metabolically deprived. This sucking of energy might be also part of the mechanism of disease.

3. What could be the magnetic field inducing the kHz radiation as a synchrotron radiation?
 - (a) For instance, kHz frequency and its harmonics could correspond to the cyclotron frequencies of proton in magnetic field which field strength slightly above that for Earth's magnetic field (750 Hz frequency corresponds to field strength of B_E , where $B_E = .5$ Gauss, the nominal strength of Earth's magnetic field). A possible problem is that the thickness of the flux tubes would be about cell size for Earth's magnetic field from flux quantization and even larger for dark matter with a large value of Planck constant. Of course, the flux tubes could make themselves thinner temporarily and leak through the pores.
 - (b) If the flux tube is assumed to have thickness of order 20-100 nm, the magnetic field for ordinary value of \hbar would be of order .1 Tesla from flux quantization and in the case of DNA the cyclotron frequencies would not depend much on the length of DNA fragment since the it carries a constant charge density. Magnetic field of order .2 Tesla would give cyclotron frequency of order kHz from the fact that the field strength of .2 Gauss gives frequency of about .1 Hz. This correspond to a magnetic field with flux tube thickness ~ 125 nm, which

happens to be the upper limit for the porosity. Dark magnetic flux tubes with large \hbar are however thicker and the leakage might involve a temporary phase transition to a phase with ordinary value of \hbar reducing the thickness of the flux tube. Perhaps some genes (adhesin) plus corresponding magnetic bodies representing DNA in terms of cyclotron frequencies depending slightly on precise weight of the DNA sequence and thus coding it correspond to the frequency of cyclotron radiation are the sought for nano-structures.

4. While developing a model for homeopathy based on dark matter I ended up with the idea that dark matter consisting of nuclear strings of neutrons and protons with a large value of \hbar and having thus a zoomed up size of nucleon could be involved. The really amazing finding was that nucleons as three quark systems allow to realize vertebrate code in terms of states formed from entangled quarks [47] described also in this chapter! One cannot decompose codons to letters as in the case of the ordinary genetic code but codons are analogous to symbols representing entire words in Chinese. The counterparts of DNA, RNA, and aminoacids emerge and genetic code has a concrete meaning as a map between quantum states.

Without any exaggeration this connection between dark hadronic physics and biology has been one of the greatest surprises of my professional life. It suggests that dark matter in macroscopic quantum phase realizes genetic code at the level of nuclear physics and biology only provides one particular (or probably very many as I have proposed) representations of it. If one takes this seriously one can imagine that genetic information is represented by these dark nuclear strings of nanoscopic size and that there exists a mechanism translating the dark nuclei to ordinary DNA and RNA sequences and thus to biological matter. This would explain the claimed regeneration of the infected cells.

5. Genetic code at dark matter level would have far reaching implications. For instance, living matter - or rather, the magnetic bodies controlling it - could purposefully perform genetic engineering. This forces me to spit out another really dirty word, "Lamarckism"! We have of course learned that mutations are random. The basic objection against Lamarckism is that there is no known mechanism which would transfer the mutations to germ cells. In the homeopathic Universe of TGD the mutations could be however performed first for the dark nucleon sequences. After this these sequences would diffuse to germ cells just like homeopathic remedies do, and after this are translated to DNA or RNA and attach to DNA.

10.6.5 Burning water and photosynthesis

For a physicist liberated from the blind belief in reductionism, biology transforms to a single gigantic anomaly about which recent day physics cannot say much. During years I have constructed several models for these anomalies helping to develop a more detailed view about how the new physics predicted by quantum TGD could allow to understand biology and consciousness.

The basic problem is of course the absence of systematic experimentation so that it is possible to imagine many new physics scenarios. For this reason the article series of Mae-Wan Ho [84, 75, 94, 97] in ISIS was a very pleasant surprise, and already now has helped considerably in the attempts to develop the ideas further.

The first article "Water electric" [84] told about the formation of exclusion zones around hydrophilic surfaces, typically gels in the experiments considered [103]. The zones were in potential of about 100 meV with respect to surroundings (same order of magnitude as membrane potential) and had thickness ranging to hundreds of micrometers (the size of a large cell): the standard physics would suggest only few molecular layers instead of millions. Sunlight induced the effect. This finding allow to develop TGD based vision about how proto cells emerged and also the model for chiral selection in living matter by combining the finding with the anomalies of water about which I had learned earlier.

The article "Can water burn?" [94] tells about the discovery of John Kanzius -a retired broadcast engineer and inventor. Kanzius found that water literally burns if subjected to a radio frequency radiation at frequency of 13.56 MHz [79]. The mystery is of course how so low frequency can induce burning. The article "The body does burn water" [97] notices that plant cells burn water routinely in photosynthesis and that also animal cells burn water but the purpose is now to generate hydrogen peroxide which kills bacteria (some readers might recall from childhood how hydrogen peroxide was

used to sterilize wounds!). Hence the understanding of how water burns is very relevant for the understanding of photosynthesis and even workings of the immune system.

Living matter burns water routinely

Photosynthesis burns water by decomposing water to hydrogen and oxygen and liberating oxygen. Oxygen from CO_2 in atmosphere combines with the oxygen of H_2O to form O_2 molecules whereas H from H_2O combines with carbon to form hydrocarbons serving as energy sources for animals which in turn produce CO_2 . This process is fundamental for aerobic life. There is also a simpler variant of photosynthesis in which oxygen is not produced and applied by an-aerobic life forms. The article "Living with Oxygen" by Mae-Wan Ho gives a nice overall view about the role of oxygen [101]. As a matter fact, also animals burn water but they do this to produce hydrogen peroxide H_2O_2 which kills very effectively bacteria.

Burning of water has been studied as a potential solution for how to utilize the solar energy to produce hydrogen serving as a natural fuel [75]. The reaction $O_2 + H_2 \rightarrow 2H_2O$ occurs spontaneously and liberates energy of about 1.23 eV. The reverse process $2H_2 \rightarrow H_2O_2 + H_2$ in the presence of sunlight means burning of water, and could provide the manner to store solar energy. The basic reaction $2H_2O + 4h\nu \leftrightarrow H_2O_2 + H_2$ stores the energy of four photons. What really happens in this process is far from being completely understood. Quite generally, the mechanisms making possible extreme efficiency of bio-catalysis remain poorly understood. Here new physics might be involved. I have discussed models for photosynthesis and $ADP \leftrightarrow ATP$ process involved with the utilization of the biochemical energy already earlier [49].

How water could burn in TGD Universe?

The new results could help to develop a more detailed model about what happens in photosynthesis. The simplest TGD inspired sketch for what might happen in the burning of water goes as follows.

1. Assume that 1/4 of water molecules are partially dark (in sense of nonstandard value of Planck constant) or at least at larger space-time sheets in atto-second scale [47, 51, 49, 50]. This would explain the $H_{1.5}O$ formula explaining the results of neutron diffraction and electron scattering.
2. The question is what this exotic fraction of water precisely is. The models for water electret, exclusion zones and chiral selection lead to concrete ideas about this. Electrons assignable to the H atoms of (partially) dark H_2O reside at space-time sheet $k_e = 151$ (this p-adic length scale corresponds to 10 nm, the thickness of cell membrane). At least the hydrogen atom for this fraction of water molecules is exotic and findings from neutron and electron scattering suggest that both proton and electron are at non-standard space-time sheets but not necessarily at the same space-time sheet. The model for the burning requires that electron and proton are at different space-time sheets in the initial situation.
3. Suppose all four electrons are kicked to the space-time sheet of protons of the exotic hydrogen atoms labeled by k_p . This requires the energy $E_\gamma = (1 - 2^{-n})E_0(k_p)$ (the formula involves idealizations). At this space-time sheet protons and electrons are assumed to combine spontaneously to form two H_2 atoms. Oxygen atoms in turn are assumed to combine spontaneously to form O_2 .
4. For $k_f = 148$ and $n = 3$ minimum energy needed would be $4E_\gamma = 4 \times .4 = 1.6$ eV. For $k_p = 149$ (thickness of lipid layer) and $n = 2$ one would have $4E_\gamma = 4 \times .3462 = 1.385$ eV whereas $H_2O_2 + H_2 \rightarrow 2H_2O$ liberates energy 1.23 eV. Therefore the model in which electrons are at cell membrane space-time sheet and protons at the space-time sheet assignable to single lipid layer of cell membrane suggests itself. This would also mean that the basic length scales of cell are already present in the structure of water. Notice that there is no need to assume that Planck constant differs from its standard value.

There is no need to add, that the model is an unashamed oversimplification of the reality. It might however catch the core mechanism of photosynthesis.

Burning of salt water induced by RF radiation

Engineer John Kanzius has made a strange discovery [79]: salt water in the test tube radiated by radiowaves at harmonics of a frequency $f=13.56$ MHz burns. Temperatures about 1500 K, which correspond to .15 eV energy have been reported. One can irradiate also hand but nothing happens. The original discovery of Kanzius was the finding that radio waves could be used to cure cancer by destroying the cancer cells. The proposal is that this effect might provide new energy source by liberating chemical energy in an exceptionally effective manner. The power is about 200 W so that the power used could explain the effect if it is absorbed in resonance like manner by salt water.

Mae-Wan Ho's article "Can water Burn?" [94] provides new information about burning salt water [79], in particular reports that the experiments have been replicated. The water is irradiated using polarized radio frequency light at frequency 13.56 MHz. The energy of radio frequency quantum is $E_{rf} = .561 \times 10^{-7}$ eV and provides only a minor fraction $E_{rf}/E = .436 \times 10^{-7}$ of the needed energy which is $E = 1.23$ eV for single $2H_2O \rightarrow H_2O_2 + H_2$ event. The structure of water has been found to change, in particular something happens to O-H bonds. The Raman spectrum of the water has changed in the energy range [0.37, 0.43] eV. Recall that the range of metabolic energy quanta $E(k, n) = (1 - 2^{-n})E_0(k)$ varies for electron in the range [.35, .46] eV in the model for the formation of exclusion zone induced by light. Therefore the photons assigned to changes in Raman spectrum might be associated with the transfer of electrons between space-time sheets.

The energies of photons involved are very small, multiples of 5.6×10^{-8} eV and their effect should be very small since it is difficult to imagine what resonant molecular transition could cause the effect. This leads to the question whether the radio wave beam could contain a considerable fraction of dark photons for which Planck constant is larger so that the energy of photons is much larger. The underlying mechanism would be phase transition of dark photons with large Planck constant to ordinary photons with shorter wavelength coupling resonantly to some molecular degrees of freedom and inducing the heating. Microwave oven of course comes in mind immediately.

As I made this proposal, I did not realize the connection with photosynthesis and actual burning of water. The recent experimental findings suggest that dark radio frequency photons transform to photons inducing splitting of water as in photosynthesis so that that one should have $r = \hbar/\hbar_0 = E_{rf}/4E$. One could say that large number of radio wave photons combine to form a single bundle of photons forming a structure analogous to what mathematician calls covering space. In the burning event the dark photon would transform to ordinary photon with the same energy. This process would thus transform low energy photons to high energy protons with the ratio $r = \hbar/\hbar_0$.

Therefore the mechanism for the burning of water in the experiment of Kanzius could be a simple modification of the mechanism behind burning of water in photosynthesis.

1. Some fraction of dark radio frequency photons are dark or are transformed to dark photons in water and have energies around the energy needed to kick electrons to smaller space-time sheets .4 eV. After this they are transformed to ordinary photons and induce the above process. Their in-elastic scattering from molecules (that is Raman scattering) explains the observation of Raman scattered photons. For a fixed value of \hbar the process would occur in resonant manner since only few metabolic quanta are allowed.
2. How dark radio frequency photons could be present or could be produced in water? Cyclotron radiation assignable to say electrons in magnetic field comes in mind. If the cyclotron radiation is associated with electrons it requires a magnetic field of 4.8 Gauss the cyclotron frequency is 13.56 MHz. This is roughly ten times the nominal value $B_E = .5$ Gauss of the Earth's magnetic field and 24 times the value of dark magnetic field $B_d = .4B_E = .2$ Gauss needed to explain the effects of ELF em fields on vertebrate brain. Maybe dark matter at flux tubes of Earth's magnetic field with Planck constant equal to $\hbar/\hbar_0 = \frac{1}{4} \frac{E}{E_{rf}}$ transforms radio frequency photons to dark photons or induces resonantly the generation of cyclotron photons, which in turn leak out from magnetic flux tubes and form ordinary photons inducing the burning of water. $E_\gamma = .4$ eV would give $\hbar/\hbar_0 = 1.063 \times 2^{21}$ and $E_\gamma = .36$ eV would give $\hbar/\hbar_0 = .920 \times 2^{21}$.
3. Magnetic fields of magnitude .2 Gauss are in central role in TGD based model of living matter and there are excellent reasons to expect that this mechanism could be involved also with processes involved with living matter. There is indeed evidence for this. The experiments of Gariaev demonstrated that the irradiation of DNA with 2 eV laser photons (which correspond

to one particular metabolic energy quantum) induced generation of radio wave photons having unexpected effects on living matter (enhanced metabolic activity) [112], and that even a realization of genetic code in terms of the time variation of polarization direction could be involved. TGD based model [46, 41] identifies radio-wave photons as dark photons with same energy as possessed by incoming visible photons so that a transformation of ordinary photons to dark photons would have been in question. The model assumed hierarchy of values of magnetic fields in accordance with the idea about onion like structure of the magnetic body.

There are several questions to be answered.

1. Is there some trivial explanation for why salt must be present or is new physics involved also here. What comes in mind are Cooper pairs dark Na^+ ions (or their exotic counterparts which are bosons) carrying Josephson currents through the cell membrane in the model of the cell membrane as a Josephson junction which is almost vacuum extremal of Kähler action. In the experimental arrangement leading to the generation of exclusion zones the pH of water was important control factor, and it might be that the presence of salt has an analogous role to that of protons.
2. Does this effect occur also for solutions of other molecules and other solutes than water? This can be tested since the rotational spectra are readily calculable from data which can be found at net.
3. Are the radio wave photons dark or does water - which is very special kind of liquid - induce the transformation of ordinary radio wave photons to dark photons by fusing $r = \hbar/\hbar_0$ radio wave massless extremals (MEs) to single ME. Does this transformation occur for all frequencies? This kind of transformation might play a key role in transforming ordinary EEG photons to dark photons and partially explain the special role of water in living systems.
4. Why the radiation does not induce spontaneous combustion of living matter which contains salt. And why cancer cells seem to burn: is salt concentration higher inside them? As a matter fact, there are reports about [105]. One might hope that there is a mechanism inhibiting this since otherwise military would be soon developing new horror weapons unless it is doing this already now. Is it that most of salt is ionized to Na^+ and Cl^- ions so that spontaneous combustion can be avoided? And how this relates to the sensation of spontaneous burning [81] - a very painful sensation that some part of body is burning?
5. Is the energy heating solely due to rotational excitations? It might be that also a "dropping" of ions to larger space-time sheets is induced by the process and liberates zero point kinetic energy. The dropping of proton from $k=137$ ($k=139$) atomic space-time sheet liberates about .5 eV (0.125 eV). The measured temperature corresponds to the energy .15 eV. This dropping is an essential element of remote metabolism and provides universal metabolic energy quanta. It is also involved with TGD based models of "free energy" phenomena. No perpetuum mobile is predicted since there must be a mechanism driving the dropped ions back to the original space-time sheets.

Recall that one of the empirical motivations for the hierarchy of Planck constants came from the observed quantum like effects of ELF em fields at EEG frequencies on vertebrate brain and also from the correlation of EEG with brain function and contents of consciousness difficult to understand since the energies of EEG photons are ridiculously small and should be masked by thermal noise.

10.7 Connection with mono-atomic elements, cold fusion, and sono-luminescence?

Anomalies are treasures for a theoretician and during years I have been using quite a bundle of reported anomalies challenging the standard physics as a test bed for the TGD vision about physics. The so called mono-atomic elements, cold fusion, and sonofusion represent examples of this kind of anomalies not taken seriously by most standard physicists. In the following the possibility that dark matter as large \hbar phase could allow to understand these anomalies.

Of course, I hear the angry voice of the skeptic reader blaming me for a complete lack of source criticism and the skeptic reader is right. I however want to tell him that I am not a soldier in troops of either skeptics or new-agers. My attitude is "let us for a moment assume that these findings are real..." and look for the consequences in this particular theoretical framework.

10.7.1 Mono-atomic elements as dark matter and high T_c super-conductors?

The ideas related to many-sheeted space-time began to develop for a decade ago. The stimulation came from a contact by Barry Carter who told me about so called mono-atomic elements, typically transition metals (precious metals), including Gold. According to the reports these elements, which are also called ORMEs ("orbitally rearranged monoatomic elements") or ORMUS, have following properties.

1. ORMEs were discovered and patented by David Hudson [57] are peculiar elements belonging to platinum group (platinum, palladium, rhodium, iridium, ruthenium and osmium) and to transition elements (gold, silver, copper, cobalt and nickel).
2. Instead of behaving as metals with valence bonds, ORMEs have ceramic like behavior. Their density is claimed to be much lower than the density of the metallic form.
3. They are chemically inert and poor conductors of heat and electricity. The chemical inertness of these elements have made their chemical identification very difficult.
4. One signature is the infra red line with energy of order $.05 eV$. There is no text book explanation for this behavior. Hudson also reports that these elements became visible in emission spectroscopy in which elements are posed in strong electric field after time which was 6 times longer than usually.

The pioneering observations of David Hudson [57] - if taken seriously - suggest an interpretation as an exotic super-conductor at room temperature having extremely low critical magnetic fields of order of magnetic field of Earth, which of course is in conflict with the standard wisdom about super-conductivity. After a decade and with an impulse coming from a different contact related to ORMEs, I decided to take a fresh look on Hudson's description for how he discovered ORMEs [57] with dark matter in my mind. From experience I can tell that the model to be proposed is probably not the final one but it is certainly the simplest one.

There are of course endless variety of models one can imagine and one must somehow constrain the choices. The key constraints used are following.

1. Only valence electrons determining the chemical properties appear in dark state and the model must be consistent with the general model of the enhanced conductivity of DNA assumed to be caused by large \hbar valence electrons with $r = \hbar/\hbar_0 = n$, $n = 5, 6$ assignable with aromatic rings. $r = 6$ for valence electrons would explain the report of Hudson about anomalous emission spectroscopy.
2. This model cannot explain all data. If ORMEs are assumed to represent very simple form of living matter also the presence electrons having $\hbar/\hbar_0 = 2^{k11}$, $k = 1$, can be considered and would be associated with high T_c super-conductors whose model predicts structures with thickness of cell membrane. This would explain the claims about very low critical magnetic fields destroying the claimed superconductivity.

Below I reproduce Hudson's own description here in a somewhat shortened form and emphasize that must not forget professional skepticism concerning the claimed findings.

Basic findings of Hudson

Hudson was recovering gold and silver from old mining sources. Hudson had learned that something strange was going on with his samples. In molten lead the gold and silver recovered but when "I held the lead down, I had nothing". Hudson tells that mining community refers to this as "ghost-gold", a non-assayable, non-identifiable form of gold.

Then Hudson decided to study the strange samples using emission spectroscopy. The sample is put between carbon electrodes and arc between them ionizes elements in the sample so that they radiate at specific frequencies serving as their signatures. The analysis lasts 10-15 seconds since for longer times lower electrode is burned away. The sample was identified as Iron, Silicon, and Aluminum. Hudson spent years to eliminate Fe, Si, and Al. Also other methods such as Cummings Microscopy, Diffraction Microscopy, and Fluorescent Microscopy were applied and the final conclusion was that there was nothing left in the sample in spectroscopic sense.

After this Hudson returned to emission spectroscopy but lengthened the time of exposure to electric field by surrounding the lower Carbon electrode with Argon gas so that it could not burn. This allowed to reach exposure times up to 300 s. The sample was silent up to 90 s after which emission lines of Palladium (Pd) appeared; after 110 seconds Platinum (Pt); at 130 seconds Ruthenium (Ru); at about 140-150 seconds Rhodium; at 190 seconds Iridium; and at 220 seconds Osmium appeared. This is known as fractional vaporization.

Hudson reports the boiling temperatures for the metals in the sample having in mind the idea that the emission begins when the temperature of the sample reaches boiling temperature inspired by the observation that elements become visible in the order which is same as that for boiling temperatures.

The boiling temperatures for the elements appearing in the sample are given by the following table.

Element	<i>Ca</i>	<i>Fe</i>	<i>Si</i>	<i>Al</i>	<i>Pd</i>	<i>Rh</i>
$T_B/^\circ C$	1420	1535	2355	2327	>2200	2500
Element	<i>Ru</i>	<i>Pt</i>	<i>Ir</i>	<i>Os</i>	<i>Ag</i>	<i>Au</i>
$T_B/^\circ C$	4150	4300	> 4800	> 5300	1950	2600

Table 2. Boiling temperatures of elements appearing in the samples of Hudson.

Hudson experimented also with commercially available samples of precious metals and found that the lines appear within 15 seconds, then follows a silence until lines re-appear after 90 seconds. Note that the ratio of these time scales is 6. The presence of some exotic form of these metals suggests itself: Hudson talks about mono-atomic elements.

Hudson studied specifically what he calls mono-atomic gold and claims that it does not possess metallic properties. Hudson reports that the weight of mono-atomic gold, which appears as a white powder, is 4/9 of the weight of metallic gold. Mono-atomic gold is claimed to behave like super-conductor.

Hudson does not give a convincing justification for why his elements should be mono-atomic so that in following this attribute will be used just because it represents established convention. Hudson also claims that the nuclei of mono-atomic elements are in a high spin state. I do not understand the motivations for this statement.

Claims of Hudson about ORMES as super conductors

The claims of Hudson that ORMES are super conductors [57] are in conflict with the conventional wisdom about super conductors.

1. The first claim is that ORMES are super conductors with gap energy about $E_g = .05$ eV and identifies photons with this energy resulting from the formation of Cooper pairs. This energy happens to correspond one of the absorption lines in high T_c superconductors.
2. ORMES are claimed to be super conductors of type II with critical fields H_{c1} and H_{c2} of order of Earth's magnetic field having the nominal value $.5 \times 10^{-4}$ Tesla [57]. The estimates for the critical parameters for the ordinary super conductors suggests for electronic super conductors critical fields, which are about .1 Tesla and thus by a factor $\sim 2^{12}$ larger than the critical fields claimed by Hudson.
3. It is claimed that ORME particles can levitate even in Earth's magnetic field. The latter claim looks at first completely nonsensical. The point is that the force giving rise to the levitation is

roughly the gradient of the would-be magnetic energy in the volume of levitating super conductor. The gradient of average magnetic field of Earth is of order B/R , R the radius of Earth and thus extremely small so that genuine levitation cannot be in question.

Minimal model

Consider now a possible TGD inspired model for these findings assuming for definiteness that the basic Hudson's claims are literally true.

1. In what sense mono-atomic elements could be dark matter?

The simplest option suggested by the applicability of emission spectroscopy and chemical inertness is that mono-atomic elements correspond to ordinary atoms for which valence electrons are dark electrons with large value of $r = \hbar/\hbar_0$. Suppose that the emission spectroscopy measures the energies of dark photons from the transitions of dark electrons transforming to ordinary photons before the detection by de-coherence increasing the frequency by r . The size of dark electrons and temporal duration of basic processes would be zoomed up by r .

Since the time scale after which emission begins is scaled up by a factor 6, there is a temptation to conclude that $r = 6$ holds true. Note that $n = 6$ corresponds to Fermat polygon and is thus preferred number theoretically in TGD based model for preferred values of \hbar [39]. The simplest possibility is that the group G_b is trivial group and $G_a = A_6$ or D_6 so that ring like structures containing six dark atoms are suggestive.

This brings in mind the model explaining the anomalous conductivity of DNA by large \hbar valence electrons of aromatic rings of DNA. The zooming up of spatial sizes might make possible exotic effects and perhaps even a formation of atomic Bose-Einstein condensates of Cooper pairs. Note however that in case of DNA $r = 6$ not gives only rise to conductivity but not super-conductivity and that $r = 6$ cannot explain the claimed very low critical magnetic field destroying the super-conductivity.

2. Loss of weight

The claimed loss of weight by a factor $p \simeq 4/9$ is a very significant hint if taken seriously. The proposed model implies that the density of the partially dark phase is different from that of the ordinary phase but is not quantitative enough to predict the value of p . The most plausible reason for the loss of weight would be the reduction of density induced by the replacement of ordinary chemistry with $r = 6$ chemistry for which the Compton length of valence electrons would increase by this factor.

3. Is super-conductivity possible?

The overlap criterion is favorable for super-conductivity since electron Compton lengths would be scaled up by factor $n_a = 6, n_b = 1$. For $r = \hbar/\hbar_0 = n_a = 6$ Fermi energy would be scaled up by $n_a^2 = 36$ and if the same occurs for the gap energy, T_c would increase by a factor 36 from that predicted by the standard BCS theory. Scaled up conventional super-conductor having $T_c \sim 10$ K would be in question (conventional super-conductors have critical temperatures below 20 K). 20 K upper bound for the critical temperature of these superconductors would allow 660 K critical temperature for their dark variants!

For large enough values of r the formation of Cooper pairs could be favored by the thermal instability of valence electrons. The binding energies would behave as $E = r^2 Z_{eff}^2 E_0/n^2$, where Z_{eff} is the screened nuclear charge seen by valence electrons, n the principal quantum number for the valence electron, and E_0 the ground state energy of hydrogen atom. This gives binding energy smaller than thermal energy at room temperature for $r > (Z_{eff}/n)\sqrt{2E_0/3T_{room}} \simeq 17.4 \times (Z_{eff}/n)$. For $n = 5$ and $Z_{eff} < 1.7$ this would give thermal instability for $r = 6$.

Interestingly, the reported .05 eV infrared line corresponds to the energy assignable to cell membrane voltage at criticality against nerve pulse generation, which suggests a possible connection with high T_c superconductors for which also this line appears and is identified in terms of Josephson energy. .05 eV line appears also in high T_c superconductors. This interpretation does not exclude the interpretation as gap energy. The gap energy of the corresponding BCS super-conductor would be scaled down by $1/r^2$ and would correspond to 14 K temperature for $r = 6$.

Also high T_c super-conductivity could involve the transformation of nuclei at the stripes containing the holes to dark matter and the formation of Cooper pairs could be due to the thermal instability of valence electrons of Cu atoms (having $n = 4$). The rough extrapolation for the critical temperature for

cuprate superconductor would be $T_c(Cu) = (n_{Cu}/n_{Rh})^2 T_c(Rh) = (25/36)T_c(Rh)$. For $T_c(Rh) = 300$ K this would give $T_c(Cu) = 192$ K: according to Wikipedia cuprate perovskite has the highest known critical temperature which is 138 K. Note that quantum criticality suggests the possibility of several values of (n_a, n_b) so that several kinds of super-conductivities might be present.

ORMEs as partially dark matter, high T_c super conductors, and high T_c super-fluids

The appearance of .05 eV photon line suggest that same phenomena could be associated with ORMES and high T_c super-conductors. The strongest conclusion would be that ORMES are T_c super-conductors and that the only difference is that Cu having single valence electron is replaced by a heavier atom with single valence electron. In the following I shall discuss this option rather independently from the minimal model.

1. ORME super-conductivity as quantum critical high T_c superconductivity

ORMES are claimed to be high T_c superconductors and the identification as quantum critical superconductors seems to make sense.

1. According to the model of high T_c superconductors as quantum critical systems, the properties of Cooper pairs should be more or less universal so that the observed absorption lines discussed in the section about high T_c superconductors should characterize also ORMES. Indeed, the reported 50 meV photon line corresponds to a poorly understood absorption line in the case of high T_c cuprate super conductors having in TGD framework an interpretation as a transition in which exotic Cooper pair is excited to a higher energy state. Also Copper is a transition metal and is one of the most important trace elements in living systems [86]. Thus the Cooper pairs could be identical in both cases. ORMES are claimed to be superconductors of type II and quantum critical superconductors are predicted to be of type II under rather general conditions.
2. The claimed extremely low value of H_c is also consistent with the high T_c superconductivity. The supra currents in the interior of flux tubes of radius of order $L_w = .4 \mu\text{m}$ are BCS type supra currents with large \hbar so that T_c is by a factor 2^{14} ($127 - 113 = 14$ is inspired by the Mersenne hypothesis for the preferred p-adic length scales) higher than expected and H_c is reduced by a factor 2^{-10} . This indeed predicts the claimed order of magnitude for the critical magnetic field.
3. The problem is that $r = 2^{14}$ is considerably higher than $r = 6$ suggested by the minimum model explaining the emission spectroscopic results of Hudson. Of course, several values of \hbar are possible so that internal consistency would be achieved if ORMES are regarded as a very simple form of living matter with relatively small value of r and giving up the claim about the low value of critical magnetic field.
4. The electronic configurations of Cu and Gold are chemically similar. Gold has electronic configuration $[Xe, 4f^{14}5d^{10}]6s$ with one valence electron in s state whereas Copper corresponds to $3d^{10}4s$ ground state configuration with one valence electron. This encourages to think that the doping by holes needed to achieve superconductivity induces the dropping of these electrons to $k = 151$ space-time sheets and gives rise to exotic Cooper pairs. Also this model assumes the phase transition of some fraction of Cu nuclei to large \hbar phase and that exotic Cooper pairs appear at the boundary of ordinary and large \hbar phase.

More generally, elements having one electron in s state plus full electronic shells are good candidates for doped high T_c superconductors. Both Cu and Au atoms are bosons. More generally, if the atom in question is boson, the formation of atomic Bose-Einstein condensates at Cooper pair space-time sheets is favored. Thus elements with odd value of A and Z possessing full shells plus single s wave valence electron are of special interest. The six stable elements satisfying these conditions are ${}^5\text{Li}$, ${}^{39}\text{K}$, ${}^{63}\text{Cu}$, ${}^{85}\text{Rb}$, ${}^{133}\text{Cs}$, and ${}^{197}\text{Au}$.

2. "Levitation" and loss of weight

The model of high T_c superconductivity predicts that some fraction of Cu atoms drops to the flux tube with radius $L_w = .4 \mu\text{m}$ and behaves as a dark matter. This is expected to occur also in the case of other transition metals such as Gold. The atomic nuclei at this space-time sheet have high

charges and make phase transition to large \hbar phase and form Bose-Einstein condensate and superfluid behavior results. Electrons in turn form large \hbar variant of BCS type superconductor. These flux tubes are predicted to be negatively charged because of the Bose-Einstein condensate of exotic Cooper pairs at the boundaries of the flux tubes having thickness L (151). The average charge density equals to the doping fraction times the density of Copper atoms.

The first explanation would be in terms of super-fluid behavior completely analogous to the ability of ordinary superfluids to defy gravity. Second explanation is based on the electric field of Earth which causes an upwards directed force on negatively charged BE condensate of exotic Cooper pairs and this force could explain both the apparent levitation and partial loss of weight. The criterion for levitation is $F_e = 2eE/x \geq F_{gr} = Am_p g$, where $g \simeq 10 \text{ m}^2/\text{s}$ is gravitational acceleration at the surface of Earth, A is the atomic weight and m_p proton mass, E the strength of electric field, and x is the number of atoms at the space-time sheet of a given Cooper pair. The condition gives $E \geq 5 \times 10 - 10Ax \text{ V/m}$ to be compared with the strength $E = 10^2 - 10^4 \text{ V/m}$ of the Earths' electric field.

An objection against the explanation for the effective loss of weight is that it depends on the strength of electric field which varies in a wide range whereas Hudson claims that the reduction factor is constant and equal to 4/9. A more mundane explanation would be in terms of a lower density of dark Gold. This explanation is quite plausible since there is no atomic lattice structure since nuclei and electrons form their own large \hbar phases.

4. The effects on biological systems

Some monoatomic elements such as White Gold are claimed to have beneficial effects on living systems [57]. 5 per cent of brain tissue of pig by dry matter weight is claimed to be Rhodium and Iridium. Cancer cells are claimed to be transformed to healthy ones in presence of ORMEs. The model for high T_c super conductivity predicts that the flux tubes along which interior and boundary supra currents flow has same structure as neuronal axons. Even the basic length scales are very precisely the same. On basis of above considerations ORMEs are reasonable candidates for high T_c superconductors and perhaps even super fluids.

The common mechanism for high T_c , ORME- and bio- super-conductivities could explain the biological effects of ORMEs.

1. In unhealthy state superconductivity might fail at the level of cell membrane, at the level of DNA or in some longer length scales and would mean that cancer cells are not anymore able to communicate. A possible reason for a lost super conductivity or anomalously weak super conductivity is that the fraction of ORME atoms is for some reason too small in unhealthy tissue.
2. The presence of ORMEs could enhance the electronic bio- superconductivity which for some reason is not fully intact. For instance, if the lipid layers of cell membrane are, not only wormhole-, but also electronic super conductors and cancer involves the loss of electronic super-conductivity then the effect of ORMEs would be to increase the number density of Cooper pairs and make the cell membrane super conductor again. Similar mechanism might work at DNA level if DNA:s are super conductors in "active" state.

5. Is ORME super-conductivity associated with the magnetic flux tubes of dark magnetic field $B_d = 0.2 \text{ Gauss}$?

The general model for the ionic super-conductivity in living matter, which has developed gradually during the last few years and will be discussed in detail later, was originally based on the assumption that super-conducting particles reside at the super-conducting magnetic flux tubes of Earth's magnetic field with the nominal value $B_E = .5 \text{ Gauss}$. It became later clear that the explanation of ELF em fields on vertebrate brain requires $B_d = .2 \text{ Gauss}$ rather than $B_E = .5 \text{ Gauss}$ [43]. The interpretation was as dark magnetic field $B_d = .2 \text{ Gauss}$. The model of EEG led also to the hypothesis that Mersenne primes and their Gaussian counterparts define preferred p-adic length scales and their dark counterparts. This hypothesis replaced the earlier $r = 2^{11k}$ hypothesis.

For $r = 2^{127-113=14}$ the predicted radius $L_w = .4 \mu\text{m}$ is consistent with the radius of neuronal axons. If one assumes that the radii of flux tubes are given by this length scale irrespective of the value of r , one must replace the quantization condition for the magnetic flux with a more general condition in which the magnetic flux is compensated by the contribution of the supra current flowing

around the flux tube: $\oint (p - eA) \cdot dl = n\hbar$ and assume $n = 0$. The supra currents would be present inside living organism but in the faraway region where flux quanta from organism fuse together, the quantization conditions $e \int B \cdot dS = n\hbar$ would be satisfied.

The most natural interpretation would be that these flux tubes topologically condense at the flux tubes of B_E . Both bosonic ions and the Cooper pairs of electrons or of fermionic ions can act as charge carriers so that actually an entire zoo of super-conductors is predicted. There is even some support for the view that even molecules and macromolecules can drop to the magnetic flux tubes [49].

Nuclear physics anomalies and ORMEs

At the homepage of Joe Champion [60] information about claimed nuclear physics anomalies can be found.

1) The first anomaly is the claimed low temperature cold fusion mentioned at the homepage of Joe Champion [60]. For instance, Champion claims that Mercury ($Z=80$), decays by emission of proton and neutrons to Gold with $Z=79$ in the electrochemical arrangement described in [60].

2) Champion mentions also the anomalous production of Cadmium isotopes electrochemically in presence of Palladium reported by Tadahiko Mizuno.

The simplest explanation of the anomalies would be based on genuine nuclear reactions. The interaction of dark nuclei with ordinary nuclei at the boundary between the two phases would make possible genuine nuclear transmutations since the Coulomb wall hindering usually cold fusion and nuclear transmutations would be absent (Trojan horse mechanism). Both cold fusion and reported nuclear transmutations in living matter could rely on this mechanism as suggested in [23, 47, 16].

Possible implications

The existence of exotic atoms could have far reaching consequences for the understanding of bio-systems. If Hudson's claims about super-conductor like behavior are correct, the formation of exotic atoms in bio-systems could provide the needed mechanism of electronic super-conductivity. One could even argue that the formation of exotic atoms is the magic step transforming chemical evolution to biological evolution.

Equally exciting are the technological prospects. If the concept works it could be possible to manufacture exotic atoms and build room temperature super conductors and perhaps even artificial life some day. It is very probable that the process of dropping electron to the larger space-time sheet requires energy and external energy feed is necessary for the creation of artificial life. Otherwise the Earth and other planets probably have developed silicon based life for long time ago. Ca, K and Na ions have central position in the electrochemistry of cell membranes. They could actually correspond to exotic ions obtained by dropping some valence electrons from $k = 137$ atomic space-time sheet to larger space-time sheets. For instance, the $k = 149$ space-time sheet of lipid layers could be in question.

The status of ORMEs is far from certain and their explanation in terms of exotic atomic concept need not be correct. The fact is however that TGD predicts exotic atoms: if they are not observed TGD approach faces the challenge of finding a good explanation for their non-observability.

10.7.2 Connection with cold fusion?

The basic prediction of TGD is a hierarchy of fractally scaled variants of non-asymptotically free QCD like theories and that color dynamics is fundamental even for our sensory qualia (visual colors identified as increments of color quantum numbers in quantum jump). The model for ORMEs suggest that exotic protons obey QCD like theory in the size scale of atom. If this identification is correct, QCD like dynamics might be studied some day experimentally in atomic or even macroscopic length scales of order cell size and there would be no need for ultra expensive accelerators! The fact that Palladium is one of the "mono-atomic" elements used also in cold fusion experiments as a target material [62, 61] obviously puts bells ringing.

What makes possible cold fusion?

I have proposed that cold fusion might be based on Trojan horse mechanism in which incoming and target nuclei feed their em gauge fluxes to different space-time sheets so that electromagnetic Coulomb wall disappears [23]. If part of Palladium nuclei are "partially dark", this is achieved. Another mechanism could be the de-localization of protons to a larger volume than nuclear volume induced by the increase of \hbar_{eff} meaning that reaction environment would differ dramatically from that appearing in the usual nuclear reactions and the standard objections against cold fusion would not apply anymore [23]: this delocalization could correspond to the darkness of electromagnetic field bodies of protons.

A third proposal is perhaps the most elegant and relies on the nuclear string model [47] predicting a large number of exotic nuclei obtained by allowing the color bonds connecting nucleons to have all possible em charges 1, 0, 1. Many ordinary heavy nuclei would be exotic in the sense that some protons would correspond to protons plus negatively charged color bonds. The exchange of an exotic weak boson between D and Pd nuclei transforming D nuclei to exotic neutral D nuclei would occur. The range of the exotic weak interaction correspond to atomic length scale meaning that it behaves as massless particle below this length scale. For instance, W boson could be $r = 2^{24}$ dark variant of $k = 113$ weak boson for which the dark variant of p-adic scale would correspond to the atomic scale $k = 137$ but also other options are possible.

How standard objections against cold fusion can be circumvented?

The following arguments against cold fusion are from an excellent review article by Storms [39].

1. Coulomb wall requires an application of higher energy. Now electromagnetic Coulomb wall disappears in both models.
2. If a nuclear reaction should occur, the immediate release of energy can not be communicated to the lattice in the time available. In the recent case the time scale is however multiplied by the factor $r = n_a$ and the situation obviously changes. For $n_a = 2^{24}$ the time scale corresponding to MeV energy becomes that corresponding to keV energy which is atomic time scale.
3. When such an energy is released under normal conditions, energetic particles are emitted along with various kinds of radiation, only a few of which are seen by various CANR (Chemically Assisted Nuclear Reactions) studies. In addition, gamma emission must accompany helium, and production of neutrons and tritium, in equal amounts, must result from any fusion reaction. None of these conditions is observed during the claimed CANR effect, no matter how carefully or how often they have been sought. The large value of $\hbar(M^4)$ implying large Compton lengths for protons making possible geometric coupling of gamma rays to condensed matter would imply that gamma rays do not leave the system. If only protons form the quantum coherent state then fusion reactions do not involve the protons of the cathode at all and production of ${}^3\text{He}$ and thus of neutrons in the fusion of D and exotic D .
4. The claimed nuclear transmutation reactions (reported to occur also in living matter [69]) are very difficult to understand in standard nuclear physics framework.
 - (a) The model of [23] allows them since protons of different nuclei can re-arrange in many different manners when the dark matter state decays back to normal.
 - (b) Nuclear string model [47] allows transmutations too. For instance, neutral exotic tritium produced in the reactions can fuse with Pd and other nuclei.
5. Many attempts to calculate fusion rates based on conventional models fail to support the claimed rates within PdD (Palladium-Deuterium). The atoms are simply too far apart. This objections also fails for obvious reasons.

Mechanisms of cold fusion

One can deduce a more detailed model for cold fusion from observations, which are discussed systematically in [39] and in the references discussed therein.

1. A critical phenomenon is in question. The average D/Pd ratio must be in the interval (.85, .90). The current must be over-critical and must flow a time longer than a critical time. The effect occurs in a small fraction of samples. D at the surface of the cathode is found to be important and activity tends to concentrate in patches. The generation of fractures leads to the loss of the anomalous energy production. Even the shaking of the sample can have the same effect. The addition of even a small amount of H_2O to the electrolyte (protons to the cathode) stops the anomalous energy production.

- (a) These findings are consistent the view that patches correspond to a macroscopic quantum phase involving delocalized nuclear protons. The added ordinary protons and fractures could serve as a seed for a phase transition leading to the ordinary phase [23].
- (b) An alternative interpretation is in terms of the formation of neutral exotic D and exotic Pd via exchange of exotic, possibly dark, W bosons massless below atomic length scale [47].

2. When D_2O is used as an electrolyte, the process occurs when PdD acts as a cathode but does not seem to occur when it is used as anode. This suggests that the basic reaction is between the ordinary deuterium $D = pn$ of electrolyte with the exotic nucleus of the cathode. Denote by \hat{p} the exotic proton and by $\hat{D} = n\hat{p}$ exotic deuterium at the cathode.

For ordinary nuclei fusions to tritium and 3He occur with approximately identical rates. The first reaction produces neutron and 3He via $D+D \rightarrow n+{}^3He$, whereas second reaction produces proton and tritium by 3H via $D + D \rightarrow p + {}^3H$. The prediction is that one neutron per each tritium nucleus should be produced. Tritium can be observed by its beta decay to 3He and the ratio of neutron flux is several orders of magnitude smaller than tritium flux as found for instance by Tadahiko Mizuno and his collaborators (Mizuno describes the experimental process leading to this discovery in his book [70]). Hence the reaction producing 3He cannot occur significantly in cold fusion which means a conflict with the basic predictions of the standard nuclear physics.

- (a) The explanation discussed in [23] is that the proton in the target deuterium \hat{D} is in the exotic state with large Compton length and the production of 3He occurs very slowly since \hat{p} and p correspond to different space-time sheets. Since neutrons and the proton of the D from the electrolyte are in the ordinary state, Coulomb barrier is absent and tritium production can occur. The mechanism also explains why the cold fusion producing 3He and neutrons does not occur using water instead of heavy water.
 - (b) Nuclear string model [47] model predicts that only neutral exotic tritium is produced considerably when incoming deuterium interacts with neutral exotic deuterium in the target.
3. The production of 4He has been reported although the characteristic gamma rays have not been detected.

- (a) 4He can be produced in reactions such as $D + \hat{D} \rightarrow {}^4He$ in the model of [23].
- (b) Nuclear string model [23] does not allow direct production of 4He in D-D collisions.

4. Also more complex reactions between D and Pd for which protons are in exotic state can occur. These can lead to the reactions transforming the nuclear charge of Pd and thus to nuclear transmutations.

Both model explain nuclear transmutations. In nuclear string model [23] the resulting exotic tritium can fuse with Pd and other nuclei and produce nuclear transmutations.

The reported occurrence of nuclear transmutation such as ${}^{23}Na + {}^{16}O \rightarrow {}^{39}K$ in living matter [69] allowing growing cells to regenerate elements K, Mg, Ca, or Fe, could be understood in nuclear string model if also neutral exotic charge states are possible for nuclei in living matter. The experimental signature for the exotic ions would be cyclotron energy spectrum containing besides the standard lines also lines with ions with anomalous mass number. This could be seen as a splitting of lines. For instance, exotic variants of ions such Na^+ , K^+ , Cl^- , Ca^{++} with anomalous mass numbers should exist. It would be easy to mis-interpret the situation unless the actual strength of the magnetic field is not checked.

5. Gamma rays, which should be produced in most nuclear reactions such as ${}^4\text{He}$ production to guarantee momentum conservation are not observed.
 - (a) The explanation of the model of [23] is that the recoil momentum goes to the macroscopic quantum phase and eventually heats the electrolyte system. This provides obviously the mechanism by which the liberated nuclear energy is transferred to the electrolyte difficult to imagine in standard nuclear physics framework.
 - (b) In nuclear string model [47] ${}^4\text{He}$ is not produced at all.
6. Both models explain why neutrons are not produced in amounts consistent with the anomalous energy production. The addition of water to the electrolyte is however reported to induce neutron bursts.
 - (a) In the model of [23] a possible mechanism is the production of neutrons in the phase transition $\hat{p} \rightarrow p$. $\hat{D} \rightarrow p + n$ could occur as the proton contracts back to the ordinary size in such a manner that it misses the neutron. This however requires energy of 2.23 MeV if the rest masses of \hat{D} and D are same. Also $\hat{D} + \hat{D} \rightarrow n + {}^3\text{He}$ could be induced by the phase transition to ordinary matter when \hat{p} transformed to p does not combine with its previous neutron partner to form D but recombines with \hat{D} to form ${}^3\hat{\text{H}}e \rightarrow {}^3\text{He}$ so that a free neutron is left.
 - (b) Nuclear string model [47] would suggest that the collisions of protons of water with exotic D produce neutron and ordinary D . This requires the transformation of negatively charged color bond between p and n of target D to a neutral color bond between incoming p and neutron of target.

10.7.3 Sono-luminescence, classical Z^0 force, and hydrodynamic hierarchy of p-adic length scales

Sono-luminescence [76] is a peculiar phenomenon, which might provide an application for the hydrodynamical hierarchy. The radiation pressure of a resonant sound field in a liquid can trap a small gas bubble at a velocity node. At a sufficiently high sound intensity the pulsations of the bubble are large enough to prevent its contents from dissolving in the surrounding liquid. For an air bubble in water, a still further increase in intensity causes the phenomenon of sono-luminescence above certain threshold for the sound intensity. What happens is that the minimum and maximum radii of the bubble decrease at the threshold and picosecond flash of broad band light extending well into ultraviolet is emitted. Rather remarkably, the emitted frequencies are emitted simultaneously during very short time shorter than 50 picoseconds, which suggests that the mechanism involves formation of coherent states of photons. The transition is very sensitive to external parameters such as temperature and sound field amplitude.

A plausible explanation for the sono-luminescence is in terms of the heating caused by shock waves launched from the boundary of the adiabatically contracting bubble [76]. The temperature jump across a strong shock is proportional to the square of Mach number and increases with decreasing bubble radius. After the reflection from the minimum radius $R_s(\text{min})$ the outgoing shock moves into the gas previously heated by the incoming shock and the increase of the temperature after focusing is approximately given by $T/T_0 = M^4$, where M is Mach number at focusing and $T_0 \sim 300\text{ K}$ is the temperature of the ambient liquid. The observed spectrum of sono-luminescence is explained as a brehmstrahlung radiation emitted by plasma at minimum temperature $T \sim 10^5\text{ K}$. There is a fascinating possibility that sono-luminescence relates directly to the classical Z^0 force.

Even standard model reproduces nicely the time development of the bubble and sono-luminescence spectrum and explains sensitivity to the external parameters [76]. The problem is to understand how the length scales are generated and explain the jump-wise transition to sono-luminescence and the decrease of the bubble radius at sono-luminescence: ordinary hydrodynamics predicts continuous increase of the bubble radius. The length scales are the ambient radius R_0 (radius of the bubble, when gas is in pressure of 1 atm) and the minimum radius $R_s(\text{min})$ of the shock wave determining the temperature reached in shock wave heating. Zero radius is certainly not reached since shock front is susceptible to instabilities.

p-Adic length scale hypothesis and the length scales sono-luminescence

Since p-adic length scale hypothesis introduces a hierarchy of hydrodynamics with each hydrodynamics characterized by a p-adic cutoff length scale there are good hopes of achieving a better understanding of these length scales in TGD. The change in bubble size in turn could be understood as a change in the 'primary' condensation level of the bubble.

1. The bubble of air is characterized by its primary condensation level k . The minimum size of the bubble at level k must be larger than the p-adic length scale $L(k)$. This suggests that the transition to photo-luminescence corresponds to the change in the primary condensation level of the air bubble. In the absence of photo-luminescence the level can be assumed to be $k = 163$ with $L(163) \sim .76 \mu m$ in accordance with the fact that the minimum bubble radius is above $L(163)$. After the transition the primary condensation level of the air bubble one would have $k = 157$ with $L(157) \sim .07 \mu m$. In the transition the minimum radius of the bubble decreases below $L(163)$ but should not decrease below $L(157)$: this hypothesis is consistent with the experimental data [76].
2. The particles of hydrodynamics at level k have minimum size $L(k_{prev})$. For $k = 163$ one has $k_{prev} = 157$ and for $k = 157$ $k_{prev} = 151$ with $L(151) \sim 11.8 nm$. It is natural to assume that the minimum size of the particle at level k gives also the minimum radius for the spherical shock wave since hydrodynamic approximation fails below this length scale. This means that the minimum radius of the shock wave decreases from $R_s(min, 163) = L(157)$ to $R_s(min, 157) = L(151)$ in the transition to sono-luminescence. The resulting minimum radius is $11 nm$ and much smaller than the radius $.1 \mu m$ needed to explain the observed radiation if it is emitted by plasma.

A quantitative estimate goes along lines described in [76].

1. The radius of the spherical shock is given by

$$R_s = At^\alpha, \quad (10.7.1)$$

where t is the time to the moment of focusing and α depends on the equation of state (for water one has $\alpha \sim .7$).

2. The collapse rate of the adiabatically compressing bubble obeys

$$\frac{dR}{dt} = c_0 \left(\frac{2}{3\gamma} \frac{\rho_0}{\rho} \left(\frac{R_m}{R_0} \right)^3 \right)^{1/2}, \quad (10.7.2)$$

where c_0 is the sound velocity in gas, γ is the heat capacity ratio and ρ_0/ρ is the ratio of densities of the ambient gas and the liquid.

3. Assuming that the shock is moving with velocity c_0 of sound in gas, when the radius of the bubble is equal to the ambient radius R_0 one obtains from previous equations for the Mach number M and for the radius of the shock wave

$$\begin{aligned} M &= \frac{\frac{dR_s}{dt}}{c_0} = (t_0/t)^{\alpha-1}, \\ R_s &= R_0(t/t_0)^\alpha, \\ t_0 &= \frac{\alpha R_0}{c_0}. \end{aligned} \quad (10.7.1)$$

where t_0 is the time that elapses between the moment, when the bubble radius is R_0 and the instant, when the shock would focus to zero radius in the ideal case. For $R_0 = L(167)$ (order of magnitude is this) and for $R_s(min) = L(151)$ one obtains $R_0/R_s(min) = 256$ and $M \simeq 10.8$ at the minimum shock radius.

4. The increase of the temperature immediately after the focusing is approximately given by

$$\frac{T}{T_0} \simeq M^4 = \left(\frac{R_0}{R_s}\right)^{\frac{4(1-\alpha)}{\alpha}} \simeq 1.3 \cdot 10^4 . \quad (10.7.1)$$

For $T_0 = 300 \text{ K}$ this gives $T \simeq 4 \cdot 10^6 \text{ K}$: the temperature is far below the temperature needed for fusion.

In principle the further increase of the temperature can lead to further transitions. The next transition would correspond to the transition $k = 157 \rightarrow k = 151$ with the minimum size of particle changing as $L(k_{prev}) \rightarrow L(149)$. The next transition corresponds to the transition to $k = 149$ and $L(k_{prev}) \rightarrow L(141)$. The values of the temperatures reached depend on the ratio of the ambient size R_0 of the bubble and the minimum radius of the shock wave. The fact that R_0 is expected to be of the order of $L(k_{next})$ suggests that the temperatures achieved are not sufficiently high for nuclear fusion to take place.

Could sonoluminescence involve the formation of a phase near vacuum extremals?

In TGD inspired model of cell membrane [27] a key role is played by almost vacuum extremals for which the induced Kähler field is very small. Vacuum extremals are accompanied by a strong classical Z^0 field proportional to classical electromagnetic field and given by $Z^0 = -2\gamma/p$, $p = \sin^2(\theta_W)$. One could also imagine that em field is vanishing in which case Z^0 field is proportional to Kähler field and also strong because of $Z^0 = 6J/p$, $p = \sin^2(\theta_W)$ proportionality. In this case also classical color fields are present. It is however not clear whether these fields can be realized as preferred extremals of Kähler action.

The classical Z^0 field should have a source and the vacuum polarization in the sense that flux tubes are generated with many fermion state and its conjugate at its opposite ends would generate it. The Compton scale of weak bosons must correspond to $L(157)$ so that either dark variants of ordinary weak bosons or their light variants would be in question. Both would be effectively massless below $L(157)$. The simplest situation corresponds to many-neutrino state for vacuum extremals but also many quark states are possible when em field for the flux tube vanishes.

The length scales involved correspond to Gaussian Mersennes $M_{G,k} = (1+i)^k - 1$ and together with $k = 151$ and $k = 167$ define biologically important length scales [27]. The p-adically scaled up variants and dark variants of of QCD and weak physics haven been conjectured to play key role in biology between length scales 10 nm (cell membrane thickness) and 2.5 μm (the size scale of nucleus). This motivates the question whether a nearly vacuum extremal phase (as far as induced gauge fields are considered) accompanies the transition changing the p-adic length scale associated with the bubble from $k = 163$ to $k = 157$. The acceleration in the strong Z^0 field associated with the flux tubes could generate the visible light as brehmstrahlung radiation, perhaps also Z^0 and W brehmstrahlung could be generated and would decay to photons and charged particles and generate a plasma in this manner. If the weak scale is given by $k_W = 157$, the mass scale of weak bosons is $2^{-31} \simeq 10^{-9}/2$ times smaller than that of ordinary weak bosons (about 50 eV which corresponds to a temperature of $5 \times 10^5 \text{ K}$). A further transition to $k = 151$ would correspond to gauge boson mass scale 400 eV and temperature or order $4 \times 10^6 \text{ K}$.

10.8 Dark atomic physics

Dark matter might be relevant also for atomic physics and in the sequel some speculations along these lines are represented. Previous considerations assumed that only field bodies can be dark and this is assumed also now. The notion of dark atom depends strongly on the precise meaning of the generalized imbedding space and I have considered several options.

1. The first option was based on the singular coverings $CD \times CP_2 \rightarrow CD/G_a \times CP_2/G_b$. This approach has a concrete connection to the quantization and the selection of quantization axes

correlates closely with the identification of groups G_a and G_b . The questionable assumption is that elementary particle like partonic 2-surfaces remain invariant under the cyclic groups $G_a \times G_b$.

2. The next proposal was that both factor spaces and coverings of H are possible. For this option the notion of covering is somewhat unsatisfactory because it lacks concreteness. Singular factor of CD and CP_2 spaces make possible all rational values of Planck constant and one loses the vision about evolution as drift to the sectors of imbedding space characterized by increasing value of Planck constant.
3. The last proposal is based on the realization that basic quantum TGD could well explain the hierarchy of Planck constants in terms of singular covering spaces emerging naturally when the time derivatives of the imbedding space coordinates are many-valued functions of the canonical momentum densities. In this framework singular factors spaces are not possible and the formula $r \equiv \hbar/\hbar_0 = n_a n_b$ emerges naturally as well as charge fractionization. One also ends up to a unique recipe for how to obtain binding energies in this kind of situation and the results are consistent with the earlier formulas deduced on purely formal arguments. Groups G_a and G_b do not directly correspond to subgroups of isometry groups but the fractionization of quantum numbers implied by the scaling of Planck constant implies that wave functions for the selected quantization axes behave as if the maximal cyclic subgroups of G_a and G_b had a geometric meaning.

For covering space option fermion number is fractionized. The group algebra of $G_a \times G_b$ defines $n_a n_b$ single particle wave functions in the covering. The simplest option is that total fermion number is integer valued so that the many-sheeted structure is analogous to a full Fermi sphere containing $n_a n_b$ fermions with fractional fermion number $1/n_a n_b$. A more general option allows states with fractional total fermion number varying from $1/n_a n_b$ to 1. One could generalize the condition about integer fermion number so that it holds for the entire quantum state involving several covering regions and the condition would correspond to the $G_a \times G_b$ singletness of the physical states.

10.8.1 Dark atoms and dark cyclotron states

The development of the notion of dark atom involves many side tracks which make me blush. The first naive guess was that dark atom would be obtained by simply replacing Planck constant with its scaled counterpart in the basic formulas and interpreting the results geometrically. After some obligatory twists and turns it became clear that this assumption is indeed the most plausible one. The main source of confusion has been the lack of precise view about what the hierarchy of Planck constants means at the level of imbedding space at space-time.

The rules are very simple when one takes the singular coverings assigned to the many-valuedness of the time-derivatives of imbedding space coordinates as functions of canonical momentum densities as a starting point.

1. The mass and charge of electron are fractionized as is also the reduced mass in Schrödinger equation. This implies the replacements $e \rightarrow e/r$, $m \rightarrow m/r$, and $\hbar \rightarrow r\hbar_0$, $r = n_a n_b$, in the general formula for the binding energy assigned with single sheet of the covering. If maximal number $n_a n_b$ are present corresponding to a full "Fermi sphere", the total binding energy is r times the binding energy associated with single sheet.
2. In the case of hydrogen atom the proportionality $E \propto m/\hbar^2$ implies that the binding energy for single sheet of the covering scales as $E \rightarrow E/(n_a n_b)^3$ and maximal binding energy scales as $E \rightarrow E/(n_a n_b)^2$. This conforms with the naive guess. For high values of the nuclear charge Z it can happen that the binding energy is larger than the rest mass and fractionization might take place when binding energy is above critical fraction of the rest mass.
3. In the case of cyclotron energies one must decide what happens to the magnetic flux. Magnetic flux quantization states that the flux is proportional to \hbar for each sheet separately. Hence one has $\Phi \rightarrow r\Phi$ for each sheet and the total flux scales as r^2 . Since the dimensions of the flux quantum are scaled up by r the natural scaling of the size of flux quantum is by r^2 . Therefore the quantization of the magnetic flux requires the scaling $B \rightarrow B/r$. The cyclotron energy for

single sheet satisfies $E \propto \hbar q B / m$ and since both mass m and charge q become fractional, the energy E for single sheet remains invariant whereas total cyclotron energy is scaled up by r in accordance with the original guess and the assumption used in applications.

4. Dark cyclotron states are expected to be stable up to temperatures which are r times higher than for ordinary cyclotron states. The states of dark hydrogen atoms and its generalizations are expected to be stable at temperatures scaled down by $1/r^2$ in the first approximation.
5. Similar arguments allow to deduce the values of binding energies in the general case once the formula of the binding energy given by standard quantum theory is known.

The most general option allows fractional atoms with proton and electron numbers varying from $1/r$ to 1. One can imagine also the possibility of fractional molecules. The analogs of chemical bonds between fractional hydrogen atoms with $N - k$ and k fractional electrons and protons can be considered and would give rise to a full shell of fractional electrons possessing an exceptional stability. These states would have proton and electron numbers equal to one.

Catalytic sites are one possible candidate for fractal electrons and catalyst activity might be perhaps understood as a strong tendency of fractal electron and its conjugate to fuse to form an ordinary electron.

10.8.2 Could q-Laguerre equation relate to the claimed fractionation of the principal quantum number for hydrogen atom?

The so called hydrino atom concept of Randell Mills [93] represents one of the notions related to free energy research not taken seriously by the community of university physicists. What is claimed that hydrogen atom can exist as scaled down variants for which binding energies are much higher than usually due to the large Coulombic energy. The claim is that the quantum number n having integer values $n = 0, 1, 2, 3, \dots$ and characterizing partially the energy levels of the hydrogen atom can have also inverse integer values $n = 1/2, 1/3, \dots$. The claim of Mills is that the laboratory BlackLight Inc. led by him can produce a plasma state in which transitions to these exotic bound states can occur and liberate as a by-product usable energy.

The National Aeronautic and Space Administration has dispatched mechanical engineering professor Anthony Marchese from Rowan University to BlackLight's labs in Cranbury, NJ, to investigate whether energy plasmas-hot, charged gases-produced by Mills might be harnessed for a new generation of rockets. Marchese reported back to his sponsor, the NASA Institute for Advanced Concepts, that indeed the plasma was so far unexplainably energetic. An article about the findings of Mills and collaborators have been accepted for publication in Journal of Applied Physics so that there are reasons to take seriously the experimental findings of Mills and collaborators even if one does not take seriously the theoretical explanations.

The fractionized principal quantum number n claimed by Mills [93] is reported to have at least the values $n = 1/k$, $k = 2, 3, 4, 5, 6, 7, 10$. First explanation would be in terms of Planck constant having also values smaller than \hbar_0 possible if singular factor spaces of causal diamond CD and CP_2 are allowed. q -Deformations of ordinary quantum mechanics are suggested strongly by the hierarchy of Jones inclusion associated with the hyper-finite factor of type II_1 about which WCW spinors are a basic example. This motivates the attempt to understand the claimed fractionization in terms of q -analog of hydrogen atom. The safest interpretation for them would be as states which can exist in ordinary imbedding space (and also in other branches)

The Laguerre polynomials appearing in the solution of Schrödinger equation for hydrogen atom possess quantum variant, so called q -Laguerre polynomials [56], and one might hope that they would allow to realize this semiclassical picture at the level of solutions of appropriately modified Schrödinger equation and perhaps also resolve the difficulty associated with $n = 1/2$. Unfortunately, the polynomials discussed in [56] correspond to $0 < q \leq 1$ rather than complex values of $q = \exp(i\pi/m)$ on circle and the extrapolation of the formulas for energy eigenvalues gives complex energies.

q -Laguerre equation for $q = \exp(i\pi/m)$

The most obvious modification of the Laguerre equation for S -wave states (which are the most interesting by semiclassical argument) in the complex case is based on the replacement

$$\begin{aligned}
\partial_x &\rightarrow \frac{1}{2}(\partial_x^q + \partial_x^{\bar{q}}) \\
\partial_x^q f &= \frac{f(qx) - f(x)}{(q-1)x} , \\
q &= \exp(i\pi/m)
\end{aligned} \tag{10.8-1}$$

to guarantee hermiticity. When applied to the Laguerre equation

$$x \frac{d^2 L_n}{dx^2} + (1-x) \frac{dL_n}{dx} = nL_n , \tag{10.8.0}$$

and expanding L_n into Taylor series

$$L_n(x) = \sum_{n \geq 0} l_n x^n , \tag{10.8.1}$$

one obtains difference equation

$$\begin{aligned}
a_{n+1} l_{n+1} + b_n l_n &= 0 , \\
a_{n+1} &= \frac{1}{4R_1^2} [R_{2n+1} - R_{2n} + 2R_{n+1}R_1 + 3R_1] + \frac{1}{2R_1} [R_{n+1} + R_1] \\
b_n &= \frac{R_n}{2R_1} - n^q + \frac{1}{2} , \\
R_n &= 2\cos[(n-1)\pi/m] - 2\cos[n\pi/m] .
\end{aligned} \tag{10.8-1}$$

Here n^q is the fractionized principal quantum number determining the energy of the q-hydrogen atom. One cannot pose the difference equation on l_0 since this together with the absence of negative powers of x would imply the vanishing of the entire solution. This is natural since for first order difference equations lowest term in the series should be chosen freely.

Polynomial solutions of q-Laguerre equation

The condition that the solution reduces to a polynomial reads as

$$b_n = 0 \tag{10.8.0}$$

and gives

$$n^q = \frac{1}{2} + \frac{R_n}{2R_1} , \tag{10.8.1}$$

For $n = 1$ one has $n^q = 1$ so that the ground state energy is not affected. At the limit $N \rightarrow \infty$ one obtains $n^q \rightarrow n$ so that spectrum reduces to that for hydrogen atom. The periodicity $R_{n+2Nk} = R_n$ reflects the corresponding periodicity of the difference equation which suggests that only the values $n \leq 2m - 1$ belong to the spectrum. Spectrum is actually symmetric with respect to the middle point $[N/2]$ which suggests that only $n < [m/2]$ corresponds to the physical spectrum. An analogous phenomenon occurs for representations of quantum groups [19]. When m increases the spectrum approaches integer valued spectrum and one has $n > 1$ so that no fractionization in the desired sense occurs for polynomial solutions.

Non-polynomial solutions of q-Laquerre equation

One might hope that non-polynomial solutions associated with some fractional values of n^q near to those claimed by Mills might be possible. Since the coefficients a_n and b_n are periodic, one can express the solution ansatz as

$$\begin{aligned} L_n(x) &= P_a^{(2m)}(x) \sum_k a^k x^{2mk} = P_a^{(2m)}(x) \frac{1}{1 - ax^{2m}} , \\ P_a^{(2m)}(x) &= \sum_{k=0}^{2m-1} l_k x^k , \\ a &= \frac{l_{2m}}{l_0} , \end{aligned} \tag{10.8.0}$$

This solution behaves as $1/x$ asymptotically but has pole at $x_\infty = (1/a)^{1/2m}$ for $a > 0$. The expression for $l_{2m}/l_0 = a$ is

$$a = \prod_{k=1}^{2m} \frac{b_{2m-k}}{a_{2m-k+1}} . \tag{10.8.1}$$

This can be written more explicitly as

$$\begin{aligned} a &= (2R_1)^{2m} \prod_{k=1}^{2m} X_k , \\ X_k &= \frac{R_{2m-k} + (-2n^q + 1)R_1}{R_{4m-2k+1} - R_{4m-2k} + 4R_{2m-k+1}R_1 + 2R_1^2 + 3R_1} , \\ R_n &= 2\cos[(n-1)\pi/m] - 2\cos[n\pi/m] . \end{aligned} \tag{10.8.-1}$$

This formula is a specialization of a more general formula for $n = 2m$ and resulting ratios l_n/l_0 can be used to construct $P_a^{(2m)}$ with normalization $P_a^{(2m)}(0) = 1$.

Results of numerical calculations

Numerical calculations demonstrate following.

1. For odd values of m one has $a < 0$ so that a a continuous spectrum of energies seems to result without any further conditions.
2. For even values of m a has a positive sign so that a pole results.

For even value of m it could happen that the polynomial $P_a^{(2m)}(x)$ has a compensating zero at x_∞ so that the solution would become square integrable. The condition for reads explicitly

$$P_a^{(2m)}\left(\left(\frac{1}{a}\right)^{\frac{1}{2m}}\right) = 0 . \tag{10.8.0}$$

If $P_a^{(2m)}(x)$ has zeros there are hopes of finding energy eigen values satisfying the required conditions. Laguerre polynomials and also q-Laguerre polynomials must posses maximal number of real zeros by their orthogonality implied by the hermiticity of the difference equation defining them. This suggests that also $P_a^{(2m)}(x)$ possesses them if a does not deviate too much from zero. Numerical calculations demonstrate that this is the case for $n^q < 1$.

For ordinary Laguerre polynomials the naive estimate for the position of the most distant zero in the units used is larger than n but not too much so. The naive expectation is that L_{2m} has largest

zero somewhat above $x = 2m$ and that same holds true a small deformation of L_{2m} considered now since the value of the parameter a is indeed very small for $n^q) < 1$. The ratio $x_\infty/2m$ is below .2 for $m \leq 10$ so that this argument gives good hopes about zeros of desired kind.

One can check directly whether x_∞ is near to zero for the experimentally suggested candidates for $n^q)$. The table below summarizes the results of numerical calculations.

1. The table gives the exact eigenvalues $1/n_q)$ with a 4-decimal accuracy and corresponding approximations $1/n_{\simeq}^q) = k$ for $k = 3, \dots, 10$. For a given value of m only single eigenvalue $n^q) < 1$ exists. If the observed anomalous spectral lines correspond to single electron transitions, the values of m for them must be different. The value of m for which $n^q) \simeq 1/k$ approximation is optimal is given with boldface. The value of k increases as m increases. The lowest value of m allowing the desired kind of zero of $P^{2m})$ is $m = 18$ and for $k \in \{3, 10\}$ the allowed values are in range $18, \dots, 38$.
2. $n^q) = 1/2$ does not appear as an approximate eigenvalue so that for even values of m quantum calculation produces same disappointing result as the classical argument. Below it will be however found that $n^q) = 1/2$ is a universal eigenvalue for odd values of m .

m	$1/n_{\simeq}^q)$	$1/n^q)$	m	$1/n_{\simeq}^q)$	$1/n^q)$
18	3	2.7568	30	8	7.5762
20	4	3.6748	32	8	8.3086
22	5	4.5103	34	9	9.0342
24	5	5.3062	36	10	9.7529
26	6	6.0781	38	10	10.4668
28	7	6.8330			

Table3. The table gives the approximations $1/n_{\simeq}^q) = 1/k$ and corresponding exact values $1/n^q)$ in the range $k = 3, \dots, 10$ for which $P_a^{2m})(x_\infty)$ is nearest to zero. The corresponding values of $m = 2k$ vary in the range, $k = 18, \dots, 38$. For odd values of m the value of the parameter a is negative so that there is no pole. Boldface marks for the best approximation by $1/n_{\simeq}^q) = k$.

How to obtain $n^q) = 1/2$ state?

For odd values of m the quantization recipe fails and physical intuition tells that there must be some manner to carry out quantization also now. The following observations give a hunch about be the desired condition.

1. For the representations of quantum groups only the first m spins are realized [19]. This suggests that there should exist a symmetry relating the coefficients l_n and l_{n+m} and implying $n^q) = 1/2$ for odd values of m . This symmetry would remove also the double degeneracy associated with the almost integer eigenvalues of $n^q)$. Also other fractional states are expected on basis of physical intuition.
2. For $n^q) = 1/2$ the recursion formula for the coefficients l_n involves only the coefficients R_m .
3. The coefficients R_k have symmetries $R_k = R_{k+2m}$ and $R_{k+m} = -R_m$.

There is indeed this kind of symmetry. From the formula

$$\begin{aligned}
 \frac{l_n}{l_0} &= (2R_1)^n \prod_{k=1}^n X_k \ , \\
 X_k &= \frac{R_{n-k} + (-2n^q) + 1)R_1}{[R_{2n-2k+1} - R_{n-2k} + 4R_{n-k+1}R_1 + 2R_1^2 + 3R_1]} \tag{10.8.0}
 \end{aligned}$$

one finds that for $n^q) = 1/2$ the formula giving l_{n+m} in terms of l_n changes sign when n increases by one unit

$$\begin{aligned}
 A_{n+1} &= (-1)^m A_n \ , \\
 A_n &= \prod_{k=1}^m \frac{b_{n+m-k}}{a_{n+m-k+1}} = \prod_{k=1}^m (2R_1)^m \prod_{k=1}^m X_{k+n} \ .
 \end{aligned}
 \tag{10.8-1}$$

The change of sign is essentially due to the symmetries $a_{n+m} = -a_n$ and $b_{n+m} = b_n$. This means that the action of translations on A_n in the space of indices n are represented by group Z_2 .

This symmetry implies $a = l_{2m}/l_0 = -(l_m)(l_0)^2$ so that for $n^q = 1/2$ the polynomial in question has a special form

$$\begin{aligned}
 P_a^{2m} &= P_a^m(1 - Ax^m) \ , \\
 A &= A_0 \ .
 \end{aligned}
 \tag{10.8-1}$$

The relationship $a = -A^2$ implies that the solution reduces to a form containing the product of m^{th} (rather than $(2m)^{th}$) order polynomial with a geometric series in x^m (rather than x^{2m}):

$$L_{1/2}(x) = \frac{P_a^m(x)}{1 + Ax^m} \ .
 \tag{10.8.0}$$

Hence the n first terms indeed determine the solution completely. For even values of m one obtains similar result for $n^q = 1/2$ but now A is negative so that the solution is excluded. This result also motivates the hypothesis that for the counterparts of ordinary solutions of Laguerre equation sum (even m) or difference (odd m) of solutions corresponding to n and $2m - n$ must be formed to remove the non-physical degeneracy.

This argument does not exclude the possibility that there are also other fractional values of n allowing this kind of symmetry. The condition for symmetry would read as

$$\begin{aligned}
 \prod_{k=1}^m (R_k + \epsilon R_1) &= \prod_{k=1}^m (R_k - \epsilon R_1) \ , \\
 \epsilon &= (2n^q) - 1 \ .
 \end{aligned}
 \tag{10.8.0}$$

The condition states that the odd part of the polynomial in question vanishes. Both ϵ and $-\epsilon$ solutions so that n^q and $1 - n^q$ are solutions. If one requires that the condition holds true for all values of m then the comparison of constant terms in these polynomials allows to conclude that $\epsilon = 0$ is the only universal solution. Since ϵ is free parameter, it is clear that the m :th order polynomial in question has at most m solutions which could correspond to other fractionized eigenvalues expected to be present on basis of physical intuition.

This picture generalizes also to the case of even n so that also now solutions of the form of Eq. 10.8.0 are possible. In this case the condition is

$$\prod_{k=1}^m (R_k + \epsilon R_1) = - \prod_{k=1}^m (R_k - \epsilon R_1) \ .
 \tag{10.8.1}$$

Obviously $\epsilon = 0$ and thus $n = 1/2$ fails to be a solution to the eigenvalue equation in this case. Also now one has the spectral symmetry $n_{\pm} = 1/2 \pm \epsilon$.

The symmetry $R_n = (-1)^m R_{n+m-1} = (-1)^m R_{n-m-1} = (-1)^m R_{m-n+1}$ can be applied to show that the polynomials associated with ϵ and $-\epsilon$ contain both the terms $R_n - \epsilon$ and $R_n + \epsilon$ as factors except for odd m for $n = (m + 1)/2$. Hence the values of n can be written for even values of m as

$$n^q(n) = \frac{1}{2} \pm \frac{R_n}{2R_1} \ , \ n = 1, \dots, \frac{m}{2} \ ,
 \tag{10.8.2}$$

and for odd values of m as

$$\begin{aligned} n_{\pm}^q(n) &= \frac{1}{2} \pm \frac{R_n}{2R_1}, \quad n = 1, \dots, \frac{m+1}{2} - 1, \\ n^q &= 1/2. \end{aligned} \quad (10.8.2)$$

Plus sign obviously corresponds to the solutions which reduce to polynomials and to $n^q \simeq n$ for large m . The explicit expression for n^q reads as

$$n_{\pm}^q(n) = \frac{1}{2} \pm \frac{(\sin^2(\pi(n-1)/2m) - \sin^2(\pi n/2m))}{2\sin^2(\pi/2m)}. \quad (10.8.3)$$

At the limit of large m one has

$$n_{+}^q(n) \simeq n, \quad n_{-}^q(n) \simeq 1 - n. \quad (10.8.4)$$

so that the fractionization $n \simeq 1/k$ claimed by Mills is not obtained at this limit. The minimum for $|n^q|$ satisfies $|n^q| < 1$ and its smallest value $|n^q| = .7071$ corresponds to $m = 4$. Thus these zeros cannot correspond to $n^q \simeq 1/k$ yielded by the numerical computation for even values of m based on the requirement that the zero of P^{2m} cancels the pole of the geometric series.

Some comments

Some closing comments are in order.

1. An open question is whether there are also zeros $|n^q| > 1$ satisfying $P_a^{2m}((1/a)^{1/2m}) = 0$ for even values of m .
2. The treatment above is not completely general since only s-waves are discussed. The generalization is however a rather trivial replacement $(1-x)d/dx \rightarrow (l+1-x)d/dx$ in the Laguerre equation to get associated Laguerre equation. This modifies only the formula for a_{n+1} in the recursion for l_n so that expression for n^q , which depends on b_n 's only, is not affected. Also the product of numerators in the formula for the parameter $a = l_{2m}/l_0$ remains invariant so that the general spectrum has the spectral symmetry $n^q \rightarrow 1 - n^q$. The only change to the spectrum occurs for even values of m and is due to the dependence of $x_{\infty} = (1/a)^{1/2m}$ on l and can be understood in the semiclassical picture. It might happen that the value of l is modified to its q counterpart corresponding to q-Legendre functions.
3. The model could partially explain the findings of Mills and $n^q \simeq 1/k$ for $k > 2$ also fixes the value of corresponding m to a very high degree so that one would have direct experimental contact with generalized imbedding space, spectrum of Planck constants, and dark matter. The fact that the fractionization is only approximately correct suggests that the states in question could be possible for all sectors of imbedding space appear as intermediate states into sectors in which the spectrum of hydrogen atom is scaled by $n_b/n_a = k = 2, 3, \dots$.
4. The obvious question is whether q-counterparts of angular momentum eigenstates ($idf_m/d\phi = mf_m$) are needed and whether they make sense. The basic idea of construction is that the phase transition changing \hbar does not involve any other modifications except fractionization of angular momentum eigenvalues and momentum eigenvalues having purely geometric origin. One can however ask whether it is possible to identify q-plane waves as ordinary plane waves. Using the definition $L_z = 1/2(\partial_u^q + \partial_{\bar{u}}^q)$, $u = \exp(i\phi)$, one obtains $f_n = \exp(in\phi)$ and eigenvalues as $n^q = R_n/R_1 \rightarrow n$ for $m \rightarrow \infty$. Similar construction applies in the case of momentum components.

Bibliography

Books about TGD

- [1] M. Pitkänen (2006), *Topological Geometroynamics: Overview*.
http://tgd.wippiespace.com/public_html/tgdview/tgdview.html.
- [2] M. Pitkänen (2006), *Quantum Physics as Infinite-Dimensional Geometry*.
http://tgd.wippiespace.com/public_html/tgdgeom/tgdgeom.html.
- [3] M. Pitkänen (2006), *Physics in Many-Sheeted Space-Time*.
http://tgd.wippiespace.com/public_html/tgdclass/tgdclass.html.
- [4] M. Pitkänen (2006), *p-Adic length Scale Hypothesis and Dark Matter Hierarchy*.
http://tgd.wippiespace.com/public_html/paddark/paddark.html.
- [5] M. Pitkänen (2006), *Quantum TGD*.
http://tgd.wippiespace.com/public_html/tgdquant/tgdquant.html.
- [6] M. Pitkänen (2006), *TGD as a Generalized Number Theory*.
http://tgd.wippiespace.com/public_html/tgdnumber/tgdnumber.html.
- [7] M. Pitkänen (2006), *TGD and Fringe Physics*.
http://tgd.wippiespace.com/public_html/freenergy/freenergy.html.

Books about TGD Inspired Theory of Consciousness and Quantum Biology

- [8] M. Pitkänen (2006), *TGD Inspired Theory of Consciousness*.
http://tgd.wippiespace.com/public_html/tgdconsc/tgdconsc.html.
- [9] M. Pitkänen (2006), *Bio-Systems as Self-Organizing Quantum Systems*.
http://tgd.wippiespace.com/public_html/bioselforg/bioselforg.html.
- [10] M. Pitkänen (2006), *Quantum Hardware of Living Matter*.
http://tgd.wippiespace.com/public_html/bioware/bioware.html.
- [11] M. Pitkänen (2006), *Bio-Systems as Conscious Holograms*.
http://tgd.wippiespace.com/public_html/hologram/hologram.html.
- [12] M. Pitkänen (2006), *Genes and Memes*.
http://tgd.wippiespace.com/public_html/genememe/genememe.html.
- [13] M. Pitkänen (2006), *Magnetospheric Consciousness*.
http://tgd.wippiespace.com/public_html/magnconsc/magnconsc.html.
- [14] M. Pitkänen (2006), *Mathematical Aspects of Consciousness Theory*.
http://tgd.wippiespace.com/public_html/mathconsc/mathconsc.html.
- [15] M. Pitkänen (2006), *TGD and EEG*.
http://tgd.wippiespace.com/public_html/tgdeeg/tgdeeg.html.

References to the chapters of the books about TGD

- [16] The chapter *TGD as a Generalized Number Theory: Infinite Primes* of [6].
http://tgd.wippiespace.com/public_html/tgdnumber/tgdnumber.html#visionc.
- [17] The chapter *TGD and Cosmology* of [3].
http://tgd.wippiespace.com/public_html/tgdclass/tgdclass.html#cosmo.
- [18] The chapter *Dark Forces and Living Matter* of [4].
http://tgd.wippiespace.com/public_html/paddark/paddark.html#darkforces.
- [19] The chapter *Quantum Hall effect and Hierarchy of Planck Constants* [5].
http://tgd.wippiespace.com/public_html/tgdquant/tgdquant.html#anyontgd.
- [20] The chapter *Nuclear String Model* of [4].
http://tgd.wippiespace.com/public_html/paddark/paddark.html#nuclstring.
- [21] The chapter *General Ideas about Many-Sheeted Space-Time: Part I* of [3].
http://tgd.wippiespace.com/public_html/tgdclass/tgdclass.html#topcond.
- [22] The chapter *Does TGD Predict the Spectrum of Planck Constants?* of [5].
http://tgd.wippiespace.com/public_html/tgdquant/tgdquant.html#Planck.
- [23] The chapter *Is it Possible to Understand Coupling Constant Evolution at Space-Time Level?* of [5].
http://tgd.wippiespace.com/public_html/tgdquant/tgdquant.html#rgflow.
- [24] The chapter *Cosmic Strings* of [3].
http://tgd.wippiespace.com/public_html/tgdclass/tgdclass.html#cstrings.
- [25] The chapter *p-Adic Particle Massivation: Hadron Masses* of [4].
http://tgd.wippiespace.com/public_html/paddark/paddark.html#mass3.
- [26] The chapter *p-Adic Particle Massivation: Elementary particle Masses* of [4].
http://tgd.wippiespace.com/public_html/paddark/paddark.html#mass2.
- [27] The chapter *TGD as a Generalized Number Theory: Infinite Primes* of [6].
http://tgd.wippiespace.com/public_html/tgdnumber/tgdnumber.html#visionc.
- [28] The chapter *p-Adic Particle Massivation: New Physics* of [4].
http://tgd.wippiespace.com/public_html/paddark/paddark.html#mass4.
- [29] The chapter *TGD and Cosmology* of [3].
http://tgd.wippiespace.com/public_html/tgdclass/tgdclass.html#cosmo.
- [30] The chapter *The Recent Status of Leptohadron Hypothesis* of [4].
http://tgd.wippiespace.com/public_html/paddark/paddark.html#leptc.
- [31] The chapter *TGD and Astrophysics* of [3].
http://tgd.wippiespace.com/public_html/tgdclass/tgdclass.html#astro.
- [32] The chapter *The Relationship Between TGD and GRT* of [3].
http://tgd.wippiespace.com/public_html/tgdclass/tgdclass.html#tgdgrt.
- [33] The chapter *Does the Modified Dirac Equation Define the Fundamental Action Principle?* of [2].
http://tgd.wippiespace.com/public_html/tgdgeom/tgdgeom.html#Dirac.
- [34] The chapter *Massless States and Particle Massivation* of [4].
http://tgd.wippiespace.com/public_html/paddark/paddark.html#mless.
- [35] The chapter *TGD and Nuclear Physics* of [4].
http://tgd.wippiespace.com/public_html/paddark/paddark.html#padnucl.

- [36] The chapter *Construction of Quantum Theory: S-matrix* of [5].
http://tgd.wippiespace.com/public_html/tgdquant/tgdquant.html#towards.
- [37] The chapter *Was von Neumann Right After All* of [5].
http://tgd.wippiespace.com/public_html/tgdquant/tgdquant.html#vNeumann.
- [38] The chapter *Basic Extremals of Kähler Action* of [3].
http://tgd.wippiespace.com/public_html/tgdclass/tgdclass.html#class.
- [39] The chapter *The Notion of Free Energy and Many-Sheeted Space-Time Concept* of [7].
http://tgd.wippiespace.com/public_html/freenergy/freenergy.html#freenergy.
- [40] The chapter *Appendix A: Quantum Groups and Related Structures* of [5].
http://tgd.wippiespace.com/public_html/tgdquant/tgdquant.html#bialgebra.

References to the chapters of the books about TGD Inspired Theory of Consciousness and Quantum Biology

- [41] The chapter *Three new physics realizations of the genetic code and the role of dark matter in bio-systems* of [12].
http://tgd.wippiespace.com/public_html/genememe/genememe.html#dnatqccodes.
- [42] The chapter *Homeopathy in Many-Sheeted Space-Time* of [11].
http://tgd.wippiespace.com/public_html/hologram/hologram.html#homeoc.
- [43] The chapter *Quantum Model for Nerve Pulse* of [15].
http://tgd.wippiespace.com/public_html//tgdeeg/tgdeeg/tgdeeg.html#pulse.
- [44] The chapter *The Notion of Wave-Genome and DNA as Topological Quantum Computer* of [12].
http://tgd.wippiespace.com/public_html/genememe/genememe.html#gari.
- [45] The chapter *Dark Matter Hierarchy and Hierarchy of EEGs* of [15].
http://tgd.wippiespace.com/public_html/tgdeeg/tgdeeg.html#eegdark.
- [46] The chapter *Bio-Systems as Conscious Holograms* of [11].
http://tgd.wippiespace.com/public_html/hologram/hologram.html#hologram.
- [47] The chapter *DNA as Topological Quantum Computer* of [12].
http://tgd.wippiespace.com/public_html/genememe/genememe.html#dnatqc.
- [48] The chapter *Three new physics realizations of the genetic code and the role of dark matter in bio-systems* of [12].
http://tgd.wippiespace.com/public_html/genememe/genememe.html#dnatqccodes.
- [49] The chapter *Macroscopic Quantum Coherence and Quantum Metabolism as Different Sides of the Same Coin* of [11].
http://tgd.wippiespace.com/public_html/hologram/hologram.html#metab.
- [50] The chapter *General Theory of Qualia* of [11].
http://tgd.wippiespace.com/public_html/hologram/hologram.html#qualia.
- [51] The chapter *Macro-Temporal Quantum Coherence and Spin Glass Degeneracy* of [11].
http://tgd.wippiespace.com/public_html/hologram/hologram.html#macro.
- [52] The chapter
em Quantum Model of EEG of [15].
http://tgd.wippiespace.com/public_html/tgdeeg/tgdeeg.html#eegII.
- [53] The chapter *p-Adic Physics as Physics of Cognition and Intention* of [8].
http://tgd.wippiespace.com/public_html/tgdconsc/tgdconsc.html#cognic.

Appendices and references to some older books

- [54] M. Pitkänen (2006) *Basic Properties of CP_2 and Elementary Facts about p -Adic Numbers*
http://tgd.wippiespace.com/public_html/pdfpool/append.pdf.

Articles related to TGD

- [55] M. Pitkänen (2007), *Further Progress in Nuclear String Hypothesis*, http://tgd.wippiespace.com/public_html/articles/nuclstring.pdf.

Mathematics

- [56] D. S. Moak (1981), *The q -analogue of the Laguerre polynomials*. J. Math. Anal. Appl. 81 20 - 47.
- [57] P. A. M. Dirac (1939), *A New Notation for Quantum Mechanics*. Proceedings of the Cambridge Philosophical Society, 35: 416-418.
 J. E. Roberts (1966), *The Dirac Bra and Ket Formalism*. Journal of Mathematical Physics, 7: 1097-1104.
 Halvorson, Hans and Clifton, Rob (2001).

Theoretical physics

Particle and nuclear physics

- [58] C. Rolfs *et al* (2006), *First hints on a change of the ^{22}Na β decay half-life in the metal Pd*, Eur. Phys. J. A 28, 251.
- [59] T. Ludham and L. McLerran (2003), *What Have We Learned From the Relativistic Heavy Ion Collider?*, Physics Today, October issue.
<http://www.physicstoday.org/vol-56/iss-10/p48.html>.
- [60] <http://www.netzone.com/~discpub/>. References to cold fusion anomalies and documents about the anomalies claimed by J. Champion and some other researchers can be found from this homepage.
- [61] E. Storms (1996), *Review of cold fusion effect*.
<http://www.jse.com/storms/1.html>.
 E. Storms (1998), *Cold Fusion Revisited*,
<http://home.netcom.com/~storms2/review5.html>.
- [62] Jed Rothwell(1996).
Some recent developments in cold fusion,
<http://ourworld.compuserve.com/homepages/JedRothwell/brieftec.htm>.
Report on The Second International Low Energy Nuclear Reactions Conference Holiday Inn, College Station, Texas, September 13-14, 1996.
<http://ourworld.compuserve.com/homepages/JedRothwell/ilenrc2s.htm>,
Review of the Sixth International Conference on Cold Fusion (ICCF6),
<http://ourworld.compuserve.com/homepages/JedRothwell/iccf6rev.htm>.
- [63] R. P. Taleyarkhan *et al* (2006), *Nuclear Emissions During Self-Nucleated Acoustic Cavitation*.
<http://adsabs.harvard.edu/abs/2006PhRvL..96c4301T>.
 For material about sono-fusion see <http://members.nuvox.net/~on.jwclymer/snf/>.
- [64] C. Rolfs and W. S. Rodney (1988), *Cauldrons in the Cosmos* (Chicago, IL: University of Chicago Press).

- [65] H. J. Assenbaum, K. Langanke and C. Rolfs (1987), *Z. Phys. A* 327, 461.
- [66] E. Storms (2001), *Cold fusion, an objective assessment*, <http://home.netcom.com/~storms2/review8.html>.
- [67] C. Rolfs *et al* (2006), *High-Z electron screening, the cases $^{50}\text{V}(p,n)^{50}\text{Cr}$ and $^{176}\text{Lu}(p,n)$* , *J. Phys. G: Nuclear. Part Phys.* 32 489. *Eur. Phys. J. A* 28, 251-252.
- [68] P. G. Hansen(1993), *Nuclear structure at the drip lines*, *Nuclear Phys. A*, Vol. 553.
- [69] C. L. Kervran (1972), *Biological Transmutations*. Swan House Publishing Co.
- [70] T. Mizuno *et al* (2002), *Hydrogen Evolution by Plasma Electolysis in Aqueous solution*, *Japanese Journal of Applied Physics*, Vol. 44, No 1A, pp. 396-401.
- [71] D. B. Kaplan, A. E. Nelson and N. Weiner (2004), *Neutrino Oscillations as a Probe of Dark Energy*, hep-ph/0401099.
- [72] C. J. T. de Grotthuss (1806), *Sur la decomposition de l'eau et des corps qu'elle tient en dissolution a l'aide de l'electricite galvanique*. *Ann. Chim.* LVIII (1806), 54-74.

Condensed matter physics

- [73] *Fractional quantum Hall Effect*. http://en.wikipedia.org/wiki/Fractional_quantum_Hall_effect.
Fractional Quantum Hall Effect. <http://www.warwick.ac.uk/~phsbf/fqhe.htm>.
- [74] *Mpemba effect*. http://en.wikipedia.org/wiki/Mpemba_effect.
- [75] Mae-Wan Ho (2009), *Making Fuel from Water*. Institute of Science in Society report. <http://www.i-sis.org.uk/makingFuelFromWater.php>.
- [76] B. R. Barber *et al* (1994), *Phys. Rev. Lett.* , Vol 72 , No 9, p, 1380.
- [77] R. Matthews (1997), *Wacky Water*. *New Scientist* 154 (2087):4043, 21 June.
- [78] J-C. Li and D.K. Ross (1993), *Evidence of Two Kinds of Hydrogen Bonds in Ices*. J-C. Li and D.K. Ross, *Nature*, 365, 327-329.
- [79] *Burning salt water*. <http://www.youtube.com/watch?v=aGgOATfoBgo>.
- [80] P. Ball (2005), *A new kind of alchemy*. *New Scientist*, 16 April issue. <http://www.newscientist.com/channel/fundamentals/mg18624951.800>.
- [81] *Spontaneous burning*. http://www.ncbi.nlm.nih.gov/sites/entrez?cmd=Retrieve&db=PubMed&list_uids=6149513&dopt=AbstractPlus.
- [82] *Tutorials: Lense flare*. <http://www.cambridgeincolour.com/tutorials/lens-flare.htm>.
- [83] M. Dolev, M. Heiblum, V. Umansky, Ady Stern, and D. Mahalu *Nature* (2008), *Observation of a quarter of an electron charge at the $\nu = 5/2$ quantum Hall state*. *Nature*, vol 452, p 829.
- [84] Mae-Wan Ho (2009), *Water electric*. Institute of Science in Society report. <http://www.i-sis.org.uk/WaterElectric.php>.
- [85] *Copper*. <http://en.wikipedia.org/wiki/Copper>.
- [86] *Copper*. <http://en.wikipedia.org/wiki/Copper>.
- [87] W. D. Knight *et al* (1984), *Phys.Rev. Lett.* 52, 2141.
- [88] *Faraday effect*. http://en.wikipedia.org/wiki/Faraday_effect.

- [89] R. A. Cowley (2004), *Neutron-scattering experiments and quantum entanglement*. Physica B 350 (2004) 243-245.
- [90] J. B. Miller *et al*(2007), *Fractional Quantum Hall effect in a quantum point contact at filling fraction 5/2*. arXiv:cond-mat/0703161v2.
- [91] G. Cantatore *et al* (2005), *Experimental observation of optical rotation generated in vacuum by a magnetic field*. arXiv-org hep-exp/0507107.
See also S. Battersby (2006), *Let there be dark*. New Scientist, vol. 191, No 2560, 15 July, 2006.
- [92] J.K. Jain(1989), Phys. Rev. Lett. 63, 199.
- [93] R. Mills *et al*(2003), *Spectroscopic and NMR identification of novel hybrid ions in fractional quantum energy states formed by an exothermic reaction of atomic hydrogen with certain catalysts*. <http://www.blacklightpower.com/techpapers.html> .
- [94] Mae-Wan Ho (2009), *Can Water burn*. Institute of Science in Society report. <http://www.i-sis.org.uk/canWaterBurn.php>.
- [95] R. B. Laughlin (1990), Phys. Rev. Lett. 50, 1395.
- [96] D. Monroe (2008), *Know Your Anyons*. New Scientist, vol 200, No 2676.
- [97] Mae-Wan Ho (2009), *The body does burn water*. Institute of Science in Society report. <http://www.i-sis.org.uk/theBodyDoesBurnWater.php>.
- [98] M. Chaplin (2005), *Water Structure and Behavior*. <http://www.lsbu.ac.uk/water/index.html>.
For 41 anomalies see <http://www.lsbu.ac.uk/water/anmlies.html>.
For the icosahedral clustering see <http://www.lsbu.ac.uk/water/clusters.html>.
- [99] J. K. Borchardt(2003), *The chemical formula H2O - a misnomer*. The Alchemist 8 Aug (2003).
- [100] R. Moreh, R. C. Block, Y. Danon, and M. Neumann (2005), *Search for anomalous scattering of keV neutrons from H2O-D2O mixtures*. Phys. Rev. Lett. 94, 185301.
- [101] Mae-Wan Ho (2009), *Living with Oxygen*. Institute of Science in Society report.<http://www.i-sis.org.uk/livingWithOxygen.php>.
- [102] *Lense flare*. http://en.wikipedia.org/wiki/Lens_flare.
- [103] Zheng, Jian-ming, Pollack, G. (2003), *Long-range forces extending from polymer-gel surfaces*. <http://arxiv.org/abs/cond-mat/0305093>.
- [104] *Camera*.<http://en.wikipedia.org/wiki/Camera>.
Digital camera.http://en.wikipedia.org/wiki/Digital_camera.
Lense. [http://en.wikipedia.org/wiki/Lens_\(optics\)](http://en.wikipedia.org/wiki/Lens_(optics)).
Aberrations. [http://en.wikipedia.org/wiki/Lens_\(optics\)#Aberrations](http://en.wikipedia.org/wiki/Lens_(optics)#Aberrations).
- [105] *Spontaneous human combustion*. <http://www.alternativescience.com/spontaneous-human-combustion-burning-issue.htm>.
- [106] A. W. Castleman *et al* (2005), *Al Cluster Superatoms as Halogens in Polyhalides and as Alkaline Earths in Iodide Salts*. Science, 307, 231-235.

Cosmology and astrophysics

- [107] D. Da Roacha and L. Nottale (2003), *Gravitational Structure Formation in Scale Relativity*. astro-ph/0310036.

Fringe physics

- [108] For the descriptions of Hudson's findings see *Mono-atomic elements*, <http://www.halexandria.org/dward479.htm>, and *David Hudson at IFNS*, <http://www.halexandria.org/dward467.htm>.

Biology related references

- [109] L. Montagnier, J. Aissa, S. Ferris, J.-L. Montagnier, and C. Lavall'e (2009). *Electromagnetic Signals Are Produced by Aqueous Nanostructures Derived from Bacterial DNA Sequences*. Interdiscip. Sci. Comput. Life Sci.. <http://www.springerlink.com/content/0557v31188m3766x/>.
- [110] P. Gariaev *et al* (2000), *The DNA-wave-biocomputer*. CASYS'2000, Fourth International Conference on Computing Anticipatory Systems, Liege, 2000. Abstract Book, Ed. M. Dubois.
- [111] H. R. Chinnery, E. Pearlman, and P. G. McMenamain (2008), *Cutting Edge: Membrane Nanotubes In Vivo: A Feature of MHC Class II+ Cells in the Mouse Cornea*. J. Immunol., May 2008; 180: 5779 - 5783. A. Anantaswamy (2008), *Tunnelling nanotubes: Life's secret network*. <http://www.newscientist.com/article/mg20026821.400-tunnelling-nanotubes-lifes-secret-network.html>. See also <http://matpitka.blogspot.com/2008/11/tunnelling-nanotubes-lifes-secret.html>.
- [112] P. P. Gariaev *et al*(2002), *The spectroscopy of bio-photons in non-local genetic regulation*. Journal of Non-Locality and Remote Mental Interactions, Vol 1, Nr 3. <http://www.emergentmind.org/gariaevI3.htm>.

Chapter 11

Dark Forces and Living Matter

11.1 Introduction

The unavoidable presence of classical long ranged weak (and also color) gauge fields in TGD Universe has been a continual source of worries for more than two decades. The basic question has been whether electro-weak charges of elementary particles are screened in electro-weak length scale or not. The TGD based view about dark matter assumes that weak charges are indeed screened for ordinary matter in electro-weak length scale but that dark electro-weak bosons correspond to much longer symmetry breaking length scale.

The large value of \hbar in dark matter phase implies that Compton lengths and -times are scaled up. In particular, the sizes of nucleons and nuclei become of order atom size so that dark nuclear physics would have direct relevance for condensed matter physics. It becomes impossible to make a reductionistic separation between nuclear physics and condensed matter physics and chemistry anymore. This view forces a profound re-consideration of the earlier ideas in nuclear and condensed physics context. It however seems that most of the earlier ideas related to the classical Z^0 force and inspired by anomaly considerations survive in a modified form.

In its original form this chapter was an attempt to concretize and develop ideas related to dark matter by using some experimental inputs with emphasis on the predicted interaction between the new nuclear physics and condensed matter. As the vision about dark matter became more coherent and the nuclear string model developed in its recent form, it became necessary to update the chapter and throw away the obsolete material. I dare hope that the recent representation is more focused than the earlier one.

11.1.1 Evidence for long range weak forces and new nuclear physics

There is a lot of experimental evidence for long range electro-weak forces, dark matter, and exotic nuclear physics giving valuable guidelines in the attempts to build a coherent theoretical scenario.

Cold fusion

Cold fusion [39] is a phenomenon involving new nuclear physics and the known selection rules give strong constraints when one tries to understand the character of dark nuclear matter. The simplest model for cold fusion found hitherto is based on the nuclear string model [47] and will be taken as the basis of the considerations of this chapter. Also comparisons with the earlier variant of model of cold fusion [23] will be made in the section about cold fusion.

Large parity breaking effects

Large parity breaking effects in living matter indicate the presence of long ranged weak forces, and the reported nuclear transmutations in living matter [40, 41] suggest that new nuclear physics plays a role also now. For instance, the Gaussian Mersennes $(1+i)^k - 1$ for $k = 113, 151, 157163, 167$ could correspond to weak length scales and four biologically important length scales in the range 10 nm-25 μm , which seem to relate directly to the coiling hierarchy of DNA double strands. Quantum criticality

of living matter against phase transitions between different values of Planck constant suggests that zeros of Riemann Zeta can appear as conformal weights of particles in living matter.

Anomalies of the physics of water

The physics of water involves a large number of anomalies and life depends in an essential manner on them. As many as 41 anomalies are discussed in the excellent web page "Water Structure and Behavior" of M. Chaplin [47]. The fact that the physics of heavy water differs much more from that of ordinary water as one might expect on basis of different masses of water molecules suggests that dark nuclear physics is involved.

1. The finding that one hydrogen atom per two water molecules remain effectively invisible in neutron and electron interactions in attosecond time scale [47, 51] suggests that water is partially dark. These findings have been questioned in [49] and thought to be erroneous in [50]. If the findings are real, dark matter phase made of super-nuclei consisting of protons connected by dark color bonds could explain them as perhaps also the clustering of water molecules predicting magic numbers of water molecules in clusters. If so, dark nuclear physics could be an essential part of condensed matter physics and biochemistry. For instance, the condensate of dark protons might be essential for understanding the properties of bio-molecules and even the physical origin of van der Waals radius of atom in van der Waals equation of state.
2. The observation that the binding energy of dark color bond for $n = 2^{11} = 1/v_0$ of the scaling of \hbar corresponds to the bond energy .5 eV of hydrogen bond raises the fascinating possibility that hydrogen bonds is accompanied by a color bond between proton and oxygen nucleus. Also more general chemical bonds might be accompanied by color bonds so that dark color physics might be an essential part of molecular physics. Color bonds might be also responsible for the formation of liquid phase and thus solid state. Dark weak bonds between nuclei could be involved and might be responsible for the repulsive core of van der Waals force and be part of molecular physics too. There is evidence for two kinds of hydrogen bonds [46, 56]: a possible identification is in terms of p-adic scaling of hydrogen bonds by a factor 2. This kind of doubling is predicted by nuclear string model [47].
3. Tetrahedral water clusters consisting of 14 water molecules would contain 8 dark protons which corresponds to a magic number for a dark nucleus consisting of protons. Icosahedral water clusters in turn consist of 20 tetrahedral clusters. This raises the question whether fractally scaled up super-nuclei could be in question. If one accepts the vision about dark matter hierarchy based in Jones inclusions to be discussed briefly later, tetrahedral and icosahedral structures of water could correspond directly to the unique genuinely 3-dimensional $G_a = E_6$ and E_8 coverings of CP_2 with $n_a = 3$ and $n_a = 5$ assignable to dark electrons. Icosahedral structures are also very abundant in living matter, mention only viruses.

Other anomalies

There are also other anomalies which might relate to the hierarchy of Planck constants and also to dark weak forces.

1. Exotic chemistries

Exotic chemistries [52] in which clusters of atoms of given given type mimic the chemistry of another element. These systems behave as if nuclei would form a jellium (constant charge density) defining a harmonic oscillator potential for electrons. Magic numbers correspond to full electron shells analogous to noble gas elements. It is difficult to understand why the constant charge density approximation works so well. If nuclear protons are in large $\hbar(M^4)$ phase with $n_F = 3 \times 2^{11}$, the electromagnetic sizes of nuclei would be about 2.4 Angstroms and the approximation would be natural.

As a matter, fact nuclear string model predicts that the nuclei can have as many as $3A$ exotic charge states obtained by giving neutral color bond charge ± 1 : this would give rise to quite different kind of alchemy [47] revealing itself in cold fusion.

2. Free energy anomalies

The anomalies reported by free energy researchers such as over unity energy production in devices involving repeated formation and dissociation of H_2 molecules based on the original discovery of Nobelist Irwing Langmuir [55] (see for instance [60]) suggest that part of H atoms might end up to dark matter phase liberating additional energy. The "mono-atomic" elements of Hudson suggest also dark nuclear physics [57]. There is even evidence for macroscopic transitions to dark phase [61, 59, 58].

3. Tritium beta decay anomaly and findings of Shnoll

Tritium beta decay anomaly [44, 66, 51, 56] suggests exotic nuclear physics related to weak interactions. The evidence for the variation of the rates of nuclear and chemical processes correlating with astrophysical periods [42] could be understood in terms of weak fields created by dark matter and affect by astrophysical phenomena.

11.1.2 Dark rules

I have done a considerable amount of trials and errors in order to identify the basic rules allowing to understand what it means to be dark matter is and what happens in the phase transition to dark matter. It is good to try to summarize the basic rules of p-adic and dark physics allowing to avoid obvious contradictions.

The notion of field body

The notion of "field body" implied by topological field quantization is essential. There would be em, Z^0 , W , gluonic, and gravitonic field bodies, each characterized by its one prime. The motivation for considering the possibility of separate field bodies seriously is that the notion of induced gauge field means that all induced gauge fields are expressible in terms of four CP_2 coordinates so that only single component of a gauge potential allows a representation as an independent field quantity. Perhaps also separate magnetic and electric field bodies for each interaction and identifiable as flux quanta must be considered. This kind of separation requires that the fermionic content of the flux quantum (say fermion and anti-fermion at the ends of color flux tube) is such that it conforms with the quantum numbers of the corresponding boson.

What is interesting that the conceptual separation of interactions to various types would have a direct correlate at the level of space-time topology. From a different perspective inspired by the general vision that many-sheeted space-time provides symbolic representations of quantum physics, the very fact that we make this conceptual separation of fundamental interactions could reflect the topological separation at space-time level.

The p-adic mass calculations for quarks encourage to think that the p-adic length scale characterizing the mass of particle is associated with its electromagnetic body and in the case of neutrinos with its Z^0 body. Z^0 body can contribute also to the mass of charged particles but the contribution would be small. It is also possible that these field bodies are purely magnetic for color and weak interactions. Color flux tubes would have exotic fermion and anti-fermion at their ends and define colored variants of pions. This would apply not only in the case of nuclear strings but also to molecules and larger structures so that scaled variants of elementary particles and standard model would appear in all length scales as indeed implied by the fact that classical electro-weak and color fields are unavoidable in TGD framework.

One can also go further and distinguish between magnetic field body of free particle for which flux quanta start and return to the particle and "relative field" bodies associated with pairs of particles. Very complex structures emerge and should be essential for the understanding the space-time correlates of various interactions. In a well-defined sense they would define space-time correlate for the conceptual analysis of the interactions into separate parts. In order to minimize confusion it should be emphasized that the notion of field body used in this chapter relates to those space-time correlates of interactions, which are more or less *static* and related to the formation of *bound states*.

What dark variant of elementary particle means

It is not at all clear what the notion of dark variant of elementary particle or of larger structures could mean.

1. Are only field bodies dark?

One variety of dark particle is obtained by making some of the field bodies dark by increasing the value of Planck constant. This hypothesis could be replaced with the stronger assumption that elementary particles are maximally quantum critical systems so that they are same irrespective of the value of the Planck constant. Elementary particles would be represented by partonic 2-surfaces, which belong to the universal orbifold singularities remaining invariant by all groups $G_a \times G_b$ for a given choice of quantization axes. If $G_a \times G_b$ is assumed to leave invariant the choice of the quantization axes, it must be of the form $Z_{n_a} \times Z_{n_b} \subset SO(3) \times SU(3)$. Partonic 2-surface would belong to $M^2 \times CP_2/U(1) \times U(1)$, where M^2 is spanned by the quantization axis of angular momentum and the time axis defining the rest system.

A different manner to say this is that the CP_2 type extremal representing particle would suffer multiple topological condensation on its field bodies so that there would be no separate "particle space-time sheet".

Darkness would be restricted to particle interactions. The value of the Planck constant would be assigned to a particular interaction between systems rather than system itself. This conforms with the original finding that gravitational Planck constant satisfies $\hbar = GM_1M_2/v_0$, $v_0 \simeq 2^{-11}$. Since each interaction can give rise to a hierarchy dark phases, a rich variety of partially dark phases is predicted. The standard assumption that dark matter is visible only via gravitational interactions would mean that gravitational field body would not be dark for this particular dark matter.

Complex combinations of dark field bodies become possible and the dream is that one could understand various phases of matter in terms of these combinations. All phase transitions, including the familiar liquid-gas and solid-liquid phase transitions, could have a unified description in terms of dark phase transition for an appropriate field body. At mathematical level Jones inclusions would provide this description.

The book metaphor for the interactions at space-time level is very useful in this framework. Elementary particles correspond to ordinary value of Planck constant analogous to the ordinary sheets of a book and the field bodies mediating their interactions are the same space-time sheet or at dark sheets of the book.

2. Can also elementary particles be dark?

Also dark elementary particles themselves rather than only the flux quanta could correspond to dark space-time sheet defining multiple coverings of $H/G_a \times G_b$. This would mean giving up the maximal quantum criticality hypothesis in the case of elementary particles. These sheets would be exact copies of each other. If single sheet of the covering contains topologically condensed space-time sheet, also other sheets contain its exact copy.

The question is whether these copies of space-time sheet defining classical identical systems can carry different fermionic quantum numbers or only identical fermionic quantum numbers so that the dark particle would be exotic many-fermion system allowing an apparent violation of statistics (N fermions in the same state).

Even if one allows varying number of fermions in the same state with respect to a basic copy of sheet, one ends up with the notion of N -atom in which nuclei would be ordinary but electrons would reside at the sheets of the covering. The question is whether symbolic representations essential for understanding of living matter could emerge already at molecular level via the formation of N -atoms.

Criterion for the transition to dark phase

The criterion $\alpha Q_1 Q_2 > 1$ for the transition to dark matter phase relates always to the interaction between two systems and the interpretation is that when the field strength characterizing the interaction becomes too strong, the interaction is mediated by dark space-time sheets which define $n = n(G_a) \times n(G_b)$ -fold covering of $M^4 \times CP_2/G_a \times G_b$. The sharing of flux between different space-time sheets reduces the field strength associated with single sheet below the critical value.

Mersenne hypothesis

The generalization of the imbedding space means a book like structure for which the pages are products of singular coverings or factor spaces of CD (causal diamond defined as intersection of future and past directed light-cones) and of CP_2 [39]. This predicts that Planck constants are rationals and that given value of Planck constant corresponds to an infinite number of different pages of the Big Book,

which might be seen as a drawback. If only singular covering spaces are allowed the values of Planck constant are products of integers and given value of Planck constant corresponds to a finite number of pages given by the number of decompositions of the integer to two different integers.

TGD inspired quantum biology and number theoretical considerations suggest preferred values for $r = \hbar/\hbar_0$. For the most general option the values of \hbar are products and ratios of two integers n_a and n_b . Ruler and compass integers defined by the products of distinct Fermat primes and power of two are number theoretically favored values for these integers because the phases $\exp(i2\pi/n_i)$, $i \in \{a, b\}$, in this case are number theoretically very simple and should have emerged first in the number theoretical evolution via algebraic extensions of p-adics and of rationals. p-Adic length scale hypothesis favors powers of two as values of r .

One can however ask whether a more precise characterization of preferred Mersennes could exist and whether there could exist a stronger correlation between hierarchies of p-adic length scales and Planck constants. Mersenne primes $M_k = 2^k - 1$, $k \in \{89, 107, 127\}$, and Gaussian Mersennes $M_{G,k} = (1 + i)k - 1$, $k \in \{113, 151, 157, 163, 167, 239, 241, \dots\}$ are expected to be physically highly interesting and up to $k = 127$ indeed correspond to elementary particles. The number theoretical miracle is that all the four p-adic length scales with $k \in \{151, 157, 163, 167\}$ are in the biologically highly interesting range 10 nm-2.5 μ m). The question has been whether these define scaled up copies of electro-weak and QCD type physics with ordinary value of \hbar . The proposal that this is the case and that these physics are in a well-defined sense induced by the dark scaled up variants of corresponding lower level physics leads to a prediction for the preferred values of $r = 2^{k_d}$, $k_d = k_i - k_j$.

What induction means is that dark variant of exotic nuclear physics induces exotic physics with ordinary value of Planck constant in the new scale in a resonant manner: dark gauge bosons transform to their ordinary variants with the same Compton length. This transformation is natural since in length scales below the Compton length the gauge bosons behave as massless and free particles. As a consequence, lighter variants of weak bosons emerge and QCD confinement scale becomes longer.

This proposal will be referred to as Mersenne hypothesis. It leads to strong predictions about EEG [43] since it predicts a spectrum of preferred Josephson frequencies for a given value of membrane potential and also assigns to a given value of \hbar a fixed size scale having interpretation as the size scale of the body part or magnetic body. Also a vision about evolution of life emerges. Mersenne hypothesis is especially interesting as far as new physics in condensed matter length scales is considered: this includes exotic scaled up variants of the ordinary nuclear physics and their dark variants. Even dark nucleons are possible and this gives justification for the model of dark nucleons predicting the counterparts of DNA, RNA, tRNA, and aminoacids as well as realization of vertebrate genetic code [48].

These exotic nuclear physics with ordinary value of Planck constant could correspond to ground states that are almost vacuum extremals corresponding to homologically trivial geodesic sphere of CP_2 near criticality to a phase transition changing Planck constant. Ordinary nuclear physics would correspond to homologically non-trivial geodesic sphere and far from vacuum extremal property. For vacuum extremals of this kind classical Z^0 field proportional to electromagnetic field is present and this modifies dramatically the view about cell membrane as Josephson junction. The model for cell membrane as almost vacuum extremal indeed led to a quantitative breakthrough in TGD inspired model of EEG and is therefore something to be taken seriously. The safest option concerning empirical facts is that the copies of electro-weak and color physics with ordinary value of Planck constant are possible only for almost vacuum extremals - that is at criticality against phase transition changing Planck constant.

11.1.3 Weak form of electric magnetic duality, screening of weak charges, and color confinement?

TGD predicts the presence of long range classical weak fields and color fields and one should understand classically why quarks and leptons do not couple to these fields above weak boson length scale. Why the quarks inside ordinary nuclei do not generate long range weak fields and do not couple to them? Obviously the weak charges of quarks must be screened so that only electromagnetic charge remains. The extreme non-linearity of field equations in principle allows non-vanishing vacuum charge densities making possible this kind of screening. I have not been able to develop any detailed model for this.

A rather attractive looking explanation came with the discovery of electric-magnetic duality leading to a considerable progress in the understanding of basic quantum TGD. The basic implication of the

duality is that Kähler electric charges of wormhole throats representing particles are proportional to Kähler magnetic charges so that the CP_2 projections of the wormhole throats are homologically non-trivial. The Kähler magnetic charges do not create long range monopole fields if they are neutralized by wormhole throats carrying opposite monopole charges and weak isospin neutralizing the axial isospin of the particle's wormhole throat. One could speak of confinement of weak isospin. The weak field bodies of elementary fermions would be replaced with string like objects with a length of order W boson Compton length. Electro-magnetic flux would be feeded to electromagnetic field body where it would be feeded to larger space-time sheets. Similar mechanism could apply in the case of color quantum numbers.

One of the basic questions closely related to the weak screening have been whether it is possible to have a weak analog of the ordinary atom - say neutrino atom. Formally one can of course construct this kind of model and I have indeed done this. The recent view about the screening of weak forces does not however allow neutrino atoms since the weak gauge fluxes flow along flux tubes and are screened by opposite charges at their end rather than being spherically symmetric Coulomb fields. Elementary particles themselves can be regarded as string like objects neutralized above weak boson Compton length. The size of the magnetic flux tubes however scales as $\sqrt{\hbar}$ so that large values of \hbar it is in principle possible to zoom up the elementary particles and see what their interior looks like. This applies to both weak and color forces and might some day make possible study of elementary particles without gigantic accelerators.

11.1.4 Dark weak forces and almost vacuum extremals

TGD suggests strongly the presence of long range weak force and the large parity breaking in living matter realized as chiral selection provides support for it. One would however like some more concrete quantitative evidence for the conjecture that the classical weak forces are indeed there. This kind of evidence comes from the model of cell membrane based on the hypothesis that cell membrane correspond to almost vacuum extremal.

1. Induced Kähler form vanishes for vacuum extremals. The condition for vanishing implies that classical Z^0 and electromagnetic fields are proportional to each other so that induced spinor field couples to both these fields. The assumption is that the quarks of nuclei and possibly also neutrinos correspond to a large value of Planck constant and therefore couple to the classical Z^0 field. Atomic electrons would not have these couplings. This modifies dramatically the model for the cell membrane as a Josephson junction and raises the scale of Josephson energies from IR range just above thermal threshold to visible and ultraviolet. The amazing finding is that the Josephson energies for biologically important ions correspond to the energies assigned to the peak frequencies in the biological activity spectrum of photoreceptors in retina suggesting. This suggests that almost vacuum extremals and thus also classical Z^0 fields are in a central role in the understanding of the functioning of the cell membrane and of sensory qualia. This would also explain the large parity breaking effects in living matter.
2. A further conjecture is that EEG and its predicted fractally scaled variants which same energies in visible and UV range but different scales of Josephson frequencies correspond to Josephson photons with various values of Planck constant. The decay of dark ELF photons with energies of visible photons would give rise to bunches of ordinary ELF photons. Biophotons in turn could correspond to ordinary visible photons resulting in the phase transition of these photons to photons with ordinary value of Planck constant. This leads to a very detailed view about the role of dark electromagnetic radiation in biomatter and also to a model for how sensory qualia are realized [33, 27, 43].

What darkness means in the case of nuclei is that the "weak" field bodies of quarks are dark so that the size scale assignable to them is of order cell size. This does not affect their electromagnetic field bodies so that it is possible to speak about ions in the ordinary sense of the word. If the size scale of a given part of field body corresponds to the Compton length proportional to the p-adic length scale scaled up by $\sqrt{\hbar}$ then cell membrane thickness as a Compton scale for the field body of weak bosons means rather large value of $\hbar \sim 2^{151-89} = 2^{62}\hbar_0$. This would scale down 10^{14} Hz frequency of visible photons to about 10^{-4} Hz

11.2 Weak form electric-magnetic duality and color and weak forces

The notion of electric-magnetic duality [65] was proposed first by Olive and Montonen and is central in $\mathcal{N} = 4$ supersymmetric gauge theories. It states that magnetic monopoles and ordinary particles are two different phases of theory and that the description in terms of monopoles can be applied at the limit when the running gauge coupling constant becomes very large and perturbation theory fails to converge. The notion of electric-magnetic self-duality is more natural since for CP_2 geometry Kähler form is self-dual and Kähler magnetic monopoles are also Kähler electric monopoles and Kähler coupling strength is by quantum criticality renormalization group invariant rather than running coupling constant. The notion of electric-magnetic (self-)duality emerged already two decades ago in the attempts to formulate the Kähler geometric of world of classical worlds. Quite recently a considerable step of progress took place in the understanding of this notion [22]. What seems to be essential is that one adopts a weaker form of the self-duality applying at partonic 2-surfaces. What this means will be discussed in the sequel.

Every new idea must be of course taken with a grain of salt but the good sign is that this concept leads to precise predictions. The point is that elementary particles do not generate monopole fields in macroscopic length scales: at least when one considers visible matter. The first question is whether elementary particles could have vanishing magnetic charges: this turns out to be impossible. The next question is how the screening of the magnetic charges could take place and leads to an identification of the physical particles as string like objects identified as pairs magnetic charged wormhole throats connected by magnetic flux tubes.

1. The first implication is a new view about electro-weak massivation reducing it to weak confinement in TGD framework. The second end of the string contains particle having electroweak isospin neutralizing that of elementary fermion and the size scale of the string is electro-weak scale would be in question. Hence the screening of electro-weak force takes place via weak confinement realized in terms of magnetic confinement.
2. This picture generalizes to the case of color confinement. Also quarks correspond to pairs of magnetic monopoles but the charges need not vanish now. Rather, valence quarks would be connected by flux tubes of length of order hadron size such that magnetic charges sum up to zero. For instance, for baryonic valence quarks these charges could be $(2, -1, -1)$ and could be proportional to color hyper charge.
3. The highly non-trivial prediction making more precise the earlier stringy vision is that elementary particles are string like objects in electro-weak scale: this should become manifest at LHC energies.
4. The weak form electric-magnetic duality together with Beltrami flow property of Kähler leads to the reduction of Kähler action to Chern-Simons action so that TGD reduces to almost topological QFT and that Kähler function is explicitly calculable. This has enormous impact concerning practical calculability of the theory.
5. One ends up also to a general solution ansatz for field equations from the condition that the theory reduces to almost topological QFT. The solution ansatz is inspired by the idea that all isometry currents are proportional to Kähler current which is integrable in the sense that the flow parameter associated with its flow lines defines a global coordinate. The proposed solution ansatz would describe a hydrodynamical flow with the property that isometry charges are conserved along the flow lines (Beltrami flow). A general ansatz satisfying the integrability conditions is found. The solution ansatz applies also to the extremals of Chern-Simons action and to the conserved currents associated with the modified Dirac equation defined as contractions of the modified gamma matrices between the solutions of the modified Dirac equation. The strongest form of the solution ansatz states that various classical and quantum currents flow along flow lines of the Beltrami flow defined by Kähler current (Kähler magnetic field associated with Chern-Simons action). Intuitively this picture is attractive. A more general ansatz would allow several Beltrami flows meaning multi-hydrodynamics. The integrability conditions boil down to two scalar functions: the first one satisfies massless d'Alembert equation in the induced

metric and the the gradients of the scalar functions are orthogonal. The interpretation in terms of momentum and polarization directions is natural.

6. The general solution ansatz works for induced Kähler Dirac equation and Chern-Simons Dirac equation and reduces them to ordinary differential equations along flow lines. The induced spinor fields are simply constant along flow lines of induced spinor field for Dirac equation in suitable gauge. Also the generalized eigen modes of the modified Chern-Simons Dirac operator can be deduced explicitly if the throats and the ends of space-time surface at the boundaries of CD are extremals of Chern-Simons action. Chern-Simons Dirac equation reduces to ordinary differential equations along flow lines and one can deduce the general form of the spectrum and the explicit representation of the Dirac determinant in terms of geometric quantities characterizing the 3-surface (eigenvalues are inversely proportional to the lengths of strands of the flow lines in the effective metric defined by the modified gamma matrices).

11.2.1 Could a weak form of electric-magnetic duality hold true?

Holography means that the initial data at the partonic 2-surfaces should fix the configuration space metric. A weak form of this condition allows only the partonic 2-surfaces defined by the wormhole throats at which the signature of the induced metric changes. A stronger condition allows all partonic 2-surfaces in the slicing of space-time sheet to partonic 2-surfaces and string world sheets. Number theoretical vision suggests that hyper-quaternionicity *resp.* co-hyperquaternionicity constraint could be enough to fix the initial values of time derivatives of the imbedding space coordinates in the space-time regions with Minkowskian *resp.* Euclidian signature of the induced metric. This is a condition on modified gamma matrices and hyper-quaternionicity states that they span a hyper-quaternionic sub-space.

Definition of the weak form of electric-magnetic duality

One can also consider alternative conditions possibly equivalent with this condition. The argument goes as follows.

1. The expression of the matrix elements of the metric and Kähler form of WCW in terms of the Kähler fluxes weighted by Hamiltonians of δM_{\pm}^4 at the partonic 2-surface X^2 looks very attractive. These expressions however carry no information about the 4-D tangent space of the partonic 2-surfaces so that the theory would reduce to a genuinely 2-dimensional theory, which cannot hold true. One would like to code to the WCW metric also information about the electric part of the induced Kähler form assignable to the complement of the tangent space of $X^2 \subset X^4$.
2. Electric-magnetic duality of the theory looks a highly attractive symmetry. The trivial manner to get electric magnetic duality at the level of the full theory would be via the identification of the flux Hamiltonians as sums of of the magnetic and electric fluxes. The presence of the induced metric is however troublesome since the presence of the induced metric means that the simple transformation properties of flux Hamiltonians under symplectic transformations -in particular color rotations- are lost.
3. A less trivial formulation of electric-magnetic duality would be as an initial condition which eliminates the induced metric from the electric flux. In the Euclidian version of 4-D YM theory this duality allows to solve field equations exactly in terms of instantons. This approach involves also quaternions. These arguments suggest that the duality in some form might work. The full electric magnetic duality is certainly too strong and implies that space-time surface at the partonic 2-surface corresponds to piece of CP_2 type vacuum extremal and can hold only in the deep interior of the region with Euclidian signature. In the region surrounding wormhole throat at both sides the condition must be replaced with a weaker condition.
4. To formulate a weaker form of the condition let us introduce coordinates (x^0, x^3, x^1, x^2) such (x^1, x^2) define coordinates for the partonic 2-surface and (x^0, x^3) define coordinates labeling partonic 2-surfaces in the slicing of the space-time surface by partonic 2-surfaces and string world sheets making sense in the regions of space-time sheet with Minkowskian signature. The assumption about the slicing allows to preserve general coordinate invariance. The weakest

condition is that the generalized Kähler electric fluxes are apart from constant proportional to Kähler magnetic fluxes. This requires the condition

$$J^{03}\sqrt{g_4} = K J_{12} . \quad (11.2.1)$$

A more general form of this duality is suggested by the considerations of [37] reducing the hierarchy of Planck constants to basic quantum TGD and also reducing Kähler function for preferred extremals to Chern-Simons terms [63] at the boundaries of CD and at light-like wormhole throats. This form is following

$$J^{n\beta}\sqrt{g_4} = K\epsilon \times \epsilon^{n\beta\gamma\delta} J_{\gamma\delta}\sqrt{g_4} . \quad (11.2.2)$$

Here the index n refers to a normal coordinate for the space-like 3-surface at either boundary of CD or for light-like wormhole throat. ϵ is a sign factor which is opposite for the two ends of CD . It could be also opposite of opposite at the opposite sides of the wormhole throat. Note that the dependence on induced metric disappears at the right hand side and this condition eliminates the potentials singularity due to the reduction of the rank of the induced metric at wormhole throat.

5. Information about the tangent space of the space-time surface can be coded to the configuration space metric with loosing the nice transformation properties of the magnetic flux Hamiltonians if Kähler electric fluxes or sum of magnetic flux and electric flux satisfying this condition are used and K is symplectic invariant. Using the sum

$$J_e + J_m = (1 + K)J , \quad (11.2.3)$$

where J can denotes the Kähler magnetic flux, makes it possible to have a non-trivial configuration space metric even for $K = 0$, which could correspond to the ends of a cosmic string like solution carrying only Kähler magnetic fields. This condition suggests that it can depend only on Kähler magnetic flux and other symplectic invariants. Whether local symplectic coordinate invariants are possible at all is far from obvious, If the slicing itself is symplectic invariant then K could be a non-constant function of X^2 depending on string world sheet coordinates. The light-like radial coordinate of the light-cone boundary indeed defines a symplectically invariant slicing and this slicing could be shifted along the time axis defined by the tips of CD .

Electric-magnetic duality physically

What could the weak duality condition mean physically? For instance, what constraints are obtained if one assumes that the quantization of electro-weak charges reduces to this condition at classical level?

1. The first thing to notice is that the flux of J over the partonic 2-surface is analogous to magnetic flux

$$Q_m = \frac{e}{\hbar} \oint B dS = n .$$

n is non-vanishing only if the surface is homologically non-trivial and gives the homology charge of the partonic 2-surface.

2. The expressions of classical electromagnetic and Z^0 fields in terms of Kähler form [46] read as

$$\begin{aligned}\gamma &= \frac{eF_{em}}{\hbar} = 3J - \sin^2(\theta_W)R_{03} \ , \\ Z^0 &= \frac{g_Z F_Z}{\hbar} = 2R_{03} \ .\end{aligned}\tag{11.2.3}$$

Here R_{03} is one of the components of the curvature tensor in vielbein representation and F_{em} and F_Z correspond to the standard field tensors. From this expression one can deduce

$$J = \frac{e}{3\hbar}F_{em} + \sin^2(\theta_W)\frac{g_Z}{6\hbar}F_Z \ .\tag{11.2.4}$$

3. The weak duality condition when integrated over X^2 implies

$$\begin{aligned}\frac{e^2}{3\hbar}Q_{em} + \frac{g_Z^2 p}{6}Q_{Z,V} &= K \oint J = Kn \ , \\ Q_{Z,V} &= \frac{I_V^3}{2} - Q_{em} \ , \ p = \sin^2(\theta_W) \ .\end{aligned}\tag{11.2.4}$$

Here the vectorial part of the Z^0 charge rather than as full Z^0 charge $Q_Z = I_L^3 + \sin^2(\theta_W)Q_{em}$ appears. The reason is that only the vectorial isospin is same for left and right handed components of fermion which are in general mixed for the massive states.

The coefficients are dimensionless and expressible in terms of the gauge coupling strengths and using $\hbar = r\hbar_0$ one can write

$$\begin{aligned}\alpha_{em}Q_{em} + p\frac{\alpha_Z}{2}Q_{Z,V} &= \frac{3}{4\pi} \times rnK \ , \\ \alpha_{em} &= \frac{e^2}{4\pi\hbar_0} \ , \ \alpha_Z = \frac{g_Z^2}{4\pi\hbar_0} = \frac{\alpha_{em}}{p(1-p)} \ .\end{aligned}\tag{11.2.4}$$

4. There is a great temptation to assume that the values of Q_{em} and Q_Z correspond to their quantized values and therefore depend on the quantum state assigned to the partonic 2-surface. The linear coupling of the modified Dirac operator to conserved charges implies correlation between the geometry of space-time sheet and quantum numbers assigned to the partonic 2-surface. The assumption of standard quantized values for Q_{em} and Q_Z would be also seen as the identification of the fine structure constants α_{em} and α_Z . This however requires weak isospin invariance.

The value of K from classical quantization of Kähler electric charge

The value of K can be deduced by requiring classical quantization of Kähler electric charge.

1. The condition that the flux of $F^{03} = (\hbar/g_K)J^{03}$ defining the counterpart of Kähler electric field equals to the Kähler charge g_K would give the condition $K = g_K^2/\hbar$, where g_K is Kähler coupling constant which should invariant under coupling constant evolution by quantum criticality. Within experimental uncertainties one has $\alpha_K = g_K^2/4\pi\hbar_0 = \alpha_{em} \simeq 1/137$, where α_{em} is finite structure constant in electron length scale and \hbar_0 is the standard value of Planck constant.

2. The quantization of Planck constants makes the condition highly non-trivial. The most general quantization of r is as rationals but there are good arguments favoring the quantization as integers corresponding to the allowance of only singular coverings of CD and CP_2 . The point is that in this case a given value of Planck constant corresponds to a finite number pages of the "Big Book". The quantization of the Planck constant implies a further quantization of K and would suggest that K scales as $1/r$ unless the spectrum of values of Q_{em} and Q_Z allowed by the quantization condition scales as r . This is quite possible and the interpretation would be that each of the r sheets of the covering carries (possibly same) elementary charge. Kind of discrete variant of a full Fermi sphere would be in question. The interpretation in terms of anyonic phases [24] supports this interpretation.
3. The identification of J as a counterpart of eB/\hbar means that Kähler action and thus also Kähler function is proportional to $1/\alpha_K$ and therefore to \hbar . This implies that for large values of \hbar Kähler coupling strength $g_K^2/4\pi$ becomes very small and large fluctuations are suppressed in the functional integral. The basic motivation for introducing the hierarchy of Planck constants was indeed that the scaling $\alpha \rightarrow \alpha/r$ allows to achieve the convergence of perturbation theory: Nature itself would solve the problems of the theoretician. This of course does not mean that the physical states would remain as such and the replacement of single particles with anyonic states in order to satisfy the condition for K would realize this concretely.

The weak form of electric-magnetic duality has surprisingly strong implications for basic view about quantum TGD as following considerations show.

11.2.2 Magnetic confinement, the short range of weak forces, and color confinement

The weak form of electric-magnetic duality has surprisingly strong implications if one combines it with some very general empirical facts such as the non-existence of magnetic monopole fields in macroscopic length scales.

How can one avoid macroscopic magnetic monopole fields?

Monopole fields are experimentally absent in length scales above order weak boson length scale and one should have a mechanism neutralizing the monopole charge. How electroweak interactions become short ranged in TGD framework is still a poorly understood problem. What suggests itself is the neutralization of the weak isospin above the intermediate gauge boson Compton length by neutral Higgs bosons. Could the two neutralization mechanisms be combined to single one?

1. In the case of fermions and their super partners the opposite magnetic monopole would be a wormhole throat. If the magnetically charged wormhole contact is electromagnetically neutral but has vectorial weak isospin neutralizing the weak vectorial isospin of the fermion only the electromagnetic charge of the fermion is visible on longer length scales. The distance of this wormhole throat from the fermionic one should be of the order weak boson Compton length. An interpretation as a bound state of fermion and a wormhole throat state with the quantum numbers of a neutral Higgs boson would therefore make sense. The neutralizing throat would have quantum numbers of $X_{-1/2} = \nu_L \bar{\nu}_R$ or $X_{1/2} = \bar{\nu}_L \nu_R$. $\nu_L \bar{\nu}_R$ would not be neutral Higgs boson (which should correspond to a wormhole contact) but a super-partner of left-handed neutrino obtained by adding a right handed neutrino. This mechanism would apply separately to the fermionic and anti-fermionic throats of the gauge bosons and corresponding space-time sheets and leave only electromagnetic interaction as a long ranged interaction.
2. One can of course wonder what is the situation situation for the bosonic wormhole throats feeding gauge fluxes between space-time sheets. It would seem that these wormhole throats must always appear as pairs such that for the second member of the pair monopole charges and I_V^3 cancel each other at both space-time sheets involved so that one obtains at both space-time sheets magnetic dipoles of size of weak boson Compton length. The proposed magnetic character of fundamental particles should become visible at TeV energies so that LHC might have surprises in store!

Magnetic confinement and color confinement

Magnetic confinement generalizes also to the case of color interactions. One can consider also the situation in which the magnetic charges of quarks (more generally, of color excited leptons and quarks) do not vanish and they form color and magnetic singlets in the hadronic length scale. This would mean that magnetic charges of the state $q_{\pm 1/2} - X_{\mp 1/2}$ representing the physical quark would not vanish and magnetic confinement would accompany also color confinement. This would explain why free quarks are not observed. To how degree then quark confinement corresponds to magnetic confinement is an interesting question.

For quark and antiquark of meson the magnetic charges of quark and antiquark would be opposite and meson would correspond to a Kähler magnetic flux so that a stringy view about meson emerges. For valence quarks of baryon the vanishing of the net magnetic charge takes place provided that the magnetic net charges are $(\pm 2, \mp 1, \mp 1)$. This brings in mind the spectrum of color hyper charges coming as $(\pm 2, \mp 1, \mp 1)/3$ and one can indeed ask whether color hyper-charge correlates with the Kähler magnetic charge. The geometric picture would be three strings connected to single vertex. Amusingly, the idea that color hypercharge could be proportional to color hyper charge popped up during the first year of TGD when I had not yet discovered CP_2 and believed on $M^4 \times S^2$.

p-Adic length scale hypothesis and hierarchy of Planck constants defining a hierarchy of dark variants of particles suggest the existence of scaled up copies of QCD type physics and weak physics. For p-adically scaled up variants the mass scales would be scaled by a power of $\sqrt{2}$ in the most general case. The dark variants of the particle would have the same mass as the original one. In particular, Mersenne primes $M_k = 2^k - 1$ and Gaussian Mersennes $M_{G,k} = (1 + i)^k - 1$ has been proposed to define zoomed copies of these physics. At the level of magnetic confinement this would mean hierarchy of length scales for the magnetic confinement.

One particular proposal is that the Mersenne prime M_{89} should define a scaled up variant of the ordinary hadron physics with mass scaled up roughly by a factor $2^{(107-89)/2} = 512$. The size scale of color confinement for this physics would be same as the weak length scale. It would look more natural that the weak confinement for the quarks of M_{89} physics takes place in some shorter scale and M_{61} is the first Mersenne prime to be considered. The mass scale of M_{61} weak bosons would be by a factor $2^{(89-61)/2} = 2^{14}$ higher and about 1.6×10^4 TeV. M_{89} quarks would have virtually no weak interactions but would possess color interactions with weak confinement length scale reflecting themselves as new kind of jets at collisions above TeV energies.

In the biologically especially important length scale range 10 nm -2500 nm there are as many as four Gaussian Mersennes corresponding to $M_{G,k}$, $k = 151, 157, 163, 167$. This would suggest that the existence of scaled up scales of magnetic-, weak- and color confinement. An especially interesting possibly testable prediction is the existence of magnetic monopole pairs with the size scale in this range. There are recent claims about experimental evidence for magnetic monopole pairs [77].

Magnetic confinement and stringy picture in TGD sense

The connection between magnetic confinement and weak confinement is rather natural if one recalls that electric-magnetic duality in super-symmetric quantum field theories means that the descriptions in terms of particles and monopoles are in some sense dual descriptions. Fermions would be replaced by string like objects defined by the magnetic flux tubes and bosons as pairs of wormhole contacts would correspond to pairs of the flux tubes. Therefore the sharp distinction between gravitons and physical particles would disappear.

The reason why gravitons are necessarily stringy objects formed by a pair of wormhole contacts is that one cannot construct spin two objects using only single fermion states at wormhole throats. Of course, also super partners of these states with higher spin obtained by adding fermions and anti-fermions at the wormhole throat but these do not give rise to graviton like states [23]. The upper and lower wormhole throat pairs would be quantum superpositions of fermion anti-fermion pairs with sum over all fermions. The reason is that otherwise one cannot realize graviton emission in terms of joining of the ends of light-like 3-surfaces together. Also now magnetic monopole charges are necessary but now there is no need to assign the entities X_{\pm} with gravitons.

Graviton string is characterized by some p-adic length scale and one can argue that below this length scale the charges of the fermions become visible. Mersenne hypothesis suggests that some Mersenne prime is in question. One proposal is that gravitonic size scale is given by electronic

Mersenne prime M_{127} . It is however difficult to test whether graviton has a structure visible below this length scale.

What happens to the generalized Feynman diagrams is an interesting question. It is not at all clear how closely they relate to ordinary Feynman diagrams. All depends on what one is ready to assume about what happens in the vertices. One could of course hope that zero energy ontology could allow some very simple description allowing perhaps to get rid of the problematic aspects of Feynman diagrams.

1. Consider first the recent view about generalized Feynman diagrams which relies zero energy ontology. A highly attractive assumption is that the particles appearing at wormhole throats are on mass shell particles. For incoming and outgoing elementary bosons and their super partners they would be positive it resp. negative energy states with parallel on mass shell momenta. For virtual bosons they the wormhole throats would have opposite sign of energy and the sum of on mass shell states would give virtual net momenta. This would make possible twistor description of virtual particles allowing only massless particles (in 4-D sense usually and in 8-D sense in TGD framework). The notion of virtual fermion makes sense only if one assumes in the interaction region a topological condensation creating another wormhole throat having no fermionic quantum numbers.
2. The addition of the particles X^\pm replaces generalized Feynman diagrams with the analogs of stringy diagrams with lines replaced by pairs of lines corresponding to fermion and $X_{\pm 1/2}$. The members of these pairs would correspond to 3-D light-like surfaces glued together at the vertices of generalized Feynman diagrams. The analog of 3-vertex would not be splitting of the string to form shorter strings but the replication of the entire string to form two strings with same length or fusion of two strings to single string along all their points rather than along ends to form a longer string. It is not clear whether the duality symmetry of stringy diagrams can hold true for the TGD variants of stringy diagrams.
3. How should one describe the bound state formed by the fermion and X^\pm ? Should one describe the state as superposition of non-parallel on mass shell states so that the composite state would be automatically massive? The description as superposition of on mass shell states does not conform with the idea that bound state formation requires binding energy. In TGD framework the notion of negentropic entanglement has been suggested to make possible the analogs of bound states consisting of on mass shell states so that the binding energy is zero [45]. If this kind of states are in question the description of virtual states in terms of on mass shell states is not lost. Of course, one cannot exclude the possibility that there is infinite number of this kind of states serving as analogs for the excitations of string like object.
4. What happens to the states formed by fermions and $X_{\pm 1/2}$ in the internal lines of the Feynman diagram? Twistor philosophy suggests that only the higher on mass shell excitations are possible. If this picture is correct, the situation would not change in an essential manner from the earlier one.

The highly non-trivial prediction of the magnetic confinement is that elementary particles should have stringy character in electro-weak length scales and could behaving to become manifest at LHC energies. This adds one further item to the list of non-trivial predictions of TGD about physics at LHC energies [20].

11.3 Dark matter hierarchy, genetic machinery, and the un-reasonable selectivity of bio-catalysis

One of the most fascinating outcomes of ideas related to the dark matter hierarchy is the notion of inherently dark fractional atom (molecule) generalizing the notion of Bose-Einstein condensate to the fermionic case. These notions might provide an elegant manner to understand the mysteries of DNA replication, transcription, and translation, and more generally, the incredible selectivity of bio-catalysis.

As often, the original idea was not quite correct. I spoke about N -atoms rather than fractional atoms. In particular, the mass of N -molecule was N times larger than that of the ordinary molecule

apart from corrections from binding energy. The more precise view about dark matter hierarchy led to the realization that fractionization of all quantum numbers occurs. In the most general case one can have fractional particles with particle number $n = k/r, k = 1, \dots, r, r = \frac{\hbar}{\hbar_0}$. This leaves the model essentially as such at formal level. The model is however much more realistic than the original one since fractional atoms have mass which is never larger than that of ordinary atom and also conforms with the recent view about the origin of the hierarchy of Planck constants.

11.3.1 Dark atoms and dark cyclotron states

The development of the notion of dark atom involves many side tracks which make me blush. The first naive guess was that dark atom would be obtained by simply replacing Planck constant with its scaled counterpart in the basic formulas and interpreting the results geometrically. After some obligatory twists and turns it became clear that this assumption is indeed the most plausible one. The main source of confusion has been the lack of precise view about what the hierarchy of Planck constants means at the level of imbedding space at space-time.

The rules are very simple when one takes the singular coverings assigned to the many-valuedness of the time-derivatives of imbedding space coordinates as functions of canonical momentum densities as a starting point.

1. The mass and charge of electron are fractionized as is also the reduced mass in Schrödinger equation. This implies the replacements $e \rightarrow e/r, m \rightarrow m/r$, and $\hbar \rightarrow r\hbar_0, r = n_a n_b$, in the general formula for the binding energy assigned with single sheet of the covering. If maximal number $n_a n_b$ are present corresponding to a full "Fermi sphere", the total binding energy is r times the binding energy associated with single sheet.
2. In the case of hydrogen atom the proportionality $E \propto m/\hbar^2$ implies that the binding energy for single sheet of the covering scales as $E \rightarrow E/(n_a n_b)^3$ and maximal binding energy scales as $E \rightarrow E/(n_a n_b)^2$. This conforms with the naive guess. For high values of the nuclear charge Z it can happen that the binding energy is larger than the rest mass and fractionization might take place when binding energy is above critical fraction of the rest mass.
3. In the case of cyclotron energies one must decide what happens to the magnetic flux. Magnetic flux quantization states that the flux is proportional to \hbar for each sheet separately. Hence one has $\Phi \rightarrow r\Phi$ for each sheet and the total flux scales as r^2 . Since the dimensions of the flux quantum are scaled up by r the natural scaling of the size of flux quantum is by r^2 . Therefore the quantization of the magnetic flux requires the scaling $B \rightarrow B/r$. The cyclotron energy for single sheet satisfies $E \propto \hbar q B/m$ and since both mass m and charge q become fractional, the energy E for single sheet remains invariant whereas total cyclotron energy is scaled up by r in accordance with the original guess and the assumption used in applications.
4. Dark cyclotron states are expected to be stable up to temperatures which are r times higher than for ordinary cyclotron states. The states of dark hydrogen atoms and its generalizations are expected to be stable at temperatures scaled down by $1/r^2$ in the first approximation.
5. Similar arguments allow to deduce the values of binding energies in the general case once the formula of the binding energy given by standard quantum theory is known.

The most general option allows fractional atoms with proton and electron numbers varying from $1/r$ to 1. One can imagine also the possibility of fractional molecules. The analogs of chemical bonds between fractional hydrogen atoms with $N - k$ and k fractional electrons and protons can be considered and would give rise to a full shell of fractional electrons possessing an exceptional stability. These states would have proton and electron numbers equal to one.

Catalytic sites are one possible candidate for fractal electrons and catalyst activity might be perhaps understood as a strong tendency of fractal electron and its conjugate to fuse to form an ordinary electron.

Connection with quantum groups?

The phase $q = \exp(i2\pi/r)$ brings unavoidably in mind the phases defining quantum groups and playing also a key role in the model of topological quantum computation [42]. Quantum groups indeed emerge from the spinor structure in the "world of classical worlds" realized as the space of 3-surfaces in $M^4 \times CP_2$ and being closely related to von Neumann algebras known as hyper-finite factors of type II₁ [34].

Only singular coverings are allowed if the hierarchy of Planck constants and corresponding hierarchy of singular coverings follows from the basic TGD. If the integer n characterizing the quantum phase allows identification with with $r = \hbar/\hbar_0$, living matter could be perhaps understood in terms of quantum deformations of the ordinary matter, which would be characterized by the quantum phases $q = \exp(i2\pi/r)$. Hence quantum groups, which have for long time suspected to have significance in elementary particle physics, might relate to the mystery of living matter and predict an entire hierarchy of new forms of matter.

How to distinguish between fractional particles and ordinary particles?

The unavoidable question is whether bio-molecules in vivo could involve actually fractional atoms molecules as their building blocks. This raises a series of related questions.

1. Could it be that we can observe only the fusion of of dark fractional fold molecules to ordinary molecules or its reversal? Is the behavior of matter matter in vivo dictated by the dark matter commentn and of matter in vitro by ordinary matter? Could just the act of observing the matter in vivo in the sense of existing science make it ordinary dead matter?
2. If fractional atoms and molecules correspond to the maximum number of fractional quanta their masses are same as for ordinary atoms and molecules and only the different binding energy photon spectrum distinguishes between them. Situation changes all fractional states are possible and one obtains scaled down spectrum as a unique signature.
3. The fusion of fractional molecules to ordinary molecules in principle allows to conclude that fractional molecule was present. Could this process mean just the replacement of DNA in vivo with DNA in vitro?

11.3.2 Spontaneous decay and completion of dark fractional atoms as a basic mechanisms of bio-chemistry?

The replication of DNA has remained for me a deep mystery and I dare to doubt that the reductionistic belief that this miraculous process is well-understood involves self deceptive elements. Of course the problem is much more general: DNA replication is only a single very representative example of the miracles of un-reasonable selectivity of the bio-catalysis. I take this fact as a justification for some free imagination inspired by the notion of dark fractional molecule.

Dark fermionic molecules can replicate via decay and spontaneous completion

Unit particle number for fractional atom or molecule means that the analog of closed electronic shell are in question so that the state is especially stable. Note that the analogy with full Fermi electronic sphere makes also sense. These atoms or molecules could decay to fractional atoms or molecules. with fractional particle numbers k/r and $(r - k)/r$.

Suppose that a fractional molecule with unit particle number decays into k/r -molecule and $(r - k)/r$ -molecule. If r is even it is possible to have $k = r - k = r/2$ and the situation is especially symmetric. If fermionic $k/r < 1$ fractional atoms or molecules are present, one can imagine that they tend to be completed to full molecules spontaneously. Thus spontaneous decay and completion would favor the spontaneous replication (or rather fractionization) and dark molecules could be ideal replicators (fractionizers) The idea that the mechanisms of spontaneous decay and completion of dark fractional particles somehow lurk behind DNA replication and various high precision bio-catalytic processes is rather attractive.

Reduction of lock and key mechanism to spontaneous completion

DNA replication and molecular recognition by the lock and key mechanism are the two mysterious processes of molecular biology. As a matter of fact, DNA replication reduces to spontaneous opening of DNA double strand and to the lock and key mechanism so that it could be enough to understand the opening of double strand in terms of spontaneous decay and lock and key mechanism in terms of spontaneous completion of fractional particle (-atom or -molecule).

Consider bio-molecules which fit like a lock and key. Suppose that they are accompanied by dark fractional atoms or molecules, to be called dark fractional particles in sequel, such that one has $k_1 + k_2 = r$ so that in the formation of bound state dark molecules combine to form r -molecule analogous to a full fermionic shell or full Fermi sea. This is expected to enhance the stability of this particular molecular complex and prefer it amongst generic combinations.

For instance, this mechanism would make it possible for nucleotide and its conjugate, DNA and mRNA molecule, and tRNA molecule and corresponding aminoacid to recognize each other. Spontaneous completion would allow to realize also the associations characterizing the genetic code as a map from RNAs to subset of RNAs and associations of this subset of RNAs with amino-acids (assuming that genetic code has evolved from RNA \rightarrow RNA code as suggested in this chapter).

As such this mechanism allows a rather limited number of different lock and key combinations unless r is very large. There is however a simple generalization allowing to increase the representative power so that lock and key mechanism becomes analogous to a password used in computers. The molecule playing the role of lock *resp.* molecule would be characterized by a set of n fractional particles with $k_1 \in \{k_{1,1}, \dots, k_{1,n}\}$ *resp.* $k_2 \in \{k_{2,1} = r - k_{1,1}, \dots, k_{2,n} = r - k_{1,n}\}$. The molecules with conjugate names would fit optimally together. Fractional molecules or fractional electrons or atoms appearing as their building blocks would be like letters of a text characterizing the name of the molecule.

The mechanism generalizes also to the case of $n > 2$ reacting molecules. The molecular complex would be defined by a partition of n copies of integer r to a sum of m integers $k_{k,i}$: $\sum_i k_{k,i} = r$.

This mechanism could provide a universal explanation for the miraculous selectivity of catalysts and this selectivity would have practically nothing to do with ordinary chemistry but would correspond to a new level of physics at which symbolic processes and representations based on dark fractional particles emerge.

Connection with the number theoretic model of genetic code?

The emergence of partitions of integers in the labelling of molecules by fractional particles suggests a connection with the number theoretical model of genetic code [33], where DNA triplets are characterized by integers $n \in \{0, \dots, 63\}$ and aminoacids by integers 0, 1 and 18 primes $p < 64$. For instance, one can imagine that the integer n means that DNA triplet is labelled by n/r -particle. $r = 64$ would be the obvious candidate for r and conjugate DNA triplet would naturally have $n_c = 64 - n$.

The model relies on number-theoretic thermodynamics for the partitions of n to a sum of integers and genetic code is fixed by the minimization of number theoretic entropy which can be also negative and has thus interpretation as information. Perhaps these partitions could correspond to states resulting in some kind of decays of n -fermion to n_k/r -fermions with $\sum_{k=1}^r n_k = n$. The n_k/r -fermions should however not correspond to separate particles but something different. A possible interpretation is that partition corresponds to a state in which n_1/r particle is topologically condensed at $n_2/r \geq n_1/r$ particle topologically condensed....at $n_k/r \geq n_{k-1}/r$ -particle. This would also automatically define a preferred ordering of the integers n_i in the partition.

An entire ensemble of labels would be present and depending on the situation codon could be labelled not only by n/r -particle but by any partition $n = \sum_{i=1}^k n_i$ corresponding to the state resulting in the decay of n/r -particle to k fractional particles.

Reduction of DNA replication to a spontaneous decay of r -particle

DNA replication could be induced by a spontaneous decay of r -particle inducing the instability of the double strand leading to a spontaneous completion of the component strands.

Strand and conjugate strand would be characterized by k_1/r -particle and $(r - k_1)/r$ -particle, which combine to form r -particle as the double strand is formed. The opening of the double strand is induced

by the decay of r -particle to k_1/r - and $(r - k_1)/r$ -particles accompanying strand and its conjugate and after this both strands would complete themselves to double strands by the completion to r -particle.

It would be basically the stability of fractional particle which would make DNA double strand stable. Usually the formation of hydrogen bonds between strands and more generally, between the atoms of stable bio-molecule, is believed to explain the stability. Since the notion of hydrogen bond is somewhat phenomenological, one cannot exclude the possibility that these two mechanisms might be closely related to each other. I have already earlier considered the possibility that hydrogen bond might involve dark protons [27]: this hypothesis was inspired by the finding that there seems to exist two kinds of hydrogen bonds [46, 56].

The reader has probably already noticed that the participating fractional molecules in the model of lock and key mechanism are like sexual partners, and if already molecules are conscious entities as TGD inspired theory of consciousness strongly suggests, one might perhaps see the formation of entangled bound states with positive number theoretic entanglement entropy accompanied by molecular experience of one-ness as molecular sex. Even more, the replication of DNA brings in also divorce and process of finding of new companions!

11.3.3 The new view about hydrogen bond and water

Concretization of the above scenario leads to a new view about hydrogen bond and the role of water in bio-catalysis.

What the fractional particles labelling bio-molecules could be?

What the dark fractional particles defining the letters for the names of various bio-molecules could be? Dark fractional hydrogen atoms are the lightest candidates for the names of bio-molecules. The fusion could give rise to the hydrogen atom appearing in hydrogen bond. One could say the fractional hydrogen atoms belong to the molecules between which the hydrogen bond is formed. In absence of bond the fractional atoms would define active catalyst sites. This mechanism would also conform with the belief that hydrogen bonds guarantee the stability of bio-molecules.

This idea is not a mere speculation. The first experimental support for the notion of dark matter [27] came from the experimental finding that water looks in atto-second time scale from the point of view of neutron diffraction and electron scattering chemically like $H_{1.5}O$: as if one fourth of protons are dark [47, 51, 49, 50]. Dark protons would be identifiable as fractional protons. Of course, also dark hydrogen atoms can be considered.

One can imagine also a second option. The model for homeopathy [32] leads to a rather concrete view about how magnetic body controls biological body and receives sensory input from it. The model relies on the idea that dark water molecule clusters and perhaps also dark exotically ionized super-nuclei formed as linear closed strings of dark protons [27] perform this mimicry. Dark proton super-nuclei are ideal for mimicking the cyclotron frequencies of ordinary atoms condensed to dark magnetic flux quanta. Of course, also partially ionized hydrogen fractional ions could perform the cyclotron mimicry of molecules with the same accuracy.

One can consider the possibility fractional molecules/atoms correspond to exotic atoms formed by electrons bound to exotically ionized dark super-nuclei: the sizes of these nuclei are however above atomic size scale so that dark electrons would move in a harmonic oscillator potential rather than Coulombic potential and form states analogous to atomic nuclei. The prediction would be the existence of magic electron numbers [27]. Amazingly, there is strong experimental evidence for the existence of this kind of many-electron states. Even more, these states are able to mimic the chemistry of ordinary atoms [52, 48, 54]. The formation of hydrogen bonds between catalyst and substrate could be the correlate for the fusion of fractional hydrogen atoms.

If the fusion process gives rise 1/1-hydrogen, its spontaneous decay to ordinary hydrogen would liberate the difference of binding energies as metabolic energy helping to overcome the energy barrier for the reaction. The liberated energy would be rather large and correspond 3.4 eV UV photon even for $r = 2$ which suggests that it does not relate with standard metabolism. For larger values of r the liberated energy rapidly approaches to the ground state energy of hydrogen. Note that the binding energy of ordinary hydrogen atom in state $n = r$ has in the lowest order approximation same energy as the ground state of dark hydrogen atom for $\hbar/\hbar_0 = r$ so that one can consider the possibility of a resonant coupling of these states.

Fractional protons and electrons have effective charge $\pm ke/r$ so that the binding regions of catalysts and reacting molecules could carry effective fractional surface charge.

This might relate in an interesting manner to the problem of how poly-electrolytes can be stable (I am grateful for Dale Trenary for pointing me the problem and for interesting discussions). For instance, DNA carries a charge of -2 units per nucleotide due to the phosphate backbone. The models trying to explain the stability involve effective binding of counter ions to the polyelectrolyte so that the resulting system has a lower charge density. The simulations of DNA condensation by Stevens [62] however predict that counter ion charge should satisfy $z > 2$ in the case of DNA. The problem is of course that protons with $z = 1$ are the natural counter ions. The positive surface charge defined by the fractional protons attached to the nucleotides of DNA strand could explain the stability.

The hydrogen atoms in hydrogen bonds as fractional hydrogen atoms and $H_{1.5}O$ formula for water

The simplest assumption is that the hydrogens associated with hydrogen bonds are actually associated with $1/1$ type dark hydrogen atoms. This hypothesis has interesting implications and could explain the formula $H_{1.5}O$ for water in atto-second time scales suggested by neutron diffraction and electron scattering [47, 51, 49, 50].

The formation of hydrogen bond would correspond to a fusion of name and conjugate name between $H_{k/r}$ -O-H atom and its conjugate $H_{(r-k)/r}$ -O-H atom. The resulting pairs would obey the chemical formula H_3-O_2 . Hence the formation of hydrogen bonds would predict the $H_{1.5}O$ formula suggested by neutron diffraction and electron scattering in atto-second time scale. This holds true only if one has complete pairing by hydrogen bonds. A more plausible explanation is that just the presence of fractional hydrogens implies the effect. Furthermore, the fraction of dark protons can depend on temperature.

The roles of water and ordered water in catalysis

The new view about hydrogen bond allows to understand the role of water in biology at qualitative level. For instance, one can

1. tentatively identify "ordered water" as a phase in which all $H_{k/r}$ atoms and their conjugates have combined to $H_{1/1}$ atoms,
2. understand why (or perhaps it is better to say "predict that") water containing $H_{k/r}$ atoms acts as a catalytic poison so that the binding sites of catalysts and reactants must be isolated from water unless the water is ordered,
3. justify the belief that gel phase involving ordered water is necessary for biological information processing,
4. understand why hydration causes hydrolysis,
5. understand the instability of DNA against decay to RNA outside nucleus.

A more more detailed sketch looks like following.

1. Suppose that at least part of water molecules appear in form $H_{k/r}$ -OH and $H_{(r-k)/r}$ -O-H. These molecules and the the molecule $H_{1/1}$ -OH₂ formed in their fusion has much smaller binding energy than ordinary water molecule and is expected to be unstable against transition to H_3O . This would suggest that the feed of metabolic energy is needed to generate the dark hydrogen atoms.

Fractional dark water molecules can join pairwise to form $H-O-(H_{1/1})-O-H \equiv H_3O_2$ with $H_{1/1}$ -atoms replacing hydrogen in hydrogen bond. Also $H_{k_1/r}$ -O- $H_{k_2/r}$ molecules are possible and could form closed strings obeying the chemical formula $O_n(H_{1/1})_n$. Also open strings with H-O:s at ends are possible. This phase of water might allow identification as "ordered water" believed to be associated with gel phase and be crucial for quantal information processing inside cell. Liquid crystal phase of water could correspond to a bundle of open vertical segments $H-O_n(H_{1/1})_{n-2}-H$ forming a 2-dimensional liquid (vertical freezing).

2. Exotic water molecules could spoil the action of both catalyst and reactant molecules by attaching to the "letters" in the name of catalyst or reactant so that the letters are not visible and catalyst and reactant cannot recognize each other anymore. Hence binding sites of catalyst and reactant must be isolated from water containing fractional water molecules. This is what Sidorova and Rau [63] suggest on basis of comparison of specific and non-specific catalysts: non-specific catalysts contain water in an isolated binding volume whereas for specific catalysts this volume is empty. An alternative mechanism hindering water molecules to attach to "letters" is that water is "ordered water" with no fractional water molecules present.
3. DNA is known to be stable against decay to RNA via hydration inside the cell but not outside. Hydration could correspond to the joining of fractional water to sites of DNA transforming it to RNA. Inside nucleus this cannot occur if water is in ordered water phase permanently.

How the first self-replicators emerged?

The identification of the first self replicator can be seen as perhaps the most fascinating and challenging problem faced by the pre-biotic model builders. Self replicator is by definition an entity which catalyzes its own replication. The analogy with the self-referential statement appearing in Gödel's theorem obvious.

In TGD framework self replication would reduce to a spontaneous decay of $H_{1/1}$ -atom to $H_{k/r}$ - and $H_{(r-k)/r}$ -atoms and their subsequent completion to $H_{1/1}$ -atoms

The picture about emergence of self-replicators would be roughly following.

1. The first self-replicating entities would have been plasmoids [66] generating $H_{1/1}$ atoms whose presence would have made possible the emergence of the first molecular self replicators. The generation of $H_{1/1}$ atoms requires metabolic energy feed. In the first approximation the decay of $H_{1,1}$ to fractional hydrogen atoms does not liberate nor require energy.
2. $H_{k/r}$ atoms would have replaced some ordinary H -atoms in some negatively charged molecules M_i (perhaps MXTP, $X = A, U, C, G$) leading to a spontaneous emergence of linear negatively charged polymers consisting of M_i . One can imagine a coding in which each X corresponds to fixed value of k or collection of the (2 hydrogen bonds or 3 hydrogen bonds depending on X). This would make the attachment of X and its conjugate to form a hydrogen bond a highly favored process.
3. $H_{k/r}$ atoms would have taken also the role of active binding sites. In ordered water conjugate molecules $M_{c,i}$ having $H_{(r-k)/r}$ atoms as labels would have had high probability to attach to the polymers made of M_i .
4. RNA molecules are good candidates for self-replicators in the presence of ordered water. The phase transition from ordinary to ordered water (which would have developed later to sol-gel phase transition) would have been an essential element of replication.

The role of water in chirality selection

In the latest New Scientist (when I am writing this) there was a news telling that chiral selection occurs in water but not in heavy water [45]. The L form of aminoacid glutamate is more stable than R in ordinary but not so in heavy water so that water environment must be responsible for the chirality selection of bio-molecules. The proposed explanation for the finding, whose importance cannot be over-estimated, was following.

1. Water molecules have two forms: orto- and para, depending on whether the nuclear spins of protons are parallel or opposite. Deuterium nuclei are spinless so that heavy water has only single form. In thermal equilibrium the fraction of orto water is 3/4 and para water 1/4.
2. Ortho-water is magnetic and if L form of aminoacid is slightly more magnetic than R, chirality selection can be understood as result of the magnetic interaction with water.

One can of course wonder how extremely short ranged weak interactions could produce strong enough effect on the magnetic moment. The situation is not made easier by the fact that magnetic interaction energies are inherently very weak and deep below the thermal threshold.

It is interesting to find whether these findings could be explained by and allow a more detailed formulation of the TGD based model for water based on the notion of fractional hydrogen atom, the new view about hydrogen bond, and the notion of dark protonic strings forming atomic sized super-nuclei carrying exotic weak charges.

1. Dark matter brings in long ranged exotic weak interactions which can produce large parity breaking effects in atomic and even longer length scales. The long ranged parity breaking weak interactions of the dark protonic super nuclei assignable to aminoacids and water could explain the chiral selection.
2. The magnetic interaction energy is scaled up by r , so that magnetic interactions could indeed play a key role. Ordinary classical magnetic fields are in TGD framework always accompanied by Z^0 magnetic fields. If aminoacids possess exotic em charge implying also exotic weak charge, one can understand the chiral breaking as being induced by the Z^0 magnetic interaction of aminoacids with the dark magnetic fields generated by water molecules or their clusters possessing a net magnetic moment. In heavy water these fields would be absent so that the experimental findings could be understood.
3. The experimental evidence that water behaves as $H_{1.5}O$ in attosecond time scales means that 1/4:th of protons of water are effectively dark. The notion of fractional hydrogen atom leads to a model of hydrogen bond predicting correctly $H_{1.5}O$ formula and the dropping of 1/4:th of protons at larger possibly dark space-time sheets. The model also predicts that the mass of $H-O-H_r-O-H \equiv 2H_{1.5}O$ hydrogen bonded pairs is very near to the mass of 2 water molecules since there are $r \simeq m_p/m_e$ electrons involved. The paired molecules have three protons and non-vanishing net nuclear spin and thus generate a magnetic field and make hydrogen bonded water a magnetic system. The natural identification would be as dark magnetic field accompanied by Z^0 magnetic field responsible for the chiral selection.

In the case of $D-O-D_r-O-D$ mass would be by about one proton mass m_p lower than mass of two D_2O molecules so that this D-bonded heavy water would look like $D_{1.25}O$ as far as masses are considered and $D_{1.5}O$ as far as neutron diffraction and electron scattering are considered. In this case no magnetic field is generated since the nuclear spin of D vanishes and no chiral breaking results. This picture explains the experimental findings. The model is not equivalent with the proposal of the experimentalists.

4. The model predicts that the protons liberated in the formation of hydrogen bonds drop to larger space-time sheets but does not specify their fate. A strong constraint comes from the requirement that the dropped particles have exotic weak charges acting as sources of the geometrically unavoidable classical Z^0 magnetic field at dark space-time sheets causing the large parity breaking. This constraint is satisfied if the protons form super-nuclei (scaled up variants of nuclei) consisting of protonic strings connected by color bonds involving exotic quark and antiquark at its ends and some of these bonds are charged (of type $u\bar{d}$ or $d\bar{u}$: this could also generate the em charge needed to make the protonic string stable).

11.4 TGD based model for cell membrane as sensory receptor

The emergence of zero energy ontology, the explanation of dark matter in terms of a hierarchy of Planck constants requiring a generalization of the notion of imbedding space, the view about life as something in the intersection of real and p-adic worlds, and the notion of number theoretic entanglement negentropy lead to the breakthrough in TGD inspired quantum biology and also to the recent view of qualia and sensory representations including hearing allowing a precise quantitative model at the level of cell membrane.

Also in the recent view long range weak forces however play a key role. They are made possible by the exotic ground state represented as almost vacuum extremal of Kähler action for which classical em and Z^0 fields are proportional to each other whereas for standard ground state classical Z^0 fields

are very weak. Neutrinos are present but it seems that they do not define cognitive representations in the time scales characterizing neural activity. Electrons and quarks for which the time scales of causal diamonds correspond to fundamental biorhythms - one of the key observations during last years- take this role.

11.4.1 Could cell correspond to almost vacuum extremal?

The question whether cell could correspond almost vacuum extremal of Kähler action was the question which led to the realization that the frequencies of peak sensitivity for photoreceptors correspond to the Josephson frequencies of biologically important ions if one accepts that the value of the Weinberg angle equals to $\sin^2(\theta_W) = .0295$ instead of the value .23 in the normal phase, in which the classical electromagnetic field is proportional to the induced Kähler form of CP_2 in a good approximation. Another implication made possible by the large value of Planck constant is the identification of Josephson photons as the counterparts of biophotons one one hand and those of EEG photons on the other hand. These observation in turn led to a detailed model of sensory qualia and of sensory receptor. Therefore the core of this argument deserves to be represented also here although it has been discussed in [27].

Cell membrane as almost vacuum extremal

Although the fundamental role of vacuum extremals for quantum criticality and life has been obvious from the beginning, it took a long time to realize how one could model living cell as this kind of system.

1. Classical electric fields are in a fundamental role in biochemistry and living biosystems are typically electrets containing regions of spontaneous electric polarization. Fröhlich [65] proposed that oriented electric dipoles form macroscopic quantum systems with polarization density serving as a macroscopic order parameter. Several theories of consciousness share this hypothesis. Experimentally this hypothesis has not been verified.
2. TGD suggests much more profound role for the unique di-electric properties of the biosystems. The presence of strong electric dipole fields is a necessary prerequisite for cognition and life and could even force the emergence of life. Strong electric fields imply also the presence of the charged wormhole BE condensates: the surface density of the charged wormholes on the boundary is essentially equal to the normal component of the electric field so that wormholes are in some sense 'square root' of the dipole condensate of Fröhlich! Wormholes make also possible pure vacuum polarization type dipole fields: in this case the magnitudes of the em field at the two space-time sheets involved are same whereas the directions of the fields are opposite. The splitting of wormhole contacts creates fermion pairs which might be interpreted as cognitive fermion pairs. Also microtubules carry strong longitudinal electric fields. This formulation emerged much before the identification of ordinary gauge bosons and their superpartners as wormhole contacts.

Cell membrane is the basic example about electret and one of the basic mysteries of cell biology is the resting potential of the living cell. Living cell membranes carry huge electric fields: something like 10^7 Volts per meter. For neuron resting potential corresponds to about .07 eV energy gained when unit charge travels through the membrane potential. In TGD framework it is not at all clear whether the presence of strong electromagnetic field necessitates the presence of strong Kähler field. The extremely strong electric field associated with the cell membrane is not easily understood in Maxwell's theory and almost vacuum extremal property could change the situation completely in TGD framework.

1. The configuration could be a small deformation of vacuum extremal so that the system would be highly critical as one indeed expects on basis of the general visiona about living matter as a quantum critical system. For vacuum extremals classical em and Z^0 fields would be proportional to each other. The second half of Maxwell's equations is not in general satisfied in TGD Universe and one cannot exclude the presence of vacuum charge densities in which case elementary particles as the sources of the field would not be necessarily. If one assumes that this is the case approximately, the presence of Z^0 charges creating the classical Z^0 fields is implied. Neutrinos are the most candidates for the carrier of Z^0 charge. Also nuclei could feed their weak

gauge fluxes to almost non-vacuum extremals but not atomic electrons since this would lead to dramatic deviations from atomic physics. This would mean that weak bosons would be light in this phase and also Weinberg angle could have a non-standard value.

2. There are also space-time surfaces for CP_2 projection belongs to homologically non-trivial geodesic sphere. In this case classical Z^0 field can vanish [46] and the vision has been that it is sensible to speak about two basic configurations.

- (a) Almost vacuum extremals (homologically trivial geodesic sphere).
- (b) Small deformations of non-vacuum extremals for which the gauge field has pure gauge Z^0 component (homologically non-trivial geodesic sphere).

The latter space-time surfaces are excellent candidates for configurations identifiable as TGD counterparts of standard electroweak physics. Note however that the charged part of electroweak fields is present for them.

3. To see whether the latter configurations are really possible one must understand how the gauge fields are affected in the color rotation.

- (a) The action of color rotations in the holonomy algebra of CP_2 is non-trivial and corresponds to the action in $U(2)$ sub-group of $SU(3)$ mapped to $SU(2)_L \times U(1)$. Since the induced color gauge field is proportional to Kähler form, the holonomy is necessary Abelian so that also the representation of color rotations as a sub-group of electro-weak group must correspond to a local $U(1)$ sub-group local with respect to CP_2 point.

- (b) Kähler form remains certainly invariant under color group and the right handed part of Z^0 field reducing to $U(1)_R$ sub-algebra should experience a mere Abelian gauge transformation. Also the left handed part of weak fields should experience a local $U(1)_L$ gauge rotation acting on the neutral left handed part of Z^0 in the same manner as it acts on the right handed part. This is true if the $U(1)_L$ sub-group does not depend on point of CP_2 and corresponds to Z^0 charge. If only Z^0 part of the induced gauge field is non-vanishing as it can be for vacuum extremals then color rotations cannot change the situation. If Z^0 part vanishes and non-vacuum extremal is in question, then color rotation rotation of W components mixing them but acts as a pure $U(1)$ gauge transformation on the left handed component.

- (c) It might not be without importance that for any partonic 2-surface induced electro-weak gauge fields have always $U(1)$ holonomy, which could allow to define what neutral part of induced electroweak gauge field means locally. This does not however hold true for the 4-D tangent space distribution. In any case, the cautious conclusion is that there are two phases corresponding to nearly vacuum extremals and small deformations of extremals corresponding to homologically non-trivial geodesic spheres for which the neutral part of the classical electro-weak gauge field reduces to photon field.

4. The unavoidable presence of long range Z^0 fields would explain large parity breaking in living matter, and the fact that neutrino Compton length is of the order of cell size would suggest the possibility that within neutrino Compton electro-weak gauge fields or even longer scales could behave like massless fields. The explanation would be in terms of the different ground state characterized also by a different value of Weinberg angle. For instance, of the p-adic temperature of weak bosons corresponds to $T_p = 1/2$, the mass scale would be multiplied by a factor $\sqrt{M_{89}}$ and Compton lengths of weak bosons would be around 10^{-4} meters corresponding to the size scale of a large neuron. If the value of Planck constant is also large then the Compton length increases to astrophysical scale.

5. From the equations for classical induced gauge fields in terms of Kähler form and classical Z^0 field [46]

$$\gamma = 3J - \frac{p}{2}Z^0 \quad , \quad Q_Z = I_L^3 - pQ_{em} \quad , \quad p = \sin^2(\theta_W) \quad (11.4.1)$$

it follows that for the vacuum extremals the part of the classical electro-weak force proportional to the electromagnetic charge vanishes for $p = 0$ so that only the left-handed couplings to the weak gauge bosons remain. The absence of electroweak symmetry breaking and vanishing or at least smallness of p would make sense below the Compton length of dark weak bosons. If this picture makes sense it has also implications for astrophysics and cosmology since small deformations of vacuum extremals are assumed to define the interesting extremals. Dark matter hierarchy might explain the presence of unavoidable long ranged Z^0 fields as being due to dark matter with arbitrarily large values of Planck constant so that various elementary particle Compton lengths are very long.

6. The simplest option is that the dark matter -say quarks with Compton lengths of order cell size and Planck constant of order $10^7 \hbar_0$ - are responsible for dark weak fields making almost vacuum extremal property possible. The condition that Josephson photons correspond to EEG frequencies implies $\hbar \sim 10^{13} \hbar_0$ and would mean the scaling of intermediate gauge boson Compton length to that corresponding to the size scale of a larger neuron. The quarks involved with DNA as topological quantum computer model could be in question and membrane potential might be assignable to the magnetic flux tubes. The ordinary ionic currents through cell membrane -having no coupling to classical Z^0 fields and not acting as its source- would be accompanied by compensating currents of dark fermions taking care that the almost vacuum extremal property is preserved. The outcome would be large parity breaking effects in cell scale from the left handed couplings of dark quarks and leptons to the classical Z^0 field. The flow of Na^+ ions during nerve pulse could take along same dark flux tube as the flow of dark quarks and leptons. This near vacuum extremal property might be fundamental property of living matter at dark space-time sheets at least.

1. *Could nuclei and neutrinos couple to light variants of weak gauge fields in the critical phase?*

One of the hard-to-kill ideas of quantum TGD inspired model of quantum biology is that neutrinos might have something do with hearing and cognition. This proposal looks however unrealistic in the recent vision. I would be more than happy to get rid of bio-neutrinos but the following intriguing finding does not allow me to have this luxury.

1. Assume that the endogenous magnetic field $B_{end} = .2$ Gauss is associated with a nearly vacuum extremal and therefore accompanied by $B_Z = 2B_{end}/p$. Assume for definiteness $m_\nu = .3$ eV and $p = \sin^2(\theta_W) = .23$. The neutrino cyclotron frequency is given by the following expression

$$f_\nu = \frac{m_e}{m_\nu} \frac{1}{2\sin^2(\theta_W)} f_e .$$

From $f_e \simeq .57 \times \text{MHz}$ and $p = \sin^2(\theta_W) = .23$ one obtains $E_\nu = 1.7 \times 10^{-2}$ eV, which is roughly one third to the Josephson frequency of electron assignable to cell membrane. Could Josephson frequency of cell membrane excite neutrino cyclotron transitions?

2. The model for photoreceptors to be discussed below forces to conclude that the value of Weinberg angle in the phase near vacuum extremal must be $p = .0295$ if one wants to reproduce the peak energies of photoreceptors as Josephson frequencies of basic biological ions. This would predict $E_\nu = .41$ eV, which is rather near to the metabolic energy quantum. The non-relativistic formula however fails in this case and one must use the relativistic formula giving

$$E = \sqrt{g_Z Q_Z B_Z 2\pi} \simeq .48 \text{ eV}$$

giving the metabolic energy quantum. Does this mean that Z^0 cyclotron frequency for neutrino is related to the transfer of metabolic energy using Z^0 MEs in the phase near vacuum extremals.

3. Josephson frequency is proportional to $1/\hbar$, whereas neutrino cyclotron frequency does not depend on \hbar at non-relativistic energies. For larger values of \hbar the neutrino becomes relativistic so that the mass in the formula for cyclotron frequency must be replaced with energy. This gives

$$E = \sqrt{nr^{1/2}} \sqrt{g_Z Q_Z B_Z 2\pi} \simeq r^{1/2} \times .48 \text{ eV} , \quad r = \sqrt{\hbar/\hbar_0} .$$

Here n refers to the cyclotron harmonic.

These observations raise the question whether the three frequencies with maximum response assignable to the three different types of receptors of visible light in retina could correspond to the three cyclotron frequencies assignable to the three neutrinos with different mass scales? The first objection is that the dependence on mass disappears completely at the relativistic limit. The second objection is that the required value of Planck constant is rather small and far from being enough to have electroweak boson Compton length of order cell size. One can of course ask whether the electroweak gauge bosons are actually massless inside almost vacuum extremals. If fermions -including neutrino- receive their masses from p-adic thermodynamics then massless electroweak gauge bosons would be consistent with massive fermions. Vacuum extremals are indeed analogous to the unstable extrema of Higgs potential at which the Higgs vacuum expectation vanishes so that this interpretation might make sense.

2. Ionic Josephson frequencies defined by the resting potential for nearly vacuum extremals

If cell membrane corresponds to an almost vacuum extremal, the membrane potential is replaced with an effective resting potential containing also the Z^0 contribution proportional to the ordinary resting potential. The surprising outcome is that one could understand the preferred frequencies for photo-receptors [69] as Josephson frequencies for biologically important ions. Furthermore, most Josephson energies are in visible and UV range and the interpretation in terms of biophotons is suggestive. If the value of Planck constant is large enough Josephson frequencies are in EEG frequency range so that biophotons and EEG photons could be both related to Josephson photons with large \hbar .

1. One must assume that the interior of the cell corresponds to many fermion state -either a state filled with neutrinos up to Fermi energy or Bose-Einstein condensate of neutrino Cooper pairs creating a harmonic oscillator potential. The generalization of nuclear harmonic oscillator model so that it applies to multi-neutrino state looks natural.
2. For exact vacuum extremals elementary fermions couple only via left-handed isospin to the classical Z^0 field whereas the coupling to classical em field vanishes. Both K_+, Na_+ , and Cl^- $A - Z = Z + 1$ so that by p-n pairing inside nucleus they have the weak isospin of neutron (opposite to that of neutrino) whereas Ca_{++} nucleus has a vanishing weak isospin. This might relate to the very special role of Ca_{++} ions in biology. For instance, Ca_{++} defines an action potential lasting a time of order .1 seconds whereas Na_+ defines a pulse lasting for about 1 millisecond [68]. These time scales might relate to the time scales of CDs associated with quarks and electron.
3. The basic question is whether only nuclei couple to the classical Z^0 field or whether also electrons do so. If not, then nuclei have a large effective vector coupling to em field coming from Z^0 coupling proportional to the nuclear charge increasing the value of effective membrane potential by a factor of order 100. If both electrons and nuclei couple to the classical Z^0 field, one ends up with difficulties with atomic physics. If only quarks couple to the Z^0 field and one has $Z^0 = -2\gamma/p$ for vacuum extremals, and one uses average vectorial coupling $\langle I_L^3 \rangle = \pm 1/4$ with + for proton and - for neutron, the resulting vector coupling is following

$$\begin{aligned} \left(\frac{Z-N}{4} - pZ\right)Z^0 + q_{em}\gamma &= Q_{eff}\gamma, \\ Q_{eff} &= -\frac{Z-N}{2p} + 2Z + q_{em}. \end{aligned} \quad (11.4.1)$$

Here γ denotes em gauge potential. For K^+, Cl^-, Na^+, Ca^{++} one has $Z = (19, 17, 11, 20)$, $Z - N = (-1, -1, -1, 0)$, and $q_{em} = (1, -1, 1, 2)$. Table 1 below gives the values of Josephson energies for some values of resting potential for $p = .23$. Rather remarkably, they are in IR or visible range.

$E(Ion)/eV$	$V = -40 \text{ mV}$	$V = -60 \text{ mV}$	$V = -70 \text{ mV}$
Na^+	1.01	1.51	1.76
Cl^-	1.40	2.11	2.46
K^+	1.64	2.47	2.88
Ca^{++}	1.68	2.52	2.94

Table 2. Values of the Josephson energy of cell membrane for some values of the membrane voltage for $p = .23$. The value $V = -40 \text{ mV}$ corresponds to the resting state for photoreceptors and $V = -70 \text{ mV}$ to the resting state of a typical neuron.

Are photoreceptors nearly vacuum extremals?

In Hodgkin-Huxley model ionic currents are Ohmian currents. If one accepts the idea that the cell membrane acts as a Josephson junction, there are also non-dissipative oscillatory Josephson currents of ions present, which run also during flow equilibrium for the ionic parts of the currents. A more radical possibility is that the dominating parts of the ionic currents are oscillatory Josephson currents so that no metabolic energy would be needed to take care that density gradients for ions are preserved. Also in this case both nearly vacuum extremals and extremals with nearly vanishing Z^0 field can be considered. Since sensory receptors must be highly critical the natural question is whether they could correspond to nearly vacuum extremals. The quantitative success of the following model for photoreceptors supports this idea.

Photoreceptors can be classified to three kinds of cones responsible for color vision and rods responsible for black-white vision. The peak sensitivities of cones correspond to wavelengths (405, 535, 565) nm and energies (3.06, 2.32, 2.19) eV. The maximum absorption occurs in the wave length range 420-440 nm, 534-545 nm, 564-580 nm for cones responsible for color vision and 498 nm for rods responsible black-white vision [69, 67]. The corresponding photon energies are (2.95, 2.32, 2.20) eV for color vision and to 2.49 eV for black-white vision. For frequency distribution the maxima are shifted from these since the maximum condition becomes $dI/d\lambda + 2I/\lambda = 0$, which means a shift to a larger value of λ , which is largest for smallest λ . Hence the energies for maximum absorbance are actually lower and the downwards shift is largest for the highest energy.

From Table 2 above it is clear that the energies of Josephson photons are in visible range for reasonable values of membrane voltages, which raises the question whether Josephson currents of nuclei in the classical em and Z^0 fields of the cell membrane could relate to vision.

Consider first the construction of the model.

1. Na^+ and Ca^{++} currents are known to present during the activation of the photoreceptors. Na^+ current defines the so called dark current [69] reducing the membrane resting potential below its normal value and might relate to the sensation of darkness as eyes are closed. Hodgkin-Huxley model predicts that also K^+ current is present. Therefore the Josephson energies of these three ion currents are the most plausible correlates for the three colors.
2. One ends up with the model in the following manner. For Ca^{++} the Josephson frequency does not depend on p and requiring that this energy corresponds to the energy 2.32 eV of maximal sensitivity for cones sensitive to green light fixes the value of the membrane potential during hyperpolarization to $V = .055 \text{ V}$, which is quite reasonable value. The value of the Weinberg angle parameter can be fixed from the condition that other peak energies are reproduced optimally. The result of $p = .0295$.

The predictions of the model come as follows summarized also by the Table 3 below.

1. The resting potential for photoreceptors is $V = -40 \text{ mV}$ [?]. In this case all Josephson energies are below the range of visible frequencies for $p = .23$. Also for maximal hyperpolarization Na^+ Josephson energy is below the visible range for this value of Weinberg angle.
2. For $V = -40 \text{ mV}$ and $p = .0295$ required by the model the energies of Cl^- and K^+ Josephson photons correspond to red light. 2 eV for Cl^- corresponds to a basic metabolic quantum. For Na^+ and Ca^{++} the wave length is below the visible range. Na^+ Josephson energy is below visible range. This conforms with the interpretation of Na^+ current as a counterpart for the sensation of darkness.

3. For $V = -55$ mV - the threshold for the nerve pulse generation- and for $p = .0295$ the Josephson energies of Na^+ , Ca^{++} , and K^+ correspond to the peak energies for cones sensitive to red, green, and blue respectively. Also Cl^- is in the blue region. Ca^{++} Josephson energy can be identified as the peak energy for rods. The increase of the hyperpolarization to $V = -59$ mV reproduces the energy of the maximal wave length response exactly. A possible interpretation is that around the criticality for the generation of the action potential ($V \simeq -55$ mV) the qualia would be generated most intensely since the Josephson currents would be strongest and induce Josephson radiation inducing the quale in other neurons of the visual pathway at the verge for the generation of action potential. This supports the earlier idea that visual pathways defines a neural window. Josephson radiation could be interpreted as giving rise to biophotons (energy scale is correct) and to EEG photons (for large enough values of \hbar the frequency scales is that of EEG).
4. In a very bright illumination the hyperpolarization is $V = -65$ mV [?], which the normal value of resting potential. For this voltage Josephson energies are predicted to be in UV region except in case of Ca^{++} . This would suggest that only the quale 'white' is generated at the level of sensory receptor: very intense light is indeed experienced as white.

The model reproduces basic facts about vision assuming that one accepts the small value of Weinberg angle, which is indeed a natural assumption since vacuum extremals are analogous to the unstable extrema of Higgs potential and should correspond to small Weinberg angle. It deserves to be noticed that neutrino Josephson energy is 2 eV for $V = -50$ mV, which correspond to color red. 2 eV energy defines an important metabolic quantum.

Ion	Na^+	Cl^-	K^+	Ca^{++}
$E_J(.04 \text{ mV}, p = .23)/eV$	1.01	1.40	1.51	1.76
$E_J(.065 \text{ V}, p = .23)/eV$	1.64	2.29	2.69	2.73
$E_J(40 \text{ mV}, p = .0295)/eV$	1.60	2.00	2.23	1.68
$E_J(50 \text{ mV}, p = .0295)/eV$	2.00	2.49	2.79	2.10
$E_J(55 \text{ mV}, p = .0295)/eV$	2.20	2.74	3.07	2.31
$E_J(65 \text{ mV}, p = .0295)/eV$	2.60	3.25	3.64	2.73
$E_J(70 \text{ mV}, p = .0295)/eV$	2.80	3.50	3.92	2.94
$E_J(75 \text{ mV}, p = .0295)/eV$	3.00	3.75	4.20	3.15
$E_J(80 \text{ mV}, p = .0295)/eV$	3.20	4.00	4.48	3.36
$E_J(90 \text{ mV}, p = .0295)/eV$	3.60	4.50	5.04	3.78
$E_J(95 \text{ mV}, p = .0295)/eV$	3.80	4.75	5.32	3.99
Color	R	G	B	W
E_{max}	2.19	2.32	3.06	2.49
energy-interval/eV	1.77-2.48	1.97-2.76	2.48-3.10	

Table 3. The table gives the prediction of the model of photoreceptor for the Josephson energies for typical values of the membrane potential. For comparison purposes the energies E_{max} corresponding to peak sensitivities of rods and cones, and absorption ranges for rods are also given. R,G,B,W refers to red, green, blue, white. The values of Weinberg angle parameter $p = \sin^2(\theta_W)$ are assumed to be .23 and .0295. The latter value is forced by the fit of Josephson energies to the known peak energies.

It interesting to try to interpret the resting potentials of various cells in this framework in terms of the Josephson frequencies of various ions.

1. The maximum value of the action potential is +40 mV so that Josephson frequencies are same as for the resting state of photoreceptor. Note that the time scale for nerve pulse is so slow as compared to the frequency of visible photons that one can consider that the neuronal membrane is in a state analogous to that of a photoreceptor.
2. For neurons the value of the resting potential is -70 mV. Na^+ and Ca^{++} Josephson energies 2.80 eV and 2.94 eV are in the visible range in this case and correspond to blue light. This

does not mean that Ca^{++} Josephson currents are present and generate sensation of blue at neuronal level: the quale possibly generated should depend on sensory pathway. During the hyperpolarization period with -75 mV the situation is not considerably different.

3. The value of the resting potential is -95 mV for skeletal muscle cells. In this case Ca^{++} Josephson frequency corresponds to 4 eV metabolic energy quantum as the table below shows.
4. For smooth muscle cells the value of resting potential is -50 mV. In this case Na^+ Josephson frequency corresponds to 2 eV metabolic energy quantum.
5. For astroglia the value of the resting potential is -80/-90 mV for astroglia. For -80 mV the resting potential for Cl^- corresponds to 4 eV metabolic energy quantum. This suggests that glial cells could also provide metabolic energy as Josephson radiation to neurons.
6. For all other neurons except photo-receptors and red blood cells Josephson photons are in visible and UV range and the natural interpretation would be as biophotons. The biophotons detected outside body could represent sensory leakage. An interesting question is whether the IR Josephson frequencies could make possible some kind of IR vision.

11.4.2 General model for qualia and sensory receptor

The identification of quantum number increments in quantum jump for a subsystem representing subself and the capacitor model of sensory receptor are already more than decade old ideas.

The concrete realization of this vision is based on several ideas that I have developed during last five years.

1. The vision about dark matter as a hierarchy of phases partially labeled by the value of Planck constant led to the model of DNA as topological quantum computer [44]. In this model magnetic flux tubes connecting DNA nucleotides with the lipids of the cell membrane define strands of the braids defining topological quantum computations. The braid strand corresponds to so called wormhole flux tube and has quark and antiquark at its ends. u and d quarks and their antiquarks code for four DNA nucleotides in this model.
2. Zero energy ontology assigns to elementary particles so called causal diamonds (CDs). For u and d quarks and electron these time scales are (6.5, .78, 100) ms respectively, and correspond to fundamental biorhythms. Electron time scale corresponds to 10 Hz fundamental biorhythm defining also the fundamental frequency of speech organs, .78 ms to kHz cortical synchrony [72], and 160 Hz to cerebellar synchrony [70]. Elementary particles therefore seem to be directly associated with neural activity, language, and presumably also hearing. One outcome was the modification of the earlier model of memetic code involving the notion of cognitive neutrino pair by replacing the sequence of cognitive neutrino pairs with that of quark sub- CDs within electron CD . Nerve pulses could induce the magnetization direction of quark coding for bit but there are also other possibilities. The detailed implications for the model of nerve pulse [27] remain to be disentangled.
3. The understanding of the Negentropy Maximization Principle [45] and the role of negentropic entanglement in living matter together with the vision about life as something in the intersection of real and p-adic worlds was a dramatic step forward. In particular, space-like and time-like negentropic entanglement become basic aspects of conscious intelligence and are expected to be especially important for understanding the difference between speech and music.
4. The most important implication concerning the model of sensory receptors however relate to the vacuum degeneracy of Kähler action. It has been clear from the beginning that the nearly vacuum extremals of Kähler action could play key role key role in living systems. The reason is their criticality making them ideal systems for sensory perception. These extremals carry classical em and Z^0 fields related to each other by a constant factor and this could explain the large parity breaking effects characterizing living matter. The assumption that cell membranes are nearly vacuum extremals and that nuclei can feed their Z^0 charges to this kind of space-time sheets (not true for atomic electrons) in living matter leads to a modification of the model for the cell membrane as Josephson junction [27]. Also a model of photoreceptors explaining the

frequencies of peak sensitivity as ionic Josephson frequencies and allowing the dual identifications Josephson radiation as biophotons (energies) [64] and EEG radiation (frequencies) emerge since the values of Planck constant can be very large. The value of the Weinberg angle in this phase is fixed to $\sin^2(\theta_W) = .0295$, whereas in standard phase the value is given by $\sin^2(\theta_W) = .23$. The significance of this quantitative success for TGD and TGD inspired quantum biology cannot be over-estimated.

11.4.3 Some implications of the model of cell membrane as sensory receptor

The ensuing general model of how cell membrane acts as a sensory receptor has unexpected implications for the entire TGD inspired view about biology.

1. DNA as topological quantum computer model plus certain simplifying assumption leads to the conclusion that the spectrum of net quantum numbers of quark antiquark pair define the primary qualia assignable to a nucleotide-lipid pair connected by a magnetic flux tube. The most general prediction is that the net quantum numbers of two quark pairs characterize the qualia. In the latter case the qualia would be assigned to a pair of receptor cells.
2. Composite qualia result when one allows the nucleotide-lipid pairs of the membrane to be characterized by a distribution of quark-antiquark pairs. Cell membrane -or at least the axonal parts of neurons- would define a sensory representation in which is a pair of this kind defines a pixel characterized by primary qualia. Cells would be sensory homunculi and DNA defines a sensory hologram of body of or of part of it. Among other things this would give a precise content to the notion of grandma cell.
3. Josephson frequencies of biologically important ions are in one-one correspondence with the qualia and Josephson radiation could re-generate the qualia or map them to different qualia in a one-one and synesthetic manner in the neurons of the sensory pathway. For large values of Planck constant Josephson frequencies are in EEG range so that a direct connection with EEG emerges and Josephson radiation indeed corresponds to both biophotons and EEG. This would realize the notion of sensory pathway which originally seemed to me a highly non-realistic notion and led to the vision that sensory qualia can be realized only at the level of sensory organs in TGD framework.
4. At the level of brain motor action and sensory perception look like reversals of each other. In zero energy ontology motor action can be indeed seen as a time reversed sensory perception so that the model of sensory representations implies also a model for motor action. Magnetic body serves as a sensory canvas where cyclotron transitions induced by Josephson frequencies induce conscious sensory map entangling the points of the magnetic body with brain and body.

11.4.4 A general model of qualia and sensory receptor

The identification of sensory qualia in terms of quantum number increments and geometric qualia representing geometric and kinematic information in terms of moduli of CD , the assignment of sensory qualia with the membrane of sensory receptor, and capacitor model of qualia are basic ideas behind the model. The communication of sensory data to magnetic body using Josephson photons is also a key aspect of the model.

A general model of qualia

It is good to start by summarizing the general vision about sensory qualia and geometric qualia in TGD Universe.

1. The basic assumption is that sensory qualia correspond to increments of various quantum numbers in quantum jump. Standard model quantum numbers- color quantum numbers, electromagnetic charge and weak isospin, and spin are the most obvious candidates. Also cyclotron transitions changing the integer characterizing cyclotron state could correspond to some kind of quale- perhaps 'a feeling of existence'. This could make sense for the qualia of the magnetic body.

2. Geometric qualia could correspond to the increments of zero modes characterizing the induced CP_2 Kähler form of the partonic 2-surface and of the moduli characterizing the causal diamonds serving as geometric correlates of selves. This moduli space involves the position of CD and the relative position of tips as well as position in CP_2 and relative position of two CP_2 points assigned to the future and past boundaries of CD . There are good motivations for proposing that the relative positions are quantized. This gives as a special case the quantization of the scale of CD in powers of two. Position and orientation sense could represent this kind of qualia. Also kinematical qualia like sensation of acceleration could correspond to geometric qualia in generalized 4-D sense. For instance, the sensation about motion could be coded by Lorentz boosts of sub- CD representing mental image about the object.
3. One can in principle distinguish between qualia assignable to the biological body (sensory receptors in particular) and magnetic body. The basic question is whether sensory qualia can be assigned only with the sensory receptors or with sensory pathways or with both. Geometric qualia might be assignable to the magnetic body and could provide third person perspective as a geometric and kinematical map of the body and its state of motion represented using the moduli space assignable to causal diamonds (CD). This map could be provided also by the body in which case the magnetic body would only share various mental images. The simplest starting assumption consistent with neuro-science is that sensory qualia are assigned with the cell membrane of sensory receptor and perhaps also with the neurons receiving data from it carried by Josephson radiation coding for the qualia and possibly partially regenerating them if the receiving neuron has same value of membrane potential as the sensory receptor when active. Note that during nerve pulse also this values of membrane potential is achieved for some time.

Could some sensory qualia correspond to the sensory qualia of the magnetic body?

Concerning the understanding of a detailed model for how sensory qualia are generated, the basic guideline comes from the notion of magnetic body and the idea that sensory data are communicated to the magnetic body as Josephson radiation associated with the cell membrane. This leaves two options: either the primary a sensory qualia are generated at the level of sensory receptor and the resulting mental images negentropically entangle with the "feeling of existence" type mental images at the magnetic body or they can be also generated at the level of the magnetic body by Josephson radiation -possibly as cyclotron transitions. The following arguments are to-be-or-not-to-be questions about whether the primary qualia must reside at the level of sensory receptors.

1. Cyclotron transitions for various cyclotron condensates of bosonic ions or Cooper pairs of fermionic ions or elementary particles are assigned with the motor actions of the magnetic body and Josephson frequencies with the communication of the sensory data. Therefore it would not be natural to assign qualia with cyclotron transitions. On the other hand, in zero energy ontology motor action can be regarded formally as a time reversed sensory perception, which suggests that cyclotron transitions correlated with the "feeling of existence" at magnetic body entangled with the sensory mental images. They could also code for the pitch of sound as will be found but this quale is strictly speaking also a geometric quale in the 4-D framework.
2. If Josephson radiation induces cyclotron transitions, the energy of Josephson radiation must correspond to that of cyclotron transition. This means very strong additional constraint not easy to satisfy except during nerve pulse when frequencies varying from about 10^{14} Hz down to kHz range are emitted the system remains Josephson contact. Cyclotron frequencies are also rather low in general, which requires that the value of \hbar must be large in order to have cyclotron energy above the thermal threshold. This would however conform with the very beautiful dual interpretation of Josephson photons in terms of biophotons and EEG. One expects that only high level qualia can correspond to a very large values of \hbar needed.

For the sake of completeness it should be noticed that one might do without large values of \hbar if the carrier wave with frequency defined by the metabolic energy quantum assignable to the kicking and that the small modulation frequency corresponds to the cyclotron frequency. This would require that Josephson frequency corresponds to the frequency defined by the metabolic quantum. This is not consistent with the fact that very primitive organisms possess sensory systems.

3. If all primary qualia are assigned to the magnetic body, Josephson radiation must include also gluons and light counter parts of weak bosons are involved besides photons. This is quite a strong additional assumption and it will be found that the identification of sensory qualia in terms of quantum numbers of quark pair restrictes them to the cell membrane. The coding of qualia by Josephson frequencies is however possible and makes it possible to regenerate them in nervous system. The successful model explaining the peak frequencies of photoreceptors in terms of ionic cyclotron frequencies supports this view and provides a realization for an old idea about spectroscopy of consciousness which I had already been ready to give up.

Capacitor model of sensory qualia

In capacitor model of sensory receptor the increments of quantum numbers are amplified as particles with given quantum numbers flow between the plates of capacitor like system and the second plate defines the subself responsible for the mental image. The generation of complementary qualia assignable to the two plates and bringing in mind complementary colors is predicted. The capacitor is at the verge of di-electric breakdown. The interior and exterior of the receptor cell are the most plausible candidates for the capacitor plates with lipid layers defining the analog of di-electric able to changes its properties. Josephson currents generating Josephson radiation could communicate the sensory percept to the magnetic body but would not generate genuine sensory qualia there (the pitch of sound would be interpreted as a geometric quale). The coding is possible if the basic qualia correspond in one-one manner to ionic Josephson currents. There are sensory receptors which themselves do not fire (this is the case for hair cells for hearing and tactile receptor cells) and in this case the neuron next to the receptor in the sensory pathway would take the role of the quantum critical system.

The notion of sensory capacitor can be generalized. In zero energy ontology the plates could be effectively replaced with positive and negative energy parts of zero energy state or with cyclotron Bose-Einstein condensates corresponding to two different energies. Plates could also correspond to a pair of space-time sheets labeled by different p -adic primes and the generation of quale would correspond in this case to a flow of particles between the space-time sheets or magnetic flux tubes connected by contacts defining Josephson junctions.

The TGD inspired model for photoreceptors [27] relies crucially on the assumption that sensory neurons at least and probably all cell membranes correspond to nearly vacuum extremals with the value of Weinberg angle equal to $\sin^2(\theta_W) = .0295$ and weak bosons having Compton length of order cell size and ordinary value of Planck constant. This also explains the large parity breaking effects in living matter. The almost vacuum extremal property conforms with the vision about cell membrane as a quantum critical system ideal for acting as a sensory receptor.

11.4.5 Detailed model for the qualia

The proposed vision about qualia requires a lot of new physics provided by TGD. What leads to a highly unique proposal is the intriguing coincidence of fundamental elementary particle time scales with basic time scales of biology and neuro science and the model of DNA as topological quantum computer [44].

1. Zero energy ontology brings in the size scale of CD assignable to the field body of the elementary particle. Zero energy states with negentropic time-like entanglement between positive and negative energy parts of the state might provide a key piece of the puzzle. The negentropic entanglement between positive energy parts of the states associated with the sub- CD assignable to the cell membrane and sub- CD at the magnetic body is expected to be an important factor.
2. For the standard value of \hbar the basic prediction would be 1 ms second time scale of d quark, 6.5 ms time scale of u quark, and .1 second time scale of electron as basic characterizes of sensory experience if one accept the most recent estimates $m(u) = 2$ MeV and $m(d) = 5$ MeV for the quark masses [43]. These time scales correspond to 10 Hz, 160 Hz, and 1280 Hz frequencies, which all characterize neural activity (for the identification of 160 Hz frequency as cerebellar resonance frequency see [70]). Hence quarks could be the most interesting particles as far as qualia are considered and the first working hypothesis would be that the fundamental quantum number increments correspond to those for quark-anti-quark pair. The identification in terms of quantum numbers of single quark is inconsistent with the model of color qualia.

3. The model of DNA as topological quantum computer led to the proposal that DNA nucleotides are connected to the lipids of the cell membrane by magnetic flux tubes having quark and antiquark at its ends such that the u and d quarks and their antiquarks code for the four nucleotides. The outer lipid layer was also assumed to be connected by flux tubes to the nucleotide in some other cell or in cell itself.
4. The model for DNA as topological quantum computer did not completely specify whether the flux tubes are ordinary flux tubes or wormhole flux tubes with possibly opposite signs of energy assigned with the members of the flux tube pair. Although it is not necessary, one could assume that the quantum numbers of the two parallel flux tubes cancel each other so that wormhole flux tube would be characterized by quantum numbers of quark pairs at its ends. It is not even necessary to assume that the net quantum numbers of the flux tubes vanish. Color confinement however suggests that the color quantum at the opposite ends of the flux tube are of opposite sign.
 - (a) The absence of a flux tube between lipid layers was interpreted as an isolation from external world during the topological quantum computation. The emergence of the flux tube connection means halting of topological quantum computation. The flux tube connection with the external world corresponds to sensory perception at the level of DNA nucleotide in consistency with the idea that DNA plays the role of the brain of cell [29]. The total color quantum numbers at the ends of the flux tubes were assumed to sum up to zero. This means that the fusion of the flux tubes ending to the interior and exterior cell membrane to single one creates a flux tube state not localized inside cell and that the interior of cell carries net quantum numbers. The attractive interpretation is that this process represents the generation of quale of single nucleotide.
 - (b) The formation of the flux tube connection between lipid layers would involve the transformation of both quark-antiquark pairs to an intermediate state. There would be no kinematic constraints on the process nor to the mass scales of quarks. A possible mechanism for the separation of the two quark-antiquark pairs associated with the lipids from the system is double reconnection of flux tubes which leads to a situation in which the quark-antiquark pairs associated with the lipid layers are connected by short flux loops and separated to a disjoint state and there is a long wormhole flux tube connecting the nucleotides possibly belonging to different cells.
 - (c) The state of two quark pairs need not have vanishing quantum numbers and one possibility is that the quantum numbers of this state code for qualia. If the total numbers of flux tubes are vanishing also the net quantum numbers of the resulting long flux tube connecting two different cells provide equivalent coding. A stronger condition is that this state has vanishing net quantum numbers and in this case the ends of the long flux tube would carry opposite quantum numbers. The end of flux tube at DNA nucleotide would characterize the quale.
5. Two identification of primary qualia are therefore possible.
 - (a) If the flux tubes have vanishing net quantum numbers, the primary sensory quale can be assigned to single receptor cell and the flow of the quantum numbers corresponds to the extension of the system with vanishing net quantum numbers in two-cell system.
 - (b) If the net quantum numbers of the flux tube need not vanish, the resulting two cell system carries non-vanishing quantum numbers as the pair of quark-antiquark pairs removes net quantum numbers out of the system.
6. If the net quantum numbers for the flux tubes vanish always, the specialization of the sensory receptor membrane to produce a specific quale would correspond to an assignment of specific quantum numbers at the DNA ends of the wormhole flux tubes attached to the lipid layers of the cell membrane. The simplest possibility that one can imagine is that the outer lipid layer is connected to the conjugate DNA nucleotide inside same cell nucleus. This option would however assign vanishing net quantum number increments to the cell as whole and is therefore unacceptable.

7. The formation of a temporary flux tube connection with another cell is necessary during the generation of quale and the question is what kind of cell is in question. The connection of the receptor to cells along the sensory pathway are expected to be present along the entire sensory pathway from DNA nucleotide to a nucleotide in the conjugate strand of second neuron to DNA nucleotide of the third neuron.... If Josephson photons are able to regenerate the quale in second neuron this would make it possible to replicate the quale along entire sensory pathway. The problem is that Josephson radiation has polarization orthogonal to axons and must propagate along the axon whereas the flux tube connection must be orthogonal to axon. Hence the temporary flux tube connection is most naturally between receptor cells and would mean horizontal integration of receptor cells to a larger structure. A holistic process in directions parallel and orthogonal to the sensory pathway would be in question. Of course, the flux tube could be also curved and connect the receptor to the next neuron along the sensory pathway.
8. The specialization of the neuron to sensory receptor would require in the framework of positive energy ontology that -as far as qualia assignable to the electro-weak quantum numbers are considered - all DNA nucleotides are identical by the corresponds of nucleotides with quarks and antiquarks. This cannot be the case. In zero energy ontology and for wormhole flux tubes it is however enough to assume that the net electroweak quantum numbers for the quark antiquark pairs assignable to the DNA wormhole contact are same for all nucleotides. This condition is easy to satisfy. It must be however emphasized that there is no reason to require that all nucleotides involved generate same quale and at the level of neurons sensory maps assigning different qualia to different nucleotides and lipids allowing DNA to sensorily perceive the external world are possible.

The model should be consistent with the assignment of the fundamental bio-rhythms with the *CDs* of electron and quarks.

1. Quark color should be free in long enough scales and cellular length scales are required at least. The QCD in question should therefore have long enough confinement length scales. The first possibility is provided by almost vacuum extremals with a long confinement scale also at the flux tubes. Large \hbar for the cell membrane space-time sheet seems to be unavoidable and suggests that color is free in much longer length scale than cell length scale.
2. Since the length of the flux tubes connecting DNA and cell membrane is roughly 1 micrometer and by a factor of order 10^7 longer than the d quark Compton length, it seems that the value of Planck constant must be of this order for the flux tubes. This however scales up the time scale of d quark *CD* by a factor of 10^{14} to about 10^4 years! The millisecond and 160 ms time scales are much more attractive. This forces to ask what happens to the quark-anti-quark pairs at the ends of the tubes.
3. The only possibility seems to be that the reconnection process involves a phase transition in which the closed flux tube structure containing the two quark pairs assignable to the wormhole contacts at lipid layers is formed and leaks to the page of the Big Book with pages partially labeled by the values of Planck constant. This page would correspond to the standard value of Planck constant so that the corresponding d quark *CDs* would have a duration of millisecond. The reconnection leading to the ordinary situation would take place after millisecond time scale. The standard physics interpretation would be as a quantum fluctuation having this duration. This sequence of quark sub-*CDs* could define what might be called memetic codon representation of the nerve pulse sequence.
4. One can also consider the possibility is that near vacuum extremals give rise to a copy of hadron physics for which the quarks associated with the flux tubes are light. The Gaussian Mersennes corresponding to $k = 151, 157, 163, 167$ define excellent p-adic time scales for quarks and light variants of weak gauge bosons. Quark mass 5 MeV would with $k = 120$ would be replaced with $k = 163$ (167) one would have mass 1.77 eV (.44 eV). Small scaling of both masses gives 2 eV and .5 eV which correspond to basic metabolic quanta in TGD framework. For quark mass of 2 MeV with $k = 123$ $k = 163$ (167) one would give masses .8 eV (.05 eV). The latter scale correspond to Josephson energy assignable with the membrane potential in the ordinary phase.

In this case a phase transition transforming almost vacuum extremal to ordinary one takes place. What this would mean that the vacuum extremal property would hold true below much shorter p-adic length scale. In zero energy ontology the scaling up of quark masses is in principle possible. This option looks however too artificial.

11.4.6 Overall view about qualia

This picture leads to the following overall view about qualia. There are two options depending on whether single quark-antiquark pair or two of them labels the qualia. In the following only the simpler option with single quark-antiquark pair is discussed.

1. All possible pairings of spin and electroweak isospin (or em charge) define 16 basic combinations if one assumes color singletness. If arbitrary color is allowed, there is a nine-fold increase of quantum numbers decomposable to color singlet and octet qualia and further into 3×15 qualia with vanishing increments of color quantum numbers and 6×16 qualia with non-vanishing increments of color quantum numbers. The qualia with vanishing increments for electroweak quantum numbers could correspond to visual colors. If electroweak quantum numbers of the quark-anti-quark pair vanish, one has 3×7 *resp.* 6×8 combinations of colorless *resp.* colored qualia.
2. There is a huge number of various combinations of these fundamental qualia if one assumes that each nucleotide defines its own quale and fundamental qualia would be analogous to constant functions and more general qualia to general functions having values in the space with $9 \times 16 - 1$ points. Only a very small fraction of all possible qualia could be realized in living matter unless the neurons in brain provide representations of body parts or of external world in terms of qualia assignable to lipid-nucleotide pairs. The passive DNA strand would be ideal in this respect.
3. The basic classification of qualia is as color qualia, electro-weak quale, and spin quale and products of these qualia. Also combinations of color qualia and and electroweak and spin quale are possible and could define exotic sensory qualia perhaps not yet realized in the evolution. Synesthesia is usually explained in terms of sensory leakage between sensory pathways and this explanation makes sense also in TGD framework if there exists a feedback from the brain to the sensory organ. Synesthesia cannot however correspond to the product qualia: for "quantum synesthesia" cross association works in both directions and this distinguishes it from the ordinary synesthesia.
4. The idea about brain and genome as holograms encourages to ask whether neurons or equivalently DNA could correspond to sensory maps with individual lipids representing qualia combinations assignable to the points of the perceptive field. In this framework quantum synesthesia would correspond to the binding of qualia of single nucleotide (or lipid) of neuron cell membrane as a sensory representation of the external world. DNA is indeed a holographic representation of the body (gene expression of course restricts the representation to a part of organism). Perhaps it is this kind of representation also at the level of sensory experience so that all neurons could be little sensory copies of body parts as holographic quantum homunculi. In particular, in the associative areas of the cortex neurons would be quantum synesthetes experiencing the world in terms of composite qualia.
5. The number of flux tube connections generated by sensory input would code for the intensity of the quale. Josephson radiation would do the same at the level of communications to the magnetic body. Also the temporal pattern of the sequence of quale mental images matters. In the case of hearing this would code for the rhythmic aspects and pitch of the sound.

11.4.7 About detailed identification of the qualia

One can make also guesses about detailed correspondence between qualia and quantum number increments.

1. Visual colors would correspond to the increments of only color quantum numbers. Each biologically important ion would correspond to its own color increment in one-one correspondence with

the three pairs of color-charged gluons and these would correspond to blue-yellow, red-green, and black white [27]. Black-white vision would mean a restriction to the $SU(2)$ subgroup of color group. The model for the cell membrane as a nearly vacuum extremal assigns the peak frequencies corresponding to fundamental colors with biologically important ions. Josephson radiation could induce artificially the same color qualia in other neurons and this might provide a manner to communicate the qualia to the brain where they could be re-experienced at neuronal level. Some organisms are able to perceive also the polarization of light. This requires receptors sensitive to polarization. The spin of quark pair would naturally code for polarization quale.

2. Also tastes and odours define qualia with "colors". Certainly the increments of electroweak numbers are involved but since these qualia do not have any directional flavor, spin is probably not involved. This would give $c 3 \times 4$ basic combinations are possible and can certainly explain the 5 or 6 basic tastes (counted as the number of different receptors). Whether there is a finite number of odours or not has been a subject of a continual debate and it might be that odours already correspond to a distribution of primary qualia for the receptor cell. That odours are coded by nerve pulse patterns for a group of neurons [71] would conform with this picture.
3. Hearing seems to represent a rather colorless quale so that electroweak isospin suggests again itself. If we had a need to hear transversely polarized sound also spin would be involved. Cilia are involved also with hair cells acting as sensory receptors in the auditory system and vestibular system. In the case of hearing the receptor itself does not fire but induces a firing of the higher level neuron. The temporal pattern of qualia mental images could define the pitch of the sound whereas the intensity would correspond to the number of flux tube connections generated.

The modulation of Josephson frequencies -rather than Josephson frequencies as such- would code for the pitch and the total intensity of the Josephson radiation for the intensity of the sound and in fact any quale. Pitch represents non-local information and the qualia subselves should be negentropically entangled in time direction. If not, the experience corresponds to a sequence of sound pulses with no well-defined pitch and responsible for the rhythmic aspects of music. Right brain sings-left brain talks metaphor would suggest that right and left brain have different kind of specializations already at the level of sensory receptors.

4. Somato-sensory system gives rise to tactile qualia like pain, touch, temperature, proprioception (body position). There are several kinds of receptors: nociceptors, mechanoreceptors, thermoreceptors, etc... Many of these qualia have also emotional coloring and it might be that the character of entanglement involved (negentropic/entropic defines the emotional color of the quale. If this is the case, one might consider a pure quale of touch as something analogous to hearing quale. One can argue that directionality is basic aspect of some of these qualia -say sense of touch- so that spin could be involved besides electroweak quantum numbers. The distribution of these qualia for the receptor neuron might distinguish between different tactile qualia.

Bibliography

Books about TGD

- [1] M. Pitkänen (2006), *Topological Geometroynamics: Overview*.
http://tgd.wippiespace.com/public_html/tgdview/tgdview.html.
- [2] M. Pitkänen (2006), *Quantum Physics as Infinite-Dimensional Geometry*.
http://tgd.wippiespace.com/public_html/tgdgeom/tgdgeom.html.
- [3] M. Pitkänen (2006), *Physics in Many-Sheeted Space-Time*.
http://tgd.wippiespace.com/public_html/tgdclass/tgdclass.html.
- [4] M. Pitkänen (2006), *p-Adic length Scale Hypothesis and Dark Matter Hierarchy*.
http://tgd.wippiespace.com/public_html/paddark/paddark.html.
- [5] M. Pitkänen (2006), *Quantum TGD*.
http://tgd.wippiespace.com/public_html/tgdquant/tgdquant.html.
- [6] M. Pitkänen (2006), *TGD as a Generalized Number Theory*.
http://tgd.wippiespace.com/public_html/tgdnumber/tgdnumber.html.
- [7] M. Pitkänen (2006), *TGD and Fringe Physics*.
http://tgd.wippiespace.com/public_html/freenergy/freenergy.html.

Books about TGD Inspired Theory of Consciousness and Quantum Biology

- [8] M. Pitkänen (2006), *TGD Inspired Theory of Consciousness*.
http://tgd.wippiespace.com/public_html/tgdconsc/tgdconsc.html.
- [9] M. Pitkänen (2006), *Bio-Systems as Self-Organizing Quantum Systems*.
http://tgd.wippiespace.com/public_html/bioselforg/bioselforg.html.
- [10] M. Pitkänen (2006), *Quantum Hardware of Living Matter*.
http://tgd.wippiespace.com/public_html/bioware/bioware.html.
- [11] M. Pitkänen (2006), *Bio-Systems as Conscious Holograms*.
http://tgd.wippiespace.com/public_html/hologram/hologram.html.
- [12] M. Pitkänen (2006), *Genes and Memes*.
http://tgd.wippiespace.com/public_html/genememe/genememe.html.
- [13] M. Pitkänen (2006), *Magnetospheric Consciousness*.
http://tgd.wippiespace.com/public_html/magnconsc/magnconsc.html.
- [14] M. Pitkänen (2006), *Mathematical Aspects of Consciousness Theory*.
http://tgd.wippiespace.com/public_html/mathconsc/mathconsc.html.
- [15] M. Pitkänen (2006), *TGD and EEG*.
http://tgd.wippiespace.com/public_html/tgdeeg/tgdeeg.html.

References to the chapters of the books about TGD

- [16] M. Pitkänen (2006), *Physics in Many-Sheeted Space-Time*.
http://tgd.wippiespace.com/public_html/tgdclass/tgdclass.html.
- [17] The chapter *Construction of Configuration Space Kähler Geometry from Symmetry Principles* of [2].
http://tgd.wippiespace.com/public_html/tgdgeom/tgdgeom.html#compl1.
- [18] The chapter *Does the QFT Limit of TGD Have Space-Time Super-Symmetry?* of [5].
http://tgd.wippiespace.com/public_html/tgdquant/tgdquant.html#susy.
- [19] The chapter *Quantum Hall effect and Hierarchy of Planck Constants* [5].
http://tgd.wippiespace.com/public_html/tgdquant/tgdquant.html#anyontgd.
- [20] The chapter *TGD and Nuclear Physics* of [4].
http://tgd.wippiespace.com/public_html/paddark/paddark.html#padnucl.
- [21] The chapter *Nuclear String Model* of [4].
http://tgd.wippiespace.com/public_html/paddark/paddark.html#nuclstring.
- [22] The chapter *Was von Neumann Right After All* of [5].
http://tgd.wippiespace.com/public_html/tgdquant/tgdquant.html#vNeumann.
- [23] The chapter *Dark Nuclear Physics and Condensed Matter* of [4].
http://tgd.wippiespace.com/public_html/paddark/paddark.html#exonuclear.
- [24] The chapter *Identification of the Configuration Space Kähler Function* of [2].
http://tgd.wippiespace.com/public_html/tgdgeom/tgdgeom.html#kahler.
- [25] The chapter *p-Adic Particle Massivation: New Physics* of [4].
http://tgd.wippiespace.com/public_html/paddark/paddark.html#mass4.
- [26] The chapter *Does TGD Predict the Spectrum of Planck Constants?* of [5].
http://tgd.wippiespace.com/public_html/tgdquant/tgdquant.html#Planck.

References to the chapters of the books about TGD Inspired Theory of Consciousness and Quantum Biology

- [27] The chapter *Quantum Model for Nerve Pulse* of [15].
http://tgd.wippiespace.com/public_html//tgdeeg/tgdeeg/tgdeeg.html#pulse.
- [28] The chapter *Topological Quantum Computation in TGD Universe* of [12].
http://tgd.wippiespace.com/public_html/genememe/genememe.html#tqc.
- [29] The chapter *Self and Binding* of [8].
http://tgd.wippiespace.com/public_html/tgdconsc/tgdconsc.html#selfbindc.
- [30] The chapter *Dark Matter Hierarchy and Hierarchy of EEGs* of [15].
http://tgd.wippiespace.com/public_html/tgdeeg/tgdeeg.html#eegdark.
- [31] The chapter *DNA as Topological Quantum Computer* of [12].
http://tgd.wippiespace.com/public_html/genememe/genememe.html#dnatqc.
- [32] The chapter *Homeopathy in Many-Sheeted Space-Time* of [11].
http://tgd.wippiespace.com/public_html/hologram/hologram.html#homeoc.
- [33] The chapter *Could Genetic Code Be Understood Number Theoretically?* of [12].
http://tgd.wippiespace.com/public_html/genememe/genememe.html#genenumber.

- [34] The chapter *General Theory of Qualia* of [11].
http://tgd.wippiespace.com/public_html/hologram/hologram.html#qualia.
- [35] The chapter *Negentropy Maximization Principle* of [8].
http://tgd.wippiespace.com/public_html/tgdconsc/tgdconsc.html#nmpc.

Appendices and references to some older books

- [36] M. Pitkänen (2006) *Basic Properties of CP_2 and Elementary Facts about p -Adic Numbers*
http://tgd.wippiespace.com/public_html/pdfpool/append.pdf.

Articles related to TGD

- [37] M. Pitkänen (2007), *Further Progress in Nuclear String Hypothesis*, http://tgd.wippiespace.com/public_html/articles/nuclstring.pdf.

Mathematics

Theoretical physics

- [38] *Montonen Olive Duality*. http://en.wikipedia.org/wiki/Montonen-Olive_duality.

Particle and nuclear physics

- [39] E. Storms (2001), *Cold fusion, an objective assessment*,
<http://home.netcom.com/~storms2/review8.html>.
- [40] C. L. Kervran (1972), *Biological transmutations, and their applications in chemistry, physics, biology, ecology, medicine, nutrition, agriculture, geology*, Swan House Publishing Co.
- [41] P. Tompkins and C. Bird (1973), *The secret life of plants*, Harper & Row, New York.
- [42] S. E. Shnoll *et al* (1998), *Realization of discrete states during fluctuations in macroscopic processes*, Uspekhi Fisicheskikh Nauk, Vol. 41, No. 10, pp. 1025-1035.
- [43] D. T. H. Davies *et al* (2010), *Precise Charm to Strange Mass Ratio and Light Quark Masses from Full Lattice QCD*. Phys. Rev. Lett. 104, 132003. <http://prl.aps.org/abstract/PRL/v104/i13/e132003>.
A. Cho (2010), *Mass of the common quark finally nailed down*. <http://news.sciencemag.org/sciencenow/2010/04/mass-of-the-common-quark-finally.html>.
- [44] V. M. Lobashev *et al*(1996), in *Neutrino 96* (Ed. K. Enqvist, K. Huitu, J. Maalampi). World Scientific, Singapore.
- [45] J. D. Bjorken (1997), Acta Phys. Polonica B. V. 28. p. 2773.

Condensed matter physics

- [46] J-C. Li and D.K. Ross (1993), *Evidence of Two Kinds of Hydrogen Bonds in Ices*. J-C. Li and D.K. Ross, Nature, 365, 327-329.

- [47] M. Chaplin (2005), *Water Structure and Behavior*. <http://www.lsbu.ac.uk/water/index.html>.
For 41 anomalies see <http://www.lsbu.ac.uk/water/anmlies.html>.
For the icosahedral clustering see <http://www.lsbu.ac.uk/water/clusters.html>.
- [48] W. D. Knight *et al* (1984), *Phys.Rev. Lett.* 52, 2141.
- [49] R. A. Cowley (2004), *Neutron-scattering experiments and quantum entanglement*. *Physica B* 350 (2004) 243-245.
- [50] R. Moreh, R. C. Block, Y. Danon, and M. Neumann (2005), *Search for anomalous scattering of keV neutrons from H₂O-D₂O mixtures*. *Phys. Rev. Lett.* 94, 185301.
- [51] J. K. Borchardt(2003), *The chemical formula H₂O - a misnomer*. *The Alchemist* 8 Aug (2003).
- [52] P. Ball (2005), *A new kind of alchemy*. *New Scientist*, 16 April issue. <http://www.newscientist.com/channel/fundamentals/mg18624951.800>.
- [53] D. J. P. Morris *et al* (2009). *Dirac Strings and Magnetic Monopoles in Spin Ice Dy₂Ti₂O₇*. *Science*, Vol. 326, No. 5951, pp. 411-414.
H. Johnston (1010) *Magnetic monopoles spotted in spin ices*. <http://physicsworld.com/cws/article/news/40302>.
- [54] A. W. Castleman *et al* (2005), *Al Cluster Superatoms as Halogens in Polyhalides and as Alkaline Earths in Iodide Salts*. *Science*, 307, 231-235.
- [55] I. Langmuir (1915), *em The Dissociation of Hydrogen Into Atoms*. *Journal of American Chemical Society* 37, 417.
- [56] R. Matthews (1997), *Wacky Water*. *New Scientist* 154 (2087):4043, 21 June.

Fringe physics

- [57] For the descriptions of Hudson's findings see *Mono-atomic elements*, <http://www.halexandria.org/dward479.htm>, and
David Hudson at IFNS, <http://www.halexandria.org/dward467.htm>.
- [58] J. Hutchison (1994), *The Hutchison Effect Apparatus*, *Proc. of the first Symposium on New Energy*, Denber, May 1994, p. 199.
- [59] J. R. Jochmans (1979), *Strange Relics from the Depths of the Earth*, Litt.D., 1979 - pub. Forgotten Ages Research Society, Lincoln, Nebraska, USA. See also the article at http://www.delusionresistance.org/creation/antedeluvian_finds.html.
- [60] J. Naudin (2005), *Free Energy Atomic Hydrogen: the MAHG project*, <http://jlnlabs.imars.com/mahg/tests/index.htm>.
- [61] W. Corliss (1978), *Ancient Man: A Handbook of Puzzling Artifacts*, The Sourcebook Project, Glen Arm (Maryland). See also <http://www.miqel.com/text/tcookie.html> about mysterious transfers of large chunks of Earth transferred from one place to another.

Biology related references

- [62] M. J. Stevens (2001), *Simple Simulations of DNA Condensation*. *Biophys. J.*, January 2001, p. 130-139, Vol. 80, No.1.
<http://www.biophysj.org/cgi/content/full/80/1/130#E8>.
- [63] N. Y. Sidorova and D.C. Rau (2004), *Differences between EcoRI Nonspecific and "Star" Sequence Complexes Revealed by Osmotic Stress*. *Biophysical Journal* 87:2564-2576. <http://www.biophysj.org/cgi/content/full/87/4/2564>.

- [64] F. A. Popp, B.Ruth, W.Bahr, J. Boehm, P.Grass (1981), G.Grolig, M.Rattemeyer, H.G.Schmidt and P.Wulle: *Emission of Visible and Ultraviolet Radiation by Active Biological Systems*. Collective Phenomena(Gordon and Breach), 3, 187-214.
 F. A. Popp, K. H. Li, and Q. Gu (eds.) (1992): *Recent Advances in Bio-photon Research and its Applications*. World Scientific, Singapore-New Jersey.
 F.- A. Popp: *Photon-storage in biological systems, in: Electromagnetic Bio-Information*. pp.123-149. Eds. F.A.Popp, G.Becker, W.L.König, and W.Peschka. Urban & Schwarzenberg, Muenchen-Baltimore.
 F.-A. Popp (2001), *About the Coherence of Bio-photons*.
<http://www.datadiwan.de/iib/ib0201e1.htm>.
 F.-A. Popp and J.-J. Chang (2001), *Photon Sucking and the Basis of Biological Organization*.
<http://www.datadiwan.de/iib/ib0201e3.htm>.
 F.-A. Popp and Y. Yan (2001), *Delayed Luminescence of Biological Systems in Terms of States*.
<http://www.datadiwan.de/iib/pub2001-07.htm>.
- [65] Fröhlich, H. (1975) *The extraordinary dielectric properties of biological materials and the action of enzymes*. Proc. Natl. Acad. Sci. 72:4211-4215.
Ibid (1968), Int. J. Quantum Chem. 641-649.
Ibid (1970), Nature 316, 349-351.
 H. Fröhlich and F. Kremer (1983), *Coherent Excitations in Biological Systems*. Springer Verlag, New York.
- [66] E. Lozneau and M. Sanduloviciu (2003) *Minimal-cell system created in laboratory by self-organization*. Chaos, Solitons & Fractals, Volume 18, Issue 2, October, p. 335.
 See also *Plasma blobs hint at new form of life*. New Scientist vol. 179, issue 2413 - 20 September 2003, page 16.

Neuroscience

- [67] *Color vision*. http://en.wikipedia.org/wiki/Color_vision.
- [68] *Action potential*. http://en.wikipedia.org/wiki/Action_potential.
- [69] *Photoreceptor cell*. http://en.wikipedia.org/wiki/Photoreceptor_cell.
- [70] G. Cheron *et al* (2004), *Inactivation of Calcium-Binding Protein Genes Induces 160 Hz Oscillations in the Cerebellar Cortex of Alert Mice*. The Journal of Neuroscience, January 14, 2004, 24(2): 434-441.<http://www.jneurosci.org/cgi/content/full/24/2/434>.
- [71] J. P. Miller (1996), *Brain Waves Deciphered*. article about the work of Wehr and Laurent in Nature, vol 384 (14 November).

Consciousness related references

- [72] A. K. Engel *et al*(2000) *Temporal Binding, Binocular Rivalry, and Consciousness*. <http://www.phil.vt.edu/ASSC/engel/engel.html>.

Chapter 12

Super-Conductivity in Many-Sheeted Space-Time

12.1 Introduction

In this chapter various TGD based ideas related to high T_c super-conductivity are discussed studied.

1. Supra currents and Josephson currents provide excellent tools of bio-control allowing large space-time sheets to control the smaller space-time sheets. The predicted hierarchy of dark matter phases characterized by a large value of \hbar and thus possessing scaled up Compton and de Broglie wavelengths allows to have quantum control of short scales by long scales utilizing de-coherence phase transition. Quantum criticality is the basic property of TGD Universe and quantum critical super-conductivity is therefore especially natural in TGD framework. The competing phases could be ordinary and large \hbar phases and supra currents would flow along the boundary between the two phases.
2. It is possible to make a tentative identification of the quantum correlates of the sensory qualia quantum number increments associated with the quantum phase transitions of various macroscopic quantum systems [33] and various kind of Bose-Einstein condensates and super-conductors are the most relevant ones in this respect.
3. The state basis for the fermionic Fock space spanned by N creation operators can be regarded as a Boolean algebra consisting of statements about N basic statements. Hence fermionic degrees of freedom could correspond to the Boolean mind whereas bosonic degrees of freedom would correspond to sensory experiencing and emotions. The integer valued magnetic quantum numbers (a purely TGD based effect) associated with the defect regions of super conductors of type I provide a very robust information storage mechanism and in defect regions fermionic Fock basis is natural. Hence not only fermionic super-conductors but also their defects are biologically interesting [34, 30].

12.1.1 General ideas about super-conductivity in many-sheeted space-time

The notion of many-sheeted space-time alone provides a strong motivation for developing TGD based view about superconductivity and I have developed various ideas about high T_c super-conductivity [57] in parallel with ideas about living matter as a macroscopic quantum system. A further motivation and a hope for more quantitative modeling comes from the discovery of various non-orthodox super-conductors including high T_c superconductors [57, 42, 36], heavy fermion super-conductors and ferromagnetic superconductors [47, 49, 45]. The standard BCS theory does not work for these super-conductors and the mechanism for the formation of Cooper pairs is not understood. There is experimental evidence that quantum criticality [43] is a key feature of many non-orthodox super-conductors. TGD provides a conceptual framework and bundle of ideas making it possible to develop models for non-orthodox superconductors.

Quantum criticality, hierarchy of dark matters, and dynamical \hbar

Quantum criticality is the basic characteristic of TGD Universe and quantum critical superconductors provide an excellent test bed to develop the ideas related to quantum criticality into a more concrete form. The hypothesis that Planck constants in CD (causal diamond defined as the intersection of the future and past directed light-cones of M^4) and CP_2 degrees of freedom are dynamical possessing quantized spectrum given as rational multiples of minimum value of Planck constant [39, 27] adds further content to the notion of quantum criticality.

The value of \hbar is in the general case given by $\hbar = x_a x_b \hbar_0$ (as it became clear after few guesses). a refers to CD and b to CP_2 . $x_i = n_i$ holds true for singular coverings and $x_i = 1/n_i$ for singular factor spaces. n is the order of maximal cyclic subgroup $Z_n \subset G$, where G defines singular covering or factor space. In principle all rational values of $r = \hbar/\hbar_0$ are possible.

Phases with different values x_i behave like dark matter with respect to each other in the sense that they do not have direct interactions except at criticality corresponding to a leakage between different sectors of imbedding space glued together along CD or CP_2 factors. The scalings of CD and CP_2 covariant metrics are from anyonic arguments given by r^2 and 1 so that the value of effective \hbar appearing in Schrödinger equation is given by $r = x_a x_b$ and in principle can have all positive rational values. In large $\hbar(CD)$ phases various quantum time and length scales are scaled up which means macroscopic and macro-temporal quantum coherence.

Number theoretic considerations favor the hypothesis that the integers corresponding to Fermat polygons constructible using only ruler and compass and given as products $n_F = 2^k \prod_s F_s$, where $F_s = 2^{2^s} + 1$ are distinct Fermat primes, are favored. The reason would be that quantum phase $q = \exp(i\pi/n)$ is in this case expressible using only iterated square root operation by starting from rationals. The known Fermat primes correspond to $s = 0, 1, 2, 3, 4$ so that the hypothesis is very strong and predicts that p-adic length scales have satellite length scales given as multiples of n_F of fundamental p-adic length scale. $n_F = 2^{11}$ corresponds in TGD framework to a fundamental constant expressible as a combination of Kähler coupling strength, CP_2 radius and Planck length appearing in the expression for the tension of cosmic strings, and seems to be especially favored in living matter [43]. There is however no reason to assume that this would be the value of Planck constant in say high T_c super-conductivity.

The only coupling constant strength of theory is Kähler coupling constant g_K^2 which appears in the definition of the Kähler function K characterizing the geometry of the configuration space of 3-surfaces (the "world of classical worlds"). The exponent of K defines vacuum functional analogous to the exponent of Hamiltonian in thermodynamics. The allowed value(s) of g_K^2 , which is (are) analogous to critical temperature(s), is (are) determined by quantum criticality requirement. Contrary to the original hypothesis inspired by the requirement that gravitational coupling is renormalization group invariant, α_K does not seem to depend on p-adic prime whereas gravitational constant is proportional to L_p^2 . The situation is saved by the assumption that gravitons correspond to the largest non-super-astrophysical Mersenne prime M_{127} so that gravitational coupling is effectively RG invariant in p-adic coupling constant evolution [26].

$\hbar(CD)$ and $\hbar(CP_2)$ appear in the commutation and anticommutation relations of various super-conformal algebras. Only $r = \hbar/\hbar_0 = x_a x_b$ of CD and CP_2 Planck constants appears in Kähler action and is due to the fact that the CD and CP_2 metrics of the imbedding space sector with given values of Planck constants are proportional to the corresponding Planck constants [39]. This implies that Kähler function codes for radiative corrections to the classical action, which makes possible to consider the possibility that higher order radiative corrections to functional integral vanish as one might expect at quantum criticality. For a given p-adic length scale space-time sheets with all allowed values of Planck constants are possible. Hence the spectrum of quantum critical fluctuations could in the ideal case correspond to the spectrum of Planck constants coding for the scaled up values of Compton lengths and other quantal lengths and times. If so, large \hbar phases could be crucial for understanding of quantum critical superconductors, in particular high T_c superconductors. For a fixed value of $x_a x_b$ one obtains zoomed up versions of particles with size scaled up by $x_a x_b$.

A further great idea is that the transition to large \hbar phase occurs when perturbation theory based on the expansion in terms of gauge coupling constant ceases to converge: Mother Nature would take care of the problems of theoretician. The transition to large \hbar phase obviously reduces gauge coupling strength α so that higher orders in perturbation theory are reduced whereas the lowest order "classical" predictions remain unchanged. A possible quantitative formulation of the criterion is that maximal

2-particle gauge interaction strength parameterized as $Q_1 Q_2 \alpha$ satisfies the condition $Q_1 Q_2 \alpha \simeq 1$.

TGD actually predicts an infinite hierarchy of phases behaving like dark or partially dark matter with respect to the ordinary matter [28] and the value of \hbar is only one characterizer of these phases. These phases, especially so large \hbar phase, seem to be essential for the understanding of even ordinary hadronic, nuclear and condensed matter physics [28, 23, 27]. This strengthens the motivations for finding whether dark matter might be involved with quantum critical super-conductivity.

Cusp catastrophe serves as a metaphor for criticality. In the recent case temperature and doping are control variables and the tip of cusp is at maximum value of T_c . Critical region correspond to the cusp catastrophe. Quantum criticality suggests the generalization of the cusp to a fractal cusp. Inside the critical lines of cusp there are further cusps which corresponds to higher levels in the hierarchy of dark matters labeled by increasing values of \hbar and they correspond to a hierarchy of subtle quantum coherent dark matter phases in increasing length scales. The proposed model for high T_c super-conductivity involves only single value of Planck constant but it might be that the full description involves very many values of them.

Many-sheeted space-time concept and ideas about macroscopic quantum phases

Many-sheeted space-time leads to obvious ideas concerning the realization of macroscopic quantum phases.

1. The dropping of particles to larger space-time sheets is a highly attractive mechanism of super-conductivity. If space-time sheets are thermally isolated, the larger space-time sheets could be at extremely low temperature and super-conducting.
2. The possibility of large \hbar phases allows to give up the assumption that space-time sheets characterized by different p-adic length scales are thermally isolated. The scaled up versions of a given space-time sheet corresponding to a hierarchy of values of \hbar are possible such that the scale of kinetic energy and magnetic interaction energy remain same for all these space-time sheets. For the scaled up variants of space-time sheet the critical temperature for superconductivity could be higher than room temperature.
3. The idea that wormhole contacts can form macroscopic quantum phases and that the interaction of ordinary charge carriers with the wormhole contacts feeding their gauge fluxes to larger space-time sheets could be responsible for the formation of Cooper pairs, have been around for a decade [31]. The rather recent realization that wormhole contacts can be actually regarded as space-time correlates for Higgs particles suggests also a new view about the photon massivation in super-conductivity.
4. Quantum classical correspondence has turned out be a very powerful idea generator. For instance, one can ask what are the space-time correlates for various notions of condensed matter such as phonons, BCS Cooper pairs, holes, etc...

12.1.2 TGD inspired model for high T_c superconductivity

The TGD inspired model for high T_c super-conductivity relies on the notions of quantum criticality, dynamical quantized Planck constant requiring a generalization of the 8-D imbedding space to a book like structure, and many-sheeted space-time. In particular, the notion of magnetic flux tube as a carrier of supra current of central concept.

With a sufficient amount of twisting and weaving these basic ideas one ends up to concrete models for high T_c superconductors as quantum critical superconductors consistent with the qualitative facts that I am personally aware. The following minimal model looks the most realistic option found hitherto.

1. The general idea is that magnetic flux tubes are carriers of supra currents. In anti-ferromagnetic phases these flux tube structures form small closed loops so that the system behaves as an insulator. Some mechanism leading to a formation of long flux tubes must exist. Doping creates holes located around stripes, which become positively charged and attract electrons to the flux tubes.

2. The higher critical temperature T_{c1} corresponds to a formation local configurations of parallel spins assigned to the holes of stripes giving rise to a local dipole fields with size scale of the order of the length of the stripe. Conducting electrons form Cooper pairs at the magnetic flux tube structures associated with these dipole fields. The elongated structure of the dipoles favors angular momentum $L = 2$ for the pairs. The presence of magnetic field favors Cooper pairs with spin $S = 1$.
3. Stripes can be seen as 1-D metals with delocalized electrons. The interaction responsible for the energy gap corresponds to the transversal oscillations of the magnetic flux tubes inducing oscillations of the nuclei of the stripe. These transverse phonons have spin and their exchange is a good candidate for the interaction giving rise to a mass gap. This could explain the BCS type aspects of high T_c super-conductivity.
4. Above T_c supra currents are possible only in the length scale of the flux tubes of the dipoles which is of the order of stripe length. The reconnections between neighboring flux tube structures induced by the transverse fluctuations give rise to longer flux tubes structures making possible finite conductivity. These occur with certain temperature dependent probability $p(T, L)$ depending on temperature and distance L between the stripes. By criticality $p(T, L)$ depends on the dimensionless variable $x = TL/\hbar$ only: $p = p(x)$. At critical temperature T_c transverse fluctuations have large amplitude and makes $p(x_c)$ so large that very long flux tubes are created and supra currents can run. The phenomenon is completely analogous to percolation [48].
5. The critical temperature $T_c = x_c \hbar/L$ is predicted to be proportional to \hbar and inversely proportional to L (, which is indeed to be the case). If flux tubes correspond to a large value of \hbar , one can understand the high value of T_c . Both Cooper pairs and magnetic flux tube structures represent dark matter in TGD sense.
6. The model allows to interpret the characteristic spectral lines in terms of the excitation energy of the transversal fluctuations and gap energy of the Cooper pair. The observed 50 meV threshold for the onset of photon absorption suggests that below T_c also $S = 0$ Cooper pairs are possible and have gap energy about 9 meV whereas $S = 1$ Cooper pairs would have gap energy about 27 meV. The flux tube model indeed predicts that $S = 0$ Cooper pairs become stable below T_c since they cannot anymore transform to $S = 1$ pairs. Their presence could explain the BCS type aspects of high T_c super-conductivity. The estimate for $\hbar/\hbar_0 = r$ from critical temperature T_{c1} is about $r = 3$ contrary to the original expectations inspired by the model of of living system as a super-conductor suggesting much higher value. An unexpected prediction is that coherence length is actually r times longer than the coherence length predicted by conventional theory so that type I super-conductor could be in question with stripes serving as duals for the defects of type I super-conductor in nearly critical magnetic field replaced now by ferromagnetic phase.
7. TGD predicts preferred values for $r = \hbar/\hbar_0$ and the applications to bio-systems favor powers of $r = 2^{11}$. $r = 2^{11}$ predicts that electron Compton length is of order atomic size scale. Bio-superconductivity could involve electrons with $r = 2^{22}$ having size characterized by the thickness of the lipid layer of cell membrane.

At qualitative level the model explains various strange features of high T_c superconductors. One can understand the high value of T_c and ambivalent character of high T_c super conductors, the existence of pseudogap and scalings laws for observables above T_c , the role of stripes and doping and the existence of a critical doping, etc...

The model explains the observed ferromagnetic super-conductivity at quantum criticality [47]. Since long flux tubes already exist, the overcritical transverse of fluctuations of the magnetic flux tubes inducing reconnections are now not responsible for the propagation of the super currents now. The should however provide the binding mechanism of $S = 1, L = 2$ Cooper pairs via the coupling of the fluctuations to effectively one-dimensional phonons in the direction of flux tubes. Also a modulated ferromagnetic phase consisting of stripes of opposite magnetization direction allows superconductivity [47] and could be understood in terms of $S = 0$ Cooper pairs with electrons of the pair located at the neighboring stripes.

12.2 General TGD based view about super-conductivity

Today super-conductivity includes besides the traditional low temperature super-conductors many other non-orthodox ones [44]. These unorthodox super-conductors carry various attributes such as cuprate, organic, dichalcogenide, heavy fermion, bismute oxide, ruthenate, antiferromagnetic and ferromagnetic. Mario Rabinowitz has proposed a simple phenomenological theory of superfluidity and super-conductivity which helps non-specialist to get a rough quantitative overall view about super-conductivity [44].

12.2.1 Basic phenomenology of super-conductivity

The following provides the first attempt by a non-professional to form an overall view about super-conductivity.

Basic phenomenology of super-conductivity

The transition to super-conductivity occurs at critical temperature T_c and involves a complete loss of electrical resistance. Super-conductors expel magnetic fields (Meissner effect) and when the external magnetic field exceeds a critical value H_c super-conductivity is lost either completely or partially. In the transition to super-conductivity specific heat has singularity. For long time magnetism and super-conductivity were regarded as mutually exclusive phenomena but the discovery of ferromagnetic super-conductors [47, 49] has demonstrated that reality is much more subtle.

The BCS theory developed by Bardeen, Cooper, and Schrieffer in 1957 provides a satisfactory model for low T_c super-conductivity in terms of Cooper pairs. The interactions of electrons with the crystal lattice induce electron-electron interaction binding electrons to Cooper pairs at sufficiently low temperatures. The electrons of Cooper pair are at the top of Fermi sphere (otherwise they cannot interact to form bound states) and have opposite center of mass momenta and spins. The binding creates energy gap E_g determining the critical temperature T_c . The singularity of the specific heat in the transition to super-conductivity can be understood as being due to the loss of thermally excitable degrees of freedom at critical temperature so that heat capacity is reduced exponentially. BCS theory has been successful in explaining the properties of low temperature super conductors but the high temperature super-conductors discovered in 1986 and other non-orthodox superconductors discovered later remain a challenge for theorists.

The reasons why magnetic fields tend to destroy super-conductivity is easy to understand. Lorentz force induces opposite forces to the electrons of Cooper pair since the momenta are opposite. Magnetic field tends also to turn the spins in the same direction. The super-conductivity is destroyed in fields for which the interaction energy of magnetic moment of electron with field is of the same order of magnitude as gap energy $E_g \sim T_c$: $e\hbar H_c/2m \sim T_c$.

If spins are parallel, the situation changes since only Lorentz force tends to destroy the Cooper pair. In high T_c super-conductors this is indeed the case: electrons are in spin triplet state ($S = 1$) and the net orbital angular momentum of Cooper pair is $L = 2$. The fact that orbital state is not $L = 0$ state makes high T_c super-conductors much more fragile to the destructive effect of impurities than conventional super-conductors (due to the magnetic exchange force between electrons responsible for magnetism). Also the Cooper pairs of 3He superfluid are in spin triplet state but have $S = 0$.

The observation that spin triplet Cooper pairs might be possible in ferro-magnets stimulates the question whether ferromagnetism and super-conductivity might tolerate each other after all, and the answer is affirmative [49]. The article [47] provides an enjoyable summary of experimental discoveries.

Basic parameters of super-conductors from universality?

Super conductors are characterized by certain basic parameters such as critical temperature T_c and critical magnetic field H_c , densities n_c and n of Cooper pairs and conduction electrons, gap energy E_g , correlation length ξ and magnetic penetration length λ . The super-conductors are highly complex systems and calculation of these parameters from BCS theory is either difficult or impossible.

It has been suggested [44] that these parameters might be more or less universal so that they would not depend on the specific properties of the interaction responsible for the formation of Cooper pairs. The motivation comes from the fact that the properties of ordinary Bose-Einstein condensates do not depend on the details of interactions. This raises the hope that these parameters might be expressible

in terms of some basic parameters such as T_c and the density of conduction electrons allowing to deduce Fermi energy E_F and Fermi momentum k_F if Fermi surface is sphere. In [44] formulas for the basic parameters are indeed suggested based on this of argumentation assuming that Cooper pairs form a Bose-Einstein condensate.

1. The most important parameters are critical temperature T_c and critical magnetic field H_c in principle expressible in terms of gap energy. In [44] the expression for T_c is deduced from the condition that the de Broglie wavelength λ must satisfy in supra phase the condition

$$\lambda \geq 2d = 2\left(\frac{n_c}{g}\right)^{-1/D} \quad (12.2.1)$$

guaranteeing the quantum overlap of Cooper pairs. Here n_c is the density of Bose-Einstein condensate of Cooper pairs and g is the number of spin states and D the dimension of the condensate. This condition follows also from the requirement that the number of particles per energy level is larger than one (Bose-Einstein condensation).

Identifying this expression with the de Broglie wavelength $\lambda = \hbar/\sqrt{2mE}$ at thermal energy $E = (D/2)T_c$, where D is the number of degrees of freedom, one obtains

$$T_c \leq \frac{\hbar^2}{4Dm} \left(\frac{n_c}{g}\right)^{2/D} . \quad (12.2.2)$$

m denotes the effective mass of super current carrier and for electron it can be even 100 times the bare mass of electron. The reason is that the electron moves is somewhat like a person trying to move in a dense crowd of people, and is accompanied by a cloud of charge carriers increasing its effective inertia. In this equation one can consider the possibility that Planck constant is not the ordinary one. This obviously increases the critical temperature unless n_c is scaled down in same proportion in the phase transition to large \hbar phase.

2. The density of n_c Cooper pairs can be estimated as the number of fermions in Fermi shell at E_F having width Δk deducible from kT_c . For $D = 3$ -dimensional spherical Fermi surface one has

$$\begin{aligned} n_c &= \frac{1}{2} \frac{4\pi k_F^2 \Delta k}{\frac{4}{3}\pi k_F^3} n , \\ kT_c &= E_F - E(k_F - \Delta k) \simeq \frac{\hbar^2 k_F \Delta k}{m} . \end{aligned} \quad (12.2.2)$$

Analogous expressions can be deduced in $D = 2$ - and $D = 1$ -dimensional cases and one has

$$n_c(D) = \frac{D}{2} \frac{T_c}{E_F} n(D) . \quad (12.2.3)$$

The dimensionless coefficient is expressible solely in terms of n and effective mass m . In [44] it is demonstrated that the inequality 12.2.2 replaced with equality when combined with 12.2.3 gives a satisfactory fit for 16 super-conductors used as a sample.

Note that the Planck constant appearing in E_F and T_c in Eq. 12.2.3 must correspond to ordinary Planck constant \hbar_0 . This implies that equations 12.2.2 and 12.2.3 are consistent within orders of magnitudes. For $D = 2$, which corresponds to high T_c superconductivity, the substitution of n_c from Eq. 12.2.3 to Eq. 12.2.2 gives a consistency condition from which n_c disappears completely. The condition reads as

$$n\lambda_F^2 = \pi = 4g .$$

Obviously the equation is not completely consistent.

3. The magnetic penetration length λ is expressible in terms of density n_c of Cooper pairs as

$$\lambda^{-2} = \frac{4\pi e^2 n_c}{m_e} . \quad (12.2.4)$$

The ratio $\kappa \equiv \frac{\lambda}{\xi}$ determines the type of the super conductor. For $\kappa < \frac{1}{\sqrt{2}}$ one has type I super conductor with defects having negative surface energy. For $\kappa \geq \frac{1}{\sqrt{2}}$ one has type II super conductor and defects have positive surface energy. Super-conductors of type I this results in complex stripe like flux patterns maximizing their area near criticality. The super-conductors of type II have $\kappa > 1/\sqrt{2}$ and the surface energy is positive so that the flux penetrates as flux quanta minimizing their area at lower critical value H_{c1} of magnetic field and completely at higher critical value H_{c2} of magnetic field. The flux quanta contain a core of size ξ carrying quantized magnetic flux.

4. Quantum coherence length ξ can be roughly interpreted as the size of the Cooper pair or as the size of the region where it is sensible to speak about the phase of wave function of Cooper pair. For larger separations the phases of wave functions are un-correlated. The values of ξ vary in the range $10^3 - 10^4$ Angstrom for low T_c super-conductors and in the range $5 - 20$ Angstrom for high T_c super-conductors (assuming that they correspond to ordinary \hbar !) the ratio of these coherence lengths varies in the range $[50 - 2000]$, with upper bound corresponding to $n_F = 2^{11}$ for \hbar . This would give range $1 - 2$ microns for the coherence lengths of high T_c super-conductors with lowest values of coherence lengths corresponding to the highest values of coherence lengths for low temperatures super conductors.

Uncertainty Principle $\delta E \delta t = \hbar/2$ using $\delta E = E_g \equiv 2\Delta$, $\delta t = \xi/v_F$, gives an order of magnitude estimate for ξ differing only by a numerical factor from the result of a rigorous calculation given by

$$\xi = \frac{4\hbar v_F}{E_g} . \quad (12.2.5)$$

E_g is apart from a numerical constant equal to T_c : $E_g = nT_c$. Using the expression for v_F and T_c in terms of the density of electrons, one can express also ξ in terms of density of electrons.

For instance, BCS theory predicts $n = 3.52$ for metallic super-conductors and $n = 8$ holds true for cuprates [44]. For cuprates one obtains $\xi = 2n^{-1/3}$ [44]. This expression can be criticized since cuprates are Mott insulators and it is not at all clear whether a description as Fermi gas makes sense. The fact that high T_c super-conductivity involves breakdown of anti-ferromagnetic order might justify the use of Fermi gas description for conducting holes resulting in the doping.

For large \hbar the value of ξ would scale up dramatically if deduced theoretically from experimental data using this kind of expression. If the estimates for ξ are deduced from v_F and T_c purely calculationally as seems to be the case, the actual coherence lengths would be scaled up by a factor $\hbar/\hbar_0 = n_F$ if high T_c super-conductors correspond to large \hbar phase. As also found that this would also allow to understand the high critical temperature.

12.2.2 Universality of the parameters in TGD framework

Universality idea conforms with quantum criticality of TGD Universe. The possibility to express everything in terms of density of critical temperature coding for the dynamics of Cooper pair formation and the density charge carriers would make it also easy to understand how p-adic scalings and transitions to large \hbar phase affect the basic parameters. The possible problem is that the replacement of inequality of Eq. 12.2.2 with equality need not be sensible for large \hbar phases. It will be found that in many-sheeted space-time T_c does not directly correspond to the gap energy and the universality of the critical temperature follows from the p-adic length scale hypothesis.

The effect of p-adic scaling on the parameters of super-conductors

p-Adic fractality expresses as $n \propto 1/L^3(k)$ would allow to deduce the behavior of the various parameters as function of the p-adic length scale and naive scaling laws would result. For instance, E_g and T_c would scale as $1/L^2(k)$ if one assumes that the density n of particles at larger space-time sheets scales p-adically as $1/L^3(k)$. The basic implication would be that the density of Cooper pairs and thus also T_c would be reduced very rapidly as a function of the p-adic length scale. Without thermal isolation between these space-time sheets and high temperature space-time sheets there would not be much hopes about high T_c super-conductivity.

In the scaling of Planck constant basic length scales scale up and the overlap criterion for super-conductivity becomes easy to satisfy unless the density of electrons is reduced too dramatically. As found, also the critical temperature scales up so that there are excellent hopes of obtain high T_c super-conductor in this manner. The claimed short correlation lengths are not a problem since they are calculational quantities.

It is of interest to study the behavior of the various parameters in the transition to the possibly existing large \hbar variant of super-conducting electrons. Also small scalings of \hbar are possible and the considerations to follow generalize trivially to this case. Under what conditions the behavior of the various parameters in the transition to large \hbar phase is dictated by simple scaling laws?

1. Scaling of T_c and E_g

T_c and E_g remain invariant if E_g corresponds to a purely classical interaction energy remaining invariant under the scaling of \hbar . This is not the case for BCS super-conductors for which the gap energy E_g has the following expression.

$$\begin{aligned} E_g &= \hbar\omega_c \exp(-1/X) , \\ X &= n(E_F)U_0 = \frac{3}{2}N(E_F)\frac{U_0}{E_F} , \\ n(E_F) &= \frac{3}{2}\frac{N(E_F)}{E_F} . \\ \omega_c &= \omega_D = (6\pi^2)^{1/3}c_s n_n^{1/3} . \end{aligned} \tag{12.2.3}$$

Here ω_c is the width of energy region near E_F for which "phonon" exchange interaction is effective. n_n denotes the density of nuclei and c_s denotes sound velocity.

$N(E_F)$ is the total number of electrons at the super-conducting space-time sheet. U_0 would be the parameter characterizing the interaction strength of electrons of Cooper pair and should not depend on \hbar . For a structure of size $L \sim 1 \mu$ m one would have $X \sim n_a 10^{12} \frac{U_0}{E_F}$, n_a being the number of exotic electrons per atom, so that rather weak interaction energy U_0 can give rise to $E_g \sim \omega_c$.

The expression of ω_c reduces to Debye frequency ω_D in BCS theory of ordinary super conductivity. If c_s is proportional to thermal velocity $\sqrt{T_c/m}$ at criticality and if n_n remains invariant in the scaling of \hbar , Debye energy scales up as \hbar . This can imply that $E_g > E_F$ condition making scaling non-sensible unless one has $E_g \ll E_F$ holding true for low T_c super-conductors. This kind of situation would *not* require large \hbar phase for electrons. What would be needed that nuclei and phonon space-time sheets correspond to large \hbar phase.

What one can hope is that E_g scales as \hbar so that high T_c superconductor would result and the scaled up T_c would be above room temperature for $T_c > .15$ K. If electron is in ordinary phase X is automatically invariant in the scaling of \hbar . If not, the invariance reduces to the invariance of U_0 and E_F under the scaling of \hbar . If n scales like $1/\hbar^D$, E_F and thus X remain invariant. U_0 as a simplified parametrization for the interaction potential expressible as a tree level Feynman diagram is expected to be in a good approximation independent of \hbar .

It will be found that in high T_c super-conductors, which seem to be quantum critical, a high T_c variant of phonon mediated superconductivity and exotic superconductivity could be competing. This would suggest that the phonon mediated superconductivity corresponds to a large \hbar phase for nuclei scaling ω_D and T_c by a factor $r = \hbar/\hbar_0$.

Since the total number $N(E_F)$ of electrons at larger space-time sheet behaves as $N(E_F) \propto E_F^{D/2}$, where D is the effective dimension of the system, the quantity $1/X \propto E_F/n(E_F)$ appearing in the expressions of the gap energy behaves as $1/X \propto E_F^{-D/2+1}$. This means that at the limit of vanishing

electron density $D = 3$ gap energy goes exponentially to zero, for $D = 2$ it is constant, and for $D = 1$ it goes zero at the limit of small electron number so that the formula for gap energy reduces to $E_g \simeq \omega_c$. These observations suggests that the super-conductivity in question should be 2- or 1-dimensional phenomenon as in case of magnetic walls and flux tubes.

2. Scaling of ξ and λ

If n_c for high T_c super-conductor scales as $1/\hbar^D$ one would have $\lambda \propto \hbar^{D/2}$. High T_c property however suggests that the scaling is weaker. ξ would scale as \hbar for given v_F and T_c . For $D = 2$ case the this would suggest that high T_c super-conductors are of type I rather than type II as they would be for ordinary \hbar . This conforms with the quantum criticality which would be counterpart of critical behavior of super-conductors of type I in nearly critical magnetic field.

3. Scaling of H_c and B

The critical magnetization is given by

$$H_c(T) = \frac{\Phi_0}{\sqrt{8\pi}\xi(T)\lambda(T)} , \quad (12.2.4)$$

where Φ_0 is the flux quantum of magnetic field proportional to \hbar . For $D = 2$ and $n_c \propto \hbar^{-2}$ $H_c(T)$ would not depend on the value of \hbar . For the more physical dependence $n_c \propto \hbar^{-2+\epsilon}$ one would have $H_c(T) \propto \hbar^{-\epsilon}$. Hence the strength of the critical magnetization would be reduced by a factor $2^{-11\epsilon}$ in the transition to the large \hbar phase with $n_F = 2^{-11}$.

Magnetic flux quantization condition is replaced by

$$\int 2eBdS = n\hbar 2\pi . \quad (12.2.5)$$

B denotes the magnetic field inside super-conductor different from its value outside the super-conductor. By the quantization of flux for the non-super-conducting core of radius ξ in the case of super-conductors of type II $eB = \hbar/\xi^2$ holds true so that B would become very strong since the thickness of flux tube would remain unchanged in the scaling.

12.2.3 Quantum criticality and super-conductivity

The notion of quantum criticality has been already discussed in introduction. An interesting prediction of the quantum criticality of entire Universe also gives naturally rise to a hierarchy of macroscopic quantum phases since the quantum fluctuations at criticality at a given level can give rise to higher level macroscopic quantum phases at the next level. A metaphor for this is a fractal cusp catastrophe for which the lines corresponding to the boundaries of cusp region reveal new cusp catastrophes corresponding to quantum critical systems characterized by an increasing length scale of quantum fluctuations.

Dark matter hierarchy could correspond to this kind of hierarchy of phases and long ranged quantum slow fluctuations would correspond to space-time sheets with increasing values of \hbar and size. Evolution as the emergence of modules from which higher structures serving as modules at the next level would correspond to this hierarchy. Mandelbrot fractal with inversion analogous to a transformation permuting the interior and exterior of sphere with zooming revealing new worlds in Mandelbrot fractal replaced with its inverse would be a good metaphor for what quantum criticality would mean in TGD framework.

How the quantum criticality of superconductors relates to TGD quantum criticality

There is empirical support that super-conductivity in high T_c super-conductors and ferromagnetic systems [47, 45] is made possible by quantum criticality [43]. In the experimental situation quantum criticality means that at sufficiently low temperatures quantum rather than thermal fluctuations are able to induce phase transitions. Quantum criticality manifests itself as fractality and simple scaling laws for various physical observables like resistance in a finite temperature range and also above the critical temperature. This distinguishes sharply between quantum critical super conductivity from

BCS type super-conductivity. Quantum critical super-conductivity also exists in a finite temperature range and involves the competition between two phases.

The absolute quantum criticality of the TGD Universe maps to the quantum criticality of sub-systems, which is broken by finite temperature effects bringing dissipation and freezing of quantum fluctuations above length and time scales determined by the temperature so that scaling laws hold true only in a finite temperature range.

Reader has probably already asked what quantum criticality precisely means. What are the phases which compete? An interesting hypothesis is that quantum criticality actually corresponds to criticality with respect to the phase transition changing the value of Planck constant so that the competing phases would correspond to different values of \hbar . In the case of high T_c super-conductors (anti-ferromagnets) the fluctuations can be assigned to the magnetic flux tubes of the dipole field patterns generated by rows of holes with same spin direction assignable to the stripes. Below T_c fluctuations induce reconnections of the flux tubes and a formation of very long flux tubes and make possible for the supra currents to flow in long length scales below T_c . Percolation type phenomenon is in question. The fluctuations of the flux tubes below $T_{c1} > T_c$ induce transversal phonons generating the energy gap for $S = 1$ Cooper pairs. $S = 0$ Cooper pairs are predicted to stabilize below T_c .

Scaling up of de Broglie wave lengths and criterion for quantum overlap

Compton lengths and de Broglie wavelengths are scaled up by an integer n , whose preferred values correspond to $n_F = 2^k \prod_s F_s$, where $F_s = 2^{2^s} + 1$ are distinct Fermat primes. In particular, $n_F = 2^{k11}$ seem to be favored in living matter. The scaling up means that the overlap condition $\lambda \geq 2d$ for the formation of Bose-Einstein condensate can be satisfied and the formation of Cooper pairs becomes possible. Thus a hierarchy of large \hbar super-conductivities would be associated with to the dark variants of ordinary particles having essentially same masses as the ordinary particles.

Unless one assumes fractionization, the invariance of $E_F \propto \hbar_{eff}^2 n^{2/3}$ in \hbar increasing transition would require that the density of Cooper pairs in large \hbar phase is scaled down by an appropriate factor. This means that supra current intensities, which are certainly measurable quantities, are also scaled down. Of course, it could happen that E_F is scaled up and this would conform with the scaling of the gap energy.

Quantum critical super-conductors in TGD framework

For quantum critical super-conductivity in heavy fermions systems, a small variation of pressure near quantum criticality can destroy ferromagnetic (anti-ferromagnetic) order so that Curie (Neel) temperature goes to zero. The prevailing spin fluctuation theory [41] assumes that these transitions are induced by long ranged and slow spin fluctuations at critical pressure P_c . These fluctuations make and break Cooper pairs so that the idea of super-conductivity restricted around critical point is indeed conceivable.

Heavy fermion systems, such as cerium-indium alloy CeIn₃ are very sensitive to pressures and a tiny variation of density can drastically modify the low temperature properties of the systems. Also other systems of this kind, such as CeCu₂Ge₂, CeIn₃, CePd₂Si₂ are known [47, 49]. In these cases super-conductivity appears around anti-ferromagnetic quantum critical point.

The last experimental breakthrough in quantum critical super-conductivity was made in Grenoble [45]. URhGe alloy becomes super-conducting at $T_c = .280$ K, loses its super-conductivity at $H_c = 2$ Tesla, and becomes again super-conducting at $H_c = 12$ Tesla and loses its super-conductivity again at $H = 13$ Tesla. The interpretation is in terms of a phase transition changing the magnetic order inducing the long range spin fluctuations.

TGD based models of atomic nucleus [23] and condensed matter [27] assume that weak gauge bosons with Compton length of order atomic radius play an essential role in the nuclear and condensed matter physics. The assumption that condensed matter nuclei possess anomalous weak charges explains the repulsive core of potential in van der Waals equation and the very low compressibility of condensed matter phase as well as various anomalous properties of water phase, provide a mechanism of cold fusion and sono-fusion, etc. [27, 16]. The pressure sensitivity of these systems would directly reflect the physics of exotic quarks and electro-weak gauge bosons. A possible mechanism behind the phase transition to super-conductivity could be the scaling up of the sizes of the space-time sheets of nuclei.

Also the electrons of Cooper pair (and only these) could make a transition to large \hbar phase. This transition would induce quantum overlap having geometric overlap as a space-time correlate. The formation of join along boundaries bonds between neighboring atoms would be part of the mechanism. For instance, the criticality condition $4n^2\alpha = 1$ for BE condensate of n Cooper pairs would give $n = 6$ for the size of a higher level quantum unit possibly formed from Cooper pairs. If one does not assume invariance of energies obtained by fractionization of principal quantum number, this transition has dramatic effects on the spectrum of atomic binding energies scaling as $1/\hbar^2$ and practically universal spectrum of atomic energies would result [16] not depending much on nuclear charge. It seems that this prediction is non-physical.

Quantum critical super-conductors resemble superconductors of type I with $\lambda \ll \xi$ for which defects near thermodynamical criticality are complex structures looking locally like stripes of thickness λ . These structures are however dynamical in super-conducting phase. Quite generally, long range quantum fluctuations due to the presence of two competing phases would manifest as complex dynamical structures consisting of stripes and their boundaries. These patterns are dynamical rather than static as in the case of ordinary spin glass phase so that quantum spin glass or 4-D spin glass is a more appropriate term. The breaking of classical non-determinism for vacuum extremals indeed makes possible space-time correlates for quantum non-determinism and this makes TGD Universe a 4-dimensional quantum spin glass.

Could quantum criticality make possible new kinds of high T_c super-conductors?

The transition to large $\hbar = r\hbar_0$ phase increases various length scales by r and makes possible long range correlations even at high temperatures. Hence the question is whether large \hbar phase could correspond to ordinary high T_c super-conductivity. If this were the case in the case of ordinary high T_c super-conductors, the actual value of coherence length ξ would vary in the range 5 – 20 Angstrom scaled up by a factor r . For effectively D -dimensional super-conductor the density of Cooper pairs would be scaled down by an immensely small factor $1/r^D$ from its value deduced from Fermi energy.

Large \hbar phase for some nuclei might be involved and make possible large space-time sheets of size at least of order of ξ at which conduction electrons forming Cooper pairs would topologically condense like quarks around hadronic space-time sheets (in [27] a model of water as a partially dark matter with one fourth of hydrogen ions in large \hbar phase is developed).

Consider for a moment the science fictive possibility that super conducting electrons for some quantum critical super-conductors to be discovered or already discovered correspond to large \hbar phase with $\hbar = r\hbar_0$ keeping in mind that this affects only quantum corrections in perturbative approach but not the lowest order classical predictions of quantum theory. For $r \simeq n2^{k11}$ with $(n, k) = (1, 1)$ the size of magnetic body would be $L(149) = 5$ nm, the thickness of the lipid layer of cell membrane. For $(n, k) = (1, 2)$ the size would be $L(171) = 10$ μm , cell size. If the density of Cooper pairs is of same order of magnitude as in case of ordinary super conductors, the critical temperature is scaled up by 2^{k11} . Already for $k = 1$ the critical temperature of 1 K would be scaled up to $4n^2 \times 10^6$ K if n_c is not changed. This assumption is not consistent with the assumption that Fermi energy remains non-relativistic. For $n = 1$ $T_c = 400$ K would be achieved for $n_c \rightarrow 10^{-6}n_c$, which looks rather reasonable since Fermi energy transforms as $E_F \rightarrow 8 \times 10^3 E_F$ and remains non-relativistic. H_c would scale down as $1/\hbar$ and for $H_c = .1$ Tesla the scaled down critical field would be $H_c = .5 \times 10^{-4}$ Tesla, which corresponds to the nominal value of the Earth's magnetic field.

Quantum critical super-conductors become especially interesting if one accepts the identification of living matter as ordinary matter quantum controlled by macroscopically quantum coherent dark matter. One of the basic hypothesis of TGD inspired theory of living matter is that the magnetic flux tubes of the Earth's magnetic field carry a super-conducting phase and the spin triplet Cooper pairs of electrons in large \hbar phase might realize this dream. That the value of Earth's magnetic field is near to its critical value could have also biological implications.

12.2.4 Space-time description of the mechanisms of super-conductivity

The application of ideas about dark matter to nuclear physics and condensed matter suggests that dark color and weak forces should be an essential element of the chemistry and condensed matter physics. The continual discovery of new super-conductors, in particular of quantum critical superconductors, suggests that super-conductivity is not well understood. Hence super-conductivity provides an obvious

test for these ideas. In particular, the idea that wormhole contacts regarded as parton pairs living at two space-time sheets simultaneously, provides an attractive universal mechanism for the formation of Cooper pairs and is not so far-fetched as it might sound first.

Leading questions

It is good to begin with a series of leading questions. The first group of questions is inspired by experimental facts about super-conductors combined with TGD context.

1. The work of Rabinowitch [44] suggests that that the basic parameters of super-conductors might be rather universal and depend on T_c and conduction electron density only and be to a high degree independent of the mechanism of super-conductivity. This is in a sharp contrast to the complexity of even BCS model with its somewhat misty description of the phonon exchange mechanism.

Questions: Could there exist a simple universal description of various kinds of super-conductivities?

2. The new super-conductors possess relatively complex chemistry and lattice structure.
Questions: Could it be that complex chemistry and lattice structure makes possible something very simple describable in terms of quantum criticality. Could it be that the transversal oscillations magnetic flux tubes allow to understand the formation of Cooper pairs at T_{c1} and their reconnections generating very long flux tubes the emergence of supra currents at T_c ?

3. The effective masses of electrons in ferromagnetic super-conductors are in the range of 10-100 electron masses [47] and this forces to question the idea that ordinary Cooper pairs are current carriers.

Questions: Can one consider the possibility that the p-adic length scale of say electron can vary so that the actual mass of electron could be large in condensed matter systems? For quarks and neutrinos this seems to be the case [18, 17]. Could it be that the Gaussian Mersennes $(1+i)^k - 1$, $k = 151, 157, 163, 167$ spanning the p-adic lengthscale range 10 nm-2.5 μ m very relevant from the point of view of biology correspond to p-adic length especially relevant for super-conductivity?

Second group of questions is inspired by quantum classical correspondence.

1. Quantum classical correspondence in its strongest form requires that bound state formation involves the generation of join along boundaries bonds between bound particles. The weaker form of the principle requires that the particles are topologically condensed at same space-time sheet. In the case of Cooper pairs in ordinary super-conductors the length of join along boundaries bonds between electrons should be of order $10^3 - 10^4$ Angstroms. This looks rather strange and it seems that the latter option is more sensible.

Questions: Could quantum classical correspondence help to identify the mechanism giving rise to Cooper pairs?

2. Quantum classical correspondence forces to ask for the space-time correlates for the existing quantum description of phonons.

Questions: Can one assign space-time sheets with phonons or should one identify them as oscillations of say space-time sheets at which atoms are condensed? Or should the microscopic description of phonons in atomic length scales rely on the oscillations of wormhole contacts connecting atomic space-time sheets to these larger space-time sheets? The identification of phonons as wormhole contacts would be completely analogous to the similar identification of gauge bosons except that phonons would appear at higher levels of the hierarchy of space-time sheets and would be emergent in this sense. As a matter fact, even gauge bosons as pairs of fermion and antifermion are emergent structures in TGD framework and this plays fundamental role in the construction of QFT limit of TGD in which bosonic part of action is generated radiatively so that all coupling constants follow as predictions [25, 23]. Could Bose-Einstein condensates of wormhole contacts be relevant for the description of super-conductors or more general macroscopic quantum phases?

The third group of questions is inspired by the new physics predicted or by TGD.

1. TGD predicts a hierarchy of macroscopic quantum phases with large Planck constant.
 Questions: Could large values of Planck constant make possible exotic electronic super-conductivities?
 Could even nuclei possess large \hbar (super-fluidity)?
2. TGD predicts that classical color force and its quantal counterpart are present in all length scales.
 Questions: Could color force, say color magnetic force which play some role in the formation of Cooper pair. The simplest model of pair is as a space-time sheet with size of order ξ so that the electrons could be "outside" the background space-time. Could the Coulomb interaction energy of electrons with positively charged wormhole throats carrying parton numbers and feeding em gauge flux to the large space-time sheet be responsible for the gap energy? Could wormhole throats carry also quark quantum numbers. In the case of single electron condensed to single space-time sheet the em flux could be indeed fed by a pair of $u\bar{u}$ and $\bar{d}d$ type wormhole contacts to a larger space-time sheet. Could the wormhole contacts have a net color? Could the electron space-time sheets of the Cooper pair be connected by long color flux tubes to give color singlets so that dark color force would be ultimately responsible for the stability of Cooper pair?
3. Suppose that one takes seriously the ideas about the possibility of dark weak interactions with the Compton scale of weak bosons scaled up to say atomic length scale so that weak bosons are effectively massless below this length scale [27].
 Questions: Could the dark weak length scale which is of order atomic size replace lattice constant in the expression of sound velocity? What is the space-time correlate for sound velocity?

Photon massivation, coherent states of Cooper pairs, and wormhole contacts

The existence of wormhole contacts is one of the most stunning predictions of TGD. First I realized that wormhole contacts can be regarded as parton-antiparton pairs with parton and antiparton assignable to the light-like causal horizons accompanying wormhole contacts. Then came the idea that Higgs particle could be identified as a wormhole contact. It was soon followed by the identification all bosonic states as wormhole contacts [26]. Finally I understood that this applies also to their super-symmetric partners, which can be also fermion [23]. Fermions and their super-partners would in turn correspond to wormhole throats resulting in the topological condensation of small deformations of CP_2 type vacuum extremals with Euclidian signature of metric to the background space-time sheet. This framework opens the doors for more concrete models of also super-conductivity involving the effective massivation of photons as one important aspect in the case of ordinary super-conductors.

There are two types of wormhole contacts. Those of first type correspond to elementary bosons. Wormhole contacts of second kind are generated in the topological condensation of space-time sheets carrying matter and form a hierarchy. Classical radiation fields realized in TGD framework as oscillations of space-time sheets would generate wormhole contacts as the oscillating space-time sheet develops contacts with parallel space-time sheets (recall that the distance between space-time sheets is of order CP_2 size). This realizes the correspondence between fields and quanta geometrically. Phonons could also correspond to wormhole contacts of this kind since they mediate acoustic oscillations between space-time sheets and the description of the phonon mediated interaction between electrons in terms of wormhole contacts might be useful also in the case of super-conductivity. Bose-Einstein condensates of wormhole contacts might be highly relevant for the formation of macroscopic quantum phases. The formation of a coherent state of wormhole contacts would be the counterpart for the vacuum expectation value of Higgs.

The notions of coherent states of Cooper pairs and of charged Higgs challenge the conservation of electromagnetic charge. The following argument however suggests that coherent states of wormhole contacts form only a part of the description of ordinary super-conductivity. The basic observation is that wormhole contacts with vanishing fermion number define space-time correlates for Higgs type particle with fermion and antifermion numbers at light-like throats of the contact.

The ideas that a genuine Higgs type photon massivation is involved with super-conductivity and that coherent states of Cooper pairs really make sense are somewhat questionable since the conservation of charge and fermion number is lost for coherent states. A further questionable feature is that a quantum superposition of many-particle states with widely different masses would be in question. These interpretational problems can be resolved elegantly in zero energy ontology [19] in which the total conserved quantum numbers of quantum state are vanishing. In this picture the energy, fermion

number, and total charge of any positive energy state are compensated by opposite quantum numbers of the negative energy state in geometric future. This makes possible to speak about superpositions of Cooper pairs and charged Higgs bosons separately in positive energy sector.

If this picture is taken seriously, super-conductivity can be seen as providing a direct support for both the hierarchy of scaled variants of standard model physics and for the zero energy ontology.

Space-time correlate for quantum critical superconductivity

The explicit model for high T_c super-conductivity relies on quantum criticality involving long ranged quantum fluctuations inducing reconnection of flux tubes of local (color) magnetic fields associated with parallel spins associated with stripes to form long flux tubes serving as wires along which Cooper pairs flow. Essentially percolation [48] type phenomenon would be in question. The role of the doping by holes is to make room for Cooper pairs to propagate by the reconnection mechanism: otherwise Fermi statistics would prevent the propagation. Too much doping reduces the number of current carriers, too little doping leaves too little room so that there exists some optimal doping. In the case of high T_c super-conductors quantum criticality corresponds to a quite wide temperature range, which provides support for the quantum criticality of TGD Universe. The probability $p(T)$ for the formation of reconnections is what matters and exceeds the critical value at T_c .

12.2.5 Super-conductivity at magnetic flux tubes

Super-conductivity at the magnetic flux tubes of magnetic flux quanta is one the basic hypothesis of the TGD based model of living matter. There is also evidence for magnetically mediated super-conductivity in extremely pure samples [53]. The magnetic coupling was only observed at lattice densities close to the critical density at which long-range magnetic order is suppressed. Quantum criticality that long flux tubes serve as pathways along which Cooper pairs can propagate. In anti-ferromagnetic phase these pathways are short-circuited to closed flux tubes of local magnetic fields.

Almost the same model as in the case of high T_c and quantum critical super-conductivity applies to the magnetic flux tubes. Now the flux quantum contains BE condensate of exotic Cooper pairs interacting with wormhole contacts feeding the gauge flux of Cooper pairs from the magnetic flux quantum to a larger space-time sheet. The interaction of spin 1 Cooper pairs with the magnetic field of flux quantum orients their spins in the same direction. Large value of \hbar guarantees thermal stability even in the case that different space-time sheets are not thermally isolated.

The understanding of gap energy is not obvious. The transversal oscillations of magnetic flux tubes generated by spin flips of electrons define the most plausible candidate for the counterpart of phonons. In this framework phonon like states identified as wormhole contacts would be created by the oscillations of flux tubes and would be a secondary phenomenon.

Large values of \hbar allow to consider not only the Cooper pairs of electrons but also of protons and fermionic ions. Since the critical temperature for the formation of Cooper pairs is inversely proportional to the mass of the charge carrier, the replacement of electron with proton or ion would require a scaling of \hbar . If T_{c1} is proportional to \hbar^2 , this requires scaling by $(m_p/m_e)^{1/2}$. For $T_{c1} \propto \hbar$ scaling by $m_p/m_e \simeq 2^{11}$ is required. This inspired idea that powers of 2^{11} could define favored values of \hbar/\hbar_0 . This hypothesis is however rather adhoc and turned out to be too restrictive.

Besides Cooper pairs also Bose-Einstein condensates of bosonic ions are possible in large \hbar phase and would give rise to super-conductivity. TGD inspired nuclear physics predicts the existence of exotic bosonic counterparts of fermionic nuclei with given (A, Z) [47].

Superconductors at the flux quanta of the Earth's magnetic field

Magnetic flux tubes and magnetic walls are the most natural candidates for super-conducting structures with spin triplet Cooper pairs. Indeed, experimental evidence relating to the interaction of ELF em radiation with living matter suggests that bio-super-conductors are effectively 1- or 2-dimensional. $D \leq 2$ -dimensionality is guaranteed by the presence of the flux tubes or flux walls of, say, the magnetic field of Earth in which charge carries form bound states and the system is equivalent with a harmonic oscillator in transversal degrees of freedom.

The effect of Earth's magnetic field is completely negligible at the atomic space-time sheets and cannot make super conductor 1-dimensional. At cellular sized space-time sheets magnetic field makes

possible transversal the confinement of the electron Cooper pairs in harmonic oscillator states but does not explain energy gap which should be at the top of 1-D Fermi surface. The critical temperature extremely low for ordinary value of \hbar and either thermal isolation between space-time sheets or large value of \hbar can save the situation.

An essential element of the picture is that topological quantization of the magnetic flux tubes occurs. In fact, the flux tubes of Earth's magnetic field have thickness of order cell size from the quantization of magnetic flux. The observations about the effects of ELF em fields on bio-matter [61, 62] suggest that similar mechanism is at work also for ions and in fact give very strong support for bio-super conductivity based on the proposed mechanism.

Energy gaps for superconducting magnetic flux tubes and walls

Besides the formation of Cooper pairs also the Bose-Einstein condensation of charge carriers to the ground state is needed in order to have a supra current. The stability of Bose-Einstein condensate requires an energy gap $E_{g, BE}$ which must be larger than the temperature at the magnetic flux tube.

Several energies must be considered in order to understand $E_{g, BE}$.

1. The Coulombic binding energy of Cooper pairs with the wormhole contacts feeding the em flux from magnetic flux tube to a larger space-time sheet defines an energy gap which is expected to be of order $E_{g, BE} = \alpha/L(k)$ giving $E_g \sim 10^{-3}$ eV for $L(167) = 2.5 \mu\text{m}$ giving a rough estimate for the thickness of the magnetic flux tube of the Earth's magnetic field $B = .5 \times 10^{-4}$ Tesla.
2. In longitudinal degrees of freedom of the flux tube Cooper pairs can be described as particles in a one-dimensional box and the gap is characterized by the length L of the magnetic flux tube and the value of \hbar . In longitudinal degrees of freedom the difference between $n = 2$ and $n = 1$ states is given by $E_0(k_2) = 3\hbar^2/4m_e L^2(k_2)$. Translational energy gap $E_g = 3E_0(k_2) = 3\hbar^2/4m_e L^2(k_2)$ is smaller than the effective energy gap $E_0(k_1) - E_0(k_2) = \hbar^2/4m_e L^2(k_1) - \hbar^2/4m_e L^2(k_2)$ for $k_1 > k_2 + 2$ and identical with it for $k_1 = k_2 + 2$. For $L(k_2 = 151)$ the zero point kinetic energy is given by $E_0(151) = 20.8$ meV so that $E_{g, BE}$ corresponds roughly to a temperature of 180 K. For magnetic walls the corresponding temperature would be scaled by a factor of two to 360 K and is above room temperature.
3. Second troublesome energy gap relates to the interaction energy with the magnetic field. The magnetic interaction energy E_m of Cooper pair with the magnetic field consists of cyclotron term $E_c = n\hbar eB/m_e$ and spin-interaction term which is present only for spin triplet case and is given by $E_s = \pm\hbar eB/m_e$ depending on the orientation of the net spin with magnetic field. In the magnetic field $B_{end} = 2B_E/5 = .2$ Gauss ($B_E = .5$ Gauss is the nominal value of the Earth's magnetic field) explaining the effects of ELF em fields on vertebrate brain, this energy scale is $\sim 10^{-9}$ eV for \hbar_0 and $\sim 1.6 \times 10^{-5}$ eV for $\hbar = 2^{14} \times \hbar_0$.

The smallness of translational and magnetic energy gaps in the case of Cooper pairs at Earth's magnetic field could be seen as a serious obstacle.

1. Thermal isolation between different space-time sheets provides one possible resolution of the problem. The stability of the Bose-Einstein condensation is guaranteed by the thermal isolation of space-time if the temperature at the magnetic flux tube is below E_m . This can be achieved in all length scales if the temperature scales as the zero point kinetic energy in transversal degrees of freedom since it scales in the same manner as magnetic interaction energy.
2. The transition to large \hbar phase could provide a more elegant way out of the difficulty. The criterion for a sequence of transitions to a large \hbar phase could be easily satisfied if there is a large number of charge Cooper pairs at the magnetic flux tube. Kinetic energy gap remains invariant if the length of the flux tube scales as \hbar . If the magnetic flux is quantized as a multiple of \hbar and flux tube thickness scales as \hbar^2 , B must scale as $1/\hbar$ so that also magnetic energy remains invariant under the scaling. This would allow to have stability without assuming low temperature at magnetic flux tubes.

12.3 TGD based model for high T_c super conductors

High T_c superconductors are quantum critical and involve in an essential magnetic structures, they provide an attractive application of the general vision for the model of super-conductivity based on magnetic flux tubes.

12.3.1 Some properties of high T_c super conductors

Quite generally, high T_c super-conductors are cuprates with CuO layers carrying the supra current. The highest known critical temperature for high T_c superconductors is 164 K and is achieved under huge pressure of 3.1×10^5 atm for LaBaCuO. High T_c super-conductors are known to be super conductors of type II.

This is however a theoretical deduction following from the assumption that the value of Planck constant is ordinary. For $\hbar = 2^{14}\hbar_0$ (say) ξ would be scaled up accordingly and type I super-conductor would be in question. These super-conductors are characterized by very complex patterns of penetrating magnetic field near criticality since the surface area of the magnetic defects is maximized. For high T_c super-conductors the ferromagnetic phase could be regarded as an analogous to defect and would indeed have very complex structure. Since quantum criticality would be in question the stripe structure would fluctuate with time too in accordance with 4-D spin glass character.

The mechanism of high T_c super conductivity is still poorly understood [46, 54].

1. It is agreed that electronic Cooper pairs are charge carriers. It is widely accepted that electrons are in relative d-wave state rather than in s-wave (see [60] and the references mentioned in [46]). Cooper pairs are believed to be in spin triplet state and electrons combine to form $L = 2$ angular momentum state. The usual phonon exchange mechanism does not generate the attractive interaction between the members of the Cooper pair having spin. There is also a considerable evidence for BCS type Cooper pairs and two kinds of Cooper pairs could be present.
2. High T_c super conductors have spin glass like character [37]. High T_c superconductors have anomalous properties also above T_c suggesting quantum criticality implying fractal scaling of various observable quantities such as resistivity. At high temperatures cuprates are anti-ferromagnets and Mott insulators meaning freezing of the electrons. Superconductivity and conductivity are believed to occur along dynamical stripes which are antiferromagnetic defects.
3. These findings encourage to consider the interpretation in terms of quantum criticality in which some new form of super conductivity which is not based on quasiparticles is involved. This super-conductivity would be assignable with the quantum fluctuations destroying antiferromagnetic order and replacing it with magnetically disordered phase possibly allowing phonon induced super-conductivity.
4. The doping of the super-conductor with electron holes is essential for high T_c superconductivity, and there is a critical doping fraction $p = .14$ at which T_c is highest. The interpretation is that holes make possible for the Cooper pairs to propagate. There is considerable evidence that holes gather on one-dimensional stripes with thickness of order few atom sizes and lengths in the range 1-10 nm [54], which are fluctuating in time scale of 10^{-12} seconds. These stripes are also present in non-superconducting state but in this case they do not fluctuate appreciably. The most plausible TGD based interpretation is in terms of fluctuations of magnetic flux tubes allowing for the formation of long connected flux tubes making super-conductivity possible. The fact that the fluctuations would be oscillations analogous to acoustic wave and might explain the BCS type aspects of high T_c super-conductivity.
5. T_c is inversely proportional to the distance L between the stripes. A possible interpretation would be that full super-conductivity requires delocalization of electrons also with respect to stripes so that T_c would be proportional to the hopping probability of electron between neighboring stripes expected to be proportional to $1/L$ [54].

From free fermion gas to Fermi liquids to quantum critical systems

The article of Jan Zaanen [40] gives an excellent non-technical discussion of various features of high T_c super-conductors distinguishing them from BCS super-conductors. After having constructed a color flux tube model of Cooper pairs I found it especially amusing to learn that the analogy of high T_c super-conductivity as a quantum critical phenomenon involving formation of dynamical stripes to QCD in the vicinity of the transition to the confined phase leading to the generation of string like hadronic objects was emphasized also by Zaanen.

BCS super-conductor behaves in a good approximation like quantum gas of non-interacting electrons. This approximation works well for long ranged interactions and the reason is Fermi statistics plus the fact that Fermi energy is much larger than Coulomb interaction energy at atomic length scales.

For strongly interacting fermions the description as Fermi liquid (a notion introduced by Landau) has been dominating phenomenological approach. ^3He provides a basic example of Fermi liquid and already here a paradox is encountered since low temperature collective physics is that of Fermi gas without interactions with effective masses of atoms about 6 times heavier than those of real atoms whereas short distance physics is that of a classical fluid at high temperatures meaning a highly correlated collective behavior.

It should be noticed that many-sheeted space-time provides a possible explanation of the paradox. Space-time sheets containing join along boundaries blocks of ^3He atoms behave like gas whereas the ^3He atoms inside these blocks form a liquid. An interesting question is whether the ^3He atoms combine to form larger units with same spin as ^3He atom or whether the increase of effective mass by a factor of order six means that \hbar as a unit of spin is increased by this factor forcing the basic units to consist of Bose-Einstein condensate of 3 Cooper pairs.

High T_c super conductors are neither Fermi gases nor Fermi liquids. Cuprate superconductors correspond at high temperatures to doped Mott insulators for which Coulomb interactions dominate meaning that electrons are localized and frozen. Electron spin can however move and the system can be regarded as an anti-ferromagnet. CuO planes are separated by highly oxidic layers and become super-conducting when doped. The charge transfer between the two kinds of layers is what controls the degree of doping. Doping induces somehow a delocalization of charge carriers accompanied by a local melting of anti-ferromagnet.

Collective behavior emerges for high enough doping. Highest T_c results with 15 per cent doping by holes. Current flows along electron stripes. Stripes themselves are dynamical and this is essential for both conductivity and superconductivity. For completely static stripes super-conductivity disappears and quasi-insulating electron crystal results.

Dynamical stripes appear in mesoscopic time and length scales corresponding to 1-10 nm length scale and picosecond time scale. The stripes are in a well-defined sense dual to the magnetized stripe like structures in type I super-conductor near criticality, which suggests analog of type I super-conductivity. The stripes are anti-ferromagnetic defects at which neighboring spins fail to be antiparallel. It has been found that stripes are a very general phenomenon appearing in insulators, metals, and super-conducting compounds [52].

Quantum criticality is present also above T_c

Also the physics of Mott insulators above T_c reflects quantum criticality. Typically scaling laws hold true for observables. In particular, resistivity increases linearly rather than transforming from T^2 behavior to constant as would be implied by quasi-particles as current carriers. The appearance of so called pseudo-gap [38] at $T_{c1} > T_c$ conforms with this interpretation. In particular, the pseudo-gap is non-vanishing already at T_{c1} and stays constant rather than starting from zero as for quasi-particles.

Results from optical measurements and neutron scattering

Optical measurements and neutron scattering have provided especially valuable microscopic information about high T_c superconductors allowing to fix the details of TGD based quantitative model.

Optical measurements of copper oxides in non-super-conducting state have demonstrated that optical conductivity $\sigma(\omega)$ is surprisingly featureless as a function of photon frequency. Below the critical temperature there is however a sharp absorption onset at energy of about 50 meV [58]. The origin of this special feature has been a longstanding puzzle. It has been proposed that this absorption

onset corresponds to a direct generation of an electron-hole pair. Momentum conservation implies that the threshold for this process is $E_g + E$, where E is the energy of the 'gluon' which binds electrons of Cooper pair together. In the case of ordinary super-conductivity E would be phonon energy.

Soon after measurements, it was proposed that in absence of lattice excitations photon must generate two electron-hole pairs such that electrons possess opposite momenta [58]. Hence the energy of the photon would be $2E_g$. Calculations however predicted soft rather than sharp onset of absorption since pairs of electron-hole pairs have continuous energy spectrum. There is something wrong with this picture.

Second peculiar characteristic [56, 50, 51] of high T_c super conductors is resonant neutron scattering at excitation energy $E_w = 41$ meV of super conductor. This scattering occurs only below the critical temperature, in spin-flip channel and for a favored momentum exchange $(\pi/a, \pi/a)$, where a denotes the size of the lattice cube [56, 50, 51]. The transferred energy is concentrated in a remarkably narrow range around E_w rather than forming a continuum.

In [59] it is suggested that e-e resonance with spin one gives rise to this excitation. This resonance is assumed to play the same role as phonon in the ordinary super conductivity and e-e resonance is treated like phonon. It is found that one can understand the dependence of the second derivative of the photon conductivity $\sigma(\omega)$ on frequency and that consistency with neutron scattering data is achieved. The second derivative of $\sigma(\omega)$ peaks near 68 meV and assuming $E = E_g + E_w$ they found nearly perfect match using $E_g = 27$ meV. This would suggest that the energy of the excitations generating the binding between the members of the Cooper pair is indeed 41 meV, that two electron-hole pairs and excitation of the super conductor are generated in photon absorption above threshold, and that the gap energy of the Cooper pair is 27 meV. Of course, the theory of Carbotte *et al* does not force the 'gluon' to be triplet excitation of electron pair. Also other possibilities can be considered. What comes in mind are spin flip waves of the spin lattice associated with stripe behaving as spin 1 waves.

In TGD framework more exotic options become possible. The transversal fluctuations of stripes- or rather of the magnetic flux tubes associated with the stripes- could define spin 1 excitations analogous to the excitations of a string like objects. Gauge bosons are identified as wormhole contacts in quantum TGD and massive gauge boson like state containing electron-positron pair or quark-antiquark pair could be considered.

12.3.2 TGD inspired vision about high T_c superconductivity

The following general view about high T_c super-conductivity as quantum critical phenomenon suggests itself. It must be emphasized that this option is one of the many that one can imagine and distinguished only by the fact that it is the minimal option.

The interpretation of critical temperatures

The two critical temperatures T_c and $T_{c1} > T_c$ are interpreted as critical temperatures. The recent observation that there exists a spectroscopic signature of high T_c super-conductivity, which prevails up to T_{c1} [55], supports the interpretation that Cooper pairs exist already below T_{c1} but that for some reason they cannot form a coherent super-conducting state.

One can imagine several alternative TGD based models but for the minimal option is the following one.

1. T_{c1} would be the temperature for the formation of two-phase system consisting of ordinary electrons and of Cooper pairs with a large value of Planck constant explaining the high critical temperature.
2. Magnetic flux tubes are assumed to be carriers of supra currents. These flux tubes are very short in in anti-ferromagnetic phase. The holes form stripes making them positively charged so that they attract electrons. If the spins of holes tend to form parallel sequences along stripes, they generate dipole magnetic fields in scales of order stripe length at least. The corresponding magnetic flux tubes are assumed to be carriers of electrons and Cooper pairs. The flux tube structures would be closed so that the supra currents associated with these flux tubes would be trapped in closed loops above T_c .

3. Below T_{c1} transversal fluctuations of the flux tubes structures occur and can induce reconnections giving rise to longer flux tubes. Reconnection can occur in two manners. Recall that upwards going outer flux tubes of the dipole field turn downwards and eventually fuse with the dipole core. If the two dipoles have opposite directions the outer flux tube of the first (second) dipole can reconnect with the inward going part of the flux tube of second (first) dipole. If the dipoles have same direction, the outer flux tubes of the dipoles reconnect with each other. Same applies to the inwards going parts of the flux tubes and the dipoles fuse to a single deformed dipole if all flux tubes reconnect. This alternative looks more plausible. The reconnection process is in general only partial since dipole field consists of several flux tubes.
4. The reconnections for the flux tubes of neighboring almost dipole fields occur with some probability $p(T)$ and make possible finite conductivity. At T_c the system the fluctuations of the flux tubes become large and also $p(T, L)$, where L is the distance between stripes, becomes large and the reconnection leads to a formation of long flux tubes of length of order coherence length at least and macroscopic supra currents can flow. One also expects that the reconnection occurs for practically all flux tubes of the dipole field. Essentially a percolation type phenomenon [48] would be in question. Scaling invariance suggests $p_c(T, L) = p_c(TL/\hbar)$, where L is the distance between stripes, and would predict the observed $T_c \propto \hbar/L$ behavior. Large value of \hbar would explain the high value of T_c .

This model relates in an interesting manner to the vision of Zaanen [39] expressed in terms of the highway metaphor visualizing stripes as quantum highways along which Cooper pairs can move. In antiferromagnetic phase the traffic is completely jammed. The doping inducing electron holes allows to circumvent traffic jam due to the Fermi statistics generates stripes along which the traffic flows in the sense of ordinary conductivity. In TGD framework highways are replaced with flux tubes and the topology of the network of highways fluctuates due to the possibility of reconnections. At quantum criticality the reconnections create long flux tubes making possible the flow of supra currents.

The interpretation of fluctuating stripes in terms of 1-D phonons

In TGD framework the phase transition to high T_c super-conductivity would have as a correlate fluctuating stripes to which supra currents are assigned. Note that the fluctuations occur also for $T > T_c$ but their amplitude is smaller. Stripes would be parallel to the dark magnetic flux tubes along which dark electron current flows above T_c . The fluctuations of magnetic flux tubes whose amplitude increases as T_c is approached induce transverse oscillations of the atoms of stripes representing 1-D transverse phonons.

The transverse fluctuations of stripes have naturally spin one character in accordance with the experimental facts. They allow identification as the excitations having 41 meV energy and would propagate in the preferred diagonal direction $(\pi/a, \pi/a)$. Dark Cooper pairs would have a gap energy of 27 meV. Neutron scattering resonance could be understood as a generation of these 1-D phonons and photon absorption a creation of this kind of phonon and breaking of dark Cooper pair. The transverse oscillations could give rise to the gap energy of the Cooper pair below T_{c1} and for the formation of long flux tubes below T_c but one can consider also other mechanisms based on the new physics predicted by TGD.

Various lattice effects such as superconductivity-induced phonon shifts and broadenings, isotope effects in T_c , the penetration depth, infrared and photoemission spectra have been observed in the cuprates [42]. The simplest interpretation is that ordinary phonons are replaced by 1-D phonons defined by the transversal excitations of stripes but do not give rise to the binding of the electrons of the Cooper pair but to to reconnection of flux tubes.

Explanation for the spectral signatures of high T_c superconductor

The model should explain various spectral signatures of high T_c super-conductors. It seems that this is possible at qualitative level at least.

1. Below the critical temperature there is a sharp absorption onset at energy of about $E_a = 50$ meV.

2. Second characteristic [56, 50, 51] of high T_c super conductors is resonant neutron scattering at excitation energy $E_w = 41$ meV of super conductor also visible only below the critical temperature.
3. The second derivative of $\sigma(\omega)$ peaks near 68 meV and assuming $E = E_g + E_w$ they found nearly perfect match using $E_g = 27$ meV for the energy gap.

$E_g = 27$ meV has a natural interpretation as energy gap of spin 1 Cooper pair. $E_w = 41$ meV can be assigned to the transversal oscillations of magnetic flux tubes inducing 1-D transversal photons which possibly give rise to the energy gap. $E_a = 50$ meV can be understood if also $S = 0$ Cooper pair for which electrons of the pair reside dominantly at the "outer" dipole flux tube and inner dipole core. The presence of this pair might explain the BCS type aspects of high T_c super-conductivity. This identification would predict the gap energy of $S = 0$ Cooper pair to be $E_g(S = 0) = 9$ meV. Since the critical absorption onset is observed only below T_c these Cooper pairs would become thermally stable at T_c and the formation of long flux tubes should somehow stabilize them. For very long flux tubes the distance of a point of "outer" flux tube from the nearby point "inner" flux tube becomes very long along dipole flux tube. Hence the transformation of $S = 0$ pairs to $S = 1$ pairs is not possible anymore and $S = 0$ pairs are stabilized.

Model for Cooper pairs

The TGD inspired model for Cooper pairs of high T_c super-conductor involves several new physics aspects: large \hbar phases, the notion of magnetic flux tubes. One can also consider the possibility that color force predicted by TGD to be present in all length scales is present.

1. One can consider two options for the topological quantization of the dipole field. It could decompose to a flux tube pattern with a discrete rotational symmetry Z_n around dipole axis or to flux sheets identified as walls of finite thickness invariant under rotations around dipole axis. Besides this there is also inner the flux tube corresponding to the dipole core. For the flux sheet option one can speak about eigenstates of L_z . For flux tube option the representations of Z_n define the counterparts of the angular momentum eigenstates with a cutoff in L_z analogous to a momentum cutoff in lattice. The discretized counterparts of spherical harmonics make sense. The counterparts of the relative angular momentum eigenstates for Cooper pair must be defined in terms of tensor products of these rather than using spherical harmonics assignable with the relative coordinate $r_1 - r_2$. The reconnection mechanism makes sense only for the flux tube option so that it is the only possibility in the recent context.
2. Exotic Cooper pair is modeled as a pair of large \hbar electrons with zoomed up size at space-time representing the dipole field pattern associated with a sequence of holes with same spin. If the members of the pair are at diametrically opposite flux tubes or at the "inner" flux tube (dipole core) magnetic fluxes flow in same direction for electrons and spin 1 Cooper pair is favored. If they reside at the "inner" flux tube and outer flux tube, spin zero state is favored. This raises the question whether also $S = 0$ variant of the Cooper pair could be present.
3. Large \hbar is needed to explain high critical temperature. By the general argument the transition to large \hbar phase occurs in order to reduce the value of the gauge coupling strength - now fine structure constant- and thus guarantee the convergence of the perturbation theory. The generation of positive net charge along stripes indeed means strong electromagnetic interactions at stripe.

Color force in condensed matter length scales is a new physics aspect which cannot be excluded in the case that transverse oscillations of flux tubes do not bind the electrons to form a Cooper pair. Classically color forces accompany any non-vacuum extremal of Kähler action since a non-vanishing induced Kähler field is accompanied by a classical color gauge field with Abelian holonomy. Induced Kähler field is always non-vanishing when the dimension of the CP_2 projection of the space-time surface is higher than 2. One can imagine too alternative scenarios.

1. Electromagnetic flux tubes for which induced Kähler field is non-vanishing carry also classical color fields. Cooper pairs could be color singlet bound states of color octet excitations of electrons

(more generally leptons) predicted by TGD and explaining quite impressive number of anomalies [24]. These states are necessarily dark since the decay widths of gauge bosons do not allow new light fermions coupling to them. The size of these states is of order electron size scale $L(127)$ for the standard value of Planck constant. For the non-standard value of Planck constant it would be scaled up correspondingly. For $r = \hbar/\hbar_0 = 2^{14}$ the size would be around 3.3 Angströms and for $r = 2^{24}$ of order 10 nm. Color binding could be responsible for the formation of the energy gap in this case and would distinguish between ordinary two-electron states and Cooper pair. The state with minimum color magnetic energy corresponds to spin triplet state for two color octet fermions whereas for colored fermion and antifermion it corresponds to spin singlet (pion like state in hadron physics).

2. A more complex variant of this picture served as the original model for Cooper pairs. Electrons at given space-time sheet feed their gauge flux to large space-time sheet via wormhole contacts. If the wormhole throats carry quantum numbers of quark and antiquark one can say that in the simplest situation the electron space-time sheet is color singlet state formed by quark and antiquark associated with the upper throats of the wormhole contacts carrying quantum numbers of u quark and \bar{d} quark. It can also happen that the electronic space-time sheets are not color singlet but color octet in which case the situation is analogous to that above. Color force would bind the two electronic space-time sheets to form a Cooper pair. The neighboring electrons in stripe possess parallel spins and could form a pair transforming to a large \hbar Cooper pair bound by color force. The Coulombic binding energy of the charged particles with the quarks and antiquarks assignable to the two wormhole throats feeding the em gauge flux to Y^4 and color interaction would be responsible for the energy gap.

Estimate for the gap energy

If transverse oscillations are responsible for the binding of the Cooper pairs, one expects similar expression for the gap energy as in the case of BCS type super conductors. The 3-D formula for the gap energy reads as

$$\begin{aligned}
 E_g &= \hbar\omega_D \exp(-1/X) , \\
 \omega_D &= (6\pi^2)^{1/3} c_s n^{1/3} \\
 X &= n(E_F)U_0 = \frac{3}{2} N(E_F) \frac{U_0}{E_F} , \\
 n(E_F) &= \frac{3}{2} \frac{N(E_F)}{E_F} .
 \end{aligned}
 \tag{12.3-3}$$

X depends on the details of the binding mechanism for Cooper pairs and U_0 parameterizes these details.

Since only stripes contribute to high T_c super-conductivity it is natural to replace 3-dimensional formula for Debye frequency in 1-dimensional case with

$$\begin{aligned}
 E_g &= \hbar\omega \exp(-1/X) , \\
 \omega &= kc_s n .
 \end{aligned}
 \tag{12.3-3}$$

where n is the 1-dimensional density of Cooper pairs and k a numerical constant. X would now correspond to the binding dynamics at the surface of 1-D counterpart of Fermi sphere associated with the stripe.

There is objection against this formula. The large number of holes for stripes suggests that the counterpart of Fermi sphere need not make sense, and one can wonder whether it could be more advantageous to talk about the counterpart of Fermi sphere for holes and treat Cooper pair as a pair of vacancies for this "Fermi sphere". High T_c super conductivity would be 1-D conventional super-conductivity for bound states of vacancies. This would require the replacement of n with the linear density of holes along stripes, which is essentially that of nuclei.

From the known data one can make a rough estimate for the parameter X . If $E_w = hf = 41$ meV is assigned with transverse oscillations the standard value of Planck constant would give $f = f_0 = 9.8 \times 10^{12}$ Hz. In the general case one has $f = f_0/r$. If one takes the 10^{-12} second length scale of the transversal fluctuations at a face value one obtains $r = 10$ as a first guess. $E_g = 27$ meV gives the estimate

$$\exp(-1/X) = \frac{E_g}{E_w} \quad (12.3.-2)$$

giving $X = 2.39$.

The interpretation in terms of transversal oscillations suggests the dispersion relation

$$f = \frac{c_s}{L} .$$

L is the length of the approximately straight portion of the flux tube. The length of the "outer" flux tube of the dipole field is expected to be longer than that of stripe. For $L = x$ nm and $f_D \sim 10^{12}$ Hz one would obtain $c_s = 10^3 x$ m/s.

Estimate for the critical temperatures and for \hbar

One can obtain a rough estimate for the critical temperature T_{c1} by following simple argument.

1. The formula for the critical temperature proposed in the previous section generalize in 1-dimensional case to the following formula

$$T_{c1} \leq \frac{\hbar^2}{8m_e} \left(\frac{n_c}{g}\right)^2 . \quad (12.3.-1)$$

g is the number of spin degrees of freedom for Cooper pair and n_c the 1-D density of Cooper pairs. The effective one-dimensionality allows only single $L = 2$ state localized along the stripe. The $g = 3$ holds true for $S = 1$.

2. By parameterizing n_c as $n_c = (1 - p_h)/a$, $a = x$ Angstrom, and substituting the values of various parameters, one obtains

$$T_{c1} \simeq \frac{r^2(1 - p_h)^2}{9x^2} \times 6.3 \text{ meV} . \quad (12.3.0)$$

3. An estimate for p_h follows from the doping fraction p_d and the fraction p_s of parallel atomic rows giving rise to stripes one can deduce the fraction of holes for a given stripe as

$$p_h = \frac{p_d}{p_s} . \quad (12.3.1)$$

One must of course have $p_d \leq p_s$. For instance, for $p_s = 1/5$ and $p_d = 15$ per cent one obtains $p_h = 75$ per cent so that a length of four atomic units along row contains one Cooper pair on the average. For $T_{c1} = 23$ meV (230 K) this would give the rough estimate $r = 23.3$: $r = 24$ satisfies the Fermat polygon constraint. Contrary to the first guess inspired by the model of bio-superconductivity the value of \hbar would not be very much higher than its standard value. Notice however that the proportionality $T_c \propto r^2$ makes it difficult to explain T_{c1} using the standard value of \hbar .

4. One $p_h \propto 1/L$ whereas scale invariance for reconnection probability ($p = p(x = TL/\hbar)$) predicts $T_c = x_c \hbar/L = x_c p_s \hbar/a$. This implies

$$\frac{T_c}{T_{c1}} = 32\pi^2 \frac{m_e a}{\hbar_0} x^2 g^2 \frac{p_s}{(1 - (p_d/p_s)^2)^2} \frac{x_c}{r}. \quad (12.3.2)$$

This prediction allows to test the proposed admittedly somewhat ad hoc formula. For $p_d \ll p_s$ T_c/T_{c1} does behaves as $1/L$. One can deduce the value of x_c from the empirical data.

5. Note that if the reconnection probability p is a universal function of x as quantum criticality suggests and thus also x_c is universal, a rather modest increase of \hbar could allow to raise T_c to room temperature range.

The value of \hbar is predicted to be inversely proportional to the density of the Cooper pairs at the flux tube. The large value of \hbar needed in the modeling of living system as magnetic flux tube super-conductor could be interpreted in terms of phase transitions which scale up both the length of flux tubes and the distance between the Cooper pairs so that the ratio rn_c remains unchanged.

Coherence lengths

The coherence length for high T_c super conductors is reported to be 5-20 Angstroms. The naive interpretation would be as the size of Cooper pair. There is however a loophole involved. The estimate for coherence length in terms of gap energy is given by $\xi = \frac{4\hbar v_F}{E_g}$. If the coherence length is estimated from the gap energy, as it seems to be the case, then the scaling up of the Planck constant would increase coherence length by a factor $r = \hbar/\hbar_0$. $r = 24$ would give coherence lengths in the range 12 – 48 nm.

The interpretation of the coherence length would be in terms of the length of the connected flux tube structure associated with the row of holes with the same spin direction which can be considerably longer than the row itself. As a matter fact r would characterize the ratio of size scales of the "magnetic body" of the row and of row itself. The coherence lengths could relate to the p-adic length scales $L(k)$ in the range $k = 151, 152, \dots, 155$ varying in the range (10, 40] nm. $k = 151$ correspond to thickness cell membrane.

Why copper and what about other elements?

The properties of copper are somehow crucial for high T_c superconductivity since cuprates are the only known high T_c superconductors. Copper corresponds to $3d^{10}4s$ ground state configuration with one valence electron. This encourages the question whether the doping by holes needed to achieve superconductivity induces the phase transition transforming the electrons to dark Cooper pairs.

More generally, elements having one electron in s state plus full electronic shells are good candidates for doped high T_c superconductors. If the atom in question is also a boson the formation of atomic Bose-Einstein condensates at Cooper pair space-time sheets is favored. Superfluid would be in question. Thus elements with odd value of A and Z possessing full shells plus single s wave valence electron are of special interest. The six stable elements satisfying these conditions are ${}^5\text{Li}$, ${}^{39}\text{K}$, ${}^{63}\text{Cu}$, ${}^{85}\text{Rb}$, ${}^{133}\text{Cs}$, and ${}^{197}\text{Au}$.

Bibliography

Books about TGD

- [1] M. Pitkänen (2006), *Topological Geometroynamics: Overview*.
http://tgd.wippiespace.com/public_html/tgdview/tgdview.html.
- [2] M. Pitkänen (2006), *Quantum Physics as Infinite-Dimensional Geometry*.
http://tgd.wippiespace.com/public_html/tgdgeom/tgdgeom.html.
- [3] M. Pitkänen (2006), *Physics in Many-Sheeted Space-Time*.
http://tgd.wippiespace.com/public_html/tgdclass/tgdclass.html.
- [4] M. Pitkänen (2006), *p-Adic length Scale Hypothesis and Dark Matter Hierarchy*.
http://tgd.wippiespace.com/public_html/paddark/paddark.html.
- [5] M. Pitkänen (2006), *Quantum TGD*.
http://tgd.wippiespace.com/public_html/tgdquant/tgdquant.html.
- [6] M. Pitkänen (2006), *TGD as a Generalized Number Theory*.
http://tgd.wippiespace.com/public_html/tgdnumber/tgdnumber.html.
- [7] M. Pitkänen (2006), *TGD and Fringe Physics*.
http://tgd.wippiespace.com/public_html/freenergy/freenergy.html.

Books about TGD Inspired Theory of Consciousness and Quantum Biology

- [8] M. Pitkänen (2006), *TGD Inspired Theory of Consciousness*.
http://tgd.wippiespace.com/public_html/tgdconsc/tgdconsc.html.
- [9] M. Pitkänen (2006), *Bio-Systems as Self-Organizing Quantum Systems*.
http://tgd.wippiespace.com/public_html/bioselforg/bioselforg.html.
- [10] M. Pitkänen (2006), *Quantum Hardware of Living Matter*.
http://tgd.wippiespace.com/public_html/bioware/bioware.html.
- [11] M. Pitkänen (2006), *Bio-Systems as Conscious Holograms*.
http://tgd.wippiespace.com/public_html/hologram/hologram.html.
- [12] M. Pitkänen (2006), *Genes and Memes*.
http://tgd.wippiespace.com/public_html/genememe/genememe.html.
- [13] M. Pitkänen (2006), *Magnetospheric Consciousness*.
http://tgd.wippiespace.com/public_html/magnconsc/magnconsc.html.
- [14] M. Pitkänen (2006), *Mathematical Aspects of Consciousness Theory*.
http://tgd.wippiespace.com/public_html/mathconsc/mathconsc.html.
- [15] M. Pitkänen (2006), *TGD and EEG*.
http://tgd.wippiespace.com/public_html/tgdeeg/tgdeeg.html.

References to the chapters of the books about TGD

- [16] The chapter *Dark Forces and Living Matter* of [4].
http://tgd.wippiespace.com/public_html/paddark/paddark.html#darkforces.
- [17] The chapter *p-Adic Particle Massivation: Hadron Masses* of [4].
http://tgd.wippiespace.com/public_html/paddark/paddark.html#mass3.
- [18] The chapter *p-Adic Particle Massivation: Elementary particle Masses* of [4].
http://tgd.wippiespace.com/public_html/paddark/paddark.html#mass2.
- [19] The chapter *Construction of Quantum Theory: S-matrix* of [5].
http://tgd.wippiespace.com/public_html/tgdquant/tgdquant.html#towards.
- [20] The chapter *Does the QFT Limit of TGD Have Space-Time Super-Symmetry?* of [5].
http://tgd.wippiespace.com/public_html/tgdquant/tgdquant.html#susy.
- [21] The chapter *Nuclear String Model* of [4].
http://tgd.wippiespace.com/public_html/paddark/paddark.html#nuclstring.
- [22] The chapter *Massless States and Particle Massivation* of [4].
http://tgd.wippiespace.com/public_html/paddark/paddark.html#mless.
- [23] The chapter *TGD and Nuclear Physics* of [4].
http://tgd.wippiespace.com/public_html/paddark/paddark.html#padnucl.
- [24] The chapter *The Recent Status of Leptohadron Hypothesis* of [4].
http://tgd.wippiespace.com/public_html/paddark/paddark.html#leptc.
- [25] The chapter *Quantum Field Theory Limit of TGD from Bosonic Emergence* of [5].
http://tgd.wippiespace.com/public_html/tgdquant/tgdquant.html#emergence.
- [26] The chapter *Is it Possible to Understand Coupling Constant Evolution at Space-Time Level?* of [5].
http://tgd.wippiespace.com/public_html/tgdquant/tgdquant.html#rgflow.
- [27] The chapter *Dark Nuclear Physics and Condensed Matter* of [4].
http://tgd.wippiespace.com/public_html/paddark/paddark.html#exonuclear.
- [28] The chapter *General Ideas about Many-Sheeted Space-Time: Part I* of [3].
http://tgd.wippiespace.com/public_html/tgdclass/tgdclass.html#topcond.
- [29] The chapter *Does TGD Predict the Spectrum of Planck Constants?* of [5].
http://tgd.wippiespace.com/public_html/tgdquant/tgdquant.html#Planck.

References to the chapters of the books about TGD Inspired Theory of Consciousness and Quantum Biology

- [30] The chapter *Quantum Model for Hearing* of [15].
http://tgd.wippiespace.com/public_html//tgdeeg/tgdeeg/tgdeeg.html#hearing.
- [31] The chapter *Wormhole Magnetic Fields* of [10].
http://tgd.wippiespace.com/public_html/bioware/bioware.html#wormc.
- [32] The chapter *Dark Matter Hierarchy and Hierarchy of EEGs* of [15].
http://tgd.wippiespace.com/public_html/tgdeeg/tgdeeg.html#eegdark.
- [33] The chapter *General Theory of Qualia* of [11].
http://tgd.wippiespace.com/public_html/hologram/hologram.html#qualia.
- [34] The chapter *Genes and Memes* of [12].
http://tgd.wippiespace.com/public_html/genememe/genememe.html#genememec.

Articles related to TGD

- [35] M. Pitkänen (2007), *Further Progress in Nuclear String Hypothesis*, http://tgd.wippiespace.com/public_html/articles/nuclstring.pdf.

Mathematics

- [36] <http://math.ucr.edu/home/baez/quantum/ruberman.html>.

Condensed matter physics

- [37] I. Morgenstern (1990), article *Spin-Glass behavior of high T_c super conductors* in the book *Earlier and Recent Aspects of Super Conductivity* (eds. J. G. Bednorz and K. A. Muller), Springer Verlag.
- [38] M. Buchanan (2001), *Mind the pseudogap*. Nature, vol 408, January 4. <http://www.physique.usherbrooke.ca/taillefer/Projets/Nature-409008.pdf>.
- [39] J. Zaanen (2007), *Watching Rush Hour in the World of Electrons*. Science vol 315. www.sciencemag.org. <http://www.ilorentz.org/~jan/perspstripes.pdf>.
- [40] J. Zaanen (2005), *Why high T_c is exciting?*. http://www.lorentz.leidenuniv.nl/research/jan_hitc.pdf.
- [41] M. Springford (ed) (1997), *Electron: A Centenary Volume*. Cambridge University Press.
- [42] *High temperature and other unconventional superconductors*. <http://www.fkf.mpg.de/metzner/research/hightc/hightc.html>.
- [43] S. Sachdev (1999) *Quantum phase transitions (summary)*. Physics World April pp. 33-38.
- [44] M. Rabinowitz (2001), *Phenomenological Theory of Superfluidity and Super-conductivity*. <http://arxiv.org/ftp/cond-mat/papers/0104/0104059.pdf>.
- [45] F. Levy, I. Sheikin, B. Grenier, and A. D. Huxley (2005), *Magnetic Field-Induced Super-conductivity in the Ferromagnet URhGe*. Science 26, August, 1343-1346.
See also P. Rogers (2005), *Critical breakthrough*. Physics Web. <http://physicsweb.org/articles/news/9/8/17>.
- [46] J. Orenstein, *Electrons pair themselves*. Nature 401.
- [47] J. Flouquet and A. Boudin (2002), *Ferromagnetic super-conductors*. Physics Web, <http://physicsweb.org/articles/world/15/1/9>.
- [48] *Percolation*. <http://en.wikipedia.org/wiki/Percolation>.
- [49] D. Aoki *et al* (2001), *Coexistence of super-conductivity and ferromagnetism in URhGe* (restricted access), Nature 413 613-616.
S. S. Saxena *et al* (2000), *Super-conductivity at the border of itinerant electron ferromagnetism in UGe₂* (restricted access) Nature 406, 587-592.
C. Pfleiderer *et al* (2001), *Coexistence of super-conductivity and ferromagnetism in d band metal ZrZn₂* (restricted access), Nature 412 58-61.
- [50] H.A. Mooock *et al* (1993), Phys. Rev. Lett. 70, 3490.
- [51] H. S. Fong *et al* (1995), Phys. Rev. Lett. 75, 316.
- [52] V. J. Emery, S. A. Kivelson, and J. M. Tranquada (1999), *Stripe phases in high-temperature superconductors*. Perspective, Vol. 96, Issue 16, 8814-8817, August 3. <http://www.pnas.org/cgi/reprint/96/16/8814.pdf>.

- [53] N. D. Mathur *et al* (1998), *Nature* 394, 39.
See also *Magnetic superglue promotes super-conductivity*. Physics Web. <http://physicsweb.org/articles/news/2/7/3>.
- [54] J. Zaanen (2006), *Superconductivity: Quantum Stripe Search*. *Nature* vol 440, 27 April. <http://www.lorentz.leidenuniv.nl/~jan/nature03/qustripes06.pdf>.
- [55] *Scientists Detect 'Fingerprint' of High-temperature Superconductivity Above Transition Temperature*. <http://www.sciencedaily.com/releases/2009/08/090827141338.htm>.
- [56] J. Rossat-Mignot *et al* (1994), *Physica (Amsterdam)* 235 C, 59.
- [57] G. Burns (1993) *High Temperature Super Conductivity*. Academic Press, Inc.
- [58] J. Orenstein *et al* (1990), in *Electronic properties of high T_c super conductors* (ed. H. Kuzmany) 254-259. Springer, Berlin.
- [59] J. Carbotte, E. Schachinger, D. N. Basov (1999), *Nature* 401, p. 354-356.
- [60] D. A. Wollman *et al* (1993), *Experimental determination of the super-conducting pairing state in YBCO from the phase coherence of YBCO-Pb dc SQUIDS*. *Phys. Rev. Lett.* B 71, 2134-2137.

Consciousness related references

- [61] D. Yarrow (1990), *Spin the tale of the dragon*. review article on biomagnetism, <http://www.ratical.org/reatv11e/RofD2.html>.
- [62] C. F. Blackman (1994), "Effect of Electrical and Magnetic Fields on the Nervous System" in *The Vulnerable Brain and Enviromental Risks, Vol. 3, Toxins in Air and Water* (eds. R. L. Isaacson and K. F. Jensen). Plenum Press, New York, pp. 331-355.

Chapter 13

Quantum Hall effect and Hierarchy of Planck Constants

13.1 Introduction

Quantum Hall effect [74, 70, 76] occurs in 2-dimensional systems, typically a slab carrying a longitudinal voltage V causing longitudinal current j . A magnetic field orthogonal to the slab generates a transversal current component j_T by Lorentz force. j_T is proportional to the voltage V along the slab and the dimensionless coefficient is known as transversal conductivity. Classically the coefficient is proportional ne/B , where n is 2-dimensional electron density and should have a continuous spectrum. The finding that came as surprise was that the change of the coefficient as a function of parameters like magnetic field strength and temperature occurred as discrete steps of same size. In integer quantum Hall effect the coefficient is quantized to $2\nu\alpha$, $\alpha = e^2/4\pi$, such that ν is integer.

Later came the finding that also smaller steps corresponding to the filling fraction $\nu = 1/3$ of the basic step were present and could be understood if the charge of electron would have been replaced with $\nu = 1/3$ of its ordinary value. Later also QH effect with wide large range of filling fractions of form $\nu = k/m$ was observed.

The model explaining the QH effect is based on pseudo particles known as anyons [50, 70]. According to the general argument of [71] anyons have fractional charge νe . Also the TGD based model for fractionization to be discussed later suggests that the anyon charge should be νe quite generally. The braid statistics of anyon is believed to be fractional so that anyons are neither bosons nor fermions. Non-fractional statistics is absolutely essential for the vacuum degeneracy used to represent logical qubits.

In the case of Abelian anyons the gauge potential corresponds to the vector potential of the divergence free velocity field or equivalently of incompressible anyon current. For non-Abelian anyons the field theory defined by Chern-Simons action is free field theory and in well-defined sense trivial although it defines knot invariants. For non-Abelian anyons situation would be different. They would carry non-Abelian gauge charges possibly related to a symmetry breaking to a discrete subgroup H of gauge group [50] each of them defining an incompressible hydrodynamical flow. According to [60] the anyons associated with the filling fraction $\nu = 5/2$ are a good candidate for non-Abelian anyons and in this case the charge of electron is reduced to $Q = e/4$ rather than being $Q = \nu e$ [75]. This finding favors non-Abelian models [76].

Non-Abelian anyons [68, 70] are always created in pairs since they carry a conserved topological charge. In the model of [60] this charge should have values in 4-element group Z_4 so that it is conserved only modulo 4 so that charges +2 and -2 are equivalent as are also charges 3 and -1. The state of n anyon pairs created from vacuum can be show to possess 2^{n-1} -dimensional vacuum degeneracy [69]. When two anyons fuse the 2^{n-1} -dimensional state space decomposes to 2^{n-2} -dimensional tensor factors corresponding to anyon Cooper pairs with topological charges 2 and 0. The topological "spin" is ideal for representing logical qubits. Since free topological charges are not possible the notion of physical qubit does not make sense (note the analogy with quarks). The measurement of topological qubit reduces to a measurement of whether anyon Cooper pair has vanishing topological charge or not.

Topological quantum computation is perhaps the most promising application of anyons [66, 60, 61, 58, 57, 64, 59]. I have already earlier proposed the explanation of FQHE, anyons, and fractionization of quantum numbers in terms of hierarchy of Planck constants realized as a generalization of the imbedding space $H = M^4 \times CP_2$ to a book like structure [39]. The book like structure applies separately to CP_2 and to causal diamonds ($CD \subset M^4$) defined as intersections of future and past directed light-cones. The pages of the Big Book correspond to singular coverings and factor spaces of CD (CP_2) glued along 2-D subspace of CD (CP_2) and are labeled by the values of Planck constants assignable to CD and CP_2 and appearing in Lie algebra commutation relations. The observed Planck constant \hbar , whose square defines the scale of M^4 metric corresponds to the ratio of these Planck constants. The key observation is that fractional filling factor results for ordinary integer QHE if \hbar is scaled up by a rational number.

In this chapter I try to formulate more precisely this idea. The outcome is a rather detailed view about anyons on one hand, and about the Kähler structure of the generalized imbedding space on the other hand.

1. Fundamental role is played by the assumption that the Kähler gauge potential of CP_2 contains a gauge part with no physical implications in the context of gauge theories but contributing to physics in TGD framework since $U(1)$ gauge transformations are representations of symplectic transformations of CP_2 . Also in the case of CD it makes also sense to speak about Kähler gauge potential. The gauge part codes for Planck constants of CD and CP_2 and leads to the identification of anyons as states associated with partonic 2-surfaces surrounding the tip of CD and fractionization of quantum numbers. Explicit formulas relating fractionized charges to the coefficients characterizing the gauge parts of Kähler gauge potentials of CD and CP_2 are proposed based on some empirical input.
2. One important implication is that Poincare and Lorentz invariance are broken inside given CD although they remain exact symmetries at the level of the geometry of world of classical worlds (WCW). The interpretation is as a breaking of symmetries forced by the selection of quantization axis.
3. Anyons would basically correspond to matter at 2-dimensional "partonic" surfaces of macroscopic size surrounding the tip of the light-cone boundary of CD and could be regarded as gigantic elementary particle states with very large quantum numbers and by charge fractionization confined around the tip of CD . Charge fractionization and anyons would be basic characteristic of dark matter (dark only in relative sense). Hence it is not surprising that anyons would have applications going far beyond condensed matter physics. Anyonic dark matter concentrated at 2-dimensional surfaces would play key key role in the the physics of stars and black holes, and also in the formation of planetary system via the condensation of the ordinary matter around dark matter. This assumption was the basic starting point leading to the discovery of the hierarchy of Planck constants [39]. In living matter membrane like structures would represent a key example of anyonic systems as the model of DNA as topological quantum computer indeed assumes [44].
4. One of the basic questions has been whether TGD forces the hierarchy of Planck constants realized in terms of generalized imbedding space or not. The condition that the choice of quantization axes has a geometric correlate at the imbedding space level motivated by quantum classical correspondence of course forces the hierarchy: this has been clear from the beginning. It is now clear that also the first principle description of anyons requires the hierarchy in TGD Universe. The hierarchy reveals also new light to the huge vacuum degeneracy of TGD and reduces it dramatically at pages for which CD corresponds to a non-trivial covering or factor space, which suggests that mathematical existence of the theory necessitates the hierarchy of Planck constants. Also the proposed manifestation of Equivalence Principle at the level of symplectic fusion algebras as a duality between descriptions relying on the symplectic structures of CD and CP_2 [31] forces the hierarchy of Planck constants.

The first sections of the chapter contain summary about theories of quantum Hall effect appearing already in [42]. Second section is a slightly modified version of the description of the generalized imbedding space, which has appeared already in [39, 42, 44] and containing brief description of how

to understand QHE in this framework. The third section represents the basic new results about the Kähler structure of generalized imbedding space and represents the resulting model of QHE.

13.2 About theories of quantum Hall effect

The most elegant models of quantum Hall effect are in terms of anyons regarded as singularities due to the symmetry breaking of gauge group G down to a finite sub-group H , which can be also non-Abelian. Concerning the description of the dynamics of topological degrees of freedom topological quantum field theories based on Chern-Simons action are the most promising approach.

13.2.1 Quantum Hall effect as a spontaneous symmetry breaking down to a discrete subgroup of the gauge group

The system exhibiting quantum Hall effect is effectively 2-dimensional. Fractional statistics suggests that topological defects, anyons, allowing a description in terms of the representations of the homotopy group of $((R^2)^n - D)/S_n$. The gauge theory description would be in terms of spontaneous symmetry breaking of the gauge group G to a finite subgroup H by a Higgs mechanism [50, 70]. This would make all gauge degrees of freedom massive and leave only topological degrees of freedom. What is unexpected that also non-Abelian topological degrees of freedom are in principle possible. Quantum Hall effect is Abelian or non-Abelian depending on whether the group H has this property.

In the symmetry breaking $G \rightarrow H$ the non-Abelian gauge fluxes defined as non-integrable phase factors $Pexp(i \oint A_\mu dx^\mu)$ around large circles (surrounding singularities (so that field approaches a pure gauge configuration) are elements of the first homotopy group of G/H , which is H in the case that H is discrete group and G is simple. An idealized manner to model the situation [70] is to assume that the connection is pure gauge and defined by an H -valued function which is many-valued such that the values for different branches are related by a gauge transformation in H . In the general case a gauge transformation of a non-trivial gauge field by a multi-valued element of the gauge group would give rise to a similar situation.

One can characterize a given topological singularity magnetically by an element in conjugacy class C of H representing the transformation of H induced by a 2π rotation around singularity. The elements of C define states in given magnetic representation. Electrically the particles are characterized by an irreducible representations of the subgroup of $H_C \subset H$ which commutes with an arbitrarily chosen element of the conjugacy class C .

The action of $h(B)$ resulting on particle A when it makes a closed turn around B reduces in magnetic degrees of freedom to translation in conjugacy class combined with the action of element of H_C in electric degrees of freedom. Closed paths correspond to elements of the braid group $B_n(X^2)$ identifiable as the mapping class group of the punctured 2-surface X^2 and this means that symmetry breaking $G \rightarrow H$ defines a representation of the braid group. The construction of these representations is discussed in [70] and leads naturally via the group algebra of H to the so called quantum double $D(H)$ of H , which is a quasi-triangular Hopf algebra allowing non-trivial representations of braid group.

Anyons could be singularities of gauge fields, perhaps even non-Abelian gauge fields, and the latter ones could be modelled by these representations. In particular, braid operations could be represented using anyons.

13.2.2 Witten-Chern-Simons action and topological quantum field theories

The Wess-Zumino-Witten action used to model 2-dimensional critical systems consists of a 2-dimensional conformally invariant term for the chiral field having values in group G combined with 2+1-dimensional term defined as the integral of Chern-Simons 3-form over a 3-space containing 2-D space as its boundary. This term is purely topological and identifiable as winding number for the map from 3-dimensional space to G . The coefficient of this term is integer k in suitable normalization. k gives the value of central extension of the Kac-Moody algebra defined by the theory.

One can couple the chiral field $g(x)$ to gauge potential defined for some subgroup of G_1 of G . If the G_1 coincides with G , the chiral field can be gauged away by a suitable gauge transformation and the theory becomes purely topological Witten-Chern-Simons theory. Pure gauge field configuration

represented either as flat gauge fields with non-trivial holonomy over homotopically non-trivial paths or as multi-valued gauge group elements however remain and the remaining degrees of freedom correspond to the topological degrees of freedom.

Witten-Chern-Simons theories are labelled by a positive integer k giving the value of central extension of the Kac-Moody algebra defined by the theory. The connection with Wess-Zumino-Witten theory come from the fact that the highest weight states associated with the representations of the Kac-Moody algebra of WZW theory are in one-one correspondence with the representations R_i possible for Wilson loops in the topological quantum field theory.

In the Abelian case case 2+1-dimensional Chern-Simons action density is essentially the inner product $A \wedge dA$ of the vector potential and magnetic field known as helicity density and the theory in question is a free field theory. In the non-Abelian case the action is defined by the 3-form

$$\frac{k}{4\pi} \text{Tr} \left(A \wedge (dA + \frac{2}{3} A \wedge A) \right)$$

and contains also interaction term so that the field theory defined by the exponential of the interaction term is non-trivial.

In topological quantum field theory the usual n -point correlation functions defined by the functional integral are replaced by the functional averages for Diff^3 invariant quantities defined in terms of non-integrable phase factors defined by ordered exponentials over closed loops. One can consider arbitrary number of loops which can be knotted, linked, and braided. These quantities define both knot and 3-manifold invariants (the functional integral for zero link in particular). The perturbative calculation of the quantum averages leads directly to the Gaussian linking numbers and infinite number of perturbative link and not invariants.

The experience gained from topological quantum field theories defined by Chern-Simons action has led to a very elegant and surprisingly simple category theoretical approach to the topological quantum field theory [51, 56] allowing to assign invariants to knots, links, braids, and tangles and also to 3-manifolds for which braids as morphisms are replaced with cobordisms. The so called modular Hopf algebras, in particular quantum groups $Sl(2)_q$ with q a root of unity, are in key role in this approach. Also the connection between links and 3-manifolds can be understood since closed, oriented, 3-manifolds can be constructed from each other by surgery based on links [19].

Witten's article [53] "Quantum Field Theory and the Jones Polynomial" is full of ingenious constructions, and for a physicist it is the easiest and certainly highly enjoyable manner to learn about knots and 3-manifolds. For these reasons a little bit more detailed sum up is perhaps in order.

1. Witten discusses first the quantization of Chern-Simons action at the weak coupling limit $k \rightarrow \infty$. First it is shown how the functional integration around flat connections defines a topological invariant for 3-manifolds in the case of a trivial Wilson loop. Next a canonical quantization is performed in the case $X^3 = \Sigma^2 \times R^1$: in the Coulomb gauge $A_3 = 0$ the action reduces to a sum of $n = \dim(G)$ Abelian Chern-Simons actions with a non-linear constraint expressing the vanishing of the gauge field. The configuration space consists thus of flat non-Abelian connections, which are characterized by their holonomy groups and allows Kähler manifold structure.
2. Perhaps the most elegant quantal element of the approach is the decomposition of the 3-manifold to two pieces glued together along 2-manifold implying the decomposition of the functional integral to a product of functional integrals over the pieces. This together with the basic properties of Hilbert of complex numbers (to which the partition functions defined by the functional integrals over the two pieces belong) allows almost a miracle like deduction of the basic results about the behavior of 3-manifold and link invariants under a connected sum, and leads to the crucial skein relations allowing to calculate the invariants by decomposing the link step by step to a union of unknotted, unlinked Wilson loops, which can be calculated exactly for $SU(N)$. The decomposition by skein relations gives rise to a partition function like representation of invariants and allows to understand the connection between knot theory and statistical physics [52]. A direct relationship with conformal field theories and Wess-Zumino-Witten model emerges via Wilson loops associated with the highest weight representations for Kac Moody algebras.
3. A similar decomposition procedure applies also to the calculation of 3-manifold invariants using link surgery to transform 3-manifolds to each other, with 3-manifold invariants being defined as

Wilson loops associated with the homology generators of these (solid) tori using representations R_i appearing as highest weight representations of the loop algebra of torus. Surgery operations are represented as mapping class group operations acting in the Hilbert space defined by the invariants for representations R_i for the original 3-manifold. The outcome is explicit formulas for the invariants of trivial knots and 3-manifold invariant of S^3 for $G = SU(N)$, in terms of which more complex invariants are expressible.

4. For $SU(N)$ the invariants are expressible as functions of the phase $q = \exp(i2\pi/(k + N))$ associated with quantum groups [19]. Note that for $SU(2)$ and $k = 3$, the invariants are expressible in terms of Golden Ratio. The central charge $k = 3$ is in a special position since it gives rise to $k + 1 = 4$ -vertex representing naturally 2-gate physically. Witten-Chern-Simons theories define universal unitary modular functors characterizing quantum computations [61].

13.2.3 Chern-Simons action for anyons

In the case of quantum Hall effect the Chern-Simons action has been deduced from a model of electrons as a 2-dimensional incompressible fluid [74]. Incompressibility requires that the electron current has a vanishing divergence, which makes it analogous to a magnetic field. The expressibility of the current as a curl of a vector potential b , and a detailed study of the interaction Lagrangian leads to the identification of an Abelian Chern-Simons for b as a low energy effective action. This action is Abelian, whereas the anyonic realization of quantum computation would suggest a non-Abelian Chern-Simons action.

Non-Abelian Chern-Simons action could result in the symmetry breaking of a non-Abelian gauge group G , most naturally electro-weak gauge group, to a non-Abelian discrete subgroup H [50] so that states would be labelled by representations of H and anyons would be characterized magnetically H -valued non-Abelian magnetic fluxes each of them defining its own incompressible hydro-dynamical flow. As will be found, TGD predicts a non-Abelian Chern-Simons term associated with electroweak long range classical fields.

13.2.4 Topological quantum computation using braids and anyons

By the general mathematical results braids are able to code all quantum logic operations [59]. In particular, braids allow to realize any quantum circuit consisting of single particle gates acting on qubits and two particle gates acting on pairs of qubits. The coding of braid requires a classical computation which can be done in polynomial time. The coding requires that each dancer is able to remember its dancing history by coding it into its own state.

The general ideas are following.

1. The ground states of anyonic system characterize the logical qubits, One assumes non-Abelian anyons with Z_4 -valued topological charge so that a system of n anyon pairs created from vacuum allows 2^{n-1} -fold anyon degeneracy [69]. The system is decomposed into blocks containing one anyonic Cooper pair with $Q_T \in \{2, 0\}$ and two anyons with such topological charges that the net topological charge vanishes. One can say that the states $(0, 1 - 1)$ and $(0, -1, +1)$ represent logical qubit 0 whereas the states $(2, -1, -1)$ and $(2, +1, +1)$ represent logical qubit 1. This would suggest 2^2 -fold degeneracy but actually the degeneracy is 2-fold.

Free physical qubits are not possible and at least four particles are indeed necessarily in order to represent logical qubit. The reason is that the conservation of Z^4 charge would not allow mixing of qubits 1 and 0, in particular the Hadamard 1-gate generating square root of qubit would break the conservation of topological charge. The square root of qubit can be generated only if 2 units of topological charge is transferred between anyon and anyon Cooper pair. Thus qubits can be represented as entangled states of anyon Cooper pair and anyon and the fourth anyon is needed to achieve vanishing total topological charge in the batch.

2. In the initial state of the system the anyonic Cooper pairs have $Q_T = 0$ and the two anyons have opposite topological charges inside each block. The initial state codes no information unlike in ordinary computation but the information is represented by the braid. Of course, also more general configurations are possible. Anyons are assumed to evolve like free particles except during swap operations and their time evolution is described by single particle Hamiltonians.

Free particle approximation fails when the anyons are too near to each other as during braid operations. The space of logical qubits is realized as k -code defined by the 2^{n-1} ground states, which are stable against local single particle perturbations for $k = 3$ Witten-Chern-Simons action. In the more general case the stability against n -particle perturbations with $n < [k/2]$ is achieved but the gates would become $[k/2]$ -particle gates (for $k = 5$ this would give 6-particle vertices).

3. Anyonic system provides a unitary modular functor as the S-matrix associated with the anyon system whose time evolution is fixed by the pre-existing braid structure. What this means that the S-matrices associated with the braids can be multiplied and thus a unitary representation for the group formed by braids results. The vacuum degeneracy of anyon system makes this representation non-trivial. By the NP complexity of braids it is possible to code any quantum logic operation by a particular braid [57]. There exists a powerful approximation theorem allowing to achieve this coding classically in polynomial time [59]. From the properties of the R-matrices inducing gate operations it is indeed clear that two gates can be realized. The Hadamard 1-gate could be realized as 2-gate in the system formed by anyon Cooper pair and anyon.
4. In [60] the time evolution is regarded as a discrete sequence of modifications of single anyon Hamiltonians induced by swaps [58]. If the modifications define a closed loop in the space of Hamiltonians the resulting unitary operators define a representation of braid group in a dense discrete sub-group of $U(2^n)$. The swap operation is 2-local operation acting like a 2-gate and induces quantum logical operation modifying also single particle Hamiltonians. What is important that this modification maps the space of the ground states to a new one and only if the modifications correspond to a closed loop the final state is in the same code space as the initial state. What time evolution does is to affect the topological charges of anyon Cooper pairs representing qubits inside the 4-anyon batches defined by the braids.

In quantum field theory the analog but not equivalent of this description would be following. Quite generally, a given particle in the final state has suffered a unitary transformation, which is an ordered product consisting of two kinds of unitary operators. Unitary single particle operators $U_n = Pexp(i \int_{t_n}^{t_{n+1}} H_0 dt)$ are analogs of operators describing single qubit gate and play the role of anyon propagators during no-swap periods. Two-particle unitary operators $U_{swap} = Pexp(i \int H_{swap} dt)$ are analogous to four-particle interactions and describe the effect of braid operations inducing entanglement of states having opposite values of topological charge but conserving the net topological charge of the anyon pair. This entanglement is completely analogous to spin entanglement. In particular, the braid operation mixes different states of the anyon. The unitary time development operator generating entangled state of anyons and defined by the braid structure represents the operation performed by the quantum circuit and the quantum measurement in the final state selects a particular final state.

5. Formally the computation halts with a measurement of the topological charge of the left-most anyon Cooper pair when the outcome is just single bit. If decay occurs with sufficiently high probability it is concluded that the value of the computed bit is 0, otherwise 1.

13.3 Hierarchy of Planck constants and the generalization of the notion of imbedding space

In the following the recent view about structure of imbedding space forced by the quantization of Planck constant is summarized. The question is whether it might be possible in some sense to replace H or its Cartesian factors by their necessarily singular multiple coverings and factor spaces. One can consider two options: either M^4 or the causal diamond CD . The latter one is the more plausible option from the point of view of WCW geometry.

13.3.1 The evolution of physical ideas about hierarchy of Planck constants

The evolution of the physical ideas related to the hierarchy of Planck constants and dark matter as a hierarchy of phases of matter with non-standard value of Planck constants was much faster than the

evolution of mathematical ideas and quite a number of applications have been developed during last five years.

1. The starting point was the proposal of Nottale [78] that the orbits of inner planets correspond to Bohr orbits with Planck constant $\hbar_{gr} = GMm/v_0$ and outer planets with Planck constant $\hbar_{gr} = 5GMm/v_0$, $v_0/c \simeq 2^{-11}$. The basic proposal [38, 27] was that ordinary matter condenses around dark matter which is a phase of matter characterized by a non-standard value of Planck constant whose value is gigantic for the space-time sheets mediating gravitational interaction. The interpretation of these space-time sheets could be as magnetic flux quanta or as massless extremals assignable to gravitons.
2. Ordinary particles possibly residing at these space-time sheet have enormous value of Compton length meaning that the density of matter at these space-time sheets must be very slowly varying. The string tension of string like objects implies effective negative pressure characterizing dark energy so that the interpretation in terms of dark energy might make sense [16]. TGD predicted a one-parameter family of Robertson-Walker cosmologies with critical or over-critical mass density and the "pressure" associated with these cosmologies is negative.
3. The quantization of Planck constant does not make sense unless one modifies the view about standard space-time is. Particles with different Planck constant must belong to different worlds in the sense local interactions of particles with different values of \hbar are not possible. This inspires the idea about the book like structure of the imbedding space obtained by gluing almost copies of H together along common "back" and partially labeled by different values of Planck constant.
4. Darkness is a relative notion in this framework and due to the fact that particles at different pages of the book like structure cannot appear in the same vertex of the generalized Feynman diagram. The phase transitions in which partonic 2-surface X^2 during its travel along X^3 leads to another page of book are however possible and change Planck constant. Particle (say photon -) exchanges of this kind allow particles at different pages to interact. The interactions are strongly constrained by charge fractionization and are essentially phase transitions involving many particles. Classical interactions are also possible. It might be that we are actually observing dark matter via classical fields all the time and perhaps have even photographed it [41].
5. The realization that non-standard values of Planck constant give rise to charge and spin fractionization and anyonization led to the precise identification of the prerequisites of anyonic phase. If the partonic 2-surface, which can have even astrophysical size, surrounds the tip of CD , the matter at the surface is anyonic and particles are confined at this surface. Dark matter could be confined inside this kind of light-like 3-surfaces around which ordinary matter condenses. If the radii of the basic pieces of these nearly spherical anyonic surfaces - glued to a connected structure by flux tubes mediating gravitational interaction - are given by Bohr rules, the findings of Nottale [78] can be understood. Dark matter would resemble to a high degree matter in black holes replaced in TGD framework by light-like partonic 2-surfaces with a minimum size of order Schwarzschild radius r_S of order scaled up Planck length $l_{Pl} = \sqrt{\hbar_{gr}G} = GM$. Black hole entropy is inversely proportional to \hbar and predicted to be of order unity so that dramatic modification of the picture about black holes is implied.
6. Perhaps the most fascinating applications are in biology. The anomalous behavior ionic currents through cell membrane (low dissipation, quantal character, no change when the membrane is replaced with artificial one) has a natural explanation in terms of dark supra currents. This leads to a vision about how dark matter and phase transitions changing the value of Planck constant could relate to the basic functions of cell, functioning of DNA and aminoacids, and to the mysteries of bio-catalysis. This leads also a model for EEG interpreted as a communication and control tool of magnetic body containing dark matter and using biological body as motor instrument and sensory receptor. One especially amazing outcome is the emergence of genetic code of vertebrates from the model of dark nuclei as nuclear strings [47, 41].

13.3.2 The most general option for the generalized imbedding space

Simple physical arguments pose constraints on the choice of the most general form of the imbedding space.

1. The fundamental group of the space for which one constructs a non-singular covering space or factor space should be non-trivial. This is certainly not possible for M^4 , CD , CP_2 , or H . One can however construct singular covering spaces. The fixing of the quantization axes implies a selection of the sub-space $H_4 = M^2 \times S^2 \subset M^4 \times CP_2$, where S^2 is geodesic sphere of CP_2 . $\hat{M}^4 = M^4 \setminus M^2$ and $\hat{CP}_2 = CP_2 \setminus S^2$ have fundamental group Z since the codimension of the excluded sub-manifold is equal to two and homotopically the situation is like that for a punctured plane. The exclusion of these sub-manifolds defined by the choice of quantization axes could naturally give rise to the desired situation.
2. CP_2 allows two geodesic spheres which left invariant by $U(2)$ resp. $SO(3)$. The first one is homologically non-trivial. For homologically non-trivial geodesic sphere $H_4 = M^2 \times S^2$ represents a straight cosmic string which is non-vacuum extremal of Kähler action (not necessarily preferred extremal). One can argue that the many-valuedness of \hbar is un-acceptable for non-vacuum extremals so that only homologically trivial geodesic sphere S^2 would be acceptable. One could go even further. If the extremals in $M^2 \times CP_2$ can be preferred non-vacuum extremals, the singular coverings of M^4 are not possible. Therefore only the singular coverings and factor spaces of CP_2 over the homologically trivial geodesic sphere S^2 would be possible. This however looks a non-physical outcome.
 - (a) The situation changes if the extremals of type $M^2 \times Y^2$, Y^2 a holomorphic surface of CP_3 , fail to be hyperquaternionic. The tangent space M^2 represents hypercomplex sub-space and the product of the modified gamma matrices associated with the tangent spaces of Y^2 should belong to M^2 algebra. This need not be the case in general.
 - (b) The situation changes also if one reinterprets the gluing procedure by introducing scaled up coordinates for M^4 so that metric is continuous at $M^2 \times CP_2$ but CD s with different size have different sizes differing by the ratio of Planck constants and would thus have only piece of lower or upper boundary in common.
3. For the more general option one would have four different options corresponding to the Cartesian products of singular coverings and factor spaces. These options can be denoted by $C-C$, $C-F$, $F-C$, and $F-F$, where C (F) signifies for covering (factor space) and first (second) letter signifies for CD (CP_2) and correspond to the spaces $(\hat{CD} \hat{\times} G_a) \times (\hat{CP}_2 \hat{\times} G_b)$, $(\hat{CD} \hat{\times} G_a) \times \hat{CP}_2/G_b$, $\hat{CD}/G_a \times (\hat{CP}_2 \hat{\times} G_b)$, and $\hat{CD}/G_a \times \hat{CP}_2/G_b$.
4. The groups G_i could correspond to cyclic groups Z_n . One can also consider an extension by replacing M^2 and S^2 with its orbit under more general group G (say tetrahedral, octahedral, or icosahedral group). One expects that the discrete subgroups of $SU(2)$ emerge naturally in this framework if one allows the action of these groups on the singular sub-manifolds M^2 or S^2 . This would replace the singular manifold with a set of its rotated copies in the case that the subgroups have genuinely 3-dimensional action (the subgroups which corresponds to exceptional groups in the ADE correspondence). For instance, in the case of M^2 the quantization axes for angular momentum would be replaced by the set of quantization axes going through the vertices of tetrahedron, octahedron, or icosahedron. This would bring non-commutative homotopy groups into the picture in a natural manner.

13.3.3 About the phase transitions changing Planck constant

There are several non-trivial questions related to the details of the gluing procedure and phase transition as motion of partonic 2-surface from one sector of the imbedding space to another one.

1. How the gluing of copies of imbedding space at $M^2 \times CP_2$ takes place? It would seem that the covariant metric of CD factor proportional to \hbar^2 must be discontinuous at the singular manifold since only in this manner the idea about different scaling factor of CD metric can make sense. On the other hand, one can always scale the M^4 coordinates so that the metric is continuous but the sizes of CD s with different Planck constants differ by the ratio of the Planck constants.
2. One might worry whether the phase transition changing Planck constant means an instantaneous change of the size of partonic 2-surface in M^4 degrees of freedom. This is not the case. Light-likeness in $M^2 \times S^2$ makes sense only for surfaces $X^1 \times D^2 \subset M^2 \times S^2$, where X^1 is light-like

geodesic. The requirement that the partonic 2-surface X^2 moving from one sector of H to another one is light-like at $M^2 \times S^2$ irrespective of the value of Planck constant requires that X^2 has single point of M^2 as M^2 projection. Hence no sudden change of the size X^2 occurs.

3. A natural question is whether the phase transition changing the value of Planck constant can occur purely classically or whether it is analogous to quantum tunneling. Classical non-vacuum extremals of Chern-Simons action have two-dimensional CP_2 projection to homologically non-trivial geodesic sphere S_I^2 . The deformation of the entire S_I^2 to homologically trivial geodesic sphere S_{II}^2 is not possible so that only combinations of partonic 2-surfaces with vanishing total homology charge (Kähler magnetic charge) can in principle move from sector to another one, and this process involves fusion of these 2-surfaces such that CP_2 projection becomes single homologically trivial 2-surface. A piece of a non-trivial geodesic sphere S_I^2 of CP_2 can be deformed to that of S_{II}^2 using 2-dimensional homotopy flattening the piece of S^2 to curve. If this homotopy cannot be chosen to be light-like, the phase transitions changing Planck constant take place only via quantum tunnelling. Obviously the notions of light-like homotopies (cobordisms) are very relevant for the understanding of phase transitions changing Planck constant.

13.3.4 How one could fix the spectrum of Planck constants?

The question how the observed Planck constant relates to the integers n_a and n_b defining the covering and factors spaces, is far from trivial and I have considered several options. The basic physical inputs are the condition that scaling of Planck constant must correspond to the scaling of the metric of CD (that is Compton lengths) on one hand and the scaling of the gauge coupling strength $g^2/4\pi\hbar$ on the other hand.

1. One can assign to Planck constant to both CD and CP_2 by assuming that it appears in the commutation relations of corresponding symmetry algebras. Algebraist would argue that Planck constants $\hbar(CD)$ and $\hbar(CP_2)$ must define a homomorphism respecting multiplication and division (when possible) by G_i . This requires $r(X) = \hbar(X)\hbar_0 = n$ for covering and $r(X) = 1/n$ for factor space or vice versa.
2. If one assumes that $\hbar^2(X)$, $X = M^4$, CP_2 corresponds to the scaling of the covariant metric tensor g_{ij} and performs an over-all scaling of H -metric allowed by the Weyl invariance of Kähler action by dividing metric with $\hbar^2(CP_2)$, one obtains the scaling of M^4 covariant metric by $r^2 \equiv \hbar^2/\hbar_0^2 = \hbar^2(M^4)/\hbar^2(CP_2)$ whereas CP_2 metric is not scaled at all.
3. The condition that \hbar scales as n_a is guaranteed if one has $\hbar(CD) = n_a\hbar_0$. This does not fix the dependence of $\hbar(CP_2)$ on n_b and one could have $\hbar(CP_2) = n_b\hbar_0$ or $\hbar(CP_2) = \hbar_0/n_b$. The intuitive picture is that n_b - fold covering gives in good approximation rise to $n_a n_b$ sheets and multiplies YM action action by $n_a n_b$ which is equivalent with the $\hbar = n_a n_b \hbar_0$ if one effectively compresses the covering to $CD \times CP_2$. One would have $\hbar(CP_2) = \hbar_0/n_b$ and $\hbar = n_a n_b \hbar_0$. Note that the descriptions using ordinary Planck constant and coverings and scaled Planck constant but contracting the covering would be alternative descriptions.

This gives the following formulas $r \equiv \hbar/\hbar_0 = r(M^4)/r(CP_2)$ in various cases.

$$\begin{array}{ccccc}
 C - C & F - C & C - F & F - F & \\
 \hline
 r & n_a n_b & \frac{n_a}{n_b} & \frac{n_b}{n_a} & \frac{1}{n_a n_b}
 \end{array}$$

13.3.5 Preferred values of Planck constants

Number theoretic considerations favor the hypothesis that the integers corresponding to Fermat polygons constructible using only ruler and compass and given as products $n_F = 2^k \prod_s F_s$, where $F_s = 2^{2^s} + 1$ are distinct Fermat primes, are favored. The reason would be that quantum phase $q = \exp(i\pi/n)$ is in this case expressible using only iterated square root operation by starting from rationals. The known Fermat primes correspond to $s = 0, 1, 2, 3, 4$ so that the hypothesis is very strong and predicts that p-adic length scales have satellite length scales given as multiples of n_F of fundamental p-adic length scale. $n_F = 2^{11}$ corresponds in TGD framework to a fundamental constant

expressible as a combination of Kähler coupling strength, CP_2 radius and Planck length appearing in the expression for the tension of cosmic strings, and the powers of 2^{11} seem to be especially favored as values of n_a in living matter [43].

13.3.6 How Planck constants are visible in Kähler action?

$\hbar(M^4)$ and $\hbar(CP_2)$ appear in the commutation and anticommutation relations of various superconformal algebras. Only the ratio of M^4 and CP_2 Planck constants appears in Kähler action and is due to the fact that the M^4 and CP_2 metrics of the imbedding space sector with given values of Planck constants are proportional to the corresponding Planck constants. This implies that Kähler function codes for radiative corrections to the classical action, which makes possible to consider the possibility that higher order radiative corrections to functional integral vanish as one might expect at quantum criticality. For a given p-adic length scale space-time sheets with all allowed values of Planck constants are possible. Hence the spectrum of quantum critical fluctuations could in the ideal case correspond to the spectrum of \hbar coding for the scaled up values of Compton lengths and other quantal lengths and times. If so, large \hbar phases could be crucial for understanding of quantum critical superconductors, in particular high T_c superconductors.

13.3.7 Could the dynamics of Kähler action predict the hierarchy of Planck constants?

The original justification for the hierarchy of Planck constants came from the indications that Planck constant could have large values in both astrophysical systems involving dark matter and also in biology. The realization of the hierarchy in terms of the singular coverings and possibly also factor spaces of CD and CP_2 emerged from consistency conditions. The formula for the Planck constant involves heuristic guess work and physical plausibility arguments. There are good arguments in favor of the hypothesis that only coverings are possible. Only a finite number of pages of the Big Book correspond to a given value of Planck constant, biological evolution corresponds to a gradual dispersion to the pages of the Big Book with larger Planck constant, and a connection with the hierarchy of infinite primes and p-adicization program based on the mathematical realization of finite measurement resolution emerges.

One can however ask whether this hierarchy could emerge directly from the basic quantum TGD rather than as a separate hypothesis. The following arguments suggest that this might be possible. One finds also a precise geometric interpretation of preferred extremal property interpreted as criticality in zero energy ontology.

1-1 correspondence between canonical momentum densities and time derivatives fails for Kähler action

The basic motivation for the geometrization program was the observation that canonical quantization for TGD fails. To see what is involved let us try to perform a canonical quantization in zero energy ontology at the 3-D surfaces located at the light-like boundaries of $CD \times CP_2$.

1. In canonical quantization canonical momentum densities $\pi_k^0 \equiv \pi_k = \partial L_K / \partial(\partial_0 h^k)$, where $\partial_0 h^k$ denotes the time derivative of imbedding space coordinate, are the physically natural quantities in terms of which to fix the initial values: once their value distribution is fixed also conserved charges are fixed. Also the weak form of electric-magnetic duality given by $J^{03} \sqrt{g_4} = 4\pi \alpha_K J_{12}$ and a mild generalization of this condition to be discussed below can be interpreted as a manner to fix the values of conserved gauge charges (not Noether charges) to their quantized values since Kähler magnetic flux equals to the integer giving the homology class of the (wormhole) throat. This condition alone need not characterize criticality, which requires an infinite number of deformations of X^4 for which the second variation of the Kähler action vanishes and implies infinite number conserved charges. This in fact gives hopes of replacing π_k with these conserved Noether charges.
2. Canonical quantization requires that $\partial_0 h^k$ in the energy is expressed in terms of π_k . The equation defining π_k in terms of $\partial_0 h^k$ is however highly non-linear although algebraic. By taking squares the equations reduces to equations for rational functions of $\partial_0 h^k$. $\partial_0 h^k$ appears in contravariant

and covariant metric at most quadratically and in the induced Kähler electric field linearly and by multiplying the equations by $\det(g_4)^3$ one can transform the equations to a polynomial form so that in principle $\partial_0 h^k$ can be obtained as a solution of polynomial equations.

3. One can always eliminate one half of the coordinates by choosing 4 imbedding space coordinates as the coordinates of the spacetime surface so that the initial value conditions reduce to those for the canonical momentum densities associated with the remaining four coordinates. For instance, for space-time surfaces representable as map $M^4 \rightarrow CP_2$ M^4 coordinates are natural and the time derivatives $\partial_0 s^k$ of CP_2 coordinates are multivalued. One would obtain four polynomial equations with $\partial_0 s^k$ as unknowns. In regions where CP_2 projection is 4-dimensional -in particular for the deformations of CP_2 vacuum extremals the natural coordinates are CP_2 coordinates and one can regard $\partial_0 m^k$ as unknowns. For the deformations of cosmic strings, which are of form $X^4 = X^2 \times Y^2 \subset M^4 \times CP_2$, one can use coordinates of $M^2 \times S^2$, where S^2 is geodesic sphere as natural coordinates and regard as unknowns E^2 coordinates and remaining CP_2 coordinates.
4. One can imagine solving one of the four polynomial equations for time derivatives in terms of other obtaining N roots. Then one would substitute these roots to the remaining 3 conditions to obtain algebraic equations from which one solves then second variable. Obviously situation is very complex without additional symmetries. The criticality of the preferred extremals might however give additional conditions allowing simplifications. The reasons for giving up the canonical quantization program was following. For the vacuum extremals of Kähler action π_k are however identically vanishing and this means that there is an infinite number of value distributions for $\partial_0 h^k$. For small deformations of vacuum extremals one might however hope a finite number of solutions to the conditions and thus finite number of space-time surfaces carrying same conserved charges.

If one assumes that physics is characterized by the values of the conserved charges one must treat the many-valuedness of $\partial_0 h^k$. The most obvious guess is that one should replace the space of space-like 4-surfaces corresponding to different roots $\partial_0 h^k = F^k(\pi_l)$ with four-surfaces in the covering space of $CD \times CP_2$ corresponding to different branches of the many-valued function $\partial_0 h^k = F(\pi_l)$ co-inciding at the ends of CD .

Do the coverings forced by the many-valuedness of $\partial_0 h^k$ correspond to the coverings associated with the hierarchy of Planck constants?

The obvious question is whether this covering space actually corresponds to the covering spaces associated with the hierarchy of Planck constants. This would conform with quantum classical correspondence. The hierarchy of Planck constants and hierarchy of covering spaces was introduced to cure the failure of the perturbation theory at quantum level. At classical level the multivaluedness of $\partial_0 h^k$ means a failure of perturbative canonical quantization and forces the introduction of the covering spaces. The interpretation would be that when the density of matter becomes critical the space-time surface splits to several branches so that the density at each branches is sub-critical. It is of course not at all obvious whether the proposed structure of the Big Book is really consistent with this hypothesis and one also consider modifications of this structure if necessary. The manner to proceed is by making questions.

1. The proposed picture would give only single integer characterizing the covering. Two integers assignable to CD and CP_2 degrees of freedom are however needed. How these two coverings could emerge?
 - (a) One should fix also the values of $\pi_k^n = \partial L_K / \partial h_n^k$, where n refers to space-like normal coordinate at the wormhole throats. If one requires that charges do not flow between regions with different signatures of the metric the natural condition is $\pi_k^n = 0$ and allows also multi-valued solution. Since wormhole throats carry magnetic charge and since weak form of electric-magnetic duality is assumed, one can assume that CP_2 projection is four-dimensional so that one can use CP_2 coordinates and regard $\partial_0 m^k$ as unknowns. The basic idea about topological condensation in turn suggests that M^4 projection can be assumed to be 4-D inside space-like 3-surfaces so that here $\partial_0 s^k$ are the unknowns. At partonic 2-surfaces one would have conditions for both π_k^0 and π_k^n . One might hope that the numbers

of solutions are finite for preferred extremals because of their symmetries and given by n_a for $\partial_0 m^k$ and by n_b for $\partial_0 s^k$. The optimistic guess is that n_a and n_b corresponds to the numbers of sheets for singular coverings of CD and CP_2 . The covering could be visualized as replacement of space-time surfaces with space-time surfaces which have $n_a n_b$ branches. n_b branches would degenerate to single branch at the ends of diagrams of the generated Feynman graph and n_a branches would degenerate to single one at wormhole throats.

- (b) This picture is not quite correct yet. The fixing of π_k^0 and π_k^n should relate closely to the effective 2-dimensionality as an additional condition perhaps crucial for criticality. One could argue that both π_k^0 and π_k^n must be fixed at X^3 and X_l^3 in order to effectively bring in dynamics in two directions so that X^3 could be interpreted as a an orbit of partonic 2-surface in space-like direction and X_l^3 as its orbit in light-like direction. The additional conditions could be seen as gauge conditions made possible by symplectic and Kac-Moody type conformal symmetries. The conditions for π_0^k would give n_b branches in CP_2 degrees of freedom and the conditions for π_k^n would split each of these branches to n_a branches.
- (c) The existence of these two kinds of conserved charges (possibly vanishing for π_k^n) could relate also very closely to the slicing of the space-time sheets by string world sheets and partonic 2-surfaces.
2. Should one then treat these branches as separate space-time surfaces or as a single space-time surface? The treatment as a single surface seems to be the correct thing to do. Classically the conserved changes would be $n_a n_b$ times larger than for single branch. Kähler action need not (but could!) be same for different branches but the total action is $n_a n_b$ times the average action and this effectively corresponds to the replacement of the \hbar_0/g_K^2 factor of the action with \hbar/g_K^2 , $r \equiv \hbar/\hbar_0 = n_a n_b$. Since the conserved quantum charges are proportional to \hbar one could argue that $r = n_a n_b$ tells only that the charge conserved charge is $n_a n_b$ times larger than without multi-valuedness. \hbar would be only effectively $n_a n_b$ fold. This is of course poor man's argument but might catch something essential about the situation.
 3. How could one interpret the condition $J^{03} \sqrt{g_4} = 4\pi \alpha_K J_{12}$ and its generalization to be discussed below in this framework? The first observation is that the total Kähler electric charge is by $\alpha_K \propto 1/(n_a n_b)$ same always. The interpretation would be in terms of charge fractionization meaning that each branch would carry Kähler electric charge $Q_K = n g_K / n_a n_b$. I have indeed suggested explanation of charge fractionization and quantum Hall effect based on this picture.
 4. The vision about the hierarchy of Planck constants involves also assumptions about imbedding space metric. The assumption that the M^4 covariant metric is proportional to \hbar^2 follows from the physical idea about \hbar scaling of quantum lengths as what Compton length is. One can always introduce scaled M^4 coordinates bringing M^4 metric into the standard form by scaling up the M^4 size of CD . It is not clear whether the scaling up of CD size follows automatically from the proposed scenario. The basic question is why the M^4 size scale of the critical extremals must scale like $n_a n_b$? This should somehow relate to the weak self-duality conditions implying that Kähler field at each branch is reduced by a factor $1/r$ at each branch. Field equations should possess a dynamical symmetry involving the scaling of CD by integer k and $J^{0\beta} \sqrt{g_4}$ and $J^{n\beta} \sqrt{g_4}$ by $1/k$. The scaling of CD should be due to the scaling up of the M^4 time interval during which the branched light-like 3-surface returns back to a non-branched one.
 5. The proposed view about hierarchy of Planck constants is that the singular coverings reduce to single-sheeted coverings at $M^2 \subset M^4$ for CD and to $S^2 \subset CP_2$ for CP_2 . Here S^2 is any homologically trivial geodesic sphere of CP_2 and has vanishing Kähler form. Weak self-duality condition is indeed consistent with any value of \hbar and implies that the vacuum property for the partonic 2-surface implies vacuum property for the entire space-time sheet as holography indeed requires. This condition however generalizes. In weak self-duality conditions the value of \hbar is free for any 2-D Lagrangian sub-manifold of CP_2 .

The branching along M^2 would mean that the branches of preferred extremals always collapse to single branch when their M^4 projection belongs to M^2 . Magnetically charged light-like throats cannot have M^4 projection in M^2 so that self-duality conditions for different values of \hbar do not lead to inconsistencies. For spacelike 3-surfaces at the boundaries of CD the condition

would mean that the M^4 projection becomes light-like geodesic. Straight cosmic strings would have M^2 as M^4 projection. Also CP_2 type vacuum extremals for which the random light-like projection in M^4 belongs to M^2 would represent this of situation. One can ask whether the degeneration of branches actually takes place along any string like object $X^2 \times Y^2$, where X^2 defines a minimal surface in M^4 . For these the weak self-duality condition would imply $\hbar = \infty$ at the ends of the string. It is very plausible that string like objects feed their magnetic fluxes to larger space-times sheets through wormhole contacts so that these conditions are not encountered.

Connection with the criticality of preferred extremals

Also a connection with quantum criticality and the criticality of the preferred extremals suggests itself. Criticality for the preferred extremals must be a property of space-like 3-surfaces and light-like 3-surfaces with degenerate 4-metric and the degeneration of the $n_a n_b$ branches of the space-time surface at the its ends and at wormhole throats is exactly what happens at criticality. For instance, in catastrophe theory roots of the polynomial equation giving extrema of a potential as function of control parameters co-incide at criticality. If this picture is correct the hierarchy of Planck constants would be an outcome of criticality and of preferred extremal property and preferred extremals would be just those multi-branched space-time surfaces for which branches co-incide at the the boundaries of $CD \times CP_2$ and at the throats.

13.4 Weak form electric-magnetic duality and its implications

The notion of electric-magnetic duality [65] was proposed first by Olive and Montonen and is central in $\mathcal{N} = 4$ supersymmetric gauge theories. It states that magnetic monopoles and ordinary particles are two different phases of theory and that the description in terms of monopoles can be applied at the limit when the running gauge coupling constant becomes very large and perturbation theory fails to converge. The notion of electric-magnetic self-duality is more natural since for CP_2 geometry Kähler form is self-dual and Kähler magnetic monopoles are also Kähler electric monopoles and Kähler coupling strength is by quantum criticality renormalization group invariant rather than running coupling constant. The notion of electric-magnetic (self-)duality emerged already two decades ago in the attempts to formulate the Kähler geometric of world of classical worlds. Quite recently a considerable step of progress took place in the understanding of this notion [22]. What seems to be essential is that one adopts a weaker form of the self-duality applying at partonic 2-surfaces. What this means will be discussed in the sequel.

Every new idea must be of course taken with a grain of salt but the good sign is that this concept leads to precise predictions. The point is that elementary particles do not generate monopole fields in macroscopic length scales: at least when one considers visible matter. The first question is whether elementary particles could have vanishing magnetic charges: this turns out to be impossible. The next question is how the screening of the magnetic charges could take place and leads to an identification of the physical particles as string like objects identified as pairs magnetic charged wormhole throats connected by magnetic flux tubes.

1. The first implication is a new view about electro-weak massivation reducing it to weak confinement in TGD framework. The second end of the string contains particle having electroweak isospin neutralizing that of elementary fermion and the size scale of the string is electro-weak scale would be in question. Hence the screening of electro-weak force takes place via weak confinement realized in terms of magnetic confinement.
2. This picture generalizes to the case of color confinement. Also quarks correspond to pairs of magnetic monopoles but the charges need not vanish now. Rather, valence quarks would be connected by flux tubes of length of order hadron size such that magnetic charges sum up to zero. For instance, for baryonic valence quarks these charges could be $(2, -1, -1)$ and could be proportional to color hyper charge.
3. The highly non-trivial prediction making more precise the earlier stringy vision is that elementary particles are string like objects in electro-weak scale: this should become manifest at LHC energies.

4. The weak form electric-magnetic duality together with Beltrami flow property of Kähler leads to the reduction of Kähler action to Chern-Simons action so that TGD reduces to almost topological QFT and that Kähler function is explicitly calculable. This has enormous impact concerning practical calculability of the theory.
5. One ends up also to a general solution ansatz for field equations from the condition that the theory reduces to almost topological QFT. The solution ansatz is inspired by the idea that all isometry currents are proportional to Kähler current which is integrable in the sense that the flow parameter associated with its flow lines defines a global coordinate. The proposed solution ansatz would describe a hydrodynamical flow with the property that isometry charges are conserved along the flow lines (Beltrami flow). A general ansatz satisfying the integrability conditions is found. The solution ansatz applies also to the extremals of Chern-Simons action and to the conserved currents associated with the modified Dirac equation defined as contractions of the modified gamma matrices between the solutions of the modified Dirac equation. The strongest form of the solution ansatz states that various classical and quantum currents flow along flow lines of the Beltrami flow defined by Kähler current (Kähler magnetic field associated with Chern-Simons action). Intuitively this picture is attractive. A more general ansatz would allow several Beltrami flows meaning multi-hydrodynamics. The integrability conditions boil down to two scalar functions: the first one satisfies massless d'Alembert equation in the induced metric and the the gradients of the scalar functions are orthogonal. The interpretation in terms of momentum and polarization directions is natural.
6. The general solution ansatz works for induced Kähler Dirac equation and Chern-Simons Dirac equation and reduces them to ordinary differential equations along flow lines. The induced spinor fields are simply constant along flow lines of induced spinor field for Dirac equation in suitable gauge. Also the generalized eigen modes of the modified Chern-Simons Dirac operator can be deduced explicitly if the throats and the ends of space-time surface at the boundaries of CD are extremals of Chern-Simons action. Chern-Simons Dirac equation reduces to ordinary differential equations along flow lines and one can deduce the general form of the spectrum and the explicit representation of the Dirac determinant in terms of geometric quantities characterizing the 3-surface (eigenvalues are inversely proportional to the lengths of strands of the flow lines in the effective metric defined by the modified gamma matrices).

13.4.1 Could a weak form of electric-magnetic duality hold true?

Holography means that the initial data at the partonic 2-surfaces should fix the configuration space metric. A weak form of this condition allows only the partonic 2-surfaces defined by the wormhole throats at which the signature of the induced metric changes. A stronger condition allows all partonic 2-surfaces in the slicing of space-time sheet to partonic 2-surfaces and string world sheets. Number theoretical vision suggests that hyper-quaternionicity *resp.* co-hyperquaternionicity constraint could be enough to fix the initial values of time derivatives of the imbedding space coordinates in the space-time regions with Minkowskian *resp.* Euclidian signature of the induced metric. This is a condition on modified gamma matrices and hyper-quaternionicity states that they span a hyper-quaternionic sub-space.

Definition of the weak form of electric-magnetic duality

One can also consider alternative conditions possibly equivalent with this condition. The argument goes as follows.

1. The expression of the matrix elements of the metric and Kähler form of WCW in terms of the Kähler fluxes weighted by Hamiltonians of δM_{\pm}^4 at the partonic 2-surface X^2 looks very attractive. These expressions however carry no information about the 4-D tangent space of the partonic 2-surfaces so that the theory would reduce to a genuinely 2-dimensional theory, which cannot hold true. One would like to code to the WCW metric also information about the electric part of the induced Kähler form assignable to the complement of the tangent space of $X^2 \subset X^4$.
2. Electric-magnetic duality of the theory looks a highly attractive symmetry. The trivial manner to get electric magnetic duality at the level of the full theory would be via the identification of

the flux Hamiltonians as sums of the magnetic and electric fluxes. The presence of the induced metric is however troublesome since the presence of the induced metric means that the simple transformation properties of flux Hamiltonians under symplectic transformations -in particular color rotations- are lost.

3. A less trivial formulation of electric-magnetic duality would be as an initial condition which eliminates the induced metric from the electric flux. In the Euclidian version of 4-D YM theory this duality allows to solve field equations exactly in terms of instantons. This approach involves also quaternions. These arguments suggest that the duality in some form might work. The full electric magnetic duality is certainly too strong and implies that space-time surface at the partonic 2-surface corresponds to piece of CP_2 type vacuum extremal and can hold only in the deep interior of the region with Euclidian signature. In the region surrounding wormhole throat at both sides the condition must be replaced with a weaker condition.
4. To formulate a weaker form of the condition let us introduce coordinates (x^0, x^3, x^1, x^2) such (x^1, x^2) define coordinates for the partonic 2-surface and (x^0, x^3) define coordinates labeling partonic 2-surfaces in the slicing of the space-time surface by partonic 2-surfaces and string world sheets making sense in the regions of space-time sheet with Minkowskian signature. The assumption about the slicing allows to preserve general coordinate invariance. The weakest condition is that the generalized Kähler electric fluxes are apart from constant proportional to Kähler magnetic fluxes. This requires the condition

$$J^{03} \sqrt{g_4} = K J_{12} . \quad (13.4.1)$$

A more general form of this duality is suggested by the considerations of [37] reducing the hierarchy of Planck constants to basic quantum TGD and also reducing Kähler function for preferred extremals to Chern-Simons terms [63] at the boundaries of CD and at light-like wormhole throats. This form is following

$$J^{n\beta} \sqrt{g_4} = K \epsilon \times \epsilon^{n\beta\gamma\delta} J_{\gamma\delta} \sqrt{g_4} . \quad (13.4.2)$$

Here the index n refers to a normal coordinate for the space-like 3-surface at either boundary of CD or for light-like wormhole throat. ϵ is a sign factor which is opposite for the two ends of CD . It could be also opposite at the opposite sides of the wormhole throat. Note that the dependence on induced metric disappears at the right hand side and this condition eliminates the potentials singularity due to the reduction of the rank of the induced metric at wormhole throat.

5. Information about the tangent space of the space-time surface can be coded to the configuration space metric with loosing the nice transformation properties of the magnetic flux Hamiltonians if Kähler electric fluxes or sum of magnetic flux and electric flux satisfying this condition are used and K is symplectic invariant. Using the sum

$$J_e + J_m = (1 + K) J_{12} , \quad (13.4.3)$$

where J denotes the Kähler magnetic flux, , makes it possible to have a non-trivial configuration space metric even for $K = 0$, which could correspond to the ends of a cosmic string like solution carrying only Kähler magnetic fields. This condition suggests that it can depend only on Kähler magnetic flux and other symplectic invariants. Whether local symplectic coordinate invariants are possible at all is far from obvious, If the slicing itself is symplectic invariant then K could be a non-constant function of X^2 depending on string world sheet coordinates. The light-like radial coordinate of the light-cone boundary indeed defines a symplectically invariant slicing and this slicing could be shifted along the time axis defined by the tips of CD .

Electric-magnetic duality physically

What could the weak duality condition mean physically? For instance, what constraints are obtained if one assumes that the quantization of electro-weak charges reduces to this condition at classical level?

1. The first thing to notice is that the flux of J over the partonic 2-surface is analogous to magnetic flux

$$Q_m = \frac{e}{\hbar} \oint B dS = n .$$

n is non-vanishing only if the surface is homologically non-trivial and gives the homology charge of the partonic 2-surface.

2. The expressions of classical electromagnetic and Z^0 fields in terms of Kähler form [46] read as

$$\begin{aligned} \gamma &= \frac{eF_{em}}{\hbar} = 3J - \sin^2(\theta_W)R_{03} , \\ Z^0 &= \frac{g_Z F_Z}{\hbar} = 2R_{03} . \end{aligned} \quad (13.4.3)$$

Here R_{03} is one of the components of the curvature tensor in vielbein representation and F_{em} and F_Z correspond to the standard field tensors. From this expression one can deduce

$$J = \frac{e}{3\hbar} F_{em} + \sin^2(\theta_W) \frac{g_Z}{6\hbar} F_Z . \quad (13.4.4)$$

3. The weak duality condition when integrated over X^2 implies

$$\begin{aligned} \frac{e^2}{3\hbar} Q_{em} + \frac{g_Z^2 p}{6} Q_{Z,V} &= K \oint J = Kn , \\ Q_{Z,V} &= \frac{I_V^3}{2} - Q_{em} , \quad p = \sin^2(\theta_W) . \end{aligned} \quad (13.4.4)$$

Here the vectorial part of the Z^0 charge rather than as full Z^0 charge $Q_Z = I_L^3 + \sin^2(\theta_W)Q_{em}$ appears. The reason is that only the vectorial isospin is same for left and right handed components of fermion which are in general mixed for the massive states.

The coefficients are dimensionless and expressible in terms of the gauge coupling strengths and using $\hbar = r\hbar_0$ one can write

$$\begin{aligned} \alpha_{em} Q_{em} + p \frac{\alpha_Z}{2} Q_{Z,V} &= \frac{3}{4\pi} \times rnK , \\ \alpha_{em} &= \frac{e^2}{4\pi\hbar_0} , \quad \alpha_Z = \frac{g_Z^2}{4\pi\hbar_0} = \frac{\alpha_{em}}{p(1-p)} . \end{aligned} \quad (13.4.4)$$

4. There is a great temptation to assume that the values of Q_{em} and Q_Z correspond to their quantized values and therefore depend on the quantum state assigned to the partonic 2-surface. The linear coupling of the modified Dirac operator to conserved charges implies correlation between the geometry of space-time sheet and quantum numbers assigned to the partonic 2-surface. The assumption of standard quantized values for Q_{em} and Q_Z would be also seen as the identification of the fine structure constants α_{em} and α_Z . This however requires weak isospin invariance.

The value of K from classical quantization of Kähler electric charge

The value of K can be deduced by requiring classical quantization of Kähler electric charge.

1. The condition that the flux of $F^{03} = (\hbar/g_K)J^{03}$ defining the counterpart of Kähler electric field equals to the Kähler charge g_K would give the condition $K = g_K^2/\hbar$, where g_K is Kähler coupling constant which should be invariant under coupling constant evolution by quantum criticality. Within experimental uncertainties one has $\alpha_K = g_K^2/4\pi\hbar_0 = \alpha_{em} \simeq 1/137$, where α_{em} is finite structure constant in electron length scale and \hbar_0 is the standard value of Planck constant.
2. The quantization of Planck constants makes the condition highly non-trivial. The most general quantization of r is as rationals but there are good arguments favoring the quantization as integers corresponding to the allowance of only singular coverings of CD and CP_2 . The point is that in this case a given value of Planck constant corresponds to a finite number of pages of the "Big Book". The quantization of the Planck constant implies a further quantization of K and would suggest that K scales as $1/r$ unless the spectrum of values of Q_{em} and Q_Z allowed by the quantization condition scales as r . This is quite possible and the interpretation would be that each of the r sheets of the covering carries (possibly same) elementary charge. Kind of discrete variant of a full Fermi sphere would be in question. The interpretation in terms of anyonic phases [24] supports this interpretation.
3. The identification of J as a counterpart of eB/\hbar means that Kähler action and thus also Kähler function is proportional to $1/\alpha_K$ and therefore to \hbar . This implies that for large values of \hbar Kähler coupling strength $g_K^2/4\pi$ becomes very small and large fluctuations are suppressed in the functional integral. The basic motivation for introducing the hierarchy of Planck constants was indeed that the scaling $\alpha \rightarrow \alpha/r$ allows to achieve the convergence of perturbation theory: Nature itself would solve the problems of the theoretician. This of course does not mean that the physical states would remain as such and the replacement of single particles with anyonic states in order to satisfy the condition for K would realize this concretely.

The weak form of electric-magnetic duality has surprisingly strong implications for basic view about quantum TGD as following considerations show.

13.4.2 Magnetic confinement, the short range of weak forces, and color confinement

The weak form of electric-magnetic duality has surprisingly strong implications if one combines it with some very general empirical facts such as the non-existence of magnetic monopole fields in macroscopic length scales.

How can one avoid macroscopic magnetic monopole fields?

Monopole fields are experimentally absent in length scales above order weak boson length scale and one should have a mechanism neutralizing the monopole charge. How electroweak interactions become short ranged in TGD framework is still a poorly understood problem. What suggests itself is the neutralization of the weak isospin above the intermediate gauge boson Compton length by neutral Higgs bosons. Could the two neutralization mechanisms be combined to single one?

1. In the case of fermions and their super partners the opposite magnetic monopole would be a wormhole throat. If the magnetically charged wormhole contact is electromagnetically neutral but has vectorial weak isospin neutralizing the weak vectorial isospin of the fermion only the electromagnetic charge of the fermion is visible on longer length scales. The distance of this wormhole throat from the fermionic one should be of the order weak boson Compton length. An interpretation as a bound state of fermion and a wormhole throat state with the quantum numbers of a neutral Higgs boson would therefore make sense. The neutralizing throat would have quantum numbers of $X_{-1/2} = \nu_L \bar{\nu}_R$ or $X_{1/2} = \bar{\nu}_L \nu_R$. $\nu_L \bar{\nu}_R$ would not be neutral Higgs boson (which should correspond to a wormhole contact) but a super-partner of left-handed neutrino obtained by adding a right handed neutrino. This mechanism would apply separately to the fermionic and anti-fermionic throats of the gauge bosons and corresponding space-time sheets and leave only electromagnetic interaction as a long ranged interaction.

2. One can of course wonder what is the situation for the bosonic wormhole throats feeding gauge fluxes between space-time sheets. It would seem that these wormhole throats must always appear as pairs such that for the second member of the pair monopole charges and I_V^3 cancel each other at both space-time sheets involved so that one obtains at both space-time sheets magnetic dipoles of size of weak boson Compton length. The proposed magnetic character of fundamental particles should become visible at TeV energies so that LHC might have surprises in store!

Magnetic confinement and color confinement

Magnetic confinement generalizes also to the case of color interactions. One can consider also the situation in which the magnetic charges of quarks (more generally, of color excited leptons and quarks) do not vanish and they form color and magnetic singles in the hadronic length scale. This would mean that magnetic charges of the state $q_{\pm 1/2} - X_{\mp 1/2}$ representing the physical quark would not vanish and magnetic confinement would accompany also color confinement. This would explain why free quarks are not observed. To how degree then quark confinement corresponds to magnetic confinement is an interesting question.

For quark and antiquark of meson the magnetic charges of quark and antiquark would be opposite and meson would correspond to a Kähler magnetic flux so that a stringy view about meson emerges. For valence quarks of baryon the vanishing of the net magnetic charge takes place provided that the magnetic net charges are $(\pm 2, \mp 1, \mp 1)$. This brings in mind the spectrum of color hyper charges coming as $(\pm 2, \mp 1, \mp 1)/3$ and one can indeed ask whether color hyper-charge correlates with the Kähler magnetic charge. The geometric picture would be three strings connected to single vertex. Amusingly, the idea that color hypercharge could be proportional to color hyper charge popped up during the first year of TGD when I had not yet discovered CP_2 and believed on $M^4 \times S^2$.

p-Adic length scale hypothesis and hierarchy of Planck constants defining a hierarchy of dark variants of particles suggest the existence of scaled up copies of QCD type physics and weak physics. For p-adically scaled up variants the mass scales would be scaled by a power of $\sqrt{2}$ in the most general case. The dark variants of the particle would have the same mass as the original one. In particular, Mersenne primes $M_k = 2^k - 1$ and Gaussian Mersennes $M_{G,k} = (1 + i)^k - 1$ has been proposed to define zoomed copies of these physics. At the level of magnetic confinement this would mean hierarchy of length scales for the magnetic confinement.

One particular proposal is that the Mersenne prime M_{89} should define a scaled up variant of the ordinary hadron physics with mass scaled up roughly by a factor $2^{(107-89)/2} = 512$. The size scale of color confinement for this physics would be same as the weak length scale. It would look more natural that the weak confinement for the quarks of M_{89} physics takes place in some shorter scale and M_{61} is the first Mersenne prime to be considered. The mass scale of M_{61} weak bosons would be by a factor $2^{(89-61)/2} = 2^{14}$ higher and about 1.6×10^4 TeV. M_{89} quarks would have virtually no weak interactions but would possess color interactions with weak confinement length scale reflecting themselves as new kind of jets at collisions above TeV energies.

In the biologically especially important length scale range 10 nm -2500 nm there are as many as four Gaussian Mersennes corresponding to $M_{G,k}$, $k = 151, 157, 163, 167$. This would suggest that the existence of scaled up scales of magnetic-, weak- and color confinement. An especially interesting possibly testable prediction is the existence of magnetic monopole pairs with the size scale in this range. There are recent claims about experimental evidence for magnetic monopole pairs [77].

Magnetic confinement and stringy picture in TGD sense

The connection between magnetic confinement and weak confinement is rather natural if one recalls that electric-magnetic duality in super-symmetric quantum field theories means that the descriptions in terms of particles and monopoles are in some sense dual descriptions. Fermions would be replaced by string like objects defined by the magnetic flux tubes and bosons as pairs of wormhole contacts would correspond to pairs of the flux tubes. Therefore the sharp distinction between gravitons and physical particles would disappear.

The reason why gravitons are necessarily stringy objects formed by a pair of wormhole contacts is that one cannot construct spin two objects using only single fermion states at wormhole throats. Of course, also super partners of these states with higher spin obtained by adding fermions and anti-

fermions at the wormhole throat but these do not give rise to graviton like states [23]. The upper and lower wormhole throat pairs would be quantum superpositions of fermion anti-fermion pairs with sum over all fermions. The reason is that otherwise one cannot realize graviton emission in terms of joining of the ends of light-like 3-surfaces together. Also now magnetic monopole charges are necessary but now there is no need to assign the entities X_{\pm} with gravitons.

Graviton string is characterized by some p-adic length scale and one can argue that below this length scale the charges of the fermions become visible. Mersenne hypothesis suggests that some Mersenne prime is in question. One proposal is that gravitonic size scale is given by electronic Mersenne prime M_{127} . It is however difficult to test whether graviton has a structure visible below this length scale.

What happens to the generalized Feynman diagrams is an interesting question. It is not at all clear how closely they relate to ordinary Feynman diagrams. All depends on what one is ready to assume about what happens in the vertices. One could of course hope that zero energy ontology could allow some very simple description allowing perhaps to get rid of the problematic aspects of Feynman diagrams.

1. Consider first the recent view about generalized Feynman diagrams which relies zero energy ontology. A highly attractive assumption is that the particles appearing at wormhole throats are on mass shell particles. For incoming and outgoing elementary bosons and their super partners they would be positive it resp. negative energy states with parallel on mass shell momenta. For virtual bosons they the wormhole throats would have opposite sign of energy and the sum of on mass shell states would give virtual net momenta. This would make possible twistor description of virtual particles allowing only massless particles (in 4-D sense usually and in 8-D sense in TGD framework). The notion of virtual fermion makes sense only if one assumes in the interaction region a topological condensation creating another wormhole throat having no fermionic quantum numbers.
2. The addition of the particles X^{\pm} replaces generalized Feynman diagrams with the analogs of stringy diagrams with lines replaced by pairs of lines corresponding to fermion and $X_{\pm 1/2}$. The members of these pairs would correspond to 3-D light-like surfaces glued together at the vertices of generalized Feynman diagrams. The analog of 3-vertex would not be splitting of the string to form shorter strings but the replication of the entire string to form two strings with same length or fusion of two strings to single string along all their points rather than along ends to form a longer string. It is not clear whether the duality symmetry of stringy diagrams can hold true for the TGD variants of stringy diagrams.
3. How should one describe the bound state formed by the fermion and X^{\pm} ? Should one describe the state as superposition of non-parallel on mass shell states so that the composite state would be automatically massive? The description as superposition of on mass shell states does not conform with the idea that bound state formation requires binding energy. In TGD framework the notion of negentropic entanglement has been suggested to make possible the analogs of bound states consisting of on mass shell states so that the binding energy is zero [45]. If this kind of states are in question the description of virtual states in terms of on mass shell states is not lost. Of course, one cannot exclude the possibility that there is infinite number of this kind of states serving as analogs for the excitations of string like object.
4. What happens to the states formed by fermions and $X_{\pm 1/2}$ in the internal lines of the Feynman diagram? Twistor philosophy suggests that only the higher on mass shell excitations are possible. If this picture is correct, the situation would not change in an essential manner from the earlier one.

The highly non-trivial prediction of the magnetic confinement is that elementary particles should have stringy character in electro-weak length scales and could behaving to become manifest at LHC energies. This adds one further item to the list of non-trivial predictions of TGD about physics at LHC energies [20].

Should $J + J_1$ appear in Kähler action?

The presence of the S^2 Kähler form J_1 in weak form of electric-magnetic duality was originally suggested by an erratic argument about the reduction to almost topological QFT to be described in

the next subsection. In any case this argument raises the question whether one could replace J with $J + J_1$ in the Kähler action. This would not affect the basic non-vacuum extremals but would modify the vacuum degeneracy of the Kähler action. Canonically imbedded M^4 would become a monopole configuration with an infinite magnetic energy and Kähler action due to the monopole singularity at the line connecting tips of the CD . Action and energy can be made small by drilling a small hole around origin. This is however not consistent with the weak form of electro-weak duality. Amusingly, the modified Dirac equation reduces to ordinary massless Dirac equation in M^4 .

This extremal can be transformed to a vacuum extremal by assuming that the solution is also a CP_2 magnetic monopole with opposite contribution to the magnetic charge so that $J + J_1 = 0$ holds true. This is achieved if one can regard space-time surface as a map $M^4 \rightarrow CP_2$ reducing to a map $(\Theta, \Phi) = (\theta, \pm\phi)$ with the sign chosen by properly projecting the homologically non-trivial $r_M = \text{constant}$ spheres of CD to the homologically non-trivial geodesic sphere of CP_2 . Symplectic transformations of $S^2 \times CP_2$ produce new vacuum extremals of this kind. Using Darboux coordinates in which one has $J = \sum_{k=1,2} P_k dQ^k$ and assuming that (P_1, Q_1) corresponds to the CP_2 image of S^2 , one can take Q_2 to be arbitrary function of P^2 which in turn is an arbitrary function of M^4 coordinates to obtain even more general vacuum extremals with 3-D CP_2 projection. Therefore the spectrum of vacuum extremals, which is very relevant for the TGD based description of gravitation in long length scales because it allows to satisfy Einstein's equations as an additional condition, looks much richer than for the original option, and it is natural to ask whether this option might make sense.

An objection is that J_1 is a radial monopole field and this breaks Lorentz invariance to $SO(3)$. Lorentz invariance is broken to $SO(3)$ for a given CD also by the presence of the preferred time direction defined by the time-like line connecting the tips of the CD becoming carrying the monopole charge but is compensated since Lorentz boosts of CD s are possible. Could one consider similar compensation also now? Certainly the extremely small breaking of Lorentz invariance and the vanishing of the monopole charge for the vacuum extremals is all that is needed at the space-time level. No new gauge fields would be introduced since only the Kähler field part of photon and Z^0 boson would receive an additional contribution.

The ultimate fate of the modification depends on whether it is consistent with the general relativistic description of gravitation. Since a breaking of spherical symmetry is involved, it is not at all clear whether one can find vacuum extremals which represent small deformations of the Reissner-Nordström metric and Robertson-Walker metric. The argument below shows that this option does not allow the imbedding of small deformations of physically plausible space-time metrics as vacuum extremals.

The basic vacuum extremal whose deformations should give vacuum extremals allowing interpretation as solutions of Einstein's equations is given by a map $M^4 \rightarrow CP_2$ projecting the r_M constant spheres S^2 of M^2 to the homologically non-trivial geodesic sphere of CP_2 . The winding number of this map is -1 in order to achieve vanishing of the induced Kähler form $J + J_1$. For instance, the following two canonical forms of the map are possible

$$\begin{aligned} (\Theta, \Psi) &= (\theta_M, -\phi_M) , \\ (\Theta, \Psi) &= (\pi - \theta_M, \phi_M) . \end{aligned} \tag{13.4.3}$$

Here (Θ, Ψ) refers to the geodesic sphere of CP_2 and (θ_M, ϕ_M) to the sphere of M^4 .

The resulting space-time surface is not flat and Einstein tensor is non-vanishing. More complex metrics can be constructed from this metric by a deformation making the CP_2 projection 3-dimensional.

Using the expression of the CP_2 line element in Eguchi-Hanson coordinates [49]

$$\frac{ds^2}{R^2} = \frac{dr^2}{F^2} + \frac{r^2}{F} (d\Psi + \cos\Theta d\Phi)^2 + \frac{r^2}{4F} (d\Theta^2 + \text{frac}{r^2} 4F \sin^2\Theta d\Phi^2) \tag{13.4.3}$$

and s the relationship $r = \tan(\Theta)$, one obtains following expression for the CP_2 metric

$$\frac{ds^2}{R^2} = d\theta_M^2 + \sin^2(\theta_M) \left[(d\phi_M + \cos(\theta)d\Phi)^2 + \frac{1}{4}(d\theta^2 + \sin^2(\theta)d\Phi^2) \right]. \quad (13.4.3)$$

The resulting metric is obtained from the metric of S^2 by replacing $d\phi^2$ which 3-D line element. The factor $\sin^2(\theta_M)$ implies that the induced metric becomes singular at North and South poles of S^2 . In particular, the gravitational potential is proportional to $\sin^2(\theta_M)$ so that gravitational force in the radial direction vanishes at equators. It is very difficult to imagine any manner to produce a small deformation of Reissner-Nordström metric or Robertson-Walker metric. Hence it seems that the vacuum extremals produce by $J + J_1$ option are not physical.

13.4.3 Could Quantum TGD reduce to almost topological QFT?

There seems to be a profound connection with the earlier unrealistic proposal that TGD reduces to almost topological quantum theory in the sense that the counterpart of Chern-Simons action assigned with the wormhole throats somehow dictates the dynamics. This proposal can be formulated also for the modified Dirac action action. I gave up this proposal but the following argument shows that Kähler action with weak form of electric-magnetic duality effectively reduces to Chern-Simons action plus Coulomb term.

1. Kähler action density can be written as a 4-dimensional integral of the Coulomb term $j_K^\alpha A_\alpha$ plus and integral of the boundary term $J^{n\beta} A_\beta \sqrt{g_4}$ over the wormhole throats and of the quantity $J^{0\beta} A_\beta \sqrt{g_4}$ over the ends of the 3-surface.
2. If the self-duality conditions generalize to $J^{n\beta} = 4\pi\alpha_K \epsilon^{n\beta\gamma\delta} J_{\gamma\delta}$ at throats and to $J^{0\beta} = 4\pi\alpha_K \epsilon^{0\beta\gamma\delta} J_{\gamma\delta}$ at the ends, the Kähler function reduces to the counterpart of Chern-Simons action evaluated at the ends and throats. It would have same value for each branch and the replacement $\hbar_0 \rightarrow r\hbar_0$ would effectively describe this. Boundary conditions would however give $1/r$ factor so that \hbar would disappear from the Kähler function! The original attempt to realize quantum TGD as an almost topological QFT was in terms of Chern-Simons action but was given up. It is somewhat surprising that Kähler action gives Chern-Simons action in the vacuum sector defined as sector for which Kähler current is light-like or vanishes.

Holography encourages to ask whether also the Coulomb interaction terms could vanish. This kind of dimensional reduction would mean an enormous simplification since TGD would reduce to an almost topological QFT. The attribute "almost" would come from the fact that one has non-vanishing classical Noether charges defined by Kähler action and non-trivial quantum dynamics in M^4 degrees of freedom. One could also assign to space-time surfaces conserved four-momenta which is not possible in topological QFTs. For this reason the conditions guaranteeing the vanishing of Coulomb interaction term deserve a detailed analysis.

1. For the known extremals j_K^α either vanishes or is light-like ("massless extremals" for which weak self-duality condition does not make sense [36]) so that the Coulombic term vanishes identically in the gauge used. The addition of a gradient to A induces terms located at the ends and wormhole throats of the space-time surface but this term must be cancelled by the other boundary terms by gauge invariance of Kähler action. This implies that the M^4 part of WCW metric vanishes in this case. Therefore massless extremals as such are not physically realistic: wormhole throats representing particles are needed.
2. The original naive conclusion was that since Chern-Simons action depends on CP_2 coordinates only, its variation with respect to Minkowski coordinates must vanish so that the WCW metric would be trivial in M^4 degrees of freedom. This conclusion is in conflict with quantum classical correspondence and was indeed too hasty. The point is that the allowed variations of Kähler function must respect the weak electro-magnetic duality which relates Kähler electric field depending on the induced 4-metric at 3-surface to the Kähler magnetic field. Therefore the dependence on M^4 coordinates creeps via a Lagrange multiplier term

$$\int \Lambda_\alpha (J^{n\alpha} - K \epsilon^{n\alpha\beta\gamma} J_{\beta\gamma}) \sqrt{g_4} d^3x . \quad (13.4.4)$$

The (1,1) part of second variation contributing to M^4 metric comes from this term.

3. This erratic conclusion about the vanishing of M^4 part WCW metric raised the question about how to achieve a non-trivial metric in M^4 degrees of freedom. The proposal was a modification of the weak form of electric-magnetic duality. Besides CP_2 Kähler form there would be the Kähler form assignable to the light-cone boundary reducing to that for $r_M = \text{constant}$ sphere - call it J^1 . The generalization of the weak form of self-duality would be $J^{n\beta} = \epsilon^{n\beta\gamma\delta} K (J_{\gamma\delta} + \epsilon J_{\gamma\delta}^1)$. This form implies that the boundary term gives a non-trivial contribution to the M^4 part of the WCW metric even without the constraint from electric-magnetic duality. Kähler charge is not affected unless the partonic 2-surface contains the tip of CD in its interior. In this case the value of Kähler charge is shifted by a topological contribution. Whether this term can survive depends on whether the resulting vacuum extremals are consistent with the basic facts about classical gravitation.
4. The Coulombic interaction term is not invariant under gauge transformations. The good news is that this might allow to find a gauge in which the Coulomb term vanishes. The vanishing condition fixing the gauge transformation ϕ is

$$j_K^\alpha \partial_\alpha \phi = -j^\alpha A_\alpha . \quad (13.4.5)$$

This differential equation can be reduced to an ordinary differential equation along the flow lines j_K by using $dx^\alpha/dt = j_K^\alpha$. Global solution is obtained only if one can combine the flow parameter t with three other coordinates- say those at the either end of CD to form space-time coordinates. The condition is that the parameter defining the coordinate differential is proportional to the covariant form of Kähler current: $dt = \phi j_K$. This condition in turn implies $d^2t = d(\phi j_K) = d\phi \wedge j_K + \phi dj_K = 0$ implying $j_K \wedge dj_K = 0$ or more concretely,

$$\epsilon^{\alpha\beta\gamma\delta} j_\beta^K \partial_\gamma j_\delta^K = 0 . \quad (13.4.6)$$

j_K is a four-dimensional counterpart of Beltrami field [62] and could be called generalized Beltrami field.

The integrability conditions follow also from the construction of the extremals of Kähler action [36]. The conjecture was that for the extremals the 4-dimensional Lorentz force vanishes (no dissipation): this requires $j_K \wedge J = 0$. One manner to guarantee this is the topologization of the Kähler current meaning that it is proportional to the instanton current: $j_K = \phi j_I$, where $j_I = *(J \wedge A)$ is the instanton current, which is not conserved for 4-D CP_2 projection. The conservation of j_K implies the condition $j_I^\alpha \partial_\alpha \phi = \partial_\alpha j^\alpha \phi$ and from this ϕ can be integrated if the integrability condition $j_I \wedge dj_I = 0$ holds true implying the same condition for j_K . By introducing at least 3 or CP_2 coordinates as space-time coordinates, one finds that the contravariant form of j_I is purely topological so that the integrability condition fixes the dependence on M^4 coordinates and this selection is coded into the scalar function ϕ . These functions define families of conserved currents $j_K^\alpha \phi$ and $j_I^\alpha \phi$ and could be also interpreted as conserved currents associated with the critical deformations of the space-time surface.

5. There are gauge transformations respecting the vanishing of the Coulomb term. The vanishing condition for the Coulomb term is gauge invariant only under the gauge transformations $A \rightarrow A + \nabla \phi$ for which the scalar function the integral $\int j_K^\alpha \partial_\alpha \phi$ reduces to a total divergence a giving an integral over various 3-surfaces at the ends of CD and at throats vanishes. This is satisfied if the allowed gauge transformations define conserved currents

$$D_\alpha(j^\alpha\phi) = 0 . \quad (13.4.7)$$

As a consequence Coulomb term reduces to a difference of the conserved charges $Q_\phi^e = \int j^0\phi\sqrt{g_4}d^3x$ at the ends of the CD vanishing identically. The change of the imons type term is trivial if the total weighted Kähler magnetic flux $Q_\phi^m = \sum \int J\phi dA$ over wormhole throats is conserved. The existence of an infinite number of conserved weighted magnetic fluxes is in accordance with the electric-magnetic duality. How these fluxes relate to the flux Hamiltonians central for WCW geometry is not quite clear.

6. The gauge transformations respecting the reduction to almost topological QFT should have some special physical meaning. The measurement interaction term in the modified Dirac interaction corresponds to a critical deformation of the space-time sheet and is realized as an addition of a gauge part to the Kähler gauge potential of CP_2 . It would be natural to identify this gauge transformation giving rise to a conserved charge so that the conserved charges would provide a representation for the charges associated with the infinitesimal critical deformations not affecting Kähler action. The gauge transformed Kähler potential couples to the modified Dirac equation and its effect could be visible in the value of Kähler function and therefore also in the properties of the preferred extremal. The effect on WCW metric would however vanish since K would transform only by an addition of a real part of a holomorphic function. Kähler function is identified as a Dirac determinant for Chern-Simons Dirac action and the spectrum of this operator should not be invariant under these gauge transformations if this picture is correct. This is achieved if the gauge transformation is carried only in the Dirac action corresponding to the Chern-Simons term: this assumption is motivated by the breaking of time reversal invariance induced by quantum measurements. The modification of Kähler action can be guessed to correspond just to the Chern-Simons contribution from the instanton term.
7. A reasonable looking guess for the explicit realization of the quantum classical correspondence between quantum numbers and space-time geometry is that the deformation of the preferred extremal due to the addition of the measurement interaction term is induced by a $U(1)$ gauge transformation induced by a transformation of $\delta CD \times CP_2$ generating the gauge transformation represented by ϕ . This interpretation makes sense if the fluxes defined by Q_ϕ^m and corresponding Hamiltonians affect only zero modes rather than quantum fluctuating degrees of freedom.

To sum up, one could understand the basic properties of WCW metric in this framework. Effective 2-dimensionality would result from the existence of an infinite number of conserved charges in two different time directions (genuine conservation laws plus gauge fixing). The infinite-dimensional symmetric space for given values of zero modes corresponds to the Cartesian product of the WCWs associated with the partonic 2-surfaces at both ends of CD and the generalized Chern-Simons term decomposes into a sum of terms from the ends giving single particle Kähler functions and to the terms from light-like wormhole throats giving interaction term between positive and negative energy parts of the state. Hence Kähler function could be calculated without any knowledge about the interior of the space-time sheets and TGD would reduce to almost topological QFT as speculated earlier. Needless to say this would have immense boost to the program of constructing WCW Kähler geometry.

13.4.4 A general solution ansatz based on almost topological QFT property

The basic vision behind the ansatz is the reduction of quantum TGD to almost topological field theory. This requires that the flow parameters associated with the flow lines of isometry currents and Kähler current extend to global coordinates. This leads to integrability conditions implying generalized Beltrami flow and Kähler action for the preferred extremals reduces to Chern-Simons action when weak electro-weak duality is applied as boundary conditions. The strongest form of the hydrodynamical interpretation requires that all conserved currents are parallel to Kähler current. In the more general case one would have several hydrodynamic flows. Also the braidings (several of them for the most general ansatz) assigned with the light-like 3-surfaces are naturally defined by the flow lines of conserved currents. The independent behavior of particles at different flow lines can be seen

as a realization of the complete integrability of the theory. In free quantum field theories on mass shell Fourier components are in a similar role but the geometric interpretation in terms of flow is of course lacking. This picture should generalize also to the solution of the modified Dirac equation.

Basic field equations

Consider first the equations at general level.

1. The breaking of the Poincare symmetry due to the presence of monopole field occurs and leads to the isometry group $T \times SO(3) \times SU(3)$ corresponding to time translations, rotations, and color group. The Cartan algebra is four-dimensional and field equations reduce to the conservation laws of energy E , angular momentum J , color isospin I_3 , and color hypercharge Y .
2. Quite generally, one can write the field equations as conservation laws for I, J, I_3 , and Y .

$$D_\alpha [D_\beta (J^{\alpha\beta} H_A) - j_K^\alpha H^A + T^{\alpha\beta} j_A^l h_{kl} \partial_\beta h^l] = 0 . \quad (13.4.8)$$

The first term gives a contraction of the symmetric Ricci tensor with antisymmetric Kähler form and vanishes so that one has

$$D_\alpha [j_K^\alpha H^A - T^{\alpha\beta} j_A^k h_{kl} \partial_\beta h^l] = 0 . \quad (13.4.9)$$

For energy one has $H_A = 1$ and energy current associated with the flow lines is proportional to the Kähler current. Its divergence vanishes identically.

3. One can express the divergence of the term involving energy momentum tensor as as sum of terms involving $j_K^\alpha J_{\alpha\beta}$ and contraction of second fundamental form with energy momentum tensor so that one obtains

$$j_K^\alpha D_\alpha H^A = j_K^\alpha J_{\alpha\beta} j_\beta^A + T^{\alpha\beta} H_{\alpha\beta}^k j_k^A . \quad (13.4.10)$$

Hydrodynamical solution ansatz

The characteristic feature of the solution ansatz would be the reduction of the dynamics to hydrodynamics analogous to that for a continuous distribution of particles initially at the end of X^3 of the light-like 3-surface moving along flow lines defined by currents j_A satisfying the integrability condition $j_A \wedge dj_A = 0$. Field theory would reduce effectively to particle mechanics along flow lines with conserved charges defined by various isometry currents. The strongest condition is that all isometry currents j_A and also Kähler current j_K are proportional to the same current j . The more general option corresponds to multi-hydrodynamics.

Conserved currents are analogous to hydrodynamical currents in the sense that the flow parameter along flow lines extends to a global space-time coordinate. The conserved current is proportional to the gradient $\nabla\Phi$ of the coordinate varying along the flow lines: $J = \Psi\nabla\Phi$ and by a proper choice of Ψ one can allow to have conservation. The initial values of Ψ and Φ can be selected freely along the flow lines beginning from either the end of the space-time surface or from wormhole throats.

If one requires hydrodynamics also for Chern-Simons action (effective 2-dimensionality is required for preferred extremals), the initial values of scalar functions can be chosen freely only at the partonic 2-surfaces. The freedom to chose the initial values of the charges conserved along flow lines at the partonic 2-surfaces means the existence of an infinite number of conserved charges so that the theory would be integrable and even in two different coordinate directions. The basic difference as compared to ordinary conservation laws is that the conserved currents are parallel and their flow parameter extends to a global coordinate.

1. The most general assumption is that the conserved isometry currents

$$J_A^\alpha = j_K^\alpha H^A - T^{\alpha\beta} j_A^k h_{kl} \partial_\beta h^l \quad (13.4.11)$$

and Kähler current are integrable in the sense that $J_A \wedge J_A = 0$ and $j_K \wedge j_K = 0$ hold true. One could imagine the possibility that the currents are not parallel.

2. The integrability condition $dJ_A \wedge J_A = 0$ is satisfied if one one has

$$J_A = \Psi_A d\Phi_A . \quad (13.4.12)$$

The conservation of J_A gives

$$d * (\Psi_A d\Phi_A) = 0 . \quad (13.4.13)$$

This would mean separate hydrodynamics for each of the currents involved. In principle there is not need to assume any further conditions and one can imagine infinite basis of scalar function pairs (Ψ_A, Φ_A) since criticality implies infinite number deformations implying conserved Noether currents.

3. The conservation condition reduces to d'Alembert equation in the induced metric if one assumes that $\nabla\Psi_A$ is orthogonal with every $d\Phi_A$.

$$d * d\Phi_A = 0 , \quad d\Psi_A \cdot d\Phi_A = 0 . \quad (13.4.14)$$

Taking $x = \Phi_A$ as a coordinate the orthogonality condition states $g^{xj} \partial_j \Psi_A = 0$ and in the general case one cannot solve the condition by simply assuming that Ψ_A depends on the coordinates transversal to Φ_A only. These conditions bring in mind $p \cdot p = 0$ and $p \cdot e$ condition for massless modes of Maxwell field having fixed momentum and polarization. $d\Phi_A$ would correspond to p and $d\Psi_A$ to polarization. The condition that each isometry current corresponds its own pair (Ψ_A, Φ_A) would mean that each isometry current corresponds to independent light-like momentum and polarization. Ordinary free quantum field theory would support this view whereas hydrodynamics and QFT limit of TGD would support single flow.

These are the most general hydrodynamical conditions that one can assume. One can consider also more restricted scenarios.

1. The strongest ansatz is inspired by the hydrodynamical picture in which all conserved isometry charges flow along same flow lines so that one would have

$$J_A = \Psi_A d\Phi . \quad (13.4.15)$$

In this case same Φ would satisfy simultaneously the d'Alembert type equations.

$$d * d\Phi = 0 , \quad d\Psi_A \cdot d\Phi = 0. \quad (13.4.16)$$

This would mean that the massless modes associated with isometry currents move in parallel manner but can have different polarizations. The spinor modes associated with light-light like 3-surfaces carry parallel four-momenta, which suggest that this option is correct. This allows a very general family of solutions and one can have a complete 3-dimensional basis of functions Ψ_A with gradient orthogonal to $d\Phi$.

2. Isometry invariance under $T \times SO(3) \times SU(3)$ allows to consider the possibility that one has

$$J_A = k_A \Psi_A d\Phi_{G(A)} , \quad d*(d\Phi_{G(A)}) = 0 , \quad d\Psi_A \cdot d\Phi_{G(A)} = 0 . \quad (13.4.17)$$

where $G(A)$ is T for energy current, $SO(3)$ for angular momentum currents and $SU(3)$ for color currents. Energy would thus flow along its own flux lines, angular momentum along its own flow lines, and color quantum numbers along their own flow lines. For instance, color currents would differ from each other only by a numerical constant. The replacement of Ψ_A with $\Psi_{G(A)}$ would be too strong a condition since Killing vector fields are not related by a constant factor.

To sum up, the most general option is that each conserved current J_A defines its own integrable flow lines defined by the scalar function pair (Ψ_A, Φ_A) . A complete basis of scalar functions satisfying the d'Alembert type equation guaranteeing current conservation could be imagined with restrictions coming from the effective 2-dimensionality reducing the scalar function basis effectively to the partonic 2-surface. The diametrically opposite option corresponds to the basis obtained by assuming that only single Φ is involved.

The proposed solution ansatz can be compared to the earlier ansatz [37] stating that Kähler current is topologized in the sense that for $D(CP_2) = 3$ it is proportional to the identically conserved instanton current (so that 4-D Lorentz force vanishes) and vanishes for $D(CP_2) = 4$ (Maxwell phase). This hypothesis requires that instanton current is Beltrami field for $D(CP_2) = 3$. In the recent case the assumption that also instanton current satisfies the Beltrami hypothesis in strong sense (single function Φ) generalizes the topologization hypothesis for $D(CP_2) = 3$. As a matter fact, the topologization hypothesis applies to isometry currents also for $D(CP_2) = 4$ although instanton current is not conserved anymore.

Can one require the extremal property in the case of Chern-Simons action?

Effective 2-dimensionality is achieved if the ends and wormhole throats are extremals of Chern-Simons action. The strongest condition would be that space-time surfaces allow orthogonal slicings by 3-surfaces which are extremals of Chern-Simons action.

Also in this case one can require that the flow parameter associated with the flow lines of the isometry currents extends to a global coordinate. Kähler magnetic field $B = *J$ defines a conserved current so that all conserved currents would flow along the field lines of B and one would have 3-D Beltrami flow. Note that in magnetohydrodynamics the standard assumption is that currents flow along the field lines of the magnetic field.

For wormhole throats light-likeness causes some complications since the induced metric is degenerate and the contravariant metric must be restricted to the complement of the light-like direction. This means that d'Alembert equation reduces to 2-dimensional Laplace equation. For space-like 3-surfaces one obtains the counterpart of Laplace equation with partonic 2-surfaces serving as sources. The interpretation in terms of analogs of Coulomb potentials created by 2-D charge distributions would be natural.

13.4.5 Hydrodynamic picture in fermionic sector

Super-symmetry inspires the conjecture that the hydrodynamical picture applies also to the solutions of the modified Dirac equation.

4-dimensional modified Dirac equation and hydrodynamical picture

Consider first the solutions of of the induced spinor field in the interior of space-time surface.

1. The local inner products of the modes of the induced spinor fields define conserved currents

$$\begin{aligned} D_\alpha J_{mn}^\alpha &= 0 , \\ J_{mn}^\alpha &= \bar{u}_m \hat{\Gamma}^\alpha u_n , \\ \hat{\Gamma}^\alpha &= \frac{\partial L_K}{\partial(\partial_\alpha h^k)} \Gamma_k . \end{aligned} \quad (13.4.16)$$

The conjecture is that the flow parameters of also these currents extend to a global coordinate so that one would have in the completely general case the condition

$$\begin{aligned} J_{mn}^\alpha &= \Phi_{mn} d\Psi_{mn} \ , \\ d*(d\Phi_{mn}) &= 0 \ , \ \nabla\Psi_{mn} \cdot \Phi_{mn} = 0 \ . \end{aligned} \quad (13.4.16)$$

The condition $\Phi_{mn} = \Phi$ would mean that the massless modes propagate in parallel manner and along the flow lines of Kähler current. The conservation condition along the flow line implies that the current component J_{mn} is constant along it. Everything would reduce to initial values at the ends of the space-time sheet boundaries of CD and 3-D modified Dirac equation would reduce everything to initial values at partonic 2-surfaces.

2. One might hope that the conservation of these super currents for all modes is equivalent with the modified Dirac equation. The modes u_n appearing in Ψ in quantized theory would be kind of "square roots" of the basis Φ_{mn} and the challenge would be to deduce the modes from the conservation laws.
3. The quantization of the induced spinor field in 4-D sense would be fixed by those at 3-D space-like ends by the fact that the oscillator operators are carried along the flow lines as such so that the anti-commutator of the induced spinor field at the opposite ends of the flow lines at the light-like boundaries of CD is in principle fixed by the anti-commutations at the either end. The anti-commutations at 3-D surfaces cannot be fixed freely since one has 3-D Chern-Simons flow reducing the anti-commutations to those at partonic 2-surfaces.

The following argument suggests that induced spinor fields are in a suitable gauge simply constant along the flow lines of the Kähler current just as massless spinor modes are constant along the geodesic in the direction of momentum.

1. The modified gamma matrices are of form $T_k^\alpha \Gamma^k$, $T_k^\alpha = \partial L_K / \partial(\partial_\alpha h^k)$. The H-vectors T_k^α can be expressed as linear combinations of a subset of Killing vector fields j_A^k spanning the tangent space of H . For CP_2 the natural choice are the 4 Lie-algebra generators in the complement of $U(2)$ sub-algebra. For CD one can use generator time translation and three generators of rotation group $SO(3)$. The completeness of the basis defined by the subset of Killing vector fields gives completeness relation $h_l^k = j^{Ak} j_{Ak}$. This implies $T^{\alpha k} = T^{\alpha k} j_A^k j_A^k = T^{\alpha A} j_A^k$. One can define gamma matrices Γ_A as $\Gamma_k j_A^k$ to get $T_k^\alpha \Gamma^k = T^{\alpha A} \Gamma_A$.
2. This together with the condition that all isometry currents are proportional to the Kähler current (or if this vanishes to same conserved current- say energy current) satisfying Beltrami flow property implies that one can reduce the modified Dirac equation to an ordinary differential equation along flow lines. The quantities T^{tA} are constant along the flow lines and one obtains

$$T^{tA} j_A D_t \Psi = 0 \ . \quad (13.4.17)$$

By choosing the gauge suitably the spinors are just constant along flow lines so that the spinor basis reduces by effective 2-dimensionality to a complete spinor basis at partonic 2-surfaces.

Generalized eigen modes for the modified Chern-Simons Dirac equation and hydrodynamical picture

Hydrodynamical picture helps to understand also the construction of generalized eigen modes of 3-D Chern-Simons Dirac equation.

The general form of generalized eigenvalue equation for Chern-Simons Dirac action

Consider first the the general form and interpretation of the generalized eigenvalue equation assigned with the modified Dirac equation for Chern-Simons action [33]. This is of course only an approximation since an additional contribution to the modified gamma matrices from the Lagrangian multiplier term guaranteeing the weak form of electric-magnetic duality must be included.

1. The modified Dirac equation for Ψ is consistent with that for its conjugate if the coefficient of the instanton term is real and one uses the Dirac action $\bar{\Psi}(D^\rightarrow - D^\leftarrow)\Psi$ giving modified Dirac equation as

$$D_{C-S}\Psi + \frac{1}{2}(D_\alpha \hat{\Gamma}_{C-S}^\alpha)\Psi = 0 . \quad (13.4.18)$$

As noticed, the divergence $D_\alpha \hat{\Gamma}_{C-S}^\alpha$ does not contain second derivatives in the case of Chern-Simons action. In the case of Kähler action they occur unless field equations equivalent with the vanishing of the divergence term are satisfied. The extremals of Chern-Simons action provide a natural manner to define effective 2-dimensionality.

Also the fermionic current is conserved in this case, which conforms with the idea that fermions flow along the light-like 3-surfaces. If one uses the action $\bar{\Psi}D^\rightarrow\Psi$, $\bar{\Psi}$ does not satisfy the Dirac equation following from the variational principle and fermion current is not conserved.

2. The generalized eigen modes of D_{C-S} should be such that one obtains the counterpart of Dirac propagator which is purely algebraic and does not therefore depend on the coordinates of the throat. This is satisfied if the generalized eigenvalues are expressible in terms of covariantly constant combinations of gamma matrices and here only M^4 gamma matrices are possible. Therefore the eigenvalue equation would read as

$$D\Psi = \lambda^k \gamma_k \Psi , \quad D = D_{C-S} + \frac{1}{2} D_\alpha \hat{\Gamma}_{C-S}^\alpha , \quad D_{C-S} = \hat{\Gamma}_{C-S}^\alpha D_\alpha . \quad (13.4.18)$$

Here the covariant derivatives D_α contain the measurement interaction term as an apparent gauge term. For extremals one has

$$D = D_{C-S} . \quad (13.4.19)$$

Covariant constancy allows to take the square of this equation and one has

$$(D^2 + [D, \lambda^k \gamma_k])\Psi = \lambda^k \lambda_k \Psi . \quad (13.4.20)$$

The commutator term is analogous to magnetic moment interaction.

3. The generalized eigenvalues correspond to $\lambda = \sqrt{\lambda^k \lambda_k}$ and Dirac determinant is defined as a product of the eigenvalues and conjecture to give the exponent of Kähler action reducing to Chern-Simons term. λ is completely analogous to mass. λ_k cannot be however interpreted as ordinary four-momentum: for instance, number theoretic arguments suggest that λ_k must be restricted to the preferred plane $M^2 \subset M^4$ interpreted as a commuting hyper-complex plane of complexified quaternions. For incoming lines this mass would vanish so that all incoming particles irrespective their actual quantum numbers would be massless in this sense and the propagator is indeed that for a massless particle. Note that the eigen-modes define the boundary values for the solutions of $D_K\Psi = 0$ so that the values of λ indeed define the counterpart of the momentum space.

This transmutation of massive particles to effectively massless ones might make possible the application of the twistor formalism as such in TGD framework [30]. $N = 4$ SUSY is one of the very few gauge theory which might be UV finite but it is definitely unphysical due to the masslessness of the basic quanta. Could the resolution of the interpretational problems be that the four-momenta appearing in this theory do not directly correspond to the observed four-momenta?

2. *Inclusion of the constraint term*

As already noticed one must include also the constraint term due to the weak form of electric-magnetic duality and this changes somewhat the above simple picture.

1. At the 3-dimensional ends of the space-time sheet and at wormhole throats the 3-dimensionality allows to introduce a coordinate varying along the flow lines of Kähler magnetic field $B = *J$. In this case the integrability conditions state that the flow is Beltrami flow. Note that the value of B^α along the flow line defining magnetic flux appearing in anti-commutation relations is constant. This suggests that the generalized eigenvalue equation for the Chern-Simons action reduces to a collection of ordinary apparently independent differential equations associated with the flow lines beginning from the partonic 2-surface. This indeed happens when the CP_2 projection is 2-dimensional. In this case it however seems that the basis u_n is not of much help.
2. The conclusion is wrong: the variations of Chern-Simons action are subject to the constraint that electric-magnetic duality holds true expressible in terms of Lagrange multiplier term

$$\int \Lambda_\alpha (J^{n\alpha} - K \epsilon^{n\alpha\beta\gamma} J_{\beta\gamma}) \sqrt{g_4} d^3x . \tag{13.4.21}$$

This gives a constraint force to the field equations and also a dependence on the induced 4-metric so that one has only almost topological QFT. This term also guarantees the M^4 part of WCW Kähler metric is non-trivial. The condition that the ends of space-time sheet and wormhole throats are extrema of Chern-Simons action subject to the electric-magnetic duality constraint is strongly suggested by the effective 2-dimensionality. Without the constraint term Chern-Simons action would vanish for its extremals so that Kähler function would be identically zero.

This term implies also an additional contribution to the modified gamma matrices besides the contribution coming from Chern-Simons action so that the first guess for the modified Dirac operator would not be quite correct. This contribution is of exactly of the same general form as the contribution for any general coordinate invariant action. The dependence of the induced metric on M^4 degrees of freedom guarantees that also M^4 gamma matrices are present. In the following this term will not be considered.

3. When the contribution of the constraint term to the modified gamma matrices is neglected, the explicit expression of the modified Dirac operator D_{C-S} associated with the Chern-Simons term is given by

$$\begin{aligned} D &= \hat{\Gamma}^\mu D_\mu + \frac{1}{2} D_\mu \hat{\Gamma}^\mu , \\ \hat{\Gamma}^\mu &= \frac{\partial L_{C-S}}{\partial_\mu h^k} \Gamma_k = \epsilon^{\mu\alpha\beta} [2J_{kl} \partial_\alpha h^l A_\beta + J_{\alpha\beta} A_k] \Gamma^k D_\mu , \\ D_\mu \hat{\Gamma}^\mu &= B_K^\alpha (J_{k\alpha} + \partial_\alpha A_k) , \\ B_K^\alpha &= \epsilon^{\alpha\beta\gamma} J_{\beta\gamma} , \quad J_{k\alpha} = J_{kl} \partial_\alpha s^l , \quad \hat{\epsilon}^{\alpha\beta\gamma} = \epsilon^{\alpha\beta\gamma} \sqrt{g_3} . \end{aligned} \tag{13.4.19}$$

For the extremals of Chern-Simons action one has $D_\alpha \hat{\Gamma}^\alpha = 0$. Analogous condition holds true when the constraining contribution to the modified gamma matrices is added.

3. *Generalized eigenvalue equation for Chern-Simons Dirac action*

Consider now the Chern-Simons Dirac equation in more detail assuming that the inclusion of the constraint contribution to the modified gamma matrices does not induce any complications. Assume also extremal property for Chern-Simons action with constraint term and Beltrami flow property.

1. For the extremals the Chern-Simons Dirac operator (constraint term not included) reduces to a one-dimensional Dirac operator

$$D_{C-S} = \hat{\epsilon}^{r\alpha\beta} [2J_{k\alpha}A_\beta + J_{\alpha\beta}A_k] \Gamma^k D_r . \quad (13.4.20)$$

Constraint term implies only a modification of the modified gamma matrices but the form of the operator remains otherwise same when extrema are in question so that one has $D_\alpha \hat{\Gamma}^\alpha = 0$.

2. For the extremals of Chern-Simons action the general solution of the modified Chern-Simons Dirac equation ($\lambda^k = 0$) is covariantly constant with respect to the coordinate r :

$$D_r \Psi = 0 . \quad (13.4.21)$$

The solution to this condition can be written immediately in terms of a non-integrable phase factor $P \exp(i \int A_r dr)$, where integration is along curve with constant transversal coordinates. If $\hat{\Gamma}^v$ is light-like vector field also $\hat{\Gamma}^v \Psi_0$ defines a solution of D_{C-S} . This solution corresponds to a zero mode for D_{C-S} and does not contribute to the Dirac determinant (suggested to give rise to the exponent of Kähler function identified as Kähler action). Note that the dependence of these solutions on transversal coordinates of X_i^3 is arbitrary which conforms with the hydrodynamic picture. The solutions of Chern-Simons-Dirac are obtained by similar integration procedure also when extremals are not in question.

The formal solution associated with a general eigenvalue λ can be constructed by integrating the eigenvalue equation separately along all coordinate curves. This makes sense if r indeed assigned to possibly light-like flow lines of B^α or more general Beltrami field possible induced by the constraint term. There are very strong consistency conditions coming from the conditions that Ψ in the interior is constant along the flow lines of Kähler current and continuous at the ends and throats (call them collectively boundaries), where Ψ has a non-trivial variation along the flow lines of B^α .

1. This makes sense only if the flow lines of the Kähler current are transversal to the boundaries so that the spinor modes at boundaries dictate the modes of the spinor field in the interior. Effective 2-dimensionality means that the spinor modes in the interior can be calculated either by starting from the throats or from the ends so that the data at either upper or lower partonic 2-surfaces dictates everything in accordance with zero energy ontology.
2. This gives an infinite number of commuting diagrams stating that the flow-line time evolution along flow lines along wormhole throats from lower partonic 2-surface to the upper one is equivalent with the flow-line time evolution along the lower end of space-time surface to interior, then along interior to the upper end of the space-time surface and then back to the upper partonic 2-surface. If the space-time surface allows a slicing by partonic 2-surfaces these conditions can be assumed for any pair of partonic 2-surfaces connected by Chern-Simons flow evolution.
3. Since the time evolution along interior keeps the spinor field as constant in the proper gauge and since the flow evolutions at the lower and upper ends are in a reverse direction, there is a strong attemptation to assume that the spinor field at the ends of the of the flow lines of Kähler magnetic field are identical apart from a gauge transformation. This leads to a particle-in-box quantization of the values of the pseudo-mass (periodic boundary conditions). These conditions will be assumed in the sequel.

These assumptions lead to the following picture about the generalized eigen modes.

1. By choosing the gauge so that covariant derivative reduces to ordinary derivative and using the constancy of $\hat{\Gamma}^r$, the solution of the generalized eigenvalue equation can be written as

$$\begin{aligned} \Psi &= \exp(iL(r)\hat{\Gamma}^r\lambda^k\Gamma_k)\Psi_0 , \\ L(r) &= \int_0^r \frac{1}{\sqrt{\hat{g}^{rr}}}dr . \end{aligned} \tag{13.4.21}$$

$L(r)$ can be regarded as the along flux line as defined by the effective metric defined by modified gamma matrices. If λ_k is linear combination of Γ^0 and Γ^{rM} it anti-commutes with Γ^r which contains only CP_2 gamma matrices so that the pseudo-momentum is a priori arbitrary.

2. When the constraint term taking care of the electric-magnetic duality is included, also M^4 gamma matrices are present. If they are in the orthogonal complement of a preferred plane $M^2 \subset M^4$, anti-commutativity is achieved. This assumption cannot be fully justified yet but conforms with the general physical vision. There is an obvious analogy with the condition that polarizations are in a plane orthogonal to M^2 . The condition indeed states that only transversal deformations define quantum fluctuating WCW degrees of freedom contributing to the WCW Kähler metric. In M^8-H duality the preferred plane M^2 is interpreted as a hyper-complex plane belonging to the tangent space of the space-time surface and defines the plane of non-physical polarizations. Also a generalization of this plane to an integrable distribution of planes $M^2(x)$ has been proposed and one must consider also now the possibility of a varying plane $M^2(x)$ for the pseudo-momenta. The scalar function Φ appearing in the general solution ansatz for the field equations satisfies massless d'Alembert equation and its gradient defines a local light-like direction at space-time-level and hence a 2-D plane of the tangent space. Maybe the projection of this plane to M^4 could define the preferred M^2 . The minimum condition is that these planes are defined only at the ends of space-time surface and at wormhole throats.

3. If one accepts this hypothesis, one can write

$$\begin{aligned} \Psi &= \left[\cos(L(r)\lambda) + i\sin(\lambda(r))\hat{\Gamma}^r\lambda^k\Gamma_k \right] \Psi_0 , \\ \lambda &= \sqrt{\lambda_k\lambda^k} . \end{aligned} \tag{13.4.21}$$

4. Boundary conditions should fix the spectrum of masses. If the the flow lines of Kähler current coincide with the flow lines of Kähler magnetic field or more general Beltrami current at wormhole throats one ends up with difficulties since the induced spinor fields must be constant along flow lines and only trivial eigenvalues are possible. Hence it seems that the two Beltrami fields must be transversal. This requires that at the partonic 2-surfaces the value of the induced spinor mode in the interior coincides with its value at the throat. Since the induced spinor fields in interior are constant along flow lines, one must have

$$\exp(i\lambda L(r_{max})) = 1 . \tag{13.4.22}$$

This implies that one has essentially particle in a box with size defined by the effective metric

$$\lambda_n = \frac{n2\pi}{L(r_{max})} . \tag{13.4.23}$$

5. This condition cannot however hold true simultaneously for all points of the partonic 2-surfaces since $L(r_{max})$ depends on the point of the surface. In the most general case one can consider only a subset consisting of the points for which the values of $L(r_{max})$ are rational multiples of the value of $L(r_{max})$ at one of the points -call it L_0 . This implies the notion of number theoretical braid. Induced spinor fields are localized to the points of the braid defined by the flow lines of

the Kähler magnetic field (or equivalently, any conserved current- this resolves the longstanding issue about the identification of number theoretical braids). The number of the included points depends on measurement resolution characterized somehow by the number rationals which are allowed. Only finite number of harmonics and sub-harmonics of L_0 are possible so that for integer multiples the number of points is finite. If $n_{max}L_0$ and L_0/n_{min} are the largest and smallest lengths involved, one can argue that the rationals n_{max}/n , $n = 1, \dots, n_{max}$ and n/n_{min} , $n = 1, \dots, n_{min}$ are the natural ones.

6. One can consider also algebraic extensions for which L_0 is scaled from its reference value by an algebraic number so that the mass scale m must be scaled up in similar manner. The spectrum comes also now in integer multiples. p-Adic mass calculations predicts mass scales to the inverses of square roots of prime and this raises the expectation that \sqrt{n} harmonics and sub-harmonics of L_0 might be necessary. Notice however that pseudo-momentum spectrum is in question so that this argument is on shaky grounds.

There is also the question about the allowed values of (λ_0, λ_3) for a given value of λ . This issue will be discussed in the next section devoted to the attempt to calculate the Dirac determinant assignable to this spectrum: suffice it to say that integer valued spectrum is the first guess implying that the pseudo-momenta satisfy $n_0^2 - n_3^2 = n^2$ and therefore correspond to Pythagorean triangles. What is remarkable that the notion of number theoretic braid pops up automatically from the Beltrami flow hypothesis.

13.5 How to define Dirac determinant?

The basic challenge is to define Dirac determinant hoped to give rise to the exponent of Kähler action associated with the preferred extremal. The reduction to almost topological QFT gives this kind of expression in terms of Chern-Simons action and one might hope of obtaining even more concrete expression from the Chern-Simons Dirac determinant. The calculation of the previous section allowed to calculate the most general spectrum of the modified Dirac operator. If the number of the eigenvalues is infinite as the naive expectation is then Dirac determinant diverges if calculated as the product of the eigenvalues and one must calculate it by using some kind of regularization procedure. Zeta function regularization is the natural manner to do this.

The following arguments however lead to a concrete vision how the regularization could be avoided and a connection with infinite primes. In fact, the manifestly finite option and the option involving zeta function regularization give Kähler functions differing only by a scaling factor and only the manifestly finite option satisfies number theoretical constraints coming from p-adicization. An explicit expression for the Dirac determinant in terms of geometric data of the orbit of the partonic 2-surface emerges.

Arithmetic quantum field theory defined by infinite emerges naturally. The lines of the generalized Feynman graphs are characterized by infinite primes and the selection rules correlating the geometries of the lines of the generalized Feynman graphs corresponds to the conservation of the sum of number theoretic momenta $\log(p_i)$ assignable to sub-braids corresponding to different primes p_i assignable to the orbit of parton. This conforms with the vision that infinite primes indeed characterize the geometry of light-like 3-surfaces and therefore also of space-time sheets. The eigenvalues of the modified Dirac operator are proportional $1/\sqrt{p_i}$ where p_i are the primes appearing in the definition of the p-adic prime and the interpretation as analogs of Higgs vacuum expectation values makes sense and is consistent with p-adic length scale hypothesis and p-adic mass calculations. It must be emphasized that all this is essentially due to single basic hypothesis, namely the reduction of quantum TGD to almost topological QFT guaranteed by the Beltrami ansatz for field equations and by the weak form of electric-magnetic duality.

13.5.1 Dirac determinant when the number of eigenvalues is infinite

At first sight the general spectrum looks the only reasonable possibility but if the eigenvalues correlate with the geometry of the partonic surface as quantum classical correspondence suggests, this conclusion might be wrong. The original hope was the number of eigenvalues would be finite so that also determinant would be finite automatically. There were some justifications for this hope in the definition of Dirac determinant based on the dimensional reduction of D_K as $D_K = D_{K,3} + D_1$ and

the identification of the generalized eigenvalues as those assigned to $D_{K,3}$ as analogs of energy eigenvalues assignable to the light-like 3-surface. It will be found that number theoretic input could allow to achieve a manifest finiteness in the case of D_{C-S} and that this option is the only possible one if number theoretic universality is required.

If there are no constraints on the eigenvalue spectrum of D_{C-S} for a given partonic orbit, the naive definition of the determinant gives an infinite result and one must define Dirac determinant using ζ function regularization implying that Kähler function reduces to the derivative of the zeta function $\zeta_D(s)$ -call it Dirac Zeta- associated with the eigenvalue spectrum.

Consider now the situation when the number of eigenvalues is infinite.

1. In this kind of situation zeta function regularization is the standard manner to define the Dirac determinant. What one does is to assign zeta function to the spectrum- let us call it Dirac zeta function and denote by $\zeta_D(s)$ - as

$$\zeta_D(s) = \sum_k \lambda_k^{-s} . \tag{13.5.1}$$

If the eigenvalue λ_k has degeneracy g_k it appears g_k times in the sum. In the case of harmonic oscillator one obtains Riemann zeta for which sum representation converges only for $Re(s) \geq 1$. Riemann zeta can be however analytically continued to the entire complex plane and the idea is that this can be done also in the more general case.

2. By the basic conjecture Kähler function corresponds to the logarithm of the Dirac determinant and equals to the sum of the logarithms of the eigenvalues

$$K = \log(\prod \lambda_k) = -\frac{d\zeta_D}{ds} \Big|_{s=0} . \tag{13.5.2}$$

The expression on the left hand side diverges if taken as such but the expression on the right had side based on the analytical continuation of the zeta function is completely well-defined and finite quantity. Note that the replacement of eigenvalues λ_k by their powers λ_k^n -or equivalently the increase of the degeneracy by a factor n - brings in only a factor n to K : $K \rightarrow nK$.

3. Dirac determinant involves in the minimal situation only the integer multiples of pseudo-mass scale $\lambda = 2\pi/L_{min}$. One can consider also rational and even algebraic multiples $qL_{min} < L_{max}$, $q \geq 1$, of L_{min} so that one would have several integer spectra simultaneously corresponding to different braids. Here L_{min} and L_{max} are the extrema of the braid strand length determined in terms of the effective metric as $L = \int (\hat{g}^{rr})^{-1/2} dr$. The question what multiples are involved will be needed later.
4. Each rational or algebraic multiple of L_{min} gives to the zeta function a contribution which is of same form so that one has

$$\zeta_D = \sum_q \zeta(\log(qx)s) , \quad x = \frac{L_{min}}{R} , \quad 1 \leq q < \frac{L_{max}}{L_{min}} . \tag{13.5.3}$$

Kähler function can be expressed as

$$K = \sum_n \log(\lambda_n) = -\frac{d\zeta_D(s)}{ds} = -\sum_q \log(qx) \frac{d\zeta(s)}{ds} \Big|_{s=0} , \quad x = \frac{L_{min}}{R} . \tag{13.5.4}$$

What is remarkable that the number theoretical details of ζ_D determine only the overall scaling factor of Kähler function and thus the value of Kähler coupling strength, which would be purely number theoretically determined if the hypothesis about the role of infinite primes is correct. Also the value of R is irrelevant since it does not affect the Kähler metric.

5. The dependence of Kähler function on WCW degrees of freedom would be coded completely by the dependence of the length scales qL_{min} on the complex coordinates of WCW: note that this dependence is different for each scale. This is reminiscent of the coding of the shape of the drum (or more generally - manifold) by the spectrum of its eigen frequencies. Now Kähler geometry would code for the dependence of the spectrum on the shape of the drum defined by the partonic 2-surface and the 4-D tangent space distribution associated with it.

What happens at the limit of vacuum extremals serves as a test for the identification of Kähler function as Dirac determinant. The weak form of electric magnetic duality implies that all components of the induced Kähler field vanish simultaneously if Kähler magnetic field cancels. In the modified Chern-Simons Dirac equation one obtains $L = \int (\hat{g}^{rr})^{-1/2} dr$. The modified gamma matrix $\hat{\Gamma}^r$ approaches a finite limit when Kähler magnetic field vanishes

$$\hat{\Gamma}^r = \epsilon^{r\beta\gamma} (2J_{\beta k} A_\gamma + J_{\beta\gamma} A_k) \Gamma^k \rightarrow 2\epsilon^{r\beta\gamma} J_{\beta k} \Gamma^k . \quad (13.5.5)$$

The relevant component of the effective metric is \hat{g}^{rr} and is given by

$$\hat{g}^{rr} = (\hat{\Gamma}^r)^2 = 4\epsilon^{r\beta\gamma} \epsilon^{r\mu\nu} J_{\beta k} J_\mu{}^k A_\gamma A_\nu . \quad (13.5.6)$$

The limit is non-vanishing in general and therefore the eigenvalues remain finite also at this limit as also the parameter $L_{min} = \int (\hat{g}^{rr})^{-1/2} dr$ defining the minimum of the length of the braid strand defined by Kähler magnetic flux line in the effective metric unless \hat{g}^{rr} goes to zero everywhere inside the partonic surface. Chern-Simons action and Kähler action vanish for vacuum extremals so that in this case one could require that Dirac determinant approaches to unity in a properly chosen gauge. Dirac determinant should approach to unit for vacuum extremals indeed approaches to unity since there are no finite eigenvalues at the limit $\hat{g}^{rr} = 0$.

13.5.2 Hyper-octonionic primes

Before detailed discussion of the hyper-octonionic option it is good to consider the basic properties of hyper-octonionic primes.

1. Hyper-octonionic primes are of form

$$\Pi_p = (n_0, n_3, n_1, n_2, \dots, n_7) , \quad \Pi_p^2 = n_0^2 - \sum_i n_i^2 = p \text{ or } p^2 . \quad (13.5.7)$$

2. Hyper-octonionic primes have a standard representation as hyper-complex primes. The Minkowski norm squared factorizes into a product as

$$n_0^2 - n_3^2 = (n_0 + n_3)(n_0 - n_3) . \quad (13.5.8)$$

If one has $n_3 \neq 0$, the prime property implies $n_0 - n_3 = 1$ so that one obtains $n_0 = n_3 + 1$ and $2n_3 + 1 = p$ giving

$$(n_0, n_3) = ((p+1)/2, (p-1)/2) . \quad (13.5.8)$$

Note that one has $(p+1)/2$ odd for $p \bmod 4 = 1$ and $(p+1)/2$ even for $p \bmod 4 = 3$. The difference $n_0 - n_3 = 1$ characterizes prime property.

If n_3 vanishes the prime prime property implies equivalence with ordinary prime and one has $n_0^2 = p^2$. These hyper-octonionic primes represent particles at rest.

3. The action of a discrete subgroup $G(p)$ of the octonionic automorphism group G_2 generates form hyper-complex primes with $n_3 \neq 0$ further hyper-octonionic primes $\Pi(p, k)$ corresponding to the same value of n_0 and p and for these the integer valued projection to M^2 satisfies $n_0^2 - n_3^2 = n > p$. It is also possible to have a state representing the system at rest with $(n_0, n_3) = ((p + 1)/2, 0)$ so that the pseudo-mass varies in the range $[\sqrt{p}, (p + 1)/2]$. The subgroup $G(n_0, n_3) \subset SU(3)$ leaving invariant the projection (n_0, n_3) generates the hyper-octonionic primes corresponding to the same value of mass for hyper-octonionic primes with same Minkowskian length p and pseudo-mass $\lambda = n \geq \sqrt{p}$.
4. One obtains two kinds of primes corresponding to the lengths of pseudo-momenta equal to p or \sqrt{p} . The first kind of particles are always at rest whereas the second kind of particles can be brought at rest only if one interprets the pseudo-momentum as M^2 projection. This brings in mind the secondary p-adic length scales assigned to causal diamonds (CDs) and the primary p-adic lengths scales assigned to particles.

If the M^2 projections of hyper-octonionic primes with length \sqrt{p} characterize the allowed basic momenta, ζ_D is sum of zeta functions associated with various projections which must be in the limits dictated by the geometry of the orbit of the partonic surface giving upper and lower bounds L_{max} and L_{min} on the length L . L_{min} is scaled up to $\sqrt{n_0^2 - n_3^2} L_{min}$ for a given projection (n_0, n_3) . In general a given M^2 projection (n_0, n_3) corresponds to several hyper-octonionic primes since $SU(3)$ rotations give a new hyper-octonionic prime with the same M^2 projection. This leads to an inconsistency unless one has a good explanation for why some basic momentum can appear several times. One might argue that the spinor mode is degenerate due to the possibility to perform discrete color rotations of the state. For hyper complex representatives there is no such problem and it seems favored. In any case, one can look how the degeneracy factors for given projection can be calculated.

1. To calculate the degeneracy factor $D(n)$ associated with given pseudo-mass value $\lambda = n$ one must find all hyper-octonionic primes Π , which can have projection in M^2 with length n and sum up the degeneracy factors $D(n, p)$ associated with them:

$$\begin{aligned}
 D(n) &= \sum_p D(n, p) , \\
 D(n, p) &= \sum_{n_0^2 - n_3^2 = p} D(p, n_0, n_3) , \\
 n_0^2 - n_3^2 &= n , \quad \Pi_p^2(n_0, n_3) = n_0^2 - n_3^2 - \sum_i n_i^2 = n - \sum_i n_i^2 = p .
 \end{aligned}
 \tag{13.5.7}$$

2. The condition $n_0^2 - n_3^2 = n$ allows only Pythagorean triangles and one must find the discrete subgroup $G(n_0, n_3) \subset SU(3)$ producing hyper-octonions with integer valued components with length p and components (n_0, n_3) . The points at the orbit satisfy the condition

$$\sum n_i^2 = p - n .
 \tag{13.5.8}$$

The degeneracy factor $D(p, n_0, n_3)$ associated with given mass value n is the number of elements of in the coset space $G(n_0, n_3, p)/H(n_0, n_3, p)$, where $H(n_0, n_3, p)$ is the isotropy group of given hyper-octonionic prime obtained in this manner. For $n_0^2 - n_3^2 = p^2$ $D(n_0, n_3, p)$ obviously equals to unity.

13.5.3 Three basic options for the pseudo-momentum spectrum

The calculation of the scaling factor of the Kähler function requires the knowledge of the degeneracies of the mass squared eigen values. There are three options to consider.

First option: all pseudo-momenta are allowed

If the degeneracy for pseudo-momenta in M^2 is same for all mass values- and formally characterizable by a number N telling how many 2-D pseudo-momenta reside on mass shell $n_0^2 - n_3^2 = m^2$. In this case zeta function would be proportional to a sum of Riemann Zetas with scaled arguments corresponding to scalings of the basic mass m to m/q .

$$\zeta_D(s) = N \sum_q \zeta(\log(qx)s) , \quad x = \frac{L_{min}}{R} . \quad (13.5.9)$$

This option provides no idea about the possible values of $1 \leq q \leq L_{max}/L_{min}$. The number N is given by the integral of relativistic density of states $\int dk/2\sqrt{k^2 + m^2}$ over the hyperbola and is logarithmically divergent so that the normalization factor N of the Kähler function would be infinite.

Second option: All integer valued pseudomomenta are allowed

Second option is inspired by number theoretic vision and assumes integer valued components for the momenta using $m_{max} = 2\pi/L_{min}$ as mass unit. p-Adicization motivates also the assumption that momentum components using m_{max} as mass scale are integers. This would restrict the choice of the number theoretical braids.

Integer valuedness together with masses coming as integer multiples of m_{max} implies $(\lambda_0, \lambda_3) = (n_0, n_3)$ with on mass shell condition $n_0^2 - n_3^2 = n^2$. Note that the condition is invariant under scaling. These integers correspond to Pythagorean triangles plus the degenerate situation with $n_3 = 0$. There exists a finite number of pairs (n_0, n_3) satisfying this condition as one finds by expressing n_0 as $n_0 = n_3 + k$ giving $2n_3k + k^2 = p^2$ giving $n_3 < n^2/2, n_0 < n^2/2 + 1$. This would be enough to have a finite degeneracy $D(n) \geq 1$ for a given value of mass squared and ζ_D would be well defined. ζ_D would be a modification of Riemann zeta given by

$$\begin{aligned} \zeta_D &= \sum_q \zeta_1(\log(qx)s) , \quad x = \frac{L_{min}}{R} , \\ \zeta_1(s) &= \sum g_n n^{-s} , \quad g_n \geq 1 . \end{aligned} \quad (13.5.9)$$

For generalized Feynman diagrams this option allows conservation of pseudo-momentum and for loops no divergences are possible since the integral over two-dimensional virtual momenta is replaced with a sum over discrete mass shells containing only a finite number of points. This option looks thus attractive but requires a regularization. On the other hand, the appearance of a zeta function having a strong resemblance with Riemann zeta could explain the finding that Riemann zeta is closely related to the description of critical systems. This point will be discussed later.

Third option: Infinite primes code for the allowed mass scales

According to the proposal of [17, 48] the hyper-complex parts of hyper-octonionic primes appearing in their infinite counterparts correspond to the M^2 projections of real four-momenta. This hypothesis suggests a very detailed map between infinite primes and standard model quantum numbers and predicts a universal mass spectrum [17]. Since pseudo-momenta are automatically restricted to the plane M^2 , one cannot avoid the question whether they could actually correspond to the hyper-octonionic primes defining the infinite prime. These interpretations need not of course exclude each other. This option allows several variants and at this stage it is not possible to exclude any of these options.

1. One must choose between two alternatives for which pseudo-momentum corresponds to hyper-complex prime serving as a canonical representative of a hyper-octonionic prime or a projection of hyper-octonionic prime to M^2 .
2. One must decide whether one allows a) only the momenta corresponding to hyper-complex primes, b) also their powers (p-adic fractality), or c) all their integer multiples ("Riemann option").

One must also decide what hyper-octonionic primes are allowed.

1. The first guess is that all hyper-complex/hyper-octonionic primes defining length scale $\sqrt{p}L_{min} \leq L_{max}$ or $pL_{min} \leq L_{max}$ are allowed. p-Adic fractality suggests that also the higher p-adic length scales $p^{n/2}L_{min} < L_{max}$ and $p^n L_{min} < L_{max}$, $n \geq 1$, are possible.

It can however happen that no primes are allowed by this criterion. This would mean vanishing Kähler function which is of course also possible since Kähler action can vanish (for instance, for massless extremals). It seems therefore safer to allow also the scale corresponding to the trivial prime $(n_0, n_3) = (1, 0)$ (1 is formally prime because it is not divisible by any prime different from 1) so that at least L_{min} is possible. This option also allows only rather small primes unless the partonic 2-surface contains vacuum regions in which case L_{max} is infinite: in this case all primes would be allowed and the exponent of Kähler function would vanish.

2. The hypothesis that only the hyper-complex or hyper-octonionic primes appearing in the infinite hyper-octonionic prime are possible looks more reasonable since large values of p would be possible and could be identified in terms of the p-adic length scale hypothesis. All hyper-octonionic primes appearing in infinite prime would be possible and the geometry of the orbit of the partonic 2-surface would define an infinite prime. This would also give a concrete physical interpretation for the earlier hypothesis that hyper-octonionic primes appearing in the infinite prime characterize partonic 2-surfaces geometrically. One can also identify the fermionic and purely bosonic primes appearing in the infinite prime as braid strands carrying fermion number and purely bosonic quantum numbers. This option will be assumed in the following.

13.5.4 Expression for the Dirac determinant for various options

The expressions for the Dirac determinant for various options can be deduced in a straightforward manner. Numerically Riemann option and manifestly finite option do not differ much but their number theoretic properties are totally different.

Riemann option

All integer multiples of these basic pseudo-momenta would be allowed for Riemann option so that ζ_D would be sum of Riemann zetas with arguments scaled by the basic pseudo-masses coming as inverses of the basic length scales for braid strands. For the option involving only hyper-complex primes the formula for ζ_D reads as

$$\zeta_D = \zeta(\log(x_{mins})) + \sum_{i,n} \zeta(\log(x_{i,n}s)) + \sum_{i,n} \zeta(\log(y_{i,n}s)) ,$$

$$x_{i,n} = p_i^{n/2} x_{min} \leq x_{max} , \quad p_i \geq 3 , \quad y_{i,n} = p_i^n x_{min} \leq x_{max} \cdot p_i \geq 2 ,$$
(13.5.9)

L_{max} resp. L_{min} is the maximal resp. minimal length $L = \int (\hat{g}^{rr})^{-1/2} dr$ for the braid strand defined by the flux line of the Kähler magnetic field in the effective metric. The contributions correspond to the effective hyper-complex prime $p_1 = (1, 0)$ and hyper-complex primes with Minkowski lengths \sqrt{p} ($p \geq 3$) and p , $p \geq 2$. If also higher p-adic length scales $L_n = p^{n/2}L_{min} < L_{max}$ and $L_n = p^n L_{min} < L_{max}$, $n > 1$, are allowed there is no further restriction on the summation. For the restricted option only L_n , $n = 0, 2$ is allowed.

The expressions for the Kähler function and its exponent reads as

$$K = k(\log(x_{min})) + \sum_i \log(x_i) + \sum_i \log(y_i) ,$$

$$\exp(K) = \left(\frac{1}{x_{min}}\right)^k \times \prod_i \left(\frac{1}{x_i}\right)^k \times \prod_i \left(\frac{1}{y_i}\right)^k ,$$

$$x_i \leq x_{max} , \quad y_i \leq x_{max} , \quad k = -\frac{d\zeta(s)}{ds} \Big|_{s=0} = \frac{1}{2} \log(2\pi) \simeq .9184 .$$
(13.5.7)

From the point of view of p-adicization program the appearance of strongly transcendental numbers in the normalization factor of ζ_D is not a well-come property.

If the scaling of the WCW Kähler metric by $1/k$ is a legitimate procedure it would allow to get rid of the transcendental scaling factor k and this scaling would cancel also the transcendental from the exponent of Kähler function. The scaling is not however consistent with the view that Kähler coupling strength determines the normalization of the WCW metric.

This formula generalizes in a rather obvious manner to the cases when one allows M^2 projections of hyper-octonionic primes.

Manifestly finite options

The options for which one does not allow summation over all integer multiples of the basic momenta characterized by the canonical representatives of hyper-complex primes or their projections to M^2 are manifestly finite. They differ from the Riemann option only in that the normalization factor $k \simeq .9184$ defined by the derivative Riemann Zeta at origin is replaced with $k = 1$. This would mean manifest finiteness of ζ_D . Kähler function and its exponent are given by

$$K = k(\log(x_{min}) + \sum_i \log(x_i) + \sum_i \log(y_i)) , \quad x_i \leq x_{max} , \quad y_i \leq x_{max} ,$$

$$\exp(K) = \frac{1}{x_{min}} \times \prod_i \frac{1}{x_i} \times \prod_i \frac{1}{y_i} .$$
(13.5.6)

Numerically the Kähler functions do not differ much since their ratio is .9184. Number theoretically these functions are however completely different. The resulting dependence involves only square roots of primes and is an algebraic function of the lengths p_i and rational function of x_{min} . p-Adicization program would require rational values of the lengths x_{min} in the intersection of the real and p-adic worlds if one allows algebraic extension containing the square roots of the primes involved. Note that in p-adic context this algebraic extension involves two additional square roots for $p > 2$ if one does not want square root of p . Whether one should allow for R_p also extension based on \sqrt{p} is not quite clear. This would give 8-D extension.

For the more general option allowing all projections of hyper-complex primes to M^2 the general form of Kähler function is same. Instead of pseudo-masses coming as primes and their square roots one has pseudomasses coming as square roots of some integers $n \leq p$ or $n \leq p^2$ for each p . In this case the conservation laws are not so strong.

Note that in the case of vacuum extremals $x_{min} = \infty$ holds true so that there are no primes satisfying the condition and Kähler function vanishes as it indeed should.

More concrete picture about the option based on infinite primes

The identification of pseudo-momenta in terms of infinite primes suggests a rather concrete connection between number theory and physics.

1. One could assign the finite hyper-octonionic primes Π_i making the infinite prime to the sub-braids identified as Kähler magnetic flux lines with the same length L in the effective metric. The primes assigned to the finite part of the infinite prime correspond to single fermion and some number of bosons. The primes assigned to the infinite part correspond to purely bosonic states assignable to the purely bosonic braid strands. Purely bosonic state would correspond to the action of a WCW Hamiltonian to the state.

This correspondence can be expanded to include all quantum numbers by using the pair of infinite primes corresponding to the "vacuum primes" $X \pm 1$, where X is the product of all finite primes [17]. The only difference with respect to the earlier proposal is that physical momenta would be replaced by pseudo-momenta.

2. Different primes p_i appearing in the infinite prime would correspond to their own sub-braids. For each sub-braid there is a N -fold degeneracy of the generalized eigen modes corresponding

to the number N of braid strands so that many particle states are possible as required by the braid picture.

3. The correspondence of infinite primes with the hierarchy of Planck constants could allow to understand the fermion-many boson states and many boson states assigned with a given finite prime in terms of many-particle states assigned to n_a and n_b -sheeted singular covering spaces of CD and CP_2 assignable to the two infinite primes. This interpretation requires that only single p-adic prime p_i is realized as quantum state meaning that quantum measurement always selects a particular p-adic prime p_i (and corresponding sub-braid) characterizing the p-adicity of the quantum state. This selection of number field behind p-adic physics responsible for cognition looks very plausible.
4. The correspondence between pairs of infinite primes and quantum states [17] allows to interpret color quantum numbers in terms of the states associated with the representations of a finite subgroup of $SU(3)$ transforming hyper-octonionic primes to each other and preserving the M^2 pseudo-momentum. Same applies to $SO(3)$. The most natural interpretation is in terms of wave functions in the space of discrete $SU(3)$ and $SO(3)$ transforms of the partonic 2-surface. The dependence of the pseudo-masses on these quantum numbers is natural so that the projection hypothesis finds support from this interpretation.
5. The infinite prime characterizing the orbit of the partonic 2-surface would thus code which multiples of the basic mass $2\pi/L_{min}$ are possible. Either the M^2 projections of hyper-octonionic primes or their hyper-complex canonical representatives would fix the basic M^2 pseudo-momenta for the corresponding number theoretic braid associated. In the reverse direction the knowledge of the light-like 3-surface, the CD and CP_2 coverings, and the number of the allowed discrete $SU(3)$ and $SU(2)$ rotations of the partonic 2-surface would dictate the infinite prime assignable to the orbit of the partonic 2-surface.

One would also like to understand whether there is some kind of conservation laws associated with the pseudo-momenta at vertices. The arithmetic QFT assignable to infinite primes would indeed predict this kind of conservation laws.

1. For the manifestly finite option the ordinary conservation of pseudo-momentum conservation at vertices is not possible since the addition of pseudo-momenta does not respect the condition $n_0 - n_3 = 1$. In fact, this difference in the sum of hyper-complex prime momenta tells how many momenta are present. If one applies the conservation law to the sum of the pseudo-momenta corresponding to different primes and corresponding braids, one can have reactions in which the number of primes involved is conserved. This would give the selection rule $\sum_1^N p_i = \sum_1^N p_f$. These reactions have interpretation in terms of the geometry of the 3-surface representing the line of the generalized Feynman diagram.
2. Infinite primes define an arithmetic quantum field theory in which the total momentum defined as $\sum n_i \log(p_i)$ is a conserved quantity. As matter fact, each prime p_i would define a separately conserved momentum so that there would be an infinite number of conservation laws. If the sum $\sum_i \log(p_i)$ is conserved in the vertex, the primes p_i associated with the incoming particle are shared with the outgoing particles so that also the total momentum is conserved. This looks the most plausible option and would give very powerful number theoretical selection rules at vertices since the collection of primes associated with incoming line would be union of the collections associated with the outgoing lines and also total pseudo-momentum would be conserved.
3. For the both Riemann zeta option and manifestly finite options the arithmetic QFT associated with infinite primes would be realized at the level of pseudo-momenta meaning very strong selection rules at vertices coding for how the geometries of the partonic lines entering the vertex correlate. WCW integration would reduce for the lines of Feynman diagram to a sum over light-like 3-surfaces characterized by (x_{min}, x_{max}) with a suitable weighting factor and the exponent of Kähler function would give an exponential damping as a function of x_{min} .

Which option to choose?

One should be able to make two choices. One must select between hyper-complex representations and the projections of hyper-octonionic primes and between the manifestly finite options and the one producing Riemann zeta?

Hyper-complex option seems to be slightly favored over the projection option.

1. The appearance of the scales $\sqrt{p_i}x_{min}$ and possibly also their p^n multiples brings in mind p-adic length scales coming as $\sqrt{p^n}$ multiples of CP_2 length scale. The scales $p_i x_{min}$ associated with hyper-complex primes reducing to ordinary primes in turn bring in mind the size scales assignable to CDs . The hierarchy of Planck constants implies also $\hbar/\hbar_0 = \sqrt{n_a n_b}$ multiples of these length scales but mass scales would not depend on n_a and n_b [21]. For large values of p the pseudo-momenta are almost light-like for hyper-complex option whereas the projection option allows also states at rest.
2. Hyper-complex option predicts that only the p-adic pseudo-mass scales appear in the partition function and is thus favored by the p-adic length scale hypothesis. Projection option predicts also the possibility of the mass scales (not all of them) coming as $1/\sqrt{n}$. These mass scales are however not predicted by the hierarchy of Planck constants.
3. The same pseudo-mass scale can appear several times for the projection option. This degeneracy corresponds to the orbit of the hyper-complex prime under the subgroup of $SU(3)$ respecting integer property. Similar statement holds true in the case of $SO(3)$: these groups are assigned to the two infinite primes characterizing parton. The natural assignment of this degeneracy is to the discrete color rotational and rotational degrees associated with the partonic 2-surface itself rather than spinor modes at fixed partonic 2-surface. That the pseudo-mass would depend on color and angular momentum quantum numbers would make sense.

Consider next the arguments in favor of the manifestly finite option.

1. The manifestly finite option is admittedly more elegant than the one based on Riemann zeta and also guarantees that no additional loop summations over pseudo-momenta are present. The strongest support for the manifestly finite option comes from number theoretical universality.
2. One could however argue that the restriction of the pseudo-momenta to a finite number is not consistent with the modified Dirac-Chern-Simons equation. Quantum classical correspondence however implies correlation between the geometry of the partonic orbits and the pseudo-momenta and the summation over all prime valued pseudo-momenta is present but with a weighting factor coming from Kähler function implying exponential suppression.

The Riemann zeta option could be also defended.

1. The numerical difference of the normalization factors of the Kähler function is however only about 8 per cent and quantum field theorists might interpret the replacement the length scales x_i and y_i with x_i^d and y_i^d , $d \simeq .9184$, in terms of an anomalous dimension of these length scales. Could one say that radiative corrections mean the scaling of the original preferred coordinates so that one could still have consistency with number theoretic universality?
2. Riemann zeta with a non-vanishing argument could have also other applications in quantum TGD. Riemann zeta has interpretation as a partition function and the zeros of partition functions have interpretation in terms of phase transitions. The quantum criticality of TGD indeed corresponds to a phase transition point. There is also experimental evidence that the distribution of zeros of zeta corresponds to the distribution of energies of quantum critical systems in the sense that the energies correspond to the imaginary parts of the zeros of zeta [54].

The first explanation would be in terms of the analogs of the harmonic oscillator coherent states with integer multiple of the basic momentum taking the role of occupation number of harmonic oscillator and the zeros $s = 1/2 + iy$ of ζ defining the values of the complex coherence parameters. TGD inspired strategy for the proof of Riemann hypothesis indeed leads to the identification of the zeros as coherence parameters rather than energies as in the case of Hilbert-Polya hypothesis

[32] and the vanishing of the zeta at zero has interpretation as orthogonality of the state with respect to the state defined by a vanishing coherence parameter interpreted as a tachyon. One should demonstrate that the energies of quantum states can correspond to the imaginary parts of the coherence parameters.

Second interpretation could be in terms of quantum critical zero energy states for which the "complex square root of density matrix" defines time-like entanglement coefficients of M -matrix. The complex square roots of the probabilities defined by the coefficient of harmonic oscillator states (perhaps identifiable in terms of the multiples of pseudo-momentum) in the coherent state defined by the zero of ζ would define the M -matrix in this situation. Energy would correspond also now to the imaginary part of the coherence parameter. The norm of the state would be completely well-defined.

Representation of configuration Kähler metric in terms of eigenvalues of D_{C-S}

A surprisingly concrete connection of the configuration space metric in terms of generalized eigenvalue spectrum of D_{C-S} results. From the general expression of Kähler metric in terms of Kähler function

$$G_{k\bar{l}} = \partial_k \partial_{\bar{l}} K = \frac{\partial_k \partial_{\bar{l}} \exp(K)}{\exp(K)} - \frac{\partial_k \exp(K)}{\exp(K)} \frac{\partial_{\bar{l}} \exp(K)}{\exp(K)}, \quad (13.5.7)$$

and from the expression of $\exp(K) = \prod_i \lambda_i$ as the product of finite number of eigenvalues of D_{C-S} , the expression

$$G_{k\bar{l}} = \sum_i \frac{\partial_k \partial_{\bar{l}} \lambda_i}{\lambda_i} - \frac{\partial_k \lambda_i}{\lambda_i} \frac{\partial_{\bar{l}} \lambda_i}{\lambda_i} \quad (13.5.8)$$

for the configuration space metric follows. Here complex coordinates refer to the complex coordinates of configuration space. Hence the knowledge of the eigenvalue spectrum of $D_{C-S}(X^3)$ as function of some complex coordinates of configuration space allows to deduce the metric to arbitrary accuracy. If the above arguments are correct the calculation reduces to the calculation of the derivatives of $\log(\sqrt{p}L_{min}/R)$, where L_{min} is the length of the Kähler magnetic flux line between partonic 2-surfaces with respect to the effective metric defined by the anti-commutators of the modified gamma matrices. Note that these length scales have different dependence on WCW coordinates so that one cannot reduce everything to L_{min} . Therefore one would have explicit representation of the basic building brick of WCW Kähler metric in terms of the geometric data associated with the orbit of the partonic 2-surface.

The formula for the Kähler action of CP_2 type vacuum extremals is consistent with the Dirac determinant formula

The first killer test for the formula of Kähler function in terms of the Dirac determinant based on infinite prime hypothesis is provided by the action of CP_2 type vacuum extremals. One of the first attempts to make quantitative predictions in TGD framework was the prediction for the gravitational constant. The argument went as follows.

1. For dimensional reasons gravitational constant must be proportional to p-adic length scale squared, where p characterizes the space-time sheet of the graviton. It must be also proportional to the square of the vacuum function for the graviton representing a line of generalized Feynman diagram and thus to the exponent $\exp(-2K)$ of Kähler action for topologically condensed CP_2 type vacuum extremals with very long projection. If topological condensation does not reduce much of the volume of CP_2 type vacuum extremal, the action is just Kähler action for CP_2 itself. This gives

$$\hbar_0 G = L_p^2 \exp(2L_K(CP_2)) = pR^2 \exp(2L_K(CP_2)) . \quad (13.5.9)$$

- Using as input the constraint $\alpha_K \simeq \alpha_{em} \sim 1/137$ for Kähler coupling strengths coming from the comparison of the TGD prediction for the rotation velocity of distant galaxies around galactic nucleus and the p-adic mass calculation for the electron mass, one obtained the result

$$\exp(2L_K(CP_2)) = \frac{1}{p \times \prod_{p_i \leq 23} p_i} . \quad (13.5.10)$$

The product contains the product of all primes smaller than 24 ($p_i \in \{2, 3, 5, 7, 11, 13, 17, 19, 23\}$). The expression for the Kähler function would be just of the form predicted by the Dirac determinant formula with L_{min} replaced with CP_2 length scale. As a matter fact, this was the first indication that particles are characterized by several p-adic primes but that only one of them is "active". As explained, the number theoretical state function reduction explains this.

- The same formula for the gravitational constant would result for any prime p but the value of Kähler coupling strength would depend on prime p logarithmically for this option. I indeed proposed that this formula fixes the discrete evolution of the Kähler coupling strength as function of p-adic prime from the condition that gravitational constant is renormalization group invariant quantity but gave up this hypothesis later. It is wisest to keep an agnostic attitude to this issue.
- I also made numerous brave attempts to deduce an explicit formula for Kähler coupling strength. The general form of the formula is

$$\frac{1}{\alpha_K} = k \log(K^2), \quad K^2 = p \times 2 \times 3 \times 5 \dots \times 23 . \quad (13.5.11)$$

The problem is the exact value of k cannot be known precisely and the guesses for its value depend on what one means with number theoretical universality. Should Kähler action be a rational number? Or is it Kähler function which is rational number (it is for the Dirac determinant option in this particular case). Is Kähler coupling strength $g_K^2/4\pi$ or g_K^2 a rational number? Some of the guesses were $k = \pi/4$ and $k = 137/107$. The facts that the value of Kähler action for the line of a generalized diagram is not exactly CP_2 action and the value of α_K is not known precisely makes these kind of attempts hopeless in absence of additional ideas.

Also other elementary particles -in particular exchanged bosons- should involve the exponent of Kähler action for CP_2 type vacuum extremal. Since the values of gauge couplings are gigantic as compared to the expression of the gravitational constant the value of Kähler action must be rather small form them. CP_2 type vacuum extremals must be short in the sense that L_{min} in the effective metric is very short. Note however that the p-adic prime characterizing the particle according to p-adic mass calculations would be large also now. One can of course ask whether this p-adic prime characterizes the gravitational space-time sheets associated with the particle and not the particle itself. The assignment of p-adic mass calculations with thermodynamics at gravitational space-time sheets of the particle would be indeed natural. The value of α_K would depend on p in logarithmic manner for this option. The topological condensation of could also eat a lot of CP_2 volume for them.

Eigenvalues of D_{C-S} as vacuum expectations of Higgs field?

Infinite prime hypothesis implies the analog of p-adic length scale hypothesis but since pseudo-momenta are in question, this need not correspond to the p-adic length scale hypothesis for the actual masses justified by p-adic thermodynamics. Note also that L_{min} does not correspond to CP_2 length scale. This is actually not a problem since the effective metric is not M^4 metric and one can quite well consider the possibility that L_{min} corresponds to CP_2 length scale in the the induced metric. The reason is that light-like 3- surface is in question the distance along the Kähler magnetic flux line reduces essentially to a distance along the partonic 2-surface having size scale of order CP_2 length for the partonic 2-surfaces identified as wormhole throats. Therefore infinite prime can code for genuine

p-adic length scales associated with the light-like 3-surface and quantum states would correspond by number theoretical state function reduction hypothesis to single ordinary prime.

Support for this identification comes also from the expression of gravitational constant deduced from p-adic length scale hypothesis. The result is that gravitational constant is assumed to be proportional to have the expression $G = L_p^2 \exp(-2S_K(CP_2))$, where p characterizes graviton or the space-time sheet mediating gravitational interaction and exponent gives Kähler action for CP_2 type vacuum extremal representing graviton. The argument allows to identify the p-adic prime $p = M_{127}$ associated with electron (largest Mersenne prime which does not correspond to super-astronomical length scale) as the p-adic prime characterizing also graviton. The exponent of Kähler action is proportional to $1/p$ which conforms with the general expression for Kähler function. I have considered several identifications of the numerical factor and one of them has been as product of primes $2 \leq p \leq 23$ assuming that somehow the primes $\{2, \dots, 23, p\}$ characterize graviton. This guess is indeed consistent with the prediction of the infinite-prime hypothesis.

The first guess inspired by the p-adic mass calculations is that the squares λ_i^2 of the eigenvalues of D_{C-S} could correspond to the conformal weights of ground states. Another natural physical interpretation of λ is as an analog of the Higgs vacuum expectation. The instability of the Higgs=0 phase would correspond to the fact that $\lambda = 0$ mode is not localized to any region in which ew magnetic field or induced Kähler field is non-vanishing. By the previous argument one would have order of magnitude estimate $h_0 = \sqrt{2\pi/L_{min}}$.

1. The vacuum expectation value of Higgs is only proportional to the scale of λ . Indeed, Higgs and gauge bosons as elementary particles correspond to wormhole contacts carrying fermion and anti-fermion at the two wormhole throats and must be distinguished from the space-time correlate of its vacuum expectation as something proportional to λ . For free fermions the vacuum expectation value of Higgs does not seem to be even possible since free fermions do not correspond to wormhole contacts between two space-time sheets but possess only single wormhole throat (p-adic mass calculations are consistent with this). If fermion suffers topological condensation as indeed assumed to do in interaction region, a wormhole contact is generated and makes possible the generation of Higgs vacuum expectation value.
2. Physical considerations suggest that the vacuum expectation of Higgs field corresponds to a particular eigenvalue λ_i of modified Chern-Simons Dirac operator so that the eigenvalues λ_i would define TGD counterparts for the minima of Higgs potential. For the minimal option one has only a finite number of pseudo-mass eigenvalues inversely proportional \sqrt{p} so that the identification as a Higgs vacuum expectation is consistent with the p-adic length scale hypothesis. Since the vacuum expectation of Higgs corresponds to a condensate of wormhole contacts giving rise to a coherent state, the vacuum expectation cannot be present for topologically condensed CP_2 type vacuum extremals representing fermions since only single wormhole throat is involved. This raises a hen-egg question about whether Higgs contributes to the mass or whether Higgs is only a correlate for massivation having description using more profound concepts. From TGD point of view the most elegant option is that Higgs does not give rise to mass but Higgs vacuum expectation value accompanies bosonic states and is naturally proportional to λ_i . With this interpretation λ_i could give a contribution to both fermionic and bosonic masses.
3. If the coset construction for super-symplectic and super Kac-Moody algebra implying Equivalence Principle is accepted, one encounters what looks like a problem. p-Adic mass calculations require negative ground state conformal weight compensated by Super Virasoro generators in order to obtain massless states. The tachyonicity of the ground states would mean a close analogy with both string models and Higgs mechanism. λ_i^2 is very natural candidate for the ground state conformal weights identified but would have wrong sign. Therefore it seems that λ_i^2 can define only a deviation of the ground state conformal weight from negative value and is positive.
4. In accordance with this λ_i^2 would give constant contribution to the ground state conformal weight. What contributes to the thermal mass squared is the deviation of the ground state conformal weight from half-odd integer since the negative integer part of the total conformal weight can be compensated by applying Virasoro generators to the ground state. The first guess motivated by cyclotron energy analogy is that the lowest conformal weights are of form $h_c = -n/2 + \lambda_i^2$ where the negative contribution comes from Super Virasoro representation. The

negative integer part of the net conformal weight can be canceled using Super Virasoro generators but Δh_c would give to mass squared a contribution analogous to Higgs contribution. The mapping of the real ground state conformal weight to a p-adic number by canonical identification involves some delicacies.

5. p-Adic mass calculations are consistent with the assumption that Higgs type contribution is vanishing (that is small) for fermions and dominates for gauge bosons. This requires that the deviation of λ_i^2 with smallest magnitude from half-odd integer value in the case of fermions is considerably smaller than in the case of gauge bosons in the scale defined by p-adic mass scale $1/L(k)$ in question. Somehow this difference could relate to the fact that bosons correspond to pairs of wormhole throats.

Is there a connection between p-adic thermodynamics, hierarchy of Planck constants, and infinite primes

The following observations suggest that there might be an intrinsic connection between p-adic thermodynamics, hierarchy of Planck constants, and infinite primes.

1. p-Adic thermodynamics [26] is based on string mass formula in which mass squared is proportional to conformal weight having values which are integers apart from the contribution of the conformal weight of vacuum which can be non-integer valued. The thermal expectation in p-adic thermodynamics is obtained by replacing the Boltzman weight $\exp(-E/T)$ of ordinary thermodynamics with p-adic conformal weight p^{n/T_p} , where n is the value of conformal weight and $1/T_p = m$ is integer values inverse p-adic temperature. Apart from the ground state contribution and scale factor p-adic mass squared is essentially the expectation value

$$\langle n \rangle = \frac{\sum_n g(n) n p^{\frac{n}{T_p}}}{\sum_n g(n) p^{\frac{n}{T_p}}} . \quad (13.5.12)$$

$g(n)$ denotes the degeneracy of a state with given conformal weight and depends only on the number of tensor factors in the representations of Virasoro or Super-Virasoro algebra. p-Adic mass squared is mapped to its real counterpart by canonical identification $\sum x_n p^n \rightarrow \sum x_n p^{-n}$. The real counterpart of p-adic thermodynamics is obtained by the replacement $p^{-\frac{n}{T_p}}$ and gives under certain additional assumptions in an excellent accuracy the same results as the p-adic thermodynamics.

2. An intriguing observation is that one could interpret p-adic and real thermodynamics for mass squared also in terms of number theoretic thermodynamics for the number theoretic momentum $\log(p^n) = n \log(p)$. The expectation value for this differs from the expression for $\langle n \rangle$ only by the factor $\log(p)$.
3. In the proposed characterization of the partonic orbits in terms of infinite primes the primes appearing in infinite prime are identified as p-adic primes. For minimal option the p-adic prime characterizes \sqrt{p} - or p - multiple of the minimum length L_{min} of braid strand in the effective metric defined by modified Chern-Simons gamma matrix. One can consider also $(\sqrt{p})^n$ and p^n (p-adic fractality)- and even integer multiples of L_{min} if they are below L_{max} . If light-like 3-surface contains vacuum regions arbitrary large p :s are possible since for these one has $L_{min} \rightarrow \infty$. Number theoretic state function reduction implies that only single p can be realized -one might say "is active"- for a given quantum state. The powers p_i^n appearing in the infinite prime have interpretation as many particle states with total number theoretic momentum $n_i \log(p)_i$. For the finite part of infinite prime one has one fermion and $n_i - 1$ bosons and for the bosonic part n_i bosons. The arithmetic QFT associated with infinite primes - in particular the conservation of the number theoretic momentum $\sum n_i \log(p)_i$ - would naturally describe the correlations between the geometries of light-like 3-surfaces representing the incoming lines of the vertex of generalized Feynman diagram. As a matter fact, the momenta associated with different primes are separately conserved so that one has infinite number of conservation laws.

4. One must assign two infinite primes to given partonic two surface so that one has for a given prime p two integers n_+ and n_- . Also the hierarchy of Planck constants assigns to a given page of the Big Book two integers and one has $\hbar = n_a n_b \hbar_0$. If one has $n_a = n_+$ and $n_b = n_-$ then the reactions in which given initial number theoretic momenta $n_{\pm, i} \log(p_i)$ is shared between final states would have concrete interpretation in terms of the integers n_a, n_b characterizing the coverings of incoming and outgoing lines.

Note that one can also consider the possibility that the hierarchy of Planck constants emerges from the basic quantum TGD. Basically due to the vacuum degeneracy of Kähler action the canonical momentum densities correspond to several values of the time derivatives of the imbedding space coordinates so that for a given partonic 2-surface there are several space-time sheets with same conserved quantities defined by isometry currents and Kähler current. This forces the introduction of N -fold covering of $CD \times CP_2$ in order to describe the situation. The splitting of the partonic 2-surface into N pieces implies a charge fractionization during its travel to the upper end of CD . One can also develop an argument suggesting that the coverings factorize to coverings of CD and CP_2 so that the number of the sheets of the covering is $N = n_a n_b$ [37].

These observations make one wonder whether there could be a connection between p-adic thermodynamics, hierarchy of Planck constants, and infinite primes.

1. Suppose that one accepts the identification $n_a = n_+$ and $n_b = n_-$. Could one perform a further identification of these integers as non-negative conformal weights characterizing physical states so that conservation of the number theoretic momentum for a given p-adic prime would correspond to the conservation of conformal weight. In p-adic thermodynamics this conformal weight is sum of conformal weights of 5 tensor factors of Super-Virasoro algebra. The number must be indeed five and one could assign them to the factors of the symmetry group. One factor for color symmetries and two factors of electro-weak $SU(2)_L \times U(1)$ are certainly present. The remaining two factors could correspond to transversal degrees of freedom assignable to string like objects but one can imagine also other identifications [26].
2. If this interpretation is correct, a given conformal weight $n = n_a = n_+$ (say) would correspond to all possible distributions of five conformal weights n_i , $i = 1, \dots, 5$ between the n_a sheets of covering of CD satisfying $\sum_{i=1}^5 n_i = n_a = n_+$. Single sheet of covering would carry only unit conformal weight so that one would have the analog of fractionization also now and a possible interpretation would be in terms of the instability of states with conformal weight $n > 1$. Conformal thermodynamics would also mean thermodynamics in the space of states determined by infinite primes and in the space of coverings.
3. The conformal weight assignable to the CD would naturally correspond to mass squared but there is also the conformal weight assignable to CP_2 and one can wonder what its interpretation might be. Could it correspond to the expectation of pseudo mass squared characterizing the generalized eigenstates of the modified Dirac operator? Note that one should allow in the spectrum also the powers of hyper-complex primes up to some maximum power $p^{n_{max}/2} \leq L_{max}/L_{min}$ so that Dirac determinant would be non-vanishing and Kähler function finite. From the point of conformal invariance this is indeed natural.

13.6 Quantum Hall effect, charge fractionization, and hierarchy of Planck constants

In this section the most recent view about the relationship between dark matter hierarchy and quantum Hall effect is discussed. This discussion leads to a more realistic view about FQHE allowing to formulate precisely the conditions under which anyons emerge, describes the fractionization of electric and magnetic charges in terms of the delicacies of the Kähler gauge potential of generalized imbedding space, and relates the TGD based model to the original model of Laughlin. The discussion allows also to sharpen the vision about the formulation of quantum TGD itself.

13.6.1 Quantum Hall effect

Recall first the basic facts. Quantum Hall effect (QHE) [74, 70, 67] is an essentially 2-dimensional phenomenon and occurs at the end of current carrying region for the current flowing transversally along the end of the wire in external magnetic field along the wire. For quantum Hall effect transversal Hall conductance characterizing the 2-dimensional current flow is dimensionless and quantized and given by

$$\sigma_{xy} = 2\nu\alpha_{em} ,$$

ν is so called filling factor telling the number of filled Landau levels in the magnetic field. In the case of integer quantum Hall effect (IQHE) ν is integer valued. For fractional quantum Hall effect (FQHE) ν is rational number. Laughlin introduced his many-electron wave function predicting fractional quantum Hall effect for filling fractions $\nu = 1/m$ [74]. The further attempts to understand FQHE led to the notion of anyon by Wilzeck [70]. Anyon has been compared to a vortex like excitation of a dense 2-D electron plasma formed by the current carriers. ν is inversely proportional to the magnetic flux and the fractional filling factor can be also understood in terms of fractional magnetic flux.

The starting point of the quantum field theoretical models is the effective 2-dimensionality of the system implying that the projective representations for the permutation group of n objects are representations of braid group allowing fractional statistics. This is due to the non-trivial first homotopy group of 2-dimensional manifold containing punctures. Quantum field theoretical models allow to assign to the anyon like states also magnetic charge, fractional spin, and fractional electric charge.

Topological quantum computation [66, 60, 42, 44] is one of the most fascinating applications of FQHE. It relies on the notion of braids with strands representing the orbits of anyons. The unitary time evolution operator coding for topological computation is a representation of the element of the element of braid group represented by the time evolution of the braid. It is essential that the group involved is non-Abelian so that the system remembers the order of elementary braiding operations (exchange of neighboring strands). There is experimental evidence that $\nu = 5/2$ anyons possessing fractional charge $Q = e/4$ are non-Abelian [75, 76].

During last year I have been developing a model for DNA as topological quantum computer [44]. Therefore it is of considerable interest to find whether TGD could provide a first principle description of anyons and related phenomena. The introduction of a hierarchy of Planck constants realized in terms of generalized imbedding space with a book like structure is an excellent candidate in this respect [39]. As a rule the encounters between real world and quantum TGD have led to a more precise quantitative articulation of basic notions of quantum TGD and the same might happen also now.

13.6.2 A simple model for fractional quantum Hall effect

The generalization of the imbedding space suggests that it could possible to understand fractional quantum Hall effect [67] at the level of basic quantum TGD as integer QHE for non-standard value of Planck constant.

The formula for the quantized Hall conductance is given by

$$\begin{aligned} \sigma &= \nu \times \frac{e^2}{h} , \\ \nu &= \frac{n}{m} . \end{aligned} \tag{13.6.0}$$

Series of fractions in $\nu = 1/3, 2/5, 3/7, 4/9, 5/11, 6/13, 7/15, \dots, 2/3, 3/5, 4/7, 5/9, 6/11, 7/13, \dots, 5/3, 8/5, 11/7, 14/9, \dots, 4/3, 7/5, 10/7, 13/9, \dots, 1/5, 2/9, 3/13, \dots, 2/7, 3/11, \dots, 1/7, \dots$ with odd denominator have been observed as are also $\nu = 1/2$ and $\nu = 5/2$ states with even denominator [67].

The model of Laughlin [74] cannot explain all aspects of FQHE. The best existing model proposed originally by Jain is based on composite fermions resulting as bound states of electron and even number of magnetic flux quanta [73]. Electrons remain integer charged but due to the effective magnetic field electrons appear to have fractional charges. Composite fermion picture predicts all the observed fractions and also their relative intensities and the order in which they appear as the quality of sample improves.

Before proposing the TGD based model of FQHE as IQHE with non-standard value of Planck constant, it is good to represent a simple explanation of IQHE effect. Choose the coordinates of the current carrying slab so that x varies in the direction of Hall current and y in the direction of the main current. For IQHE the value of Hall conductivity is given by $\sigma = j_y/E_x = n_e ev/vB = n_e e/B = Ne^2/hBS = Ne^2/mh$, where m characterizes the value of magnetized flux and N is the total number of electrons in the current. In the Landau gauge $A_y = xB$ one can assume that energy eigenstates are momentum eigenstates in the direction of current and harmonic oscillator Gaussians in x -direction in which Hall current runs. This gives

$$\Psi \propto \exp(iky)H_n(x + kl^2)\exp(-\frac{(x+kl^2)^2}{2l^2}) , \quad l^2 = \frac{\hbar}{eB} . \tag{13.6.1}$$

Only the states for which the oscillator Gaussian differs considerably from zero inside slab are important so that the momentum eigenvalues are in good approximation in the range $0 \leq k \leq k_{max} = L_x/l^2$. Using $N = (L_y/2\pi) \int_0^{k_{max}} dk$ one obtains that the total number of momentum eigenstates associated with the given value of n is $N = eBdL_xL_y/h = n$. If ν Landau states are filled, the value of σ is $\sigma = \nu e^2/h$.

The interpretation of FQHE as IQHE with non standard value of Planck constant could explain also the fractionization of charge, spin, and electron number. There are $2 \times 2 = 4$ combinations of covering and factor spaces of CP_2 and three of them can lead to the increase or at least fractionization of the Planck constant required by FQHE.

1. The prediction for the filling fraction in FQHE would be

$$\nu = \nu_0 \frac{\hbar_0}{\hbar} , \quad \nu_0 = 1, 2, \dots . \tag{13.6.2}$$

ν_0 denotes the number of filled Landau levels.

2. Let us denote the options as C-C, C-F, F-C, F-F, where the first (second) letter tells whether a singular covering or factor space of CD (CP_2) is in question. The observed filling fractions are consistent with options C-C, C-F, and F-C for which CD or CP_2 or both correspond to a singular covering space. The values of ν in various cases are given by the following table.

Option	C – C	C – F	F – C
ν	$\frac{\nu_0}{n_a n_b}$	$\frac{\nu_0 n_b}{n_a}$	$\frac{\nu_0 n_a}{n_b}$

(13.6.2)

There is a complete symmetry under the exchange of CD and CP_2 as far as values of ν are considered.

3. All three options are consistent with observations. Charge fractionization allows only the options C – C and F – C. If one believes the general arguments stating that also spin is fractionized in FQHE then only the option C – C, for which charge and spin units are equal to $1/n_b$ and $1/n_a$ respectively, remains. For C – C option one must allow $\nu_0 > 1$.
4. Both $\nu = 1/2$ and $\nu = 5/2$ state has been observed [67, 72]. The fractionized charge is believed to be $e/4$ in the latter case [75, 76]. This requires $n_b = 4$ allowing only (C, C) and (F, C) options. $n_i \geq 3$ holds true if coverings and factor spaces are correlates for Jones inclusions and this gives additional constraint. The minimal values of (ν_0, n_a, n_b) are (2, 1, 4) for $\nu = 1/2$ and (10, 1, 4) for $\nu = 5/2$ for both C – C and F – C option. Filling fraction 1/2 corresponds in the composite fermion model and also experimentally to the limit of zero magnetic field [73]. $n_b = 2$ would be inconsistent with the observed fractionization of electric charge for $\nu = 5/2$ and with the vision inspired by Jones inclusions implying $n_i \geq 3$.

5. A possible problematic aspect of the TGD based model is the experimental absence of even values of m except $m = 2$ (Laughlin's model predicts only odd values of m). A possible explanation is that by some symmetry condition possibly related to fermionic statistics (as in Laughlin model) both n_a and n_b must be odd. This would require that $m = 2$ case differs in some manner from the remaining cases.
6. Large values of m in $\nu = n/m$ emerge as B increases. This can be understood from flux quantization. One has $e \int B dS = n\hbar$. By using actual fractional charge $e_F = e/n_b$ in the flux factor would give for (C, C) option $e_F \int B dS = nn_a \hbar_0$. The interpretation is that each of the n_b sheets contributes one unit to the flux for e . Note that the value of magnetic field at given sheet is not affected so that the build-up of multiple covering seems to keep magnetic field strength below critical value.
7. The understanding of the thermal stability is not trivial. The original FQHE was observed in 80 mK temperature corresponding roughly to a thermal energy of $T \sim 10^{-5}$ eV. For graphene the effect is observed at room temperature. Cyclotron energy for electron is (from $f_e = 6 \times 10^5$ Hz at $B = .2$ Gauss) of order thermal energy at room temperature in a magnetic field varying in the range 1-10 Tesla. This raises the question why the original FQHE requires such a low temperature. A possible explanation is that since FQHE involves several values of Planck constant, it is quantum critical phenomenon and is characterized by a critical temperature. The differences of single particle energies associated with the phase with ordinary Planck constant and phases with different Planck constant would characterize the transition temperature.

13.6.3 Description of QHE in terms of hierarchy of Planck constants

The proportionality $\sigma_{xy} \propto \alpha_{em} \propto 1/\hbar$ suggests an explanation of FQHE [70, 74, 67] in terms of the hierarchy of Planck constants. Perhaps filling factors and magnetic fluxes are actually integer valued but the value of Planck constant defining the unit of magnetic flux is changed from its standard value - to its rational multiple in the most general case. The killer test for the hypothesis is to find whether higher order perturbative QED corrections in powers of α_{em} are reduced from those predicted by QED in QHE phase. The proposed general principle governing the transition to large \hbar phase is states that Nature loves lazy theoreticians: if perturbation theory fails to converge, a phase transition increasing Planck constant occurs and guarantees the convergence. Geometrically the phase transition corresponds to the leakage of 3-surface from a given 8-D page to another one in the Big Book having singular coverings and factor spaces of $CD \times CP_2$ as pages. Only cove

The hierarchy of Planck constants strongly suggests the emergence of quantum groups and fractionalization of quantum numbers [19]. The challenge is to figure out the details and see whether this framework is consistent with what is known about FQHE. At least the following questions pop up immediately in the mind of physicist.

1. What the effective 2-dimensionality of the system exhibiting QHE corresponds in TGD framework?
2. What happens in the phase transition leading to the phase exhibiting QHE effect?
3. What are the counterparts anyons? How the fractional electric and magnetic charges emerge at classical and quantum level in the two descriptions?

The TGD inspired description of charge fractionization is based on the weak form of electric-magnetic duality and the reduction of the hierarchy of Planck constants to the basic quantum TGD. Also now one can raise a series of questions.

1. Electric magnetic duality provides a natural description of charge quantization and fractionization. The explanation for the hierarchy of Planck constants predicts that all charges- even Noether charges- are fractionized in the same manner and come as multiples of $1/n_a$ and $1/n_b$. Does this prediction make sense physically?
2. Does the singular gauge part $\Delta A = d\Phi$ of Kähler gauge potential whose exponent is n_a - (n_b -) valued function of appropriate angle coordinates of M^4 and CP_2 provide a description of charge

fractionization for a given sheet of the covering associated with a given value of Planck constant? Does this description reduce to the measurement interaction term which is indeed effective gauge part added to the Kähler gauge potential of either space-time surface or of wormhole throats or ends of space-time surface.

3. The Chern-Simons action associated with the induced Kähler gauge potential is Abelian: is this consistent with the non-Abelian character of the braiding matrix?

In the following I try to summarize the basic ideas giving hopes about a coherent description of quantum Hall effect and charge and spin fractionization in TGD framework.

Hierarchy of Planck constants and book like structure of imbedding space

TGD leads to a description for the hierarchy of Planck constants in terms of the generalization of $CD \times CP_2$ to book like structure. To be more precise, the generalization takes place for any region $CD \times CP_2 \subset H$, where CD corresponds to a causal diamond defined as an intersection of future and past directed light-cones of M^4 . CD s play key role in the formulation of quantum TGD in zero energy ontology in which the light-like boundaries of CD connected by light-like 3-surfaces can be said to be carriers of positive and negative energy parts of zero energy states. They are also crucial for TGD inspired theory of consciousness, in particular for understanding the relationship between experienced and geometric time [40].

1. *Should one postulate the hierarchy of Planck constants separately?*

In the most general case both CD and CP_2 are replaced with a book like structure consisting of singular coverings and factor spaces associated with them. A simple geometric argument identifying the square of Planck constant as scaling factor of the covariant metric tensor of M^4 (or actually CD) leads in the most general case to the identification of Planck constant as the ratio $\hbar/\hbar_0 = x_a x_b$, where $x = n$ holds true for a singular covering of X and $x = 1/n$ holds true for a singular factor space. x is the order of the maximal cyclic subgroup of the covering/divisor group $G \subset SO(3)$. The order of G can be thus larger than n . As a consequence, the spectrum of Planck constants is in principle rational-valued. \hbar_0 is unique since it corresponds to the unit of rational numbers.

2. *Does the hierarchy follow from the basic quantum TGD?*

The proposed option is too general if one believes on the argument reducing the hierarchy of Planck constants to the basic quantum TGD. Recall that the argument goes as follows.

1. By the extreme non-linearity of the Kähler action the correspondence between the time derivatives of the imbedding space coordinates and canonical momentum densities is many-to-one. This leads naturally to the introduction of covering spaces of $CD \times CP_2$, which are singular in the sense that the sheets of the covering co-incide at the ends of CD and at wormhole throats. One can say that quantum criticality means also the instability of the 3-surfaces defined by the throats and the ends against the decay to several space-time sheets and consequent charge fractionization. The interpretation is as an instability caused by too strong density of mass and making perturbative description possible since the matter density at various branches is reduced. The nearer the vacuum extremal the system is, the lower the mass density needed to induce the instability is and the larger is the number of sheets resulting in this manner is.
2. The singular regions of the covering are regions in which the integer characterizing the multiple-valuedness of the time derivatives of the imbedding space coordinates as functions of canonical momentum densities is reduced from the maximal value. The reduction to single sheeted covering could (but need not!) take place over any Lagrangian manifold of CP_2 rather than only over a homologically trivial geodesic sphere and would thus directly correspond to the vacuum degeneracy of Kähler action. One can also imagine the reduction of the integer characterizing multivaluedness to a smaller value different from one in non-vacuum regions.
3. In M^4 degrees of freedom branching to a single sheeted covering can occur over any partonic 2-surface which does not enclose the tip of CD . In this case the Kähler gauge potential would contain a singular gauge term having an archetypal form $\Delta A = d\phi/n_a$ at say upper hemisphere so that the magnetic flux would receive a non-vanishing contribution from North pole and give

rise to a fractionized Kähler magnetic and therefore also to Kähler electric charge. This term is pure gauge for all partonic 2-surface not containing the tip of CD . Thus one species of anyons would be associated with this kind of partonic 2-surfaces. Second species would correspond to singular gauge transforms about which example would be $\Delta A = d\Psi/n_b$, where Ψ is the angle coordinate associated with a homologically non-trivial geodesic sphere. The modification of the Kähler gauge potential could be interpreted in terms of a measurement interaction term added to the Dirac action and their sum at the ends would give rise to the non-fractional contribution to the measurement interaction term. This kind of term would be also associated with Noether charges such as 4-momentum. Depending on whether one considers the end of space-time sheet or at wormhole throat, the measurement interaction term would be given as $1/n_b$ or $1/n_a$ multiple of the measurement interaction term in absence of branching and would be more complex than the simple archetypal forms. The general form of the measurement interaction term is discussed in [55].

4. Classically the fractional Noether charges would emerge from Chern-Simons representation of Kähler function with the Lagrangian multiplier term realizing the weak form of electric-magnetic duality as a constraint. The latter term would be responsible for the non-vanishing values of four-momentum and angular momentum. The isometry charges in CP_2 degrees of freedom would receive a contribution also from the Chern-Simons term.
5. The situation can be described mathematically either by using effectively only single sheet but an integer multiple of Planck constant or many-sheeted covering and ordinary value of Planck constant. In [39] the argument that this indeed leads to hierarchy of Planck constants including charge fractionization is developed in detail. The restriction to singular coverings is consistent with the experimental constraints and means that only integer valued Planck constants are possible. A given value of Planck constant corresponds only to a finite number of the pages of the Big Book and that the evolution by quantum jumps is analogous to a diffusion at half-line and tends to increase the value of Planck constant.
6. The following argument would suggest a direct connection between vacuum degeneracy, coverings, and the hierarchy of infinite primes. For vacuum extremal the number of sheets is formally infinite but the sheets are in a well-define sense "passive". On the other hand, by the arguments of [55] the numbers n_a and n_b for sheets correspond to powers p^{n_a} and p^{n_b} for a prime appearing in infinite prime characterizing the partonic 3-surface and having interpretation as particle numbers. The unit infinite primes $X \pm 1$ correspond to the two basic infinite primes having interpretation as fermionic vacua are interpreted as Dirac sea: the numbers of bosons and fermions are vanishing for them. This suggests that the fermions of Dirac sea correspond to the "passive" sheets. This raises the question whether one could characterize the infinite degeneracy associated with vacuum extremals by these two infinite primes and non-vacuum extremals by infinite primes for which boson and fermion numbers are non-vanishing. The two infinite primes would correspond to CD and CP_2 degrees of freedom. They could also correspond to the space-time sheets of Euclidian and Minkowskian signature of the induced metric meeting at the wormhole throat at which the induced 4-metric is degenerate. Bose-Einstein condensate of n_i bosons ($i = a, b$) or fermion plus $n_i - 1$ bosons would correspond to n_i sheets of covering.

Arithmetic quantum field theory allows infinite number of conservation laws corresponding to the conservation of the number theoretic momentum $p = \sum_i n_i \log(p_i)$ which forces separate conservation of each number theoretic momentum $n_i \log(p_i)$ since the logarithms of primes are linearly independent in the realm of rationals. This conservation law could correlate the partonic lines arriving in the interaction vertices and state that the total number of sheets of the covering is conserved although it can be shared by several partonic space-time sheets in the final state.

The reduction of the hierarchy of Planck constants to basic quantum TGD is of course only an interesting idea and the best strategy to proceed is to develop objections against it.

1. The branching of partonic 2-surfaces at the ends of space-time sheets and wormhole throats is analogous to the branching of the line of Feynman graph. The 3-D lines of generalized Feynman graphs indeed branch at the vertices and this leads to the basic objection against the proposed interpretation of the fractionization. Could one consider the possibility that branching

corresponds to what happens in the vertices of Feynman diagrams? This cannot not seem to be the case. The point is that canonical momentum densities are identical so that also the conserved classical Noether and Kähler charges associated with various branches should be the same.

2. The value of gravitational Planck constant is enormous and one would mean enormously many-fold branching of partonic 2-surfaces of astrophysical size. Does this really make sense? Is this simply due the fact that the basic parameter GM_1M_2 characterizing the strength of gravitational interaction is much larger than unity so that perturbation theory in terms of it fails to converge and the splitting to \hbar_{gr}/\hbar_0 sheets guarantees that the perturbation theory at each sheet converges.
3. One can also ask whether the fractional charges can be observed directly since it seems that only the partonic 2-surfaces at the ends of the space-time sheet are observable.
4. Perhaps the most serious objection relates to the basic intuition about scaling of quantum lengths by \hbar since this scaling is fundamental for all predictions in the model of quantum biology. It is not obvious why the basic quantum lengths in M^4 degrees of freedom - in particular the size scale of CD - should be scaled up by $n_a n_b$. Could this scaling up result dynamically or can one find some simple kinematic argument forcing the size scale spectrum of CD s? Kinematic argument is more plausible and indeed exists. Suppose that one can speak about plane waves $\exp(inEt/\hbar_0)$, where t is proper time coordinate associated with the line connecting the tips of CD . Periodic boundary conditions at $t = T$ imply $E = n\hbar_0/2\pi T$ where T is the proper time distance between the tips of CD . Suppose that \hbar_0 is replaced with its $n_a n_b$ multiple in the plane wave. As a consequence, the plane waves for sheets and for same value of E do not anymore satisfy periodic boundary conditions at $t = T$ anymore. These conditions are however satisfied for $t = n_a n_b T$.

3. Connection with quantum measurement theory

The hierarchy of Planck constants relates closely to quantum measurement theory. The selection of quantization axis implied by the gauge terms ΔA proportional to appropriate angle coordinates has a direct correlate at the level of imbedding space geometry. This means breaking of isometries of H for a given CD with preferred choice time axis (rest frame) and quantization axis of spin. For CP_2 the choice of the quantization axes of color hyper charge and isospin imply symmetry breaking $SU(3) \rightarrow U(2) \rightarrow U(1) \times U(1)$. The "world of classical worlds" (WCW) is union over all Poincare and color translates of given $CD \times CP_2$ so that these symmetries are not lost at the level of WCW although the loss can happen at the level of quantum states.

4. How the different sectors of the generalized imbedding space are glued together?

Intuitively the scaling of Planck constant scales up quantum lengths, in particular the size of CD . This looks trivial but one one must describe precisely what is involved to check internal consistency and also to understand how to model the quantum phase transitions changing Planck constant. The first manner to understand the situation is to consider CD with a fixed range of M^4 coordinates. The scaling up of the covariant Kähler metric of CD by $r^2 = (\hbar/\hbar_0)^2$ scales up the size of CD by r . Another manner to see the situation is by scaling up the linear M^4 coordinates by r for the larger CD so that M^4 metric becomes same for both CD s. The smaller CD is glued to the larger one isometrically together along $(M^2 \cap CD) \subset CD$ anywhere in the interior of the larger CD . What happens is non-trivial for the following reasons.

1. The singular coverings (and possibly also factor spaces) are different and M^4 scaling is not a symmetry of the Kähler action so that the preferred extrema in the two cases do not relate by a simple scaling. The interpretation is in terms of the coding of the radiative corrections in powers of \hbar to the shape of the preferred extremals. This becomes clear from the representation of Kähler action in which M^4 coordinates have the same range for two CD s but M^4 metric differs by r^2 factor.
2. In common M^4 coordinates the M^4 gauge part A_a of CP_2 Kähler potential for the larger CD differs by a factor $1/r$ from that for the smaller CD . This guarantees the invariance of four-momentum assignable to Chern-Simons action in the phase transition changing \hbar . The resulting

discontinuity of A_a at M^2 is analogous to a static voltage difference between the two CD s and M^2 could be seen as an analog of Josephson junction. In absence of dissipation (expected in quantum criticality) the Kähler voltage could generate oscillatory fermion, em, and Z^0 Josephson currents between the two CD s. Fermion current would flow in opposite directions for fermions and antifermions and also for quarks and leptons since Kähler gauge potential couples to quarks and leptons with opposite signs. In presence of dissipation fermionic currents would be ohmic and could force quarks and leptons and matter and antimatter to different pages of the Big Book. Quarks inside hadrons could have nonstandard value of Planck constant.

Measurement interaction term as gauge transform of Kähler gauge potential and description of charge fractionization in terms of singular gauge transforms

The introduction of a gauge part to the Kähler gauge potential of the imbedding space looks somewhat tricky idea. Can one really assign non-trivial physics to a mere gauge transformation? This is certainly the case if the gauge transformation is singular and induces a fractional Kähler magnetic charge and by electric-magnetic duality also a fractional Kähler electric charge. The introduction of a measurement interaction term as a formal gauge transform of the Kähler gauge potential only in Dirac Kähler action or Kähler Chern-Simons Dirac action but not both provides a second manner to achieve a non-trivial physical effect. It is good to summarize the background in more detail before continuing.

The idea about description of quantum Hall effect in terms of a gauge part of Kähler gauge potential emerged from the idea that Chern-Simons action for Kähler gauge potential (equivalently the for induced classical color gauge field proportional to the Kähler form) could define TGD as an almost topological QFT. It turned out however that Kähler action and the corresponding modified Dirac action containing also Chern-Simons boundary term with the constraint term coming from electric-magnetic duality are the fundamental actions. The general ansatz for the classical field equations based on the proportionality of Kähler current to instanton current reduces TGD to almost topological QFT with action reducing to Chern-Simons term with a Lagrangian multiplier term guaranteeing the weak form of electric-magnetic duality. This term is of extreme importance since the extremals of mere Chern-Simons action would give rise to identically vanishing Kähler function and Kähler metric and WCW metric would not have any M^4 part even if one gives up the extremality condition.

The measurement interaction term which corresponds to a gauge part of the Kähler gauge potential and can be added either to the interior part of Kähler Dirac action (and Kähler action) or to the Chern-Simons Dirac action. The measurement interaction term therefore modifies the physics and is visible also in the classical dynamics by the proportionality of Kähler current to instanton current. Note that the modification of Chern-Simons term assigned to the ends of the space-time sheet and to wormhole throats affects the space-time sheet since the Kähler action changes.

For Noether charges the Lagrangian multiplier term guaranteeing the weak form of electric magnetic duality in Chern-Simons action gives rise to non-vanishing Noether charges also in M^4 degrees of freedom. The proposed view about the basic process behind the charge fractionization implies that all charges are fractionized in basically the same manner although it seems that M^4 charges are n_b multiples and CP_2 charges n_a multiples of $1/n_a n_b$. Also in this case the additional of a formal gauge term would realize the fractionization at the level of couplings and total anomalous coupling would correspond to a non-singular gauge transformation of A .

One can imagine several kinds of pseudo gauge transformations appearing in the measurement interaction term.

1. The first kind of gauge transformation corresponds to a gauge change for A_μ with no reference to the fact that it is a projection of CP_2 Kähler gauge potential. It is not clear whether measurement interaction could be induced also by this kind of gauge transform. In any case, the proposed form of measurement interaction can be interpreted in terms of a gauge transform at the level of imbedding space [55]
2. Second kind of gauge transformations are induced by the symplectic transformations of $\delta M_\pm^4 \times CP_2$ and in general affect the induced metric and thus the gravitational properties of the system in the case of non-vacuum extremals. Furthermore, there exist no symplectic transformation allowing to eliminate the "gauge part" of A in $M^2 \subset M^4$ or gauge part in $CD \setminus M^2$ or $CP_2 \setminus S^2$ if it corresponds to a scalar function which is discontinuous. $\Delta A_\phi = k\phi$, $k \neq n$, where ϕ is an angle variable in M^4 or CP_2 would represent a canonical example of this.

3. Third kind of gauge transform would characterize the pages of the Big Book and give rise to fractional Kähler magnetic charge and by definition would not be reducible to a gauge transform induced by a symplectic transformation. This raises the idea that the gauge parts of A in CD and CP_2 could characterize the pages of the Big Book and thus the charge fractionization. In particular in the case of coverings one might argue that ΔA must be pure gauge in the covering implying $k = m/n_a$ or $k = m/n_b$.

The simplest hypothesis is that the ordinary measurement interaction term for trivial covering is simply scaled down by $1/n_a n_b$ in the interior of the space-time sheet and by $1/n_b$ or $1/n_a$ at its ends and at throats where n_b or n_a sheets co-incide. With this interpretation ΔA would provide a description of physics at a particular sheet of covering and there would be no need to introduce anything new at the level of imbedding space geometry since the coverings of the imbedding space would provide only a formal tool to describe the situation caused by the extreme non-linearity of the Kähler action.

13.6.4 In what kind of situations do anyons emerge?

Charge fractionization is a fundamental piece of quantum TGD and should be extremely general phenomenon and the basic characteristic of dark matter known to contribute 95 per cent to the matter of Universe.

1. In TGD framework scaling $\hbar = m\hbar_0$ implies the scaling of the unit of angular momentum for m -fold covering of CD only if the many particle state is Z_m singlet. Z_m singletness for many particle states allows of course non-singletness for single particle states. For factor spaces of CD -if present- the scaling $\hbar \rightarrow \hbar/m$ is compensated by the scaling $l \rightarrow ml$ for $L_z = l\hbar$ guaranteeing invariance under rotations by multiples of $2\pi/m$. Again one can pose the invariance condition on many-particle states but not to individual particles so that genuine physical effect is in question.
2. There is analogy with Z_3 -singletness holding true for many quark states and one cannot completely exclude the possibility that quarks are actually fractionally charged leptons with $m = 3$ -covering of CP_2 reducing the value of Planck constant [34, 39] so that quarks would be anyonic dark matter with smaller Planck constant and the impossibility to observe quarks directly would reduce to the impossibility for them to exist at our space-time sheet. Confinement would in this picture relate to the fractionization requiring that the 2-surface associated with quark must surround the tip of CD . Whether this option really works remains an open question. In any case, TGD anyons are quite generally confined around the tip of CD .
3. The model of DNA as topological quantum computer [44] assumes that DNA nucleotides are connected by magnetic flux tubes to the lipids of the cell membrane. In this case, p-adically scaled down u and d quarks and their antiquarks are assumed to be associated with the ends of the flux tubes and provide a representation of DNA nucleotides. Quantum Hall states would be associated with partonic 2-surfaces assignable to the lipid layers of the cell and nuclear membranes and also endoplasmic reticulum filling the cell interior and making it macroscopic quantum system and explaining also its stability. The entire system formed in this manner would be single extremely complex anyonic surface and the coherent behavior of living system would result from the fusion of anyonic 2-surfaces associated with cells to larger anyonic surfaces giving rise to organs and organisms and maybe even larger macroscopically quantum coherent connected systems. An interesting possibility is that the ends of the flux tubes assumed to connect DNA nucleotides to lipids of various membranes carry instead of u, d and their antiquarks fractionally charged electrons and neutrinos and their anti-particles having $n_b = 3$ and large value of n_a .

In astrophysical scales gigantic values of Planck constants would be realized meaning coverings with huge number of sheets. This conforms with the fact that for vacuum extremals the coverings would be formally infinitely many sheeted.

1. Quite generally, one would expect that dark matter and its anyonic forms emerge in situations where the density of plasma like state of matter is very high so that N -fold cover of CD reduces the density of matter by $1/N$ factor at given sheet of covering and thus also the repulsive

Coulomb energy. Plasma state resulting in QHE is one example of this. The interiors of neutron stars and black hole like structures are extreme examples of this, and I have proposed that black holes are dark matter with a gigantic value of gravitational Planck constant implying that black hole entropy -which is proportional to $1/\hbar$ - is of the same order of magnitude and even smaller as the entropy assignable to the spin of elementary particle. If the covering results from the basic quantum TGD this entropy would characterize single sheet of the covering only. The fact that there are $n_a n_b$ sheets would mean that the total entropy has just the standard value! Could this mean that entropy is the critical contrple parameter which splits the 3-surface into parallel sheets?

2. The confinement of matter inside black hole could have interpretation in terms of macroscopic anyonic 2-surfaces containing the topologically condensed elementary particles. This conforms with the TGD inspired model for the final state of star [35] inspiring the conjecture that even ordinary stars could possess onion like structure with thin layers with radii given by p-adic length scale hypothesis.
3. The idea about hierarchy of Planck constants was inspired by the finding that planetary orbits can be regarded as Bohr orbits [78, 39]: the explanation was that visible matter has condensed around dark matter at spherical cells or tubular structures around planetary orbits. This led to the proposal that planetary system has formed through this kind of condensation process around spherical shells or flux tubes surrounding planetary orbits and containing dark matter.

The question why dark matter would concentrate around flux tubes surrounding planetary orbits was not answered. The answer could be that dark matter is anyonic matter at partonic 2-surfaces whose light-like orbits define the basic geometric objects of quantum TGD. These partonic 2-surfaces could contain a central spherical anyonic 2-surface connected by radial flux tubes to flux tubes surrounding the orbits of planets and other massive objects of solar system to form connected anyonic surfaces analogous to elementary particles.

4. If factor spaces appear in M^4 degrees of freedom, they give rise to $Z_n \subset G_a$ symmetries. In astrophysical systems the large value of \hbar necessarily requires a large value of n_a for CD coverings as the considerations of [27] - in particular the model for graviton dark graviton emission and detection - forces to conclude. The same conclusion follows also from the absence of evidence for exact orbifold type symmetries in M^4 degrees of freedom for dark matter in astrophysical scales.

Coverings alone are enough to produce rational number valued spectrum for \hbar consistent with the observed spectrum of ν , and one must keep in mind that the applications of theory do not allow to decide whether singular factor spaces are really needed and that the reduction of the hierarchy of Planck constants to basic quantum TGD for coverings disfavors the factor spaces. The possibility to interpret evolution in terms of the increase of Planck constant also favors coverings-only option.

13.6.5 What happens in FQHE?

This picture suggest following description for what would happen in QHE in TGD Universe accepting the C-C option implied by the basic quantum TGD.

1. Light-like 3-surfaces - locally random light-like orbits of partonic 2-surfaces- are identifiable as very tiny wormhole throats in the case of elementary particles. This is the case for electrons in particular. Partonic surfaces can be also large, even macroscopic, and the size scales up in the scaling of Planck constant. To avoid confusion, it must be emphasized that light-likeness is with respect to the induced metric and does not imply expansion with light velocity in Minkowski space since the contribution to the induced metric implying light-likeness typically comes from CP_2 degrees of freedom. Strong classical gravitational fields are present near the wormhole throats. Second important point is that regions of space-time surface with Euclidian signature of the induced metric are implied: CP_2 type extremals representing elementary particles and having light-like random curve as CP_2 projection represents basic example of this. Hence rather exotic gravitational physics is predicted to manifest itself in everyday length scales.

2. The simplest identification for what happens in the phase transition to quantum Hall phase is that the end of wire carrying the Hall current corresponds to a partonic 2-surface having a macroscopic size. The electrons in the current correspond to similar 2-surfaces but with size of elementary particle for the ordinary value of Planck constant. As the electrons meet the end of the wire, the tiny wormhole throats of electrons suffer topological condensation to the boundary. One can say that one very large elementary particle having very high electron number is formed.
3. Fractionization occurs for charges in CP_2 degrees of freedom with unit $1/n_a$. If the end of the wire forms part of a spherical surface surrounding the tip of the CD involved fractionization occurs also in CD degrees of freedom so that electrons can become carriers of anomalous electric and magnetic charges. If not then the total spin is n_a multiple of fundamental spin unit.

One of the basic question was whether it is possible to describe non-Abelian FQHE in TGD framework.

1. Chern- Simons action for Kähler gauge potential is Abelian. This raises the question whether the representations of the number theoretical braid group are also Abelian. Since there is evidence for non-Abelian anyons, one might argue that this means a failure of the proposed approach. There are however many reasons to expect that braid group representations are non-Abelian. The action is for induced Kähler form rather than primary Maxwell field, $U(1)$ gauge symmetry is transformed to a dynamical symmetry (symplectic transformations of CP_2 representing isometries of WCW and definitely non-Abelian), and the particles of the theory belong to the representations of electro-weak and color gauge groups naturally defining the representations of braid group.
2. The finite subgroups of $SU(2)$ defining covering and factor groups are in the general case non-commutative subgroups of $SU(2)$ since the hierarchies of coverings and factors spaces are assumed to correspond to the two hierarchy of Jones inclusions to which one can assign ADE Lie algebras by McKay correspondence. The ADE Lie algebras define effective gauge symmetries having interpretation in terms of finite measurement resolution described in terms of Jones inclusion so that extremely rich structures are expected. The question arises whether the covering option implied by the basic quantum TGD allows coverings defined by finite groups. There seems to be no obvious reason why this could not be the case.

An interesting challenge is to relate concrete models of FQHE to the proposed description. Here only some comments about Laughlin's wave function are made.

1. In the description provided by Laughlin wave function FQHE results from a minimization of Coulomb energy. In TGD framework the tunneling to the page of H with m sheets of covering has the same effect since the density of electrons is reduced by $1/m$ factor.
2. The formula $\nu \propto e^2 N_e / e \int B dS$ with scaling up of magnetic flux by $\hbar/h_0 = m$ implies effective fractional filling factor. The scaling up of magnetic flux results from the presence of m sheets carrying magnetic field with same strength. Since the N_e electrons are shared between m sheets, the filling factor is fractional when one restricts the consideration to single sheet as one indeed does.
3. Laughlin wave function makes sense for $\nu = 1/m$, m odd, and is m :th power of the many electron wave function for IQHE and expressible as the product $\prod_{i < j} (z_i - z_j)^m$, where z represents complex coordinate for the anyonic plane. The relative orbital angular momenta of electrons satisfy $L_z \geq m$ if the value of Planck constant is standard. If Laughlin wave function makes sense also in TGD framework, then m :th power implies that many-electron wave function is singlet with respect to Z_m acting in covering and the value of relative angular momentum indeed satisfies $L_z \geq m\hbar_0$ just as in Laughlin's theory.

Bibliography

Books about TGD

- [1] M. Pitkänen (2006), *Topological Geometroynamics: Overview*.
http://tgd.wippiespace.com/public_html/tgdview/tgdview.html.
- [2] M. Pitkänen (2006), *Quantum Physics as Infinite-Dimensional Geometry*.
http://tgd.wippiespace.com/public_html/tgdgeom/tgdgeom.html.
- [3] M. Pitkänen (2006), *Physics in Many-Sheeted Space-Time*.
http://tgd.wippiespace.com/public_html/tgdclass/tgdclass.html.
- [4] M. Pitkänen (2006), *p-Adic length Scale Hypothesis and Dark Matter Hierarchy*.
http://tgd.wippiespace.com/public_html/paddark/paddark.html.
- [5] M. Pitkänen (2006), *Quantum TGD*.
http://tgd.wippiespace.com/public_html/tgdquant/tgdquant.html.
- [6] M. Pitkänen (2006), *TGD as a Generalized Number Theory*.
http://tgd.wippiespace.com/public_html/tgdnumber/tgdnumber.html.
- [7] M. Pitkänen (2006), *TGD and Fringe Physics*.
http://tgd.wippiespace.com/public_html/freenergy/freenergy.html.

Books about TGD Inspired Theory of Consciousness and Quantum Biology

- [8] M. Pitkänen (2006), *TGD Inspired Theory of Consciousness*.
http://tgd.wippiespace.com/public_html/tgdconsc/tgdconsc.html.
- [9] M. Pitkänen (2006), *Bio-Systems as Self-Organizing Quantum Systems*.
http://tgd.wippiespace.com/public_html/bioselforg/bioselforg.html.
- [10] M. Pitkänen (2006), *Quantum Hardware of Living Matter*.
http://tgd.wippiespace.com/public_html/bioware/bioware.html.
- [11] M. Pitkänen (2006), *Bio-Systems as Conscious Holograms*.
http://tgd.wippiespace.com/public_html/hologram/hologram.html.
- [12] M. Pitkänen (2006), *Genes and Memes*.
http://tgd.wippiespace.com/public_html/genememe/genememe.html.
- [13] M. Pitkänen (2006), *Magnetospheric Consciousness*.
http://tgd.wippiespace.com/public_html/magnconsc/magnconsc.html.
- [14] M. Pitkänen (2006), *Mathematical Aspects of Consciousness Theory*.
http://tgd.wippiespace.com/public_html/mathconsc/mathconsc.html.
- [15] M. Pitkänen (2006), *TGD and EEG*.
http://tgd.wippiespace.com/public_html/tgdeeg/tgdeeg.html.

References to the chapters of the books about TGD

- [16] The chapter *TGD and Cosmology* of [3].
http://tgd.wippiespace.com/public_html/tgdclass/tgdclass.html#cosmo.
- [17] The chapter *TGD as a Generalized Number Theory: Infinite Primes* of [6].
http://tgd.wippiespace.com/public_html/tgdnumber/tgdnumber.html#visionc.
- [18] The chapter *p-Adic Particle Massivation: Elementary particle Masses* of [4].
http://tgd.wippiespace.com/public_html/paddark/paddark.html#mass2.
- [19] The chapter *Appendix A: Quantum Groups and Related Structures* of [5].
http://tgd.wippiespace.com/public_html/tgdquant/tgdquant.html#bialgebra.
- [20] The chapter *p-Adic Particle Massivation: New Physics* of [4].
http://tgd.wippiespace.com/public_html/paddark/paddark.html#mass4.
- [21] The chapter *TGD as a Generalized Number Theory: p-Adicization Program* of [6].
http://tgd.wippiespace.com/public_html/tgdnumber/tgdnumber.html#visiona.
- [22] The chapter *Construction of Configuration Space Kähler Geometry from Symmetry Principles* of [2].
http://tgd.wippiespace.com/public_html/tgdgeom/tgdgeom.html#compl1.
- [23] The chapter *Does the QFT Limit of TGD Have Space-Time Super-Symmetry?* of [5].
http://tgd.wippiespace.com/public_html/tgdquant/tgdquant.html#susy.
- [24] The chapter *Quantum Hall effect and Hierarchy of Planck Constants* [5].
http://tgd.wippiespace.com/public_html/tgdquant/tgdquant.html#anyontgd.
- [25] The chapter *Nuclear String Model* of [4].
http://tgd.wippiespace.com/public_html/paddark/paddark.html#nuclstring.
- [26] The chapter *Massless States and Particle Massivation* of [4].
http://tgd.wippiespace.com/public_html/paddark/paddark.html#mless.
- [27] The chapter *Quantum Astrophysics* of [3].
http://tgd.wippiespace.com/public_html/tgdclass/tgdclass.html#gastro.
- [28] M. Pitkänen (2006), *Physics in Many-Sheeted Space-Time*.
http://tgd.wippiespace.com/public_html/tgdclass/tgdclass.html.
- [29] The chapter *Does the Modified Dirac Equation Define the Fundamental Action Principle?* of [2].
http://tgd.wippiespace.com/public_html/tgdgeom/tgdgeom.html#Dirac.
- [30] The chapter *Twistors, N=4 Super-Conformal Symmetry, and Quantum TGD* of [5].
http://tgd.wippiespace.com/public_html/tgdquant/tgdquant.html#twistor.
- [31] The chapter *Category Theory and Quantum TGD* of [5].
http://tgd.wippiespace.com/public_html/tgdquant/tgdquant.html#categorynew.
- [32] The chapter *Riemann Hypothesis and Physics* of [6].
http://tgd.wippiespace.com/public_html/tgdnumber/tgdnumber.html#riema.
- [33] The chapter *Configuration Space Spinor Structure* of [2].
http://tgd.wippiespace.com/public_html/tgdgeom/tgdgeom.html#cspin.
- [34] The chapter *Was von Neumann Right After All* of [5].
http://tgd.wippiespace.com/public_html/tgdquant/tgdquant.html#vNeumann.
- [35] The chapter *The Relationship Between TGD and GRT* of [3].
http://tgd.wippiespace.com/public_html/tgdclass/tgdclass.html#tgdgrt.

- [36] The chapter *Basic Extremals of Kähler Action* of [3].
http://tgd.wippiespace.com/public_html/tgdclass/tgdclass.html#class.
- [37] The chapter *Identification of the Configuration Space Kähler Function* of [2].
http://tgd.wippiespace.com/public_html/tgdgeom/tgdgeom.html#kahler.
- [38] The chapter *TGD and Astrophysics* of [3].
http://tgd.wippiespace.com/public_html/tgdclass/tgdclass.html#astro.
- [39] The chapter *Does TGD Predict the Spectrum of Planck Constants?* of [5].
http://tgd.wippiespace.com/public_html/tgdquant/tgdquant.html#Planck.

References to the chapters of the books about TGD Inspired Theory of Consciousness and Quantum Biology

- [40] The chapter *About Nature of Time* of [8].
http://tgd.wippiespace.com/public_html/tgdconsc/tgdconsc.html#timenature.
- [41] The chapter *The Notion of Wave-Genome and DNA as Topological Quantum Computer* of [12].
http://tgd.wippiespace.com/public_html/genememe/genememe.html#gari.
- [42] The chapter *Topological Quantum Computation in TGD Universe* of [12].
http://tgd.wippiespace.com/public_html/genememe/genememe.html#tqc.
- [43] The chapter *Dark Matter Hierarchy and Hierarchy of EEGs* of [15].
http://tgd.wippiespace.com/public_html/tgdeeg/tgdeeg.html#eegdark.
- [44] The chapter *DNA as Topological Quantum Computer* of [12].
http://tgd.wippiespace.com/public_html/genememe/genememe.html#dnatqc.
- [45] The chapter *Negentropy Maximization Principle* of [8].
http://tgd.wippiespace.com/public_html/tgdconsc/tgdconsc.html#nmpc.

Appendices and references to some older books

- [46] M. Pitkänen (2006) *Basic Properties of CP_2 and Elementary Facts about p -Adic Numbers*
http://tgd.wippiespace.com/public_html/pdfpool/append.pdf.

Articles related to TGD

- [47] M. Pitkänen (2007), *Further Progress in Nuclear String Hypothesis*, http://tgd.wippiespace.com/public_html/articles/nucstring.pdf.
- [48] M. Pitkänen (2010), *Physics as Generalized Number Theory III: Infinite Primes*. Prespacetime Journal July Vol. 1 Issue 4 Page 153-181.
- [49] M. Pitkänen (2010), *The Geometry of CP_2 and its Relationship to Standard Model*. Prespacetime Journal July Vol. 1 Issue 4 Page 182-192.

Mathematics

- [50] M. de Wild Propitius and F. A. Bais (1996), *Discrete Gauge Theories*. hep-th/9511201.
- [51] S. Sawin (1995), *Links, Quantum Groups, and TQFT's*. q-alg/9506002.

- [52] C. N. Yang, M. L. Ge (1989), *Braid Group, Knot Theory, and Statistical Mechanics*. World Scientific.
- [53] E. Witten (1989), *Quantum field theory and the Jones polynomial*. *Comm. Math. Phys.* 121 , 351-399.
- [54] *The Riemann zeta function interpreted as partition function*. <http://www.secamlocal.ex.ac.uk/people/staff/mrwatkin//zeta/physics2.htm>.
- [55] P. A. M. Dirac (1939), *A New Notation for Quantum Mechanics*. *Proceedings of the Cambridge Philosophical Society*, 35: 416-418.
 J. E. Roberts (1966), *The Dirac Bra and Ket Formalism*. *Journal of Mathematical Physics*, 7: 1097-1104.
 Halvorson, Hans and Clifton, Rob (2001),
- [56] V. Jones (2003), *In and around the origin of quantum groups*. arXiv:math.OA/0309199.
 C. Kassel (1995), *Quantum Groups*. Springer Verlag.
 C. Gomez, M. Ruiz-Altaba, G. Sierra (1996), *Quantum Groups and Two-Dimensional Physics*. Cambridge University Press.

Theoretical physics

- [57] M. H. Freedman (1998), *P/NP, and the quantum field computer*, *Proc. Natl. Acad. Sci. USA* 95, no. 1, 98-101.
- [58] M. H. Freedman (2001), *Quantum Computation and the localization of Modular Functors*, *Found. Comput. Math.* 1, no 2, 183-204.
- [59] A. Kitaev (1997), *Quantum computations: algorithms and error correction*, *Russian Math. Survey*, 52:61, 1191-1249.
- [60] M. Freedman, A. Kitaev, M. Larson, Z. Wang (200?), www.arxiv.org/quant-ph/0101025.
- [61] M. Freedman, H. Larsen, and Z. Wang (2002), *A modular functor which is universal for quantum computation*, *Found. Comput. Math.* 1, no 2, 183-204. *Comm. Math. Phys.* 227, no 3, 605-622. [quant-ph/0001108](http://arxiv.org/quant-ph/0001108).
 M. H. Freedman (2001), *Quantum Computation and the localization of Modular Functors*, *Found. Comput. Math.* 1, no 2, 183-204.
 M. H. Freedman (1998), *P/NP, and the quantum field computer*, *Proc. Natl. Acad. Sci. USA* 95, no. 1, 98-101.
- [62] A. Lakhakia (1994), *Beltrami Fields in Chiral Media*, Series in Contemporary Chemical Physics - Vol. 2, World Scientific, Singapore.
 D. Reed (1995), in *Advanced Electromagnetism: Theories, Foundations, Applications*, edited by T. Barrett (Chap. 7), World Scientific, Singapore.
 O. I Bogoyavlenskij (2003), *Exact unsteady solutions to the Navier-Stokes equations and viscous MHD equations*. *Phys. Lett. A*, 281-286.
 J. Etnyre and R. Ghrist (2001), *An index for closed orbits in Beltrami field*. [ArXiv:math.DS/0101010](http://arxiv.org/math.DS/0101010).
 G. E. Marsh (1995), *Helicity and Electromagnetic Field Topology* in *Advanced Electromagnetism*, Eds. T. W. Barrett and D. M. Grimes, World Scientific.
- [63] *Chern-Simons theory*. http://en.wikipedia.org/wiki/ChernSimons_theory.
- [64] A. Kitaev (1997), *Annals of Physics*, vol 303, p.2. See also *Fault tolerant quantum computation by anyons*, [quant-ph/9707021](http://arxiv.org/quant-ph/9707021).
 A. Kitaev (1997), *Quantum computations: algorithms and error correction*, *Russian Math. Survey*, 52:61, 1191-1249.
- [65] *Montonen Olive Duality*. http://en.wikipedia.org/wiki/Montonen-Olive_duality.

Particle and nuclear physics

- [66] E. Samuel (2002), *Ghost in the Atom*, New Scientist, vol 176 issue 2366 - 26 October 2002, page 30.

Condensed matter physics

- [67] *Fractional quantum Hall Effect*. http://en.wikipedia.org/wiki/Fractional_quantum_Hall_effect.
Fractional Quantum Hall Effect. <http://www.warwick.ac.uk/~phsbn/fqhe.htm>.
- [68] G. Moore and N. Read (1991), *Non-Abelians in the fractional quantum Hall effect*. Nucl. Phys. B360, 362-396.
- [69] C. Nayak and F. Wilczek (1996), *2n-quasihole states realize 2^{n-1} -dimensional spinor braiding statistics in paired quantum Hall states*. Nucl. Phys. B479, 529-533.
- [70] F. Wilczek (1990), *Fractional Statistics and Anyon Super-Conductivity*. World Scientific.
- [71] S. M. Girvin (1999), *Quantum Hall Effect, Novel Excitations and Broken Symmetries*. cond-mat/9907002.
- [72] J. B. Miller *et al*(2007), *Fractional Quantum Hall effect in a quantum point contact at filling fraction 5/2*. arXiv:cond-mat/0703161v2.
- [73] J.K. Jain(1989), Phys. Rev. Lett. 63, 199.
- [74] R. B. Laughlin (1990), Phys. Rev. Lett. 50, 1395.
- [75] M. Dolev, M. Heiblum, V. Umansky, Ady Stern, and D. Mahalu Nature (2008), *Observation of a quarter of an electron charge at the $= 5/2$ quantum Hall state*. Nature, vol 452, p 829.
- [76] D. Monroe (2008), *Know Your Anyons*. New Scientist, vol 200, No 2676.
- [77] D. J. P. Morris *et et al* (2009). *Dirac Strings and Magnetic Monopoles in Spin Ice Dy₂Ti₂O₇*. Science, Vol. 326, No. 5951, pp. 411-414.
H. Johnston (1010) *Magnetic monopoles spotted in spin ices*. <http://physicsworld.com/cws/article/news/40302>.

Cosmology and astrophysics

- [78] D. Da Roacha and L. Nottale (2003), *Gravitational Structure Formation in Scale Relativity*. astro-ph/0310036.

Chapter 1

Appendix

A-1 Basic properties of CP_2 and elementary facts about p-adic numbers

A-1.1 CP_2 as a manifold

CP_2 , the complex projective space of two complex dimensions, is obtained by identifying the points of complex 3-space C^3 under the projective equivalence

$$(z^1, z^2, z^3) \equiv \lambda(z^1, z^2, z^3) . \quad (\text{A-1.1})$$

Here λ is any non-zero complex number. Note that CP_2 can be also regarded as the coset space $SU(3)/U(2)$. The pair z^i/z^j for fixed j and $z^i \neq 0$ defines a complex coordinate chart for CP_2 . As j runs from 1 to 3 one obtains an atlas of three ordinate charts covering CP_2 , the charts being holomorphically related to each other (e.g. CP_2 is a complex manifold). The points $z^3 \neq 0$ form a subset of CP_2 homeomorphic to R^4 and the points with $z^3 = 0$ a set homeomorphic to S^2 . Therefore CP_2 is obtained by "adding the 2-sphere at infinity to R^4 ".

Besides the standard complex coordinates $\xi^i = z^i/z^3$, $i = 1, 2$ the coordinates of Eguchi and Freund [45] will be used and their relation to the complex coordinates is given by

$$\begin{aligned} \xi^1 &= z + it , \\ \xi^2 &= x + iy . \end{aligned} \quad (\text{A-1.1})$$

These are related to the "spherical coordinates" via the equations

$$\begin{aligned} \xi^1 &= r \exp(i \frac{(\Psi + \Phi)}{2}) \cos(\frac{\Theta}{2}) , \\ \xi^2 &= r \exp(i \frac{(\Psi - \Phi)}{2}) \sin(\frac{\Theta}{2}) . \end{aligned} \quad (\text{A-1.1})$$

The ranges of the variables r, Θ, Φ, Ψ are $[0, \infty], [0, \pi], [0, 4\pi], [0, 2\pi]$ respectively.

Considered as a real four-manifold CP_2 is compact and simply connected, with Euler number Euler number 3, Pontryagin number 3 and second $b = 1$.

A-1.2 Metric and Kähler structure of CP_2

In order to obtain a natural metric for CP_2 , observe that CP_2 can be thought of as a set of the orbits of the isometries $z^i \rightarrow \exp(i\alpha)z^i$ on the sphere S^5 : $\sum z^i \bar{z}^i = R^2$. The metric of CP_2 is obtained by projecting the metric of S^5 orthogonally to the orbits of the isometries. Therefore the distance between the points of CP_2 is that between the representative orbits on S^5 .

The line element has the following form in the complex coordinates

$$ds^2 = g_{a\bar{b}} d\xi^a d\bar{\xi}^b , \quad (\text{A-1.2})$$

where the Hermitian, in fact Kähler metric $g_{a\bar{b}}$ is defined by

$$g_{a\bar{b}} = R^2 \partial_a \partial_{\bar{b}} K , \quad (\text{A-1.3})$$

where the function K , Kähler function, is defined as

$$\begin{aligned} K &= \log(F) , \\ F &= 1 + r^2 . \end{aligned} \quad (\text{A-1.3})$$

The Kähler function for S^2 has the same form. It gives the S^2 metric $dzd\bar{z}/(1+r^2)^2$ related to its standard form in spherical coordinates by the coordinate transformation $(r, \phi) = (\tan(\theta/2), \phi)$.

The representation of the CP_2 metric is deducible from S^5 metric is obtained by putting the angle coordinate of a geodesic sphere constant in it and is given

$$\frac{ds^2}{R^2} = \frac{(dr^2 + r^2 \sigma_3^2)}{F^2} + \frac{r^2(\sigma_1^2 + \sigma_2^2)}{F} , \quad (\text{A-1.4})$$

where the quantities σ_i are defined as

$$\begin{aligned} r^2 \sigma_1 &= \text{Im}(\xi^1 d\xi^2 - \xi^2 d\xi^1) , \\ r^2 \sigma_2 &= -\text{Re}(\xi^1 d\xi^2 - \xi^2 d\xi^1) , \\ r^2 \sigma_3 &= -\text{Im}(\xi^1 d\bar{\xi}^1 + \xi^2 d\bar{\xi}^2) . \end{aligned} \quad (\text{A-1.3})$$

R denotes the radius of the geodesic circle of CP_2 . The vierbein forms, which satisfy the defining relation

$$s_{kl} = R^2 \sum_A e_k^A e_l^A , \quad (\text{A-1.4})$$

are given by

$$\begin{aligned} e^0 &= \frac{dr}{F} , & e^1 &= \frac{r\sigma_1}{\sqrt{F}} , \\ e^2 &= \frac{r\sigma_2}{\sqrt{F}} , & e^3 &= \frac{r\sigma_3}{F} . \end{aligned} \quad (\text{A-1.5})$$

The explicit representations of vierbein vectors are given by

$$\begin{aligned} e^0 &= \frac{dr}{F} , & e^1 &= \frac{r(\sin\Theta \cos\Psi d\Phi + \sin\Psi d\Theta)}{2\sqrt{F}} , \\ e^2 &= \frac{r(\sin\Theta \sin\Psi d\Phi - \cos\Psi d\Theta)}{2\sqrt{F}} , & e^3 &= \frac{r(d\Psi + \cos\Theta d\Phi)}{2F} . \end{aligned} \quad (\text{A-1.5})$$

The explicit representation of the line element is given by the expression

$$ds^2/R^2 = \frac{dr^2}{F^2} + \frac{r^2}{4F^2} (d\Psi + \cos\Theta d\Phi)^2 + \frac{r^2}{4F} (d\Theta^2 + \sin^2\Theta d\Phi^2) . \quad (\text{A-1.5})$$

The vierbein connection satisfying the defining relation

$$de^A = -V_B^A \wedge e^B, \quad (\text{A-1.6})$$

is given by

$$\begin{aligned} V_{01} &= -\frac{e^1}{r}, & V_{23} &= \frac{e^1}{r^2}, \\ V_{02} &= -\frac{e^2}{r}, & V_{31} &= \frac{e^2}{r}, \\ V_{03} &= (r - \frac{1}{r})e^3, & V_{12} &= (2r + \frac{1}{r})e^3. \end{aligned} \quad (\text{A-1.7})$$

The representation of the covariantly constant curvature tensor is given by

$$\begin{aligned} R_{01} &= e^0 \wedge e^1 - e^2 \wedge e^3, & R_{23} &= e^0 \wedge e^1 - e^2 \wedge e^3, \\ R_{02} &= e^0 \wedge e^2 - e^3 \wedge e^1, & R_{31} &= -e^0 \wedge e^2 + e^3 \wedge e^1, \\ R_{03} &= 4e^0 \wedge e^3 + 2e^1 \wedge e^2, & R_{12} &= 2e^0 \wedge e^3 + 4e^1 \wedge e^2. \end{aligned} \quad (\text{A-1.8})$$

Metric defines a real, covariantly constant, and therefore closed 2-form J

$$J = -ig_{a\bar{b}}d\xi^a d\bar{\xi}^b, \quad (\text{A-1.9})$$

the so called Kähler form. Kähler form J defines in CP_2 a symplectic structure because it satisfies the condition

$$J^k_r J^{rl} = -s^{kl}. \quad (\text{A-1.10})$$

The form J is integer valued and by its covariant constancy satisfies free Maxwell equations. Hence it can be regarded as a curvature form of a $U(1)$ gauge potential B carrying a magnetic charge of unit $1/2g$ (g denotes the gauge coupling). Locally one has therefore

$$J = dB, \quad (\text{A-1.11})$$

where B is the so called Kähler potential, which is not defined globally since J describes homological magnetic monopole.

It should be noticed that the magnetic flux of J through a 2-surface in CP_2 is proportional to its homology equivalence class, which is integer valued. The explicit representations of J and B are given by

$$\begin{aligned} B &= 2re^3, \\ J &= 2(e^0 \wedge e^3 + e^1 \wedge e^2) = \frac{r}{F^2} dr \wedge (d\Psi + \cos\Theta d\Phi) + \frac{r^2}{2F} \sin\Theta d\Theta d\Phi. \end{aligned} \quad (\text{A-1.10})$$

The vierbein curvature form and Kähler form are covariantly constant and have in the complex coordinates only components of type (1,1).

Useful coordinates for CP_2 are the so called canonical coordinates in which Kähler potential and Kähler form have very simple expressions

$$\begin{aligned} B &= \sum_{k=1,2} P_k dQ_k, \\ J &= \sum_{k=1,2} dP_k \wedge dQ_k. \end{aligned} \quad (\text{A-1.10})$$

The relationship of the canonical coordinates to the "spherical" coordinates is given by the equations

$$\begin{aligned}
P_1 &= -\frac{1}{1+r^2} , \\
P_2 &= \frac{r^2 \cos \Theta}{2(1+r^2)} , \\
Q_1 &= \Psi , \\
Q_2 &= \Phi .
\end{aligned} \tag{A-1.8}$$

A-1.3 Spinors in CP_2

CP_2 doesn't allow spinor structure in the conventional sense [17]. However, the coupling of the spinors to a half odd multiple of the Kähler potential leads to a respectable spinor structure. Because the delicacies associated with the spinor structure of CP_2 play a fundamental role in TGD, the arguments of Hawking are repeated here.

To see how the space can fail to have an ordinary spinor structure consider the parallel transport of the vierbein in a simply connected space M . The parallel propagation around a closed curve with a base point x leads to a rotated vierbein at x : $e^A = R_B^A e^B$ and one can associate to each closed path an element of $SO(4)$.

Consider now a one-parameter family of closed curves $\gamma(v) : v \in (0, 1)$ with the same base point x and $\gamma(0)$ and $\gamma(1)$ trivial paths. Clearly these paths define a sphere S^2 in M and the element $R_B^A(v)$ defines a closed path in $SO(4)$. When the sphere S^2 is contractible to a point e.g., homologically trivial, the path in $SO(4)$ is also contractible to a point and therefore represents a trivial element of the homotopy group $\Pi_1(SO(4)) = Z_2$.

For a homologically nontrivial 2-surface S^2 the associated path in $SO(4)$ can be homotopically nontrivial and therefore corresponds to a nonclosed path in the covering group $\text{Spin}(4)$ (leading from the matrix 1 to -1 in the matrix representation). Assume this is the case.

Assume now that the space allows spinor structure. Then one can parallel propagate also spinors and by the above construction associate a closed path of $\text{Spin}(4)$ to the surface S^2 . Now, however this path corresponds to a lift of the corresponding $SO(4)$ path and cannot be closed. Thus one ends up with a contradiction.

From the preceding argument it is clear that one could compensate the non-allowed -1 -factor associated with the parallel transport of the spinor around the sphere S^2 by coupling it to a gauge potential in such a way that in the parallel transport the gauge potential introduces a compensating -1 -factor. For a $U(1)$ gauge potential this factor is given by the exponential $\exp(i2\Phi)$, where Φ is the magnetic flux through the surface. This factor has the value -1 provided the $U(1)$ potential carries half odd multiple of Dirac charge $1/2g$. In case of CP_2 the required gauge potential is half odd multiple of the Kähler potential B defined previously. In the case of $M^4 \times CP_2$ one can in addition couple the spinor components with different chiralities independently to an odd multiple of $B/2$.

A-1.4 Geodesic sub-manifolds of CP_2

Geodesic sub-manifolds are defined as sub-manifolds having common geodesic lines with the imbedding space. As a consequence the second fundamental form of the geodesic manifold vanishes, which means that the tangent vectors h_α^k (understood as vectors of H) are covariantly constant quantities with respect to the covariant derivative taking into account that the tangent vectors are vectors both with respect to H and X^4 .

In [16] a general characterization of the geodesic sub-manifolds for an arbitrary symmetric space G/H is given. Geodesic sub-manifolds are in 1-1-correspondence with the so called Lie triple systems of the Lie-algebra g of the group G . The Lie triple system t is defined as a subspace of g characterized by the closedness property with respect to double commutation

$$[X, [Y, Z]] \in t \text{ for } X, Y, Z \in t . \tag{A-1.9}$$

$SU(3)$ allows, besides geodesic lines, two nonequivalent (not isometry related) geodesic spheres. This is understood by observing that $SU(3)$ allows two nonequivalent $SU(2)$ algebras corresponding to

subgroups $SO(3)$ (orthogonal 3×3 matrices) and the usual isospin group $SU(2)$. By taking any subset of two generators from these algebras, one obtains a Lie triple system and by exponentiating this system, one obtains a 2-dimensional geodesic sub-manifold of CP_2 .

Standard representatives for the geodesic spheres of CP_2 are given by the equations

$$S_I^2 : \xi^1 = \bar{\xi}^2 \text{ or equivalently } (\Theta = \pi/2, \Psi = 0) ,$$

$$S_{II}^2 : \xi^1 = \xi^2 \text{ or equivalently } (\Theta = \pi/2, \Phi = 0) .$$

The non-equivalence of these sub-manifolds is clear from the fact that isometries act as holomorphic transformations in CP_2 . The vanishing of the second fundamental form is also easy to verify. The first geodesic manifold is homologically trivial: in fact, the induced Kähler form vanishes identically for S_I^2 . S_{II}^2 is homologically nontrivial and the flux of the Kähler form gives its homology equivalence class.

A-2 CP_2 geometry and standard model symmetries

A-2.1 Identification of the electro-weak couplings

The delicacies of the spinor structure of CP_2 make it a unique candidate for space S . First, the coupling of the spinors to the $U(1)$ gauge potential defined by the Kähler structure provides the missing $U(1)$ factor in the gauge group. Secondly, it is possible to couple different H -chiralities independently to a half odd multiple of the Kähler potential. Thus the hopes of obtaining a correct spectrum for the electromagnetic charge are considerable. In the following it will be demonstrated that the couplings of the induced spinor connection are indeed those of the GWS model [21] and in particular that the right handed neutrinos decouple completely from the electro-weak interactions.

To begin with, recall that the space H allows to define three different chiralities for spinors. Spinors with fixed H -chirality $e = \pm 1$, CP_2 -chirality l, r and M^4 -chirality L, R are defined by the condition

$$\begin{aligned} \Gamma\Psi &= e\Psi , \\ e &= \pm 1 , \end{aligned} \tag{A-2.0}$$

where Γ denotes the matrix $\Gamma_9 = \gamma_5 \times \gamma_5$, $1 \times \gamma_5$ and $\gamma_5 \times 1$ respectively. Clearly, for a fixed H -chirality CP_2 - and M^4 -chiralities are correlated.

The spinors with H -chirality $e = \pm 1$ can be identified as quark and lepton like spinors respectively. The separate conservation of baryon and lepton numbers can be understood as a consequence of generalized chiral invariance if this identification is accepted. For the spinors with a definite H -chirality one can identify the vielbein group of CP_2 as the electro-weak group: $SO(4) = SU(2)_L \times SU(2)_R$.

The covariant derivatives are defined by the spinorial connection

$$A = V + \frac{B}{2}(n_+ 1_+ + n_- 1_-) . \tag{A-2.1}$$

Here V and B denote the projections of the vielbein and Kähler gauge potentials respectively and $1_+(-)$ projects to the spinor H -chirality $+(-)$. The integers n_{\pm} are odd from the requirement of a respectable spinor structure.

The explicit representation of the vielbein connection V and of B are given by the equations

$$\begin{aligned} V_{01} &= -\frac{e^1}{r} , & V_{23} &= \frac{e^1}{r} , \\ V_{02} &= -\frac{e^2}{r} , & V_{31} &= \frac{e^2}{r} , \\ V_{03} &= (r - \frac{1}{r})e^3 , & V_{12} &= (2r + \frac{1}{r})e^3 , \end{aligned} \tag{A-2.2}$$

and

$$B = 2re^3 , \tag{A-2.3}$$

respectively. The explicit representation of the vielbein is not needed here.

Let us first show that the charged part of the spinor connection couples purely left handedly. Identifying Σ_3^0 and Σ_2^1 as the diagonal (neutral) Lie-algebra generators of $SO(4)$, one finds that the charged part of the spinor connection is given by

$$A_{ch} = 2V_{23}I_L^1 + 2V_{13}I_L^2, \quad (\text{A-2.4})$$

where one have defined

$$\begin{aligned} I_L^1 &= \frac{(\Sigma_{01} - \Sigma_{23})}{2}, \\ I_L^2 &= \frac{(\Sigma_{02} - \Sigma_{13})}{2}. \end{aligned} \quad (\text{A-2.4})$$

A_{ch} is clearly left handed so that one can perform the identification

$$W^\pm = \frac{2(e^1 \pm ie^2)}{r}, \quad (\text{A-2.5})$$

where W^\pm denotes the charged intermediate vector boson.

Consider next the identification of the neutral gauge bosons γ and Z^0 as appropriate linear combinations of the two functionally independent quantities

$$\begin{aligned} X &= re^3, \\ Y &= \frac{e^3}{r}, \end{aligned} \quad (\text{A-2.5})$$

appearing in the neutral part of the spinor connection. We show first that the mere requirement that photon couples vectorially implies the basic coupling structure of the GWS model leaving only the value of Weinberg angle undetermined.

To begin with let us define

$$\begin{aligned} \bar{\gamma} &= aX + bY, \\ \bar{Z}^0 &= cX + dY, \end{aligned} \quad (\text{A-2.5})$$

where the normalization condition

$$ad - bc = 1,$$

is satisfied. The physical fields γ and Z^0 are related to $\bar{\gamma}$ and \bar{Z}^0 by simple normalization factors.

Expressing the neutral part of the spinor connection in term of these fields one obtains

$$\begin{aligned} A_{nc} &= [(c+d)2\Sigma_{03} + (2d-c)2\Sigma_{12} + d(n_+1_+ + n_-1_-)]\bar{\gamma} \\ &+ [(a-b)2\Sigma_{03} + (a-2b)2\Sigma_{12} - b(n_+1_+ + n_-1_-)]\bar{Z}^0. \end{aligned} \quad (\text{A-2.4})$$

Identifying Σ_{12} and $\Sigma_{03} = 1 \times \gamma_5 \Sigma_{12}$ as vectorial and axial Lie-algebra generators, respectively, the requirement that γ couples vectorially leads to the condition

$$c = -d. \quad (\text{A-2.5})$$

Using this result plus previous equations, one obtains for the neutral part of the connection the expression

$$A_{nc} = \gamma Q_{em} + Z^0(I_L^3 - \sin^2\theta_W Q_{em}) . \quad (\text{A-2.6})$$

Here the electromagnetic charge Q_{em} and the weak isospin are defined by

$$\begin{aligned} Q_{em} &= \Sigma^{12} + \frac{(n_+1_+ + n_-1_-)}{6} , \\ I_L^3 &= \frac{(\Sigma^{12} - \Sigma^{03})}{2} . \end{aligned} \quad (\text{A-2.6})$$

The fields γ and Z^0 are defined via the relations

$$\begin{aligned} \gamma &= 6d\bar{\gamma} = \frac{6}{(a+b)}(aX + bY) , \\ Z^0 &= 4(a+b)\bar{Z}^0 = 4(X - Y) . \end{aligned} \quad (\text{A-2.6})$$

The value of the Weinberg angle is given by

$$\sin^2\theta_W = \frac{3b}{2(a+b)} , \quad (\text{A-2.7})$$

and is not fixed completely. Observe that right handed neutrinos decouple completely from the electro-weak interactions.

The determination of the value of Weinberg angle is a dynamical problem. The angle is completely fixed once the YM action is fixed by requiring that action contains no cross term of type γZ^0 . Pure symmetry non-broken electro-weak YM action leads to a definite value for the Weinberg angle. One can however add a symmetry breaking term proportional to Kähler action and this changes the value of the Weinberg angle.

To evaluate the value of the Weinberg angle one can express the neutral part F_{nc} of the induced gauge field as

$$F_{nc} = 2R_{03}\Sigma^{03} + 2R_{12}\Sigma^{12} + J(n_+1_+ + n_-1_-) , \quad (\text{A-2.8})$$

where one has

$$\begin{aligned} R_{03} &= 2(2e^0 \wedge e^3 + e^1 \wedge e^2) , \\ R_{12} &= 2(e^0 \wedge e^3 + 2e^1 \wedge e^2) , \\ J &= 2(e^0 \wedge e^3 + e^1 \wedge e^2) , \end{aligned} \quad (\text{A-2.7})$$

in terms of the fields γ and Z^0 (photon and Z - boson)

$$F_{nc} = \gamma Q_{em} + Z^0(I_L^3 - \sin^2\theta_W Q_{em}) . \quad (\text{A-2.8})$$

Evaluating the expressions above one obtains for γ and Z^0 the expressions

$$\begin{aligned} \gamma &= 3J - \sin^2\theta_W R_{03} , \\ Z^0 &= 2R_{03} . \end{aligned} \quad (\text{A-2.8})$$

For the Kähler field one obtains

$$J = \frac{1}{3}(\gamma + \sin^2\theta_W Z^0) . \quad (\text{A-2.9})$$

Expressing the neutral part of the symmetry broken YM action

$$\begin{aligned} L_{ew} &= L_{sym} + f J^{\alpha\beta} J_{\alpha\beta} , \\ L_{sym} &= \frac{1}{4g^2} Tr(F^{\alpha\beta} F_{\alpha\beta}) , \end{aligned} \quad (\text{A-2.9})$$

where the trace is taken in spinor representation, in terms of γ and Z^0 one obtains for the coefficient X of the γZ^0 cross term (this coefficient must vanish) the expression

$$\begin{aligned} X &= -\frac{K}{2g^2} + \frac{fp}{18} , \\ K &= Tr [Q_{em}(I_L^3 - \sin^2\theta_W Q_{em})] , \end{aligned} \quad (\text{A-2.9})$$

In the general case the value of the coefficient K is given by

$$K = \sum_i \left[-\frac{(18 + 2n_i^2)\sin^2\theta_W}{9} \right] , \quad (\text{A-2.10})$$

where the sum is over the spinor chiralities, which appear as elementary fermions and n_i is the integer describing the coupling of the spinor field to the Kähler potential. The cross term vanishes provided the value of the Weinberg angle is given by

$$\sin^2\theta_W = \frac{9 \sum_i 1}{(fg^2 + 2 \sum_i (18 + n_i^2))} . \quad (\text{A-2.11})$$

In the scenario where both leptons and quarks are elementary fermions the value of the Weinberg angle is given by

$$\sin^2\theta_W = \frac{9}{(\frac{fg^2}{2} + 28)} . \quad (\text{A-2.12})$$

The bare value of the Weinberg angle is $9/28$ in this scenario, which is quite close to the typical value $9/24$ of GUTs [19].

A-2.2 Discrete symmetries

The treatment of discrete symmetries C, P, and T is based on the following requirements:

- Symmetries must be realized as purely geometric transformations.
- Transformation properties of the field variables should be essentially the same as in the conventional quantum field theories [22].

The action of the reflection P on spinors is given by

$$\Psi \rightarrow P\Psi = \gamma^0 \otimes \gamma^0 \Psi . \quad (\text{A-2.13})$$

in the representation of the gamma matrices for which γ^0 is diagonal. It should be noticed that W and Z^0 bosons break parity symmetry as they should since their charge matrices do not commute with the matrix of P .

The guess that a complex conjugation in CP_2 is associated with T transformation of the physicist turns out to be correct. One can verify by a direct calculation that pure Dirac action is invariant under T realized according to

$$\begin{aligned} m^k &\rightarrow T(M^k) , \\ \xi^k &\rightarrow \bar{\xi}^k , \\ \Psi &\rightarrow \gamma^1 \gamma^3 \otimes 1 \Psi . \end{aligned} \quad (\text{A-2.12})$$

The operation bearing closest resemblance to the ordinary charge conjugation corresponds geometrically to complex conjugation in CP_2 :

$$\begin{aligned}\xi^k &\rightarrow \bar{\xi}^k, \\ \Psi &\rightarrow \Psi^\dagger \gamma^2 \gamma^0 \otimes 1.\end{aligned}\tag{A-2.12}$$

As one might have expected symmetries CP and T are exact symmetries of the pure Dirac action.

A-3 Basic facts about induced gauge fields

Since the classical gauge fields are closely related in TGD framework, it is not possible to have space-time sheets carrying only single kind of gauge field. For instance, em fields are accompanied by Z^0 fields for extremals of Kähler action. Weak forces is however absent unless the space-time sheets contains topologically condensed exotic weakly charged particles responding to this force. Same applies to classical color forces. The fact that these long range fields are present forces to assume that there exists a hierarchy of scaled up variants of standard model physics identifiable in terms of dark matter.

Classical em fields are always accompanied by Z^0 field and some components of color gauge field. For extremals having homologically non-trivial sphere as a CP_2 projection em and Z^0 fields are the only non-vanishing electroweak gauge fields. For homologically trivial sphere only W fields are non-vanishing. Color rotations does not affect the situation.

For vacuum extremals all electro-weak gauge fields are in general non-vanishing although the net gauge field has $U(1)$ holonomy by 2-dimensionality of the CP_2 projection. Color gauge field has $U(1)$ holonomy for all space-time surfaces and quantum classical correspondence suggest a weak form of color confinement meaning that physical states correspond to color neutral members of color multiplets.

A-3.1 Induced gauge fields for space-times for which CP_2 projection is a geodesic sphere

If one requires that space-time surface is an extremal of Kähler action and has a 2-dimensional CP_2 projection, only vacuum extremals and space-time surfaces for which CP_2 projection is a geodesic sphere, are allowed. Homologically non-trivial geodesic sphere correspond to vanishing W fields and homologically non-trivial sphere to non-vanishing W fields but vanishing γ and Z^0 . This can be verified by explicit examples.

$r = \infty$ surface gives rise to a homologically non-trivial geodesic sphere for which e_0 and e_3 vanish imply the vanishing of W field. For space-time sheets for which CP_2 projection is $r = \infty$ homologically non-trivial geodesic sphere of CP_2 one has

$$\gamma = \left(\frac{3}{4} - \frac{\sin^2(\theta_W)}{2}\right) Z^0 \simeq \frac{5Z^0}{8}.$$

The induced W fields vanish in this case and they vanish also for all geodesic sphere obtained by $SU(3)$ rotation.

$Im(\xi^1) = Im(\xi^2) = 0$ corresponds to homologically trivial geodesic sphere. A more general representative is obtained by using for the phase angles of standard complex CP_2 coordinates constant values. In this case e^1 and e^3 vanish so that the induced em, Z^0 , and Kähler fields vanish but induced W fields are non-vanishing. This holds also for surfaces obtained by color rotation. Hence one can say that for non-vacuum extremals with 2-D CP_2 projection color rotations and weak symmetries commute.

A-3.2 Space-time surfaces with vanishing em, Z^0 , or Kähler fields

In the following the induced gauge fields are studied for general space-time surface without assuming the extremal property. In fact, extremal property reduces the study to the study of vacuum extremals and surfaces having geodesic sphere as a CP_2 projection and in this sense the following arguments are somewhat obsolete in their generality.

Space-times with vanishing em, Z^0 , or Kähler fields

The following considerations apply to a more general situation in which the homologically trivial geodesic sphere and extremal property are not assumed. It must be emphasized that this case is possible in TGD framework only for a vanishing Kähler field.

Using spherical coordinates (r, Θ, Ψ, Φ) for CP_2 , the expression of Kähler form reads as

$$\begin{aligned} J &= \frac{r}{F^2} dr \wedge (d\Psi + \cos(\Theta)d\Phi) + \frac{r^2}{2F} \sin(\Theta)d\Theta \wedge d\Phi , \\ F &= 1 + r^2 . \end{aligned} \quad (\text{A-3.0})$$

The general expression of electromagnetic field reads as

$$\begin{aligned} F_{em} &= (3 + 2p) \frac{r}{F^2} dr \wedge (d\Psi + \cos(\Theta)d\Phi) + (3 + p) \frac{r^2}{2F} \sin(\Theta)d\Theta \wedge d\Phi , \\ p &= \sin^2(\Theta_W) , \end{aligned} \quad (\text{A-3.0})$$

where Θ_W denotes Weinberg angle.

a) The vanishing of the electromagnetic fields is guaranteed, when the conditions

$$\begin{aligned} \Psi &= k\Phi , \\ (3 + 2p) \frac{1}{r^2 F} (d(r^2)/d\Theta)(k + \cos(\Theta)) + (3 + p) \sin(\Theta) &= 0 , \end{aligned} \quad (\text{A-3.0})$$

hold true. The conditions imply that CP_2 projection of the electromagnetically neutral space-time is 2-dimensional. Solving the differential equation one obtains

$$\begin{aligned} r &= \sqrt{\frac{X}{1-X}} , \\ X &= D \left[\left| \frac{k+u}{C} \right| \right]^\epsilon , \\ u &\equiv \cos(\Theta) , \quad C = k + \cos(\Theta_0) , \quad D = \frac{r_0^2}{1+r_0^2} , \quad \epsilon = \frac{3+p}{3+2p} , \end{aligned} \quad (\text{A-3.1})$$

where C and D are integration constants. $0 \leq X \leq 1$ is required by the reality of r . $r = 0$ would correspond to $X = 0$ giving $u = -k$ achieved only for $|k| \leq 1$ and $r = \infty$ to $X = 1$ giving $|u+k| = [(1+r_0^2)/r_0^2]^{(3+2p)/(3+p)}$ achieved only for

$$\text{sign}(u+k) \times \left[\frac{1+r_0^2}{r_0^2} \right]^{\frac{3+2p}{3+p}} \leq k+1 ,$$

where $\text{sign}(x)$ denotes the sign of x .

The expressions for Kähler form and Z^0 field are given by

$$\begin{aligned} J &= -\frac{p}{3+2p} X du \wedge d\Phi , \\ Z^0 &= -\frac{6}{p} J . \end{aligned} \quad (\text{A-3.1})$$

The components of the electromagnetic field generated by varying vacuum parameters are proportional to the components of the Kähler field: in particular, the magnetic field is parallel to the Kähler magnetic field. The generation of a long range Z^0 vacuum field is a purely TGD based feature not encountered in the standard gauge theories.

b) The vanishing of Z^0 fields is achieved by the replacement of the parameter ϵ with $\epsilon = 1/2$ as becomes clear by considering the condition stating that Z^0 field vanishes identically. Also the relationship $F_{em} = 3J = -\frac{3}{4} \frac{r^2}{F} du \wedge d\Phi$ is useful.

c) The vanishing Kähler field corresponds to $\epsilon = 1, p = 0$ in the formula for em neutral space-times. In this case classical em and Z^0 fields are proportional to each other:

$$\begin{aligned} Z^0 &= 2e^0 \wedge e^3 = \frac{r}{F^2}(k+u) \frac{\partial r}{\partial u} du \wedge d\Phi = (k+u) du \wedge d\Phi \ , \\ r &= \sqrt{\frac{X}{1-X}} \ , \ X = D|k+u| \ , \\ \gamma &= -\frac{p}{2} Z^0 \ . \end{aligned} \tag{A-3-2}$$

For a vanishing value of Weinberg angle ($p = 0$) em field vanishes and only Z^0 field remains as a long range gauge field. Vacuum extremals for which long range Z^0 field vanishes but em field is non-vanishing are not possible.

The effective form of CP_2 metric for surfaces with 2-dimensional CP_2 projection

The effective form of the CP_2 metric for a space-time having vanishing em, Z^0 , or Kähler field is of practical value in the case of vacuum extremals and is given by

$$\begin{aligned} ds_{eff}^2 &= (s_{rr}(\frac{dr}{d\Theta})^2 + s_{\Theta\Theta})d\Theta^2 + (s_{\Phi\Phi} + 2ks_{\Phi\Psi})d\Phi^2 = \frac{R^2}{4}[s_{\Theta\Theta}^{eff}d\Theta^2 + s_{\Phi\Phi}^{eff}d\Phi^2] \ , \\ s_{\Theta\Theta}^{eff} &= X \times \left[\frac{\epsilon^2(1-u^2)}{(k+u)^2} \times \frac{1}{1-X} + 1 - X \right] \ , \\ s_{\Phi\Phi}^{eff} &= X \times [(1-X)(k+u)^2 + 1 - u^2] \ , \end{aligned} \tag{A-3-3}$$

and is useful in the construction of vacuum imbedding of, say Schwartzchild metric.

Topological quantum numbers

Space-times for which either em, Z^0 , or Kähler field vanishes decompose into regions characterized by six vacuum parameters: two of these quantum numbers (ω_1 and ω_2) are frequency type parameters, two (k_1 and k_2) are wave vector like quantum numbers, two of the quantum numbers (n_1 and n_2) are integers. The parameters ω_i and n_i will be referred as electric and magnetic quantum numbers. The existence of these quantum numbers is not a feature of these solutions alone but represents a much more general phenomenon differentiating in a clear cut manner between TGD and Maxwell's electrodynamics.

The simplest manner to avoid surface Kähler charges and discontinuities or infinities in the derivatives of CP_2 coordinates on the common boundary of two neighboring regions with different vacuum quantum numbers is topological field quantization, 3-space decomposes into disjoint topological field quanta, 3-surfaces having outer boundaries with possibly macroscopic size.

Under rather general conditions the coordinates Ψ and Φ can be written in the form

$$\begin{aligned} \Psi &= \omega_2 m^0 + k_2 m^3 + n_2 \phi + \text{Fourier expansion} \ , \\ \Phi &= \omega_1 m^0 + k_1 m^3 + n_1 \phi + \text{Fourier expansion} \ . \end{aligned} \tag{A-3-3}$$

m^0, m^3 and ϕ denote the coordinate variables of the cylindrical M^4 coordinates) so that one has $k = \omega_2/\omega_1 = n_2/n_1 = k_2/k_1$. The regions of the space-time surface with given values of the vacuum parameters ω_i, k_i and n_i and m and C are bounded by the surfaces at which space-time surface becomes ill-defined, say by $r > 0$ or $r < \infty$ surfaces.

The space-time surface decomposes into regions characterized by different values of the vacuum parameters r_0 and Θ_0 . At $r = \infty$ surfaces n_2, ω_2 and m can change since all values of Ψ correspond to the same point of CP_2 : at $r = 0$ surfaces also n_1 and ω_1 can change since all values of Φ correspond to same point of CP_2 , too. If $r = 0$ or $r = \infty$ is not in the allowed range space-time surface develops a boundary.

This implies what might be called topological quantization since in general it is not possible to find a smooth global imbedding for, say a constant magnetic field. Although global imbedding exists

it decomposes into regions with different values of the vacuum parameters and the coordinate u in general possesses discontinuous derivative at $r = 0$ and $r = \infty$ surfaces. A possible manner to avoid edges of space-time is to allow field quantization so that 3-space (and field) decomposes into disjoint quanta, which can be regarded as structurally stable units a 3-space (and of the gauge field). This doesn't exclude partial join along boundaries for neighboring field quanta provided some additional conditions guaranteeing the absence of edges are satisfied.

For instance, the vanishing of the electromagnetic fields implies that the condition

$$\Omega \equiv \frac{\omega_2}{n_2} - \frac{\omega_1}{n_1} = 0 \quad , \quad (\text{A-3.-2})$$

is satisfied. In particular, the ratio ω_2/ω_1 is rational number for the electromagnetically neutral regions of space-time surface. The change of the parameter n_1 and n_2 (ω_1 and ω_2) in general generates magnetic field and therefore these integers will be referred to as magnetic (electric) quantum numbers.

A-4 p-Adic numbers and TGD

A-4.1 p-Adic number fields

p-Adic numbers (p is prime: 2,3,5,...) can be regarded as a completion of the rational numbers using a norm, which is different from the ordinary norm of real numbers [18]. p-Adic numbers are representable as power expansion of the prime number p of form:

$$x = \sum_{k \geq k_0} x(k)p^k, \quad x(k) = 0, \dots, p-1 \quad . \quad (\text{A-4.1})$$

The norm of a p-adic number is given by

$$|x| = p^{-k_0(x)} \quad . \quad (\text{A-4.2})$$

Here $k_0(x)$ is the lowest power in the expansion of the p-adic number. The norm differs drastically from the norm of the ordinary real numbers since it depends on the lowest pinary digit of the p-adic number only. Arbitrarily high powers in the expansion are possible since the norm of the p-adic number is finite also for numbers, which are infinite with respect to the ordinary norm. A convenient representation for p-adic numbers is in the form

$$x = p^{k_0} \varepsilon(x) \quad , \quad (\text{A-4.3})$$

where $\varepsilon(x) = k + \dots$ with $0 < k < p$, is p-adic number with unit norm and analogous to the phase factor $\exp(i\phi)$ of a complex number.

The distance function $d(x, y) = |x - y|_p$ defined by the p-adic norm possesses a very general property called ultra-metricity:

$$d(x, z) \leq \max\{d(x, y), d(y, z)\} \quad . \quad (\text{A-4.4})$$

The properties of the distance function make it possible to decompose R_p into a union of disjoint sets using the criterion that x and y belong to same class if the distance between x and y satisfies the condition

$$d(x, y) \leq D \quad . \quad (\text{A-4.5})$$

This division of the metric space into classes has following properties:

a) Distances between the members of two different classes X and Y do not depend on the choice of points x and y inside classes. One can therefore speak about distance function between classes.

b) Distances of points x and y inside single class are smaller than distances between different classes.

c) Classes form a hierarchical tree.

Notice that the concept of the ultra-metricity emerged in physics from the models for spin glasses and is believed to have also applications in biology [20]. The emergence of p-adic topology as the topology of the effective space-time would make ultra-metricity property basic feature of physics.

A-4.2 Canonical correspondence between p-adic and real numbers

The basic challenge encountered by p-adic physicist is how to map the predictions of the p-adic physics to real numbers. p-Adic probabilities provide a basic example in this respect. Identification via common rationals and canonical identification and its variants have turned out to play a key role in this respect.

Basic form of canonical identification

There exists a natural continuous map $I : R_p \rightarrow R_+$ from p-adic numbers to non-negative real numbers given by the "pinary" expansion of the real number for $x \in R$ and $y \in R_p$ this correspondence reads

$$\begin{aligned}
 y &= \sum_{k>N} y_k p^k \rightarrow x = \sum_{k<N} y_k p^{-k} , \\
 y_k &\in \{0, 1, \dots, p-1\} .
 \end{aligned}
 \tag{A-4.5}$$

This map is continuous as one easily finds out. There is however a little difficulty associated with the definition of the inverse map since the pinary expansion like also decimal expansion is not unique ($1 = 0.999\dots$) for the real numbers x , which allow pinary expansion with finite number of pinary digits

$$\begin{aligned}
 x &= \sum_{k=N_0}^N x_k p^{-k} , \\
 x &= \sum_{k=N_0}^{N-1} x_k p^{-k} + (x_N - 1)p^{-N} + (p-1)p^{-N-1} \sum_{k=0,\dots} p^{-k} .
 \end{aligned}
 \tag{A-4.4}$$

The p-adic images associated with these expansions are different

$$\begin{aligned}
 y_1 &= \sum_{k=N_0}^N x_k p^k , \\
 y_2 &= \sum_{k=N_0}^{N-1} x_k p^k + (x_N - 1)p^N + (p-1)p^{N+1} \sum_{k=0,\dots} p^k \\
 &= y_1 + (x_N - 1)p^N - p^{N+1} ,
 \end{aligned}
 \tag{A-4.3}$$

so that the inverse map is either two-valued for p-adic numbers having expansion with finite pinary digits or single valued and discontinuous and non-surjective if one makes pinary expansion unique by choosing the one with finite pinary digits. The finite pinary digit expansion is a natural choice since in the numerical work one always must use a pinary cutoff on the real axis.

The topology induced by canonical identification

The topology induced by the canonical identification in the set of positive real numbers differs from the ordinary topology. The difference is easily understood by interpreting the p-adic norm as a norm in the set of the real numbers. The norm is constant in each interval $[p^k, p^{k+1})$ (see Fig. A-4.2) and is equal to the usual real norm at the points $x = p^k$: the usual linear norm is replaced with a piecewise constant norm. This means that p-adic topology is coarser than the usual real topology and the higher the value of p is, the coarser the resulting topology is above a given length scale. This hierarchical ordering of the p-adic topologies will be a central feature as far as the proposed applications of the p-adic numbers are considered.

Ordinary continuity implies p-adic continuity since the norm induced from the p-adic topology is rougher than the ordinary norm. p-Adic continuity implies ordinary continuity from right as is clear already from the properties of the p-adic norm (the graph of the norm is indeed continuous from right). This feature is one clear signature of the p-adic topology.

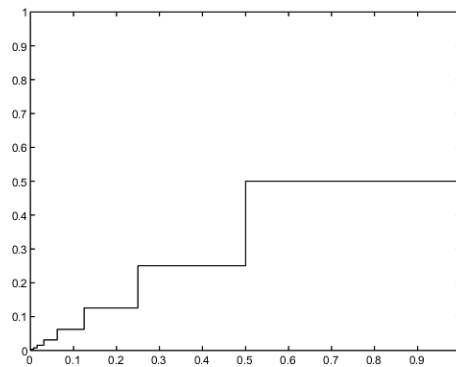


Figure 1: The real norm induced by canonical identification from 2-adic norm.

The linear structure of the p-adic numbers induces a corresponding structure in the set of the non-negative real numbers and p-adic linearity in general differs from the ordinary concept of linearity. For example, p-adic sum is equal to real sum only provided the summands have no common binary digits. Furthermore, the condition $x +_p y < \max\{x, y\}$ holds in general for the p-adic sum of the real numbers. p-Adic multiplication is equivalent with the ordinary multiplication only provided that either of the members of the product is power of p . Moreover one has $x \times_p y < x \times y$ in general. The p-Adic negative -1_p associated with p-adic unit 1 is given by $(-1)_p = \sum_k (p-1)p^k$ and defines p-adic negative for each real number x . An interesting possibility is that p-adic linearity might replace the ordinary linearity in some strongly nonlinear systems so these systems would look simple in the p-adic topology.

These results suggest that canonical identification is involved with some deeper mathematical structure. The following inequalities hold true:

$$\begin{aligned} (x + y)_R &\leq x_R + y_R , \\ |x|_p |y|_R &\leq (xy)_R \leq x_R y_R , \end{aligned} \tag{A-4.3}$$

where $|x|_p$ denotes p-adic norm. These inequalities can be generalized to the case of $(R_p)^n$ (a linear vector space over the p-adic numbers).

$$\begin{aligned} (x + y)_R &\leq x_R + y_R , \\ |\lambda|_p |y|_R &\leq (\lambda y)_R \leq \lambda_R y_R , \end{aligned} \tag{A-4.3}$$

where the norm of the vector $x \in T_p^n$ is defined in some manner. The case of Euclidian space suggests the definition

$$(x_R)^2 = \left(\sum_n x_n^2 \right)_R . \quad (\text{A-4.4})$$

These inequalities resemble those satisfied by the vector norm. The only difference is the failure of linearity in the sense that the norm of a scaled vector is not obtained by scaling the norm of the original vector. Ordinary situation prevails only if the scaling corresponds to a power of p .

These observations suggests that the concept of a normed space or Banach space might have a generalization and physically the generalization might apply to the description of some non-linear systems. The nonlinearity would be concentrated in the nonlinear behavior of the norm under scaling.

Modified form of the canonical identification

The original form of the canonical identification is continuous but does not respect symmetries even approximately. This led to a search of variants which would do better in this respect. The modification of the canonical identification applying to rationals only and given by

$$I_Q(q = p^k \times \frac{r}{s}) = p^k \times \frac{I(r)}{I(s)} \quad (\text{A-4.5})$$

is uniquely defined for rationals, maps rationals to rationals, has also a symmetry under exchange of target and domain. This map reduces to a direct identification of rationals for $0 \leq r < p$ and $0 \leq s < p$. It has turned out that it is this map which most naturally appears in the applications. The map is obviously continuous locally since p-adically small modifications of r and s mean small modifications of the real counterparts.

Canonical identification is in a key role in the successful predictions of the elementary particle masses. The predictions for the light elementary particle masses are within extreme accuracy same for I and I_Q but I_Q is theoretically preferred since the real probabilities obtained from p-adic ones by I_Q sum up to one in p-adic thermodynamics.

Generalization of number concept and notion of imbedding space

TGD forces an extension of number concept: roughly a fusion of reals and various p-adic number fields along common rationals is in question. This induces a similar fusion of real and p-adic imbedding spaces. Since finite p-adic numbers correspond always to non-negative reals n -dimensional space R^n must be covered by 2^n copies of the p-adic variant R_p^n of R^n each of which projects to a copy of R_+^n (four quadrants in the case of plane). The common points of p-adic and real imbedding spaces are rational points and most p-adic points are at real infinity.

For a given p-adic space-time sheet most points are literally infinite as real points and the projection to the real imbedding space consists of a discrete set of rational points: the interpretation in terms of the unavoidable discreteness of the physical representations of cognition is natural. Purely local p-adic physics implies real p-adic fractality and thus long range correlations for the real space-time surfaces having enough common points with this projection.

p-Adic fractality means that M^4 projections for the rational points of space-time surface X^4 are related by a direct identification whereas CP_2 coordinates of X^4 at these points are related by I , I_Q or some of its variants implying long range correlates for CP_2 coordinates. Since only a discrete set of points are related in this manner, both real and p-adic field equations can be satisfied and there are no problems with symmetries. p-Adic effective topology is expected to be a good approximation only within some length scale range which means infrared and UV cutoffs. Also multi-p-fractality is possible.

Bibliography

Books about TGD

- [1] M. Pitkänen (2006), *Topological Geometroynamics: Overview*.
http://tdg.wippiespace.com/public_html/tgdview/tgdview.html.
- [2] M. Pitkänen (2006), *Quantum Physics as Infinite-Dimensional Geometry*.
http://tdg.wippiespace.com/public_html/tgdgeom/tgdgeom.html.
- [3] M. Pitkänen (2006), *Physics in Many-Sheeted Space-Time*.
http://tdg.wippiespace.com/public_html/tgdclass/tgdclass.html.
- [4] M. Pitkänen (2006), *p-Adic length Scale Hypothesis and Dark Matter Hierarchy*.
http://tdg.wippiespace.com/public_html/paddark/paddark.html.
- [5] M. Pitkänen (2006), *Quantum TGD*.
http://tdg.wippiespace.com/public_html/tgdquant/tgdquant.html.
- [6] M. Pitkänen (2006), *TGD as a Generalized Number Theory*.
http://tdg.wippiespace.com/public_html/tgdnumber/tgdnumber.html.
- [7] M. Pitkänen (2006), *TGD and Fringe Physics*.
http://tdg.wippiespace.com/public_html/freenergy/freenergy.html.

Books about TGD Inspired Theory of Consciousness and Quantum Biology

- [8] M. Pitkänen (2006), *TGD Inspired Theory of Consciousness*.
http://tdg.wippiespace.com/public_html/tgdconsc/tgdconsc.html.
- [9] M. Pitkänen (2006), *Bio-Systems as Self-Organizing Quantum Systems*.
http://tdg.wippiespace.com/public_html/bioselforg/bioselforg.html.
- [10] M. Pitkänen (2006), *Quantum Hardware of Living Matter*.
http://tdg.wippiespace.com/public_html/bioware/bioware.html.
- [11] M. Pitkänen (2006), *Bio-Systems as Conscious Holograms*.
http://tdg.wippiespace.com/public_html/hologram/hologram.html.
- [12] M. Pitkänen (2006), *Genes and Memes*.
http://tdg.wippiespace.com/public_html/genememe/genememe.html.
- [13] M. Pitkänen (2006), *Magnetospheric Consciousness*.
http://tdg.wippiespace.com/public_html/magnconsc/magnconsc.html.
- [14] M. Pitkänen (2006), *Mathematical Aspects of Consciousness Theory*.
http://tdg.wippiespace.com/public_html/mathconsc/mathconsc.html.
- [15] M. Pitkänen (2006), *TGD and EEG*.
http://tdg.wippiespace.com/public_html/tgdeeg/tgdeeg.html.

Mathematics

- [16] Helgason, S. (1962): *Differential Geometry and Symmetric Spaces*. Academic Press, New York.
- [17] Pope, C., N. (1980): *Eigenfunctions and Spin^c Structures on CP₂* D.A.M.T.P. preprint.
- [18] Z. I. Borevich and I. R. Shafarevich (1966) ,*Number Theory*. Academic Press.

Theoretical physics

- [19] Zee, A. (1982): *The Unity of Forces in the Universe* World Science Press, Singapore.
- [20] G. Parisi (1992) *Field Theory, Disorder and Simulations*, World Scientific.
- [21] Huang, K. (1982): *Quarks, Leptons & Gauge Fields*. World Scientific.
- [22] Björken, J. and Drell, S. (1965): *Relativistic Quantum Fields*. Mc-Graw-Hill, New York.

Index

- CP_2 spinor Laplacian, 146, 168, 189
- CP_2 spinor harmonic, 156
- H -chirality, 719
- δM_+^4 , 150
- , 715

- Abelian anyon, 653
- Abelian differentials of the first kind, 107
- acceleration mechanism, 307
- Aleph anomaly, 186
- algebraic continuation, 154
- algebraic genus, 79
- anticommutation relations, 626
- axions, 536

- Babbha scattering, 346
- Beraha numbers, 405
- Betti number, 715
- Big Bang, 290
- biological transmutations, 475
- Black hole-elementary particle analogy, 160
- Boltzmann weight, 131
- braid groups, 655
- braiding, 414
- breaking of isospin symmetry, 498
- burning salt water, 475

- c, 715
- Cabibbo angle, 168, 196, 201
- Calabi-Yau manifold, 79
- canonical homology basis, 105
- Cartan algebra, 44, 250
- causal determinant, 187
- causal diamond, 154
- CDF, 172, 367, 373
- CDF anomaly, 346
- cellular water, 298, 304
- Centauro events, 244, 259, 303
- central charge, 657
- central extension, 655
- chemical qualia, 249
- Chern-Simons action, 129
- Chern-Simons term, 657
- Chilbolton, 406
- Christoffel symbol, 157
- CKM matrix, 145, 169, 185
- classical chaos, 221
- classical color gauge fields, 406

- cobordism, 656
- coiled structure, 410
- cold fusion, 410
- color constancy, 190, 422
- color Coulombic energy, 169
- color electric flux tubes, 407
- color force, 293, 294
- color glass condensate, 287
- color magnetic flux tube, 293
- color magnetic interaction energy, 413, 417
- condensate level, 373
- cones, 110
- configuration space spinor, 369
- conformal algebra, 130
- conformal confinement, 291
- conformal field theory, 419
- conjugacy class, 655
- conserved vector current, 192, 194
- constituent quark masses, 171
- coordinates of Eguchi and Freund, 715
- coset construction, 128
- cosmic expansion, 244
- cosmic rays, 294, 298
- cosmological constant, 139
- covariantly constant, 717
- covariantly constant right handed neutrino, 144
- Coxeter number, 165, 186
- CP breaking, 164
- critical cosmologies, 286, 290
- critical line, 441, 627
- current quark masses, 171, 192
- cusps, 627
- Cutkosky rules, 75

- dark neutrinos, 410, 434
- dark nuclear strings, 452, 501
- de-coherence, 471
- de-coherence time, 306
- defect regions, 625
- Dehn twist, 106
- delta function, 263, 264, 383
- Dirac determinant, 110
- direct CP breaking, 244, 252
- DNA as topological quantum computer, 497
- dual of the canonical homology basis, 106

- Ed Witten, 655
- effective 2-dimensionality, 80, 217

- effective p-adic topology, 130
 electric-magnetic duality, 589
 electro-weak couplings, 166, 222, 253, 719
 electro-weak interactions, 719
 elementary particle horizon, 217
 exotic atoms, 534
 exotic particles, 117
 exotic Super Virasoro representations, 244

 family replication phenomenon, 247, 248, 310
 Fermat primes, 295
 fermionic statistics, 309
 Feynman graph, 404, 487
 Fibonacci numbers, 481
 final state of the star, 497
 flag-manifold qualia, 108
 Fock space, 119, 625
 Fourier transform, 339, 341, 360
 fractional electric charge, 698
 functor, 657

 gamma ray bursts, 300, 308, 370
 gap energy, 560
 Gaussian integer, 202
 Gaussian Mersenne, 161
 Gaussian primes, 161, 403
 Gell-Mann-Okubo mass formula, 186, 192, 247
 generalized Feynman diagram, 172
 generalized Feynman diagrams, 70, 310
 generalized imbedding space, 371
 genus-generation correspondence, 246
 Geodesic sub-manifolds, 718
 gravitational collapse, 296
 GSI anomaly, 494

 hadron masses, 169, 185
 hadronic string tension, 218, 293
 hadronization, 244, 290, 293
 Hagedorn temperature, 293, 294
 heavy-ion collision, 339, 340, 347
 height function, 110
 helicity density, 656
 hierarchy of infinite primes, 426
 Higgs mechanism, 127, 158
 high T_c superconductivity, 560, 562
 highest weight representation, 656
 Hodge numbers, 79
 holomorphic function, 149
 holonomy, 723
 holonomy group, 409, 417
 homotopy group, 718
 Hopf algebra, 655
 Hurwitz zetas, 117
 hydrophily, 500
 hyper-complex primes, 73
 hyper-finite factor of type II_1 , 118
 hyperboloid, 110

 imbedding, 341, 356
 impact parameter, 289
 induced spinor connection, 719
 infinite prime, 155
 infinite-dimensional symmetric space, 309
 inflationary cosmologies, 286
 inner product, 147, 316
 instanton, 375
 instanton current, 356, 383
 instanton density, 339
 intentionality in astrophysical length scales, 233
 interaction strength, 228
 intersection number, 105
 intron, 435
 inverse beta decay, 435
 isometry algebra, 44, 249

 Jacobian variety, 109, 110, 257
 jets, 257
 Jones index, 121, 625
 Josephson junction, 590

 Kähler action, 76
 Kähler form, 717
 Kähler function, 309, 716
 Kähler geometry, 253
 Kähler metric, 716
 Kähler potential, 717
 Kaluza-Klein, 142
 Kanarev, 253
 kaon-antikaon system, 252
 Karmen anomaly, 338, 489
 Kervran, 488
 Killing vector fields, 44, 249
 knot, 409
 knot invariants, 653
 Kurie plot, 430

 Lagrangian, 252, 253
 Landau level, 698
 Langlands program, 120
 length scale cutoff, 363
 lepto-baryon, 223, 338, 343
 lepto-hadron, 145, 369, 370
 lepto-hadrons, 244, 337
 lepto-pion, 258, 293, 337–339, 355, 356
 lepto-pion production, 356, 357
 lepto-hadron physics, 293
 levitation, 560
 Lie triple system, 718
 light-like boundary, 292
 line element, 715
 link, 308, 405
 link invariants, 656
 lithium problem, 475
 Lorentz group, 150

 Möbius transformation, 107

- magic number, 409
 magnetic monopole, 421, 717
 Majorana, 142
 Majorana neutrino, 435
 Majorana spinors, 42, 248
 Mapping class group, 106
 mapping class group, 105
 mass distribution of top quark, 186
 measurement interaction, 44, 250
 Mersenne primes, 161
 Mersenne primes and mass scales, 298
 metric determinant, 413
 microwave heating, 494
 Minkowskian signature, 129
 model for hadron masses, 185, 186, 224, 237
 modified Dirac equation, 43, 44, 248, 249
 modular contribution to mass squared, 156
 modular degrees of freedom, 120
 modular invariance, 112
 module, 159
 moduli space, 120
 mRNA, 499
 MSSM, 252
- neutrino masses, 116, 162
 neutrino mixing, 162, 164
 nuclear string hypothesis, 451
- color glass condensate, 292
 orbifold singularities, 510
 order parameter, 306
 orthopositronium, 339, 345, 350
 orthopositronium anomaly, 345
 oscillator operator, 130
- p-adic coupling constant evolution, 104
 p-Adic length scale hypothesis, 160
 p-adic mass squared, 145
 p-adic temperature, 104
 p-adicization, 149
 parallel transport, 718
 parity breaking effects, 352
 parity breaking effects in living matter, 407
 particle massivation, 127
 partonic 2-surfaces, 70, 120
 partons, 128
 PCAC hypothesis, 338, 341
 percolation, 628
 perturbative QCD, 188, 200, 201
 Polyakov, 111
 Pomeron, 223
 Pontryagin number, 715
 production amplitude, 340, 341
 propagator, 259, 310
 protein folding, 453
 proton spin crisis, 214, 254
 pseudo-momentum, 73
- pseudoscalar, 170, 186
 Pythagorean phase, 203
- quantum computation, 297, 426
 quantum critical superconductors, 626, 627
 quantum-classical correspondence, 288
 quark-gluon plasma, 266, 286
 quasars, 300
- rapidity, 263, 287, 288
 rational numbers, 185
 reconnection, 628
 Regge slope, 265, 294
 region momentum, 73
 Relativistic Heavy Ion Collider, 286
 renormalization group equations, 314, 318
 residue calculus, 360, 384, 385
 RHIC, 286
 RHIC events, 293, 296, 411
 Riemann zeta, 117
 Robertson-Walker cosmologies, 289
 ruler-and-compass integers, 295
 Rutherford cross section, 407
- scaled up Compton length, 534
 scaled up copies of neutrinos, 193
 scaled up variants of light quarks, 185, 224
 Schwarzschild radius, 295, 301
 sea quark, 254, 256, 408
 second quantization, 426
 sigma model, 172, 220, 316
 slicing, 43, 249
 sono-luminescence, 437, 438, 440
 space-time super-symmetry, 248
 spectrum of Planck constants, 626
 spin glass degeneracy, 453
 spin puzzle of proton, 188, 215, 223
 spin-spin splitting, 188, 189
 spin-spin splittings for hadron masses, 231
 spinor connection, 720
 spinor harmonics, 141
 spinor Laplacian, 143
 spinor structure, 718
 stopping codons, 500
 string tension, 103
 stringy propagator, 44, 249
 stripe, 264
 super Kac-Moody algebra, 128
 super nova, 168
 super Virasoro conditions, 141
 super-potential, 251
 super-symplectic algebra, 128
 super-symplectic invariance, 160
 superconductivity, 439
 SUSY QFT, 41
 symmetric space, 203
 symplectic fusion algebra, 654

- symplectic modular group, 106
- symplectic structure, 106, 717
- symplectic transformation, 150
- synchrotron radiation, 495

- tachyonic ground state, 187
- Teichmueller parameters, 105
- Teichmuller parameters, 156
- tensor factor, 128
- tensor product, 136
- tetraneutron, 370, 408, 526
- thermal contribution to mass squared, 157
- thermodynamical model for topological mixing,
207
- theta parameter, 41
- time evolution, 158
- time like entanglement, 495
- topological condensate, 403
- topological evaporation, 245
- topological mixing, 168, 169, 185
- topological mixing of quarks, 168, 189
- transcription, 499
- tritium beta decay anomaly, 429, 434
- tRNA, 500
- tunneling, 414, 428
- twistor space, 76

- unitarity, 147, 164
- unitarity conditions, 198, 203, 206

- vacuum energy, 484
- vacuum functional, 100, 135
- valence quark, 169, 170
- vapor phase, 263
- vielbein group, 719
- vierbein, 716
- vierbein connection, 716
- Virasoro algebra, 129

- warping, 412
- water memory, 497
- WCW, 42, 248, 309
- Weinberg angle, 721
- Wess-Zumino-Witten model, 656
- world of classical worlds, 142

- zero modes, 110